

**Studies on the
Biosynthesis and Structure Elucidation
of Terpene Natural Products
by Isotopic Labeling Experiments**

Kumulative Dissertation zur Erlangung des
Doktorgrades (Dr. rer. nat.)

der

Mathematisch-Naturwissenschaftlichen Fakultät der
Rheinischen Friedrich-Wilhelms-Universität Bonn

vorgelegt von

Lena Barra

aus Braunschweig

Bonn 2017

Angefertigt mit der Genehmigung der Mathematisch-Naturwissenschaftlichen Fakultät
der Rheinischen Friedrich-Wilhelms-Universität Bonn

1. Gutachter: Prof. Dr. Jeroen S. Dickschat

2. Gutachter: Prof. Dr. Arne Lützen

Tag der Promotion: 18.02.2018

Erscheinungsjahr: 2019

Die vorliegende Arbeit wurde in der Zeit vom 01.09.2013 bis 30.06.2014 am Institut für Organische Chemie der Technischen Universität Carolo-Wilhelmina zu Braunschweig und in der Zeit vom 01.07.2014 bis 31.10.2017 am Kekulé-Institut für Organische Chemie und Biochemie der Rheinischen Friedrich-Wilhelms-Universität Bonn unter der Leitung von Herrn Prof. Dr. J. S. Dickschat angefertigt.

Vorveröffentlichungen der Dissertation

Teilergebnisse aus dieser Promotionsschrift wurden mit Genehmigung der Mathematisch-Naturwissenschaftlichen Fakultät, vertreten durch den Mentor Prof. Dr. Jeroen S. Dickschat, in folgenden Beiträgen vorab veröffentlicht:

Publikationen

- [1] L. Barra, B. Schulz, J. S. Dickschat, *Pogostol Biosynthesis by the Endophytic Fungus *Geniculosporium**, *ChemBioChem* **2014**, *15*, 2379-2383.
- [2] C. A. Citron, P. Rabe, L. Barra, C. Nakano, T. Hoshino, J. S. Dickschat, *Synthesis of Isotopically Labelled Oligoprenyl Diphosphates and Their Application in Mechanistic Investigations of Terpene Cyclases*, *Eur. J. Org. Chem.* **2014**, 7684-7691.
- [3] C. A. Citron, L. Barra, J. Wink, J. S. Dickschat, *Volatiles from Nineteen Recently Genome Sequenced Actinomycetes*, *Org. Biomol. Chem.* **2015**, *13*, 2673-2683.
- [4] L. Barra, K. Ibrom, J. S. Dickschat, *Structural Revision and Elucidation of the Biosynthesis of Hypodoratoxide by ^{13}C , ^{13}C COSY NMR Spectroscopy*, *Angew. Chem. Int. Ed.* **2015**, *54*, 6637-6640.
L. Barra, K. Ibrom, J. S. Dickschat, *Strukturrevision und Aufklärung der Biosynthese von Hypodoratoxid durch ein ^{13}C , ^{13}C -COSY-NMR-Experiment*, *Angew. Chem.* **2015**, *127*, 6737-6740.
- [5] P. Rabe, L. Barra, J. Rinkel, R. Riclea, C. A. Citron, T. A. Klapschinski, A. Janusko, J. S. Dickschat, *Conformational Analysis, Thermal Rearrangement, and EI-MS Fragmentation Mechanism of (1(10)E,4E,6S,7R)-Germacradien-6-ol by ^{13}C -Labeling Experiments*, *Angew. Chem. Int. Ed.* **2015**, *54*, 13448-13451.
P. Rabe, L. Barra, J. Rinkel, R. Riclea, C. A. Citron, T. A. Klapschinski, A. Janusko, J. S. Dickschat, *Konformationsanalyse, thermische Umlagerung und EI-MS-Fragmentierungsmechanismus von (1(10)E,4E,6S,7R)-Germacradien-6-ol durch ^{13}C -Markierungsexperimente*, *Angew. Chem.* **2015**, *127*, 13649-13653.
- [6] P. Rabe, J. Rinkel, T. A. Klapschinski, L. Barra, J. S. Dickschat, *A method for investigating the stereochemical course of terpene cyclisations*, *Org. Biomol. Chem.* **2016**, *14*, 158-164.
- [7] M. M. Mohseni, T. Höver, L. Barra, M. Kaiser, P. C. Dorrestein, J. S. Dickschat, T. F. Schäberle, *Discovery of a Mosaic-Like Biosynthetic Assembly Line with a Decarboxylative Off-Loading Mechanism through a Combination of Genome Mining and Imaging*, *Angew. Chem. Int. Ed.* **2016**, *55*, 13611-13614.

- M. M. Mohseni, T. Höver, L. Barra, M. Kaiser, P. C. Dorrestein, J. S. Dickschat, T. F. Schäberle, *Entdeckung einer Mosaik-ähnlichen Biosynthesemaschinerie mit einem decarboxylierenden Entladungsmechanismus durch die Kombination von Genom-Mining und bildgebenden Verfahren*, *Angew. Chem.* **2016**, *128*, 13809-13813.
- [8] L. Barra, J. S. Dickschat, *Sceptrin – Enantioselective Synthesis of a Tetrasubstituted all-trans Cyclobutane Key Intermediate*, *Eur. J. Org. Chem.* **2017**, 4566-4571.
- [9] L. Barra, P. Barac, G. M. König, M. Crüsemann, J. S. Dickschat, *Volatiles from the fungal microbiome of the marine sponge Callyspongia cf. flammaea*, *Org. Biomol. Chem.* **2017**, *15*, 7411-7421.
- [10] L. Barra, J. S. Dickschat, *Harzianone Biosynthesis by the Biocontrol Fungus Trichoderma*, *ChemBioChem*, **2017**, accepted.

Acknowledgments

Mein aufrichtiger Dank gilt:

Meinem Doktorvater Professor Dr. Jeroen S. Dickschat, für die Aufnahme in seinen Arbeitskreis und besonders für die stete Diskussionsbereitschaft, die hilfreichen Ideen sowie die andauernde Unterstützung und Motivation.

Den Mitgliedern der Prüfungskommission: Prof. Dr. Arne Lützen, Prof. Dr. Gabriele M. König sowie Prof. Dr. Robert Glaum.

Den aktuellen und ehemaligen Mitgliedern der Arbeitsgruppe: Dr. Ramona Riclea, Dr. Nelson L. Brock, Dr. Christian A. Citron, Dr. Susanne M. Wickel, Dr. Patrick Rabe, Tao Wang, Dr. Khomaizon A. K. Pahirulzaman, Ersin Celik, Erik Daniel, Etilia Dolja, Tim A. Klapschinski, Jan Rinkel, Lukas Lauterbach, Britta Nubbemeyer, Thomas Schmitz, meiner Bachelorstudentin Marie Reuter-Schniete, Dr. Zhongfeng Ye, Simone Gaeta und besonders meinem "Laborehemann" Immo Burkhardt.

Mein Dank gilt außerdem meinen Kooperationspartnern: Prof. Dr. Gabriele M. König, Prof. Dr. Till F. Schäberle, Dr. Barbara Schulz, Dr. Kerstin Ibrom, Dr. Mahsa M. Mohseni, Dr. Max Crüsemann und Paul Barac.

Danken möchte ich den Mitarbeitern der analytischen Abteilungen in Braunschweig und Bonn: Dr. Kerstin Ibrom, Petra Holba Schulz, Gabriele Krafft, Karin Kadhim, Andreas Schneider, Dr. Senada Nozinovic, Claus Schmidt, Ulrike Weynand, Karin Prochnicki, Hannelore Spitz und Dr. Marianne Engeser.

Außerdem möchte ich meinen Freunden danken, die mich direkt oder indirekt im Laufe der letzten Jahre unterstützt haben: Axel, Immo, Kathi, Jule, Carsten und Paul.

Mein ganz besonderer Dank gilt meinen Eltern Klaus und Manuela Barra, ohne eure Unterstützung wäre dies hier nicht möglich gewesen, sowie dem Rest der Familie: Dieter und Inge Handel, Grete Barra, Laura Barra, Ela Reinhold, Christian Handel, Stefan Wieneber, Tatjana Reuter, Familie Richter und Familie Reuter.

Danke

PREFACE

This cumulative doctoral thesis is divided into two main sections, chapter 1 and chapters 2 to 11. The first chapter comprises an introduction into the topic by giving an overview on the scientific knowledge. A strong focus was laid on terpene natural products and their biosynthetic machinery. Nonribosomal peptide/polyketide biosynthesis, the isotope tracer technique and an introduction into volatile natural products is also given.

The following second section contains the scientific results obtained during the course of this doctoral thesis. It is comprised of ten chapters, each representing one scientific publication. In every chapter, an introduction and a summary are given, explaining the relationship between the individual parts and their scientific significance. Chapters 2 to 6 contain publications revolving around the identification and biosynthesis of terpenes and other volatile natural products from microorganisms. A focus is made on the *in vivo* application of synthetic isotopically labeled precursors. Chapters 7 to 10 comprise publications revolving around the design, synthesis and application of isotopically labeled substrates for *in vitro* studies with recombinant enzymes. The publications in Chapter 7, 8 and 9 are already included in cumulative doctoral theses from Dr. Christian A. Citron (TU Braunschweig, Chapter 7) and Dr. Patrick Rabe (University of Bonn, Chapter 7, 8, and 9) and are only supplementary to this thesis. A statement on my contribution to the work is given priorly to every chapter. The last chapter (chapter 11) describes a method for the synthesis of a tetrasubstituted, pseudosymmetric cyclobutane derivative, which was developed during studies towards a total synthesis for a fungal sesquiterpene. Reprints of all mentioned publications are given in the appendix of this thesis.

Table of Contents

1	State of Scientific Knowledge	1
1.1	Terpene Natural Products	1
1.2	Biosynthesis of Terpenes	2
1.2.1	Biosynthesis of DMAPP and IPP	4
1.2.1.1	The Mevalonate Pathway	4
1.2.1.2	The Deoxyxylulose Phosphate Pathway	6
1.2.1.3	Pharmacological Implications	8
1.2.2	Biosynthesis of Polyisoprenoid Chains	9
1.2.3	Terpene Cyclization	9
1.2.3.1	Mechanistic Details - Taxadiene Synthase	11
1.3	NRPS/PKS-Derived Natural Products	13
1.4	Isotope Tracer Technique	16
1.4.1	<i>In Vivo</i> Labeling – Siphonazole Biosynthesis	16
1.4.2	<i>In Vitro</i> Labeling – Corvol Ether Biosynthesis	19
1.5	Volatile Natural Products	22
1.5.1	Capturing Volatile Natural Products from Microorganisms	23
2	Pogostol Biosynthesis by the Endophytic Fungus <i>Geniculosporium</i>	25
3	Structural Revision and Elucidation of the Biosynthesis of Hypodoratoxide by ¹³C, ¹³C COSY NMR Spectroscopy	29
4	Harzianone Biosynthesis by the Biocontrol Fungus <i>Trichoderma</i>	32
5	Volatiles from the Fungal Microbiome of the Marine Sponge <i>Callyspongia cf. flammea</i>	35
6	Volatiles from Nineteen Recently Genome Sequenced Actinomycetes	39
7	Synthesis of Isotopically Labelled Oligoprenyl Diphosphates and Their Application in Mechanistic Investigations of Terpene Cyclases	42
8	Conformational Analysis, Thermal Rearrangement, and EI-MS Fragmentation Mechanism of (1(10)<i>E</i>,4<i>E</i>,6<i>S</i>,7<i>R</i>)-Germacradien-6-ol by ¹³C-Labeling Experiments	45
9	A Method for Investigating the Stereochemical Course of Terpene Cyclisations	45

10	Discovery of a Mosaic-Like Biosynthetic Assembly Line with a Decarboxylative Off-Loading Mechanism through a Combination of Genome Mining and Imaging	49
11	Sceptrin – Enantioselective Synthesis of a Tetrasubstituted all- <i>trans</i> Cyclobutane Key Intermediate	52
12	References.....	57
13	Appendix A – J	68

1 State of Scientific Knowledge

1.1 Terpene Natural Products

Terpenes make up the biggest class of natural products, with over 50,000 known structures isolated from all kingdoms of life.^[1] They all share a common biosynthetic origin and are composed of 2-methyl-1,3-butadiene, so called isoprene units. This concept was firstly recognized by Otto Wallach in 1887 and later described by Leopold Ruzicka as the “isoprene rule”.^[2,3] According to the number of C₅ units, the terpenoids are subdivided into (C₅) hemi-, (C₁₀) mono-, (C₁₅) sesqui-, (C₂₀) di-, (C₂₅) sester-, (C₃₀) tri-, and (C₄₀) tetraterpenes. Important and interesting examples for each subdivision are discussed in the following section.

Only about 25 naturally occurring hemiterpenoids are known from nature.^[4] One prominent example is isoprene (1), released by plants with an annual rate of 500 – 750 Tg, one of the most abundant volatile natural product on earth (Figure 1).^[5]

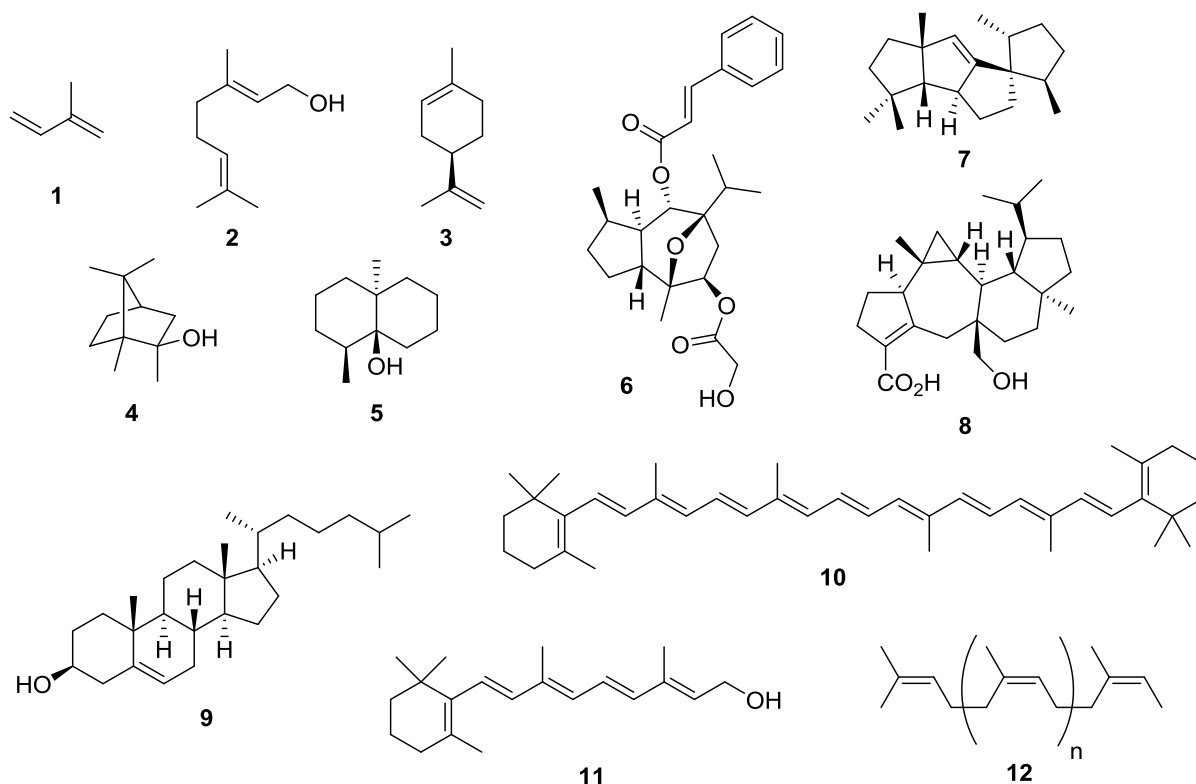


Figure 1. Selection of known hemi-, mono-, sesqui-, di-, tri- and tetraterpenes.

Geraniol (**2**) is an acyclic, linear monoterpene consisting of two isoprene building blocks and can be found as an ingredient in rose oil (*Rosa damascene*) inhabiting a characteristic flowery smell.^[1] (*R*)-(+)-limonene (**3**) is an example for a monocyclic monoterpene and can be found in essential oils from citrus fruits, exhibiting a characteristic smell of oranges.^[1] The methylated monoterpene 2-methylisoborneol (2-MIB, **4**) and the degraded sesquiterpene geosmin (**5**) are together responsible for the characteristic smell of forest earth and both terpenes are produced by soil-dwelling bacteria of the genus *Streptomyces*.^[6,7] The terpene hydrocarbon backbones often occur as highly decorated terpenoids, carrying various functional groups, as can be seen for the guaiane sesquiterpenoid englerine A (**6**). Englerin A was isolated from the African plant *Phyllanthus engleri*, indigenous to Tanzania and Zimbabwe and exhibits high activity against renal cancer cells.^[8] The tetracyclic diterpene spiroviolene (**7**), isolated from *Streptomyces violens*^[9] and the fungal sesterterpene asperterpenoid A (**8**) are recent examples for highly complex polycyclic terpenoids.^[10] Interestingly, an oxidation product of **7** was recently isolated from the deep-sea-derived fungus *Penicillium granulatum*.^[11] Cholesterol (**9**) is a triterpene steroid, a constituent of all cell membranes in animal tissues. It is also a precursor for human steroid hormones, bile acids and vitamin D.^[12] Another biologically important terpene is the tetraterpene β -carotene (**10**). Due to the extended π -system, strong red-orange coloration is observed and **10** and analogues are widely used in the food industry as coloring agents. β -Carotene is the precursor of retinol (**11**), also known as vitamin A₁, the universal chromophore essential for the mammalian process of sight.^[13] Lastly, polyisoprenes (**12**, $n > 8$) exist in nature and are known as natural rubber. This polymer is harvested from the Brazilian rubber tree (*Hevea brasiliensis*) and is used to manufacture a wide range of products, for example tires for automobiles or aircrafts.^[14]

1.2 Biosynthesis of Terpenes

The biosynthesis of terpenoid natural products can be sectioned into four general steps. The first step comprises the generation of the central biological C₅-units dimethylallyl pyrophosphate (DMAPP, **13**) and isopentenyl pyrophosphate (IPP, **14**). They either arise from the mevalonate pathway (MV pathway) or the deoxyxylulose phosphate pathway (DOX pathway). In bacteria, algae and protozoen, the DOX

pathway is employed, whereas in higher eukaryotes like fungi and animals the mevalonate pathway is utilized. In plants both metabolic pathways co-occur: the mevalonate pathway is localized in the cytosol, whereas the DOX pathway is found in the chloroplasts.^[15] The subsequent second step involves coupling of the C₅-monomers **13** and **14** to linear oligoprenyl diphosphates. The chain length is thereby controlled by the operating synthase, yielding geranyl diphosphate (**15**, GPP, n = 1), farnesyl diphosphate (**16**, FPP, n = 2), geranylgeranyl diphosphate (**17**, GGPP, n = 3) or geranylgeranyl farnesyl diphosphate (**18**, GFPP, n = 3). In the third step, the linear achiral precursors are converted by designated terpene synthases into linear or (poly)cyclic terpenes. In a subsequent fourth step, the obtained terpenes can be further functionalized by one or more tailoring enzymes, like P450-monooxygenases, NAD(P)⁺ and flavin dependent oxidoreductases, acetyltransferases or methyltransferases. This final step often introduces the specific bioactivity into the metabolite (Figure 2).^[4,15]

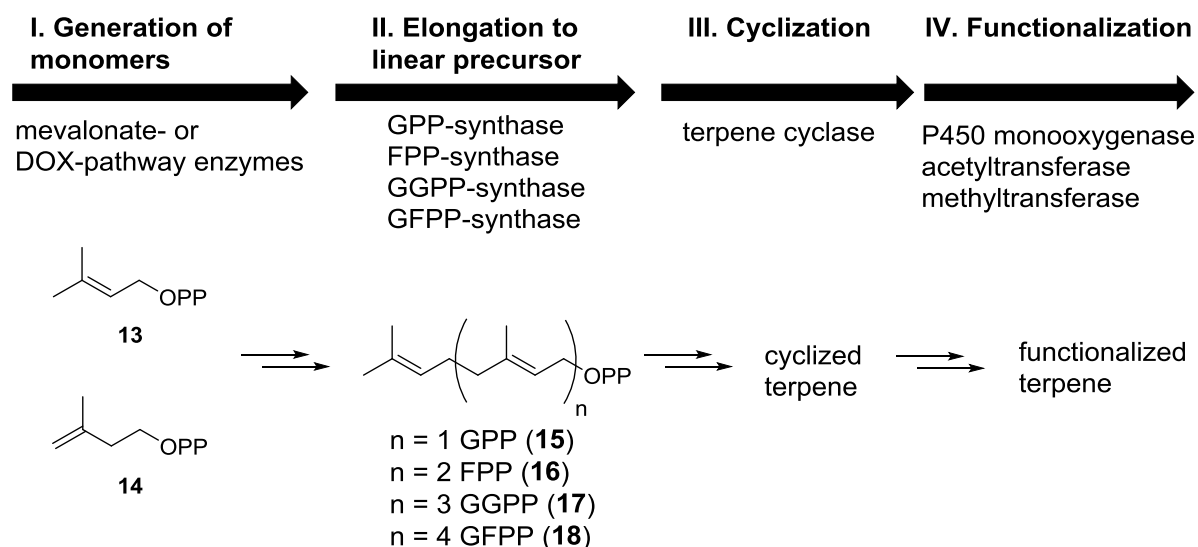


Figure 2. Overview of the biogenetic steps during terpene biosynthesis.

The linear precursor for all triterpenes, squalene (**19**) is produced by dimerization of two FPP units, catalyzed by a squalene synthase. Similarly, condensation of two GGPP units gives phytoene (**20**), the precursor of all tetraterpenes (Figure 3). The biosynthetic details of tri- and tetraterpenes are not covered in this thesis.

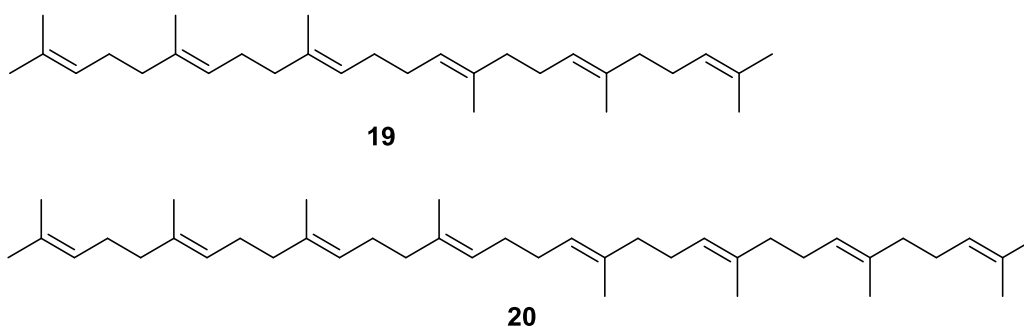


Figure 3. Structure of squalene (**19**) and phytoene (**20**).

1.2.1 Biosynthesis of DMAPP and IPP

1.2.1.1 The Mevalonate Pathway

The discovery of the mevalonate pathway was achieved in the course of investigating steroid metabolism and was awarded with a Nobel Prize to Feodor Lynen and Konrad Bloch in 1964 and John Cornforth in 1975.^[16,17] This essential metabolic pathway links the primary metabolism to isoprenoid biosynthesis by the central metabolite acetyl coenzyme A (acetyl-CoA, **21**). Overall, six enzymes convert three units of **21** firstly to IPP (**14**) and a seventh enzyme can isomerize **14** into DMAPP (**13**) (Figure 4).

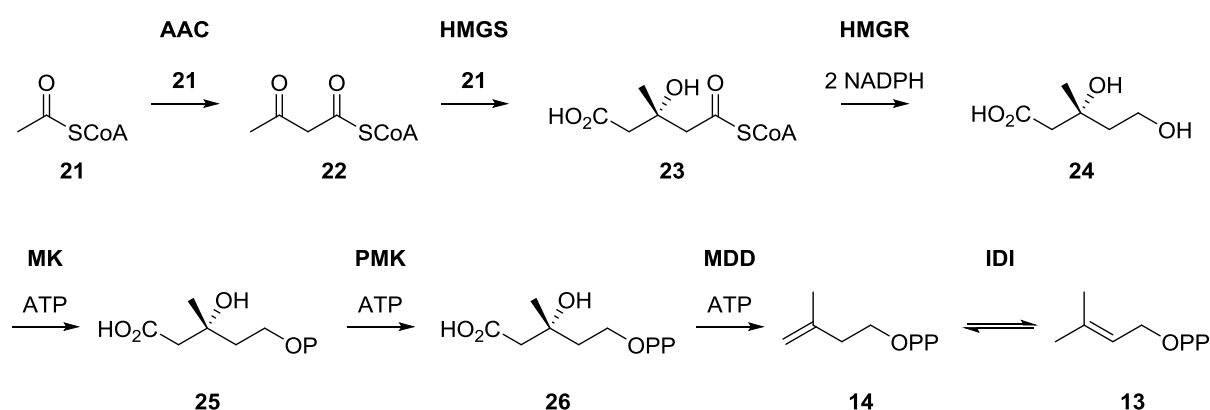


Figure 4. Depiction of the mevalonate pathway. AAC: acetyl-CoA synthase; HMGS: hydroxymethylglutaryl-CoA synthase; HMGR: hydroxymethylglutaryl-CoA reductase; MK: mevalonate kinase; PMK: phosphomevalonate kinase, MDD: diphosphomevalonate decarboxylase; IDI: isopentenyl diphosphate isomerase; NADPH: nicotinamide adenine dinucleotide phosphate; ATP: adenosine triphosphate.

The first reaction is catalyzed by the enzyme acetoacetyl-CoA synthase (AAC), which connects two acetyl-CoA (**21**) units in a biological Claisen reaction to form

β -keto thioester **22**. A third acetyl-CoA (**21**) is attached to **22** in a stereospecific aldol addition by the 3-hydroxy-3-methylglutaryl-CoA synthase (HMGS),^[18] followed by reduction to the central metabolite mevalonic acid (**24**), catalyzed by the 3-hydroxy-3-methylglutaryl-CoA reductase (HMGR).^[19] The stereochemical course of the aldol reaction was firstly studied by Theodor Lynen by growing *Mycobacterium* spp. on media containing *rac*-**24** as a single carbon source. He was able to show that only (+)-(*R*)-**24** was consumed by the organism, observed from enrichment of the antipodal (-)-(*S*)-**24** in the culture.^[20] Two subsequent phosphorylation steps of the primary alcohol function of **24** by a mevalonate kinase (MK) and phosphomevalonate kinase (PMK) yield diphosphate **26**.^[21] Subsequently, IPP (**14**) is generated by an ATP assisted decarboxylative-elimination reaction, catalyzed by the mevalonate 5-diphosphate decarboxylase (MDD).^[22,21b] At last, IPP (**14**) is isomerized to DMAPP (**13**) by the isopentenyl diphosphate isomerase (IDI) (Figure 4).^[23]

The stereochemical details of the MDD catalyzed decarboxylation-elimination reaction were analyzed by isotopic labeling experiments, employing (*2R*)- and (*2S*)-(*2*-²H)-**24**. Determination of the label incorporation into **14** demonstrated that the *pro-R* proton (H_R) in **26** is turned into H_Z in **14** and the *pro-S* proton (H_S) into H_E .^[24] Here, ATP assists the *anti*-elimination of H_2O without covalently binding to **26** (Figure 5A).

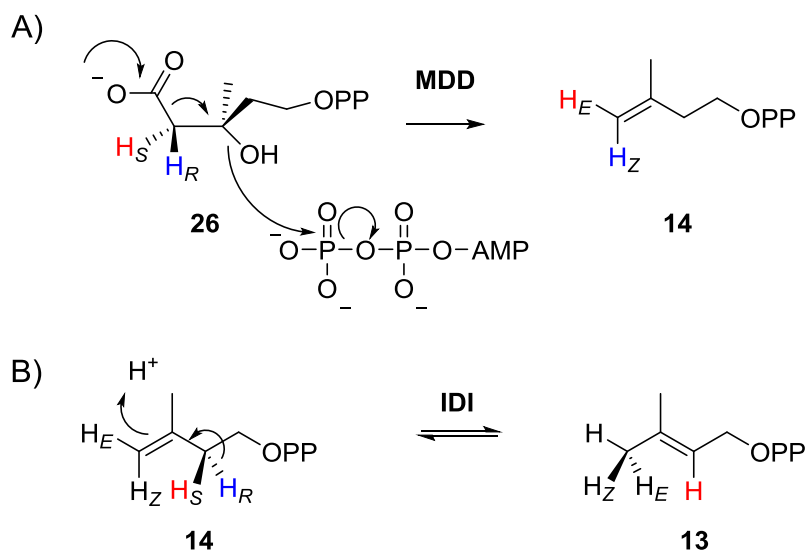


Figure 5. Stereochemical details of A) the MDD mediated reaction; B) the IDI-reaction. MDD: diphosphomevalonate decarboxylase; IDI: isopentenyl diphosphate isomerase.

The enzyme IDI converts IPP (**14**) into DMAPP (**13**) by a protonation-deprotonation sequence. The H_R proton in **14** is thereby selectively abstracted (Figure 5B).

1.2.1.2 The Deoxyxylulose Phosphate Pathway

An alternative pathway for isoprenoid biosynthesis was subsequently discovered, which also gave an explanation for observed inconsistencies in labeling patterns after feeding experiments, like in the biosynthesis of ubiquinones in *Escherichia coli*.^[25] Key experiments have been conducted by Michel Rohmer and Duilio Arigoni in the 1990s.^[26] The deoxyxylulose phosphate pathway starts with pyruvic acid (**27**) and D-glyceraldehyde-3-phosphate (**28**), which are converted under decarboxylation into 1-deoxy-D-xylulose-5-phosphate (**29**) in a thiamine pyrophosphate mediated reaction, which is catalyzed by the 1-deoxy-D-xylulose-5-phosphate synthase (DXPS) (Figure 6).^[27]

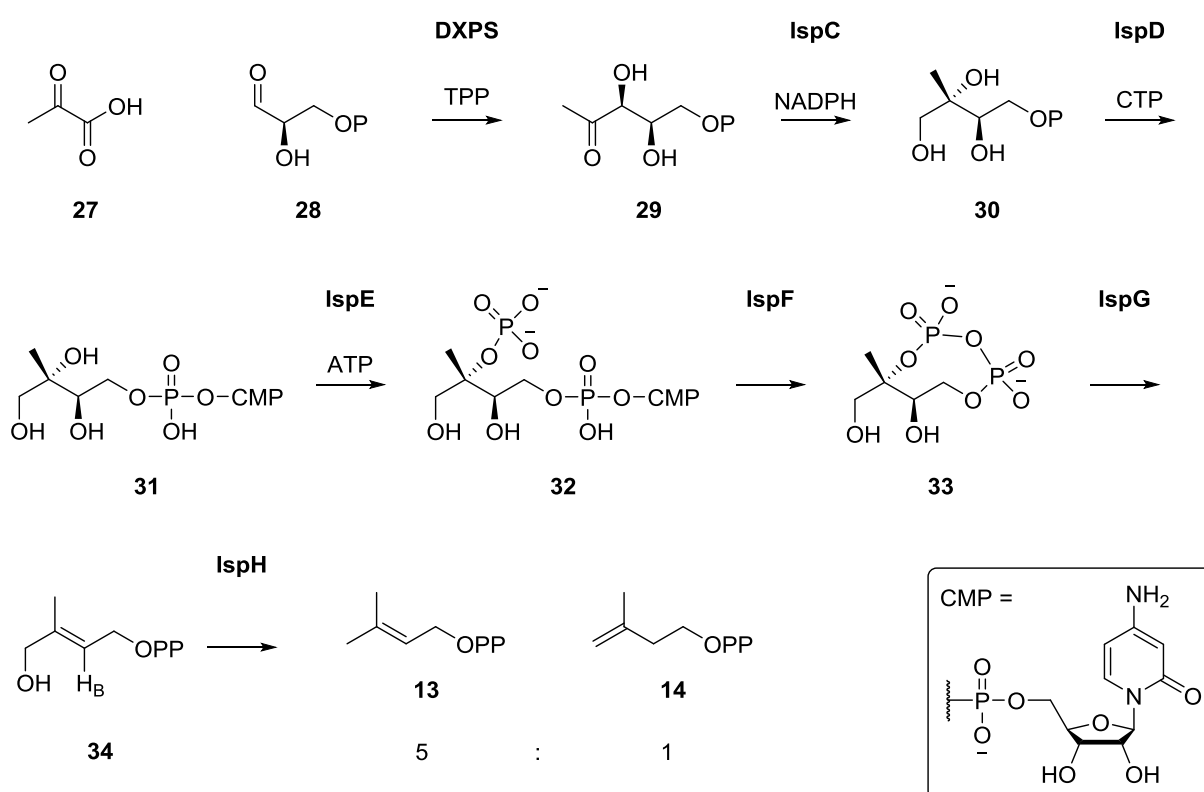


Figure 6. The deoxyxylulose phosphate pathway. DXPS: 1-deoxy-D-xylulose-5-phosphate synthase; IspC: 1-deoxy-D-xylulose 5-phosphate reductoisomerase; IspD: 4-diphosphocytidyl-2-C-methyl-D-erythritol synthase; IspE: 4-diphosphocytidyl-2-C-methyl-D-erythritol kinase; IspF: 2-C-methyl-D-erythritol-2,4-cyclodiphosphate synthase; IspG: 4-hydroxy-3-methylbut-2-enyl diphosphate synthase; IspH: 4-hydroxy-3-methylbut-2-enyl diphosphate reductase.

In the next step, the branched-chain structure, equivalent to the isoprene unit, is introduced by a reductoisomerase (IspC), generating 2-C-methyl-D-erythritol-4-phosphate (**30**).^[28] The primary phosphate group in **30** is substituted with a cytidine diphosphate, catalyzed by the 4-diphosphocytidyl-2-C-methyl-D-erythritol synthase

(IspD),^[29] followed by phosphorylation of the tertiary alcohol by the 4-diphosphocytidyl-2-*C*-methyl-D-erythritol kinase (IspE).^[30] Intermediate **32** is transformed into a highly unusual 8-membered cyclic phosphoanhydride (**33**), the only known cyclic diphosphate from nature, by the 2-*C*-methyl-D-erythritol-2,4-cyclodiphosphate synthase (IspF).^[31] By elimination of water and transfer of two electrons, 4-hydroxy-3-methyl-but-2-enyl diphosphate (**34**) is generated by IspG.^[32] The final step is catalyzed by the 4-hydroxy-3-methylbut-2-enyl diphosphate synthase (IspH), yielding DMAPP (**13**) and IPP (**14**) in a ratio of 5:1 by elimination of water and reduction.^[33]

The second step in the DOX-pathway is catalyzed by the reductoisomerase IspC and involves a complex rearrangement to aldehyde intermediate **35** prior to reduction. For this transformation, two possible mechanisms are discussed in the literature: a concerted α -ketol rearrangement consisting of initial deprotonation of the C3 hydroxyl group, followed by 1,2-alkyl migration from C4 to C2 (Figure 7A), or a stepwise mechanism by a retroaldol/aldol sequence (Figure 7B). A study by LIU, employing deuterated isotopologues of **29** and determination of secondary kinetic isotope effects, points to the occurrence of a stepwise mechanism via the bimolecular intermediate **A**.^[34]

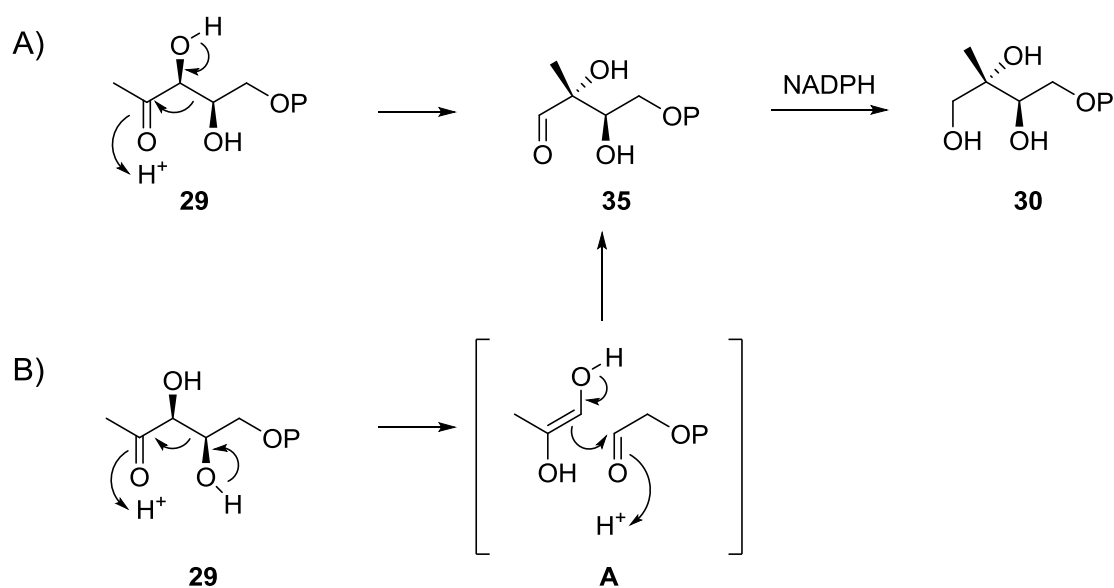


Figure 7. Possible mechanisms for IspC-reaction.

1.2.1.3 Pharmacological Implications

Knowledge about the details of early terpenoid biosynthetic pathways is not only indispensable for the design of feeding experiments, but also offers opportunities for the development of pharmaceutical therapeutics.^[35] The differing biogenesis of terpenes in mammalian cells to that in prokaryotes, like the tuberculosis pathogen *Mycobacterium tuberculosis* or the protozoan malaria parasite *Plasmodium falciparum*, opens up possibilities for a selective inhibition of these pathogens without disturbing the human metabolism. Fosmidomycin (**36**) and its derivative FR-900098 (**37**) were found to be highly potent inhibitors of the reductoisomerase IspC of the deoxyxylulose phosphate pathway^[36], which was shown for *M. tuberculosis*^[37] *in vitro* and for *P. falciparum* *in vitro* and *in vivo*.^[38] A lack of acute toxicity and genotoxicity further supports pre-clinical and clinical development (Figure 8).^[39]

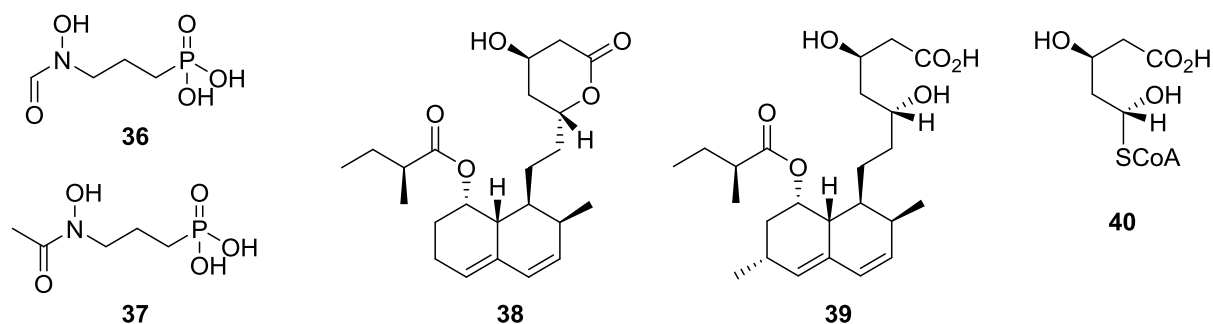


Figure 8. Structures of isoprenoid biosynthesis inhibitors (**36-39**) and mevaldyl-CoA (**40**).

A second pharmacologically important example is the use of statins for the treatment of hypocholesterolemia, a major risk for the development of coronary heart disease. High levels of cholesterol (**9**), a steroid produced via the mevalonate pathway in mammals, can be lowered by inhibition of the HMG-CoA reductase (HMGR).^[40] The first highly potent HMG-CoA reductase inhibitor was the polyketide compactin (**38**), isolated from *Penicillium citrinum* in 1977.^[41] The related lovastatin (**39**), isolated from *Aspergillus terreus*,^[42] was the first cholesterol-lowering agent approved for clinical use.^[40] Its structural similarity to mevaldyl-CoA (**40**), an intermediate towards mevalonic acid (**24**), is shown in Figure 8.

1.2.2 Biosynthesis of Polyisoprenoid Chains

The linear oligoprenyl diphosphates are synthesized by prenyltransferases, also called polyisoprenoid diphosphate synthases, catalyzing consecutive prenyl chain elongations. These enzymes mediate the coupling between DMAPP (**13**) and IPP (**14**) via a nucleophilic substitution reaction. Thereby, the allylic diphosphate in DMAPP is abstracted and the allylic cation is attacked by the terminal, electron-rich double bond in IPP, followed by a stereoselective deprotonation of the H_R-proton at C2 (Figure 9).

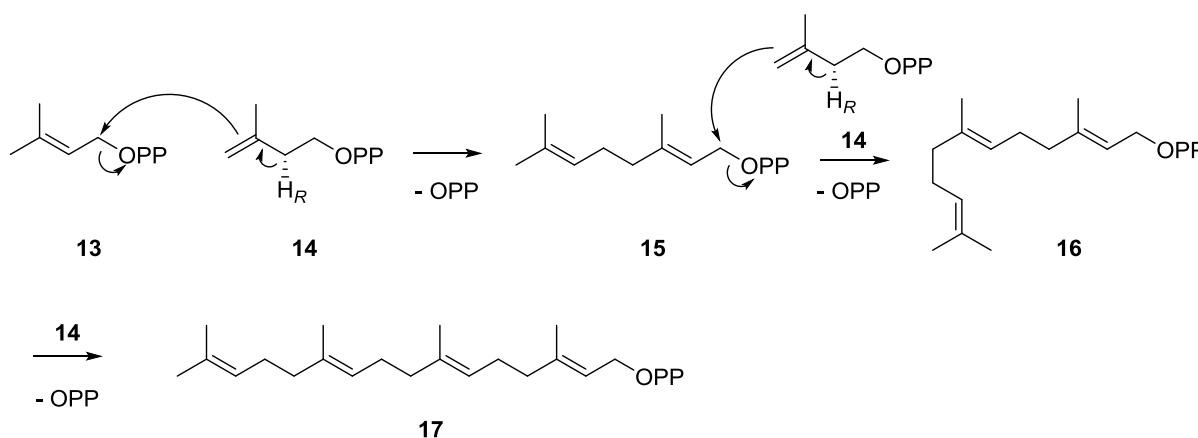


Figure 9. Mechanism of the oligoprenyl chain formation from DMAPP (**13**) and IPP (**14**).

In the course of this reaction, one DMAPP (**13**) is extended by IPP (**14**) to form GPP (**15**), the linear precursor for all monoterpenes. A second elongation by addition of another IPP-extender unit following the same mechanism yields FPP (**16**), the universal sesquiterpene, and a third addition of **14** yields GGPP (**17**), the diterpene precursor. The actual chain length and structure of the enzyme product depends on the nature of the catalyzing prenyltransferase. The first enzyme structurally and chemically characterized was the FPP-synthase, a prototypal representative for regular chain elongating oligoprenyl diphosphate synthases.^[43]

1.2.3 Terpene Cyclization

The final terpene carbon backbone is constructed from the linear oligoprenyl diphosphates by a carbocation-mediated cyclization cascade. The responsible enzymes catalyzing these reactions are called terpene synthases, often referred to

as terpene cyclases. Terpene cyclases can be subdivided into two classes, type I and type II cyclases.^[44] On amino acid level, terpene cyclases of type I can be identified from their conserved motifs DDxx(D,E) and the NSE-triad (ND(L/I/V)xSxxxE). This aspartate-rich sequences effectuate binding of a cationic co-factor, in most cases a trinuclear magnesium metal cluster, responsible for coordination of the diphosphate moiety, present in all type I terpene cyclase substrates. The binding initiates pyrophosphate abstraction accompanied by formation of a reactive allylic cation, the starting point for the subsequent domino reaction. Recently, a new effector triad, including a highly conserved pyrophosphate sensor, an effector and a linker, was recognized during crystallographic studies on the bacterial selina-4(15),7(11)-diene synthase.^[45]

In contrast, terpene cyclases of type II initiate cyclization by protonation of a double bond or a previously formed epoxide and share the conserved DxDD motif. After formation of the initial reactive cation, the subsequent conformationally and stereochemically precise cyclization reaction is guided by amino acid residues inside the active center of a terpene cyclase, which confer an overall shape to the cavity, serving as a template for the precursor conformation. The mechanistic reaction steps resemble the reactivity of carbocation chemistry such as nucleophilic attack of double bonds, proton transfer reactions, hydride shifts and alkyl shifts. In the terminating step, a carbocation is either quenched by deprotonation or attack of an exogenous nucleophile, in most cases water.^[46,4]

In 2017 LIU and coworkers discovered a new family of diterpene cyclases, closely related to the UbiA superfamily of intramembrane prenyltransferases, which usually catalyze the formation of ubiquinones, menaquinones, plastoquinones, hemes, chlorophylls, vitamin E and structural lipids. Analysis of their protein sequences led to the identification of two highly conserved motifs: Nxxx(G/A)xxxD and DxxxD.^[47] A detailed analysis of the mechanism and function of this new class of terpene cyclases remains to be conducted.

1.2.3.1 Mechanistic Details - Taxadiene Synthase

Important insights into the structural and chemical features of terpene cyclases were obtained from X-ray crystallographic data. The first reported terpene cyclase structure was the pentalenene synthase from *Streptomyces* UC5319, published by CHRISTIANSON in 1997.^[48] In this chapter, the mechanistic details of a type I terpene cyclase are exemplary illustrated by the taxadiene synthase (TXS), catalyzing the formation of taxa-4(5),11(12)diene (**41**) from GGPP (**17**), reported by CHRISTIANSON in 2011.^[49]

The TXS was co-crystallized with substrate analogue 2-fluorogeranylgeranyl diphosphate (FGP). The active site with bound substrate is shown in Figure 10A and a detailed view of the molecular recognition site is shown in Figure 10B.^[49] The active center of TXS exhibits conserved motifs typical for class I terpene cyclases with the amino acid sequences **D**⁶¹³**DMAD**⁶¹⁷ and **N**⁷⁵⁷**DTKT**⁷⁶¹**YQAE**⁷⁶⁵. Cofactor ions Mg^{2+}_A and Mg^{2+}_C are coordinated by D613 and D617, whereas N757, T761 and E765 complex Mg^{2+}_B , building up the binding site for the diphosphate moiety of GGPP (Figure 10B).

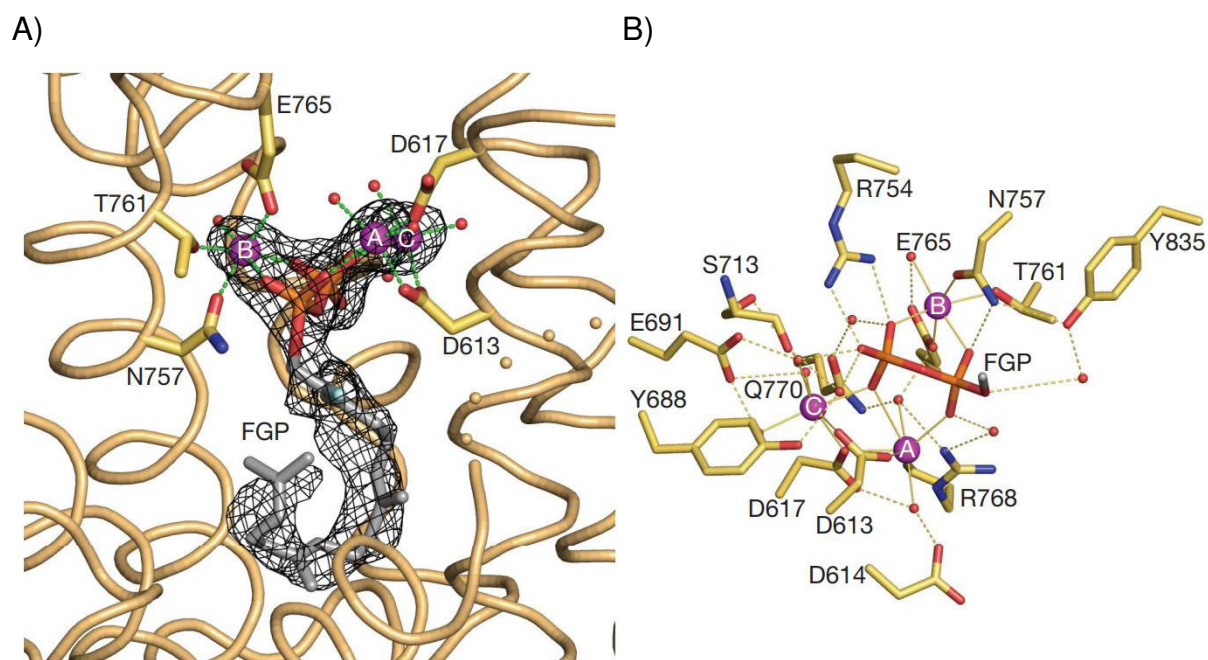
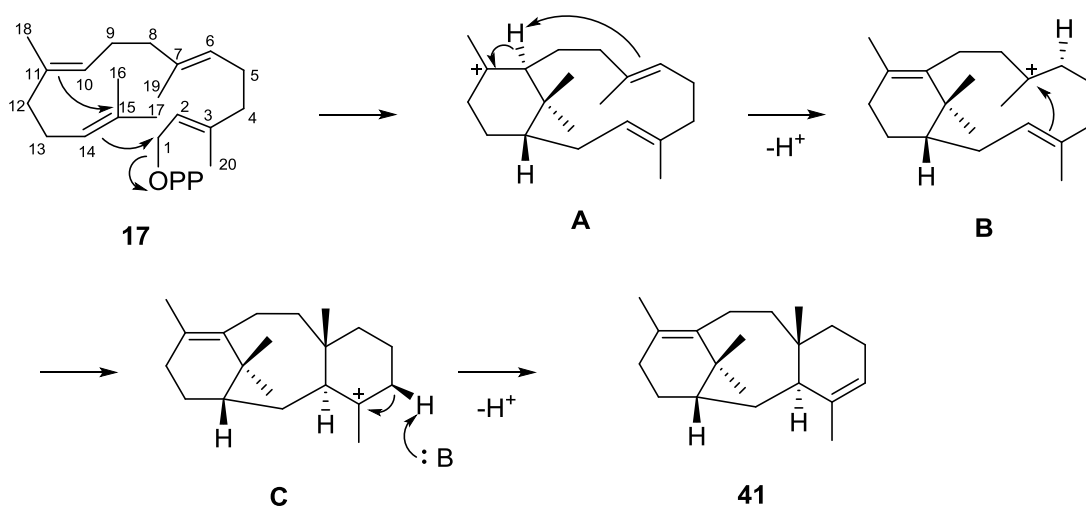


Figure 10. X-ray crystal structure of taxadiene synthase. A) Active site with bound substrate analogue and B) close-up view of the phosphate binding site (FGP is shortened to one carbon (grey)). Metal coordination is shown as thin solid lines, hydrogen bond interactions are indicated by thin dashed lines. Atoms are colored as follows: carbon=yellow, nitrogen=blue, oxygen=red, phosphorus=orange. Mg^{2+} -ions (A, B, C)=purple spheres, water=red spheres.^[49]

Coordination of the diphosphate is also assisted by hydrogen bonds to R754 and N757, as well as hydrogen bonds with Y688, E691, Y835, S713, R768 and Q770 mediated by water. The overall shape of the enzyme pocket determines the fate of the activated substrate and in case of the TXS, taxadiene (**41**) is formed.

The cyclization mechanism of GGPP to **41** can be explained by the following reaction cascade: attack of the terminal C14/C15-double bond in GGPP (**17**) to the allylic cation, generated after pyrophosphate-abstraction, yields an isopropyl cation, which is subsequently attacked by the neighboring double bond C10/C11 to form bicyclic intermediary verticillen-12-yl cation **A** (Scheme 1).



Scheme 1. Cyclization mechanism of GGPP (**17**) to taxa-4(5),11(12)diene (**41**).

Via a proton transfer reaction, verticillen-8-yl cation **B** is formed, from which a transannular attack of double bond C2/C3 generates taxen-4-yl cation **C**. The reaction cascade is terminated by deprotonation, mediated by a basic residue in the enzyme pocket, thereby generating the final product **41**. Different polar amino acid residues or the extruded PP_i are discussed to assist this terminating deprotonation.^[49]

1.3 NRPS/PKS-Derived Natural Products

Nonribosomal peptides are oligopeptides with a linear, circular or branched structure, often consisting of less than 20 amino acids. Besides DNA-encoded regular amino acids, highly modified building blocks are frequently observed carrying additional acyl-, methyl- or glycosyl groups, exhibiting epimerized stereocenters or are condensed to heterocycles.^[50] Many bioactive NRPS-derived natural products are known and used for medicinal purposes. A prominent example is the antibiotic vancomycin (**42**), isolated from *Amycolatopsis orientalis* (Figure 11).^[51]

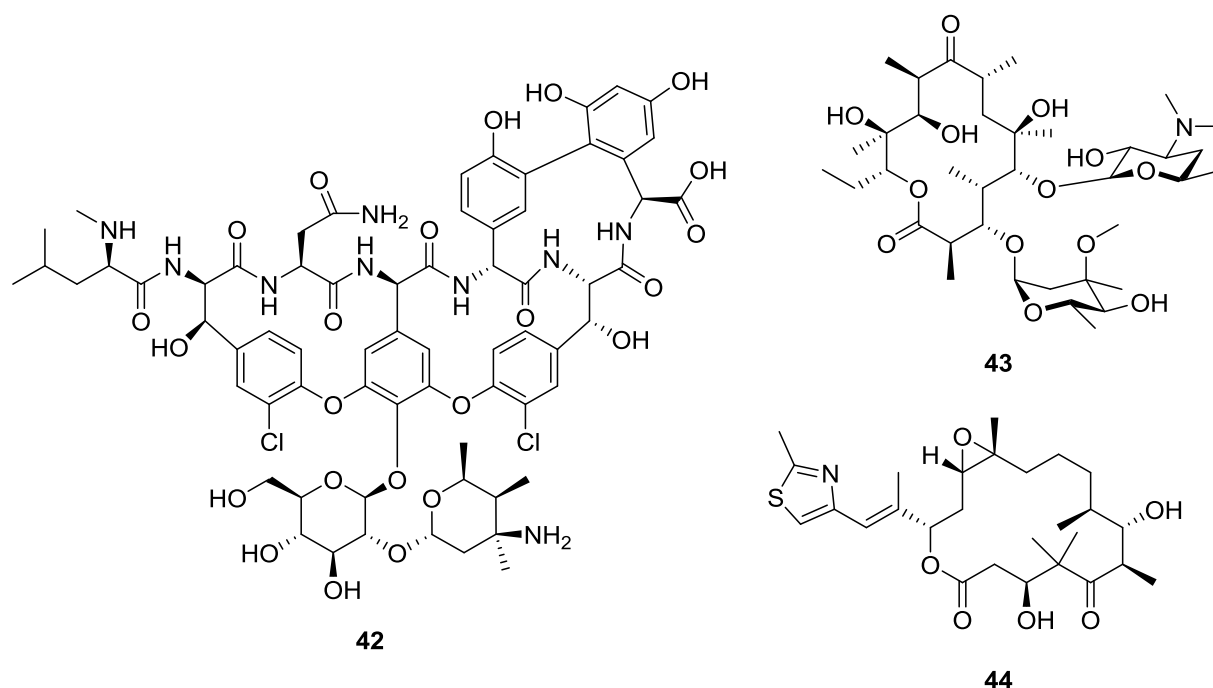
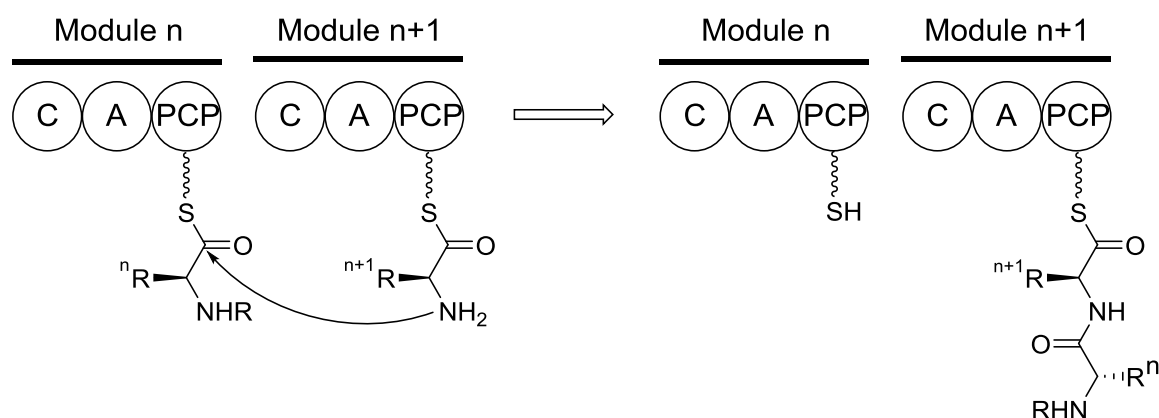


Figure 11. Examples for NRPs, PKs and NRPs/PKs hybrid natural products.

Nonribosomal peptides are biosynthetically generated by nonribosomal peptide synthases (NRPS), large megaenzymes functioning as assembly lines on a molecular level.^[52] They have a modular architecture, in which every module is responsible for the assembly and modification of one building block. The first module initiates the assembly line by loading of the starter unit. All subsequent modules extend this starter by one further building block and the last module terminates the assembly line and releases the product from the enzyme. Each extender module comprises at least three functional domains, an adenylation- (A), thiolation- (PCP) and condensation (C) domain. The loading module usually contains only an A and a PCP domain. The adenylation domain is responsible for selection and activation of

the respective building block by converting the amino acid into aminoacyl adenylates using ATP. The activated amino acid is then transferred to the peptidyl carrier protein (PCP), forming an aminoacyl thioester. The PCP domain carries a phosphopantetheine residue, resembling a flexible arm and enabling the growing chain to reach the active sites of the enzyme. The condensation domain then catalyzes the transpeptidation between the PCP-loaded amino acid of module n and module $n+1$ (Figure 12A).^[50]

A) NRPS



B) PKS

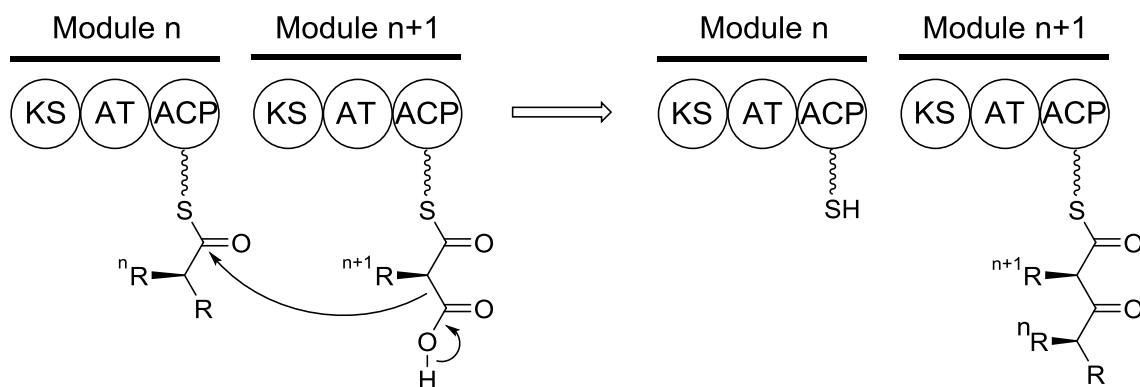


Figure 12. Schematic representation of A) a NRPS and B) a PKS assembly line.

The modules often do not only consist of these core domains, but can have additional specialized domains, like epimerization, methylation, cyclization, reduction or oxidation domains, enabling production of highly specialized bioactive natural products. The termination step is usually catalyzed by a thioesterase, breaking the bond of the oligopeptide to the NRPS, often under intramolecular cyclization by nucleophilic attack of an amino group in the assembled amino acid chain.^[53]

The biosynthesis of polyketide natural products follows the same modular logic but differs in the employed building blocks. Instead of amino acids, short carboxylic acids like malonyl-CoA are sequentially condensed. The responsible multifunctional megaenzymes are called polyketide synthases (PKS). Similar to NRPSs, three core domains exist within each module of a PKS. Selection of the incorporated building block is catalyzed by an acyltransferase (AT), selecting a distinct building block and transferring it onto the acyl carrier protein (ACP). The ACP domain is also comprised of a flexible phosphopantetheine moiety. The condensation of two building blocks is catalyzed by a ketoacyl synthase (KS), which connects the building block with the extender unit under decarboxylation (Figure 12B). Similar to NRPS, PKS modules can also contain additional tailoring domains, like a ketoreductase, dehydratase, an enoyl reductase or *O*- and *C*-methylation domains. The off-loading of the polyketide chain is also achieved by a thioesterase for most cases.^[50,52,53] Many clinically used drugs are PKS-derived natural products, like the antibiotic erythromycin (**43**) (Figure 11).^[54]

Additional diversification in nature was achieved by the evolutionary combination of NRPS and PKS biosynthetic machineries to NRPS/PKS hybrids.^[50,52] An important example for a natural product originating from such a hybrid machinery is the clinically used anticancer agent epothilone B (**44**) isolated from *Sorangium cellulosum* (Figure 11).^[55]

1.4 Isotope Tracer Technique

“The single most important technical advance that transformed biochemistry in the 20th century was the isotope tracer technique. Without it, the rapid growth of our knowledge of biosynthesis would be simply inconceivable.” (E. P. Kennedy)^[56]

The investigation of biochemically processes on a molecular level strongly relies on appropriate tracer techniques, enabling to follow the fate of specific atoms or molecules through complex metabolic processes. The first idea of tracing a metabolite through a biochemical transformation was exemplified by Franz Knoop in 1904, who studied the fate of fatty acids in metabolism by introducing a phenylring in the ω -position of even and uneven fatty acids.^[57] Such a “chemical labeling” of metabolites can however affect the overall chemistry of a compound and therefore alter its biochemical processing. The groundbreaking discovery of isotopes by Frederik Soddy and Francis Aston, awarded with a Nobel Prize in 1921 and 1922, paved the way for the development of the isotope tracer technique.^[58] Isotopes of one element differ in their number of neutrons and therefore in their physical properties. However, their overall chemical behavior is not altered or only to a limited extent (kinetic isotope effect). In the 1940s and 1950s Rudolf Schoenheimer, Konrad Bloch, John Cornforth and Georg Papják were pioneers in biochemistry and the discovery of metabolic pathways by using isotope tracer techniques. They employed heavy water ($^2\text{H}_2\text{O}$) and radioactive ^{14}C -labeled isotopomers to study metabolic pathways.^[56] The invention of pulsed Fourier-transform nuclear magnetic resonance spectroscopic methods in the 1970s revolutionized the applicability and scope of stable isotope tracer techniques^[59] and continuous to be of great importance for studying biochemical processes.^[60]

1.4.1 *In Vivo* Labeling – Siphonazole Biosynthesis

Siphonazole (**45**) was isolated from the Gram-negative gliding bacterium *Herpetosiphon* sp., belonging to the phylum Chloroflexi. It exhibits a linear arrangement of unusual building blocks, pointing to a PKS/NRPS-derived natural product (Figure 13).^[61]

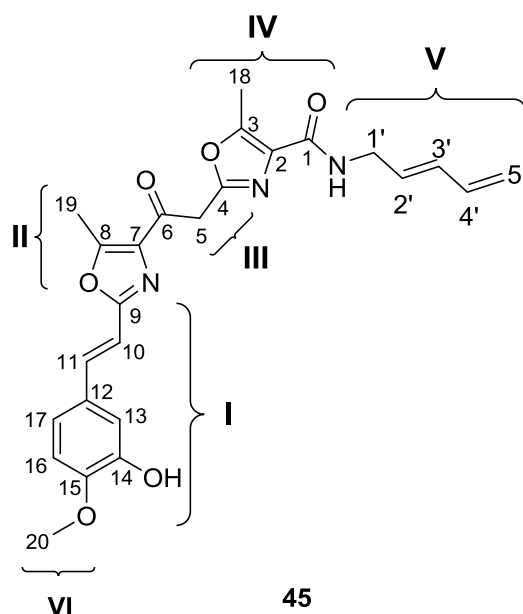


Figure 13. Structure of Siphonazole (**45**).

Building block I consists of an aromatic benzene ring and a C₃-side chain, with an additional C₁-element at one of the aromatic hydroxyl functions (Building block VI). The two presumably threonine-derived oxazole rings (II and IV) are connected via a C₂-unit (III) and an additional C₅N-group, carrying an unusual terminal diene structure, is incorporated (Figure 13). The biogenetic origin of these building blocks was hypothesized to arise from phenylalanine-derived cinnamic acid for I, threonine-derived oxazole moieties II and IV and acetate for the linkage III. Building block V was hypothesized to arise either from a lysine precursor, resembling a C₅N-building block, or by condensation of propionate and glycine. To address this hypothesis, feeding experiments using ¹³C- and ¹⁵N-labeled precursors were conducted.

Feeding of (1-¹³C)acetate, which is transformed into the central metabolite (1-¹³C)acetyl-CoA, revealed incorporation into C4, C9, C11, C2' and C4' of **45** (Figure 14A).

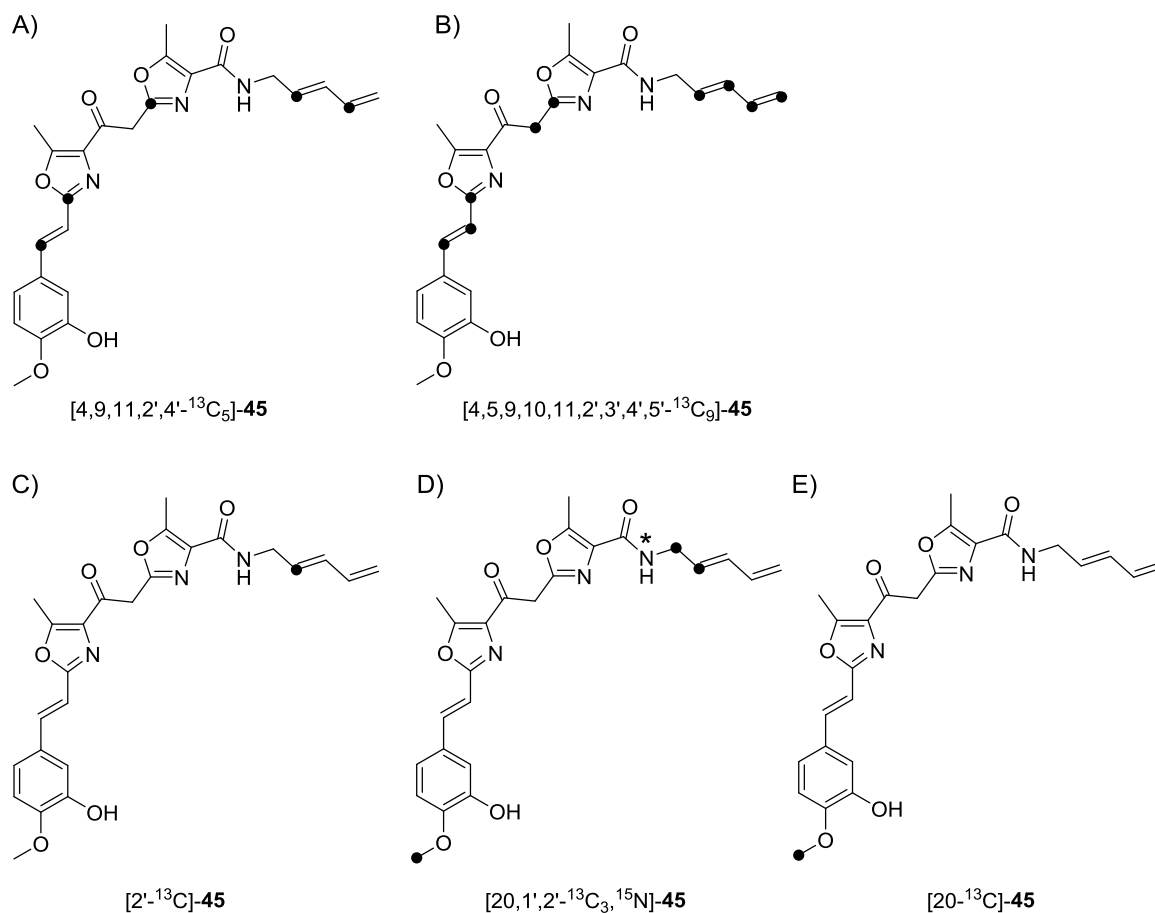


Figure 14. Label incorporation into siphonazole (**45**) after feeding of A) (1- ^{13}C)acetate; B) (1,2- $^{13}\text{C}_2$)acetate; C) (1- ^{13}C)glycine; D) (1,2- $^{13}\text{C}_2$, ^{15}N)glycine; E) (*methyl*- ^{13}C)methionine. Black dots indicate ^{13}C -incorporation; asterisks indicate ^{15}N -incorporation.

The observed labeling in building block I (C9 and C11) clearly ruled out a cinammic acid origin, since only labeling of C9 would be expected. Cinammic acid is derived from phenylalanine, which itself is build up from two phosphoenolpyruvate units and D-erythrose-4-phosphate via the shikimate pathway. (1- ^{13}C)Acetyl-CoA is transformed into (1- ^{13}C)phosphoenolpyruvate, which would lead to labeling of only C9 since one ^{13}C -label is lost during a decarboxylation step from prephenic acid to phenylpyruvic acid, the precursor to phenylalanine. The findings also rule out an acetate-derived origin of the aromatic ring, since no labeling in the benzene ring of **45** was detected. The results therefore point to a benzoic acid building block, connected to an acetate unit. The incorporation into C4 is in line with an acetyl-CoA-derived linkage of the oxazole building blocks. Incorporation into the homodiene side chain was detected in C2' and C4' position. A complementing experiment was conducted

using (1,2-¹³C₂)acetate, which was in line with feeding of the singly labeled acetyl-CoA (Figure 14B). Interestingly, an intact C₂-unit was detected in position C3'-C4'.

To further analyze the biogenetic origin of the side chain, labeled (1-¹³C)glycine and (1,2-¹³C₂, ¹⁵N)glycine were fed to *Herpetosiphon*, both leading to incorporation resembling a glycine-derived moiety for C1' and C2' (Figure 14C and D).

The remaining three carbon atoms in the side chain were thought to arise from propionyl-CoA, but surprisingly (1-¹³C)propionate was not incorporated into the carbon backbone of **45**. Taking into account, that labeling of C2' and C4' had been detected after feeding of (1-¹³C)acetate (labeling of the glycine-derived C2' position can be explained by an intensive metabolism via (1-¹³C)oxaloacetate (tca cycle) and (1-¹³C)-3-phosphoglycerate (gluconeogenesis) to (1-¹³C)glycine) and that C3' and C4' resemble an intact acetate unit, it was concluded, that the side chain must have been composed of glycine and two acetate units, from which one carbon is lost by decarboxylation.

Lastly, feeding of (*methyl*-¹³C)methionine proved that C20 originates from S-adenosylmethionine, the universal biological methylation agent (Figure 14E).

1.4.2 *In Vitro* Labeling – Corvol Ether Biosynthesis

The detailed understanding of the underlying mechanism of terpene cyclases resembles an important field in terpene natural product research. The product scope of these enzymes is up to now highly difficult to predict solely on their protein- or nucleic acid sequence. Besides the evaluation of structural biology data by computational studies using quantum chemical calculations, the investigation of terpene cyclization mechanisms, using isotope tracer techniques can further contribute to this research field.^[62] Corvol ethers A (**47**) and B (**46**) were recently characterized as the enzyme products of a sesquiterpene cyclase from *Kitasatospora setae* and are produced in a 1:3 ratio, respectively (Figure 15).^[63]

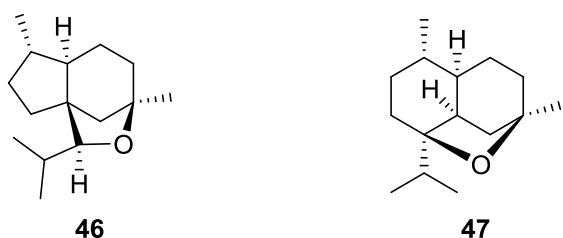


Figure 15. Structures of corvol ether A (**47**) and B (**46**).

Their biosynthesis was intensively investigated by *in vitro* incubation of isotopically labeled FPP isotopomers with the recombinant enzyme obtained by heterologous expression in *E. coli*. The formation of corvol ether can be envisaged by the following cyclization mechanism. After initial pyrophosphate abstraction from FPP (**16**) nerolidol diphosphate (**48**) is generated, enabling 1,10-cyclization towards isopropyl cation **A**. A subsequent 1,3-hydride shift to allylic cation **B**, followed by a double bond shift and attack of water gives neutral intermediate germacrene D-4-ol (**49**) (Figure 16).

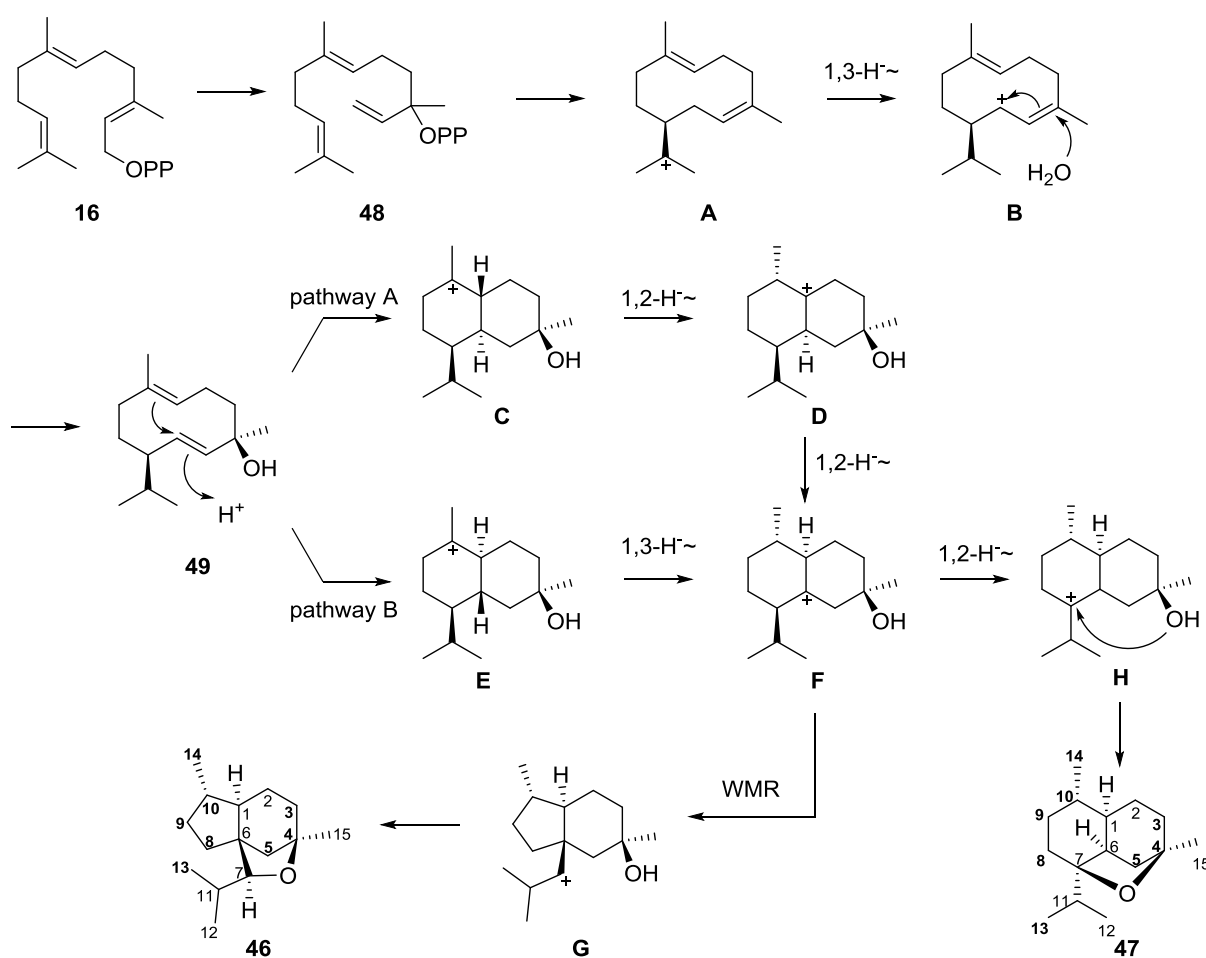
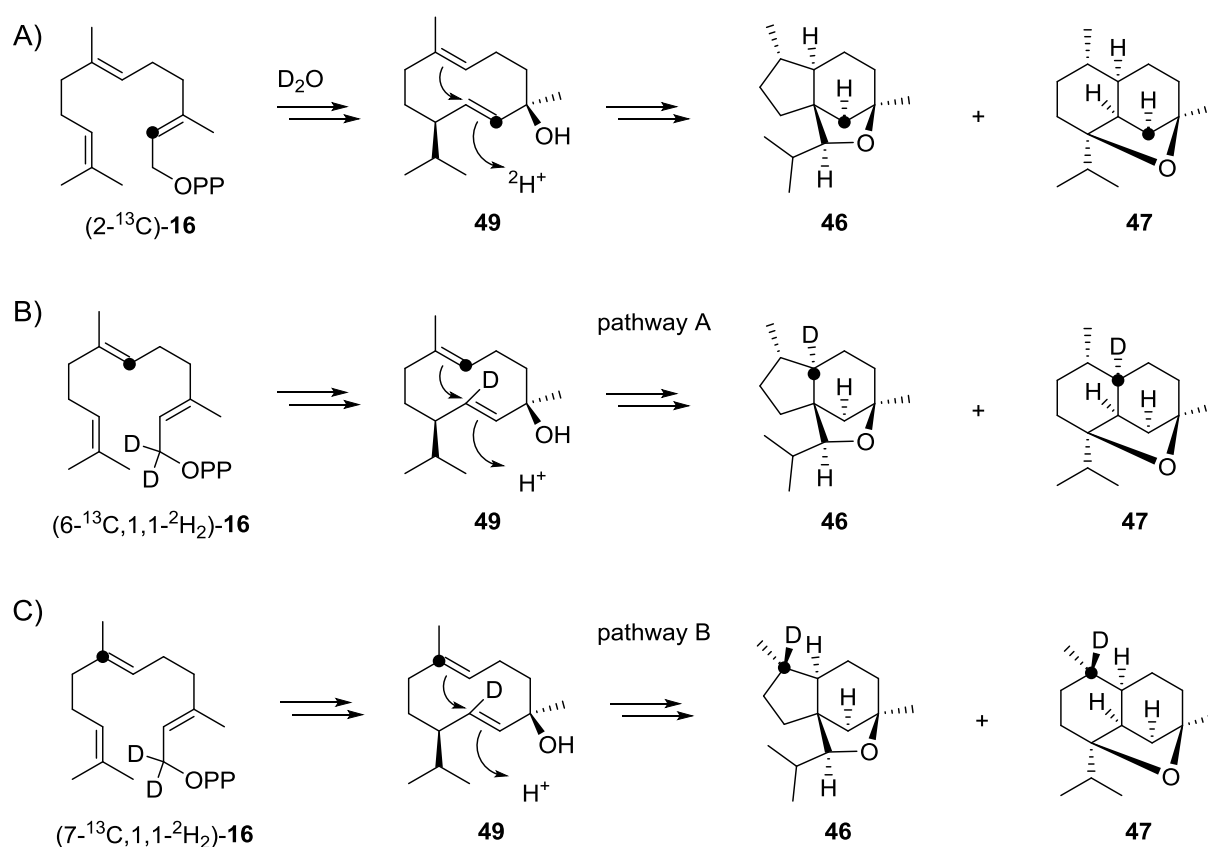


Figure 16. Biosynthesis of corvol ether A (**44**) and B (**43**).

The transannular second ring closer mediated by protonation opens up two possible pathways for the generation of central intermediate **F** towards corvol ether A or B. Formation of **C** would require two subsequent suprafacial 1,2-hydride shifts, whereas formation of stereoisomer **E** necessitates one suprafacial 1,3-hydride shift to explain the stereochemical outcome in **46** and **47**. The main product of the corvol ether synthase, **46** is formed from **F** by a Wagner-Meerwein rearrangement (WMR) to cationic intermediate **G**, followed by intramolecular attack of the hydroxyl group. The formation of the second product **47** can be explained by a 1,2-hydride shift instead of the WMR to cation **H** also followed by an intramolecular attack of the alcohol moiety.

To verify the proposed cyclization mechanism and experimentally prove the postulated steps, three labeling experiments were designed and conducted.^[64] The presence of neutral intermediate **49** was investigated by incubation of synthetic (2-¹³C)-**16** with corvol ether synthase in D₂O (Scheme 2A).



Scheme 2. Labeling experiments for corvol ether biosynthesis studies.

Since neutral intermediates require a reprotonation step to regenerate a cationic reactive center in the carbon backbone, this proton gets ^2H -labeled, when the reaction is carried out in D_2O . The position of deuterium can be detected by a triplet signal for the bound carbon atom in the corresponding ^{13}C -NMR spectrum caused by ^1H , ^{13}C heteronuclear coupling. When the respective carbon atom is additionally ^{13}C -labeled, the ^{13}C -NMR signal is strongly enhanced, allowing for analysis of only minute amounts of material. The outcome of the incubation experiment indeed revealed a triplet signal for the respective carbon atom, giving evidence for the presence of **49**. Additionally, labeling experiments were designed to distinguish between the two possible pathways from **49** to **F**. By incubation of $(6\text{-}^{13}\text{C}, 1, 1\text{-}^2\text{H}_2)\text{-16}$ the fate of the proton in C5 position can be followed (Scheme 2B). Pathway A should lead to ^2H -labeling of C1, which is also ^{13}C -labeled, whereas in pathway B the deuterium is shifted in the C10 position. The outcome was analyzed by ^{13}C -NMR spectroscopy and revealed a strong triplet signal for C1, which demonstrates the occurrence of two subsequent 1,2-hydride shifts instead of one 1,3-hydride shift. This finding was further supported by the complementary experiment with $(7\text{-}^{13}\text{C}, 1, 1\text{-}^2\text{H}_2)\text{-16}$ leading to a strong triplet for C10 (Scheme 2C).

1.5 Volatile Natural Products

Volatile compounds are typically small (up to C_{20}) and have therefore a low molecular mass (100-500 Daltons), high vapour pressure and a low boiling point. Volatiles are produced by nearly all living organisms and can exhibit diverse functions for the producing organism.^[65]

The sulfur volatile dimethyl sulfide (DMS, **50**) is produced by marine bacteria of the Roseobacter clade by degradation of the algal metabolite dimethylsulfoniopropionate. DMS is released from the ocean into the atmosphere by 2×10^7 tons per year. Its oxidation products dimethylsulfate and sulfate influence the planets climate by acting as cloud condensation nuclei and participate in the global sulfur cycle. DMS is also the main contributor for the typical smell of the seaside and is a potent chemoattractant for birds (Figure 17).^[66]

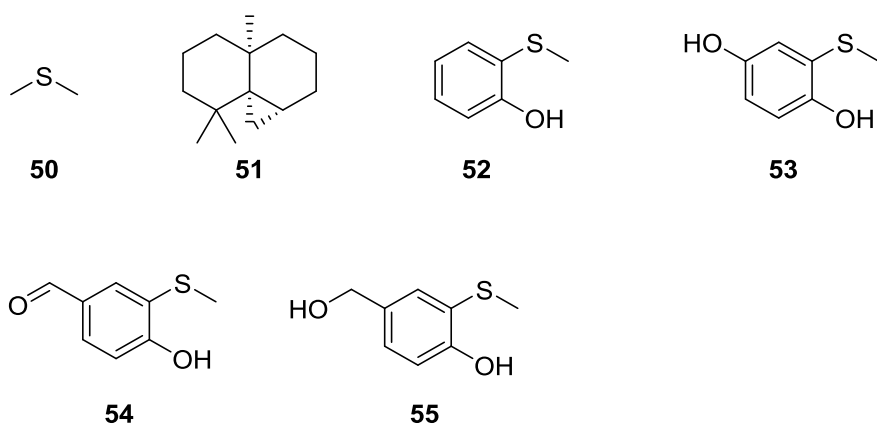


Figure 17. Examples of bioactive volatile metabolites from bacteria, fungi, plants and insects.

Another interesting volatile metabolite is the sesquiterpene (–)-thujopsene (**51**), produced by the ectomycorrhizal fungus *Laccaria bicolor*. *L. bicolor* is a mutualistic fungus associated with the roots of plants e.g. *Populus* or *Arabidopsis*. It was shown, that **51** is the key signaling compound emitted by the fungus to initiate plant lateral root production, prior to direct contact pre-colonization.^[67] Volatiles are also produced by almost all plants and often act as chemical defense compounds against herbivores.^[68] In many cases, not only a single compound exhibits a certain bioactivity, but a whole set of different chemicals. Recently, the semiochemicals **52-55** have been identified from the spider orchid *Caladenia crebra* and were shown to attract the male thynnine wasp *Campylothynnus flavopictus* for pollination by mimicking the female wasps pheromone cocktail.^[69]

1.5.1 Capturing Volatile Natural Products from Microorganisms

Besides their biological importance, the analysis of volatile natural products is associated with certain obstacles. Classical extraction-isolation techniques employed for natural product isolation require concentration steps to remove the employed solvent during which volatiles are easily lost. Therefore, special techniques are necessary for compound sampling. Additionally, volatiles often occur as complex mixtures and in rather low yields, demanding for elaborate chromatographic and highly sensitive analytical methods.^[70] For the sampling of biogenic volatiles, two main techniques have evolved: the closed-loop-stripping apparatus (CLSA)^[71] and the use of a solid phase micro extraction fibre (SPME) (Figure 18).^[72]

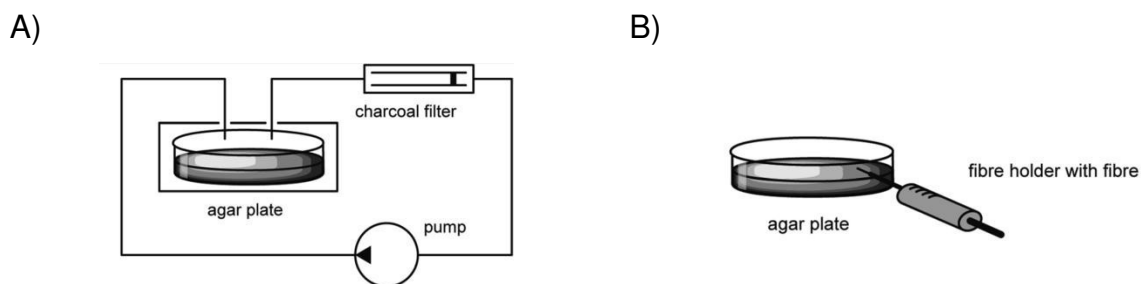


Figure 18. Sampling techniques for the trapping of volatiles: A) CLSA; B) SPME.

A CLSA is a closed glass vessel, in which a grown agar plate culture can be introduced. A connected pump blows a constant airflow over the culture and through a charcoal filter on which the emitted volatiles get trapped and concentrated. This filter is subsequently extracted with suitable solvents (e.g. dichloromethane) and the amounts of material are sufficient for GC/MS analysis. Alternatively, a SPME-fibre can be employed for trapping of emitted volatiles. The fibre is coated with poly(dimethylsiloxane), acting as an adsorber medium, and can be held directly above a biological sample. The adsorbed compounds can be analyzed by GC/MS, thereby making use of thermal desorption inside the injector chamber.

2 Pogostol Biosynthesis by the Endophytic Fungus *Geniculosporium*

Lena Barra, Dr. Barbara Schulz and Prof. Dr. Jeroen S. Dickschat*

ChemBioChem **2014**, *15*, 2379-2383.

Reprinted from *ChemBioChem* **2014**, *15*, 2379-2383 with kind permission from John Wiley and Sons.

Introduction

Fungi are prolific producers of volatile terpenes with hundreds of identified compounds from various fungal genera like *Aspergillus*, *Penicillium*, *Trichoderma* or *Fusarium*.^[65c] The homomonoterpenoid 2-methylisoborneol (2-MIB, **4**), firstly isolated from a Streptomycete, as already discussed in the introduction (Chapter 1.1),^[7] was found to be also produced by *Aspergillus*^[73] and *Penicillium*.^[74] The sesquiterpene β -caryophyllene (**56**) is produced by *Talaromyces wortmannii* and shows plant growth promoting properties.^[75] Besides terpenes with direct effects in their environments, the terpene carbon backbone is often used as a precursor towards highly functionalized bioactive compounds like the aristolochene (**57**) derived toxin PR-Toxin (**58**) from *Penicillium roqueforti* (Figure 19).^[76]

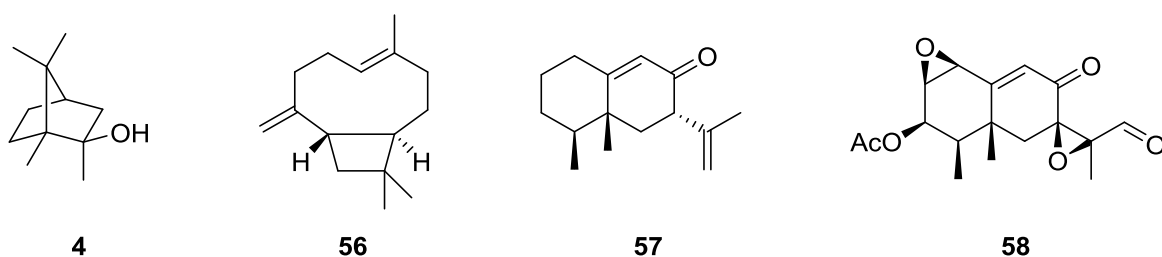


Figure 19. Examples of volatile terpenes from fungi.

The GC/MS based identification of volatile terpenes relies on comparison of the measured respective mass spectra and retention indices to electronic mass spectral libraries and tabulated literature data. This approach is limited by incomplete published data, the occurrence of stereoisomers, which can exhibit highly similar mass spectra and retention indices, or completely unknown terpenes. Alternatively, a mass spectrum deviated reference compound could be used as a standard, but only a few compounds are commercially available and the development of a total synthesis for complex organic molecules like terpenes is highly laborious. In those cases, access to ^{13}C -NMR data is desirable to gain additional structural information of the analyte. The sampling of volatile metabolites by CLSA usually yields material in the sub-microgram range, too little for NMR spectroscopic methods. Additionally, terpenes often occur in a complex mixture with other volatile organic compounds from various classes, further preventing the sufficient application of NMR techniques.

To circumvent these problems, a suitable ^{13}C -labeled biosynthetic precursor can be fed to the organism, leading to selective labeling of distinct carbon atoms in the final natural product. These ^{13}C -labeled atoms appear with strongly enhanced intensities in the respective ^{13}C -NMR spectrum enabling access to ^{13}C -NMR data with only minute amounts of material as obtained from CLSA headspace extracts. The CLSA/NMR technique was firstly employed in the analysis of the stereochemical course in 2-MIB biosynthesis in *Micromonospora olivasterospora* by feeding of (1- ^{13}C)-1-deoxy-D-xylulose.^[77]

Summary

The CLSA/NMR technique was systematically developed for the identification of volatile terpenes from fungal sources. Fungi employ the mevalonate pathway for the generation of the isoprenoid monomers DMAPP and IPP (Chapter 1.2.1), enabling feeding experiments with mevalonolactone, the δ -lactone of mevalonic acid, leading to sufficient incorporation into the produced terpenes.^[78] Therefore, a robust synthesis starting from commercially available ^{13}C -labeled ethyl acetoacetate developed by ZAMIR et al.^[79] was tested and employed for the generation of singly and doubly ^{13}C -labeled mevalonolactone isotopomers **59a-59d** (Figure 20). Synthesis of (2,6- $^{13}\text{C}_2$)-**59e** was achieved by a previously developed route in our workgroup^[80] and (4- ^{13}C)-**59f** was synthesized by a procedure developed by CANE.^[81]

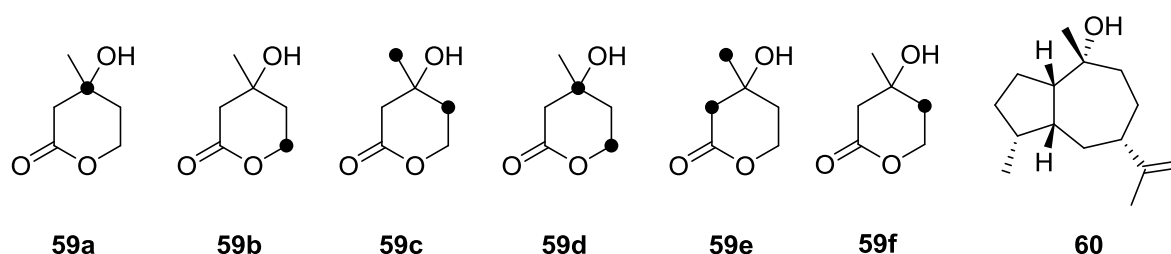


Figure 20. Synthesized ^{13}C -labeled mevalonolactone isotopomers **59a-59f** and structure of the identified sesquiterpene pogostol (**60**). Black dots indicate ^{13}C -label,

Feeding of labeled precursors to the endophytic fungus *Geniculosporium* sp. isolated from *Cistus monspeliensis* and analyses of the headspace extracts obtained from CLSA sampling by GC/MS revealed high incorporation into a sesquiterpene alcohol.

The structure of the terpene was analyzed by sequential feeding of all six mevalonolactone isotopomers, collection of the emitted volatile bouquet by CLSA, extraction of the charcoal filter with CDCl_3 and direct analyses of the extracts by ^{13}C -NMR spectroscopy. The results gave access to the complete ^{13}C -NMR data of the sesquiterpene alcohol, which could be identified and distinguished from its stereoisomers as pogostol (**60**) by comparison to literature data. The results additionally gave insight into the cyclization mechanism of **60**, including stereochemical aspects.

3 Structural Revision and Elucidation of the Biosynthesis of Hypodoratoxide by ^{13}C , ^{13}C COSY NMR Spectroscopy

Lena Barra, Dr. Kerstin Ibrom and Prof. Dr. Jeroen S. Dickschat*

Angew. Chem. Int. Ed. **2015**, *54*, 6637-6640.

Reprinted from *Angew. Chem. Int. Ed.* **2015**, *54*, 6637-6640 with kind permission from John Wiley and Sons.

Introduction

The CLSA/NMR technique is a highly useful method for the identification of volatile terpenes produced by microorganisms. The access to ^{13}C -NMR data of only little amounts of material based on *in vivo* ^{13}C -labeling of the natural product gives valuable information about the analyte. However, a direct access to the connectivity of the labeled carbon atoms can not be obtained, rendering a direct approach to the structure. Alternatively, isolation of the natural product in preparative amounts and standard NMR spectroscopic methods can be established. Isolation is often highly laborious for volatile organic compounds like mono- or sesquiterpenes, due to low yields and material loss during concentration steps. Additionally, interpretation of NMR and 2D NMR data of complex (poly)cyclic hydrocarbons is often difficult due to strong overlapping of chemical shifts. Direct access to the connectivity of a carbon backbone can be obtained from ^{13}C , ^{13}C -INADEQUATE experiments, but for that high amounts of material are necessary.

Summary

The mycophylus fungus *Hypomyces odoratus* produces a sesquiterpene, which was isolated by ABRAHAM and shown to have phytotoxic and antifungal activity.^[82] Its structure was analyzed by various 2D NMR methods leading to the eremophilane ether **61** (Figure 21).

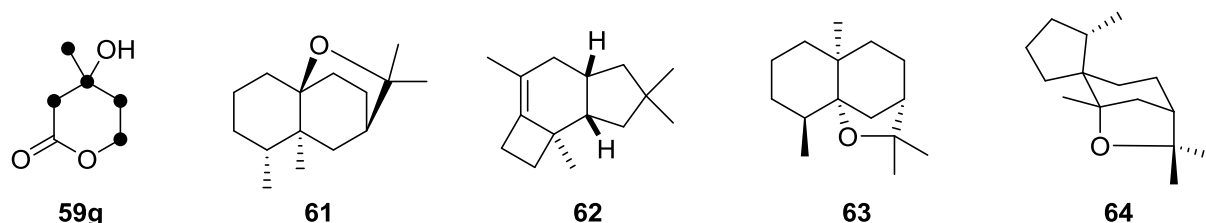


Figure 21. Structure of (2,3,4,5,6- $^{13}\text{C}_5$)-**59g** and volatile terpenes from *H. odoratus*: initial structure of hypodoratoxide (**61**), protoillud-6-ene (**62**), *cis*-dihydroagarofuran (**63**), revised structure of hypodoratoxide (**64**). Black dots indicate ^{13}C -label.

During our analysis of the volatiles of *H. odoratus* three terpenes were detected, from which the two minor compounds could be identified as protoillud-6-ene (**62**) and *cis*-dihydroagarofuran (**63**) based on their GC/MS data. The major compound was

identified by feeding of (2,3,4,5,6-¹³C₅)mevalonolactone (**59g**), which was synthesized from ethyl (1,2,3,4-¹³C₄)acetoacetate and (2-¹³C)ethyl acetate.^[79] Label incorporation by 16% to [¹³C₁₅]hypodoratoxide allowed the measurement of a ¹³C, ¹³C-COSY-NMR spectrum, from which the planary structure could be deduced by one-bond ¹³C, ¹³C-homonuclear coupling. The obtained structure of hypodoratoxide was different to the previously reported structure showing a 5,6,5-tricyclic ringsystem, a spirocenter and a cyclic ether moiety (**64**) (Figure 21). In order to support the structural revision of hypodoratoxide, **64** was isolated in preparative amounts and 2D NMR analysis was conducted. It could be shown, that the false structure elucidation of **64** was caused by misinterpretation of HMBC correlations, due to the strong overlapping of proton signals. This demonstrates, that ¹³C-labeling not only assists structure elucidation but can be even superior to standard methods. The relative configuration of **64** could be established by NOESY interpretation and the absolute configuration was tentatively deduced from identification and isolation of the biosynthetically related *cis*-dihydroagarofuran (**63**). Additionally, the complex biosynthetic cyclization mechanism of hypodoratoxide was analyzed by feeding of (3-¹³C)-**59a** and (4,6-¹³C₂)-**59c**, proving the occurrence of a Wagner-Meerwein rearrangement (WMR) and a methyl shift.

4 Harzianone Biosynthesis by the Biocontrol Fungus *Trichoderma*

Lena Barra and Prof. Dr. Jeroen S. Dickschat*

ChemBioChem, 2017, 18, accepted.

Reprinted from *ChemBioChem*, 2017, 18, DOI: 10.1002/cbic.201700462 with kind permission from John Wiley and Sons.

Introduction

As illustrated in the previous chapters, many interesting volatile natural products can be isolated from microbial sources and isotopically labeled biosynthetic precursors can help to elucidate their structures and give valuable insights into their biosynthesis. Fungi of the genus *Trichoderma* are opportunistic, avirulent plant symbionts common in soil and wood habitats. They are used in agriculture as biocontrol agents where they are able to increase crop productivity due to their mycoparasitic and antibiotic potential against different plant pathogens.^[83] Identified volatiles from *Trichoderma* spp.^[84] include 6-pentyl- α -pyrone (**65**), which was recently shown to improve pathogen resistance in *Arabidopsis*,^[85] the sesquiterpene alcohol α -acorenol (**66**), along with acorenone (**67**) and related acorane sesquiterpenes **68**, **69** and **70** (Figure 22).^[86]

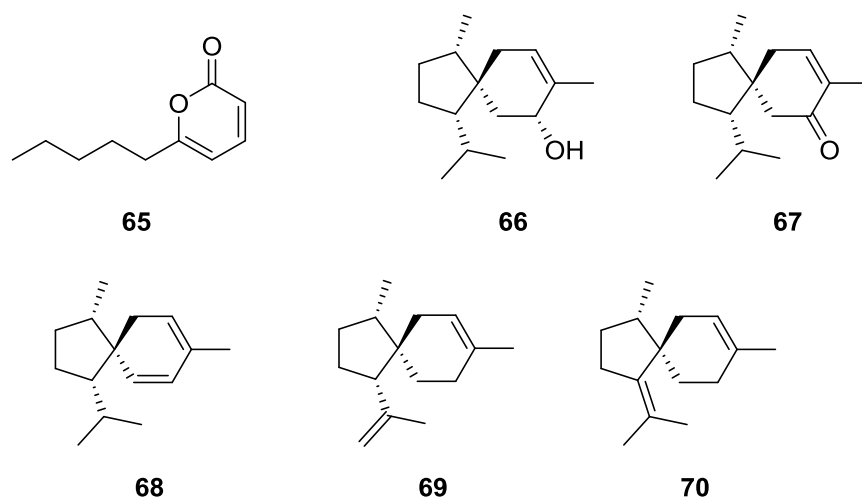


Figure 22. Examples of known volatiles from *Trichoderma*.

The biosynthesis of the acorane sesquiterpenes has been studied by feeding experiments with deuterated mevalonolactone isotopomers and analysis of the resulting GC/MS data.^[86b,87] Accompanied by the presented volatiles, an oxidated diterpene was observed in the analyzed *Trichoderma* strains, which could not be identified in the course of these studies.

Summary

The observed volatile diterpene was detected during the analysis of all seven *Trichoderma* strains (*Trichoderma* sp. 34, *T. asperellum*, *T. citrinoviride*, *T. harzianum*, *T. longibrachiatum*, *T. viride*, *T. reesei* QM6a) and identified by a combination of ^{13}C , ^{13}C -COSY-NMR spectroscopy of *in vivo* [$^{13}\text{C}_{15}$]labeled diterpene and classic NMR spectroscopic methods. The deduced structure was identical to the literature known harzianone (**71**), previously isolated from *Trichoderma*. It consists of a unique tetracyclic 4,7,5,6-membered ring system and is known to exhibit antibacterial and cytotoxic activity.^[88] A series of related harziane diterpenes (**72-76**) has also been reported (Figure 23).^[89]

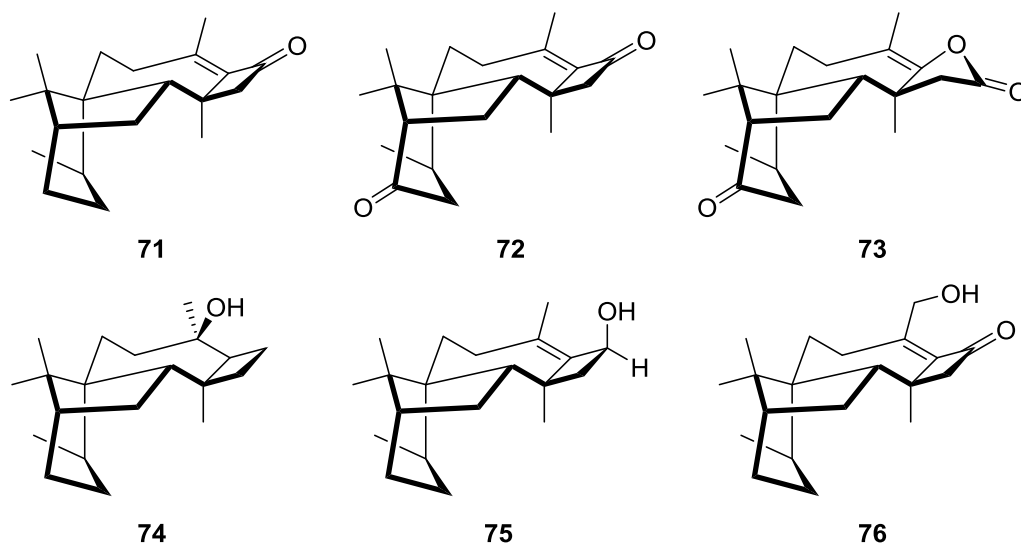


Figure 23. Structures of the identified diterpene harzianone (**71**) and related harziane diterpenes **72-76** reported in the literature.

The cyclization mechanism of **71** was studied by feeding of a series of ^{13}C -labeled mevalonolactone isotopologues and a 1,2-hydride shift was followed by feeding of ^2H -labeled isotopologues of **50**. The results revealed a concise biosynthesis for **71**, sharing similarities to taxadiene (**41**) biosynthesis of early cyclization steps (Chapter 1.2.3.1). The common production of **71** in all analyzed *Trichoderma* strains indicates a conserved occurrence of the respective terpene synthase within the genus *Trichoderma*.

5 Volatiles from the Fungal Microbiome of the Marine Sponge *Callyspongia cf. flammea*

Lena Barra, Paul Barac, Prof. Dr. Gabriele M. König, Dr. Max Crüseemann and Prof.
Dr. Jeroen S. Dickschat*

Org. Biomol. Chem. **2017**, *15*, 7411-7421.

Reprinted from *Org. Biomol. Chem.* **2017**, *15*, 7411-7421 with kind permission from
The Royal Society of Chemistry.

Introduction

As illustrated in chapter 1.5 volatile metabolites are of great importance for all living organisms and can have many different functions for signalling, chemical defense or pathogen control. They are particularly important for communication among microbes and between microbes and their eukaryotic hosts, where they can have antimicrobial properties, effects on bacterial quorum sensing, motility, gene expression and antibiotic resistance.^[90] Marine sponges, the most ancient living animals on our planet, are sessile filter feeding organisms, occurring in almost any aquatic habitat. They are known to inhabit highly complex dense microbial communities consisting of bacteria, fungi and archaea.^[91] Many bioactive natural products have been isolated from sponges or their microbes^[92] but only little is known about volatiles from these animals or their associated microbial communities. The bread-crumb sponge (*Halichondria panicea*) from the North Sea (Clever Bank) emits a strong stench, causing sickness and nausea among fishermen. The olfactory source was traced back to three volatile sulfur compounds, dimethyl disulfide (**77**), dimethyl trisulfide (**78**) and methylbenzylsulfide (**79**) (Figure 24).^[93] A similar study was conducted on volatiles from the stinker-sponge (*Ircinia felix*), emitting a sulfur-garlic stench. Among 59 detected volatile compounds, the three metabolites DMS (**50**), methyl isocyanide (**80**) and methyl isothiocyanate (**81**) were identified as the odour source. Metabolites **50**, **80** and **81** are continuously released by the sponge and the concentration drastically increases after tissue wounding.^[94] The released volatiles are discussed to act as chemical defense compounds, protecting the sponge from predators. However, their metabolic origin is unknown.

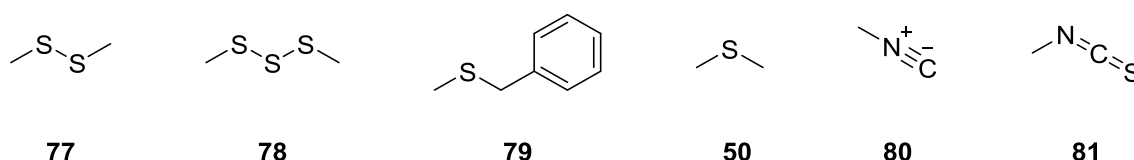


Figure 24. Volatiles from sponges.

A series of studies on volatiles emitted by Antarctic sponge-associated bacteria is reported in the literature and the volatile bouquet was shown to be active against the

human pathogen *Burkholderia*.^[95] The volatiles from sponge-associated fungi have not been investigated so far.

Summary

The volatile metabolites from five fungal strains, previously isolated from the Australian marine sponge *Callyspongia* cf. *flammea*^[96] were investigated. A closed-loop-stripping apparatus was used for sampling and the obtained headspace extracts were analyzed by GC/MS. In total 48 compounds were identified from various compound classes e.g. alkanes, alcohols, ketones and aldehydes, terpenes and aromatic compounds. The highly methylated isotorquatone (**82**) along with two desmethyl analogues (**83** and **84**) were identified by synthesis of reference compounds. The *para*-*O*-desmethyl derivative **84** is a new natural product and was named dichotomone (Figure 25).

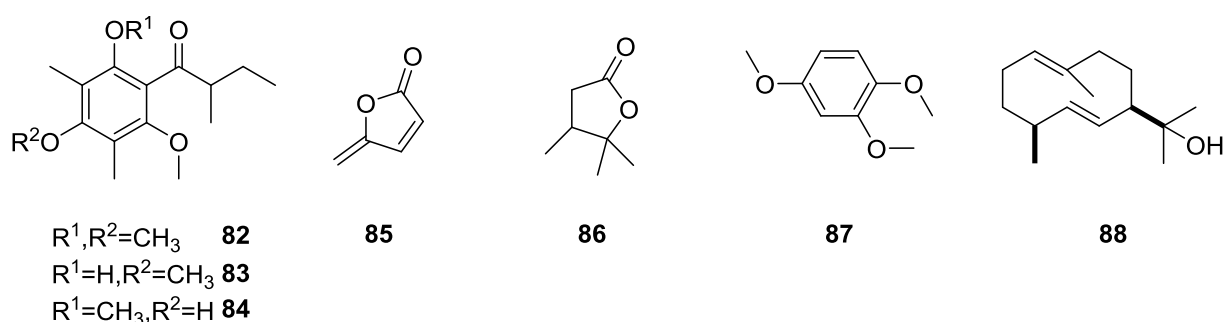


Figure 25. Selection of identified bioactive volatiles from the analyzed sponge-associated fungi.

The absolute configuration of **82** was deduced by an asymmetric synthesis and revealed the natural occurrence of **82** as a mixture of enantiomers (40% *ee*) with (*R*)-(-)-**82** as the major component. The biosynthetic origin of **82** was addressed by feeding experiments with isotopically labeled ($2\text{-}^{13}\text{C}$)acetate and (*methyl*- $^2\text{H}_3$)methionine, pointing to a polyketide biosynthetic machinery and *S*-adenosylmethionine-derived methylgroups. The obtained synthetic compounds were tested for activity against Gram-positive bacteria (*Bacillus megaterium*), Gram-negative bacteria (*E. coli*) and algae (*Chlorella fusca*). Racemic isotorquatone

showed algicidal activity but not the synthesized (*S*)-(+)-enantiomer, pointing to (*R*)-(-)-**82** as being the bioactive enantiomer. The algicidal activity of isotorquatone hints at a possible ecological function in the sponge-microbiome community. Other interesting identified volatiles are the quorum sensing inhibitor protoanemonine (**85**), the phytopathogenic lactone **86**, kairomone **87** and the sesquiterpene (1(10)*E*,5*E*)-germacradien-11-ol (**88**).

6 Volatiles from Nineteen Recently Genome Sequenced Actinomycetes

Dr. Christian A. Citron, Lena Barra, Dr. Joachim Wink, Prof. Dr. Jeroen S. Dickschat*

Org. Biomol. Chem. **2015**, *13*, 2673-2683.

Reprinted from *Org. Biomol. Chem.* **2015**, *13*, 2673-2683 with kind permission from The Royal Society of Chemistry.

Introduction

Actinomycetes are Gram-positive filamentous actinobacteria, occurring in both soil and marine ecosystems. They are known for their tremendous production of bioactive substances, reflected by their large genomes, containing numerous genes for secondary metabolism.^[97] They are used in agriculture, biotechnology and medicine and two-thirds of all known antibiotics originate from these bacteria.^[98] Many actinomycetes have been studied in regard of their volatile metabolites^[65a,99] leading to the identification of new interesting natural products, like the antibacterial butenolide (**89**),^[100] the unusual γ - and (ω -3)-methyl branched fatty acid **90**,^[101] the antimycin derived blastmycinone **91**^[102] or streptopyridine (**92**) (Figure 26).^[103] However, the most abundant and widespread volatile compounds from actinomycetes are the terpenoids geosmin (**5**) and 2-methylisoborneol (**4**), already introduced in chapter 1.1.^[6]

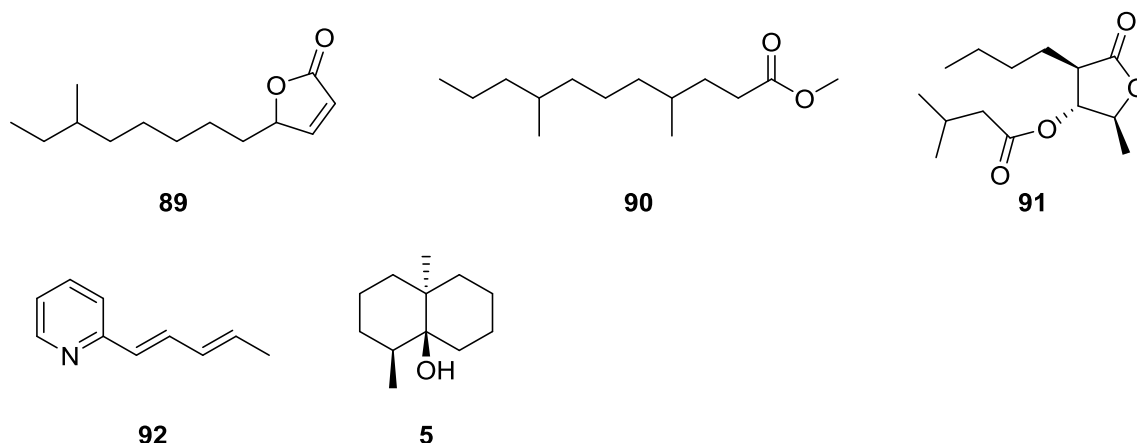


Figure 26. Selection of volatiles identified from actinomycetes.

Summary

The volatile constituents of 19 actinomycetes were investigated by trapping with a CLSA and analyses of the headspace extracts by GC/MS. In total 178 compounds were identified from different compound classes. Two particularly interesting metabolites, the insect pheromone frontalin (**93**) and the plant compound 1-nitro-2-phenylethane (**94**) were identified (Figure 27).

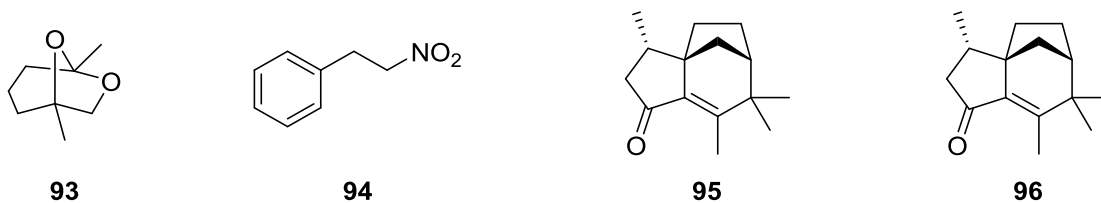


Figure 27. Frontalin (**93**) identified from *S. varsoviensis* and 1-nitro-2-phenylethane (**94**) from *S. afghaniensis* and *S. prunicolor* and structure of *epi*-isozizaene (**95**) and albaflavenone (**96**).

The occurrence of insect pheromones in bacteria, as can also be seen for conophtorin and chalcogran identified from streptomycetes, suggests that the true origin of pheromones, at least in some cases, could be the metabolism of insect-associated bacteria.^[104] Nitrocompound **94**, so far only known from different plants e.g. tomato,^[105] has interesting bioactivities and antifungal, antinociceptive, bradycardiac, vasorelaxant, anti-inflammatory, anticonvulsant and anxiolytic activity has been reported.^[106] Its biosynthetic origin was studied by feeding experiments with isotopically labeled precursors, pointing to a phenylalanine-derived metabolite. Formation of **94** could be explained by a PLP assisted decarboxylation of phenylalanine and subsequent oxidation of the amino group in phenylethylamine. Also, a series of terpenes were identified from the analyzed organisms, e.g. *epi*-isozizaene (**95**), the carbon precursor towards the antibiotic albaflavenone (**96**). Since all 19 analyzed strains were recently genome sequenced and the genetic information is available from public databases, a correlation between the encoded terpene cyclases and the identified produced terpenes was conducted.

7 Synthesis of Isotopically Labelled Oligoprenyl Diphosphates and Their Application in Mechanistic Investigations of Terpene Cyclases

Dr. Christian A. Citron, Dr. Patrick Rabe, Lena Barra, Prof. Dr. Chiaki Nakano, Prof.
Dr. Tsutomu Hoshino and Prof. Dr. Jeroen S. Dickschat*
Eur. J. Org. Chem. **2014**, 7684-7691.

This publication was also part of a cumulative dissertation by Dr. Patrick Rabe at the University of Bonn and Dr. Christian A. Citron, Technical University of Braunschweig and only supplements this thesis. My contribution to this work comprises the synthesis of a few unlabeled substrates for completion of the systematic table of isolated yields.

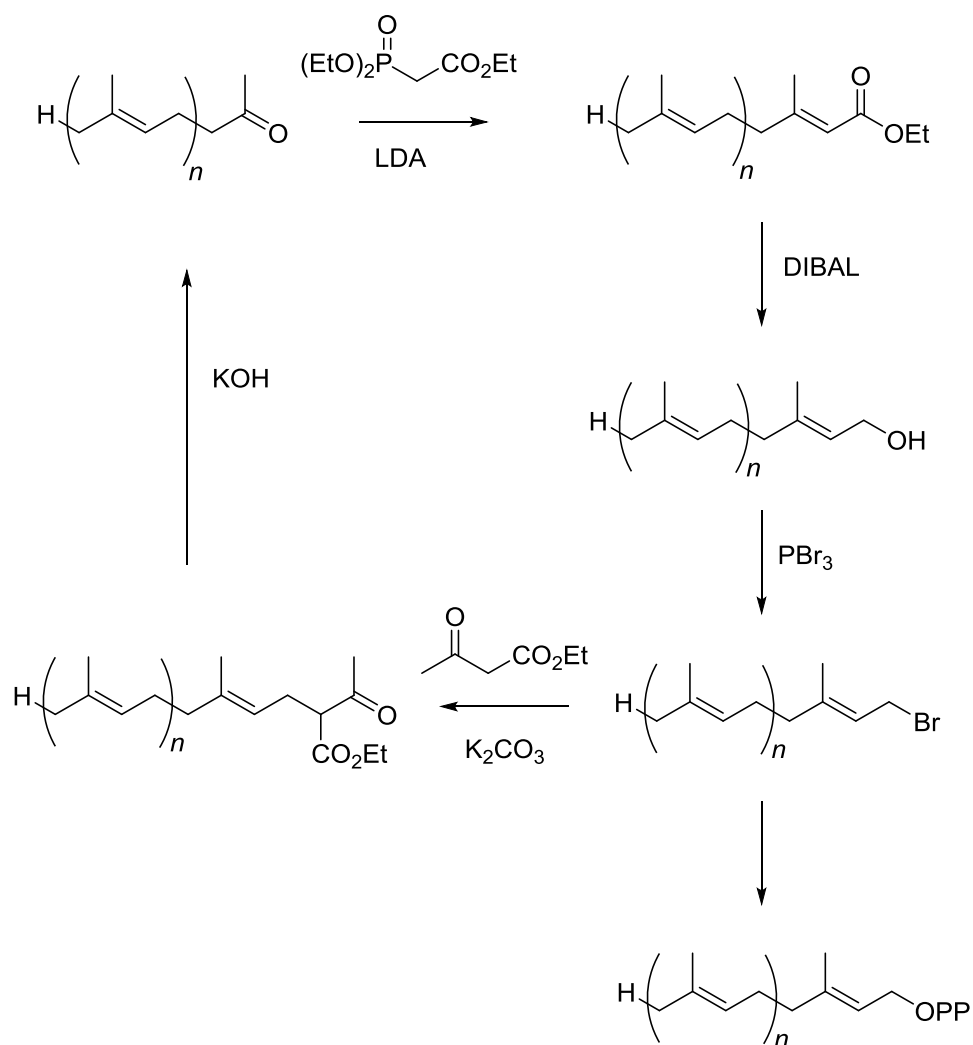
Reprinted from *Eur. J. Org. Chem.* **2014**, 7684-7691 with kind permission from John Wiley and Sons.

Introduction

Classic isotopic labeling experiments in combination with modern NMR spectroscopic methods remain a powerful tool for the investigation of molecular biochemical processes (Chapter 1.4). Terpene cyclases are remarkable enzymes in terms of the structural complexity they create from one achiral linear precursor in only one enzymatic reaction. To study the mechanism underlying these transformations, labeling experiments, which enable the tracking of specific atoms, with stable isotopes can be carried out (Chapter 1.4.2). Therefore, robust, flexible and reliable synthetic methodologies have to be developed, which enable the synthesis of isotopically labeled compounds from commercially available building blocks.

Summary

A systematic synthetic route towards oligoprenyl diphosphates, based on the employment of three simple building blocks, acetone, triethyl phosphonoacetate and ethyl acetoacetate was developed. The synthesis enables selective labeling of every position of the linear terpene precursor. Isotopomers of the required building blocks are either commercially available or can be easily generated thereof. The synthesis makes use of a cyclic sequence, resembling subsequent elongation by five carbon atoms in every cycle (Scheme 3).



Scheme 3. Schematic representation of the developed synthetic route.

The scope of this synthetic route was demonstrated by the synthesis of $[14\text{-}^2\text{H}]$ GGPP, which was used for incubation experiments with the tuberculosinyl diphosphate synthase from *Mycobacterium tuberculosis*. The experiments allowed for following of the stereochemical course of the initial protonation step, revealing attack from the *Si* face.

8 Conformational Analysis, Thermal Rearrangement, and EI-MS Fragmentation Mechanism of (1(10)*E*,4*E*,6*S*,7*R*)-Germacradien-6-ol by ¹³C-Labeling Experiments

Dr. Patrick Rabe, Lena Barra, Jan Rinkel, Dr. Ramona Riclea, Dr. Christian A. Citron, Tim A. Klapschinski, Aron Janusko and Prof. Dr. Jeroen S. Dickschat*

Angew. Chem. Int. Ed. **2015**, *54*, 13448-13451.

This publication was also part of a cumulative dissertation by Dr. Patrick Rabe at the University of Bonn and only supplements this thesis. My contribution to this work comprises the synthesis of (¹³C₁₅)-labeled FPP and a series of (¹³C₁)-labeled isotopomers.

Reprinted from *Angew. Chem. Int. Ed.* **2015**, *54*, 13448-13451 with kind permission from John Wiley and Sons.

&

9 A Method for Investigating the Stereochemical Course of Terpene Cyclisations

Dr. Patrick Rabe, Jan Rinkel, Tim A. Klapschinski, Lena Barra, Prof. Dr. Jeroen S. Dickschat*

Org. Biomol. Chem. **2016**, *14*, 158-164.

This publication was also part of a cumulative dissertation by Dr. Patrick Rabe at the University of Bonn and Dr. Christian A. Citron, Technical University of Braunschweig and only supplements this thesis. My contribution to this work comprises the synthesis of one labeled substrate, employed for *in vitro* experiments in this study.

Reprinted from *Org. Biomol. Chem.* **2016**, *14*, 158-164 with kind permission from The Royal Society of Chemistry.

Introduction

Biotechnological methods and the next generation sequencing technologies have revolutionized natural products research, with thousands of genome sequences available from public databases. The identification of genes encoding for terpene synthases can be achieved by utilizing a Basic Local Alignment Search Tool (BLAST), enabling the identification of genes by their homology.^[107] The targeted genes can be amplified by polymerase chain reaction and cloned into heterologous expression hosts, like *E. coli*. After purification, the recombinant proteins can be used for *in vitro* experiments and the substrate scope can be tested by incubation with suitable substrates e.g. GPP, FPP or GGPP. The obtained enzyme products have to be purified and their structure has to be identified or elucidated. By 2016 over 600 bacterial terpene cyclases have been identified from genome sequencing data, from which about 50 have been biochemically characterized. By phylogenetic analyses of known genes to predicted terpene cyclase genes, resulting in grouping of closely related families, round about 300 further enzymes could be identified in regard of their product specificity.^[46,108]

Summary

Five terpene cyclase genes are encoded in the genome of the actinomycete *Streptomyces pratensis*, from which a geosmin,^[109] 2-methylisoborneol,^[110] 7-*epi*- α -eudesmol,^[111] and *epi*-cubanol^[112] synthase has been characterized before. The product of the terpene cyclase from the fifth gene was identified in this publication and its chemical properties were thoroughly investigated by isotopic labeling experiments. Therefore the gene was cloned into the heterologous expression host *E. coli* and incubation of the purified expressed enzyme with the sesquiterpene precursor FPP led to the production of (1(10)*E*,4*E*)-germacradien-6-ol (**97**), identified from GC/MS data. Analysis of the respective ¹H- and ¹³C-NMR data, measured at room temperature, showed unclear and broad signals for the terpenoid. When measured at -50 °C or 0 °C, two sets of clearly resolved signals were observed, resembling the occurrence of two conformers (**97a** and **97b**), also known from literature data (Figure 28).^[113] In order to fully elucidate the NMR data, all singly labeled (¹³C)FPP isotopomers and the fully ¹³C-labeled (¹³C₁₅)FPP were synthesized

by the route described in Chapter 7.^[114] By incubation of singly labeled (^{13}C)FPP with the recombinant germacradien-6-ol synthase and analysis of the resulting singly labeled terpene by ^{13}C -NMR spectroscopy, two sharp signals, belonging to **97a** and **97b** were obtained. By sequential incubation of all 15 isotopomers of FPP, all ^{13}C signals in the NMR spectrum belonging to one carbon atom of **97** could be deduced. To differentiate between the two conformers, incubation with fully labeled ($^{13}\text{C}_{15}$)FPP was conducted. The resulting fully ^{13}C -labeled terpene ($^{13}\text{C}_{15}$)-**97** was subjected to ^{13}C , ^{13}C -COSY-NMR spectroscopy. The results enabled the assignment of the ^{13}C signals to the corresponding conformer **97a** or **97b** by analysis of the C,C-connectivities deduced from the obtained cross peaks.

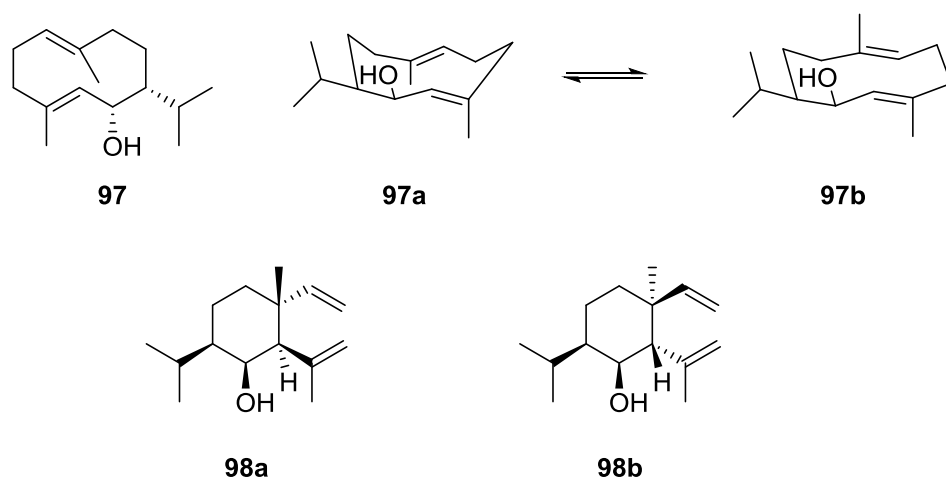


Figure 28. Structure of the identified sesquiterpene (1(10)*E*,4*E*)-germacradien-6-ol (**97**) from *S. pratensis* and its interconvertible conformers **97a** and **97b**. Thermal rearrangement products **98a** and **98b**.

Apart from the interesting NMR properties, (1(10)*E*,4*E*)-germacradien-6-ol (**97**) also showed reactivity for undergoing a thermal Cope-rearrangement, as was observed from two sideproducts in the respective gaschromatogram, caused by the high temperature impact in the GC/MS injector. Their structures were elucidated after microwave assisted synthesis from **97** and were identified as shyobunol (**98a**) and 5,10-di-*epi*-shyobunol (**98b**). Additionally, the EI-MS (electron ionization mass spectrometry) fragmentation mechanism of **97** was studied by GC/MS and GC/MS² experiments employing all enzymatically generated (^{13}C)-**97** isotopomers.

Additionally, three putative terpene cyclase genes from *S. scabei*, *S. venezuelae* and *S. clavuligerus* were identified and cloned into the expression host *E. coli*. The expressed purified enzymes were incubated with GPP, FPP and GGPP and revealed in all three cases the conversion of FPP into a sesquiterpene. The three terpenes were isolated and their structures were elucidated by NMR spectroscopic methods, leading to the identification of the two new natural products neomeranol B (**99**) from *S. scabei* and isodauc-8-en-11-ol (**100**) for *S. venezuelae*. The terpene cyclase from *S. clavuligerus* produced the known terpene (+)-(4*S*,5*S*,7*R*,10*S*)-intermedeol (**101**) (Figure 29).^[115]

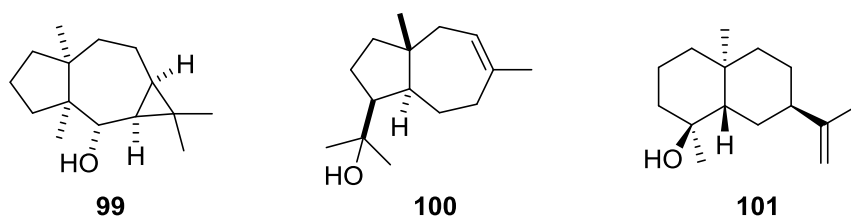


Figure 29. Structures of the identified terpenes neomeranol B (**99**), isodauc-8-en-11-ol (**100**) and intermedeol (**101**).

The cyclization mechanisms of **99**, **100** and **101** were studied by incubation experiments with ^{13}C -labeled FPP isotopomers. The biosyntheses of **99** and **101** proceed via neutral intermediates, requiring reprotonation prior to subsequent attack of an olefinic double bond. A highly sensitive method to follow the stereochemical course of these reprotonation steps was developed. Therefore, a ^{13}C -label was introduced in the reprotonated carbon position by employing a (^{13}C)FPP isotopomer labeled in the appropriate position. The enzyme reaction was carried out in D_2O , leading to a stereoselective deuteration of the respective carbon atom. The outcome of the experiment was analyzed by recording a $^1\text{H},^{13}\text{C}$ -HSQC spectrum, revealing which of the diastereotopic protons got deuterated by a missing crosspeak.

10 Discovery of a Mosaic-Like Biosynthetic Assembly Line with a Decarboxylative Off-Loading Mechanism through a Combination of Genome Mining and Imaging

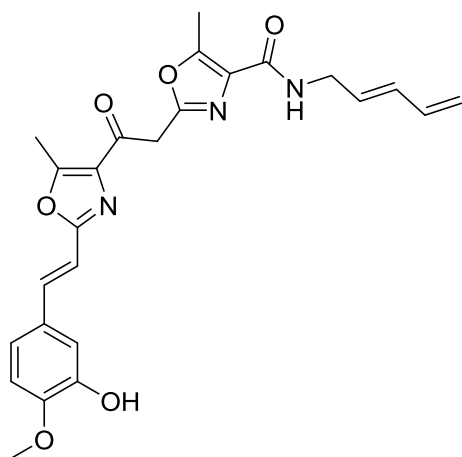
Dr. Mahsa M. Mohseni, Dr. Thomas Höver, Lena Barra, Marcel Kaiser, Prof. Dr. Pieter C. Dorrestein, Prof. Dr. Jeroen S. Dickschat and Prof. Dr. Till F. Schäberle*

Angew. Chem. Int. Ed. **2016**, *55*, 13611-13614.

Reprinted from *Angew. Chem. Int. Ed.* **2016**, *55*, 13611-13614 with kind permission from John Wiley and Sons.

Introduction

The identification of the biosynthetic gene cluster (BGC) responsible for the assembly of a certain natural product is nowadays a key step in natural product research. Access to the BGC provides the opportunity for high-level overproduction in heterologous hosts to improve isolatable yields, the genetic manipulation to generate novel derivatives or detailed mechanistic investigations by expression of recombinant enzymes. This research is particularly important in terms of the quest for new bioactive compounds, which can be exploited for therapeutic uses.^[116] Compared to well studied bacteria genera like streptomycetes or myxobacteria, *Herpetosiphon* spp. belonging to the phylum Chloroflexi have not been thoroughly investigated before. The PKS/NRPS-derived natural product siphonazole (**45**), isolated from *Herpetosiphon* sp. C060 is one recent example and is already introduced in Chapter 1.4.1 (Figure 30).^[61]



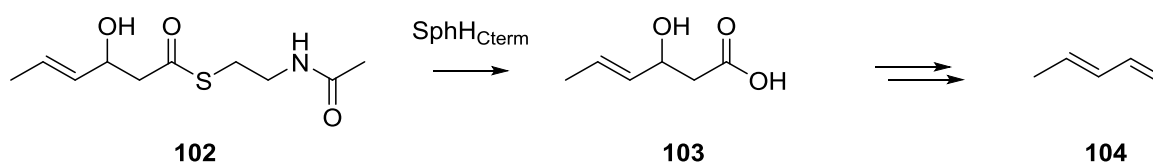
45

Figure 30. Structure of siphonazole (**45**).

Summary

The gene cluster from *Herpetosiphon* sp. B060, responsible for the biosynthesis of siphonazole (**45**) was identified by genome-mining in combination with imaging mass spectrometry (IMS). By bioinformatic screening of the draft genome, two candidate NRPS/PKS hybrid gene clusters were discovered, from which one could be excluded

based on the substrate specificity of the encoded adenylation domains. The second cluster carries adenylation domains predicted to be specific for glycine and threonine, both building blocks in siphonazole biosynthesis. Additionally, oxidation domains are encoded within this cluster, essential for oxazole formation. In total 10 genes *spha* to *sphJ* consisting of 12 core modules were identified and linked to siphonazole biosynthesis by activity tests. Besides the mosaic-like assembly line, the termination step in the biosynthesis of this natural product is highly unusual and the mechanism of the decarboxylative release mechanism was studied by *in vitro* experiments. Therefore, recombinant enzymes SphJ, the thioesterase domain and SphH_{Cterm}, the C-terminal hydrolase domain, were incubated with substrate mimic **102**. The resulting enzyme product, the volatile pentadiene (**104**), was trapped by using the SPME-technique and detected by GC/MS. The results demonstrate that SphH_{Cterm} alone is responsible for product release and SphJ acts as a proof-reading function, which is further supported from bioinformatic predictions. The mechanism of the decarboxylation-dehydration sequence was studied by a labeling experiment, pointing to an initial thioesterase hydrolysis to acid **103** catalyzed by SphH_{Cterm} followed by spontaneous or concerted dehydration and decarboxylation (Scheme 4).



Scheme 4. Possible mechanism for product off-loading in siphonazole biosynthesis.

The bioactivity of siphonazole (**45**) was studied and activity against the malaria pathogen *Plasmodium falciparum* was detected. The evolutionary background of the encoded gene cluster is discussed, as well as the possible application of SphH_{Cterm} for synthetic biology.

11 Sceptin – Enantioselective Synthesis of a Tetrasubstituted *all-trans* Cyclobutane Key Intermediate

Lena Barra and Prof. Dr. Jeroen S. Dickschat*

Eur. J. Org. Chem. **2017**, 4566-4571.

Reprinted from *Eur. J. Org. Chem.* **2017**, 4566-4571 with kind permission from John Wiley and Sons.

Introduction

The cyclobutane skeleton is a highly strained and yet widespread structural motif in nature and can be found in almost all classes of natural products, namely terpenes, alkaloids, fatty acids, nucleosides or polyketides.^[117] A particularly intriguing group among them are the cyclobutane-centered symmetric or often rather pseudo-symmetric natural products. They can be seen as dimers formed by an intermolecular [2+2] cycloaddition, either by homo- or heterodimerization. The sponge-derived pyrrole-imidazole alkaloid Sceptrin (**105**) was isolated in 1981 by FAULKNER and CLARDY from the marine sponge *Agelas sceptrum*.^[118] Its structure consists of two hymenidin (**106**) subunits which are connected in a head-to-head manner with an all-*trans* configured cyclobutane core. Sceptrin exhibits antimicrobial activity by disrupting cell membranes of eukaryotic and prokaryotic cells, anti-muscarinic and anti-histaminic activities and inhibits cell motility of cancer cell lines without showing cytotoxicity at comparable concentrations.^[119] Apart from sceptrin (**105**) a series of related compounds can be isolated from different *Agelas* species, for example nakamuric acid^[120] (**107**) and ageliferin^[121] (**108**), which can be rationalized as the [4+2] cycloaddition product of **106** (Figure 31).

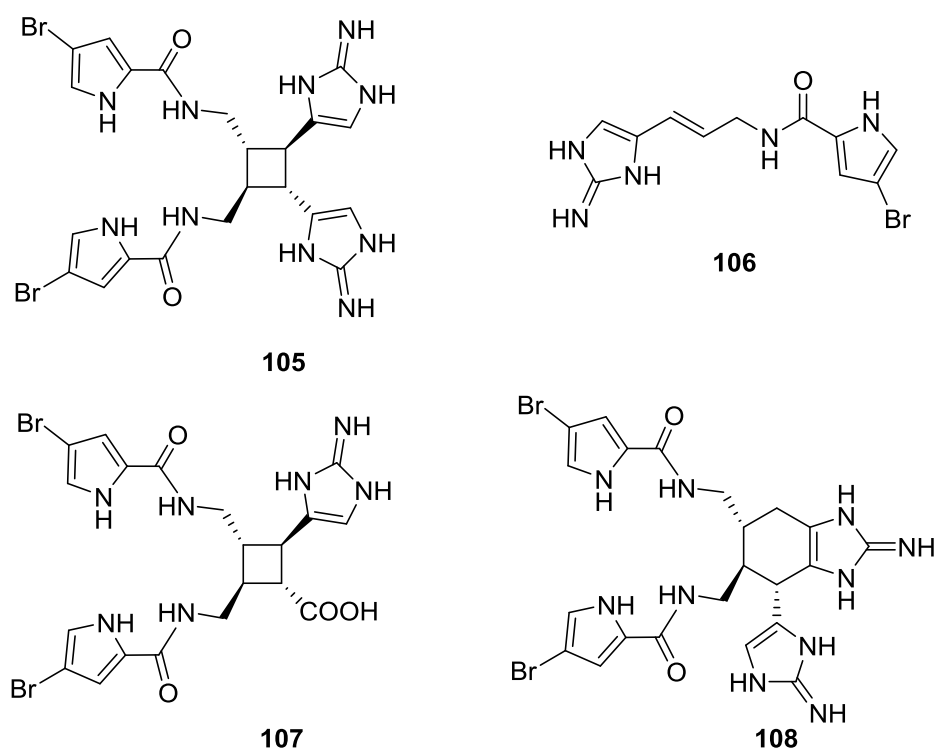
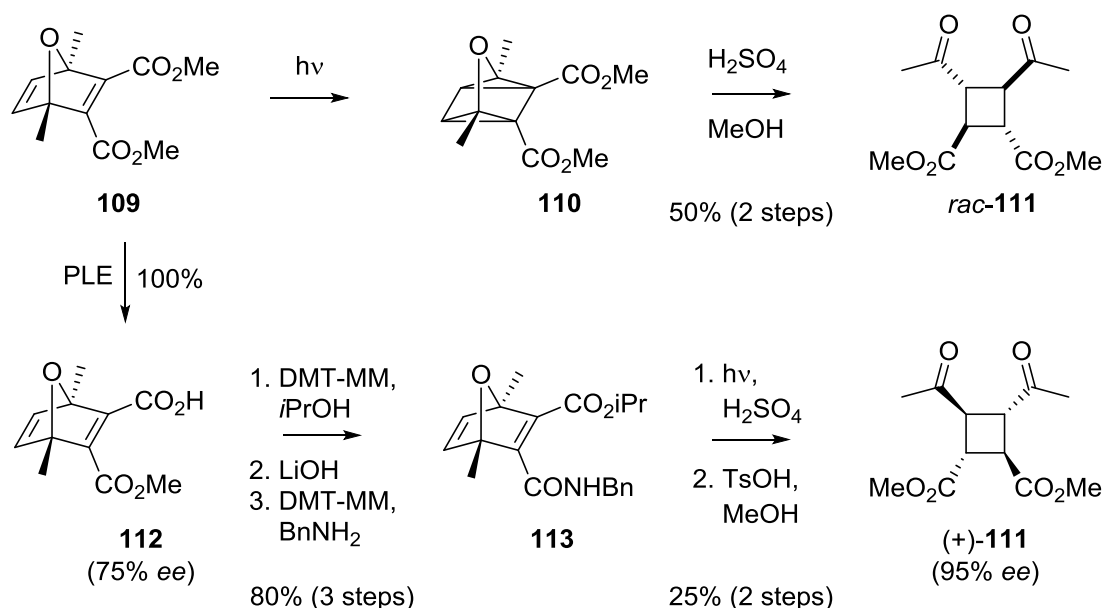


Figure 31. Structures of sceptrin (**105**), hymenidin (**106**), nakamuric acid (**107**) and ageliferin (**108**). Revised structures (2014) are shown.

From a synthetic point of view chiral cyclobutane centered natural products are challenging targets since methods for asymmetric construction of cyclobutane scaffolds are limited.^[122] The first total synthesis of *rac*-sceptrin was developed by BARAN in 2004 and was based on the formation of a tetrasubstituted cyclobutane skeleton containing suitable reactive side chains, which subsequently were transformed into **105** in 12 linear steps. The cyclobutane ring was synthesized by an intramolecular [2+2] photocycloaddition of oxo-bridged compound **109**, which can be obtained from a Diels-Alder reaction of dimethyl acetylenedicarboxylate and 2,5-dimethylfuran, to the highly reactive oxaquadricyclane species **110**, followed by an acid induced fragmentation and epimerization to all-*trans* cyclobutane *rac*-**111**.^[123] An asymmetric variation of this reaction could be achieved by the desymmetrization of *meso*-compound **109** to acid **112** using pig liver esterase (PLE) in quantitative yield and 75% *ee*. Subsequent esterification, selective saponification and amidation with benzylamine to **113** allowed for the conservation of the implemented stereo information to obtain (+)-**111** after irradiation, acid induced fragmentation and methanolysis under simultaneous epimerization. The enantiomeric excess was increased to 95% by recrystallization after photolysis. Thus, (+)-**111** was synthesized over 7 steps with an overall yield of 20% (Scheme 5).^[124]

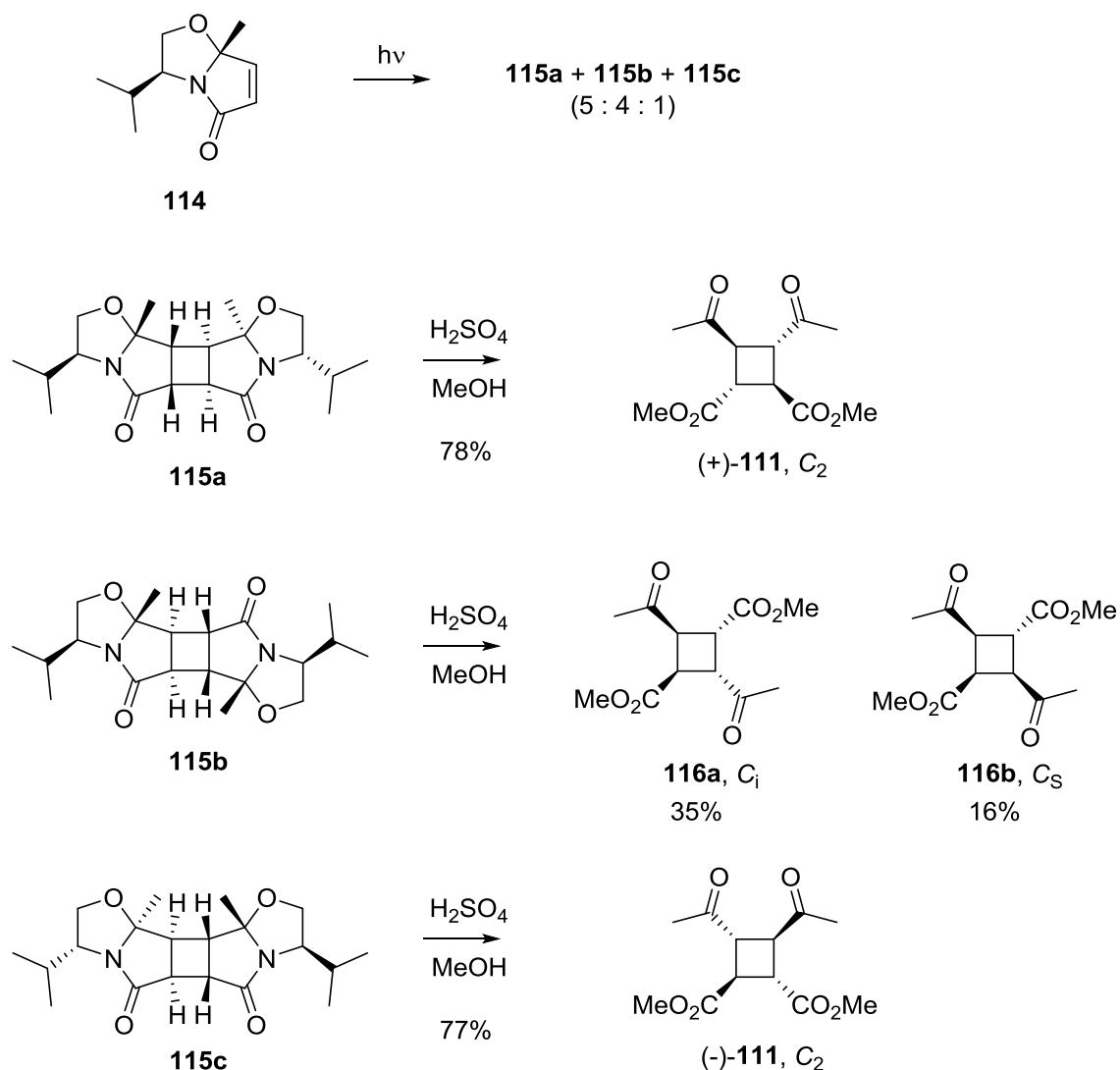


Scheme 5. Synthesis of *rac*-all-*trans* cyclobutane **111** and asymmetric approach to (+)-**111** developed by BARAN. The absolute configuration of (+)-**111** is shown according to the revised structure of sceptrin (**105**).

The opposite enantiomer (–)-**111** could be synthesized analogously after direct amidation of **112** with benzylamine. The absolute configurations of cyclobutanes (–)-**111** and (+)-**111** were assigned by conversion to scep trin and comparison of CD-spectra and optical rotary powers to the natural sample. Since the absolute configuration of **105** was wrongly assigned in 1981, which was shown in 2014 by CHEN and BARAN, also the configurations of (–)-**111** and (+)-**111** should be incorrect.^[125] This finding stands in disagreement with a crystal structure, which was obtained to determine the absolute configuration of **112**. However, as concluded by the authors, the desymmetrization of **109** could only be achieved with an ee of 75%, therefore a single-crystal of the minor enantiomer could have been obtained and subjected to X-ray analysis. In addition, the fragmentation mechanism of **110** to **111** has not been elucidated, therefore the absolute configurations of (+)-**111** and (–)-**111** have not been unambiguously assigned yet.

Summary

During studies towards the total synthesis of the cyclobutane containing volatile terpene koraiol,^[126] an alternative synthesis for both enantiomers of **111** was discovered. Irradiation of photoactive valine-derived enone **114**, originally developed for stereoselective cyclopropanations and cyclobutanations by MEYERS,^[127] led to the formation of two major (**115a** and **115b**) and one minor photodimer (**115c**) (Scheme 6).



Scheme 6. Alternative approach to key intermediate (+)- and (-)-**111**.

Their structures were elucidated by 2D NMR spectroscopy, symmetry considerations and analyses of their methanolysis products. Additionally, a crystal structure could be obtained for the major photodimer **115a**. Methanolyses of the chiral auxiliary yielded cyclobutane (+)-**111** for **115a**, two achiral compounds (**116a** and **116b**) for **115b** and (-)-**111** for **115c**. Their formation can be explained by cleavage of the chiral auxiliary and fast epimerization in α -position to the methyl ketones, instead of the methyl esters. This observation was supported from a deuterium exchange experiment and the occurrence of a high enantiomeric excess of 98% for **111**. The absolute configuration of (+)-**111** can thus be delineated from the prearrangement in **115a** and was additionally shown by X-ray diffraction analysis.

12 References

- [1] E. Breitmaier, *Terpenes*, WILEY-VCH, Weinheim, **2006**.
- [2] O. Wallach, *Liebigs. Ann. Chem.* **1887**, 239, 1.
- [3] a) L. Ruzicka, M. Stoll, *Helv. Chim. Acta* **1922**, 5, 923; b) L. Ruzicka *Experientia* **1953**, 9, 357.
- [4] N. L. Brock, J. S. Dickschat, *Biosynthesis of Terpenoids*, in: *Handbook of Natural Products*, K. G. Ramawat, J.-M. Mérillon (Eds.), Springer, **2013**, 2693.
- [5] A. Guenther, T. Karl, P. Harley, C. Wiedinmyer, P. I. Palmer, C. Geron, *Atmos. Chem. Phys.* **2006**, 6, 3181.
- [6] N. N. Gerber, H. A. Lechevalier, *Appl. Microbiol.* **1965**, 13, 935.
- [7] a) L. L. Medsker, D. Jenkins, J. F. Thomas, C. Koch, *Environ. Sci. Technol.* **1969**, 3, 476; b) R. Bentley, R. Meganathan, *FEBS Lett.* **1981**, 125, 220.
- [8] a) R. Ratnayake, D. Covell, T. T. Ransom, K. R. Gustafson, J. A. Beutler, *Org. Lett.* **2009**, 11, 57; b) J. A. Beutler, R. Ratnayake, D. Covell, T. R. Johnson, WO 2009/088854, **2009**.
- [9] P. Rabe, J. Rinkel, E. Dolja, T. Schmitz, B. Nubbemeyer, T. H. Luu, J. S. Dickschat, *Angew. Chem. Int. Ed.* **2017**, 56, 2776.
- [10] T. Mitsuhashi, J. Rinkel, M. Okado, I. Abe, J. S. Dickschat, *Chem. Eur. J.* **2017**, 23, 10053.
- [11] S. Niu, Z.-W. Fan, C.-L. Xie, Q. Liu, Z.-H. Luo, G. Liu, X.-W. Yang, *J. Nat. Prod.* **2017**, 80, 2174.
- [12] a) D. E. Vance, H. van den Bosch, *Biochim. Biophys. Acta* **2000**, 1529, 1; b) M. Wang, M. R. Briggs, *Chem. Rev.* **2004**, 104, 119; c) S. Nagpal, J. Lu, M. F. Boehm, *Curr. Med. Chem.* **2001**, 8, 1661; d) D. Steinberg, *J. Lipid Res.* **2006**, 47, 1339.
- [13] a) M. Lidén, U. Eriksson, *J. Biol. Chem.* **2006**, 281, 13001; b) M. G. Leuenberger, C. Engeloch-Jarret, W.-D. Woggon, *Angew. Chem. Int. Ed.* **2001**, 40, 2614.
- [14] K. Cornish, *Nat. Prod. Rep.* **2001**, 18, 182.
- [15] a) D. A. Bochar, J. Freisen, C. V. Stauffacher, V. W. Rodwell, in *Comprehensive Natural Products Chemistry*, D. E. Cane (Eds.), Vol. 2, Pergamon, Oxford, **1999**, 15.

- [16] a) F. Lynen, *Angew. Chem.* **1965**, 77, 929; b) K. Bloch, *Angew. Chem.* **1965**, 77, 944.
- [17] J. W. Cornforth, *Angew. Chem.* **1976**, 88, 550.
- [18] a) H. Rudney, J. J. Ferguson, *J. Am. Chem. Soc.* **1957**, 79, 5580; b) H. Rudney, *J. Biol. Chem.* **1957**, 227, 363; c) H. Rudney, J. J. Ferguson, *J. Biol. Chem.* **1959**, 234, 1076.
- [19] a) J. Knappe, E. Ringelmann, F. Lynen, *Biochem. Z.* **1959**, 332, 195; b) I. F. Durr, H. Rudney, *J. Biol. Chem.* **1960**, 235, 2572; c) M. Eberle, D. Arigoni, *Helv. Chim. Acta.* **1960**, 43, 1508.
- [20] F. Lynen, M. Graßl, *Hoppe-Seyler's Z. Physiol. Chem.* **1958**, 313, 291.
- [21] a) T. T. Tchen, *J. Am. Chem. Soc.* **1957**, 79, 6344; b) S. Chaykin, J. Law, A. H. Phillips, T. T. Chen, K. Bloch, *Proc. Natl. Acad. Sci. U.S.A.* **1958**, 44, 998; c) U. Henning, E. M. Möslein, F. Lynen, *Arch. Biochem. Biophys.* **1959**, 83, 259; d) W. D. Loomis, J. Battaile, *Biochim. Biophys. Acta.* **1963**, 67, 54.
- [22] a) F. Lynen, H. Eggerer, U. Henning, I. Kessel, *Angew. Chem.* **1958**, 70, 734; b) K. Bloch, S. Chaykin, A. H. Phillips, A. de Waard, *J. Biol. Chem.* **1959**, 234, 2595.
- [23] a) B. W. Agranoff, H. Eggerer, U. Henning, F. Lynen, *J. Am. Chem. Soc.* **1959**, 81, 1254; b) J. W. Cornforth, R. H. Cornforth, G. Popják, L. Yengoyan, *J. Biol. Chem.* **1966**, 241, 3970; c) J. W. Cornforth, R. H. Cornforth, C. Donninger, G. Popják, *Proc. R. Soc. London Ser. B* **1966**, 163, 492; d) K. Clifford, J. W. Cornforth, R. Mallaby, G. T. Phillips, *J. Chem. Soc. D Chem. Commun.* **1971**, 1599.
- [24] J. W. Cornforth, R. H. Cornforth, G. Popják, L. Yengoyan, *J. Biol. Chem.* **1966**, 241, 3970.
- [25] S. Pandian, S. Saengchjan, T. S. Raman, *Biochem. J.* **1981**, 675; b) D. Zhou, R. H. White, *Biochem. J.* **1991**, 273, 627.
- [26] M. Rohmer, *Nat. Prod. Rep.* **1999**, 16, 565.
- [27] a) M. Rohmer, M. Seemann, S. Horbach, S. Bringer-Meyer, H. Sahn, *J. Am. Chem. Soc.* **1996**, 118, 2564; b) L. M. Lois, N. Campos, S. R. Putra, K. Danielsen, M. Rohmer, A. Boronat, *Proc. Natl. Acad. Sci. U.S.A.* **1998**, 95, 2105.

- [28] T. Kuzuyama, S. Takahashi, H. Watanabe, H. Seto, *Tetrahedron Lett.* **1998**, *39*, 4509.
- [29] T. Kuzuyama, M. Takagi, K. Kaneda, T. Dairi, H. Seto, *Tetrahedron Lett.* **2000**, *41*, 703.
- [30] T. Kuzuyama, M. Takagi, K. Kaneda, H. Watanabe, T. Dairi, H. Seto, *Tetrahedron Lett.* **2000**, *41*, 2925.
- [31] M. Takagi, T. Kuzuyama, K. Kaneda, H. Watanabe, T. Dairi, H. Seto, *Tetrahedron Lett.* **2000**, *41*, 3395.
- [32] a) S. Hecht, W. Eisenreich, P. Adam, S. Amslinger, K. Kis, A. Bacher, D. Arigoni, F. Rohdich, *Proc. Natl. Acad. Sci. U.S.A.* **2001**, *98*, 14837; b) A.-K. Kollas, E. C. Duin, M. Eberl, B. Altincicek, M. Hintz, A. Reichenberg, D. Henschker, A. Henne, I. Steinbrecher, D. N. Ostrovsky, R. Hedderich, E. Beck, H. Jomaa, J. Wiesner, *FEBS Lett.* **2002**, *532*, 432; c) M. Seemann, B. Tse Sum Bui, M. Wolff, D. Tritsch, N. Campos, A. Boronat, A. Marquet, M. Rohmer, *Angew. Chem. Int. Ed.* **2002**, *41*, 4337.
- [33] a) F. Rohdich, S. Hecht, K. Gärtner, P. Adam, C. Krieger, S. Amslinger, D. Arigoni, A. Bacher, W. Eisenreich, *Proc. Natl. Acad. Sci. U.S.A.* **2002**, *99*, 1158; b) M. Wolff, M. Seemann, B. Tse Sum Bui, Y. Frapart, D. Tritsch, A. Garcia Estrabot, M. Rodriguez-Concepcion, A. Boronat, A. Marquet, M. Rohmer, *FEBS Lett.* **2003**, *541*, 115; c) C. A. Citron, N. L. Brock, P. Rabe, J. S. Dickschat, *Angew. Chem. Int. Ed.* **2012**, *51*, 4053.
- [34] J. W. Munos, X. Pu, S. O. Mansoorabadi, H. J. Kim, H.-W. Liu, *J. Am. Chem. Soc.* **2009**, *131*, 2048.
- [35] E. Oldfield, *Acc. Chem. Res.* **2010**, *43*, 1216.
- [36] T. Kuzuyama, T. Shimizu, S. Takahashi, H. Seto, *Tetrahedron Lett.* **1998**, *39*, 7913.
- [37] M. Andaloussi, L. M. Henriksson, A. Wieckowska, M. Lindh, C. Björkelid, A. M. Larsson, S. Suresh, H. Iyer, B. R. Srinivasa, T. Bergfors, T. Unge, S. L. Mowbray, M. Larhed, T. A. Jones, A. Karlén, *J. Med. Chem.* **2011**, *54*, 4964.
- [38] H. Jomaa, J. Wiesner, S. Sanderbrand, B. Altincicek, C. Weidemeyer, M. Hintz, I. Türbachova, M. Eberl, J. Zeidler, H. K. Lichtenthaler, D. Soldati, E. Beck, *Science* **1999**, *285*, 1573.

- [39] J. Wiesner, C. Ziemann, M. Hintz, A. Reichenberg, R. Ortmann, M. Schlitzer, R. Fuhst, N. Timmesfeld, A. Vilcinskis, H. Jomaa, *Virulence* **2016**, 7, 718.
- [40] J. A. Tobert, *Nat. Rev. Drug Discov.* **2003**, 2, 517.
- [41] a) A. Endo, M. Kuroda, Y. Tsujita, *J. Antibiot. (Tokyo)* **1976**, 29, 1346; b) A. Endo, Y. Tsujita, M. Kuroda, K. Tanzawa, *Eur. J. Biochem.* **1977**, 77, 31.
- [42] A. W. Alberts, J. Chen, G. Kuron, V. Hunt, J. Huff, C. Hoffman, J. Rothrock, M. Lopez, H. Joshua, E. Harris, A. Patchett, R. Monaghan, S. Currie, E. Stapley, G. Albers-Schonberg, O. Hensens, J. Hirshfield, K. Hoogsteen, J. Liesch, J. Springer, *Proc. Natl. Acad. Sci. U.S.A.* **1980**, 77, 3957.
- [43] a) L. C. Tarshis, M. Yan, C. D. Poulter, J. C. Sacchettini, *Biochemistry* **1994**, 33, 10871; b) L. C. Tarshis, P. J. Proteau, B. A. Kellogg, J. C. Sacchettini, C. D. Poulter, *Proc. Natl. Acad. Sci. U.S.A.* **1996**, 93, 15018; c) H. V. Thulasiram, C. D. Poulter, *J. Am. Chem. Soc.* **2006**, 128, 15819; d) K. Ogura, T. Koyama, *Chem. Rev.* **1998**, 98, 1263.
- [44] D. W. Christianson, *Chem. Rev.* **2017**, 117, 11570.
- [45] P. Baer, P. Rabe, K. Fischer, C. A. Citron, T. A. Klapschinski, M. Groll, J. S. Dickschat, *Angew. Chem. Int. Ed.* **2014**, 53, 7652.
- [46] J. S. Dickschat, *Nat. Prod. Rep.* **2016**, 33, 87.
- [47] Y.-L. Yang, S. Zhang, K. Ma, Y. Xu, Q. Tao, Y. Chen, J. Chen, S. Guo, J. Ren, W. Wang, Y. Tao, W.-B. Yin, H. Liu, *Angew. Chem. Int. Ed.* **2017**, 56, 4749.
- [48] C. A. Lesburg, G. Zhai, D. E. Cane, D. W. Christianson, *Science* **1997**, 277, 1820.
- [49] M. Köksal, Y. Jin, R. M. Coates, R. Croteau, D. W. Christianson, *Nature* **2011** 469, 116.
- [50] L. Du, C. Sánchez, B. Shen, *Metab. Eng.* **2001**, 3, 78.
- [51] a) R. C. G. R. Anderson, H. M. Higgins, C. D. Pettinga, *Cincinnati J. Med.* **1961**, 42, 49; b) D. P. Levine, *Clin. Infect. Dis.* **2006**, 42, 5; c) C. T. Walsh, *Science* **2004**, 303, 1805.
- [52] K. J. Weissman, *Nat. Chem. Biol.* **2015**, 11, 660.
- [53] L. Du, L. Lou, *Nat. Prod. Rep.* **2010**, 27, 255.
- [54] R. L. Bunch, J. M. McGuire, US2653899, **1953**.
- [55] a) G. Höfle, N. Bedorf, H. Steinmetz, D. Schomburg, K. Gerth, H. Reichenbach, *Angew. Chem. Int. Ed.* **1996**, 35, 1567; b) M. A. Jordan, L. Wilson, *Nat. Rev. Cancer* **2004**, 4, 253.

- [56] E. P. Kennedy, *J. Biol. Chem.* **2001**, *276*, 42619.
- [57] C. A. Hutchison, D. W. Stewart, H. C. Urey, *J. Chem. Phys.* **1940**, *8*, 532.
- [58] a) F. Soddy, *The origins of the conceptions of isotopes*, Nobel Prize Lecture, **1922**. b) F. W. Aston, *Mass spectra and isotopes*, Nobel Prize Lecture, **1922**.
- [59] T. J. Simpson, *Chem. Soc. Rev.* **1987**, *16*, 123.
- [60] a) J. Rinkel, J. S. Dickschat, *Beilstein J. Org. Chem.* **2015**, *11*, 2493; b) J. S. Dickschat, *Eur. J. Org. Chem.* **2017**, 4872.
- [61] M. Nett, Ö. Erol, S. Kehraus, M. Köck, A. Krick, E. Eguereva, E. Neu, G. M. König, *Angew. Chem. Int. Ed.* **2006**, *45*, 3863.
- [62] a) D. J. Tantillo, *Nat. Prod. Rep.* **2011**, *28*, 1035; b) T. E. O'Brien, S. J. Bertolani, D. J. Tantillo, J. B. Siegel, *Chem. Sci.* **2016**, *7*, 4009; c) S. R. Hare, D. J. Tantillo, *Beilstein J. Org. Chem.* **2016**, *12*, 377.
- [63] P. Rabe, K. A. K. Pahirulzaman, J. S. Dickschat, *Angew. Chem. Int. Ed.* **2015**, *54*, 6041.
- [64] P. Rabe, A. Janusko, B. Goldfuss, J. S. Dickschat, *ChemBioChem* **2016**, *17*, 146.
- [65] a) S. Schulz, J. S. Dickschat, *Nat. Prod. Rep.* **2007**, *24*, 814; b) S. Schulz, J. S. Dickschat, B. Kunze, I. Wagner-Döbler, R. Diestel, F. Sasse, *Mar. Drugs* **2010**, *8*, 2976; c) J. S. Dickschat, *Nat. Prod. Rep.* **2017**, *34*, 310; d) O. Tyc, C. Song, J. S. Dickschat, M. Vos, P. Garbeva, *Trends Microbiol.* **2017**, *25*, 280.
- [66] A. R. J. Curson, J. D. Todd, M. J. Sullivan, A. W. B. Johnston, *Nat. Rev. Microbiol.* **2011**, *9*, 849.
- [67] F. A. Ditengou, A. Müller, M. Rosenkranz, J. Felten, H. Lasok, M. M. van Doorn, V. Legué, K. Palme, J.-P. Schnitzler, A. Polle, *Nat. Commun.* **2015**, *6*, 6279.
- [68] P. W. Paré, J. H. Tumlinson, *Plant Physiol.* **1999**, *121*, 325.
- [69] B. Bohmann, R. D. Phillips, G. R. Flematti, R. A. Barrow, R. Peakall, *Angew. Chem. Int. Ed.* **2017**, *56*, 8455.
- [70] J. S. Dickschat, *Nat. Prod. Rep.* **2014**, *31*, 838.
- [71] a) K. Grob, F. Zürcher, *J. Chromatogr. A* **1976**, *117*, 285; b) W. Boland, P. Ney, L. Jänicke, G. Gassmann, A "closed-loop-stripping" technique as a versatile tool for metabolic studies of volatiles, in *Analysis of volatiles: methods and applications*, ed. P. Schreier, Walter de Gruyter & Co., Berlin,

- 1984**, pp. 371-380.
- [72] a) C. L. Arthur, J. Pawliszyn, *Anal. Chem.* **1990**, *62*, 2145; b) Z. Zhang, J. Pawliszyn, *Anal. Chem.* **1993**, *65*, 1843.
- [73] B.-E. Priegnitz, U. Brandt, K. A. K. Pahirulzaman, J. S. Dickschat, A. Fleißner, *Eukaryotic Cell*, **2015**, *14*, 602.
- [74] a) T. Nilsson, T. O. Larsen, L. Montanarella, J. O. Madsen, *J. Microbiol. Methods* **1996**, *25*, 245; b) T. O. Larsen, J. C. Frisvad, *Mycol. Res.* **1995**, *99*, 1153.
- [75] Y. Yamagiwa, Y. Inagaki, Y. Ichinose, K. Toyoda, M. Hyakumachi, T. Shiraishi, *J. Gen. Plant Pathol.* **2011**, *77*, 336.
- [76] a) R. D. Wei, P. E. Still, E. B. Smalley, H. K. Schnoes, F. M. Strong, *Appl. Microbiol.* **1973**, *25*, 111; b) R. D. Wei, H. K. Schnoes, P. A. Hart, F. M. Strong, *Tetrahedron* **1975**, *31*, 109.
- [77] N. L. Brock, S. R. Ravella, S. Schulz, J. S. Dickschat, *Angew. Chem. Int. Ed.* **2013**, *52*, 2100.
- [78] a) D. E. Wolf, C. H. Hoffman, P. E. Aldrich, H. R. Skeggs, L. D. Wright, K. Folkers, *J. Am. Chem. Soc.* **1957**, *79*, 1486; b) J. R. Hanson, *J. Chem. Res.* **2008**, 241.
- [79] L. O. Zamir, C.-D. Nguyen, *J. Label. Compd. Radiopharm.* **1988**, *25*, 1189.
- [80] J. S. Dickschat, C. A. Citron, N. L. Brock, R. Riclea, H. Kuhz, *Eur. J. Org. Chem.* **2011**, 3339.
- [81] D. E. Cane, R. H. Levin, *J. Am. Chem. Soc.* **1976**, *98*, 1183.
- [82] a) B. Kühne, H.-P. Hanssen, W.-R. Abraham, V. Wray, *Phytochemistry* **1991**, *30*, 1463; b) I. Urbasch, B. Kühne, H.-P. Hanssen, W.-R. Abraham, *Planta Med.* **1991**, *57*, A18.
- [83] a) G. E. Harman, C. R. Howell, A. Viterbo, I. Chet, M. Lorito, *Nat. Rev. Microbiol.* **2004**, *2*, 43; b) C. M. F. Vos, K. De Cremer, B. P. A. Cammue, B. DeConinck, *Mol. Plant Pathol.* **2015**, *16*, 400.
- [84] N. Stoppacher, B. Kluger, S. Zeilinger, R. Krska, R. Schumacher, *J. Microbiol. Methods* **2010**, *81*, 187.
- [85] a) R. P. Collins, A. F. Halim, *J. Agric. Food Chem.* **1972**, *20*, 437; b) M. Kottb, T. Gigolashvili, D. K. Großkinsky, B. Piechulla, *Front. Microbiol.* **2015**, *6*, 1.

- [86] a) Q. Huang, Y. Tezuka, Y. Hatanaka, T. Kikuchi, A. Nishi, K. Tubaki, *Chem. Pharm. Bull.* **1995**, *43*, 1035; b) C. A. Citron, R. Riclea, N. L. Brock, J. S. Dickschat, *RSC Advances* **2011**, *1*, 290.
- [87] C. A. Citron, J. S. Dickschat, *Org. Biomol. Chem.* **2013**, *11*, 7447.
- [88] F.-P. Miao, X.-R. Liang, X.-L. Yin, G. Wang, N.-Y. Ji, *Org. Lett.* **2012**, *14*, 3815.
- [89] a) E. L. Ghisalberti, D. C. R. Hockless, C. Rowland, A. H. White, *J. Nat. Prod.* **1992**, *11*, 1690; b) S. Chantrapromma, C. Jeerapong, W. Phupong, C. K. Quah, H.-K. Fun, *Acta. Cryst.* **2014**, *E70*, o408-o409; c) E. Adelin, C. Servy, M.-T. Martin, G. Arcile, B. I. Iorga, P. Retailleau, M. Bonfill, J. Ouazzani, *Phytochemistry* **2014**, *97*, 55.
- [90] R. Schmidt, V. Cordovez, W. de Boer, J. Raaijmakers, P. Garbeva, *ISME J.* **2015**, *9*, 2329.
- [91] M. W. Taylor, R. Radax, D. Steger, M. Wagner, *Microbiol. Mol. Biol. Rev.* **2007**, *71*, 295.
- [92] a) C. C. P. Hardoim, R. Costa, *Mar. Drugs* **2014**, *12*, 5089; b) W. H. Gerwick, B. S. Moore, *Cell Chem. Biol.* **2012**, *19*, 85.
- [93] C. Christophersen, U. Anthoni, P. H. Nielsen, N. Jacobsen, O. S. Tendal, *Biochem. Syst. Ecol.* **1989**, *17*, 459.
- [94] C. Duque, A. Bonilla, E. Bautista, S. Zea, *Biochem. Syst. Ecol.* **2001**, *29*, 459.
- [95] a) R. Romoli, M. C. Papaleo, D. de Pascale, M. L. Tutino, L. Michaud, A. L. Giudice, R. Fani, G. Bartolucci, *J. Mass. Spectrom.* **2011**, *46*, 1051; b) M. C. Papaleo, R. Romoli, G. Bartolucci, I. Maida, E. Perrin, M. Fondi, V. Orlandini, A. Mengoni, G. Emiliani, M. L. Tutino, E. Parrilli, D. de Pascale, L. Michaud, A. L. Giudice, R. Fani, *N. Biotechnol.* **2013**, *30*, 824; c) V. Orlandini, I. Maida, M. Fondi, E. Perrin, M. C. Papaleo, E. Bosi, D. de Pascale, M. L. Tutino, L. Michaud, A. L. Giudice, R. Fani, *Microbiol. Res.* **2014**, *169*, 593.
- [96] U. Höller, A. D. Wright, G. F. Matthée, G. M. König, S. Draeger, H.-J. Aust, B. Schulz, *Mycol. Res.* **2000**, *104*, 1354.
- [97] S. D. Bentley, K. F. Chater, A.-M. Cerdeno-Tárraga, G. L. Challis, N. R. Thomson, K. D. James, D. E. Harris, M. A. Quail, H. Kieser, D. Harper, A. Bateman, S. Brown, G. Chandra, C. W. Chen, M. Collins, A. Cronin, A. Fraser, A. Goble, J. Hidalgo, T. Hornsby, S. Howarth, C.-H. Huang, T. Kieser,

- L. Larke, L. Murphy, K. Oliver, S. O'Neil, E. Rabbinowitsch, M.-A. Rajandream, K. Rutherford, S. Rutter, K. Seeger, D. Saunders, S. Sharp, R. Squares, S. Squares, K. Taylor, T. Warren, A. Wietzorrek, J. Woodward, B. G. Barrell, J. Parkhill, D. A. Hopwood, *Nature* **2002**, *417*, 141.
- [98] A. van der Meij, S. F. Worsley, M. I. Hutchings, G. P. van Wezel, *FEMS Microbiol. Rev.* **2017**, *41*, 392.
- [99] C. A. Citron, P. Rabe, J. S. Dickschat, *J. Nat. Prod.* **2012**, *75*, 1765.
- [100] J. S. Dickschat, T. Martens, T. Brinkhoff, M. Simon, S. Schulz, *Chem. Biodivers.* **2005**, *2*, 837.
- [101] J. S. Dickschat, H. Bruns, R. Riclea, *Beilstein J. Org. Chem.* **2011**, *7*, 1697.
- [102] R. Riclea, B. Aigle, P. Leblond, I. Schoenian, D. Spiteller, J. S. Dickschat, *ChemBioChem* **2012**, *13*, 1635.
- [103] U. Groenhagen, M. Maczka, J. S. Dickschat, S. Schulz, *Beilstein J. Org. Chem.* **2014**, *10*, 1421.
- [104] a) S. Haeder, R. Wirth, H. Herz, D. Spiteller, *Proc. Natl. Acad. Sci. U.S.A.* **2009**, *106*, 4742; b) D.-C. Oh, M. Poulsen, C. M. Currie, J. Clardy, *Nat. Chem. Biol.* **2009**, *5*, 391; c) J. M. Crawford, J. Clardy, *Chem. Commun.* **2011**, *47*, 7559.
- [105] R. G. Buttery, R. Teranishi, R. A. Flath, L. C. Ling, *ACS Symp. Ser.* **1989**, *388*, 213.
- [106] a) J.-M. Oger, P. Richomme, H. Guinaudeau, J. P. Bouchara, A. Fournet, *J. Essent. Oil Res.* **1994**, *6*, 493; b) A. B. de Lima, M. B. Santana, A. S. Cardoso, J. K. R. da Silva, J. G. S. Maia, J. C. T. Carvalho, P. J. C. Sousa, *Phytomedicine* **2009**, *16*, 555; c) R. J. Bezerra de Siqueira, F. I. Bulcão Macedo, L. de Fátima Leal Interaminense, G. Pinto Duarte, P. J. Caldas Magalhães, T. Silva Brito, J. K. R. da Silva, J. G. S. Maia, P. J. C. Sousa, J. H. Leal-Cardoso, S. Lahlou, *Eur. J. Pharmacol.* **2010**, *638*, 90; d) L. de Fátima Leal Interaminense, F. E. dos Ramos-Alves, R. J. Bezerra de Siqueira, F. E. Xavier, G. Pinto Duarte, P. J. Caldas Magalhães, J. G. S. Maia, P. J. C. Sousa, S. Lahlou, *Eur. J. Pharm. Sci.* **2013**, *48*, 709; e) J. K. L. Vale, A. B. Lima, B. G. Pinheiro, A. S. Cardoso, J. K. R. Silva, J. G. S. Maia, G. E. P. de Sousa, A. B. F. da Silva, P. J. C. Sousa, R. S. Borges, *Planta Med.* **2013**, *79*, 628; f) I. A. Oyemitan, C. A. Elusiyan, M. A. Akanmu, T. A. Olugbade,

- Phytomedicine* **2013**, *20*, 1315.
- [107] S. F. Altschul, T. L. Madden, A. A. Schäffer, J. Zhang, Z. Zhang, W. Miller, D. Lipman, *J. Nucleic Acids Res.* **1997**, *25*, 3389.
- [108] P. Rabe, J. Rinkel, T. A. Klapschinski, L. Barra, J. S. Dickschat, *Org. Biomol. Chem.* **2016**, *14*, 158.
- [109] J. Jiang, X. He, D. E. Cane, *Nat. Chem. Biol.* **2007**, *3*, 711.
- [110] a) M. Komatsu, M. Tsuda, S. Omura, H. Oikawa, H. Ikeda, *Proc. Natl. Acad. Sci. U.S.A.* **2008**, *105*, 7422; b) W. K. W. Chou, I. Fanizza, T. Uchiyama, M. Komatsu, H. Ikeda, D. E. Cane, *J. Am. Chem. Soc.* **2010**, *132*, 8850.
- [111] P. Rabe, J. S. Dickschat, *Angew. Chem. Int. Ed.* **2013**, *52*, 1810.
- [112] C. Nakano, T. Tezuka, S. Horinouchi, Y. Ohnishi, *J. Antibiot.* **2012**, *65*, 551.
- [113] a) A. F. Barrero, M. M. Herrador, J. F. Quilez, R. Alvarez-Manzaneda, D. Portal, J. A. Gavin, D. G. Gravalos, M. S. J. Simmonds, W. M. Blaney, *Phytochemistry* **1999**, *51*, 529; b) J. A. Faraldos, S. Wu, J. Chappell, R. M. Coates, *Tetrahedron* **2007**, *63*, 7733.
- [114] C. A. Citron, P. Rabe, L. Barra, C. Nakano, T. Hoshino, J. S. Dickschat, *Eur. J. Org. Chem.* **2014**, 7684.
- [115] a) A. San Feliciano, M. Medarde, B. Del Rey, J. M. M. Del Corral, A. F. Barrero, *Phytochemistry* **1990**, *29*, 3207; b) R. P. W. Kesselmanns, J. B. P. A. Wijnberg, A. J. Minnaard, R. E. Walinga, A. de Groot, *J. Org. Chem.* **1991**, *56*, 7237.
- [116] a) P. J. Rutledge, G. L. Challis, *Nature Rev. Microbiol.* **2015**, *13*, 1; b) N. Ziemert, M. Alanjary, T. Weber, *Nat. Prod. Rep.* **2016**, *33*, 988.
- [117] a) Y. J. Hong, D. J. Tantillo, *Chem. Soc. Rev.* **2014**, *43*, 5042; b) Y.-Y. Fan, X.-H. Gao, J.-M. Yue, *Sci. China Chem.* **2016**, *59*, 1126; c) V. M. Dembitsky, *Phytomedicine* **2014**, *21*, 1559.
- [118] R. P. Walker, D. J. Faulkner, D. Van Engen, J. Clardy, *J. Am. Chem. Soc.* **1981**, *103*, 6772.
- [119] a) V. S. Bernan, D. M. Roll, C. M. Ireland, M. Greenstein, W. M. Maiese, D. A. Steinberg, *J. Antimicrob. Chemother.* **1993**, *32*, 539; b) R. Rosa, W. Silva, G. Escalona de Motta, A. D. Rodriguez, J. J. Morales, M. Ortiz, *Experientia* **1992**, *48*, 885; c) R. Mohammed, J. Peng, M. Kelly, M. T. Hamann, *J. Nat. Prod.* **2006**, *69*, 1739; d) A. Vassas, G. Bourdy, J. J. Paillard, J. Lavayre, M. Pais, J.

- C. Quirion, C. Debitus, *Planta Med.* **1996**, *62*, 28; e) P. A. Keifer, R. E. Schwartz, M. E. S. Koker, R. G. Hughes, D. Rittschof, K. L. Rinehart, *J. Org. Chem.* **1991**, *56*, 2965; f) A. D. Rodriguez, M. J. Lear, J. J. La Clair, *J. Am. Chem. Soc.* **2008**, *130*, 7256; g) A. Cipres, D. P. O'Malley, K. Li, D. Finlay, P. S. Baran, K. Vuori, *ACS Chem. Biol.* **2010**, *5*, 195.
- [120] C. Eder, P. Proksch, V. Wray, R. W. M. van Soest, E. Ferdinandus, L. A. Pattisina, Sudarsono, *J. Nat. Prod.* **1999**, *62*, 1295.
- [121] J. Kobayashi, M. Tsuda, T. Murayama, H. Nakamura, Y. Ohizumi, M. Ishibashi, M. Iwamura, T. Ohta, S. Nozoe, *Tetrahedron* **1990**, *46*, 5579.
- [122] a) S. Poplata, A. Troster, Y.-Q. Zou, T. Bach, *Chem. Rev.* **2016**, *116*, 9748; b) W. R. Gutekunst, P. S. Baran, *J. Org. Chem.* **2014**, *79*, 2430; c) T. Bach, J. P. Hehn, *Angew. Chem. Int. Ed.* **2011**, *50*, 1000; *Angew. Chem.* **2011**, *123*, 1032; d) E. Lee-Ruff, G. Mladenova, *Chem. Rev.* **2003**, *103*, 1449.
- [123] P. S. Baran, A. L. Zografos, D. P. O'Malley, *J. Am. Chem. Soc.* **2004**, *126*, 3726.
- [124] P. S. Baran, K. Li, D. P. O'Malley, C. Mitsos, *Angew. Chem. Int. Ed.* **2006**, *45*, 255.
- [125] Z. Ma, X. Wang, X. Wang, R. A. Rodriguez, C. E. Moore, S. Gao, X. Tan, Y. Ma, A. L. Rheinglod, P. S. Baran, C. Chen, *Science* **2014**, *346*, 219.
- [126] a) V. A. Khan, Y. V. Gatilov, Z. V. Dubovanko, V. A. Pentegova, *Chem. Nat. Compd.* **1979**, *15*, 572; b) N. L. Brock, K. Huss, B. Tudzynski, J. S. Dickschat, *ChemBioChem* **2013**, *14*, 311.
- [127] a) A. I. Meyers, S. A. Fleming *J. Am. Chem. Soc.* **1986**, *108*, 306; b) A. I. Meyers, J. L. Romine, S. A. Fleming *J. Am. Chem. Soc.* **1988**, *110*, 7245.

13 Appendix A – J

Appendix A

Pogostol Biosynthesis by the Endophytic Fungus
Geniculosporium

DOI: 10.1002/cbic.201402298

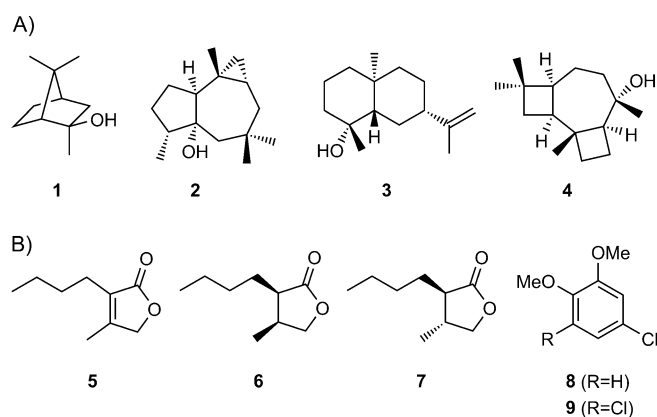
Pogostol Biosynthesis by the Endophytic Fungus *Geniculosporium*

Lena Barra,^[a] Barbara Schulz,^[b] and Jeroen S. Dickschat^{*[a]}

Six ¹³C-labelled isotopomers of mevalonolactone were synthesised and used in feeding experiments with the endophytic fungus *Geniculosporium*. The high incorporation rates of ¹³C-label into a sesquiterpene that was found in headspace extracts of the fungus enabled unambiguous identification of this volatile as pogostol without the need for compound purification, simply by collecting the volatile fraction with a closed-loop stripping apparatus followed by direct ¹³C NMR analysis (CLSA-NMR). The feeding experiments also gave insights into the biosynthesis of pogostol, including stereochemical aspects of the terpene cyclisation reaction. The possible biological function of pogostol is discussed.

Volatiles that are emitted by living organisms can be efficiently captured on charcoal filters by the use of a closed-loop stripping apparatus (CLSA). The experimental setup consists of a chamber containing a biological sample, and an air stream maintained by a pump and directed over the sample and then through the charcoal filter. The filter can then simply be extracted with an organic solvent, and the extract can be analysed by GC/MS.^[1] This technique was originally developed in 1973 by Grob and Zürcher for trace analysis of volatile contaminants in water samples,^[2,3] and has since been successfully applied in studies on volatile natural products, for example, those from insects,^[4] bacteria^[5,6] and fungi.^[7] Unambiguous compound identification by GC/MS requires knowledge of the analyte's mass spectrum. For automated database searches, the mass spectra of thousands of compounds are collected in large electronic libraries.^[8,9] In cases where several constitutional or stereoisomers of a compound have very similar mass spectra, the analyte can only be identified by additional comparison of its retention index to published retention indices. Ideally, positive compound identification in such cases requires knowledge of the retention indices of all eligible isomers. If this is not the case, synthesis of all isomers for direct comparison is a solution,^[10,11] but this is highly laborious and impractical, especially with highly complex volatile natural products,

such as most sesquiterpenes. An alternative approach is to purify the compound from culture extracts for structure elucidation by NMR spectroscopy. However, with volatiles significant losses in concentration steps can render the purification process unsuccessful. The major advantage of the CLSA technique is non-invasive detection of trace components in complex mixtures that cannot be analysed by NMR. Thus, to obtain NMR data from compounds in CLSA headspace extracts, we recently reported a new method; this combines feeding with ¹³C-labelled precursors and CLSA headspace extraction for ¹³C NMR analysis (CLSA-NMR).^[12–15] The fed precursor must be one that is only incorporated into volatiles from a certain compound class (e.g., mevalonolactone or deoxyxylulose, only into terpenes). If incorporation rates are high, ¹³C NMR analysis of the CLSA headspace extract results in a set of strongly enhanced ¹³C NMR signals, and only of compounds from a particular class. By using this method, the volatiles 2-methylisoborneol (**1**),^[12] isoafrikanol (**2**),^[13] eudesma-11-en-4 α -ol (**3**)^[14] and koraïol (**4**)^[15] were identified in headspace extracts of different actinomycetes and ascomycete fungi (Scheme 1 A), and stereo-



Scheme 1. A) Volatiles identified from actinomycetes and ascomycete fungi by CLSA-NMR. B) Previously identified volatiles from *Geniculosporium* sp.

chemical aspects of their biosynthesis were elucidated. Here, we report the synthesis of ¹³C-labelled mevalonolactone isotopomers, their use in feeding experiments with the endophytic fungus *Geniculosporium* sp., the identification of pogostol in headspace extracts and investigation of its biosynthesis by CLSA-NMR.

In previous investigations, we identified a series of structurally related lactones (**5–7**; Scheme 1 B) and two chlorinated veratrole derivatives (**8** and **9**) by GC/MS in headspace extracts of *Geniculosporium* sp., an endophytic fungus that had been

[a] L. Barra, Prof. Dr. J. S. Dickschat
Kekulé-Institut für Organische Chemie und Biochemie
Rheinische Friedrich-Wilhelms-Universität Bonn
Gerhard-Domagk-Strasse 1, 53121 Bonn (Germany)
E-mail: dickschat@uni-bonn.de

[b] Dr. B. Schulz
Institut für Mikrobiologie
Technische Universität Braunschweig
Spielmannstrasse 7, 38106 Braunschweig (Germany)

Supporting information for this article is available on the WWW under <http://dx.doi.org/10.1002/cbic.201402298>.

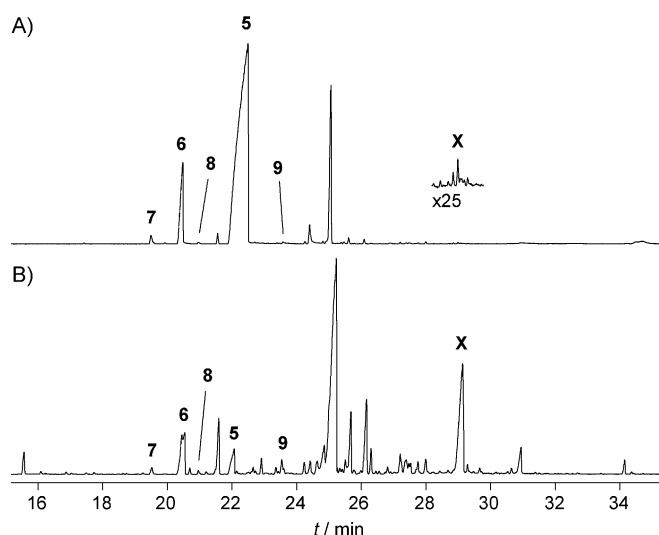
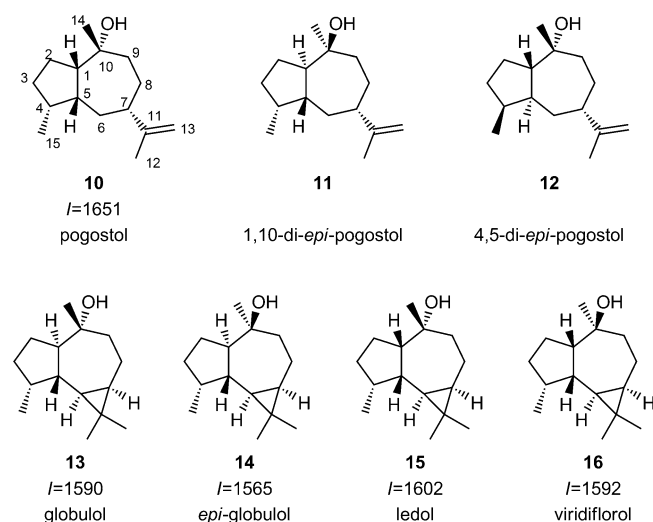


Figure 1. Total ion chromatograms of headspace extracts from *Geniculosporium* sp. cultured on potato-carrot agar medium at 20 °C, A) after three weeks of incubation, and B) after five weeks of incubation with feeding of mevalonolactone (5 mM) after four weeks. Peak numbers refer to compounds in Scheme 2. The intensity scales of chromatograms A and B are directly comparable.

isolated from *Cistus monspeliensis* and was grown on potato-carrot medium for three weeks at 20 °C (Figure 1A).^[7,10] A few other unidentified compounds and traces of a sesquiterpene alcohol "X" were also detected. The mass spectrum of the alcohol was most similar to that of pogostol (**10**) in the database, but as the quality of the mass spectrum of the trace compound X was poor, the next best matches, globulol (**13**) and *epi*-globulol (**14**), could not be excluded (Scheme 2 and Figure S1 in the Supporting Information). The structures of their stereoisomers, ledol (**15**) and viridiflorol (**16**), were excluded

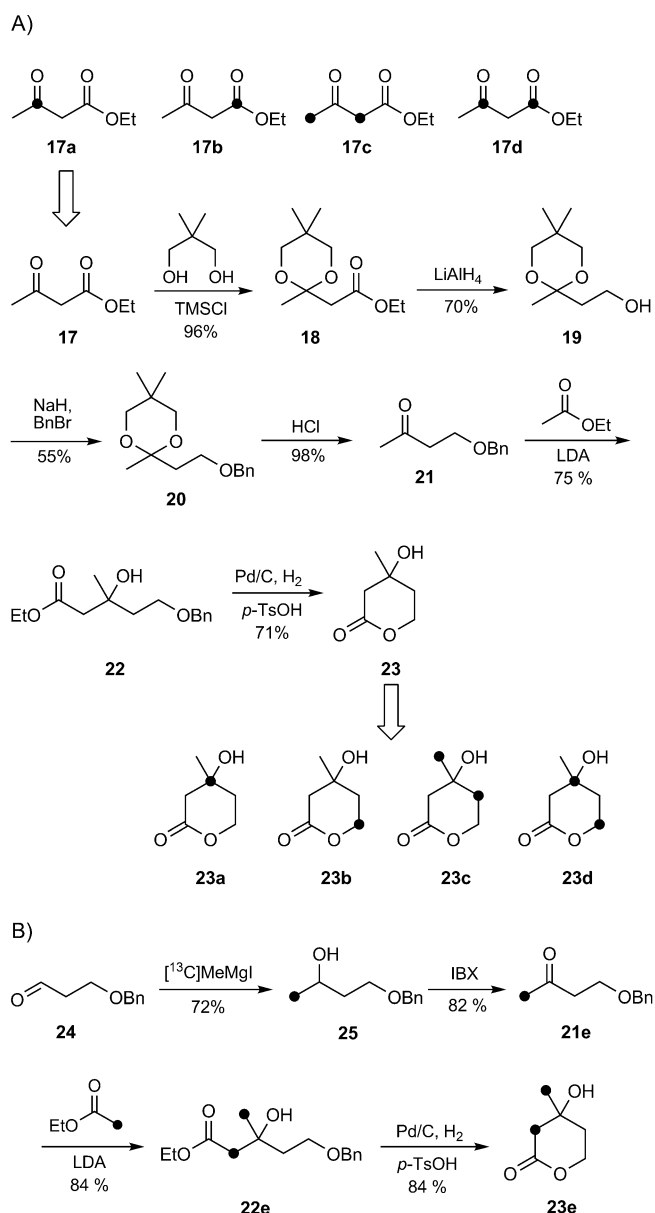


Scheme 2. Pogostol (**10**) and structurally related isomers. The retention index *I* for commercially available **14** (Sigma-Aldrich; analysed by GC-MS under the same conditions as the headspace extracts, vide infra) was determined on a HP5-MS fused silica capillary column. Retention indices of the other compounds are for a BP5 column and were taken from ref. [9].

based on their mass spectra (data not shown). Also, the retention index of X (*I*=1659) matched best that of **10** (*I*=1651), whereas the retention indices of **13**–**16** deviated significantly.^[9] Unfortunately, published mass spectra and retention indices for all other stereoisomers of pogostol and of globulol were not available, so these compounds were also candidate structures for X. The ¹³C NMR data for all five compounds^[16–20] and the two pogostol stereoisomers (**11** and **12**)^[21] have been reported, and therefore we strived to confirm the identities of X and **10** by obtaining ¹³C NMR data for X by CLSA-NMR (note: the originally published structure of **10**^[22] was later found to be incorrect^[21] and then corrected;^[23] in ref. [17] the wrong structure is shown for **13**). Therefore, we had to find culture conditions under which the production of X was significantly enhanced. The production of X was much higher after five weeks of incubation with feeding of mevalonolactone (5 mM) after four weeks (Figure 1B), thus suggesting that the availability of terpenoid monomers was limiting.

For further investigations on the structure of X by CLSA-NMR, a series of ¹³C-labelled isotopomers of mevalonolactone was synthesised from commercially available ¹³C-labelled ethyl acetoacetate isotopomers by a known route (Zamir and Nguyen,^[24] Scheme 3A). The route was first tested with unlabelled material, thus revealing that the reported yields were accessible. Ethyl acetoacetate (**17**) was converted into ketal **18** by reaction with neopentyl glycol and trimethylchlorosilane. Subsequent reduction with LiAlH₄ to alcohol **19** and protection of the hydroxy function gave the benzyl ether **20**, which was transformed into ketone **21** by acid deprotection. Aldol reaction with the ester enolate of ethyl acetate yielded ester **22**, which upon catalytic hydrogenation and treatment with *p*-toluenesulfonic acid provided mevalonolactone in 19% yield via six steps. This reliable protocol allowed us to convert commercially available isotopomers of ethyl acetoacetate **17a–d** into the corresponding mevalonolactones **23a–d**. For the synthesis of **23e** we used a route that we previously developed for the synthesis of deuterated isotopomers of mevalonolactone (Scheme 3B).^[25] Starting from the aldehyde **24**, reaction with [¹³C]methylmagnesium iodide yielded the alcohol **25**, which was oxidised with IBX to ketone **21e**. This was transformed into mevalonolactone **23e** (as above). Finally, [¹³C]mevalonolactone (**23f**) was synthesised by a reported procedure (Cane and Levin).^[26]

All six mevalonolactone isotopomers (**23a–f**) were fed to agar plate cultures of *Geniculosporium* sp., and the volatiles emitted by these agar plate cultures were trapped on charcoal by CLSA. The charcoal filter was extracted with CDCl₃ daily for one week. The extracts were collected in an NMR tube and subjected to ¹³C NMR analysis (¹³C NMR and DEPT spectra; results in Figure 2). Each feeding experiment resulted in the incorporation of labelling at three or six carbons of X, depending on whether a singly or doubly labelled mevalonolactone isotopomer was fed. This resulted in a set of strongly enhanced ¹³C NMR signals. These signals perfectly matched the chemical shifts of **10**, whereas the chemical shifts of its known stereoisomers revealed significant differences (Table S1). The ¹³C NMR shifts of **13** and its known stereoisomers also did not match. In



Scheme 3. Synthesis of ^{13}C -labelled isotopomers of mevalonolactone. A) Synthesis of isotopomers **23a–d** starting from ethyl acetoacetate according to Zamir and Nguyen.^[24] The yields are those obtained in the synthesis of unlabelled **23**. (For yields with labelled compounds see the Supporting Information.) B) Synthesis of **23e** by a route that was previously developed in our laboratories.^[25] Black dots indicate ^{13}C -labelled carbons.

particular, the presence of signals for olefinic carbons in the experiments with **23a** and **23c–e** clearly ruled out **13–16** and their unknown stereoisomers. Based on these data, the identity of **X** as pogostol was unequivocally established. The full biosynthetic pathway for the incorporation of label from **23** into **10** is presented in Scheme S1.

The obtained data were also used to investigate the biosynthesis of **10** (Scheme 4). The conversion of farnesyl diphosphate (FPP) into **10** proceeds most likely first through a 1,10-cyclisation to the (*E,E*)-germacradienyl cation (**26**), which might proceed via nerolidyl diphosphate (not shown), and deprotonation to germacrene A (**27**). Its reprotonation initiates a second cyclisation to cation **28**, which is trapped with water to yield **10**. Feeding of **23f** resulted in labelling of FPP at C-2, C-6 and C-10 (converted into C-5, C-1 and C-7 of **10**). A C–C single bond between C-5 and C-1 is formed by the second ring clo-

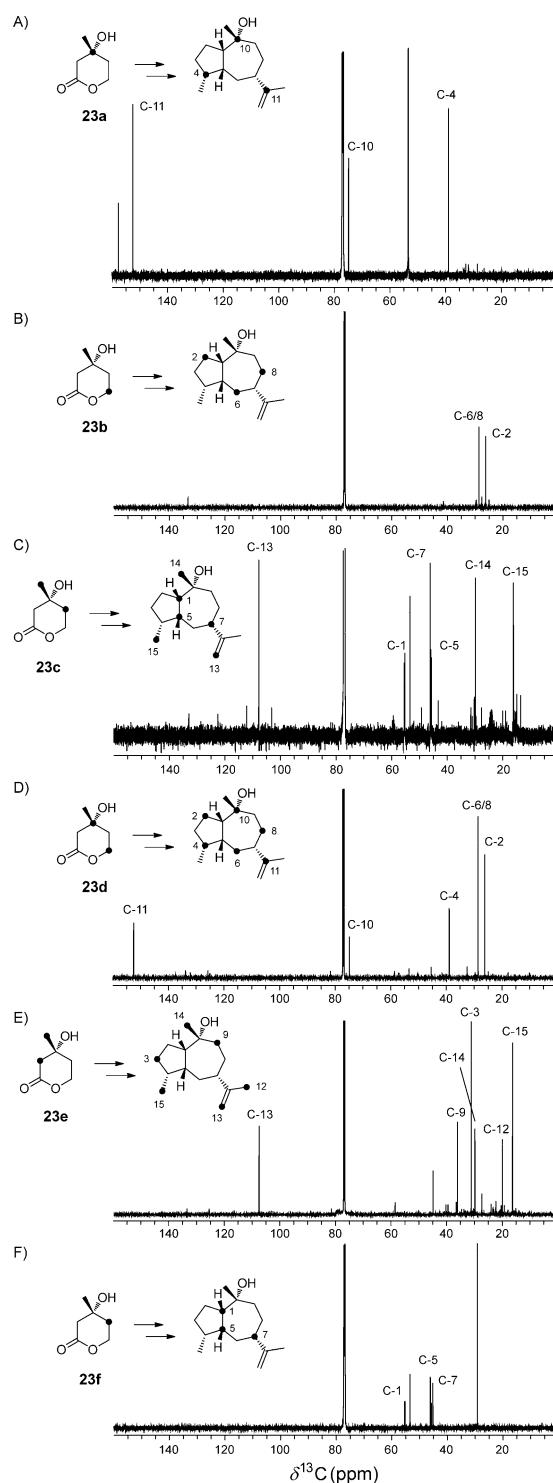
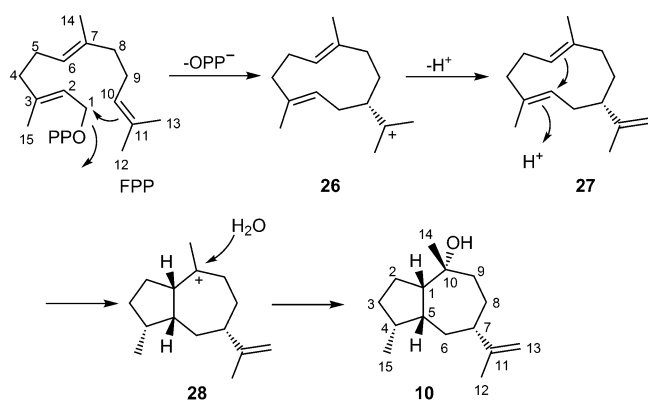


Figure 2. Results of feeding experiments with synthetic mevalonolactone isotopomers **23a–f**. The ^{13}C NMR spectra were obtained in CLSA-NMR experiments from crude extracts. Chemical shifts of ^{13}C signals, multiplicities and coupling constants for $^n\text{J}(\text{C},\text{C})$ couplings are summarised in Table S1.

nation to germacrene A (**27**). Its reprotonation initiates a second cyclisation to cation **28**, which is trapped with water to yield **10**. Feeding of **23f** resulted in labelling of FPP at C-2, C-6 and C-10 (converted into C-5, C-1 and C-7 of **10**). A C–C single bond between C-5 and C-1 is formed by the second ring clo-



Scheme 4. Biosynthesis of pogostol (**10**).

sure, thus resulting in doublets in the respective ^{13}C NMR signals (coupling constant $^1J(\text{C,C})=33.1$ Hz), thereby confirming the biosynthesis of **10** as shown in Scheme 4. Feeding experiments with **23c** and **23e** gave insights into the stereochemical course of the terpene cyclisation. The methyl group of mevalonolactone that is labelled in these two isotopomers is converted into the terminal (*Z*)-methyl group of FPP (C-13). Both feeding experiments showed that the deprotonation step of the terpene cyclisation to the neutral intermediate **27** proceeds with stereospecific deprotonation of C-13 and not C-12 of FPP, thus ending up as the olefinic C-13 of **10**. This suggests that free rotation around the C-10/C-11 single bond in cation **26** is not possible, as similarly observed in the biosynthesis of 2-methylisoborneol.^[12] A possible explanation is cation- π stabilisation^[27] of cation **26** with an adjacent aromatic amino acid residue in the active centre of the terpene cyclase, similarly to other terpene cyclisation reactions.^[28–31]

Stereochemical questions in terpene biosynthesis have frequently been solved by isotopic labelling.^[32] Other compound classes can be investigated by related methods; for example, Bode and co-workers recently presented a combined strategy of gene knockout and cultivation in D_2O to identify *D*-amino acids in nonribosomally synthesised peptides.^[33] Pogostol was first isolated from patchouli (*Pogostemon cablin*),^[34] and was recently reported in the endophytic fungus *Biscogniauxia nummularia* from the plum yew *Cephalotaxus harringtonia*, where it co-occurs with its oxidation product xylaranone (xylaranone arises by oxidation at C-3 of **10** to the corresponding ketone).^[23] Both **10** and xylaranone were shown to inhibit seed germination by *Raphanus sativus* (radish)—the particularly strong activity of xylaranone is comparable to that of glyphosate. Intrigued by this we reanalysed our *Geniculosporium* headspace extracts for the presence of oxidation products of **10**. We observed traces of candidate compounds, but the amounts were too small for detection by CLSA-NMR in the ^{13}C NMR spectra, and the mass spectra did not match database spectra in our mass spectral libraries. In an ecological context, both sesquiterpenoids **10** and xylaranone secreted by the endophytes might be directed towards the endophyte's host. In particular, endophytic fungi produce herbicidal metabolites that are assumed to play a role in maintaining a balance of an-

tagonisms between host and endophyte.^[35–37] Seed germination inhibiting metabolites such as **10** and xylaranone might also benefit the host plant by inhibiting the proliferation of other species in the area. Currently, the toxic effects of glyphosate towards humans have become a concern and have prompted discussion as to whether glyphosate should be substituted. Natural germination inhibitors such as **10** and xylaranone might be suitable alternatives and could be made available by biotechnological approaches in the near future.

Experimental Section

Culture conditions and feeding experiment: The endophytic fungus *Geniculosporium* sp. 9910, isolated from the leaves of *Cistus monspeliensis*, was cultivated for three weeks (without feeding) or four weeks (feeding experiment) on potato-carrot agar medium^[38] (20 mL) in glass petri dishes at 20 °C. For the feeding experiments, cultures were supplemented with an aqueous solution of mevalonolactone isotopomer (**23a–f**, 10 mg in sterile-filtered water (200 μL)). The resulting solution was injected with a syringe (10 μL) into the agar. The cultures were incubated at 20 °C for a further day, and collection of the volatiles was by use of a closed-loop stripping apparatus as described previously.^[39] For the feeding experiments, collection of volatiles was continued for the next seven days. The charcoal filter was extracted every 24 h with of CDCl_3 (50 μL). The extracts were combined and analysed by ^{13}C NMR and DEPT spectroscopy. Spectra were recorded on an AV II-600 spectrometer (150 MHz; Bruker) and referenced to TMS.

GC-MS analysis of headspace extracts: CLSA headspace extracts were obtained from *Geniculosporium*, with or without feeding of mevalonolactone isotopomers, and analysed by GC-MS (total ion chromatograms in Figure 1). GC-MS analyses were carried out on an HP7890A GC system (Agilent) connected to an HP5975C Mass Selective Detector equipped with a HP-5 MS fused silica capillary column (30 m \times 0.22 mm, 0.25 μm ; Agilent): inlet pressure 67 kPa, He 23.3 mL min^{-1} , injection volume 1 μL , injector 250 °C, transfer line 300 °C, electron energy 70 eV. The GC was programmed as follows: 50 °C (5 min isothermic), then increasing (5 °C min^{-1}) to 320 °C, operated in splitless mode (60 s valve time), He 1.2 mL min^{-1} .

Acknowledgements

Funding by the Deutsche Forschungsgemeinschaft with an Emmy Noether grant (DI1536/1–3) and a Heisenberg grant (DI1536/4–1) is gratefully acknowledged.

Keywords: isotopic labeling • NMR • terpenoids • trace analysis • volatiles

- [1] J. S. Dickschat, *Nat. Prod. Rep.* **2014**, *31*, 838–861.
- [2] K. Grob, *J. Chromatogr.* **1973**, *84*, 255–273.
- [3] K. Grob, F. Zürcher, *J. Chromatogr.* **1976**, *117*, 285–294.
- [4] W. Boland, P. Ney, L. Jänicke, G. Grassmann in *Analysis of Volatiles: Method, Applications* (Ed.: P. Schreiber), Walter de Gruyter, Berlin, **1984**, pp. 371–380.
- [5] S. Schulz, J. Fuhlendorff, H. Reichenbach, *Tetrahedron* **2004**, *60*, 3863–3872.
- [6] C. A. Citron, J. Gleitzmann, G. Laurenzano, R. Pukall, J. S. Dickschat, *ChemBioChem* **2012**, *13*, 202–214.

- [7] C. A. Citron, S. M. Wickel, B. Schulz, S. Draeger, J. S. Dickschat, *Eur. J. Org. Chem.* **2012**, 6636–6646.
- [8] D. Joulain, W. A. König, *The Atlas of Spectral Data of Sesquiterpene Hydrocarbons*, E. B. Verlag, Hamburg, **1998**.
- [9] R. P. Adams, *Identification of Essential Oil Components by Gas Chromatography/Mass Spectrometry*, Allured, Carol Stream, **2009**.
- [10] T. Wang, P. Rabe, C. A. Citron, J. S. Dickschat, *Beilstein J. Org. Chem.* **2013**, *9*, 2767–2777.
- [11] C. A. Citron, P. Rabe, J. S. Dickschat, *J. Nat. Prod.* **2012**, *75*, 1765–1776.
- [12] N. L. Brock, S. R. Ravella, S. Schulz, J. S. Dickschat, *Angew. Chem. Int. Ed.* **2013**, *52*, 2100–2104; *Angew. Chem.* **2013**, *125*, 2154–2158.
- [13] R. Riclea, C. A. Citron, J. Rinkel, J. S. Dickschat, *Chem. Commun.* **2014**, *50*, 4228–4230.
- [14] N. L. Brock, J. S. Dickschat, *ChemBioChem* **2013**, *14*, 1189–1193.
- [15] C. A. Citron, N. L. Brock, B. Tudzynski, J. S. Dickschat, *Chem. Commun.* **2014**, *50*, 5224–5226.
- [16] A. A. Stierle, D. B. Stierle, E. Goldstein, K. Parker, T. Bugni, C. Baarson, J. Gress, D. Blake, *J. Nat. Prod.* **2003**, *66*, 1097–1100.
- [17] M. L. Bolte, J. Bowers, W. D. Crow, D. M. Paton, A. Sakurai, N. Takahashi, M. Ujiie, S. Yoshida, *Agric. Biol. Chem.* **1984**, *48*, 373–376.
- [18] H. J. M. Gijzen, K. Kanai, G. A. Stork, J. B. P. A. Wijnberg, R. V. A. Orru, C. G. J. M. Seelen, S. M. van der Kerk, A. de Groot, *Tetrahedron* **1990**, *46*, 7237–7246.
- [19] H. J. M. Gijzen, J. B. P. A. Wijnberg, G. A. Stork, A. de Groot, M. A. de Waard, J. G. M. van Nistelrooy, *Tetrahedron* **1992**, *48*, 2465–2476.
- [20] A. San Feliciano, M. Medarde, M. Gordaliza, E. del Olmo, J. M. M. del Corral, *Phytochemistry* **1989**, *28*, 2717–2721.
- [21] K. I. Booker-Milburn, H. Jenkins, J. P. H. Charmant, P. Mohr, *Org. Lett.* **2003**, *5*, 3309–3312.
- [22] P. Weyerstahl, H. Marschall, U. Splittgerber, D. Wolf, *Flavour Fragrance J.* **2000**, *15*, 153–173.
- [23] S. Amand, A. Langenfeld, A. Blond, J. Dupont, B. Nay, S. Prado, *J. Nat. Prod.* **2012**, *75*, 798–801.
- [24] L. O. Zamir, C.-D. Nguyen, *J. Labelled Compd. Radiopharm.* **1988**, *25*, 1189–1196.
- [25] J. S. Dickschat, C. A. Citron, N. L. Brock, R. Riclea, H. Kuhz, *Eur. J. Org. Chem.* **2011**, 3339–3346.
- [26] D. E. Cane, R. H. Levin, *J. Am. Chem. Soc.* **1976**, *98*, 1183–1188.
- [27] D. A. Dougherty, *Science* **1996**, *271*, 163–168.
- [28] P. Baer, P. Rabe, K. Fischer, C. A. Citron, T. A. Klapschinski, M. Groll, J. S. Dickschat, *Angew. Chem. Int. Ed.* **2014**, *53*, 7652–7656; *Angew. Chem.* **2014**, *126*, 7783–7787.
- [29] M. J. Rynkiewicz, D. E. Cane, D. W. Christianson, *Proc. Natl. Acad. Sci. USA* **2001**, *98*, 13543–13548.
- [30] C. A. Lesburg, G. Zhai, D. E. Cane, D. W. Christianson, *Science* **1997**, *277*, 1820–1824.
- [31] J. M. Caruthers, I. Kang, M. J. Rynkiewicz, D. E. Cane, D. W. Christianson, *J. Biol. Chem.* **2000**, *275*, 25533–25539.
- [32] J. S. Dickschat, *Nat. Prod. Rep.* **2011**, *28*, 1917–1936.
- [33] C. Kegler, F. I. Nollmann, T. Ahrendt, F. Fleischhacker, E. Bode, H. B. Bode, *ChemBioChem* **2014**, *15*, 826–828.
- [34] H. Hikino, K. Ito, T. Takemoto, *Chem. Pharm. Bull.* **1968**, *16*, 1608–1610.
- [35] S. Peters, S. Draeger, H.-J. Aust, B. Schulz, *Mycologia* **1998**, *90*, 360–367.
- [36] B. Schulz, C. Boyle, S. Draeger, A.-K. Römmert, K. Krohn, *Mycol. Res.* **2002**, *106*, 996–1004.
- [37] B. Schulz, C. Boyle, *Mycol. Res.* **2005**, *109*, 661–686.
- [38] U. Höller, A. D. Wright, G. F. Matthée, G. M. König, S. Draeger, H.-J. Aust, B. Schulz, *Mycol. Res.* **2000**, *104*, 1354–1365.
- [39] J. S. Dickschat, S. C. Wenzel, H. B. Bode, R. Müller, S. Schulz, *ChemBioChem* **2004**, *5*, 778–787.

Received: June 10, 2014

Published online on September 3, 2014

CHEMBIOCHEM

Supporting Information

© Copyright Wiley-VCH Verlag GmbH & Co. KGaA, 69451 Weinheim, 2014

Pogostol Biosynthesis by the Endophytic Fungus *Geniculosporium*

Lena Barra,^[a] Barbara Schulz,^[b] and Jeroen S. Dickschat^{*[a]}

cbic_201402298_sm_miscellaneous_information.pdf

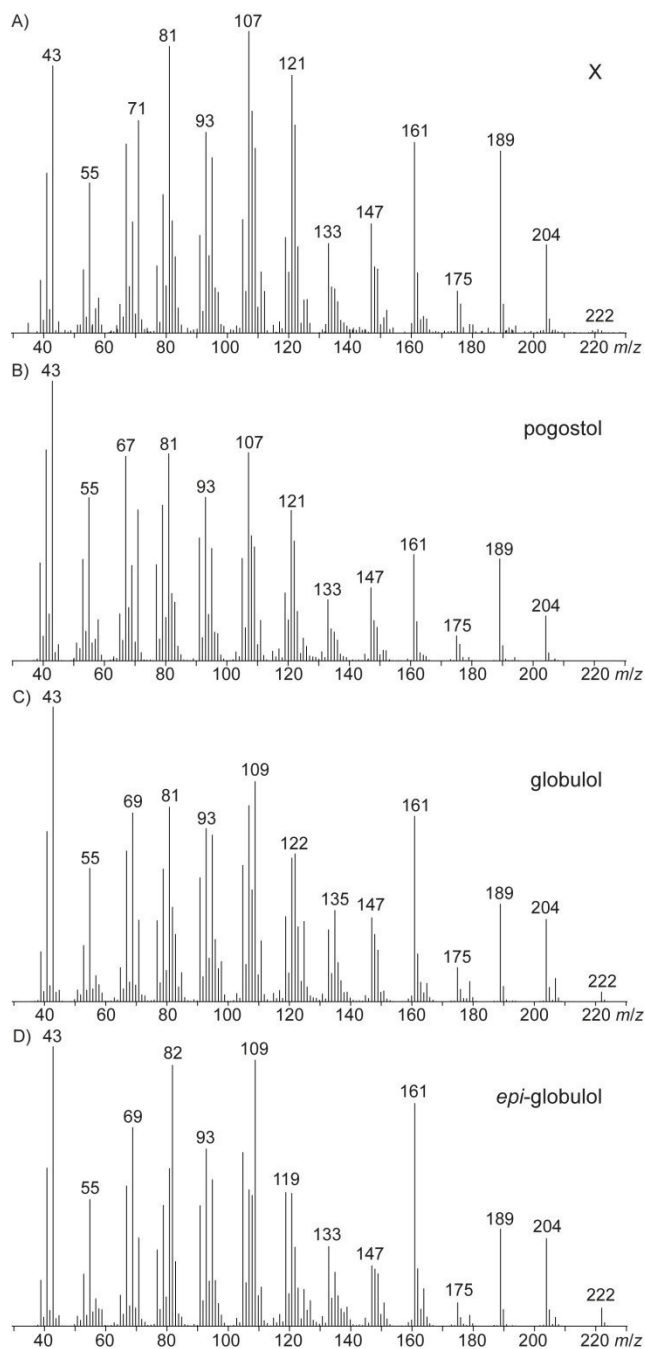


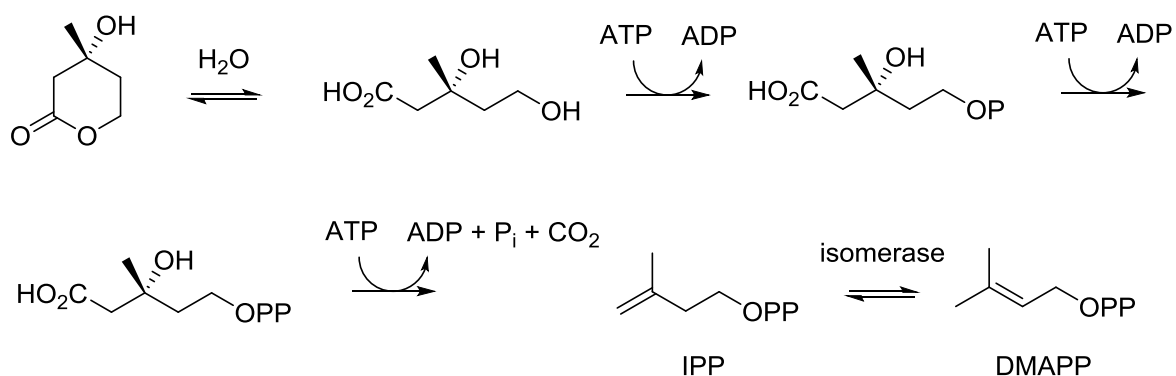
Figure 1. Mass spectra of **X**, pogostol (**10**), globulol (**13**), and *epi*-globulol (**14**).

Table 1. Results of CLSA-NMR experiments and comparison to ¹³C-NMR data of **10** and structurally related known compounds.

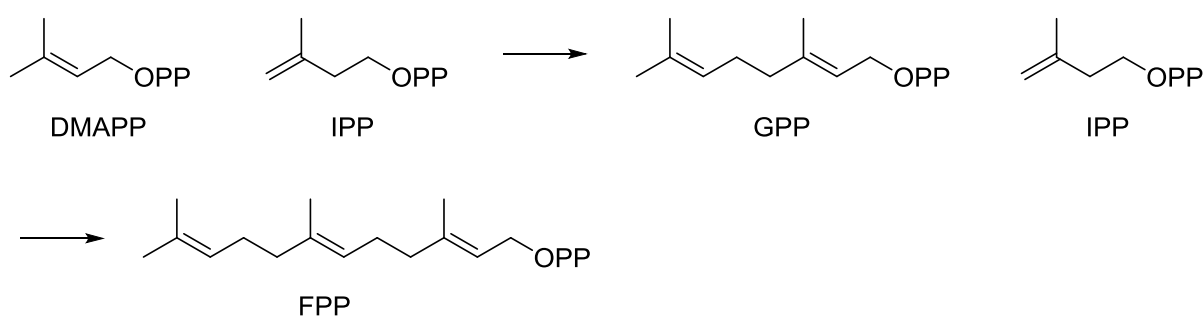
23a ^[a]	23b ^[a]	23c ^[a]	23d ^[a]	23e ^[a]	23f ^[a]	10 ^[b]	11 ^[b]	12 ^[b]	13 ^[b]	14 ^[b]	15 ^[b]	16 ^[b]
		16.2 CH ₃ , d ² J=1.7		16.2 CH ₃ , s		16.1 CH ₃ C-15	14.6 CH ₃	15.4 CH ₃	16.4 CH ₃	15.8 CH ₃	15.2 CH ₃	16.1 CH ₃ C-15
				19.9 CH ₃ , d ² J=3.1		19.9 CH ₃ C-12	20.8 CH ₃	20.5 CH ₃	16.6 CH ₃	16.6 CH ₃	15.7 CH ₃	16.3 CH ₃ C-12
	26.2 CH ₂ , s		26.2 CH ₂ , s			26.1 CH ₂ C-2	25.2 CH ₂	25.9 CH ₂	19.5 CH ₂	19.1 CH ₂	19.2 C _q	18.4 C _q C-11
	28.53 CH ₂ , s		28.52 CH ₂ , s			28.5 CH ₂ C-8	28.0 CH ₂	26.1 CH ₂	20.7 CH ₃	20.6 C _q	20.1 CH ₂	18.9 CH ₂ C-8
	28.55 CH ₂ , s		28.53 CH ₂ , s			28.5 CH ₂ C-6	30.0 CH ₃	31.1 CH ₃	20.7 CH ₃	26.6 CH ₂	23.1 CH	22.5 CH C-7
		29.8 CH ₃ , s		29.8 CH ₃ , d ² J=2.3		29.7 CH ₃ C-14	34.1 CH ₂	33.6 CH ₂	26.0 CH ₂	27.1 CH	24.4 CH ₂	25.9 CH ₂ C-3
				31.1 CH ₂ , s		31.1 CH ₂ C-3	37.8 CH ₂	33.8 CH ₂	26.7 CH	28.7 CH ₃	24.7 CH	28.7 CH ₃ C-13
				36.1 CH ₂ , d ² J=2.3		36.0 CH ₂ C-9	38.9 CH	38.3 CH	28.9 CH	28.9 CH	28.4 CH ₃	28.7 CH C-6
38.9 CH, d ³ J=3.3			38.9 CH, d ³ J=3.3			38.9 CH C-4	41.1 CH	38.8 CH	29.0 CH	31.3 CH ₃	30.3 CH ₃	29.3 CH ₂ C-9
		45.8 CH, dd ¹ J=33.3 ² J=1.5			45.8 CH, d ¹ J=33.1	45.8 CH C-5	42.8 CH ₂	43.5 CH ₂	34.9 C _q	34.6 CH ₂	30.6 CH ₂	32.1 CH ₃ C-14
		46.1 CH, d ² J=2.1			46.1 CH, s	46.1 CH C-7	50.0 CH	45.0 CH	36.8 CH ₂	35.8 CH	38.2 CH	37.9 CH ₂ C-2
		55.3 CH, d ¹ J=33.3			55.3 CH, d ¹ J=33.1	55.3 CH C-1	52.6 CH	53.5 CH	40.0 CH	37.5 CH	39.0 CH ₂	38.5 CH C-4
74.9 C _q , d ³ J=3.3			74.9 C _q , d ³ J=3.2			74.9 C _q C-10	74.1 C _q	72.7 C _q	45.2 CH ₂	42.9 CH ₂	40.5 CH	39.8 CH C-5
		107.8 CH ₂ , d ² J=2.1		107.8 CH ₂ , d ² J=3.1		107.7 CH ₂ C-13	108.3 CH ₂	108.5 CH ₂	57.1 CH	55.9 CH	53.5 CH	58.4 CH C-1
152.5 C _q , s			152.5 C _q , t ² J=1.2			152.4 C _q C-11	151.8 C _q	152.1 C _q	74.5 C _q	72.3 C _q	74.7 C _q	74.6 C _q C-10

[a] Observed ¹³C-NMR signals after feeding of mevalonolactones **23a-f**. Multiplicities (s=singlet, d=doublet, t=triplet) and coupling constants (in Hz) are for ⁿJ(C,C) couplings. Results of DEPT spectra are indicated by CH₃, CH₂, CH, and C_q. [b] Assigned ¹³C-NMR data according to references [1-6].

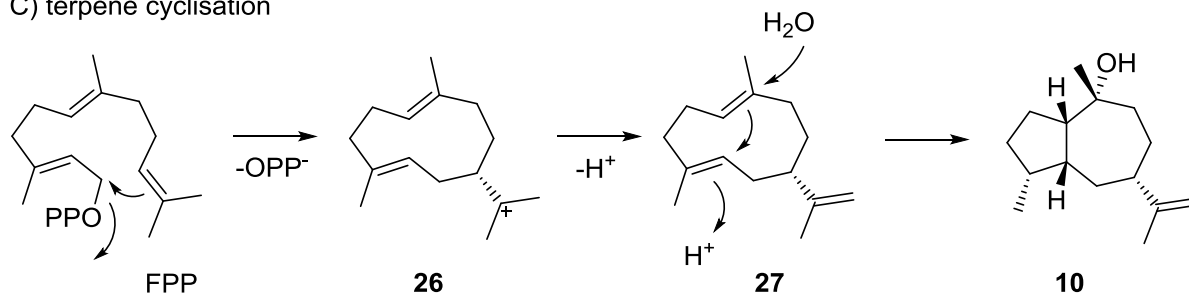
A) mevalonate pathway



B) polyisoprenoid biosynthesis



C) terpene cyclisation



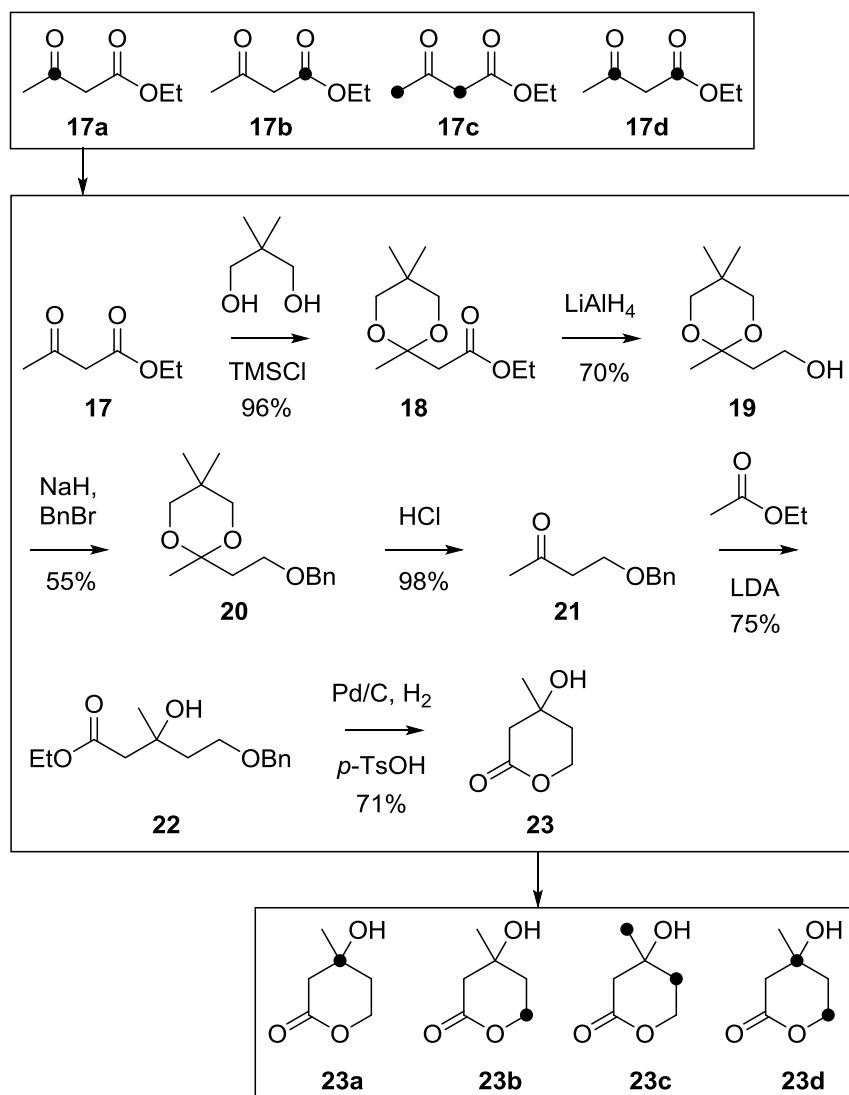
Scheme 1. Biosynthetic pathway from mevalonolactone **23** to pogostol **10**. The biosynthesis involves three stages, i. e. A) mevalonate pathway from **23** to the isoprenoid monomers isopentenyl diphosphate (IPP) and dimethylallyl diphosphate (DMAPP), B) polyisoprenoid biosynthesis via geranyl diphosphate (GPP) to farnesyl diphosphate (FPP), and C) terpene cyclisation of FPP to **10**.

Synthesis of isotopomers of mevalonolactone (23a-f)

General synthetic methods.

Chemicals were obtained from Acros Organics (Geel, Belgium) or Sigma Aldrich Chemie GmbH (Steinheim, Germany) and used without purification. All non-aqueous reactions were performed under an inert atmosphere (N_2) in flame-dried flasks. Solvents were purified by distillation and dried according to standard methods. In case of general procedures, the relative amounts of the reagents are given as equivalents (eq) with respect to their molar ratios. Relative amounts of solvents are indicated by final concentrations of the transformed starting material (set to 1.0 eq). Thin-layer chromatography was performed with 0.2 mm precoated plastic sheets Polygram® Sil G/UV254 (Machery-Nagel). Column chromatography was carried out using Merck silica gel 60 (70-200 mesh). 1H NMR and ^{13}C NMR spectra were recorded on Bruker DRX-400 (400 MHz), AV III-400 (400 MHz) or AV II-600 (600 MHz) spectrometers, and were referenced against TMS ($\delta = 0.00$ ppm) for 1H -NMR and $CDCl_3$ ($\delta = 77.01$ ppm) for ^{13}C -NMR. IR spectra were recorded with a Bruker Tensor 27 ATR (attenuated total reflectance). GC-MS analyses of synthetic compounds were carried out with a HP 6890 gas chromatograph connected to a HP 5973 inert mass detector fitted with a BPX-5 fused silica capillary column (25 m, 0.25 mm i. d., 0.25 μm film). Instrumental parameters were (1) inlet pressure, 77.1 kPa, He 23.3 mL min^{-1} , (2) injection volume, 2 μL , (3) transfer line, 300 $^{\circ}C$, and (4) electron energy 70 eV. The GC was programmed as follows: 5 min at 50 $^{\circ}C$ increasing at 10 $^{\circ}C$ min^{-1} to 320 $^{\circ}C$, and operated in split mode (20:1, 60 s valve time). The carrier gas was He at 1 mL min^{-1} . Retention indices (I) were determined from a homologous series of n-alkanes (C_8 - C_{38}).

Synthesis of mevalonolactones **23a-d**



Scheme 22. Synthesis of mevalonolactones **23a-d**. The indicated yields were obtained in a test synthesis of the unlabelled compound. For yields of labelled compounds vide infra.

The synthesis of the mevalonolactones **23a-d** was performed according to the procedure of Zamir and Nguyen (Scheme 2).^[7] Briefly, the commercially available isotopomers of ^{13}C -labelled ethyl acetoacetate (**17**) were protected with neopentyl glycol to give the ketals **18**. This was followed by a reduction with LiAlH_4 to the corresponding alcohols **19** and protection with benzyl bromide to give **20**. Subsequent removal of the ketal function yielded the ketones **21** which were used in aldol reactions with ethyl acetate to give the esters **22**. Removal of the benzyl group with Pd/C in a hydrogen atmosphere and acidic lactonization yielded the mevalonolactones **23**.

General procedure for the synthesis of isotopomers of 18. Freshly distilled TMSCl (4.4 eq) was added to a 0.5 M solution of ethyl acetoacetate (**17**, 1 eq) and neopentyl glycol (2.2 eq) in dry dichloromethane. The reaction mixture was heated to reflux overnight, followed by neutralisation with an aqueous solution of NaHCO₃ (5 wt %) and extraction with dichloromethane. The organic phase was dried with MgSO₄ and the solvent was removed under reduced pressure. The crude product was purified by flash chromatography with ethyl acetate-hexane (1:10 v/v, *R_f* = 0.2) to yield the isotopomers of **18** as colourless oils.

Ethyl [3-¹³C]-2-(2,5,5-trimethyl-1,3-dioxan-2-yl)acetate (18a). Yield: 1.61 g (7.4 mmol, 97%). GC (BPX-5): *I* = 1352. ¹H-NMR (400 MHz, CDCl₃, TMS): δ = 4.15 (q, ³*J*(H,H) = 7.1 Hz, 2H, CH₂), 3.56 (dd, ²*J*(H,H) = 11.4 Hz, ³*J*(C,H) = 3.8 Hz, 2H, 2 CH₂), 3.50 (dd, ²*J*(H,H) = 11.4 Hz, ³*J*(C,H) = 4.4 Hz, 2H, 2 CH₂), 2.78 (d, ²*J*(C,H) = 5.9 Hz, 2H, CH₂), 1.54 (d, ²*J*(C,H) = 4.8 Hz, 3H, CH₃), 1.26 (t, ³*J*(H,H) = 7.1 Hz, 3H, CH₃), 0.98 (s, 3H, CH₃), 0.94 (s, 3H, CH₃) ppm. ¹³C-NMR (100 MHz, CDCl₃): δ = 169.5 (d, ²*J*(C,C) = 0.7 Hz, C_q), 97.3 (s, ¹³C_q), 70.6 (d, ²*J*(C,C) = 1.9 Hz, 2 CH₂), 60.5 (s, CH₂), 41.6 (d, ¹*J*(C,C) = 44.3 Hz, CH₂), 29.9 (d, ³*J*(C,C) = 2.2 Hz, C_q), 22.8 (d, ¹*J*_{C,C} = 47.6 Hz, CH₃), 22.6 (s, CH₃), 22.5 (s, CH₃), 14.2 (s, CH₃) ppm. MS (EI, 70 eV): *m/z* (%) = 203 (7), 202 (46), 132 (40), 130 (100), 104 (19), 86 (43), 69 (69), 44 (100).

Ethyl [1-¹³C]-2-(2,5,5-trimethyl-1,3-dioxan-2-yl)acetate (18b). Yield: 0.98 g (4.5 mmol, 59%). GC (BPX-5): *I* = 1352. ¹H-NMR (400 MHz, CDCl₃, TMS): δ = 4.15 (dq, ³*J*(H,H) = 7.2 Hz, ³*J*(C,H) = 3.2 Hz, 2H, CH₂), 3.56 (d, ²*J*(H,H) = 11.5 Hz, 2H, 2 CH₂), 3.50 (d, ²*J*(H,H) = 11.5 Hz, 2H, 2 CH₂), 2.78 (d, ²*J*(C,H) = 6.9 Hz, 2H, CH₂), 1.54 (s, 3H, CH₃), 1.26 (t, ³*J*(H,H) = 7.1 Hz, 3H, CH₃), 0.97 (s, 3H, CH₃), 0.94 (s, 3H, CH₃) ppm. ¹³C-NMR (100 MHz, CDCl₃): δ = 169.7 (s, ¹³C_q), 97.5 (s, C_q), 70.8 (s, 2 CH₂), 60.7 (d, ²*J*(C,C) = 2.5 Hz, CH₂), 41.7 (d, ¹*J*(C,C) = 58.8 Hz, CH₂), 30.0 (s, C_q), 22.8 (s, CH₃), 22.6 (s, CH₃), 22.5 (s, CH₃), 14.2 (d, ³*J*(C,C) = 2.0 Hz, CH₃) ppm. MS (EI, 70 eV): *m/z* (%) = 203 (4), 202 (40), 132 (36), 129 (94), 117 (22), 104 (17), 86 (39), 69 (61), 43 (100).

[2-¹³C]Ethyl 2-(2,5,5-[2-¹³C]trimethyl-1,3-dioxan-2-yl)acetate (18c). Yield: 1.62 g (7.4 mmol, 98%). GC (BPX-5): *I* = 1350. ¹H-NMR (400 MHz, CDCl₃, TMS): δ = 4.16 (q, ³*J*(H,H) = 7.1 Hz, 2H, CH₂), 3.57 (d, ²*J*(H,H) = 11.4 Hz, 2H, 2 CH₂), 3.51 (d, ²*J*(H,H) = 11.4 Hz, 2H, 2 CH₂), 2.79 (dd, ¹*J*(C,H) = 130.1 Hz, ³*J*(C,H) = 3.2 Hz, 2H,

CH₂), 1.55 (dd, $^1J(\text{C,H}) = 127.4$ Hz, $^3J(\text{C,H}) = 3.0$ Hz, 3H, CH₃), 1.27 (t, $^3J(\text{H,H}) = 7.1$ Hz, 3H, CH₃), 0.99 (s, 3H, CH₃), 0.95 (s, 3H, CH₃) ppm. ¹³C-NMR (100 MHz, CDCl₃): $\delta = 169.5$ (d, $^1J(\text{C,C}) = 58.9$ Hz, C_q), 97.3 (dd, $^1J(\text{C,C}) = 44.2$ Hz, $^1J(\text{C,C}) = 47.3$ Hz, C_q), 70.6 (dd, $^3J(\text{C,C}) = 1.7$ Hz, $^3J(\text{C,C}) = 1.7$ Hz, 2 CH₂), 60.5 (s, CH₂), 41.6 (d, $^2J(\text{C,C}) = 4.0$ Hz, ¹³CH₂), 29.9 (s, C_q), 22.8 (d, $^2J(\text{C,C}) = 4.0$ Hz, ¹³CH₃), 22.6 (s, CH₃), 22.5 (s, CH₃), 14.2 (s, CH₃) ppm. MS (EI, 70 eV): m/z (%) = 202 (30), 133 (29), 130 (100), 116 (18), 105 (14), 87 (37), 69 (57), 56 (34), 44 (99), 43 (25), 41 (42).

[1-¹³C]Ethyl [2-¹³C]-2-(2,5,5-trimethyl-1,3-dioxan-2-yl)acetate (18d). Yield: 1.44 g (6.6 mmol, 87%). GC (BPX-5): $t = 1353$. ¹H-NMR (400 MHz, CDCl₃, TMS): $\delta = 4.15$ (dq, $^3J(\text{H,H}) = 7.2$ Hz, $^3J(\text{C,H}) = 3.2$ Hz, 2H, CH₂), 3.56 (dd, $^2J(\text{H,H}) = 11.4$ Hz, $^3J(\text{C,H}) = 3.8$ Hz, 2H, 2 CH₂), 3.50 (dd, $^2J(\text{H,H}) = 11.4$ Hz, $^3J(\text{C,H}) = 3.8$ Hz, 2H, 2 CH₂), 2.78 (dd, $^2J(\text{C,H}) = 6.3$ Hz, $^2J(\text{C,H}) = 6.3$ Hz, 2H, CH₂), 1.54 (d, $^2J(\text{C,H}) = 4.8$ Hz, 3H, CH₃), 1.26 (t, $^3J(\text{H,H}) = 7.2$ Hz, 3H, CH₃), 0.98 (s, 3H, CH₃), 0.94 (s, 3H, CH₃) ppm. ¹³C-NMR (100 MHz, CDCl₃): $\delta = 169.5$ (d, $^2J(\text{C,C}) = 0.7$ Hz, ¹³C_q), 97.3 (d, $^2J(\text{C,C}) = 0.7$ Hz, ¹³C_q), 70.6 (d, $^2J(\text{C,C}) = 2.0$ Hz, 2 CH₂), 60.5 (d, $^2J(\text{C,C}) = 2.4$ Hz, CH₂), 41.6 (dd, $^1J(\text{C,C}) = 59.0$ Hz, $^1J(\text{C,C}) = 44.3$ Hz, CH₂), 29.9 (d, $^3J(\text{C,C}) = 2.5$ Hz, C_q), 22.8 (d, $^1J(\text{C,C}) = 47.6$ Hz, CH₃), 22.6 (s, CH₃), 22.5 (s, CH₃), 14.2 (d, $^3J(\text{C,C}) = 2.1$ Hz, CH₃) ppm. MS (EI, 70 eV): m/z (%) = 203 (67), 133 (64), 130 (100), 117 (42), 105 (31), 87 (63), 69 (78), 56 (62), 44 (91).

General procedure for the synthesis of isotopomers of 20. A 1.5 M solution of the respective isotopomer of **18** (1 eq) in dry THF at 0 °C was added to a 1.5 M suspension of LiAlH₄ (1 eq) in dry THF. The mixture was stirred at room temperature for 2 h and then quenched by the addition of water under stirring until a white suspension was formed. The mixture was filtered and the obtained filtrate was dried over MgSO₄. The solvent was removed under reduced pressure and the residue was purified by flash chromatography with ethyl acetate-hexane (1:2 v/v, $R_f = 0.2$). The resulting alcohol **19** was used immediately in the next step. The alcohol (1 eq) was added dropwise at 0 °C to a 0.5 M suspension of NaH (1.1 eq) in dry DMF. After stirring for 15 min benzyl bromide (1 eq) was added dropwise. The reaction mixture was stirred at room temperature overnight, quenched by the addition of water, and extracted with dichloromethane. The combined organic layers were washed with water, dried over MgSO₄ and the solvent was removed under reduced pressure. The

residue was purified by flash chromatography with ethyl acetate-hexane (1:10 v/v, R_f = 0.3) to yield the isotopomers of **20** as colourless oils.

[2-¹³C]-2-(2-(Benzyloxy)ethyl)-2,5,5-trimethyl-1,3-dioxane (20a). Yield: 1.41 g (5.3 mmol, 72%). GC (BPX-5): I = 1880. ¹H-NMR (400 MHz, C₆D₆, TMS): δ = 7.36-7.05 (m, 5H, 5 CH), 4.36 (s, 2H, CH₂), 3.74 (dt, ³ J (H,H) = 7.2 Hz, ³ J (C,H) = 2.8 Hz, 2H, CH₂), 3.33 (dd, ² J (H,H) = 11.3 Hz, ³ J (C,H) = 3.1 Hz, 2H, 2 CH₂), 3.26 (dd, ² J (H,H) = 11.3 Hz, ³ J (C,H) = 4.8 Hz, 2H, 2 CH₂), 2.26 (dt, ³ J (H,H) = 7.3 Hz, ² J (C,H) = 5.1 Hz, 2H, CH₂), 1.36 (d, ² J (C,H) = 4.5 Hz, 3H, CH₃), 0.83 (s, 3H, CH₃), 0.62 (s, 3H, CH₃) ppm. ¹³C-NMR (100 MHz, C₆D₆): δ = 139.5 (s, C_q), 128.5 (s, 2 CH), 127.7 (s, 2 CH), 127.5 (s, CH), 98.3 (s, ¹³C_q), 73.1 (s, CH₂), 70.3 (d, ² J (C,C) = 2.0 Hz, 2 CH₂), 66.6 (s, CH₂), 38.6 (d, ¹ J (C,C) = 46.5 Hz, CH₂), 29.8 (d, ³ J (C,C) = 2.5 Hz, C_q), 22.8 (s, CH₃), 22.4 (s, CH₃), 21.1 (d, ¹ J (C,C) = 46.2 Hz, CH₃) ppm. MS (EI, 70 eV): m/z (%) = 250 (20), 178 (2), 161 (6), 130 (70), 107 (26), 91 (100), 69 (43), 56 (32), 44 (64).

[4-¹³C]-2-(2-(Benzyloxy)ethyl)-2,5,5-trimethyl-1,3-dioxane (20b). Yield: 0.38 g (1.6 mmol, 35%). GC (BPX-5): I = 1879. ¹H-NMR (400 MHz, CDCl₃, TMS): δ = 7.37-7.23 (m, 5H, 5 CH), 4.50 (d, ³ J (C,H) = 3.9 Hz, 2H, CH₂), 3.64 (dt, ¹ J (C,H) = 141.9 Hz, ³ J (H,H) = 7.3 Hz, 2H, CH₂), 3.53 (d, ² J (H,H) = 11.4 Hz, 2H, 2 CH₂), 3.45 (d, ² J (H,H) = 11.4 Hz, 2H, 2 CH₂), 2.10 (dt, ³ J (H,H) = 7.4 Hz, ² J (C,H) = 5.7 Hz, 2H, CH₂), 1.40 (s, 3H, CH₃), 0.97 (s, 3H, CH₃), 0.91 (s, 3H, CH₃) ppm. ¹³C-NMR (100 MHz, CDCl₃): δ = 138.5 (d, ³ J (C,C) = 2.9 Hz, C_q), 128.3 (s, 2 CH), 127.7 (s, 2 CH), 127.5 (s, CH), 98.1 (s, C_q), 73.1 (d, ² J (C,C) = 1.4 Hz, CH₂), 70.3 (s, 2 CH₂), 66.2 (s, ¹³CH₂), 37.9 (d, ¹ J (C,C) = 39.3 Hz, CH₂), 29.9 (s, C_q), 22.7 (s, CH₃), 22.6 (s, CH₃), 21.4 (s, CH₃) ppm. MS (EI, 70 eV): m/z (%) = 250 (18), 159 (5), 129 (74), 107 (21), 91 (100), 69 (40), 56 (17), 43 (61).

2-(2-(Benzyloxy)-[1-¹³C]ethyl)-2,5,5-[2-¹³C]trimethyl-1,3-dioxane (20c). Yield: 0.91 g (3.4 mmol, 53%). GC (BPX-5): I = 1884. ¹H-NMR (400 MHz, CDCl₃, TMS): δ = 7.37-7.23 (m, 5H, 5 CH), 4.51 (s, 2H, CH₂), 3.64 (dt, ² J (C,H) = 2.9 Hz, ³ J (H,H) = 7.3 Hz, 2H, 2 CH₂), 3.53 (d, ² J (H,H) = 11.3 Hz, 2H, 2 CH₂), 3.45 (d, ² J (H,H) = 11.3 Hz, 2H, CH₂), 2.10 (ddt, ¹ J (C,H) = 126.9 Hz, ³ J (H,H) = 7.4 Hz, ³ J (C,H) = 3.0 Hz, 2H, CH₂), 1.40 (dd, ¹ J (C,H) = 126.6 Hz, ³ J (C,H) = 3.0 Hz, 3H, CH₃), 0.97 (s, 3H, CH₃), 0.91 (s, 3H, CH₃) ppm. ¹³C-NMR (100 MHz, CDCl₃): δ = 138.5 (s, C_q), 128.3 (s, 2 CH), 127.7 (s, 2 CH), 127.5 (s, CH), 98.1 (dd, ¹ J (C,C) = 46.3 Hz, ¹ J (C,C) = 46.3 Hz, C_q), 73.1 (d, ³ J (C,C) = 3.7 Hz, CH₂), 70.3 (dd, ³ J (C,C) = 1.7 Hz, ³ J (C,C) = 1.7 Hz, 2

CH₂), 66.2 (dd, $^1J(\text{C,C}) = 39.3$ Hz, $^3J(\text{C,C}) = 0.9$ Hz, CH₂), 37.3 (d, $^2J(\text{C,C}) = 3.7$ Hz, $^{13}\text{CH}_2$), 29.9 (s, C_q), 22.7 (s, CH₃), 22.6 (s, CH₃), 21.3 (d, $^2J(\text{C,C}) = 3.7$ Hz, $^{13}\text{CH}_3$). MS (EI, 70 eV): m/z (%) = 250 (45), 179 (5), 160 (16), 130 (95), 107 (48), 91 (100), 69 (71), 56 (32), 44 (85).

[2- ^{13}C]-2-([2- ^{13}C]-2-(Benzyloxy)ethyl)-2,5,5-trimethyl-1,3-dioxane (20d). Yield: 0.71 g (2.7 mmol, 40%). GC (BPX-5): $t = 1884$. $^1\text{H-NMR}$ (400 MHz, d₆-DMSO, TMS): $\delta = 7.39$ -7.23 (m, 5H, 5 CH), 4.44 (d, $^3J(\text{C,H}) = 3.9$ Hz, 2H, CH₂), 3.54 (ddt, $^1J(\text{C,H}) = 141.5$ Hz, $^3J(\text{H,H}) = 7.3$ Hz, $^3J(\text{C,H}) = 2.4$ Hz, 2H, CH₂), 3.47 (dd, $^2J(\text{H,H}) = 11.3$ Hz, $^3J(\text{C,H}) = 2.9$ Hz, 2H, 2 CH₂), 3.38 (dd, $^2J(\text{H,H}) = 11.3$ Hz, $^3J(\text{C,H}) = 5.0$ Hz, 2H, 2 CH₂), 1.96 (m, 2H, CH₂), 1.32 (d, $^2J(\text{C,H}) = 4.5$ Hz, 3H, CH₃), 0.91 (s, 3H, CH₃), 0.82 (s, 3H, CH₃) ppm. $^{13}\text{C-NMR}$ (100 MHz, d₆-DMSO): $\delta = 138.6$ (d, $^3J(\text{C,C}) = 3.0$ Hz, C_q), 128.2 (s, 2 CH), 127.4 (s, 2 CH), 127.3 (s, CH), 97.5 (s, $^{13}\text{C}_q$), 71.9 (d, $^2J(\text{C,C}) = 1.1$ Hz, CH₂), 69.2 (d, $^2J(\text{C,C}) = 1.9$ Hz, 2 CH₂), 65.5 (s, $^{13}\text{CH}_2$), 37.3 (dd, $^1J(\text{C,C}) = 46.0$ Hz, $^1J(\text{C,C}) = 39.2$ Hz, CH₂), 29.5 (d, $^3J(\text{C,C}) = 2.4$ Hz, C_q), 22.4 (s, CH₃), 22.0 (s, CH₃), 21.0 (d, $^1J(\text{C,C}) = 46.3$ Hz, CH₃) ppm. MS (EI, 70 eV): m/z (%) = 251 (23), 143 (24), 130 (100), 107 (49), 91 (84), 79 (59), 69 (57), 57 (50), 44 (79).

General procedure for the synthesis of isotopomers of 21. A 1 M solution of HCl in water (0.5 mL/mmol) was added to a 0.2 M solution of the respective isotopomer of **20** (1 eq) in MeOH. The reaction mixture was stirred at room temperature for 15 min and then neutralized with an aqueous solution of NaHCO₃ (5 wt%). The aqueous layer was extracted three times with Et₂O and the combined extracts were dried over MgSO₄. The solvent was removed under reduced pressure and the residue purified by flash chromatography with ethyl acetate-hexane (1:5 v/v, $R_f = 0.2$) to yield the isotopomers of **21** as colourless oils.

[2- ^{13}C]-4-(Benzyloxy)butan-2-one (21a). Yield: 0.84 g (4.7 mmol, 89%). GC (BPX-5): $t = 1462$. $^1\text{H-NMR}$ (400 MHz, CDCl₃, TMS): $\delta = 7.38$ -7.24 (m, 5H, 5 CH), 4.51 (s, 2H, CH₂), 3.74 (dt, $^3J(\text{H,H}) = 6.3$ Hz, $^3J(\text{C,H}) = 4.4$ Hz, 2H, CH₂), 2.71 (dt, $^2J(\text{C,H}) = 5.8$ Hz, $^3J(\text{H,H}) = 6.1$ Hz, 2H, CH₂), 2.18 (d, $^2J(\text{C,H}) = 5.9$ Hz, 3H, CH₃) ppm. $^{13}\text{C-NMR}$ (100 MHz, CDCl₃): $\delta = 207.1$ (s, $^{13}\text{C}_q$), 138.1 (s, C_q), 128.4 (s, 2 CH), 127.7 (s, 2 CH), 127.6 (s, CH), 73.2 (s, CH₂), 65.2 (d, $^2J(\text{C,C}) = 1.6$ Hz, CH₂), 43.7 (d, $^1J(\text{C,C}) = 40.0$ Hz, CH₂), 30.4 (d, $^1J(\text{C,C}) = 40.9$ Hz, CH₃) ppm. MS (EI, 70 eV): m/z (%) = 179 (1), 120 (24), 107 (63), 91 (100), 79 (30), 65 (31), 44 (76).

[4-¹³C]-4-(Benzyloxy)butan-2-one (21b). Yield: 0.28 g (1.5 mmol, 98%). GC (BPX-5): *I* = 1461. ¹H-NMR (400 MHz, CDCl₃, TMS): δ = 7.38-7.24 (m, 5H, 5 CH), 4.51 (d, ³*J*(C,H) = 4.3 Hz, 2H, CH₂), 3.74 (dt, ¹*J*(C,H) = 144.5 Hz, ³*J*(H,H) = 6.3 Hz, 2H, CH₂), 2.72 (dt, ²*J*(C,H) = 4.9 Hz, ³*J*(H,H) = 6.3 Hz, 2H, CH₂), 2.18 (s, 3H, CH₃) ppm. ¹³C-NMR (100 MHz, CDCl₃): δ = 207.1 (d, ²*J*(C,C) = 1.7 Hz, C_q), 138.0 (d, ³*J*(C,C) = 2.9 Hz, C_q), 128.4 (s, 2 CH), 127.7 (s, 2 CH), 127.6 (s, CH), 73.2 (d, ²*J*(C,C) = 1.3 Hz, CH₂), 65.2 (s, ¹³CH₂), 43.7 (d, ¹*J*(C,C) = 39.8 Hz, CH₂), 30.4 (s, CH₃) ppm. MS (EI, 70 eV): *m/z* (%) = 121 (13), 120 (13), 107 (59), 91 (100), 79 (27), 65 (27), 43 (67).

[1,3-¹³C₂]-4-(Benzyloxy)butan-2-one (21c). Yield: 0.61 g (3.4 mmol, 99%). GC (BPX-5): *I* = 1468. ¹H-NMR (400 MHz, CDCl₃, TMS): δ = 7.38-7.24 (m, 5H, 5 CH), 4.51 (s, 2H, CH₂), 3.74 (dt, ³*J*(H,H) = 6.3 Hz, ²*J*(C,H) = 2.8 Hz, 2H, CH₂), 2.72 (dt, ¹*J*(C,H) = 126.0 Hz, ³*J*(H,H) = 6.2 Hz, 2H, CH₂), 2.18 (dd, ¹*J*(C,H) = 127.3 Hz, ³*J*(C,H) = 1.5 Hz, 3H, CH₃) ppm. ¹³C-NMR (100 MHz, CDCl₃): δ = 138.1 (s, C_q), 128.4 (s, 2 CH), 127.7 (s, 2 CH), 127.6 (s, CH), 73.2 (d, ³*J*(C,C) = 3.9 Hz, CH₂), 65.2 (d, ¹*J*(C,C) = 39.9 Hz, CH₂), 43.7 (d, ²*J*(C,C) = 13.9 Hz, ¹³CH₂), 30.4 (d, ²*J*(C,C) = 13.9 Hz, ¹³CH₃) ppm. MS (EI, 70 eV): *m/z* (%) = 121 (26), 120 (27), 107 (83), 92 (30), 91 (100), 79 (50), 65 (50), 58 (27), 44 (88).

[2,4-¹³C₂]-4-(Benzyloxy)butan-2-one (21d). Yield: 0.39 g (2.2 mmol, 81%). GC (BPX-5): *I* = 1459. ¹H-NMR (400 MHz, CDCl₃, TMS): δ = 7.38-7.25 (m, 5H, 5 CH), 4.51 (d, ³*J*(C,H) = 4.3 Hz, 2H, CH₂), 3.74 (ddt, ¹*J*(C,H) = 143.0 Hz, ³*J*(H,H) = 6.3 Hz, ³*J*(C,H) = 4.4 Hz, 2H, CH₂), 2.72 (m, 2H, CH₂), 2.18 (d, ²*J*(C,H) = 5.9 Hz, 3H, CH₃) ppm. ¹³C-NMR (100 MHz, CDCl₃): δ = 207.1 (d, ²*J*(C,C) = 1.7 Hz, ¹³C_q), 138.1 (d, ³*J*(C,C) = 2.9 Hz, C_q), 128.4 (s, 2 CH), 127.7 (s, 2 CH), 127.6 (s, CH), 73.2 (d, ²*J*(C,C) = 1.6 Hz, CH₂), 65.2 (d, ²*J*(C,C) = 1.7 Hz, ¹³CH₂), 43.7 (dd, ¹*J*(C,C) = 40.0 Hz, ¹*J*(C,C) = 40.0 Hz, CH₂), 30.4 (d, ¹*J*(C,C) = 40.7 Hz, CH₃) ppm. MS (EI, 70 eV): *m/z* (%) = 121 (15), 120 (15), 107 (66), 91 (100), 79 (31), 74 (21), 65 (35), 59 (15), 51 (16), 44 (87).

General procedure for the preparation of the isotopomers of 22. A 1.6 M solution of n-butyllithium (2.1 eq) in hexane was added at 0 °C to a 0.2 M solution of diisopropylamine (2.1 eq) in dry THF. The mixture was stirred for 1 h and then cooled to -78°C. A solution of ethyl acetate (2.1 eq, 0.4 M) in dry THF was added dropwise and the reaction was stirred for 30 min. Subsequently, a solution of the respective

isotopomer of **21** (1 eq, 0.3 M) in dry THF was added dropwise. The reaction mixture was stirred for 45 min, quenched by the addition of water and allowed to warm to room temperature. The mixture was extracted with ethyl acetate and the combined extracts were dried over MgSO₄. The solvent was removed under reduced pressure and the residue was purified by flash chromatography with ethyl acetate-hexane (1:5 v/v, *R_f* = 0.2) to yield the isotopomers of **22** as colourless oils.

Ethyl [3-¹³C]-5-(benzyloxy)-3-hydroxy-3-methylpentanoate (22a). Yield: 0.98 g (3.7 mmol, 79%). GC (BPX-5): *I* = 1918. ¹H-NMR (400 MHz, CDCl₃, TMS): δ = 7.38-7.26 (m, 5H, 5 CH), 4.50 (s, 2H, CH₂), 4.14 (dq, ³*J*(H,H) = 7.1 Hz, ¹*J*(H,H) = 10.8 Hz, 1H, CH₂), 4.13 (dq, ³*J*(H,H) = 7.1 Hz, ¹*J*(H,H) = 10.8 Hz, 1H, CH₂), 3.95 (d, ²*J*(C,H) = 2.8 Hz, 1H, OH), 3.69 (m, 2H, CH₂), 2.58 (dd, ²*J*(H,H) = 15.3 Hz, ²*J*(C,H) = 4.9 Hz, 1H, CH₂), 2.49 (dd, ²*J*(H,H) = 15.3 Hz, ²*J*(C,H) = 4.4 Hz, 1H, CH₂), 1.91 (m, 2H, CH₂), 1.28 (d, ²*J*(C,H) = 4.2 Hz, 3H, CH₃), 1.25 (dd, ³*J*(H,H) = 7.2 Hz, ³*J*(H,H) = 7.2 Hz, 3H, CH₃) ppm. ¹³C-NMR (100 MHz, CDCl₃): δ = 172.4 (d, ²*J*(C,C) = 1.1 Hz, C_q), 138.0 (s, C_q), 128.4 (s, 2 CH), 127.7 (s, CH), 127.6 (s, 2 CH), 73.3 (s, CH₂), 70.8 (s, ¹³C_q), 66.9 (d, ²*J*(C,C) = 1.1 Hz, CH₂), 60.5 (s, CH₂), 45.5 (d, ¹*J*(C,C) = 37.3 Hz, CH₂), 40.3 (d, ¹*J*(C,C) = 38.8 Hz, CH₂), 27.1 (d, ¹*J*(C,C) = 40.2 Hz, CH₃), 14.1 (s, CH₃) ppm. MS (EI, 70 eV): *m/z* (%) = 180 (2), 161 (27), 143 (18), 131 (11), 107 (9), 91 (100), 65 (16), 44 (25).

Ethyl [5-¹³C]-5-(benzyloxy)-3-hydroxy-3-methylpentanoate (22b). Yield: 0.08 g (0.4 mmol, 71%). GC (BPX-5): *I* = 1917. ¹H-NMR (400 MHz, CDCl₃, TMS): δ = 7.39-7.26 (m, 5H, 5 CH), 4.50 (d, ³*J*(C,H) = 4.0 Hz, 2H, CH₂), 4.14 (dq, ³*J*(H,H) = 7.1 Hz, ²*J*(H,H) = 10.8 Hz, 1H, CH₂), 4.13 (dq, ³*J*(H,H) = 7.1 Hz, ²*J*(H,H) = 10.8 Hz, 1H, CH₂), 3.97 (s, 1H, OH), 3.68 (dt, ¹*J*(C,H) = 141.2 Hz, ³*J*(H,H) = 6.1 Hz, 2H, CH₂), 2.58 (d, ²*J*(H,H) = 15.3 Hz, 1H, CH₂), 2.50 (d, ²*J*(H,H) = 15.3 Hz, 1H, CH₂), 1.91 (m, 2H, CH₂), 1.21 (s, 3H, CH₃), 1.18 (dd, ³*J*(H,H) = 7.1 Hz, ³*J*(H,H) = 7.1 Hz, 3H, CH₃) ppm. ¹³C-NMR (100 MHz, CDCl₃): δ = 172.4 (s, C_q), 138.0 (d, ³*J*(C,C) = 2.8 Hz, C_q), 128.4 (s, 2 CH), 127.7 (s, CH), 127.6 (s, 2 CH), 73.2 (d, ²*J*(C,C) = 1.3 Hz, CH₂), 70.7 (d, ²*J*(C,C) = 1.3 Hz, C_q), 66.9 (s, ¹³CH₂), 60.5 (s, CH₂), 45.5 (d, ³*J*(C,C) = 2.1 Hz, CH₂), 40.3 (d, ¹*J*(C,C) = 38.8 Hz, CH₂), 27.1 (d, ³*J*(C,C) = 2.2 Hz, CH₃), 14.1 (s, CH₃) ppm. MS (EI, 70 eV): *m/z* (%) = 180 (2), 161 (28), 143 (17), 131 (9), 112 (9), 91 (100), 65 (13), 43 (21).

Ethyl [4-¹³C₂]-5-(benzyloxy)-3-hydroxy-3-[¹³C]methylpentanoate (22c). Yield: 0.74 g (2.8 mmol, 82%). GC (BPX-5): *I* = 1919. ¹H-NMR (400 MHz, CDCl₃, TMS): δ = 7.38-7.26 (m, 5H, 5 CH), 4.50 (s, 2H, CH₂), 4.14 (dq, ²*J*(H,H) = 10.8 Hz, ³*J*(H,H) = 7.1 Hz, 1H, CH₂), 4.13 (dq, ²*J*(H,H) = 10.8 Hz, ³*J*(H,H) = 7.1 Hz, 1H, CH₂), 3.95 (t, ³*J*(C,H) = 3.1 Hz, ³*J*(C,H) = 3.1 Hz, 1H, OH), 3.68 (dt, ³*J*(C,H) = 6.2 Hz, ²*J*(C,H) = 2.9 Hz, 2H, CH₂), 2.58 (ddd, ²*J*(H,H) = 15.3 Hz, ³*J*(C,H) = 3.2 Hz, ³*J*(C,H) = 3.2 Hz, 1H, CH₂), 2.50 (ddd, ²*J*(H,H) = 15.3 Hz, ³*J*(C,H) = 3.0 Hz, ³*J*(C,H) = 3.0 Hz, 1H, CH₂), 1.91 (m, ¹*J*(C,H) = 125.8 Hz, 2H, CH₂), 1.29 (dd, ¹*J*(C,H) = 126.2 Hz, ³*J*(C,H) = 3.7 Hz, 3H, CH₃), 1.25 (dd, ³*J*(H,H) = 7.2 Hz, ³*J*(H,H) = 7.2 Hz, 3H, CH₃) ppm. ¹³C-NMR (100 MHz, CDCl₃): δ = 172.4 (dd, ³*J*(C,C) = 2.1 Hz, ³*J*(C,C) = 2.1 Hz, C_q), 138.0 (s, C_q), 128.4 (s, 2 CH), 127.7 (s, CH), 127.6 (s, 2 CH), 73.3 (d, ³*J*(C,C) = 3.6 Hz, CH₂), 70.8 (dd, ¹*J*(C,C) = 40 Hz, ¹*J*(C,C) = 38 Hz, C_q), 67.0 (dd, ¹*J*(C,C) = 39.4 Hz, ³*J*(C,C) = 1.7 Hz, CH₂), 60.5 (s, CH₂), 45.6 (dd, ²*J*(C,C) = 1.7 Hz, ²*J*(C,C) = 1.7 Hz, CH₂), 40.4 (d, ²*J*(C,C) = 1.4 Hz, ¹³CH₂), 27.2 (d, ²*J*(C,C) = 1.5 Hz, ¹³CH₃), 14.2 (s, CH₃) ppm. MS (EI, 70 eV): *m/z* (%) = 181 (2), 162 (28), 144 (18), 132 (11), 113 (9), 91 (100), 65 (16), 44 (26).

Ethyl [3,5-¹³C₂]-5-(benzyloxy)-3-hydroxy-3-methylpentanoate (22d). Yield: 0.42 g (1.6 mmol, 72%). GC (BPX-5): *I* = 1912. ¹H-NMR (400 MHz, CDCl₃, TMS): δ = 7.36-7.25 (m, 5H, 5 CH), 4.50 (d, ³*J*(C,H) = 4.0 Hz, 2H, CH₂), 4.14 (dq, ²*J*(H,H) = 10.8 Hz, ³*J*(H,H) = 7.2 Hz, 1H, CH₂), 4.13 (dq, ²*J*(H,H) = 10.8 Hz, ³*J*(H,H) = 7.2 Hz, 1H, CH₂), 3.95 (s, 1H, OH), 3.69 (dm, ¹*J*(C,H) = 141.4 Hz, 2H, CH₂), 2.58 (dd, ²*J*(H,H) = 15.4 Hz, ²*J*(C,H) = 4.6 Hz, 1H, CH₂), 2.50 (dd, ²*J*(H,H) = 15.4 Hz, ²*J*(C,H) = 4.4 Hz, 1H, CH₂), 1.91 (m, 2H, CH₂), 1.29 (d, ²*J*(C,H) = 4.2 Hz, 3H, CH₃), 1.25 (dd, ³*J*(H,H) = 7.2 Hz, ³*J*(H,H) = 7.2 Hz, 3H, CH₃) ppm. ¹³C-NMR (100 MHz, CDCl₃): δ = 172.4 (d, ²*J*(C,C) = 1.1 Hz, C_q), 138.0 (d, ³*J*(C,C) = 2.7 Hz, C_q), 128.4 (s, 2 CH), 127.7 (s, CH), 127.6 (s, 2 CH), 73.2 (d, ²*J*(C,C) = 1.5 Hz, CH₂), 70.7 (d, ²*J*(C,C) = 1.1 Hz, ¹³C_q), 66.9 (d, ²*J*(C,C) = 1.1 Hz, ¹³CH₂), 60.5 (s, CH₂), 45.5 (d, ¹*J*(C,C) = 37.3 Hz, CH₂), 40.3 (dd, ¹*J*(C,C) = 38.8 Hz, ¹*J*(C,C) = 38.8 Hz, CH₂), 27.1 (dd, ¹*J*(C,C) = 40.2 Hz, ³*J*(C,C) = 2.2 Hz, CH₃), 14.1 (s, CH₃) ppm. MS (EI, 70 eV): *m/z* (%) = 162 (22), 144 (13), 132 (10), 113 (7), 107 (8), 98 (8), 91 (100), 86 (12), 77 (13), 65 (20), 44 (30).

General procedure for the synthesis of isotopomers of 23. Pd/C (5 wt%, 0.05 eq) was added to a solution of the respective isotopomer of **22** (1 eq, 0.1 M) in MeOH. The mixture was then stirred at 40 °C under a hydrogen atmosphere (40 bar) for 2 h.

The Pd/C catalyst was filtered off and the solvent was removed under reduced pressure. The residue was dissolved in dichloromethane (0.1 M) and a catalytic amount (0.01 eq) of *p*-TsOH was added. The reaction mixture was stirred at room temperature overnight. The solvent was removed under reduced pressure and the residue was purified by flash chromatography with ethyl acetate-hexane (1:1 v/v, R_f = 0.1) to yield the isotopomers of **23** as colourless oils.

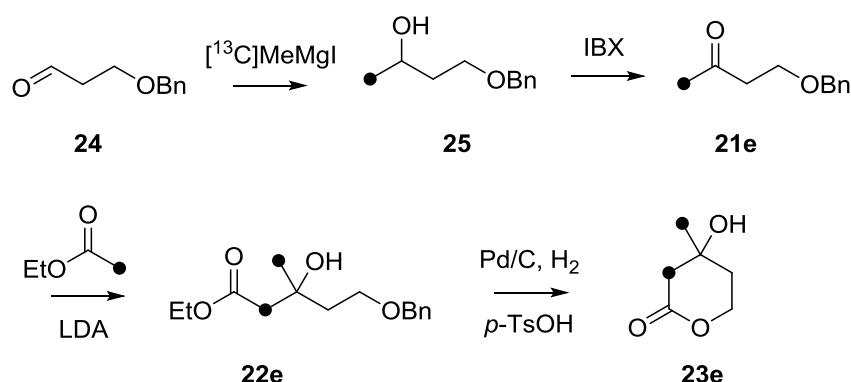
[3-¹³C]Mevalonolactone (23a). Yield: 0.37 g (2.8 mmol, 76%). GC (BPX-5, MSTFA): I = 1389. ¹H-NMR (400 MHz, CDCl₃, TMS): δ = 4.61 (m, 1H, CH₂), 4.35 (m, 1H, CH₂), 2.67 (m, ² J (H,H) = 17.4 Hz, ² J (C,H) = 5.0 Hz, 1H, CH₂), 2.52 (dd, ² J (H,H) = 17.4 Hz, ² J (C,H) = 5.0 Hz, 1H, CH₂), 2.48 (s, 1H, OH), 1.90 (m, 2H, CH₂), 1.36 (d, ² J (C,H) = 4.3 Hz, 3H, CH₃) ppm. ¹³C-NMR (100 MHz, CDCl₃): δ = 170.8 (d, ² J (C,C) = 1.8 Hz, C_q), 68.1 (s, ¹³C_q), 66.4 (d, ² J (C,C) = 2.3 Hz, CH₂), 44.6 (d, ¹ J (C,C) = 36.6 Hz, CH₂), 35.8 (d, ¹ J (C,C) = 37.0 Hz, CH₂), 29.1 (d, ¹ J (C,C) = 39.6 Hz, CH₃) ppm. MS (EI, 70 eV, MSTFA): m/z (%) = 188 (18), 161 (7), 146 (100), 145 (39), 116 (88), 101 (15), 75 (77), 73 (50), 45 (36).

[5-¹³C]Mevalonolactone (23b). Yield: 0.05 g (0.4 mmol, 74%). GC (BPX-5, MSTFA): I = 1389. ¹H-NMR (400 MHz, CDCl₃, TMS): δ = 4.67 (m, ¹ J (C,H) = 150.6 Hz, 1H, CH₂), 4.29 (m, ¹ J (C,H) = 150.6 Hz, 1H, CH₂), 2.67 (d, ² J (H,H) = 17.4 Hz, 1H, CH₂), 2.51 (d, ² J (H,H) = 17.4 Hz, CH₂), 1.92 (m, 2H, CH₂), 1.39 (s, 3H, CH₃). ¹³C-NMR (100 MHz, CDCl₃): δ = 170.9 (s, C_q), 68.0 (d, ² J (C,C) = 2.4 Hz, C_q), 66.1 (s, ¹³CH₂), 44.6 (d, ³ J (C,C) = 1.8 Hz, CH₂), 35.8 (d, ¹ J (C,C) = 34.6 Hz, CH₂), 29.6 (d, ³ J (C,C) = 2.4 Hz, CH₃) ppm. MS (EI, 70 eV): m/z (%) = 188 (21), 157 (8), 146 (100), 145 (37), 115 (82), 102 (20), 75 (77), 45 (36).

[4,6-¹³C₂]Mevalonolactone (23c). Yield: 0.27 g (2.1 mmol, 75%). GC (BPX-5, MSTFA): I = 1385. ¹H-NMR (400 MHz, CDCl₃, TMS): δ = 4.61 (m, 1H, CH₂), 4.35 (m, 1H, CH₂), 2.67 (m, ² J (H,H) = 17.4 Hz, 1H, CH₂), 2.53 (ddd, ² J (H,H) = 17.4 Hz, ³ J (C,H) = 1.9 Hz, ³ J (C,H) = 1.9 Hz, 1H, CH₂), 2.08 (m, 1H, CH₂), 1.76 (m, 1H, CH₂), 1.40 (dd, ¹ J (C,H) = 126.3 Hz, ³ J (C,H) = 4.2 Hz, 3H, CH₃) ppm. ¹³C-NMR (100 MHz, CDCl₃): δ = 170.5 (dd, ³ J (C,C) = 3.6 Hz, ³ J (C,C) = 3.6 Hz, C_q), 68.2 (dd, ¹ J (C,C) = 39.8 Hz, ¹ J (C,C) = 37.2 Hz, C_q), 66.0 (dd, ¹ J (C,C) = 34.5 Hz, ³ J (C,C) = 2.3 Hz, CH₂), 44.7 (d, ² J (C,C) = 2.7 Hz, CH₂), 35.9 (d, ² J (C,C) = 1.8 Hz, ¹³CH₂), 29.8 (d, ² J (C,C) = 1.8 Hz, ¹³CH₃) ppm. MS (EI, 70 eV, MSTFA): m/z (%) = 189 (12), 147 (100), 145 (39), 117 (47), 116 (48), 75 (51), 73 (45), 45 (24).

[3,5-¹³C₂]Mevalonolactone (23d). Yield: 0.15 g (1.1 mmol, 73%). GC (BPX-5, MSTFA): *I* = 1389. ¹H-NMR (300 MHz, CDCl₃, TMS): δ = 4.58 (m, ¹*J*(C,H) = 150.6 Hz, 1H, CH₂), 4.34 (m, ¹*J*(C,H) = 150.6 Hz, 1H, CH₂), 2.67 (m, ²*J*(H,H) = 17.4 Hz, 1H, CH₂), 2.52 (dd, ²*J*(H,H) = 17.4 Hz, ²*J*(C,H) = 2.8 Hz, 1H, CH₂), 2.08 (s, 1H, OH) 1.90 (m, 2H, CH₂), 1.40 (d, ²*J*(C,H) = 4.4 Hz, 3H, CH₃) ppm. ¹³C-NMR (75 MHz, CDCl₃): δ = 171.9 (s, C_q), 68.2 (d, ²*J*(C,C) = 2.3 Hz, ¹³C_q), 66.0 (d, ²*J*(C,C) = 2.3 Hz, ¹³CH₂), 44.7 (dd, ¹*J*(C,C) = 36.6 Hz, ³*J*(C,C) = 1.8 Hz, CH₂), 35.6 (dd, ¹*J*(C,C) = 37.1 Hz, ¹*J*(C,C) = 34.8 Hz, CH₂), 29.1 (dd, ¹*J*(C,C) = 40.1 Hz, ³*J*(C,C) = 2.3 Hz, CH₃) ppm. MS (EI, 70 eV, MSTFA): *m/z* (%) = 189 (44), 158 (22), 147 (100), 131 (25), 116 (96), 102 (37), 75 (80), 45 (44).

Synthesis of [2,6-¹³C₂]mevalonolactone (**23e**)



Scheme 3. Synthesis of [2,6-¹³C]mevalonolactone (**23e**).

The synthesis of [2,6-¹³C₂]mevalonolactone (**23e**) was performed according to a previously published procedure that was developed in our laboratories for the synthesis of deuterated isotopomers of mevalonolactone (Scheme 3).^[8] Therefore, the aldehyde **24** was used in a Grignard reaction with [¹³C]methyl iodide to yield the alcohol **25**. Oxidation to the corresponding ketone **21e** was performed using IBX. The subsequent steps towards **23e** were according to those presented in Scheme 1.

Synthesis of [1-¹³C]-4-(benzyloxy)-2-butanol (25**).** Magnesium (185 mg, 7.7 mmol, 1.1 eq) was covered with dry Et₂O (2 mL) and a solution of [¹³C]methyl iodide (1.10 g, 7.7 mmol, 1.1 eq) in dry Et₂O (5 mL) was added dropwise. The reaction mixture was stirred at room temperature for 15 min until the magnesium was consumed and then cooled to 0 °C. A solution of the aldehyde **24** (1.03 g, 7.0 mmol, 1.0 eq) in dry Et₂O (5 mL) was added dropwise and the reaction mixture was stirred for 2 h at room temperature. The mixture was quenched with a saturated aqueous NH₄Cl solution (50 mL) and extracted with Et₂O (3 x 50 mL). The organic layers were dried over MgSO₄ and the solvent was removed under reduced pressure. The residue was purified by flash chromatography using ethyl acetate-hexane (1:3 v/v, *R_f* = 0.2) to yield **25** as a colourless oil (0.90 g, 5.0 mmol, 72%). GC (BPX-5): *I* = 1467. ¹H-NMR (400 MHz, CDCl₃, TMS): δ = 7.37-7.25 (m, 5H, 5 CH), 4.52 (s, 2H, CH₂), 4.05-3.97 (m, 1H, CH), 3.74 (ddd, ²*J*(H,H) = 9.3 Hz, ³*J*(H,H) = 5.8 Hz, ³*J*(H,H) = 4.8 Hz, 1H, CH₂), 3.64 (ddd, ²*J*(H,H) = 9.1 Hz, ³*J*(H,H) = 8.6 Hz, ³*J*(H,H) = 4.6 Hz, 1H, CH₂), 2.65 (br s, 1H, OH), 1.83-1.67 (m, 2H, CH₂), 1.20 (dd, ¹*J*(C,H) = 125.9 Hz, ³*J*(H,H) = 6.3 Hz, 3H, ¹³CH₃) ppm. ¹³C-NMR (100 MHz, CDCl₃): δ = 137.9 (s, C_q), 128.4 (s, 2 CH),

127.7 (s, CH), 127.6 (s, 2 CH), 73.2 (s, CH₂), 69.0 (d, ³J(C,C) = 3.9 Hz, CH), 67.4 (d, ¹J(C,C) = 39.2 Hz, CH), 38.1 (s, CH₂), 23.3 (s, ¹³CH₃) ppm. MS (EI, 70 eV): *m/z* (%) = 181 (<1) [M]⁺, 162 (21), 120 (21), 108 (13), 107 (52), 105 (16), 92 (23), 91 (100), 79 (39), 78 (11), 77 (24), 65 (30), 57 (19), 51 (13), 46 (22), 44 (16).

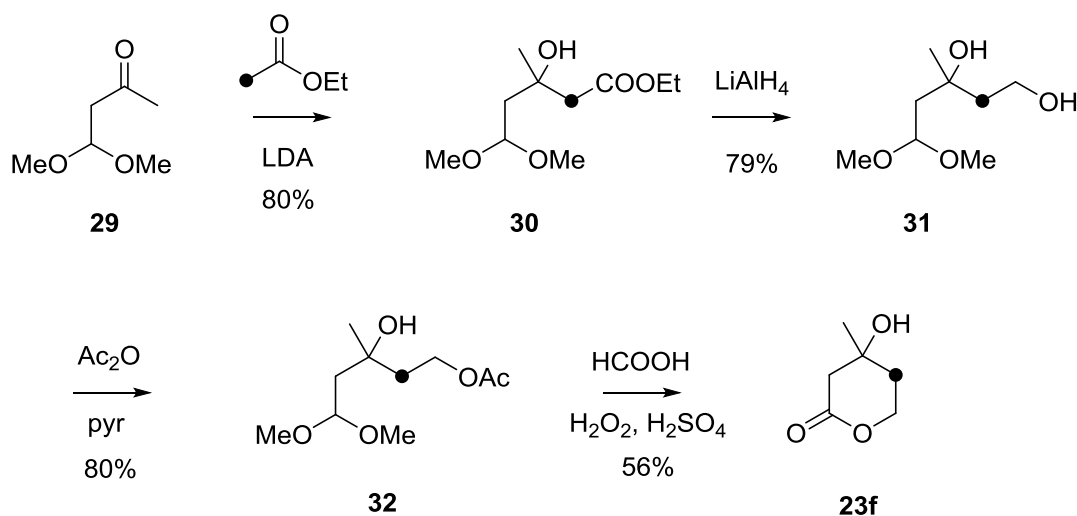
Synthesis of [1-¹³C]-4-(benzyloxy)-2-butanone (21e). To a solution of IBX (1.54 g, 5.5 mmol, 1.1 eq) in dry DMSO (55 mL) was added alcohol **25** (0.90 g, 5.0 mmol, 1 eq). The reaction mixture was stirred for 3 h at room temperature, then quenched by the addition of water (250 mL) and extracted with Et₂O (3 x 250 mL). The combined organic layers were washed with water (3 x 250 mL) and dried with MgSO₄. The solvent was removed under reduced pressure and the residue was purified by flash chromatography with ethyl acetate-hexane (1:5 v/v, *R_f* = 0.2) to yield **21e** (0.71 g, 4.1 mmol, 82%) as colourless oil. GC (BPX-5): *I* = 1461. ¹H-NMR (400 MHz, CDCl₃, TMS): δ = 7.38-7.25 (m, 5H, 5 CH), 4.51 (s, 2H, CH₂), 3.74 (t, ³J(H,H) = 6.3 Hz, 2H, CH₂), 2.72 (t, ³J(H,H) = 6.3 Hz, 2H, CH₂), 2.18 (d, ¹J(C,H) = 127.3 Hz, 3H, ¹³CH₃) ppm. ¹³C-NMR (100 MHz, CDCl₃): δ = 207.1 (d, ¹J(C,C) = 40.7 Hz, C_q), 138.0 (s, C_q), 128.4 (s, 2 CH), 127.7 (s, 2 CH), 127.6 (s, CH), 73.2 (s, CH₂), 65.3 (s, CH₂), 43.7 (d, ²J(C,C) = 13.9 Hz, CH₂), 30.4 (s, ¹³CH₃) ppm. MS (EI, 70 eV): *m/z* (%) = 179 (<1) [M]⁺, 120 (19), 107 (55), 91 (100), 79 (30), 77 (29), 65 (33), 44 (81).

Synthesis of ethyl [2,6-¹³C₂]-5-(benzyloxy)-3-hydroxy-3-methylpentanoate (22e). The conversion of **21e** into the ester **22e** was carried out as described above for the synthesis of the isotopomers **22a-d**. The labelled ester [2-¹³C]ethyl acetate was used. Yield: 0.90 g (3.5 mmol, 82%). GC (BPX-5): *I* = 1916. ¹H-NMR (400 MHz, CDCl₃, TMS): δ = 7.39-7.25 (m, 5H, 5 CH), 4.50 (s, 2H, CH₂), 4.14 (dq, ²J(H,H) = 10.3 Hz, ³J(H,H) = 7.1 Hz, 1H, CH₂), 4.13 (dq, ²J(H,H) = 10.3 Hz, ³J(H,H) = 7.1 Hz, 1H, CH₂), 3.69 (m, 2H, CH₂), 2.58 (ddd, ¹J(C,H) = 128.9 Hz, ²J(H,H) = 15.4 Hz, ³J(C,H) = 3.7 Hz, 1H, CH₂), 2.50 (ddd, ¹J(C,H) = 128.3 Hz, ²J(H,H) = 15.4 Hz, ³J(C,H) = 3.2 Hz, 1H, CH₂), 1.91 (m, 2H, CH₂), 1.28 (dd, ¹J(C,H) = 126.2 Hz, ³J(C,H) = 4.1 Hz, 3H, CH₃), 1.25 (dd, ³J(H,H) = 7.1 Hz, ³J(H,H) = 7.1 Hz, 3H, CH₃) ppm. ¹³C-NMR (100 MHz, CDCl₃): δ = 172.4 (dd, ¹J(C,C) = 56.8 Hz, ³J(C,C) = 2.1 Hz, C_q), 138.0 (s, C_q), 128.4 (s, 2 CH), 127.7 (s, CH), 127.6 (s, 2 CH), 73.2 (s, CH₂), 70.7 (dd, ¹J(C,C) = 40.1 Hz, ¹J(C,C) = 37.6 Hz, C_q), 66.9 (dd, ³J(C,C) = 4.2 Hz, ³J(C,C) = 2.1 Hz, CH₂), 60.5 (s, CH₂), 45.5 (d, ²J(C,C) = 2.2 Hz, ¹³CH₂), 40.4 (dd, ²J(C,C) = 1.4 Hz, ²J(C,C) = 1.4 Hz,

CH₂), 27.1 (d, ²J(C,C) = 2.2 Hz, ¹³CH₃), 14.1 (s, CH₃). MS (EI, 70 eV): *m/z* (%) = 180 (2), 161 (24), 144 (12), 107 (10), 91 (100), 65 (12), 44 (24).

Synthesis of [2,6-¹³C₂]mevalonolactone (23e). The conversion of **22e** into **23e** was carried out as described above for the isotopomers **23a-d**. Yield: 0.95 g (0.72 mmol, 84%). GC (BPX-5, MSTFA): *I* = 1381. ¹H-NMR (400 MHz, CDCl₃, TMS): δ = 4.61 (ddd, ²J(H,H) = 11.2 Hz, ³J(H,H) = 9.2 Hz, ³J(H,H) = 5.5 Hz, 1H, CH₂), 4.35 (ddd, ²J(H,H) = 11.2 Hz, ³J(H,H) = 5.1 Hz, ³J(H,H) = 4.1 Hz, 1H, CH₂), 2.69 (m, ¹J(C,H) = 133.0 Hz, ²J(H,H) = 17.3 Hz, 1H, CH₂), 2.52 (ddd, ¹J(C,H) = 126.6 Hz, ²J(H,H) = 17.3 Hz, ³J(C,H) = 2.4 Hz, 1H, CH₂), 2.20 (br s, 1H, OH), 1.98-1.85 (m, 2H, CH₂), 1.40 (dd, ¹J(C,H) = 126.2 Hz, ³J(C,H) = 4.4 Hz, 3H, CH₃) ppm. ¹³C-NMR (100 MHz, CDCl₃): δ = 170.7 (dd, ¹J(C,C) = 51.6 Hz, ³J(C,C) = 3.6 Hz, C_q), 68.1 (dd, ¹J(C,C) = 36.5 Hz, ¹J(C,C) = 40.0 Hz, C_q), 66.0 (dd, ³J(C,C) = 2.0 Hz, ³J(C,C) = 2.0 Hz, ³J(C,C) = 2.0 Hz, CH₂), 44.7 (d, ²J(C,C) = 2.7 Hz, ¹³CH₂), 35.8 (d, ²J(C,C) = 1.7 Hz, 29.7 (d, ²J(C,C) = 2.7 Hz, ¹³CH₃) ppm. MS (EI, 70 eV, MSTFA): *m/z* (%) = 189 (10), 161 (19), 146 (100), 144 (36), 116 (39), 101 (17), 75 (75), 40 (52).

Synthesis of [4-¹³C]mevalonolactone (**23f**)



Scheme 4. Synthesis of [4-¹³C]mevalonolactone (**23f**).

The synthesis of [4-¹³C]mevalonolactone (**23f**) was performed according to the procedure of Cane and Levin (Scheme 4).^[9] Briefly, acetoacetaldehyde dimethylacetal (**29**) was used in an aldol reaction with [2-¹³C]ethyl acetate to yield ester **30**. Subsequent reduction with LiAlH₄ to the corresponding alcohol **31** was followed by conversion into the acetate ester **32** with acetic anhydride in pyridine. The resulting material was directly converted into **23f** with sulfuric acid and hydrogen peroxide in formic acid.

Synthesis of ethyl [2-¹³C]-3-hydroxy-3-methyl-5,5-dimethoxypentanoate (30**).** A solution of n-butyllithium in hexane (1.6 M, 5.3 mL, 8.4 mmol, 1.1 eq) was added at 0°C to a solution of diisopropylamine (850 mg, 8.4 mmol, 1.1 eq) in dry THF (2 mL). The mixture was stirred for 1 h and then cooled to -78°C. A solution of [2-¹³C]ethyl acetate (750 mg, 8.4 mmol, 1.1 eq) in dry THF (2 mL) was added dropwise and the reaction mixture was stirred for 30 min. Subsequently, a solution of acetoacetaldehyde dimethylacetal (**29**, 1.01 g, 7.6 mmol, 1.0 eq) in dry THF (1 mL) was added dropwise. The reaction mixture was stirred for 45 min, quenched with sat. aqueous NH₄Cl solution (50 mL) and allowed to warm to room temperature. The aqueous layer was extracted with Et₂O (3 x 50 mL) and the combined extracts were dried with MgSO₄. The solvent was removed under reduced pressure and the residue was purified by flash chromatography with ethyl acetate-hexane (1:4 v/v, *R_f* = 0.2) to yield the target compound **30** (1.35 g, 6.1 mmol, 80%) as a colourless oil. GC (BPX-

5): $I = 1406$. $^1\text{H-NMR}$ (400 MHz, C_6D_6 , TMS): $\delta = 4.67$ (t, $^3J(\text{H,H}) = 5.4$ Hz, 1H, CH), 4.03 (d, $^3J(\text{C,H}) = 2.1$ Hz, 1H, OH), 3.87 (q, $^3J(\text{H,H}) = 7.1$ Hz, 2H, CH_2), 3.05 (s, 6H, 2 CH_3), 2.56 (dd, $^1J(\text{C,H}) = 129.4$ Hz, $^2J(\text{H,H}) = 15.5$ Hz, 1H, CH_2), 2.39 (dd, $^1J(\text{C,H}) = 129.0$ Hz, $^2J(\text{H,H}) = 15.5$ Hz, 1H, CH_2), 1.97 (ddd, $^2J(\text{H,H}) = 14.1$ Hz, $^3J(\text{H,H}) = 5.3$ Hz, $^3J(\text{C,H}) = 3.0$ Hz, 1H, CH_2), 1.94 (ddd, $^2J(\text{H,H}) = 14.1$ Hz, $^3J(\text{H,H}) = 5.3$ Hz, $^3J(\text{C,H}) = 3.7$ Hz, 1H, CH_2), 1.30 (d, $^3J(\text{C,H}) = 4.1$ Hz, 3H, CH_3), 0.90 (t, $^3J(\text{H,H}) = 7.1$ Hz, 3H, CH_3) ppm. $^{13}\text{C-NMR}$ (100 MHz, C_6D_6): $\delta = 172.4$ (d, $^1J(\text{C,C}) = 57.5$ Hz, C_q), 102.5 (d, $^3J(\text{C,C}) = 1.9$ Hz, CH), 69.6 (d, $^1J(\text{C,C}) = 37.8$ Hz, C_q), 60.3 (s, CH_2), 52.5 (s, CH_3), 52.4 (s, CH_3), 45.7 (s, $^{13}\text{CH}_2$), 43.7 (d, $^2J(\text{C,C}) = 1.7$ Hz, CH_2), 28.2 (d, $^2J(\text{C,C}) = 2.3$ Hz, CH_3), 14.1 (s, CH_3) ppm. MS (EI, 70 eV): m/z (%) = 188 (3), 174 (15), 172 (34), 158 (11), 132 (28), 118 (14), 101 (32), 86 (43), 75 (100), 58 (53), 43 (100).

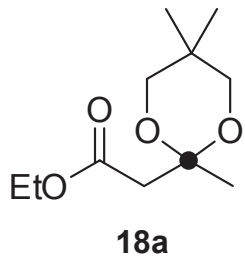
Synthesis of [2- ^{13}C]-3-methyl-5,5-dimethoxypentane-1,3-diol (31). A 1.5 M solution of **30** (1.35 g, 6.1 mmol, 1.0 eq) in dry THF (1 mL) was added at 0 °C to a suspension of LiAlH_4 (460 mg, 12.2 mmol, 2.0 eq) in dry THF (10 mL). The reaction mixture was stirred at room temperature for 2 h and then quenched by the addition of water under stirring until a white suspension was formed. The mixture was filtered and the obtained filtrate was dried over MgSO_4 . The solvent was removed under reduced pressure and the residue was purified by flash chromatography with ethyl acetate-hexane (2:1 v/v, $R_f = 0.2$) to yield the target compound **31** (0.86 g, 4.8 mmol, 79%) as colourless oil. GC (BPX-5, MSTFA): $I = 1500$. $^1\text{H-NMR}$ (400 MHz, C_6D_6 , TMS): $\delta = 4.53$ (t, $^3J(\text{H,H}) = 5.8$ Hz, 1H, CH), 3.84 (d, $^3J(\text{C,H}) = 3.3$ Hz, 1H, OH), 3.82 (m, 1H, CH_2), 3.75 (m, 1H, CH_2), 3.32 (br s, 1H, OH), 3.02 (s, 3H, CH_3), 3.01 (s, 3H, CH_3), 1.86 (ddd, $^2J(\text{H,H}) = 14.4$ Hz, $^3J(\text{H,H}) = 6.4$ Hz, $^3J(\text{C,H}) = 2.3$ Hz, 1H, CH_2), 1.61 (ddd, $^2J(\text{H,H}) = 14.4$ Hz, $^3J(\text{H,H}) = 5.3$ Hz, $^3J(\text{C,H}) = 3.0$ Hz, 1H, CH_2), 1.66 (ddd, $^1J(\text{C,H}) = 125.1$ Hz, $^2J(\text{H,H}) = 14.3$ Hz, $^3J(\text{H,H}) = 4.6$ Hz, 1H, CH_2), 1.48 (ddd, $^1J(\text{C,H}) = 124.1$ Hz, $^2J(\text{H,H}) = 14.3$ Hz, $^3J(\text{H,H}) = 4.3$ Hz, 1H, CH_2), 1.13 (d, $^3J(\text{C,H}) = 3.8$ Hz, 3H, CH_3) ppm. $^{13}\text{C-NMR}$ (100 MHz, C_6D_6): $\delta = 102.6$ (d, $^3J(\text{C,C}) = 2.7$ Hz, CH), 71.9 (d, $^1J(\text{C,C}) = 38.8$ Hz, C_q), 59.5 (d, $^1J(\text{C,C}) = 36.8$ Hz, CH_2), 52.6 (s, CH_3), 52.3 (s, CH_3), 43.7 (s, CH_2), 43.3 (s, $^{13}\text{CH}_2$), 27.2 (d, $^2J(\text{C,C}) = 1.5$ Hz, CH_3) ppm. MS (EI, 70 eV, MSTFA): m/z (%) = 234 (24), 147 (23), 133 (23), 116 (19), 103 (29), 89 (25), 75 (100).

Synthesis of [2-¹³C]-3-methyl-5,5-dimethoxypentane-1,3-diol-1-acetate (32). The diol **31** (0.86 g, 4.8 mmol) was dissolved in dry pyridine (20 mL) and the solution was cooled to 4 °C. Ac₂O (20 mL) was added and the reaction mixture was stirred overnight at 4 °C. The mixture was concentrated under reduced pressure and the residue was purified by flash chromatography with ethyl acetate-hexane (1:2 v/v, *R_f* = 0.2) to yield the target compound **32** (0.84 g, 3.8 mmol, 80%) as a colourless oil. GC (BPX-5): *I* = 1479. ¹H-NMR (400 MHz, C₆D₆, TMS): δ = 4.50 (dd, ³*J*(H,H) = 5.5 Hz, ³*J*(H,H) = 6.1 Hz, 1H, CH), 4.30 (dt, ³*J*(H,H) = 7.2, ²*J*(C,H) = 2.7 Hz, 2H, CH₂), 3.14 (br s, 1H, OH), 2.99 (s, 6H, 2 CH₃), 1.78 (ddt, ¹*J*(C,H) = 126.3 Hz, ²*J*(H,H) = 13.9 Hz, ³*J*(H,H) = 7.2 Hz, 1H, CH₂), 1.75 (ddd, ²*J*(H,H) = 14.4 Hz, ³*J*(H,H) = 6.1 Hz, ³*J*(C,H) = 2.0 Hz, 1H, CH₂), 1.72 (ddt, ¹*J*(C,H) = 126.3 Hz, ²*J*(H,H) = 13.9 Hz, ³*J*(H,H) = 7.3 Hz, 1H, CH₂), 1.68 (s, 3H, CH₃), 1.63 (ddd, ²*J*(H,H) = 14.4 Hz, ³*J*(H,H) = 5.5 Hz, ³*J*(C,H) = 3.2 Hz, 1H, CH₂), 1.08 (d, ³*J*(C,H) = 3.8 Hz, 3H, CH₃) ppm. ¹³C-NMR (100 MHz, C₆D₆): δ = 170.2 (d, ³*J*(C,C) = 1.8 Hz, C_q), 102.6 (d, ³*J*(C,C) = 2.8 Hz, CH), 69.6 (d, ¹*J*(C,C) = 39.2 Hz, C_q), 61.2 (d, ¹*J*(C,C) = 39.2 Hz, CH₂), 52.5 (s, CH₃), 52.3 (s, CH₃), 43.3 (d, ²*J*(C,C) = 1.5 Hz, CH₂), 41.3 (s, ¹³CH₂), 27.6 (d, ²*J*(C,C) = 1.8 Hz, CH₃), 20.6 (s, CH₃) ppm. MS (EI, 70 eV): *m/z* (%) = 174 (2), 132 (9), 114 (9), 101 (34), 75 (89), 58 (32), 43 (100).

Synthesis of [4-¹³C]mevalonolactone (23f). Formic acid (4 mL), an aqueous solution of H₂O₂ (30 wt%, 12 mL) and an aqueous solution of H₂SO₄ (1%, 4 mL) were added to the acetate ester **32** (0.84 g, 3.8 mmol). The reaction mixture was heated to reflux for 1 h and then quenched by the addition of anhydrous K₂CO₃ (200 mg). The mixture was concentrated under reduced pressure and the residue was purified by flash chromatography with ethyl acetate-hexane (1:1 v/v, *R_f* = 0.2) to yield the target compound **23f** (0.28 g, 2.1 mmol, 56%) as colourless oil. GC (BPX-5, MSTFA): *I* = 1382. ¹H-NMR (400 MHz, CDCl₃, TMS): δ = 4.61 (dddd, ²*J*(H,H) = 11.2 Hz, ³*J*(H,H) = 9.2 Hz, ³*J*(H,H) = 5.5 Hz, ²*J*(C,H) = 2.7 Hz, 1H, CH₂), 4.39-4.32 (m, 1H, CH₂), 2.67 (m, ²*J*(H,H) = 17.4 Hz, 1H, CH₂), 2.53 (dd, ²*J*(H,H) = 17.4 Hz, ³*J*(C,H) = 1.6 Hz, 1H, CH₂), 1.90 (m, ¹*J*(C,H) = 127.7 Hz, 2H, CH₂), 1.41 (d, ³*J*(C,H) = 4.2 Hz, 3H, CH₃) ppm. ¹³C-NMR (100 MHz, CDCl₃): δ = 170.4 (d, ³*J*(C,C) = 3.5 Hz, C_q), 68.2 (d, ¹*J*(C,C) = 37.3 Hz, C_q), 66.0 (d, ¹*J*(C,C) = 34.5 Hz, CH₂), 44.7 (s, CH₂), 35.9 (s, ¹³CH₂), 29.8 (d, ²*J*(C,C) = 1.7 Hz, CH₃) ppm. MS (EI, 70 eV, MSTFA): *m/z* (%) = 188 (20), 159 (7), 146 (100), 115 (51), 102 (15), 75 (51), 45 (19).

References

- [1] A. A. Stierle, D. B. Stierle, E. Goldstein, K. Parker, T. Bugni, C. Baarson, J. Gress, D. Blake, *J. Nat. Prod.* **2003**, *66*, 1097-1100.
- [2] M. L. Bolte, J. Bowers, W. D. Crow, D. M. Paton, A. Sakurai, N. Takahashi, M. Ujiie, S. Yoshida, *Agric. Biol. Chem.* **1984**, *48*, 373-376.
- [3] H. J. M. Gijsen, K. Kanai, G. A. Stork, J. B. P. A. Wijnberg, R. V. A. Orru, C. G. J. M. Seelen, S. M. van der Kerk, A. de Groot, *Tetrahedron* **1990**, *46*, 7237-7246.
- [4] H. J. M. Gijsen, J. B. P. A. Wijnberg, G. A. Stork, A. de Groot, M. A. de Waard, J. G. M. van Nistelrooy, *Tetrahedron* **1992**, *48*, 2465-2476.
- [5] A. San Feliciano, M. Medarde, M. Gordaliza, E. del Olmo, J. M. M. del Corral, *Phytochemistry* **1989**, *28*, 2717-2721.
- [6] K. I. Booker-Milburn, H. Jenkins, J. P. H. Charmant, P. Mohr, *Org. Lett.* **2003**, *5*, 3309-3312.
- [7] L. O. Zamir, C.-D. Nguyen, *J. Label. Compd. Radiopharm.* **1988**, *25*, 1189-1196.
- [8] J. S. Dickschat, C. A. Citron, N. L. Brock, R. Riclea, H. Kuhz, *Eur. J. Org. Chem.* **2011**, 3339-3346.
- [9] D. E. Cane, R. H. Levin, *J. Am. Chem. Soc.* **1976**, *98*, 1183-1188.

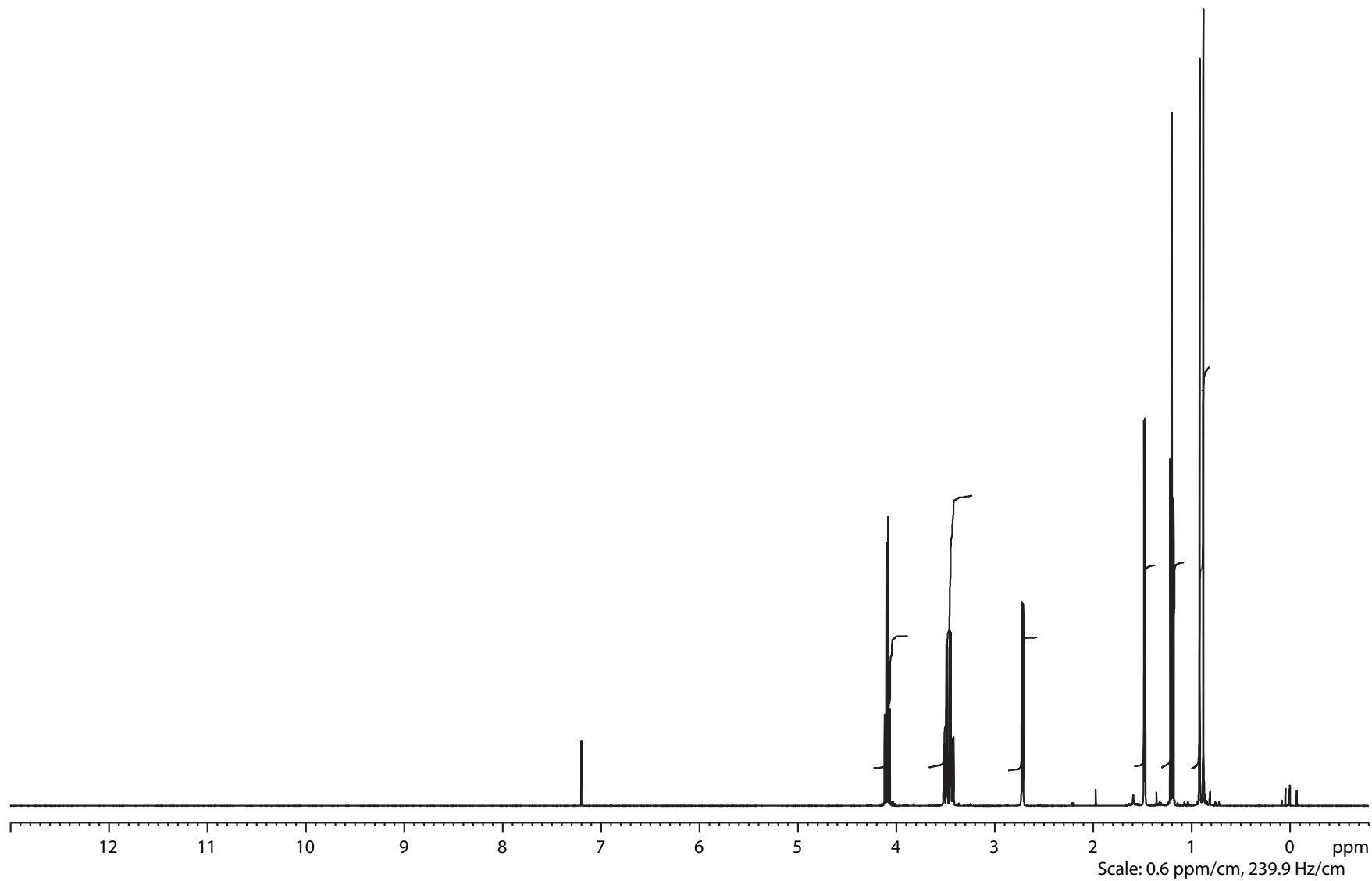


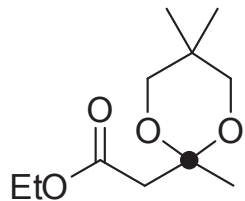
Current Data Parameters
 NAME bae119842_od
 EXPNO 1
 PROCNO 1

F2 - Acquisition Parameters
 Date_ 20130223
 Time 6.11
 INSTRUM drx400
 PROBHD 5 mm QNP 1H/13
 PULPROG zg30
 TD 65536
 SOLVENT CDCl3
 NS 64
 DS 2
 SWH 8278.146 Hz
 FIDRES 0.126314 Hz
 AQ 3.9584243 sec
 RG 90.5
 DW 60.400 usec
 DE 6.00 usec
 TE 298.2 K
 D1 1.00000000 sec
 TD0 1

==== CHANNEL f1 =====
 NUC1 1H
 P1 10.20 usec
 PL1 -2.00 dB
 SFO1 399.8924689 MHz

F2 - Processing parameters
 SI 32768
 SF 399.8900368 MHz
 SR 36.77 Hz
 WDW EM
 SSB 0
 LB 0.00 Hz
 GB 0
 PC 1.40





18a

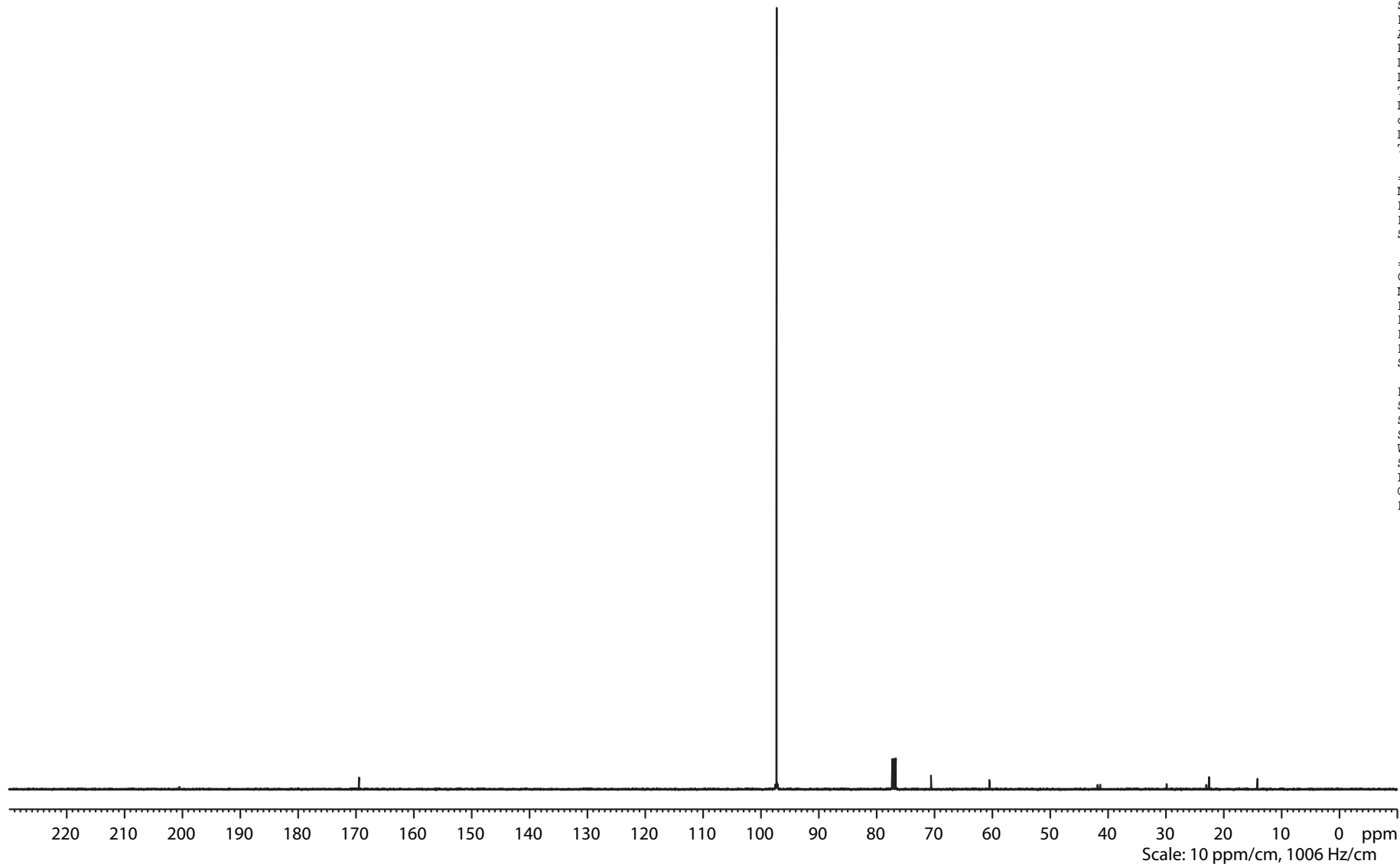
Current Data Parameters
 NAME bae119842_od
 EXPNO 2
 PROCNO 1

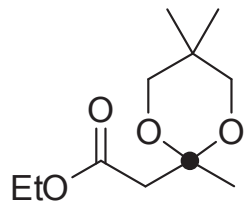
F2 - Acquisition Parameters
 Date_ 20130223
 Time 6.20
 INSTRUM drx400
 PROBHD 5 mm QNP 1H/13
 PULPROG zgpg30
 TD 131072
 SOLVENT CDCl3
 NS 96
 DS 4
 SWH 26315.789 Hz
 FIDRES 0.200774 Hz
 AQ 2.4904180 sec
 RG 9195.2
 DW 19.000 usec
 DE 6.00 usec
 TE 299.2 K
 D1 2.00000000 sec
 d11 0.03000000 sec
 DELTA 1.89999998 sec
 TD0 1

==== CHANNEL f1 =====
 NUC1 13C
 P1 11.00 usec
 PL1 -3.00 dB
 SFO1 100.5635842 MHz

==== CHANNEL f2 =====
 CPDPRG2 waltz16
 NUC2 1H
 PCPD2 80.00 usec
 PL2 -2.00 dB
 PL12 16.06 dB
 PL13 16.06 dB
 SFO2 399.8915996 MHz

F2 - Processing parameters
 SI 65536
 SF 100.5524238 MHz
 SR 2.76 Hz
 WDW EM
 SSB 0
 LB 1.00 Hz
 GB 0
 PC 1.40





18a

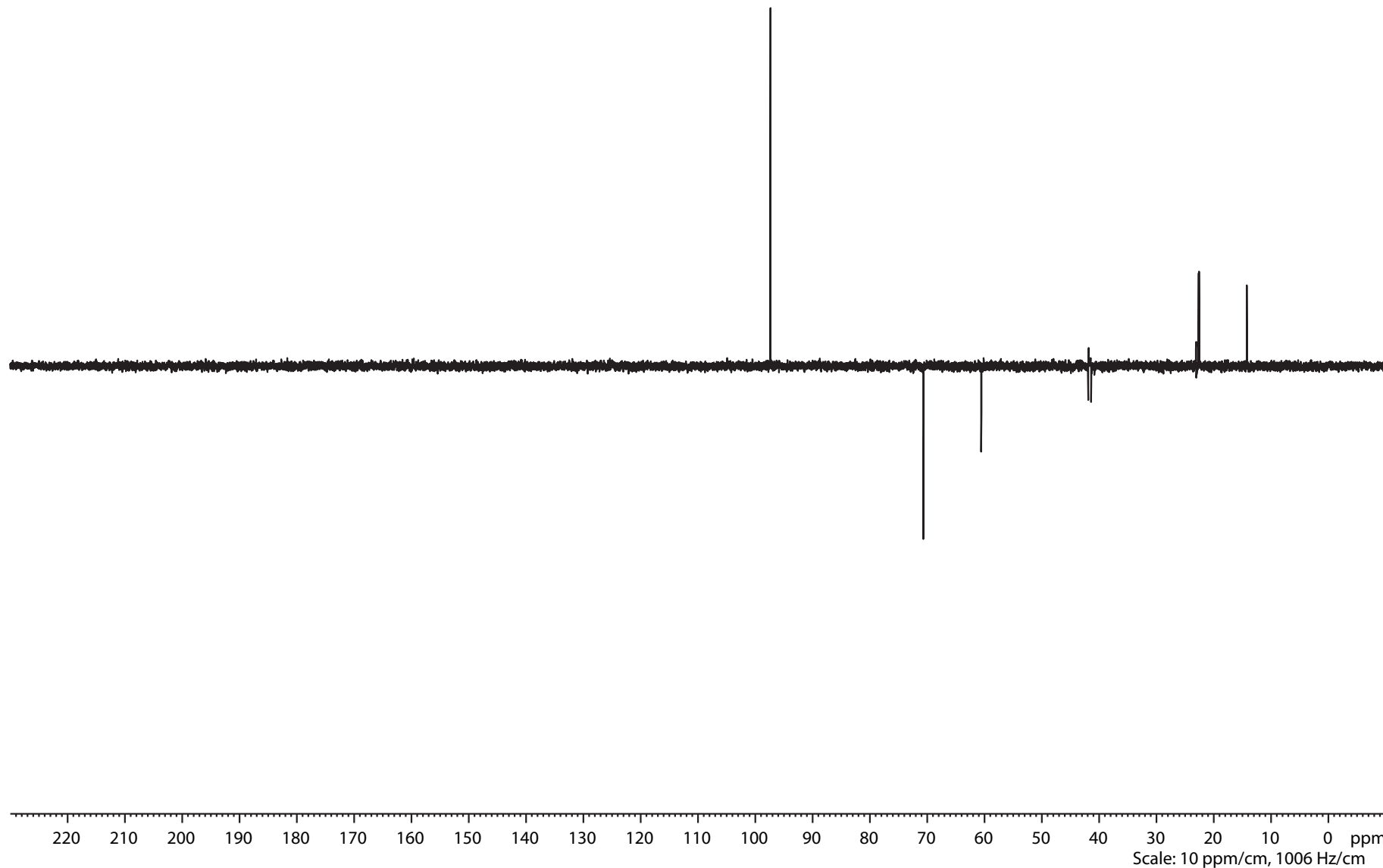
Current Data Parameters
 NAME bae119842_od
 EXPNO 3
 PROCNO 1

F2 - Acquisition Parameters
 Date_ 20130223
 Time 6.28
 INSTRUM drx400
 PROBHD 5 mm QNP 1H/13
 PULPROG dept135
 TD 131072
 SOLVENT CDCl3
 NS 96
 DS 4
 SWH 26315.789 Hz
 FIDRES 0.200774 Hz
 AQ 2.4904180 sec
 RG 8192
 DW 19.000 usec
 DE 7.00 usec
 TE 298.2 K
 CNST2 145.0000000
 D1 2.00000000 sec
 d2 0.00344828 sec
 d12 0.00002000 sec
 DELTA 0.00001401 sec
 TD0 1

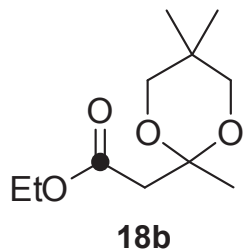
==== CHANNEL f1 =====
 NUC1 13C
 P1 11.00 usec
 p2 22.00 usec
 PL1 -3.00 dB
 SFO1 100.5635842 MHz

==== CHANNEL f2 =====
 CPDPRG2 waltz16
 NUC2 1H
 P3 10.00 usec
 p4 20.00 usec
 PCPD2 80.00 usec
 PL2 -2.00 dB
 PL12 16.06 dB
 SFO2 399.8915996 MHz

F2 - Processing parameters
 SI 65536
 SF 100.5524178 MHz
 SR -3.20 Hz
 WDW EM
 SSB 0
 LB 1.00 Hz
 GB 0
 PC 1.40



Scale: 10 ppm/cm, 1006 Hz/cm



```

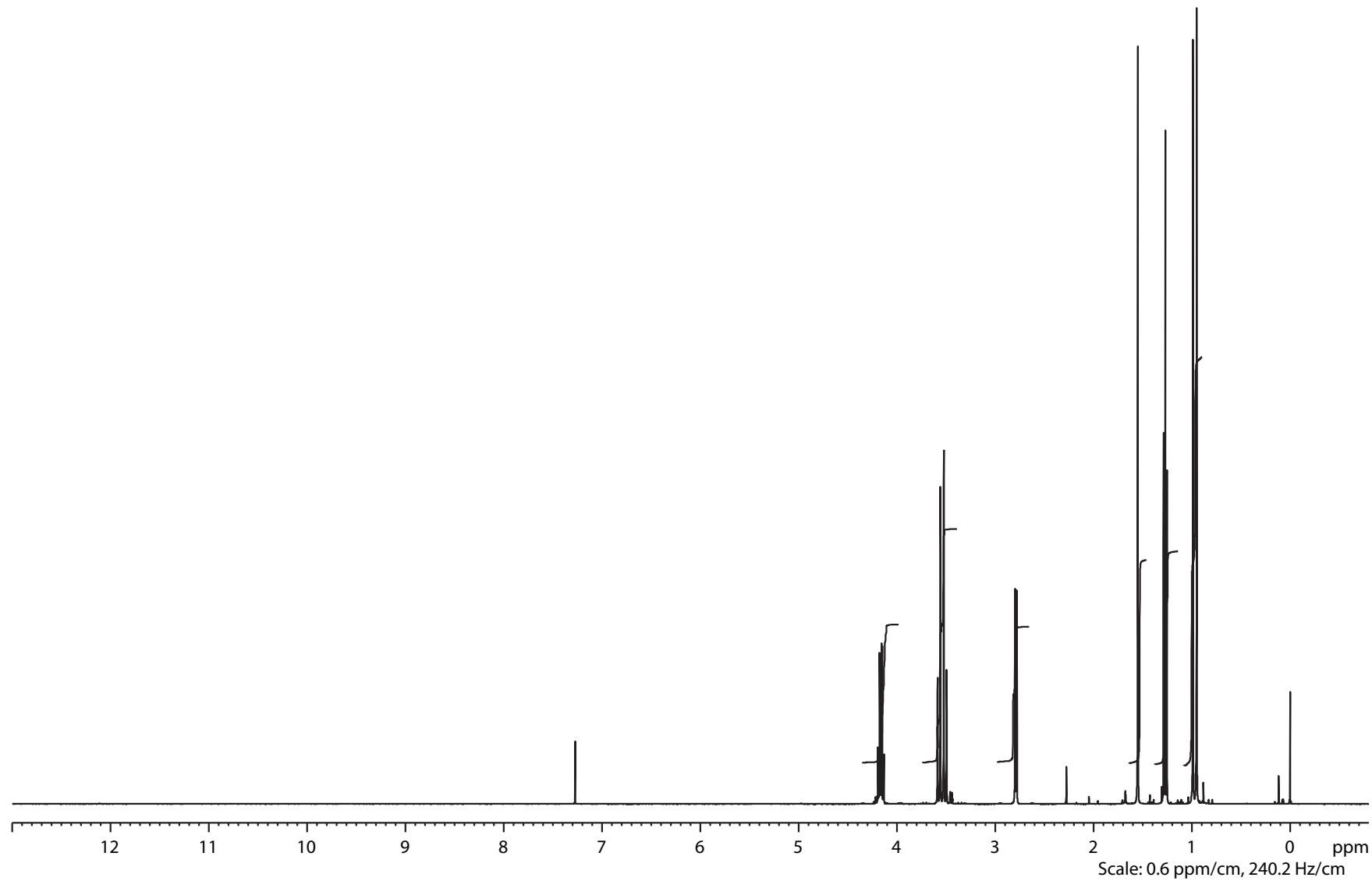
NAME      bae120069_od
EXPNO     1
PROCNO    1
Date_     20130312
Time      2.19
INSTRUM   AVIII400
PROBHD    5 mm PABBO BB-
PULPROG   zg30
TD         65536
SOLVENT   CDCl3
NS         64
DS         2
SWH        8223.685 Hz
FIDRES     0.125483 Hz
AQ         3.9846387 sec
RG         64
DW         60.800 usec
DE         6.50 usec
TE         295.7 K
D1         1.00000000 sec
TD0        1

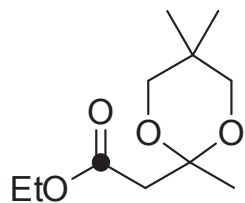
```

```

===== CHANNEL f1 =====
NUC1       1H
P1         10.33 usec
PL1        -4.00 dB
SFO1       400.4024726 MHz
SI         32768
SF         400.4000129 MHz
SR         12.90 Hz
WDW        EM
SSB        0
LB         0.00 Hz
GB         0
PC         1.40
F1P        13.000 ppm
F2P        -0.800 ppm

```





18b

```

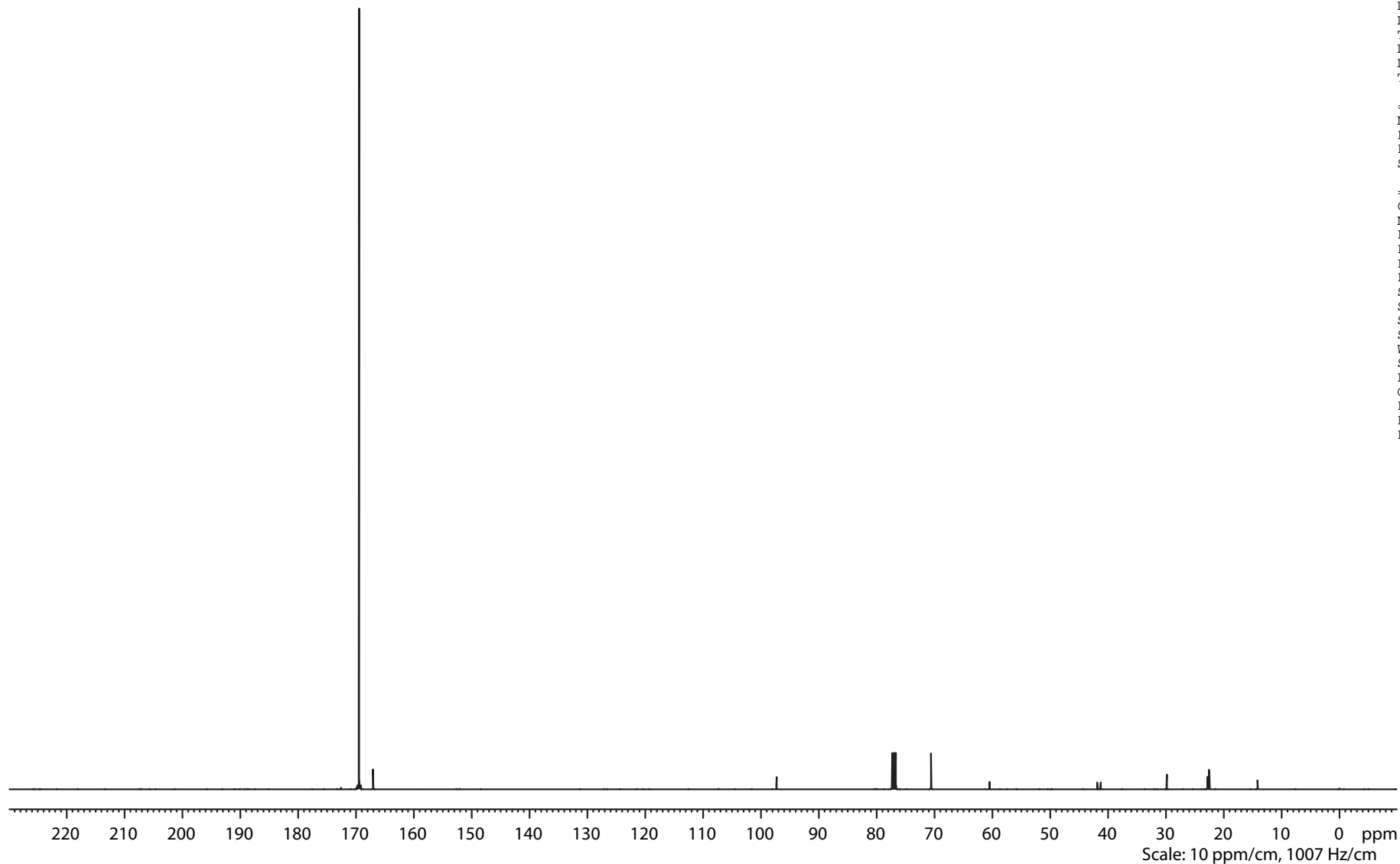
NAME      bae120069_od
EXPNO     2
PROCNO    1
Date_     20130312
Time      3.39
INSTRUM   AVIII400
PROBHD    5 mm PABBO BB-
PULPROG   zgpg30
TD         131072
SOLVENT   CDCl3
NS         1024
DS         4
SWH        26315.789 Hz
FIDRES     0.200774 Hz
AQ         2.4904180 sec
RG         80.6
DW         19.000 usec
DE         6.50 usec
TE         297.0 K
D1         2.00000000 sec
D11        0.03000000 sec
TD0        1
  
```

```

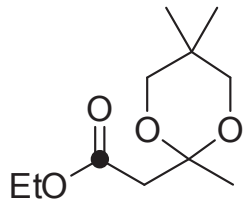
===== CHANNEL f1 =====
NUC1       13C
P1         8.50 usec
PL1        -3.00 dB
SFO1       100.6918371 MHz
  
```

```

===== CHANNEL f2 =====
CPDPRG2    waltz16
NUC2        1H
PCPD2       80.00 usec
PL2         -4.00 dB
PL12        13.78 dB
PL13        14.00 dB
SFO2        400.4016016 MHz
SI          65536
SF          100.6806648 MHz
SR           3.83 Hz
WDW         EM
SSB         0
LB          1.00 Hz
GB          0
PC          1.40
F1P         230.000 ppm
F2P         -10.000 ppm
  
```



Scale: 10 ppm/cm, 1007 Hz/cm



18b

```

NAME      bae120069_od
EXPNO     3
PROCNO    1
Date_     20130312
Time      3.48
INSTRUM   AVIII400
PROBHD    5 mm PABBO BB-
PULPROG   dept135
TD         131072
SOLVENT   CDCl3
NS         96
DS         4
SWH        26315.789 Hz
FIDRES     0.200774 Hz
AQ         2.4904180 sec
RG         2050
DW         19.000 usec
DE         6.50 usec
TE         296.4 K
CNST2     145.0000000
D1         2.00000000 sec
D2         0.00344828 sec
D12        0.00002000 sec
TD0        5

```

```

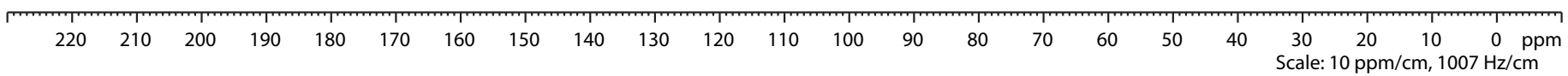
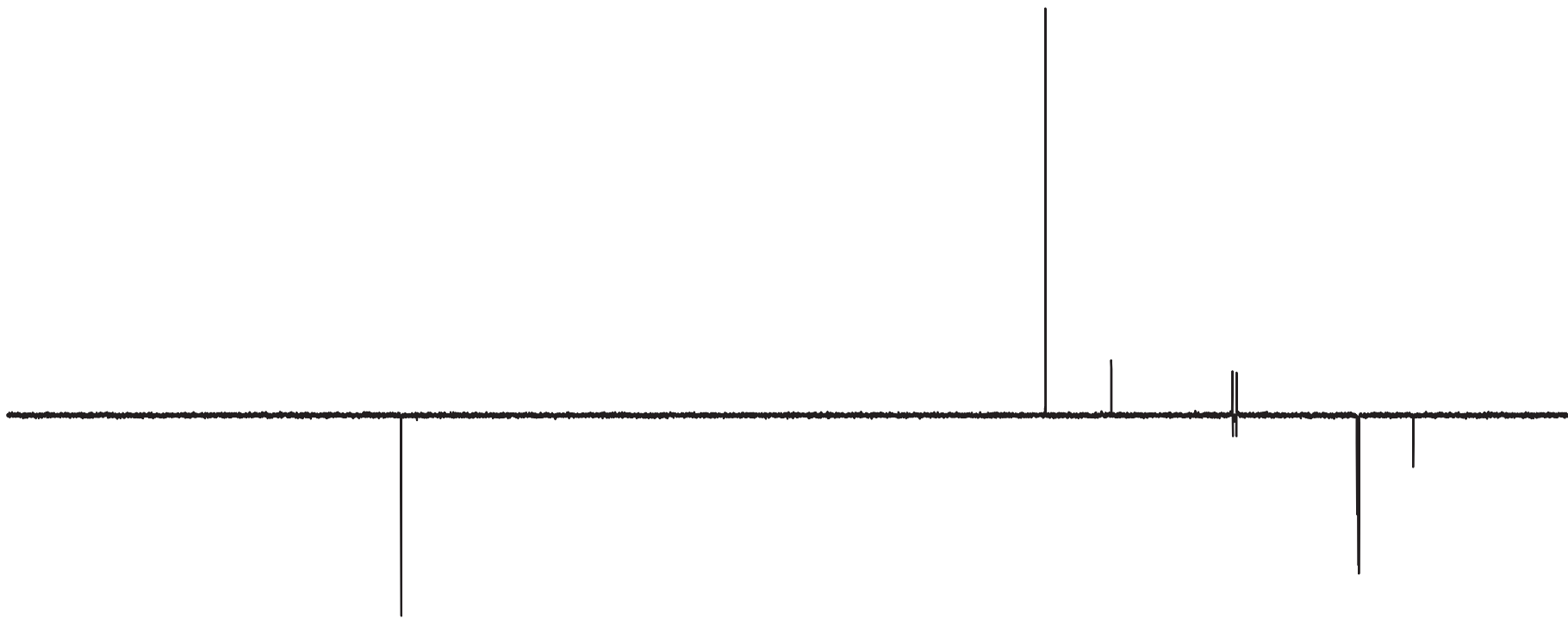
===== CHANNEL f1 =====
NUC1       13C
P1         8.50 usec
P2         17.00 usec
PL1        -3.00 dB
SFO1       100.6918371 MHz

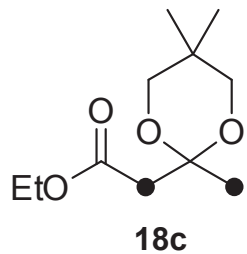
```

```

===== CHANNEL f2 =====
CPDPRG2    waltz16
NUC2       1H
P3         10.33 usec
P4         20.66 usec
PCPD2      80.00 usec
PL2        -4.00 dB
PL12       13.78 dB
SFO2       400.4016016 MHz
SI         65536
SF         100.6806578 MHz
SR         -3.20 Hz
WDW        EM
SSB        0
LB         1.00 Hz
GB         0
PC         1.40
F1P        230.000 ppm
F2P        -10.000 ppm

```



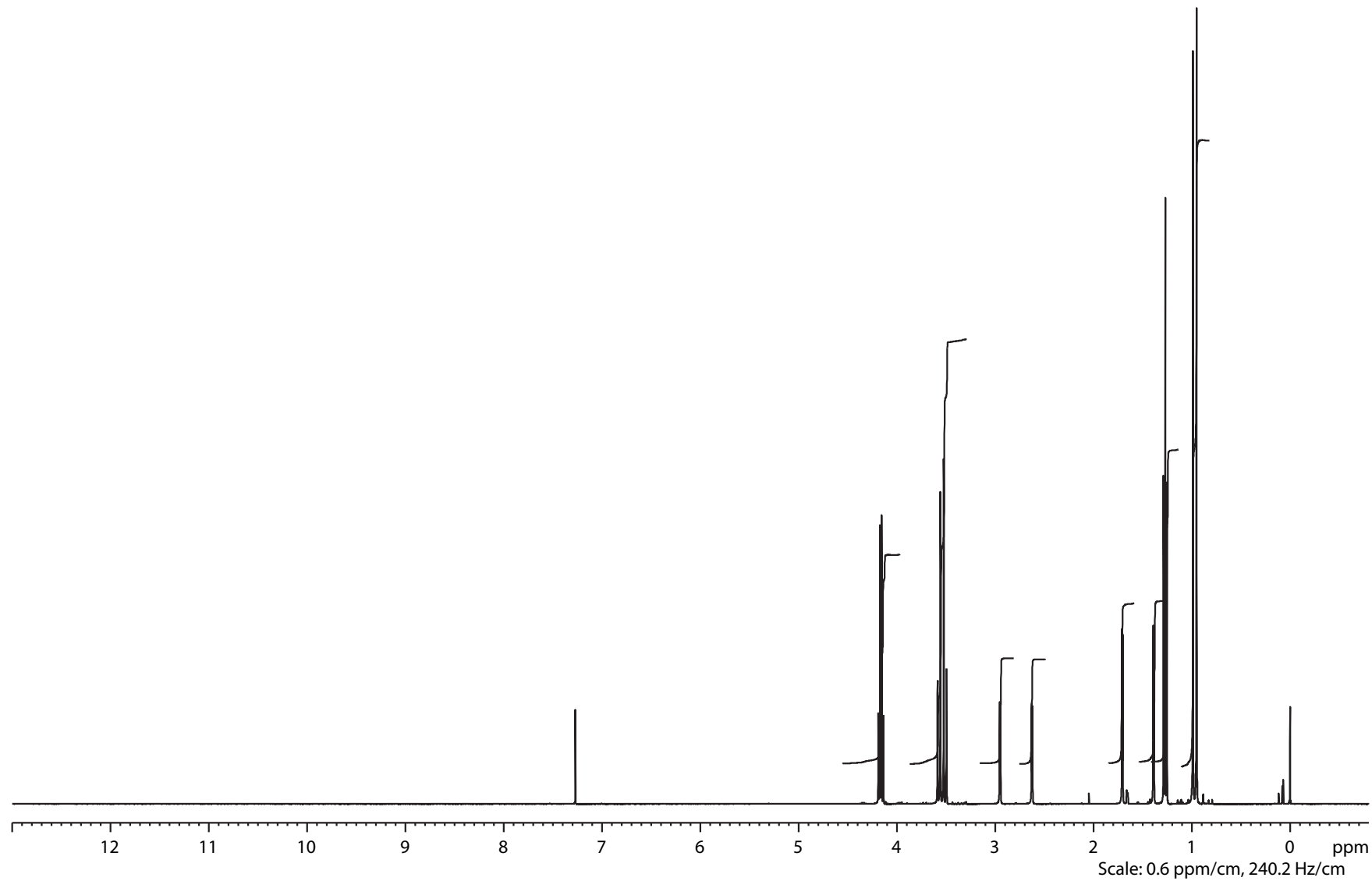


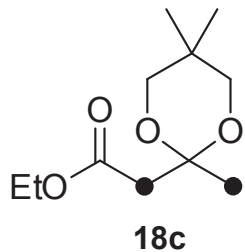
```

NAME      bae120391_od
EXPNO     1
PROCNO    1
Date_     20130410
Time      16.02
INSTRUM   AVIII400
PROBHD    5 mm PABBO BB-
PULPROG   zg30
TD         65536
SOLVENT   CDCl3
NS         64
DS         2
SWH        8223.685 Hz
FIDRES     0.125483 Hz
AQ         3.9846387 sec
RG         71.8
DW         60.800 usec
DE         6.50 usec
TE         296.7 K
D1         1.00000000 sec
TD0        1
  
```

```

===== CHANNEL f1 =====
NUC1      1H
P1         10.33 usec
PL1        -4.00 dB
SFO1      400.4024726 MHz
SI         32768
SF         400.4000140 MHz
SR         13.96 Hz
WDW        EM
SSB        0
LB         0.00 Hz
GB         0
PC         1.40
F1P        13.000 ppm
F2P        -0.800 ppm
  
```





```

NAME      bae120391_od
EXPNO     2
PROCNO    1
Date_     20130410
Time      20.00
INSTRUM   AVIII400
PROBHD    5 mm PABBO BB-
PULPROG   zgpg30
TD         131072
SOLVENT   CDCl3
NS         3072
DS         4
SWH        26315.789 Hz
FIDRES     0.200774 Hz
AQ         2.4904180 sec
RG         71.8
DW         19.000 usec
DE         6.50 usec
TE         298.2 K
D1         2.00000000 sec
D11        0.03000000 sec
TD0        1

```

```

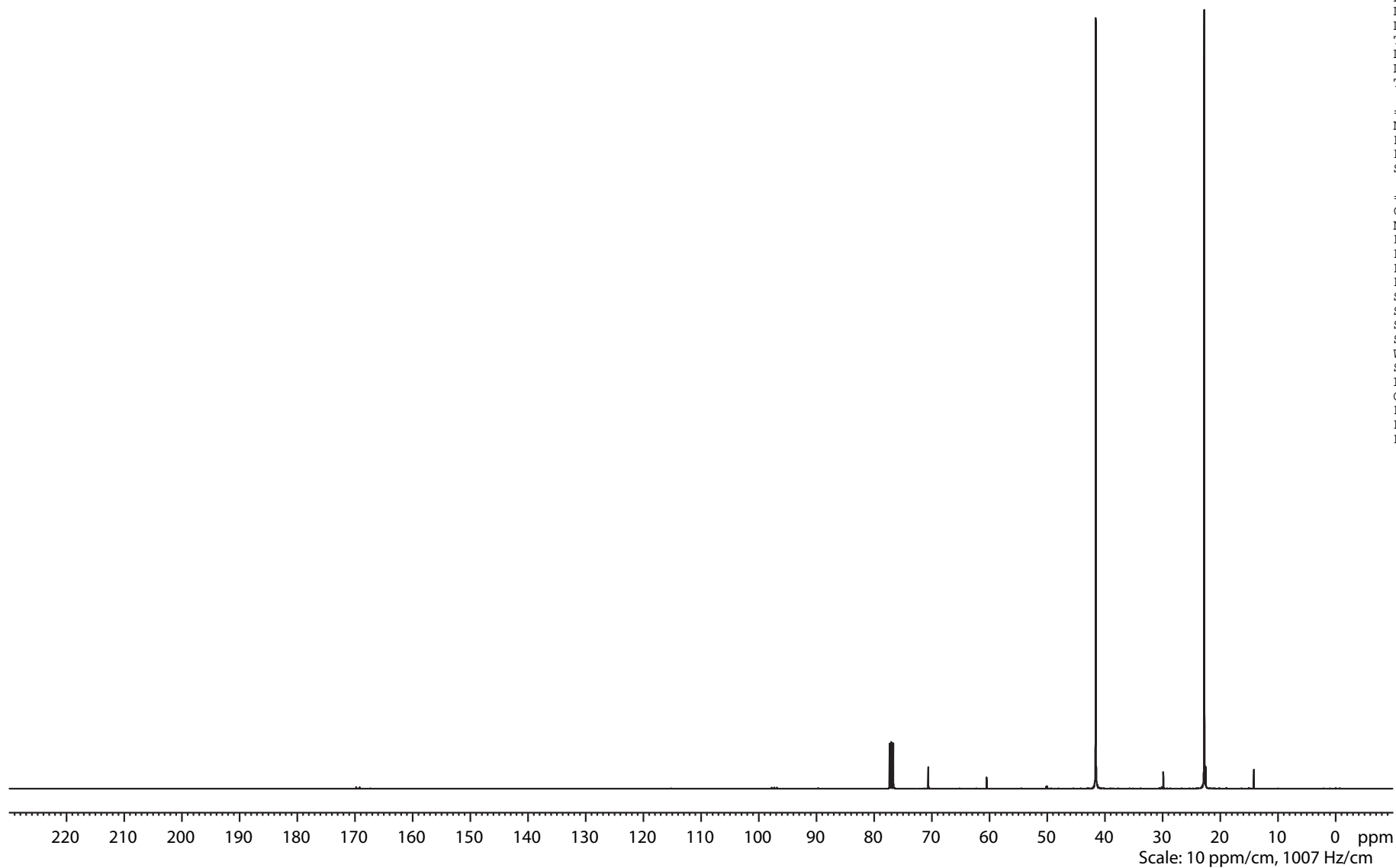
===== CHANNEL f1 =====
NUC1       13C
P1         8.50 usec
PL1        -3.00 dB
SFO1       100.6918371 MHz

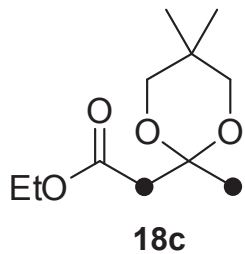
```

```

===== CHANNEL f2 =====
CPDPRG2    waltz16
NUC2       1H
PCPD2      80.00 usec
PL2        -4.00 dB
PL12       13.78 dB
PL13       14.00 dB
SFO2       400.4016016 MHz
SI         65536
SF         100.6806641 MHz
SR         3.14 Hz
WDW        EM
SSB        0
LB         1.00 Hz
GB         0
PC         1.40
F1P        230.000 ppm
F2P        -10.000 ppm

```





```

NAME      bae120391_od
EXPNO     3
PROCNO    1
Date_     20130410
Time      20.44
INSTRUM   AVIII400
PROBHD    5 mm PABBO BB-
PULPROG   dept135
TD         131072
SOLVENT   CDCl3
NS         512
DS         4
SWH        26315.789 Hz
FIDRES     0.200774 Hz
AQ         2.4904180 sec
RG         2050
DW         19.000 usec
DE         6.50 usec
TE         297.5 K
CNST2     145.0000000
D1         2.00000000 sec
D2         0.00344828 sec
D12        0.00002000 sec
TD0        1

```

```

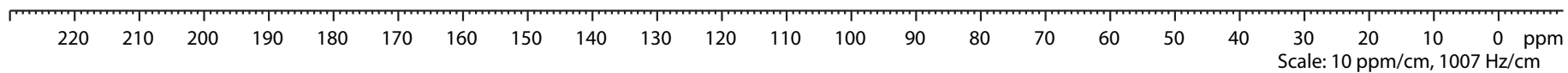
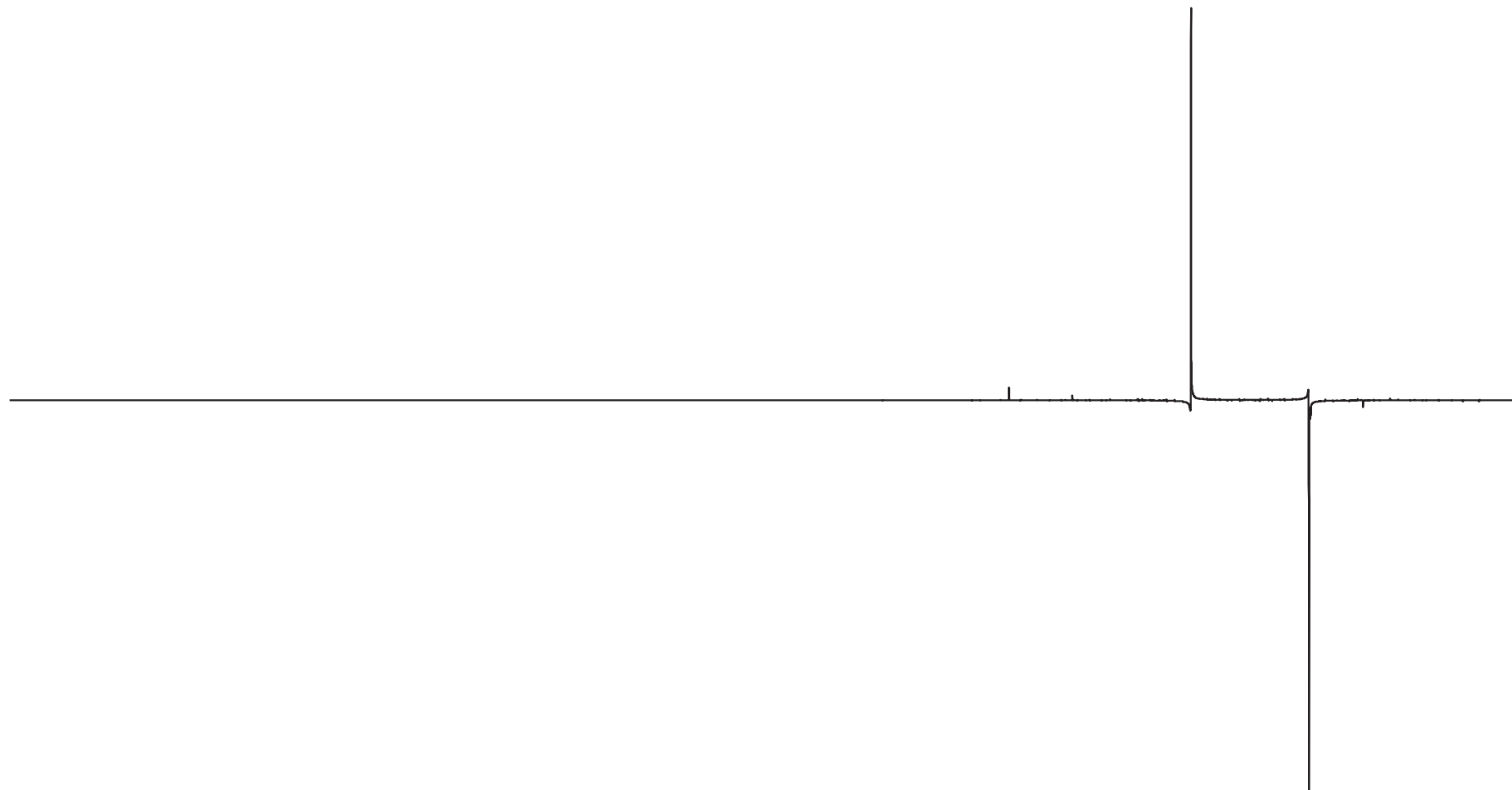
===== CHANNEL f1 =====
NUC1       13C
P1         8.50 usec
P2         17.00 usec
PL1        -3.00 dB
SFO1       100.6919063 MHz

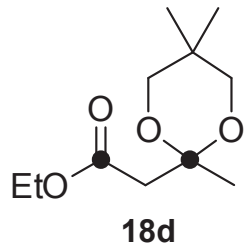
```

```

===== CHANNEL f2 =====
CPDPRG2    waltz16
NUC2        1H
P3          10.33 usec
P4          20.66 usec
PCPD2       80.00 usec
PL2         -4.00 dB
PL12        13.78 dB
SFO2        400.4016016 MHz
SI          65536
SF          100.6806578 MHz
SR          -3.20 Hz
WDW         EM
SSB         0
LB          1.00 Hz
GB          0
PC          1.40
F1P         230.000 ppm
F2P         -10.000 ppm

```



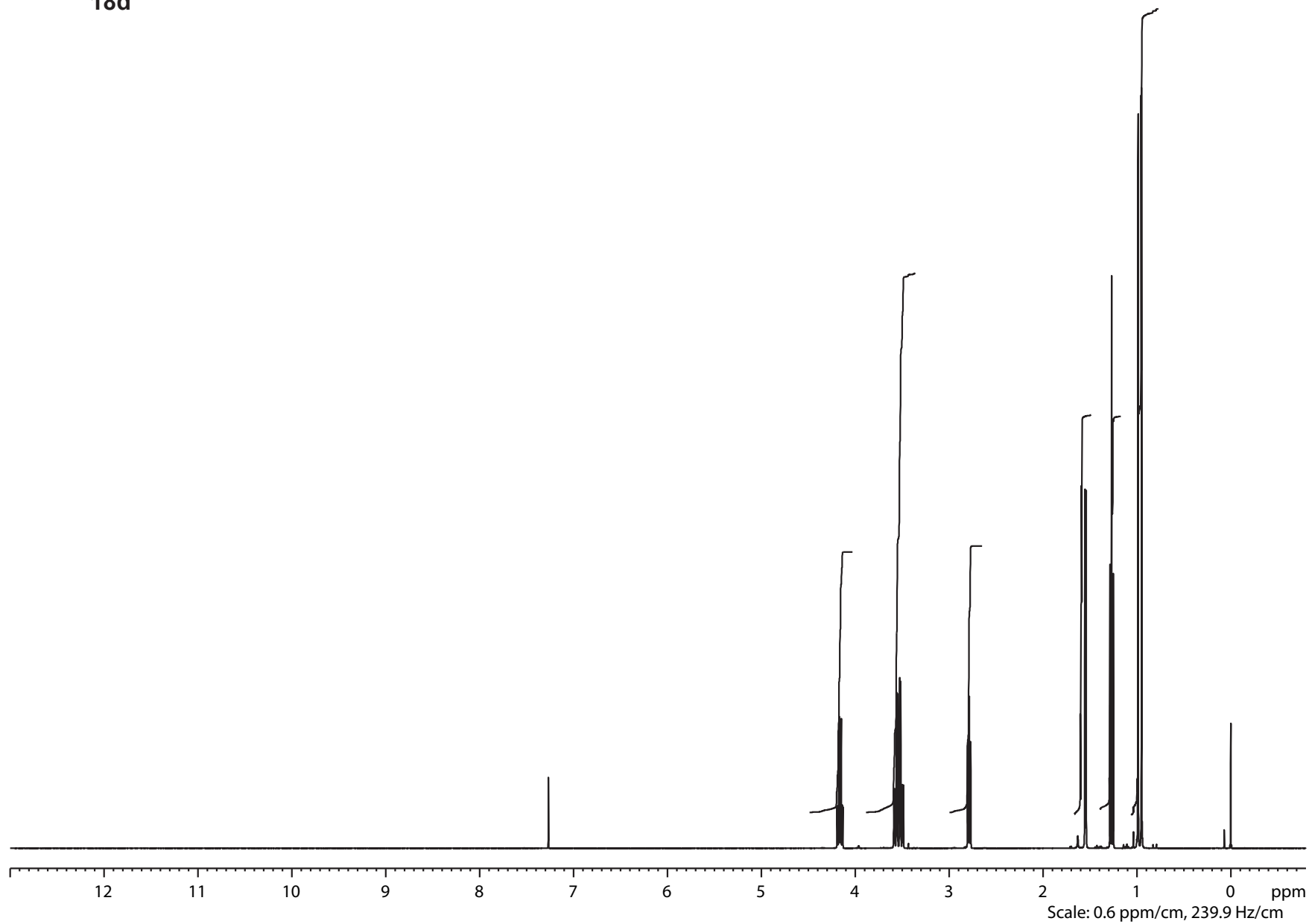


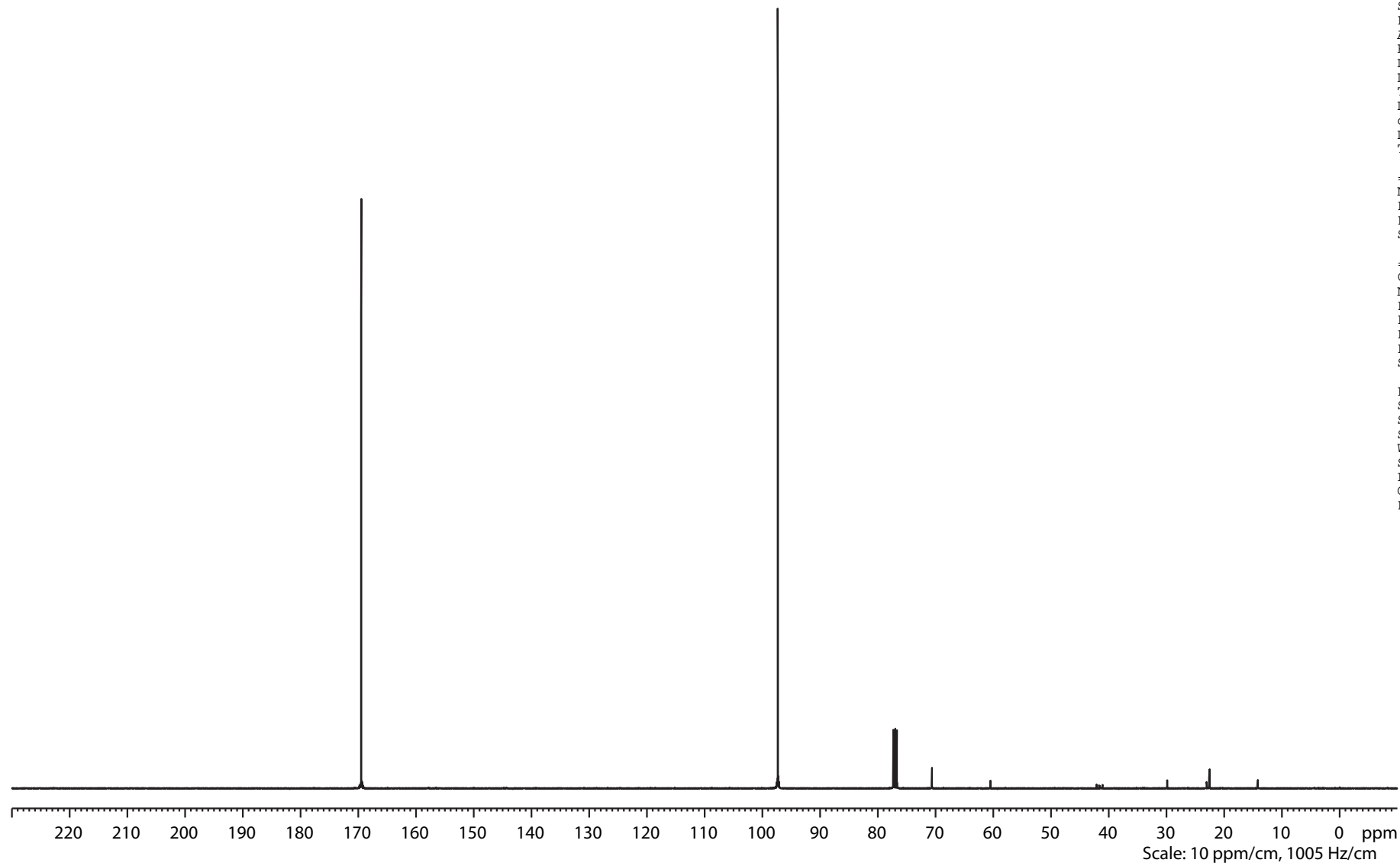
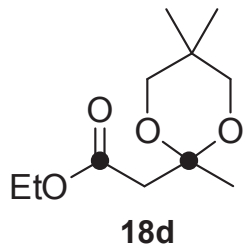
Current Data Parameters
 NAME bae121723_od
 EXPNO 1
 PROCNO 1

F2 - Acquisition Parameters
 Date_ 20130822
 Time 8.45
 INSTRUM drx400
 PROBHD 5 mm QNP 1H/13
 PULPROG zg30
 TD 65536
 SOLVENT CDCl3
 NS 64
 DS 2
 SWH 8278.146 Hz
 FIDRES 0.126314 Hz
 AQ 3.9584243 sec
 RG 114
 DW 60.400 usec
 DE 6.00 usec
 TE 299.2 K
 D1 1.00000000 sec
 TD0 1

==== CHANNEL f1 =====
 NUC1 1H
 P1 10.20 usec
 PL1 -2.00 dB
 SFO1 399.8724688 MHz

F2 - Processing parameters
 SI 32768
 SF 399.8700109 MHz
 SR 10.91 Hz
 WDW EM
 SSB 0
 LB 0.00 Hz
 GB 0
 PC 1.40





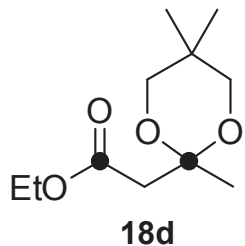
Current Data Parameters
 NAME bae121723_od
 EXPNO 2
 PROCNO 1

F2 - Acquisition Parameters
 Date_ 20130822
 Time 9.06
 INSTRUM drx400
 PROBHD 5 mm QNP 1H/13
 PULPROG zgpg30
 TD 131072
 SOLVENT CDCl3
 NS 960
 DS 4
 SWH 26315.789 Hz
 FIDRES 0.200774 Hz
 AQ 2.4904180 sec
 RG 8192
 DW 19.000 usec
 DE 6.00 usec
 TE 300.2 K
 D1 2.00000000 sec
 d11 0.03000000 sec
 DELTA 1.89999998 sec
 TD0 1

==== CHANNEL f1 =====
 NUC1 13C
 P1 11.00 usec
 PL1 -3.00 dB
 SFO1 100.5585542 MHz

==== CHANNEL f2 =====
 CPDPRG2 waltz16
 NUC2 1H
 PCPD2 80.00 usec
 PL2 -2.00 dB
 PL12 16.06 dB
 PL13 16.06 dB
 SFO2 399.8715995 MHz

F2 - Processing parameters
 SI 65536
 SF 100.5473939 MHz
 SR 1.89 Hz
 WDW EM
 SSB 0
 LB 1.00 Hz
 GB 0
 PC 1.40



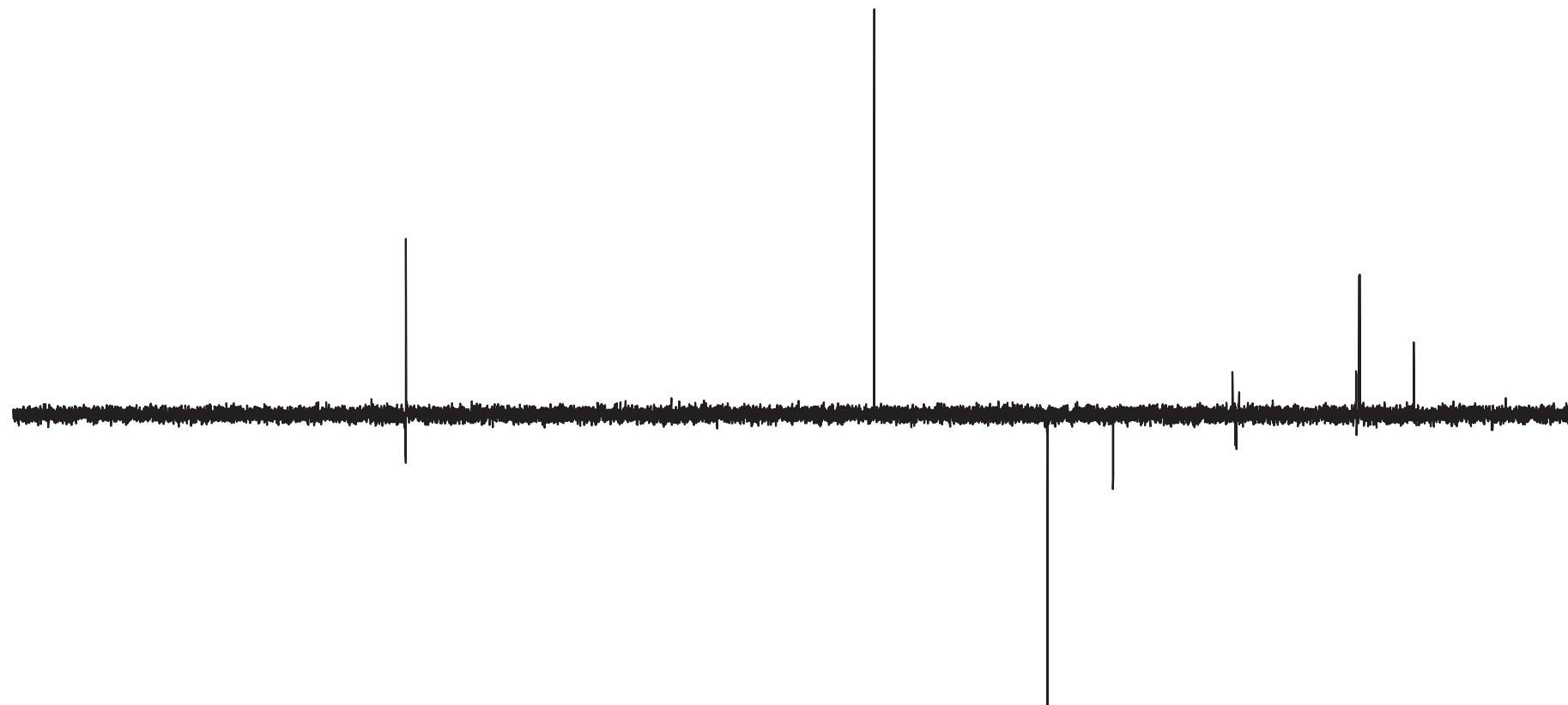
Current Data Parameters
 NAME bae121723_od
 EXPNO 3
 PROCNO 1

F2 - Acquisition Parameters
 Date_ 20130822
 Time 10.04
 INSTRUM drx400
 PROBHD 5 mm QNP 1H/13
 PULPROG dept135
 TD 131072
 SOLVENT CDCl3
 NS 160
 DS 4
 SWH 26315.789 Hz
 FIDRES 0.200774 Hz
 AQ 2.4904180 sec
 RG 9195.2
 DW 19.000 usec
 DE 7.00 usec
 TE 300.2 K
 CNST2 145.0000000
 D1 2.00000000 sec
 d2 0.00344828 sec
 d12 0.00002000 sec
 DELTA 0.00001401 sec
 TD0 1

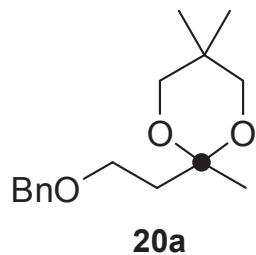
==== CHANNEL f1 =====
 NUC1 13C
 P1 11.00 usec
 p2 22.00 usec
 PL1 -3.00 dB
 SFO1 100.5585542 MHz

==== CHANNEL f2 =====
 CPDPRG2 waltz16
 NUC2 1H
 P3 10.00 usec
 p4 20.00 usec
 PCPD2 80.00 usec
 PL2 -2.00 dB
 PL12 16.06 dB
 SFO2 399.8715995 MHz

F2 - Processing parameters
 SI 65536
 SF 100.5473888 MHz
 SR -3.20 Hz
 WDW EM
 SSB 0
 LB 1.00 Hz
 GB 0
 PC 1.40



220 210 200 190 180 170 160 150 140 130 120 110 100 90 80 70 60 50 40 30 20 10 0 ppm
 Scale: 10 ppm/cm, 1005 Hz/cm

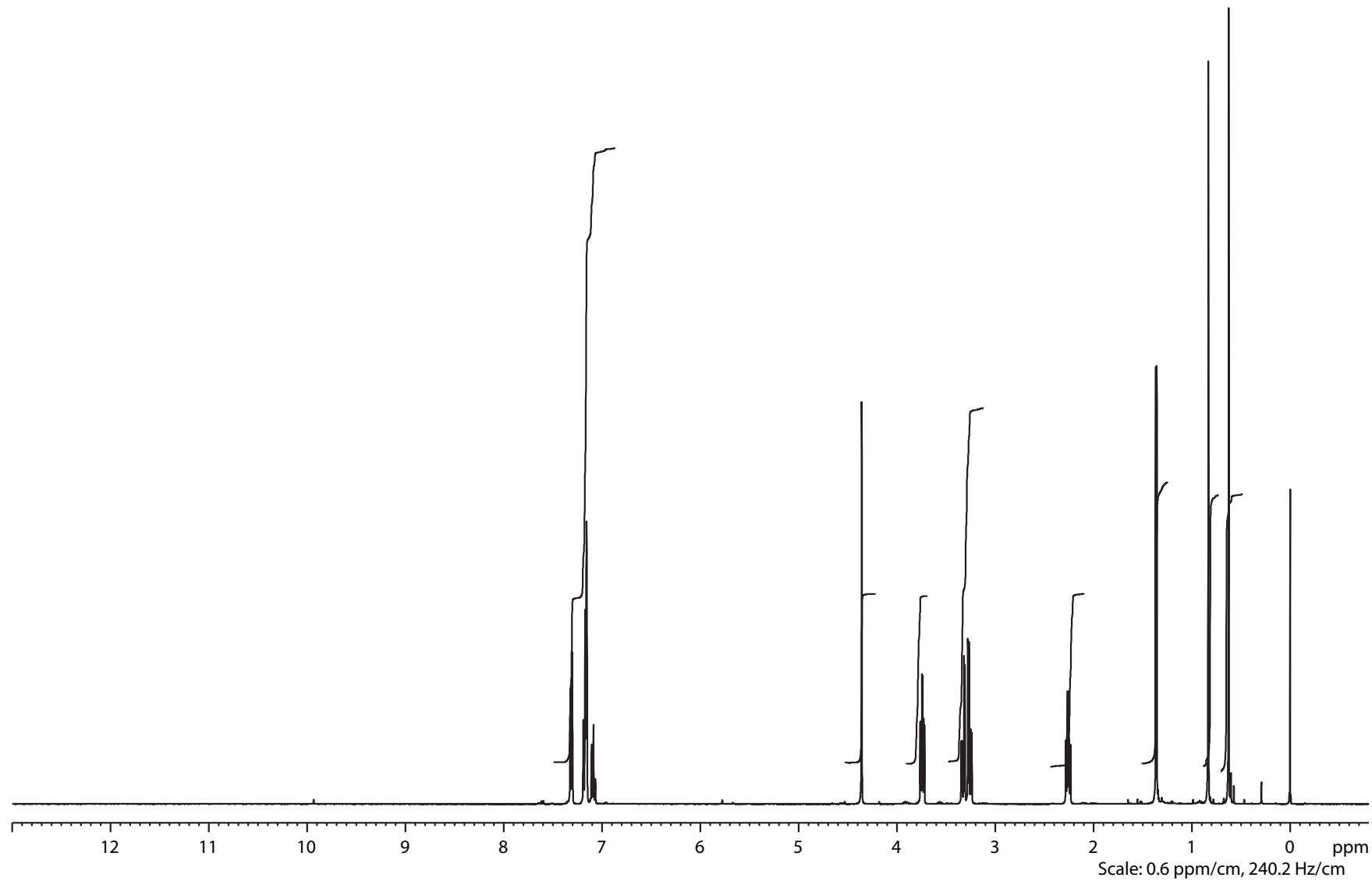


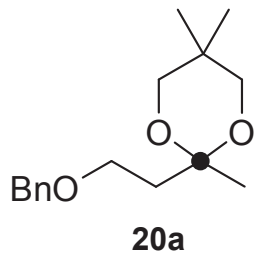
```

NAME      bae122964_od
EXPNO     1
PROCNO    1
Date_     20140120
Time      23.44
INSTRUM   AVIII400
PROBHD    5 mm PABBO BB-
PULPROG   zg30
TD         65536
SOLVENT   C6D6
NS         64
DS         2
SWH        8223.685 Hz
FIDRES     0.125483 Hz
AQ         3.9846387 sec
RG         57
DW         60.800 usec
DE         6.50 usec
TE         296.0 K
D1         1.00000000 sec
TD0        1
  
```

```

===== CHANNEL f1 =====
NUC1      1H
P1         10.33 usec
PL1        -4.00 dB
SFO1      400.4024726 MHz
SI         32768
SF         400.3999996 MHz
SR         -0.42 Hz
WDW        EM
SSB        0
LB         0.00 Hz
GB         0
PC         1.40
F1P        13.000 ppm
F2P        -0.800 ppm
  
```





```

NAME      bae122964_od
EXPNO     2
PROCNO    1
Date_     20140121
Time      2.21
INSTRUM   AVIII400
PROBHD    5 mm PABBO BB-
PULPROG   zgpg30
TD         131072
SOLVENT   C6D6
NS         2048
DS         4
SWH        26315.789 Hz
FIDRES     0.200774 Hz
AQ         2.4904180 sec
RG         80.6
DW         19.000 usec
DE         6.50 usec
TE         297.5 K
D1         2.00000000 sec
D11        0.03000000 sec
TD0        1

```

```

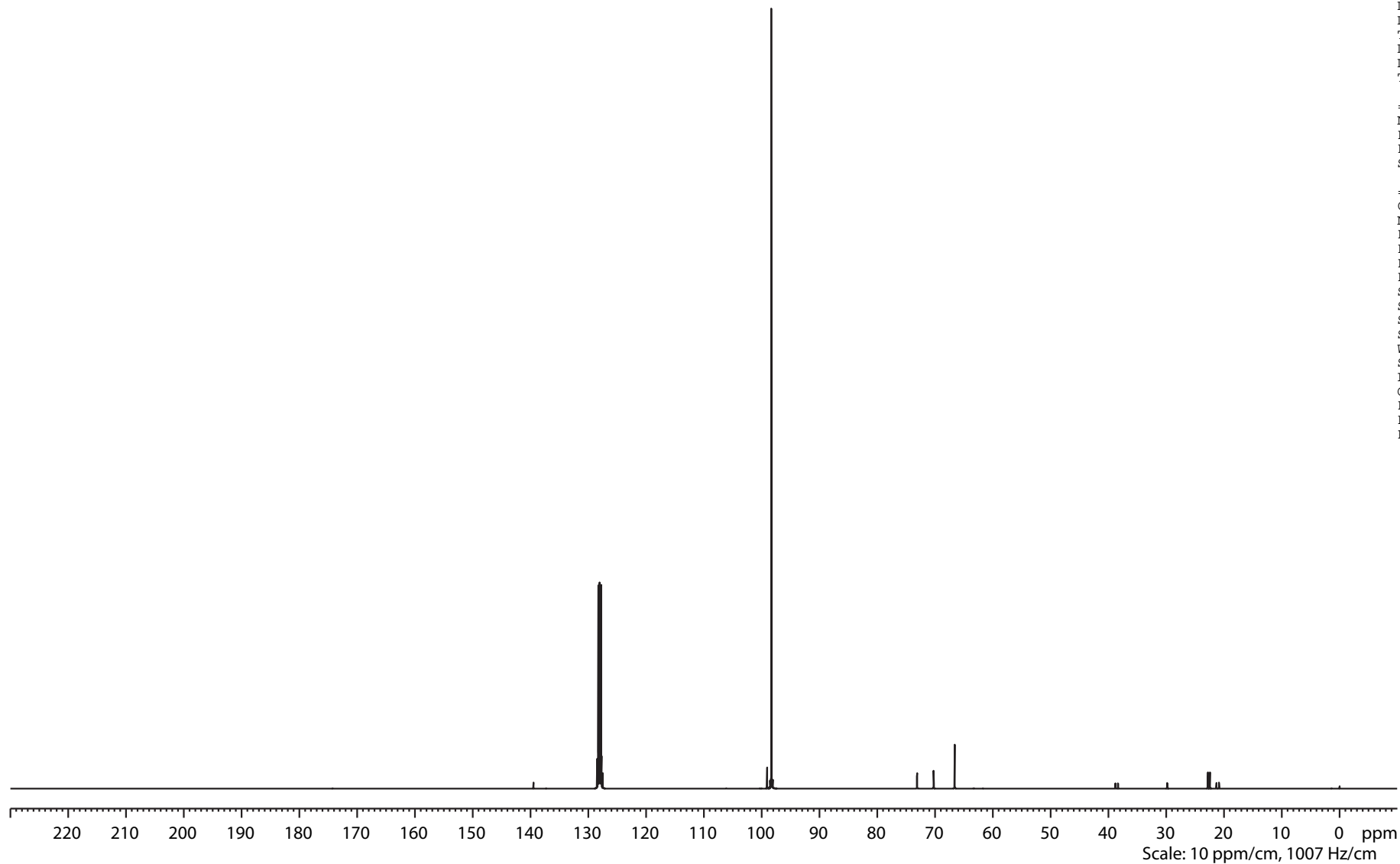
===== CHANNEL f1 =====
NUC1       13C
P1         8.50 usec
PL1        -3.00 dB
SFO1       100.6918371 MHz

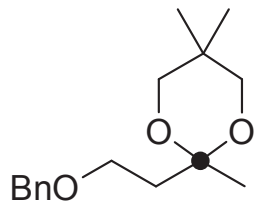
```

```

===== CHANNEL f2 =====
CPDPRG2    waltz16
NUC2       1H
PCPD2      80.00 usec
PL2        -4.00 dB
PL12       13.78 dB
PL13       14.00 dB
SFO2       400.4016016 MHz
SI         65536
SF         100.6806256 MHz
SR         -35.36 Hz
WDW        EM
SSB        0
LB         1.00 Hz
GB         0
PC         1.40
F1P        230.000 ppm
F2P        -10.000 ppm

```





20a

```

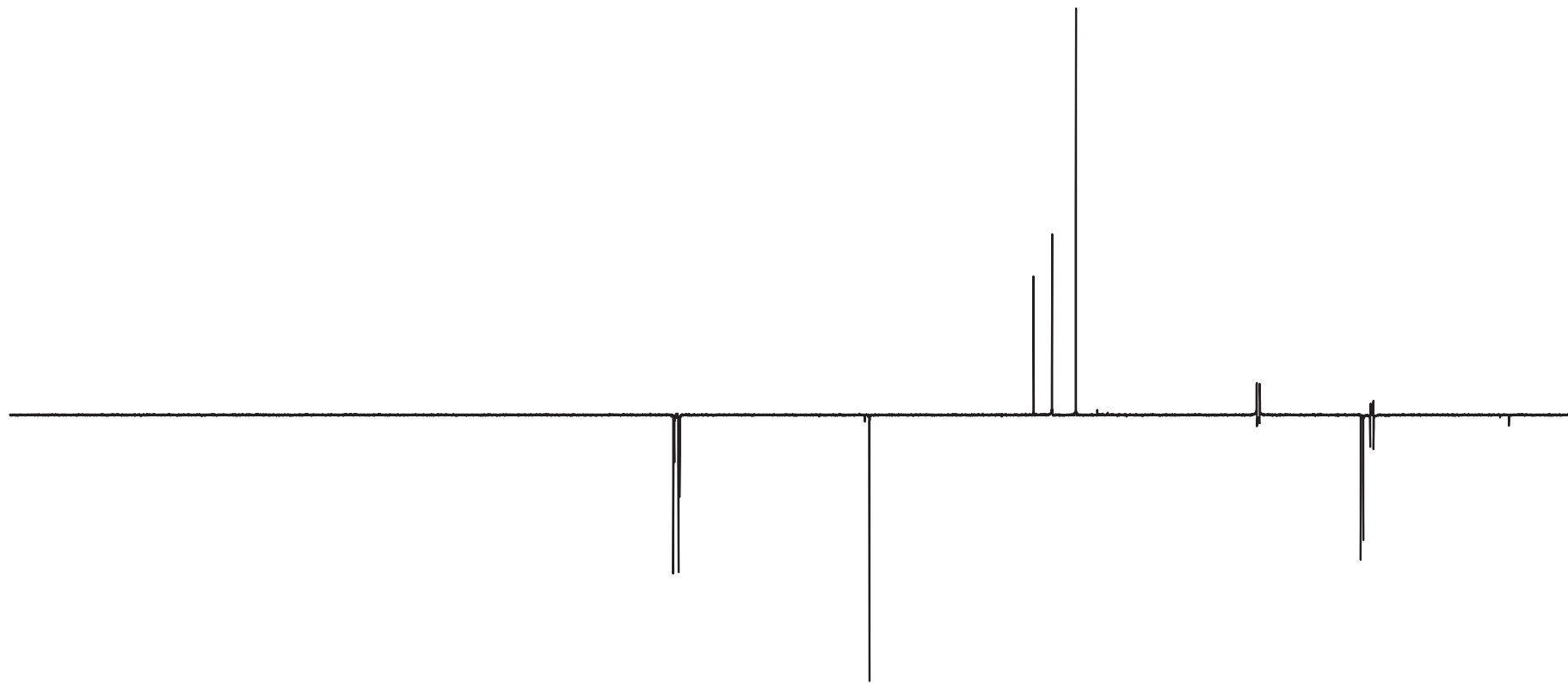
NAME      bae122964_od
EXPNO     3
PROCNO    1
Date_     20140121
Time      3.41
INSTRUM   AVIII400
PROBHD    5 mm PABBO BB-
PULPROG   dept135
TD         131072
SOLVENT   C6D6
NS         1024
DS         4
SWH        26315.789 Hz
FIDRES     0.200774 Hz
AQ         2.4904180 sec
RG         2050
DW         19.000 usec
DE         6.50 usec
TE         296.7 K
CNST2     145.0000000
D1         2.00000000 sec
D2         0.00344828 sec
D12        0.00002000 sec
TD0        1
  
```

```

===== CHANNEL f1 =====
NUC1       13C
P1         8.50 usec
P2         17.00 usec
PL1        -3.00 dB
SFO1       100.6919063 MHz
  
```

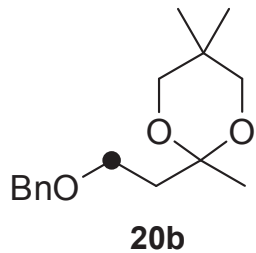
```

===== CHANNEL f2 =====
CPDPRG2    waltz16
NUC2       1H
P3         10.33 usec
P4         20.66 usec
PCPD2      80.00 usec
PL2        -4.00 dB
PL12       13.78 dB
SFO2       400.4016016 MHz
SI         65536
SF         100.6806731 MHz
SR         12.12 Hz
WDW        EM
SSB        0
LB         1.00 Hz
GB         0
PC         1.40
F1P        230.000 ppm
F2P        -10.000 ppm
  
```



220 210 200 190 180 170 160 150 140 130 120 110 100 90 80 70 60 50 40 30 20 10 0 ppm

Scale: 10 ppm/cm, 1007 Hz/cm



```

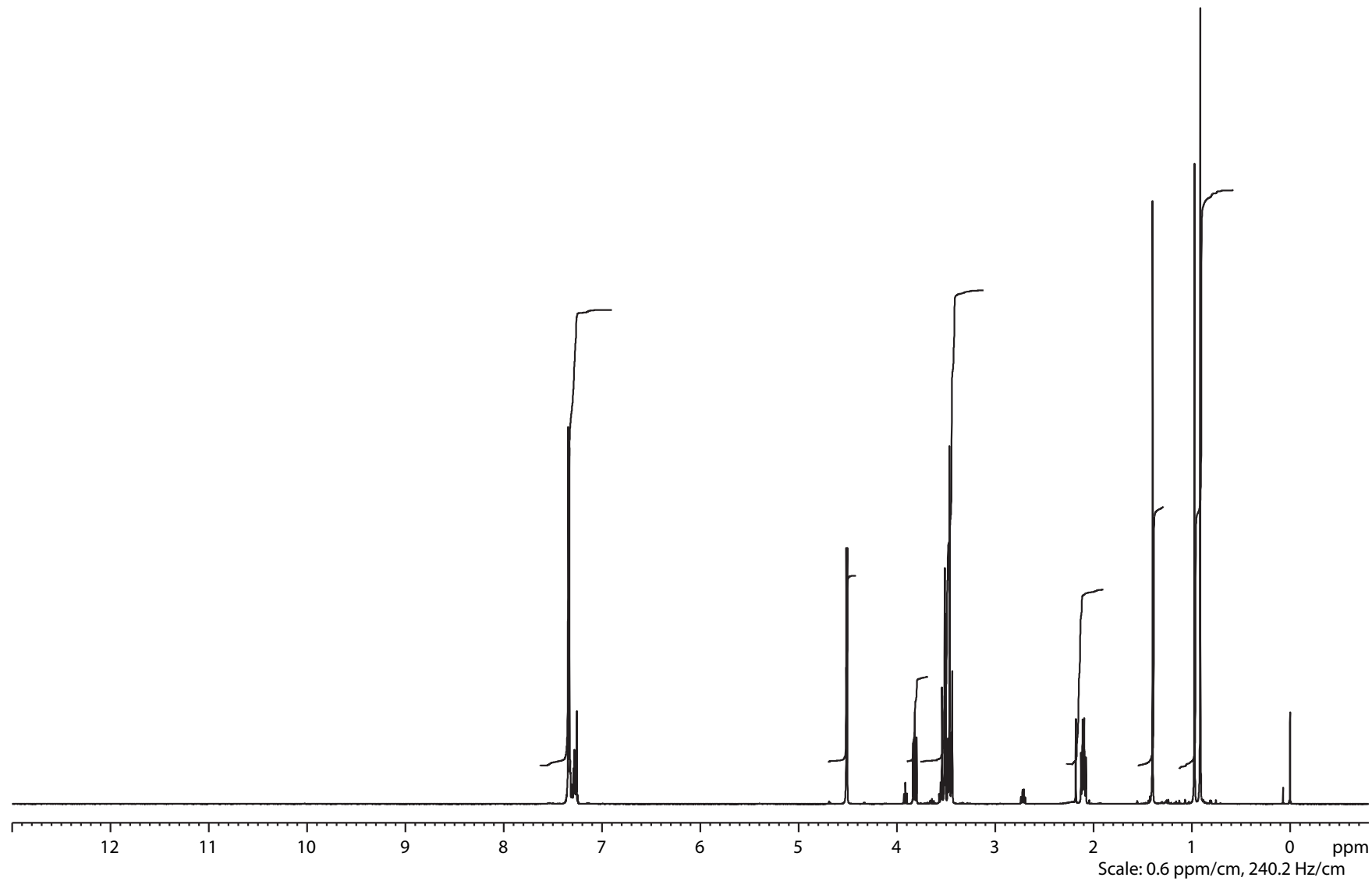
NAME      bae120166_od
EXPNO     1
PROCNO    1
Date_     20130319
Time      19.33
INSTRUM   AVIII400
PROBHD    5 mm PABBO BB-
PULPROG   zg30
TD         65536
SOLVENT   CDCl3
NS         64
DS         2
SWH        8223.685 Hz
FIDRES     0.125483 Hz
AQ         3.9846387 sec
RG         64
DW         60.800 usec
DE         6.50 usec
TE         296.2 K
D1         1.00000000 sec
TD0        1

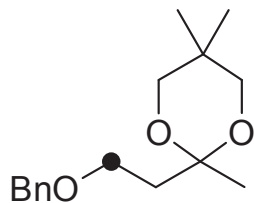
```

```

===== CHANNEL f1 =====
NUC1       1H
P1         10.33 usec
PL1        -4.00 dB
SFO1       400.4024726 MHz
SI         32768
SF         400.4000200 MHz
SR         20.01 Hz
WDW        EM
SSB        0
LB         0.00 Hz
GB         0
PC         1.40
F1P        13.000 ppm
F2P        -0.800 ppm

```



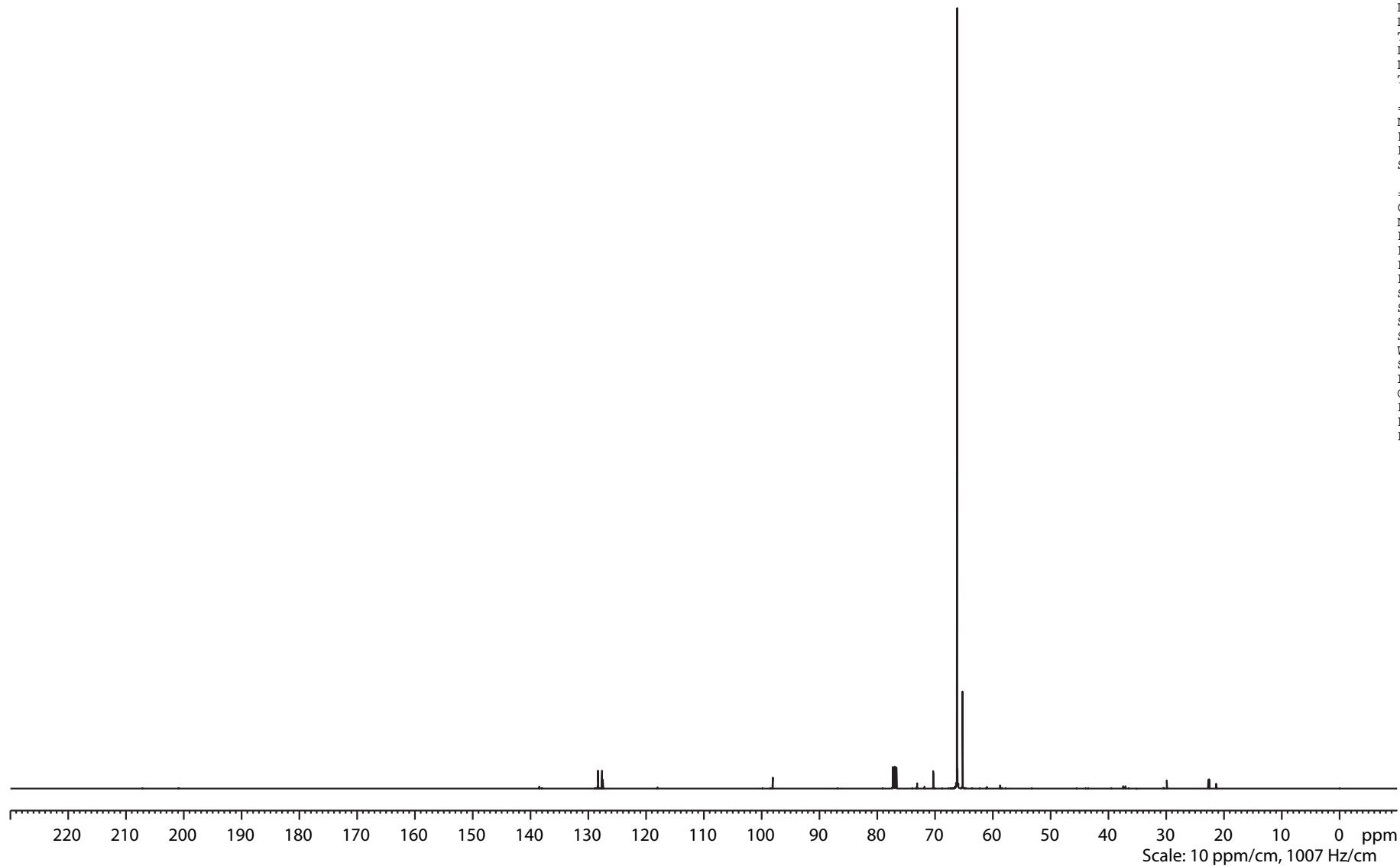


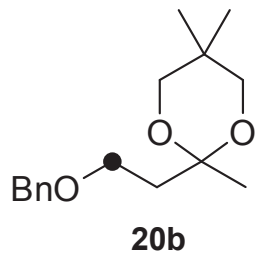
20b

NAME bae120166_od
EXPNO 2
PROCNO 1
Date_ 20130319
Time_ 20.53
INSTRUM AVIII400
PROBHD 5 mm PABBO BB-
PULPROG zgpg30
TD 131072
SOLVENT CDCl3
NS 1024
DS 4
SWH 26315.789 Hz
FIDRES 0.200774 Hz
AQ 2.4904180 sec
RG 90.5
DW 19.000 usec
DE 6.50 usec
TE 297.5 K
D1 2.00000000 sec
D11 0.03000000 sec
TD0 1

==== CHANNEL f1 =====
NUC1 13C
P1 8.50 usec
PL1 -3.00 dB
SFO1 100.6918371 MHz

==== CHANNEL f2 =====
CPDPRG2 waltz16
NUC2 1H
PCPD2 80.00 usec
PL2 -4.00 dB
PL12 13.78 dB
PL13 14.00 dB
SFO2 400.4016016 MHz
SI 65536
SF 100.6806650 MHz
SR 4.00 Hz
WDW EM
SSB 0
LB 1.00 Hz
GB 0
PC 1.40
F1P 230.000 ppm
F2P -10.000 ppm





```

NAME      bae120166_od
EXPNO     3
PROCNO    1
Date_     20130319
Time      21.02
INSTRUM   AVIII400
PROBHD    5 mm PABBO BB-
PULPROG   dept135
TD         131072
SOLVENT   CDCl3
NS         96
DS         4
SWH        26315.789 Hz
FIDRES     0.200774 Hz
AQ         2.4904180 sec
RG         2050
DW         19.000 usec
DE         6.50 usec
TE         296.9 K
CNST2     145.0000000
D1         2.00000000 sec
D2         0.00344828 sec
D12        0.00002000 sec
TD0        5

```

```

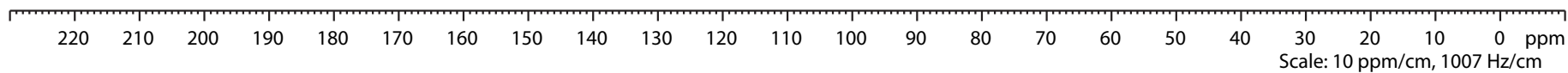
===== CHANNEL f1 =====
NUC1       13C
P1         8.50 usec
P2         17.00 usec
PL1        -3.00 dB
SFO1       100.6918371 MHz

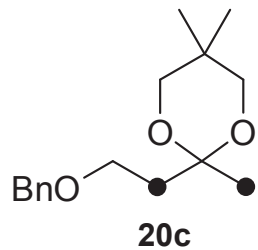
```

```

===== CHANNEL f2 =====
CPDPRG2    waltz16
NUC2       1H
P3         10.33 usec
P4         20.66 usec
PCPD2      80.00 usec
PL2        -4.00 dB
PL12       13.78 dB
SFO2       400.4016016 MHz
SI         65536
SF         100.6806578 MHz
SR         -3.20 Hz
WDW        EM
SSB        0
LB         1.00 Hz
GB         0
PC         1.40
F1P        230.000 ppm
F2P        -10.000 ppm

```



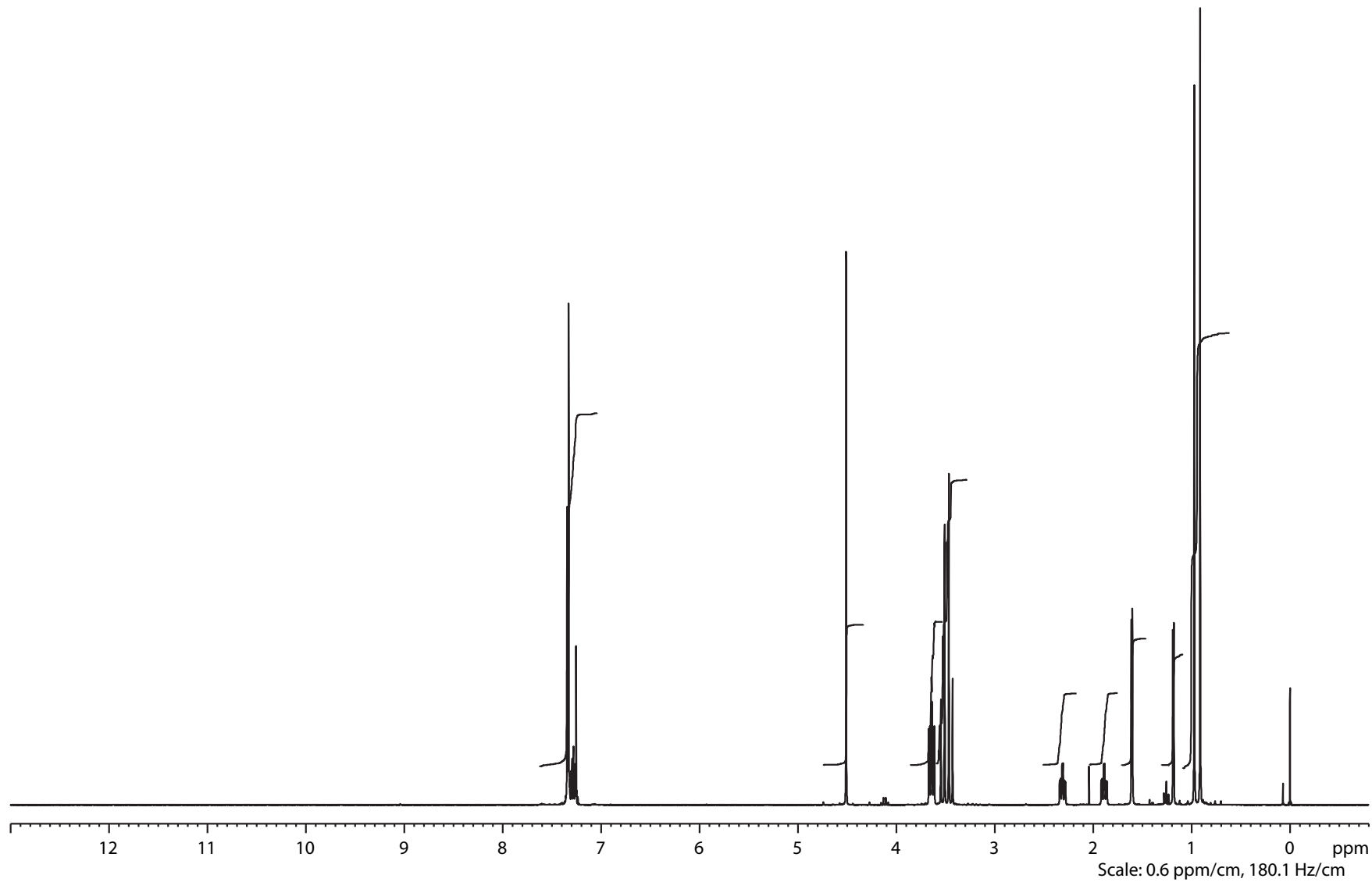


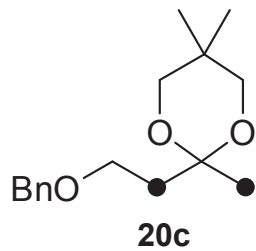
```

NAME      bae-130412-194108_od
EXPNO     1
PROCNO    1
Date_     20130412
Time      19.50
INSTRUM   av300
PROBHD    5 mm PABBO BB-
PULPROG   zg30
TD         49152
SOLVENT   CDCl3
NS         32
DS         2
SWH        6203.474 Hz
FIDRES     0.126210 Hz
AQ         3.9617012 sec
RG         128
DW         80.600 usec
DE         6.00 usec
TE         298.2 K
D1         1.00000000 sec
TD0        1
  
```

```

===== CHANNEL f1 =====
NUC1       1H
P1         12.00 usec
PL1        -1.00 dB
SFO1       300.1318530 MHz
SI         32768
SF         300.1300137 MHz
SR         13.68 Hz
WDW        EM
SSB        0
LB         0.00 Hz
GB         0
PC         1.40
F1P        13.000 ppm
F2P        -0.800 ppm
  
```





```

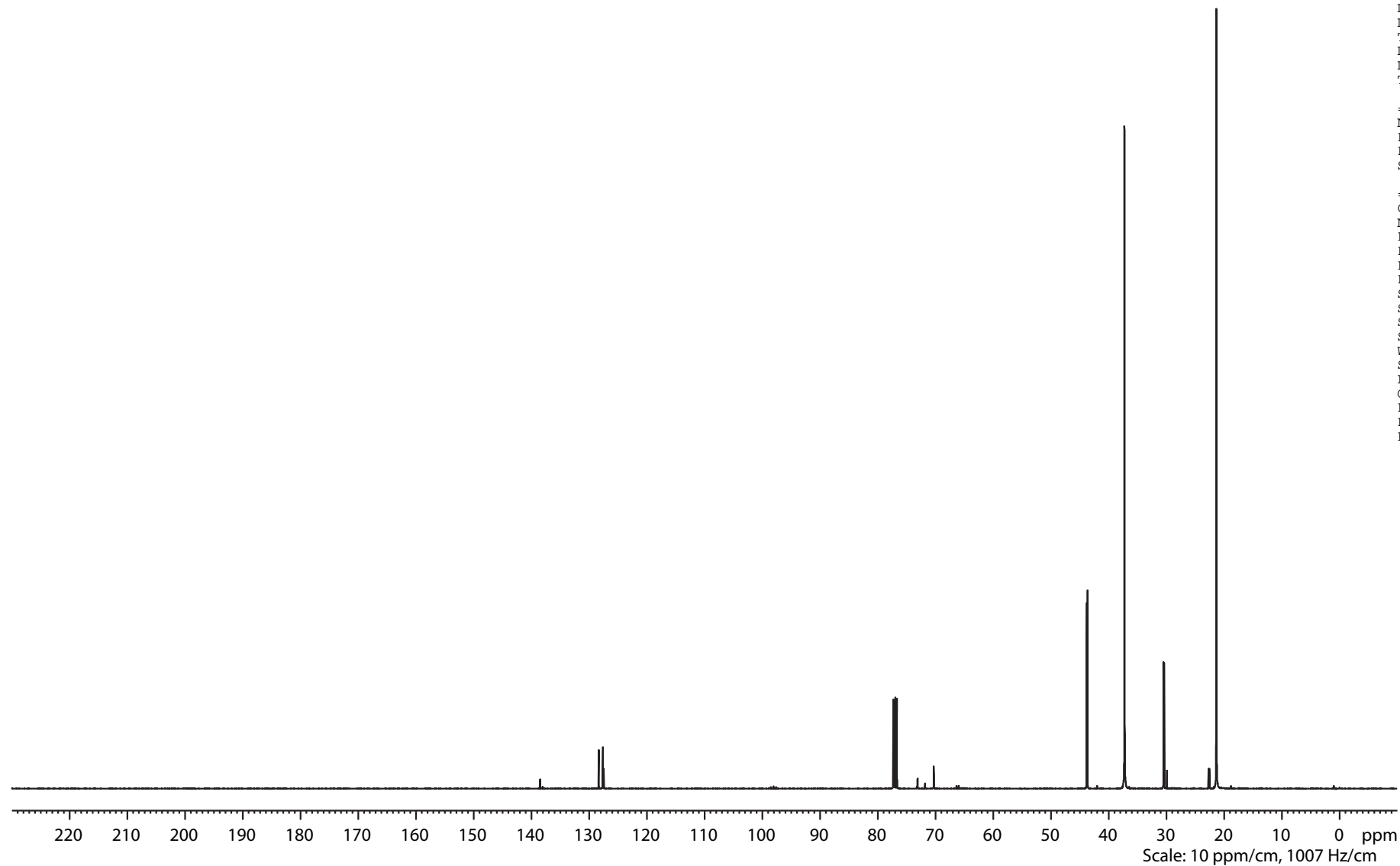
NAME      bae120505_od
EXPNO     2
PROCNO    1
Date_     20130418
Time      10.36
INSTRUM   AVIII400
PROBHD    5 mm PABBO BB-
PULPROG   zgpg30
TD         131072
SOLVENT   CDCl3
NS         3072
DS         4
SWH        26315.789 Hz
FIDRES     0.200774 Hz
AQ         2.4904180 sec
RG         80.6
DW         19.000 usec
DE         6.50 usec
TE         298.8 K
D1         2.00000000 sec
D11        0.03000000 sec
TD0        1
  
```

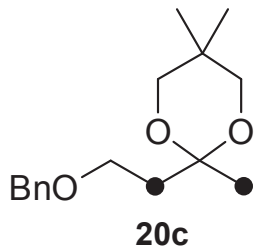
```

===== CHANNEL f1 =====
NUC1       13C
P1         8.50 usec
PL1        -3.00 dB
SFO1       100.6918371 MHz
  
```

```

===== CHANNEL f2 =====
CPDPRG2    waltz16
NUC2        1H
PCPD2       80.00 usec
PL2         -4.00 dB
PL12        13.78 dB
PL13        14.00 dB
SFO2        400.4016016 MHz
SI          65536
SF          100.6806645 MHz
SR           3.45 Hz
WDW         EM
SSB         0
LB           1.00 Hz
GB           0
PC           1.40
F1P         230.000 ppm
F2P         -10.000 ppm
  
```





```

NAME      bae120505_od
EXPNO     3
PROCNO    1
Date_     20130418
Time      10.45
INSTRUM   AVIII400
PROBHD    5 mm PABBO BB-
PULPROG   dept135
TD         131072
SOLVENT   CDCl3
NS         96
DS         4
SWH        26315.789 Hz
FIDRES     0.200774 Hz
AQ         2.4904180 sec
RG         2050
DW         19.000 usec
DE         6.50 usec
TE         298.3 K
CNST2     145.0000000
D1         2.00000000 sec
D2         0.00344828 sec
D12        0.00002000 sec
TD0        5

```

```

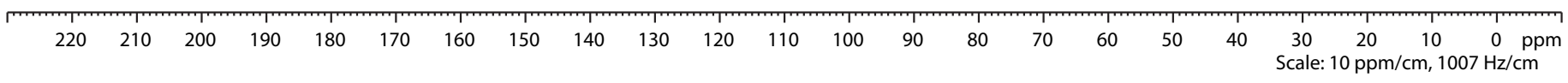
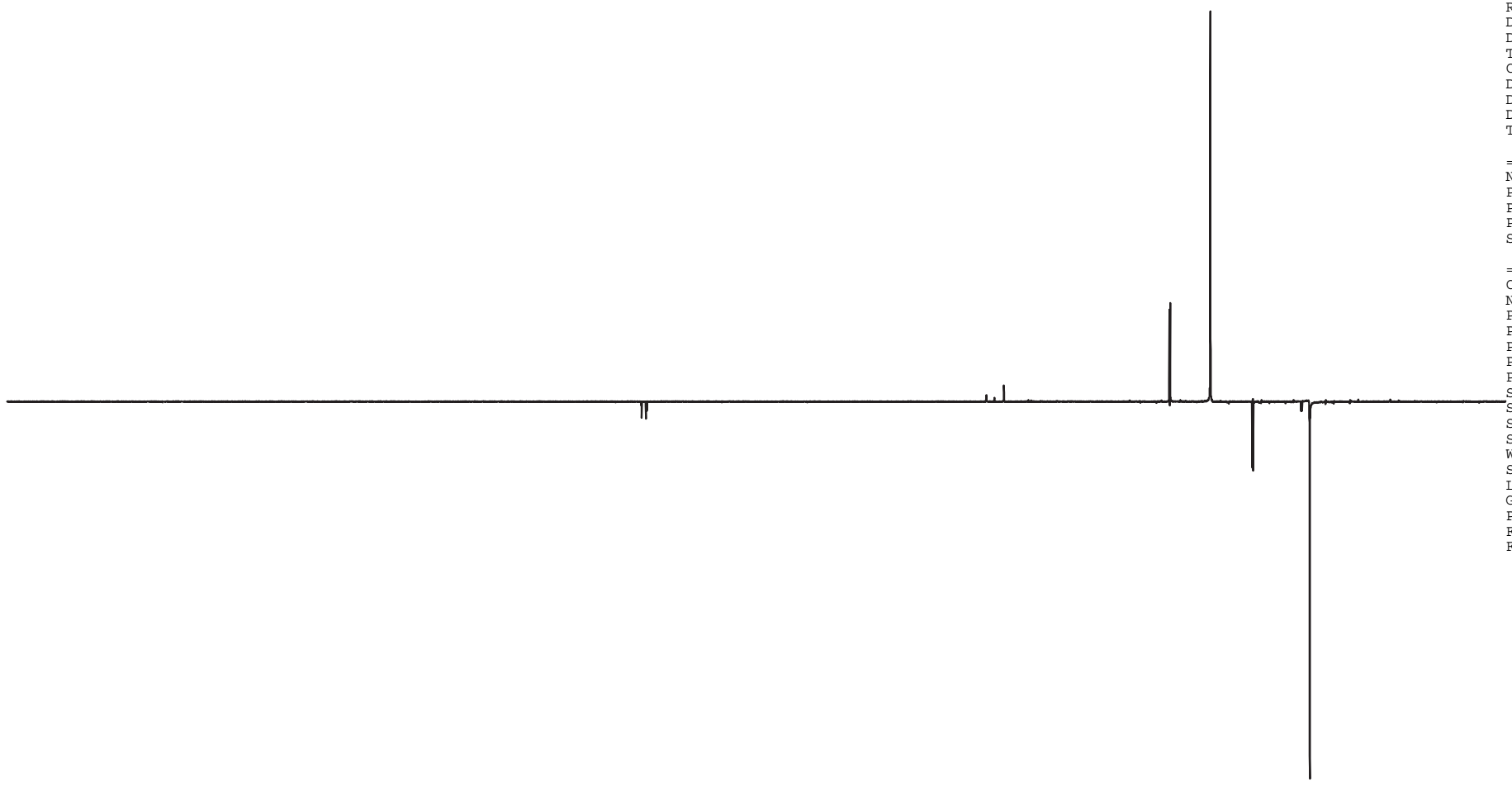
===== CHANNEL f1 =====
NUC1       13C
P1         8.50 usec
P2         17.00 usec
PL1        -3.00 dB
SFO1       100.6918371 MHz

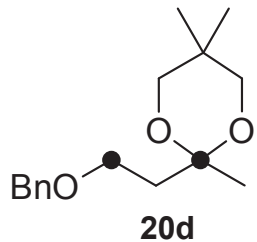
```

```

===== CHANNEL f2 =====
CPDPRG2    waltz16
NUC2        1H
P3          10.33 usec
P4          20.66 usec
PCPD2       80.00 usec
PL2         -4.00 dB
PL12        13.78 dB
SFO2        400.4016016 MHz
SI          65536
SF          100.6806578 MHz
SR          -3.20 Hz
WDW         EM
SSB         0
LB          1.00 Hz
GB          0
PC          1.40
F1P         230.000 ppm
F2P         -10.000 ppm

```





```

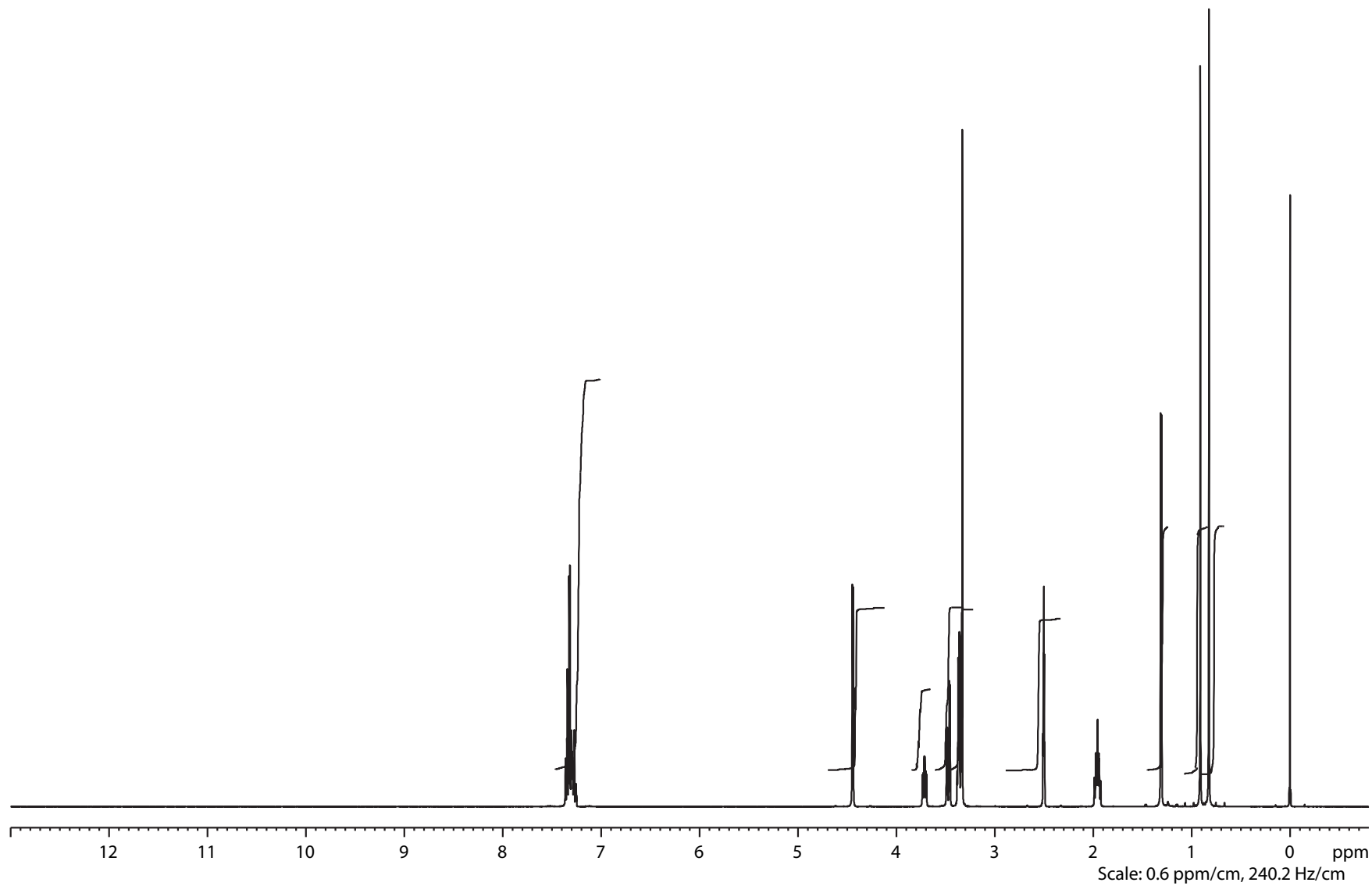
NAME      bae122468_od
EXPNO     1
PROCNO    1
Date_     20131104
Time      18.48
INSTRUM   AVIII400
PROBHD    5 mm PABBO BB-
PULPROG   zg30
TD         65536
SOLVENT   DMSO
NS         64
DS         2
SWH        8223.685 Hz
FIDRES     0.125483 Hz
AQ         3.9846387 sec
RG         114
DW         60.800 usec
DE         6.50 usec
TE         296.8 K
D1         1.00000000 sec
TD0        1

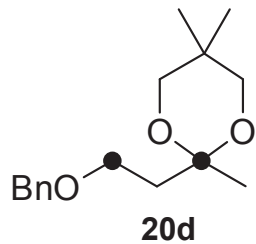
```

```

===== CHANNEL f1 =====
NUC1      1H
P1        10.33 usec
PL1       -4.00 dB
SFO1      400.4024726 MHz
SI         32768
SF         400.4000046 MHz
SR         4.61 Hz
WDW        EM
SSB        0
LB         0.00 Hz
GB         0
PC         1.40
F1P        13.000 ppm
F2P        -0.800 ppm

```





```

NAME      bae122468_od
EXPNO     2
PROCNO    1
Date_     20131104
Time      20.08
INSTRUM   AVIII400
PROBHD    5 mm PABBO BB-
PULPROG   zgpg30
TD         131072
SOLVENT   DMSO
NS         1024
DS         4
SWH        26315.789 Hz
FIDRES     0.200774 Hz
AQ         2.4904180 sec
RG         101
DW         19.000 usec
DE         6.50 usec
TE         298.1 K
D1         2.00000000 sec
D11        0.03000000 sec
TD0        1

```

```

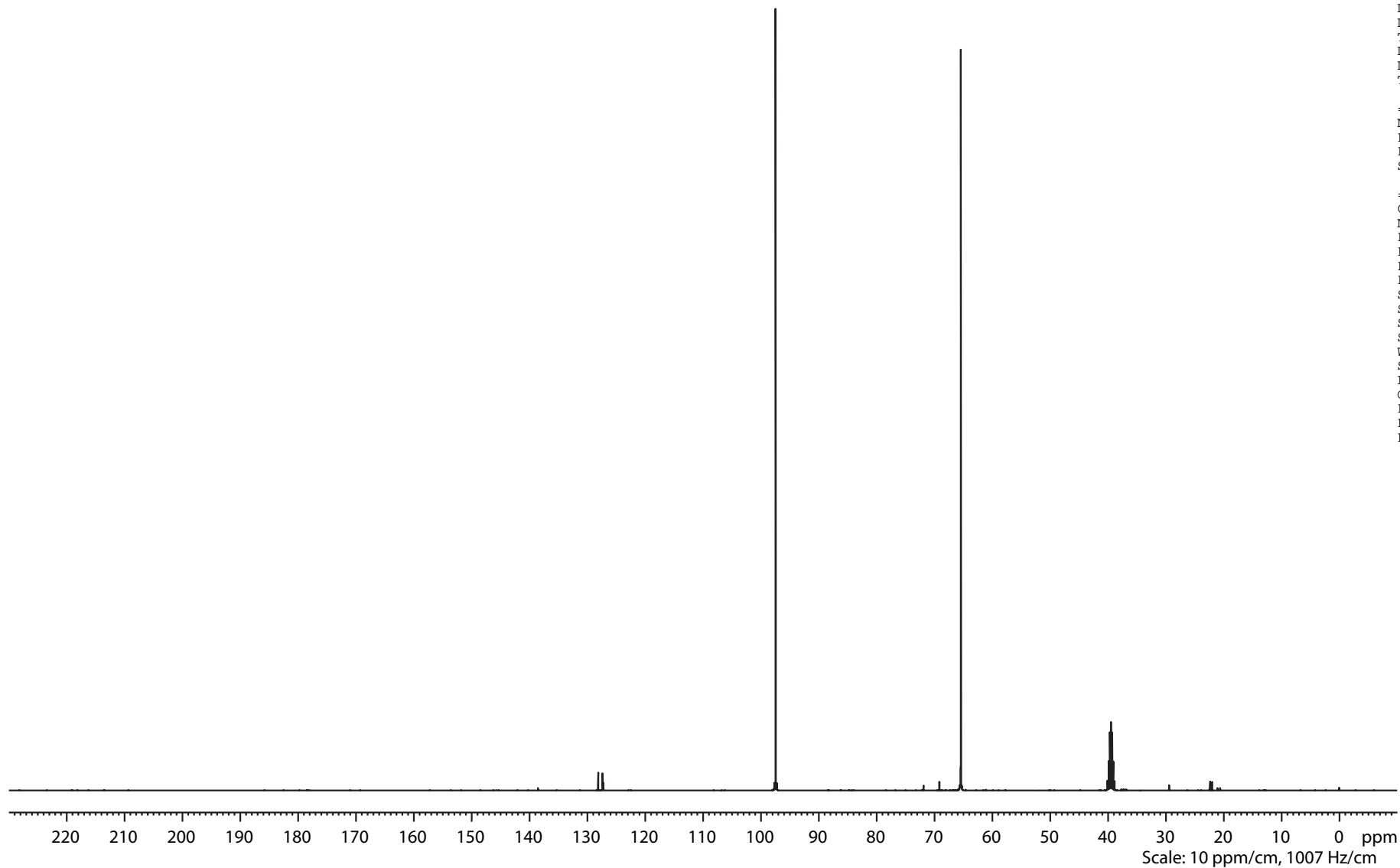
===== CHANNEL f1 =====
NUC1      13C
P1        8.50 usec
PL1       -3.00 dB
SFO1      100.6918371 MHz

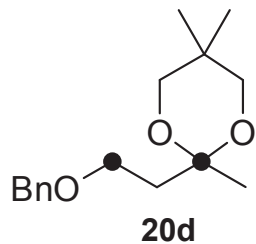
```

```

===== CHANNEL f2 =====
CPDPRG2   waltz16
NUC2      1H
PCPD2     80.00 usec
PL2       -4.00 dB
PL12      13.78 dB
PL13      14.00 dB
SFO2      400.4016016 MHz
SI        65536
SF        100.6807122 MHz
SR        51.24 Hz
WDW       EM
SSB       0
LB        1.00 Hz
GB        0
PC        1.40
F1P       230.000 ppm
F2P       -10.000 ppm

```





```

NAME      bae122468_od
EXPNO     3
PROCNO    1
Date_     20131104
Time      21.27
INSTRUM   AVIII400
PROBHD    5 mm PABBO BB-
PULPROG   dept135
TD         131072
SOLVENT   DMSO
NS         1024
DS         4
SWH        26315.789 Hz
FIDRES     0.200774 Hz
AQ         2.4904180 sec
RG         2050
DW         19.000 usec
DE         6.50 usec
TE         297.3 K
CNST2     145.0000000
D1         2.00000000 sec
D2         0.00344828 sec
D12        0.00002000 sec
TD0        1

```

```

===== CHANNEL f1 =====
NUC1       13C
P1         8.50 usec
P2         17.00 usec
PL1        -3.00 dB
SFO1       100.6919063 MHz

```

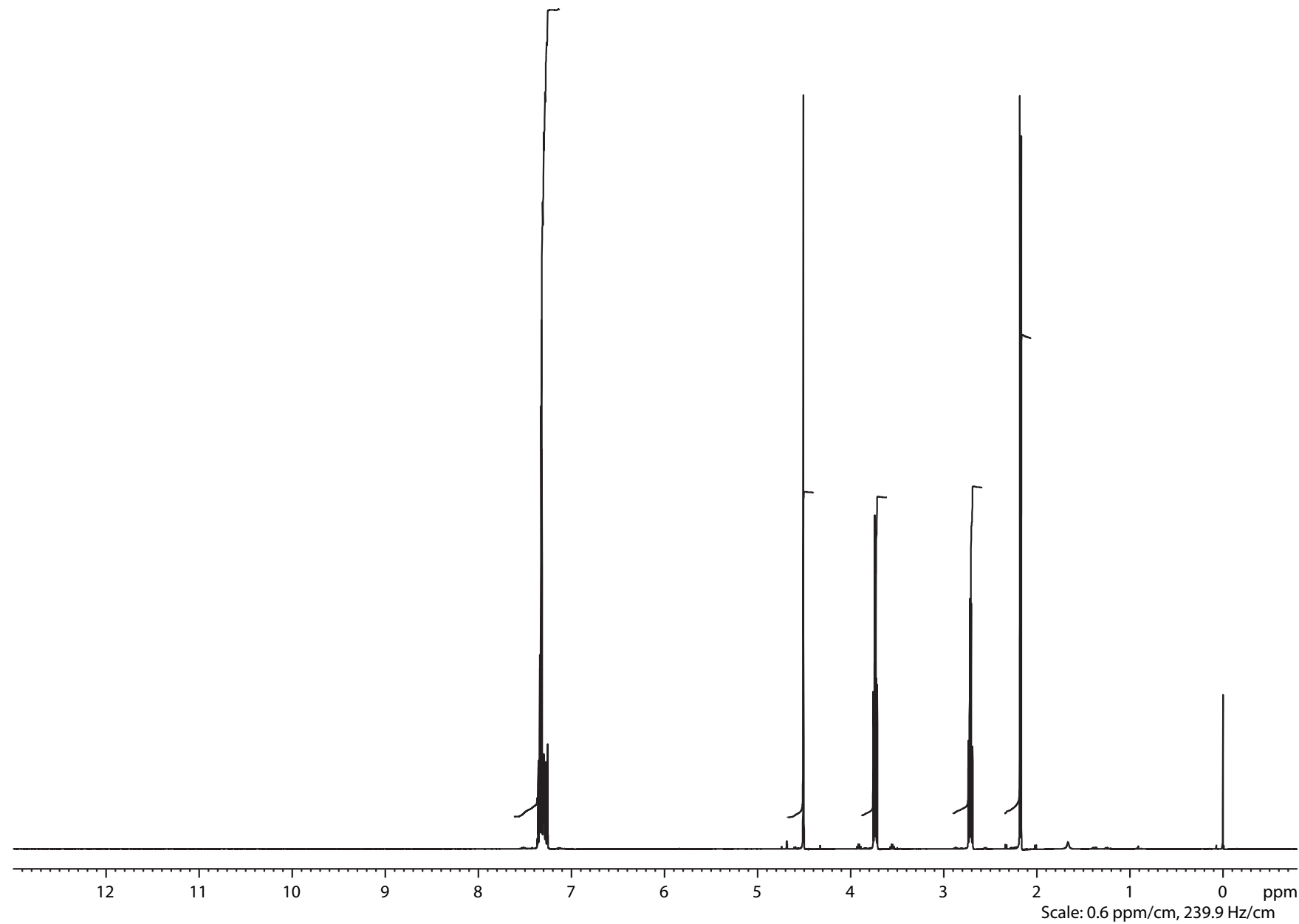
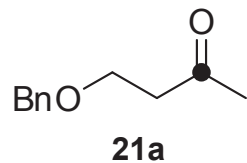
```

===== CHANNEL f2 =====
CPDPRG2   waltz16
NUC2       1H
P3         10.33 usec
P4         20.66 usec
PCPD2     80.00 usec
PL2        -4.00 dB
PL12       13.78 dB
SFO2       400.4016016 MHz
SI         65536
SF         100.6807369 MHz
SR         75.85 Hz
WDW        EM
SSB        0
LB         1.00 Hz
GB         0
PC         1.40
F1P        230.000 ppm
F2P        -10.000 ppm

```



220 210 200 190 180 170 160 150 140 130 120 110 100 90 80 70 60 50 40 30 20 10 0 ppm
 Scale: 10 ppm/cm, 1007 Hz/cm

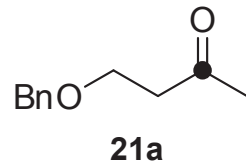


Current Data Parameters
NAME bae119978_od
EXPNO 1
PROCNO 1

F2 - Acquisition Parameters
Date_ 20130304
Time 14.09
INSTRUM drx400
PROBHD 5 mm QNP 1H/13
PULPROG zg30
TD 65536
SOLVENT CDCl3
NS 64
DS 2
SWH 8278.146 Hz
FIDRES 0.126314 Hz
AQ 3.9584243 sec
RG 101.6
DW 60.400 usec
DE 6.00 usec
TE 299.2 K
D1 1.00000000 sec
TD0 1

==== CHANNEL f1 =====
NUC1 1H
P1 10.20 usec
PL1 -2.00 dB
SFO1 399.8924689 MHz

F2 - Processing parameters
SI 32768
SF 399.8900152 MHz
SR 15.19 Hz
WDW EM
SSB 0
LB 0.00 Hz
GB 0
PC 1.40



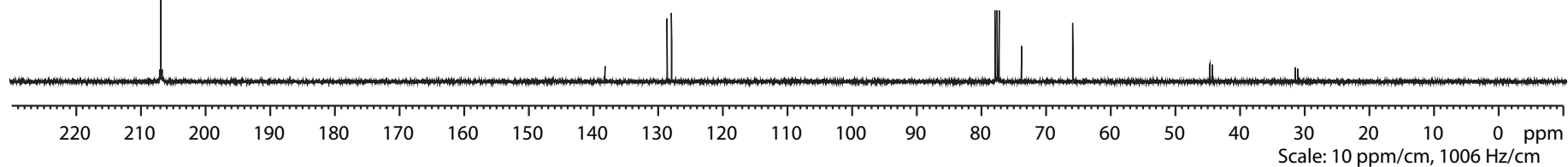
Current Data Parameters
 NAME bae119978_od
 EXPNO 2
 PROCNO 1

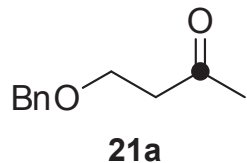
F2 - Acquisition Parameters
 Date_ 20130304
 Time 14.18
 INSTRUM drx400
 PROBHD 5 mm QNP 1H/13
 PULPROG zgpg30
 TD 131072
 SOLVENT CDCl3
 NS 96
 DS 4
 SWH 26315.789 Hz
 FIDRES 0.200774 Hz
 AQ 2.4904180 sec
 RG 9195.2
 DW 19.000 usec
 DE 6.00 usec
 TE 299.2 K
 D1 2.00000000 sec
 d11 0.03000000 sec
 DELTA 1.89999998 sec
 TD0 1

===== CHANNEL f1 =====
 NUC1 13C
 P1 11.00 usec
 PL1 -3.00 dB
 SFO1 100.5635842 MHz

===== CHANNEL f2 =====
 CPDPRG2 waltz16
 NUC2 1H
 PCPD2 80.00 usec
 PL2 -2.00 dB
 PL12 16.06 dB
 PL13 16.06 dB
 SFO2 399.8915996 MHz

F2 - Processing parameters
 SI 65536
 SF 100.5524261 MHz
 SR 5.11 Hz
 WDW EM
 SSB 0
 LB 1.00 Hz
 GB 0
 PC 1.40





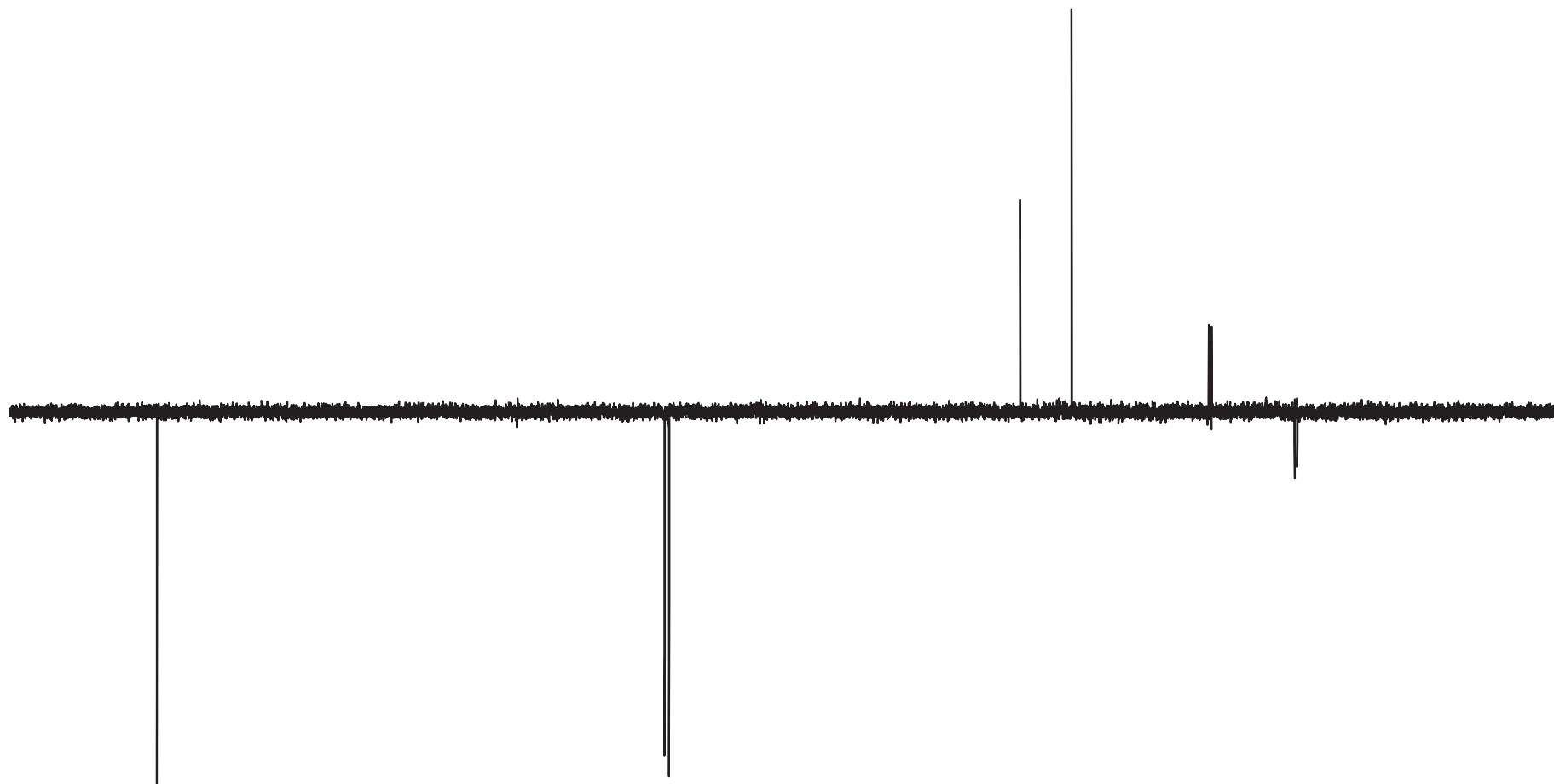
Current Data Parameters
 NAME bae119978_od
 EXPNO 3
 PROCNO 1

F2 - Acquisition Parameters
 Date_ 20130304
 Time 14.26
 INSTRUM drx400
 PROBHD 5 mm QNP 1H/13
 PULPROG dept135
 TD 131072
 SOLVENT CDCl3
 NS 96
 DS 4
 SWH 26315.789 Hz
 FIDRES 0.200774 Hz
 AQ 2.4904180 sec
 RG 7298.2
 DW 19.000 usec
 DE 7.00 usec
 TE 299.2 K
 CNST2 145.0000000
 D1 2.0000000 sec
 d2 0.00344828 sec
 d12 0.00002000 sec
 DELTA 0.00001401 sec
 TD0 1

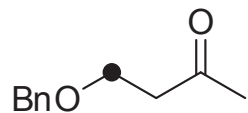
===== CHANNEL f1 =====
 NUC1 13C
 P1 11.00 usec
 p2 22.00 usec
 PL1 -3.00 dB
 SFO1 100.5635842 MHz

===== CHANNEL f2 =====
 CPDPRG2 waltz16
 NUC2 1H
 P3 10.00 usec
 p4 20.00 usec
 PCPD2 80.00 usec
 PL2 -2.00 dB
 PL12 16.06 dB
 SFO2 399.8915996 MHz

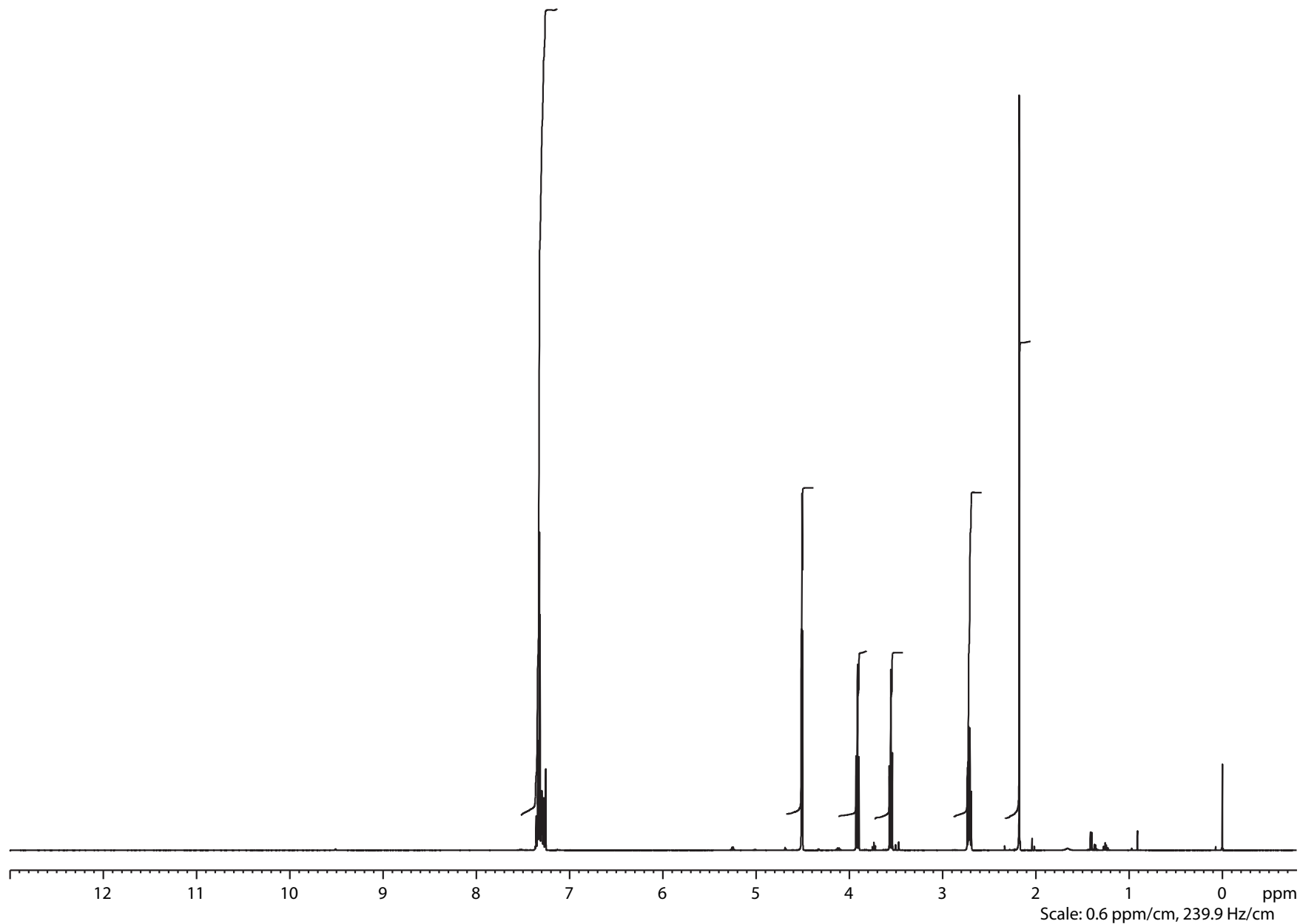
F2 - Processing parameters
 SI 65536
 SF 100.5524178 MHz
 SR -3.20 Hz
 WDW EM
 SSB 0
 LB 1.00 Hz
 GB 0
 PC 1.40



220 210 200 190 180 170 160 150 140 130 120 110 100 90 80 70 60 50 40 30 20 10 0 ppm
 Scale: 10 ppm/cm, 1006 Hz/cm



21b

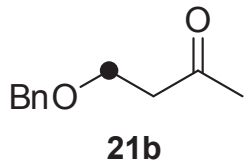


Current Data Parameters
NAME bae120225_od
EXPNO 1
PROCNO 1

F2 - Acquisition Parameters
Date_ 20130323
Time 15.57
INSTRUM drx400
PROBHD 5 mm QNP 1H/13
PULPROG zg30
TD 65536
SOLVENT CDCl3
NS 64
DS 2
SWH 8278.146 Hz
FIDRES 0.126314 Hz
AQ 3.9584243 sec
RG 114
DW 60.400 usec
DE 6.00 usec
TE 298.2 K
D1 1.00000000 sec
TD0 1

==== CHANNEL f1 =====
NUC1 1H
P1 10.20 usec
PL1 -2.00 dB
SFO1 399.8924689 MHz

F2 - Processing parameters
SI 32768
SF 399.8900149 MHz
SR 14.88 Hz
WDW EM
SSB 0
LB 0.00 Hz
GB 0
PC 1.40



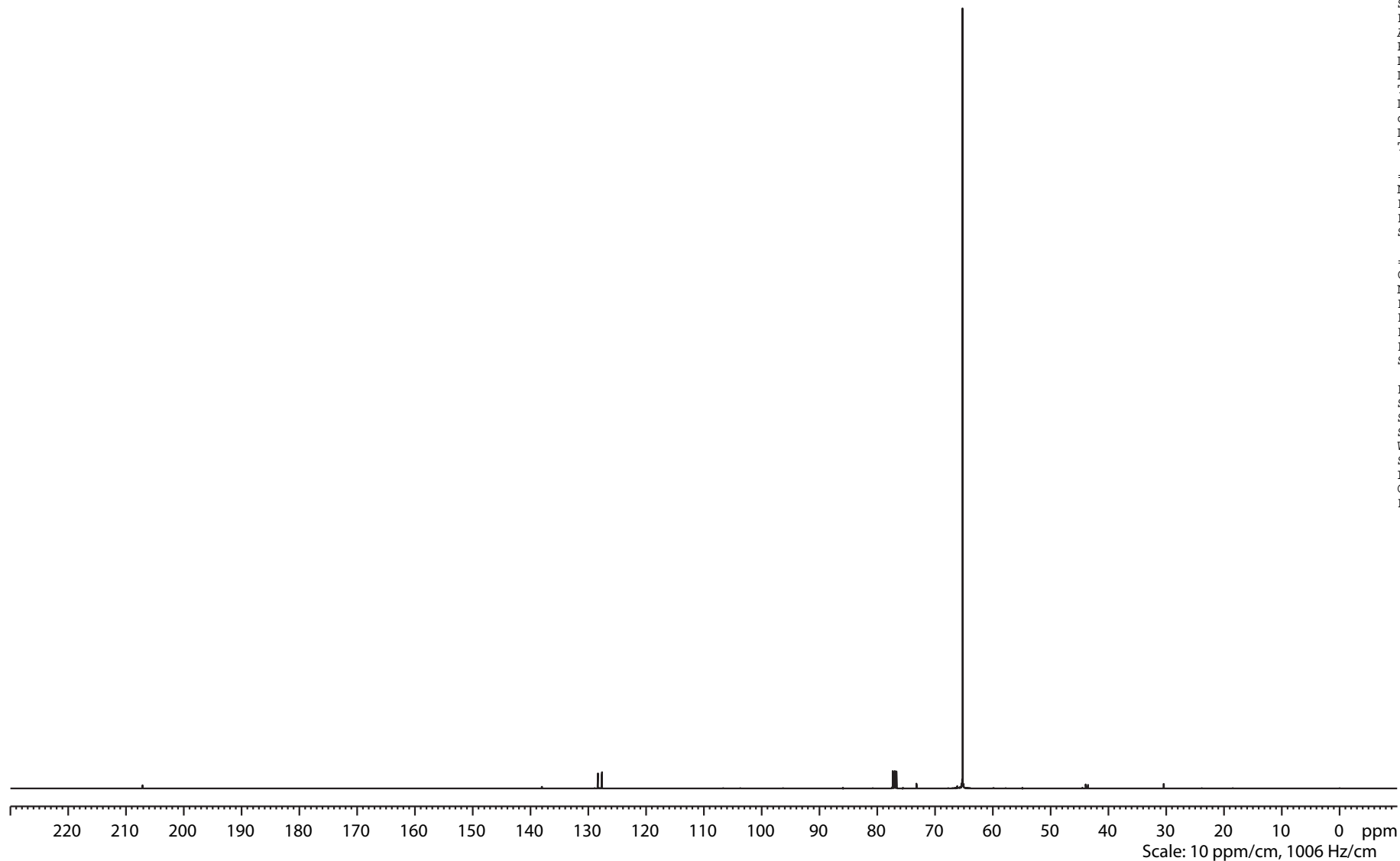
Current Data Parameters
 NAME bae120225_od
 EXPNO 2
 PROCNO 1

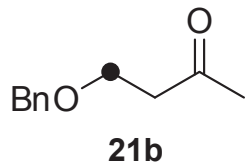
F2 - Acquisition Parameters
 Date_ 20130323
 Time 18.34
 INSTRUM drx400
 PROBHD 5 mm QNP 1H/13
 PULPROG zgpg30
 TD 131072
 SOLVENT CDCl3
 NS 2048
 DS 4
 SWH 26315.789 Hz
 FIDRES 0.200774 Hz
 AQ 2.4904180 sec
 RG 8192
 DW 19.000 usec
 DE 6.00 usec
 TE 299.2 K
 D1 2.00000000 sec
 d11 0.03000000 sec
 DELTA 1.89999998 sec
 TD0 1

==== CHANNEL f1 =====
 NUC1 13C
 P1 11.00 usec
 PL1 -3.00 dB
 SFO1 100.5635842 MHz

==== CHANNEL f2 =====
 CPDPRG2 waltz16
 NUC2 1H
 PCPD2 80.00 usec
 PL2 -2.00 dB
 PL12 16.06 dB
 PL13 16.06 dB
 SFO2 399.8915996 MHz

F2 - Processing parameters
 SI 65536
 SF 100.5524256 MHz
 SR 4.61 Hz
 WDW EM
 SSB 0
 LB 1.00 Hz
 GB 0
 PC 1.40





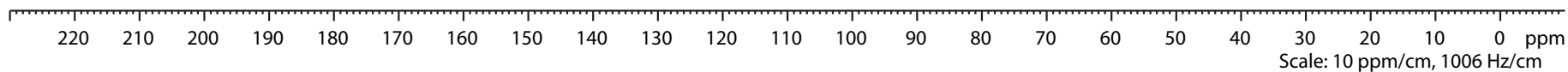
Current Data Parameters
 NAME bae120225_od
 EXPNO 3
 PROCNO 1

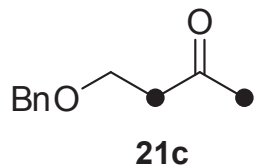
F2 - Acquisition Parameters
 Date_ 20130323
 Time 19.52
 INSTRUM drx400
 PROBHD 5 mm QNP 1H/13
 PULPROG dept135
 TD 131072
 SOLVENT CDCL3
 NS 1024
 DS 4
 SWH 26315.789 Hz
 FIDRES 0.200774 Hz
 AQ 2.4904180 sec
 RG 4597.6
 DW 19.000 usec
 DE 7.00 usec
 TE 299.2 K
 CNST2 145.0000000
 D1 2.00000000 sec
 d2 0.00344828 sec
 d12 0.00002000 sec
 DELTA 0.00001401 sec
 TD0 1

===== CHANNEL f1 =====
 NUC1 13C
 P1 11.00 usec
 p2 22.00 usec
 PL1 -3.00 dB
 SFO1 100.5635842 MHz

===== CHANNEL f2 =====
 CPDPRG2 waltz16
 NUC2 1H
 P3 10.00 usec
 p4 20.00 usec
 PCPD2 80.00 usec
 PL2 -2.00 dB
 PL12 16.06 dB
 SFO2 399.8915996 MHz

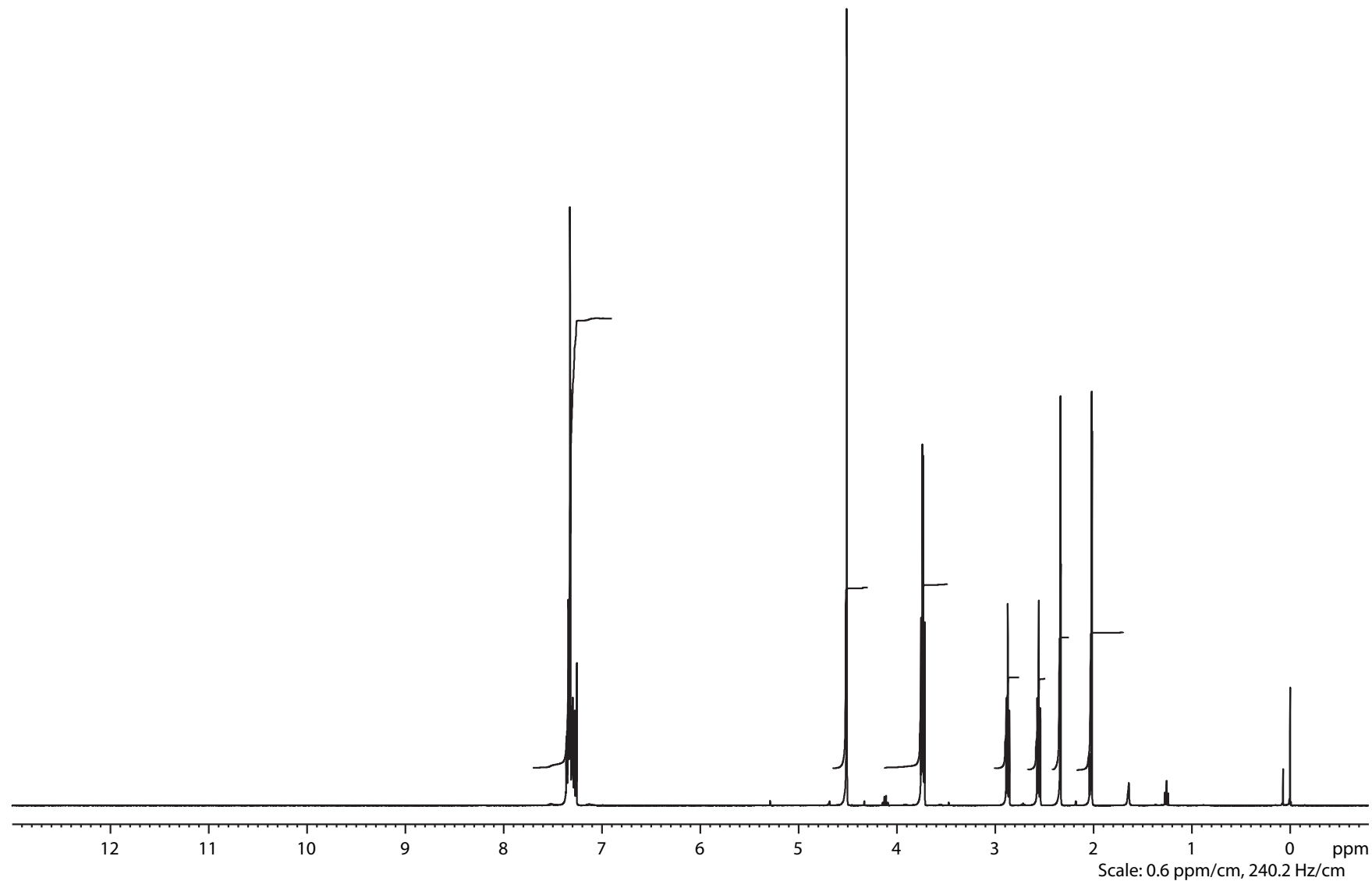
F2 - Processing parameters
 SI 65536
 SF 100.5525401 MHz
 SR 119.09 Hz
 WDW EM
 SSB 0
 LB 1.00 Hz
 GB 0
 PC 1.40

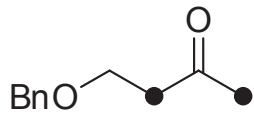




NAME bae120533_od
EXPNO 1
PROCNO 1
Date_ 20130419
Time_ 18.45
INSTRUM AVIII400
PROBHD 5 mm PABBO BB-
PULPROG zg30
TD 65536
SOLVENT CDCl3
NS 64
DS 2
SWH 8223.685 Hz
FIDRES 0.125483 Hz
AQ 3.9846387 sec
RG 128
DW 60.800 usec
DE 6.50 usec
TE 297.2 K
D1 1.0000000 sec
TD0 1

==== CHANNEL f1 =====
NUC1 1H
P1 10.33 usec
PL1 -4.00 dB
SFO1 400.4024726 MHz
SI 32768
SF 400.4000194 MHz
SR 19.40 Hz
WDW EM
SSB 0
LB 0.00 Hz
GB 0
PC 1.40
F1P 13.000 ppm
F2P -0.800 ppm



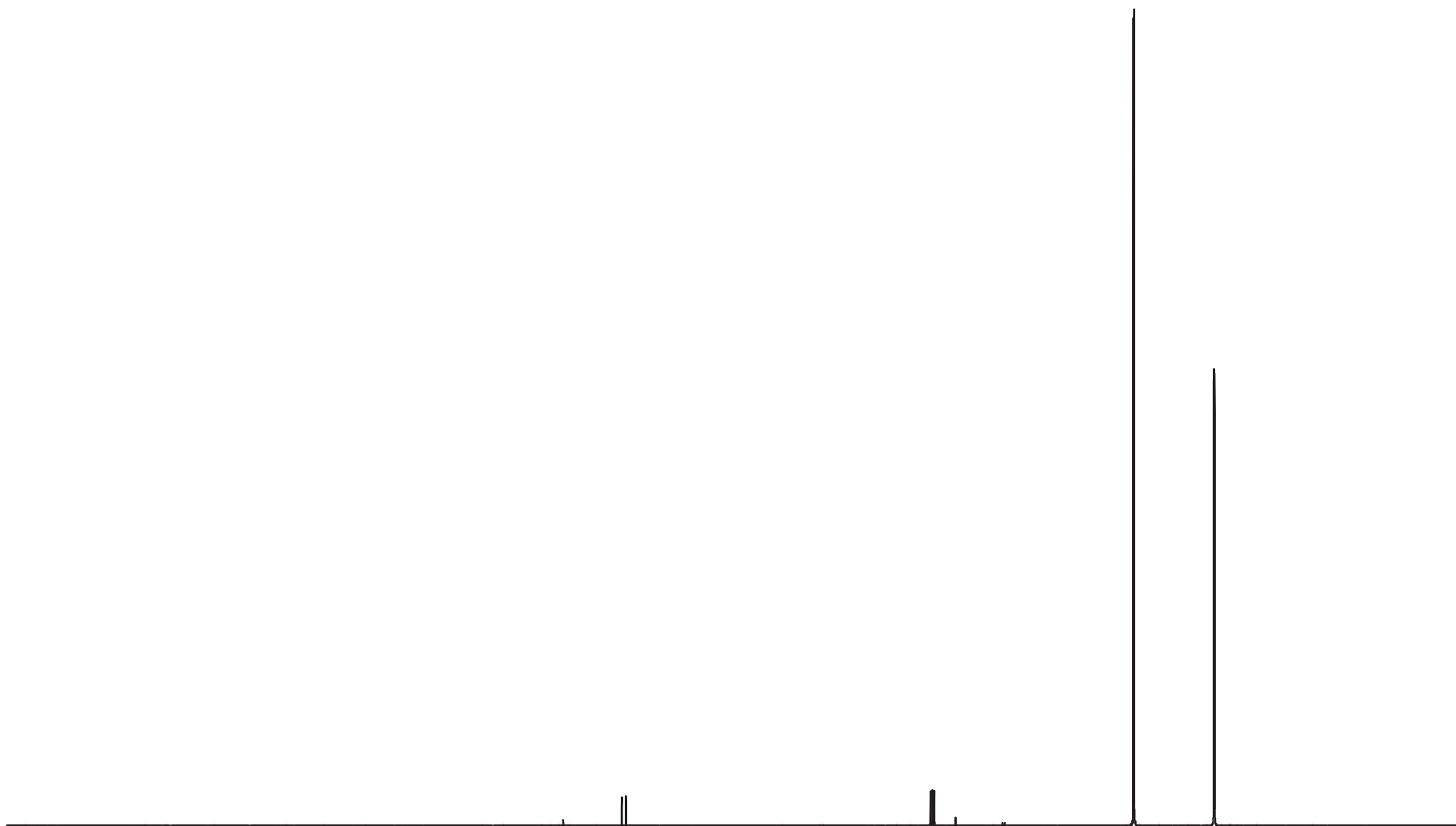


21c

NAME bae120533_od
EXPNO 2
PROCNO 1
Date_ 20130419
Time_ 18.54
INSTRUM AVIII400
PROBHD 5 mm PABBO BB-
PULPROG zgpg30
TD 131072
SOLVENT CDCl3
NS 96
DS 4
SWH 26315.789 Hz
FIDRES 0.200774 Hz
AQ 2.4904180 sec
RG 90.5
DW 19.000 usec
DE 6.50 usec
TE 298.4 K
D1 2.00000000 sec
D11 0.03000000 sec
TD0 10

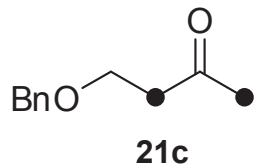
==== CHANNEL f1 =====
NUC1 13C
P1 8.50 usec
PL1 -3.00 dB
SFO1 100.6918371 MHz

==== CHANNEL f2 =====
CPDPRG2 waltz16
NUC2 1H
PCPD2 80.00 usec
PL2 -4.00 dB
PL12 13.78 dB
PL13 14.00 dB
SFO2 400.4016016 MHz
SI 65536
SF 100.6806661 MHz
SR 5.13 Hz
WDW EM
SSB 0
LB 1.00 Hz
GB 0
PC 1.40
F1P 230.000 ppm
F2P -10.000 ppm



220 210 200 190 180 170 160 150 140 130 120 110 100 90 80 70 60 50 40 30 20 10 0 ppm

Scale: 10 ppm/cm, 1007 Hz/cm



```

NAME      bae120533_od
EXPNO     3
PROCNO    1
Date_     20130419
Time      19.03
INSTRUM   AVIII400
PROBHD    5 mm PABBO BB-
PULPROG   dept135
TD         131072
SOLVENT   CDCl3
NS         96
DS         4
SWH        26315.789 Hz
FIDRES     0.200774 Hz
AQ         2.4904180 sec
RG         2050
DW         19.000 usec
DE         6.50 usec
TE         297.9 K
CNST2     145.0000000
D1         2.00000000 sec
D2         0.00344828 sec
D12        0.00002000 sec
TD0        5

```

```

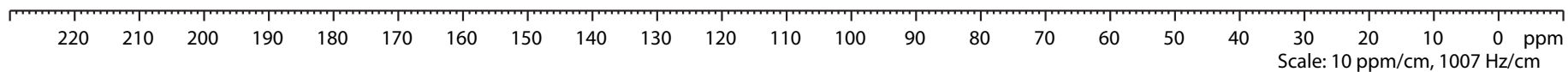
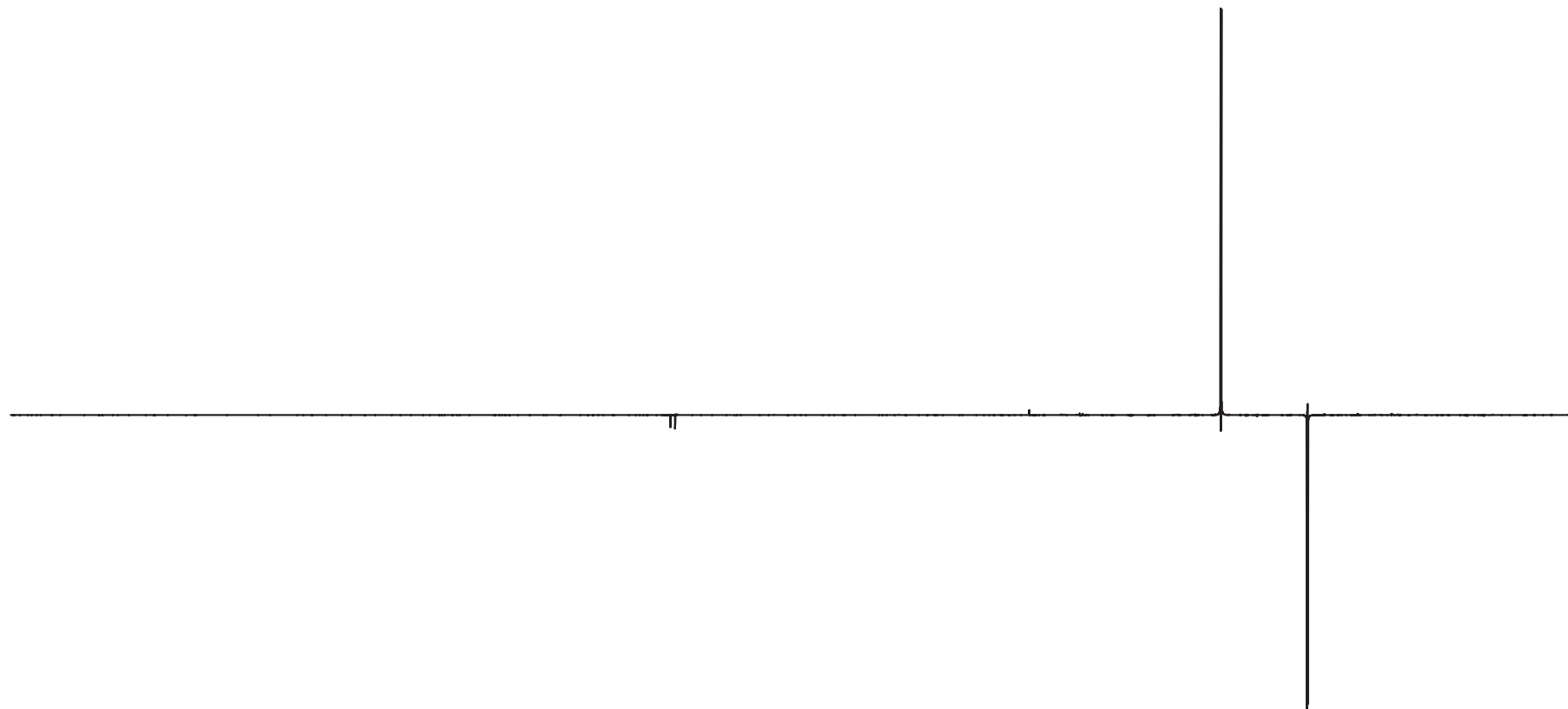
===== CHANNEL f1 =====
NUC1       13C
P1         8.50 usec
P2         17.00 usec
PL1        -3.00 dB
SFO1       100.6918371 MHz

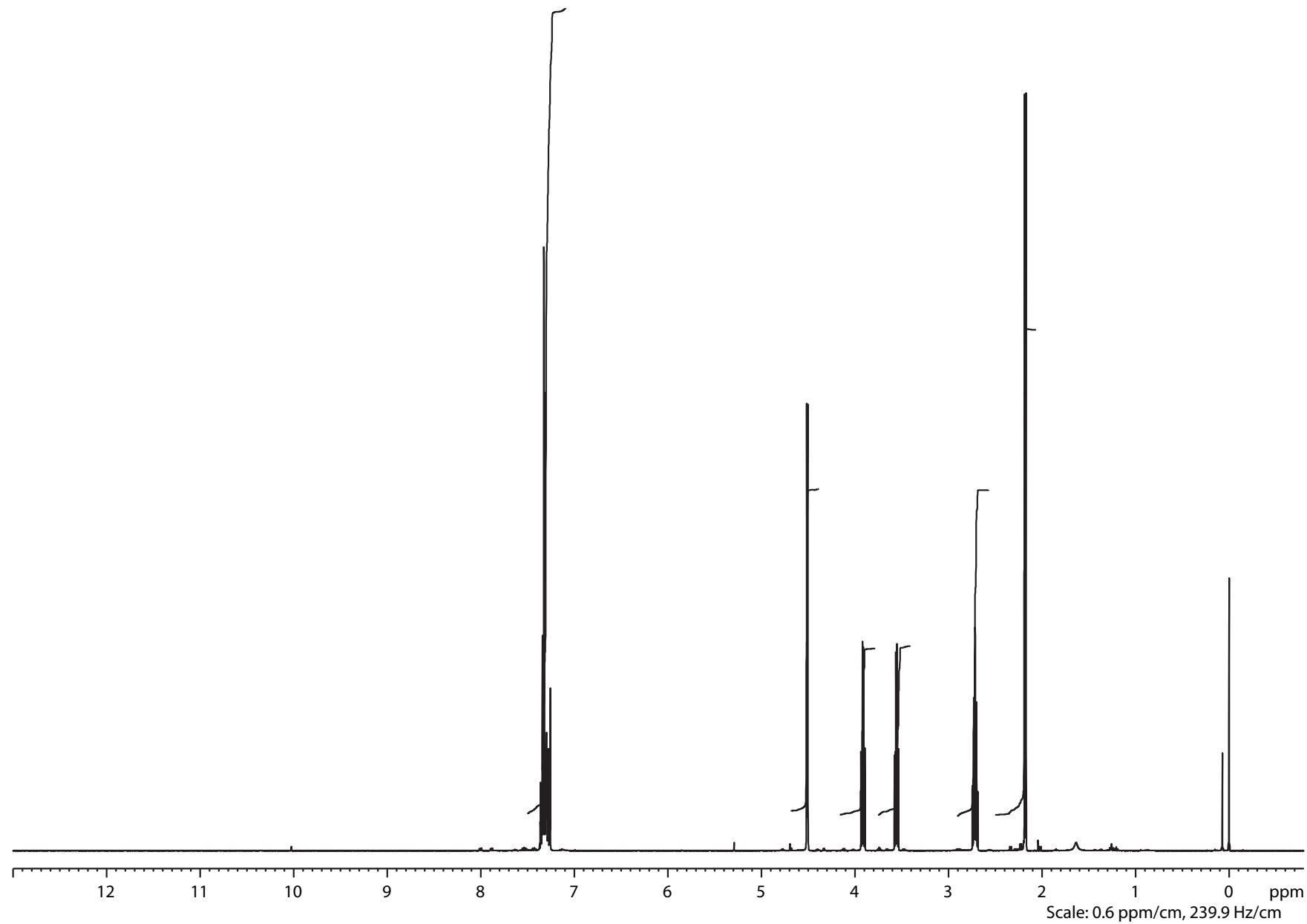
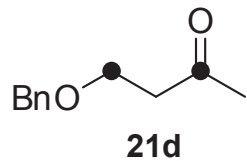
```

```

===== CHANNEL f2 =====
CPDPRG2    waltz16
NUC2        1H
P3          10.33 usec
P4          20.66 usec
PCPD2       80.00 usec
PL2         -4.00 dB
PL12        13.78 dB
SFO2        400.4016016 MHz
SI          65536
SF          100.6806578 MHz
SR          -3.20 Hz
WDW         EM
SSB         0
LB          1.00 Hz
GB          0
PC          1.40
F1P         230.000 ppm
F2P         -10.000 ppm

```



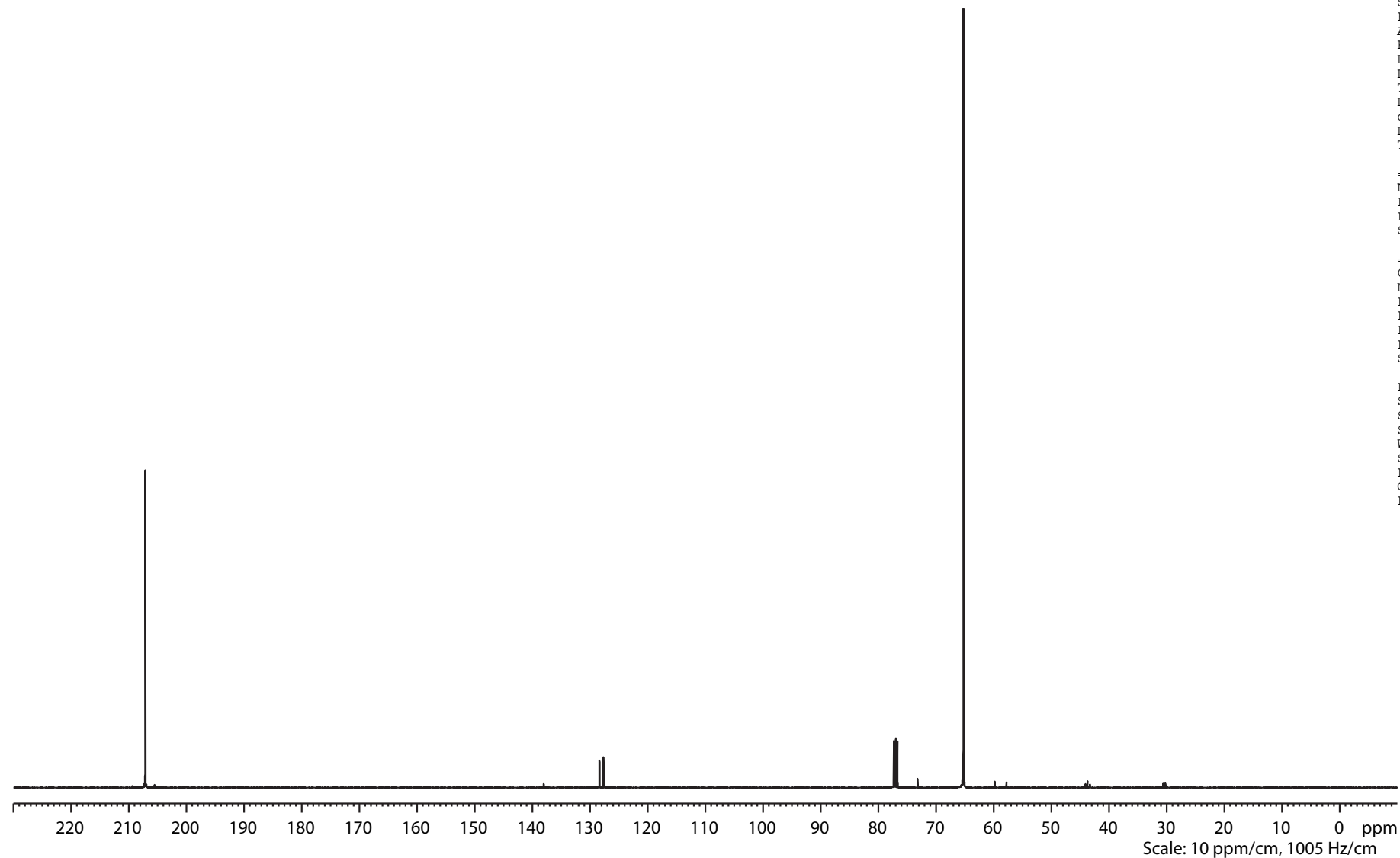
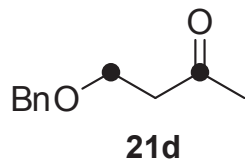


Current Data Parameters
NAME bae122541_od
EXPNO 1
PROCNO 1

F2 - Acquisition Parameters
Date_ 20131112
Time 23.47
INSTRUM drx400
PROBHD 5 mm QNP 1H/13
PULPROG zg30
TD 65536
SOLVENT CDCl3
NS 64
DS 2
SWH 8278.146 Hz
FIDRES 0.126314 Hz
AQ 3.9584243 sec
RG 143.7
DW 60.400 usec
DE 6.00 usec
TE 298.2 K
D1 1.00000000 sec
TD0 1

==== CHANNEL f1 =====
NUC1 1H
P1 10.20 usec
PL1 -2.00 dB
SFO1 399.8524687 MHz

F2 - Processing parameters
SI 32768
SF 399.8500161 MHz
SR 16.15 Hz
WDW EM
SSB 0
LB 0.00 Hz
GB 0
PC 1.40



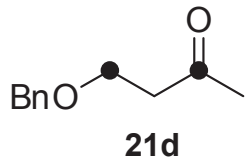
Current Data Parameters
NAME bae122541_od
EXPNO 2
PROCNO 1

F2 - Acquisition Parameters
Date_ 20131113
Time 2.23
INSTRUM drx400
PROBHD 5 mm QNP 1H/13
PULPROG zgpg30
TD 131072
SOLVENT CDCl3
NS 2048
DS 4
SWH 26315.789 Hz
FIDRES 0.200774 Hz
AQ 2.4904180 sec
RG 8192
DW 19.000 usec
DE 6.00 usec
TE 299.2 K
D1 2.00000000 sec
d11 0.03000000 sec
DELTA 1.89999998 sec
TD0 1

==== CHANNEL f1 =====
NUC1 13C
P1 11.00 usec
PL1 -3.00 dB
SFO1 100.5535241 MHz

==== CHANNEL f2 =====
CPDPRG2 waltz16
NUC2 1H
PCPD2 80.00 usec
PL2 -2.00 dB
PL12 16.06 dB
PL13 16.06 dB
SFO2 399.8515994 MHz

F2 - Processing parameters
SI 65536
SF 100.5423670 MHz
SR 3.97 Hz
WDW EM
SSB 0
LB 1.00 Hz
GB 0
PC 1.40



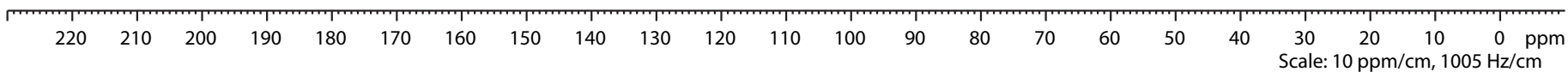
Current Data Parameters
 NAME bae122541_od
 EXPNO 3
 PROCNO 1

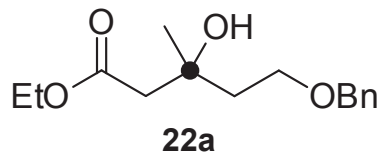
F2 - Acquisition Parameters
 Date_ 20131113
 Time 3.42
 INSTRUM drx400
 PROBHD 5 mm QNP 1H/13
 PULPROG dept135
 TD 131072
 SOLVENT CDCL3
 NS 1024
 DS 4
 SWH 26315.789 Hz
 FIDRES 0.200774 Hz
 AQ 2.4904180 sec
 RG 6502
 DW 19.000 usec
 DE 7.00 usec
 TE 299.2 K
 CNST2 145.0000000
 D1 2.00000000 sec
 d2 0.00344828 sec
 d12 0.00002000 sec
 DELTA 0.00001401 sec
 TD0 1

==== CHANNEL f1 =====
 NUC1 13C
 P1 11.00 usec
 p2 22.00 usec
 PL1 -3.00 dB
 SFO1 100.5535241 MHz

==== CHANNEL f2 =====
 CPDPRG2 waltz16
 NUC2 1H
 P3 10.00 usec
 p4 20.00 usec
 PCPD2 80.00 usec
 PL2 -2.00 dB
 PL12 16.06 dB
 SFO2 399.8515994 MHz

F2 - Processing parameters
 SI 65536
 SF 100.5424858 MHz
 SR 122.75 Hz
 WDW EM
 SSB 0
 LB 1.00 Hz
 GB 0
 PC 1.40



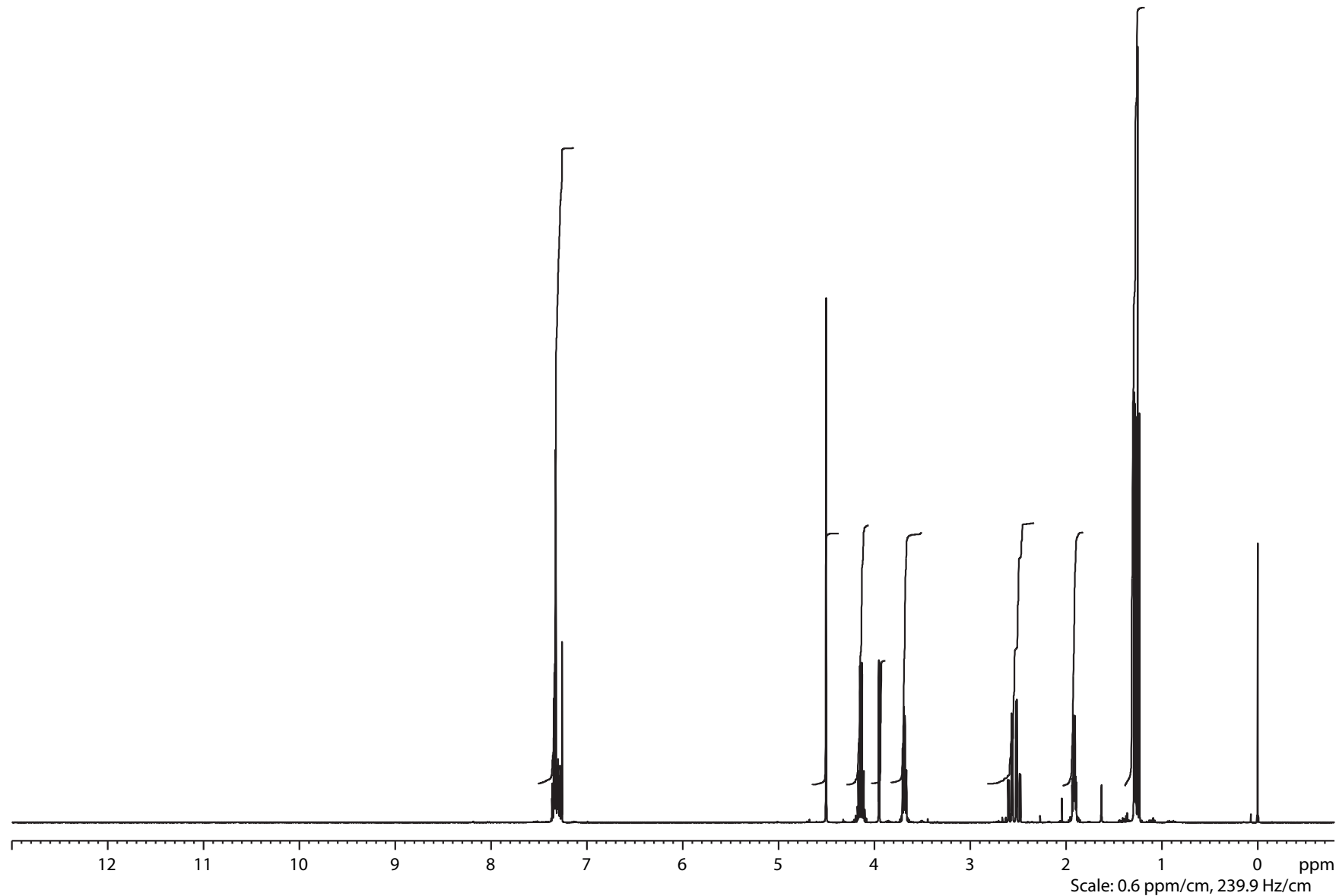


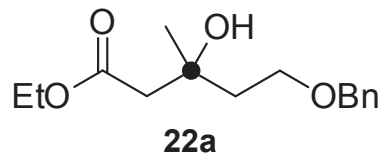
Current Data Parameters
 NAME bae123035_od
 EXPNO 1
 PROCNO 1

F2 - Acquisition Parameters
 Date_ 20140128
 Time 23.45
 INSTRUM drx400
 PROBHD 5 mm QNP 1H/13
 PULPROG zg30
 TD 65536
 SOLVENT CDCl3
 NS 64
 DS 2
 SWH 8278.146 Hz
 FIDRES 0.126314 Hz
 AQ 3.9584243 sec
 RG 128
 DW 60.400 usec
 DE 6.00 usec
 TE 298.2 K
 D1 1.00000000 sec
 TD0 1

==== CHANNEL f1 =====
 NUC1 1H
 P1 10.20 usec
 PL1 -2.00 dB
 SFO1 399.8524687 MHz

F2 - Processing parameters
 SI 32768
 SF 399.8500156 MHz
 SR 15.62 Hz
 WDW EM
 SSB 0
 LB 0.00 Hz
 GB 0
 PC 1.40





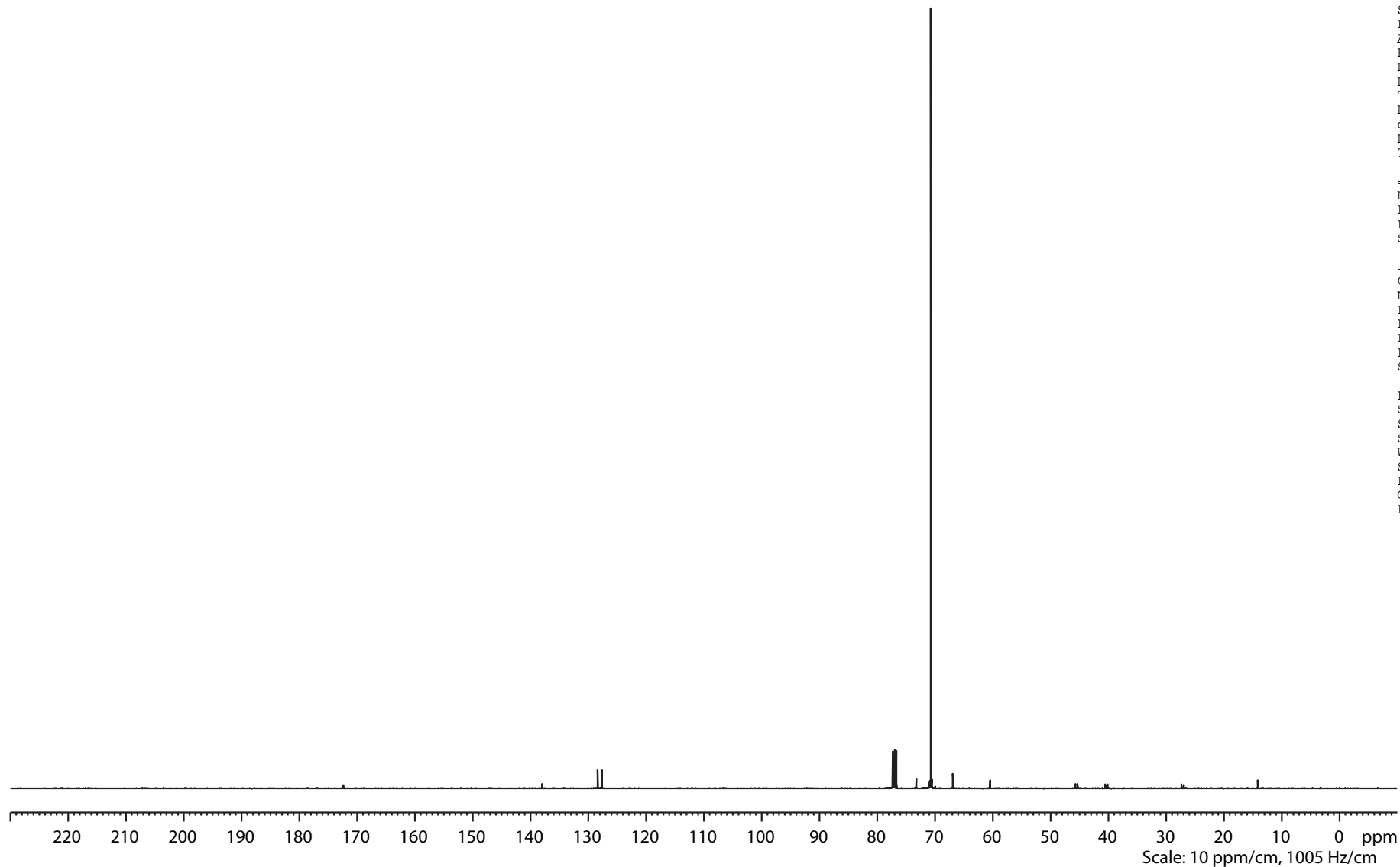
Current Data Parameters
 NAME bae123035_od
 EXPNO 2
 PROCNO 1

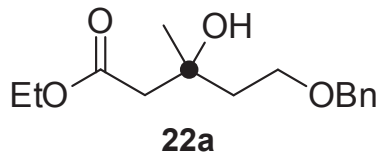
F2 - Acquisition Parameters
 Date_ 20140129
 Time 3.40
 INSTRUM drx400
 PROBHD 5 mm QNP 1H/13
 PULPROG zgpg30
 TD 131072
 SOLVENT CDCl3
 NS 3072
 DS 4
 SWH 26315.789 Hz
 FIDRES 0.200774 Hz
 AQ 2.4904180 sec
 RG 9195.2
 DW 19.000 usec
 DE 6.00 usec
 TE 299.2 K
 D1 2.00000000 sec
 d11 0.03000000 sec
 DELTA 1.89999998 sec
 TD0 1

==== CHANNEL f1 =====
 NUC1 13C
 P1 11.00 usec
 PL1 -3.00 dB
 SFO1 100.5535241 MHz

==== CHANNEL f2 =====
 CPDPRG2 waltz16
 NUC2 1H
 PCPD2 80.00 usec
 PL2 -2.00 dB
 PL12 16.06 dB
 PL13 16.06 dB
 SFO2 399.8515994 MHz

F2 - Processing parameters
 SI 65536
 SF 100.5423665 MHz
 SR 3.46 Hz
 WDW EM
 SSB 0
 LB 1.00 Hz
 GB 0
 PC 1.40





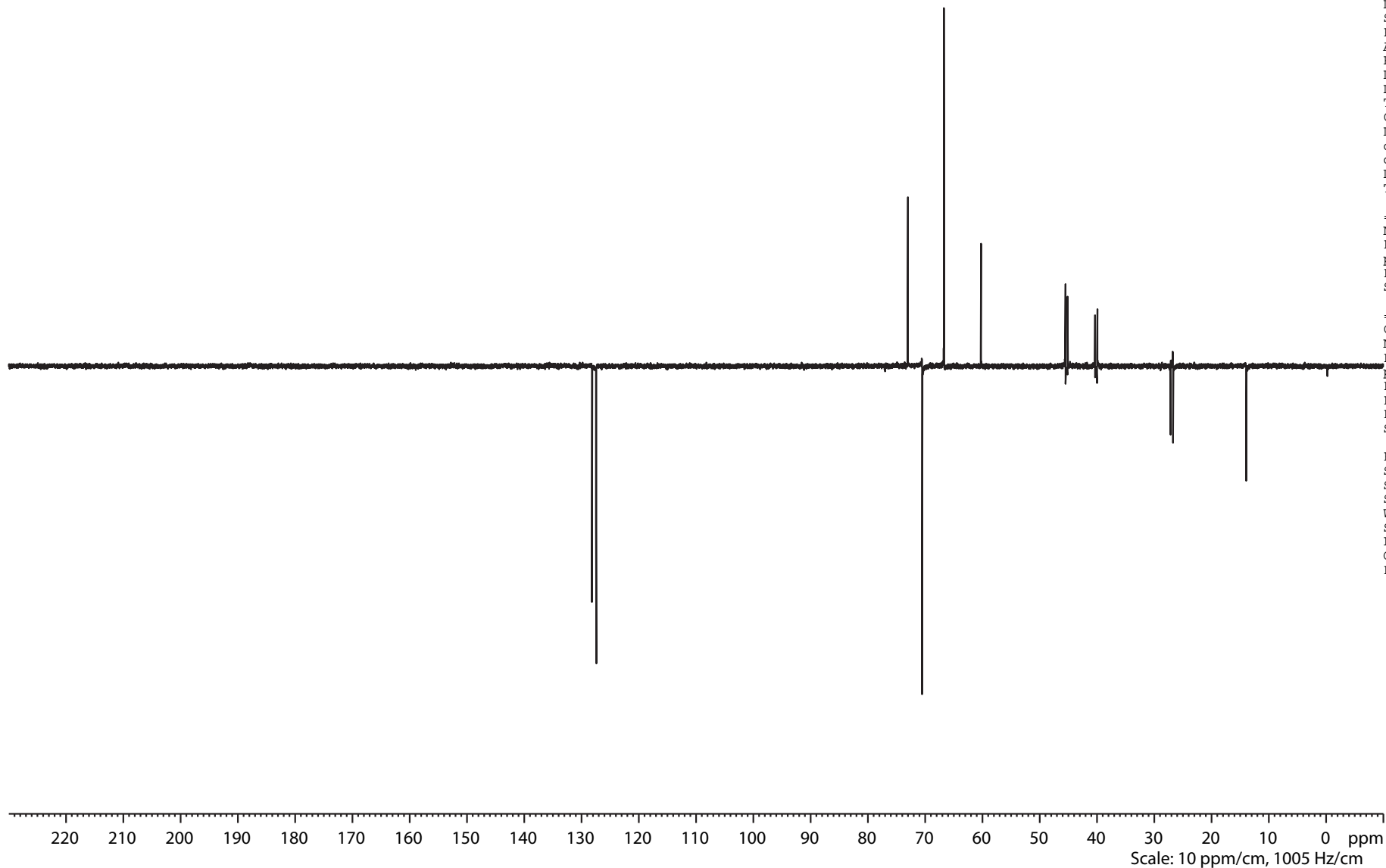
Current Data Parameters
 NAME bae123035_od
 EXPNO 3
 PROCNO 1

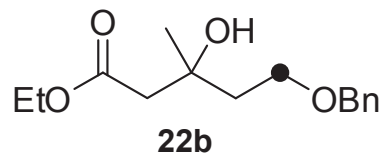
F2 - Acquisition Parameters
 Date_ 20140129
 Time 6.16
 INSTRUM drx400
 PROBHD 5 mm QNP 1H/13
 PULPROG dept135
 TD 131072
 SOLVENT CDCl3
 NS 2048
 DS 4
 SWH 26315.789 Hz
 FIDRES 0.200774 Hz
 AQ 2.4904180 sec
 RG 9195.2
 DW 19.000 usec
 DE 7.00 usec
 TE 299.2 K
 CNST2 145.0000000
 D1 2.00000000 sec
 d2 0.00344828 sec
 d12 0.00002000 sec
 DELTA 0.00001401 sec
 TD0 1

===== CHANNEL f1 =====
 NUC1 13C
 P1 11.00 usec
 p2 22.00 usec
 PL1 -3.00 dB
 SFO1 100.5535241 MHz

===== CHANNEL f2 =====
 CPDPRG2 waltz16
 NUC2 1H
 P3 10.00 usec
 p4 20.00 usec
 PCPD2 80.00 usec
 PL2 -2.00 dB
 PL12 16.06 dB
 SFO2 399.8515994 MHz

F2 - Processing parameters
 SI 65536
 SF 100.5423873 MHz
 SR 24.27 Hz
 WDW EM
 SSB 0
 LB 1.00 Hz
 GB 0
 PC 1.40





```

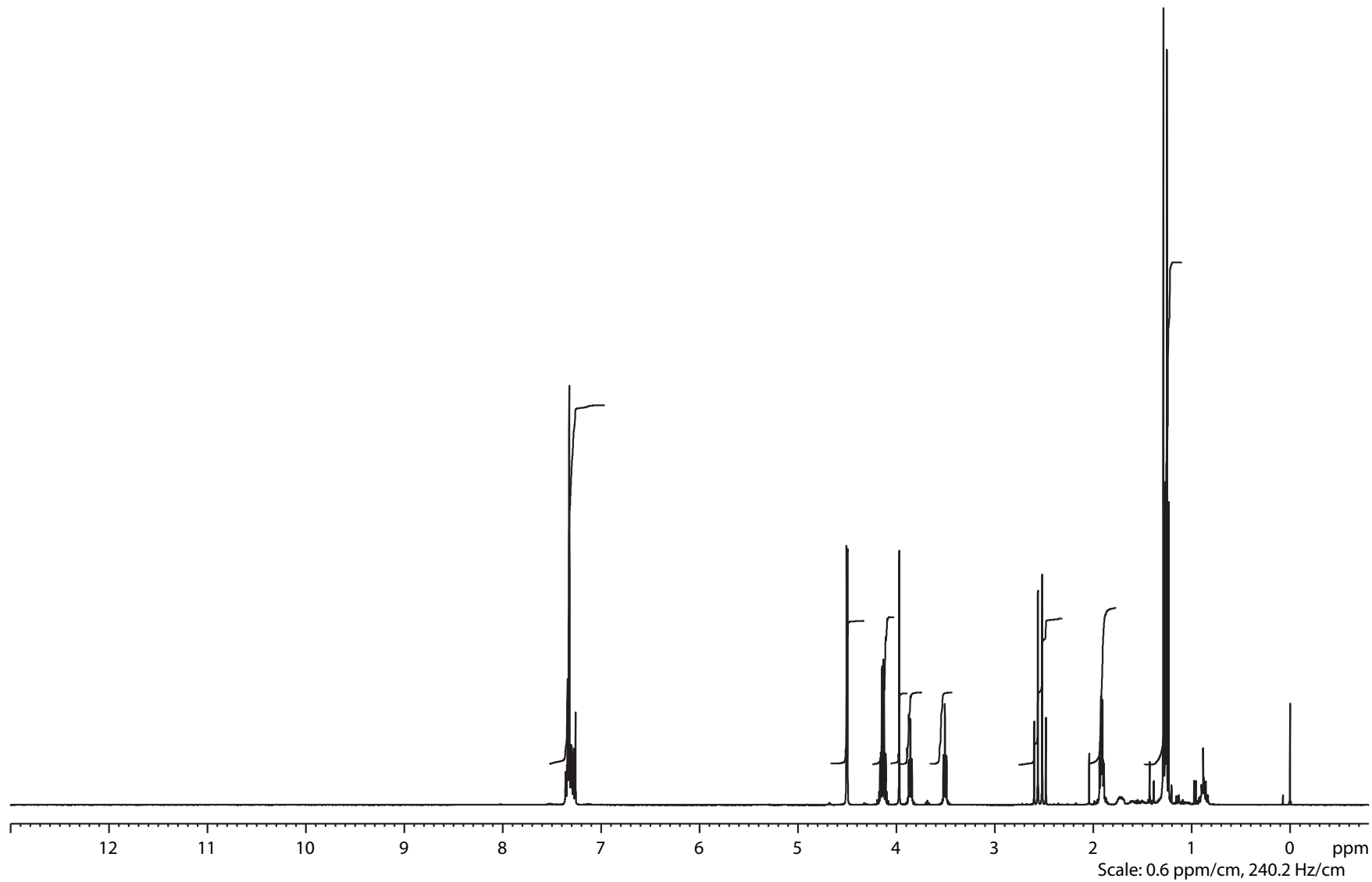
NAME      bae123830_od
EXPNO     1
PROCNO    1
Date_     20140404
Time      19.11
INSTRUM   AVIII400
PROBHD    5 mm PABBO BB-
PULPROG   zg30
TD         65536
SOLVENT   CDCl3
NS         64
DS         2
SWH        8223.685 Hz
FIDRES     0.125483 Hz
AQ         3.9846387 sec
RG         57
DW         60.800 usec
DE         6.50 usec
TE         297.0 K
D1         1.00000000 sec
TD0        1

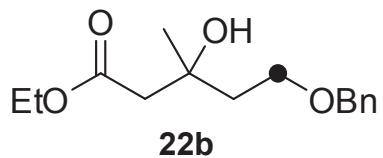
```

```

===== CHANNEL f1 =====
NUC1      1H
P1        10.33 usec
PL1       -4.00 dB
SFO1      400.4024726 MHz
SI         32768
SF         400.4000182 MHz
SR         18.23 Hz
WDW        EM
SSB        0
LB         0.00 Hz
GB         0
PC         1.40
F1P        13.000 ppm
F2P        -0.800 ppm

```





```

NAME      bae123830_od
EXPNO     2
PROCNO    1
Date_     20140404
Time      23.06
INSTRUM   AVIII400
PROBHD    5 mm PABBO BB-
PULPROG   zgpg30
TD         131072
SOLVENT   CDCl3
NS         3072
DS         4
SWH        26315.789 Hz
FIDRES     0.200774 Hz
AQ         2.4904180 sec
RG         101
DW         19.000 usec
DE         6.50 usec
TE         298.5 K
D1         2.00000000 sec
D11        0.03000000 sec
TD0        1

```

```

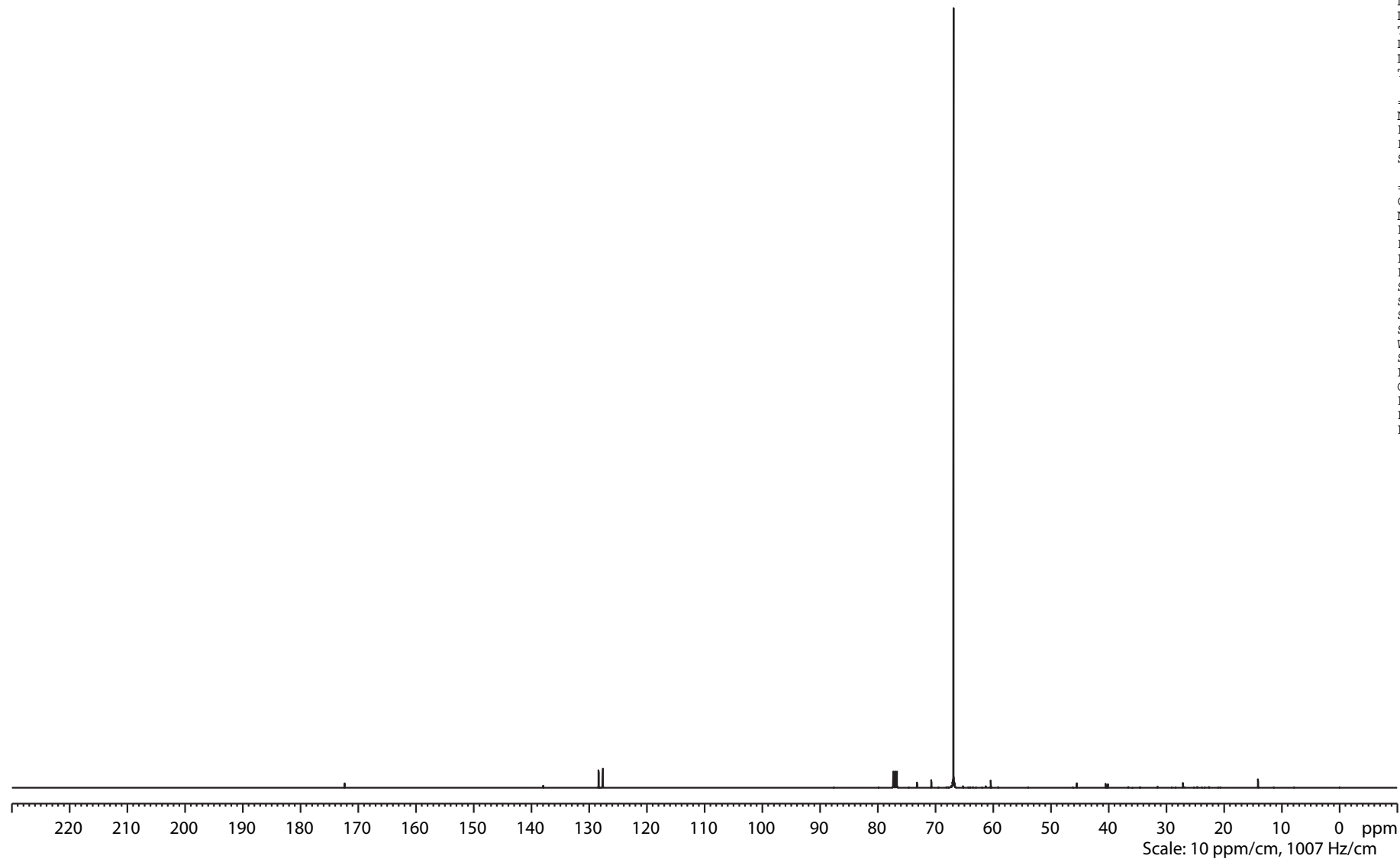
===== CHANNEL f1 =====
NUC1      13C
P1        8.50 usec
PL1       -3.00 dB
SFO1      100.6918371 MHz

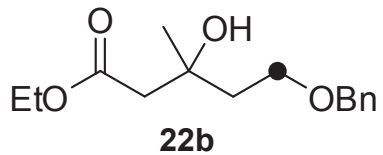
```

```

===== CHANNEL f2 =====
CPDPRG2   waltz16
NUC2      1H
PCPD2     80.00 usec
PL2       -4.00 dB
PL12      13.78 dB
PL13      14.00 dB
SFO2      400.4016016 MHz
SI        65536
SF        100.6806663 MHz
SR         5.31 Hz
WDW       EM
SSB       0
LB        1.00 Hz
GB        0
PC        1.40
F1P       230.000 ppm
F2P       -10.000 ppm

```





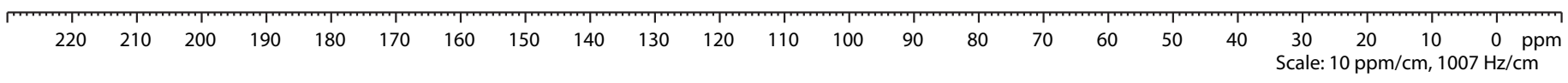
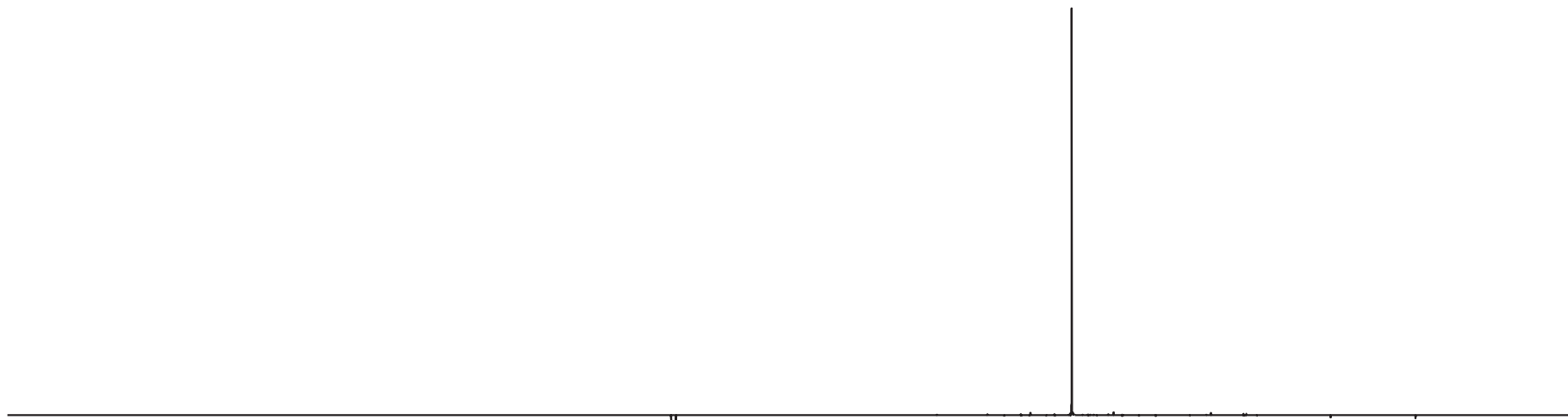
```

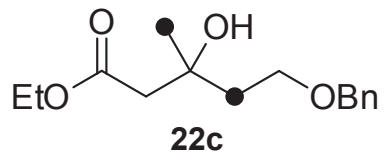
NAME      bae123830_od
EXPNO     3
PROCNO    1
Date_     20140405
Time      1.43
INSTRUM   AVIII400
PROBHD    5 mm PABBO BB-
PULPROG   dept135
TD         131072
SOLVENT   CDCl3
NS         2048
DS         4
SWH        26315.789 Hz
FIDRES     0.200774 Hz
AQ         2.4904180 sec
RG         2050
DW         19.000 usec
DE         6.50 usec
TE         297.6 K
CNST2     145.0000000
D1         2.00000000 sec
D2         0.00344828 sec
D12        0.00002000 sec
TD0        1

===== CHANNEL f1 =====
NUC1       13C
P1         8.50 usec
P2         17.00 usec
PL1        -3.00 dB
SFO1       100.6919063 MHz

===== CHANNEL f2 =====
CPDPRG2    waltz16
NUC2       1H
P3         10.33 usec
P4         20.66 usec
PCPD2      80.00 usec
PL2        -4.00 dB
PL12       13.78 dB
SFO2       400.4016016 MHz
SI         65536
SF         100.6806908 MHz
SR         29.80 Hz
WDW        EM
SSB        0
LB         1.00 Hz
GB         0
PC         1.40
F1P        230.000 ppm
F2P        -10.000 ppm

```



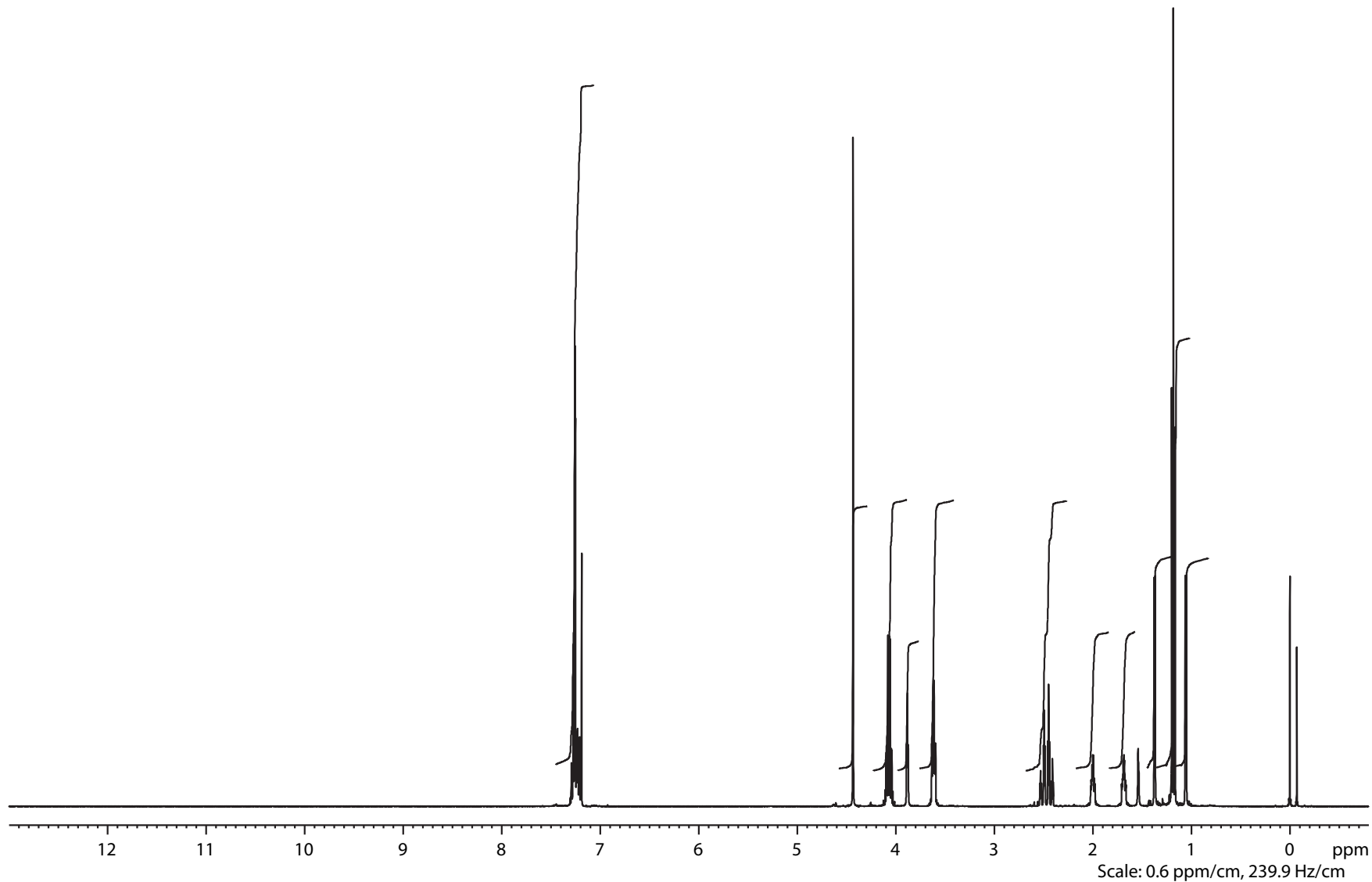


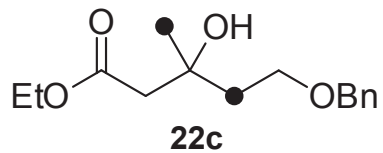
Current Data Parameters
 NAME bae120553_od
 EXPNO 1
 PROCNO 1

F2 - Acquisition Parameters
 Date_ 20130422
 Time 13.12
 INSTRUM drx400
 PROBHD 5 mm QNP 1H/13
 PULPROG zg30
 TD 65536
 SOLVENT CDCl3
 NS 64
 DS 2
 SWH 8278.146 Hz
 FIDRES 0.126314 Hz
 AQ 3.9584243 sec
 RG 181
 DW 60.400 usec
 DE 6.00 usec
 TE 299.2 K
 D1 1.00000000 sec
 TD0 1

==== CHANNEL f1 =====
 NUC1 1H
 P1 10.20 usec
 PL1 -2.00 dB
 SFO1 399.8924689 MHz

F2 - Processing parameters
 SI 32768
 SF 399.8900417 MHz
 SR 41.71 Hz
 WDW EM
 SSB 0
 LB 0.00 Hz
 GB 0
 PC 1.40





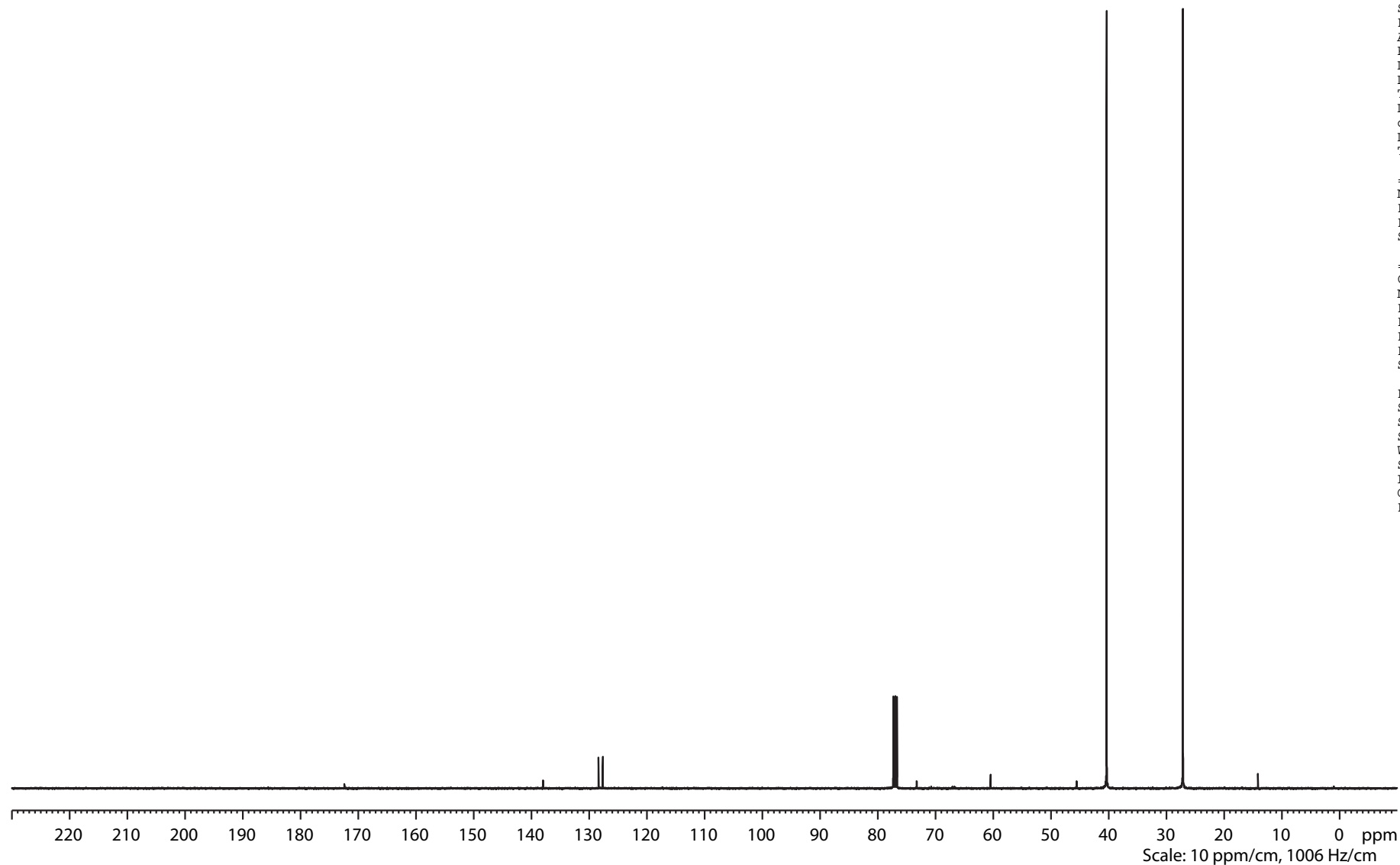
Current Data Parameters
 NAME bae120553_od
 EXPNO 2
 PROCNO 1

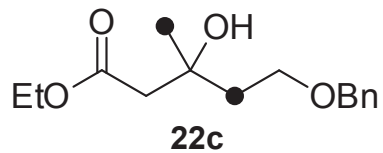
F2 - Acquisition Parameters
 Date_ 20130422
 Time 14.31
 INSTRUM drx400
 PROBHD 5 mm QNP 1H/13
 PULPROG zgpg30
 TD 131072
 SOLVENT CDCl3
 NS 1024
 DS 4
 SWH 26315.789 Hz
 FIDRES 0.200774 Hz
 AQ 2.4904180 sec
 RG 9195.2
 DW 19.000 usec
 DE 6.00 usec
 TE 300.2 K
 D1 2.00000000 sec
 d11 0.03000000 sec
 DELTA 1.89999998 sec
 TD0 1

===== CHANNEL f1 =====
 NUC1 13C
 P1 11.00 usec
 PL1 -3.00 dB
 SFO1 100.5635842 MHz

===== CHANNEL f2 =====
 CPDPRG2 waltz16
 NUC2 1H
 PCPD2 80.00 usec
 PL2 -2.00 dB
 PL12 16.06 dB
 PL13 16.06 dB
 SFO2 399.8915996 MHz

F2 - Processing parameters
 SI 65536
 SF 100.5524233 MHz
 SR 2.27 Hz
 WDW EM
 SSB 0
 LB 1.00 Hz
 GB 0
 PC 1.40





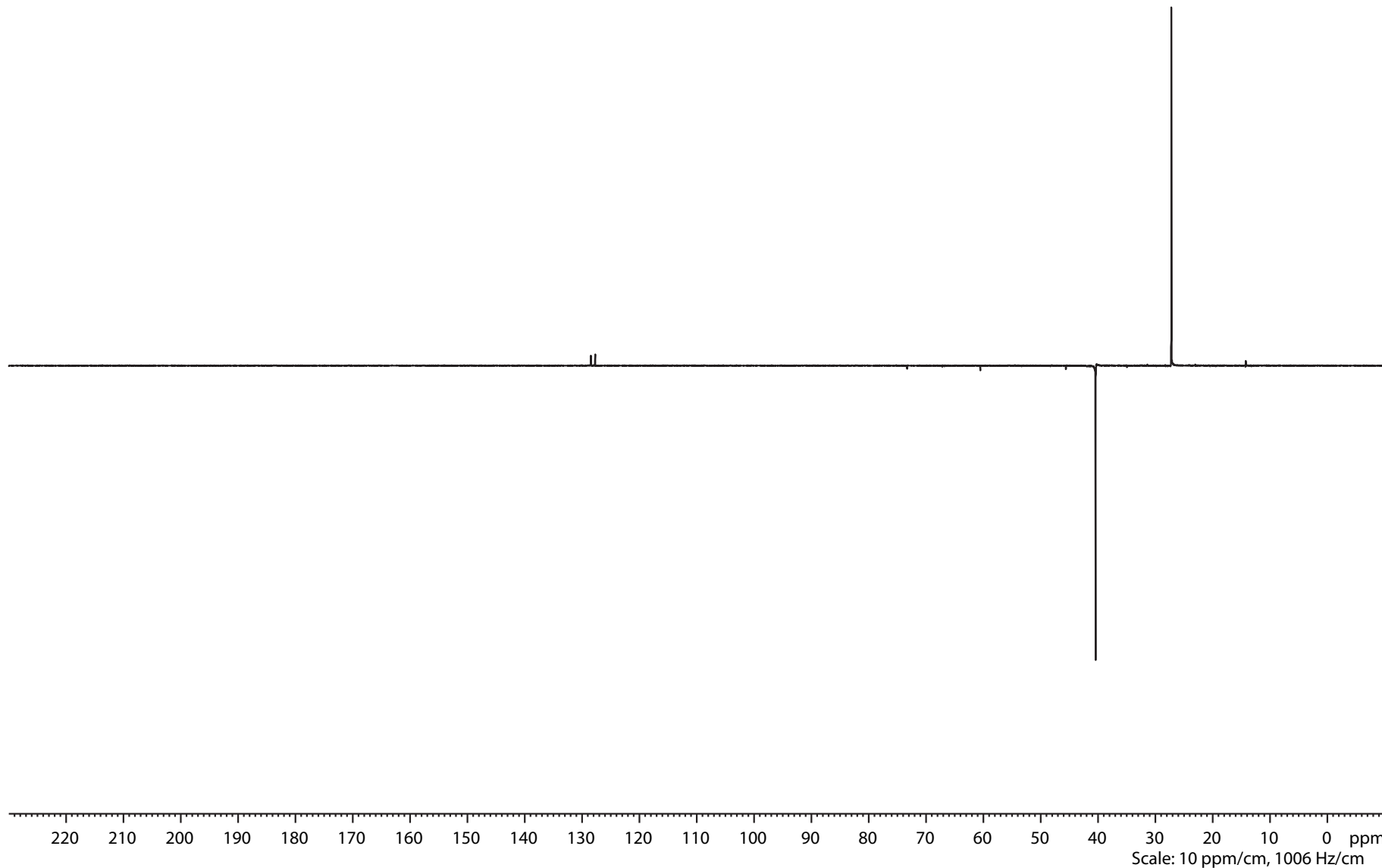
Current Data Parameters
 NAME bae120553_od
 EXPNO 3
 PROCNO 1

F2 - Acquisition Parameters
 Date_ 20130422
 Time 15.11
 INSTRUM drx400
 PROBHD 5 mm QNP 1H/13
 PULPROG dept135
 TD 131072
 SOLVENT CDCl3
 NS 512
 DS 4
 SWH 26315.789 Hz
 FIDRES 0.200774 Hz
 AQ 2.4904180 sec
 RG 8192
 DW 19.000 usec
 DE 7.00 usec
 TE 299.2 K
 CNST2 145.0000000
 D1 2.00000000 sec
 d2 0.00344828 sec
 d12 0.00002000 sec
 DELTA 0.00001401 sec
 TD0 1

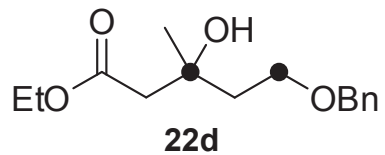
===== CHANNEL f1 =====
 NUC1 13C
 P1 11.00 usec
 p2 22.00 usec
 PL1 -3.00 dB
 SFO1 100.5635842 MHz

===== CHANNEL f2 =====
 CPDPRG2 waltz16
 NUC2 1H
 P3 10.00 usec
 p4 20.00 usec
 PCPD2 80.00 usec
 PL2 -2.00 dB
 PL12 16.06 dB
 SFO2 399.8915996 MHz

F2 - Processing parameters
 SI 65536
 SF 100.5524178 MHz
 SR -3.20 Hz
 WDW EM
 SSB 0
 LB 1.00 Hz
 GB 0
 PC 1.40



Scale: 10 ppm/cm, 1006 Hz/cm

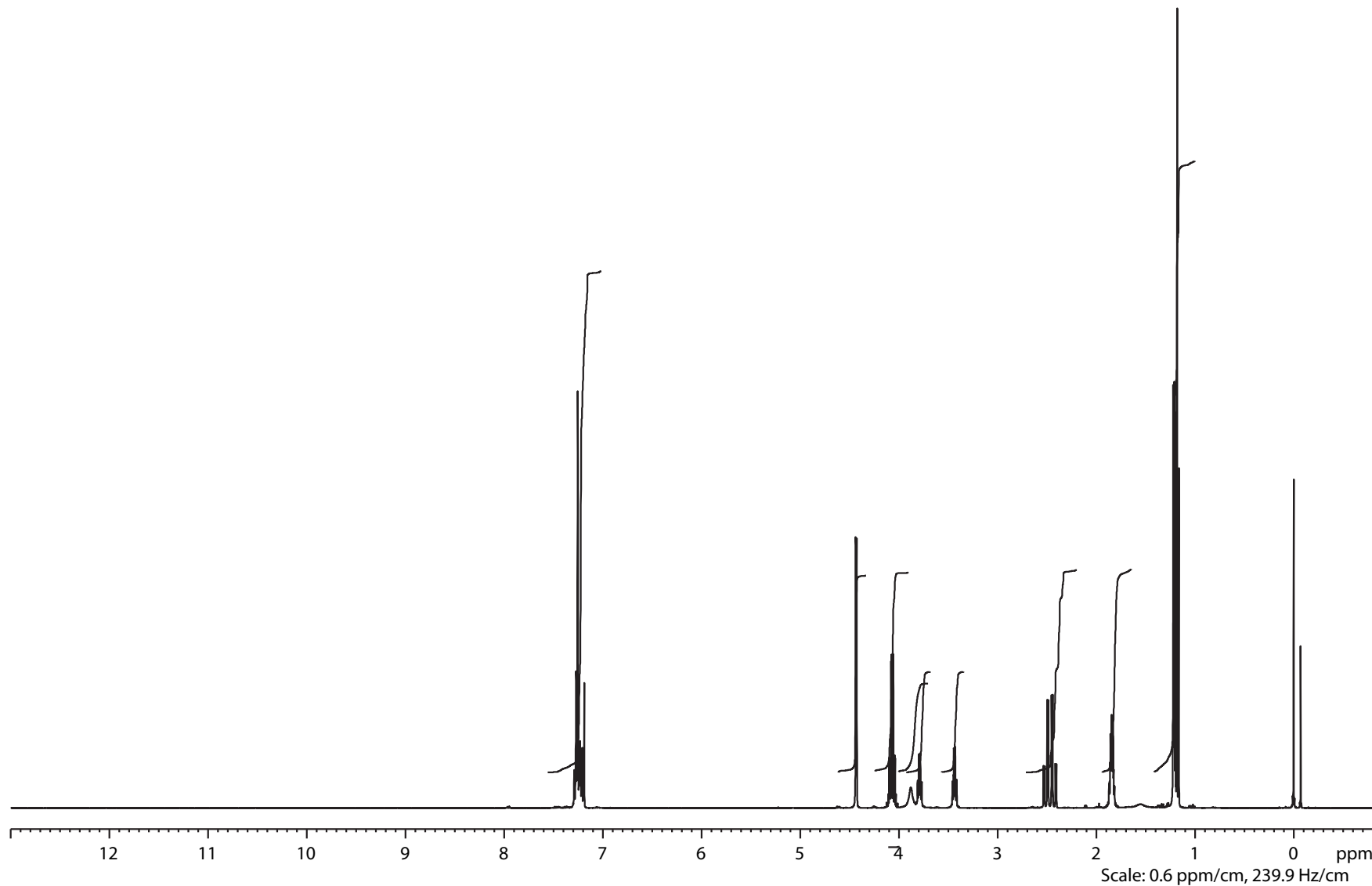


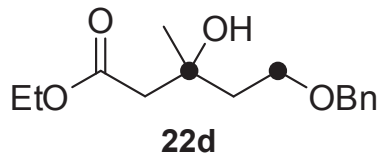
Current Data Parameters
 NAME bae122796_od
 EXPNO 1
 PROCNO 1

F2 - Acquisition Parameters
 Date_ 20131212
 Time 18.22
 INSTRUM drx400
 PROBHD 5 mm QNP 1H/13
 PULPROG zg30
 TD 65536
 SOLVENT CDCl3
 NS 64
 DS 2
 SWH 8278.146 Hz
 FIDRES 0.126314 Hz
 AQ 3.9584243 sec
 RG 161.3
 DW 60.400 usec
 DE 6.00 usec
 TE 298.2 K
 D1 1.00000000 sec
 TD0 1

==== CHANNEL f1 =====
 NUC1 1H
 P1 10.20 usec
 PL1 -2.00 dB
 SFO1 399.8524687 MHz

F2 - Processing parameters
 SI 32768
 SF 399.8500439 MHz
 SR 43.88 Hz
 WDW EM
 SSB 0
 LB 0.00 Hz
 GB 0
 PC 1.40





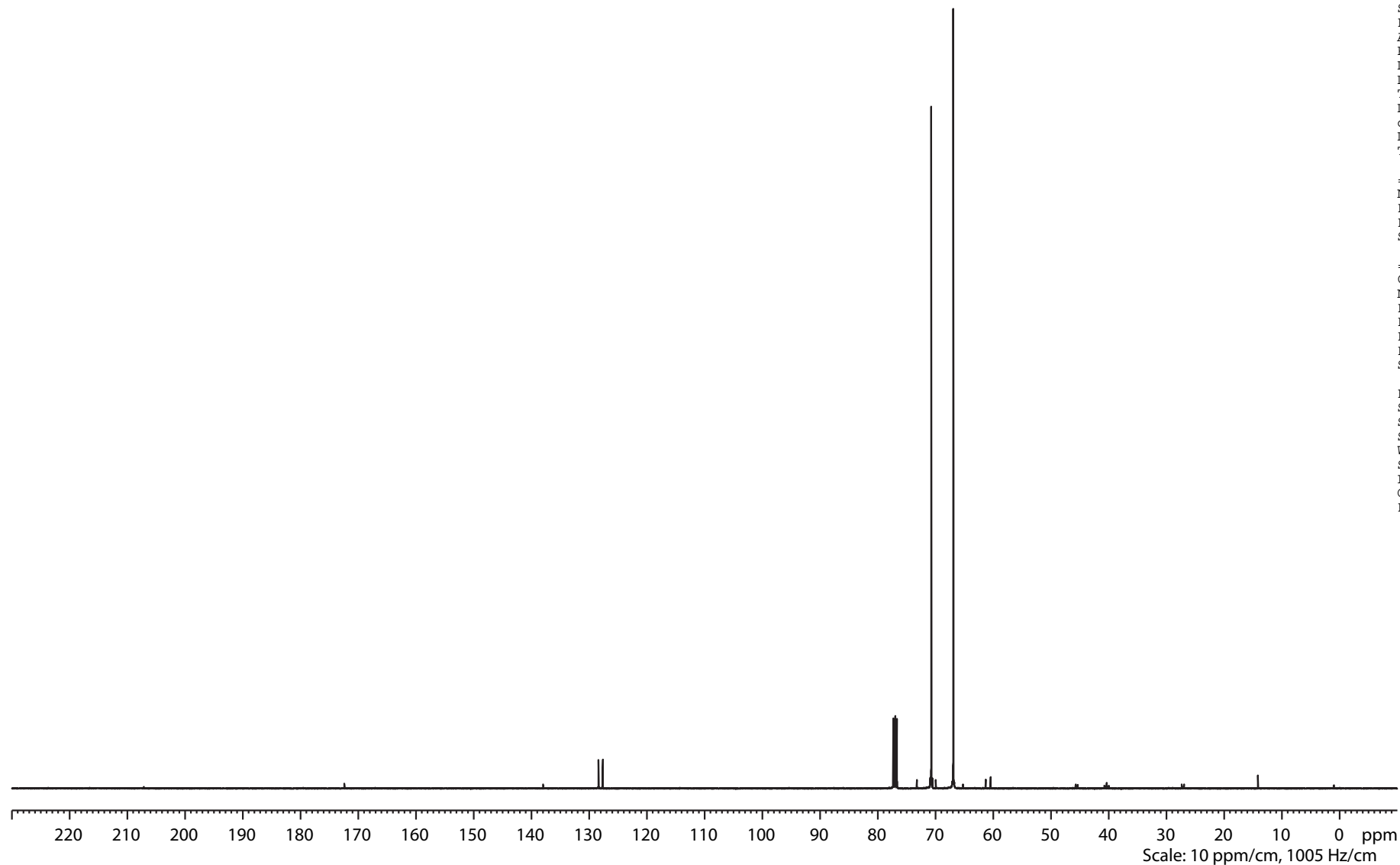
Current Data Parameters
 NAME bae122796_od
 EXPNO 2
 PROCNO 1

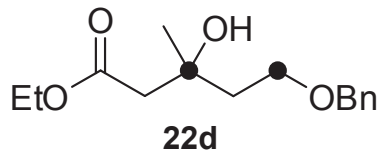
F2 - Acquisition Parameters
 Date_ 20131212
 Time 20.58
 INSTRUM drx400
 PROBHD 5 mm QNP 1H/13
 PULPROG zgpg30
 TD 131072
 SOLVENT CDCl3
 NS 2048
 DS 4
 SWH 26315.789 Hz
 FIDRES 0.200774 Hz
 AQ 2.4904180 sec
 RG 9195.2
 DW 19.000 usec
 DE 6.00 usec
 TE 299.2 K
 D1 2.00000000 sec
 d11 0.03000000 sec
 DELTA 1.89999998 sec
 TD0 1

==== CHANNEL f1 =====
 NUC1 13C
 P1 11.00 usec
 PL1 -3.00 dB
 SFO1 100.5535241 MHz

==== CHANNEL f2 =====
 CPDPRG2 waltz16
 NUC2 1H
 PCPD2 80.00 usec
 PL2 -2.00 dB
 PL12 16.06 dB
 PL13 16.06 dB
 SFO2 399.8515994 MHz

F2 - Processing parameters
 SI 65536
 SF 100.5423662 MHz
 SR 3.16 Hz
 WDW EM
 SSB 0
 LB 1.00 Hz
 GB 0
 PC 1.40





```

Current Data Parameters
NAME      bae122796_od
EXPNO     3
PROCNO    1

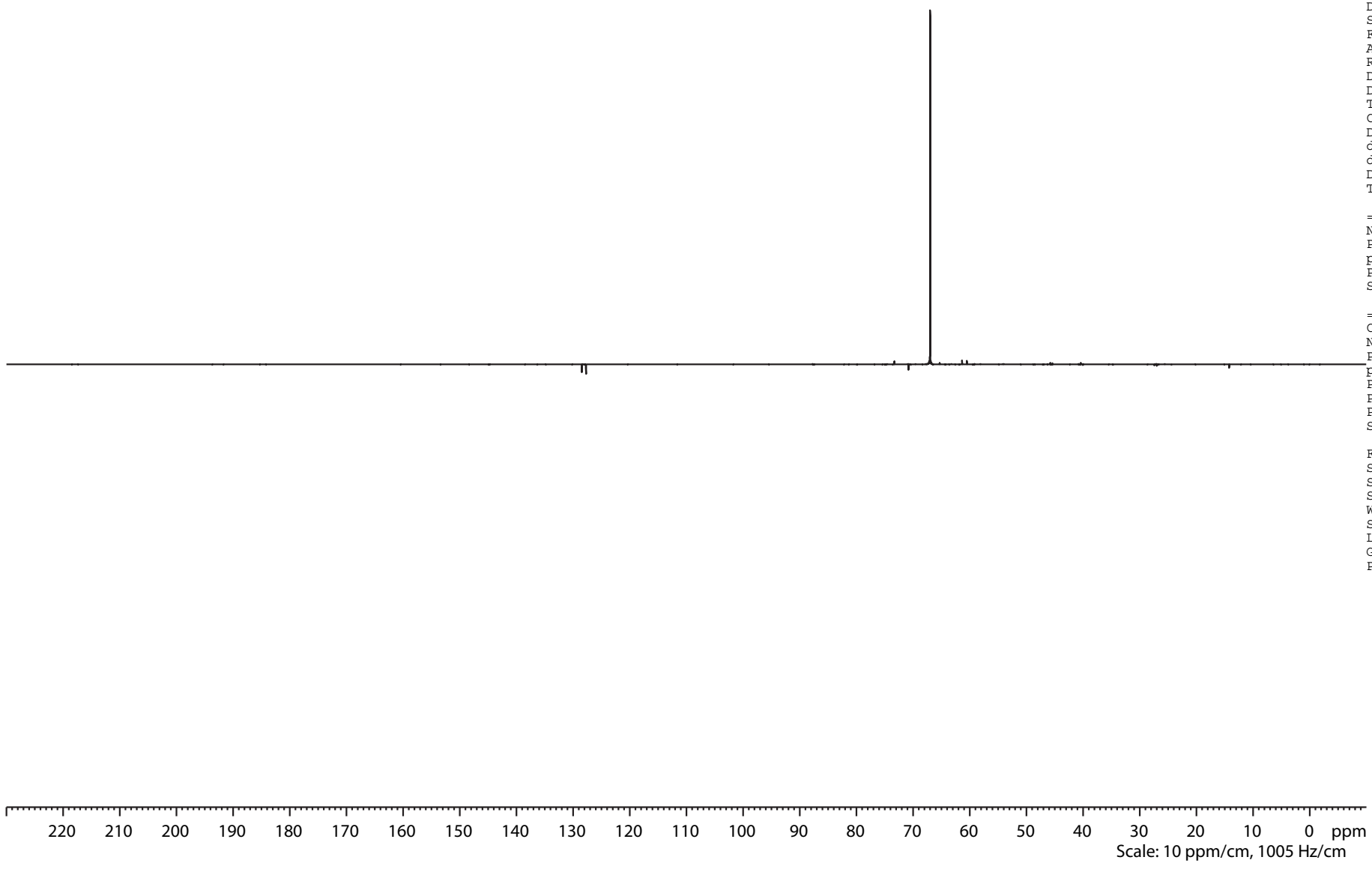
F2 - Acquisition Parameters
Date_     20131212
Time      22.17
INSTRUM   drx400
PROBHD    5 mm QNP 1H/13
PULPROG   dept135
TD         131072
SOLVENT   CDCl3
NS         1024
DS         4
SWH        26315.789 Hz
FIDRES     0.200774 Hz
AQ         2.4904180 sec
RG         8192
DW         19.000 usec
DE         7.00 usec
TE         299.2 K
CNST2     145.0000000
D1         2.0000000 sec
d2         0.00344828 sec
d12        0.00002000 sec
DELTA     0.00001401 sec
TD0        1

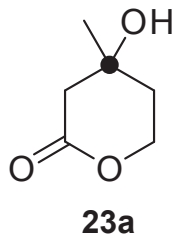
===== CHANNEL f1 =====
NUC1       13C
P1         11.00 usec
p2         22.00 usec
PL1        -3.00 dB
SFO1       100.5535241 MHz

===== CHANNEL f2 =====
CPDPRG2    waltz16
NUC2       1H
P3         10.00 usec
p4         20.00 usec
PCPD2      80.00 usec
PL2        -2.00 dB
PL12       16.06 dB
SFO2       399.8515994 MHz

F2 - Processing parameters
SI         65536
SF         100.5423598 MHz
SR         -3.20 Hz
WDW        EM
SSB        0
LB         1.00 Hz
GB         0
PC         1.40

```



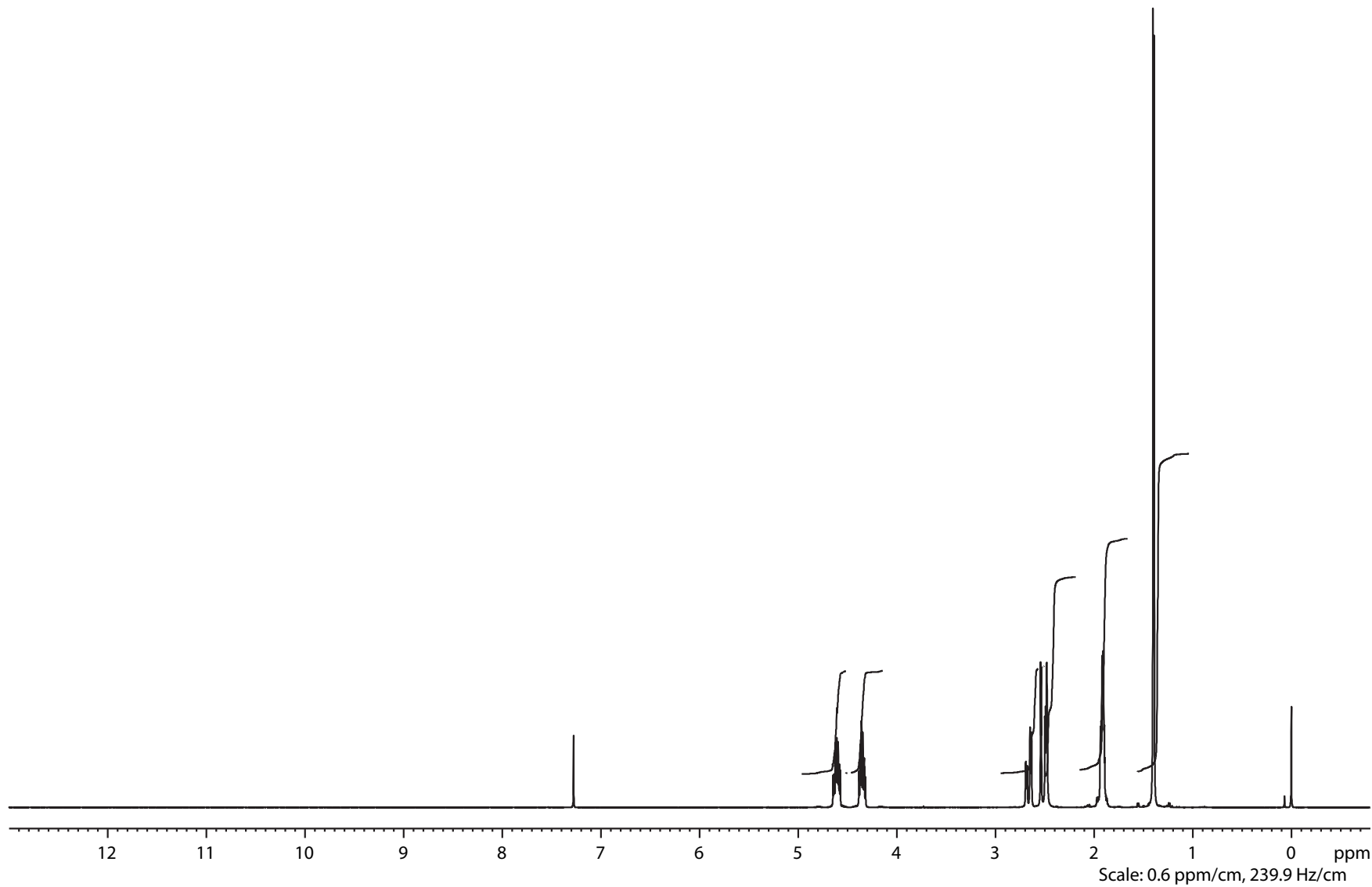


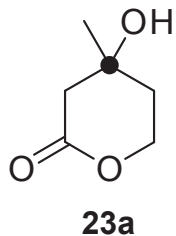
Current Data Parameters
NAME bae123137_od
EXPNO 1
PROCNO 1

F2 - Acquisition Parameters
Date_ 20140209
Time 1.30
INSTRUM drx400
PROBHD 5 mm QNP 1H/13
PULPROG zg30
TD 65536
SOLVENT CDCl3
NS 64
DS 2
SWH 8278.146 Hz
FIDRES 0.126314 Hz
AQ 3.9584243 sec
RG 128
DW 60.400 usec
DE 6.00 usec
TE 299.2 K
D1 1.00000000 sec
TD0 1

==== CHANNEL f1 =====
NUC1 1H
P1 10.20 usec
PL1 -2.00 dB
SFO1 399.8524687 MHz

F2 - Processing parameters
SI 32768
SF 399.8500084 MHz
SR 8.37 Hz
WDW EM
SSB 0
LB 0.00 Hz
GB 0
PC 1.40





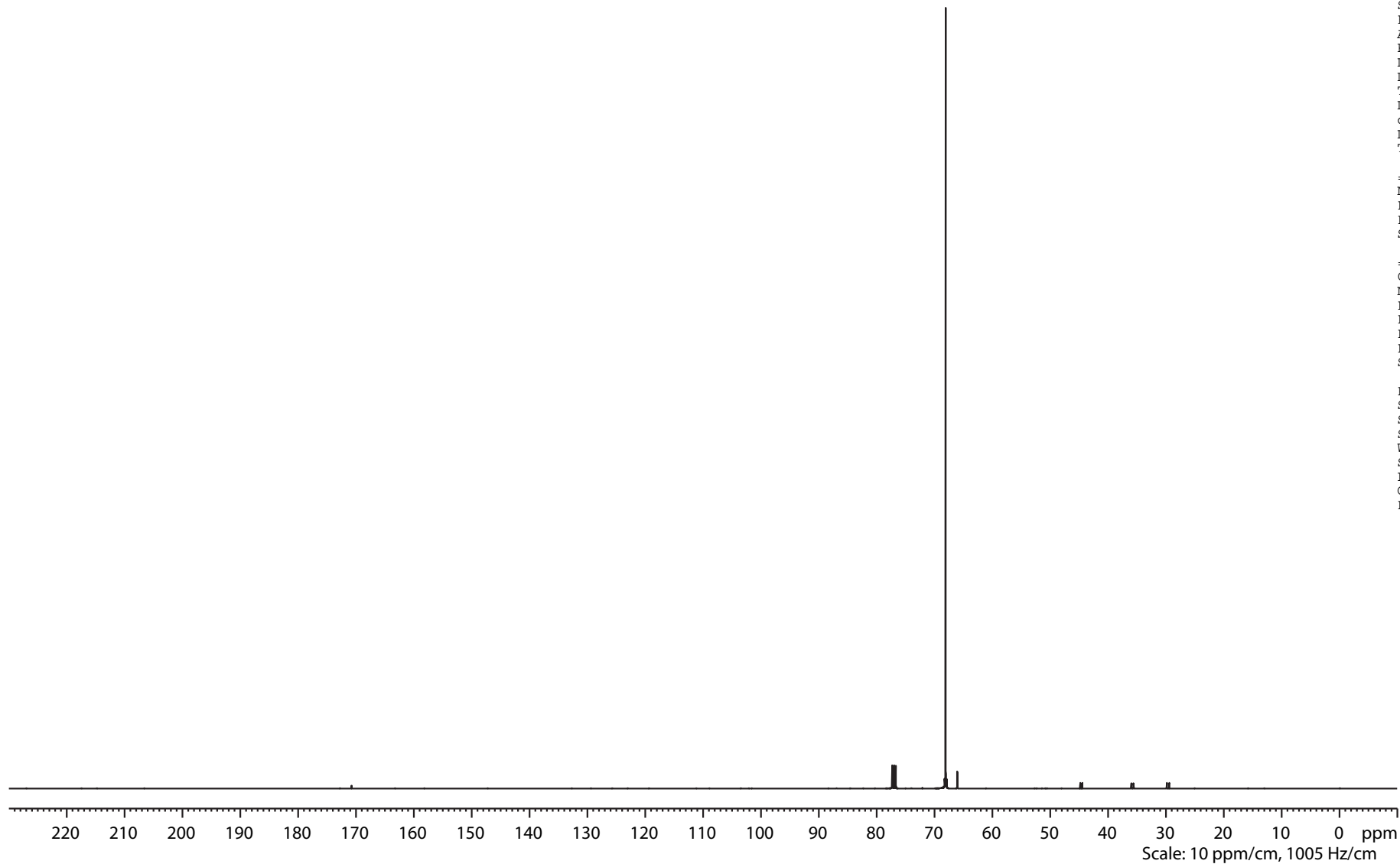
Current Data Parameters
 NAME bae123137_od
 EXPNO 2
 PROCNO 1

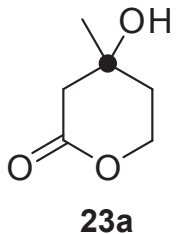
F2 - Acquisition Parameters
 Date_ 20140209
 Time 4.06
 INSTRUM drx400
 PROBHD 5 mm QNP 1H/13
 PULPROG zgpg30
 TD 131072
 SOLVENT CDCl3
 NS 2048
 DS 4
 SWH 26315.789 Hz
 FIDRES 0.200774 Hz
 AQ 2.4904180 sec
 RG 9195.2
 DW 19.000 usec
 DE 6.00 usec
 TE 300.2 K
 D1 2.00000000 sec
 d11 0.03000000 sec
 DELTA 1.89999998 sec
 TD0 1

==== CHANNEL f1 =====
 NUC1 13C
 P1 11.00 usec
 PL1 -3.00 dB
 SFO1 100.5535241 MHz

==== CHANNEL f2 =====
 CPDPRG2 waltz16
 NUC2 1H
 PCPD2 80.00 usec
 PL2 -2.00 dB
 PL12 16.06 dB
 PL13 16.06 dB
 SFO2 399.8515994 MHz

F2 - Processing parameters
 SI 65536
 SF 100.5423683 MHz
 SR 5.33 Hz
 WDW EM
 SSB 0
 LB 1.00 Hz
 GB 0
 PC 1.40





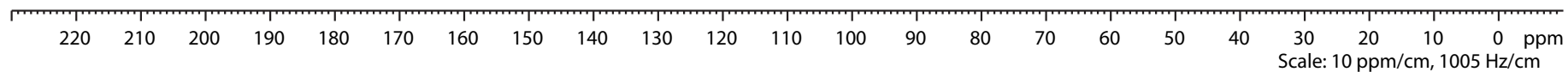
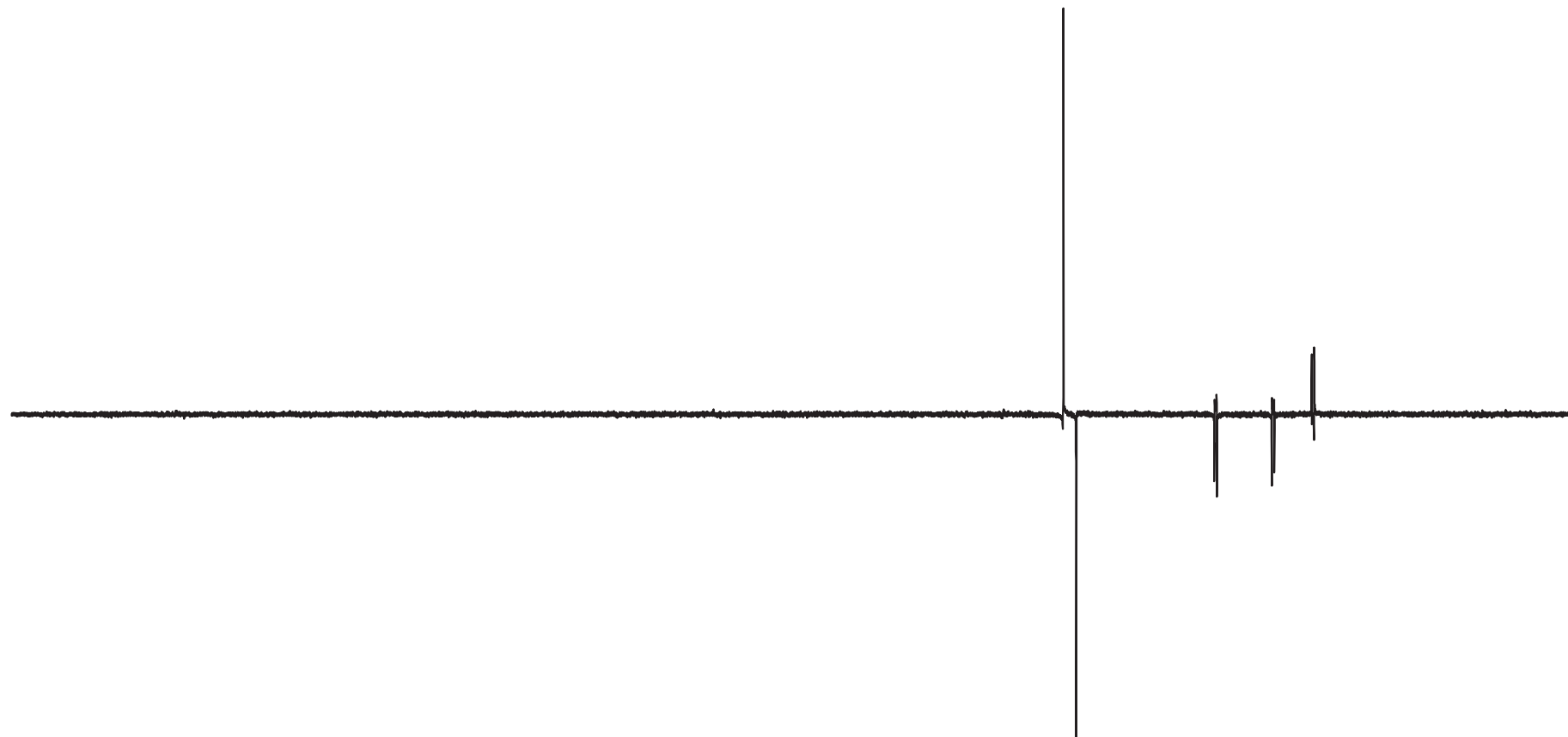
Current Data Parameters
 NAME bae123137_od
 EXPNO 3
 PROCNO 1

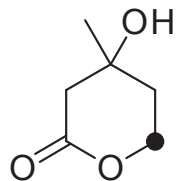
F2 - Acquisition Parameters
 Date_ 20140209
 Time 5.25
 INSTRUM drx400
 PROBHD 5 mm QNP 1H/13
 PULPROG dept135
 TD 131072
 SOLVENT CDCl3
 NS 1024
 DS 4
 SWH 26315.789 Hz
 FIDRES 0.200774 Hz
 AQ 2.4904180 sec
 RG 8192
 DW 19.000 usec
 DE 7.00 usec
 TE 299.2 K
 CNST2 145.0000000
 D1 2.0000000 sec
 d2 0.00344828 sec
 d12 0.00002000 sec
 DELTA 0.00001401 sec
 TD0 1

==== CHANNEL f1 =====
 NUC1 13C
 P1 11.00 usec
 p2 22.00 usec
 PL1 -3.00 dB
 SFO1 100.5535241 MHz

==== CHANNEL f2 =====
 CPDPRG2 waltz16
 NUC2 1H
 P3 10.00 usec
 p4 20.00 usec
 PCPD2 80.00 usec
 PL2 -2.00 dB
 PL12 16.06 dB
 SFO2 399.8515994 MHz

F2 - Processing parameters
 SI 65536
 SF 100.5423598 MHz
 SR -3.20 Hz
 WDW EM
 SSB 0
 LB 1.00 Hz
 GB 0
 PC 1.40

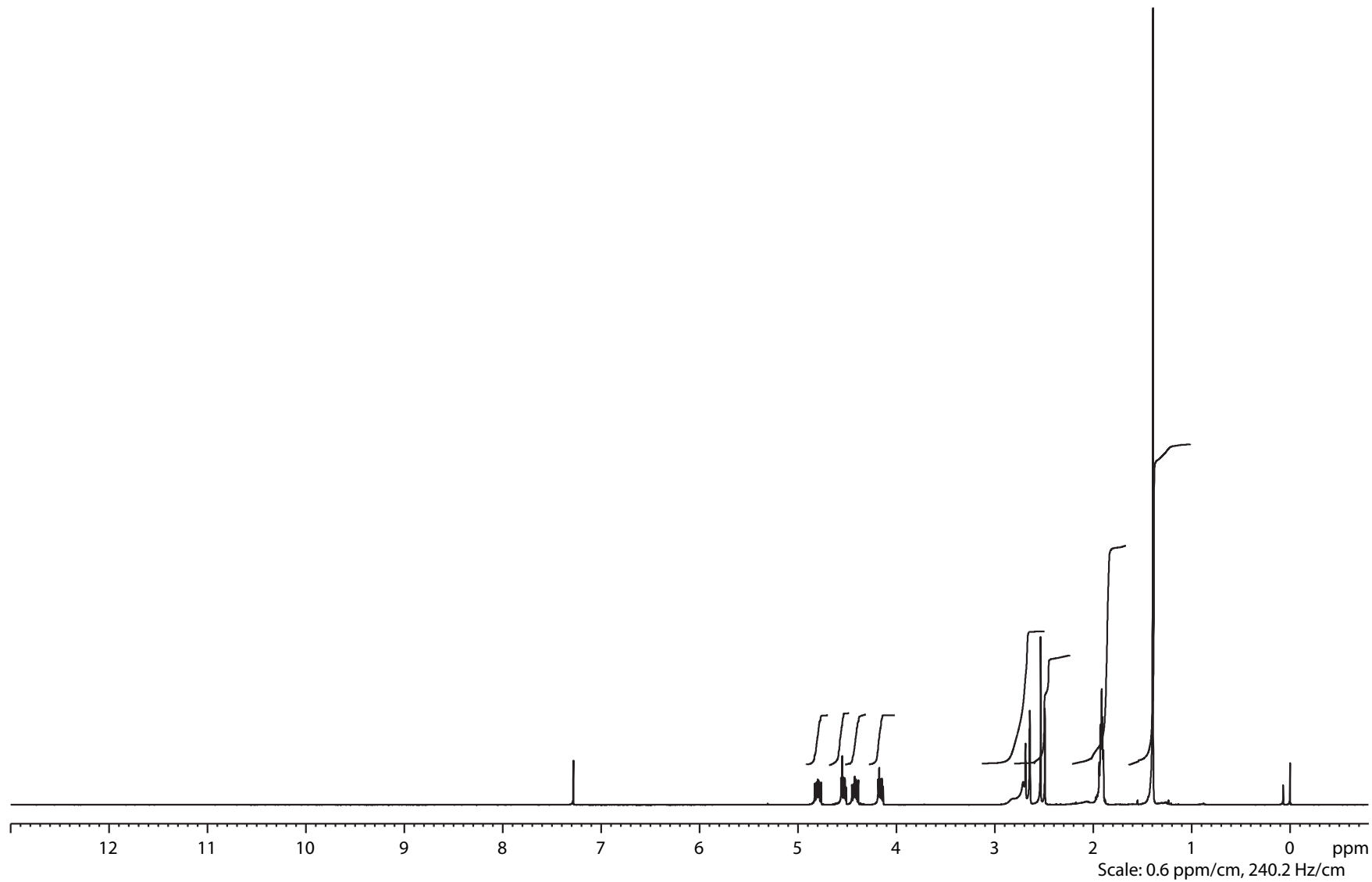


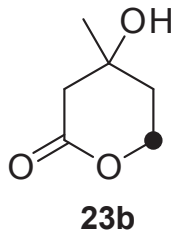


23b

NAME bae123987_od
EXPNO 1
PROCNO 1
Date_ 20140424
Time_ 15.48
INSTRUM AVIII400
PROBHD 5 mm PABBO BB-
PULPROG zg30
TD 65536
SOLVENT CDCl3
NS 64
DS 2
SWH 8223.685 Hz
FIDRES 0.125483 Hz
AQ 3.9846387 sec
RG 64
DW 60.800 usec
DE 6.50 usec
TE 297.3 K
D1 1.00000000 sec
TD0 1

==== CHANNEL f1 =====
NUC1 1H
P1 10.33 usec
PL1 -4.00 dB
SFO1 400.4024726 MHz
SI 32768
SF 400.4000089 MHz
SR 8.88 Hz
WDW EM
SSB 0
LB 0.00 Hz
GB 0
PC 1.40
F1P 13.000 ppm
F2P -0.800 ppm





```

NAME      bae123987_od
EXPNO     2
PROCNO    1
Date_     20140424
Time      17.08
INSTRUM   AVIII400
PROBHD    5 mm PABBO BB-
PULPROG   zgpg30
TD         131072
SOLVENT   CDCl3
NS         1024
DS         4
SWH        26315.789 Hz
FIDRES     0.200774 Hz
AQ         2.4904180 sec
RG         90.5
DW         19.000 usec
DE         6.50 usec
TE         299.0 K
D1         2.00000000 sec
D11        0.03000000 sec
TD0        1

```

```

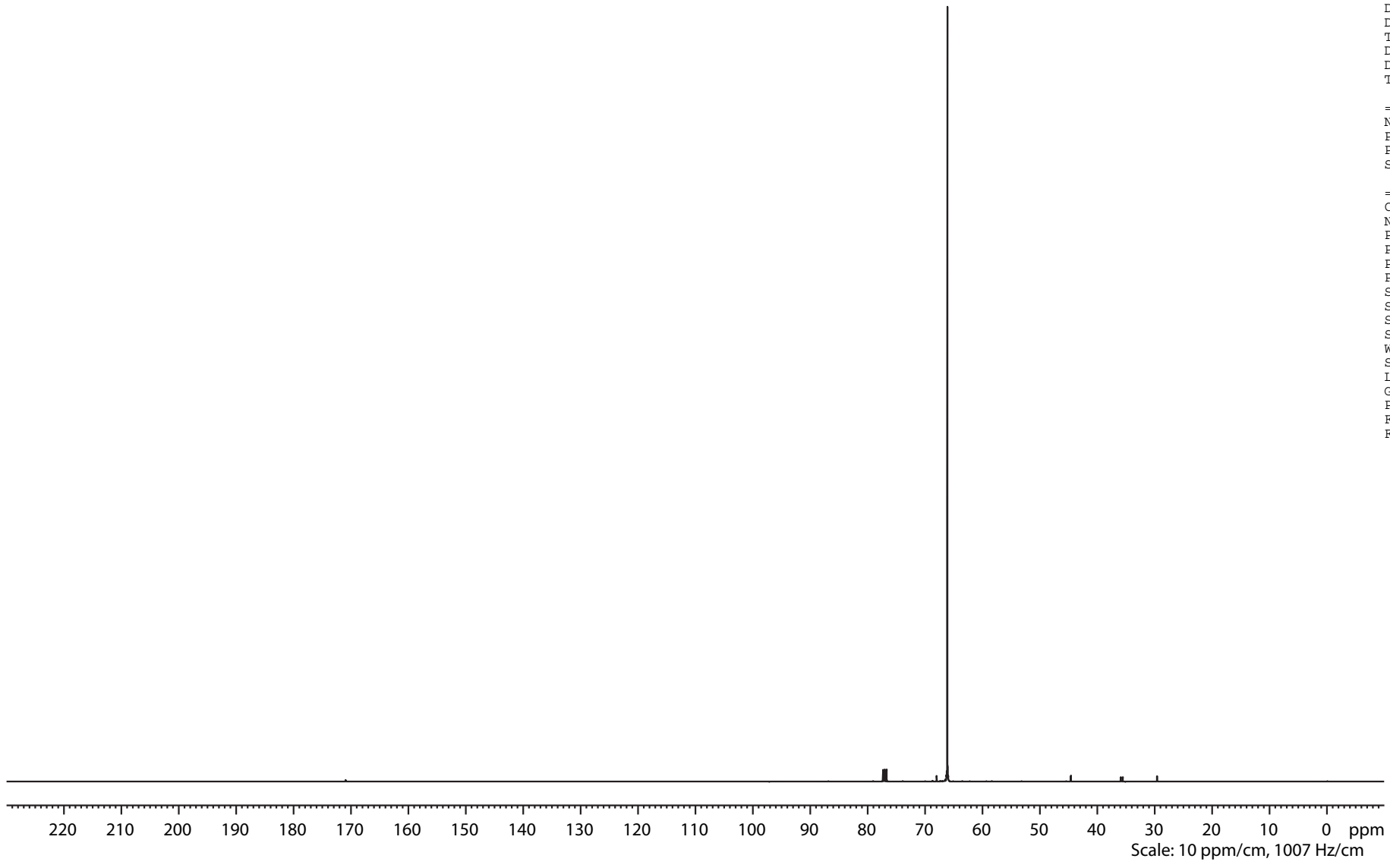
===== CHANNEL f1 =====
NUC1       13C
P1         8.50 usec
PL1        -3.00 dB
SFO1       100.6918371 MHz

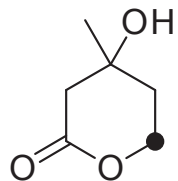
```

```

===== CHANNEL f2 =====
CPDPRG2    waltz16
NUC2       1H
PCPD2      80.00 usec
PL2        -4.00 dB
PL12       13.78 dB
PL13       14.00 dB
SFO2       400.4016016 MHz
SI         65536
SF         100.6806681 MHz
SR         7.07 Hz
WDW         EM
SSB         0
LB         1.00 Hz
GB         0
PC         1.40
F1P        230.000 ppm
F2P        -10.000 ppm

```





23b

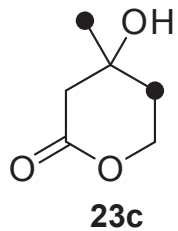
NAME bae123987_od
EXPNO 3
PROCNO 1
Date_ 20140424
Time_ 17.49
INSTRUM AVIII400
PROBHD 5 mm PABBO BB-
PULPROG dept135
TD 131072
SOLVENT CDCl3
NS 512
DS 4
SWH 26315.789 Hz
FIDRES 0.200774 Hz
AQ 2.4904180 sec
RG 2050
DW 19.000 usec
DE 6.50 usec
TE 298.4 K
CNST2 145.0000000
D1 2.00000000 sec
D2 0.00344828 sec
D12 0.00002000 sec
TD0 1

==== CHANNEL f1 =====
NUC1 13C
P1 8.50 usec
P2 17.00 usec
PL1 -3.00 dB
SFO1 100.6919063 MHz

==== CHANNEL f2 =====
CPDPRG2 waltz16
NUC2 1H
P3 10.33 usec
P4 20.66 usec
PCPD2 80.00 usec
PL2 -4.00 dB
PL12 13.78 dB
SFO2 400.4016016 MHz
SI 65536
SF 100.6806152 MHz
SR -45.83 Hz
WDW EM
SSB 0
LB 1.00 Hz
GB 0
PC 1.40
F1P 230.000 ppm
F2P -10.000 ppm



220 210 200 190 180 170 160 150 140 130 120 110 100 90 80 70 60 50 40 30 20 10 0 ppm
Scale: 10 ppm/cm, 1007 Hz/cm

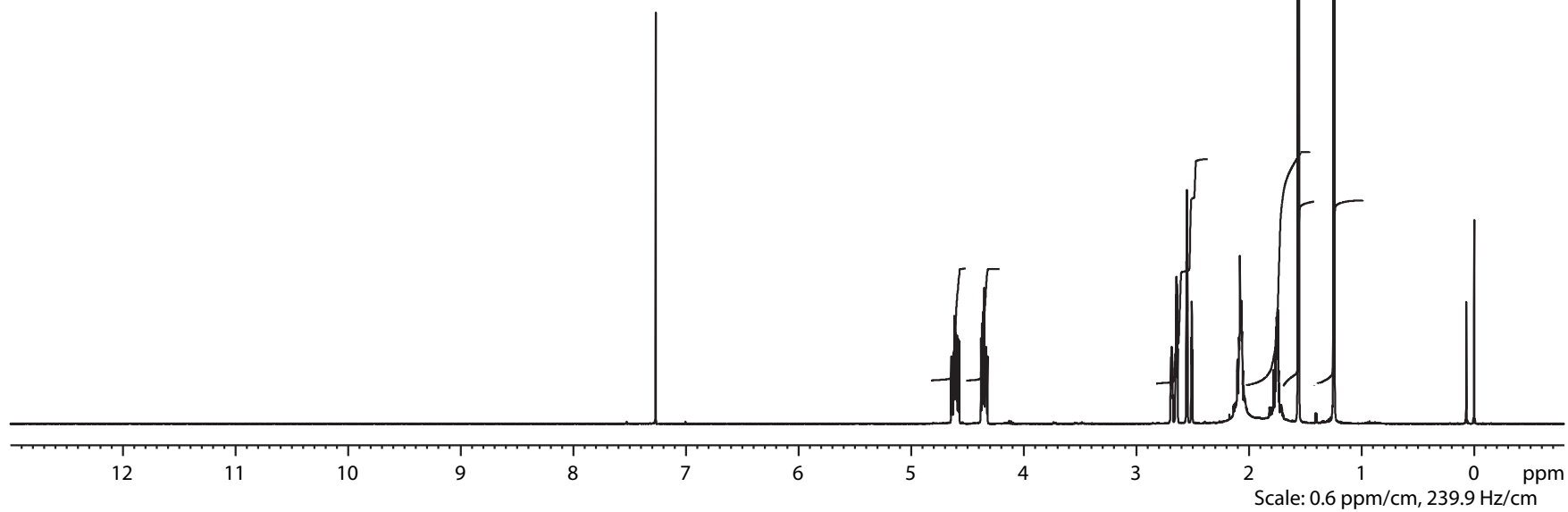


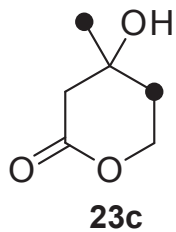
Current Data Parameters
NAME bae120588_od
EXPNO 1
PROCNO 1

F2 - Acquisition Parameters
Date_ 20130426
Time 19.01
INSTRUM drx400
PROBHD 5 mm QNP 1H/13
PULPROG zg30
TD 65536
SOLVENT CDCl3
NS 64
DS 2
SWH 8278.146 Hz
FIDRES 0.126314 Hz
AQ 3.9584243 sec
RG 228.1
DW 60.400 usec
DE 6.00 usec
TE 299.2 K
D1 1.00000000 sec
TD0 1

==== CHANNEL f1 =====
NUC1 1H
P1 10.20 usec
PL1 -2.00 dB
SFO1 399.8924689 MHz

F2 - Processing parameters
SI 32768
SF 399.8900099 MHz
SR 9.86 Hz
WDW EM
SSB 0
LB 0.00 Hz
GB 0
PC 1.40





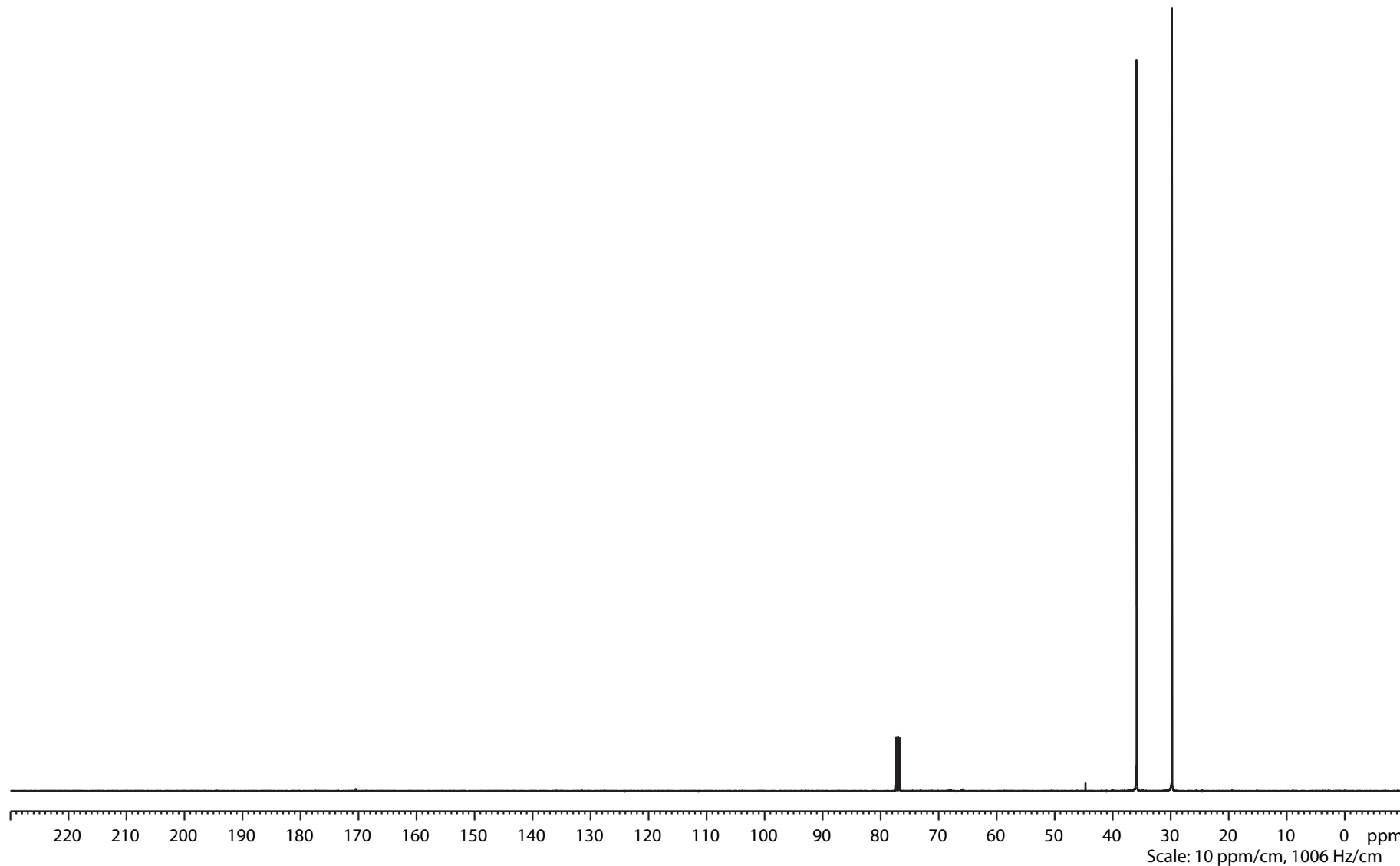
Current Data Parameters
 NAME bae120588_od
 EXPNO 2
 PROCNO 1

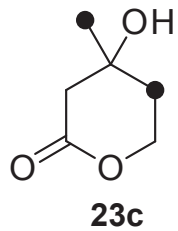
F2 - Acquisition Parameters
 Date_ 20130426
 Time 20.20
 INSTRUM drx400
 PROBHD 5 mm QNP 1H/13
 PULPROG zgpg30
 TD 131072
 SOLVENT CDCL3
 NS 1024
 DS 4
 SWH 26315.789 Hz
 FIDRES 0.200774 Hz
 AQ 2.4904180 sec
 RG 8192
 DW 19.000 usec
 DE 6.00 usec
 TE 300.2 K
 D1 2.00000000 sec
 d11 0.03000000 sec
 DELTA 1.89999998 sec
 TD0 1

==== CHANNEL f1 =====
 NUC1 13C
 P1 11.00 usec
 PL1 -3.00 dB
 SFO1 100.5635842 MHz

==== CHANNEL f2 =====
 CPDPRG2 waltz16
 NUC2 1H
 PCPD2 80.00 usec
 PL2 -2.00 dB
 PL12 16.06 dB
 PL13 16.06 dB
 SFO2 399.8915996 MHz

F2 - Processing parameters
 SI 65536
 SF 100.5524240 MHz
 SR 2.95 Hz
 WDW EM
 SSB 0
 LB 1.00 Hz
 GB 0
 PC 1.40





Current Data Parameters
 NAME bae120588_od
 EXPNO 3
 PROCNO 1

F2 - Acquisition Parameters
 Date_ 20130426
 Time 21.00
 INSTRUM drx400
 PROBHD 5 mm QNP 1H/13
 PULPROG dept135
 TD 131072
 SOLVENT CDCl3
 NS 512
 DS 4
 SWH 26315.789 Hz
 FIDRES 0.200774 Hz
 AQ 2.4904180 sec
 RG 5792.6
 DW 19.000 usec
 DE 7.00 usec
 TE 299.2 K
 CNST2 145.0000000
 D1 2.00000000 sec
 d2 0.00344828 sec
 d12 0.00002000 sec
 DELTA 0.00001401 sec
 TD0 1

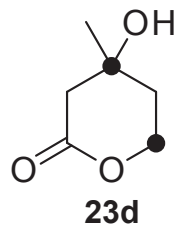
==== CHANNEL f1 =====
 NUC1 13C
 P1 11.00 usec
 p2 22.00 usec
 PL1 -3.00 dB
 SFO1 100.5635842 MHz

==== CHANNEL f2 =====
 CPDPRG2 waltz16
 NUC2 1H
 P3 10.00 usec
 p4 20.00 usec
 PCPD2 80.00 usec
 PL2 -2.00 dB
 PL12 16.06 dB
 SFO2 399.8915996 MHz

F2 - Processing parameters
 SI 65536
 SF 100.5524178 MHz
 SR -3.20 Hz
 WDW EM
 SSB 0
 LB 1.00 Hz
 GB 0
 PC 1.40



220 210 200 190 180 170 160 150 140 130 120 110 100 90 80 70 60 50 40 30 20 10 0 ppm
 Scale: 10 ppm/cm, 1006 Hz/cm

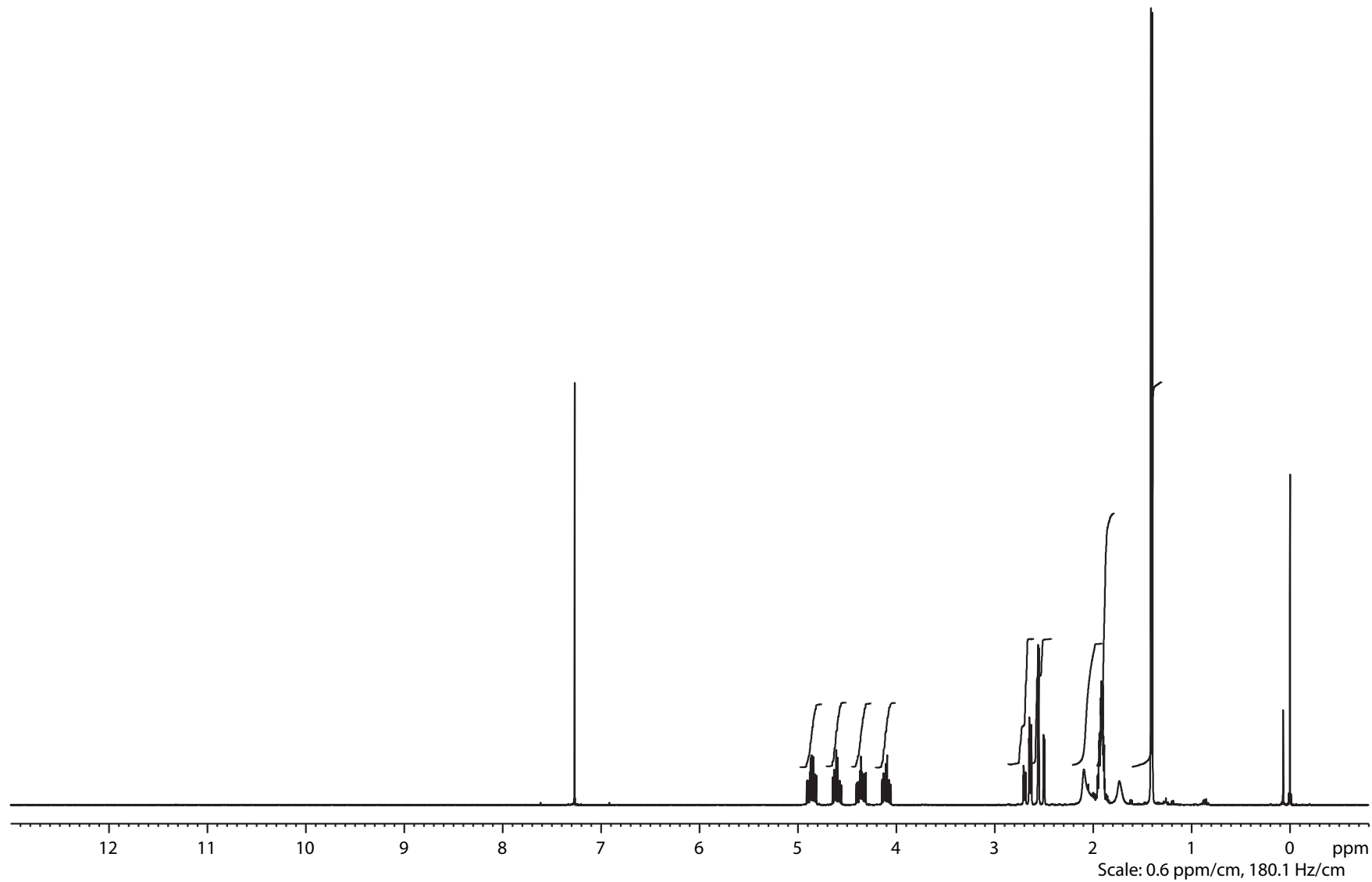


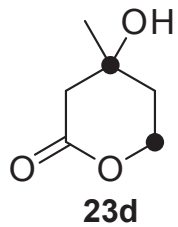
```

NAME      bae-131220-094451_od
EXPNO     1
PROCNO    1
Date_     20131220
Time      10.20
INSTRUM   av300
PROBHD    5 mm PABBO BB-
PULPROG   zg30
TD         49152
SOLVENT   CDCl3
NS         32
DS         2
SWH        6203.474 Hz
FIDRES     0.126210 Hz
AQ         3.9617012 sec
RG         203
DW         80.600 usec
DE         6.00 usec
TE         296.2 K
D1         1.00000000 sec
TD0        1
  
```

```

===== CHANNEL f1 =====
NUC1      1H
P1        12.00 usec
PL1       -1.00 dB
SFO1     300.1318530 MHz
SI        32768
SF        300.1300094 MHz
SR        9.40 Hz
WDW       EM
SSB       0
LB        0.00 Hz
GB        0
PC        1.40
F1P       13.000 ppm
F2P       -0.800 ppm
  
```





```

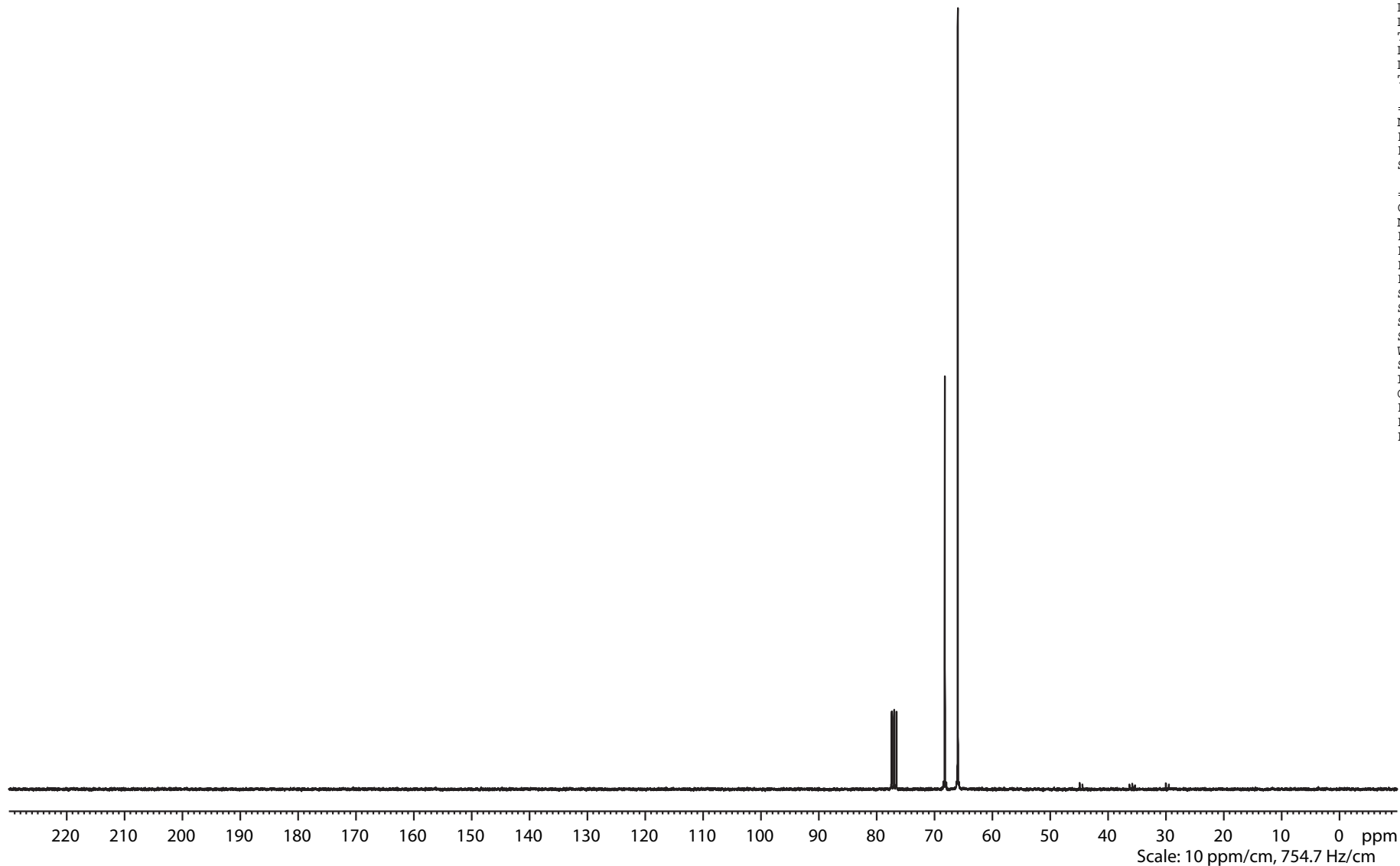
NAME      bae-131220-094451_od
EXPNO     2
PROCNO    1
Date_     20131220
Time      10.35
INSTRUM   av300
PROBHD    5 mm PABBO BB-
PULPROG   zgpg30
TD         98304
SOLVENT   CDCl3
NS         152
DS         4
SWH        19736.842 Hz
FIDRES     0.200774 Hz
AQ         2.4904180 sec
RG         512
DW         25.333 usec
DE         6.00 usec
TE         297.2 K
D1         2.00000000 sec
D11        0.03000000 sec
TD0        1
  
```

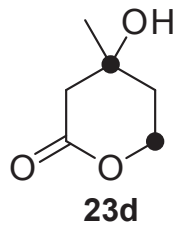
```

===== CHANNEL f1 =====
NUC1       13C
P1         9.60 usec
PL1        -1.00 dB
SFO1       75.4761254 MHz
  
```

```

===== CHANNEL f2 =====
CPDPRG2    waltz16
NUC2       1H
PCPD2      80.00 usec
PL2         -1.00 dB
PL12       15.98 dB
PL13       16.00 dB
SFO2       300.1312005 MHz
SI         65536
SF         75.4677525 MHz
SR         3.50 Hz
WDW         EM
SSB         0
LB         1.00 Hz
GB         0
PC         1.40
F1P        230.000 ppm
F2P        -10.000 ppm
  
```





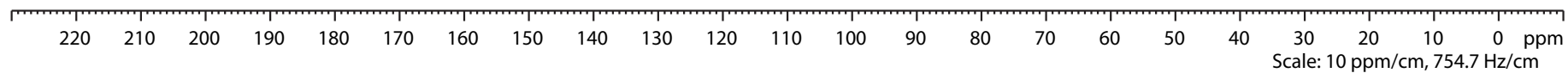
```

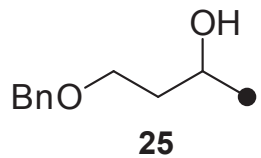
NAME      bae-131220-094451_od
EXPNO     3
PROCNO    1
Date_     20131220
Time      10.43
INSTRUM   av300
PROBHD    5 mm PABBO BB-
PULPROG   dept135
TD         98304
SOLVENT   CDCl3
NS         76
DS         4
SWH        19736.842 Hz
FIDRES     0.200774 Hz
AQ         2.4904180 sec
RG         1030
DW         25.333 usec
DE         6.00 usec
TE         297.2 K
CNST2     145.0000000
D1         2.00000000 sec
D2         0.00344828 sec
D12        0.00002000 sec
TD0        1

===== CHANNEL f1 =====
NUC1       13C
P1         9.60 usec
P2         19.20 usec
PL1        -1.00 dB
SFO1       75.4761254 MHz

===== CHANNEL f2 =====
CPDPRG2    waltz16
NUC2       1H
P3         11.60 usec
P4         23.20 usec
PCPD2      80.00 usec
PL2        -1.00 dB
PL12       15.98 dB
SFO2       300.1312005 MHz
SI         65536
SF         75.4677466 MHz
SR         -2.41 Hz
WDW        EM
SSB        0
LB         1.00 Hz
GB         0
PC         1.40
F1P        230.000 ppm
F2P        -10.000 ppm

```





```

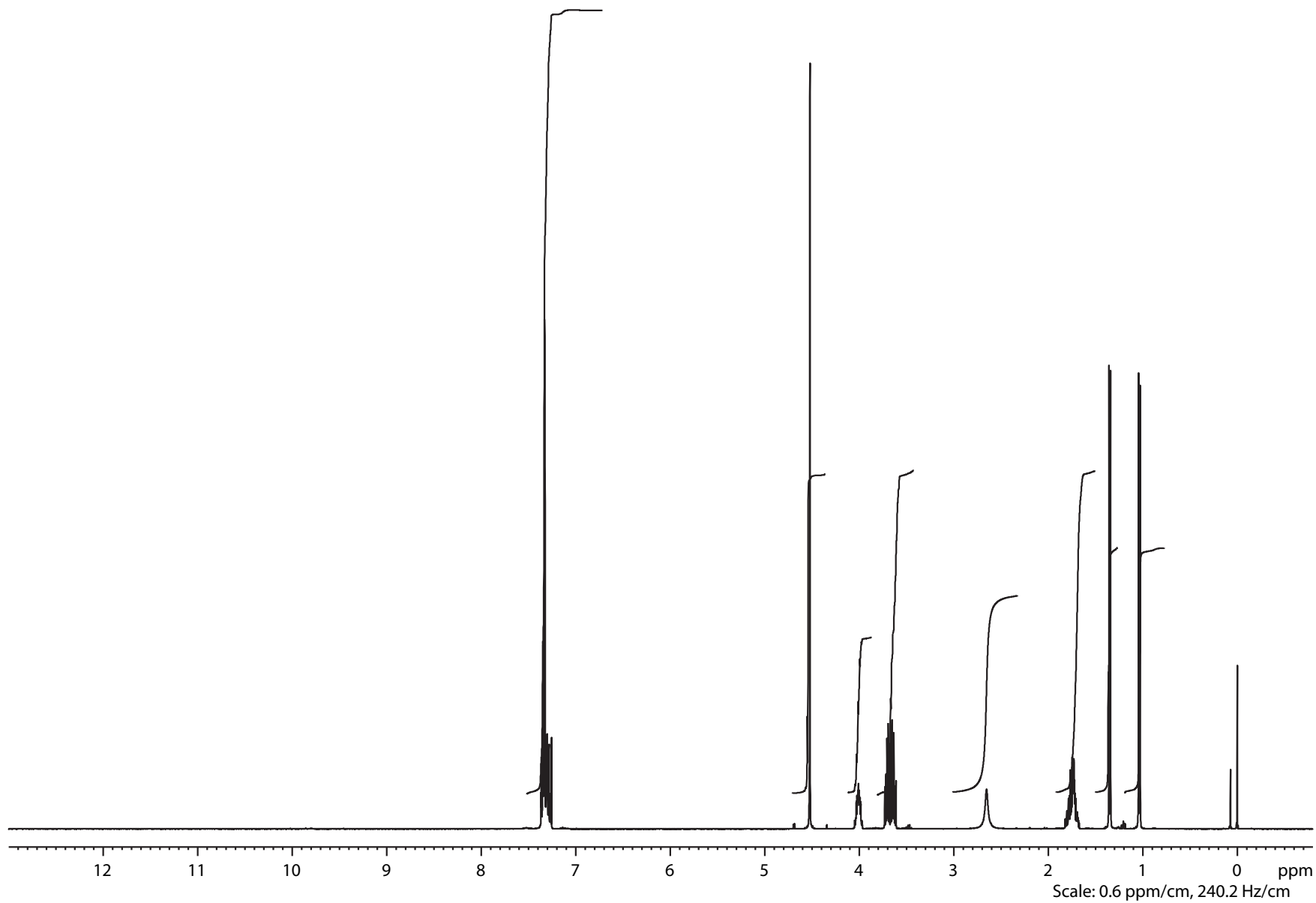
NAME      bae122178_od
EXPNO     1
PROCNO    1
Date_     20131008
Time      17.38
INSTRUM   AVIII400
PROBHD    5 mm PABBO BB-
PULPROG   zg30
TD         65536
SOLVENT   CDCl3
NS         64
DS         2
SWH        8223.685 Hz
FIDRES     0.125483 Hz
AQ         3.9846387 sec
RG         71.8
DW         60.800 usec
DE         6.50 usec
TE         297.7 K
D1         1.00000000 sec
TD0        1

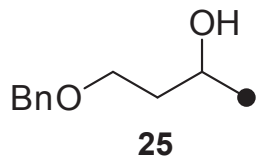
```

```

===== CHANNEL f1 =====
NUC1      1H
P1        10.33 usec
PL1       -4.00 dB
SFO1      400.4024726 MHz
SI        32768
SF         400.4000202 MHz
SR         20.15 Hz
WDW        EM
SSB        0
LB         0.00 Hz
GB         0
PC         1.40
F1P        13.000 ppm
F2P        -0.800 ppm

```





```

NAME      bae122178_od
EXPNO     2
PROCNO    1
Date_     20131008
Time      20.16
INSTRUM   AVIII400
PROBHD    5 mm PABBO BB-
PULPROG   zgpg30
TD         131072
SOLVENT   CDCl3
NS         2048
DS         4
SWH        26315.789 Hz
FIDRES     0.200774 Hz
AQ         2.4904180 sec
RG         90.5
DW         19.000 usec
DE         6.50 usec
TE         298.8 K
D1         2.00000000 sec
D11        0.03000000 sec
TD0        1

```

```

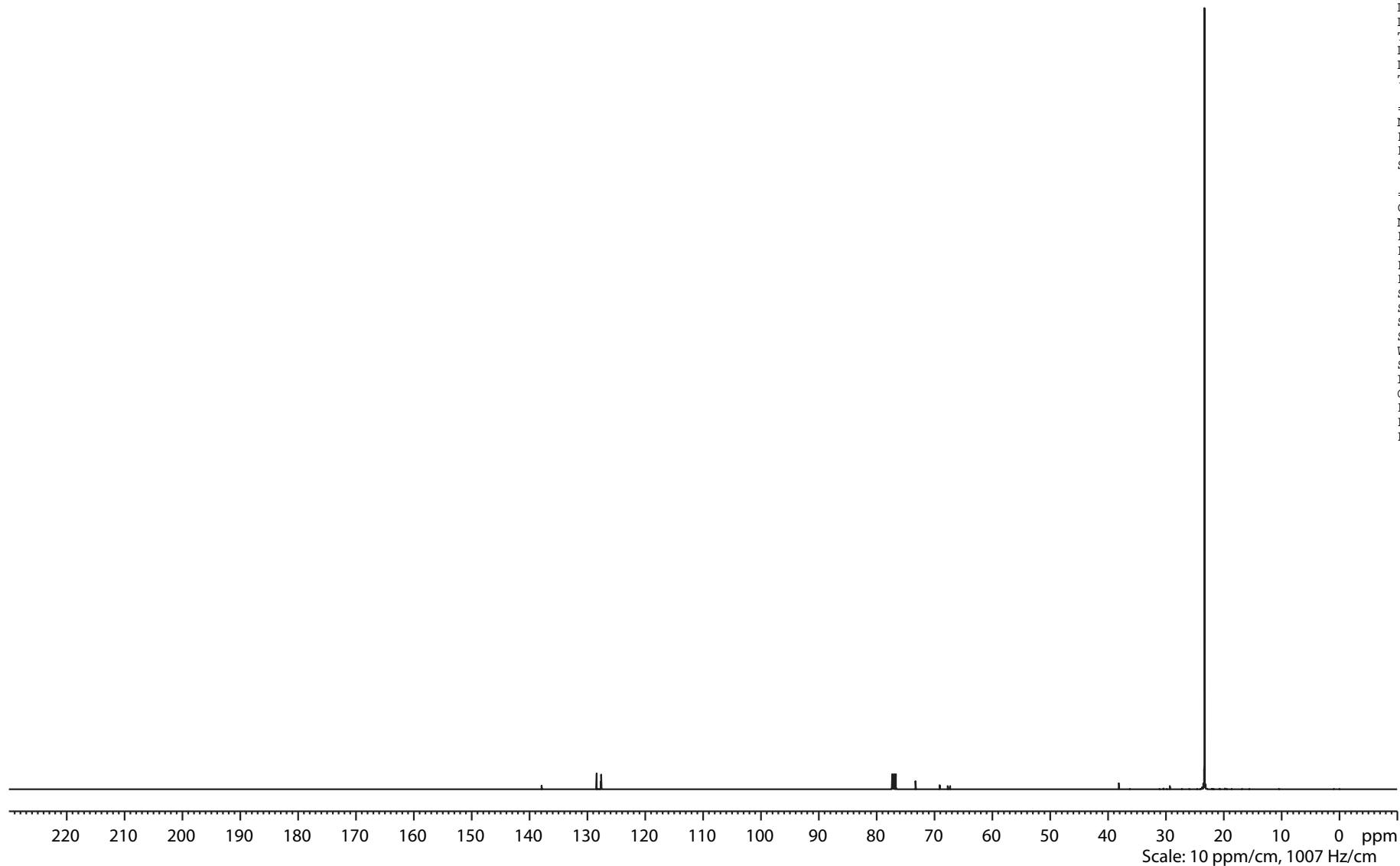
===== CHANNEL f1 =====
NUC1       13C
P1         8.50 usec
PL1        -3.00 dB
SFO1       100.6918371 MHz

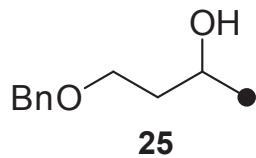
```

```

===== CHANNEL f2 =====
CPDPRG2    waltz16
NUC2        1H
PCPD2       80.00 usec
PL2         -4.00 dB
PL12        13.78 dB
PL13        14.00 dB
SFO2        400.4016016 MHz
SI          65536
SF          100.6806664 MHz
SR          5.37 Hz
WDW         EM
SSB         0
LB          1.00 Hz
GB          0
PC          1.40
F1P         230.000 ppm
F2P         -10.000 ppm

```





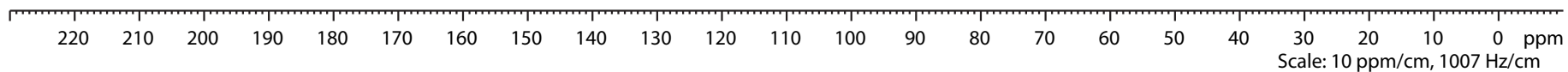
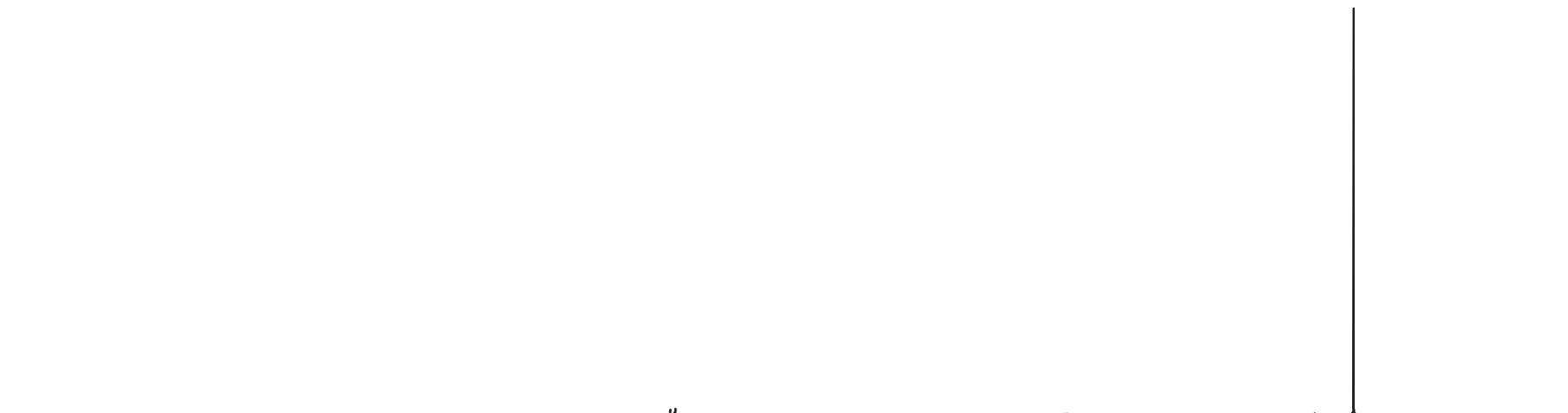
```

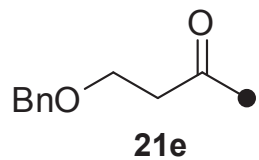
NAME      bae122178_od
EXPNO     3
PROCNO    1
Date_     20131008
Time      21.35
INSTRUM   AVIII400
PROBHD    5 mm PABBO BB-
PULPROG   dept135
TD         131072
SOLVENT   CDCl3
NS         1024
DS         4
SWH        26315.789 Hz
FIDRES     0.200774 Hz
AQ         2.4904180 sec
RG         2050
DW         19.000 usec
DE         6.50 usec
TE         298.0 K
CNST2     145.0000000
D1         2.00000000 sec
D2         0.00344828 sec
D12        0.00002000 sec
TD0        1

===== CHANNEL f1 =====
NUC1       13C
P1         8.50 usec
P2         17.00 usec
PL1        -3.00 dB
SFO1       100.6919063 MHz

===== CHANNEL f2 =====
CPDPRG2    waltz16
NUC2       1H
P3         10.33 usec
P4         20.66 usec
PCPD2      80.00 usec
PL2        -4.00 dB
PL12       13.78 dB
SFO2       400.4016016 MHz
SI         65536
SF         100.6806578 MHz
SR         -3.20 Hz
WDW        EM
SSB        0
LB         1.00 Hz
GB         0
PC         1.40
F1P        230.000 ppm
F2P        -10.000 ppm

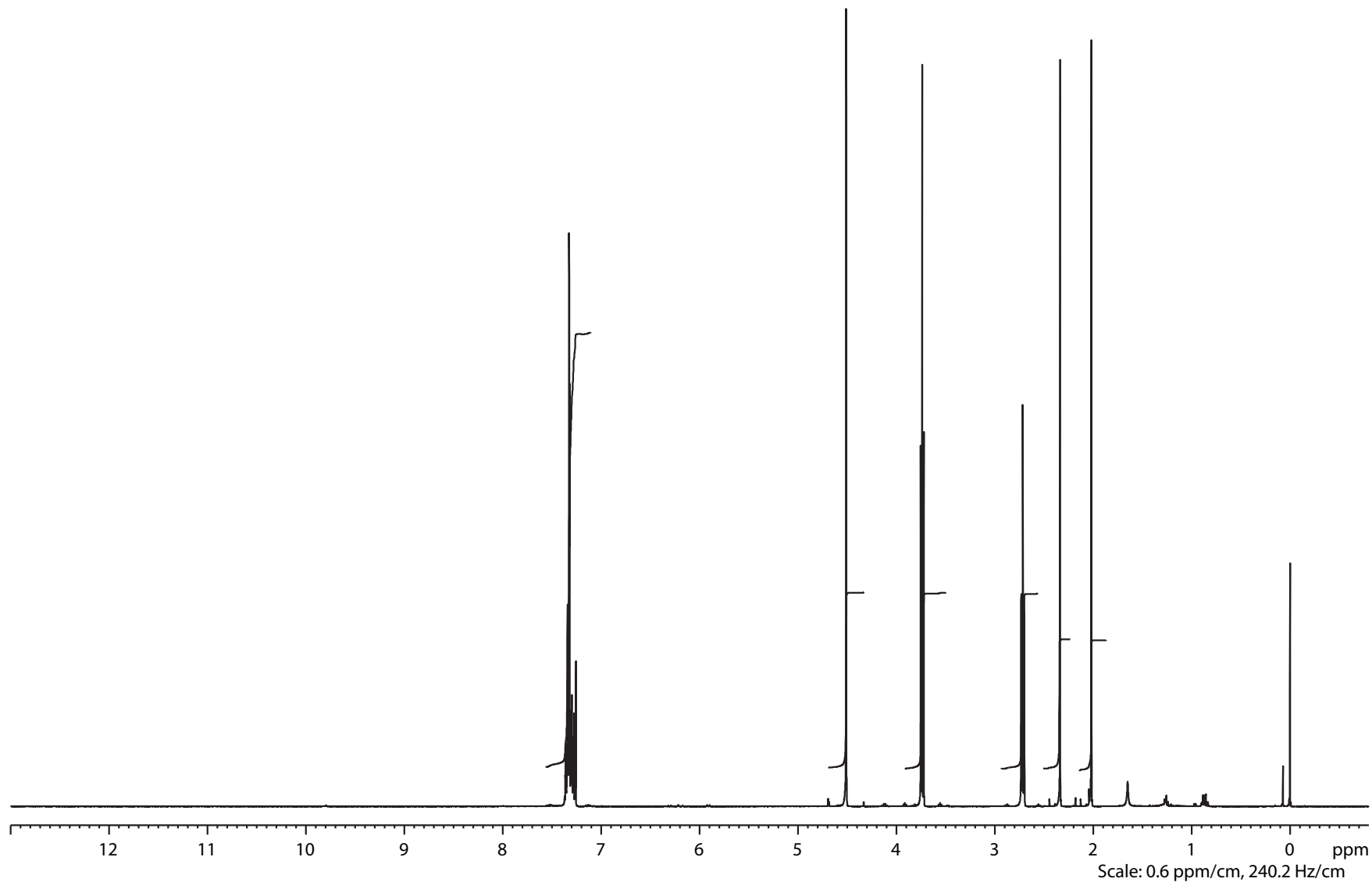
```

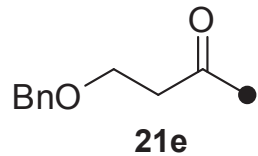




NAME bae122177_od
EXPNO 1
PROCNO 1
Date_ 20131008
Time_ 13.32
INSTRUM AVIII400
PROBHD 5 mm PABBO BB-
PULPROG zg30
TD 65536
SOLVENT CDCl3
NS 64
DS 2
SWH 8223.685 Hz
FIDRES 0.125483 Hz
AQ 3.9846387 sec
RG 144
DW 60.800 usec
DE 6.50 usec
TE 297.4 K
D1 1.00000000 sec
TD0 1

==== CHANNEL f1 =====
NUC1 1H
P1 10.33 usec
PL1 -4.00 dB
SFO1 400.4024726 MHz
SI 32768
SF 400.4000194 MHz
SR 19.42 Hz
WDW EM
SSB 0
LB 0.00 Hz
GB 0
PC 1.40
F1P 13.000 ppm
F2P -0.800 ppm





```

NAME      bae122177_od
EXPNO     2
PROCNO    1
Date_     20131008
Time      16.10
INSTRUM   AVIII400
PROBHD    5 mm PABBO BB-
PULPROG   zgpg30
TD         131072
SOLVENT   CDCl3
NS         2048
DS         4
SWH        26315.789 Hz
FIDRES     0.200774 Hz
AQ         2.4904180 sec
RG          90.5
DW          19.000 usec
DE          6.50 usec
TE          299.3 K
D1          2.00000000 sec
D11         0.03000000 sec
TD0         1

```

```

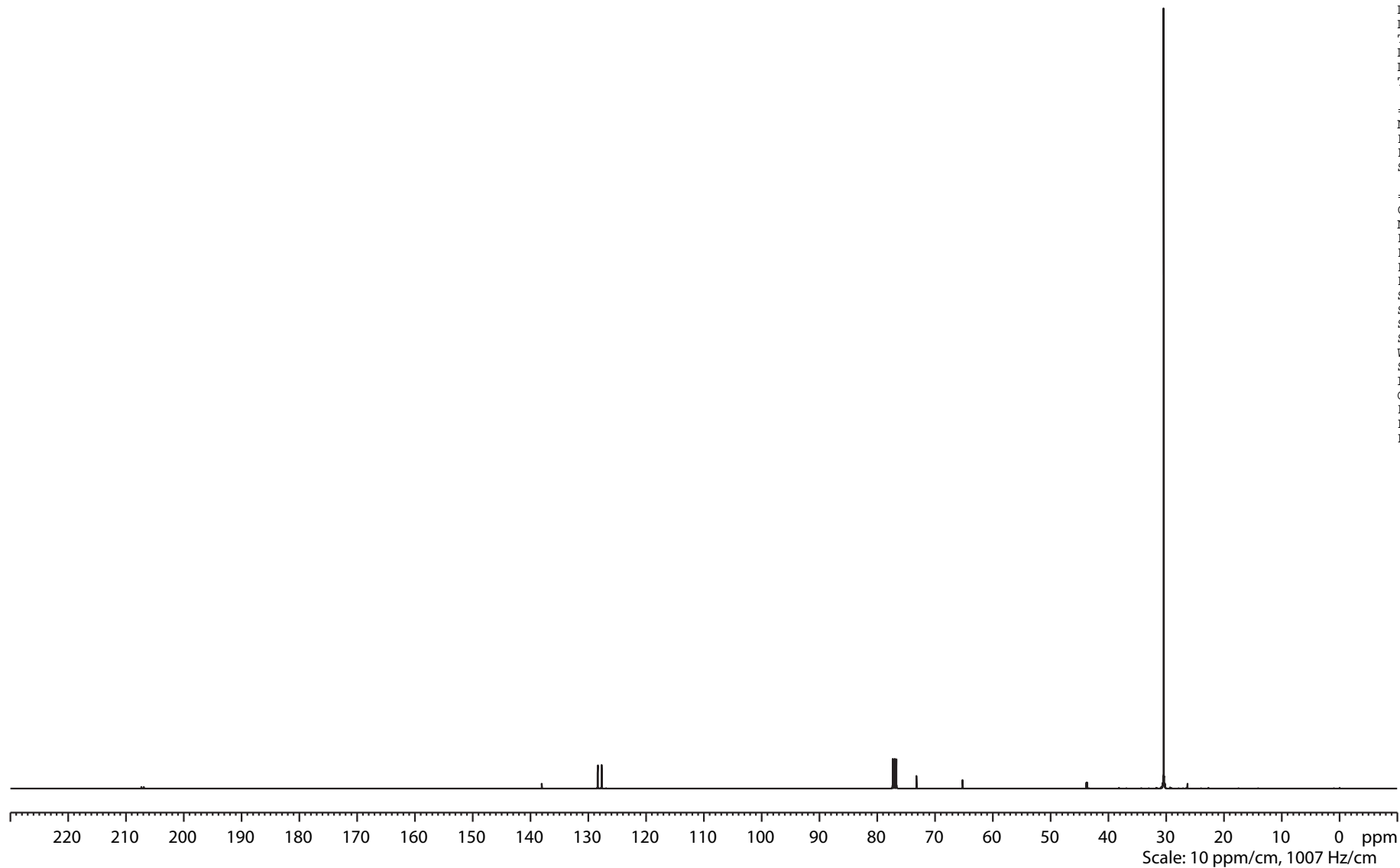
===== CHANNEL f1 =====
NUC1       13C
P1         8.50 usec
PL1        -3.00 dB
SFO1       100.6918371 MHz

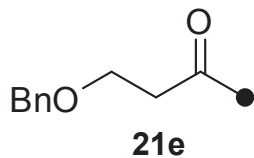
```

```

===== CHANNEL f2 =====
CPDPRG2    waltz16
NUC2        1H
PCPD2       80.00 usec
PL2         -4.00 dB
PL12        13.78 dB
PL13        14.00 dB
SFO2        400.4016016 MHz
SI          65536
SF           100.6806655 MHz
SR           4.51 Hz
WDW          EM
SSB           0
LB           1.00 Hz
GB           0
PC           1.40
F1P          230.000 ppm
F2P          -10.000 ppm

```





```

NAME      bae122177_od
EXPNO     3
PROCNO    1
Date_     20131008
Time      17.29
INSTRUM   AVIII400
PROBHD    5 mm PABBO BB-
PULPROG   dept135
TD        131072
SOLVENT   CDCl3
NS        1024
DS        4
SWH       26315.789 Hz
FIDRES    0.200774 Hz
AQ        2.4904180 sec
RG        2050
DW        19.000 usec
DE        6.50 usec
TE        298.5 K
CNST2     145.0000000
D1        2.00000000 sec
D2        0.00344828 sec
D12       0.00002000 sec
TD0       1

```

```

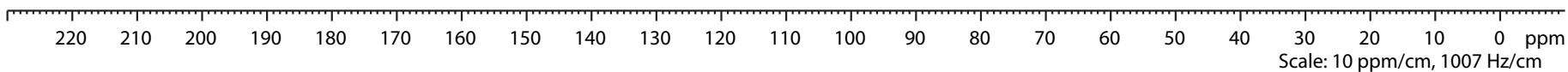
===== CHANNEL f1 =====
NUC1      13C
P1        8.50 usec
P2        17.00 usec
PL1       -3.00 dB
SFO1     100.6919063 MHz

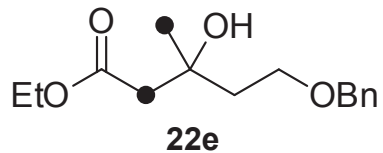
```

```

===== CHANNEL f2 =====
CPDPRG2   waltz16
NUC2      1H
P3        10.33 usec
P4        20.66 usec
PCPD2     80.00 usec
PL2       -4.00 dB
PL12      13.78 dB
SFO2     400.4016016 MHz
SI        65536
SF        100.6806578 MHz
SR        -3.20 Hz
WDW       EM
SSB       0
LB        1.00 Hz
GB        0
PC        1.40
F1P       230.000 ppm
F2P       -10.000 ppm

```



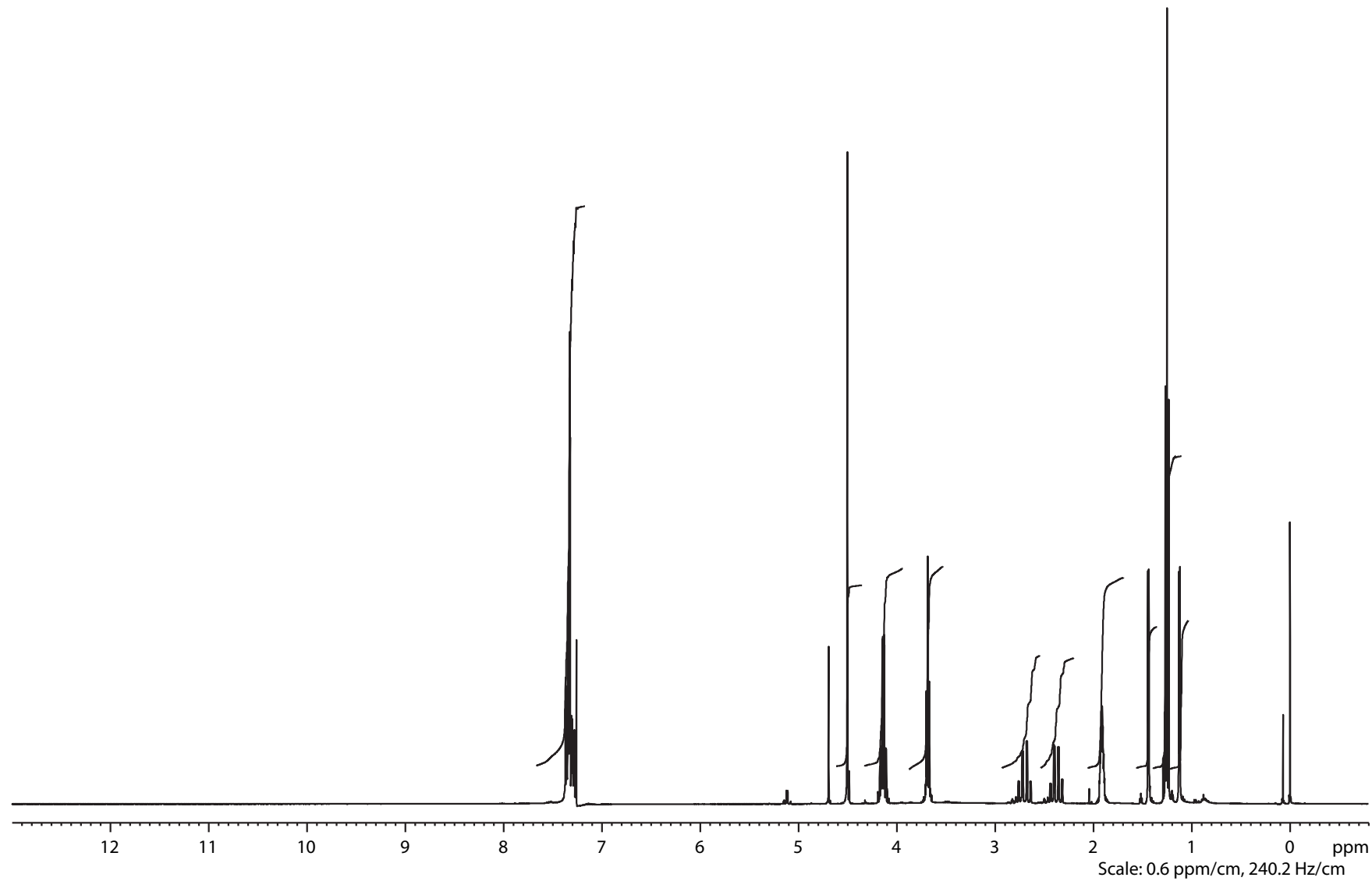


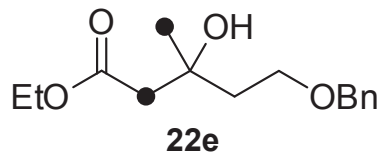
```

NAME      bae122196_od
EXPNO     1
PROCNO    1
Date_     20131010
Time      13.48
INSTRUM   AVIII400
PROBHD    5 mm PABBO BB-
PULPROG   zg30
TD         65536
SOLVENT   CDCl3
NS         64
DS         2
SWH        8223.685 Hz
FIDRES     0.125483 Hz
AQ         3.9846387 sec
RG         71.8
DW         60.800 usec
DE         6.50 usec
TE         295.2 K
D1         1.00000000 sec
TD0        1
  
```

```

===== CHANNEL f1 =====
NUC1      1H
P1        10.33 usec
PL1       -4.00 dB
SFO1      400.4024726 MHz
SI         32768
SF         400.4000186 MHz
SR         18.63 Hz
WDW        EM
SSB        0
LB         0.00 Hz
GB         0
PC         1.40
F1P        13.000 ppm
F2P        -0.800 ppm
  
```





```

NAME      bae122196_od
EXPNO     2
PROCNO    1
Date_     20131010
Time      16.26
INSTRUM   AVIII400
PROBHD    5 mm PABBO BB-
PULPROG   zgpg30
TD         131072
SOLVENT   CDCl3
NS         2048
DS         4
SWH        26315.789 Hz
FIDRES     0.200774 Hz
AQ         2.4904180 sec
RG          90.5
DW          19.000 usec
DE           6.50 usec
TE          296.6 K
D1          2.00000000 sec
D11         0.03000000 sec
TD0         1

```

```

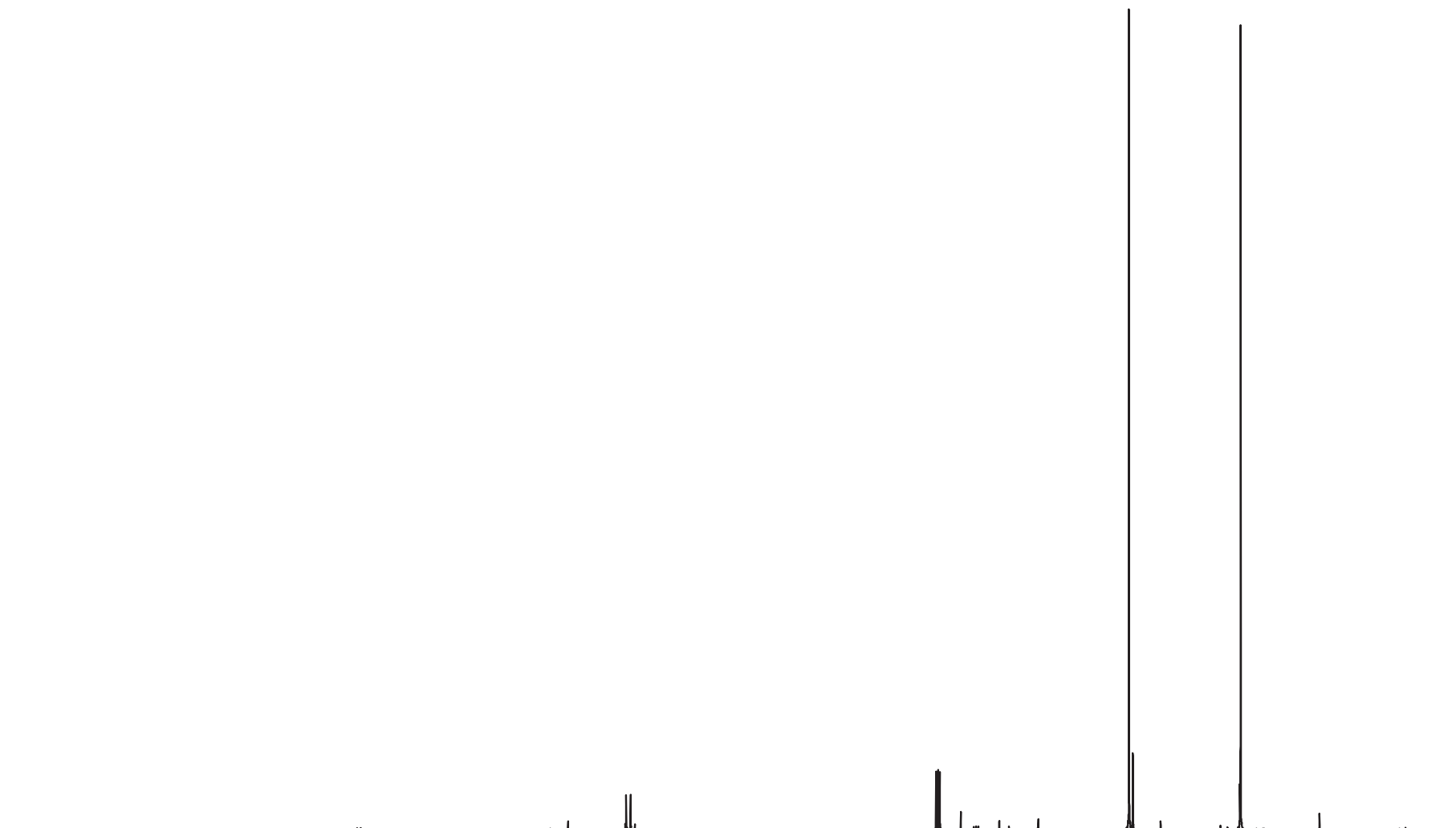
===== CHANNEL f1 =====
NUC1       13C
P1          8.50 usec
PL1         -3.00 dB
SFO1       100.6918371 MHz

```

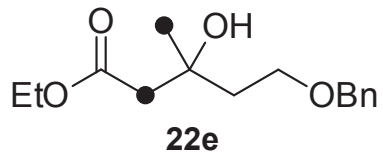
```

===== CHANNEL f2 =====
CPDPRG2    waltz16
NUC2        1H
PCPD2       80.00 usec
PL2         -4.00 dB
PL12        13.78 dB
PL13        14.00 dB
SFO2       400.4016016 MHz
SI          65536
SF          100.6806662 MHz
SR           5.20 Hz
WDW          EM
SSB          0
LB           1.00 Hz
GB           0
PC           1.40
F1P         230.000 ppm
F2P         -10.000 ppm

```



220 210 200 190 180 170 160 150 140 130 120 110 100 90 80 70 60 50 40 30 20 10 0 ppm
 Scale: 10 ppm/cm, 1007 Hz/cm



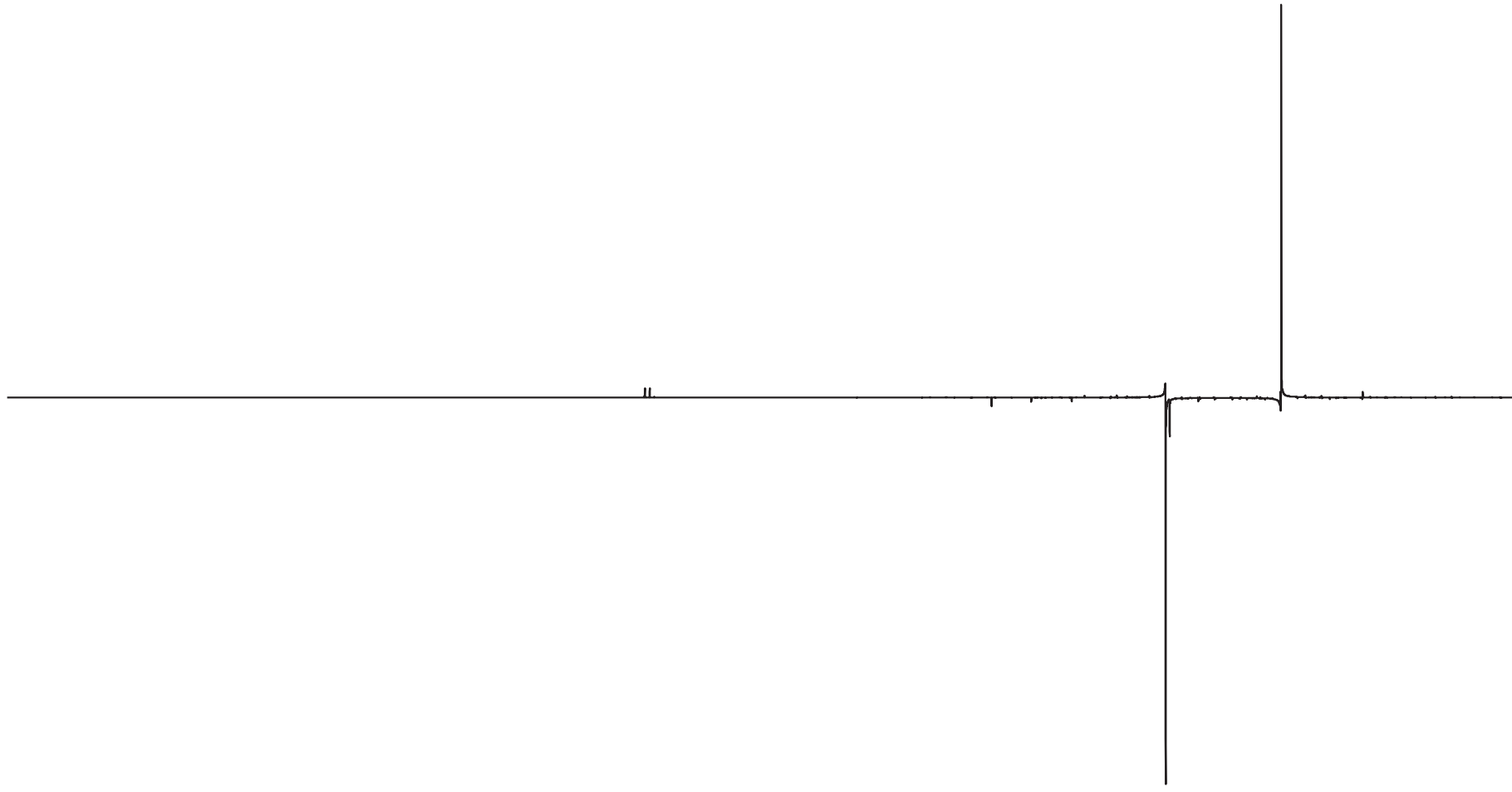
```

NAME      bae122196_od
EXPNO     3
PROCNO    1
Date_     20131010
Time      17.06
INSTRUM   AVIII400
PROBHD    5 mm PABBO BB-
PULPROG   dept135
TD         131072
SOLVENT   CDCl3
NS         512
DS         4
SWH        26315.789 Hz
FIDRES     0.200774 Hz
AQ         2.4904180 sec
RG         2050
DW         19.000 usec
DE         6.50 usec
TE         295.9 K
CNST2     145.0000000
D1         2.00000000 sec
D2         0.00344828 sec
D12        0.00002000 sec
TD0        1

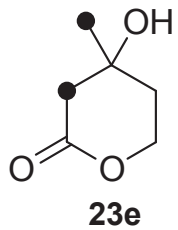
===== CHANNEL f1 =====
NUC1       13C
P1         8.50 usec
P2         17.00 usec
PL1        -3.00 dB
SFO1       100.6919063 MHz

===== CHANNEL f2 =====
CPDPRG2    waltz16
NUC2       1H
P3         10.33 usec
P4         20.66 usec
PCPD2      80.00 usec
PL2        -4.00 dB
PL12       13.78 dB
SFO2       400.4016016 MHz
SI         65536
SF         100.6806578 MHz
SR         -3.20 Hz
WDW        EM
SSB        0
LB         1.00 Hz
GB         0
PC         1.40
F1P        230.000 ppm
F2P        -10.000 ppm

```

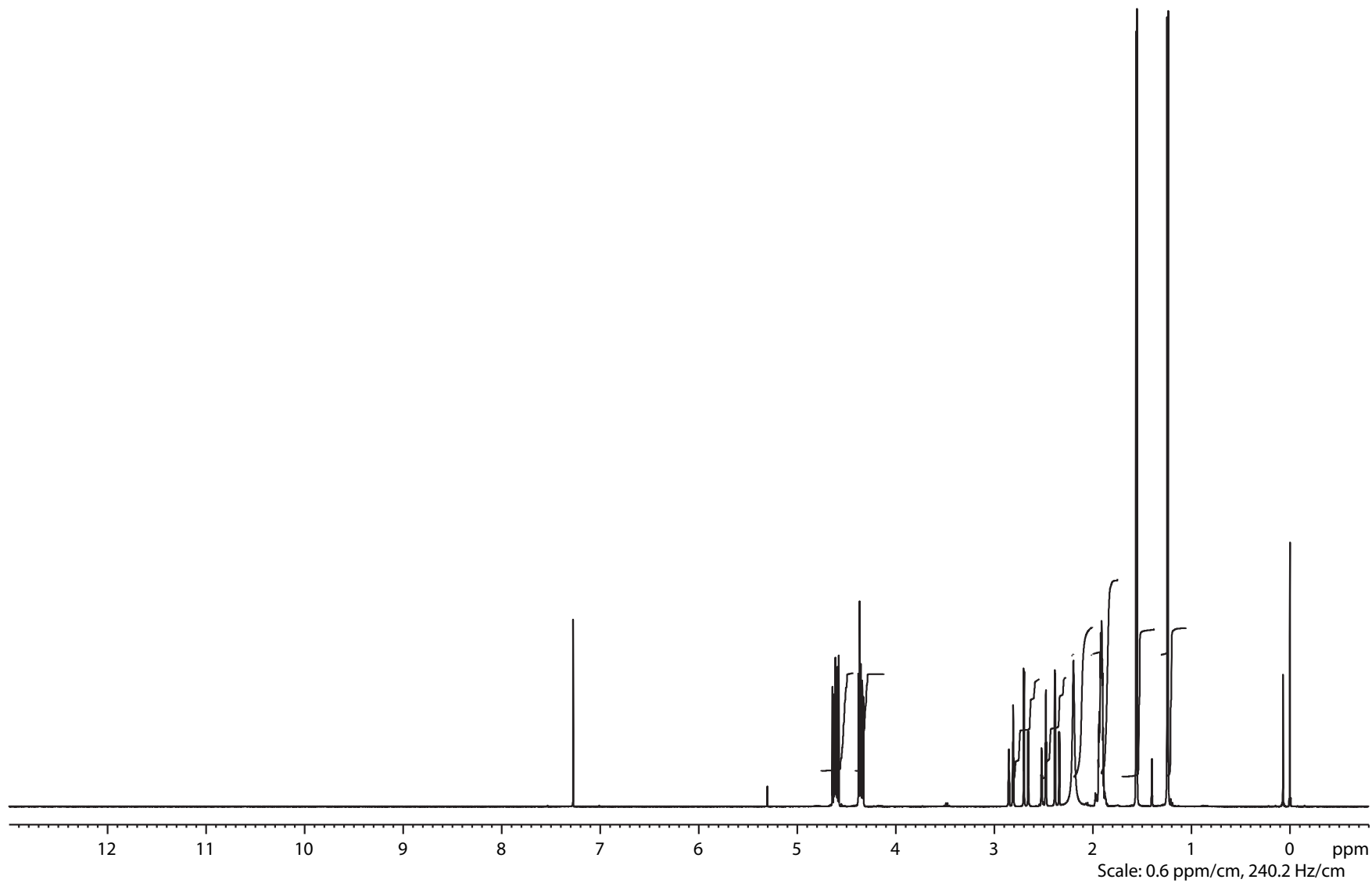


220 210 200 190 180 170 160 150 140 130 120 110 100 90 80 70 60 50 40 30 20 10 0 ppm
 Scale: 10 ppm/cm, 1007 Hz/cm

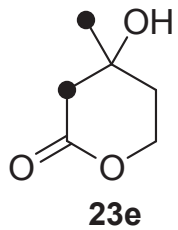


NAME bae121642_od
EXPNO 1
PROCNO 1
Date_ 20130814
Time_ 12.57
INSTRUM AVIII400
PROBHD 5 mm PABBO BB-
PULPROG zg30
TD 65536
SOLVENT CDCl3
NS 64
DS 2
SWH 8223.685 Hz
FIDRES 0.125483 Hz
AQ 3.9846387 sec
RG 101
DW 60.800 usec
DE 6.50 usec
TE 297.6 K
D1 1.0000000 sec
TD0 1

==== CHANNEL f1 =====
NUC1 1H
P1 10.33 usec
PL1 -4.00 dB
SFO1 400.4024726 MHz
SI 32768
SF 400.4000123 MHz
SR 12.34 Hz
WDW EM
SSB 0
LB 0.00 Hz
GB 0
PC 1.40
F1P 13.000 ppm
F2P -0.800 ppm



Scale: 0.6 ppm/cm, 240.2 Hz/cm



```

NAME      bae121642_od
EXPNO     2
PROCNO    1
Date_     20130814
Time      14.16
INSTRUM   AVIII400
PROBHD    5 mm PABBO BB-
PULPROG   zgpg30
TD         131072
SOLVENT   CDCl3
NS         1024
DS         4
SWH        26315.789 Hz
FIDRES     0.200774 Hz
AQ         2.4904180 sec
RG         90.5
DW         19.000 usec
DE         6.50 usec
TE         299.1 K
D1         2.00000000 sec
D11        0.03000000 sec
TD0        1

```

```

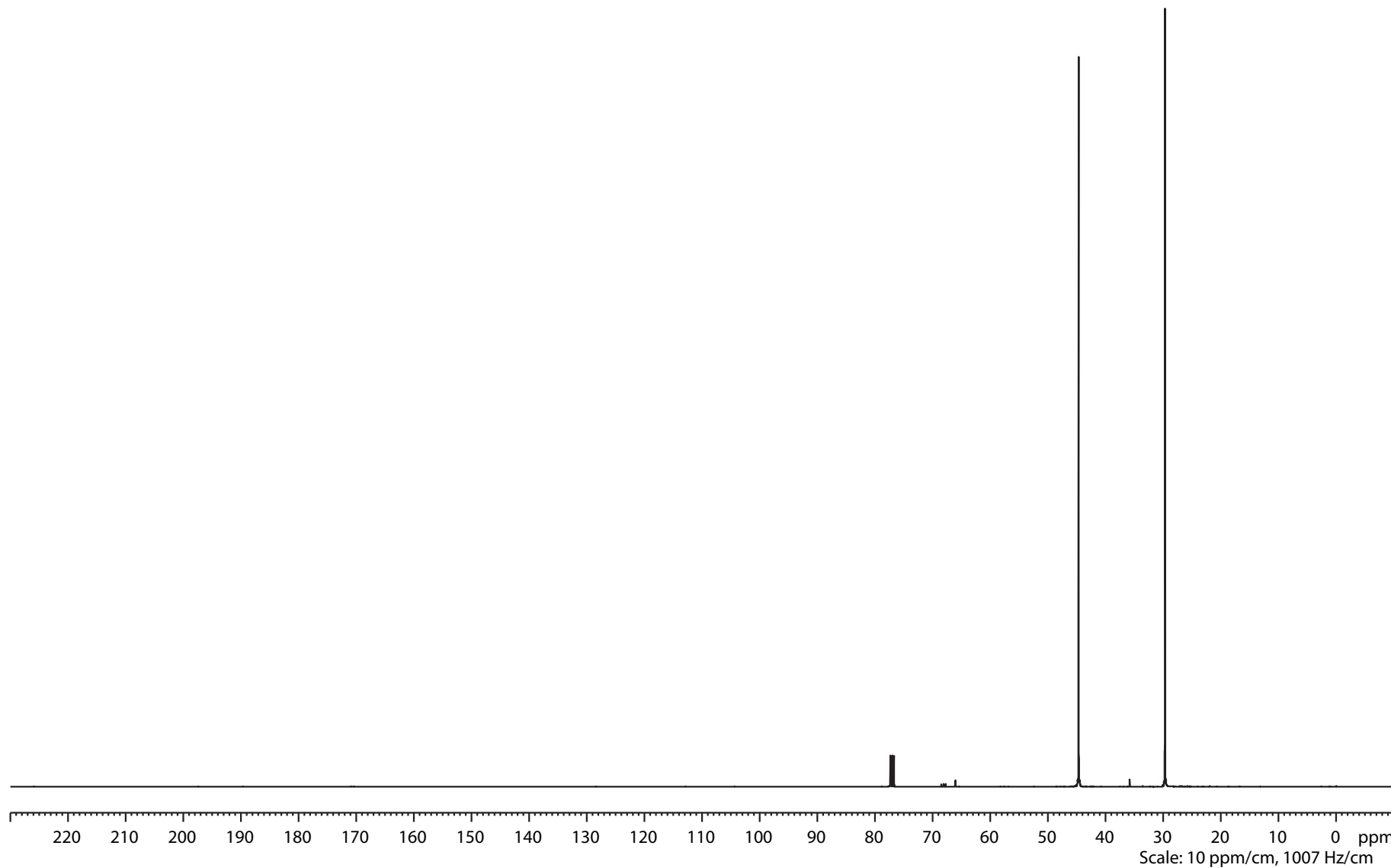
===== CHANNEL f1 =====
NUC1      13C
P1        8.50 usec
PL1       -3.00 dB
SFO1      100.6918371 MHz

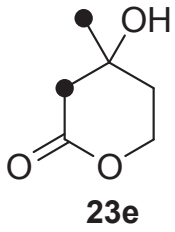
```

```

===== CHANNEL f2 =====
CPDPRG2   waltz16
NUC2      1H
PCPD2     80.00 usec
PL2       -4.00 dB
PL12      13.78 dB
PL13      14.00 dB
SFO2      400.4016016 MHz
SI        65536
SF        100.6806659 MHz
SR         4.91 Hz
WDW       EM
SSB       0
LB        1.00 Hz
GB        0
PC        1.40
F1P       230.000 ppm
F2P       -10.000 ppm

```





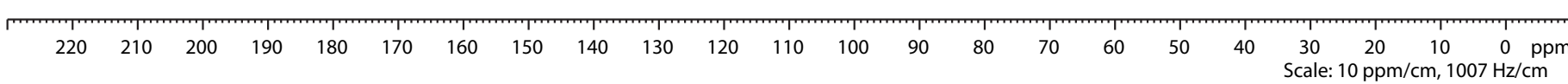
```

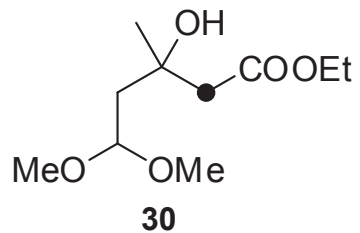
NAME      bae121642_od
EXPNO     3
PROCNO    1
Date_     20130814
Time      14.26
INSTRUM   AVIII400
PROBHD    5 mm PABBO BB-
PULPROG   dept135
TD         131072
SOLVENT   CDCl3
NS         96
DS         4
SWH        26315.789 Hz
FIDRES     0.200774 Hz
AQ         2.4904180 sec
RG         2050
DW         19.000 usec
DE         6.50 usec
TE         298.5 K
CNST2     145.0000000
D1         2.00000000 sec
D2         0.00344828 sec
D12        0.00002000 sec
TD0        5

===== CHANNEL f1 =====
NUC1       13C
P1         8.50 usec
P2         17.00 usec
PL1        -3.00 dB
SFO1       100.6918371 MHz

===== CHANNEL f2 =====
CPDPRG2    waltz16
NUC2       1H
P3         10.33 usec
P4         20.66 usec
PCPD2      80.00 usec
PL2        -4.00 dB
PL12       13.78 dB
SFO2       400.4016016 MHz
SI         65536
SF         100.6806578 MHz
SR         -3.20 Hz
WDW        EM
SSB        0
LB         1.00 Hz
GB         0
PC         1.40
F1P        230.000 ppm
F2P        -10.000 ppm

```



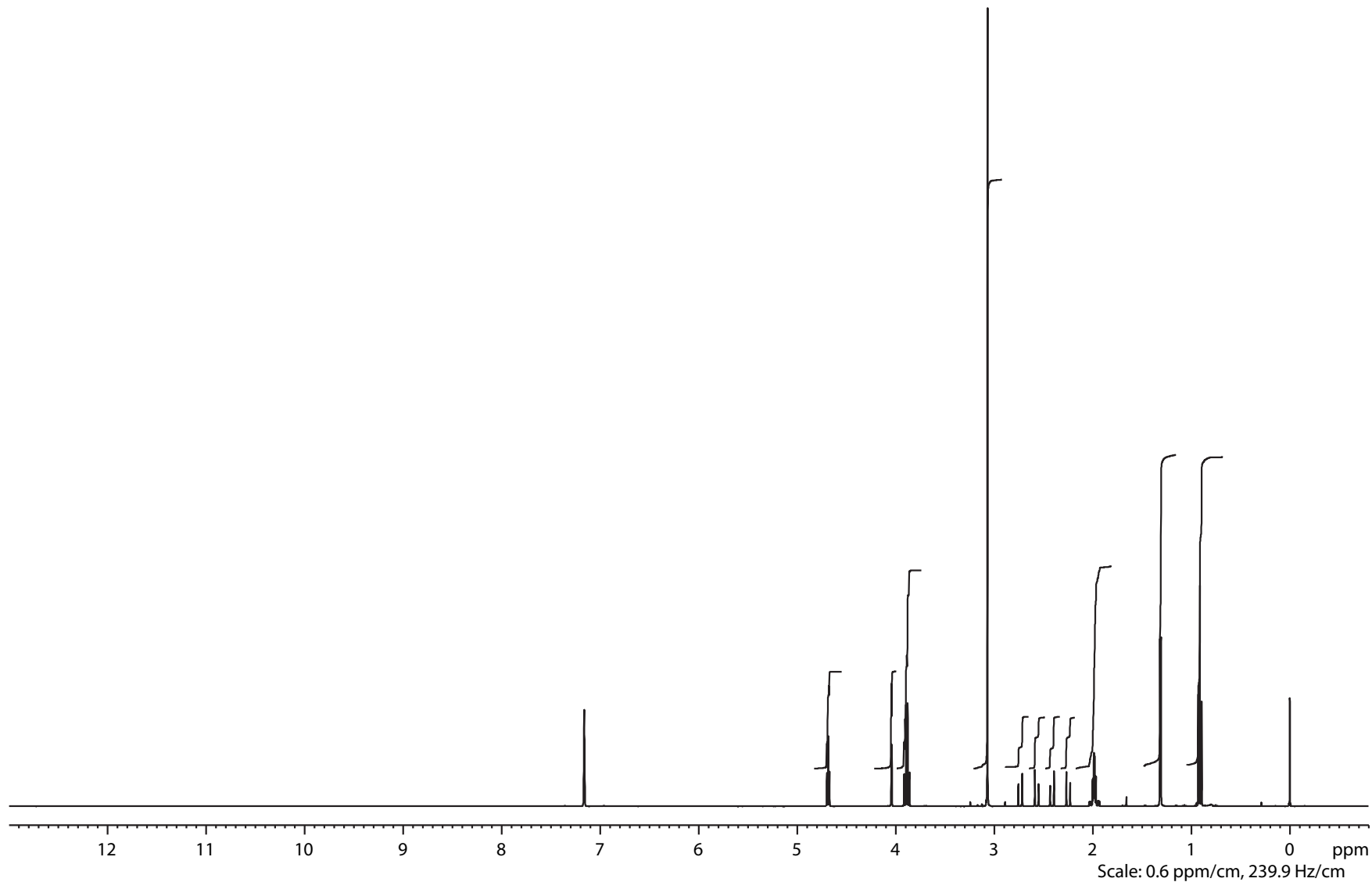


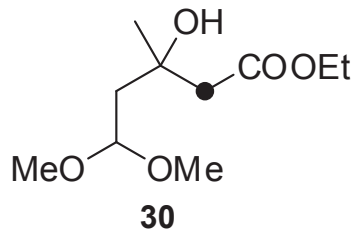
Current Data Parameters
 NAME bae122580_od
 EXPNO 1
 PROCNO 1

F2 - Acquisition Parameters
 Date_ 20131116
 Time 6.13
 INSTRUM drx400
 PROBHD 5 mm QNP 1H/13
 PULPROG zg30
 TD 65536
 SOLVENT C6D6
 NS 64
 DS 2
 SWH 8278.146 Hz
 FIDRES 0.126314 Hz
 AQ 3.9584243 sec
 RG 90.5
 DW 60.400 usec
 DE 6.00 usec
 TE 298.2 K
 D1 1.00000000 sec
 TD0 1

==== CHANNEL f1 =====
 NUC1 1H
 P1 10.20 usec
 PL1 -2.00 dB
 SFO1 399.8524687 MHz

F2 - Processing parameters
 SI 32768
 SF 399.8499931 MHz
 SR -6.95 Hz
 WDW EM
 SSB 0
 LB 0.00 Hz
 GB 0
 PC 1.40





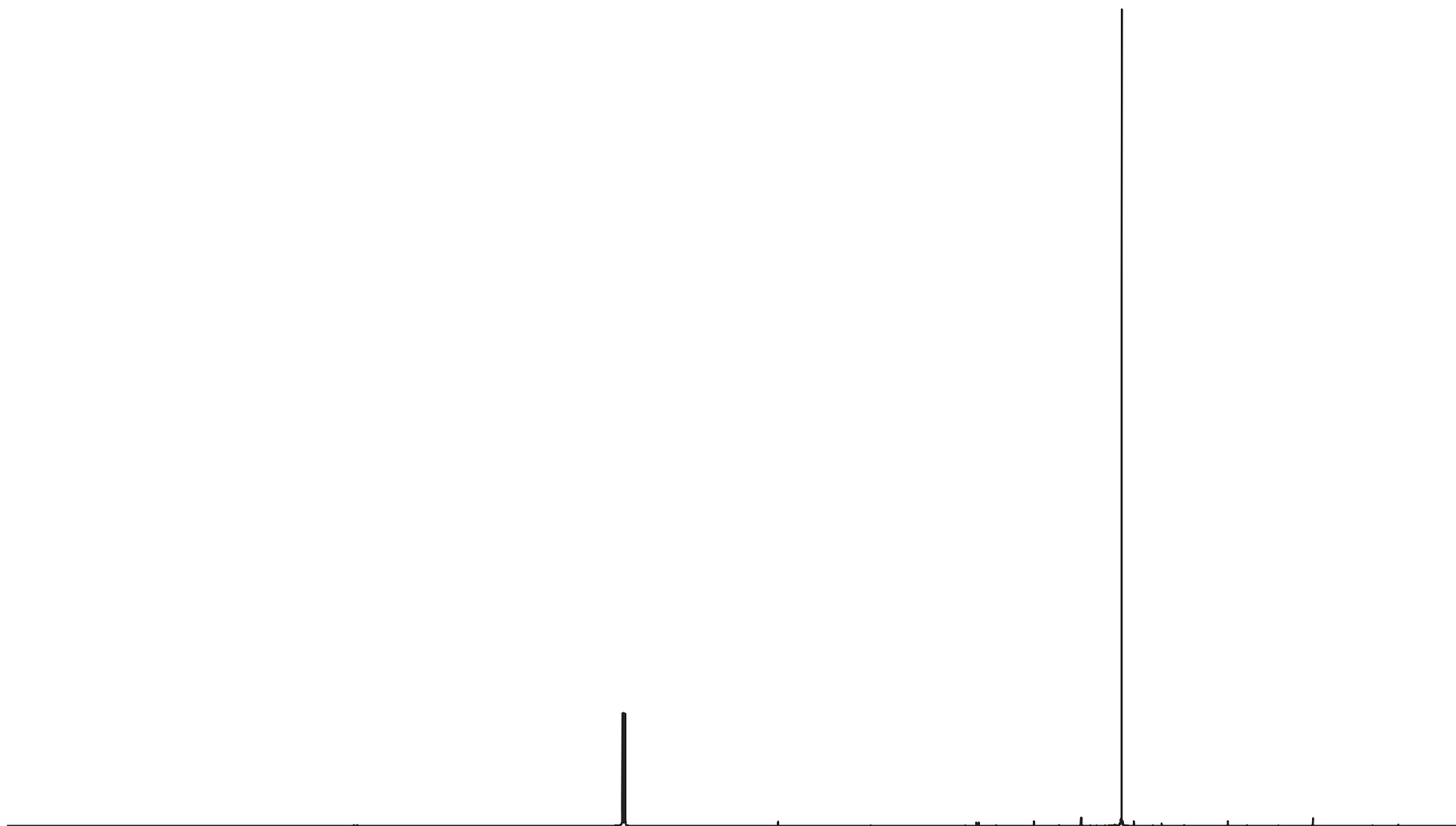
Current Data Parameters
 NAME bae122580_od
 EXPNO 2
 PROCNO 1

F2 - Acquisition Parameters
 Date_ 20131116
 Time 10.07
 INSTRUM drx400
 PROBHD 5 mm QNP 1H/13
 PULPROG zgpg30
 TD 131072
 SOLVENT C6D6
 NS 3072
 DS 4
 SWH 26315.789 Hz
 FIDRES 0.200774 Hz
 AQ 2.4904180 sec
 RG 6502
 DW 19.000 usec
 DE 6.00 usec
 TE 299.2 K
 D1 2.00000000 sec
 d11 0.03000000 sec
 DELTA 1.89999998 sec
 TD0 1

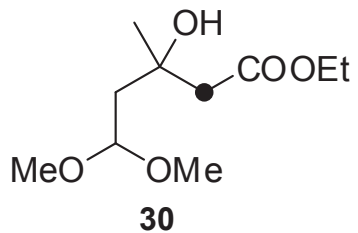
==== CHANNEL f1 =====
 NUC1 13C
 P1 11.00 usec
 PL1 -3.00 dB
 SFO1 100.5535241 MHz

==== CHANNEL f2 =====
 CPDPRG2 waltz16
 NUC2 1H
 PCPD2 80.00 usec
 PL2 -2.00 dB
 PL12 16.06 dB
 PL13 16.06 dB
 SFO2 399.8515994 MHz

F2 - Processing parameters
 SI 65536
 SF 100.5423261 MHz
 SR -36.87 Hz
 WDW EM
 SSB 0
 LB 1.00 Hz
 GB 0
 PC 1.40



220 210 200 190 180 170 160 150 140 130 120 110 100 90 80 70 60 50 40 30 20 10 0 ppm
 Scale: 10 ppm/cm, 1005 Hz/cm



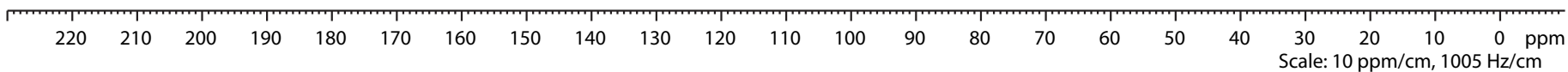
Current Data Parameters
 NAME bae122580_od
 EXPNO 3
 PROCNO 1

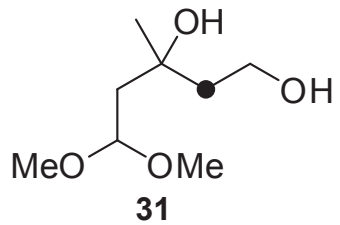
F2 - Acquisition Parameters
 Date_ 20131116
 Time 12.43
 INSTRUM drx400
 PROBHD 5 mm QNP 1H/13
 PULPROG dept135
 TD 131072
 SOLVENT C6D6
 NS 2048
 DS 4
 SWH 26315.789 Hz
 FIDRES 0.200774 Hz
 AQ 2.4904180 sec
 RG 7298.2
 DW 19.000 usec
 DE 7.00 usec
 TE 298.2 K
 CNST2 145.0000000
 D1 2.00000000 sec
 d2 0.00344828 sec
 d12 0.00002000 sec
 DELTA 0.00001401 sec
 TD0 1

==== CHANNEL f1 =====
 NUC1 13C
 P1 11.00 usec
 p2 22.00 usec
 PL1 -3.00 dB
 SFO1 100.5535241 MHz

==== CHANNEL f2 =====
 CPDPRG2 waltz16
 NUC2 1H
 P3 10.00 usec
 p4 20.00 usec
 PCPD2 80.00 usec
 PL2 -2.00 dB
 PL12 16.06 dB
 SFO2 399.8515994 MHz

F2 - Processing parameters
 SI 65536
 SF 100.5423557 MHz
 SR -7.29 Hz
 WDW EM
 SSB 0
 LB 1.00 Hz
 GB 0
 PC 1.40



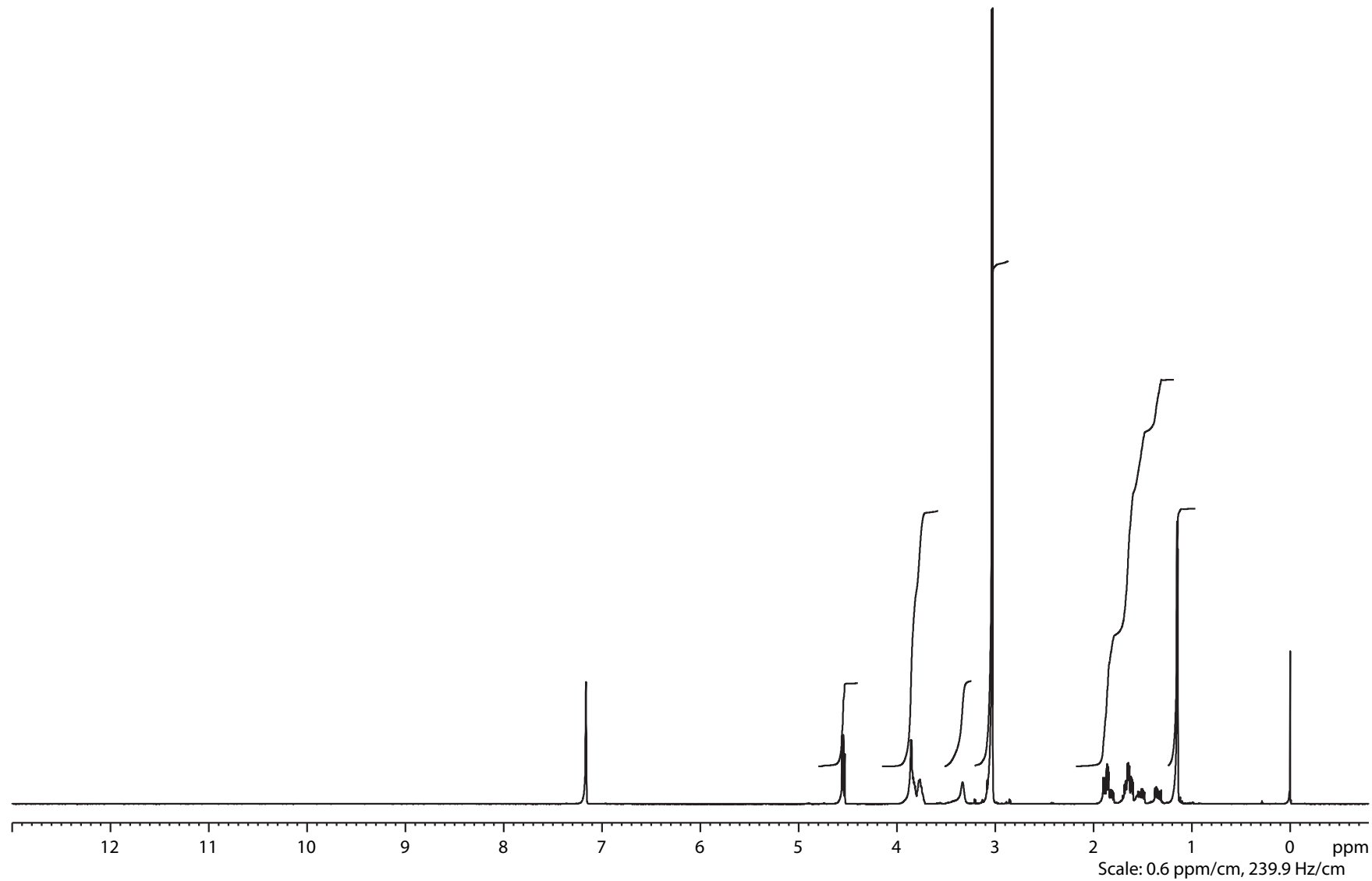


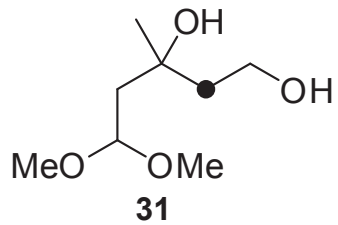
Current Data Parameters
 NAME bae122597_od
 EXPNO 1
 PROCNO 1

F2 - Acquisition Parameters
 Date_ 20131118
 Time 14.27
 INSTRUM drx400
 PROBHD 5 mm QNP 1H/13
 PULPROG zg30
 TD 65536
 SOLVENT C6D6
 NS 64
 DS 2
 SWH 8278.146 Hz
 FIDRES 0.126314 Hz
 AQ 3.9584243 sec
 RG 71.8
 DW 60.400 usec
 DE 6.00 usec
 TE 298.2 K
 D1 1.00000000 sec
 TD0 1

==== CHANNEL f1 =====
 NUC1 1H
 P1 10.20 usec
 PL1 -2.00 dB
 SFO1 399.8524687 MHz

F2 - Processing parameters
 SI 32768
 SF 399.8499921 MHz
 SR -7.87 Hz
 WDW EM
 SSB 0
 LB 0.00 Hz
 GB 0
 PC 1.40





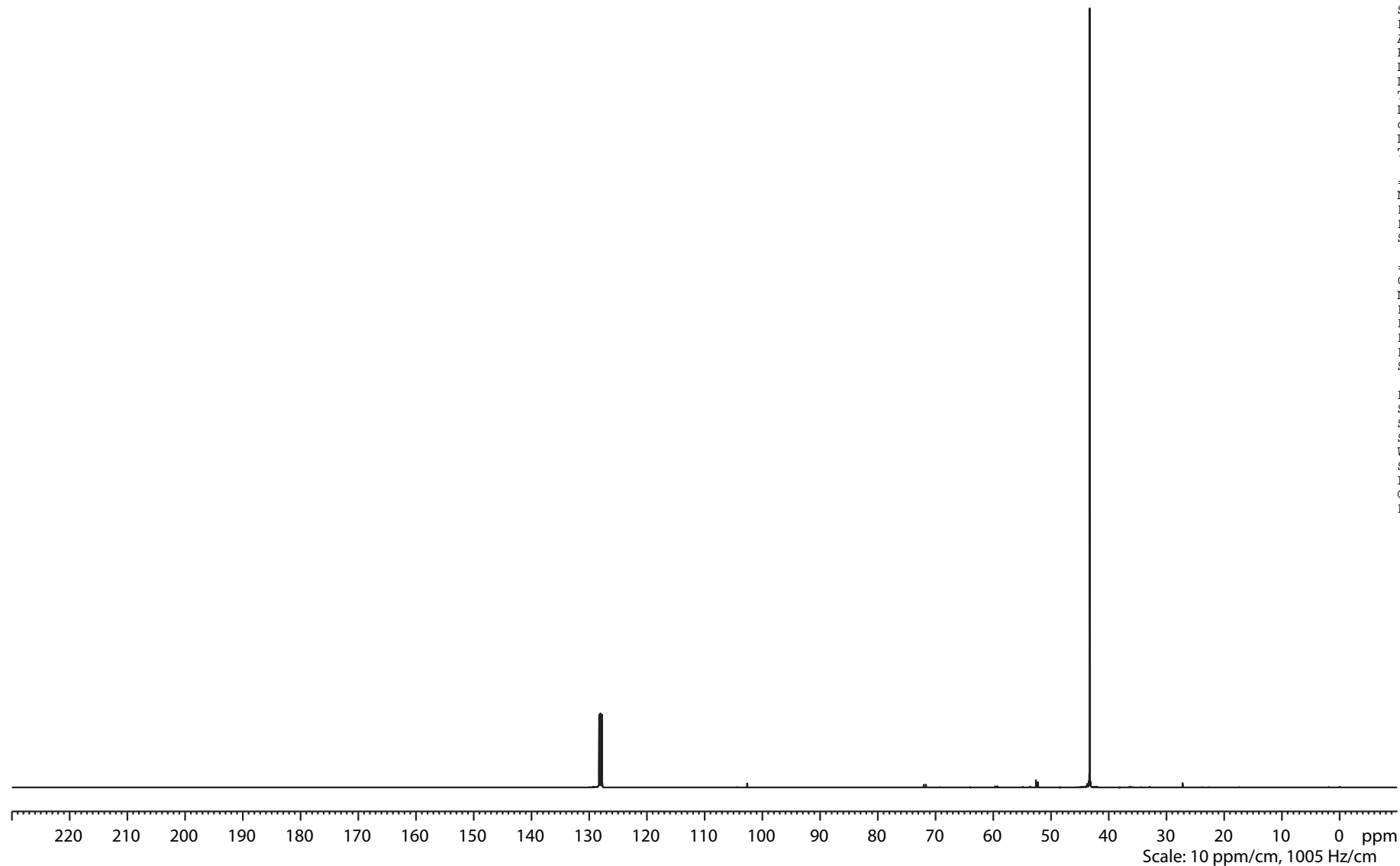
Current Data Parameters
 NAME bae122597_od
 EXPNO 2
 PROCNO 1

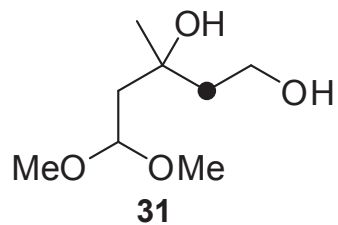
F2 - Acquisition Parameters
 Date_ 20131118
 Time 14.30
 INSTRUM drx400
 PROBHD 5 mm QNP 1H/13
 PULPROG zgpg30
 TD 131072
 SOLVENT C6D6
 NS 2048
 DS 4
 SWH 26315.789 Hz
 FIDRES 0.200774 Hz
 AQ 2.4904180 sec
 RG 5792.6
 DW 19.000 usec
 DE 6.00 usec
 TE 299.2 K
 D1 2.00000000 sec
 d11 0.03000000 sec
 DELTA 1.89999998 sec
 TD0 1

==== CHANNEL f1 =====
 NUC1 13C
 P1 11.00 usec
 PL1 -3.00 dB
 SFO1 100.5535241 MHz

==== CHANNEL f2 =====
 CPDPRG2 waltz16
 NUC2 1H
 PCPD2 80.00 usec
 PL2 -2.00 dB
 PL12 16.06 dB
 PL13 16.06 dB
 SFO2 399.8515994 MHz

F2 - Processing parameters
 SI 65536
 SF 100.5423263 MHz
 SR -36.68 Hz
 WDW EM
 SSB 0
 LB 1.00 Hz
 GB 0
 PC 1.40





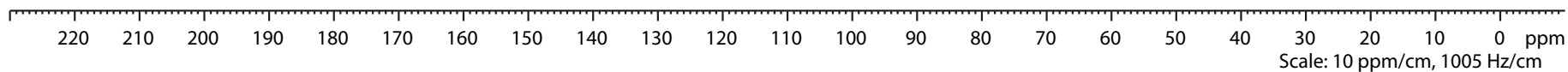
Current Data Parameters
 NAME bae122597_od
 EXPNO 3
 PROCNO 1

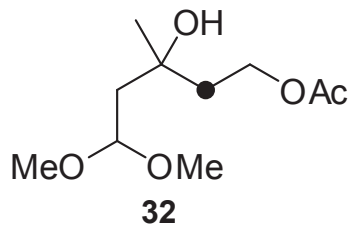
F2 - Acquisition Parameters
 Date_ 20131118
 Time 18.23
 INSTRUM drx400
 PROBHD 5 mm QNP 1H/13
 PULPROG dept135
 TD 131072
 SOLVENT C6D6
 NS 1024
 DS 4
 SWH 26315.789 Hz
 FIDRES 0.200774 Hz
 AQ 2.4904180 sec
 RG 6502
 DW 19.000 usec
 DE 7.00 usec
 TE 299.2 K
 CNST2 145.0000000
 D1 2.00000000 sec
 d2 0.00344828 sec
 dI2 0.00002000 sec
 DELTA 0.00001401 sec
 TD0 1

==== CHANNEL f1 =====
 NUC1 13C
 P1 11.00 usec
 p2 22.00 usec
 PL1 -3.00 dB
 SFO1 100.5535241 MHz

==== CHANNEL f2 =====
 CPDPRG2 waltz16
 NUC2 1H
 P3 10.00 usec
 p4 20.00 usec
 PCPD2 80.00 usec
 PL2 -2.00 dB
 PL12 16.06 dB
 SFO2 399.8515994 MHz

F2 - Processing parameters
 SI 65536
 SF 100.5423558 MHz
 SR -7.22 Hz
 WDW EM
 SSB 0
 LB 1.00 Hz
 GB 0
 PC 1.40



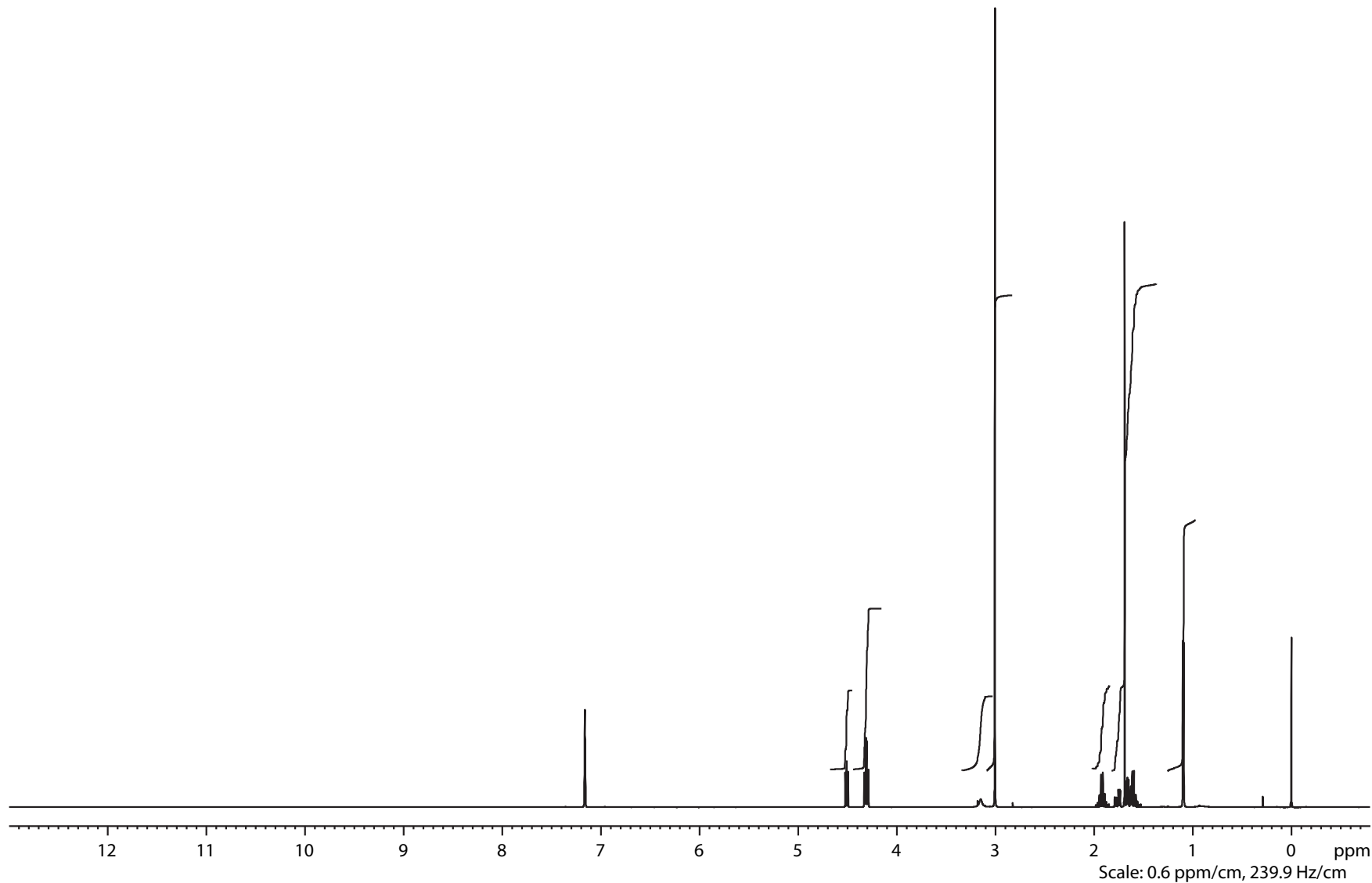


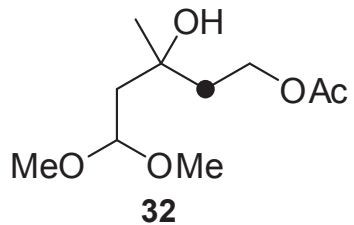
Current Data Parameters
 NAME bae122630_od
 EXPNO 1
 PROCNO 1

F2 - Acquisition Parameters
 Date_ 20131120
 Time 18.36
 INSTRUM drx400
 PROBHD 5 mm QNP 1H/13
 PULPROG zg30
 TD 65536
 SOLVENT C6D6
 NS 64
 DS 2
 SWH 8278.146 Hz
 FIDRES 0.126314 Hz
 AQ 3.9584243 sec
 RG 90.5
 DW 60.400 usec
 DE 6.00 usec
 TE 298.2 K
 D1 1.00000000 sec
 TD0 1

==== CHANNEL f1 =====
 NUC1 1H
 P1 10.20 usec
 PL1 -2.00 dB
 SFO1 399.8524687 MHz

F2 - Processing parameters
 SI 32768
 SF 399.8499932 MHz
 SR -6.79 Hz
 WDW EM
 SSB 0
 LB 0.00 Hz
 GB 0
 PC 1.40





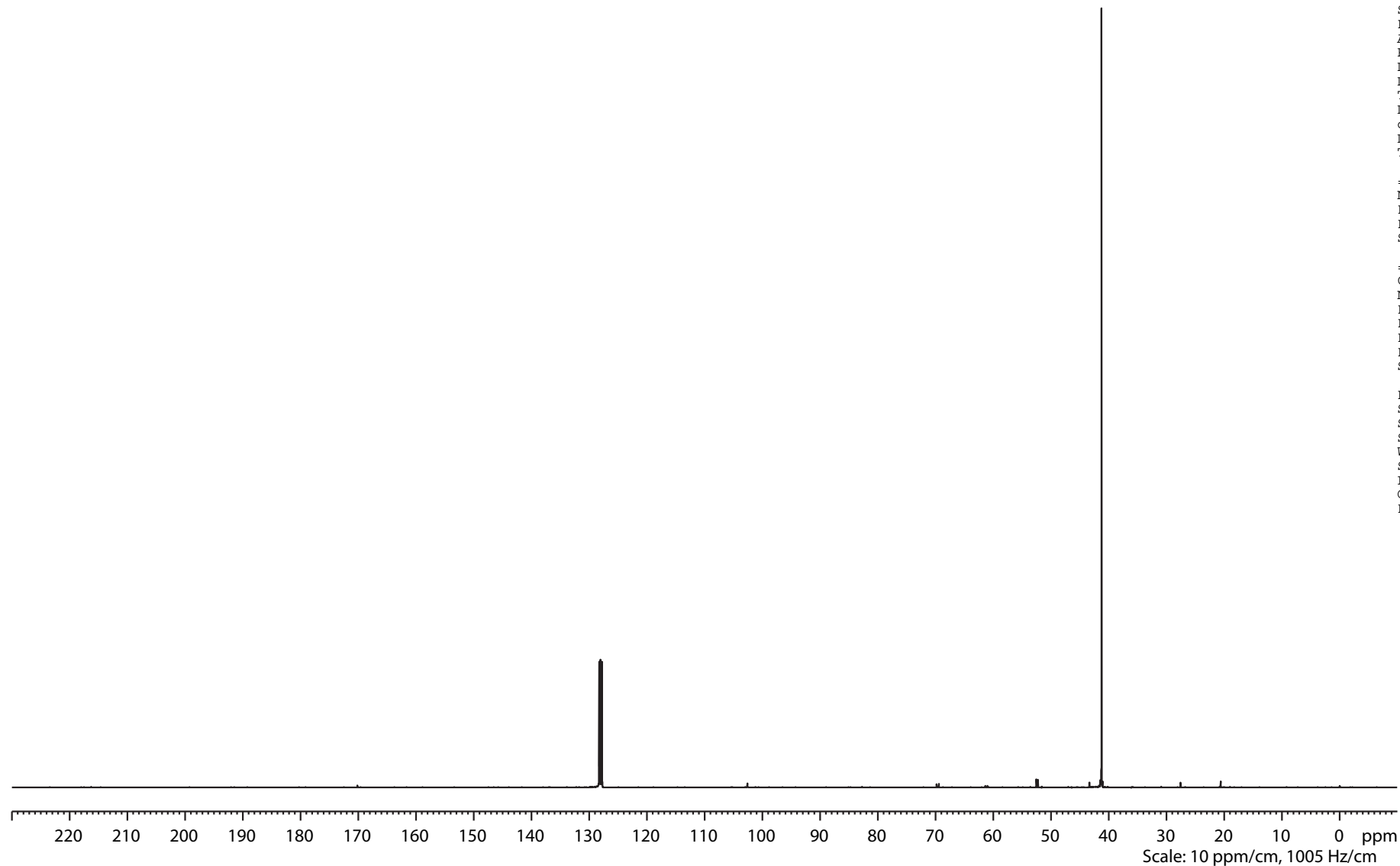
Current Data Parameters
 NAME bae122630_od
 EXPNO 2
 PROCNO 1

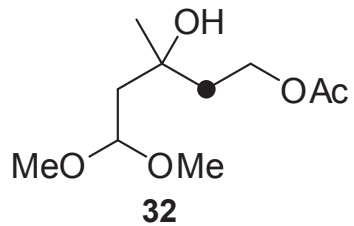
F2 - Acquisition Parameters
 Date_ 20131120
 Time 21.12
 INSTRUM drx400
 PROBHD 5 mm QNP 1H/13
 PULPROG zgpg30
 TD 131072
 SOLVENT C6D6
 NS 2048
 DS 4
 SWH 26315.789 Hz
 FIDRES 0.200774 Hz
 AQ 2.4904180 sec
 RG 6502
 DW 19.000 usec
 DE 6.00 usec
 TE 299.2 K
 D1 2.00000000 sec
 d11 0.03000000 sec
 DELTA 1.89999998 sec
 TD0 1

==== CHANNEL f1 =====
 NUC1 13C
 P1 11.00 usec
 PL1 -3.00 dB
 SFO1 100.5535241 MHz

==== CHANNEL f2 =====
 CPDPRG2 waltz16
 NUC2 1H
 PCPD2 80.00 usec
 PL2 -2.00 dB
 PL12 16.06 dB
 PL13 16.06 dB
 SFO2 399.8515994 MHz

F2 - Processing parameters
 SI 65536
 SF 100.5423263 MHz
 SR -36.71 Hz
 WDW EM
 SSB 0
 LB 1.00 Hz
 GB 0
 PC 1.40





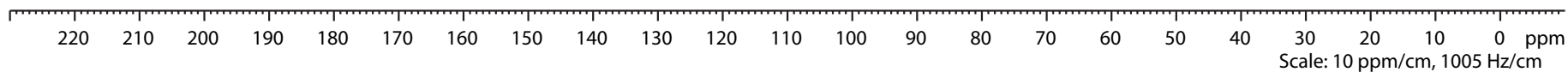
Current Data Parameters
 NAME bae122630_od
 EXPNO 3
 PROCNO 1

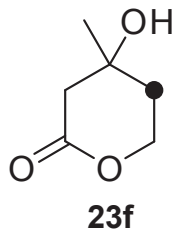
F2 - Acquisition Parameters
 Date_ 20131120
 Time 22.31
 INSTRUM drx400
 PROBHD 5 mm QNP 1H/13
 PULPROG dept135
 TD 131072
 SOLVENT C6D6
 NS 1024
 DS 4
 SWH 26315.789 Hz
 FIDRES 0.200774 Hz
 AQ 2.4904180 sec
 RG 6502
 DW 19.000 usec
 DE 7.00 usec
 TE 299.2 K
 CNST2 145.0000000
 D1 2.00000000 sec
 d2 0.00344828 sec
 dI2 0.00002000 sec
 DELTA 0.00001401 sec
 TD0 1

==== CHANNEL f1 =====
 NUC1 13C
 P1 11.00 usec
 p2 22.00 usec
 PL1 -3.00 dB
 SFO1 100.5535241 MHz

==== CHANNEL f2 =====
 CPDPRG2 waltz16
 NUC2 1H
 P3 10.00 usec
 p4 20.00 usec
 PCPD2 80.00 usec
 PL2 -2.00 dB
 PL12 16.06 dB
 SFO2 399.8515994 MHz

F2 - Processing parameters
 SI 65536
 SF 100.5423557 MHz
 SR -7.27 Hz
 WDW EM
 SSB 0
 LB 1.00 Hz
 GB 0
 PC 1.40



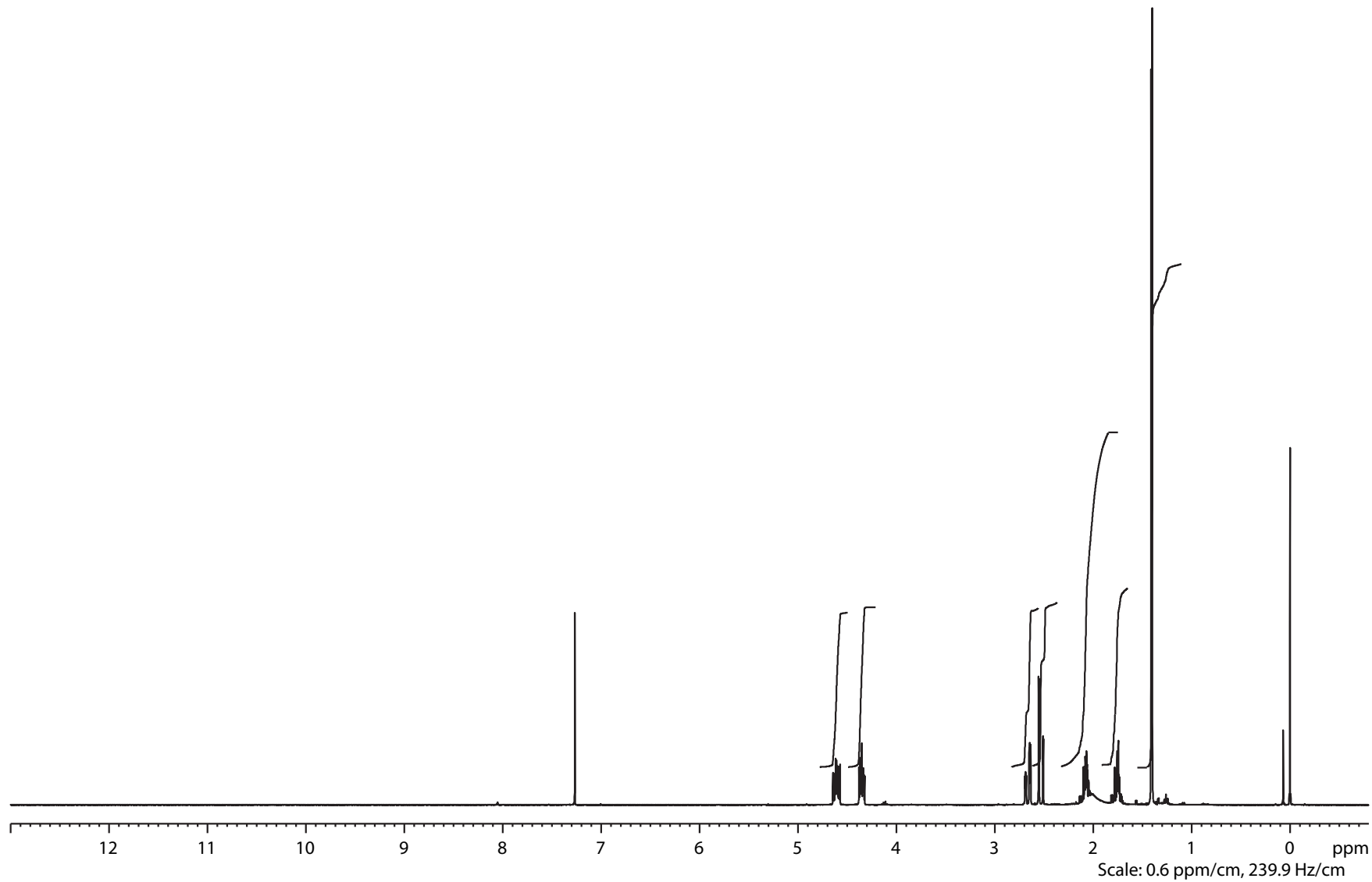


Current Data Parameters
NAME bae123108_od
EXPNO 1
PROCNO 1

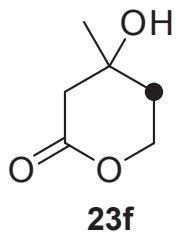
F2 - Acquisition Parameters
Date_ 20140206
Time 7.04
INSTRUM drx400
PROBHD 5 mm QNP 1H/13
PULPROG zg30
TD 65536
SOLVENT CDCl3
NS 64
DS 2
SWH 8278.146 Hz
FIDRES 0.126314 Hz
AQ 3.9584243 sec
RG 203.2
DW 60.400 usec
DE 6.00 usec
TE 299.2 K
D1 1.00000000 sec
TD0 1

==== CHANNEL f1 =====
NUC1 1H
P1 10.20 usec
PL1 -2.00 dB
SFO1 399.8524687 MHz

F2 - Processing parameters
SI 32768
SF 399.8500121 MHz
SR 12.11 Hz
WDW EM
SSB 0
LB 0.00 Hz
GB 0
PC 1.40



Scale: 0.6 ppm/cm, 239.9 Hz/cm



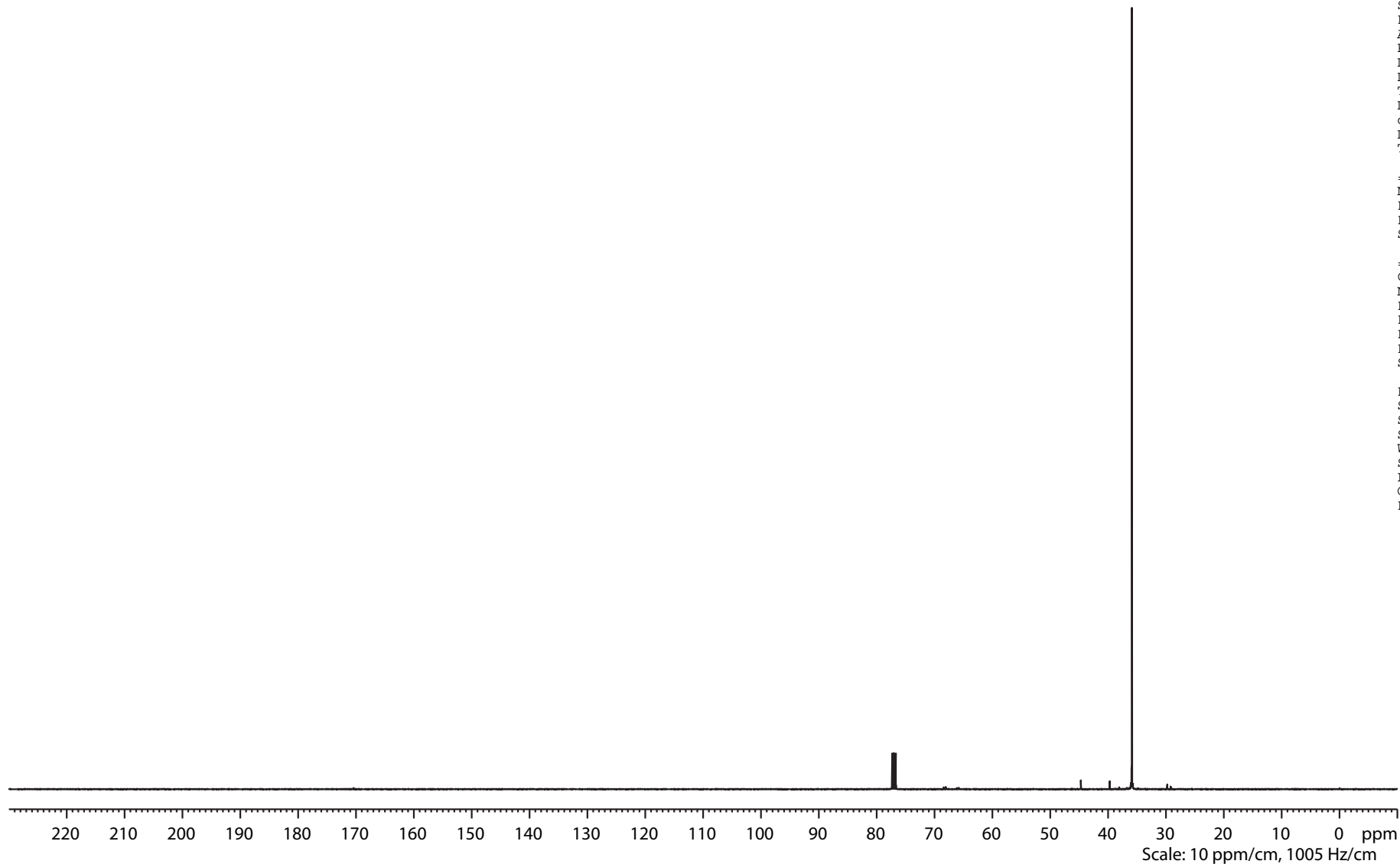
Current Data Parameters
NAME bae123108_od
EXPNO 2
PROCNO 1

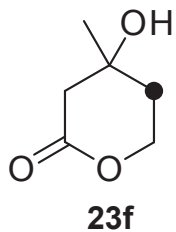
F2 - Acquisition Parameters
Date_ 20140206
Time 8.23
INSTRUM drx400
PROBHD 5 mm QNP 1H/13
PULPROG zgpg30
TD 131072
SOLVENT CDCL3
NS 1024
DS 4
SWH 26315.789 Hz
FIDRES 0.200774 Hz
AQ 2.4904180 sec
RG 9195.2
DW 19.000 usec
DE 6.00 usec
TE 299.2 K
D1 2.00000000 sec
d11 0.03000000 sec
DELTA 1.89999998 sec
TD0 1

==== CHANNEL f1 =====
NUC1 13C
P1 11.00 usec
PL1 -3.00 dB
SFO1 100.5535241 MHz

==== CHANNEL f2 =====
CPDPRG2 waltz16
NUC2 1H
PCPD2 80.00 usec
PL2 -2.00 dB
PL12 16.06 dB
PL13 16.06 dB
SFO2 399.8515994 MHz

F2 - Processing parameters
SI 65536
SF 100.5423664 MHz
SR 3.38 Hz
WDW EM
SSB 0
LB 1.00 Hz
GB 0
PC 1.40





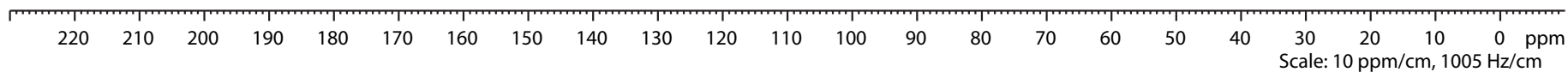
Current Data Parameters
 NAME bae123108_od
 EXPNO 3
 PROCNO 1

F2 - Acquisition Parameters
 Date_ 20140206
 Time 9.03
 INSTRUM drx400
 PROBHD 5 mm QNP 1H/13
 PULPROG dept135
 TD 131072
 SOLVENT CDCl3
 NS 512
 DS 4
 SWH 26315.789 Hz
 FIDRES 0.200774 Hz
 AQ 2.4904180 sec
 RG 9195.2
 DW 19.000 usec
 DE 7.00 usec
 TE 299.2 K
 CNST2 145.0000000
 D1 2.0000000 sec
 d2 0.00344828 sec
 d12 0.00002000 sec
 DELTA 0.00001401 sec
 TD0 1

==== CHANNEL f1 =====
 NUC1 13C
 P1 11.00 usec
 p2 22.00 usec
 PL1 -3.00 dB
 SFO1 100.5535241 MHz

==== CHANNEL f2 =====
 CPDPRG2 waltz16
 NUC2 1H
 P3 10.00 usec
 p4 20.00 usec
 PCPD2 80.00 usec
 PL2 -2.00 dB
 PL12 16.06 dB
 SFO2 399.8515994 MHz

F2 - Processing parameters
 SI 65536
 SF 100.5423598 MHz
 SR -3.20 Hz
 WDW EM
 SSB 0
 LB 1.00 Hz
 GB 0
 PC 1.40



Appendix B

Structural Revision and Elucidation of the Biosynthesis of
Hypodoratoxide by ^{13}C , ^{13}C COSY NMR Spectroscopy

Structural Revision and Elucidation of the Biosynthesis of Hypodoratoxide by ^{13}C , ^{13}C COSY NMR Spectroscopy

Lena Barra, Kerstin Ibrom, and Jeroen S. Dickschat*

Abstract: Feeding of (2,3,4,5,6- $^{13}\text{C}_5$)mevalonolactone to the fungus *Hypomyces odoratus* resulted in a completely labeled sesquiterpene ether. The connectivity of the carbon atoms was easily deduced from a ^{13}C , ^{13}C COSY spectrum, revealing a structure that was different from the previously reported structure of hypodoratoxide, even though the reported ^{13}C NMR data matched. A structural revision of hypodoratoxide is thus presented. Its absolute configuration was tentatively assigned from its co-metabolite *cis*-dihydroagarofuran. Its biosynthesis was investigated by feeding of (3- ^{13}C)- and (4,6- $^{13}\text{C}_2$)mevalonolactone, which gave insights into the complex rearrangement of the carbon skeleton during terpene cyclization by analysis of the ^{13}C , ^{13}C couplings.

The mountaintop of molecular diversity within secondary metabolites is represented by the more than 50000 known terpenes from all kingdoms of life. Their biosynthesis involves complex reactions that are usually catalyzed by a single terpene cyclase, which converts a linear precursor, such as geranyl diphosphate (GPP), farnesyl diphosphate (FPP), or geranylgeranyl diphosphate (GGPP), into a terpene hydrocarbon or alcohol. This conversion proceeds via cationic intermediates in a domino reaction with several elementary steps, such as cyclizations, hydride and proton shifts, Wagner–Meerwein rearrangements, and fragmentations, resulting in (poly)cyclic frameworks with several stereogenic centers.^[1] The initial product can be modified by oxygenases or acyl transferases, for example, to generate a highly functionalized terpenoid. The structural complexity of terpenoids renders their structure elucidation difficult, and although structural data of terpene cyclases have contributed significantly to our understanding of terpene biosynthesis,^[2–9] it is challenging to gain insights into the intricate mechanisms of terpene cyclizations. Herein, we present an approach that addresses both problems by feeding of ^{13}C -labeled precursors and ^{13}C , ^{13}C correlation spectroscopy (COSY).

In our continued research program on the biosynthesis of bacterial and fungal terpenes, we noticed that the production of one major sesquiterpene **1** by the fungus *Hypomyces*

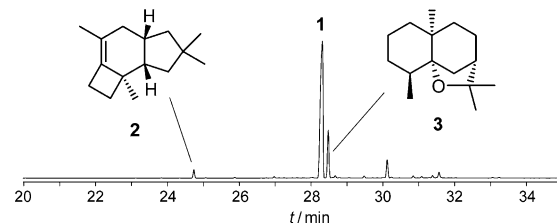


Figure 1. Total ion chromatogram of a headspace extract from *Hypomyces odoratus* DSM 11934.

odoratus DSM 11934 was accompanied by traces of other sesquiterpenes (Figure 1). Two of these co-metabolites were identified by GC/MS as protoillud-6-ene (**2**) and *cis*-dihydroagarofuran (**3**; for mass spectra of **1–3**, see the Supporting Information, Figure S1).^[10,11] For the structure elucidation of **1**, (2,3,4,5,6- $^{13}\text{C}_5$)mevalonolactone was synthesized according to a known procedure (Scheme S1).^[12,13] In this isotopologue of mevalonolactone, all five carbon atoms that are incorporated into terpenes are labeled. The compound was fed to *H. odoratus*, from which [$^{13}\text{C}_{15}$]-**1** was subsequently isolated (16% incorporation; the material was mainly a mixture of unlabeled and completely labeled **1**, see Figure S2A). This allowed for the structure elucidation of **1** by ^{13}C , ^{13}C COSY analysis, which revealed its planar structure (Figure 2).

For the elucidation of the relative configuration, unlabeled **1** was isolated in a yield of 15 mg L⁻¹, and a full set of NMR spectroscopic data, including ^1H , ^{13}C , ^{13}C -DEPT-135, ^1H , ^1H COSY, HSQC, HMBC, and NOESY spectra, was recorded. Comparison of the ^{13}C chemical shifts of **1** (in CDCl_3) to the chemical shifts of previously reported hypodoratoxide (in C_6D_6)^[14] suggested that **1** and hypodoratoxide are identical, which was confirmed by re-examination of the ^{13}C NMR spectrum of **1** in C_6D_6 (Table 1) and comparison of the mass spectra. However, as the ^{13}C , ^{13}C COSY spectrum disagreed with the reported structure **4** of hypodoratoxide,^[14] a structural revision was required. The detected HMBC correlations were in agreement with the structure delineated from the ^{13}C , ^{13}C COSY spectrum (Figure 3), while the overlap of signals from several protons in the ^1H NMR spectrum may have caused misinterpretations of HMBC correlations. As this is a general problem in the structure elucidation of structurally complex natural products, our findings demonstrate the advantage of a ^{13}C , ^{13}C -COSY-based structure elucidation.

The relative configuration of **1** was determined by NOESY spectroscopy (Figure 4). Key correlations were observed between H7 ($\delta = 1.57$ ppm) and H11 ($\delta = 1.25$), placing these on the same face of **1**. This finding was

[*] L. Barra, Prof. Dr. J. S. Dickschat
 Kekulé-Institut für Organische Chemie und Biochemie
 Rheinische Friedrich-Wilhelms-Universität Bonn
 Gerhard-Domagk-Strasse 1, 53121 Bonn (Germany)
 E-mail: dickschat@uni-bonn.de

Dr. K. Ibrom
 Institut für Organische Chemie, TU Braunschweig
 Hagenring 30, 38106 Braunschweig (Germany)

Supporting information for this article is available on the WWW under <http://dx.doi.org/10.1002/anie.201501765>.

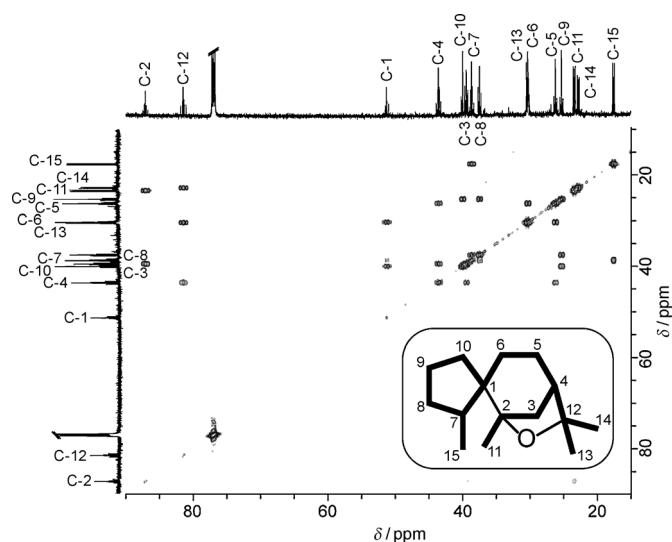


Figure 2. ^{13}C , ^{13}C COSY spectrum of $[\text{C}_{15}^{13}]$ -**1** in CDCl_3 . All neighboring carbon atoms along the bold lines of **1** showed cross-peaks, with the exception of the two neighboring quaternary carbon atoms. The reason for the missing signal is that spin relaxation of quaternary carbon atoms is generally slower than for other carbon atoms. The C1–C2 bond was instead inferred from the multiplicities of the signals (Figure S3). An enlarged version of this Figure is presented as Figure S4.

corroborated by a correlation between $\text{H}_{6_{\text{eq}}}$ ($\delta = 1.47$ ppm) and H_{15} ($\delta = 1.03$ ppm), which are in similar positions on the opposite face. The equatorial position of $\text{H}_{6_{\text{eq}}}$ was deduced from a correlation between $\text{H}_{6_{\text{ax}}}$ ($\delta = 1.65$ ppm) and H_{14} ($\delta =$

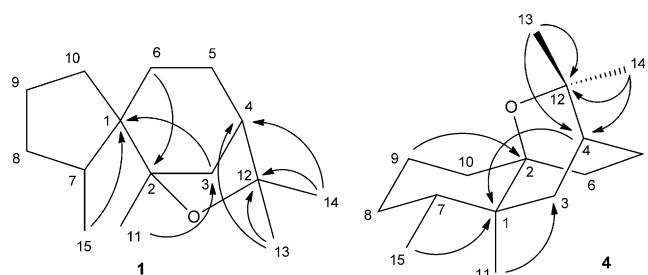


Figure 3. Key HMBC correlations of hypodoratoxide and their interpretation for the revised (**1**) and reported structure (**4**). Carbon atom numbering of **1** is based on IUPAC systematic nomenclature, whereas carbon numbering of **4** followed the reported assignment of ^{13}C NMR signals (Table 1). Note that some of the interpretations of HMBC correlations in the original work involve different hydrogen atoms than in this work (e.g., the correlation $\text{H}_9/\text{C}2$ is now interpreted as $\text{H}_6/\text{C}2$; the ^1H NMR signals of H_9 and H_6 overlap).

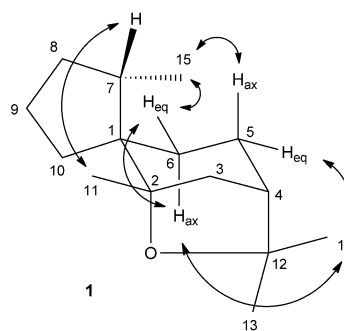


Figure 4. Key NOESY correlations of hypodoratoxide (**1**).

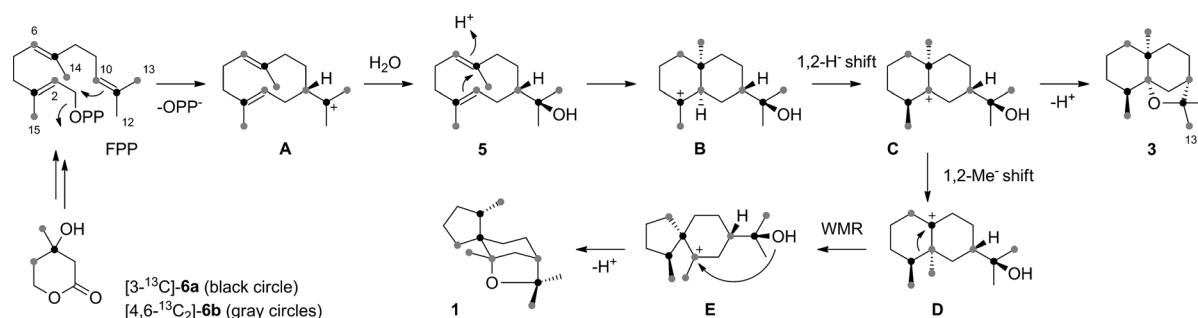
Table 1: ^1H NMR data of **1** and comparison of the ^{13}C NMR data of **1** and hypodoratoxide in C_6D_6 .

$\text{C}^{\text{[a]}}$	$^1\text{H}^{\text{[b]}}$	$^{13}\text{C}^{\text{[c]}}$	$^{13}\text{C}^{\text{[c]}}$
	1	1	hypodoratoxide ^[14]
2		86.7 (C_q)	86.7 (C_q)
12		81.3 (C_q)	81.3 (C_q)
1		51.7 (C_q)	51.8 (C_q)
4	1.64, m	44.0 (CH)	44.0 (CH)
10	2.34, dddd, $^2J = 13.6$, $^3J = 7.0$, 1.9, $^4J = 1.9$ 1.05, m	40.5 (CH_2)	40.5 (CH_2)
3	1.75, ddd, $^2J = 11.7$, $^3J = 4.6$, $^4J = 2.5$ 1.62, d, $^2J = 11.8$	39.8 (CH_2)	39.9 (CH_2)
7	1.57, m	38.9 (CH)	38.9 (CH)
8	1.73, m 1.08, m	38.0 (CH_2)	37.9 (CH_2)
6	1.65, m 1.47, m	30.9 (CH_2)	30.9 (CH_2)
13	1.18, s	30.8 (CH_3)	30.7 (CH_3)
5	1.55, m 1.43, m	26.8 (CH_2)	26.8 (CH_2)
9	1.47, m 1.23, dddd, $^2J = 12.0$, $^3J = 12.0$, 12.0, 7.1, 6.1	25.9 (CH_2)	25.8 (CH_2)
11	1.25, s	23.9 (CH_3)	23.9 (CH_3)
14	1.29, s	23.2 (CH_3)	23.1 (CH_3)
15	1.03, d, $^3J = 6.8$	17.8 (CH_3)	17.8 (CH_3)

[a] Carbon numbering as shown in Figure 3. [b] Chemical shifts δ in ppm; multiplicity m: s = singlet, d = doublet, m = multiplet; coupling constants nJ refer to couplings via n bonds and are given in Hertz. [c] Chemical shifts δ in ppm; carbon assignments (CH_3 , CH_2 , CH , and C_q) were delineated from a DEPT spectrum.

1.29 ppm). The configuration of the spiro center, that is, the counter-clockwise orientation of the C1, C7, C8, C9, and C10 carbon atoms when looking at **1** as depicted in Figure 4, was evident from a correlation between the axial $\text{H}_{5_{\text{ax}}}$ atom ($\delta = 1.43$ ppm) and H_{15} [the equatorial orientation of $\text{H}_{5_{\text{eq}}}$ ($\delta = 1.55$ ppm) was delineated from its correlation to H_{14}].

A proposed mechanism for the enzymatic conversion of FPP into **1** is shown in Scheme 1. The reaction starts with the cyclization of FPP to the (*E,E*)-germacradienyl cation (**A**), which is attacked by water to yield hedycaryol (**5**). Its protonation initiates a cyclization to cation **B**, which is followed by a 1,2-hydride migration to yield **C**. A subsequent 1,2-methyl shift results in **D**, which gives rise to **1** upon Wagner–Meerwein rearrangement with ring contraction to **E** and intramolecular attack of the



Scheme 1. Biosynthesis of hypodoratoxide (**1**). Gray and black circles indicate ^{13}C -labeled carbon atoms from two individual feeding experiments. PP=diphosphate, WMR=Wagner–Meerwein rearrangement.

hydroxy group at the cationic center with inversion of configuration. The formation of side product **3** is explained by intramolecular attack of the hydroxy group at the cationic center in **C** with retention of configuration (Figure 1). The relative configuration of **3** is in line with that of **1**. Knowledge of the absolute configuration of **3** would point to the absolute configuration of **C**, from which the absolute configuration of **1** could be inferred. Therefore, 18 mg of **3** were isolated from *H. odoratus* with a yield of 3 mg L^{-1} . Its ^{13}C NMR spectroscopic data matched those reported for *cis*-dihydroagarofuran (**3**),^[15] confirming the GC/MS-based identification. The optical activity of isolated (+)-**3** pointed to the absolute configuration that is shown in Scheme 1, which is opposite to that of (–)-**3** from *Prostanthera ovalifolia* (Lamiaceae),^[16] while this is the first report of (+)-**3** from a natural source. Consequently, the absolute configuration of hypodoratoxide is (1*R*,2*S*,4*S*,7*S*)-**1**. This assignment is tentative because a biosynthesis of **1** and **3** by two different terpene cyclases cannot be ruled out.

The proposed cyclization mechanism for **1** was investigated in two feeding experiments with the mevalonolactone isotopologues (3- ^{13}C)-**6a** and (4,6- $^{13}\text{C}_2$)-**6b**.^[12] Feeding of **6a** resulted in the incorporation of the ^{13}C label at the C3, C7, and C11 positions of FPP (68% incorporation, Figure S2B) and allowed for interesting insights into the terpene cyclization. The proposed ring contraction from **D** to **E** was directly evident from the occurrence of doublets for the neighboring labeled carbon atoms C1 and C7 in the ^{13}C NMR spectrum (Figure 5A). Feeding of **6b** gave incorporation of labeling at the C2, C6, C10, C13, C14, and C15 positions of FPP (10% incorporation; see Figure S2C, for the carbon numbering of FPP, see Scheme 1). The ^{13}C NMR spectrum of the terpene cyclization product showed doublets for the neighboring labeled carbon atoms C2 and C11, which is indicative of the 1,2-methyl migration from intermediate **C** to **D** (Figure 5B). The incorporation of labeling almost only at the C13 position (ca. 90% of labeling from C13 of FPP) and only to a low extent at the C14 position of **1** (ca. 10%) revealed a strict stereochemical course for the attack of water at cation **A**. A similar control of the stereochemical course of terpene cyclizations in terms of the fate of the geminal methyl groups of linear terpene precursors was previously observed for other terpene cyclases.^[1,12,17–19]

The strategy of labeling a natural product by feeding of ^{13}C -labeled precursors for structure elucidation by advanced

NMR spectroscopic methods has been applied before in the cases of the diterpene miltiradiene from the lycophyte *Selaginella moellendorffii*,^[20] solwaric acids A and B from the

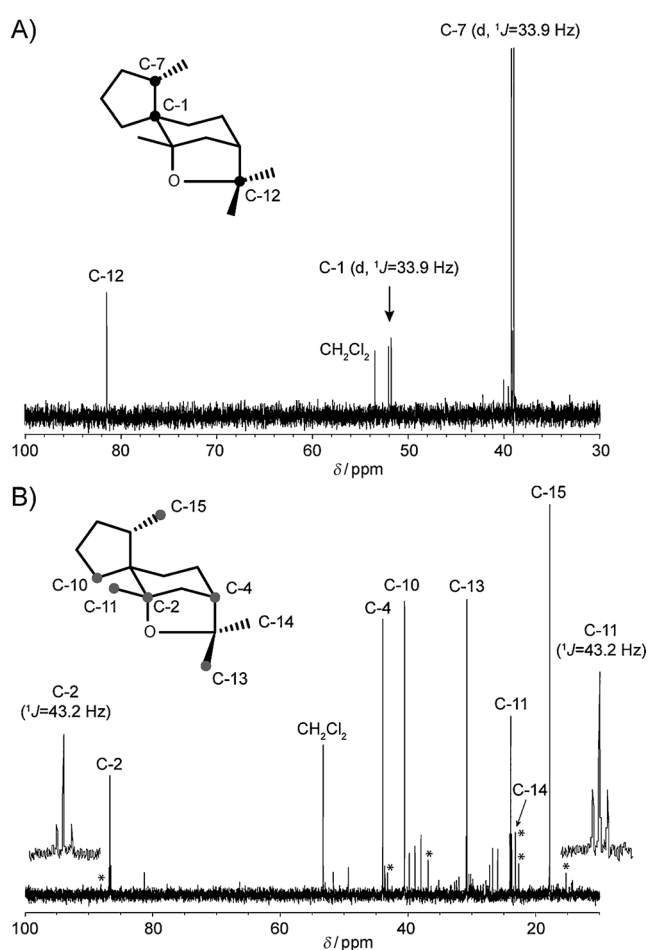


Figure 5. Investigation of the terpene cyclization mechanism by feeding experiments. A) ^{13}C NMR spectrum of [1,7,12- $^{13}\text{C}_3$]-**1** obtained after feeding of (3- ^{13}C)-**6a**. B) ^{13}C NMR spectrum of [2,4,10,11,13,15- $^{13}\text{C}_6$]-**1** obtained after feeding of (4,6- $^{13}\text{C}_2$)-**6b**. The signals for C2 and C11 are also shown in enlarged versions (width: 800%). Some of the additional ^{13}C signals are due to incorporation into the minor product **3** of the hypodoratoxide synthase (labeled with asterisks). The signal at $\delta = 23.1 \text{ ppm}$, which was assigned to a minor incorporation into the C14 position of **1**, may also partially account for incorporation into C13 of **3**.

marine actinomycete *Solwaraspora* sp. WMMB-329,^[21] and the polyketide forazoline A from marine *Actinomadura* sp. WMMB-499.^[22] Herein, we provide an example that this strategy makes structure elucidation not only easier, but can also be superior because misinterpretations of HMBC correlations are avoided.

Carefully designed feeding experiments with ¹³C-labeled precursors can give detailed insights into rearrangements of the carbon skeleton during the biosynthesis of a natural product. Whereas rearrangement-induced ¹³C,¹³C couplings have only very rarely been used to prove skeleton rearrangements,^[23] the feeding of multiply ¹³C-labeled precursors, usually (1,2-¹³C₂)acetate, and the loss of ¹³C,¹³C couplings owing to bond cleavages in rearrangements has historically been widely used.^[24] An interesting complementary approach to study the mechanisms of natural-product biosyntheses is the usage of deuterium labeling, as recently performed to follow epimerization reactions in the biosynthesis of non-ribosomal peptides.^[25,26] Another study that combines the usage of ¹³C and ²H labeling in mechanistic investigations of a terpene cyclization has recently been reported from our laboratories.^[27] These and many other previous examples demonstrate how isotopes can successfully be used to solve special problems in natural-products chemistry.

Keywords: biosynthesis · isotopic labeling · NMR spectroscopy · structure elucidation · terpenoids

How to cite: *Angew. Chem. Int. Ed.* **2015**, *54*, 6637–6640
Angew. Chem. **2015**, *127*, 6737–6740

[1] J. S. Dickschat, *Nat. Prod. Rep.* **2011**, *28*, 1917–1936.

[2] C. M. Starks, K. Back, J. Chappell, J. P. Noel, *Science* **1997**, *277*, 1815–1820.

[3] C. A. Lesburg, G. Zhai, D. E. Cane, D. W. Christianson, *Science* **1997**, *277*, 1820–1824.

[4] M. J. Rynkiewicz, D. E. Cane, D. W. Christianson, *Proc. Natl. Acad. Sci. USA* **2001**, *98*, 13543–13548.

[5] E. Y. Shishova, L. Di Constanzo, D. E. Cane, D. W. Christianson, *Biochemistry* **2007**, *46*, 1941–1951.

[6] J. A. Aaron, X. Lin, D. E. Cane, D. W. Christianson, *Biochemistry* **2010**, *49*, 1787–1797.

[7] M. Köksal, Y. Jin, R. M. Coates, R. Croteau, D. W. Christianson, *Nature* **2011**, *469*, 116–120.

[8] P. Baer, P. Rabe, C. A. Citron, C. C. de Oliveira Mann, N. Kaufmann, M. Groll, J. S. Dickschat, *ChemBioChem* **2014**, *15*, 213–216.

[9] P. Baer, P. Rabe, K. Fischer, C. A. Citron, T. A. Klapschinski, M. Groll, J. S. Dickschat, *Angew. Chem. Int. Ed.* **2014**, *53*, 7652–7656; *Angew. Chem.* **2014**, *126*, 7783–7787.

[10] H. Utsunomiya, J. Kawata, W. Chanoki, N. Shirakawa, M. Miyazawa, *J. Oleo Sci.* **2005**, *54*, 609–612.

[11] R. P. Adams, *Identification of Essential Oil Components by Gas Chromatography/Mass Spectrometry*, Allured Books, Carol Stream, **2009**.

[12] L. Barra, B. Schulz, J. S. Dickschat, *ChemBioChem* **2014**, *15*, 2379–2383.

[13] L. O. Zamir, C.-D. Nguyen, *J. Labelled Compd. Radiopharm.* **1988**, *25*, 1189–1196.

[14] B. Kühne, H.-P. Hanssen, W.-R. Abraham, V. Wray, *Phytochemistry* **1991**, *30*, 1463–1465.

[15] J.-F. Cavalli, F. Tomi, A.-F. Bernardini, J. Casanova, *Magn. Reson. Chem.* **2004**, *42*, 709–711.

[16] I. A. Southwell, D. J. Tucker, *Phytochemistry* **1993**, *33*, 857–862.

[17] X. Lin, D. E. Cane, *J. Am. Chem. Soc.* **2009**, *131*, 6332–6333.

[18] N. L. Brock, S. R. Ravella, S. Schulz, J. S. Dickschat, *Angew. Chem. Int. Ed.* **2013**, *52*, 2100–2104; *Angew. Chem.* **2013**, *125*, 2154–2158.

[19] C. A. Citron, N. L. Brock, B. Tudzynski, J. S. Dickschat, *Chem. Commun.* **2014**, *50*, 5224–5226.

[20] Y. Sugai, Y. Ueno, K. Hayashi, S. Oogami, T. Toyomasu, S. Matsumoto, M. Natsume, H. Nozaki, H. Kawaide, *J. Biol. Chem.* **2011**, *286*, 42840–42847.

[21] G. A. Ellis, T. P. Wyche, C. G. Fry, D. R. Braun, T. S. Bugni, *Mar. Drugs* **2014**, *12*, 1013–1022.

[22] T. P. Wyche, J. S. Piotrowski, Y. Hou, D. Braun, R. Deshpande, S. McIlwain, I. M. Ong, C. L. Myers, I. A. Guzei, W. M. Westler, D. R. Andes, T. S. Bugni, *Angew. Chem. Int. Ed.* **2014**, *53*, 11583–11586; *Angew. Chem.* **2014**, *126*, 11767–11770.

[23] A. P. W. Bradshaw, J. R. Hanson, M. Siversns, *J. Chem. Soc. Chem. Commun.* **1977**, 819a.

[24] T. J. Simpson, *Top. Curr. Chem.* **1998**, *195*, 1–48.

[25] H. B. Bode, D. Reimer, S. W. Fuchs, F. Kirchner, C. Dauth, C. Kegler, W. Lorenzen, A. O. Brachmann, P. Grün, *Chem. Eur. J.* **2012**, *18*, 2342–2348.

[26] B. Morinaka, A. L. Vagstad, M. J. Helf, M. Gugger, C. Kegler, M. F. Freeman, H. B. Bode, J. Piel, *Angew. Chem. Int. Ed.* **2014**, *53*, 8503–8507; *Angew. Chem.* **2014**, *126*, 8643–8647.

[27] P. Rabe, K. A. K. Pahirulzaman, J. S. Dickschat, *Angew. Chem. Int. Ed.* **2015**, DOI: 10.1002/anie.201501119; *Angew. Chem.* **2015**, DOI: 10.1002/ange.201501119.

Received: February 24, 2015

Published online: April 15, 2015

Supporting Information

German Edition: DOI:

Structural Revision and Elucidation of the Biosynthesis of Hypodoratoxide by ^{13}C , ^{13}C COSY NMR Spectroscopy

*Lena Barra, Kerstin Ibrom, and Jeroen S. Dickschat**

ange_201501765_sm_miscellaneous_information.pdf

Strain, culture conditions and feeding experiments. *Hypomyces odoratus* DSM 11934 was obtained from the Deutsche Sammlung für Mikroorganismen und Zellkulturen (DSMZ) and cultured on agar plates containing oat agar medium (30.0 g oat flakes, boiled for 10 min in 1 L water, and then charged with 15.0 g agar before autoclavation). The fungus was incubated for 4 d at 22 °C and directly subjected to headspace analysis using a closed-loop stripping apparatus (CLSA).^[1] Feeding experiments were conducted by distributing a solution of the ¹³C-labelled mevalonolactone isotopomers [2,3,4,5,6-¹³C₅]mevalonolactone (**SI-7**) or **6a** (10 mg in 0.5 mL sterile water) with a syringe over a grown agar plate culture. To increase the incorporation rates in the experiment with **6a** the agar medium was charged with lovastatin (100 mg L⁻¹) after autoclavation. The feeding experiment with **6b** was conducted by incubation of *H. odoratus* in liquid oat medium (100 mL) for 4 d at 22 °C. After growth the culture was charged with labelled material (10 mg of **6b**) and lovastatin (100 mg L⁻¹). The fed agar plate and liquid cultures were immediately subjected to a CLSA for the collection of volatiles and the charcoal filters were extracted daily with 70 µL of CDCl₃ or C₆D₆ for 1 week. The combined extracts were directly subjected to NMR analysis.

Collection of volatiles by CLSA. The volatiles emitted by *H. odoratus* grown on agar plate cultures were collected by use of a closed loop stripping apparatus (CLSA) as described previously.^[1] A circulating air flow was directed over the grown agar plate culture and through a charcoal filter (Chromtech GmbH, Idstein, Precision Charcoal Filter, 5 mg) in a closed apparatus for 1 week. The charcoal filter was extracted daily with 70 µL of either CDCl₃ or C₆D₆ and the obtained extracts were combined and analyzed by NMR spectroscopy and GC-MS.

GC/MS analysis of headspace extracts. GC-MS analyses for the headspace extracts were carried out on a HP 1890B GC system connected to a HP 5977 Mass Selective Detector fitted with a HP5-MS fused silica capillary column (30 m x 0.25 mm i.d., 0.50 µm film). Measurement conditions: inlet pressure: 77.1 kPa, He 23.3 mL/min; injection volume: 1 µL; injector: 250 °C; transfer line: 250 °C; electron energy: 70 eV. The GC was programmed as follows: 50 °C (5 min isothermic), increasing at 5 °C/min to 320 °C, and operated in split mode (10:1); carrier gas (He): 1.0 mL/min. Retention indices were determined from a homologous series of *n*-alkanes (C₈ – C₃₂). The identification of compounds was performed by comparison of mass spectra to data base spectra of commercially available libraries.

Structure elucidation of 1 by ¹³C,¹³C-COSY. The volatile material emitted by a *H. odoratus* agar plate culture in the feeding experiment with [2,3,4,5,6-¹³C₅]mevalonolactone (**SI-7**) was collected as described above and subjected to ¹³C,¹³C-COSY.

Preparative scale isolation of (+)-hypodoratoxide (1) and (+)-cis-dihydroagarofuran (3). *H. odoratus* was cultured on oat agar medium (2 L) using

large petri dishes (20 cm diameter) for 4 d. The cultures were cut in small pieces and extracted with pentane (3 x 500 mL). The combined extracts were dried with MgSO₄. After removal of the solvent the crude material (1.78 g) was purified by column chromatography using Merck silica gel 60 (0.040–0.063 mm) and pentane/diethyl ether (50:1) as eluent. Pure hypodoratoxide (30 mg) was obtained as a colourless oil. For isolation of the minor component *cis*-dihydroagarofuran *H. odoratus* was cultured on oat agar medium (6 L). The same extraction and workup procedure as described above yielded *cis*-dihydroagarofuran as a colourless oil (18 mg). Both compounds were subjected to NMR spectroscopy for full structure elucidation.

(+)-Hypodoratoxide (1). IR (ATR): $\tilde{\nu}$ = 2936 (s), 2868 (m), 1456 (m), 1377 (m), 1197 (w), 1140 (w), 1114 (w), 971 (w), 885 (s), 547 (w) cm⁻¹. $[\alpha]_{\text{D}}^{20}$ = +63.7 (*c* = 14.0, CHCl₃). GC (HP5-MS): *I* = 1512. MS (EI, 70 eV): *m/z* (%) = 222 (7), 164 (9), 149 (5), 111 (100), 95 (14), 82 (15), 67 (13), 55 (10), 43 (32).

(+)-*cis*-Dihydroagarofuran (3). $[\alpha]_{\text{D}}^{20}$ = +61.9 (*c* = 1.5, CHCl₃), the reported optical rotary power for (–)-*cis*-dihydroagarofuran is $[\alpha]_{\text{D}}^{25}$ = –87.6 (neat).^[2] GC (HP5-MS): *I* = 1520. MS (EI, 70 eV): *m/z* (%) = 222 (9), 207 (100), 189 (38), 179 (5), 164 (17), 149 (32), 137 (61), 123 (18), 109 (43), 95 (25), 81 (25), 69 (27), 55 (29), 43 (32). ¹H-NMR (400 MHz, CDCl₃): δ = 1.94 (m, 1H, CH), 1.93 (m, 1H, CH₂), 1.80 (m, 1H, CH), 1.72 (m, 1H, CH₂), 1.64 (m, 1H, CH₂), 1.62 (m, 1H, CH₂), 1.61 (m, 1H, CH₂), 1.55 (m, 1H, CH₂), 1.54 (m, 1H, CH₂), 1.53 (m, 1H, CH₂), 1.38 (m, 1H, CH₂), 1.32 (s, 3H, CH₃), 1.17 (m, 1H, CH₂), 1.15 (m, 1H, CH₂), 1.14 (s, 3H, CH₃), 0.97 (m, 1H, CH₂), 0.89 (s, 3H, CH₃), 0.83 (d, ³*J*_{H,H} = 6.7 Hz, 3H, CH₃) ppm. ¹³C-NMR (100 MHz, CDCl₃): δ = 88.5 (C_q), 81.2 (C_q), 43.0 (CH), 39.7 (C_q), 36.8 (CH₂), 35.3 (CH₂), 33.2 (CH₂), 32.6 (CH), 30.7 (CH₂), 30.1 (CH₃), 25.9 (CH₂), 23.1 (CH₃), 22.5 (CH₃), 21.6 (CH₂), 15.0 (CH₃) ppm.

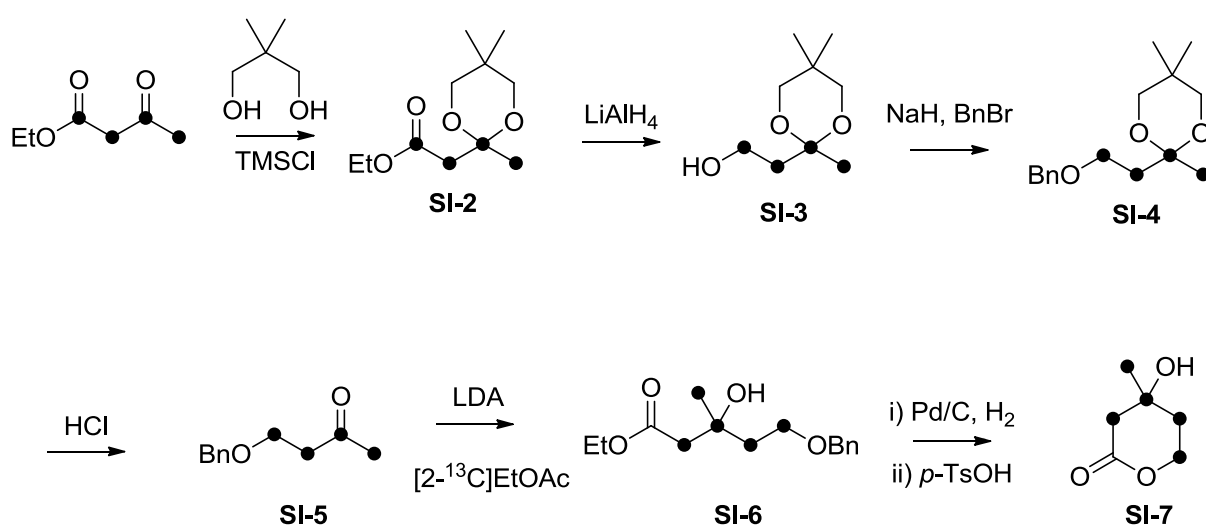
NMR spectroscopy of isolated natural products. NMR (Nuclear magnetic resonance) spectra were recorded at 20 °C on a Bruker Avance II 600 spectrometer equipped with a TCI cryo probehead (Bruker BioSpin, Rheinstetten, Germany) operating at 600.1 MHz (¹H) and 150.9 MHz (¹³C). Chemical shifts δ were referenced to internal tetramethylsilane (¹H, δ = 0.00 ppm), C₆D₆ (¹³C, δ = 128.0 ppm) or CDCl₃ (¹³C, δ = 77.0 ppm), respectively.

The techniques used to assign the ¹H and ¹³C spectra were ¹³C-DEPT-135, ¹H,¹H-COSY, ¹H,¹H-NOESY (mixing time 1s), ¹H,¹³C-HSQC, ¹H,¹³C-HMBC (optimised for *J*_{C,H} = 8 Hz), and ¹³C,¹³C-COSY (relaxation delay 2 s, proton decoupled). Bruker standard pulse programs were applied throughout and with the exception of the ¹³C,¹³C-COSY experiment pulse sequences with gradient selection were applied for the two-dimensional spectra. Digital resolutions in the two-dimensional spectra were chosen small enough to distinguish cross peaks with similar chemical shifts (if possible).

General Synthetic Methods. Chemicals were purchased from Acros Organics (Geel, Belgium) or Sigma-Aldrich Chemie GmbH (Steinheim, Germany). Solvents were purified by distillation, and dried according to standard methods. Oxygen and/or

moisture sensitive reactions were carried out under inert atmosphere (N₂) in vacuum-heated flasks with dried solvents. Thin-layer chromatography (SiO₂, TLC) was performed on 0.20 mm Macherey-Nagel silica gel plates (Polygram SIL G/UV254). Column chromatography was performed on Merck silica gel 60 (0.040–0.063 mm) using standard flash chromatographic methods. The NMR spectra of synthetic compounds were recorded on Bruker DRX-400 (400 MHz), AV III-400 (400 MHz) or AV II-300 (300 MHz) spectrometers, and were referenced against TMS ($\delta = 0.00$ ppm) for ¹H-NMR and CHCl₃ ($\delta = 77.01$ ppm) for ¹³C-NMR. GC-MS analyses were performed on a HP 1890B GC system connected to a HP 5977 Mass Selective Detector fitted with a HP5-MS fused silica capillary column (30 m x 0.25 mm i.d., 0.50 μ m film). Measurement conditions: inlet pressure: 77.1 kPa, He 23.3 mL/min; injection volume: 1 μ L; injector: 250 °C; transfer line: 250 °C; electron energy: 70 eV. The GC was programmed as follows: 50 °C (5 min isothermic), increasing at 5 °C/min to 320 °C, and operated in split mode (50:1); carrier gas (He): 1.0 mL/min. Retention indices were determined from a homologous series of *n*-alkanes (C₈ – C₃₂).

Synthesis of (2,3,4,5,6-¹³C₅)mevalonolactone. This compound was synthesised via a reported procedure by Zamir and Nguyen using the labelled building blocks ethyl (1,2,3,4-¹³C₄)acetoacetate (**SI-1**) and ethyl (2-¹³C)acetate (Scheme 1 of SI).^[3,4]



Scheme 1. Synthesis of (2,3,4,5,6-¹³C₅)mevalonolactone (**SI-7**).

Ethyl (1,2-¹³C₂)-2-(2-(¹³C)methyl-5,5-dimethyl-(2-¹³C)-1,3-dioxan-2-yl)acetate (SI-2**).** Yield: 1.63 g (7.4 mmol, 99%). GC (HP5-MS): *I* = 1342. ¹H-NMR (400 MHz, C₆D₆): δ = 3.98 (dq, ³J_{H,H} = 7.2 Hz, ³J_{C,H} = 3.2 Hz, 2H, CH₂), 3.38 (dd, ²J_{H,H} = 11.4 Hz, ³J_{C,H} = 3.7 Hz, 2H, 2 x CH₂), 3.28 (dd, ²J_{H,H} = 11.4 Hz, ³J_{C,H} = 4.6 Hz, 2H, 2 x CH₂), 2.78 (dddd, ¹J_{C,H} = 129.8 Hz, ²J_{C,H} = 6.9 Hz, ²J_{C,H} = 6.4 Hz, ³J_{C,H} = 3.5 Hz, 2H, CH₂), 1.68 (ddd, ¹J_{C,H} = 127.4 Hz, ²J_{C,H} = 4.9 Hz, ³J_{C,H} = 2.9 Hz, 3H, CH₃), 0.96 (t, ³J_{H,H} = 7.1 Hz, 3H, CH₃), 0.76 (s, 3H, CH₃), 0.67 (s, 3H, CH₃) ppm. ¹³C-NMR (100 MHz, C₆D₆): δ = 169.1 (d, ¹J_{C,C} = 59.2 Hz, C_q), 97.7 (dd, ¹J_{C,C} = 48.0 Hz, ¹J_{C,C} = 44.3 Hz,

C_q), 70.5 (dd, ²J_{C,C} = 1.9 Hz, ³J_{C,C} = 1.8 Hz, 2 x CH₂), 60.2 (d, ²J_{C,C} = 2.1 Hz, CH₂), 41.7 (ddd, ¹J_{C,C} = 59.3 Hz, ¹J_{C,C} = 44.2 Hz, ²J_{C,C} = 3.8 Hz, CH₂), 29.7 (d, ³J_{C,C} = 2.3 Hz, C_q), 23.3 (dd, ¹J_{C,C} = 47.9 Hz, ²J_{C,C} = 3.9 Hz, CH₃), 22.6 (s, CH₃), 22.4 (s, CH₃), 14.2 (d, ³J_{C,C} = 2.0 Hz, CH₃) ppm. MS (EI, 70 eV): *m/z* (%) = 204 (32), 135 (35), 131 (100), 118 (16), 107 (12), 89 (28), 69 (39), 56 (16), 45 (38).

(1,2-¹³C₂)-2-(2-(¹³C)methyl-5,5-dimethyl-(2-¹³C)-1,3-dioxan-2-yl)ethanol (SI-3).

Yield: 1.18 g (6.73 mmol, 90%). GC (HP5-MS): *I* = 1238. ¹H-NMR (400 MHz, C₆D₆): δ = 3.94 (dm, ¹J_{C,H} = 142.2 Hz, 2H, CH₂), 3.28 (d, ²J_{H,H} = 11.1 Hz, 2H, 2 x CH₂), 3.11 (dm, ²J_{H,H} = 11.1 Hz, 2H, 2 x CH₂), 2.81 (m, 1H, OH), 1.87 (dm, ¹J_{C,H} = 125.7 Hz, 2H, CH₂), 1.17 (dm, ¹J_{C,H} = 126.1 Hz, 3H, CH₃), 0.96 (s, 3H, CH₃), 0.40 (s, 3H, CH₃) ppm. ¹³C-NMR (100 MHz, C₆D₆): δ = 100.1 (ddd, ¹J_{C,C} = 46.3 Hz, ¹J_{C,C} = 46.3 Hz, ²J_{C,C} = 1.9 Hz, C_q), 70.2 (d, ²J_{C,C} = 1.9 Hz, 2 x CH₂), 58.8 (ddd, ¹J_{C,C} = 36.3 Hz, ²J_{C,C} = 1.8 Hz, ³J_{C,C} = 1.8 Hz, CH₂), 42.4 (ddd, ¹J_{C,C} = 46.8 Hz, ¹J_{C,C} = 36.3 Hz, ²J_{C,C} = 3.8 Hz, CH₂), 29.7 (d, ³J_{C,C} = 2.4 Hz, C_q), 22.8 (s, CH₃), 22.0 (s, CH₃), 19.1 (ddd, ¹J_{C,C} = 45.9 Hz, ²J_{C,C} = 3.7 Hz, ³J_{C,C} = 1.7 Hz, CH₃) ppm. MS (EI, 70 eV): *m/z* (%) = 162 (84), 131 (100), 93 (44), 76 (55), 69 (67), 56 (37), 45 (71).

2-((1,2-¹³C₂)-2-(benzyloxy)ethyl)-2-(¹³C)methyl-5,5-dimethyl-(2-¹³C)-1,3-dioxane (SI-4).

Yield: 1.17 g (4.4 mmol, 65%). GC (HP5-MS): *I* = 1871. ¹H-NMR (400 MHz, [²H₆]DMSO): δ = 7.37 - 7.25 (m, 5H, 5 x CH), 4.44 (d, ³J_{C,H} = 3.9 Hz, 2H, CH₂), 3.54 (dm, ¹J_{C,H} = 141.6 Hz, 2H, CH₂), 3.47 (dd, ²J_{H,H} = 11.3 Hz, ³J_{C,H} = 3.1 Hz, 2H, 2 x CH₂), 3.35 (m, 2H, 2 x CH₂), 1.96 (dm, ¹J_{C,H} = 126.2 Hz, 2H, CH₂), 1.31 (ddd, ¹J_{C,H} = 126.3 Hz, ²J_{C,H} = 4.5 Hz, ³J_{C,H} = 3.0 Hz, 3H, CH₃), 0.91 (s, 3H, CH₃), 0.82 (s, 3H, CH₃) ppm. ¹³C-NMR (100 MHz, [²H₆]DMSO): δ = 138.6 (d, ³J_{C,C} = 2.9 Hz, C_q), 128.2 (s, 2 x CH), 127.4 (s, 2 x CH), 127.3 (s, CH), 97.5 (dd, ¹J_{C,C} = 46.2 Hz, ¹J_{C,C} = 46.2 Hz, C_q), 71.9 (d, ²J_{C,C} = 3.2 Hz, CH₂), 69.2 (d, ²J_{C,C} = 1.8 Hz, 2 x CH₂), 65.5 (d, ¹J_{C,C} = 39.2 Hz, CH₂), 37.3 (ddd, ¹J_{C,C} = 46.1 Hz, ¹J_{C,C} = 42.9 Hz, ²J_{C,C} = 3.6 Hz, CH₂), 29.5 (d, ³J_{C,C} = 2.4 Hz, C_q), 22.4 (s, CH₃), 22.0 (s, CH₃), 20.9 (dd, ¹J_{C,C} = 46.4 Hz, ³J_{C,C} = 3.5 Hz, CH₃) ppm. MS (EI, 70 eV): *m/z* (%) = 252 (16), 164 (11), 131 (100), 107 (21), 91 (84), 76 (16), 69 (32), 45 (33).

(1,2,3,4-¹³C₄)-4-(benzyloxy)butan-2-one (SI-5).

Yield: 0.72 g (4.0 mmol, 92%). GC (HP5-MS): *I* = 1445. ¹H-NMR (400 MHz, CDCl₃): δ = 7.38 - 7.24 (m, 5H, 5 x CH), 4.51 (d, ³J_{C,H} = 4.3 Hz, 2H, CH₂), 3.74 (dm, ¹J_{C,H} = 143.1 Hz, 2H, CH₂), 2.72 (dm, ¹J_{C,H} = 126.0 Hz, 2H, CH₂), 2.18 (ddd, ¹J_{C,H} = 127.2 Hz, ²J_{C,H} = 5.9 Hz, ³J_{C,H} = 1.3 Hz, 3H, CH₃) ppm. ¹³C-NMR (100 MHz, CDCl₃): δ = 207.2 (ddd, ¹J_{C,C} = 40.4 Hz, ¹J_{C,C} = 40.0 Hz, ²J_{C,C} = 1.7 Hz, C_q), 138.1 (d, ³J_{C,C} = 2.8 Hz, C_q), 128.4 (s, 2 x CH), 127.7 (s, 2 x CH), 127.6 (s, CH), 73.2 (dd, ²J_{C,C} = 3.8 Hz, ³J_{C,C} = 1.4 Hz, CH₂), 65.2 (d, ¹J_{C,C} = 39.6 Hz, CH₂), 43.7 (ddd, ¹J_{C,C} = 39.3 Hz, ¹J_{C,C} = 39.3 Hz, ²J_{C,C} = 13.8 Hz, CH₂), 30.4 (d, ¹J_{C,C} = 40.6 Hz, ²J_{C,C} = 14.1 Hz, CH₃) ppm. MS (EI, 70 eV): *m/z* (%) = 121 (34), 107 (100), 91 (86), 79 (26), 76 (21), 65 (12), 45 (38).

Ethyl (2,3,4,5-¹³C₄)-5-(benzyloxy)-3-hydroxy-3-(¹³C)methylpentanoate (SI-6). Yield: 0.74 g (2.7 mmol, 68%). GC (HP5-MS): *I* = 1907. ¹H-NMR (400 MHz, CDCl₃): δ = 7.38 - 7.25 (m, 5H, 5 x CH), 4.51 (d, ³J_{C,H} = 4.0 Hz, 2H, CH₂), 4.14 (m, 2H, CH₂), 3.94 (m, 1H, OH), 3.69 (dm, ¹J_{C,H} = 141.9 Hz, 2H, CH₂), 2.53 (dm, ¹J_{C,H} = 129.2 Hz, 2H, CH₂), 1.91 (dm, ¹J_{C,H} = 126.4 Hz, 2H, CH₂), 1.28 (dddd, ¹J_{C,H} = 126.3 Hz, ²J_{C,H} = 4.2 Hz, ³J_{C,H} = 3.9 Hz, ³J_{C,H} = 3.9 Hz, 3H, CH₃), 1.25 (t, ³J_{H,H} = 7.2 Hz, 3H, CH₃) ppm. ¹³C-NMR (100 MHz, CDCl₃): δ = 172.4 (d, ¹J_{C,C} = 55.0 Hz, C_q), 138.0 (d, ³J_{C,C} = 2.9 Hz, C_q), 128.4 (s, 2 x CH), 127.7 (s, CH), 127.6 (s, 2 x CH), 73.2 (dd, ²J_{C,C} = 3.6 Hz, ³J_{C,C} = 1.5 Hz, CH₂), 70.7 (dddd, ¹J_{C,C} = 38.5 Hz, ¹J_{C,C} = 38.5 Hz, ¹J_{C,C} = 38.5 Hz, ²J_{C,C} = 1.0 Hz, C_q), 66.9 (dd, ¹J_{C,C} = 38.7 Hz, ²J_{C,C} = 1.4 Hz, CH₂), 60.5 (s, CH₂), 45.5 (dd, ¹J_{C,C} = 37.4 Hz, ²J_{C,C} = 2.2 Hz, CH₂), 40.3 (dd, ¹J_{C,C} = 38.4 Hz, ¹J_{C,C} = 38.4 Hz, CH₂), 27.1 (d, ¹J_{C,C} = 40.2 Hz, ²J_{C,C} = 1.8 Hz, CH₃), 14.1 (s, CH₃) ppm. MS (EI, 70 eV): *m/z* (%) = 183 (2), 164 (29), 147 (21), 134 (9), 107 (21), 101 (11), 91 (100), 79 (9), 45 (16).

(2,3,4,5,6-¹³C₅)Mevalonolactone (SI-7). Yield 0.23 g (1.7 mmol, 62%). GC (HP5-MS, MSTFA): *I* = 1375. ¹H-NMR (300 MHz, CDCl₃): δ = 4.61 (dm, ¹J_{C,H} = 150.9 Hz, 1H, CH₂), 4.36 (dm, ¹J_{C,H} = 150.3 Hz, 1H, CH₂), 2.67 (ddm, ¹J_{C,H} = 132.8 Hz, ²J_{H,H} = 17.8 Hz, 1H, CH₂), 2.52 (ddm, ¹J_{C,H} = 126.8 Hz, ²J_{H,H} = 17.5 Hz, 1H, CH₂), 2.35 (br s, 1H, OH), 1.92 (dm, ¹J_{C,H} = 130.4 Hz, 1H, CH₂), 1.33 (dddd, ¹J_{C,H} = 126.3 Hz, ²J_{C,H} = 4.3 Hz, ³J_{C,H} = 4.3 Hz, ³J_{C,H} = 4.3 Hz, 3H, CH₃) ppm. ¹³C-NMR (75 MHz, CDCl₃): δ = 170.7 (d, ¹J_{C,C} = 51.6 Hz, C_q), 68.2 (dddd, ¹J_{C,C} = 38.1 Hz, ¹J_{C,C} = 38.1 Hz, ¹J_{C,C} = 38.1 Hz, ²J_{C,C} = 2.4 Hz, C_q), 66.1 (dd, ¹J_{C,C} = 34.6 Hz, ²J_{C,C} = 2.0 Hz, CH₂), 44.6 (ddd, ¹J_{C,C} = 36.5 Hz, ²J_{C,C} = 2.3 Hz, ²J_{C,C} = 2.3 Hz, CH₂), 35.8 (ddd, ¹J_{C,C} = 35.1 Hz, ¹J_{C,C} = 35.1 Hz, ²J_{C,C} = 2.0 Hz, CH₂), 29.7 (dddd, ¹J_{C,C} = 39.8 Hz, ²J_{C,C} = 2.3 Hz, ²J_{C,C} = 2.3 Hz, ³J_{C,C} = 2.3 Hz, CH₃) ppm. MS (EI, 70 eV): *m/z* (%) = 207 (<1), 192 (16), 161 (11), 149 (100), 133 (6), 118 (86), 103 (20), 75 (78), 45 (32).

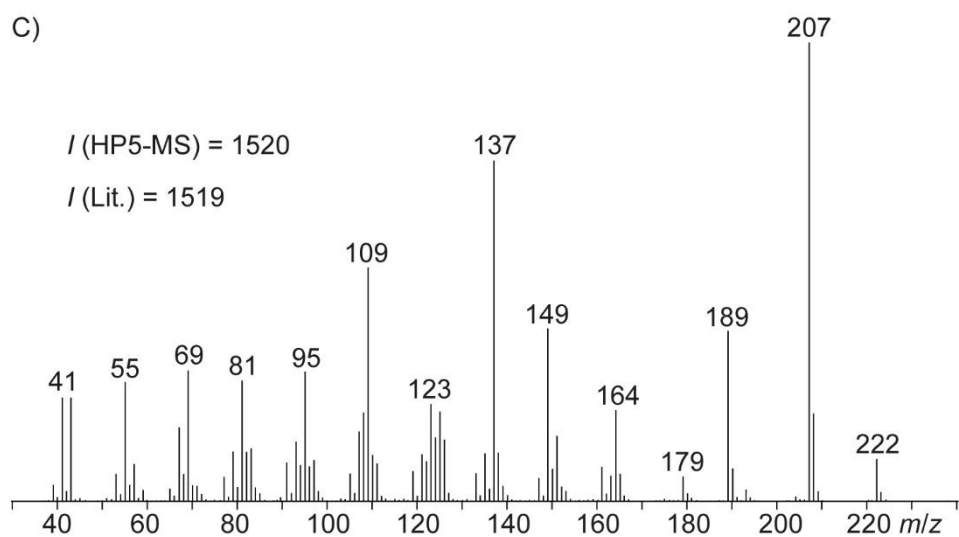
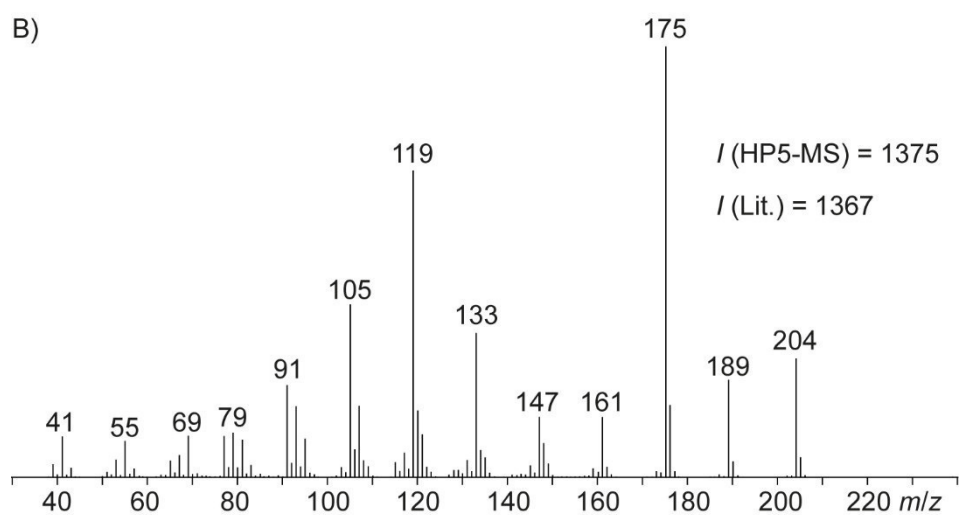
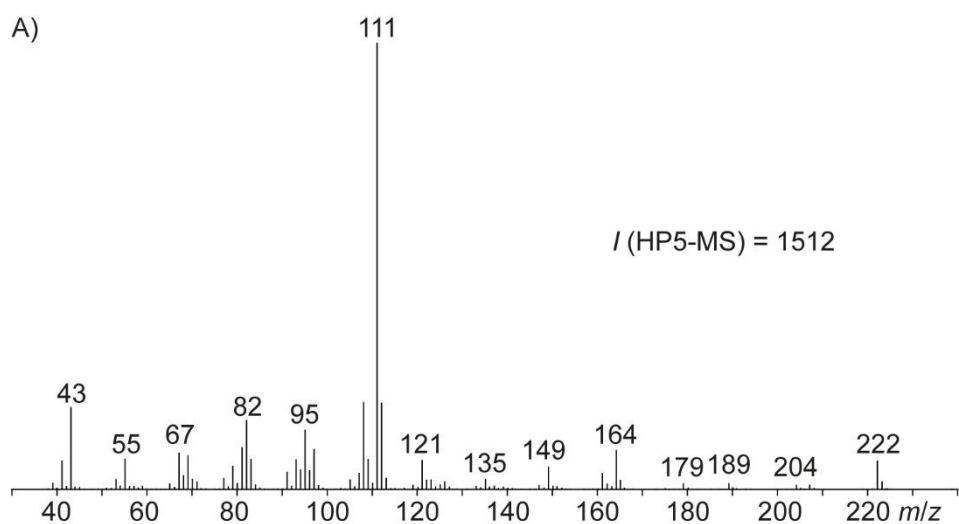


Figure 1. Mass spectra and retention indices of A) hypodoratoxide (**1**), B) protoillud-6-ene (**2**), and C) *cis*-dihydroagarofuran (**3**). Retention index literature data were taken from references [5] (compound **2**) and [6] (compound **3**).

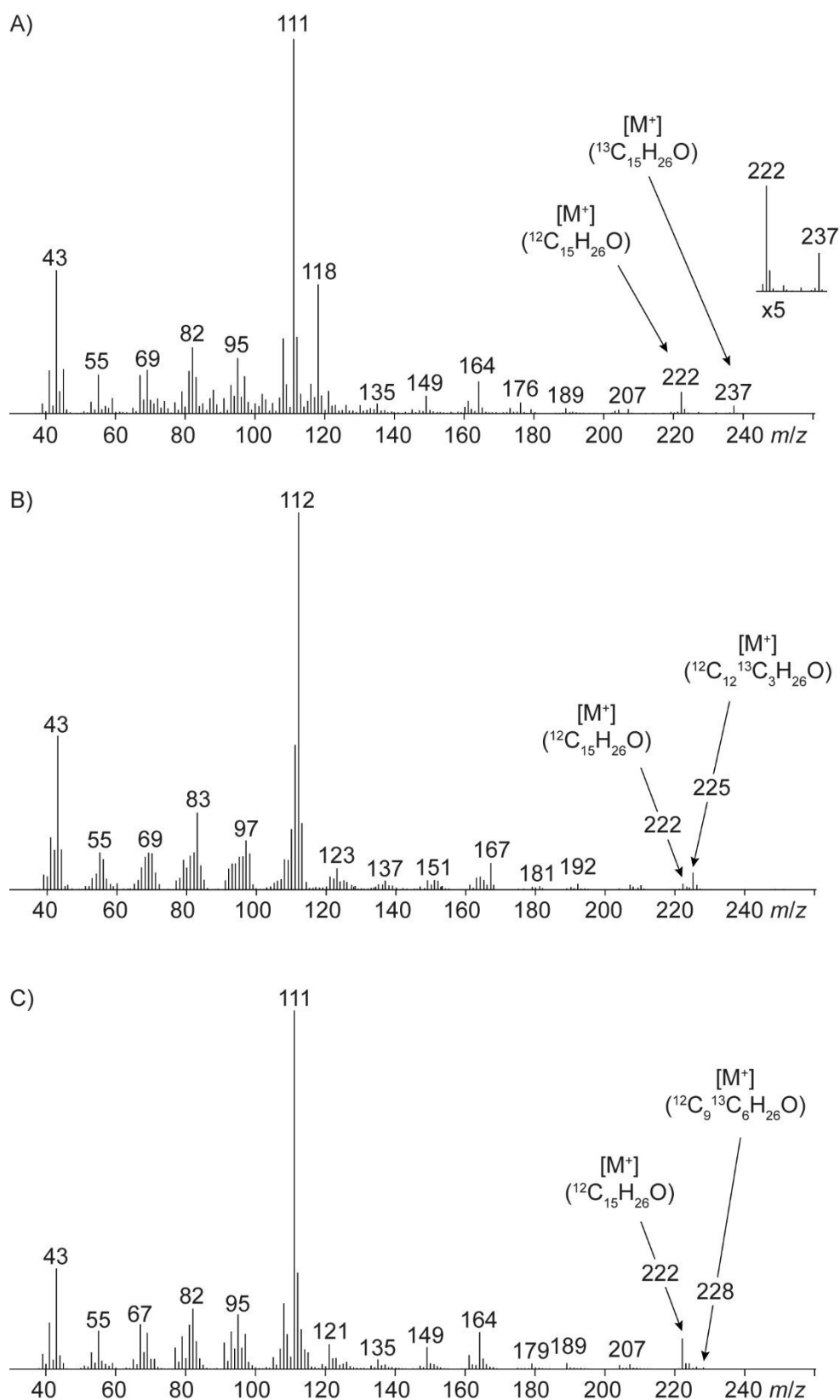


Figure 2. Mass spectra of ^{13}C -labelled **1** obtained in feeding experiments with ^{13}C -labelled isotopologs of mevalonolactone. A) Mass spectrum of $[^{13}\text{C}_{15}]\text{-1}$ obtained after feeding of (2,3,4,5,6- $^{13}\text{C}_5$)mevalonolactone, B) mass spectrum of $[^{13}\text{C}_3]\text{-1}$ obtained after feeding of (3- ^{13}C)mevalonolactone, C) mass spectrum of $[^{13}\text{C}_6]\text{-1}$ obtained after feeding of (4,6- ^{13}C)mevalonolactone.

The mass spectrum of Figure 2A shows that the labelled material is mainly a mixture of unlabelled **1** (indicated by its molecular ion at $m/z = 222$) and completely labelled [$^{13}\text{C}_{15}$]-**1** (indicated by its molecular ion at $m/z = 237$), while other expected isotopologs arising by incorporation of only one or two ^{13}C -labelled isoprene units from (2,3,4,5,6- $^{13}\text{C}_5$)mevalonolactone are missing. This finding may be explained by the special setup of the feeding experiments. First, the *H. odoratus* agar plates were incubated until the fungus was fully grown. At this point the isotopically labelled mevalonolactone was fed to the culture. The administration of the mevalonolactone may have resulted in high incorporation rates into **1**, explaining the formation of mainly [$^{13}\text{C}_{15}$]-**1**. This material was then isolated as a mixture with non-labelled **1** that was produced by the fungus before administration of (2,3,4,5,6- $^{13}\text{C}_5$)mevalonolactone.

A similar observation was made in the feeding experiment with (3- ^{13}C)mevalonolactone (Figure 2B), while the “usual” dilution and statistical distribution of administered labelling was observed in the feeding of (4,6- ^{13}C)mevalonolactone (Figure 2C). These different outcomes were also reflected by a few unsuccessful attempts during the feeding experiments. Although the feeding experiments were always conducted in the same way, the fungal cultures were obviously in different and difficult to control metabolic stages, that result in different incorporation rates and distributions of the isotopic labelling.

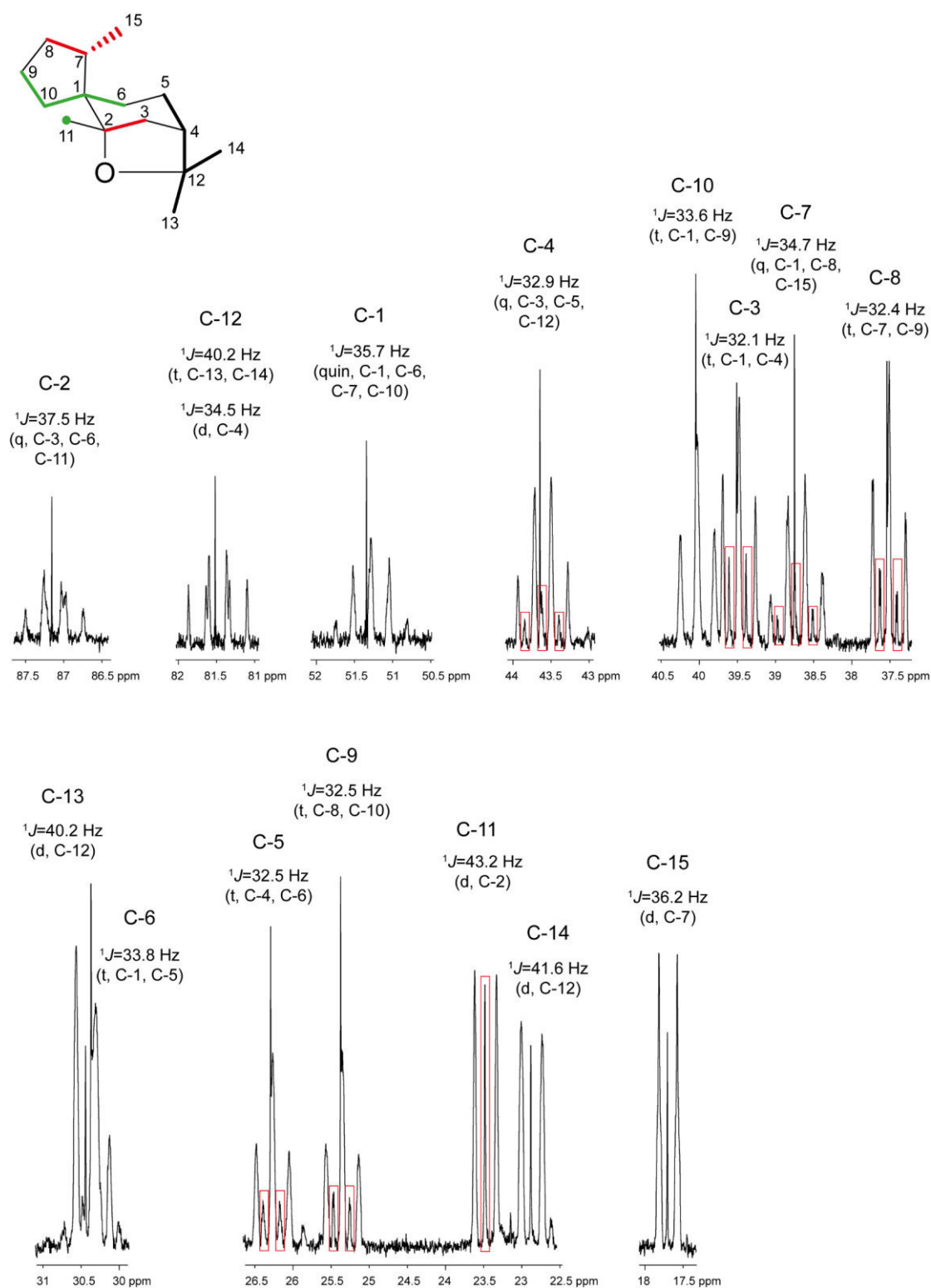


Figure 3. Detailed analysis of the coupling patterns of ^{13}C -labelled hypodoratoxide obtained in the feeding experiment with $(2,3,4,5,6\text{-}^{13}\text{C}_5)$ mevalonolactone. For each ^{13}C -signal the coupling constants, multiplicities of the main signal originating from $(^{13}\text{C}_5)$ hypodoratoxide, and the neighbouring carbons are given. The structural formula shows the three isoprene units in different colours (cf. discussion of biosynthesis in main text).

As indicated by the mass spectrum (Figure 2A of SI), the hypodoratoxide isolated from the feeding experiment with (2,3,4,5,6-¹³C₅)mevalonolactone is mainly composed of unlabelled and (¹³C₅)hypodoratoxide. While the unlabelled material leads to sharp singlets (e. g. at $\delta = 87.2$ ppm for C-2, note that the difference to the chemical shift in Table 1 of main text is due to a different solvent, CDCl₃ instead of C₆D₆), the completely labelled material shows broad multiplets from which the number of directly neighbouring carbons can be inferred (e. g. the quartet for C-2 indicated 3 neighbouring carbons, C-1, C-3 and C-11). The mass spectrum in Figure 2A of SI also shows that very little of the material is composed of only one or two ¹³C-labelled isoprene units. Thus, in rare cases two neighbouring carbons from different isoprene units may not both be labelled. This leads to additional small signals with lower multiplicities at the borders of isoprene units, shown in red boxes, e. g. for C-3 (doublet due to coupling with C-2 from the same, but not with C-4 from a different isoprene unit) and C-4 (triplett due to coupling with C-5 and C-12 from the same, but not with C-3 from a different isoprene unit). The observed pattern is in full agreement with the biosynthetic mechanism as discussed in the main text.

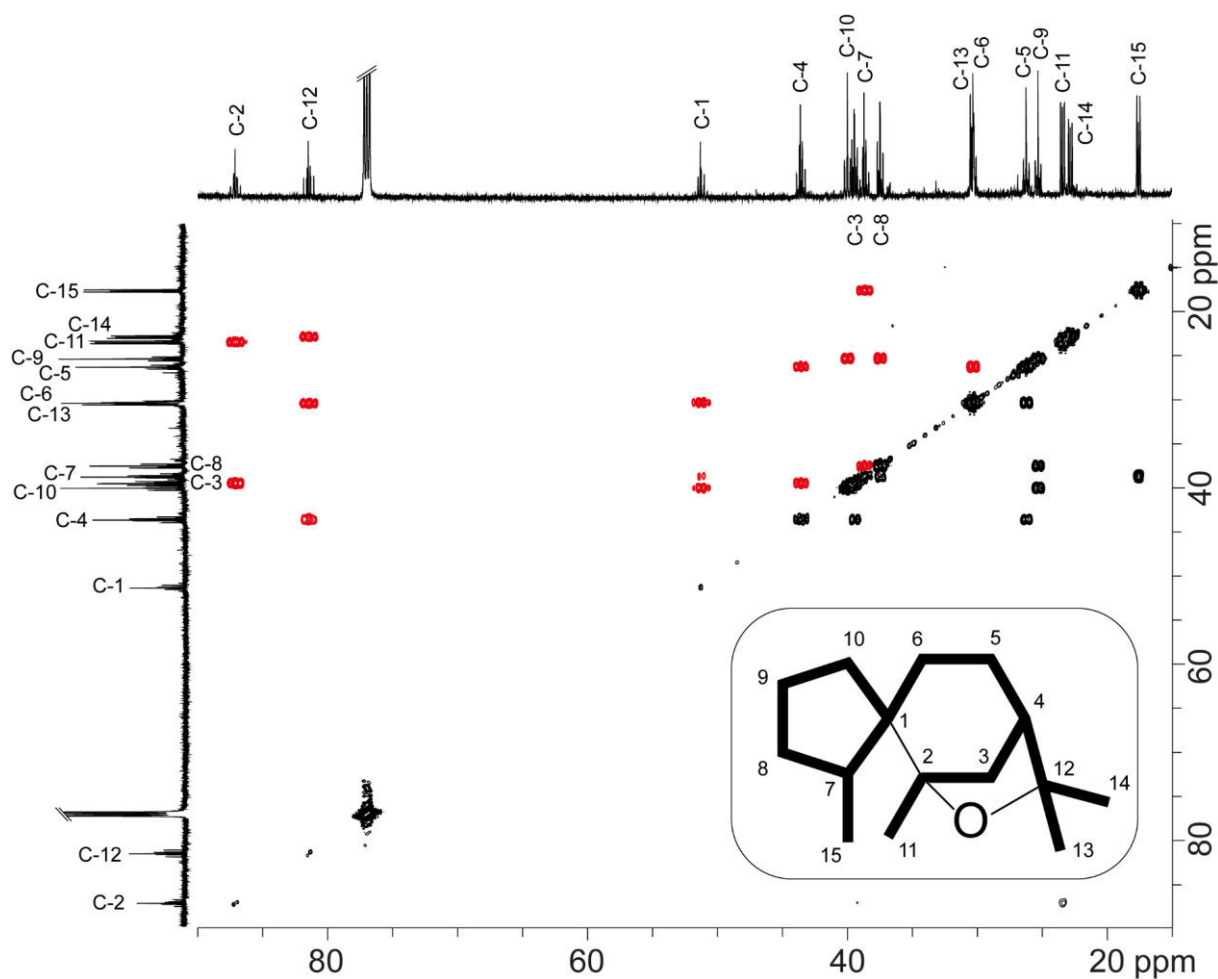
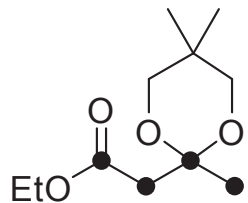


Figure 4. Enlargement of Figure 2 of main text. All relevant crosspeaks for the fifteen ^{13}C - ^{13}C -connections are shown in red (only shown for the north-western half of the ^{13}C , ^{13}C -COSY spectrum). The expected crosspeak for the 16th bond between the quaternary carbons is missing (cf. discussion in main text).

References

- [1] C. A. Citron, J. Gleitzmann, G. Laurenzano, R. Pukall, J. S. Dickschat, *ChemBioChem* **2012**, *13*, 202.
- [2] I. A. Southwell, D. J. Tucker, *Phytochemistry* **1993**, *33*, 857.
- [3] L. O. Zamir, C.-D. Nguyen, *J. Label. Compd. Radiopharm.* **1988**, *25*, 1189.
- [4] L. Barra, B. Schulz, J. S. Dickschat, *ChemBioChem* **2014**, *15*, 2379.
- [5] H. Utsunomia, J. Kawata, W. Chanoki, N. Shirakawa, M. Miyazawa, *J. Oleo Sci.* **2005**, *54*, 609-612.
- [6] R. P. Adams, *Identification of Essential Oil Components by Gas Chromatography/Mass Spectrometry*, Allured Books, Carol Stream, **2009**.



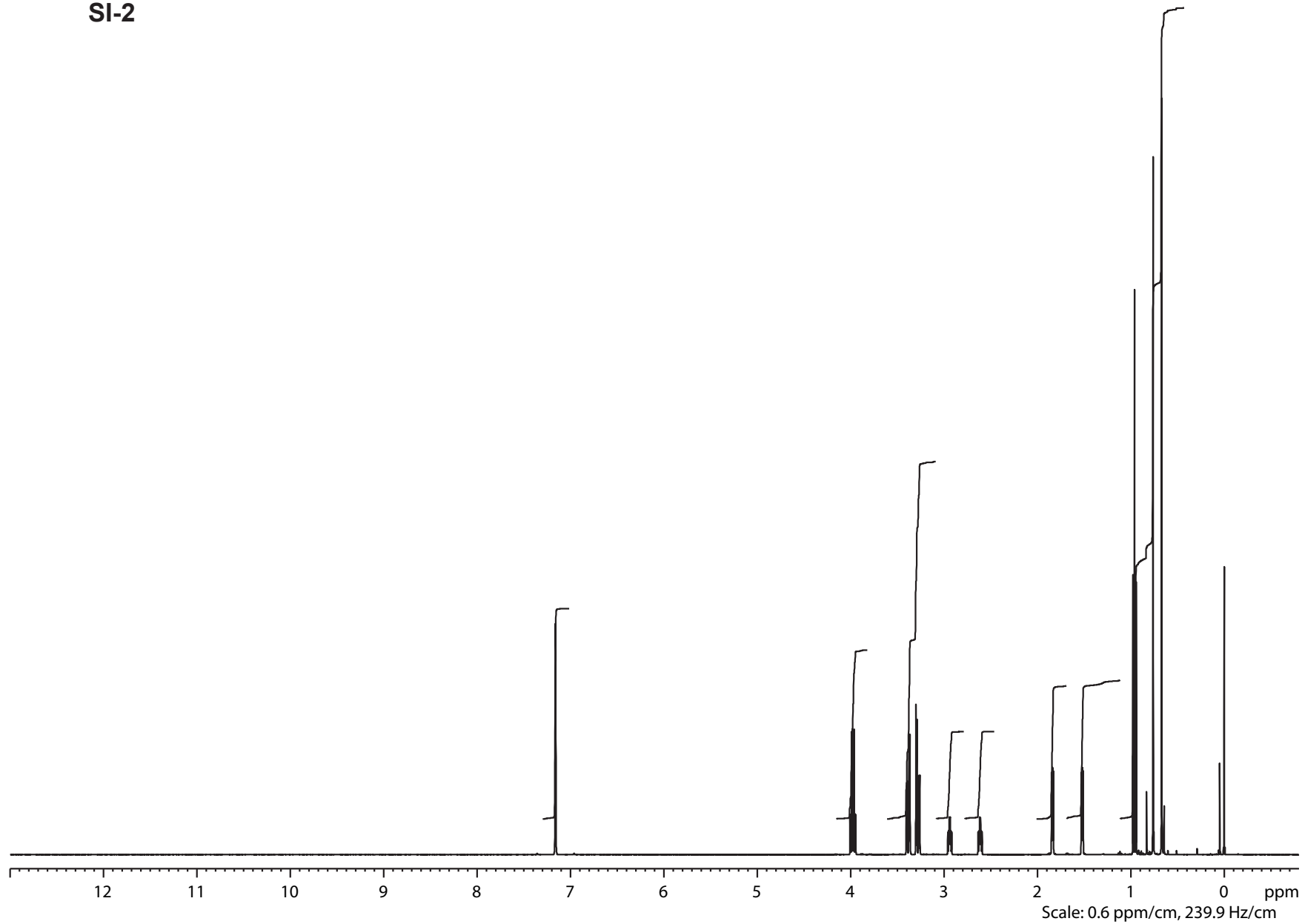
SI-2

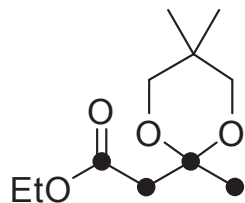
Current Data Parameters
 NAME bae123065_od
 EXPNO 1
 PROCNO 1

F2 - Acquisition Parameters
 Date_ 20140204
 Time 2.50
 INSTRUM drx400
 PROBHD 5 mm QNP 1H/13
 PULPROG zg30
 TD 65536
 SOLVENT C6D6
 NS 64
 DS 2
 SWH 8278.146 Hz
 FIDRES 0.126314 Hz
 AQ 3.9584243 sec
 RG 101.6
 DW 60.400 usec
 DE 6.00 usec
 TE 298.2 K
 D1 1.00000000 sec
 TD0 1

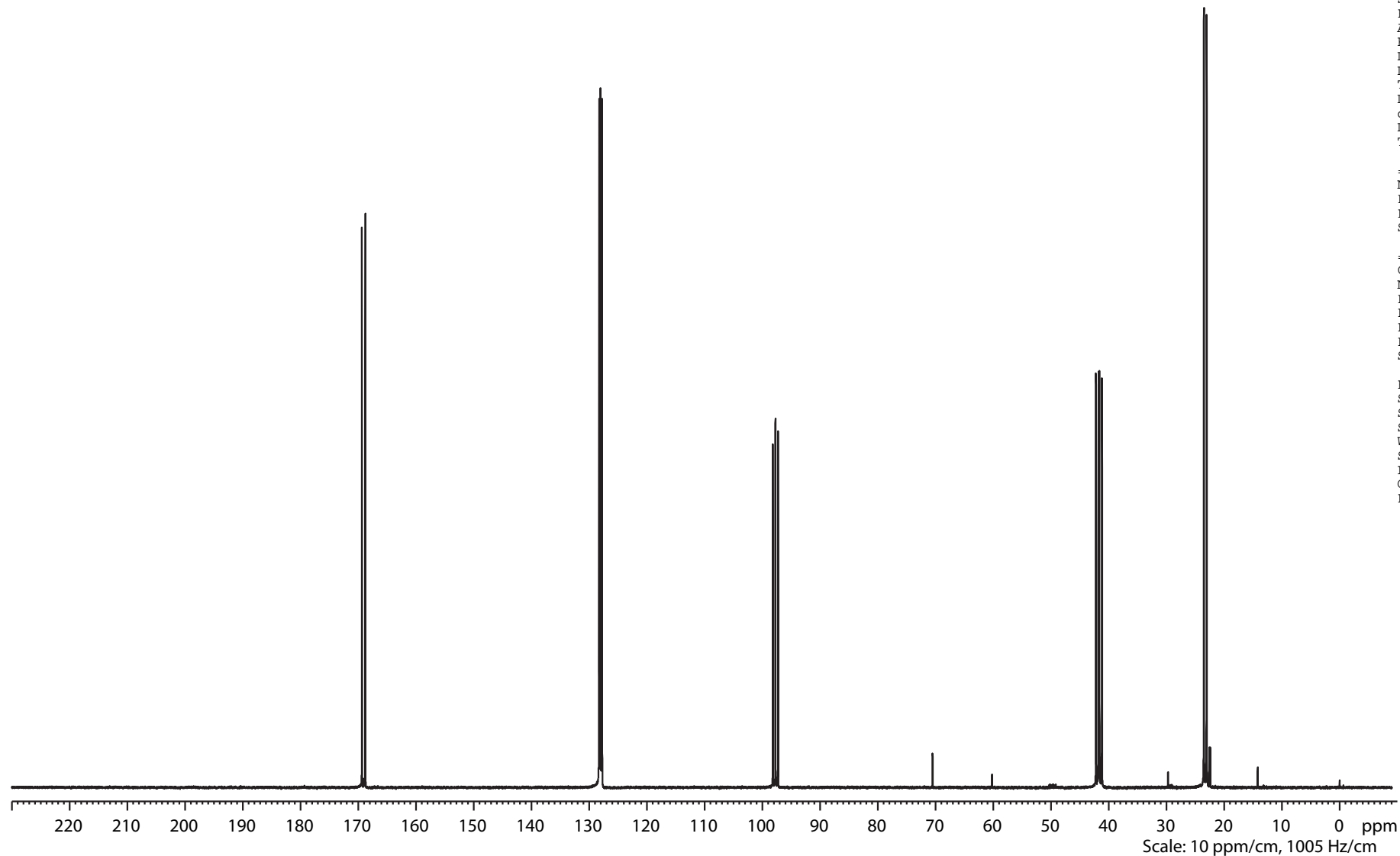
==== CHANNEL f1 =====
 NUC1 1H
 P1 10.20 usec
 PL1 -2.00 dB
 SFO1 399.8524687 MHz

F2 - Processing parameters
 SI 32768
 SF 399.8499939 MHz
 SR -6.15 Hz
 WDW EM
 SSB 0
 LB 0.00 Hz
 GB 0
 PC 1.40





SI-2



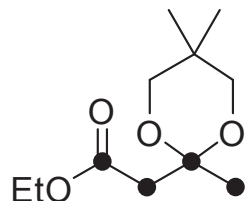
Current Data Parameters
 NAME bae123065_od
 EXPNO 2
 PROCNO 1

F2 - Acquisition Parameters
 Date_ 20140204
 Time 4.09
 INSTRUM drx400
 PROBHD 5 mm QNP 1H/13
 PULPROG zgpg30
 TD 131072
 SOLVENT C6D6
 NS 1024
 DS 4
 SWH 26315.789 Hz
 FIDRES 0.200774 Hz
 AQ 2.4904180 sec
 RG 6502
 DW 19.000 usec
 DE 6.00 usec
 TE 299.2 K
 D1 2.00000000 sec
 d11 0.03000000 sec
 DELTA 1.89999998 sec
 TD0 1

==== CHANNEL f1 =====
 NUC1 13C
 P1 11.00 usec
 PL1 -3.00 dB
 SFO1 100.5535241 MHz

==== CHANNEL f2 =====
 CPDPRG2 waltz16
 NUC2 1H
 PCPD2 80.00 usec
 PL2 -2.00 dB
 PL12 16.06 dB
 PL13 16.06 dB
 SFO2 399.8515994 MHz

F2 - Processing parameters
 SI 65536
 SF 100.5423263 MHz
 SR -36.70 Hz
 WDW EM
 SSB 0
 LB 1.00 Hz
 GB 0
 PC 1.40



SI-2

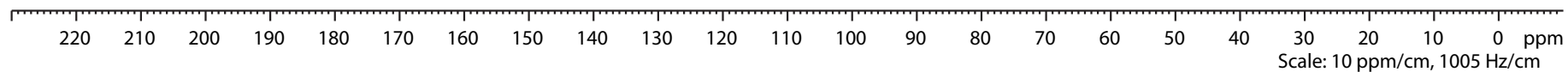
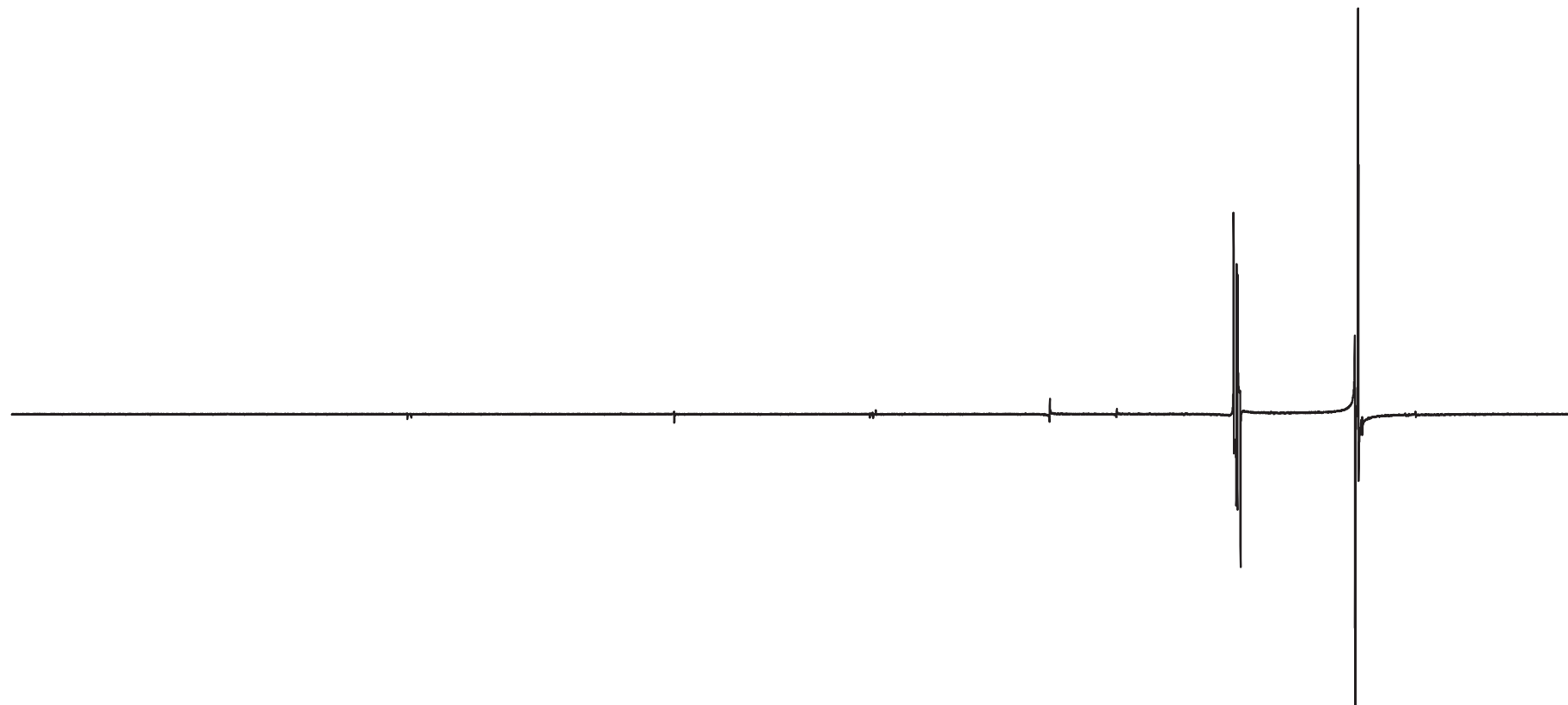
Current Data Parameters
 NAME bae123065_od
 EXPNO 3
 PROCNO 1

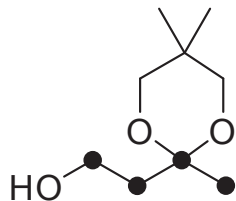
F2 - Acquisition Parameters
 Date_ 20140204
 Time 4.49
 INSTRUM drx400
 PROBHD 5 mm QNP 1H/13
 PULPROG dept135
 TD 131072
 SOLVENT C6D6
 NS 512
 DS 4
 SWH 26315.789 Hz
 FIDRES 0.200774 Hz
 AQ 2.4904180 sec
 RG 8192
 DW 19.000 usec
 DE 7.00 usec
 TE 299.2 K
 CNST2 145.0000000
 D1 2.0000000 sec
 d2 0.00344828 sec
 d12 0.00002000 sec
 DELTA 0.00001401 sec
 TD0 1

==== CHANNEL f1 =====
 NUC1 13C
 P1 11.00 usec
 p2 22.00 usec
 PL1 -3.00 dB
 SFO1 100.5535241 MHz

==== CHANNEL f2 =====
 CPDPRG2 waltz16
 NUC2 1H
 P3 10.00 usec
 p4 20.00 usec
 PCPD2 80.00 usec
 PL2 -2.00 dB
 PL12 16.06 dB
 SFO2 399.8515994 MHz

F2 - Processing parameters
 SI 65536
 SF 100.5423549 MHz
 SR -8.12 Hz
 WDW EM
 SSB 0
 LB 1.00 Hz
 GB 0
 PC 1.40





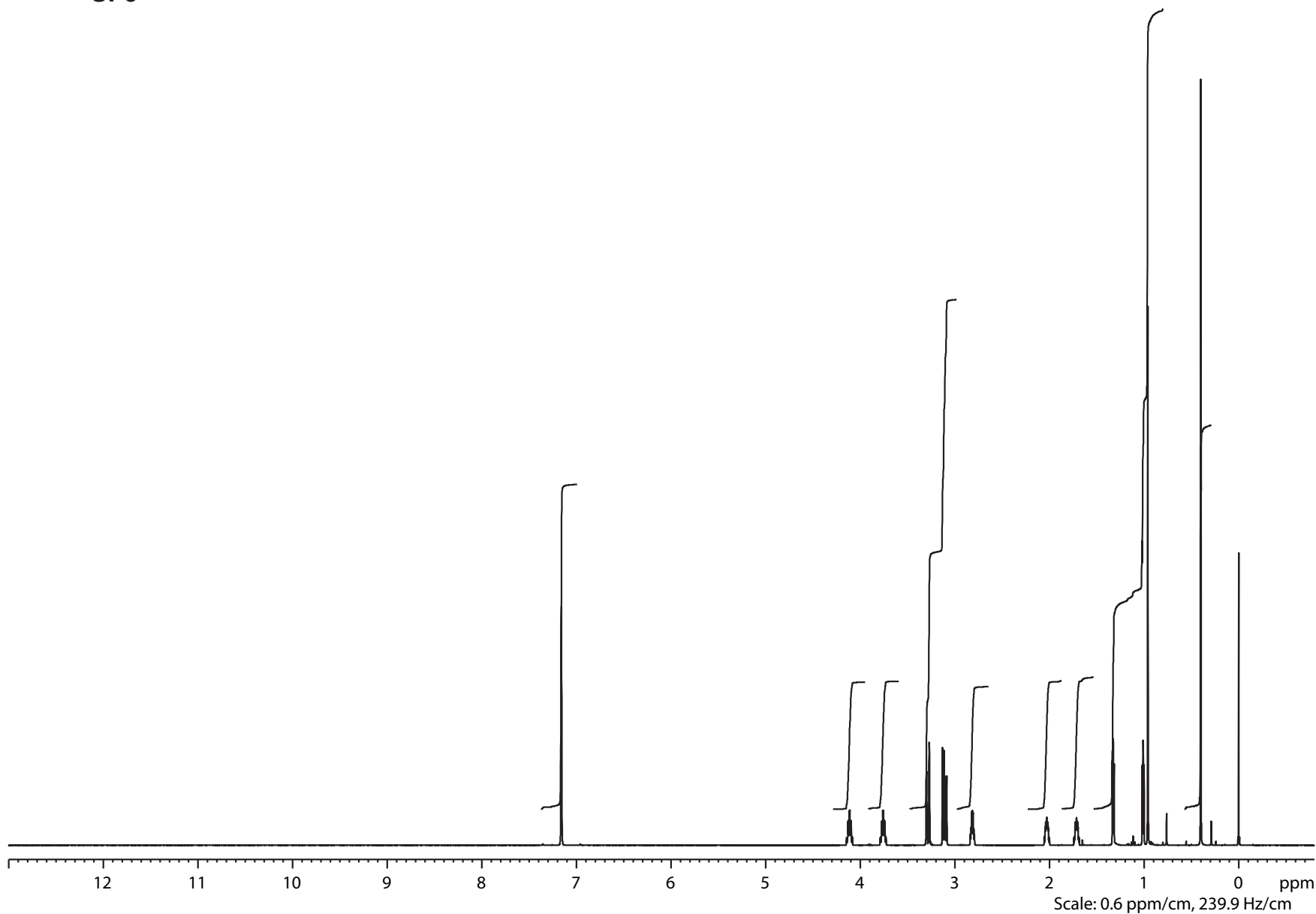
SI-3

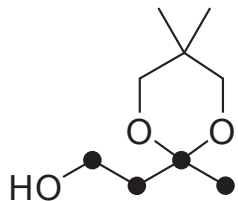
Current Data Parameters
 NAME bae123070_od
 EXPNO 1
 PROCNO 1

F2 - Acquisition Parameters
 Date_ 20140204
 Time 4.59
 INSTRUM drx400
 PROBHD 5 mm QNP 1H/13
 PULPROG zg30
 TD 65536
 SOLVENT C6D6
 NS 64
 DS 2
 SWH 8278.146 Hz
 FIDRES 0.126314 Hz
 AQ 3.9584243 sec
 RG 114
 DW 60.400 usec
 DE 6.00 usec
 TE 298.2 K
 D1 1.00000000 sec
 TD0 1

==== CHANNEL f1 =====
 NUC1 1H
 P1 10.20 usec
 PL1 -2.00 dB
 SFO1 399.8524687 MHz

F2 - Processing parameters
 SI 32768
 SF 399.8499944 MHz
 SR -5.60 Hz
 WDW EM
 SSB 0
 LB 0.00 Hz
 GB 0
 PC 1.40





SI-3

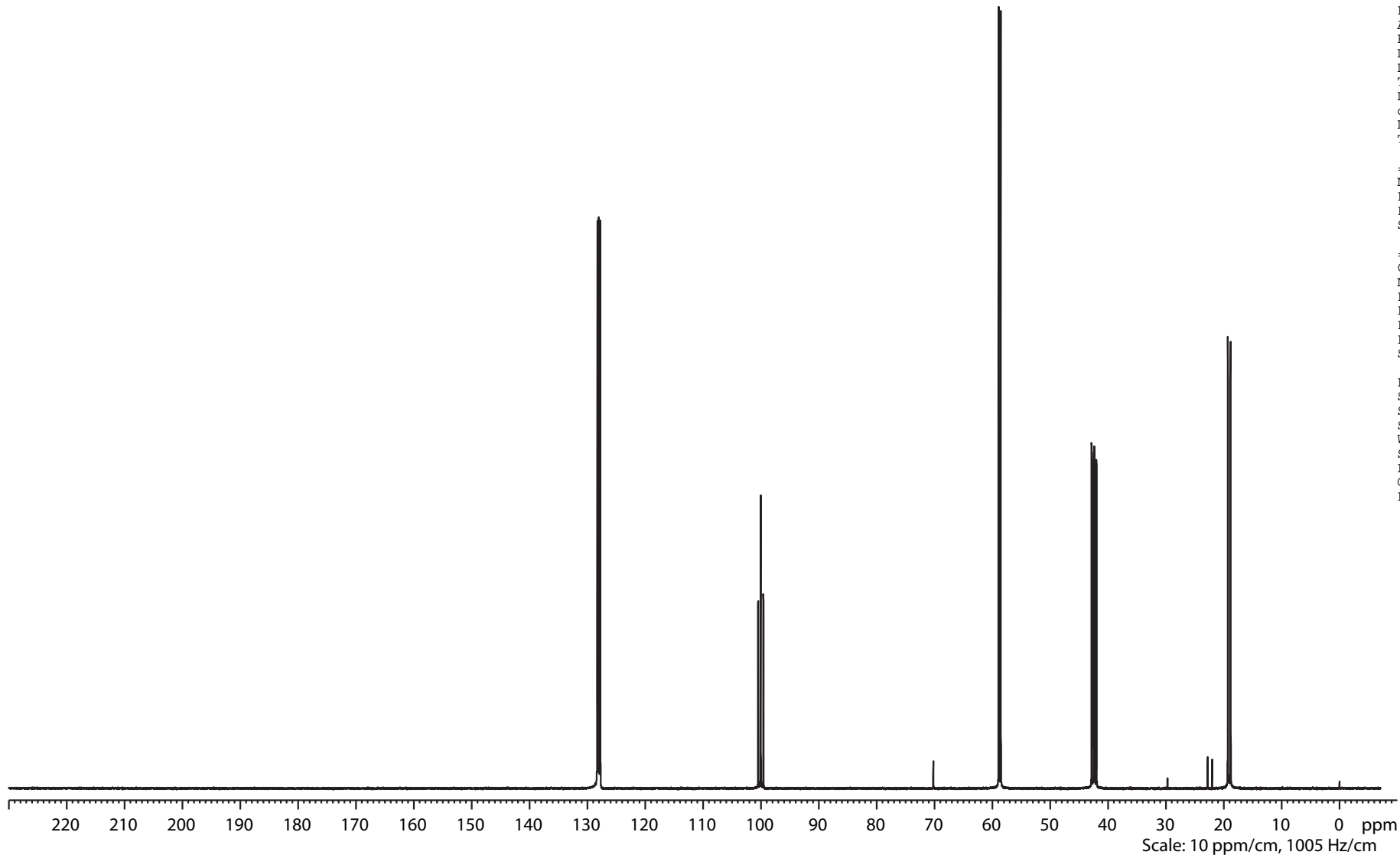
Current Data Parameters
 NAME bae123070_od
 EXPNO 2
 PROCNO 1

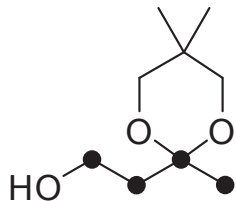
F2 - Acquisition Parameters
 Date_ 20140204
 Time 6.18
 INSTRUM drx400
 PROBHD 5 mm QNP 1H/13
 PULPROG zgpg30
 TD 131072
 SOLVENT C6D6
 NS 1024
 DS 4
 SWH 26315.789 Hz
 FIDRES 0.200774 Hz
 AQ 2.4904180 sec
 RG 4597.6
 DW 19.000 usec
 DE 6.00 usec
 TE 299.2 K
 D1 2.00000000 sec
 d11 0.03000000 sec
 DELTA 1.89999998 sec
 TD0 1

==== CHANNEL f1 =====
 NUC1 13C
 P1 11.00 usec
 PL1 -3.00 dB
 SFO1 100.5535241 MHz

==== CHANNEL f2 =====
 CPDPRG2 waltz16
 NUC2 1H
 PCPD2 80.00 usec
 PL2 -2.00 dB
 PL12 16.06 dB
 PL13 16.06 dB
 SFO2 399.8515994 MHz

F2 - Processing parameters
 SI 65536
 SF 100.5423264 MHz
 SR -36.57 Hz
 WDW EM
 SSB 0
 LB 1.00 Hz
 GB 0
 PC 1.40





SI-3

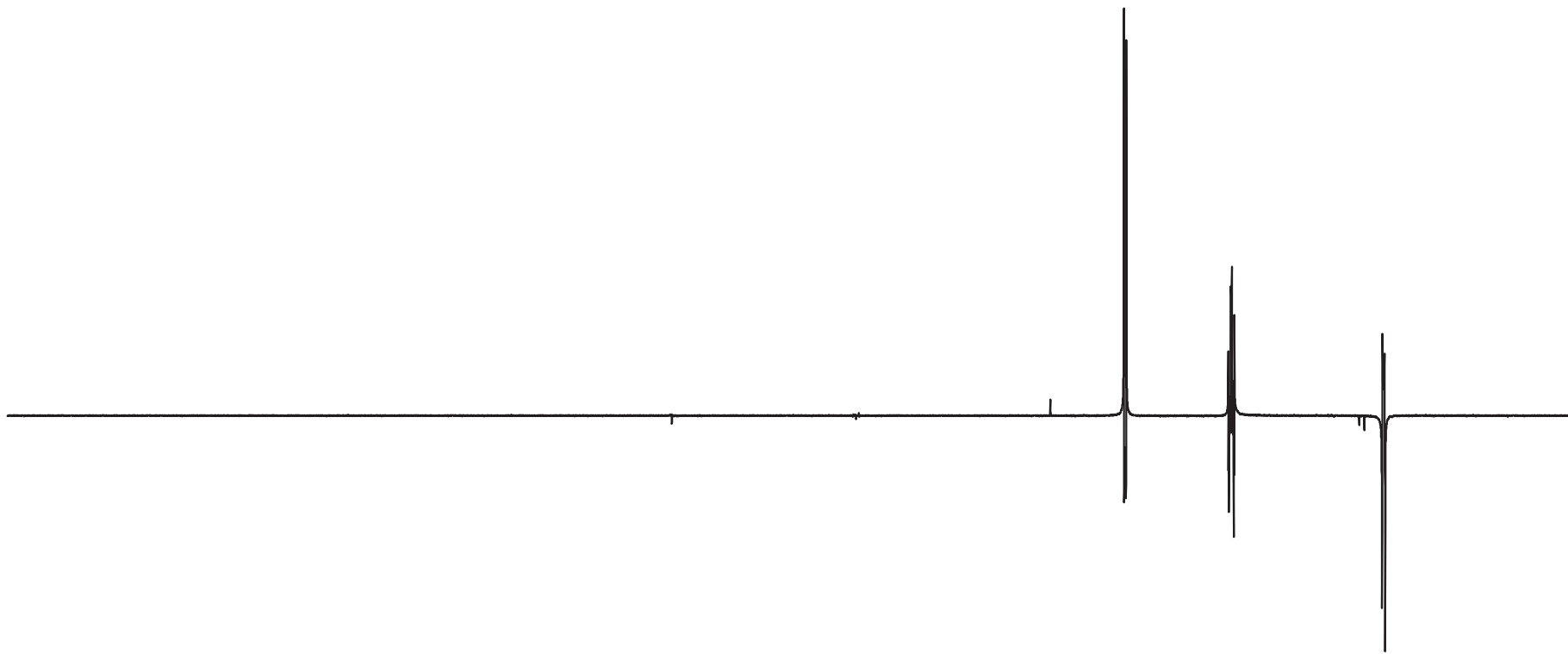
Current Data Parameters
 NAME bae123070_od
 EXPNO 3
 PROCNO 1

F2 - Acquisition Parameters
 Date_ 20140204
 Time 6.58
 INSTRUM drx400
 PROBHD 5 mm QNP 1H/13
 PULPROG dept135
 TD 131072
 SOLVENT C6D6
 NS 512
 DS 4
 SWH 26315.789 Hz
 FIDRES 0.200774 Hz
 AQ 2.4904180 sec
 RG 7298.2
 DW 19.000 usec
 DE 7.00 usec
 TE 299.2 K
 CNST2 145.0000000
 D1 2.00000000 sec
 d2 0.00344828 sec
 d12 0.00002000 sec
 DELTA 0.00001401 sec
 TD0 1

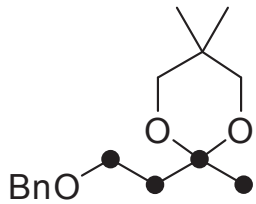
==== CHANNEL f1 =====
 NUC1 13C
 P1 11.00 usec
 p2 22.00 usec
 PL1 -3.00 dB
 SFO1 100.5535241 MHz

==== CHANNEL f2 =====
 CPDPRG2 waltz16
 NUC2 1H
 P3 10.00 usec
 p4 20.00 usec
 PCPD2 80.00 usec
 PL2 -2.00 dB
 PL12 16.06 dB
 SFO2 399.8515994 MHz

F2 - Processing parameters
 SI 65536
 SF 100.5423555 MHz
 SR -7.49 Hz
 WDW EM
 SSB 0
 LB 1.00 Hz
 GB 0
 PC 1.40



220 210 200 190 180 170 160 150 140 130 120 110 100 90 80 70 60 50 30 20 10 0 ppm
 Scale: 10 ppm/cm, 1005 Hz/cm



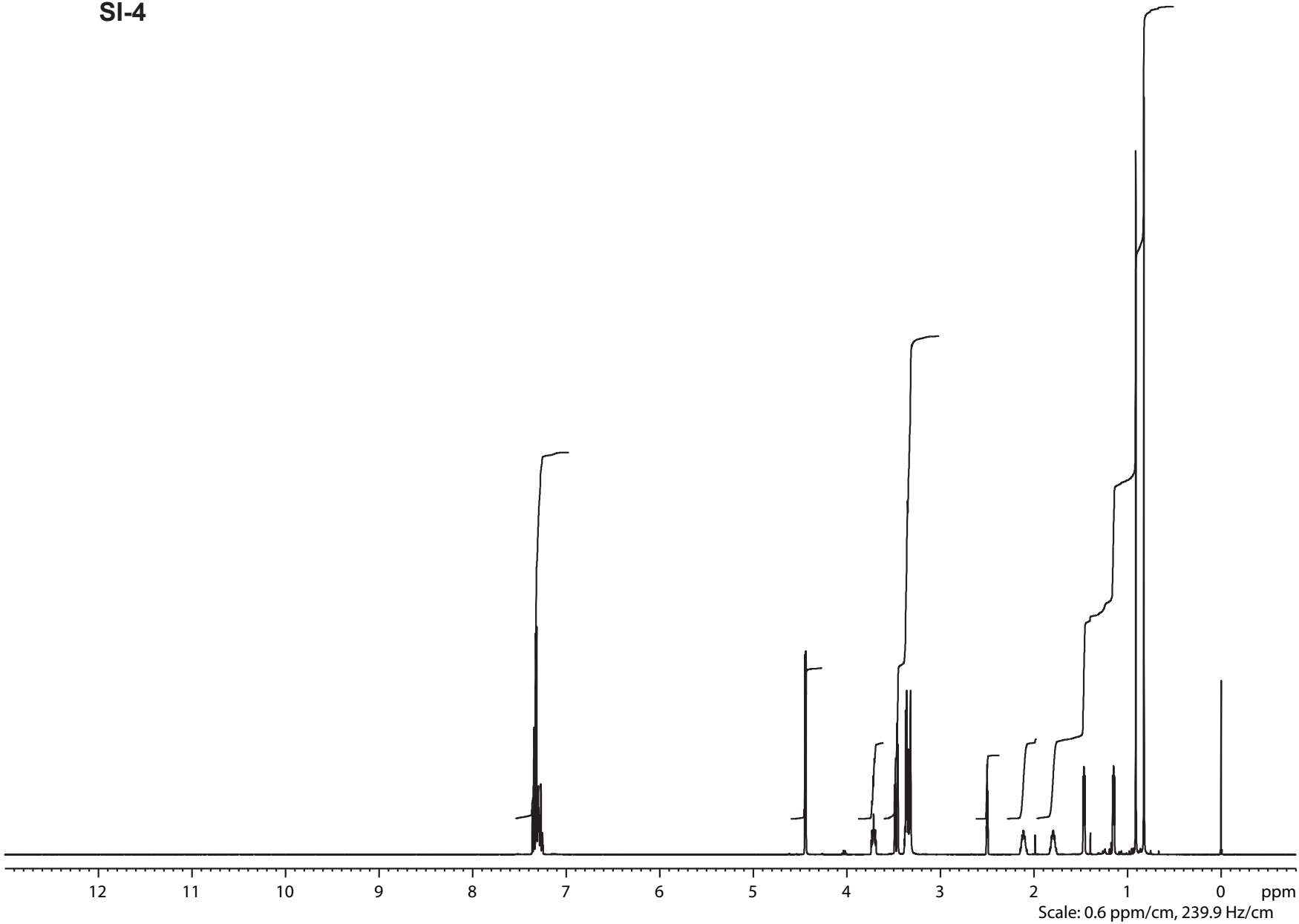
SI-4

Current Data Parameters
 NAME bae123090_od
 EXPNO 1
 PROCNO 1

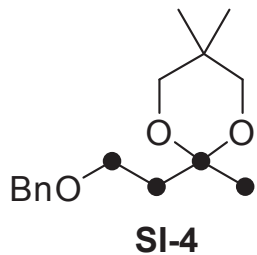
F2 - Acquisition Parameters
 Date_ 20140205
 Time 13.13
 INSTRUM drx400
 PROBHD 5 mm QNP 1H/13
 PULPROG zg30
 TD 65536
 SOLVENT DMSO
 NS 64
 DS 2
 SWH 8278.146 Hz
 FIDRES 0.126314 Hz
 AQ 3.9584243 sec
 RG 128
 DW 60.400 usec
 DE 6.00 usec
 TE 299.2 K
 D1 1.00000000 sec
 TD0 1

==== CHANNEL f1 =====
 NUC1 1H
 P1 10.20 usec
 PL1 -2.00 dB
 SFO1 399.8524687 MHz

F2 - Processing parameters
 SI 32768
 SF 399.8500049 MHz
 SR 4.87 Hz
 WDW EM
 SSB 0
 LB 0.00 Hz
 GB 0
 PC 1.40



Scale: 0.6 ppm/cm, 239.9 Hz/cm



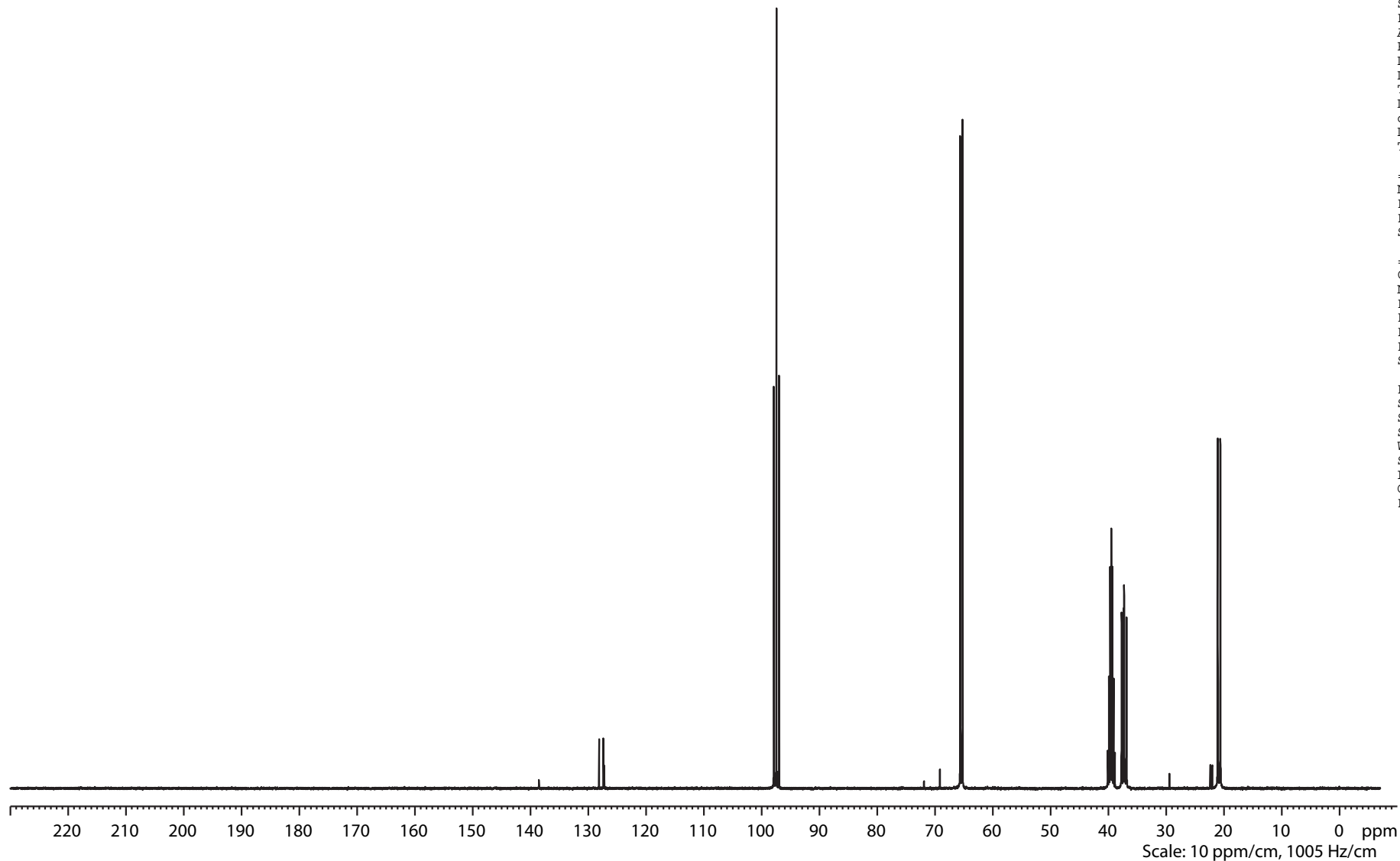
Current Data Parameters
 NAME bae123090_od
 EXPNO 2
 PROCNO 1

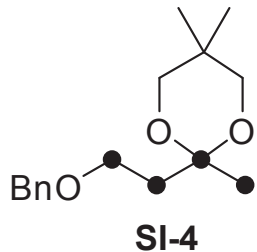
F2 - Acquisition Parameters
 Date_ 20140205
 Time 13.20
 INSTRUM drx400
 PROBHD 5 mm QNP 1H/13
 PULPROG zgpg30
 TD 131072
 SOLVENT DMSO
 NS 1024
 DS 4
 SWH 26315.789 Hz
 FIDRES 0.200774 Hz
 AQ 2.4904180 sec
 RG 8192
 DW 19.000 usec
 DE 6.00 usec
 TE 299.2 K
 D1 2.00000000 sec
 d11 0.03000000 sec
 DELTA 1.89999998 sec
 TD0 1

==== CHANNEL f1 =====
 NUC1 13C
 P1 11.00 usec
 PL1 -3.00 dB
 SFO1 100.5535241 MHz

==== CHANNEL f2 =====
 CPDPRG2 waltz16
 NUC2 1H
 PCPD2 80.00 usec
 PL2 -2.00 dB
 PL12 16.06 dB
 PL13 16.06 dB
 SFO2 399.8515994 MHz

F2 - Processing parameters
 SI 65536
 SF 100.5424152 MHz
 SR 52.18 Hz
 WDW EM
 SSB 0
 LB 1.00 Hz
 GB 0
 PC 1.40





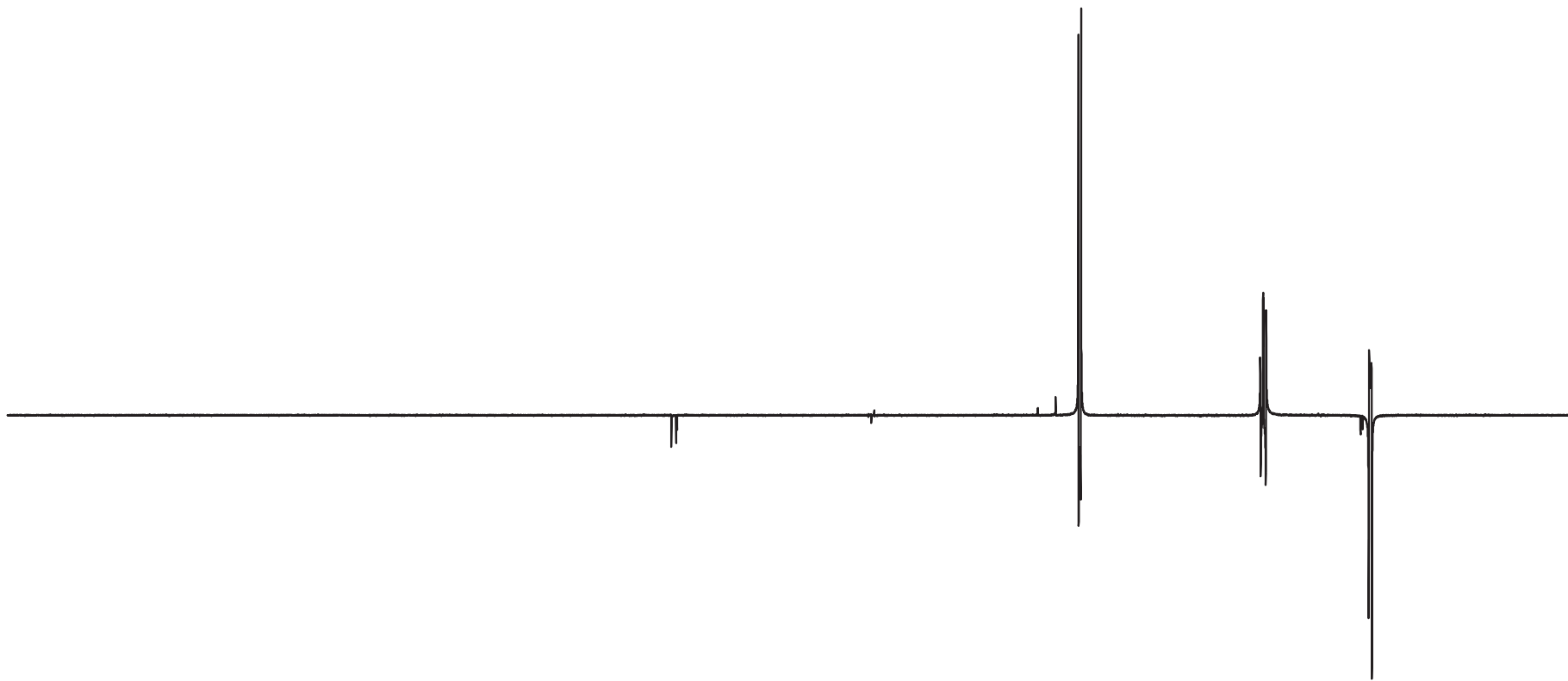
Current Data Parameters
 NAME bae123090_od
 EXPNO 3
 PROCNO 1

F2 - Acquisition Parameters
 Date_ 20140205
 Time 15.12
 INSTRUM drx400
 PROBHD 5 mm QNP 1H/13
 PULPROG dept135
 TD 131072
 SOLVENT DMSO
 NS 512
 DS 4
 SWH 26315.789 Hz
 FIDRES 0.200774 Hz
 AQ 2.4904180 sec
 RG 5792.6
 DW 19.000 usec
 DE 7.00 usec
 TE 299.2 K
 CNST2 145.0000000
 D1 2.0000000 sec
 d2 0.00344828 sec
 d12 0.00002000 sec
 DELTA 0.00001401 sec
 TD0 1

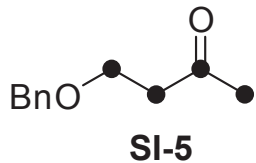
==== CHANNEL f1 =====
 NUC1 13C
 P1 11.00 usec
 p2 22.00 usec
 PL1 -3.00 dB
 SFO1 100.5535241 MHz

==== CHANNEL f2 =====
 CPDPRG2 waltz16
 NUC2 1H
 P3 10.00 usec
 p4 20.00 usec
 PCPD2 80.00 usec
 PL2 -2.00 dB
 PL12 16.06 dB
 SFO2 399.8515994 MHz

F2 - Processing parameters
 SI 65536
 SF 100.5424198 MHz
 SR 56.76 Hz
 WDW EM
 SSB 0
 LB 1.00 Hz
 GB 0
 PC 1.40



220 210 200 190 180 170 160 150 140 130 120 110 100 90 80 70 60 50 40 30 20 10 0 ppm
 Scale: 10 ppm/cm, 1005 Hz/cm

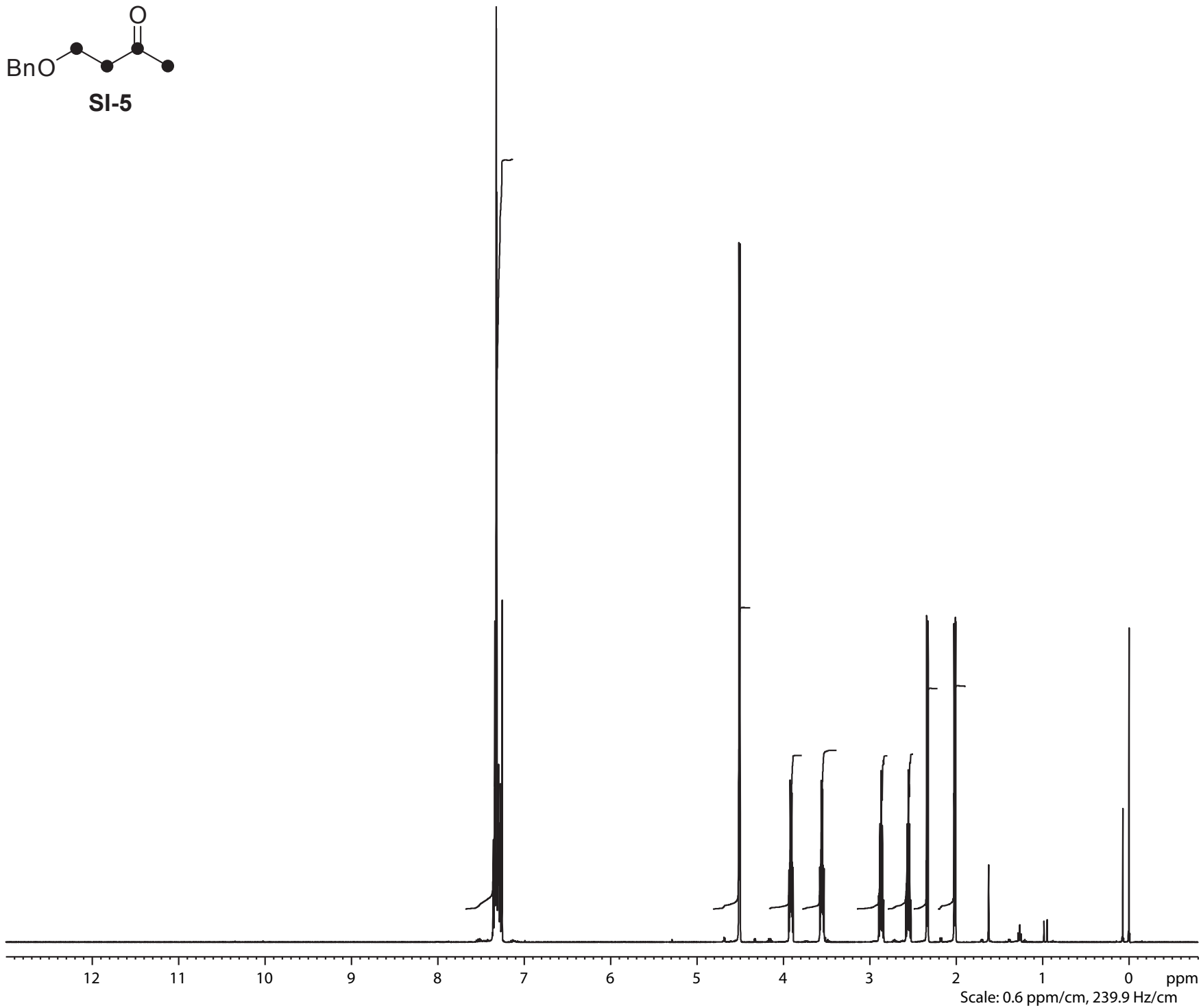


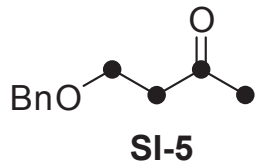
Current Data Parameters
 NAME bae123107_od
 EXPNO 1
 PROCNO 1

F2 - Acquisition Parameters
 Date_ 20140206
 Time 4.53
 INSTRUM drx400
 PROBHD 5 mm QNP 1H/13
 PULPROG zg30
 TD 65536
 SOLVENT CDCl3
 NS 64
 DS 2
 SWH 8278.146 Hz
 FIDRES 0.126314 Hz
 AQ 3.9584243 sec
 RG 143.7
 DW 60.400 usec
 DE 6.00 usec
 TE 299.2 K
 D1 1.00000000 sec
 TD0 1

===== CHANNEL f1 =====
 NUC1 1H
 P1 10.20 usec
 PL1 -2.00 dB
 SFO1 399.8524687 MHz

F2 - Processing parameters
 SI 32768
 SF 399.8500168 MHz
 SR 16.76 Hz
 WDW EM
 SSB 0
 LB 0.00 Hz
 GB 0
 PC 1.40





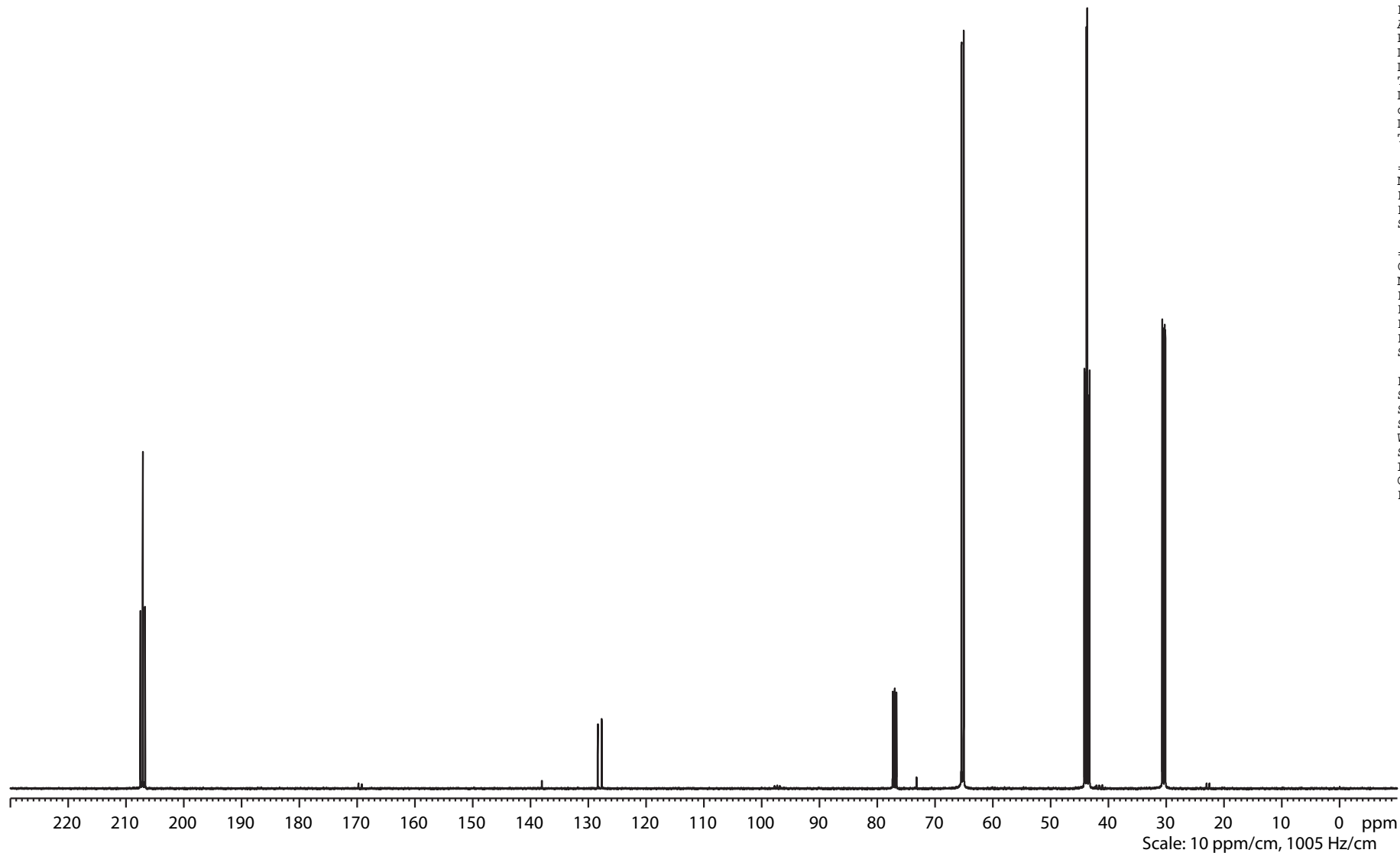
Current Data Parameters
 NAME bae123107_od
 EXPNO 2
 PROCNO 1

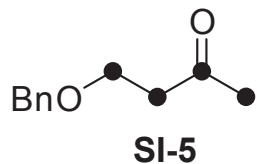
F2 - Acquisition Parameters
 Date_ 20140206
 Time 6.12
 INSTRUM drx400
 PROBHD 5 mm QNP 1H/13
 PULPROG zgpg30
 TD 131072
 SOLVENT CDCl3
 NS 1024
 DS 4
 SWH 26315.789 Hz
 FIDRES 0.200774 Hz
 AQ 2.4904180 sec
 RG 8192
 DW 19.000 usec
 DE 6.00 usec
 TE 300.2 K
 D1 2.00000000 sec
 d11 0.03000000 sec
 DELTA 1.89999998 sec
 TD0 1

===== CHANNEL f1 =====
 NUC1 13C
 P1 11.00 usec
 PL1 -3.00 dB
 SFO1 100.5535241 MHz

===== CHANNEL f2 =====
 CPDPRG2 waltz16
 NUC2 1H
 PCPD2 80.00 usec
 PL2 -2.00 dB
 PL12 16.06 dB
 PL13 16.06 dB
 SFO2 399.8515994 MHz

F2 - Processing parameters
 SI 65536
 SF 100.5423674 MHz
 SR 4.37 Hz
 WDW EM
 SSB 0
 LB 1.00 Hz
 GB 0
 PC 1.40





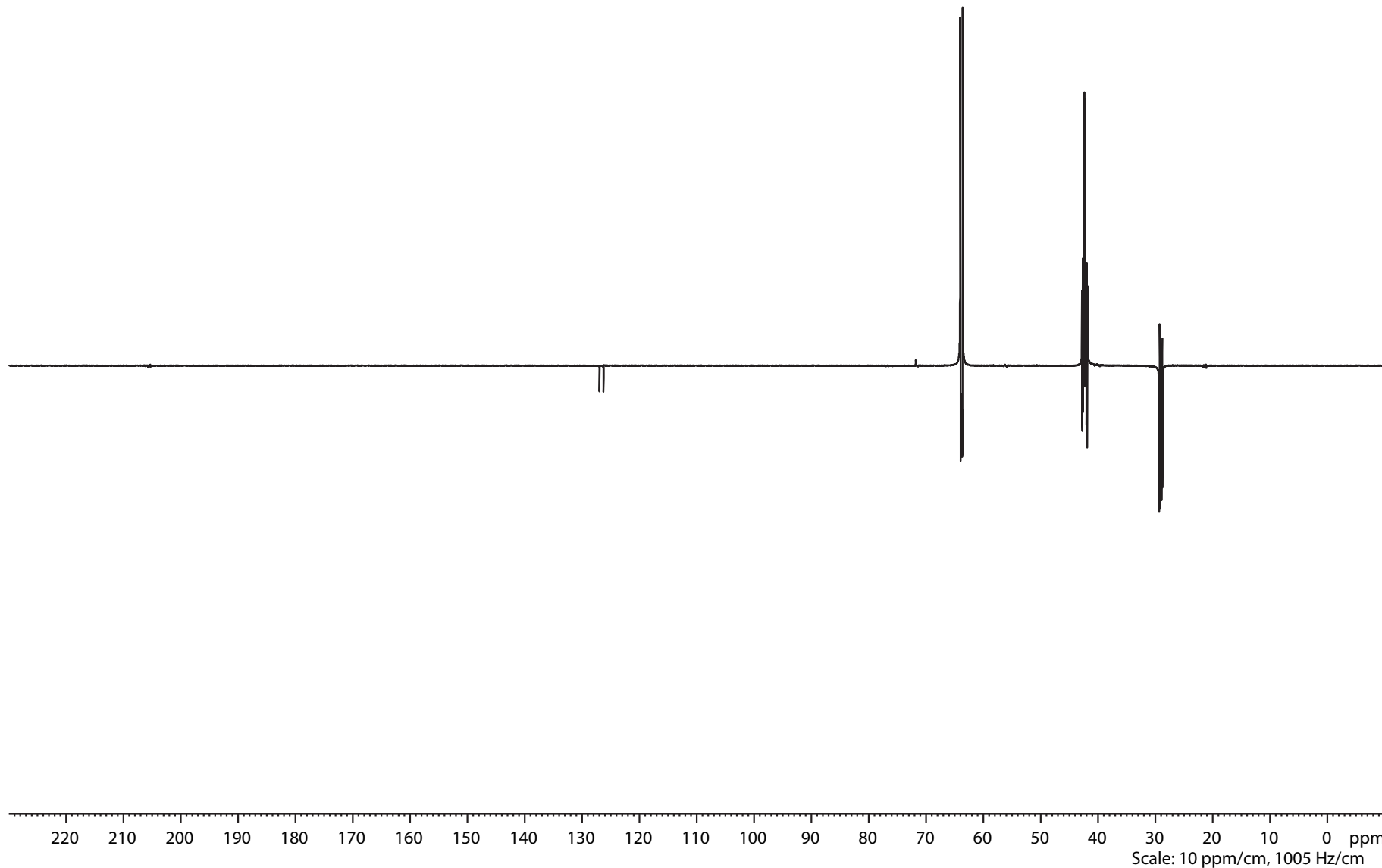
Current Data Parameters
 NAME bae123107_od
 EXPNO 3
 PROCNO 1

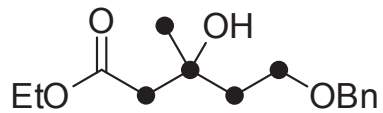
F2 - Acquisition Parameters
 Date_ 20140206
 Time 6.52
 INSTRUM drx400
 PROBHD 5 mm QNP 1H/13
 PULPROG dept135
 TD 131072
 SOLVENT CDCl3
 NS 512
 DS 4
 SWH 26315.789 Hz
 FIDRES 0.200774 Hz
 AQ 2.4904180 sec
 RG 4096
 DW 19.000 usec
 DE 7.00 usec
 TE 299.2 K
 CNST2 145.0000000
 D1 2.0000000 sec
 d2 0.00344828 sec
 d12 0.00002000 sec
 DELTA 0.00001401 sec
 TD0 1

===== CHANNEL f1 =====
 NUC1 13C
 P1 11.00 usec
 p2 22.00 usec
 PL1 -3.00 dB
 SFO1 100.5535241 MHz

===== CHANNEL f2 =====
 CPDPRG2 waltz16
 NUC2 1H
 P3 10.00 usec
 p4 20.00 usec
 PCPD2 80.00 usec
 PL2 -2.00 dB
 PL12 16.06 dB
 SFO2 399.8515994 MHz

F2 - Processing parameters
 SI 65536
 SF 100.5425081 MHz
 SR 145.13 Hz
 WDW EM
 SSB 0
 LB 1.00 Hz
 GB 0
 PC 1.40





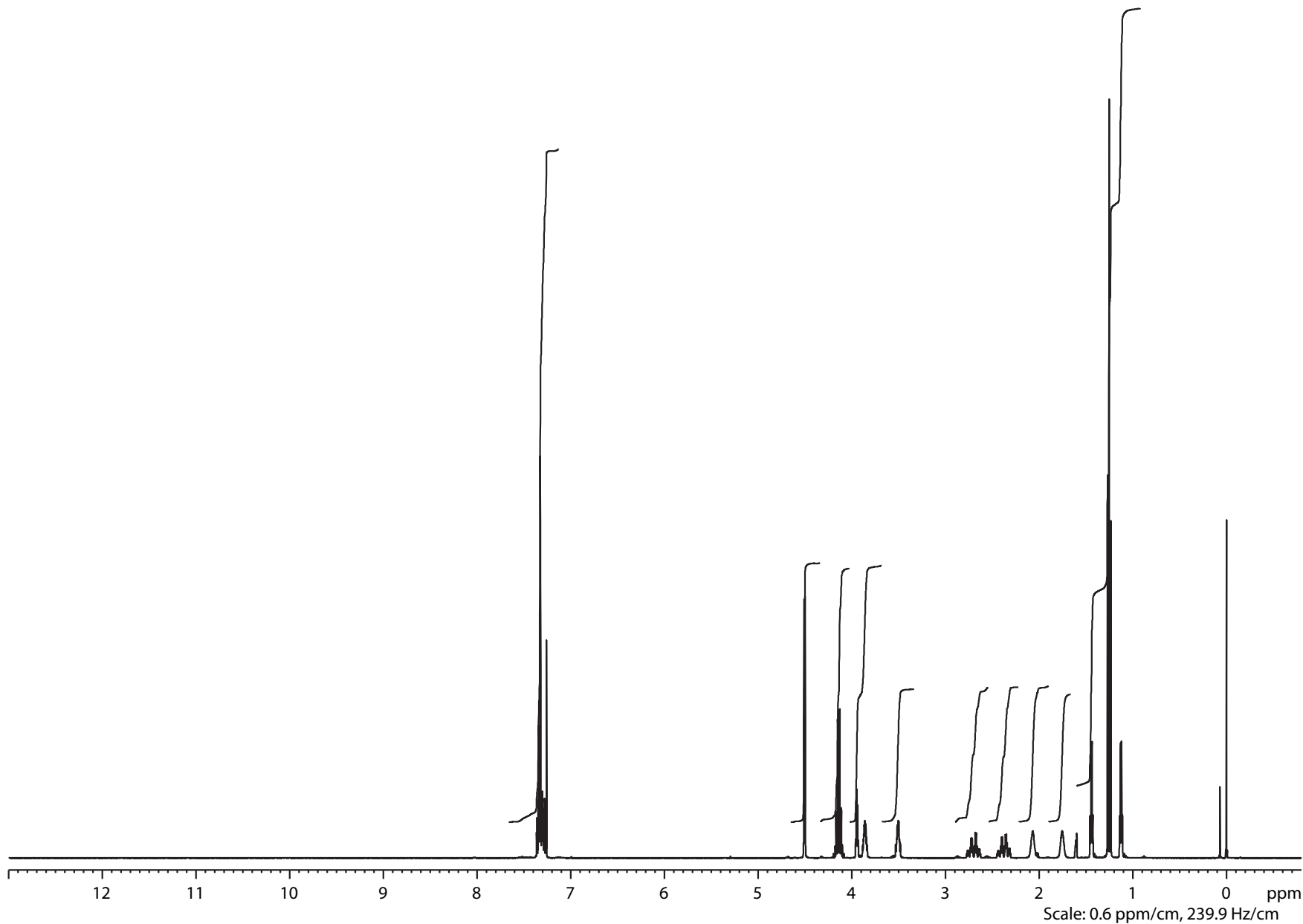
SI-6

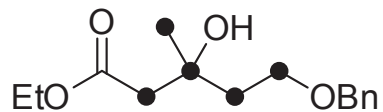
Current Data Parameters
NAME bae123190_od
EXPNO 1
PROCNO 1

F2 - Acquisition Parameters
Date_ 20140212
Time 17.22
INSTRUM drx400
PROBHD 5 mm QNP 1H/13
PULPROG zg30
TD 65536
SOLVENT CDCl3
NS 64
DS 2
SWH 8278.146 Hz
FIDRES 0.126314 Hz
AQ 3.9584243 sec
RG 143.7
DW 60.400 usec
DE 6.00 usec
TE 299.2 K
D1 1.00000000 sec
TD0 1

==== CHANNEL f1 =====
NUC1 1H
P1 10.20 usec
PL1 -2.00 dB
SFO1 399.8524687 MHz

F2 - Processing parameters
SI 32768
SF 399.8500159 MHz
SR 15.87 Hz
WDW EM
SSB 0
LB 0.00 Hz
GB 0
PC 1.40





SI-6

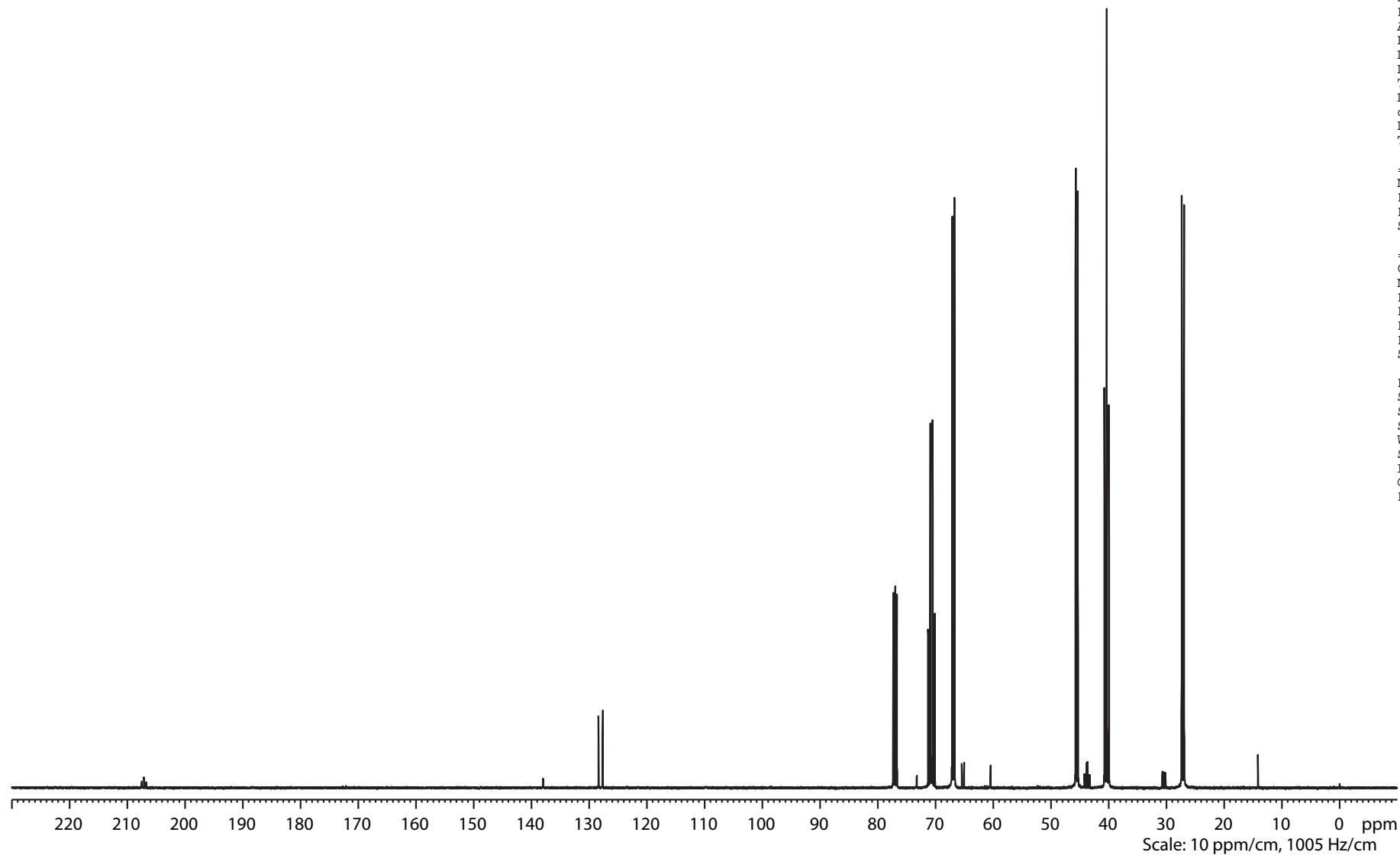
Current Data Parameters
NAME bae123190_od
EXPNO 2
PROCNO 1

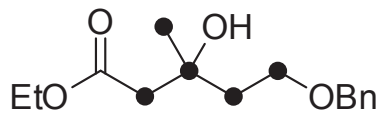
F2 - Acquisition Parameters
Date_ 20140212
Time 21.16
INSTRUM drx400
PROBHD 5 mm QNP 1H/13
PULPROG zgpg30
TD 131072
SOLVENT CDCl3
NS 3072
DS 4
SWH 26315.789 Hz
FIDRES 0.200774 Hz
AQ 2.4904180 sec
RG 8192
DW 19.000 usec
DE 6.00 usec
TE 300.2 K
D1 2.00000000 sec
d11 0.03000000 sec
DELTA 1.89999998 sec
TD0 1

==== CHANNEL f1 =====
NUC1 13C
P1 11.00 usec
PL1 -3.00 dB
SFO1 100.5535241 MHz

==== CHANNEL f2 =====
CPDPRG2 waltz16
NUC2 1H
PCPD2 80.00 usec
PL2 -2.00 dB
PL12 16.06 dB
PL13 16.06 dB
SFO2 399.8515994 MHz

F2 - Processing parameters
SI 65536
SF 100.5423658 MHz
SR 2.77 Hz
WDW EM
SSB 0
LB 1.00 Hz
GB 0
PC 1.40





SI-6

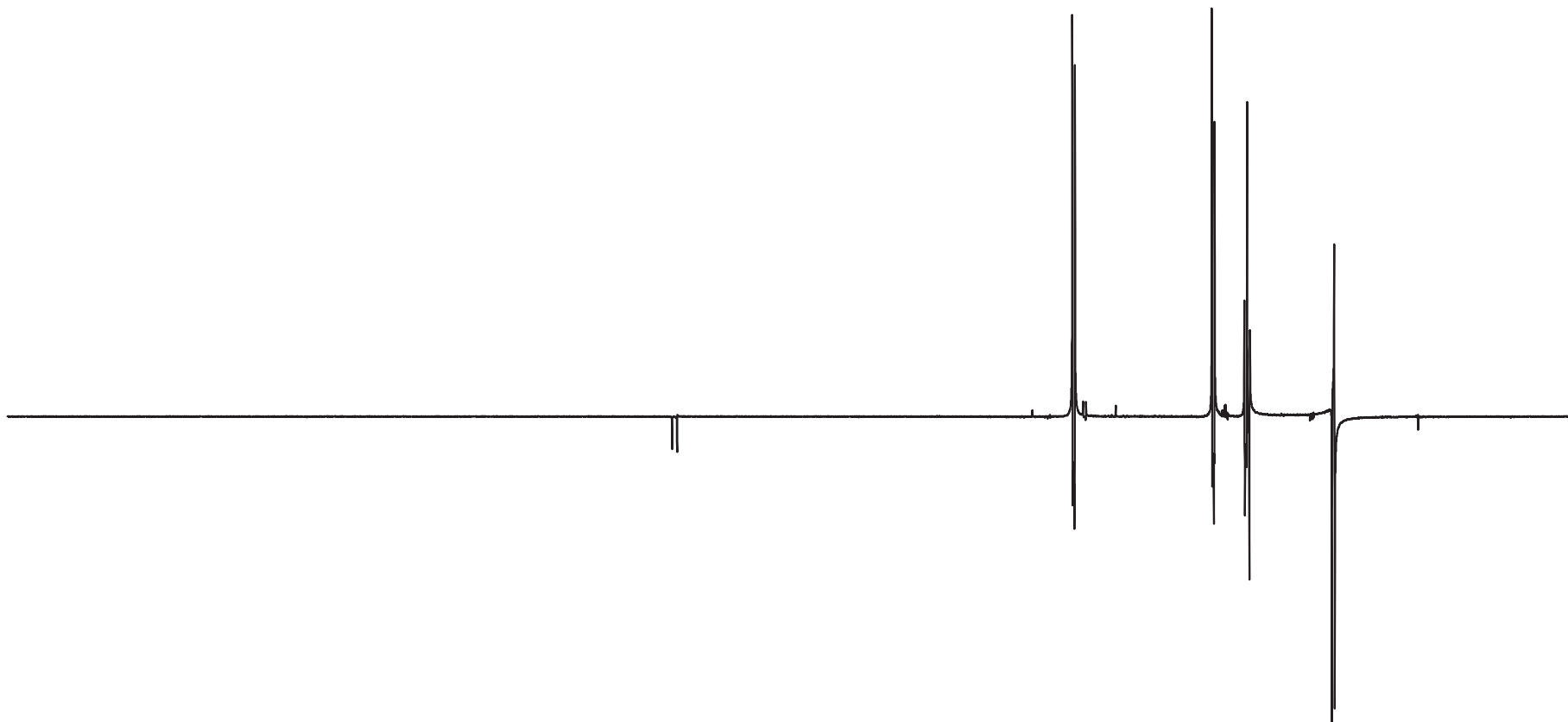
Current Data Parameters
 NAME bae123190_od
 EXPNO 3
 PROCNO 1

F2 - Acquisition Parameters
 Date_ 20140212
 Time 23.52
 INSTRUM drx400
 PROBHD 5 mm QNP 1H/13
 PULPROG dept135
 TD 131072
 SOLVENT CDCl3
 NS 2048
 DS 4
 SWH 26315.789 Hz
 FIDRES 0.200774 Hz
 AQ 2.4904180 sec
 RG 5792.6
 DW 19.000 usec
 DE 7.00 usec
 TE 299.2 K
 CNST2 145.0000000
 D1 2.0000000 sec
 d2 0.00344828 sec
 d12 0.00002000 sec
 DELTA 0.00001401 sec
 TD0 1

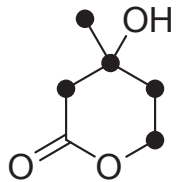
==== CHANNEL f1 =====
 NUC1 13C
 P1 11.00 usec
 p2 22.00 usec
 PL1 -3.00 dB
 SFO1 100.5535241 MHz

==== CHANNEL f2 =====
 CPDPRG2 waltz16
 NUC2 1H
 P3 10.00 usec
 p4 20.00 usec
 PCPD2 80.00 usec
 PL2 -2.00 dB
 PL12 16.06 dB
 SFO2 399.8515994 MHz

F2 - Processing parameters
 SI 65536
 SF 100.5423863 MHz
 SR 23.34 Hz
 WDW EM
 SSB 0
 LB 1.00 Hz
 GB 0
 PC 1.40



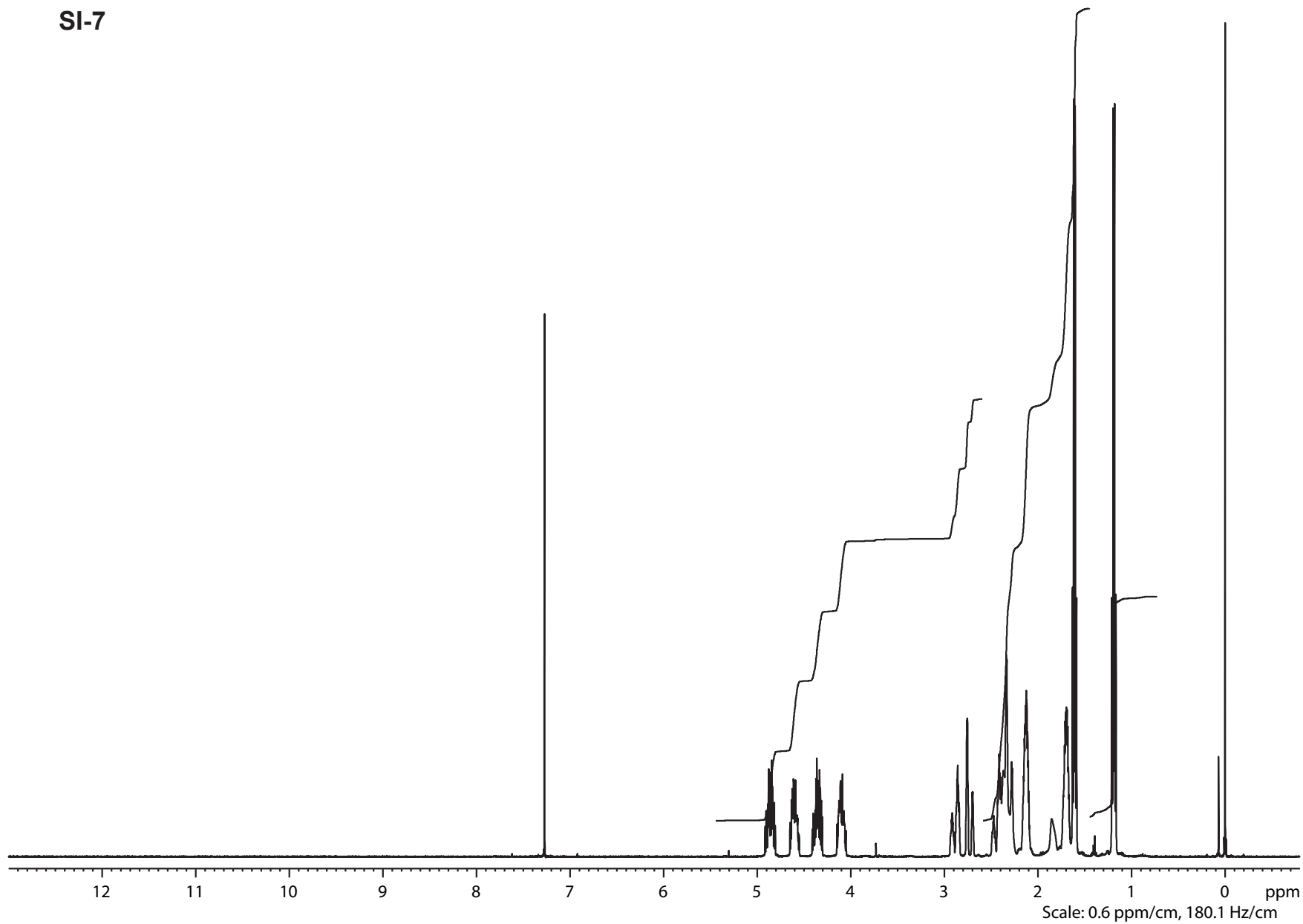
220 210 200 190 180 170 160 150 140 130 120 110 100 90 80 70 60 50 40 30 20 10 0 ppm
 Scale: 10 ppm/cm, 1005 Hz/cm

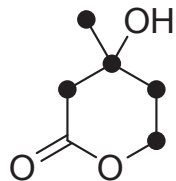


SI-7

NAME bae-140214-104957_od
EXPNO 1
PROCNO 1
Date_ 20140214
Time_ 10.57
INSTRUM av300
PROBHD 5 mm PABBO BB-
PULPROG zg30
TD 49152
SOLVENT CDCl3
NS 32
DS 2
SWH 6203.474 Hz
FIDRES 0.126210 Hz
AQ 3.9617012 sec
RG 161
DW 80.600 usec
DE 6.00 usec
TE 296.2 K
D1 1.00000000 sec
TD0 1

==== CHANNEL f1 =====
NUC1 1H
P1 12.00 usec
PL1 -1.00 dB
SFO1 300.1318530 MHz
SI 32768
SF 300.1300081 MHz
SR 8.12 Hz
WDW EM
SSB 0
LB 0.00 Hz
GB 0
PC 1.40
F1P 13.000 ppm
F2P -0.800 ppm





SI-7

```

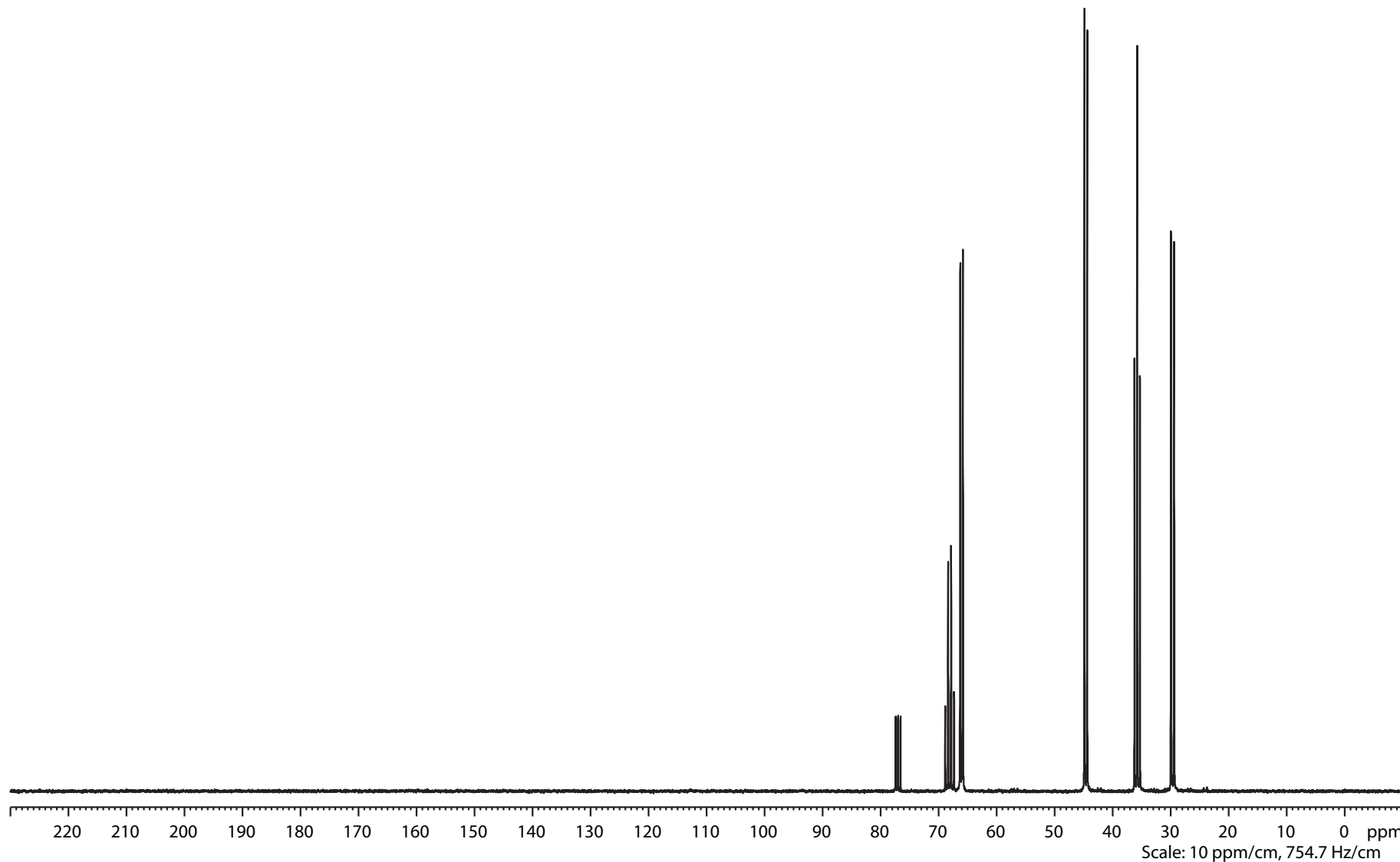
NAME      bae-140214-104957_od
EXPNO     2
PROCNO    1
Date_     20140214
Time      11.12
INSTRUM   av300
PROBHD    5 mm PABBO BB-
PULPROG   zgpg30
TD         98304
SOLVENT   CDCl3
NS         152
DS         4
SWH        19736.842 Hz
FIDRES     0.200774 Hz
AQ         2.4904180 sec
RG         362
DW         25.333 usec
DE         6.00 usec
TE         297.2 K
D1         2.00000000 sec
D11        0.03000000 sec
TD0        1
  
```

```

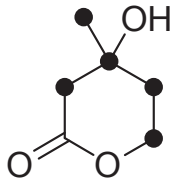
===== CHANNEL f1 =====
NUC1       13C
P1         9.60 usec
PL1        -1.00 dB
SFO1       75.4761254 MHz
  
```

```

===== CHANNEL f2 =====
CPDPRG2    waltz16
NUC2       1H
PCPD2      80.00 usec
PL2        -1.00 dB
PL12       15.98 dB
PL13       16.00 dB
SFO2       300.1312005 MHz
SI         65536
SF         75.4677532 MHz
SR         4.24 Hz
WDW         EM
SSB         0
LB         1.00 Hz
GB         0
PC         1.40
F1P        230.000 ppm
F2P        -10.000 ppm
  
```



Scale: 10 ppm/cm, 754.7 Hz/cm



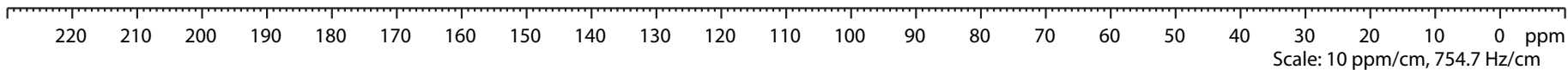
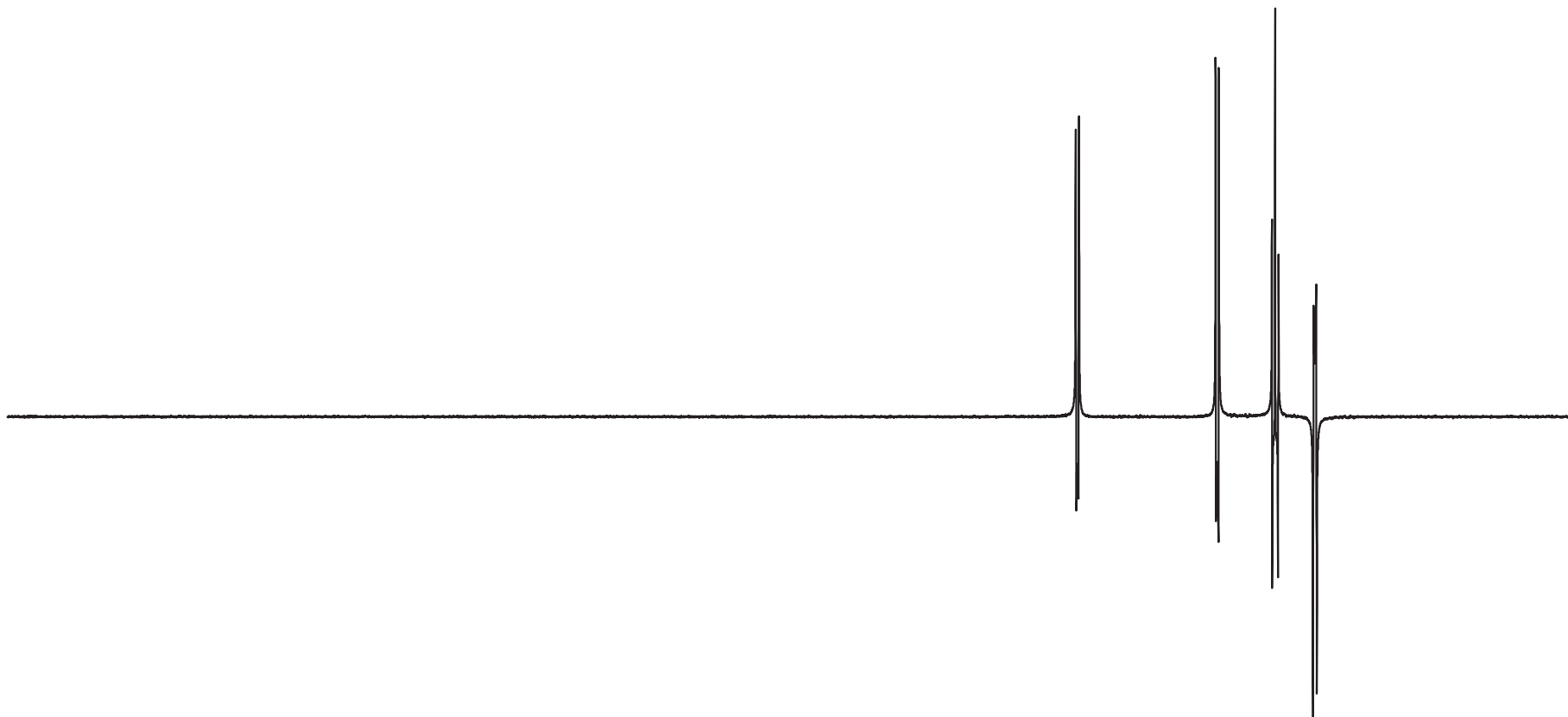
SI-7

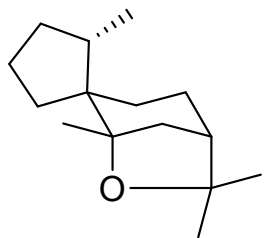
```

NAME      bae-140214-104957_od
EXPNO     3
PROCNO    1
Date_     20140214
Time      11.20
INSTRUM   av300
PROBHD    5 mm PABBO BB-
PULPROG   dept135
TD         98304
SOLVENT   CDCl3
NS         76
DS         4
SWH        19736.842 Hz
FIDRES     0.200774 Hz
AQ         2.4904180 sec
RG         1030
DW         25.333 usec
DE         6.00 usec
TE         297.2 K
CNST2     145.0000000
D1         2.00000000 sec
D2         0.00344828 sec
D12        0.00002000 sec
TD0        1

===== CHANNEL f1 =====
NUC1       13C
P1         9.60 usec
P2         19.20 usec
PL1        -1.00 dB
SFO1       75.4761254 MHz

===== CHANNEL f2 =====
CPDPRG2    waltz16
NUC2       1H
P3         11.60 usec
P4         23.20 usec
PCPD2      80.00 usec
PL2        -1.00 dB
PL12       15.98 dB
SFO2       300.1312005 MHz
SI         65536
SF         75.4677466 MHz
SR         -2.41 Hz
WDW        EM
SSB        0
LB         1.00 Hz
GB         0
PC         1.40
F1P        230.000 ppm
F2P        -10.000 ppm
  
```





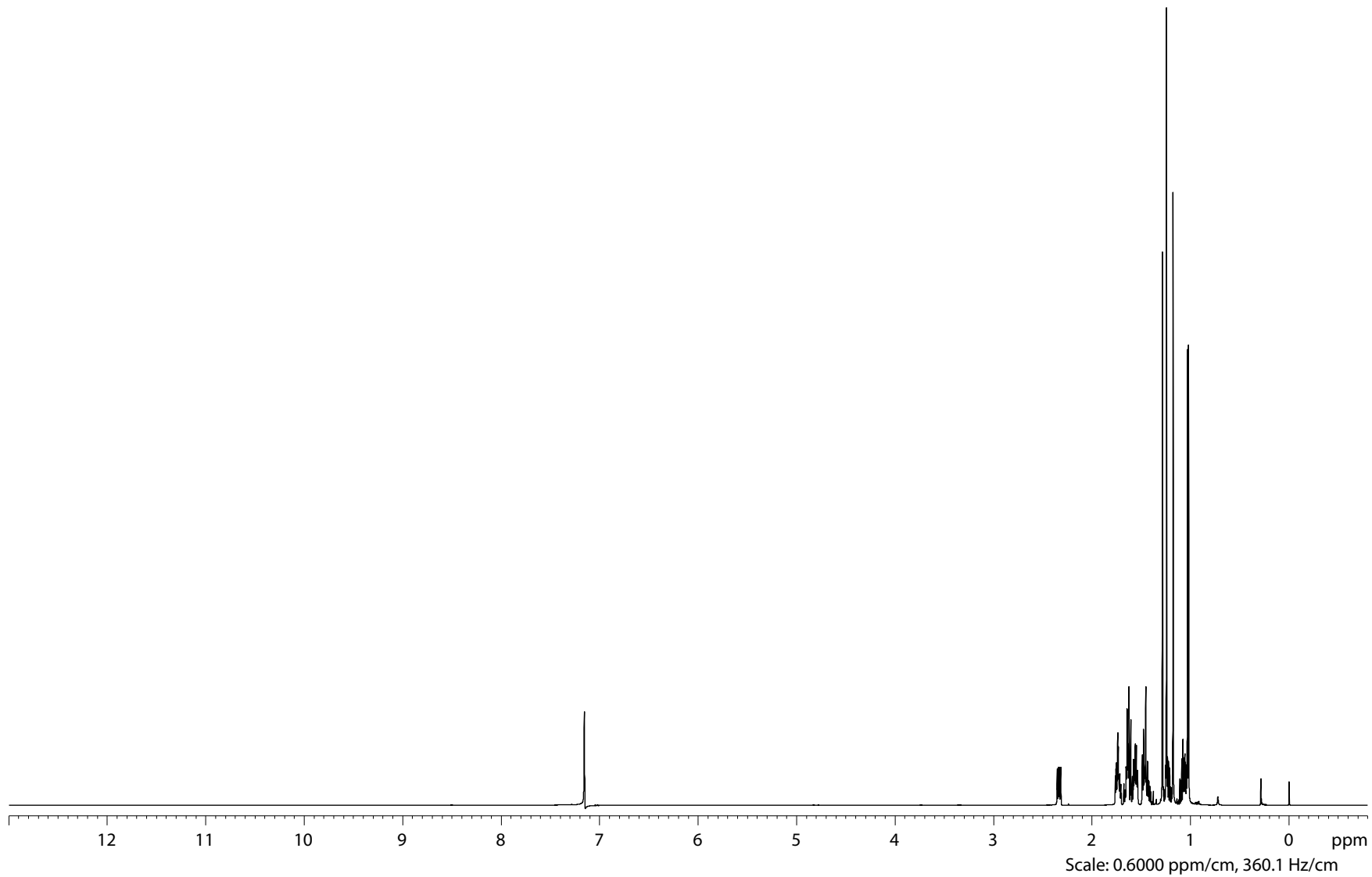
1

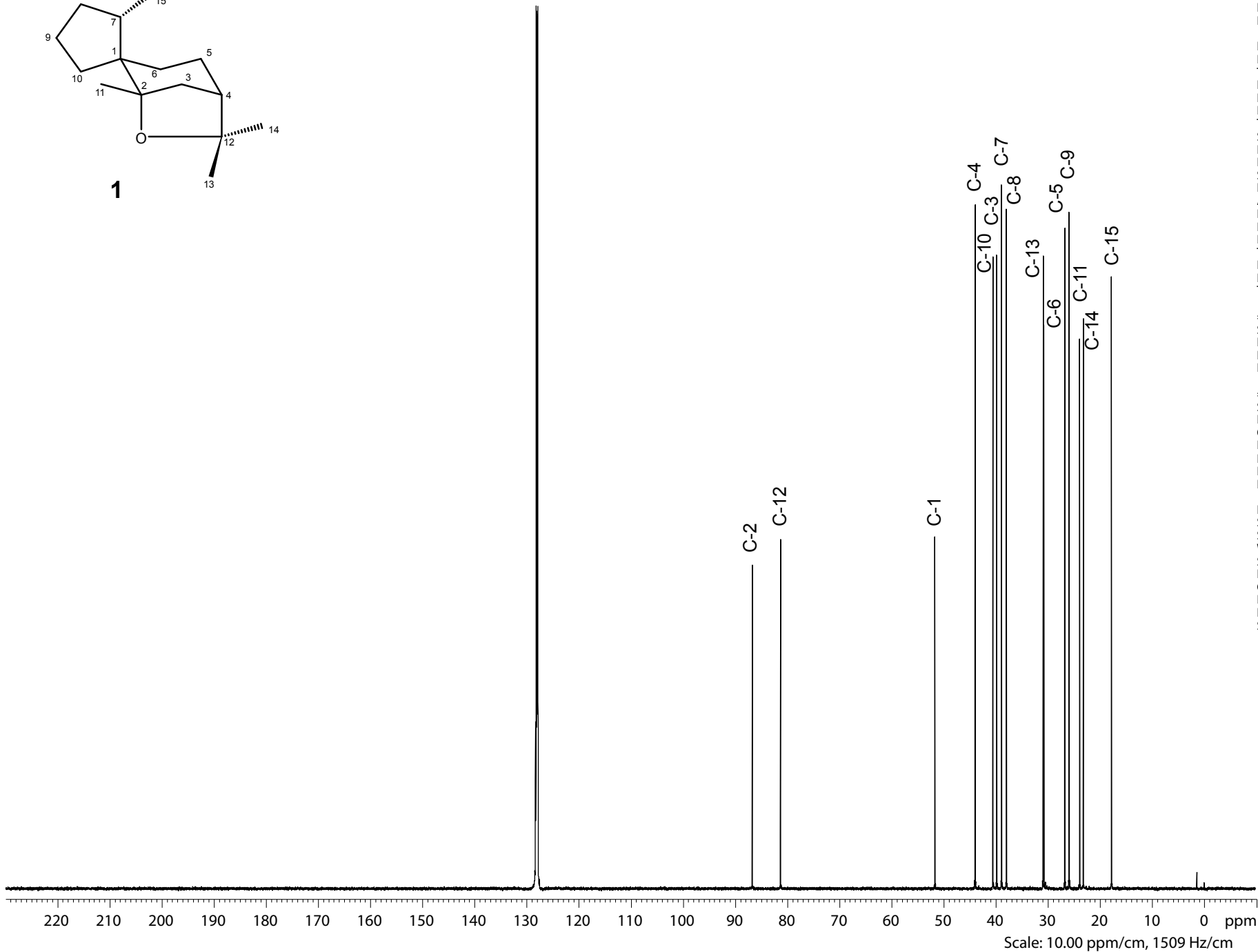
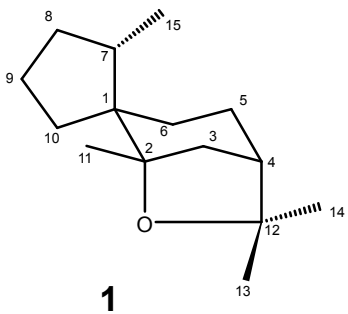
Current Data Parameters
NAME bae125470_od
EXPNO 1
PROCNO 1

F2 - Acquisition Parameters
Date_ 20141111
Time 11.24
INSTRUM av600
PROBHD 5 mm CPTCI 1H-
PULPROG zg30
TD 98304
SOLVENT C6D6
NS 64
DS 2
SWH 12335.526 Hz
FIDRES 0.125483 Hz
AQ 3.9845889 sec
RG 4
DW 40.533 usec
DE 10.00 usec
TE 303.3 K
D1 1.0000000 sec
TD0 1

===== CHANNEL f1 =====
SFO1 600.1337052 MHz
NUC1 1H
P1 7.48 usec
PLW1 6.97440004 W

F2 - Processing parameters
SI 65536
SF 600.1299991 MHz
WDW EM
SSB 0
LB 0 Hz
GB 0
PC 1.40
HZpPT 0.188225 Hz
SR -0.94 Hz





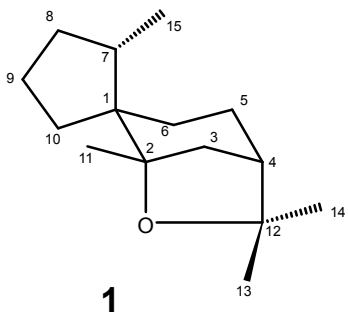
Current Data Parameters
 NAME bae125470_od
 EXPNO 7
 PROCNO 1

F2 - Acquisition Parameters
 Date_ 20141121
 Time 19.11
 INSTRUM av600
 PROBHD 5 mm CPTCI 1H-
 PULPROG zgpg30
 TD 196608
 SOLVENT C6D6
 NS 512
 DS 4
 SWH 39682.539 Hz
 FIDRES 0.201836 Hz
 AQ 2.4772608 sec
 RG 25.4
 DW 12.600 usec
 DE 18.00 usec
 TE 303.3 K
 D1 2.00000000 sec
 D11 0.03000000 sec
 TD0 1

===== CHANNEL f1 =====
 SFO1 150.9195568 MHz
 NUC1 13C
 P1 13.10 usec
 PLW1 71.87300110 W

===== CHANNEL f2 =====
 SFO2 600.1324005 MHz
 NUC2 1H
 CPDPRG[2] waltz16
 PCPD2 70.00 usec
 PLW2 6.97440004 W
 PLW12 0.10284000 W
 PLW13 0.050390000 W

F2 - Processing parameters
 SI 131072
 SF 150.9027566 MHz
 WDW EM
 SSB 0
 LB 1.00 Hz
 GB 0
 PC 1.40
 HZpPT 0.302754 Hz
 SR -52.40 Hz



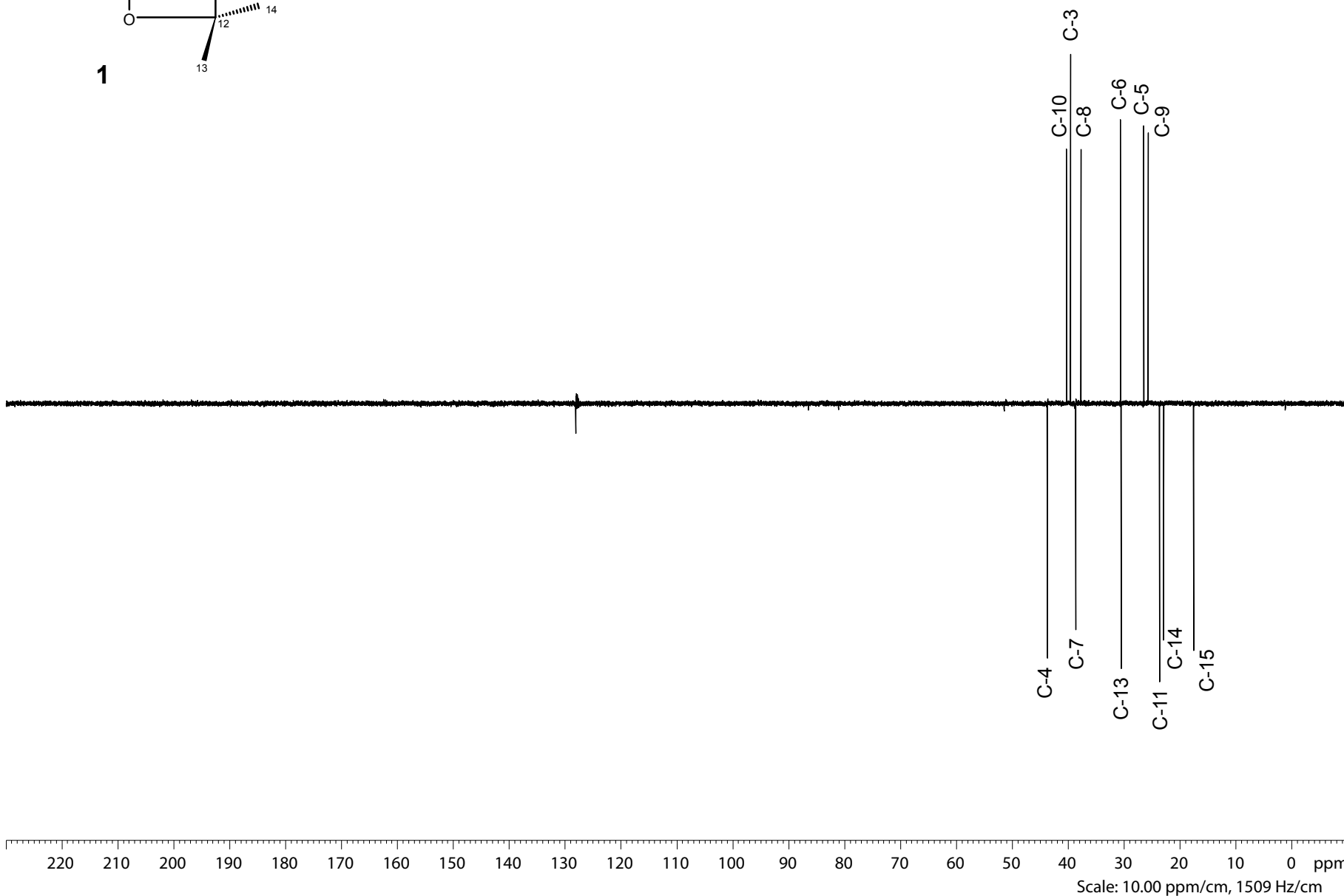
Current Data Parameters
 NAME bae125470_od
 EXPNO 8
 PROCNO 1

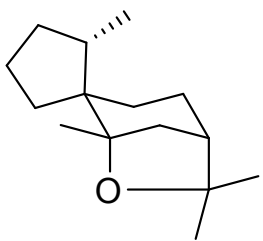
F2 - Acquisition Parameters
 Date_ 20141121
 Time 19.33
 INSTRUM av600
 PROBHD 5 mm CPTCI 1H-
 PULPROG depts135
 TD 196608
 SOLVENT C6D6
 NS 256
 DS 4
 SWH 39682.539 Hz
 FIDRES 0.201836 Hz
 AQ 2.4772608 sec
 RG 2050
 DW 12.600 usec
 DE 18.00 usec
 TE 303.3 K
 CNST2 145.0000000
 D1 2.00000000 sec
 D2 0.00344828 sec
 D12 0.00002000 sec
 TD0 1

===== CHANNEL f1 =====
 SFO1 150.9195568 MHz
 NUC1 13C
 P1 13.10 usec
 P13 2000.00 usec
 PLW0 0 W
 PLW1 71.87300110 W
 SPNAM[5] Crp60comp.4
 SPOAL5 0.500
 SPOFFS5 0 Hz
 SPW5 18.84499931 W

===== CHANNEL f2 =====
 SFO2 600.1324005 MHz
 NUC2 1H
 CPDPRG[2] waltz16
 P3 8.50 usec
 P4 17.00 usec
 PCPD2 70.00 usec
 PLW2 6.97440004 W
 PLW12 0.10284000 W

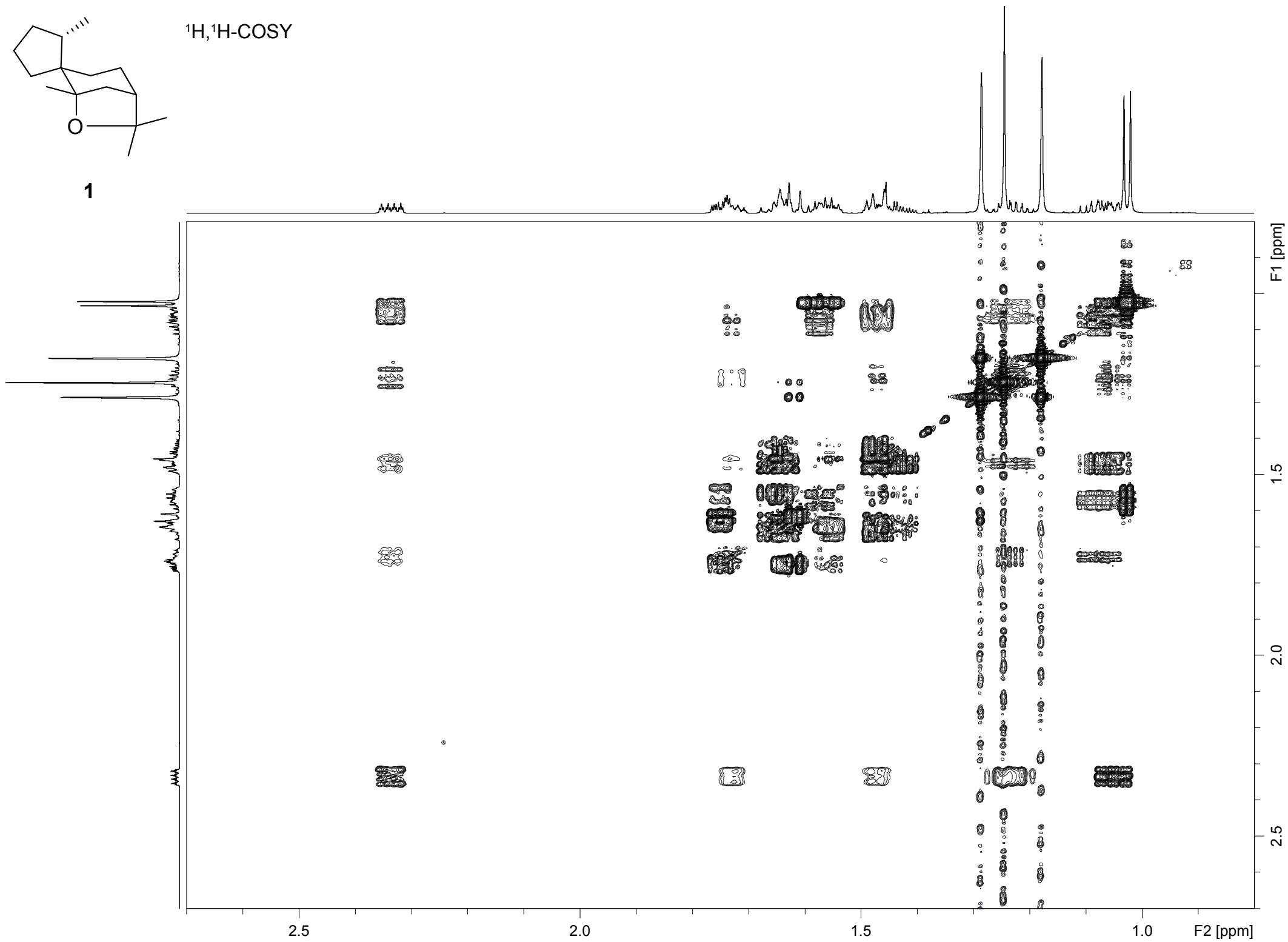
F2 - Processing parameters
 SI 131072
 SF 150.9028016 MHz
 WDW EM
 SSB 0
 LB 1.00 Hz
 GB 0
 PC 1.40
 HZpPT 0.302754 Hz
 SR -7.43 Hz



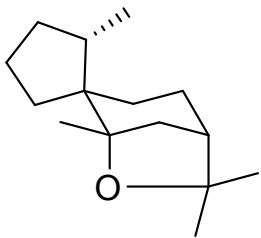


1

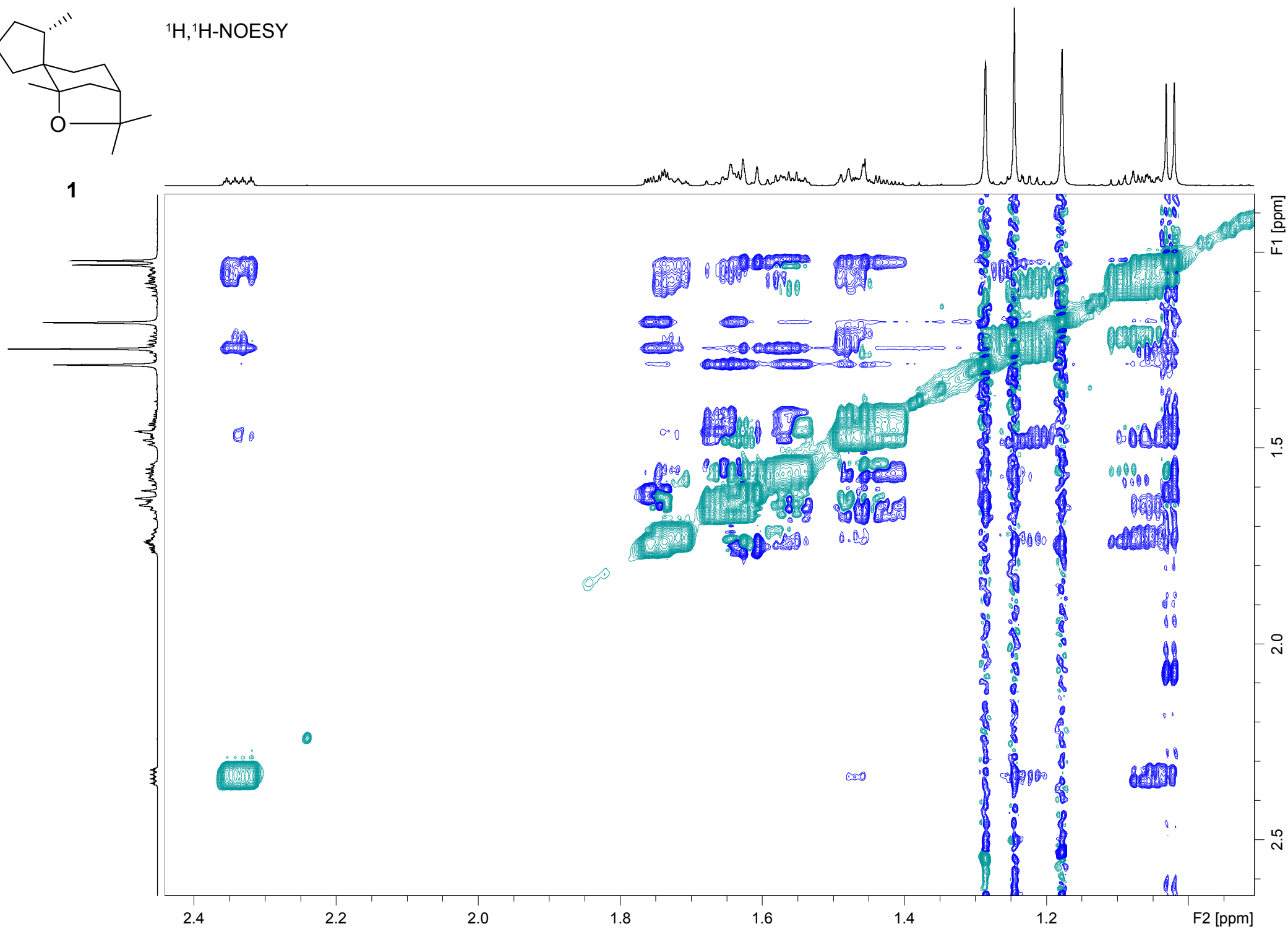
$^1\text{H}, ^1\text{H}$ -COSY

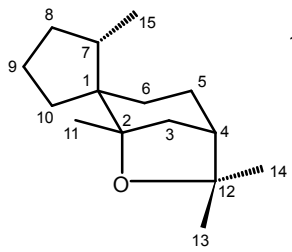


$^1\text{H}, ^1\text{H}$ -NOESY

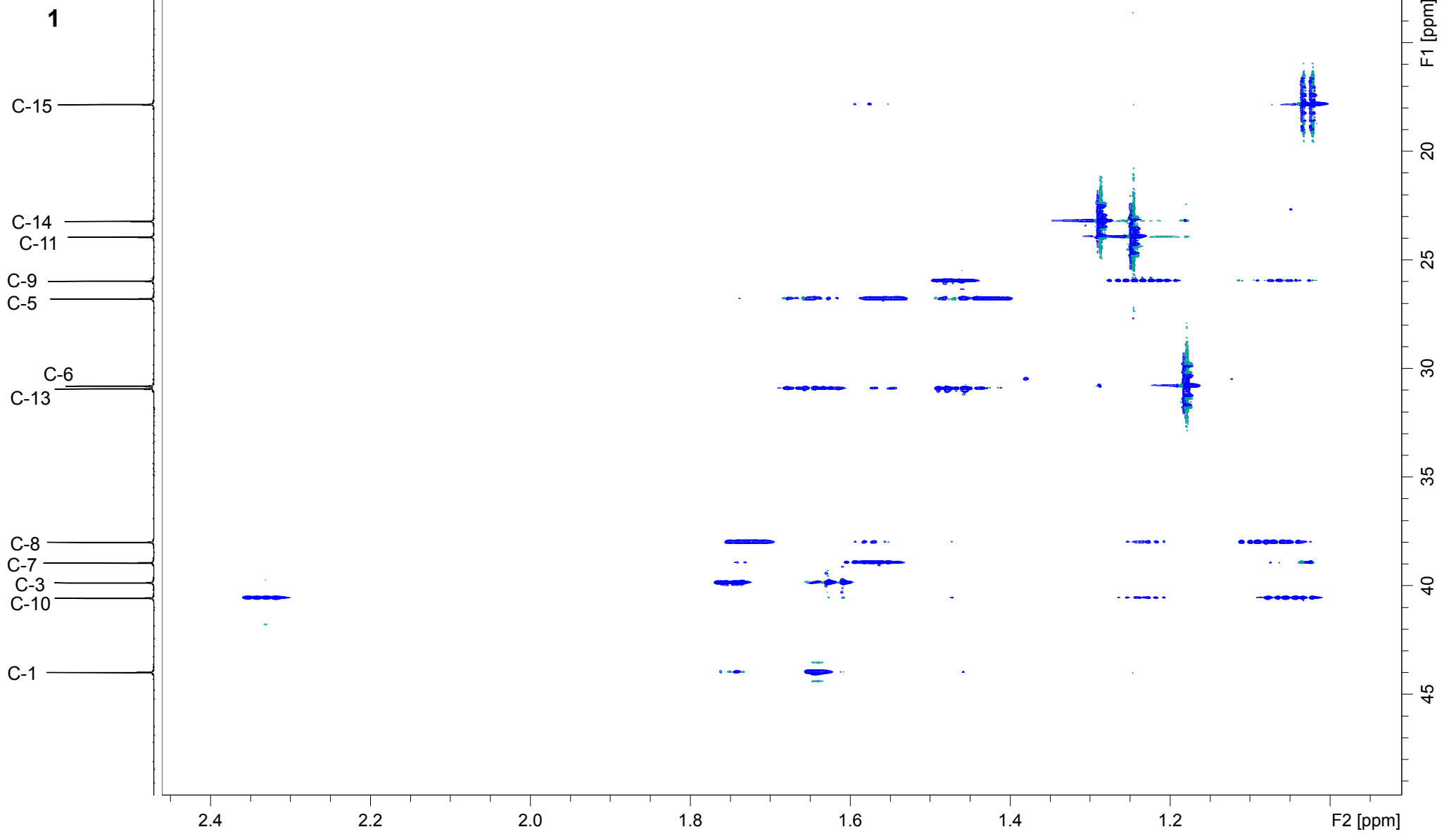


1

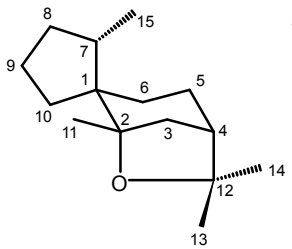




$^{13}\text{C}, ^1\text{H}$ -HSQC

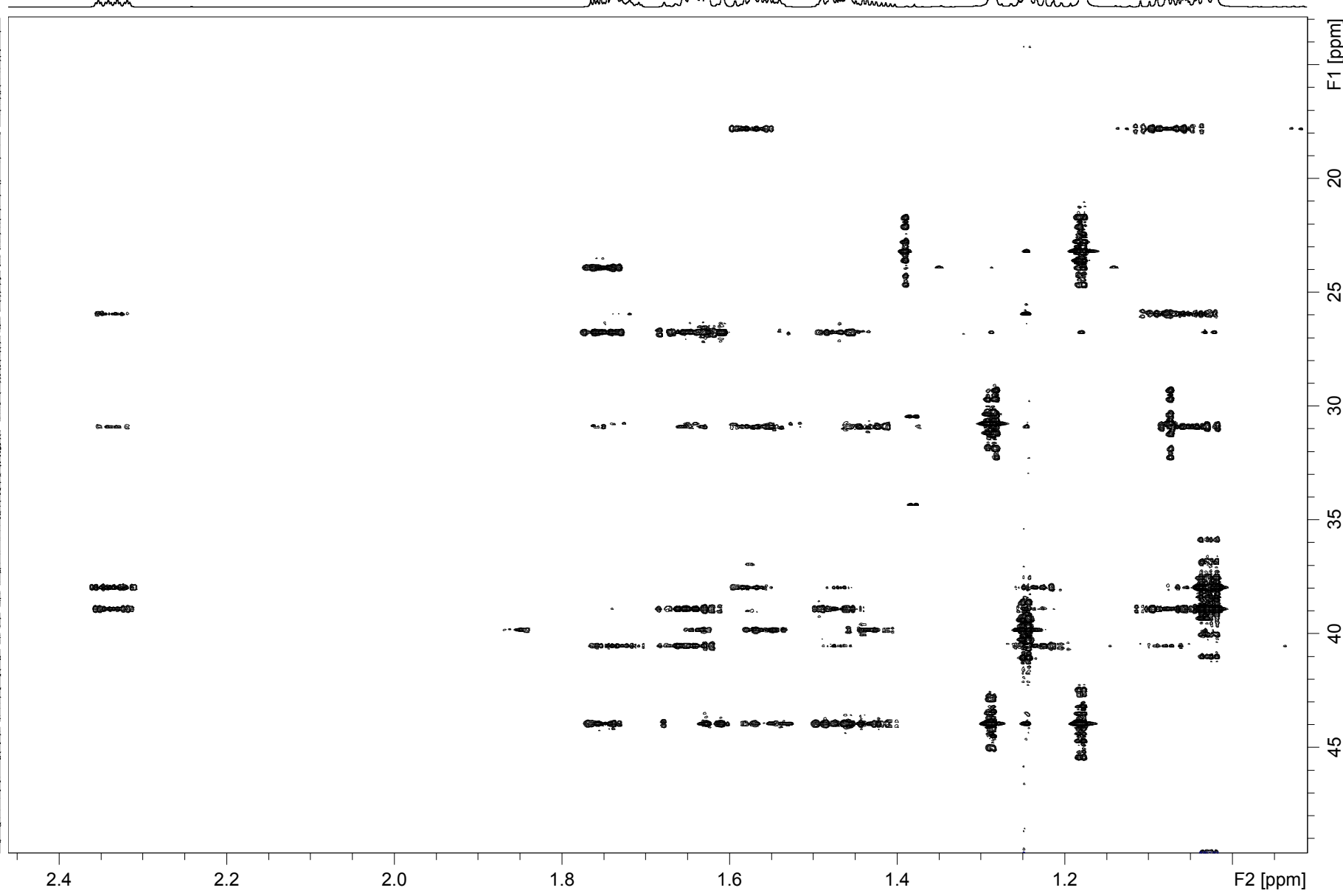


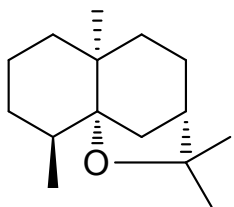
$^{13}\text{C}, ^1\text{H}$ -HMBC



1

- C-15
- C-14
- C-11
- C-9
- C-5
- C-6
- C-13
- C-8
- C-7
- C-3
- C-10
- C-1





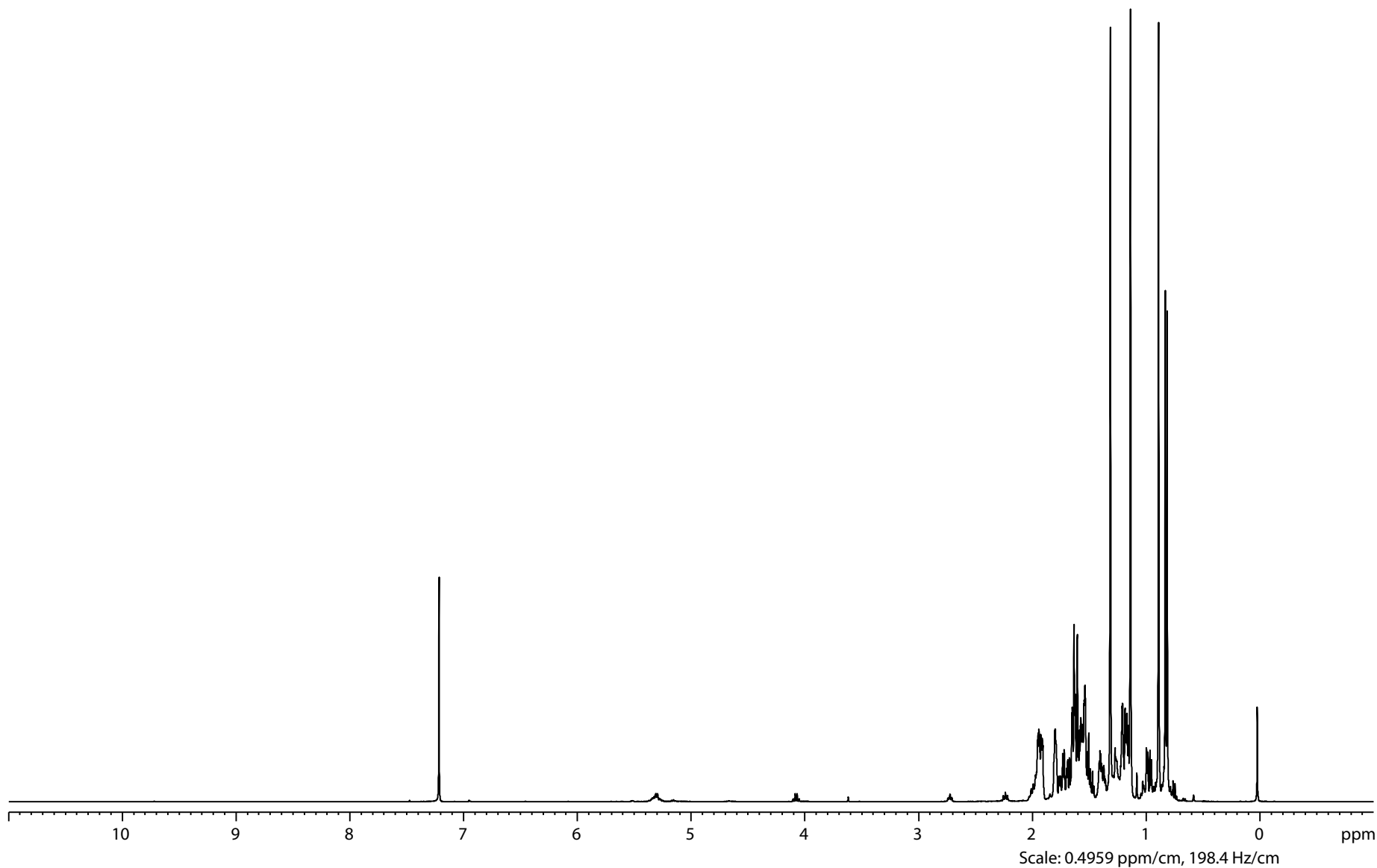
3

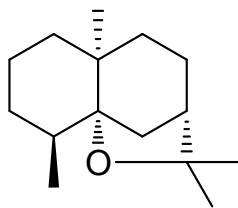
Current Data Parameters
NAME 06x4a041.15
EXPNO 10
PROCNO 1

F2 - Acquisition Parameters
Date_ 20150203
Time 9.02
INSTRUM spect
PROBHD 5 mm PABBO BB-
PULPROG zg40
TD 65536
SOLVENT CDCl3
NS 16
DS 2
SWH 8802.817 Hz
FIDRES 0.134320 Hz
AQ 3.724448 sec
RG 114
DW 56.800 usec
DE 7.50 usec
TE 298.0 K
D1 1.00000000 sec
TD0 1

===== CHANNEL f1 =====
NUC1 1H
P1 7.20 usec
PL1 0 dB
SFO1 400.1320007 MHz

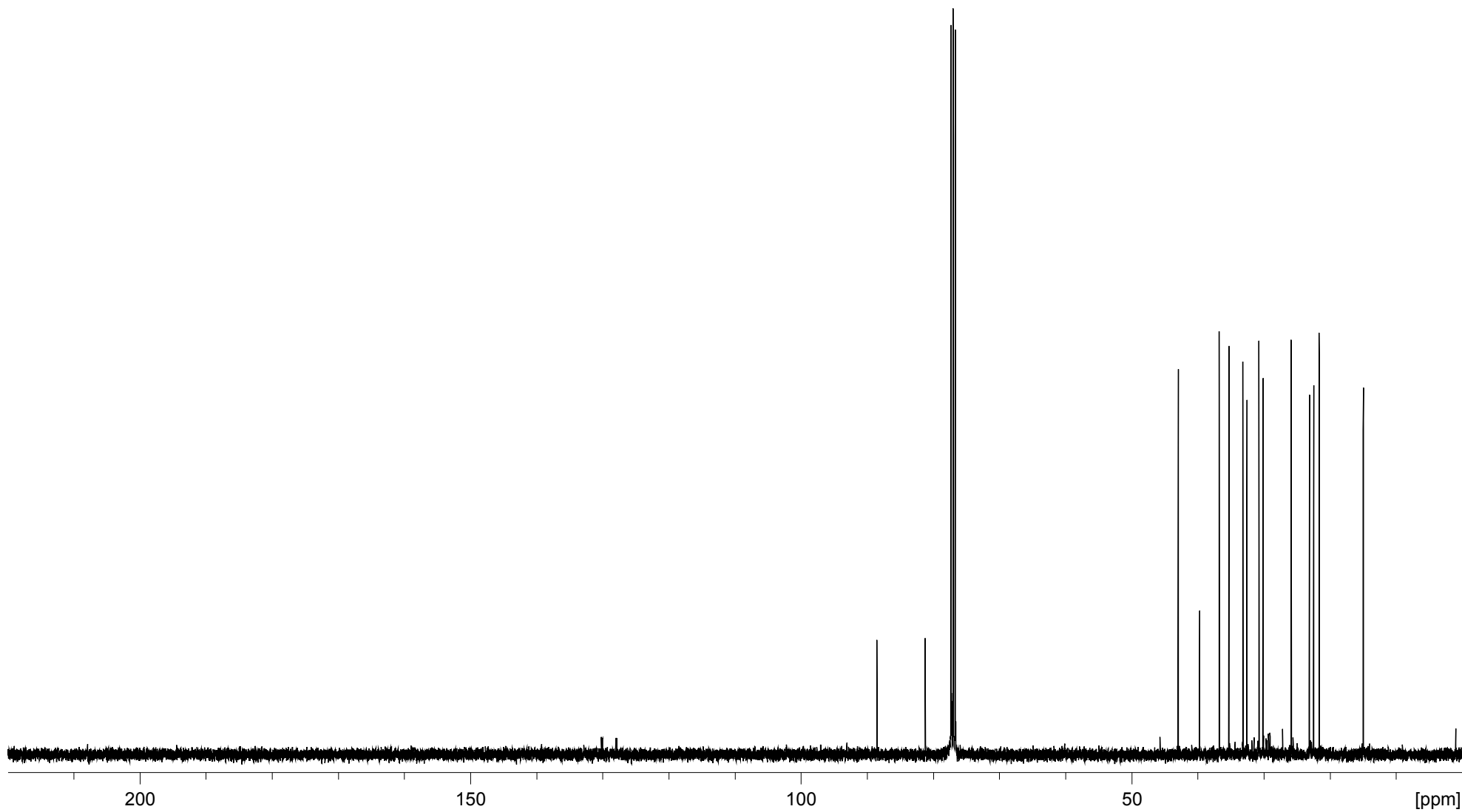
F2 - Processing parameters
SI 65536
SF 400.1300258 MHz
WDW EM
SSB 0
LB 0.30 Hz
GB 0
PC 3.00

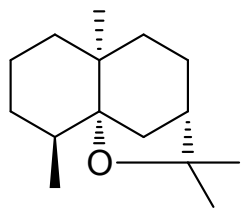




$^{13}\text{C-NMR}$ (100 MHz, CDCl_3)

3





^{13}C -DEPT-135 (100 MHz, CDCl_3)

3



200

150

100

50

[ppm]

Appendix C

Harzianone Biosynthesis by the Biocontrol Fungus *Trichoderma*

A EUROPEAN JOURNAL OF CHEMICAL BIOLOGY

CHEM **BIO** CHEM

SYNTHETIC BIOLOGY & BIO-NANOTECHNOLOGY

Accepted Article

Title: Harzianone Biosynthesis by the Biocontrol Fungus *Trichoderma*

Authors: Lena Barra and Jeroen Sidney Dickschat

This manuscript has been accepted after peer review and appears as an Accepted Article online prior to editing, proofing, and formal publication of the final Version of Record (VoR). This work is currently citable by using the Digital Object Identifier (DOI) given below. The VoR will be published online in Early View as soon as possible and may be different to this Accepted Article as a result of editing. Readers should obtain the VoR from the journal website shown below when it is published to ensure accuracy of information. The authors are responsible for the content of this Accepted Article.

To be cited as: *ChemBioChem* 10.1002/cbic.201700462

Link to VoR: <http://dx.doi.org/10.1002/cbic.201700462>

WILEY-VCH

www.chembiochem.org

A Journal of



Harzianone Biosynthesis by the Biocontrol Fungus *Trichoderma*

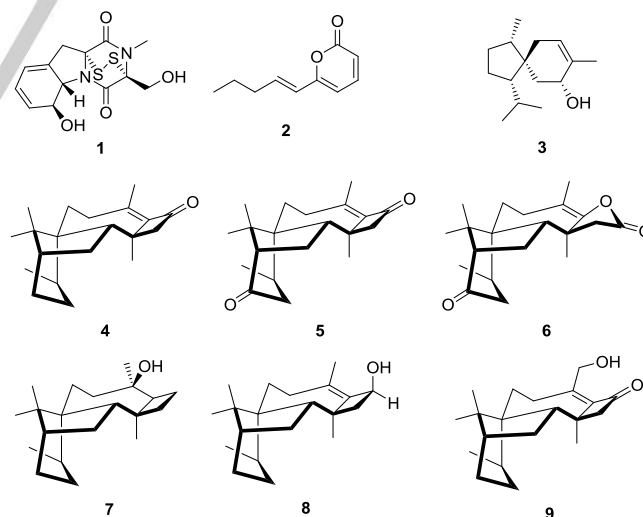
Lena Barra^[a] and Jeroen S. Dickschat*^[a]

Abstract: Analysis of the volatile terpenes produced by seven fungal strains of the genus *Trichoderma* by use of a closed-loop stripping apparatus (CLSA) revealed a common production of harzianone, a bioactive, structurally unique diterpenoid consisting of a fused tetracyclic 4,5,6,7-membered ring system. The terpene cyclization mechanism was studied by feeding experiments using selectively ¹³C- and ²H-labeled synthetic mevalonolactone isotopologues, followed by analysis of the incorporation patterns by ¹³C-NMR spectroscopy and GC/MS. The structure of harzianone was further supported from a ¹³C,¹³C-COSY experiment of the *in vivo* generated fully ¹³C-labeled diterpene.

Introduction

Fungi of the genus *Trichoderma* are widespread in soil and wood habitats and are known for their opportunistic avirulent plant beneficial attributes.^[1] They are used as environmentally friendly biocontrol agents, because of their positive effect on root growth and development, crop productivity and nutrient uptake.^[2] One aspect in the complex mechanisms of *Trichoderma*-plant-pathogen interaction is the ability of *Trichoderma* to parasitize other fungi, thereby protecting the plant from harmful phytopathogens.^[3] This ability can be attributed to the production of cellulose and chitin degrading enzymes and the production of diverse bioactive secondary metabolites.^[4] A well-known example is the diketopiperazine gliotoxine (**1**, Scheme 1) that was first isolated from *Gliocladium fimbriatum*, a fungus that was later reclassified as *T. virens*.^[5] Gliotoxine is an immunosuppressive, toxic, antimicrobial compound that plays an important role in pathogen defense.^[6] Fungi are also known as producers of volatiles with often distinct functions.^[7] A series of volatile pyrones such as **2** were isolated from *Trichoderma*,^[8] which exhibit growth inhibitory properties against phytopathogenic fungi including *Aspergillus*, *Botrytis*, *Rhizoctonia*, *Sclerotinia* and *Pyrenochaeta*.^[9] A volatile sesquiterpene alcohol that is frequently released by *Trichoderma* is tricho-acorenol (**3**) that was first identified from culture extracts of *Trichoderma koningii*.^[10] Its absolute configuration was deduced by enantioselective synthesis,^[11] and its biosynthesis was addressed by feeding experiments with isotopically labeled precursors.^[12] Furthermore, a series of structurally unique and biosynthetically related diterpenes represented by harzianone (**4**),^[13] harziandione (**5**)^[14] and

trichodermaerin (**6**)^[15] were isolated from *Trichoderma*. Notably, **5** and the related diterpenoids **7** – **9** were recently isolated from a *Trichoderma* symbiont of the taxane producing plant *Taxus baccata*.^[16] Diketone **5** is a strong antifungal compound active against the plant pathogenic fungus *Sclerotium rolfsii*,^[17] whereas ketone **4** lacks such an antifungal activity, but exhibits activity against *Escherichia coli* and *Staphylococcus aureus* and in a brine shrimp (*Artemia salina*) toxicity assay.^[13] The absolute configuration of **4** was determined by comparison of experimental to calculated ECD spectroscopic data,^[13] but so far no studies regarding the biosynthesis of this unique tetracyclic diterpene have been conducted. We have recently developed a method that combines feeding of ¹³C-labeled mevalonolactones and capturing of the resulting labeled volatile terpenes by collection with a closed-loop stripping apparatus, that allows for a direct analysis of the headspace extracts by ¹³C-NMR (CLSA-NMR).^[18] This method is especially powerful, if the biosynthesis of volatile terpenoids is to be addressed, for which the classical method of liquid culture extraction and compound isolation in preparative amounts can be significantly hampered because of the danger of compound loss during solvent evaporation steps. Furthermore, the biosynthetic investigations can be performed with only a single agar plate culture and thus require only small amounts of the expensive ¹³C-labeled precursors. Here we present our insights into harzianone (**4**) biosynthesis by application of this method to the fungus *Trichoderma*.



Scheme 1. Structures of known secondary metabolites from *Trichoderma*.

[a] Prof. Dr. J. S. Dickschat, L. Barra
Kekulé-Institut für Organische Chemie und Biochemie
Rheinische Friedrich-Wilhelms-Universität Bonn
Gerhard-Domagk-Straße 1, 53121 Bonn, Germany
E-mail: dickschat@uni-bonn.de

Supporting information for this article is given via a link at the end of the document.

Results and Discussion

The volatile terpenes released by seven fungi of the genus *Trichoderma* were analyzed by use of a CLSA (Figure 1A and Figure S1).^[19] In all headspace extracts tricho-acorenol (**3**) was

found as the main constituent, except for *T. atroviride*, which produces large amounts of **2**. Furthermore, all seven strains produced a compound with a mass spectrum that suggested the structure of an oxidized diterpene hydrocarbon, as indicated by the molecular ion at $m/z = 286$ (Figure 1B), but the mass spectrum was not included in our mass spectral libraries, preventing instantaneous compound identification. Since production of this compound was the highest in *Trichoderma* sp. 34, this strain was chosen for all further experiments.

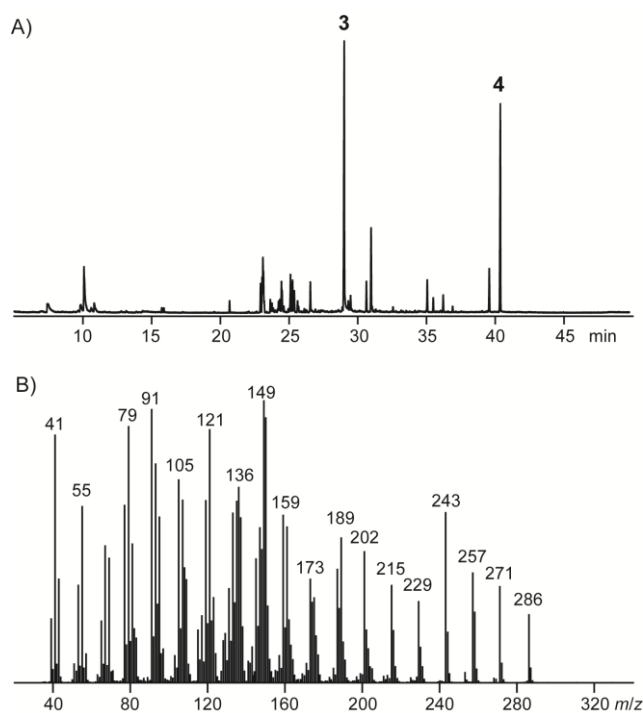


Figure 1. A) Representative total ion chromatogram of the headspace extract of *Trichoderma* sp. 34 and B) EI mass spectrum of harzianone (**4**).

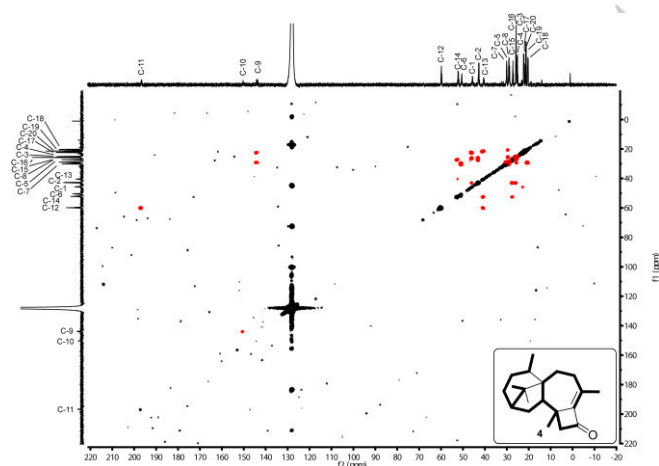


Figure 2. $^{13}\text{C}, ^{13}\text{C}$ -COSY spectrum of $(^{13}\text{C}_{20})$ -**4** in C_6D_6 and C,C connectivities deduced from the cross peaks shown in red (bold lines in structure).

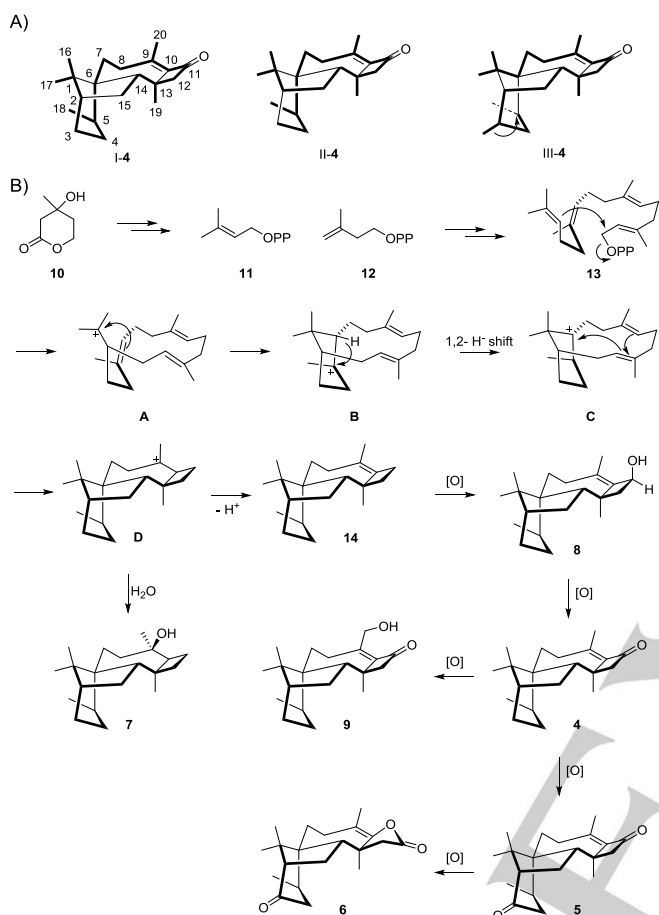
In order to identify the detected compound, its isolation by solvent extraction of agar plate cultures was tried several times, but the production was too low to obtain sufficient material for structure elucidation by NMR. Therefore, feeding experiments with $(2,3,4,5,6\text{-}^{13}\text{C}_5)$ mevalonolactone^[18f] ($(2,3,4,5,6\text{-}^{13}\text{C}_5)$ -**10**) were carried out, in which all five carbons ending up in the terpene monomers dimethylallyl diphosphate (DMAPP, **11**) and isopentenyl diphosphate (IPP, **12**) are ^{13}C -labeled. In a typical experiment 10 mg of the labeled compound were fed to a standard agar plate culture (ca. 30 mL of medium), followed by collection of volatiles by CLSA for the next seven days. The charcoal filter was extracted with 50 μL C_6D_6 every day and the collected extracts were directly used for further analysis. GC/MS analysis revealed an increased production of the diterpenoid due to the administration of the terpene precursor and a high incorporation of labeling (91% incorporation rate, Figure S2). The content of the labeled diterpene in the sample was sufficient for recording a $^{13}\text{C}, ^{13}\text{C}$ -COSY spectrum that hinted at the structure of harzianone (**4**, Figure 2). Since a few crosspeaks for correlations to quaternary carbons were missing, the isolation of non-labelled **4** was tried again from a large number of agar plates (100 plates), resulting in the isolation of 3.8 mg of pure **4**. Its structure was confirmed by ^1H -, ^{13}C -, ^{13}C -DEPT-135, $^1\text{H}, ^1\text{H}$ -COSY, $^1\text{H}, ^{13}\text{C}$ -HSQC, $^1\text{H}, ^{13}\text{C}$ -HMBC, and $^1\text{H}, ^1\text{H}$ -NOESY and comparison of recorded to literature data (Figure S4 – S10).^[13,16]

The terpene cyclization mechanism of **4** was studied by feeding of a series of synthetic ^{13}C -labeled mevalonolactones (**10**).^[18e] Three different possibilities for the fold of the diterpene precursor geranylgeranyl diphosphate (GGPP, **13**) may explain the formation of the harzianone backbone (Scheme 2A), but one of these folds as shown in I-**4** resembles the most straight forward arrangement, while the GGPP cyclization mechanisms for the substrate folds as in II-**4** and III-**4** are more difficult to understand. In order to distinguish between these possibilities, $(4,5\text{-}^{13}\text{C}_2)$ -**10** was synthesized from ethyl $(1,2\text{-}^{13}\text{C}_2)$ acetoacetate by a known procedure (Scheme S1)^[20] and fed to *Trichoderma* sp. 34, resulting in the incorporation of labeling into eight carbons of **4** with 51% incorporation rate, resulting in two contiguous spin systems, C10-11 ($^1J_{\text{C,C}} = 43.0$ Hz) and C3-2-15-14-6-7 with doublet signals for C7 and C3 ($^1J_{\text{C7,C6}} = 35.0$ Hz, $^1J_{\text{C3,C2}} = 34.0$ Hz) and doublets of doublets for the carbons at the internal positions (Figure 3A, Table S1). These findings strongly support the GGPP fold implied by I-**4** for the biosynthesis of **4**, which was further supported by similar feeding experiments with $(6\text{-}^{13}\text{C})$ -, $(2,6\text{-}^{13}\text{C}_2)$ -, $(3\text{-}^{13}\text{C})$ - and $(3,5\text{-}^{13}\text{C}_2)$ -**10** (Figures 3B-E, Table S1).

A plausible cyclization mechanism from GGPP (**13**) that is in line with all feeding experiments with the ^{13}C -labeled mevalonolactone isotopomers is illustrated in Scheme 2B. After initial abstraction of the pyrophosphate group in **13**, the allylic cation is attacked by the terminal double bond to build up a 14-membered ring system under formation of a tertiary cation **A**, which is subsequently attacked by the neighbouring double bond to form cation **B**. Intermediate **B** then undergoes a 1,2-hydride shift to **C**, followed by two cyclization steps yielding the harzianyl cation **D**. The formation of known **7** can be explained by a terminating attack of water to **D**, whereas its deprotonation may

For internal use, please do not delete. Submitted_Manuscript

yield **14**, which is a so far unknown diterpene. Subsequent allylic oxidation at C11 gives harzianone **4**, possibly via alcohol intermediate **8**. The other harzianone derivatives **5**, **6** and **9** can be explained by additional oxidations of **4**.



Scheme 2. Biosynthetic considerations for the generation of **4**. A) Different possibilities for GGPP folds (bold) to explain the formation of the harzianone skeleton. The arrow in III-**4** indicates a required carbon backbone rearrangement. B) biosynthetic mechanism to **4** and related derivatives.

The stereochemical course of the cyclization mechanism for GGPP to **4** in terms of the fate of the stereochemically distinct terminal geminal methyl groups could be followed by the feeding experiment with (6-¹³C)-**10** that results in the specific incorporation of labeling into only one of the geminal methyl groups in **4** (C16, no incorporation into C17, Figure 3B). This finding suggests that the conformation of the intermediate cation **A** is strictly controlled by the enzyme, allowing no rotation of the C1-16-17 group prior to the further cyclization to **B**, and is in line with similar results obtained for various other terpenes including 2-methylisoborneol, hypodoratoxide or pentalenolactone.^[18e,18f,21] A scrambling of labeling has so far only been observed in combination with 1,2-hydride shifts into an isopropyl group as in guaia-6,10(14)-diene and β-pinacene biosynthesis.^[22]

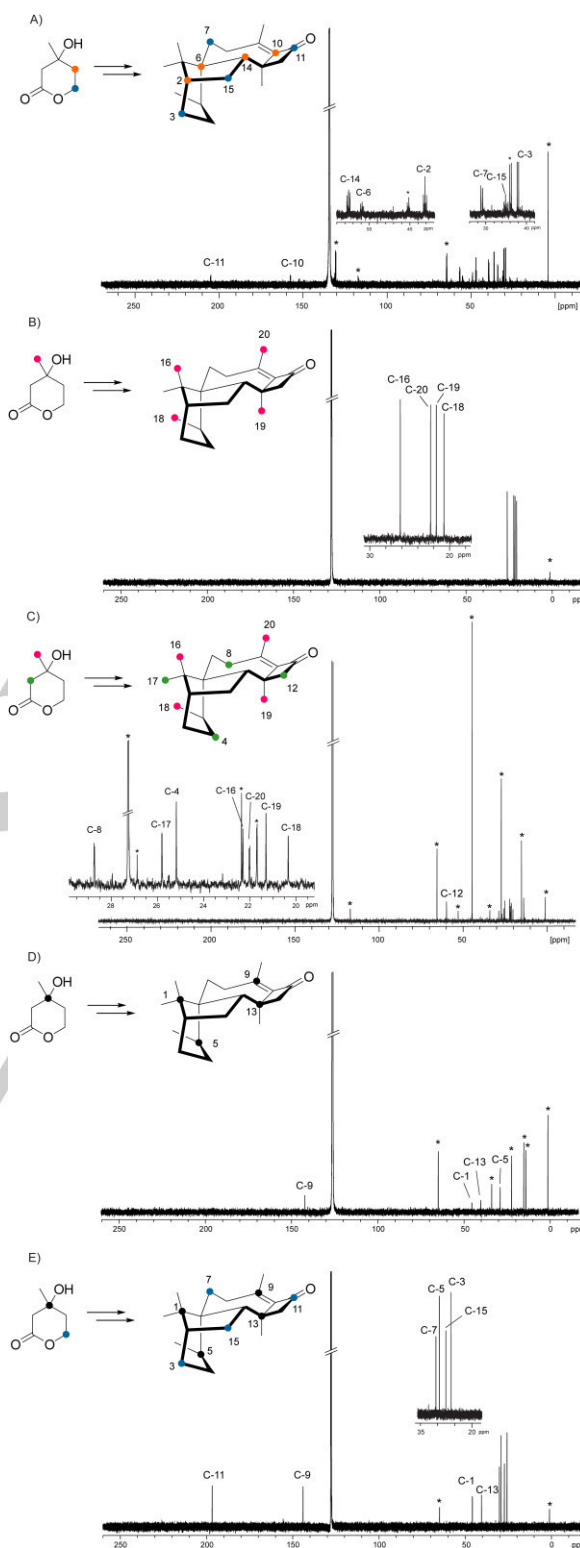
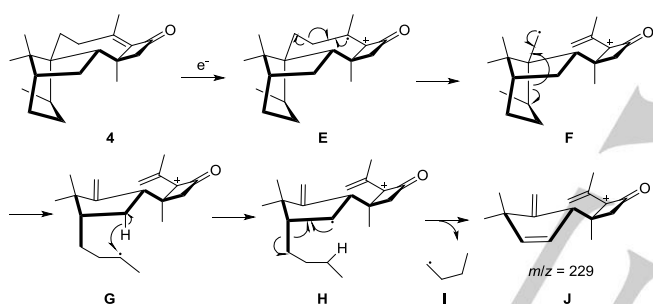


Figure 3. Results of feeding experiments. ¹³C-NMR spectra of CLSA extracts after feeding of A) (4,5-¹³C₂)-**10** (51% incorporation), B) (6-¹³C)-**10** (91% incorporation), C) (2,6-¹³C₂)-**10** (76% incorporation), D) (3-¹³C)-**10** (70% incorporation), E) (3,5-¹³C₂)-**10** (93% incorporation). Colored dots indicate ¹³C label. Asterisks indicate signals from solvent contaminations or other terpenoid signals.

For internal use, please do not delete. Submitted_Manuscript

The biosynthesis of **4** was further studied by feeding of deuterated mevalonolactones^[23] and analysis of the incorporation and fragment ions by GC/MS. The advantage of using deuterated precursors is the possible gas chromatographic separation of the obtained isotopologues of **4** due to their deuterium content (Figure S3). This allows for the interpretation of the mass spectra of the maximum deuterated isotopologues that are not overlapped with mass spectra of isotopologues with a lower deuterium content that can arise by dilution of the fed labeled material with mevalolactone synthesized by the fungus. The aim of the feeding experiments with the deuterated mevalonolactones was to prove the 1,2-hydride shift from **B** to **C** during the cyclization of GGPP to **14** as the precursor to **4**. This requires to localize the positions of incorporation of deuterium labelings from the EI mass spectra of deuterated **4**. For this purpose, an EI-MS fragmentation mechanism explaining the formation of the fragment ion at $m/z = 229$ was developed (Scheme 3). The electron impact ionization of **4** may result in radical cation **E** that can undergo two subsequent α -cleavage reactions via **F** to **G**. A hydrogen atom transfer results in **H** that produces cation **J** ($m/z = 229$) in another α -fragmentation with extrusion of a C_4H_9 radical (**I**).



Scheme 3. EI-MS fragmentation mechanism to fragment ion $m/z = 229$.

This hypothetical fragmentation mechanism was supported by the results from three feeding experiments. First, feeding of (6,6,6-²H₃)-**10** resulted in the incorporation of up to twelve deuterium atoms into **4**, as indicated by the molecular ion of $m/z = 298$. Fragment ion **J** was increased by 9 amu ($m/z = 238$, Figure 4A) which supports the suggested mechanism for its formation. Similarly, the feeding experiment with (2,2,6,6,6-²H₅)-**10** resulted in an increased molecular ion of deuterated **4** to $m/z = 306$ (Figure 4B), showing the incorporation of up to twenty deuterium atoms, fifteen of which end up in **J** (increased to $m/z = 244$), which is again in line with the mechanism of Scheme 3. Finally, feeding of (5,5,6,6,6-²H₅)-**10** produced deuterated **4** with a maximum deuterium content of eighteen deuterium atoms ($m/z = 304$, Figure 4C), two deuterium atoms are lost in the oxidation of **14** to **4**). Along the fragmentation pathway to **J** a hydrogen atom is suggested to be transferred from radical cation **G** to **H**, and this hydrogen atom is exchanged by deuterium in the feeding experiment with (5,5,6,6,6-²H₅)-**10**. As a consequence, fragment ion **J** is observed at $m/z = 241$. Taken together, all three feeding experiments support the fragmentation mechanism for **J** as shown in Scheme 3.

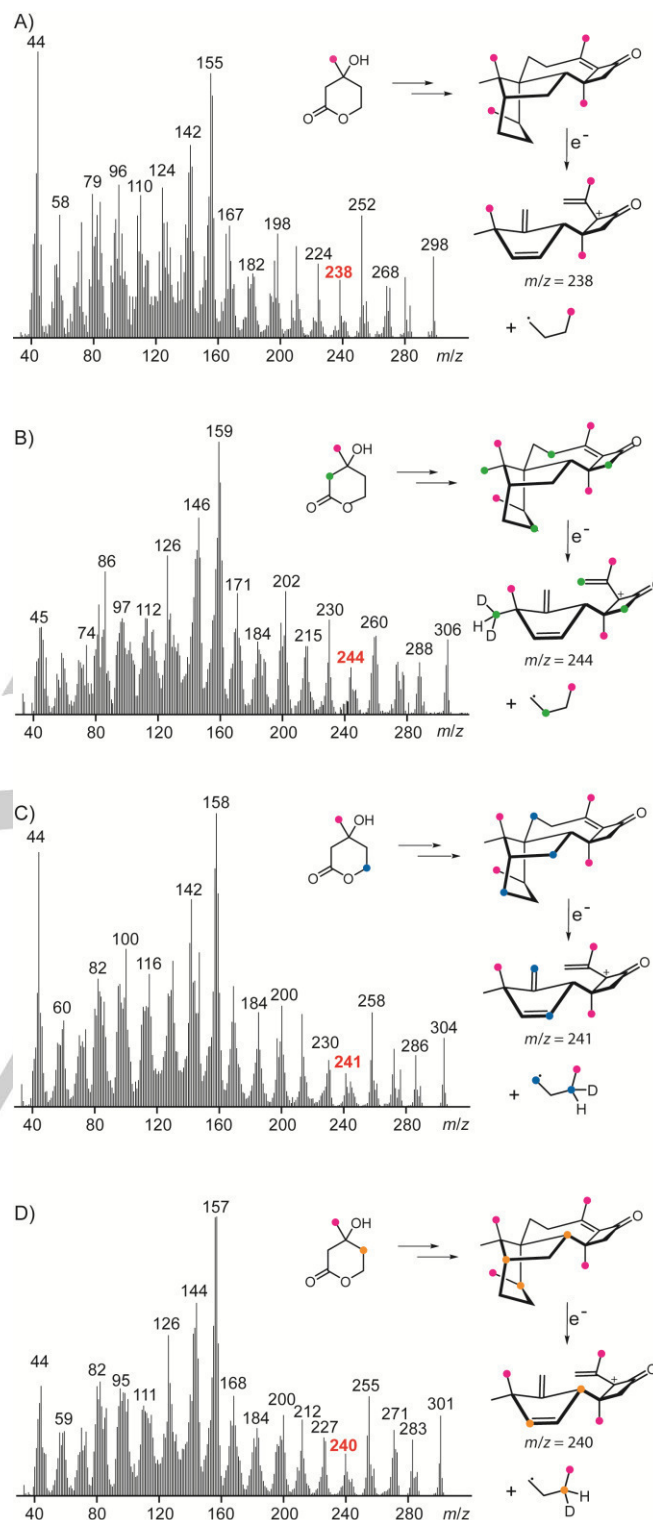


Figure 4. Results of feeding experiments with deuterated mevalonolactones. Mass spectrum of harzianone with highest deuterium incorporation after feeding of A) (6,6,6-²H₃)-**10**, B) (2,2,6,6,6-²H₅)-**10**, C) (5,5,6,6,6-²H₅)-**10**, D) (4,4,6,6,6-²H₅)-**10**. Colored dots indicate positions of ²H labelings.

For internal use, please do not delete. Submitted_Manuscript

The critical feeding experiment to follow the 1,2-hydride shift from intermediate **B** to **C** in the cyclization of GGPP to **4** was subsequently performed with (4,4,6,6,6-²H₅)-**10**. The expected labeling pattern of **4** with the maximum deuterium content is shown in Figure 4D. Notably, the 1,2-hydride shift should cause incorporation of labeling at C5 of **4**. The molecular ion of deuterated **4** was observed at $m/z = 301$, indicating the incorporation of fifteen of the sixteen deuterium atoms from GGPP into **4** (one deuterium atom is lost by the final deprotonation step from **D** to **14**). The fragment ion $m/z = 240$ shows incorporation of eleven of these deuterium atoms into **J**, in other words four deuterium atoms are extruded with fragment **I**. These findings are in line with the 1,2-hydride transfer from **B** to **C**.

Conclusions

In conclusion we analyzed the cyclization mechanism of the unique diterpene harzianone (**4**) by feeding of a series of isotopically labeled mevalonolactones. The results reveal a concise mechanism, resulting in a so far unknown diterpene, which is subsequently oxidized, presumably by a P450 monooxygenase, to harzianone (**4**) and related known terpenoids. Selective labeling of the Z-methyl group in geranylgeranyl diphosphate by feeding of (6-¹³C)-**10** revealed a strict stereochemical course for the first cyclization. The 1,2 hydride shift was monitored by selective labeling and careful analysis of EI mass spectrometric data. The early steps in harziane cyclization are identical to taxadiene biosynthesis,^[24] which may point to a shared evolutionary background of the respective terpene synthases. In this context it is interesting to note that *Trichoderma* symbionts isolated from *Taxus baccata* reportedly produce harziane diterpenes.^[16] Detection of harzianone (**4**) in all seven analyzed *Trichoderma* strains investigated in this study points to a conserved genetic occurrence of a harziane terpene synthase within this genus. Identification of the respective genes, followed by heterologous expression and *in vitro* testing are part of our ongoing investigations.

Experimental Section

Strains and growth conditions. *Trichoderma* sp. 34, *T. asperellum* 328, *T. citrinoviride* 596, *T. harzianum* 714, *T. longibrachiatum* 594 and *T. viride* 54 were obtained from Gabriele König (University of Bonn, Germany). *T. reesei* QM 6a was obtained from USDA. *T. asperellum*, *T. citrinoviride*, *T. reesei* and *T. viride* were cultivated at 28 °C in BM liquid medium (20 g malt extract per L of deionised water), and *Trichoderma* sp. 34, *T. harzianum* 714 and *T. longibrachiatum* were cultivated at 28 °C in BM-ASW liquid medium (20 g L⁻¹ malt extract, artificial sea water: 23.5 g NaCl, 10.6 g MgCl₂·6H₂O, 3.92 g Na₂SO₄, 1.47 g CaCl₂·2H₂O, 0.66 g KCl, 0.19 g NaHCO₃, 0.10 g KBr, 0.04 g SrCl₂·6H₂O, 0.03 g H₃BO₃) for 10 – 14 days, then inoculated on agar plates of BM or BM-ASW medium. The cultures were grown for 5 to 10 days and then analyzed by CLSA.

Collection of volatiles. The emitted volatiles were collected by use of a closed-loop stripping apparatus (CLSA, Chromtech GmbH, Idstein, Precision Charcoal Filter 5 mg). Sampling was conducted for 16 – 20 h and the adsorbed volatiles were eluted by extraction with analytically pure dichloromethane (40–50 μL).

Feeding experiments. Feeding experiments were performed with *Trichoderma* sp. 34 and synthetic isotopically labeled mevalonolactones (10 mg) were directly added to the medium for agar plate cultures (ca. 30 mL). *Trichoderma* sp. 34 was inoculated on the agar plates and grown for 5 – 10 days, followed by CLSA-sampling. For feeding experiments with (2,3,4,5,6-¹³C₅)-, (3-¹³C)-, (3,5-¹³C₂)-, (4,5-¹³C₂)-, (2,6-¹³C₂)- and (6-¹³C)-**10** the volatiles were collected for 7 days and daily extraction of the charcoal filter, using C₆D₆ (7 x 50 μL) as solvent was conducted. The crude extracts were directly analyzed by NMR spectroscopy. For feeding of (6,6,6-²H₃)-, (2,2,6,6,6-²H₅)-, (4,4,6,6,6-²H₅) and (5,5,6,6,6-²H₅)-**10**, sampling was conducted for 16 – 20 h and analytically pure dichloromethane was used for extraction (50 μL).

GC/MS Analysis. The obtained headspace extracts were analyzed by use of an Agilent HP7890B gas chromatograph, fitted with a HP-5MS silica capillary column (30 m, 0.25 mm i. d., 0.50 μm film), connected to a HP5977A mass detector. The GC/MS conditions were as follows: (1) inlet pressure: 77.1 kPa, He flow 23.3 mL/min; (2) injection volume: 1 μL; (3) injection mode: splitless, valve time 60 s; (4) oven temperature ramp: 5 min at 50 °C increasing at 5 °C/min to 320 °C; (5) carrier gas He at 1 mL/min; (6) transfer line: 250 °C; (7) electron energy: 70 eV. Retention indices (*I*) were determined from a homologous series of *n*-alkanes (C₈-C₄₀).

General Synthetic Methods. All chemicals were obtained from Acros Organics (Geel, Belgium), Sigma Aldrich Chemie GmbH (Steinheim, Germany) or TCI Deutschland GmbH (Eschborn, Germany). Utilized solvents were purified by distillation. Whenever necessary, reactions were carried out under inert atmosphere (Ar) using vacuum-heated flasks and dry solvents (dried according to standard protocols). Thin layer chromatography (TLC) was performed on 0.20 mm silica plates (Polygram SIL G/UV254) obtained from Macherey-Nagel (Düren, Germany). Column chromatography was performed on Merck silica gel (0.040 – 0.063 Mesh). NMR spectra were recorded on Bruker AV I (400 MHz), AV III HD Prodigy (500 MHz) and AV III HD Cryo (700 MHz) spectrometers, and were referenced against CDCl₃ (δ = 7.26 ppm), C₆D₆ (δ = 7.16 ppm) and d₆-DMSO (δ = 2.50 ppm) for ¹H NMR, and CDCl₃ (δ = 77.01 ppm), C₆D₆ (δ = 128.06 ppm) and d₆-DMSO (δ = 39.52 ppm) for ¹³C-NMR. The multiplicities are specified as follows: singlet (s), doublet (d), triplet (t), quartet (q), quintet (quin), sextet (sex), septet (sept). GC/MS analyses were carried out with an Agilent HP7890B gas chromatograph connected to a HP5977A mass detector fitted with a HP-5MS silica capillary column (30 m, 0.25 mm i. d., 0.50 μm film). The GC-MS conditions were as follows: (1) inlet pressure: 77.1 kPa, He flow 23.3 mL/min; (2) injection volume: 1 μL; (3) injection mode: split 50:1, valve time 60 s; (4) oven temperature ramp: 5 min at 50 °C increasing at 10 °C/min to 320 °C; (5) carrier gas He at 1 mL/min; (6) transfer line: 250 °C; (7) electron energy: 70 eV. Retention indices (*I*) were determined from a homologous series of *n*-alkanes (C₈-C₄₀). Optical rotary powers were recorded on a P8000 Polarimeter (Krüss).

Synthetic procedures

Synthesis of ethyl (1,2-¹³C₂)-2-(2,5,5-trimethyl-1,3-dioxan-2-yl)acetate (S1). Ethyl (1,2-¹³C₂)acetoacetate (>99% ¹³C, 1.00 g, 7.68 mmol, 1.0 equiv.) and neopentyl glycol (1.76 g, 16.9 mmol, 2.2 equiv.) were dissolved in dry dichloromethane (35 mL) and freshly distilled TMSCl (3.67 g, 33.8 mmol, 4.4 equiv.) was added. The reaction mixture

For internal use, please do not delete. Submitted_Manuscript

was heated to reflux overnight and neutralized with an aqueous solution of NaHCO₃ (5 wt %) followed by extraction with dichloromethane (3 x 10 mL). The organic layers were combined and dried with MgSO₄ and the solvent was removed under reduced pressure. The crude product was purified by column chromatography on silica gel (ethyl acetate/hexane; 1:10 v/v, *R_f* = 0.2) to yield **S1** as a colorless oil (1.64 g, 7.50 mmol, 98%). GC (BPX-5): *I* = 1349. ¹H-NMR (400 MHz, CDCl₃): δ [ppm] = 4.15 (dq, ³J_{H,H} = 7.1 Hz, ³J_{C,H} = 3.1 Hz, 2H, CH₂), 3.56 (d, ²J_{H,H} = 11.4 Hz, 2H, CHH), 3.49 (d, ²J_{H,H} = 11.4 Hz, 2H, CHH), 2.78 (dd, ¹J_{C,H} = 130.3 Hz, ²J_{C,H} = 6.9 Hz, 2H, CH₂), 1.53 (d, ³J_{C,H} = 2.9 Hz, 3H, CH₃), 1.26 (t, ³J_{H,H} = 7.1 Hz, 3H, CH₃), 0.97 (s, 3H, CH₃), 0.94 (s, 3H, CH₃). ¹³C-NMR (100 MHz, CDCl₃): δ [ppm] = 169.7 (d, ¹J_{C,C} = 58.9 Hz, C_q), 97.3 (d, ¹J_{C,C} = 44.4 Hz, C_q), 70.6 (d, ³J_{C,C} = 1.6 Hz, 2 x CH₂), 60.7 (d, ²J_{C,C} = 1.9 Hz, CH₂), 41.7 (d, ¹J_{C,C} = 58.9 Hz, CH₂), 29.9 (s, C_q), 22.8 (d, ²J_{C,C} = 4.0 Hz, CH₃), 22.6 (s, CH₃), 22.5 (s, CH₃), 14.2 (d, ³J_{C,C} = 2.0 Hz, CH₃). EI-MS (70 eV): *m/z* (%) = 203 (36), 133 (29), 129 (100), 117 (18), 105 (12), 87 (31), 69 (54), 56 (36), 43 (98), 41 (49).

Synthesis of (1,2-¹³C₂)-2-(2-(benzyloxy)ethyl)-2,5,5-trimethyl-1,3-dioxane (S2). LiAlH₄ (0.29 g, 7.50 mmol, 1.0 equiv.) was suspended in 5 mL dry THF and cooled to 0 °C. A solution of **S1** (1.64 g, 7.50 mmol, 1.0 equiv.) in 5 mL dry THF was added and the reaction was stirred at room temperature for 2 h, followed by addition of water until a white suspension was formed. The mixture was filtered and the obtained organic phase was dried with MgSO₄. The solvent was removed under reduced pressure and the crude product was purified by column chromatography (ethyl acetate/hexane; 1:2 v/v, *R_f* = 0.2). The resulting alcohol was used immediately in the next step. The alcohol (1.13 g, 6.40 mmol, 1.0 equiv.) was added dropwise at 0 °C to a suspension of NaH (0.17 g, 7.04 mmol, 1.1 equiv.) in 15 mL dry DMF. After stirring for 15 min benzyl bromide (1.09 g, 6.40 mmol, 1.0 equiv.) was added dropwise and the reaction mixture was stirred at room temperature over night. After addition of water, the mixture was extracted with dichloromethane (3 x 10 mL). The organic layers were combined and washed with water, dried over MgSO₄ and the solvent was removed under reduced pressure. The residue was purified by column chromatography on silica gel (ethyl acetate/hexane; 1:10 v/v, *R_f* = 0.3) to yield product **S2** (1.40 g, 5.10 mmol, 69% over 2 steps) as a colourless oil. GC (BPX-5): *I* = 1878. ¹H-NMR (400 MHz, *d₆*-DMSO): δ [ppm] = 7.36 - 7.23 (m, 5H, C₆H₅), 4.43 (d, ³J_{C,H} = 3.9 Hz, 2H, CH₂), 3.53 (ddt, ¹J_{C,H} = 141.5 Hz, ³J_{H,H} = 7.3 Hz, ²J_{C,H} = 2.9 Hz, 2H, CH₂), 3.46 (d, ²J_{H,H} = 11.3 Hz, 2H, CHH), 3.34 (d, ²J_{H,H} = 11.3 Hz, 2H, CHH), 1.94 (ddt, ¹J_{C,H} = 126.7 Hz, ³J_{H,H} = 6.7 Hz, ²J_{C,H} = 6.7 Hz, 2H, CH₂), 1.30 (d, ³J_{C,H} = 2.9 Hz, 3H, CH₃), 0.90 (s, 3H, CH₃), 0.81 (s, 3H, CH₃). ¹³C-NMR (100 MHz, CDCl₃): δ [ppm] = 138.6 (d, ³J_{C,C} = 3.0 Hz, C_q), 128.2 (s, 2 x CH), 127.4 (s, 2 x CH), 127.3 (s, CH), 97.5 (d, ¹J_{C,C} = 46.2 Hz, C_q), 71.9 (dd, ²J_{C,C} = 3.6 Hz, ³J_{C,C} = 1.4 Hz, CH₂), 69.2 (d, ³J_{C,C} = 1.8 Hz, 2 x CH₂), 65.6 (d, ¹J_{C,C} = 39.3 Hz, CH₂), 37.9 (d, ¹J_{C,C} = 39.3 Hz, CH₂), 29.5 (s, C_q), 22.4 (s, CH₃), 22.1 (s, CH₃), 20.9 (d, ³J_{C,C} = 3.3 Hz, CH₃). EI-MS (70 eV): *m/z* (%) = 251 (26), 179 (2), 162 (7), 129 (78), 107 (29), 91 (100), 69 (45), 56 (29), 43 (66), 41 (45).

Synthesis of (3,4-¹³C₂)-4-(benzyloxy)butan-2-one (S3). Compound **S2** (1.40 g, 5.10 mmol, 1 equiv.) was dissolved in 25 mL MeOH and 3 mL of a 1.0 M solution of HCl in water was added. The reaction was stirred at room temperature for 15 minutes followed by neutralization with an aqueous solution of NaHCO₃ (5 wt %). The aqueous phase was extracted with Et₂O (3 x 10 mL) and the combined organic layers were dried with MgSO₄. The solvent was removed under reduced pressure and the residue was purified by column chromatography on silica gel (ethyl acetate/hexane; 1:5 v/v, *R_f* = 0.2) to yield product **S3** (0.90 g, 5.00 mmol, 99%) as a colorless oil. GC (BPX-5): *I* = 1467. ¹H-NMR (400 MHz, CDCl₃): δ [ppm] = 7.37 - 7.25 (m, 5H, C₆H₅), 4.51 (d, ³J_{C,H} = 4.3 Hz, 2H, CH₂), 3.74 (ddt, ¹J_{C,H} = 143.2 Hz, ³J_{H,H} = 6.3 Hz, ²J_{C,H} = 2.8 Hz, 2H, CH₂), 2.72 (ddt, ¹J_{C,H} = 126.0 Hz, ³J_{H,H} = 6.3 Hz, ²J_{C,H} = 4.9 Hz, 2H, CH₂), 2.18

(d, ³J_{C,H} = 1.3 Hz, 3H, CH₃). ¹³C-NMR (100 MHz, CDCl₃): δ [ppm] = 207.1 (dd, ¹J_{C,C} = 40.6 Hz, ²J_{C,C} = 1.7 Hz, C_q), 138.1 (d, ³J_{C,C} = 2.9 Hz, C_q), 128.4 (s, 2 x CH), 127.7 (s, 2 x CH), 127.6 (s, CH), 73.2 (dd, ²J_{C,C} = 3.9 Hz, ³J_{C,C} = 1.4 Hz, CH₂), 65.3 (d, ¹J_{C,C} = 39.8 Hz, CH₂), 43.7 (d, ¹J_{C,C} = 39.8 Hz, CH₂), 30.4 (d, ²J_{C,C} = 14.2 Hz, CH₃). EI-MS (70 eV): *m/z* (%) = 121 (21), 107 (59), 91 (100), 79 (39), 77 (37), 65 (38), 59 (12), 43 (90).

Synthesis of ethyl (4,5-¹³C₂)-5-(benzyloxy)-3-hydroxy-3-methylpentanoate (S4). Diisopropylamine (1.06 g, 10.5 mmol, 2.1 equiv.) was dissolved in 50 mL dry THF and a 1.6 M solution of *n*-butyllithium (6.56 mL, 10.5 mmol, 2.1 equiv.) in hexane was added at 0 °C. The reaction mixture was stirred for 1 h at 0 °C and then cooled to -78 °C. A solution of ethyl acetate (0.93 g, 10.5 mmol, 2.1 equiv.) in 20 mL dry THF was added dropwise and the reaction mixture was stirred for 30 min. A solution of **S3** (0.90 g, 5.00 mmol, 1.0 equiv.) in 15 mL dry THF was added dropwise and the mixture was stirred for 1 h, quenched by addition of water and allowed to warm to room temperature. The reaction mixture was extracted with ethyl acetate (3 x 15 mL) and the combined organic layers were dried with MgSO₄. The solvent was removed under reduced pressure and the residue was purified by column chromatography on silica gel (ethyl acetate/hexane; 1:5 v/v, *R_f* = 0.2) to yield product **S4** (1.10 g, 4.10 mmol, 82%) as a colorless oil. GC (BPX-5): *I* = 1916. ¹H-NMR (400 MHz, CDCl₃): δ [ppm] = 7.33 - 7.17 (m, 5H, C₆H₅), 4.43 (d, ³J_{C,H} = 4.0 Hz, 2H, CH₂), 4.11 - 4.02 (m, 2H, CH₂), 3.90 (d, ³J_{C,H} = 2.4 Hz, 1H, OH), 3.62 (ddt, ¹J_{C,H} = 141.9 Hz, ³J_{H,H} = 6.2 Hz, ²J_{C,H} = 2.8 Hz, 2H, CH₂), 2.52 (dd, ²J_{H,H} = 15.2 Hz, ³J_{C,H} = 2.9 Hz, 1H, CHH), 2.43 (dd, ²J_{H,H} = 15.2 Hz, ³J_{C,H} = 2.9 Hz, 1H, CHH), 1.85 (ddt, ¹J_{C,H} = 126.3 Hz, ³J_{H,H} = 6.2 Hz, ²J_{C,H} = 4.6 Hz, 2H, CH₂), 1.21 (d, ³J_{C,H} = 3.7 Hz, 3H, CH₃), 1.18 (t, ³J_{H,H} = 7.1 Hz, 3H, CH₃). ¹³C-NMR (100 MHz, CDCl₃): δ [ppm] = 172.6 (d, ³J_{C,C} = 2.3 Hz, C_q), 138.1 (d, ³J_{C,C} = 2.6 Hz, C_q), 128.5 (s, 2 x CH), 127.8 (s, CH), 127.8 (s, 2 x CH), 73.4 (dd, ²J_{C,C} = 3.9 Hz, ³J_{C,C} = 1.4 Hz, CH₂), 70.9 (dd, ¹J_{C,C} = 38.5 Hz, ²J_{C,C} = 1.33 Hz, C_q), 67.1 (d, ¹J_{C,H} = 38.8 Hz, CH₂), 60.6 (s, CH₂), 45.5 (dd, ²J_{C,C} = 1.9 Hz, ³J_{C,C} = 1.9 Hz, CH₂), 40.3 (d, ¹J_{C,C} = 38.5 Hz, CH₂), 27.1 (dd, ²J_{C,C} = 1.9 Hz, ³J_{C,C} = 1.9 Hz, CH₃), 14.1 (s, CH₃). EI-MS (70 eV): *m/z* (%) = 181 (1), 162 (21), 144 (13), 132 (8), 113 (7), 91 (100), 65 (20), 43 (38).

Synthesis of (4,5-¹³C₂)mevalonolactone ((4,5-¹³C₂)-10). Compound **S4** (1.10 g, 4.10 mmol, 1 equiv.) was dissolved in 40 mL MeOH and Pd/C (5 wt %, 0.05 equiv.) was added. The mixture was stirred at 40 °C under a hydrogen atmosphere (40 bar) for 2 h. The Pd/C catalyst was removed by filtration over celite and the organic phase was concentrated under reduced pressure. The residue was dissolved in 40 mL dichloromethane and catalytic amounts of *p*-TsOH were added. The reaction mixture was stirred at room temperature over night followed by removal of the solvent under reduced pressure and purification of the residue by column chromatography (ethyl acetate/hexane; 1:1 v/v, *R_f* = 0.1) to yield (4,5-¹³C₂)-**10** (0.33 g, 2.50 mmol, 62%) as a colorless oil. GC (BPX-5, MSTFA): *I* = 1390. ¹H-NMR (400 MHz, CDCl₃): δ [ppm] = 4.53 (dm, ¹J_{C,H} = 150.4 Hz, 1H, CHH), 4.32 (dm, ¹J_{C,H} = 150.4 Hz, 1H, CHH), 2.65 (ddd, ²J_{H,H} = 17.4 Hz, ³J_{C,H} = 3.5 Hz, ⁴J_{H,H} = 1.7 Hz, 1H, CHH), 2.53 (dd, ²J_{H,H} = 17.4 Hz, ³J_{C,H} = 1.5 Hz, 1H, CHH), 1.87 (dm, ¹J_{C,H} = 130.6 Hz, 2H, CH₂), 1.32 (d, ³J_{C,H} = 4.2 Hz, 3H, CH₃). ¹³C-NMR (100 MHz, CDCl₃): δ [ppm] = 170.8 (s, C_q), 68.3 (dd, ¹J_{C,C} = 37.1 Hz, ²J_{C,C} = 2.3 Hz, C_q), 66.2 (d, ¹J_{C,C} = 34.9 Hz, CH₂), 44.5 (d, ²J_{C,C} = 1.7 Hz, CH₂), 35.0 (d, ¹J_{C,C} = 34.9 Hz, CH₂), 29.9 (dd, ²J_{C,C} = 1.9 Hz, ³J_{C,C} = 1.9 Hz, CH₃). EI-MS (70 eV, MSTFA): *m/z* (%) = 189 (12), 147 (100), 145 (39), 117 (47), 116 (48), 75 (51), 73 (45), 45 (24).

Isolation of harzianone (4). *Trichoderma* sp. 34 was precultured at 28 °C in liquid BM-ASW medium for 10 - 14 days and then inoculated on 100 agar plates using 3 L BM-ASW medium. The cultures were grown for 21 days, cut in small pieces and extracted with pentane. After removal of

For internal use, please do not delete. Submitted_Manuscript

the solvent under reduced pressure the residue was purified by column chromatography on silica gel (diethyl ether/pentane; 20:1 to 5:1 v/v, R_f = 0.3) to yield harzianone (**4**) (3.8 mg, 0.01 mmol). GC (HP-5MS) = 2280. $^1\text{H-NMR}$ (700 MHz, C_6D_6): δ [ppm] = 2.33 (d, 2J = 15.8 Hz, 1H, *CHH*), 2.24 (d, 2J = 15.8 Hz, 1H, *CHH*), 2.20 (dd, 3J = 7.8 Hz, 2J = 7.8 Hz, 1H, CH), 2.06 (s, 3H, CH_3), 2.04 (m, 1H, *CHH*), 1.97 (dd, 3J = 11.4 Hz, 3J = 8.9 Hz, 1H, CH), 1.92 (m, 1H, *CHH*), 1.86 (m, 1H, *CHH*), 1.60 (m, 1H, *CHH*), 1.51 (m, 1H, CH), 1.49 (m, 1H, *CHH*), 1.42 (m, 1H, *CHH*), 1.24 (s, 3H, CH_3), 1.21 (m, 1H, *CHH*), 1.12 (m, 1H, *CHH*), 1.11 (m, 1H, *CHH*), 1.03 (m, 1H, *CHH*), 0.94 (s, 3H, CH_3), 0.86 (d, 3J = 7.5 Hz, 3H, CH_3), 0.70 (s, 3H, CH_3). $^{13}\text{C-NMR}$ (175 MHz, C_6D_6): δ [ppm] = 197.0 (C_q), 150.8 (C_q), 144.3 (C_q), 60.2 (CH_2), 52.6 (CH), 50.9 (C_q), 46.2 (C_q), 43.2 (CH), 40.9 (C_q), 30.5 (CH_2), 29.5 (CH), 29.1 (CH_2), 27.6 (CH_2), 26.2 (CH_3), 25.7 (CH_2), 25.6 (CH_2), 22.7 (CH_3), 22.4 (CH_3), 21.7 (CH_3), 20.7 (CH_3). $[\alpha]_{\text{D}}^{21}$ = +21.0 (c 0.1, MeOH). EI-MS (70 eV): m/z (%) = 286 (23), 271 (34), 257 (40), 243 (60), 229 (30), 215 (40), 202 (46), 189 (51), 173 (34), 159 (57), 149 (100), 136 (66), 121 (89), 105 (71), 91 (94), 79 (89), 55 (60), 41 (86).

Acknowledgements

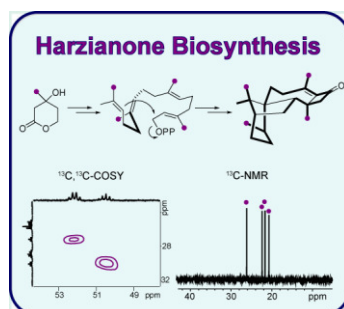
We thank Gabriele König (Bonn) for the *Trichoderma* strains. This work was funded by the DFG (DI1536/9-1).

Keywords: biosynthesis • terpenoids • isotopic labeling • mass spectrometry • NMR spectroscopy

- [1] C. P. Kubicek, G. E. Harman in *Trichoderma & Gliocladium*, Vol. 1, Taylor & Francis, London, **2002**.
- [2] G. E. Harman, C. R. Howell, A. Viterbo, I. Chet, M. Lorito, *Nature Rev. Microbiol.* **2004**, *2*, 43-56.
- [3] a) F. Vinale, K. Sivasithamparam, E. L. Ghisalberti, R. Marra, S. L. Woo, M. Lorito, *Soil Biol. Biochem.* **2008**, *40*, 1-10; b) G. E. Harman, *Phytopathology* **2006**, *96*, 190-194.
- [4] R. Hermosa, R. E. Cardoza, M. B. Rubio, S. Gutiérrez, E. Monte in *Biotechnology and Biology of Trichoderma*, (Eds.: V. Gupta, M. Schmoll, A. Herrera-Estrella, R. Upadhyay, R. Druzhinia, M. Tuohy), Elsevier, Amsterdam, **2014**.
- [5] a) R. Weindling, O. H. Emerson, *Phytopathology* **1936**, *26*, 1068-1070; b) P. W. Brian, *Nature* **1944**, *154*, 667-668.
- [6] D. H. Scharf, A. A. Brakhage, P. K. Mukherjee, *Environ. Microbiol.* **2015**, *18*, 1096-1109.
- [7] J. S. Dickschat, *Nat. Prod. Rep.* **2017**, *34*, 310-328.
- [8] a) R. P. Collins, A. F. Halim, *J. Agric. Food Chem.* **1972**, *20*, 437-438; b) M. O. Moss, R. M. Jackson, D. Rogers, *Phytochemistry* **1975**, *14*, 2706-2708; c) N. Claydon, M. Allan, J. R. Hanson, A. G. Avent, *Trans. Br. Mycol. Soc.* **1987**, *88*, 503-513; d) A. Evidente, A. Cabras, L. Maddau, S. Serra, A. Andolfi, A. Motta, *J. Agric. Food Chem.* **2003**, *51*, 6957-6960; e) J. L. Reino, R. F. Guerrero, R. Hernández-Galán, I. G. Collando, *Phytochem. Rev.* **2008**, *7*, 89-123; f) S. M. Wickel, C. A. Citron, J. S. Dickschat, *Eur. J. Org. Chem.* **2013**, 2906-2913.
- [9] a) N. Claydon, M. Allan, J. R. Hanson, A. G. Avent, *Trans. Br. Mycol. Soc.* **1987**, *88*, 503-513; b) A. Evidente, A. Cabras, L. Maddau, S. Serra, A. Andolfi, A. Motta, *J. Agric. Food Chem.* **2003**, *51*, 6957-6960; c) N. Kishimoto, S. Sugihara, K. Mochida, T. Fujita, *Biocontrol Sci.* **2005**, *10*, 31-36.
- [10] Q. Huang, Y. Tezuka, Y. Hatanaka, T. Kikuchi, A. Nishi, K. Tubaki, *Chem. Pharm. Bull.*, **1995**, *43*, 1035-1038.
- [11] N. L. Brock, J. S. Dickschat, *Eur. J. Org. Chem.* **2011**, 5167-5175.
- [12] a) C. A. Citron, R. Riclea, N. L. Brock, J. S. Dickschat, *RSC Advances* **2011**, *1*, 290-297; b) C. A. Citron, J. S. Dickschat, *Org. Biomol. Chem.* **2013**, *11*, 7447-7450.
- [13] F.-P. Miao, X.-R. Liang, X.-L. Yin, G. Wang, N.-Y. Ji, *Org. Lett.* **2012**, *14*, 3815-3817.
- [14] E. L. Ghisalberti, D. C. R. Hockless, C. Rowland, A. H. White, *J. Nat. Prod.* **1992**, *11*, 1690-1694.
- [15] S. Chantrapromma, C. Jeerapong, W. Phupong, C. K. Quah, H.-K. Fun, *Acta. Cryst.* **2014**, *E70*, o408-o409.
- [16] E. Adelin, C. Servy, M.-T. Martin, G. Arcile, B. I. Iorga, P. Retailleau, M. Bonfill, J. Ouazzani, *Phytochemistry* **2014**, *97*, 55-61.
- [17] L. Mannina, A. L. Segre, A. Ritiene, V. Fogliano, F. Vinale, G. Randazzo, L. Maddau, A. Bottalico, *Tetrahedron* **1997**, *9*, 3135-3144.
- [18] a) N. L. Brock, S. R. Ravella, S. Schulz, J. S. Dickschat, *Angew. Chem.* **2013**, *125*, 2154-2158; *Angew. Chem. Int. Ed.* **2013**, *52*, 2100-2104; b) R. Riclea, C. A. Citron, J. Rinkel, J. S. Dickschat, *ChemComm* **2014**, *50* 4228-4230; c) N. L. Brock, J. S. Dickschat, *ChemBioChem* **2013**, *14*, 1189-1193; d) C. A. Citron, N. L. Brock, B. Tudzynski, J. S. Dickschat, *ChemComm* **2014**, *50*, 5224-5226; e) L. Barra, B. Schulz, J. S. Dickschat, *ChemBioChem* **2014**, *15*, 2379-2383; f) L. Barra, K. Ibrum, J. S. Dickschat, *Angew. Chem. Int. Ed.* **2015**, *54*, 6637-6640.
- [19] a) K. Grob, F. Zürcher, *J. Chromatogr.* **1976**, *117*, 285-294; b) J. S. Dickschat, S. C. Wenzel, H. B. Bode, R. Müller, S. Schulz, *ChemBioChem* **2004**, *5*, 778-787.
- [20] L. O. Zamir, C.-D. Nguyen, *J. Label. Compd. Radiopharm.* **1988**, *25*, 1189-1196.
- [21] a) P. Rabe, J. Rinkel, B. Nubbemeyer, T. G. Köllner, F. Chen, J. S. Dickschat, *Angew. Chem. Int. Ed.* **2016**, *55*, 15420-15423; b) P. Rabe, J. Rinkel, E. Dolja, T. Schmitz, B. Nubbemeyer, T. H. Luu, J. S. Dickschat, *Angew. Chem. Int. Ed.* **2017**, *56*, 2776-2779; c) D. E. Cane, T. Rossi, A. M. Tillman, J. P. Pachlatko, *J. Am. Chem. Soc.* **1981**, *103*, 1838-1843; d) C.-M. Wang, R. Hopson, X. Lin, D. E. Cane, *J. Am. Chem. Soc.* **2009**, *131*, 8360-8361; e) N. L. Brock, S. R. Ravella, S. Schulz, J. S. Dickschat, *Angew. Chem. Int. Ed.* **2013**, *52*, 2100-2104; f) T. A. Klapschinski, P. Rabe, J. S. Dickschat, *Angew. Chem. Int. Ed.* **2016**, *55*, 10141-10144.
- [22] a) I. Burkhardt, T. Siemon, M. Henrot, L. Studt, S. Rösler, B. Tudzynski, M. Christmann, J. S. Dickschat, *Angew. Chem. Int. Ed.* **2016**, *55*, 8748-8751; b) J. Rinkel, P. Rabe, X. Chen, T. G. Köllner, F. Chen, J. S. Dickschat, *Chem. Eur. J.* **2017**, *23*, 10501-10505.
- [23] J. S. Dickschat, C. A. Citron, N. L. Brock, R. Riclea, H. Kuhz, *Eur. J. Org. Chem.* **2011**, 3339-3346.
- [24] M. Köksal, Y. Jin, R. M. Coates, R. Croteau, D. W. Christianson, *Nature* **2011**, *469*, 116-120; b) Q. Jin, D. C. Williams, M. Hezari, R. Croteau, R. M. Coates, *J. Org. Chem.* **2005**, *70*, 4667-4675; c) Y. J. Hong, D. J. Tantillo, *J. Am. Chem. Soc.* **2011**, *133*, 18249-18256.

FULL PAPER

The cyclization mechanism of the bioactive, unique tetracyclic diterpene harzianone, produced by the biocontrol fungus *Trichoderma*, was studied by feeding experiments using synthetic mevalonolactone isotopologues, capturing with a closed-loop stripping apparatus and direct analysis by ^{13}C -NMR spectroscopic methods (CLSA-NMR) or GC/MS.



Lena Barra and Jeroen S. Dickschat*

Page No. – Page No.

Harzianone Biosynthesis by the Biocontrol Fungus *Trichoderma*

CHEM**BIO**CHEM

Supporting Information

Harzianone Biosynthesis by the Biocontrol Fungus *Trichoderma*

Lena Barra and Jeroen S. Dickschat^{*[a]}

cbic_201700462_sm_miscellaneous_information.pdf

TABLE OF CONTENTS

1. CLSA HEADSPACE EXTRACTS OF TRICHODERMA STRAINS	2
2. RESULTS OF FEEDING EXPERIMENTS WITH ^{13}C -LABELED 10	3 – 4
3. SYNTHESIS OF (4,5- $^{13}\text{C}_2$)- 10	5
4. RESULTS OF FEEDING EXPERIMENTS WITH ^2H -LABELED 10	6
5. NMR SPECTRA FOR HARZIANONE (4) AND SYNTHETIC COMPOUNDS	7 – 28

1. CLSA HEADSPACE EXTRACTS OF TRICHODERMA STRAINS

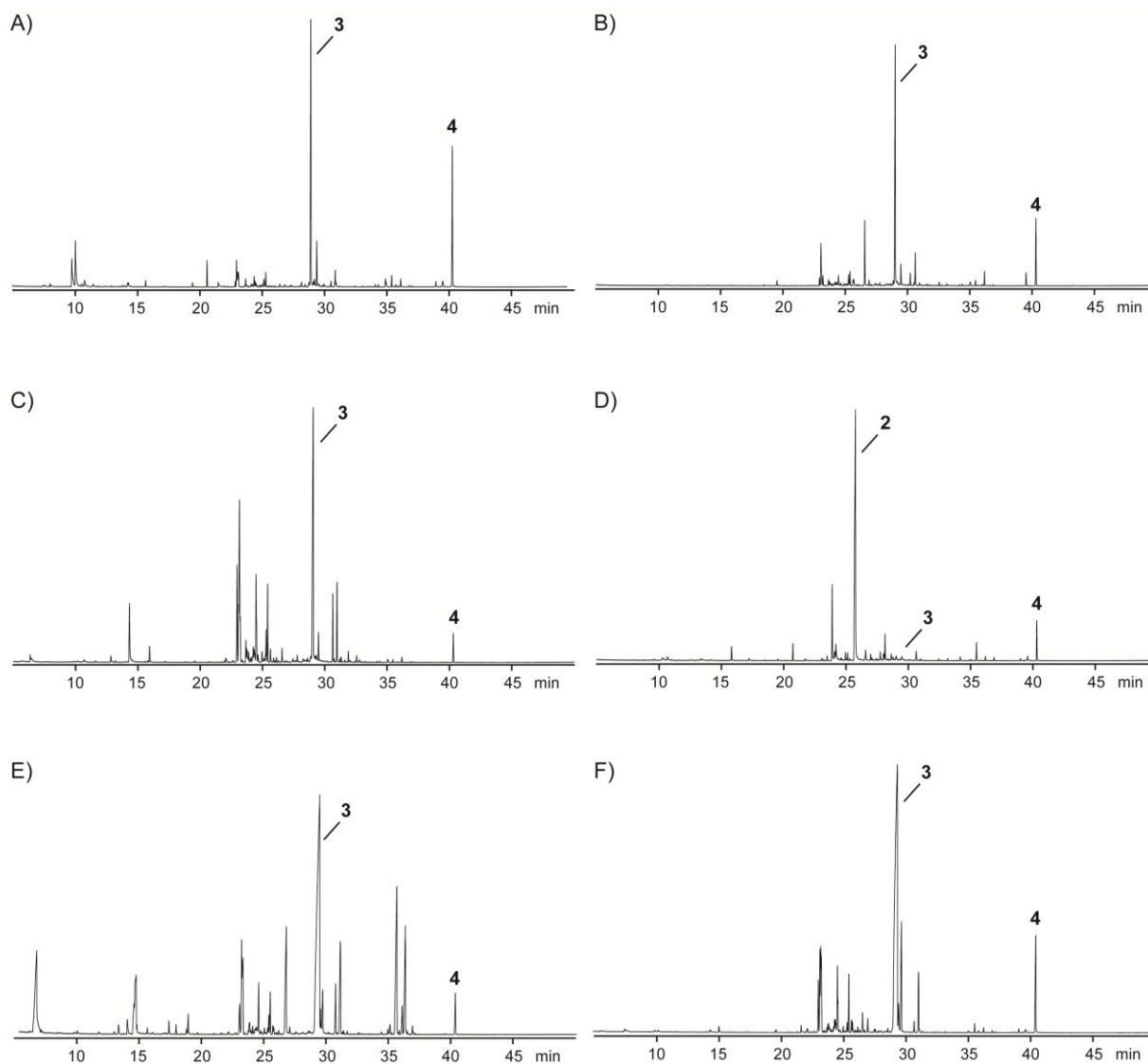
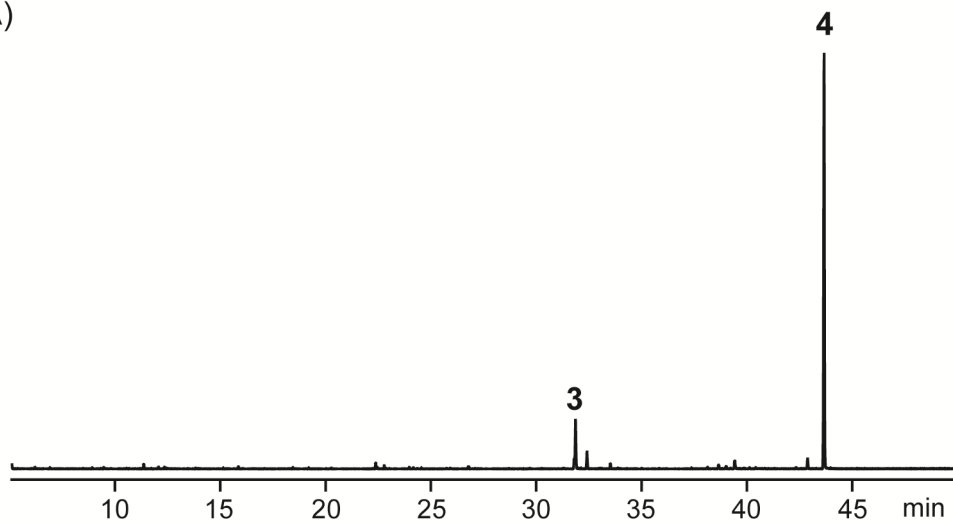


Figure S1. Total ion chromatograms of the headspace extracts of A) *T. citrinoviride*, B) *T. longibrachiatum*, C) *T. viride*, D) *T. asperellum*, E) *T. reesei* and F) *T. harzianum*. Numbers at peaks refer to compound numbers in main text.

2. RESULTS OF FEEDING EXPERIMENTS WITH ^{13}C -LABELED 10

A)



B)

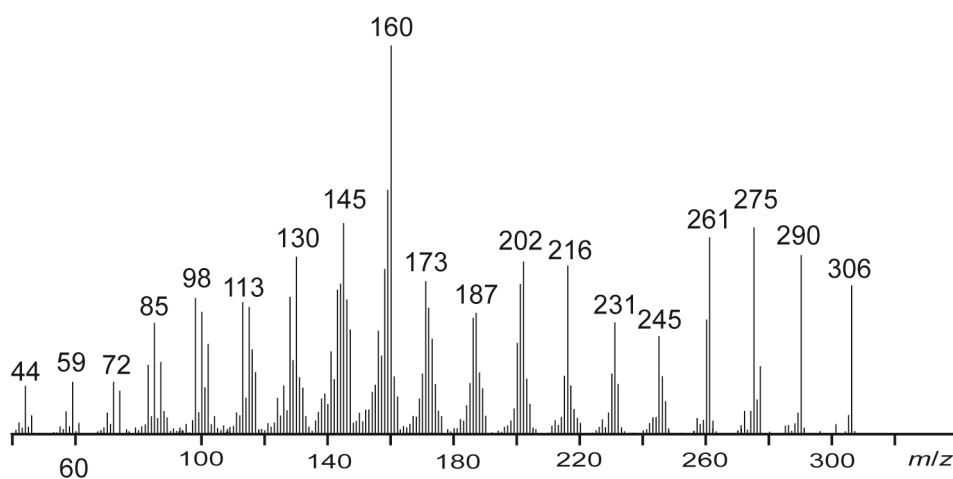


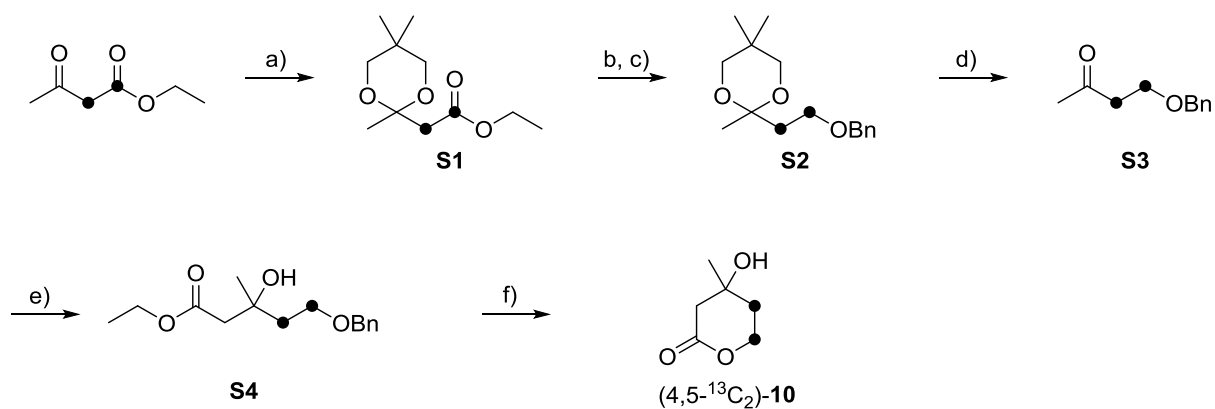
Figure S2. Result of feeding experiment with $(2,3,4,5,6-^{13}\text{C}_5)$ -10. A) Total ion chromatogram of headspace extract, B) mass spectrum of $(^{13}\text{C}_{20})$ -4.

Table S1. ^1H NMR data of **4** and comparison of ^{13}C -NMR data of **4** and feeding experiments in C_6D_6 .

$\text{C}^{[a]}$	^1H (δ , m, J) ^[b]	^{13}C (δ) ^[c]	^{13}C (δ)	^{13}C (δ)	^{13}C (δ)	^{13}C (δ)	^{13}C (δ)	^{13}C (δ)
4	4	4	(2,3,4,5,6- $^{13}\text{C}_5$)- 10	(3- ^{13}C)- 10	(3,5- $^{13}\text{C}_2$)- 10	(6- ^{13}C)- 10	(2,6- $^{13}\text{C}_2$)- 10	(4,5- $^{13}\text{C}_2$)- 10
11	-	197.0 (C _q)	197.0, dd, $^1J_{\text{C,C}}=43.0$, $^1J_{\text{C,C}}=34.0$	-	197.0, s	-	-	197.0, d, $^1J_{\text{C,C}}=43.0$
10	-	150.8 (C _q)	150.8, ddd, $^1J_{\text{C,C}}=70.0$, $^1J_{\text{C,C}}=43.0$, $^1J_{\text{C,C}}=35.0$	-	-	-	-	150.7, d, $^1J_{\text{C,C}}=43.0$
9	-	144.3 (C _q)	144.3, ddd, $^1J_{\text{C,C}}=70.0$, $^1J_{\text{C,C}}=40.0$, $^1J_{\text{C,C}}=40.0$	144.3	144.3, d, $J_{\text{C,C}}=2.1$	-	-	-
12	2.33, d, $^2J=15.8$ 2.24, d, $^2J=15.8$	60.2 (CH ₂)	60.2, dd, $^1J_{\text{C,C}}=30.0$, $^1J_{\text{C,C}}=30.0$	-	-	-	60.2, s	-
14	1.97, dd, $^3J=11.4$, $^3J=8.9$	52.6 (CH)	52.6, ddd, $^1J_{\text{C,C}}=33.0$, $^1J_{\text{C,C}}=33.0$, $^1J_{\text{C,C}}=33.0$	-	-	-	-	52.6, ddd, $^1J_{\text{C,C}}=33.0$, $^1J_{\text{C,C}}=33.0$, $^3J_{\text{C,C}}=5.3$
6	-	50.9 (C _q)	50.9, dddd, $^1J_{\text{C,C}}=35.0$, $^1J_{\text{C,C}}=35.0$, $^1J_{\text{C,C}}=35.0$, $^1J_{\text{C,C}}=35.0$	-	-	-	-	50.9, dd, $^1J_{\text{C,C}}=35.0$, $^1J_{\text{C,C}}=35.0$
1	-	46.2 (C _q)	46.2, dddd, $^1J_{\text{C,C}}=35.0$, $^1J_{\text{C,C}}=35.0$, $^1J_{\text{C,C}}=35.0$, $^1J_{\text{C,C}}=35.0$	46.2, d, $^3J_{\text{C,C}}=2.7$	46.1, d, $^3J_{\text{C,C}}=3.1$	-	-	-
2	1.51, m	43.2 (CH)	43.2, ddd, $^1J_{\text{C,C}}=34.0$, $^1J_{\text{C,C}}=34.0$, $^1J_{\text{C,C}}=34.0$	-	-	-	-	43.2, dd, $^1J_{\text{C,C}}=34.0$, $^1J_{\text{C,C}}=34.0$
13	-	40.9 (C _q)	40.9, dddd, $^1J_{\text{C,C}}=35.0$, $^1J_{\text{C,C}}=35.0$, $^1J_{\text{C,C}}=35.0$, $^1J_{\text{C,C}}=35.0$	40.9, d, $^3J_{\text{C,C}}=2.7$	40.9, d, $^3J_{\text{C,C}}=3.1$	-	-	-
7	1.49, m 1.03, m	30.5 (CH ₂)	30.5, dd, $^1J_{\text{C,C}}=35.0$, $^1J_{\text{C,C}}=35.0$	-	-	-	-	30.5, d, $^1J_{\text{C,C}}=35.0$
5	2.20, dd, $^3J=7.8$, $^3J=7.8$	29.5 (CH)	29.5, ddd, $^1J_{\text{C,C}}=34.0$, $^1J_{\text{C,C}}=34.0$, $^1J_{\text{C,C}}=34.0$	29.5, s	29.5, d, $^2J_{\text{C,C}}=0.9$	-	-	-
8	2.04, m 1.42, m	29.1 (CH ₂)	29.1, dd, $^1J_{\text{C,C}}=36.0$, $^1J_{\text{C,C}}=36.0$	-	-	-	29.1, d, $^2J_{\text{C,C}}=2.8$	-
15	1.60, m 1.12, m	27.6 (CH ₂)	27.6, dd, $^1J_{\text{C,C}}=32.0$, $^1J_{\text{C,C}}=32.0$	-	27.6, d, $^3J_{\text{C,C}}=2.9$	-	-	27.6, dd, $^1J_{\text{C,C}}=32.0$, $^1J_{\text{C,C}}=32.0$
16	0.70, s	26.2 (CH ₃)	26.2, d, $^1J_{\text{C,C}}=37$	-	-	26.2, s	26.2, d, $^2J_{\text{C,C}}=1.4$	-
3	1.86, m 1.21, m	25.7 (CH ₂)	25.7, dd, $^1J_{\text{C,C}}=34.0$, $^1J_{\text{C,C}}=34.0$	-	26.1, s	-	-	26.1, d, $^1J_{\text{C,C}}=34.0$
4	1.92, m 1.11, m	25.6 (CH ₂)	25.6, dd, $^1J_{\text{C,C}}=33.0$, $^1J_{\text{C,C}}=33.0$	-	-	-	25.6, s	-
17	0.94, s	22.7 (CH ₃)	22.7, d, $^1J_{\text{C,C}}=37.0$	-	-	-	22.7, br	-
20	2.06, s	22.4 (CH ₃)	22.4, d, $^1J_{\text{C,C}}=39.0$	-	-	22.4, s	22.4, d, $^2J_{\text{C,C}}=2.8$	-
19	1.24, s	21.7 (CH ₃)	21.7, d, $^1J_{\text{C,C}}=37.0$	-	-	21.7, s	21.7, s	-
18	0.86, d, $^3J=7.5$ Hz	20.7 (CH ₃)	20.7, d, $^1J_{\text{C,C}}=35.0$	-	-	20.7, s	20.7, s	-

[a] Carbon numbering as shown in Figure 4A. [b] Chemical shifts δ in ppm, multiplicity m: s=singlet, d=doublet, m=multiplett; coupling constants nJ are via n bonds and given in Hertz. [c] Carbon assignments (CH₃, CH₂, CH and C_q) were delineated from a DEPT spectrum.

3. SYNTHESIS OF (4,5-¹³C₂)-10



Scheme S1. Synthesis of (4,5-¹³C₂)-10. a) TMSCl, neopentyl glycol, reflux, 16 h, 98%; b) LiAlH₄, THF, 0 °C to rt, 2 h; c) NaH, BnBr, 0 °C to rt, 69% (2 steps); d) HCl/MeOH, rt, 15 min, 99%; e) LDA, ethyl acetate, -78 °C, 82%; f) Pd/C, H₂, 2 h, 40 °C, then *p*-TsOH, DCM, 68%.

4. RESULTS OF FEEDING EXPERIMENTS WITH ^2H -LABELED **10**

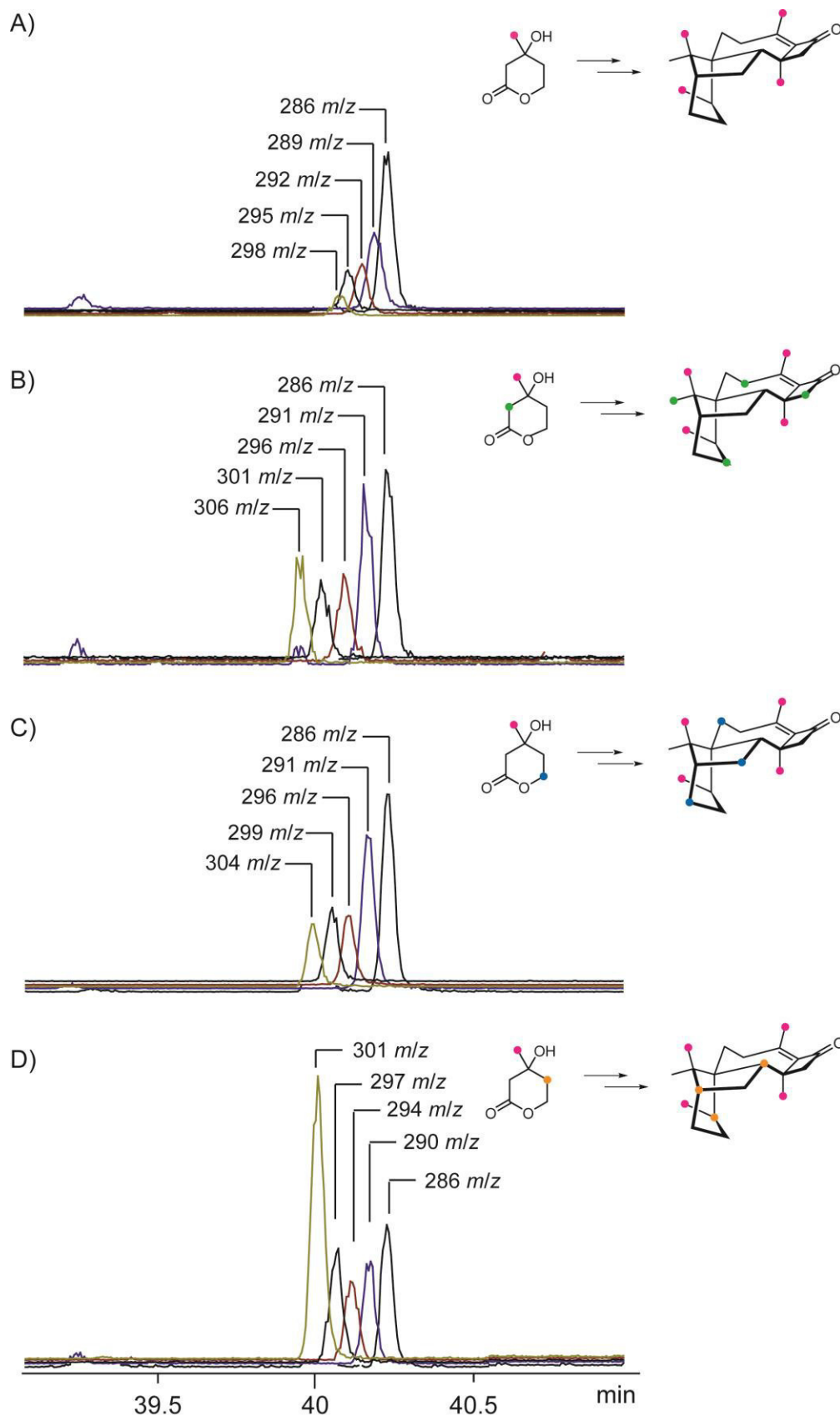


Figure S3. Extracted ion traces of isotopomers of **4** after feeding of A) (6,6,6- $^2\text{H}_3$)-**10**, B) (2,2,6,6,6- $^2\text{H}_5$)-**10**, C) (5,5,6,6,6- $^2\text{H}_5$)-**10**, D) (4,4,6,6,6- $^2\text{H}_5$)-**10**. Colored dots indicate positions of ^2H labelings.

5. NMR SPECTRA FOR HARZIANONE (4) AND SYNTHETIC COMPOUNDS

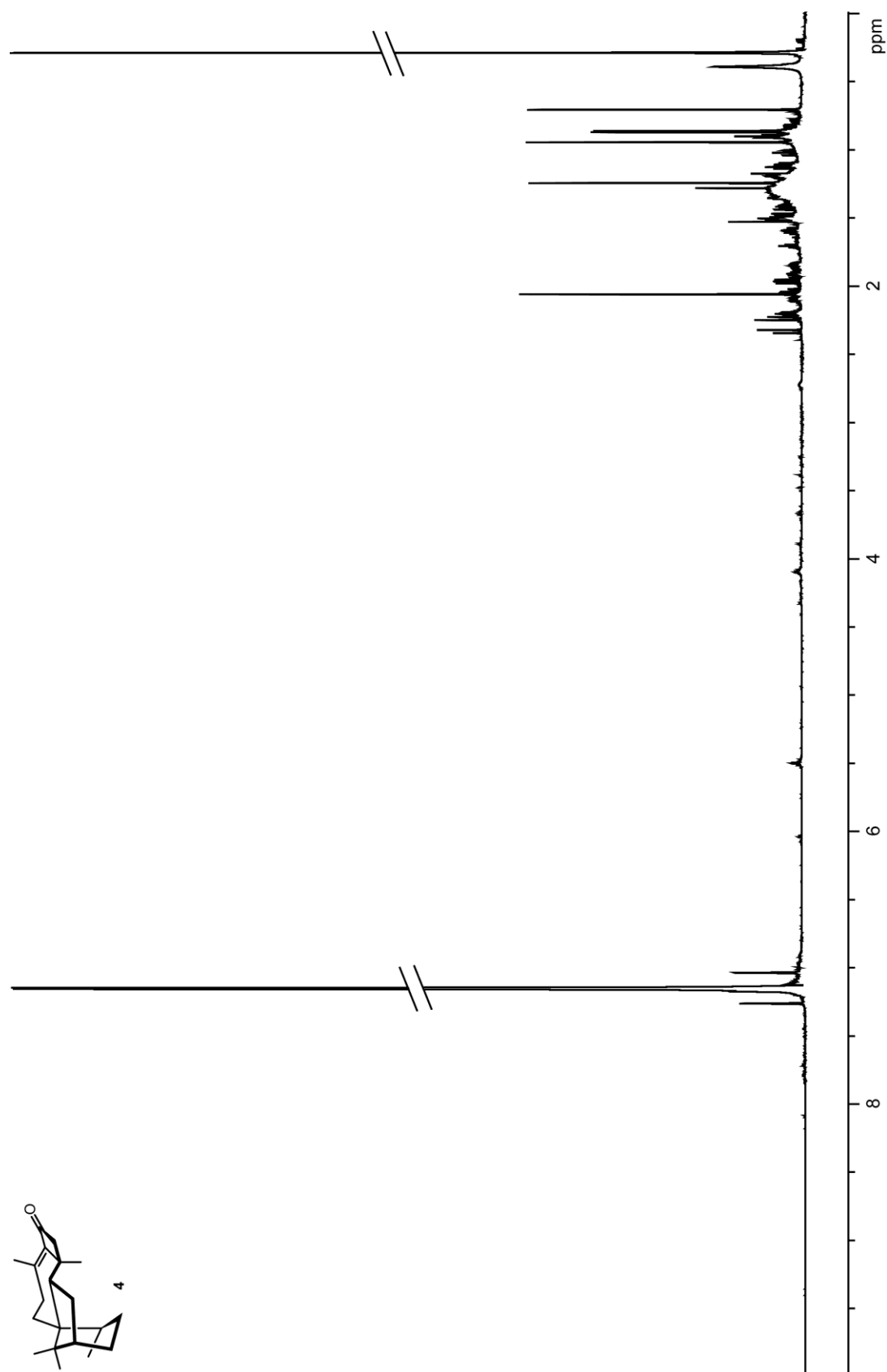
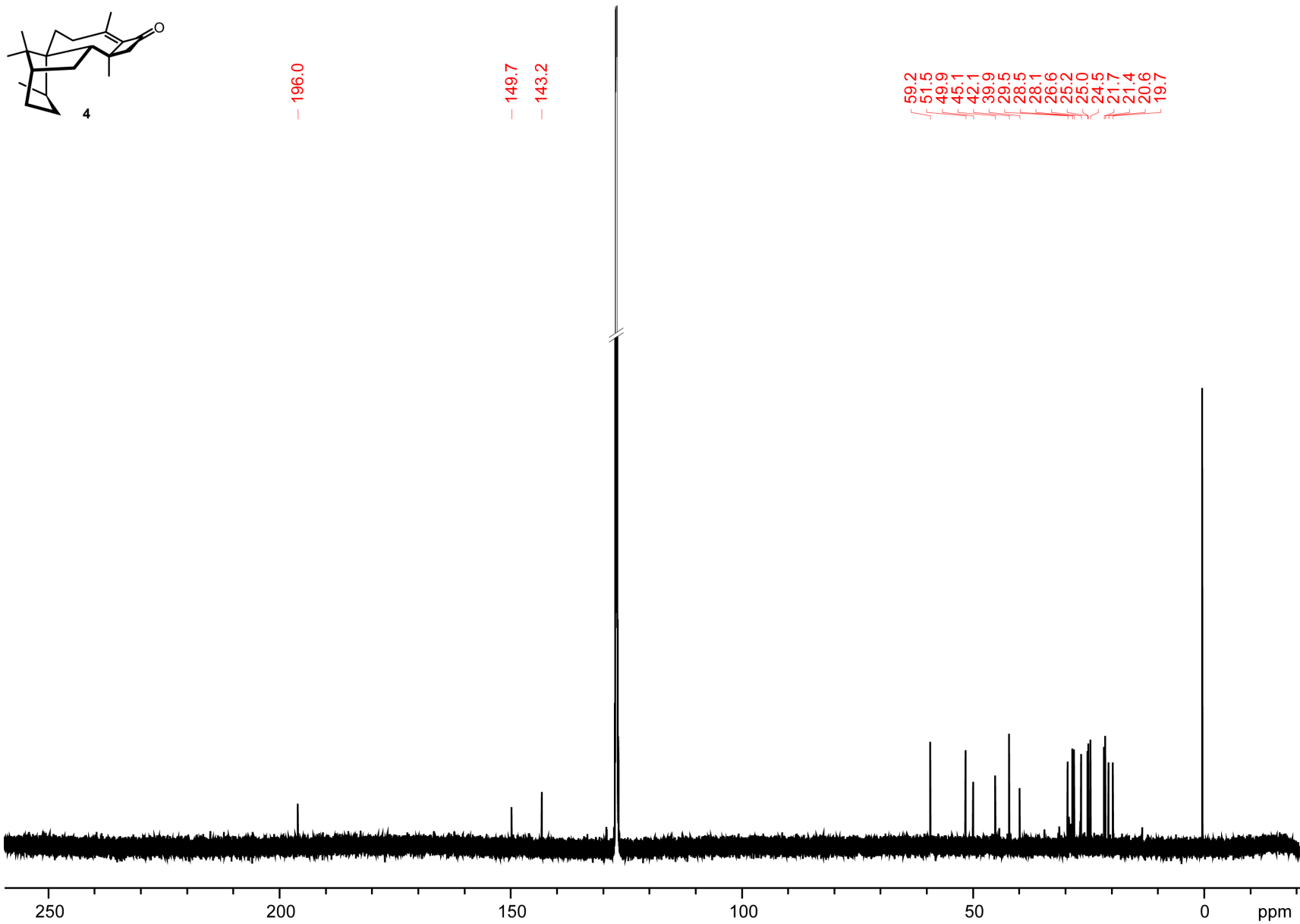


Figure S4. $^1\text{H-NMR}$ spectrum of **4** (700 MHz, C_6D_6).



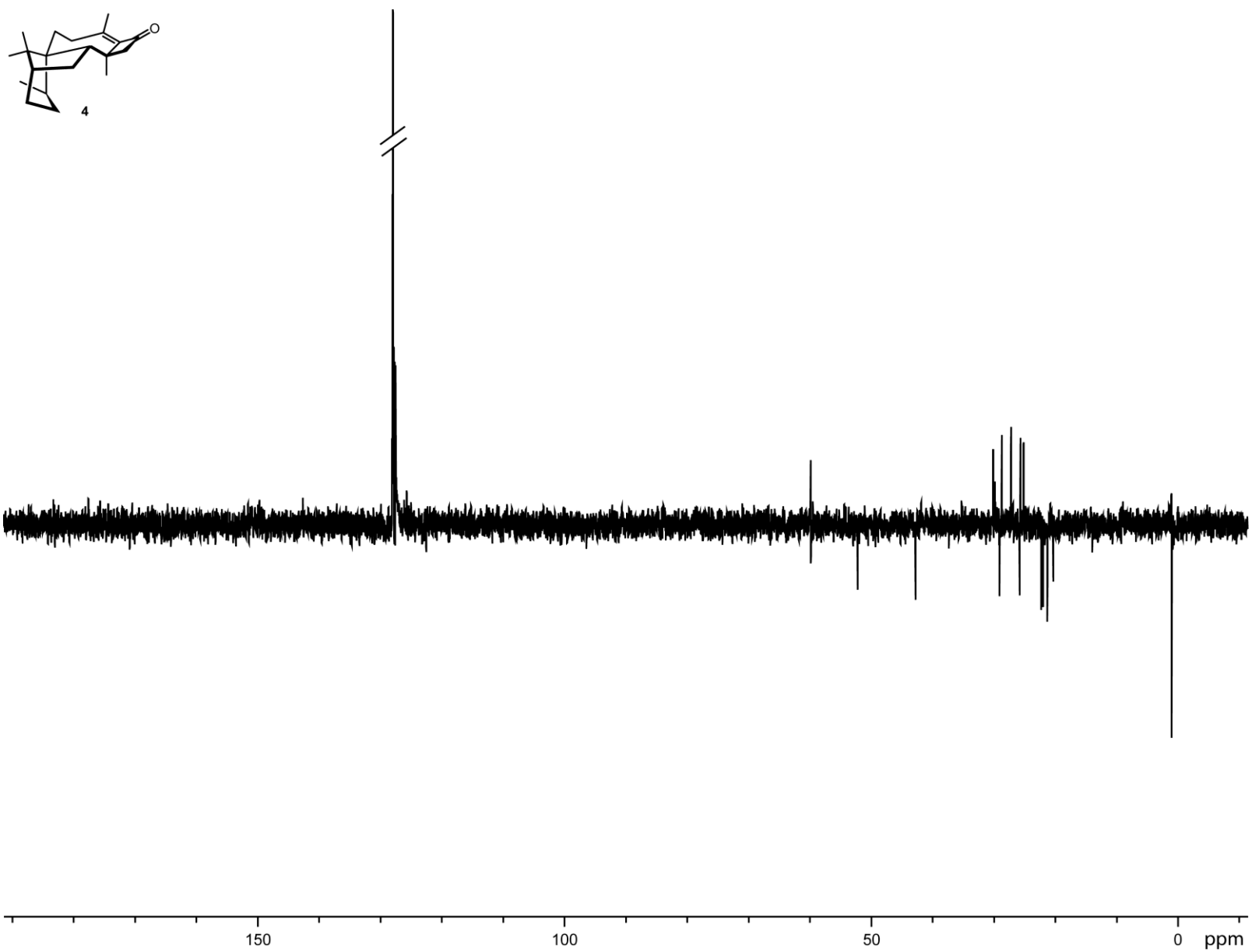
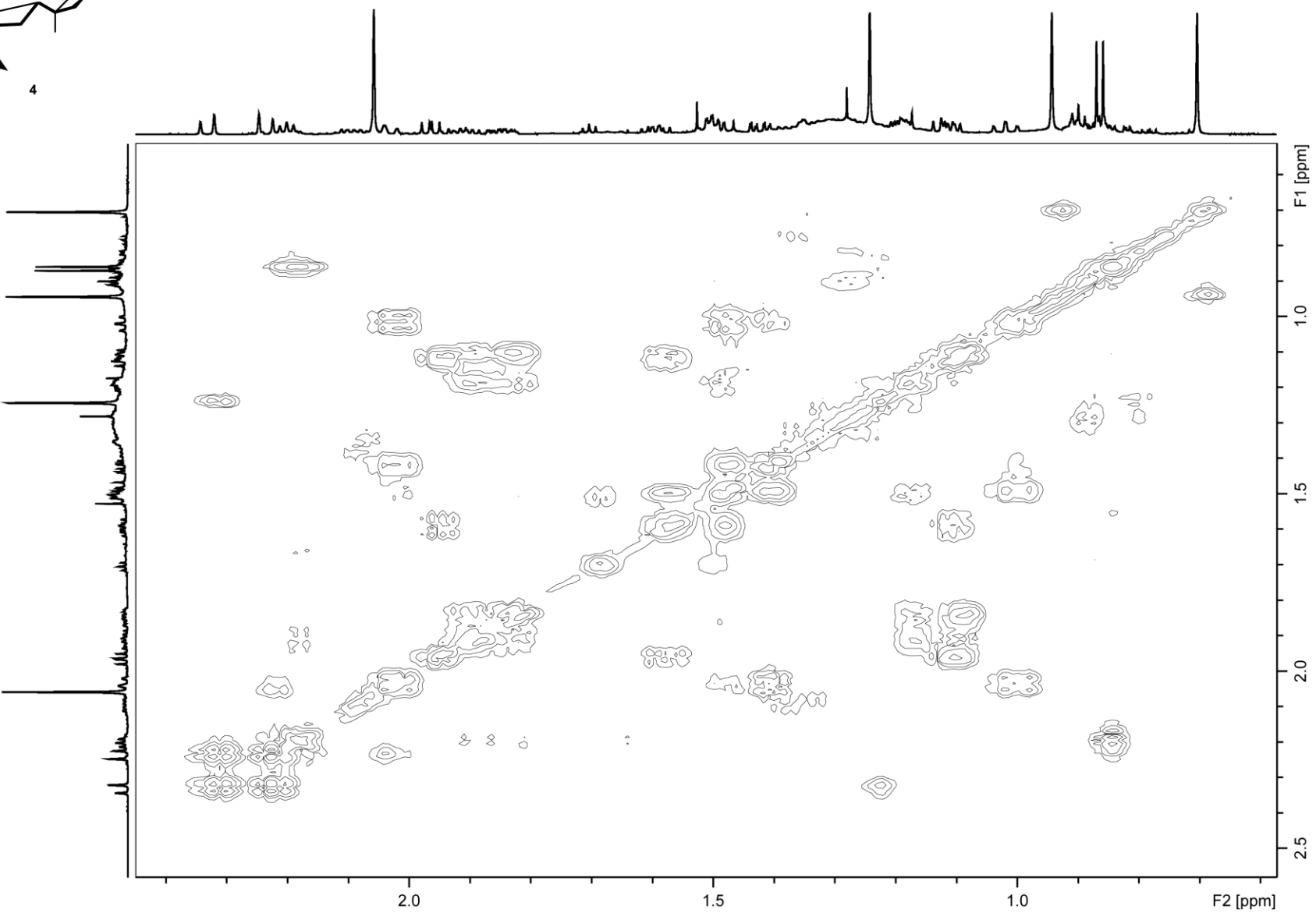
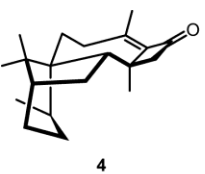


Figure S6. ^{13}C -DEPT 135 spectrum of **4** (175 MHz, C_6D_6).



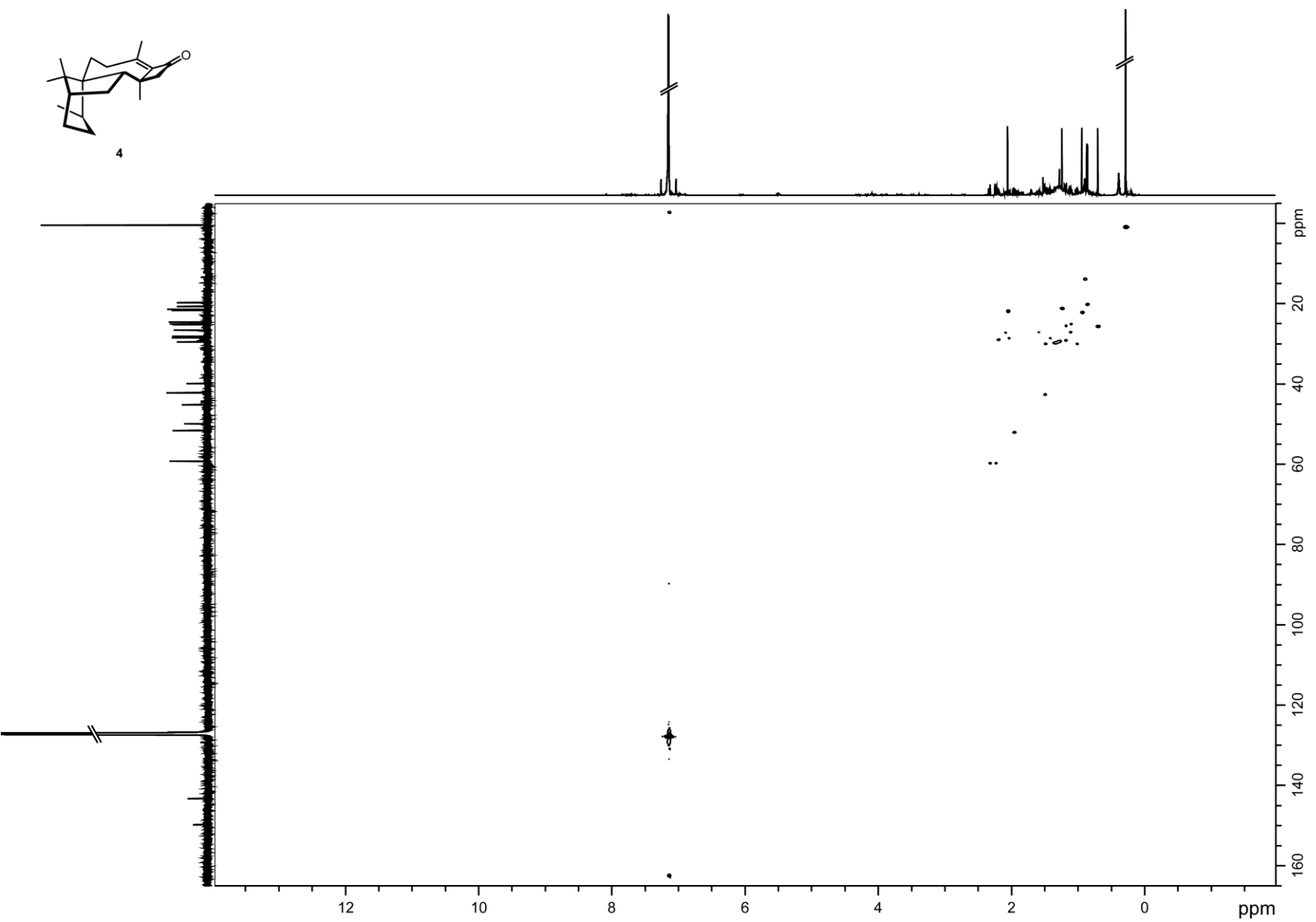


Figure S8. ^1H , ^{13}C -HSQC spectrum of **4** (C_6D_6).

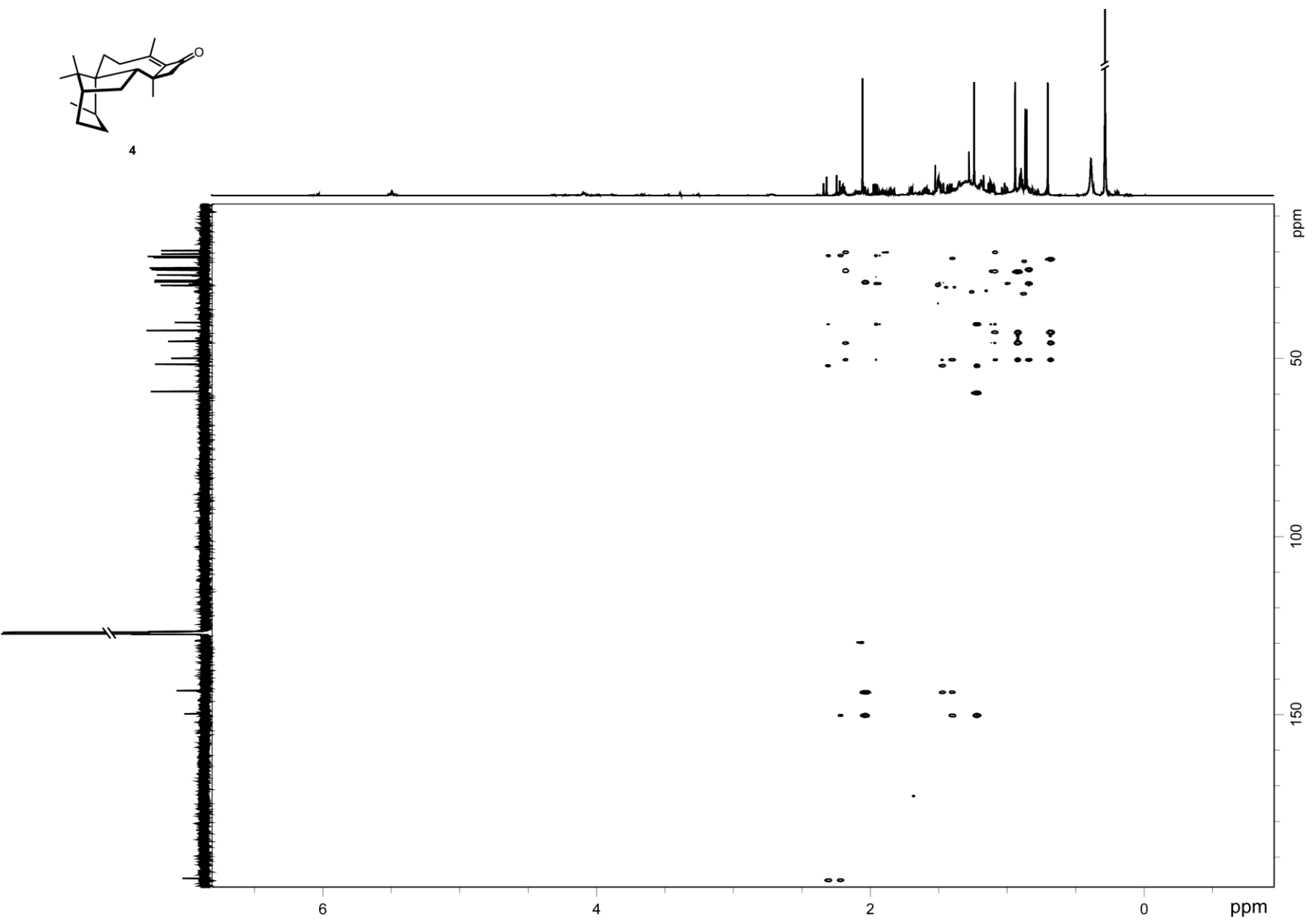


Figure S9. ^1H , ^{13}C -HMBC of **4** (C_6D_6).

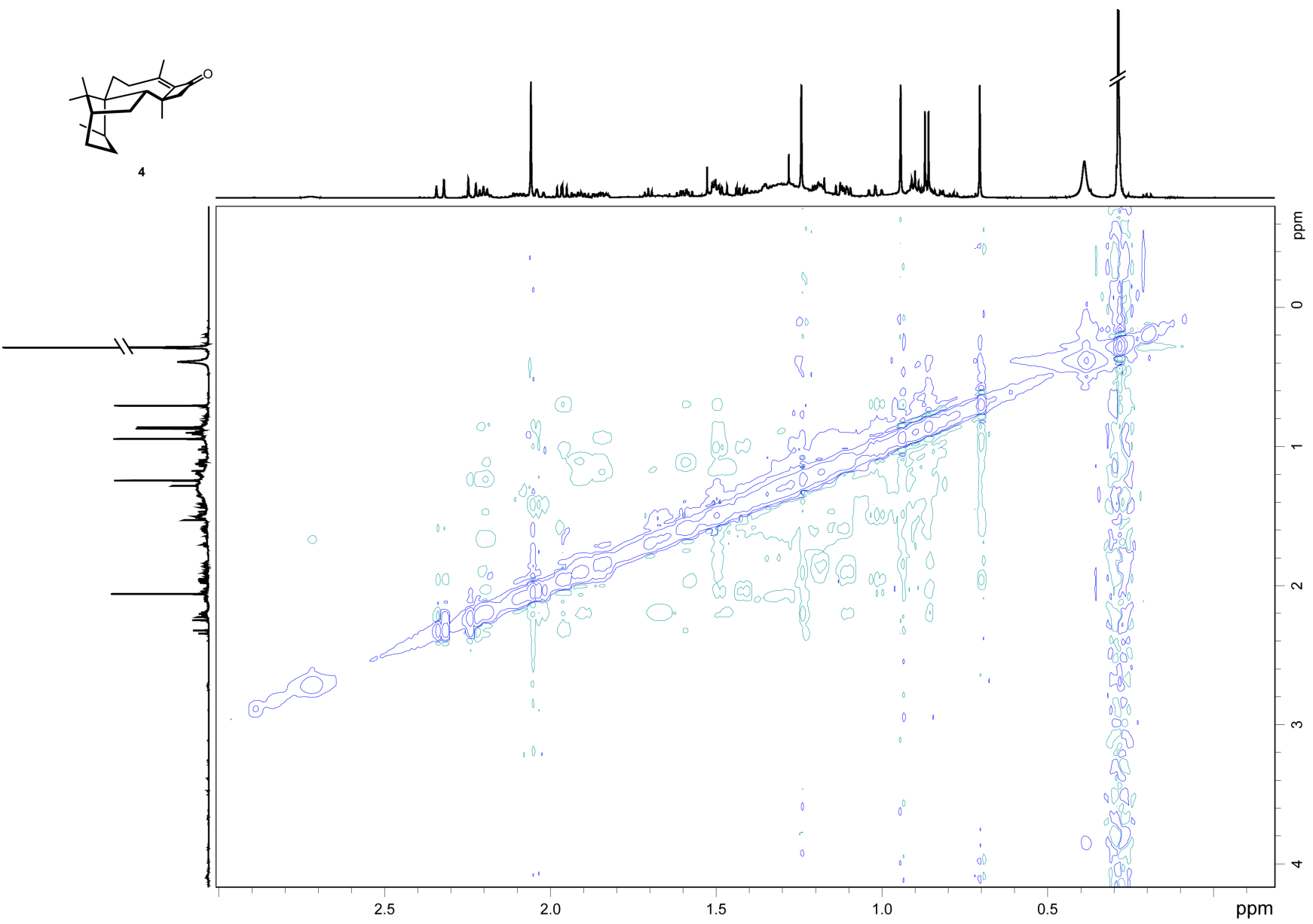


Figure S10. ^1H , ^1H -NOESY of **4** (C_6D_6).

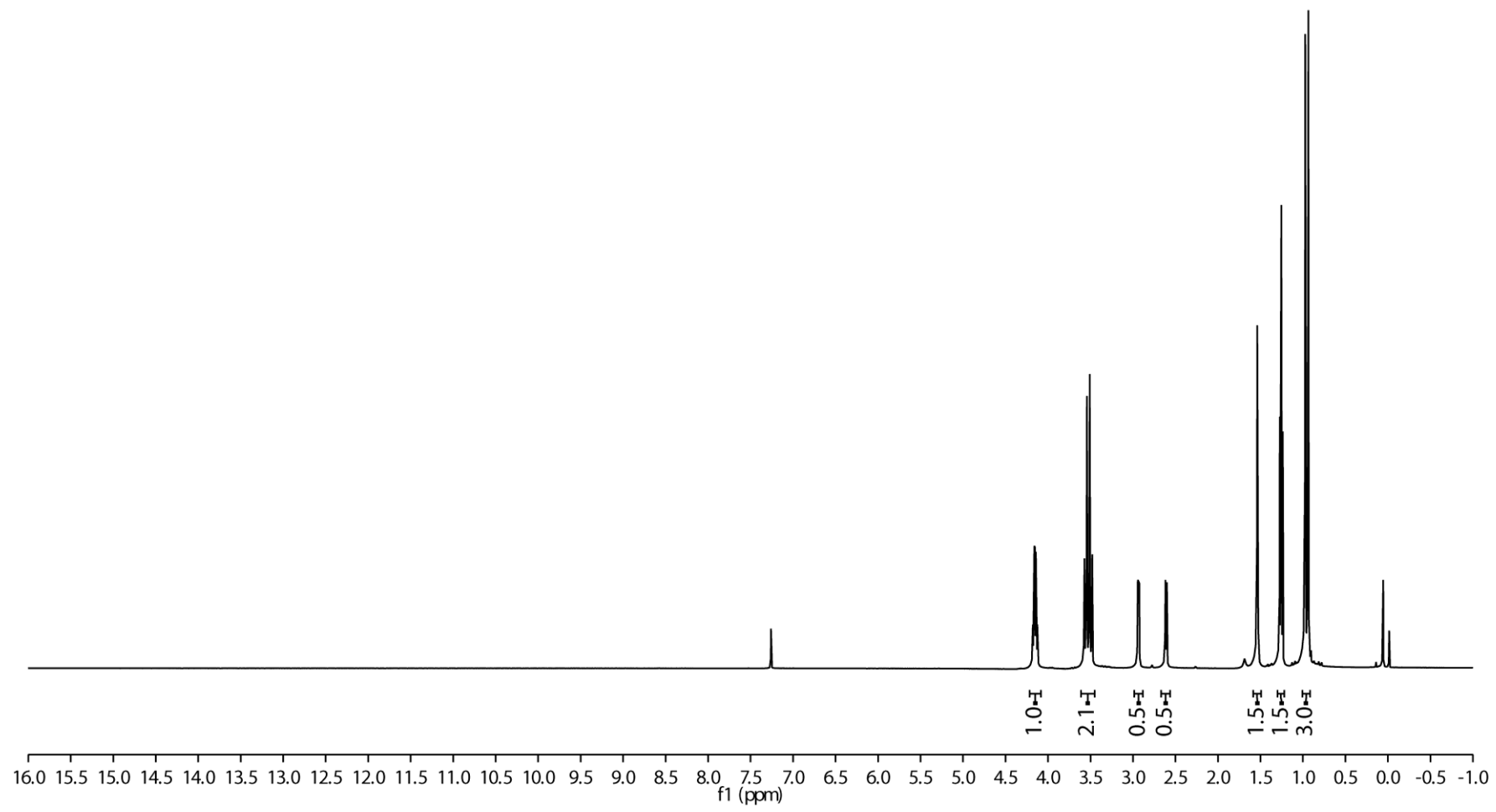
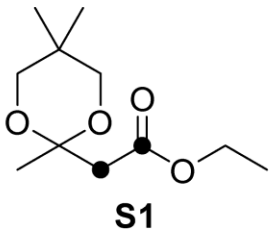


Figure S11. ¹H-NMR spectrum of **S1** (400 MHz, CDCl₃).

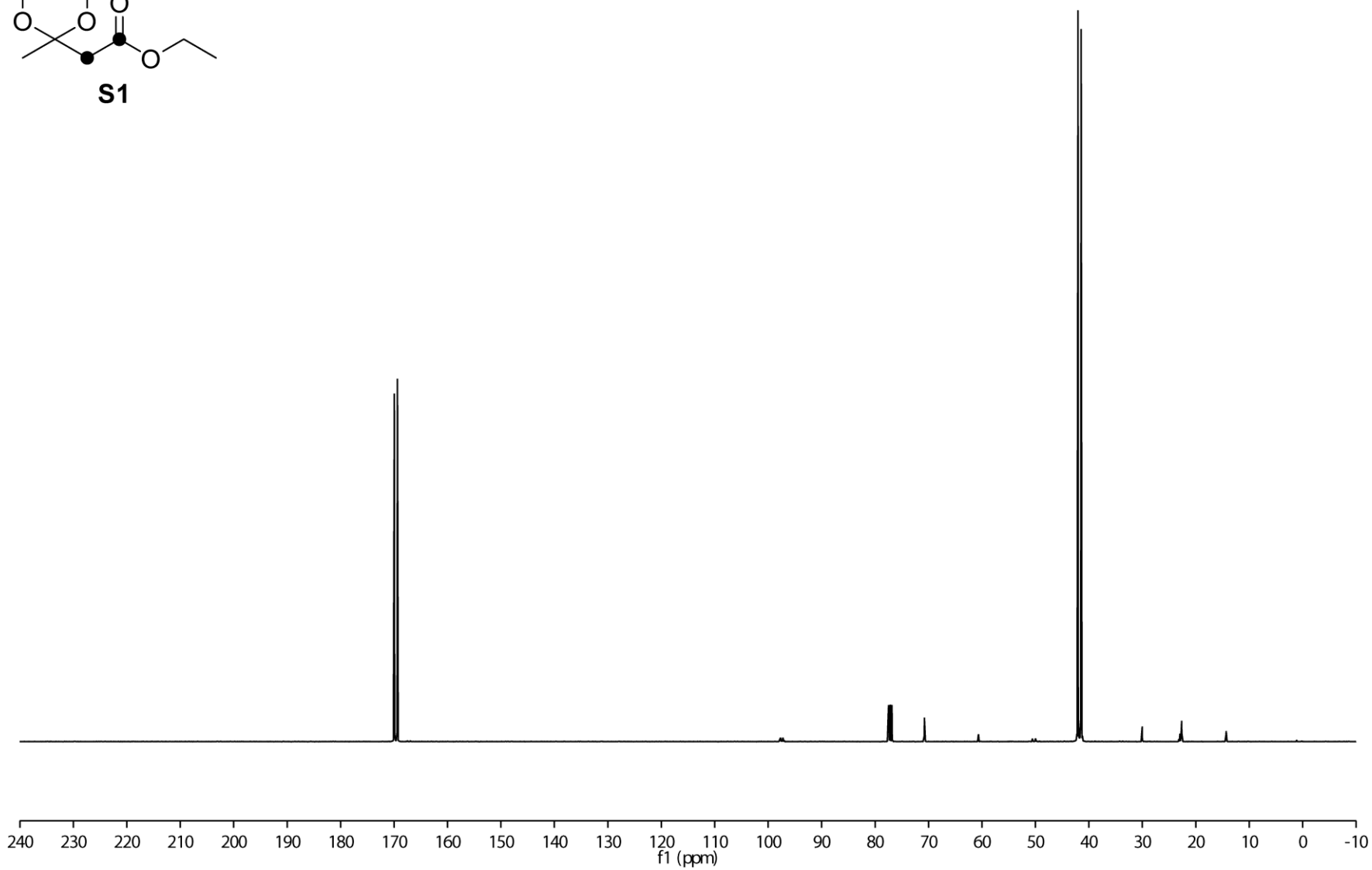
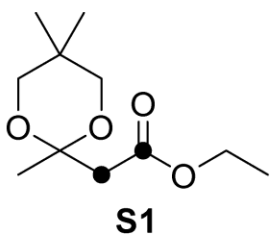


Figure S12. ^{13}C -NMR spectrum of **S1** (100 MHz, CDCl_3).

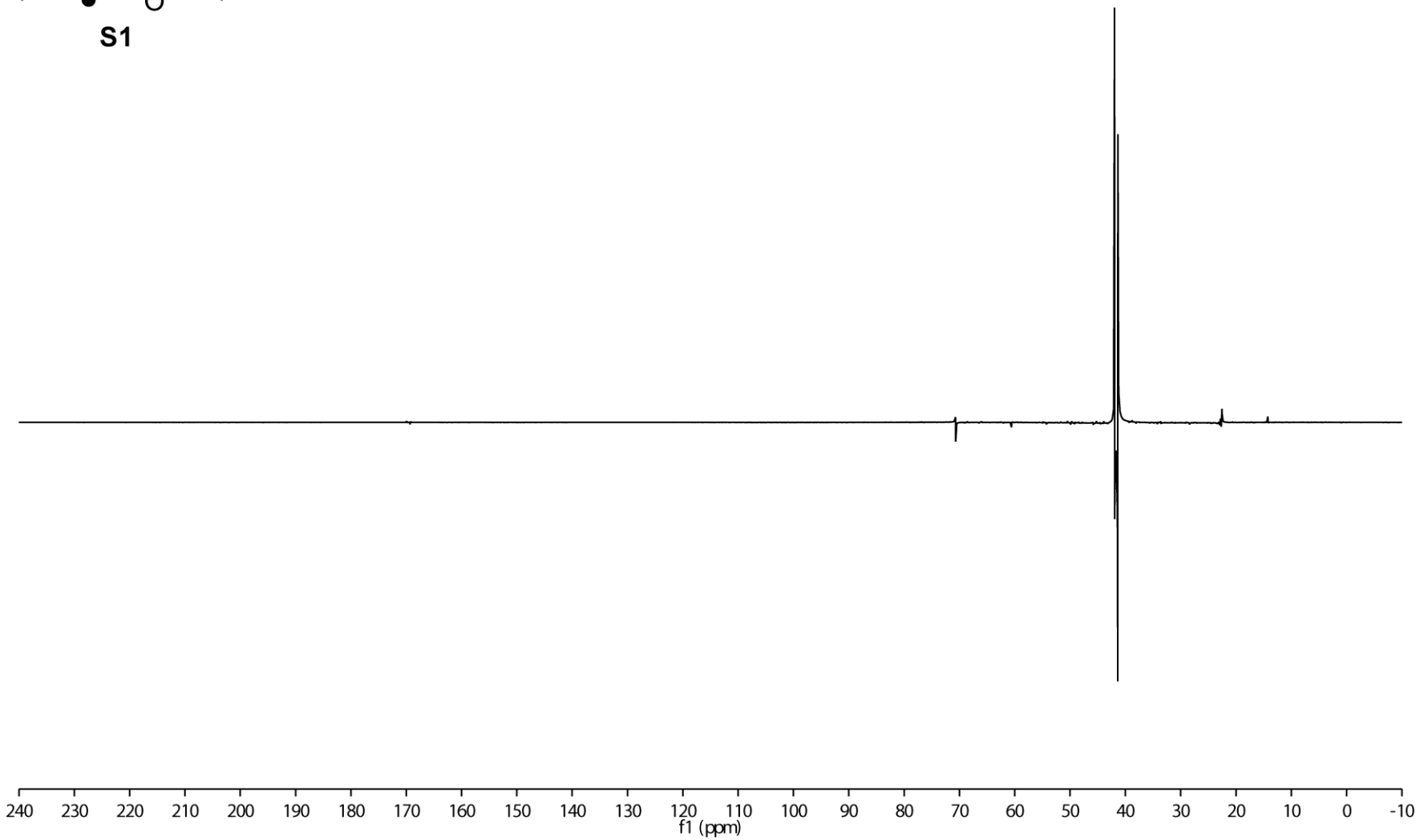
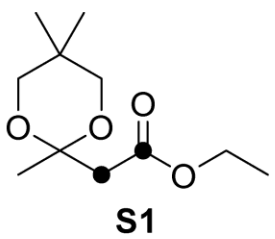


Figure S13. ^{13}C -DEPT 135 spectrum of **S1** (100 MHz, CDCl_3).

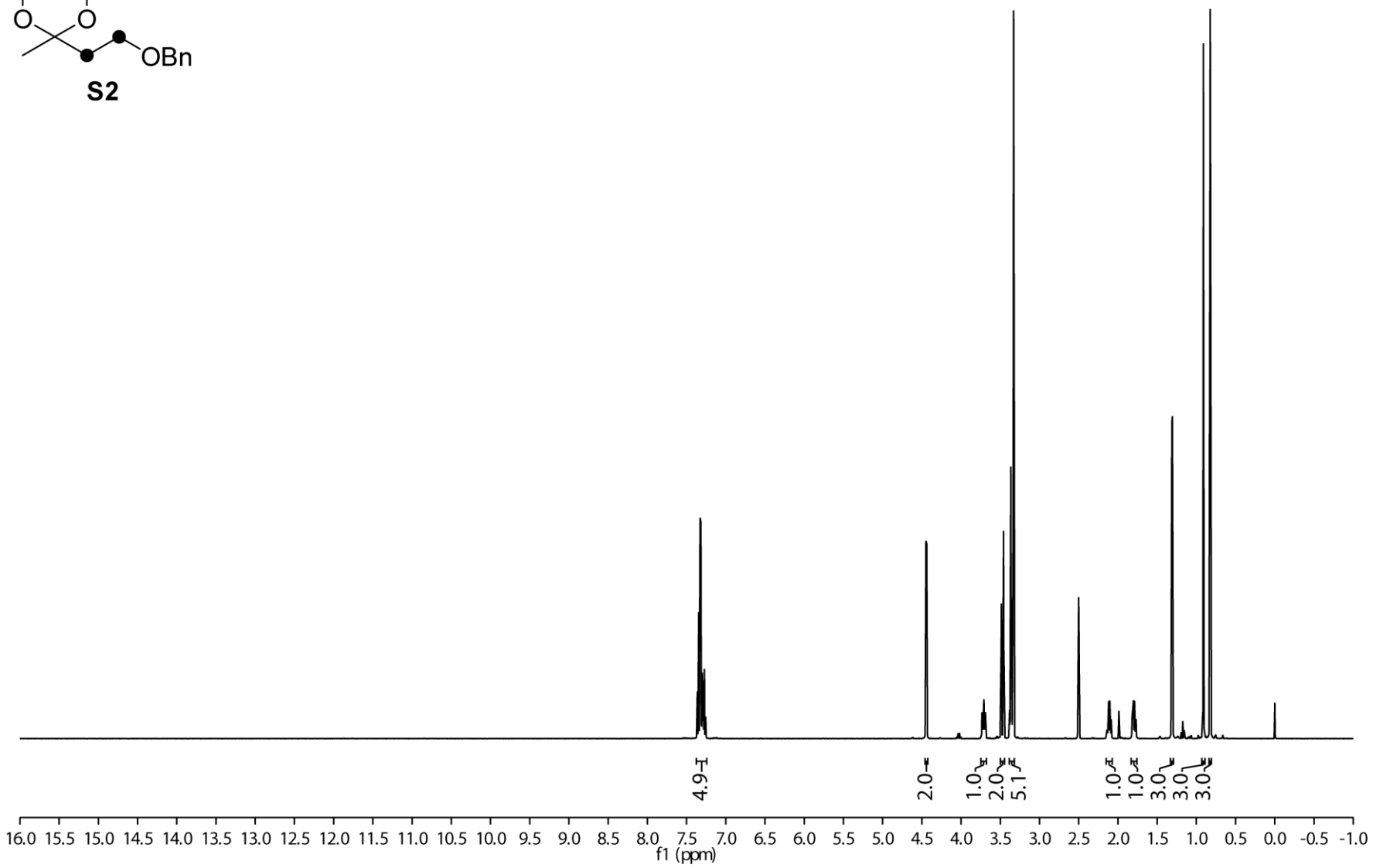
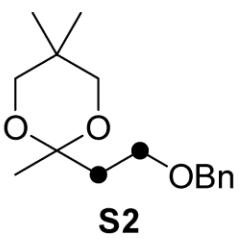


Figure S14. ¹H-NMR spectrum of **S2** (400 MHz, *d*₆-DMSO).

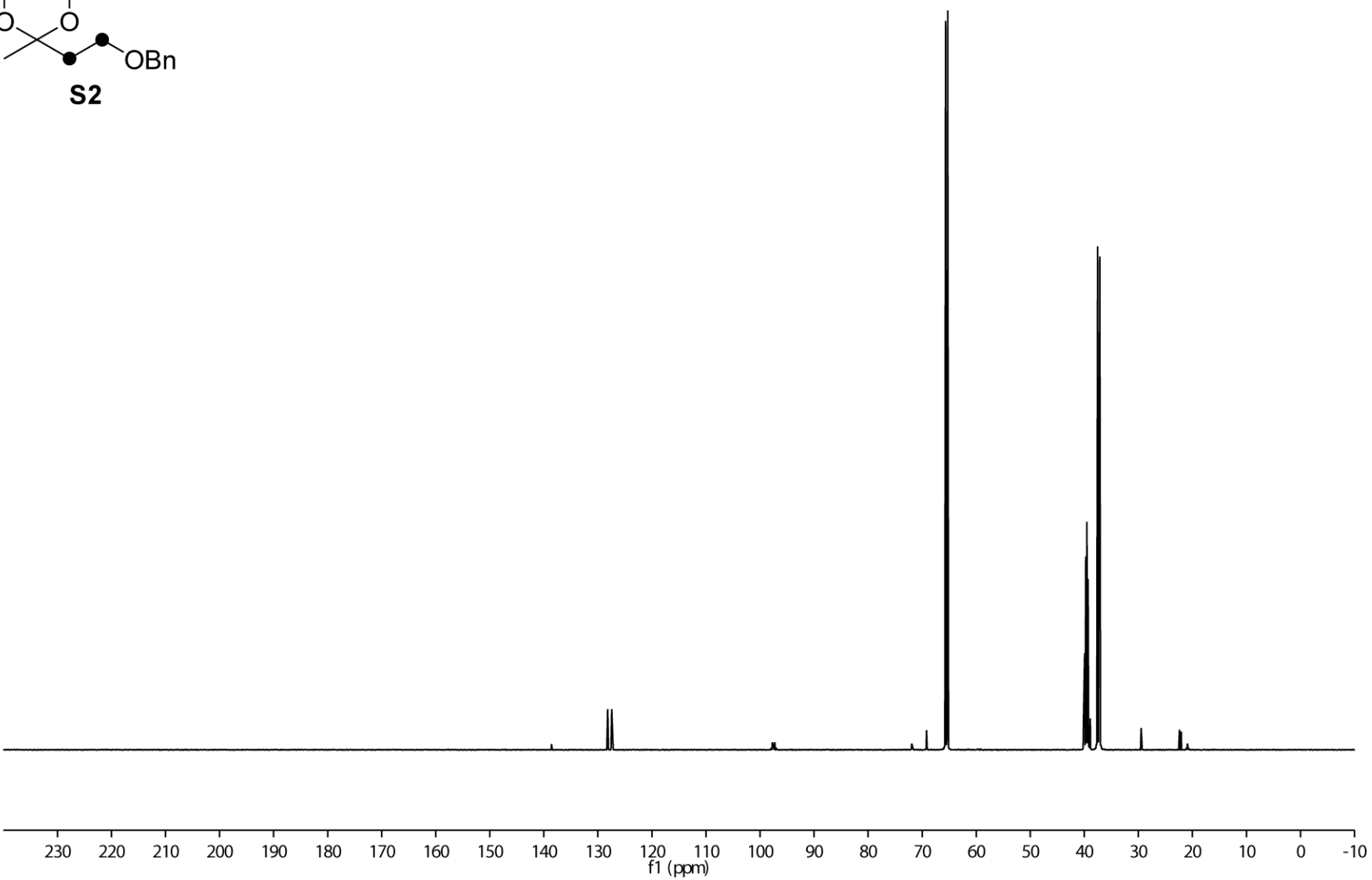
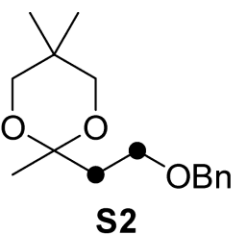


Figure S15. ¹³C-NMR spectrum of **S2** (100 MHz, d₆-DMSO).

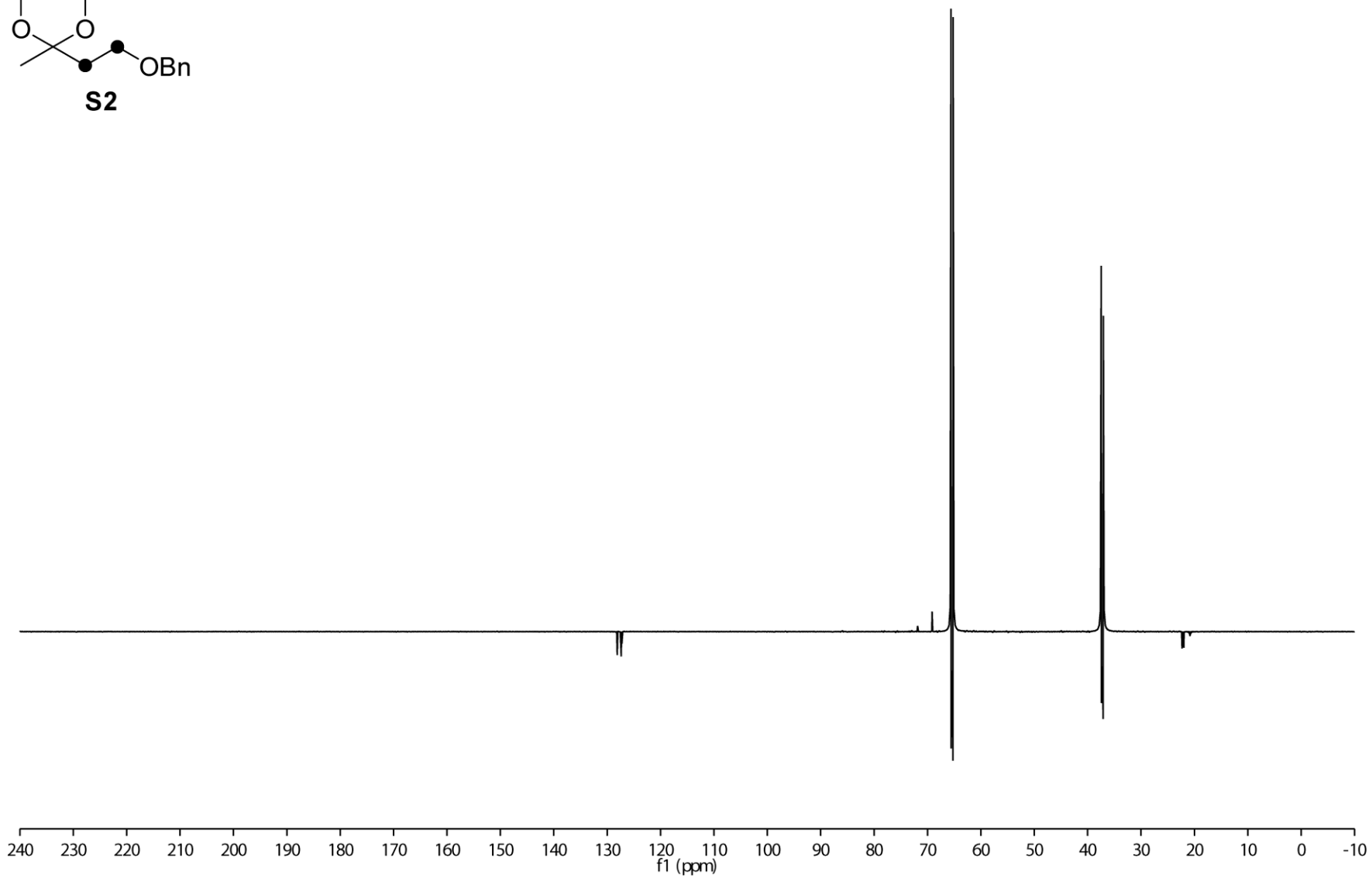
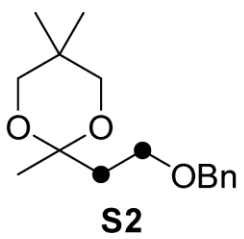


Figure S16. ^{13}C -DEPT 135 spectrum of **S2** (100 MHz, d_6 -DMSO).

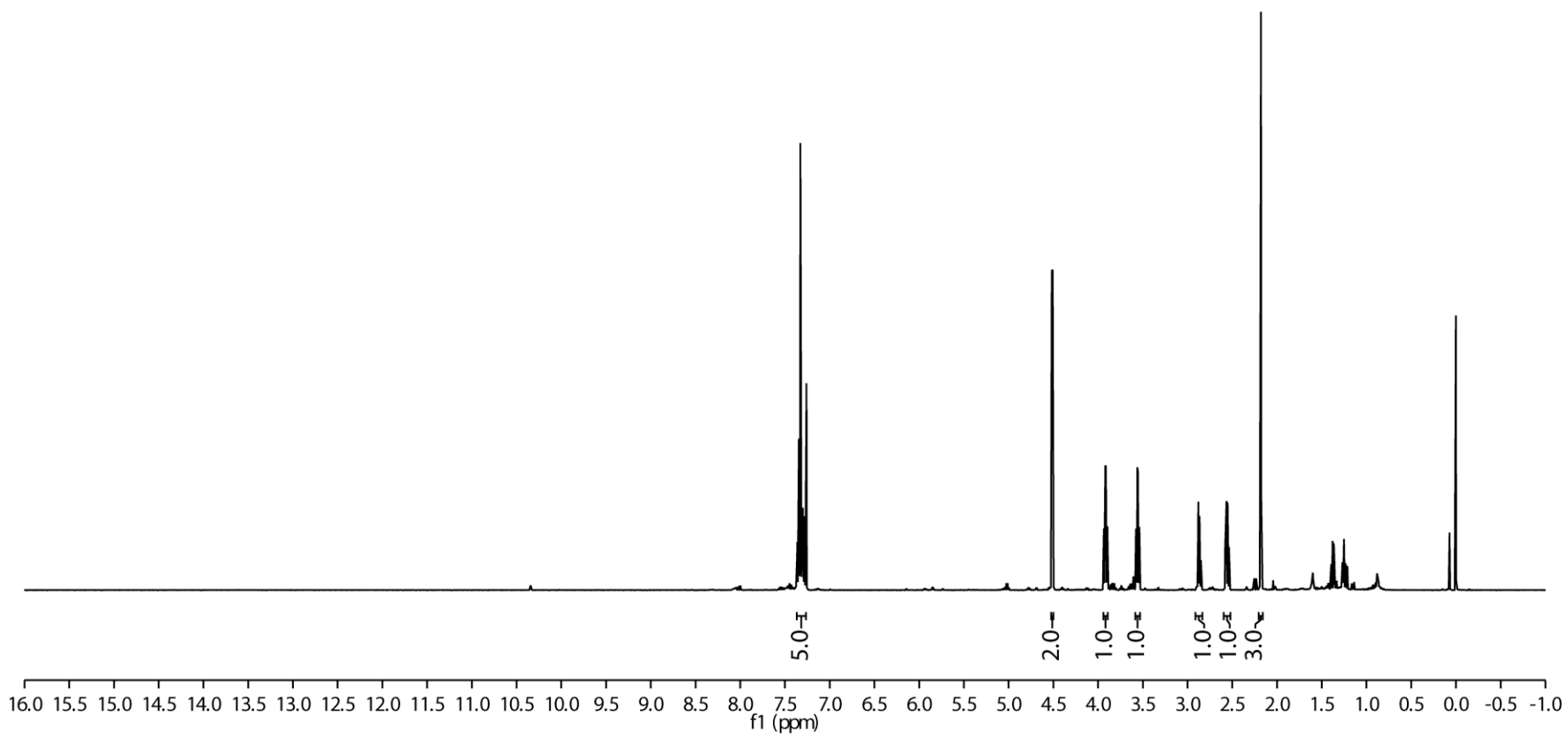
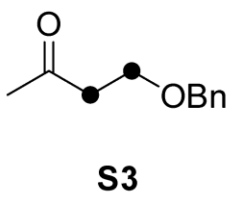
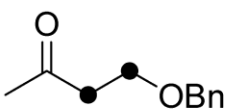


Figure S17. ¹H-NMR spectrum of **S3** (400 MHz, CDCl₃).



S3

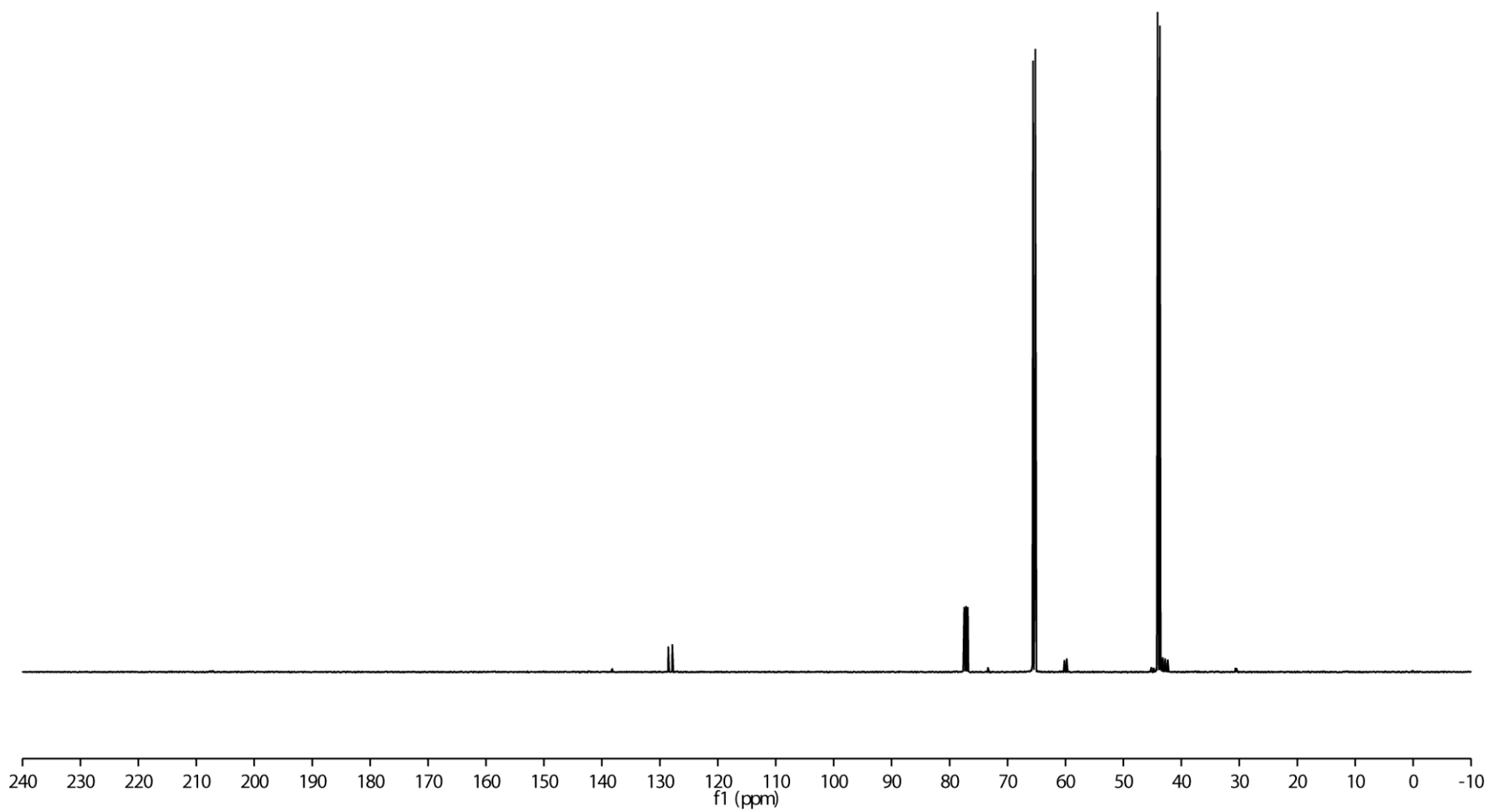
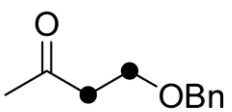


Figure S18. ^{13}C -NMR spectrum of **S3** (100 MHz, CDCl_3).



S3

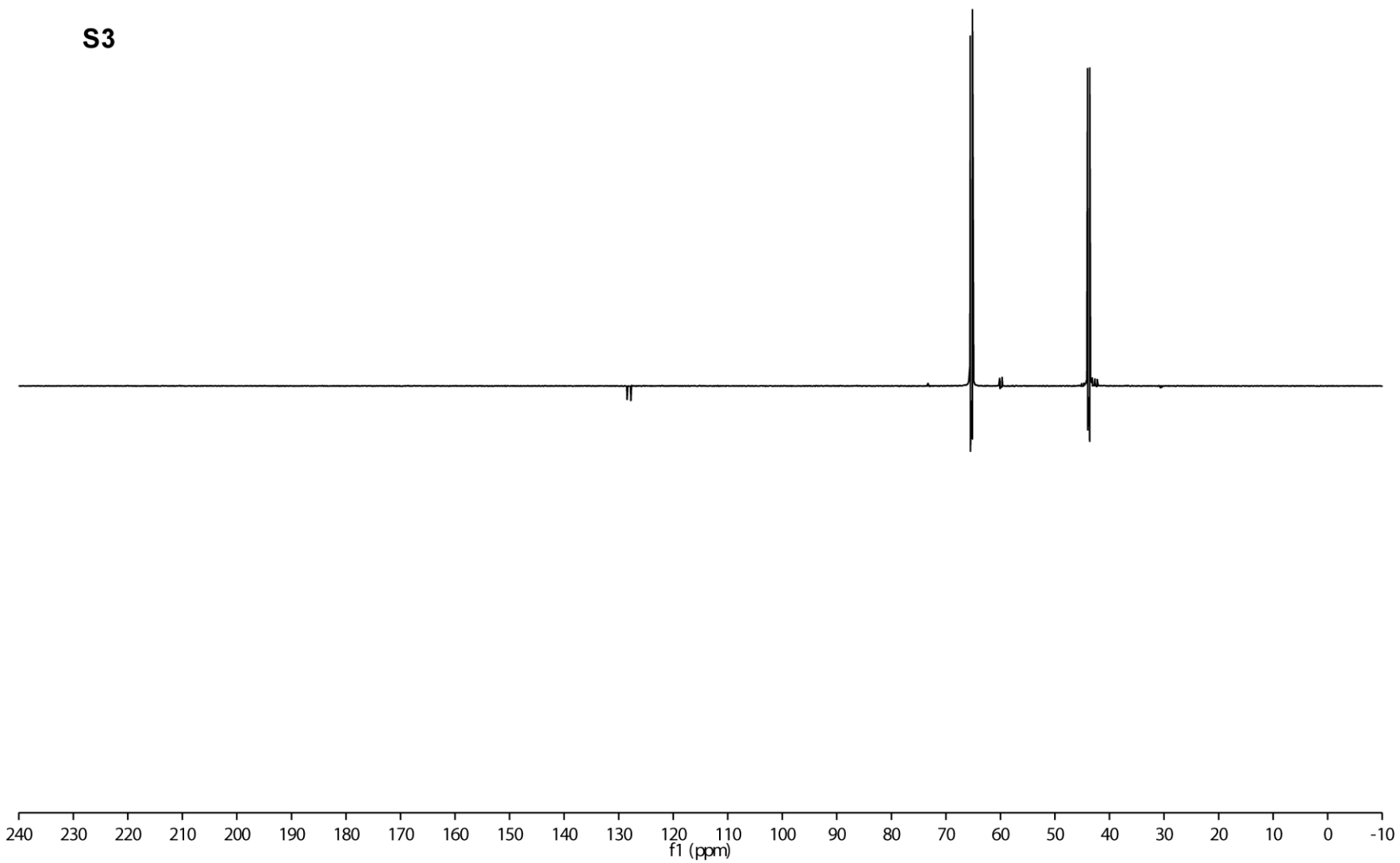


Figure S19. ¹³C-DEPT 135 spectrum of **S3** (100 MHz, CDCl₃).

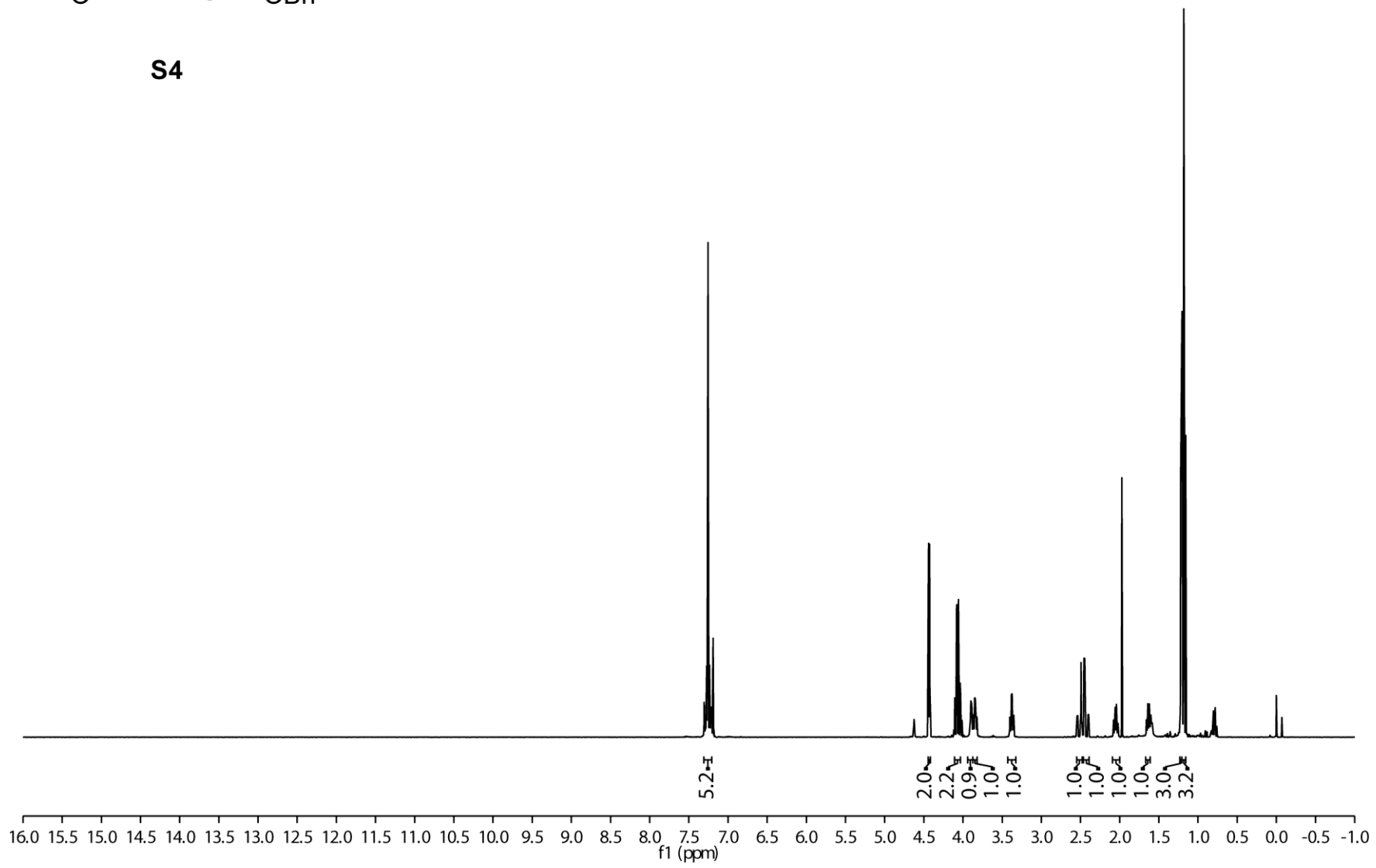
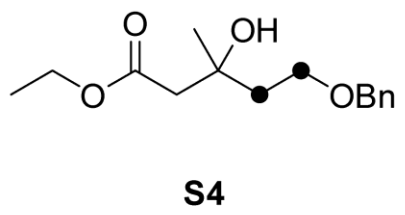


Figure S20. ¹H-NMR spectrum of **S4** (400 MHz, CDCl₃).

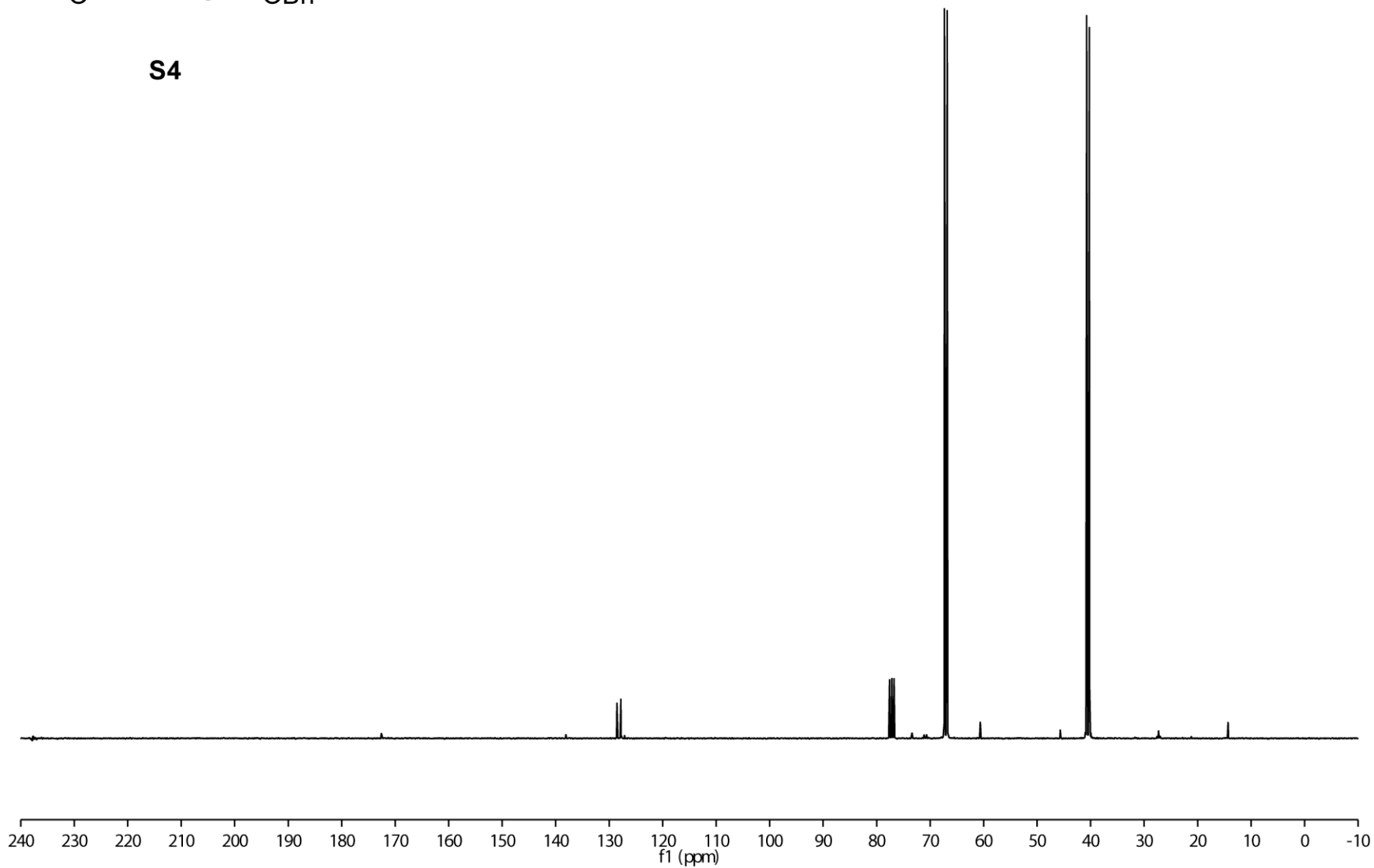
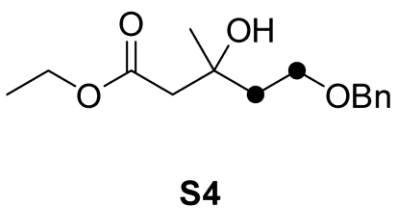


Figure S21. ¹³C-NMR spectrum of **S4** (100 MHz, CDCl₃).

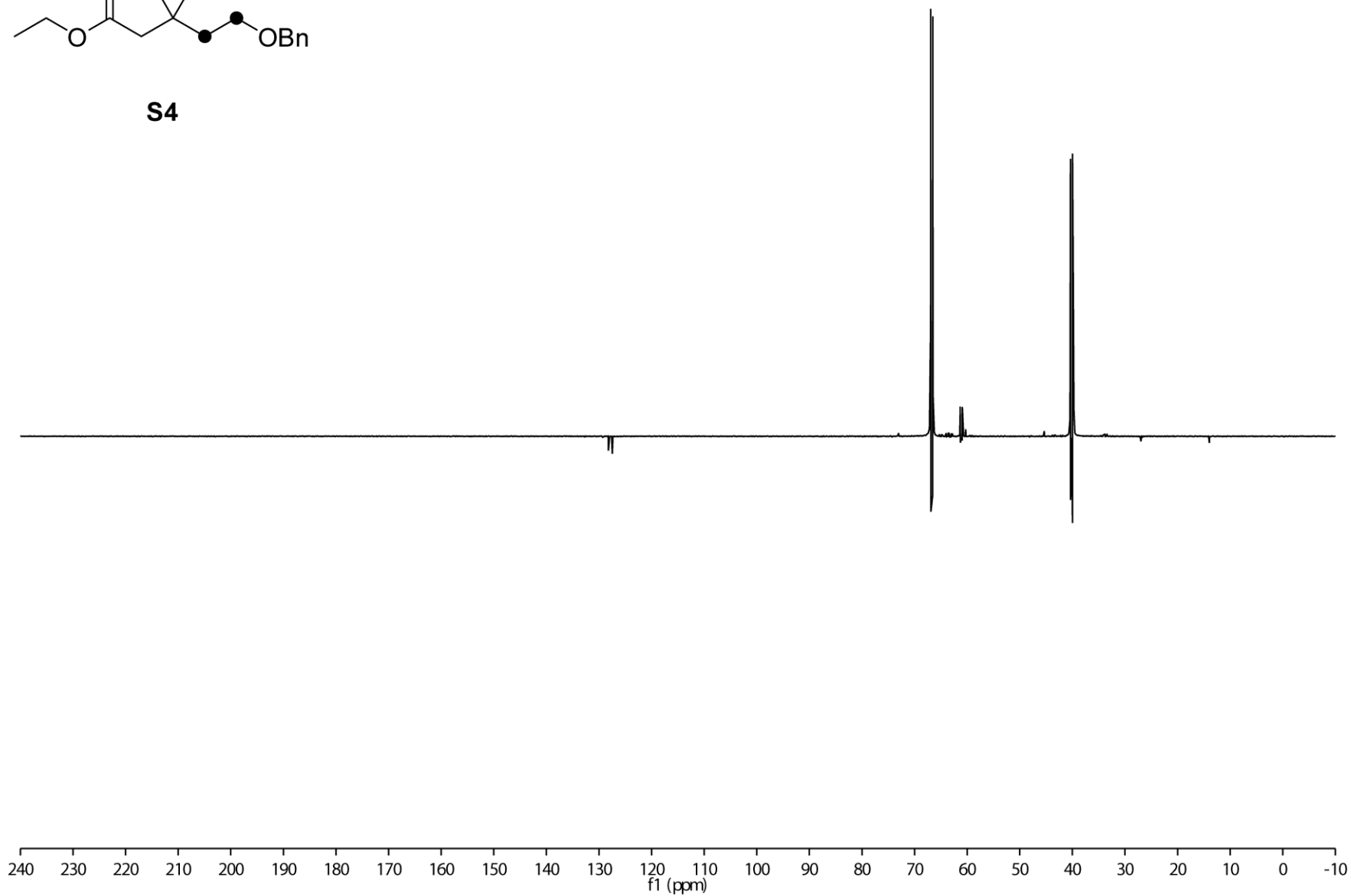
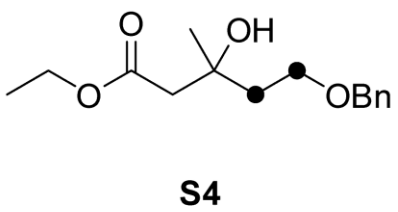


Figure S22. ^{13}C -DEPT 135 spectrum of **S4** (100 MHz, CDCl_3).

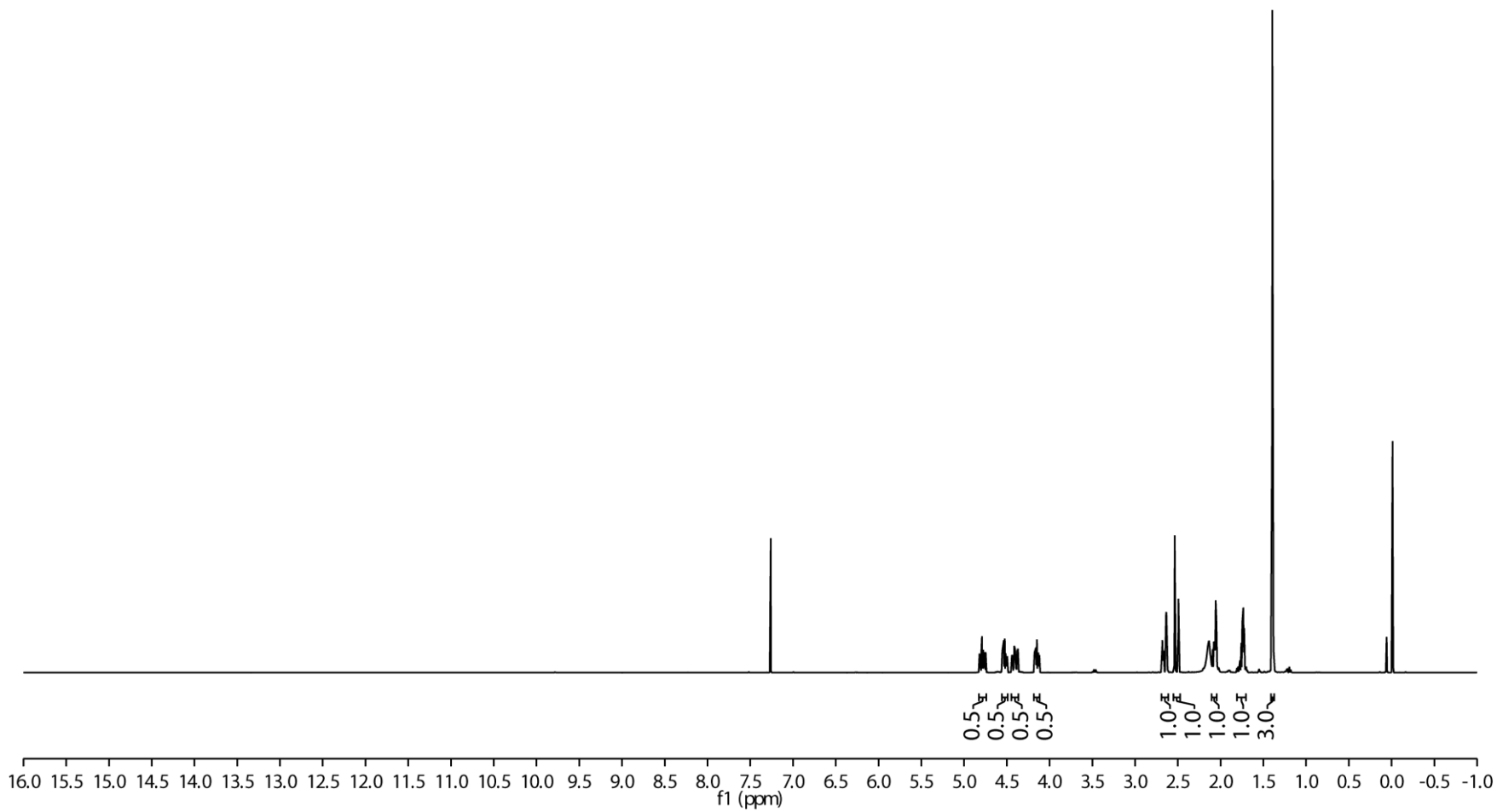
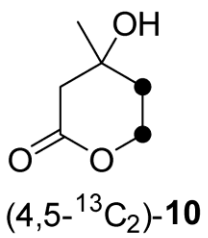


Figure S23. ¹H-NMR spectrum of (4,5-¹³C₂)-**10** (400 MHz, CDCl₃).

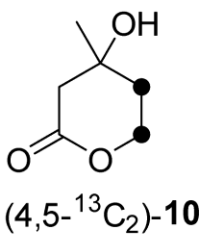
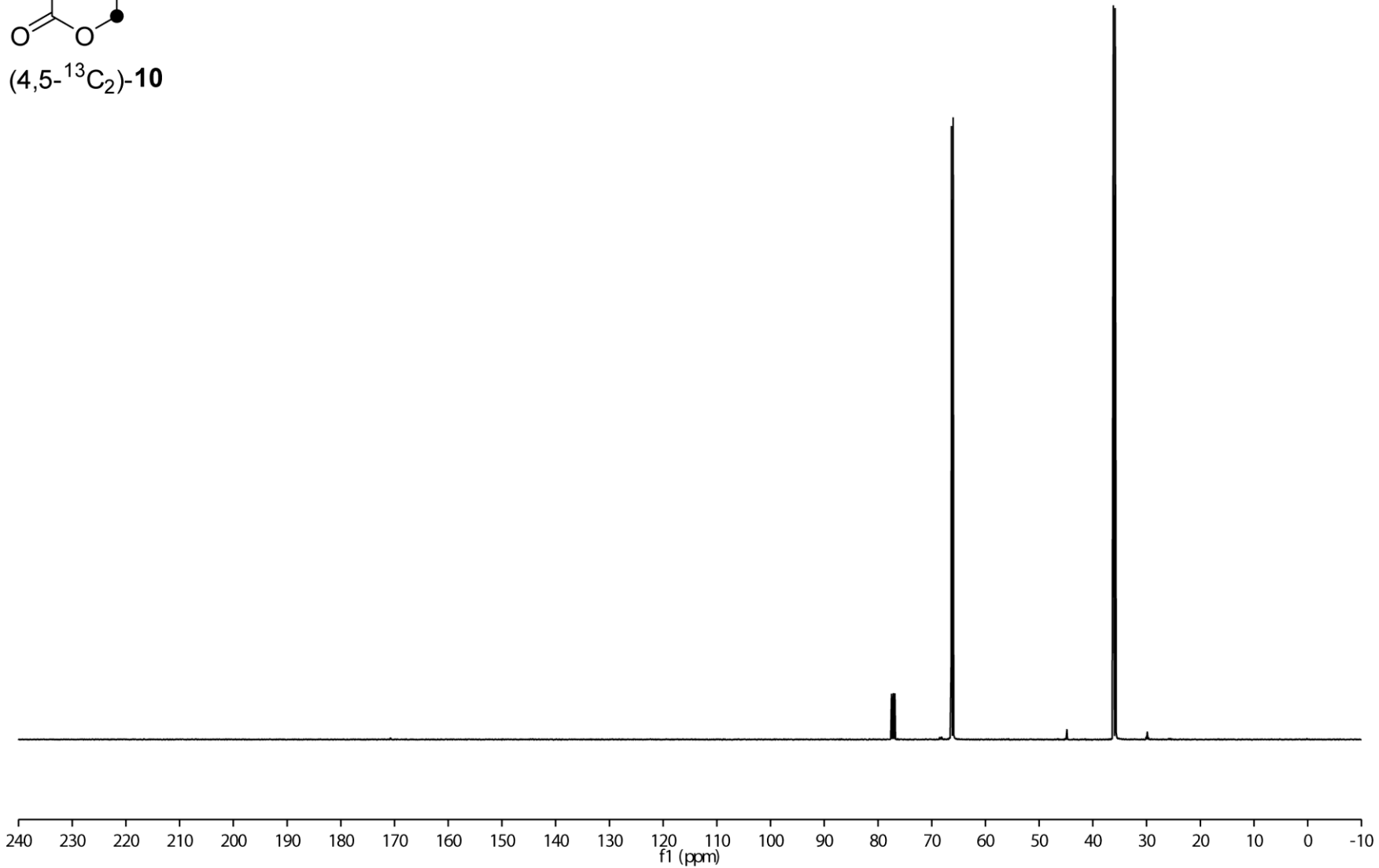


Figure S24. ¹³C-NMR spectrum of (4,5-¹³C₂)-**10** (100 MHz, CDCl₃).



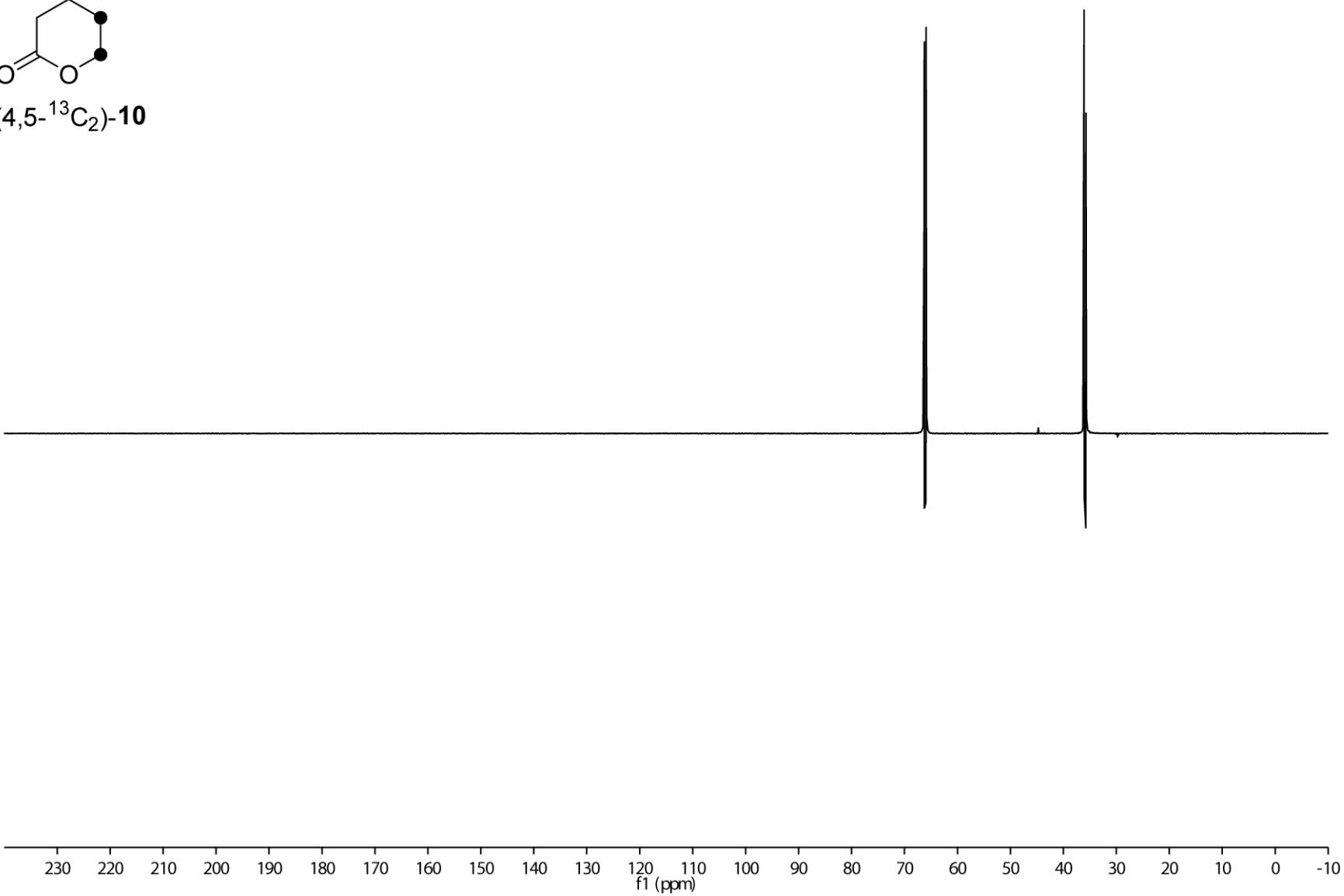
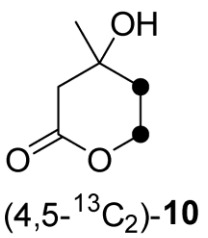


Figure S25. ¹³C-DEPT 135 spectrum of (4,5-¹³C₂)-**10** (100 MHz, CDCl₃).

Appendix D

Volatiles from the Fungal Microbiome of the Marine Sponge
Callyspongia cf. *flammea*



Cite this: *Org. Biomol. Chem.*, 2017, **15**, 7411

Volatiles from the fungal microbiome of the marine sponge *Callyspongia cf. flammea*†

Lena Barra,^a Paul Barac,^b Gabriele M. König,^b Max Crüsemann^b and Jeroen S. Dickschat *^a

The volatiles emitted by five fungal strains previously isolated from the marine sponge *Callyspongia cf. flammea* were captured with a closed-loop stripping apparatus (CLSA) and analyzed by GC-MS. Besides several widespread compounds, a series of metabolites with interesting bioactivities were found, including the quorum sensing inhibitor protoanemonin, the fungal phytotoxin 3,4-dimethylpentan-4-olide, and the insect attractant 1,2,4-trimethoxybenzene. In addition, the aromatic polyketides isotorquatone and char-tabomone that are both known from *Eucalyptus* and a new *O*-desmethyl derivative were identified. The biosynthesis of isotorquatone was studied by feeding experiments with isotopically labeled precursors and its absolute configuration was determined by enantioselective synthesis of a reference compound. Bioactivity testings showed algicidal activity for some of the identified compounds, suggesting a potential ecological function in sponge defence.

Received 25th July 2017,
Accepted 30th August 2017

DOI: 10.1039/c7ob01837a

rsc.li/obc

Introduction

Marine sponges (Porifera) belong to the most ancient living animals that have evolved during the Cryogenian period (>635 Myr ago), well before the Cambrian explosion.¹ They are sessile, filter-feeding organisms, that occur in almost any aquatic habitat from tropical reefs to the polar regions, and from the deep sea to fresh water lakes and rivers.² They exhibit highly variable and complex microbiomes consisting of bacteria, fungi and archaea³ that can account for up to 40% of the sponge tissue volume.⁴ This microbial diversity requires complex interactions between the symbionts and their host that are mediated by secondary metabolites with often strong biological activities and remarkable structural architectures.⁵ A well-known example is the pyrrole-imidazole alkaloid sceptrin (**1**) from the Caribbean sponge *Agelas sceptrum*⁶ that shows antimicrobial, anti-muscarinic and anti-histaminic activities, besides a strong inhibition of cancer cell motility,⁷ but the function of this compound in its ecological context remains elusive.⁸ Calyculin A (**2**) from the marine sponge *Discodermia calyx* is a highly cytotoxic compound and a potent inhibitor of

the protein phosphatases 1 and 2A.⁹ Notably, this polyketide is produced by the symbiotic bacterium *Entotheonella* and generated enzymatically from the pro-toxin phosphocalyculin (**3**) upon tissue wounding (Fig. 1).¹⁰ The fungus *Stachylidium* sp. 293 K04 that was isolated from the marine sponge *Callyspongia cf. flammea* produces the human leukocyte elastase inhibitor mariline A (**4**) as a mixture of enantiomers.¹¹ The tetrapeptide endolide A (**5**) containing an unusual 3-furyl-alanine subunit was isolated from the same fungus and showed affinity to the vasopressin receptor 1A.¹²

In contrast to such natural products that are typically isolated by classical extraction-isolation techniques, volatile metabolites are often overlooked, because these compounds are easily lost during concentration steps.¹³ Still, knowledge about these compounds is desirable, because volatiles can exhibit antibiotic properties or can be of critical importance *e.g.* for interspecies communication, cell-to-cell signaling, or control of pathogens¹⁴ which is of particularly high relevance in complex microbial communities as they occur in sponges. Despite these considerations studies on volatiles from sponges or their microbiomes are surprisingly rare and so far limited to investigations on bacterial symbionts. Among the few examples is a report on the North Sea sponge *Halichondria panacea* that emits a strong nauseating odour that can be traced back to a mixture of the sulfur compounds dimethyl disulfide, dimethyl trisulfide and methyl benzyl sulfide.¹⁵ Sponges of the genus *Ircinia* were found to release dimethyl sulfide, methyl isocyanide and methyl isothiocyanate that may act as chemical defense compounds.¹⁶ A series of studies on symbiotic bacteria from Antarctic sponges demonstrated the

^aKekulé-Institute for Organic Chemistry and Biochemistry, University of Bonn, Gerhard-Domagk-Straße 1, D-53121 Bonn, Germany. E-mail: dickschat@uni-bonn.de

^bInstitute of Pharmaceutical Biology, University of Bonn, Nußallee 6, D-53115 Bonn, Germany

† Electronic supplementary information (ESI) available: Table of identified volatiles, mass spectra, gas chromatograms for headspace extracts from *Sporomiella* and *Botrytis*, NMR spectra of synthetic compounds. See DOI: 10.1039/c7ob01837a

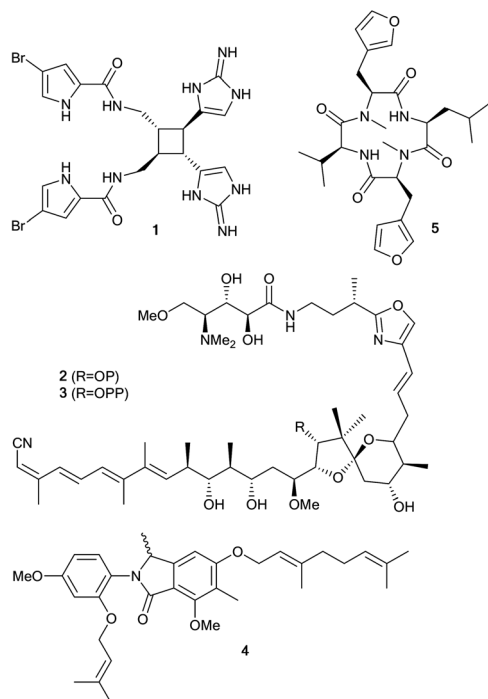


Fig. 1 Secondary metabolites from sponges and sponge associated bacteria and fungi. Structures of sceptrin (**1**), calyculin A (**2**), phosphocalyculin (**3**), marilene A (**4**) and endolide A (**5**).

production of volatiles with activity against *Burkholderia*.¹⁷ Here we present the first study on volatile metabolites produced by sponge associated fungi that were previously isolated¹⁸ from *Callyspongia* cf. *flammea*.

Results and discussion

The volatile metabolites released by *Dichotomomyces cejpilii* 293 K09, *Stachylidium* sp. 293 K04, *Botrytis* sp. 293 K02, *Emericella* sp. 293 K10, and *Sporormiella* sp. 293 K05 that were all isolated from the marine sponge *Callyspongia* cf. *flammea*¹⁸ were collected on a charcoal filter by use of a closed-loop stripping apparatus (CLSA).¹⁹ Sampling was conducted for 16–24 h and the adsorbed volatiles were eluted with dichloromethane. The obtained headspace extracts were analyzed by GC-MS and compounds were identified by comparison of their mass spectra to electronic mass spectral libraries²⁰ and comparison of their measured retention indices to reported data, with additional verification by comparison to synthetic or commercially available authentic standards in most cases. A summary of all 48 identified compounds is given in Table S1.† Two of the examined fungi, *Sporormiella* and *Botrytis*, did not show a significant emission of volatiles (Fig. S1 and S2†). The results obtained from the other three isolates are discussed here in detail.

Dichotomomyces cejpilii 293 K09

The ascomycete *D. cejpilii* 293 K09 has been intensively investigated for its rich secondary metabolism, which resulted in the

identification of indoloditerpenes,²¹ unusual steroids, aromatic isocyanides,²² gliotoxins and heveadrides.²³ Analysis of the headspace extracts obtained from this fungus also revealed a rich production of structurally diverse volatiles (Fig. 2). The most abundant compound was identified as the sesquiterpene alcohol (1(10)*E*,5*E*)-germacradien-11-ol (**14**), a known intermediate in geosmin biosynthesis, found in *Streptomyces* spp.,²⁴ myxobacteria²⁵ and liverworts.²⁶ Other identified terpenoids are dauca-4(11),8-diene (**13**), which was previously isolated from the liverwort *Bazzania trilobata*²⁷ and the acyclic terpenoid geranylacetone (**12**). The acrid plant defense compound protoanemonin (**6**) was found in minor amounts and has previously been described from plants of the buttercup family (*Ranunculaceae*) where it is enzymatically generated from the glucoside ranunculin upon lesion of plant tissue.²⁸ Protoanemonin was also found as a catabolite of the xeno-

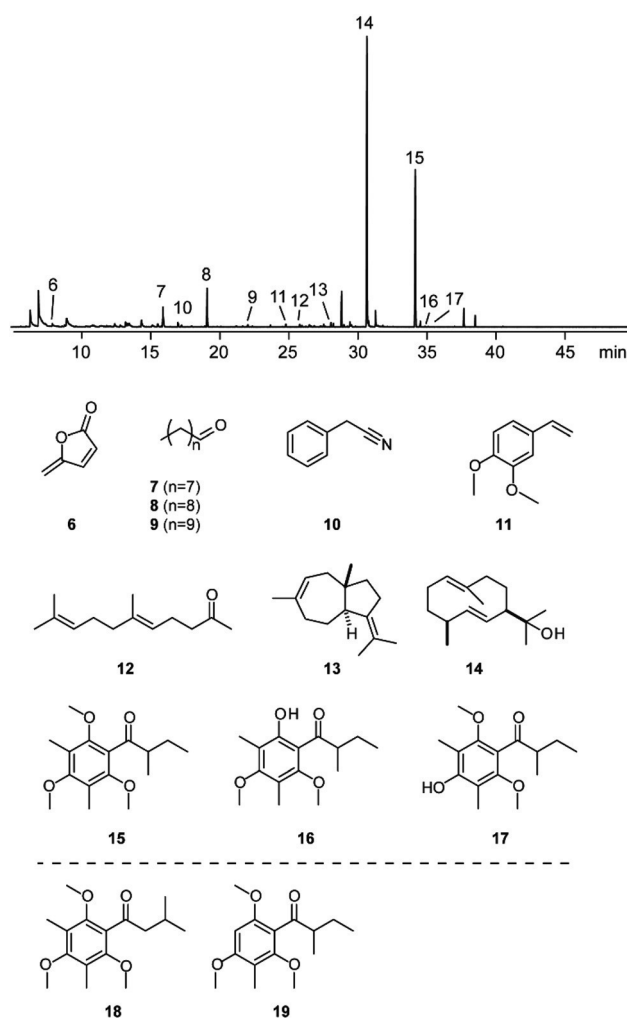


Fig. 2 Volatiles from *Dichotomomyces cejpilii*. Total ion chromatogram of the headspace extract, structures of the identified volatiles and of torquatone (**18**) and of *C*-desmethyl isotorquatone (**19**). Peak numbers in the chromatogram refer to compound numbers. The absolute configurations of **13**, **14**, **16** and **17** have not been determined, cf. main text for the absolute configuration of **15**.

biotic 4-chlorocatechol in *Pseudomonas*.²⁹ Recently, **6** was shown to act as a quorum sensing inhibitor towards *N*-acyl-L-homoserine lactones (AHLs) in *Pseudomonas* sp. B13.³⁰ The production of **6** by *D. cejpii* is interesting, as AHLs were shown to play a key role in the interaction between sponge symbiotic bacteria and their host.³¹ Additionally, protoanemonin exhibits antifungal and antibacterial properties.³²

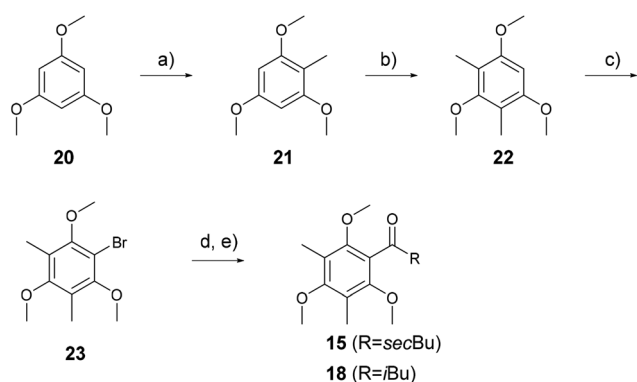
Other detected metabolites included the unbranched long-chain aldehydes nonanal (**7**), decanal (**8**) and dodecanal (**9**), and the benzene derivatives benzyl cyanide (**10**) and 3,4-dimethoxystyrene (**11**) which are all frequently observed fungal volatiles.^{14c} A particularly interesting compound, detected as the second most abundant volatile in the headspace extract of *D. cejpii*, was the highly methylated aromatic polyketide **15** along with its *O*-desmethyl derivatives **16** and **17**. Comparison of the mass spectrum of **15** to data base spectra returned the two possible structures of torquatone (**18**) and isotorquatone (**15**). Since the mass spectra and retention indices of both compounds are nearly identical (Fig. S3†), a synthesis for both isomers was performed to allow for an unambiguous structural assignment. Two successive methylations of 1,3,5-trimethoxybenzene (**20**) with methyl iodide gave access to **22** that was brominated with NBS to yield **23**.³³ Subsequent lithiation, addition to 2-methylbutyraldehyde, and oxidation with Dess–Martin periodinane resulted in **15** (Scheme 1). Compound **18** was prepared analogously from **23** and isovaleraldehyde.

Both synthetic compounds **15** and **18** were compared to the volatile emitted by *D. cejpii*, revealing the identity of **15** and the natural material by GC–MS analysis (Fig. S4†). To determine the absolute configuration of natural **15**, a stereoselective synthesis was performed using the same synthetic route as described above and employing enantiomerically pure (*S*)-2-methylbutyraldehyde.³⁴ The obtained material (*S*)-(+)-**15** (98% ee) and the racemate of **15** were used to determine the absolute configuration of natural isotorquatone by HPLC on a homochiral stationary phase, indicating that natural **15** is a

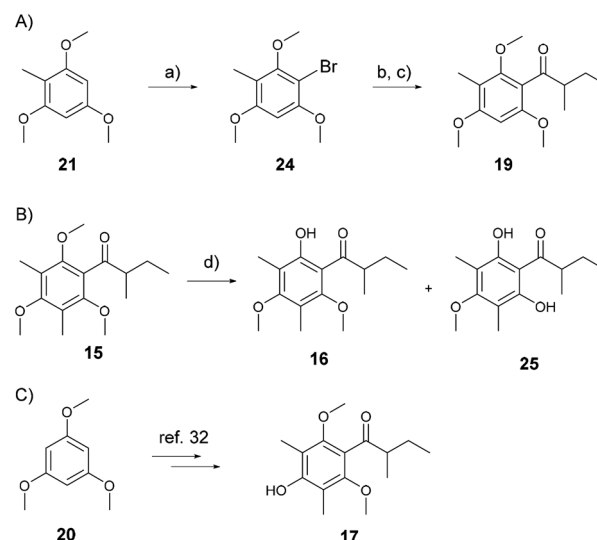
mixture of enantiomers ((40% ee in favour of (*R*)-(-)-**15**, Fig. S5†). Isotorquatone is a known constituent of the essential oils of various *Eucalyptus* species,³⁵ but the absolute configuration of the plant-derived isotorquatone is unknown.

The headspace extract of *D. cejpii* contained two additional trace compounds whose mass spectra showed a molecular ion at $m/z = 266$ and a base peak ion at $m/z = 209$ (Fig. S6†), suggesting the structures of desmethyl analogs of **15** with a missing methyl group at one of the oxygens or ring carbons. For an unambiguous structural assignment all three possible derivatives were synthesized. The *C*-desmethyl analog **19** was prepared from **21** via the same strategy as described for torquatone and isotorquatone, by omission of the methylation step to **22**. Treating (*rac*)-**15** with BBr_3 yielded the *O*-desmethyl analog **16**, in addition to the doubly *O*-demethylated compound **25**, but no *O*-demethylation of the methoxy group in *para*-position to the ketone side chain was observed. Therefore, a published synthesis for **17** over 9 steps starting from 1,3,5-trimethoxybenzene was conducted (Scheme 2).³³ Comparison of the three synthetic compounds to the natural volatiles by GC–MS resulted in the identification of **16** and **17**, but not of **19** as headspace constituents of *D. cejpii*. The isotorquatone derivative **16** (chartabomone) is known from *Eucalyptus chartaboma* and *E. miniata*,^{35b} while **17** is a new natural product that we wish to name dichotomone.

The biosynthesis of **15** was addressed in feeding experiments with isotopically labeled ($2\text{-}^{13}\text{C}$)acetate and (*methyl*- $^2\text{H}_3$)-L-methionine. Feeding of ($2\text{-}^{13}\text{C}$)acetate resulted in the incorporation of five labeled C_2 -units into **15** as indicated by the resulting mass spectrum, and feeding of (*methyl*- $^2\text{H}_3$)-L-methionine gave incorporation of labeling into six methyl groups (Fig. S7†). These findings are in line with a biosynthesis of **15**



Scheme 1 Synthesis of isotorquatone (**15**) and torquatone (**18**). (a) *s*-BuLi, 40 °C, 2 h; then MeI, –78 °C to rt, 70%; (b) *s*-BuLi, 40 °C, 2 h; then MeI, –78 °C to rt, 82%; (c) NBS, rt, 82%; (d) *t*-BuLi, –78 °C to –10 °C; then aldehyde RCHO, –78 °C, 30 min; (e) DMP, rt, 63% for **15**, 50% for **18** (2 steps). BuLi butyllithium, MeI methyl iodide, NBS *N*-bromosuccinimide, DMP Dess–Martin periodinane.



Scheme 2 Synthesis of (A) *C*-desmethyl isotorquatone (**19**), (B) chartabomone (**16**), and (C) dichotomone (**17**). (a) NBS, 0 °C to rt, 97%; (b) *t*-BuLi, –78 °C to –10 °C, then 2-methylbutyraldehyde, –78 °C, 30 min; (c) IBX, rt, 28% (2 steps); (d) BBr_3 (1.1 equiv.), –78 °C to rt, 35% of **16** and 52% of **25**. IBX 2-iodoxybenzoic acid.

by a polyketide synthase (PKS) from an acetate starter unit by four extension steps with malonyl-CoA, with full reduction of the 3-oxo function during the first and no reduction during the following chain extensions, and C-methylation during the first, third and last chain elongation (Scheme 3). Product release by a Claisen condensation and three O-methylations yield **15**. The presence of minor amounts of **16** and **17** suggests that the O-methyltransferase does not convert the complete material released from the PKS. In contrast to this finding, the polyketide synthase acts in a highly programmed fashion, as indicated by the absence of **19** which would represent a PKS product formed through an omitted C-methylation step.

Stachyldidium sp. 293 K04

Besides marilone A (**4**) and endolide A (**5**),^{11,12} a variety of other bioactive natural products has been isolated from *Stachyldidium* sp. 293 K04, including the marilonones A–C and the stachylinones A–D.^{36–38} Analysis of the volatiles from *Stachyldidium* resulted in the identification of 14 compounds (Fig. 3). The most abundant compound was 1,2,4-trimethoxybenzene (**44**) that is a known constituent of the bouquet of orchid flowers³⁹ and *Cucurbita* blossoms where it acts together with indole and (*E*)-cinnamaldehyde as an attractant for rootworm beetles.⁴⁰ The related compound 1,2-dimethoxybenzene (**41**) is only found in traces and is also known from *Aspergillus clavatus*.⁴¹ The sulphur compound benzothiazole (**43**), also a minor component, has previously been reported from *Trichoderma*⁴² and *Aspergillus*.⁴¹ Among the major components 1-octen-3-ol (**38**)

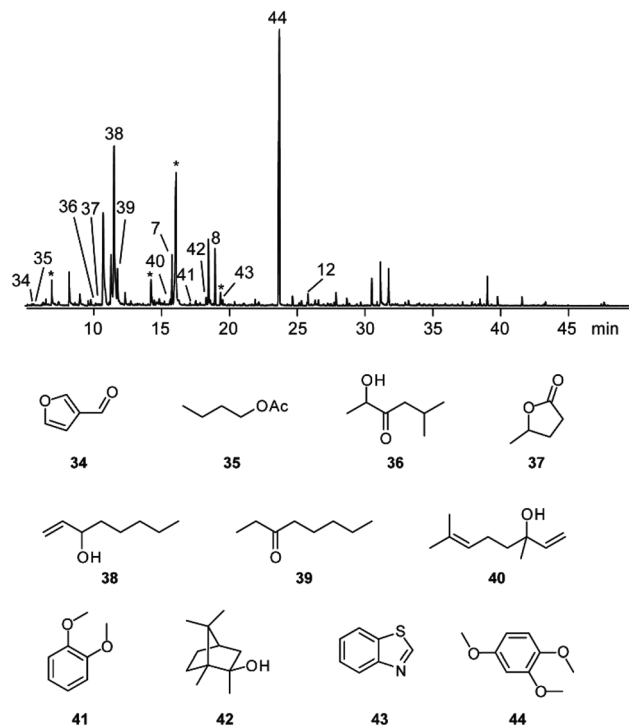
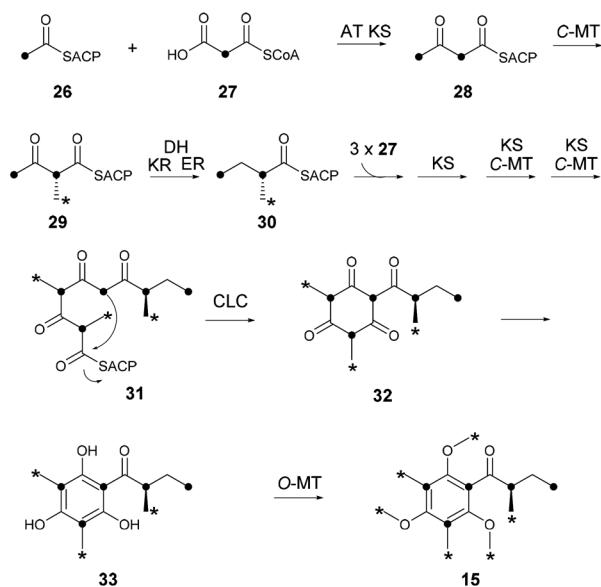


Fig. 3 Volatiles from *Stachyldidium* sp. 293 K04. Total ion chromatogram of the headspace extract of *Stachyldidium* sp. 293 K04 and structures of the identified volatiles. Asterisks indicate compounds originating from the medium. Peak numbers in the chromatogram refer to compound numbers.



Scheme 3 Biosynthetic model for **15** and labeling pattern after feeding of ($2\text{-}^{13}\text{C}$)acetate and ($\text{methyl-}^2\text{H}_3$)-L-methionine. AT = acyl transferase, C-MT = C-methyltransferase, O-MT = O-methyltransferase, DH = dehydratase, KR = ketoreductase, ER = enoylreductase, KS = ketosynthase, CLC = claisen condensation domain. Asterisks indicate completely deuterated carbons and black dots indicate ^{13}C -labeling carbons. The indicated positions for incorporation of labelling are based on mechanistic considerations for PKS biosynthesis.

was identified that is probably the most widespread fungal volatile. This compound is frequently accompanied by other C_8 metabolites such as 3-octanone (**39**).^{14c} “Matsutake alcohol” **38** was first isolated from *Tricholoma matsutake*⁴³ and its role in chemical defense is suggested by the triggered emission upon wounding of fungal fruiting bodies.⁴⁴

A rather unusual metabolite released by *Stachyldidium* is furan-3-carbaldehyde (**34**) whose production may be linked to the biosynthesis of endolide A (**5**), a natural product that is made up from the structurally related uncommon amino acid 3-furylalanine.⁴⁵ The production of terpenes including nerolidol (**40**), 2-methylisborneol (**42**) and geranyl acetone (**12**) was also observed. 2-Methylisborneol is a widespread off-flavour with a characteristic mouldy odor that is commonly found in various bacteria^{24c} and ascomycete fungi such as *Aspergillus*⁴⁶ und *Penicillium*.⁴⁷ Other identified compounds are butyl acetate (**35**), 2-hydroxy-5-methylhexan-3-one (**36**), 4-methyl- γ -butyrolactone (**37**) and the long chain aldehydes **7** and **8**.

Emericella sp. 293 K02

The fungus *Emericella* sp. 293 K02 has not been investigated with respect to its secondary metabolism. The headspace extracts contained a large number of compounds, twelve of which could be identified including the aldehydes **7**, **8**, **9** and the higher homolog dodecanal (**48**), matsutake alcohol (**38**) and its companion **39**, and benzothiazole (**43**, Fig. 4). A unique compound emitted by *Emericella* was 3,4-dimethylpentan-4-

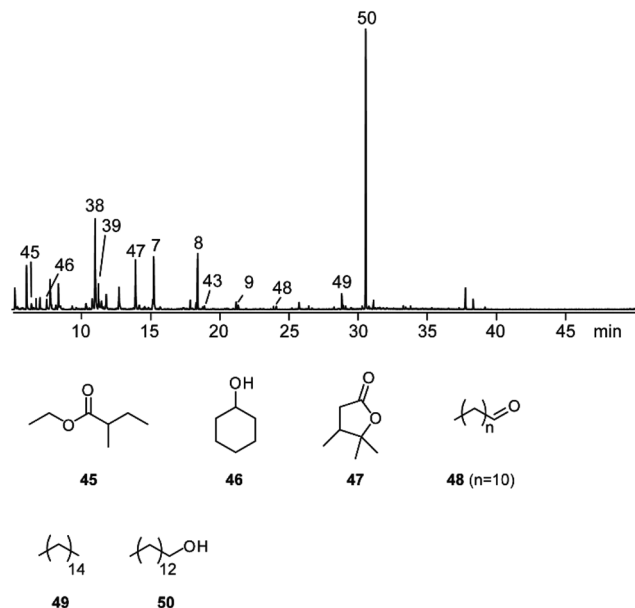


Fig. 4 Volatiles from *Emericella* sp. 293 K02. Total ion chromatogram of the headspace extract of *Emericella* sp. and structures of the identified volatiles. Peak numbers in the chromatogram refer to compound numbers.

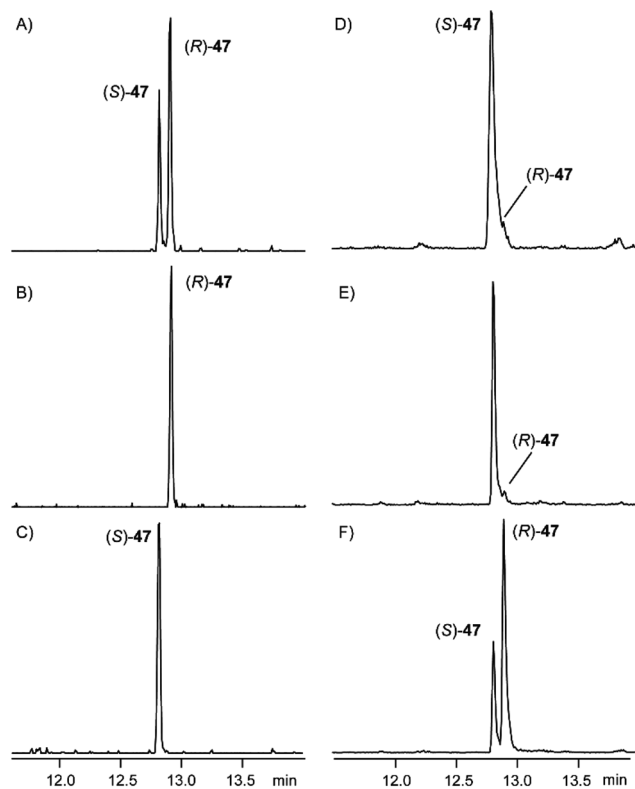


Fig. 5 Extracted ion chromatograms ($m/z = 113$) of (A) a pseudoracemic mixture of synthetic (S)- and (R)-47, (B) synthetic (R)-47, (C) synthetic (S)-47, (D) a headspace extract from *Emericella*, (E) headspace extract spiked with synthetic (S)-47, and (F) headspace extract spiked with synthetic (R)-47.

Table 1 Algicidal activity of fungal volatiles against *Chlorella fusca* (80% inhibition)

Compound	MIC ^a [$\mu\text{g mL}^{-1}$]
(<i>rac</i>)-15	31.3
(<i>S</i>)-15	125.0
16	31.3
17	>125.0
18	>125.0
19	2.0
25	15.6
2,4-Dichlorophenol ^b	1.0
CuSO ₄ ·5H ₂ O ^b	<31.3

^a Minimal inhibitory concentration. ^b Positive control.

olide (47). This lactone was previously described as a phyto-toxin that is possibly involved in the pathogenicity of the fungus *Hymenoscyphus pseudoalbidus*, the causative agent of European ash dieback. Compound testings in the laboratory revealed a strong inhibitory activity of lactone 47 against ash seed germination.⁴⁸ *H. pseudoalbidus* produces mainly the *R* enantiomer with 80% ee. Notably, the material emitted by *Emericella* is also a 1 : 10 mixture of enantiomers, but in this species (*S*)-47 is dominant (Fig. 5).

Bioactivity tests

A selection of fungal volatiles identified during the course of this study were tested for their bioactivities against bacteria and algae. While all the tested compounds showed no or only moderate activity against Gram-positive (*Bacillus megaterium*) and Gram-negative (*Escherichia coli*) bacteria (Table S2[†]), the racemate of 15 showed growth inhibitory effects towards the alga *Chlorella fusca* (Table 1). The *S* enantiomer was much less active, suggesting that the growth inhibition is mainly due to the *R* enantiomer in the racemate. Notably, the isomer torquatone (18) was inactive. The *O*-desmethyl derivative chartabomone 16 revealed a similarly strong algicidal activity as (*rac*)-15, while no activity was observed for the newly identified dichotomone 17. The strongest bioactivity was detected for the synthetic derivatives 19 and 25 (Table 1).

Conclusions

In the present study we describe the first analysis of volatiles released by sponge-associated fungi that were previously isolated from *Callyspongia* cf. *flammea*. The analyses revealed the production of several volatiles with interesting bioactivities, including a small family of polymethylated polyketides with the main compound isotorquatone (15). The observed algicidal activity of racemic 15 and its *O*-desmethyl derivative 16 may point to their involvement in protecting the sponge from algal infections, but it is difficult to judge to which extent the results from laboratory bioactivity experiments can be used to assign a function to these compounds in a complex ecosystem such as a sponge and its microbiome in their natural habitat. The occurrence of compounds such as the quorum sensing

disruptor protoanemonine (**6**) is also noteworthy and suggests a potential involvement of fungal volatiles in the intra- and interspecies communication between the multiple microorganisms in the rich sponge microbiomes. Further research will be required to deepen our understanding of the role of fungal volatiles in the complex interactions between sponges and their microbial symbionts.

Experimental

Fungal strains and growth conditions

The fungal strains investigated in this study (Table 2) were previously isolated from a marine sample of the sponge *Callyspongia* cf. *flammea*, collected on Bear Island, Sydney, Australia as reported in ref. 18. In order to obtain the volatiles, all strains were cultivated on biomalt salt medium, in 100 mm × 15 mm Petri dishes, for 14 days, at room temperature.

CLSA sampling

The volatiles were collected by use of a closed-loop stripping apparatus (CLSA).¹⁸ Sampling was conducted for 16 to 24 h at room temperature (20 °C) and under natural day and night light conditions. The charcoal filter was extracted with dichloromethane (50 µL) and the resulting headspace extracts were directly analyzed by GC-MS. All headspace samplings were carried out in duplicates.

GC-MS analysis of headspace extracts

The crude headspace extracts were analyzed by use of an Agilent HP7890B gas chromatograph, fitted with a HP-5MS silica capillary column (30 m, 0.25 mm i.d., 0.50 µm film), connected to a HP5977A mass detector. The GC-MS conditions were as follows: (1) inlet pressure: 77.1 kPa, He flow 23.3 mL min⁻¹; (2) injection volume: 1 µL; (3) injection mode: splitless, valve time 60 s; (4) oven temperature ramp: 5 min at 50 °C increasing at 5 °C min⁻¹ to 320 °C; (5) carrier gas He at 1 mL min⁻¹; (6) transfer line: 250 °C; (7) electron energy: 70 eV. Retention indices (*I*) were determined from a homologous series of *n*-alkanes (C₈–C₄₀).

Feeding experiments

Feeding experiments were performed with *D. cejpii* and isotopically enriched (2-¹³C)acetate and (methyl-²H₃)-L-methionine. The labeled compounds were directly added to the liquid agar medium (10 mM) and *D. cejpii* was inoculated for 10 days. The

emitted volatiles of the grown cultures were captured by use of a CLSA and the crude headspace extracts were analyzed by GC-MS.

General synthetic and analytical methods

All chemicals were obtained from Acros Organics (Geel, Belgium), Sigma Aldrich Chemie GmbH (Steinheim, Germany) or TCI Deutschland GmbH (Eschborn, Germany). All solvents were purified by distillation. Whenever necessary, reactions were carried out under inert atmosphere (Ar) using vacuum-heated flasks and dried solvents (dried according to standard protocols). Thin layer chromatography (TLC) was performed on 0.20 mm silica plates (Polygram SIL G/UV254) obtained from Macherey–Nagel (Düren, Germany). Column chromatography was performed on Merck silica gel (0.040–0.063 Mesh). NMR spectra were recorded on Bruker AV I (400 MHz), AV III HD Prodigy (500 MHz) and AV III HD Cryo (700 MHz) spectrometers, and were referenced against CDCl₃ (δ = 7.26 ppm) and C₆D₆ (δ = 7.16 ppm) for ¹H-NMR, and CDCl₃ (δ = 77.01 ppm) and C₆D₆ (δ = 128.06 ppm) for ¹³C-NMR. The multiplicities are specified as follows: singlet (s), doublet (d), triplet (t), quartet (q), quintet (quin), sextet (sex), septet (sept). GC-MS analyses were carried out with an Agilent HP7890B gas chromatograph connected to a HP5977A mass detector fitted with a HP-5MS silica capillary column (30 m, 0.25 mm i.d., 0.50 µm film). The GC-MS conditions were as follows: (1) inlet pressure: 77.1 kPa, He flow 23.3 mL min⁻¹; (2) injection volume: 1 µL; (3) injection mode: split 50 : 1, valve time 60 s; (4) oven temperature ramp: 5 min at 50 °C increasing at 10 °C min⁻¹ to 320 °C; (5) carrier gas He at 1 mL min⁻¹; (6) transfer line: 250 °C; (7) electron energy: 70 eV. Retention indices (*I*) were determined from a homologous series of *n*-alkanes (C₈–C₄₀). Optical rotary powers were recorded on a P8000 Polarimeter (Krüss). UV/Vis spectra were recorded on a Cary 100 UV/Vis spectrometer (Agilent). IR Spectra were measured by use of an Alpha FT-IR spectrometer from Bruker.

Synthetic procedures

1,3,5-Trimethoxy-2-methylbenzene (21). To a solution of 1,3,5-trimethoxybenzene (**20**) (5.00 g, 29.7 mmol, 1.0 equiv.) in 80 mL dry THF was slowly added a 1.4 M solution of *s*-butyllithium (31.9 mL, 44.6 mmol, 1.5 equiv.) at room temperature and stirred for 15 minutes. The reaction was heated to 40 °C and stirred for 2 h. Afterwards it was cooled to –78 °C and methyl iodide (7.40 mL, 119 mmol, 4.0 equiv.) was added slowly. The reaction was allowed to warm to room temperature and stirred over night. Addition of water was followed by extraction with Et₂O and the combined organic layers were dried with MgSO₄ and the solvent was removed under reduced pressure. The crude product was purified by column chromatography on silica gel (cyclohexane/ethyl acetate 30 : 1) and **21** was isolated as a yellowish oil (3.78 g, 20.8 mmol, 70%). *R*_f = 0.2. GC (HP-5MS): *I* = 1482. ¹H-NMR (500 MHz, CDCl₃): δ = 6.15 (s, 2H, CH), 3.81 (s, 9H, CH₃), 2.03 (s, 3H, CH₃) ppm. ¹³C-NMR (125 MHz, CDCl₃): δ = 159.1 (s, C_q), 158.9 (s, 2 × C_q), 106.9 (s, C_q), 90.7 (2 × CH), 55.8 (2 × CH₃), 55.5 (s, CH₃), 7.8 (s, CH₃) ppm. IR (ATR): $\tilde{\nu}$ = 2997, 2938, 2836, 1594, 1499, 807.

Table 2 Investigated strains from *Callyspongia* cf. *flammea*

Strain no.	Taxonomy
293 K02	<i>Botrytis</i> sp.
293 K04	<i>Stachyliidium bicolor</i>
293 K05	<i>Sporomiella</i> sp.
293 K09	<i>Dichotomomyces cejpii</i>
293 K10	<i>Emericella</i> sp.

UV/Vis (MeCN): λ_{\max} (lg ϵ): 271 (4.29), 241 (5.63) nm. EI-MS (70 eV): m/z (%) = 182 (100), 167 (21), 153 (23), 151 (25), 139 (17), 121 (22), 109 (15), 91 (14), 77 (14), 69 (14). HR-EIMS calcd for $C_{10}H_{14}O_3^+$: m/z = 182.0943, found: m/z = 182.0979.

1,3,5-Trimethoxy-2,4-dimethylbenzene (22). To a solution of **21** (2.30 g, 12.6 mmol, 1.0 equiv.) in 15 mL dry THF was slowly added a 1.4 M solution of *s*-butyllithium (13.5 mL, 19.0 mmol, 1.5 equiv.) at room temperature and stirred for 15 minutes. The reaction was heated to 40 °C and stirred for 2 h. Afterwards it was cooled to -78 °C and methyl iodide (3.20 mL, 50.5 mmol, 4.0 eq.) was added slowly. The reaction was allowed to warm to room temperature and stirred over night. Addition of water was followed by extraction with Et₂O and the combined organic layers were dried with MgSO₄ and the solvent was removed under reduced pressure. The crude product was purified by column chromatography on silica gel (cyclohexane/ethyl acetate 30 : 1) and **22** was isolated as a white crystalline solid (2.04 g, 10.4 mmol, 82%). R_f = 0.2. GC (HP-5MS): I = 1520. ¹H-NMR (500 MHz, CDCl₃): δ = 6.28 (s, 1H, CH), 3.83 (s, 6H, 2 × CH₃), 3.69 (s, 3H, CH₃), 2.11 (s, 6H, 2 × CH₃) ppm. ¹³C-NMR (125 MHz, CDCl₃): δ = 158.0 (s, C_q), 156.8 (s, 2 × C_q), 111.7 (s, 2 × C_q), 91.84 (s, CH), 60.3 (s, CH₃), 55.9 (s, 2 × CH₃), 8.7 (s, 2 × CH₃) ppm. IR (ATR): $\tilde{\nu}$ = 2985, 2938, 2840, 1593, 1495, 803. UV/Vis (MeCN): λ_{\max} (lg ϵ): 281 (4.45), 235 (4.79) nm. EI-MS (70 eV): m/z (%) = 197 (12), 196 (100), 181 (34), 165 (31), 153 (15), 138 (10), 135 (11), 121 (11), 91 (10), 77 (10). HR-EIMS calcd for $C_{11}H_{16}O_3^+$: m/z = 196.1099, found: m/z = 196.1121.

1-Bromo-2,4,6-trimethoxy-3,5-dimethylbenzene (23). To a solution of **22** (0.20 g, 1.02 mmol, 1.0 equiv.) in 6 mL dry DCM was added NBS (0.20 g, 1.12 mmol, 1.1 equiv.) and the mixture was stirred for 16 h at room temperature. The reaction was quenched with water and extracted with Et₂O and the combined organic layers were dried with MgSO₄. The solvent was removed under reduced pressure and the crude product was purified by column chromatography on silica gel (cyclohexane/ethyl acetate 20 : 1). Product **23** was isolated as a white solid (0.23 g, 0.84 mmol, 82%). R_f = 0.2. GC (HP-5MS): I = 1704. ¹H-NMR (400 MHz, CDCl₃): δ = 3.78 (s, 6H, 2 × CH₃), 3.69 (3H, CH₃), 2.23 (s, 6H, 2 × CH₃) ppm. ¹³C-NMR (100 MHz, CDCl₃): δ = 157.5 (C_q), 154.5 (2 × C_q), 122.2 (2 × C_q), 108.3 (C_q), 60.5 (2 × CH₃), 60.1 (CH₃), 10.0 (2 × CH₃) ppm. IR (ATR): $\tilde{\nu}$ = 3000, 2938, 2866, 2831, 1583, 1559. UV/Vis (MeCN): λ_{\max} (lg ϵ): 231 (4.90) nm. EI-MS (70 eV): m/z (%) = 276 (98), 274 (100), 261 (14), 259 (14), 233 (25), 231 (27), 216 (17), 165 (20), 137 (20), 77 (16). HR-EIMS calcd for $C_{11}H_{15}O_3Br^+$: m/z = 274.0205, found: m/z 274.0204.

(rac)-Isotorquatone (15). To a solution of **23** (0.23 g, 0.84 mmol, 1.0 equiv.) in 5 mL dry THF was slowly added a 1.7 M solution of *t*-butyllithium (1.00 mL, 1.67 mmol, 2.0 equiv.) at -78 °C. The reaction was warmed to -10 °C, stirred for 10 minutes and again cooled to -78 °C. Aldehyde 2-methylbutyraldehyde (0.22 g, 2.51 mmol, 3.0 equiv.) was slowly added and the reaction was stirred for 30 minutes at -78 °C. The reaction was quenched with water and extracted with Et₂O. The combined organic layers were dried with MgSO₄ and the

solvent was removed under reduced pressure. The crude product was dissolved in 5 mL dry DCM and DMP (0.36 g, 0.84 mmol, 1.0 equiv.) was added. The reaction was stirred over night at room temperature, quenched with water and extracted with Et₂O. The crude product was purified by column chromatography on silica gel (cyclohexane/ethyl acetate 20 : 1). (*rac*)-Isotorquatone **15** (0.15 g, 0.53 mmol, 63%) was isolated as a colorless oil. R_f = 0.2. GC (HP-5MS): I = 1810. ¹H-NMR (500 MHz, CDCl₃): δ = 3.72 (s, 3H, CH₃), 3.69 (s, 6H, 2 × CH₃), 2.93–2.84 (m, 1H, CH), 2.17 (s, 6H, 2 × CH₃), 1.86–1.75 (m, 1H, CHH), 1.45–1.34 (m, 1H, CHH), 1.13 (d, 3H, ³ J = 6.8 Hz, CH₃), 0.94 (t, 3H, ³ J = 7.3 Hz, CH₃) ppm. ¹³C-NMR (125 MHz, CDCl₃): δ = 209.2 (C_q), 159.0 (C_q), 153.9 (C_q), 127.2 (C_q), 121.0 (C_q), 62.5 (2 × CH₃), 60.1 (CH₃), 49.3 (CH), 25.2 (CH₂), 15.2 (CH₃), 11.7 (CH₃), 9.4 (CH₃) ppm. IR (ATR): $\tilde{\nu}$ = 2997, 2921, 2856, 1652. EI-MS (70 eV): m/z (%) = 280 (9), 225 (3), 224 (26), 223 (100), 208 (6), 193 (5), 190 (3), 179 (3), 165 (7), 91 (3). HR-EIMS calcd for $C_{16}H_{24}O_4^+$: m/z = 280.1675, found: m/z = 280.1658.

(S)-Isotorquatone ((S)-15). Synthesis of (*S*)-**15** was conducted according to the procedure for (*rac*)-**15**. Enantiomerically pure (*S*)-2-methylbutyraldehyde³³ was used for the alkylation of **23**. All recorded spectral data were identical to those for (*rac*)-**15**. [α]_D²⁰ = +4.3 (*c* 1, EtOH).

Analysis of the enantiomeric excess of 15. The enantiomeric excess of natural **15** and synthetic (*S*)-**15** was determined by analytical HPLC on a homochiral stationary phase (Fig. S2†) using the following conditions: system: Fa. Knauer GmbH (Berlin, Germany), 2 pumps P-1 HPLCplus (max. 750 bar), oven T-1 with 2 integrated 6-Port valves, photodiode array detector PDA-1 (190–1000 nm); column: Eurocel 03, 3 μ m, 4.6 mm × 250 mm; solvent: methanol/water (90/10); flow rate: 1.0 mL min⁻¹; pressure: 209 bar, temperature: 20 °C. *Dichotomomyces cejpai* 293 K09 was cultivated on MPY medium (malt extract 20 g L⁻¹, peptone from meat 2.5 g L⁻¹, yeast extract 2.5 g L⁻¹, agar 15 g L⁻¹). Cultivation was performed in 1800 mL Fernbach flasks (20 × 250 mL per flask) for 40 days at room temperature with constant artificial light exposure. Each Fernbach flask was extracted with pentane (100 mL) and the combined extracts were concentrated under reduced pressure. The crude extract was purified by column chromatography on silica gel (pentane/diethyl ether 20 : 1) and a fraction containing **15** (8 mg) was isolated and directly analyzed.

Torquatone (18). To a solution of **23** (0.05 g, 0.18 mmol, 1.0 equiv.) in 1 mL dry THF was slowly added a 1.7 M solution of *t*-butyllithium (0.22 mL, 0.36 mmol, 2.0 equiv.) at -78 °C. The reaction was warmed to -10 °C, stirred for 10 minutes and again cooled to -78 °C. Aldehyde **24** (0.05 g, 0.58 mmol, 3.0 equiv.) was slowly added and the reaction was stirred for 30 minutes at -78 °C. The reaction was quenched with water and extracted with Et₂O. The combined organic layers were dried with MgSO₄ and the solvent was removed under reduced pressure. The crude product was dissolved in 1 mL dry DCM and DMP (0.08 g, 0.18 mmol, 1.0 equiv.) was added. The reaction was stirred over night at room temperature, quenched with water and extracted with Et₂O. The crude product was

purified by column chromatography on silica gel (cyclohexane/ethyl acetate 20 : 1). Torquatone **18** (0.03 g, 0.09 mmol, 50%) was isolated as a colorless oil. $R_f = 0.2$. GC (HP-5MS): $I = 1824$. $^1\text{H-NMR}$ (500 MHz, C_6D_6): $\delta = 3.53$ (s, 6H, $2 \times \text{CH}_3$), 3.34 (s, 3H, $2 \times \text{CH}_3$), 2.73 (d, $^3J = 6.8$ Hz, 2H, CH_2), 2.42 (tsept, $^3J = 6.7$ Hz, $^3J = 6.7$ Hz, 1H, CH), 2.14 (s, 6H, $2 \times \text{CH}_3$), 0.97 (d, $^3J = 6.7$ Hz, 6H, $2 \times \text{CH}_3$) ppm. $^{13}\text{C-NMR}$ (125 MHz, C_6D_6): $\delta = 204.1$ (C_q), 159.3 (C_q), 154.3 ($2 \times \text{C}_q$), 128.6 (C_q), 121.1 ($2 \times \text{C}_q$), 62.3 ($2 \times \text{CH}_3$), 59.5 (CH_3), 54.4 (CH_2), 24.4 (CH), 22.7 ($2 \times \text{CH}_3$), 9.3 ($2 \times \text{CH}_3$) ppm. IR (ATR): $\tilde{\nu} = 2955, 2868, 1696, 1581, 1452, 1397, 1365, 1333, 1324, 1294, 1265, 1221, 1194, 1143, 1071, 1006, 990$. EI-MS (70 eV): m/z (%) = 280 (10), 223 (100), 208 (3), 196 (3), 165 (3). HR-ESIMS calcd for $\text{C}_{16}\text{H}_{25}\text{O}_4^+$: $m/z = 281.1747$, found: $m/z = 280.1747$ [$\text{M} + \text{H}$] $^+$.

2-Bromo-1,3,5-trimethoxy-4-methylbenzene (24). To a solution of **21** (0.20 g, 1.10 mmol, 1.0 equiv.) in 2 mL dry THF was added NBS (0.19 g, 1.10 mmol, 1.0 equiv.) at 0 °C. The reaction was warmed to room temperature and stirred for 14 h. Afterwards water was added and it was extracted with Et_2O . The combined organic layers were dried with MgSO_4 and the solvent was removed under reduced pressure. The crude product was purified by column chromatography on silica gel (cyclohexane/ethyl acetate 20 : 1) and **24** was isolated as a crystalline white solid (0.28 g, 1.06 mmol, 97%). $R_f = 0.2$. GC (HP-5MS): $I = 1724$. $^1\text{H-NMR}$ (500 MHz, CDCl_3): $\delta = 6.31$ (s, 1H, CH), 3.88 (s, 3H, CH_3), 3.83 (s, 3H, CH_3), 3.77 (s, 3H, CH_3), 2.13 (s, 3H, CH_3) ppm. $^{13}\text{C-NMR}$ (125 MHz, CDCl_3): $\delta = 158.3$ (C_q), 156.7 (C_q), 155.2 (C_q), 113.8 (C_q), 98.1 (C_q), 92.8 (CH), 60.5 (CH_3), 56.7 (CH_3), 55.9 (CH_3), 9.2 (CH_3) ppm. IR (ATR): $\tilde{\nu} = 2973, 2944, 2858, 1594, 1575, 805$. EI-MS (70 eV): m/z (%) = 262 (95), 260 (100), 217 (20), 182 (19), 181 (24), 152 (20), 151 (34), 123 (20), 121 (25), 77 (18). HR-EIMS calcd for $\text{C}_{10}\text{H}_{13}\text{O}_3\text{Br}^+$: $m/z = 260.0048$, found: $m/z = 260.0028$.

2-Methyl-1-(2,4,6-trimethoxy-3-methylphenyl)butan-1-one (19). To a solution of **24** (0.10 g, 0.38 mmol, 1.0 equiv.) in 1 mL dry hexane was slowly added a 1.7 M solution of *t*-butyllithium (0.45 mL, 0.77 mmol, 2.0 equiv.) at -78 °C. The reaction was warmed to -10 °C, stirred for 10 minutes and again cooled to -78 °C. 2-Methylbutyraldehyde (0.05 g, 0.58 mmol, 1.5 equiv.) was slowly added and the reaction was stirred for 30 minutes at -78 °C. The reaction was quenched with water and extracted with Et_2O . The combined organic layers were dried with MgSO_4 and the solvent was removed under reduced pressure. The crude product was dissolved in 2 mL dry DMSO and IBX (0.04 g, 0.15 mmol, 1.2 equiv.) was added at room temperature. The reaction was stirred over night and quenched with sat. aq. NaHCO_3 -solution. The mixture was extracted with Et_2O and the organic layers were dried with MgSO_4 . Purification of the crude product was done by flash chromatography (cyclohexane/ethyl acetate 5 : 1) and **19** was isolated as a colorless oil (0.03 g, 0.94 mmol, 28%). $R_f = 0.2$. GC (HP-5MS): $I = 1877$. $^1\text{H-NMR}$ (500 MHz, CDCl_3): $\delta = 6.25$ (s, 1H, CH), 3.84 (s, 3H, CH_3), 3.78 (s, 3H, CH_3), 3.69 (s, 3H, CH_3), 2.94–2.86 (m, 1H, CH), 2.06 (s, 3H, CH_3), 1.83–1.74 (m, 1H, *CHH*), 1.43–1.34 (m, 1H, *CHH*), 1.11 (d, $^3J = 7.0$ Hz, 3H, CH_3), 0.92 (t, $^3J = 7.4$ Hz, 3H, CH_3) ppm. $^{13}\text{C-NMR}$ (125 MHz, CDCl_3): $\delta = 208.8$ (C_q),

159.9 (C_q), 156.7 (C_q), 155.6 (C_q), 118.6 (C_q), 112.2 (C_q), 91.5 (CH), 62.6 (CH_3), 56.0 (CH_3), 55.8 (CH_3), 49.2 (CH), 25.5 (CH_2), 15.3 (CH_3), 11.8 (CH_3), 8.5 (CH_3) ppm. IR (ATR): $\tilde{\nu} = 2964, 2935, 2875, 2837, 1692, 1598, 805$. EI-MS (70 eV): m/z (%) = 266 (6), 209 (100), 194 (5), 165 (3), 136 (5). HR-EIMS calcd for $\text{C}_{15}\text{H}_{23}\text{O}_4^+$: $m/z = 266.1518$, found: $m/z = 266.1501$.

1-(2-Hydroxy-4,6-dimethoxy-3,5-dimethylphenyl)-2-methylbutan-1-one (16) and 1-(2,6-dihydroxy-4-methoxy-3,5-dimethylphenyl)-2-methylbutan-1-one (25). To a solution of **15** (0.05 g, 0.16 mmol, 1.0 equiv.) in dry DCM was slowly added BBr_3 (0.04 g, 0.18 mmol, 1.1 equiv.) in 0.1 mL dry DCM at -78 °C. The reaction was allowed to warm to room temperature and stirred over night. It was cooled with an ice bath, quenched with water and extracted with EtOAc . After drying with MgSO_4 the solvent was removed under reduced pressure and the crude product was purified by column chromatography on silica gel (cyclohexane/ethyl acetate 15 : 1 to 5 : 1). Compounds **16** (0.015 g, 0.06 mmol, 35%) and **25** (0.021 g, 0.08 mmol, 52%) were isolated as colorless oils. Analytical data for **16**: $R_f = 0.2$ (15 : 1). GC (HP-5MS): $I = 1855$. $^1\text{H-NMR}$ (500 MHz, CDCl_3): $\delta = 12.63$ (s, 1H, OH), 3.74 (s, 3H, CH_3), 3.72 (m, 1H, CH), 3.69 (s, 3H, CH_3), 2.15 (s, 3H, CH_3), 2.13 (s, 3H, CH_3), 1.82–1.74 (m, 1H, *CHH*), 1.48–1.38 (m, 1H, *CHH*), 1.17 (d, $^3J = 6.9$ Hz, 3H, CH_3), 0.89 (t, $^3J = 7.5$ Hz, 3H, CH_3) ppm. $^{13}\text{C-NMR}$ (125 MHz, CDCl_3): $\delta = 212.2$ (C_q), 163.2 (C_q), 160.7 (C_q), 158.6 (C_q), 115.7 (C_q), 115.5 (C_q), 111.6 (C_q), 62.4 (CH_3), 60.2 (CH_3), 45.9 (CH), 27.4 (CH_2), 17.2 (CH_3), 12.0 (CH_3), 9.3 (CH_3), 8.9 (CH_3) ppm. IR (ATR): $\tilde{\nu} = 2961, 2934, 2874, 1776, 1613, 1585, 1452, 1403, 1371, 1358, 1272, 1192, 1132, 1104, 1030, 992, 922, 904, 832, 771, 709, 580, 510$. EI-MS (70 eV): m/z (%) = 266 (M^+ , 7), 209 (100), 166 (2). HR-ESIMS calcd for $\text{C}_{15}\text{H}_{23}\text{O}_4^+$: $m/z = 267.1591$, found: $m/z = 267.1592$ [$\text{M} + \text{H}$] $^+$. Analytical data for **25**: $R_f = 0.2$ (5 : 1). GC (HP-5MS): $I = 1928$. $^1\text{H-NMR}$ (500 MHz, CDCl_3): $\delta = 13.22$ (s, 1H, OH), 5.28 (s, 1H, OH), 3.75–3.68 (m, 1H, CH), 3.69 (s, 3H, CH_3), 2.13 (s, 3H, CH_3), 2.10 (s, 3H, CH_3), 1.83–1.73 (m, 1H, *CHH*), 1.48–1.38 (m, 1H, *CHH*), 1.16 (d, $^3J = 6.8$ Hz, 3H, CH_3), 0.89 (t, $^3J = 7.5$ Hz, 3H, CH_3) ppm. $^{13}\text{C-NMR}$ (125 MHz, CDCl_3): $\delta = 211.4$ (C_q), 161.2 (C_q), 158.9 (C_q), 158.7 (C_q), 108.7 (C_q), 108.6 (C_q), 106.6 (C_q), 62.5 (CH_3), 45.5 (CH), 27.6 (CH_2), 17.4 (CH_3), 12.1 (CH_3), 8.8 (CH_3), 7.7 (CH_3) ppm. IR (ATR): $\tilde{\nu} = 3469, 2963, 2933, 2874, 1601, 1453, 1410, 1373, 1288, 1223, 1171, 1142, 1104, 1069, 1024, 989, 937, 901, 812, 773, 732, 689, 508$. EI-MS (70 eV): m/z (%) = 252 (M^+ , 6), 195 (100), 180 (3), 152 (4). HR-ESIMS calcd for $\text{C}_{14}\text{H}_{21}\text{O}_4^+$: $m/z = 253.1434$, found: $m/z = 253.1437$ [$\text{M} + \text{H}$] $^+$.

Dichotomone (17). Compound **17** was synthesized starting from 1,3,5-trimethoxybenzene (**20**) according to a literature known procedure.³² GC (HP-5MS): $I = 1885$. $^1\text{H-NMR}$ (500 MHz, CDCl_3): $\delta = 4.91$ (s br, 1H, OH), 3.68 (s, 6H, $2 \times \text{CH}_3$), 2.95–2.87 (m, 1H, CH), 2.13 (s, 6H, $2 \times \text{CH}_3$), 1.83–1.74 (m, 1H, *CHH*), 1.43–1.33 (m, 1H, *CHH*), 1.12 (d, $^3J = 7.1$ Hz, 3H, CH_3), 0.93 (t, $^3J = 7.5$ Hz, 3H, CH_3) ppm. $^{13}\text{C-NMR}$ (125 MHz, CDCl_3): $\delta = 209.1$ (C_q), 154.4 (C_q), 154.0 (C_q), 123.5 (C_q), 113.1 (C_q), 62.9 ($2 \times \text{CH}_3$), 49.3 (CH), 25.4 (CH_2), 15.3 (CH_3), 11.8 (CH_3), 8.8 (CH_3) ppm. IR (ATR): $\tilde{\nu} = 3463, 2965,$

2936, 2874, 2838, 1682, 1584, 1457, 1406, 1376, 1295, 1227, 1186, 1126, 1102, 1063, 1022, 1001, 986, 932, 877, 844, 501. EI-MS (70 eV): m/z (%) = 266 (M^+ , 7), 209 (100), 194 (11). HR-ESIMS calcd for $C_{15}H_{23}O_4^+$: m/z = 267.1591, found: m/z = 267.1592.

Analysis of the enantiomeric excess of 47. The enantiomeric excess of natural **47** and synthetic (*R*)- and (*S*)-**47**⁴⁷ was determined by GC-MS on a homochiral stationary phase (Fig. 5) using the following conditions: system: Agilent HP7890B gas-chromatograph connected to a HP5977A mass detector fitted with an Agilent CycloSil-B capillary column (30 m, 0.25–0.32 mm ID, 0.25 μ m film); The GC-MS conditions were as follows: (1) inlet pressure: 77.1 kPa, He flow 23.3 mL min⁻¹; (2) injection volume: 1 μ L; (3) injection mode: splitless, valve time 60 s; (4) oven temperature ramp: 5 min at 70 °C increasing at 10 °C min⁻¹ to 210 °C; (5) carrier gas He at 1 mL min⁻¹; (6) transfer line: 250 °C; (7) electron energy: 70 eV.

Bioactivity tests against *Chlorella fusca*

CP medium (10 mL; yeast extract 10.0 g L⁻¹, D-(+)-glucose monohydrate 10.0 g L⁻¹, 1000 mL H₂O, pH 6.2) was inoculated with *Chlorella fusca*, followed by culturing for one week under constant artificial light exposure and shaking (100 rpm) at 24 °C. The culture was diluted with sterile CP medium to a cell count of 10 000 cells per mL distributed in 96 well plates. Solutions of the test compounds (Table 1) in CP medium were added with a final concentration of 125 μ g mL⁻¹, followed by a 1 : 1 dilution series (62.5 μ g mL⁻¹, 31.3 μ g mL⁻¹, 15.6 μ g mL⁻¹, etc.). All experiments were performed in triplicate, with 3 negative controls (no compound added) and using 2,4-dichlorophenol and CuSO₄·5H₂O as positive controls. An extra plate was used as a blank control (no algae) to exclude light absorption by the medium. The incubation time was 5 days at 24 °C, with constant artificial light exposure and without shaking. OD values were measured at 560 nm using a Sunrise Tecan microplate reader plate reader. The minimal inhibitory concentration was considered the lowest concentration that led to at least 80% growth inhibition compared to the negative control.

Bioactivity tests against *B. megaterium* and *E. coli*

NP medium (10 mL; peptone from meat 7.8 g L⁻¹, peptone from casein 7.8 g L⁻¹, yeast extract 2.8 g L⁻¹, D-(+)-glucose monohydrate 1.0 g L⁻¹, NaCl 5.6 g L⁻¹, 1000 mL H₂O, pH 7.5) was inoculated with *Bacillus megaterium* DSM 32 or *Escherichia coli* DSM 498 and the cultures were grown overnight under constant shaking (200 rpm) at 30 °C. Agar plates were prepared using NP medium (with 12 g L⁻¹ agar) and the plates were inoculated with 150 μ L bacterial suspension which was evenly distributed on the surface of the agar. With the use of 200 μ L pipette tip, three small agar plugs were taken out from each agar plate and solutions of the test compounds (50 μ L, 1 mg mL⁻¹) were filled into the hole from the removed agar plugs. Ertapenem was used as a positive control. Incubation time was 24 h at 30 °C, with constant artificial light exposure. The inhibition zones were measured in mm (radii) and compared to the positive control.

Conflicts of interest

There are no conflicts to declare.

Acknowledgements

This work was funded by the Deutsche Forschungsgemeinschaft DFG (DI1536/9-1). We thank Barbara Schulz (TU Braunschweig) for *Chlorella fusca*, Marie Reuter-Schniete for contributions to the experimental work, and Ekaterina Egereva (Pharmaceutical Biology, Bonn) for fungal strains cultivations.

References

- (a) C. W. Li, J. Y. Chen and T. E. Hua, *Science*, 1998, **279**, 879–882; (b) G. D. Love, E. Grosjean, C. Stalvies, D. A. Fike, J. P. Grotzinger, A. S. Bradley, A. E. Kelly, M. Bhatia, W. Meredith, C. E. Snape, S. A. Bowring, D. J. Condon and R. E. Summons, *Nature*, 2009, **457**, 718–721.
- J. N. A. Hooper and R. W. M. van Soest, in *System Porifera: a guide to the classification of sponges*, Academic/Plenum Publishers, New York, NY, 2002.
- (a) M. W. Taylor, R. Radax, D. Steger and M. Wagner, *Microbiol. Mol. Biol. Rev.*, 2007, **71**, 295–347; (b) U. Hentschel, J. Piel, S. M. Degnan and M. W. Taylor, *Nat. Rev. Microbiol.*, 2012, **10**, 641–654; (c) T. Thomas, L. Moitinho-Silva, M. Lurgi, J. R. Björk, C. Easson, C. Astudillo-García, J. B. Olson, P. M. Erwin, S. López-Legentil, H. Luter, A. Chaves-Fonnegra, R. Costa, P. J. Schupp, L. Steindler, D. Erpenbeck, J. Gilbert, R. Knight, G. Ackermann, J. V. Lopez, M. W. Taylor, R. W. Thacker, J. M. Montoya, U. Hentschel and N. S. Webster, *Nat. Commun.*, 2016, **7**, 1–12.
- J. Vacelet, *J. Microsc. Biol. Cell.*, 1975, **23**, 271–288.
- (a) C. A. Bewley and D. J. Faulkner, *Angew. Chem., Int. Ed.*, 1998, **37**, 2162–2178; (b) U. R. Abdelmohsen, K. Bayer and U. Hentschel, *Nat. Prod. Rep.*, 2014, **31**, 381–399; (c) M. F. Mehbub, J. Lei, C. Franco and W. Zhang, *Mar. Drugs*, 2014, **12**, 4539–4577; (d) W. H. Gerwick and B. S. Moore, *Cell Chem. Biol.*, 2012, **19**, 85–98; (e) M. S. Laport, O. C. S. Santos and G. Muricy, *Curr. Pharm. Biotechnol.*, 2009, **10**, 86–105; (f) J. Piel, *Nat. Prod. Rep.*, 2004, **21**, 519–538.
- R. P. Walker, D. J. Faulkner, D. Van Engen and J. Clardy, *J. Am. Chem. Soc.*, 1981, **103**, 6772–6773.
- (a) V. S. Bernan, D. M. Roll, C. M. Ireland, M. Greenstein, W. M. Maiese and D. A. Steinberg, *J. Antimicrob. Chemother.*, 1993, **32**, 539–550; (b) R. Rosa, W. Silva, G. Escalona de Motta, A. D. Rodriguez, J. J. Morales and M. Ortiz, *Experientia*, 1992, **48**, 885–887; (c) R. Mohammed, J. Peng, M. Kelly and M. T. Hamann, *J. Nat. Prod.*, 2006, **69**, 1739–1744; (d) A. Vassas, G. Bourdy, J. J. Paillard, J. Lavayre, M. Pais, J. C. Quirion and C. Debitus, *Planta*

- Med.*, 1996, **62**, 28–30; (e) P. A. Keifer, R. E. Schwartz, M. E. S. Koker, R. G. Hughes, D. Rittschof and K. L. Rinehart, *J. Org. Chem.*, 1991, **56**, 2965–2975; (f) A. D. Rodríguez, M. J. Lear and J. J. La Clair, *J. Am. Chem. Soc.*, 2008, **130**, 7256–7258; (g) A. Cipres, D. P. O'Malley, K. Li, D. Finlay, P. S. Baran and K. Vuori, *ACS Chem. Biol.*, 2009, **5**, 195–202.
- 8 T. Lindel, *Alkaloids*, 2017, **77**, 117–219.
- 9 (a) Y. Kato, N. Fusetani, S. Matsunaga, K. Hashimoto, S. Fujita and T. Furuya, *J. Am. Chem. Soc.*, 1986, **108**, 2780–2781; (b) H. Ishihara, B. L. Martin, D. L. Brautigan, H. Karaki, H. Ozaki, Y. Kato, N. Fusetani, S. Watabe, K. Hashimoto, D. Uemura and D. J. Hartshorne, *Biochem. Biophys. Res. Commun.*, 1989, **159**, 871–877.
- 10 T. Wakimoto, Y. Egami, Y. Nakashima, Y. Wakimoto, T. Mori, T. Awakawa, T. Ito, H. Kenmoku, Y. Asakawa, J. Piel and I. Abe, *Nat. Chem. Biol.*, 2014, **10**, 648–655.
- 11 C. Almeida, Y. Hemberger, S. M. Schmitt, S. Bouhired, L. Natesan, S. Kehraus, K. Dimas, M. Gütschow, G. Bringmann and G. M. König, *Chem. – Eur. J.*, 2012, **18**, 8827–8834.
- 12 C. Almeida, F. E. Maddah, S. Kehraus, G. Schnakenburg and G. M. König, *Org. Lett.*, 2016, **18**, 528–531.
- 13 J. S. Dickschat, *Nat. Prod. Rep.*, 2014, **31**, 838–861.
- 14 (a) S. Schulz and J. S. Dickschat, *Nat. Prod. Rep.*, 2007, **24**, 814–842; (b) S. Schulz, J. S. Dickschat, B. Kunze, I. Wagner-Döbler, R. Diestel and F. Sasse, *Mar. Drugs*, 2010, **8**, 2976–2987; (c) J. S. Dickschat, *Nat. Prod. Rep.*, 2017, **34**, 310–328; (d) O. Tyc, C. Song, J. S. Dickschat, M. Vos and P. Garbeva, *Trends Microbiol.*, 2017, **25**, 280–292; (e) J. S. Dickschat, T. Martens, T. Brinkhoff, M. Simon and S. Schulz, *Chem. Biodiversity*, 2005, **2**, 837–865.
- 15 C. Christophersen, U. Anthoni, P. H. Nielsen, N. Jacobsen and O. S. Tendal, *Biochem. Syst. Ecol.*, 1989, **17**, 459–461.
- 16 C. Duque, A. Bonilla, E. Bautista and S. Zea, *Biochem. Syst. Ecol.*, 2001, **29**, 459–467.
- 17 (a) C. Christophersen, U. Anthoni, P. H. Nielsen, N. Jacobsen and O. S. Tendal, *Biochem. Syst. Ecol.*, 1989, **17**, 459–461; (b) C. Duque, A. Bonilla, E. Bautista and S. Zea, *Biochem. Syst. Ecol.*, 2001, **29**, 459–467; (c) R. Romoli, M. C. Papaleo, D. de Pascale, M. L. Tutino, L. Michaud, A. L. Giudice, R. Fani and G. Bartolucci, *J. Mass. Spectrom.*, 2011, **46**, 1051–1059; (d) M. C. Papaleo, R. Romoli, G. Bartolucci, I. Maida, E. Perrin, M. Fondi, V. Orlandini, A. Mengoni, G. Emiliani, M. L. Tutino, E. Parrilli, D. de Pascale, L. Michaud, A. L. Giudice and R. Fani, *New Biotechnol.*, 2013, **30**, 824–838; (e) V. Orlandini, I. Maida, M. Fondi, E. Perrin, M. C. Papaleo, E. Bosi, D. de Pascale, M. L. Tutino, L. Michaud, A. L. Giudice and R. Fani, *Microbiol. Res.*, 2014, **169**, 593–601.
- 18 U. Höller, A. D. Wright, G. F. Matthée, G. M. König, S. Draeger, H.-J. Aust and B. Schulz, *Mycol. Res.*, 2000, **104**, 1354–1365.
- 19 (a) K. Grob and F. Zürcher, *J. Chromatogr.*, 1976, **117**, 285–294; (b) J. S. Dickschat, S. C. Wenzel, H. B. Bode, R. Müller and S. Schulz, *ChemBioChem*, 2004, **5**, 778–787.
- 20 R. P. Adams, *Identification of Essential Oil Components by Gas Chromatography/Mass Spectrometry*, Allured, Carol Stream, 2009.
- 21 H. Harms, V. Rempel, S. Kehraus, M. Kaiser, P. Hufendiek, C. E. Müller and G. M. König, *J. Nat. Prod.*, 2014, **77**, 673–677.
- 22 H. Harms, S. Kehraus, D. Nesaei-Mosaferan, P. Hufendiek, L. Meijer and G. M. König, *Steroids*, 2015, **104**, 182–188.
- 23 H. Harms, B. Orlikova, S. Ji, D. Nesaei-Mosaferan, G. M. König and M. Diederich, *Mar. Drugs*, 2015, **13**, 4949–4966.
- 24 (a) D. Gansser, F. C. Pollak and R. G. Berger, *J. Nat. Prod.*, 1995, **58**, 1790–1793; (b) C. A. Citron, J. Gleitzmann, G. Laurenzano, R. Pukall and J. S. Dickschat, *ChemBioChem*, 2012, **13**, 202–214; (c) P. Rabe, C. A. Citron and J. S. Dickschat, *ChemBioChem*, 2013, **14**, 2345–2354; (d) C. A. Citron, L. Barra, J. Wink and J. S. Dickschat, *Org. Biomol. Chem.*, 2015, **13**, 2673–2683.
- 25 (a) J. S. Dickschat, S. C. Wenzel, H. B. Bode, R. Müller and S. Schulz, *ChemBioChem*, 2004, **5**, 778–787; (b) J. S. Dickschat, H. B. Bode, T. Mahmud, R. Müller and S. Schulz, *J. Org. Chem.*, 2005, **70**, 5174–5182.
- 26 (a) M. Toyota, T. Yoshida, J. Matsunami and Y. Asakawa, *Phytochemistry*, 1997, **44**, 293–298; (b) D. Spiteller, A. Jux, J. Piel and W. Boland, *Phytochemistry*, 2002, **61**, 827–834.
- 27 U. Warmers and W. A. König, *Phytochemistry*, 1999, **52**, 99–104.
- 28 H. W. L. Ruijgrok, The distribution of ranunculin and cyanogenetic compounds in the Ranunculaceae, in *Comparative Phytochemistry*, ed. T. Swain, Academic Press, New York, 1966, pp. 175–186.
- 29 R. Blasco, R.-M. Wittich, M. Mallavarapu, K. N. Timmis and D. H. Pieper, *J. Biol. Chem.*, 1995, **270**, 29229–29235.
- 30 R. A. B. Fazzini, M. E. Skindersoe, P. Bielecki, J. Puchalka, M. Givskov and V. A. P. Martins dos Santos, *Environ. Microbiol.*, 2012, **15**, 111–120.
- 31 M. W. Taylor, P. J. Schupp, H. J. Baillie, T. S. Charlton, R. de Nys, S. Kjelleberg and P. D. Steinberg, *Appl. Environ. Microbiol.*, 2004, **70**, 4387–4389.
- 32 (a) N. Didry, L. Dubreuil and M. Pinkas, *Phytother. Res.*, 1993, **7**, 21–24; (b) M. L. Martín, L. S. Román and A. Domínguez, *Planta Med.*, 1990, **56**, 66–69.
- 33 L. Pouységu, M. Marguerit, J. Gagnepain, G. Lyinec, A. J. Eatheron and S. Quideau, *Org. Lett.*, 2008, **10**, 5211–5214.
- 34 L. F. Tietze, R. R. Singidi, K. M. Gericke, H. Böckemeier and H. Laatsch, *Eur. J. Org. Chem.*, 2007, 5875–5878.
- 35 (a) C. Menut, J. M. Bessiere, A. D. Samate, J. Millogo-Rasolodimby and M. Nacro, *Phytochemistry*, 1999, **51**, 975–978; (b) B. F. Ireland, R. J. Goldsack, J. J. Brophy, C. J. R. Fookes and J. R. Clarkson, *J. Essent. Oil Res.*, 2004, **16**, 89–94; (c) M. Baranska, H. Schulz, S. Reitzenstein, U. Uhlemann, M. A. Strehle, H. Krüger, R. Quilitzsch, W. Foley and J. Popp, *Biopolymers*, 2004, **78**, 237–248.
- 36 C. Almeida, S. Kehraus, M. Prudêncio and G. M. König, *Beilstein J. Org. Chem.*, 2011, **7**, 1636–1642.
- 37 C. Almeida, E. Eguereva, S. Kehraus and G. M. König, *J. Nat. Prod.*, 2013, **76**, 322–326.

- 38 C. Almeida, N. Part, S. Bouhired, S. Kehraus and G. M. König, *J. Nat. Prod.*, 2011, **74**, 21–25.
- 39 L. Dormont, R. Delle-Vedove, J.-M. Bessière and B. Schatz, *Phytochemistry*, 2014, **100**, 51–59.
- 40 R. L. Metcalf and R. L. Lampman, *Proc. Natl. Acad. Sci. U. S. A.*, 1991, **88**, 1869–1872.
- 41 R. M. Seifert and A. D. King, *J. Agric. Food Chem.*, 1982, **30**, 786–790.
- 42 M. Nemcovic, L. Jakubikova, I. Viden and V. Farkas, *FEMS Microbiol. Lett.*, 2008, **284**, 231–236.
- 43 S. Murahashi, *Sci. Pap. Inst. Phys. Chem. Res.*, 1938, **34**, 155–172.
- 44 P. Spiteller, *Chem. – Eur. J.*, 2008, **14**, 9100–9110.
- 45 F. El Maddah, S. Kehraus, M. Nazir, C. Almeida and G. M. König, *J. Nat. Prod.*, 2016, **79**, 2838–2845.
- 46 B.-E. Priegnitz, U. Brandt, K. A. K. Pahirulzaman, J. S. Dickschat and A. Fleißner, *Eukaryotic Cell*, 2015, **14**, 602–615.
- 47 (a) T. Nilsson, T. O. Larsen, L. Montanarella and J. O. Madsen, *J. Microbiol. Methods*, 1996, **25**, 245–255; (b) T. O. Larsen and J. C. Frisvad, *Mycol. Res.*, 1995, **99**, 1153–1166.
- 48 C. A. Citron, C. Junker, B. Schulz and J. S. Dickschat, *Angew. Chem., Int. Ed.*, 2014, **53**, 4346–4349.

SUPPORTING INFORMATION

Volatiles from the fungal microbiome of the marine sponge
Callyspongia cf. flammea

Lena Barra,^a Paul Barac,^b Gabriele M. König,^b Max Crüseemann^b and Jeroen S.
Dickschat^{*a}

a. Kekulé-Institute for Organic Chemistry and Biochemistry, University of Bonn, Gerhard-
Domagk-Straße 1, D-53121 Bonn, Germany

E-mail: dickschat@uni-bonn.de

b. Institute of Pharmaceutical Biology, University of Bonn, Nußallee 6, D-53115 Bonn,
Germany

TABLE OF CONTENTS

1. LIST OF IDENTIFIED VOLATILES	3 - 5
2. HEADSPACE EXTRACT OF <i>Sporormiella</i> sp. 293 K05	6
3. HEADSPACE EXTRACT OF <i>Botrytis</i> sp. 293 K02	7
4. MASS SPECTRA OF ISOTORQUATONE (15) AND TORQUATONE (18)	8
5. IDENTIFICATION OF ISOTORQUATONE BY GC-MS	9
6. DETERMINATION OF THE ABSOLUTE CONFIGURATION OF 15	10
7. MASS SPECTRA OF DESMETHYL ANALOGS 16 , 17 and 19	11
8. RESULTS OF FEEDING EXPERIMENTS	12
9. BIOACTIVITY TESTS AGAINST BACTERIA	13
10. NMR SPECTRA OF SYNTHETIC COMPOUNDS	14-43

1. LIST OF IDENTIFIED VOLATILES

Table S1. Identified volatile compounds and their occurrence in the investigated strains.

Compound ^a	P	I (Lit.) ^c	Ident. ^d	occurrence (strain) ^e
furan-3-carbaldehyde (34)	816		ms, std	St
butyl acetate (35)	819	814 ¹	ms, ri, std	St
<i>furan-2-carbaldehyde</i>	835	835 ²	ms, ri, std	St
<i>2-furanmethanol</i>	854	850 ³	ms, ri, std	D, St
ethyl 2-methylbutyrate (45)	856	861 ⁴	ms, ri	E
<i>ethylbenzene</i>	860	858 ⁵	ms, ri, std	E, B
<i>m-xylene</i>	868	866 ⁵	ms, ri, std	E, B
protoanemonin (6)	881	880 ⁶	ms, ri	D
cyclohexanol (46)	886	886 ⁷	ms, ri, std	E
<i>2-acetylfuran</i>	909	909 ⁸	ms, ri, std	D, Sp
<i>2,5-hexanedione</i>	927	931 ⁹	ms, ri, std	St,
2-hydroxy-5-methylhexan-3-one (36)	942	944 ¹⁰	ms, ri	St
4-methyl- γ -butyrolactone (37)	954	958 ¹¹	ms, ri	St
<i>benzaldehyde</i>	959	952 ⁸	ms, ri, std	B, Sp
1-octen-3-ol (38)	978	975 ¹²	ms, ri, std	St, E
<i>1-ethyl-4-methylbenzene</i>	968	965 ¹³	ms, ri, std	B
3-octanon (39)	986	983 ¹⁴	ms, ri, std	St, E
6-methylhept-5-en-2-one (51)	987	981 ⁸	ms, ri, std	B
<i>1,3,4-trimethylbenzene</i>	993	995 ⁸	ms, ri, std	E, B
<i>2-acetylpyrrole</i>	1058	1054 ⁸	ms, ri, std	D, St, Sp
3,4-dimethylpentan-4-olid (47)	1064	1063 ¹⁵	ms, ri, std	E
<i>acetophenone</i>	1066	1059 ⁸	ms, ri, std	St, Sp
linalool (40)	1100	1095 ⁸	ms, ri, std	St, B
nonanal (7)	1104	1101 ¹⁶	ms, ri, std	D, St, E, B, Sp
<i>2-phenylethanol</i>	1114	1107 ⁸	ms, ri, std	St, Sp
phenylacetonitrile (10)	1138	1134 ⁸	ms, ri, std	D
1,2-dimethoxybenzene (41)	1146	1146 ¹⁷	ms, ri, std	St
2-methylisoborneol (42)	1184	1178 ⁸	ms, ri, std	St, B
decanal (8)	1202	1201 ⁸	ms, ri, std	D, St, E, B, Sp

<i>2-phenyloxyethanol</i>	1219	1221 ⁸	ms, ri	St, B, Sp
benzothiazole (43)	1224	1223 ¹⁸	ms, ri	St, E, Sp
undecanal (9)	1307	1305 ¹⁴	ms, ri, std	D, E
3,4-dimethoxystyrene (11)	1364	1368 ¹⁹	ms, ri, std	D
1,3,4-trimethoxybenzene (44)	1368	1373	ms, std	St
dodecanal (48)	1418	1411 ²⁰	ms, ri, std	E, B
geranylactone (12)	1454	1455 ²¹	ms, ri, std	D, St, B
dauca-4(11),8-diene (13)	1539	1537 ²²	ms, ri	D
hexadecane (49)	1600	1600 ⁸	ms, ri, std	E
(1(10) <i>E</i> ,5 <i>E</i>)-germacradien-11-ol (14)	1649	1638 ²³	ms, ri, std	D
tetradecanol (50)	1676	1676 ⁸	ms, ri, std	E
isotorquatone (15)	1808		ms, std	D
chartabomone (16)	1853		ms, std	D
dichotomone (17)	1884		ms, std	D

^aCompound numbers refer to compound numbers in main text. Unidentified compounds and artifacts are not listed. Compounds which have also been identified from the medium are marked in italics. ^bRetention index on a HP5-MS fused silica capillary column. ^cRetention index on the same or a similar column from tabulated data in the literature. ^dIdentification based on ms: mass spectrum (mass spectral match factor >850), ri: retention index on same or similar column (maximum deviation of 10 points), std: comparison to a synthetic or commercially available standard. ^eLetters refer to fungal strains: *D. cejpii* (D), *Stachylidium* sp. (St), *Emericella* sp. (E), *Sporormiella* sp. (Sp), *Botrytis* sp. (B).

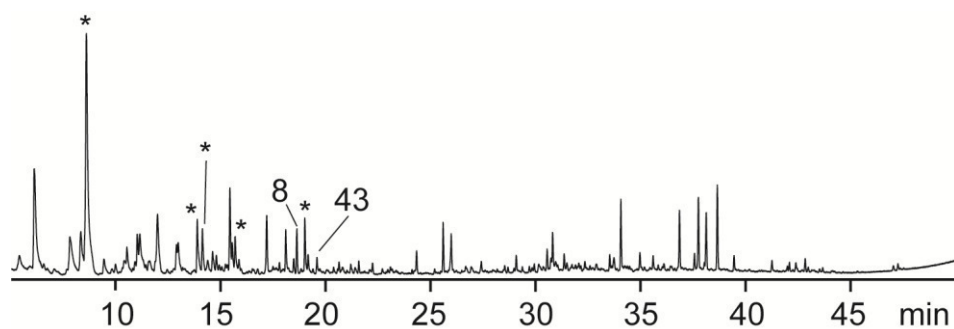
References

- 1 C. A. Citron, L. Barra, J. Wink and J. S. Dickschat, *Org. Biomol. Chem.*, 2015, **13**, 2673.
- 2 N. S. Radulovic, N. D. Dordevic and R. M. Palic, *J. Serbian Chem. Soc.*, 2010, **75**, 1653.
- 3 D. Ansorena, I. Astiasaran and J. Bello, *J. Agric. Food Chem.*, 2000, **48**, 2395.
- 4 J. C. Leffingwell and E. D. Alford, *Electron. J. Environ. Agric. Food Chem.*, 2005, **4**, 899.
- 5 E. Engel, C. Baty, D. L. Corre, I. Souchon and N. Martin, *J. Agric. Food Chem.*, 2002, **50**, 6459.
- 6 N. Radulovic, N. Dordevic, M. Markovic and R. Palic, *Bull. Chem. Soc. Ethio.*, 2010, **24**, 67.
- 7 J. A. Pino, J. Mesa, Y. Munoz, M. P. Marti and R. Marbot, *J. Agric. Food Chem.*, 2005, **53**, 2213.
- 8 R. P. Adams, *Identification of Essential Oil Components by Gas Chromatography/ Mass Spectrometry*, Allured, Carol Stream, **2009**.
- 9 I. Jerkovic and Z. Marijanovic, *Molecules*, 2010, **15**, 3744.
- 10 C. A. Citron, P. Rabe and J. S. Dickschat, *J. Nat. Prod.*, 2012, **75**, 1765.
- 11 M. Garcia-Estaban, D. Ansorena, I. Astiasaran, D. Martin and J. Ruiz, *J. Sci. Food Agric.*, 2004, **84**, 1364.
- 12 S. Cavar, M. Maksimovic and M. E. Solic, *Biologica Nyssana*, 2010, **1**, 99.
- 13 Z. Wang, M. Fingas, *J. Chromatogr. A*, 1995, **712**, 321.

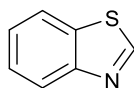
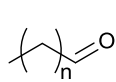
- 14 M. Miyazawa, S. Marumoto, T. Kobayashi, S. Yoshida and Y. Utsumi, *Rec. Nat. Prod.*, 2011, **5**, 221.
- 15 C. A. Citron, C. Junker, B. Schulz, J. S. Dickschat, *Angew. Chem. Int. Ed.*, 2014, **53**, 4346.
- 16 A. Bertoli, M. Lepnardi, J. Krzyzanowska, W. Oleszek, L. Pistelli, *Acta Biochem. Polonica*, 2011, **58**, 581.
- 17 W. N. Setzer, J. A. Noletto, R. O. Lawton, *Flavour Fragr. J.*, 2006, **21**, 244.
- 18 T. Nawrath, G. F. Mgode, B. Weetjens, S. H. E. Kaufmann and S. Schulz, *Beilstein J. Org. Chem.*, 2012, **8**, 290.
- 19 C. X. Zhao, X. N. Li, Y. Z. Liang, H. Z. Fang, L. F. Huang and F. Q. Guo, *Chemom. Intell. Lab. Syst.*, 2006, **82**, 218.
- 20 N. Radulovic, P. Blagojevic and R. Palic, *Molecules*, 2010, **15**, 6168.
- 21 N. E. Sandoval-Montemayor, A. Garcia, E. Elizondo-Trevino, E. Garza-Gonzales, L. Alvarez, and M. del Rayo Camacho-Corona, *Molecules*, 2012, **17**, 11173.
- 22 G. M. Petrovic, J. G. Stamenkovic, I. R. Kostevski, G. S. Stojanovic, V. D. Mitic and B. K. Zlatkovic, *Chem. Biodivers.*, 2017, DOI: 10.1002/cbdv.201600367.
- 23 P. Rabe, C. A. Citron and J. S. Dickschat, *ChemBioChem*, 2013, **14**, 2345.

2. HEADSPACE EXTRACT OF *Sporormiella* sp. 293 K05

A)



B)



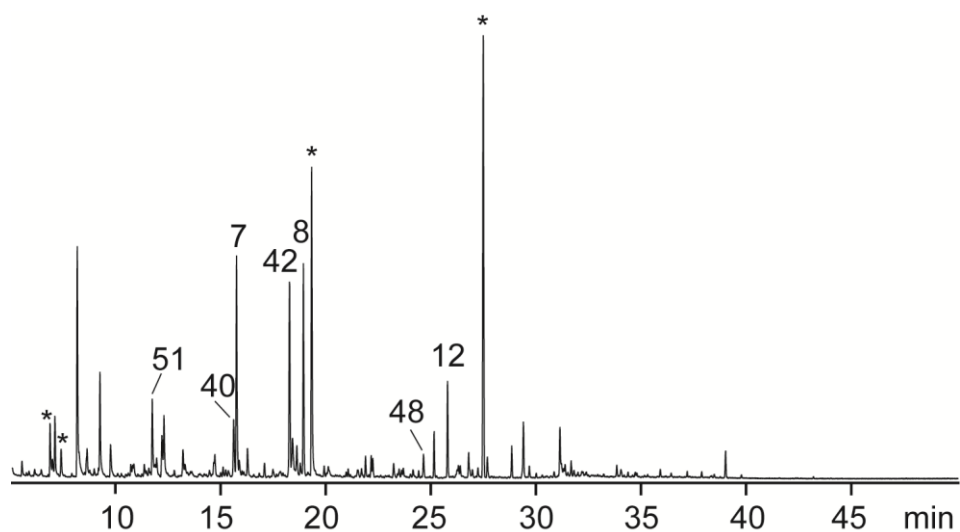
n = 8 (**8**)

43

Figure S1. Volatiles produced by *Sporormiella*. A) Gas chromatogram of the headspace extract, B) structures of the detected volatiles. Asterisks indicate compounds originating from the medium.

3. HEADSPACE EXTRACT OF *Botrytis* sp. 293 K02

A)



B)

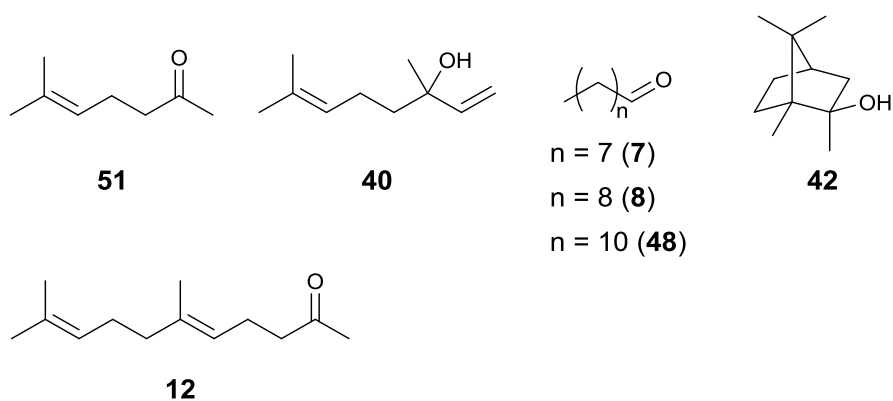


Figure S2. Volatiles produced by *Botrytis*. A) Gas chromatogram of the headspace extract, B) structures of the detected volatiles. Asterisks indicate compounds originating from the medium.

4. MASS SPECTRA OF ISOTORQUATONE (15) AND TORQUATONE (18)

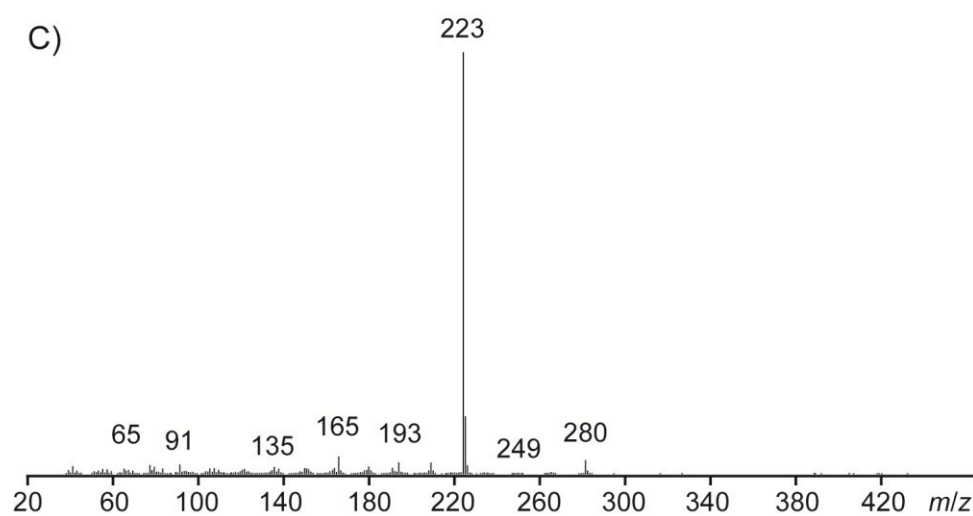
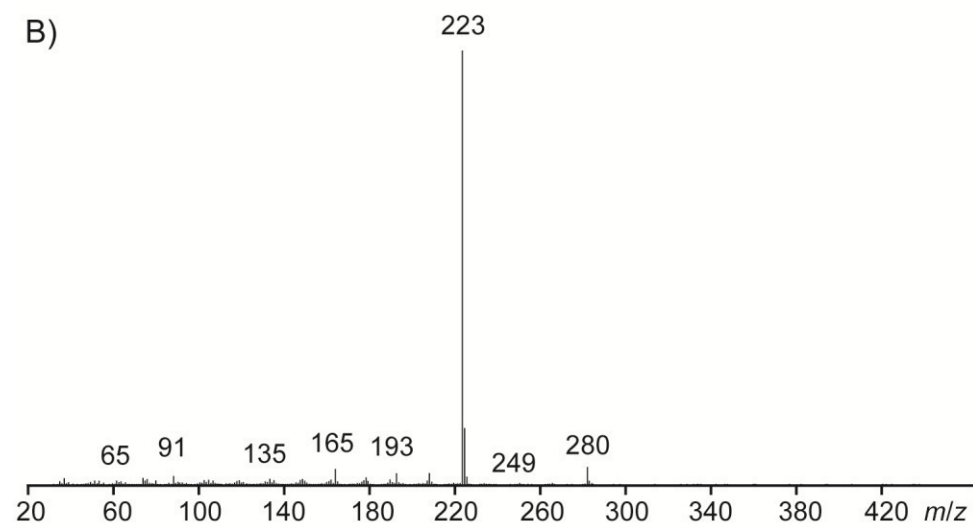
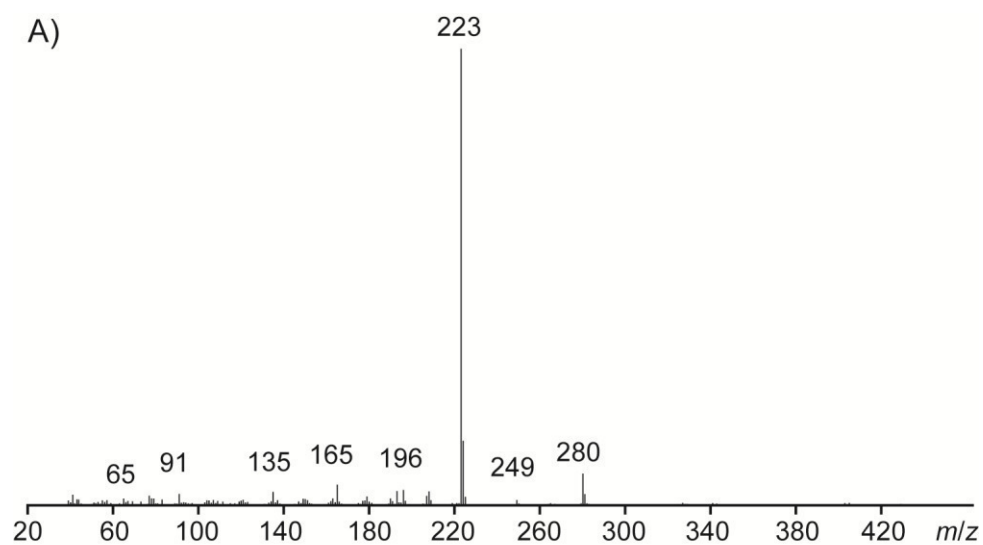


Figure S3. Mass spectra of A) synthetic isotorquatone (**15**), B) synthetic torquatone (**18**), C) natural product from *D. cejpilii* (identified as **15**).

5. IDENTIFICATION OF ISOTORQUATONE BY GC-MS

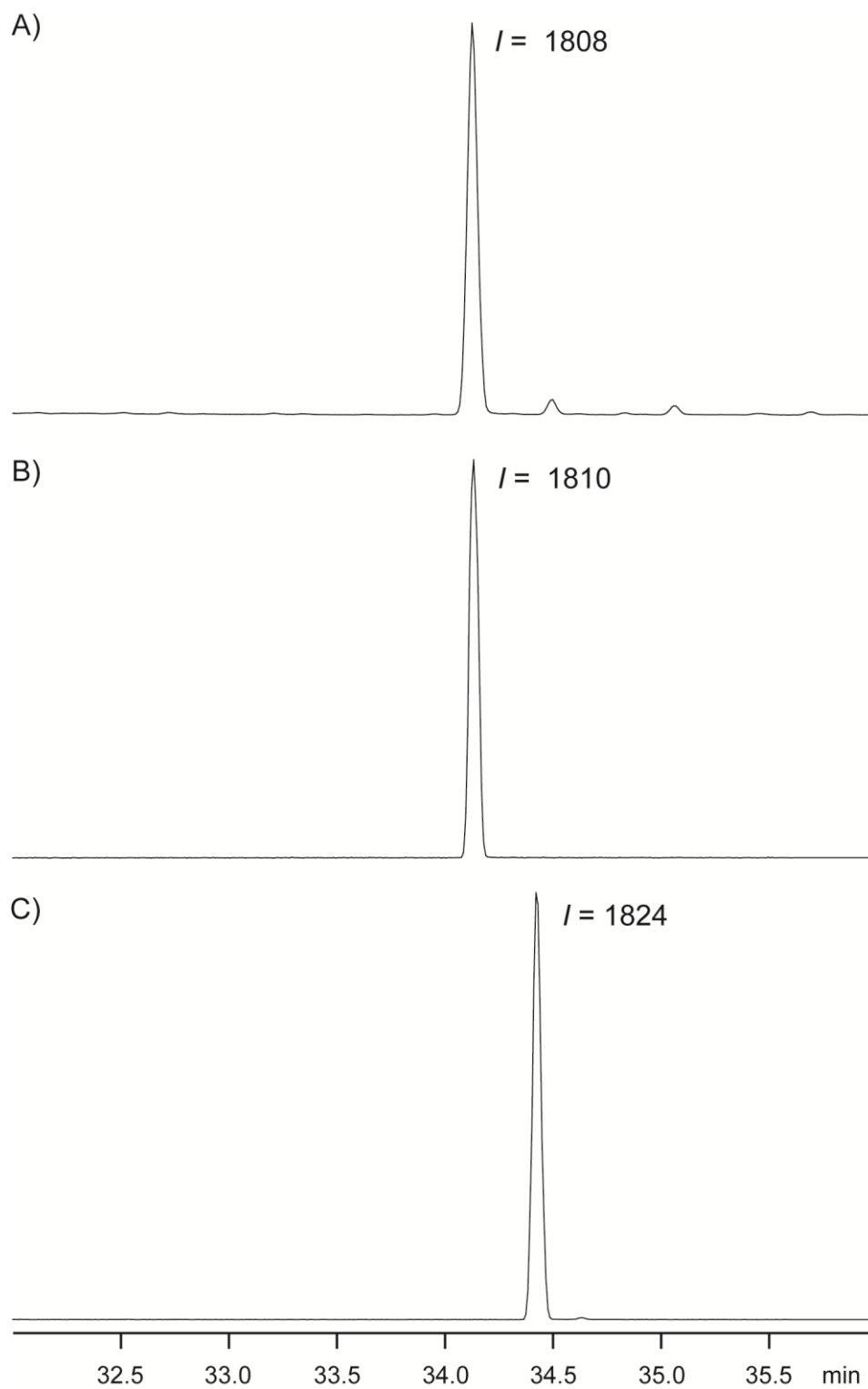


Figure S4. Total ion chromatograms of A) headspace extract of *D. cejpilii*, B) synthetic **15**, C) synthetic **18**.

6. DETERMINATION OF THE ABSOLUTE CONFIGURATION OF **15**

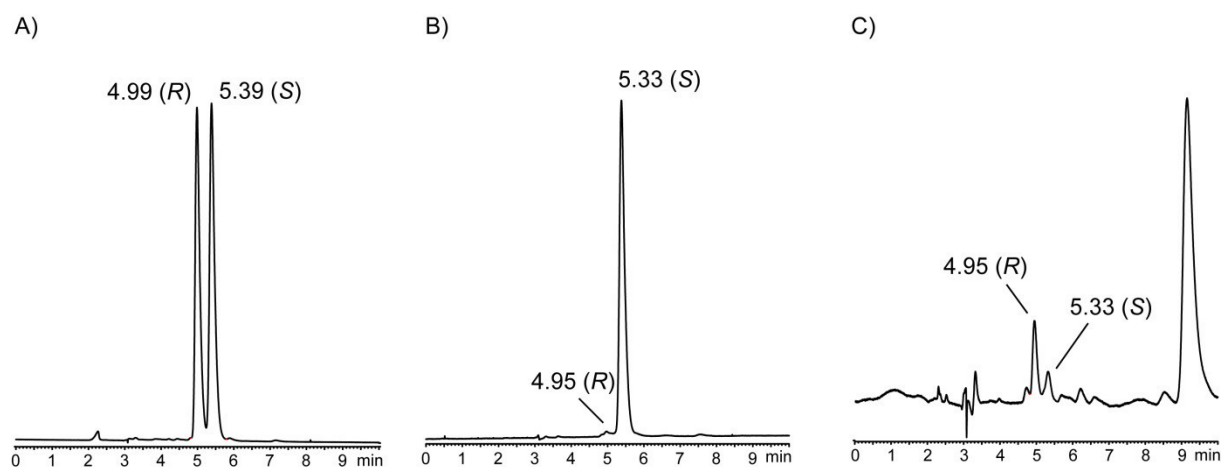


Figure S5. Analysis of the absolute configuration of **15** by HPLC on a homochiral stationary phase. A) mixture of synthetic (*R*)-**15** and (*S*)-**15**, B) synthetic (*S*)-**15**, C) natural product from *D. cejpii*.

7. MASS SPECTRA OF DESMETHYL ANALOGS 16, 17 and 19

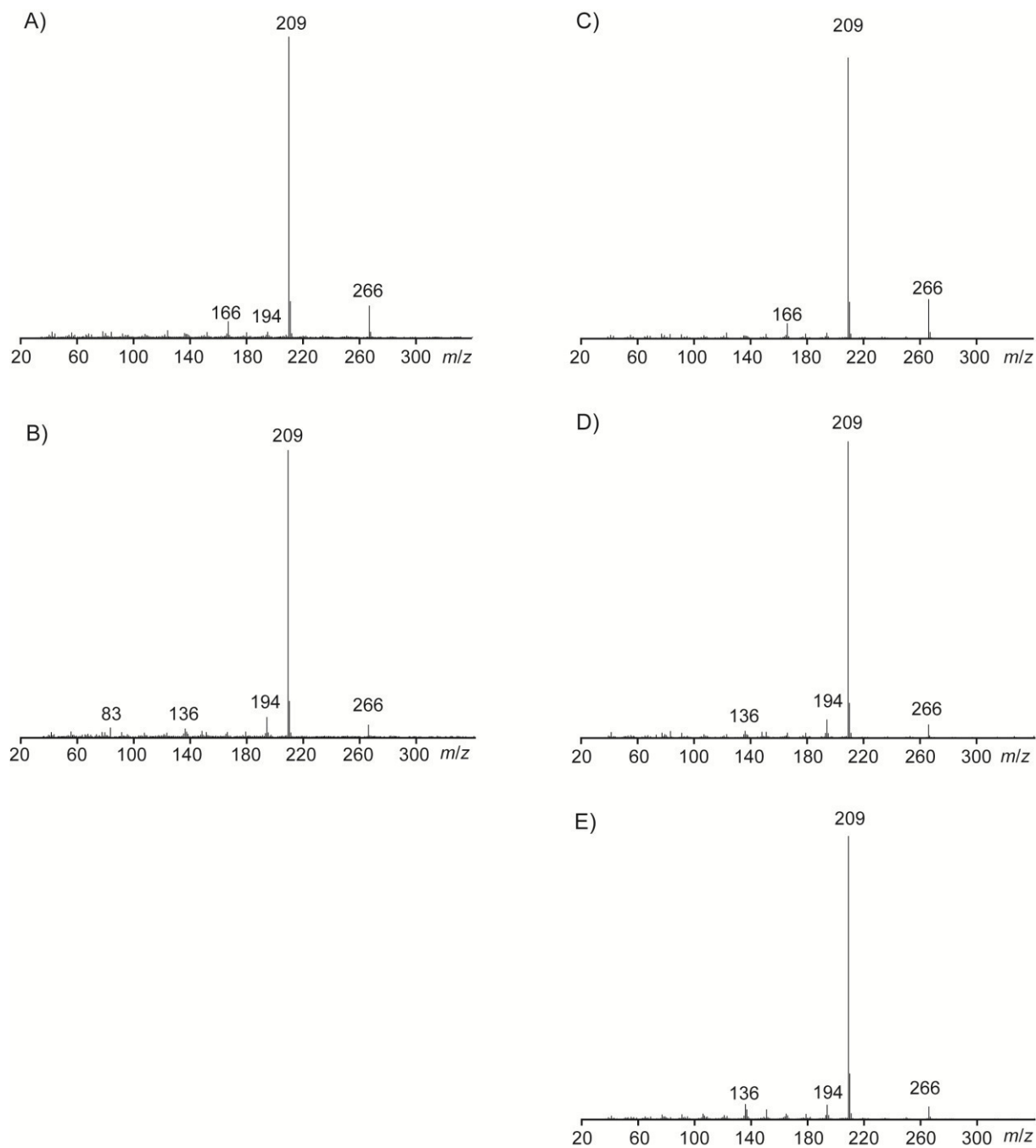


Figure S6. Mass spectra of A) natural desmethyl analogue **16**, B) natural desmethyl analogue **17**, C) synthetic **16**, D) synthetic **17**, E) synthetic **19**.

8. RESULTS OF FEEDING EXPERIMENTS

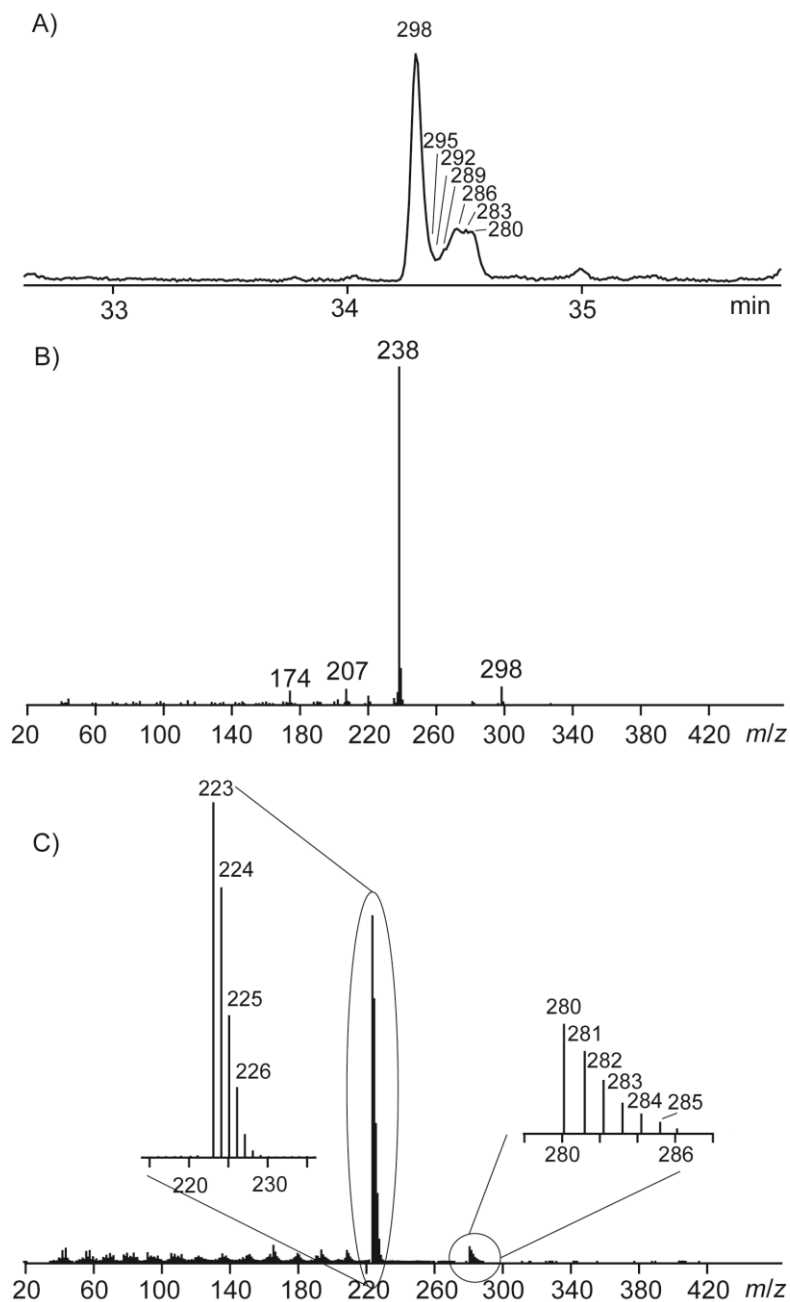


Figure S7. Results of feeding experiments in *D. ceppii*. A) Total ion chromatogram of the headspace-extract of *D. ceppii* after feeding of (methyl-²H₃)-L-methionine, B) mass spectrum of (²H₁₈)-**15** after feeding of (methyl-²H₃)-L-methionine, C) mass spectrum of **15** after feeding of (2-¹³C)acetate.

9. BIOACTIVITY TESTS AGAINST BACTERIA

Table S2. Bioactivity tests against bacteria.

Compound	<i>B. megaterium</i> DSM 32 ^a	<i>E. coli</i> DSM 498 ^a
15	0	0
(S)- 15	0	0
16	3	0
17	3	2 ^b
18	0	0
19	2 ^b	1 ^b
25	2 ^b	0
pos. control (ertapenem)	10	8

^a Radii of inhibition zones in mm, ^b partial inhibition.

10. NMR SPECTRA OF SYNTHETIC COMPOUNDS

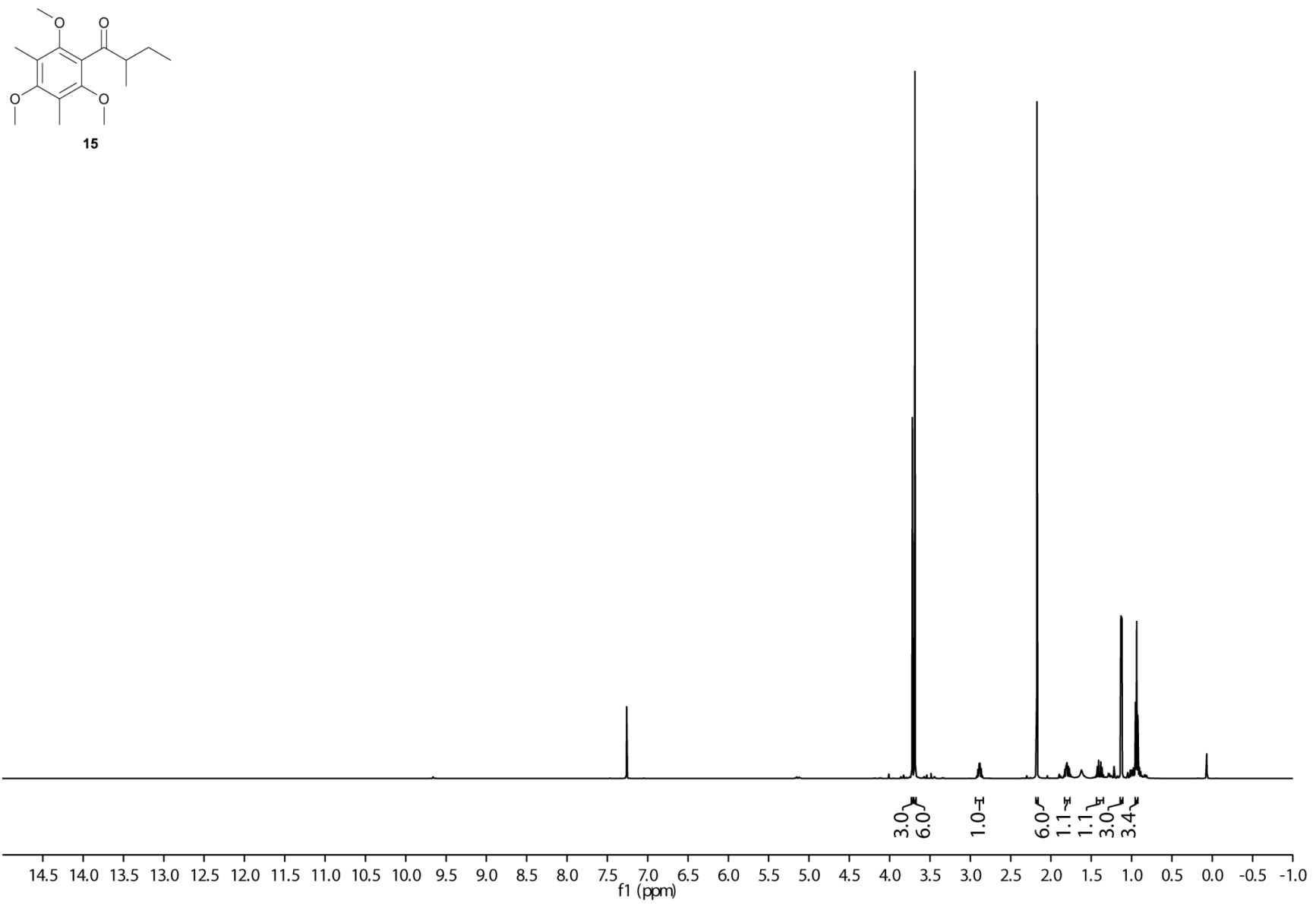
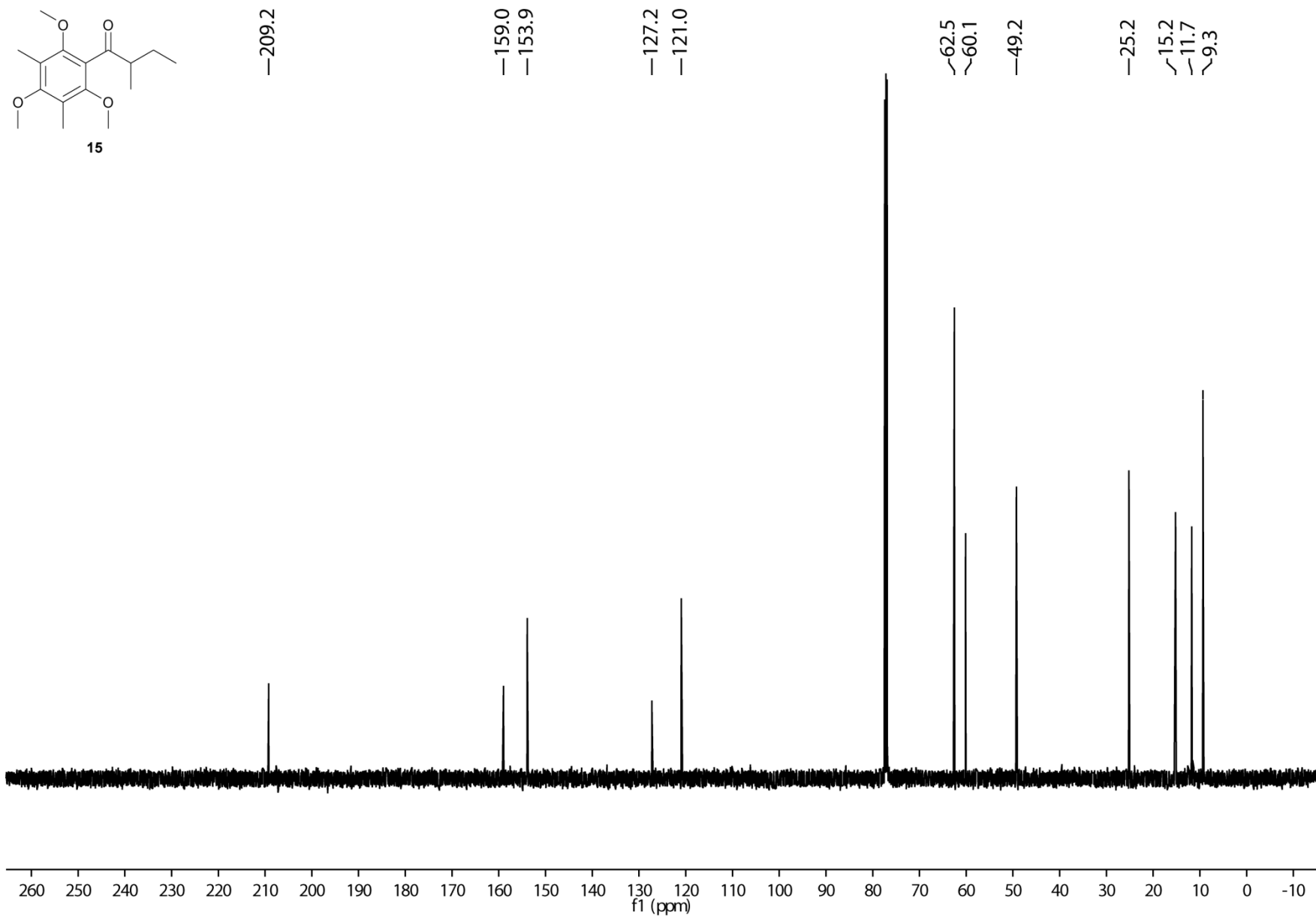
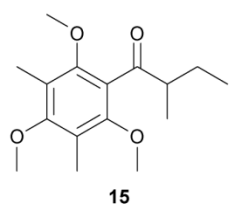


Figure S8. ¹H NMR spectrum of **15** (500 MHz, CDCl₃).



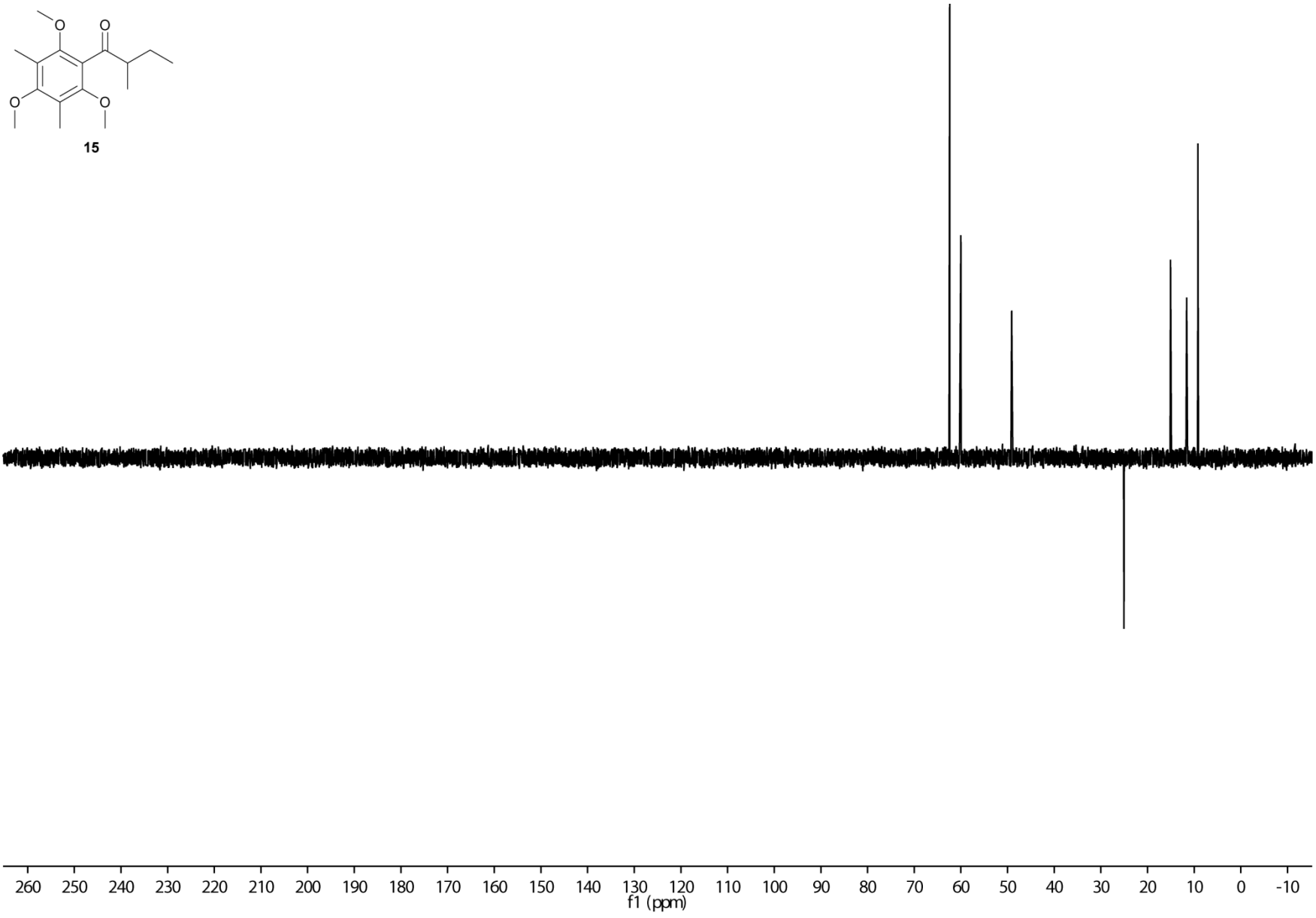
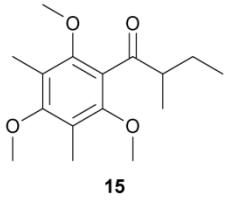


Figure S10. ¹³C DEPT 135 spectrum of **15** (125 MHz, CDCl₃).

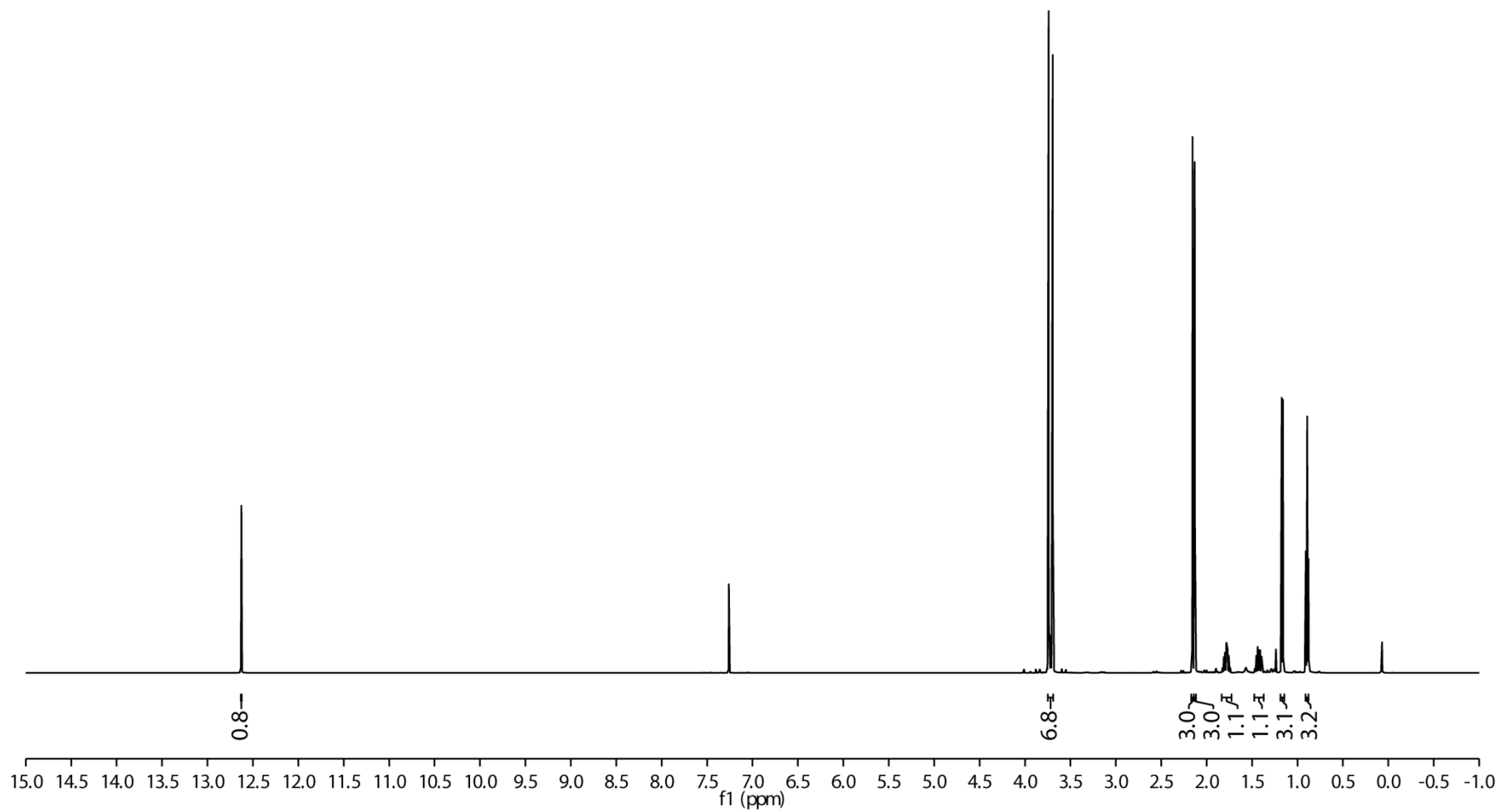
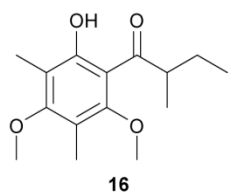
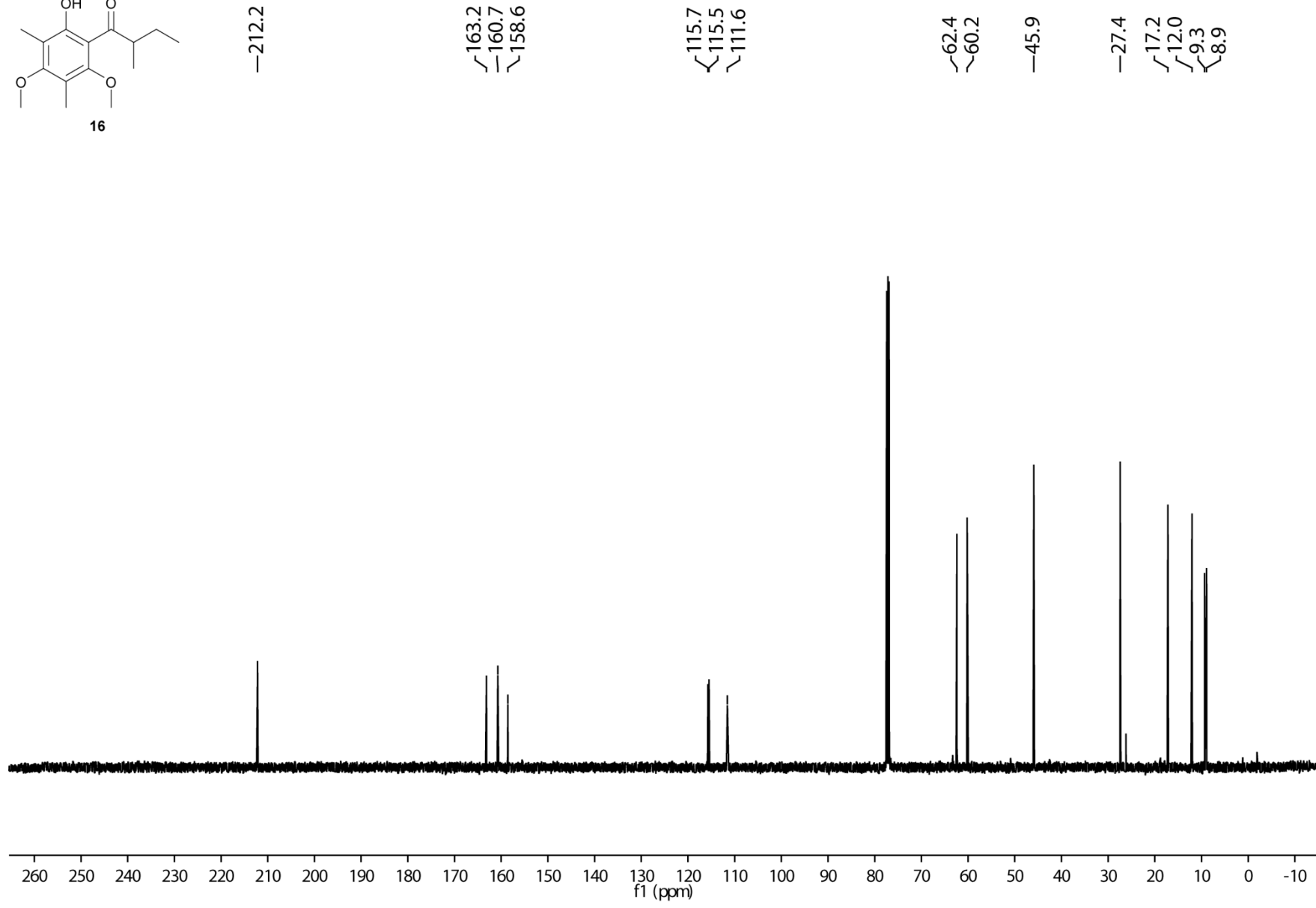


Figure S11. ¹H NMR spectrum of **16** (500 MHz, CDCl₃).

Figure S12. ^{13}C NMR spectrum of **16** (125 MHz, CDCl_3).

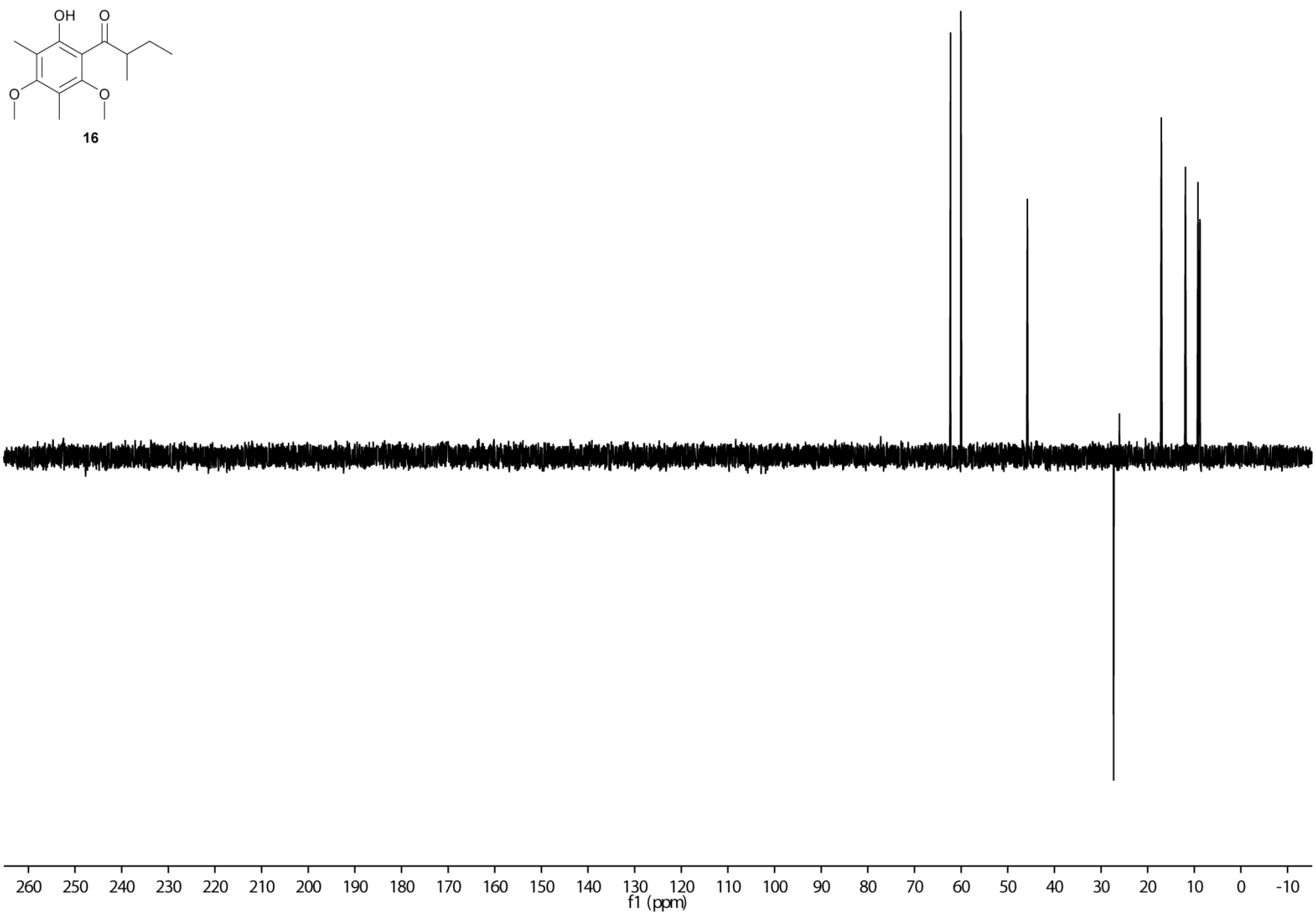
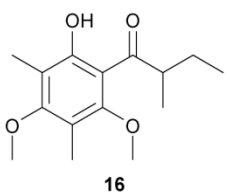


Figure S13. ¹³C DEPT 135 spectrum of **16** (125 MHz, CDCl₃).

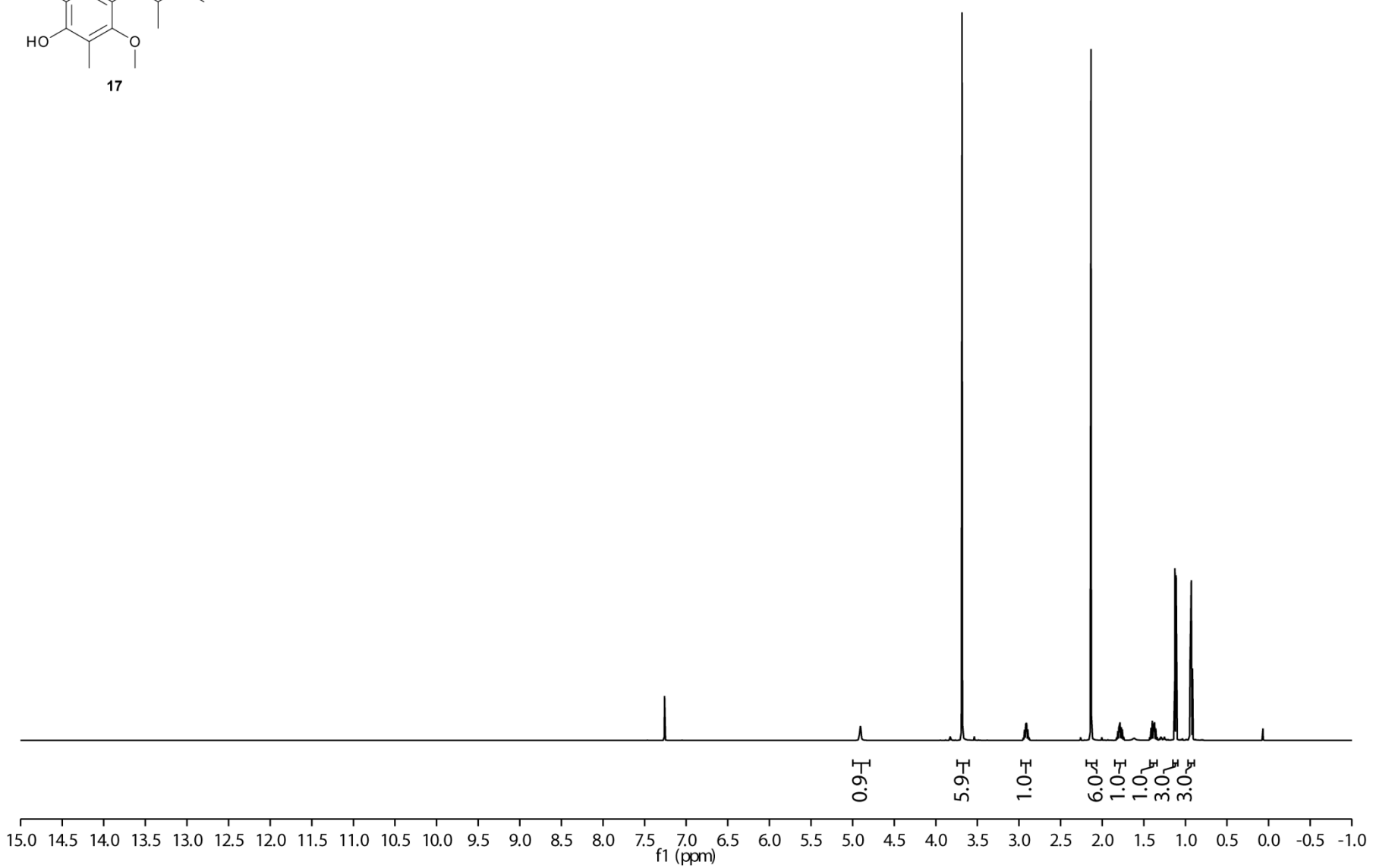
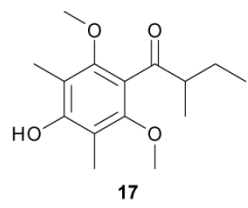


Figure S14. ¹H NMR spectrum of **17** (500 MHz, CDCl₃).

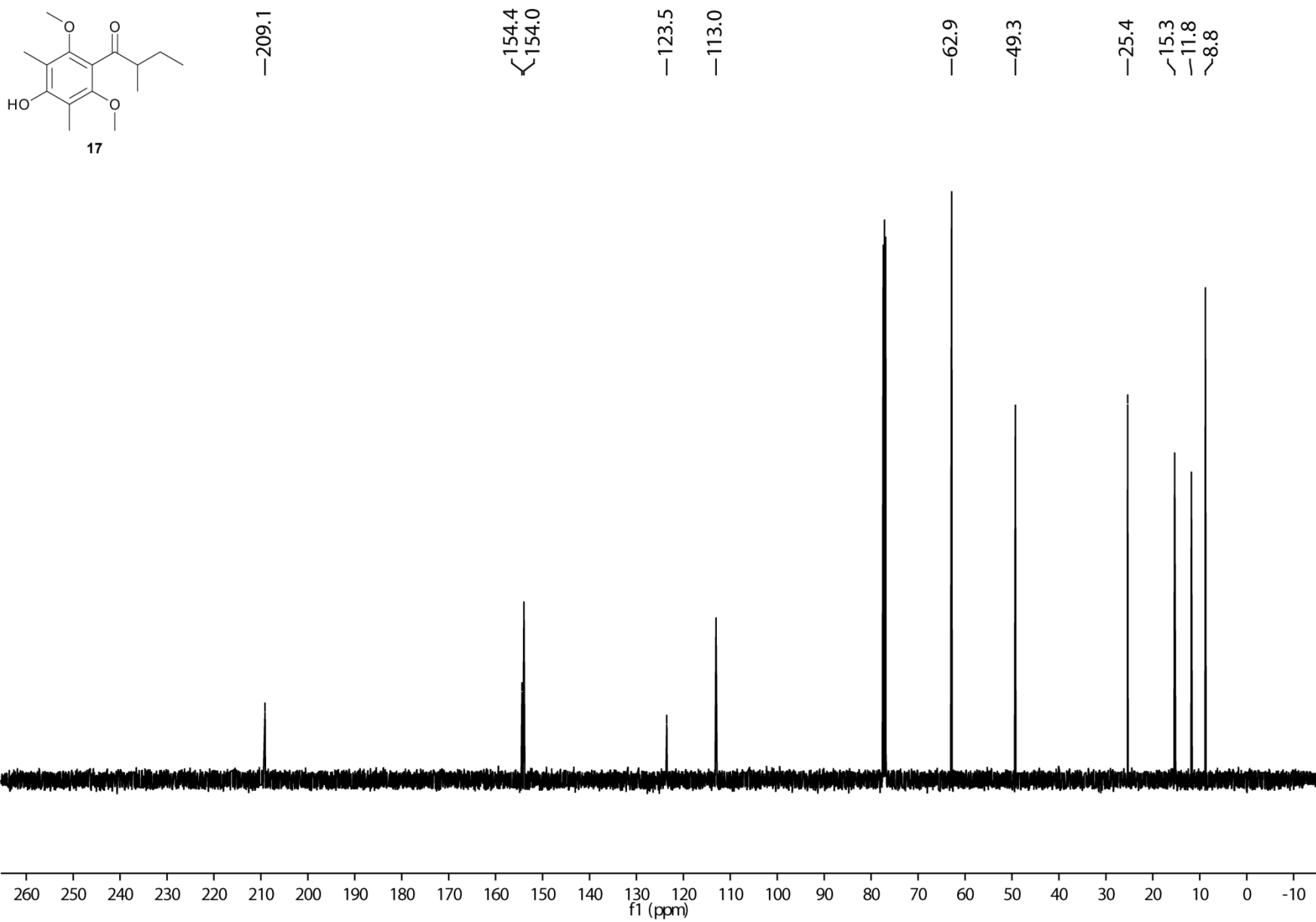
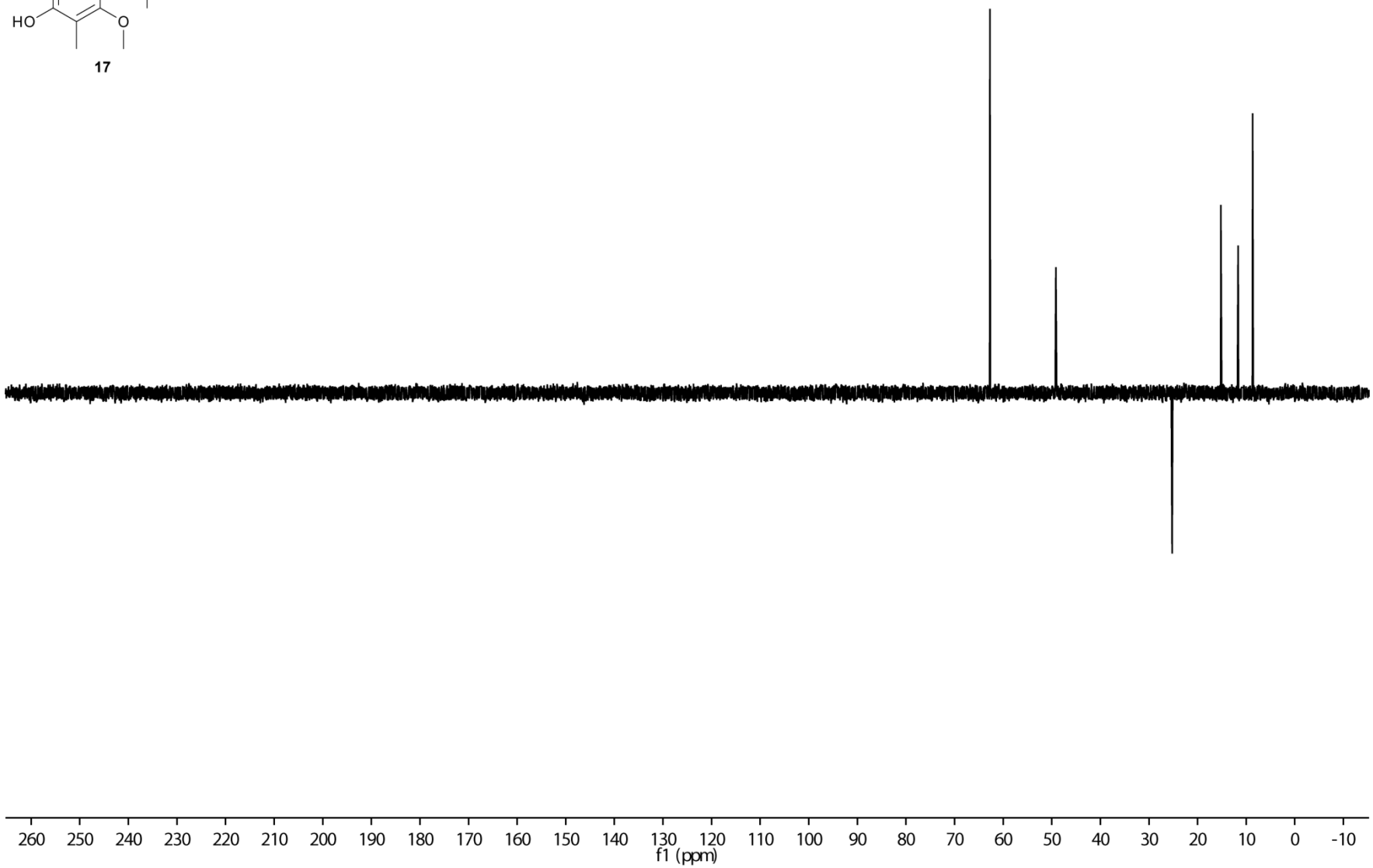
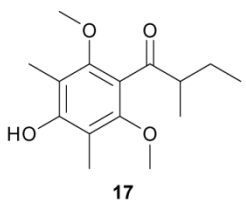


Figure S15. ¹³C NMR spectrum of **17** (125 MHz, CDCl₃).



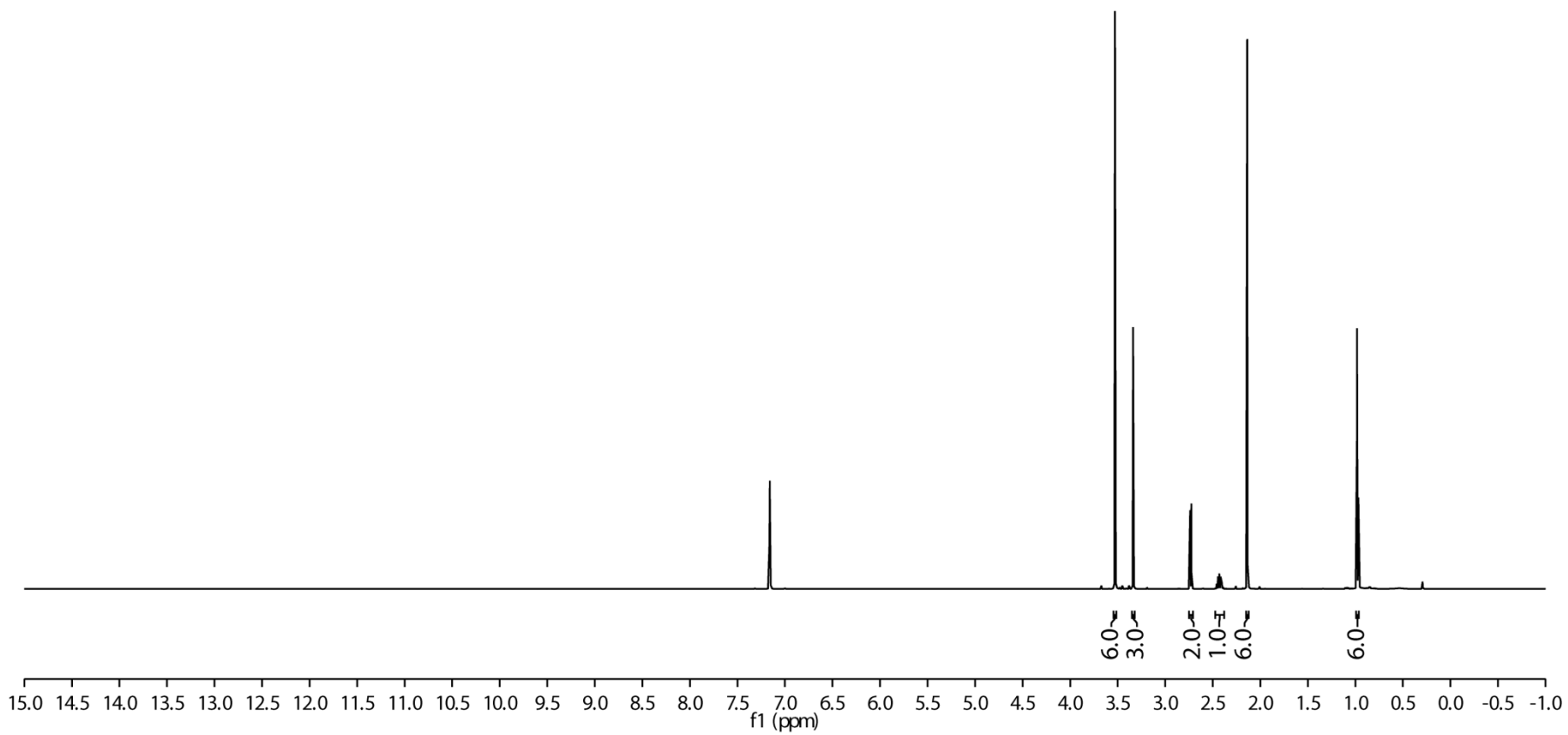
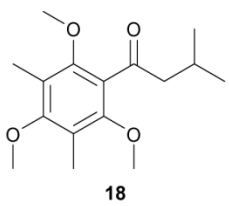


Figure S17. ^1H NMR spectrum of **18** (500 MHz, C_6D_6).

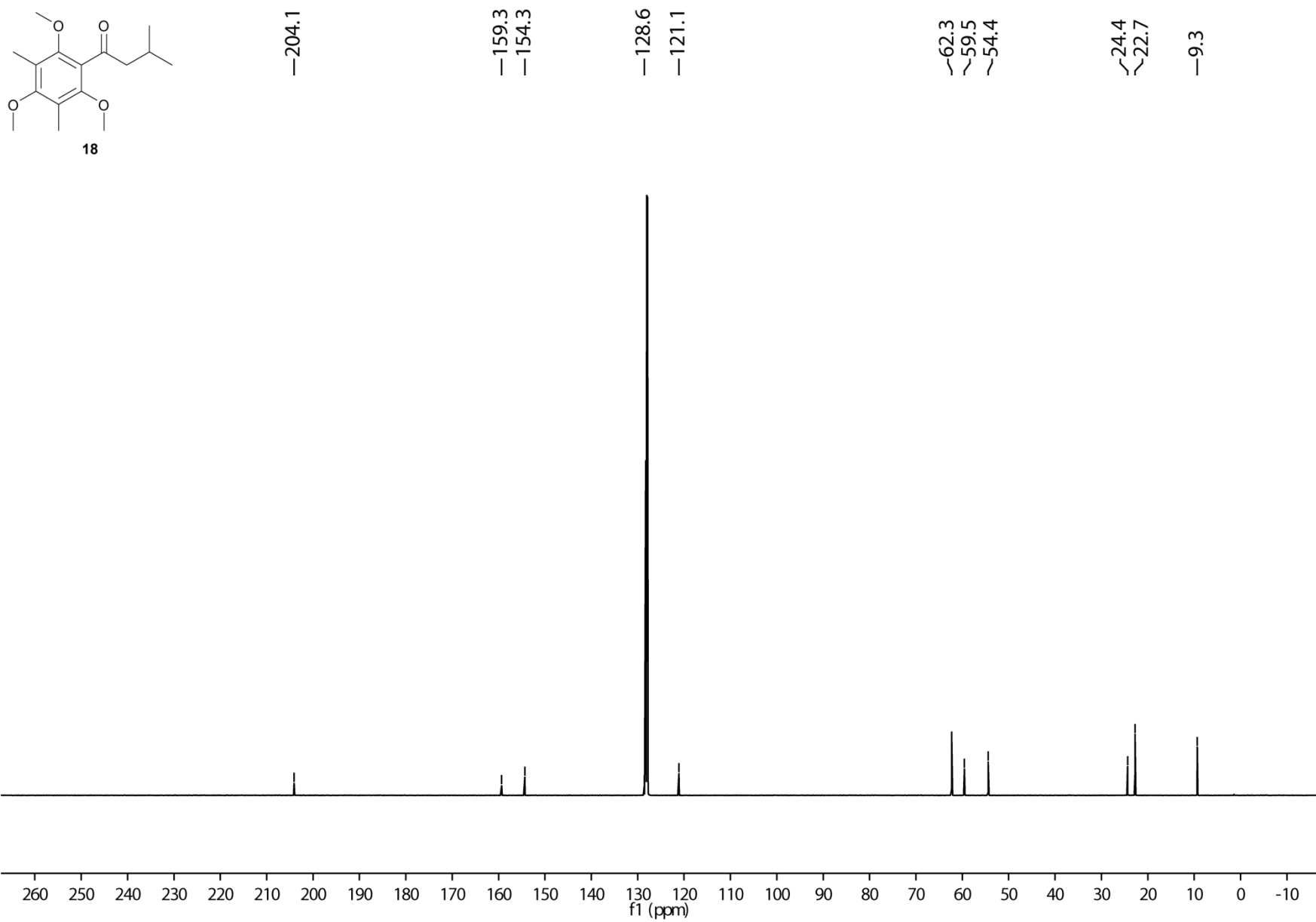


Figure S18. ¹³C NMR spectrum of **18** (125 MHz, C₆D₆).

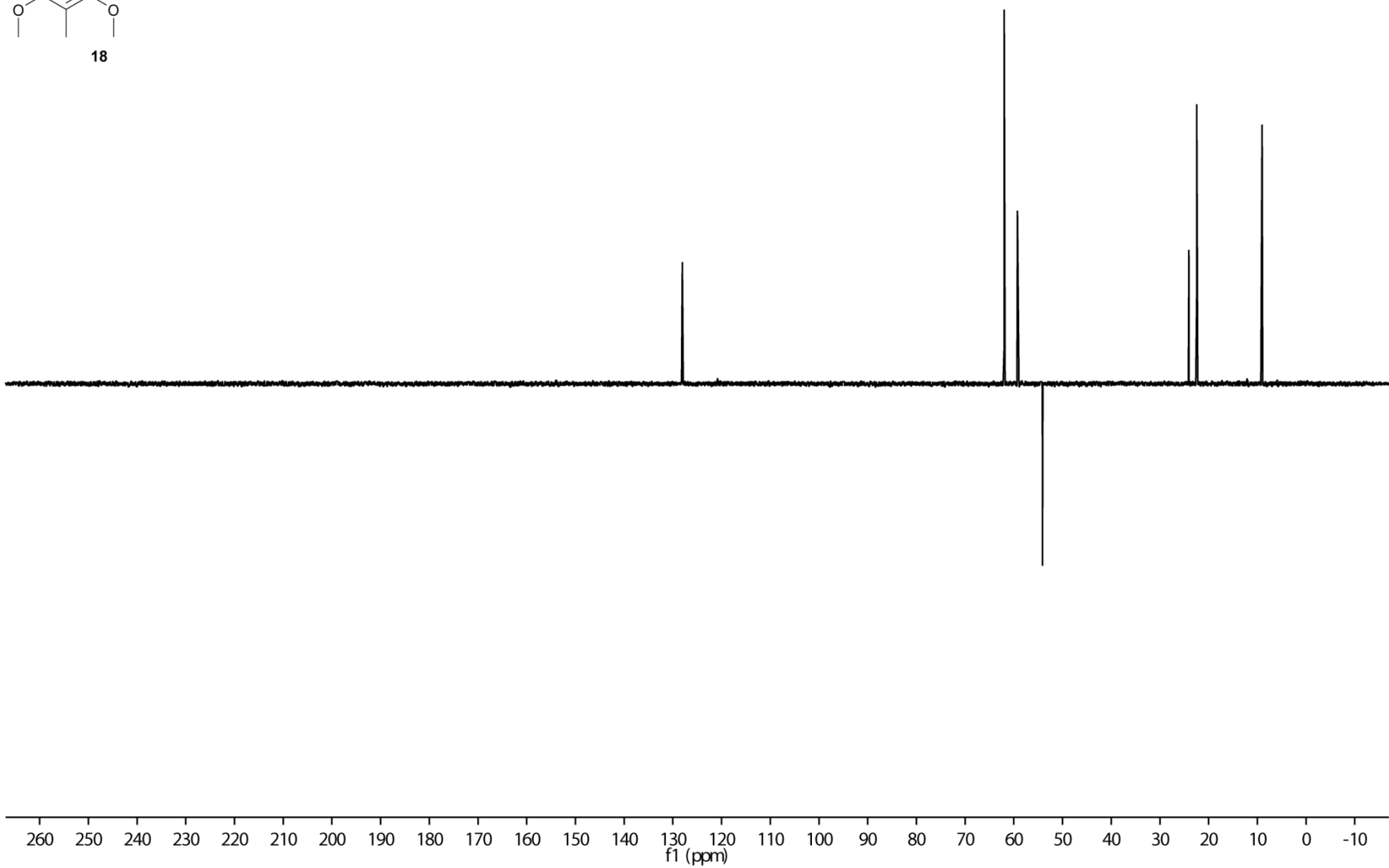
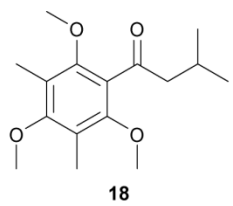


Figure S19. ^{13}C DEPT 135 spectrum of **18** (125 MHz, C_6D_6).

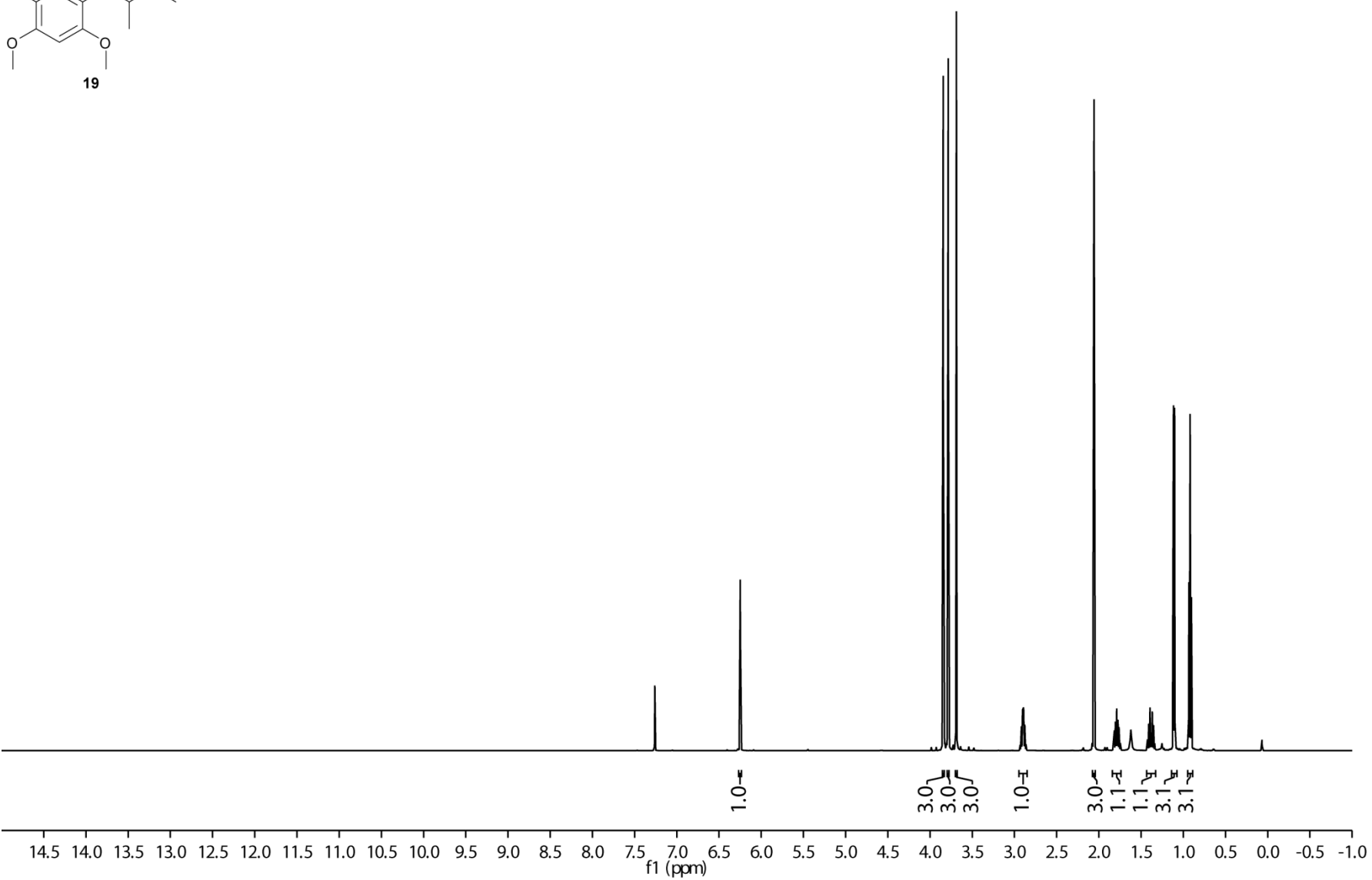
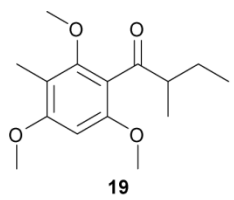
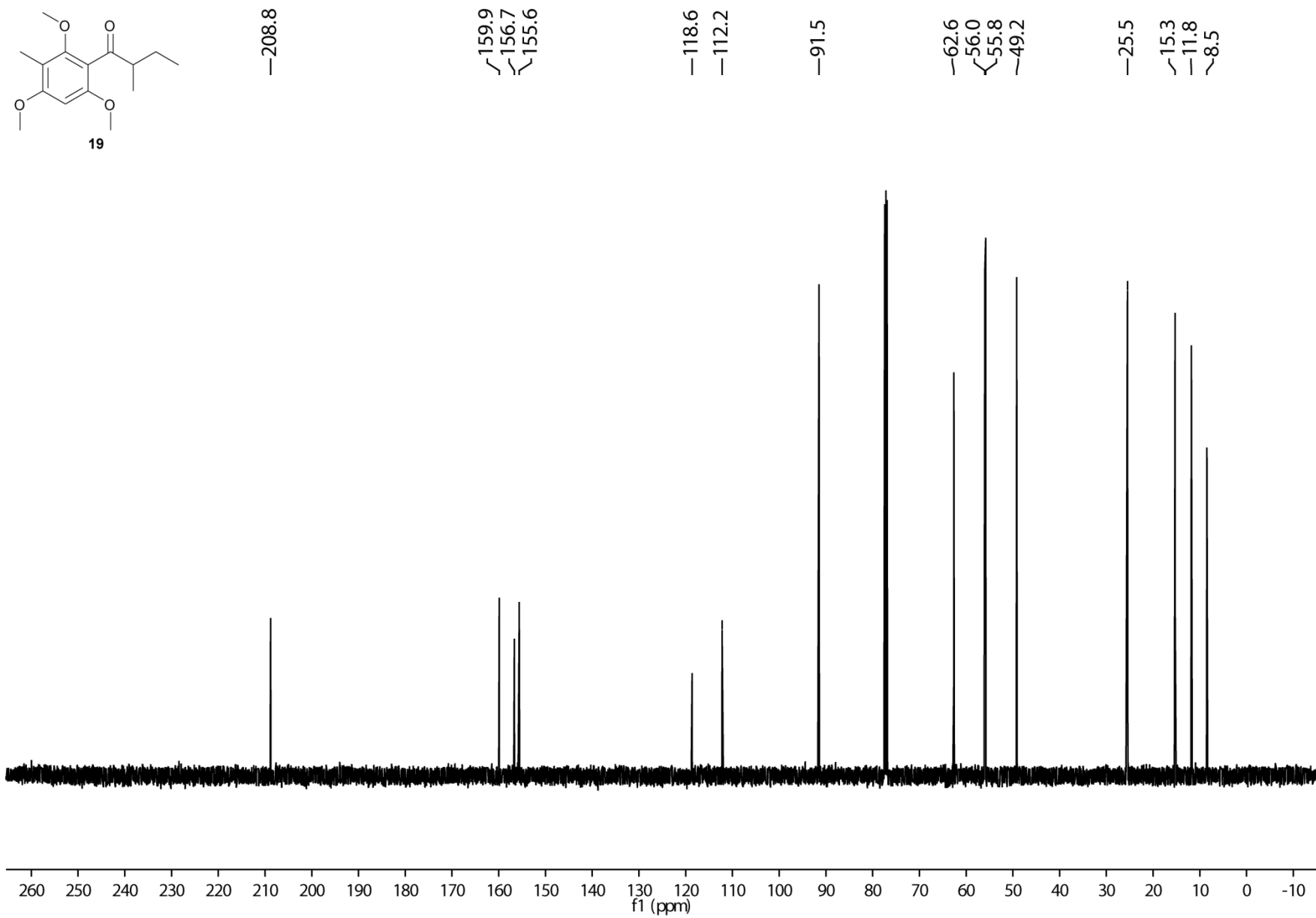


Figure S20. ^1H NMR spectrum of **19** (500 MHz, CDCl_3).



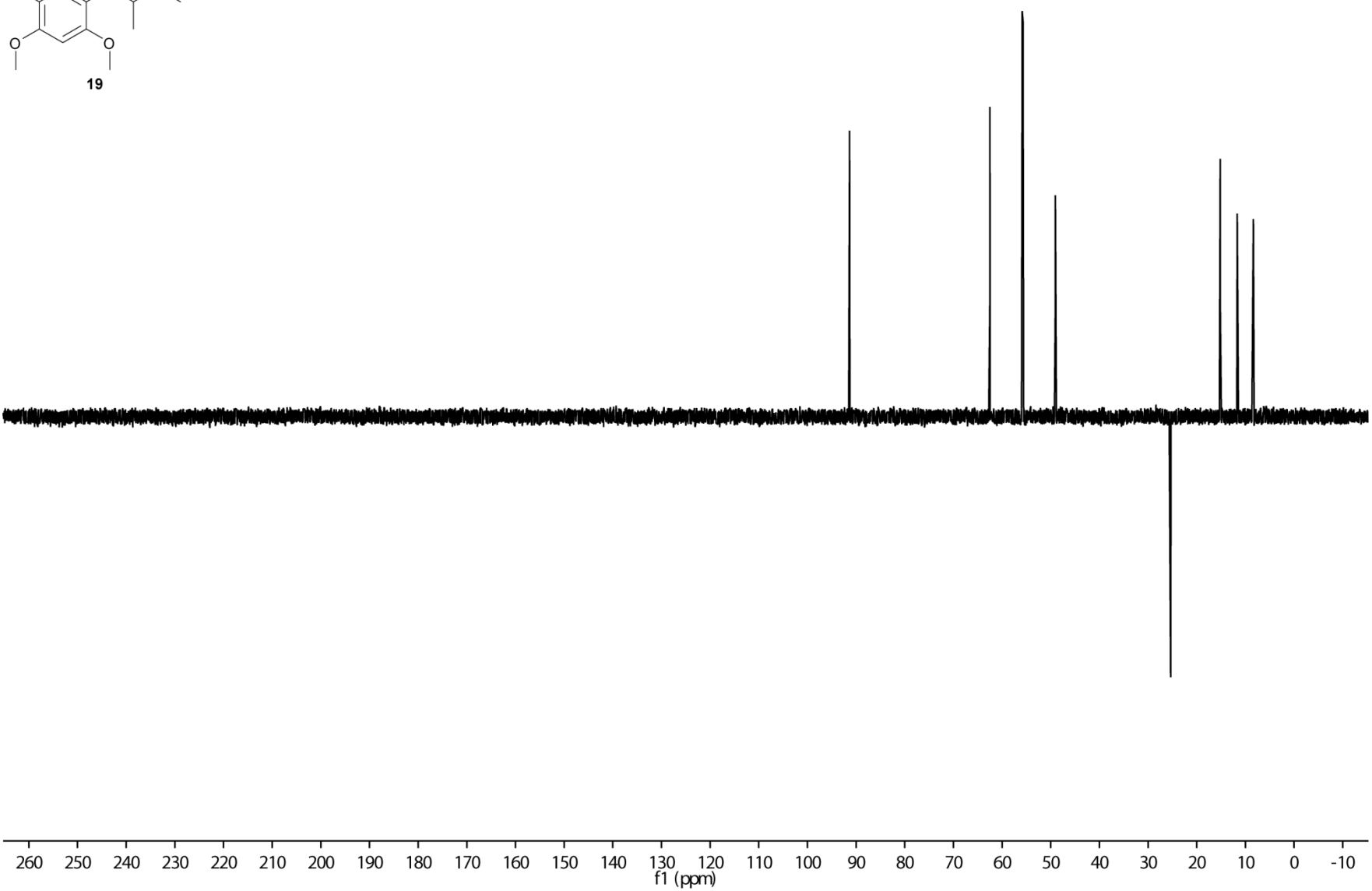
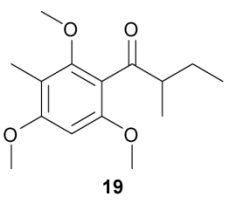


Figure S22. ¹³C DEPT 135 spectrum of **19** (125 MHz, CDCl₃).

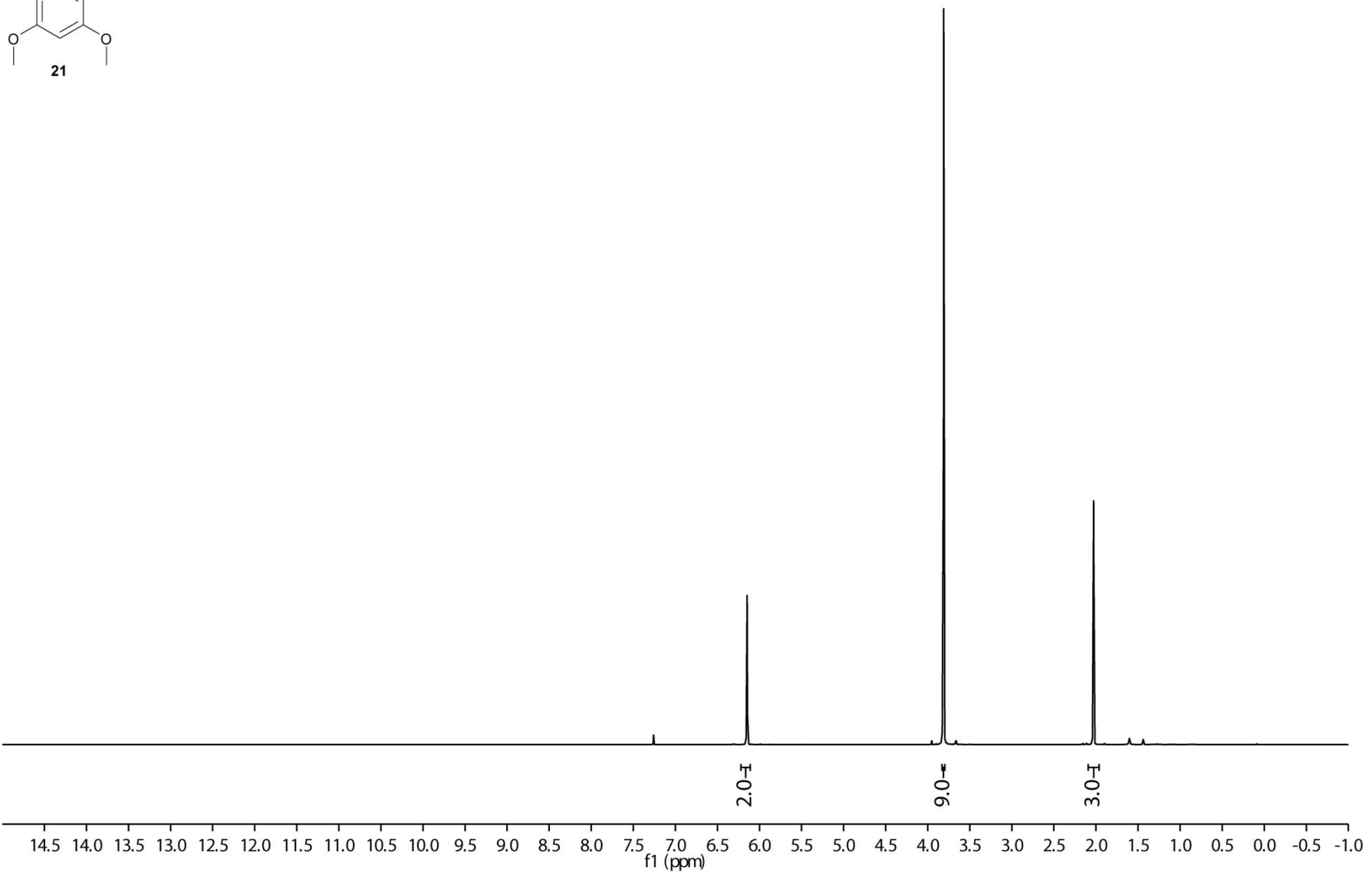
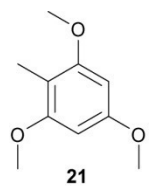


Figure S23. ^1H NMR spectrum of **21** (500 MHz, CDCl_3).

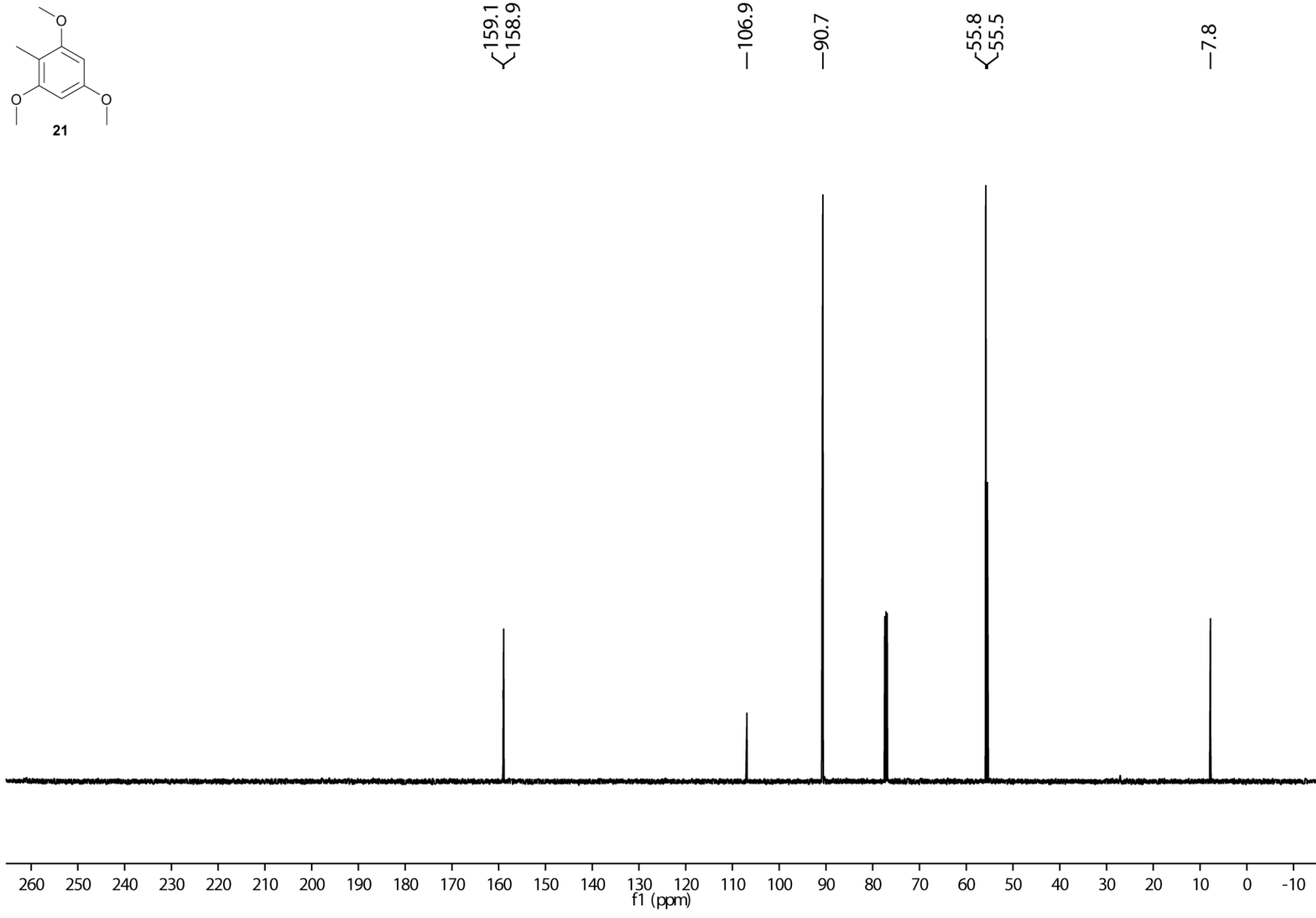
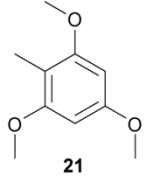


Figure S24. ¹³C NMR spectrum of **21** (125 MHz, CDCl₃).

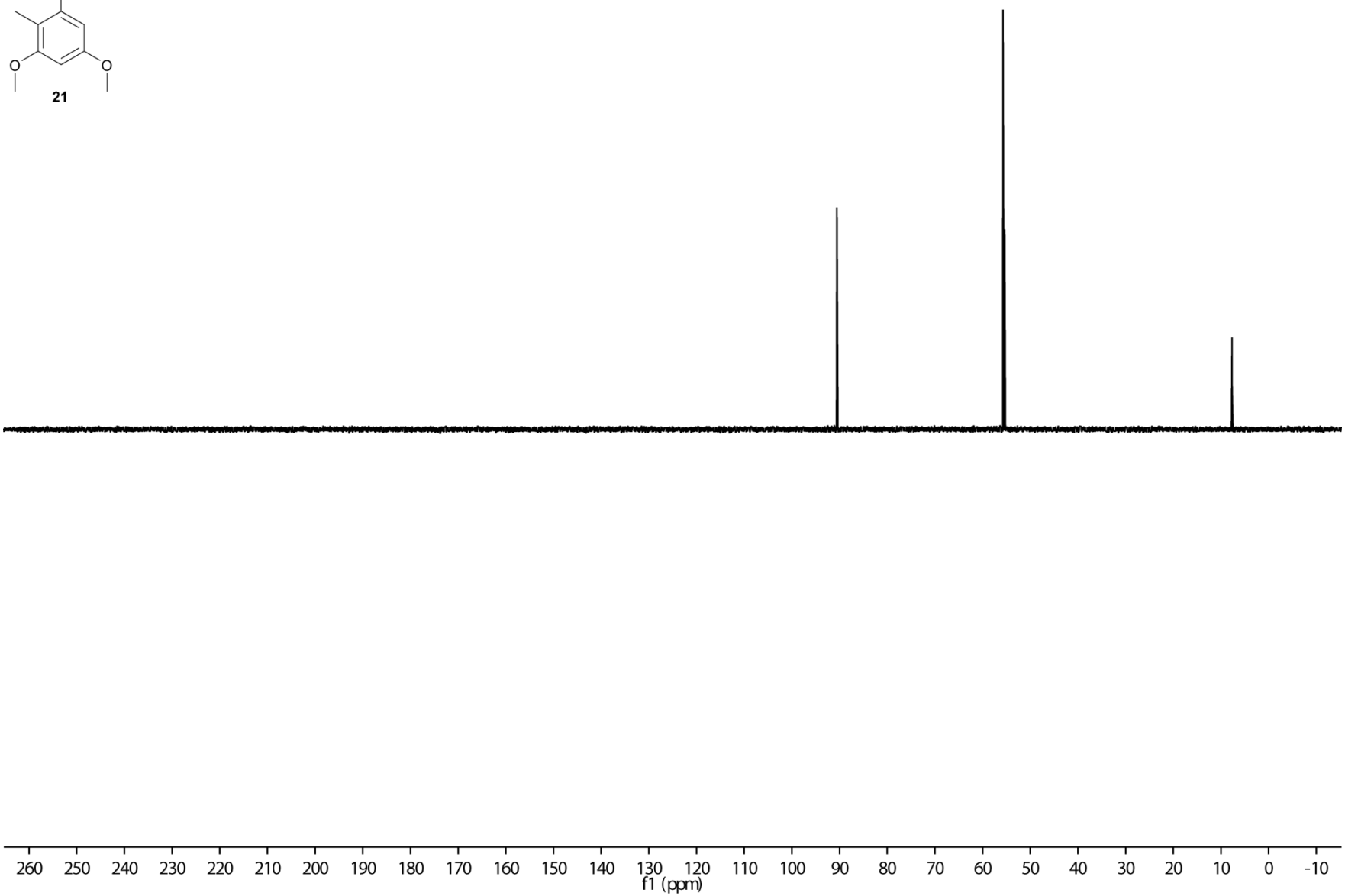
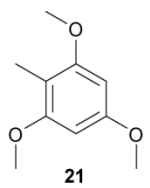


Figure S25. ¹³C DEPT 135 spectrum of **21** (125 MHz, CDCl₃).

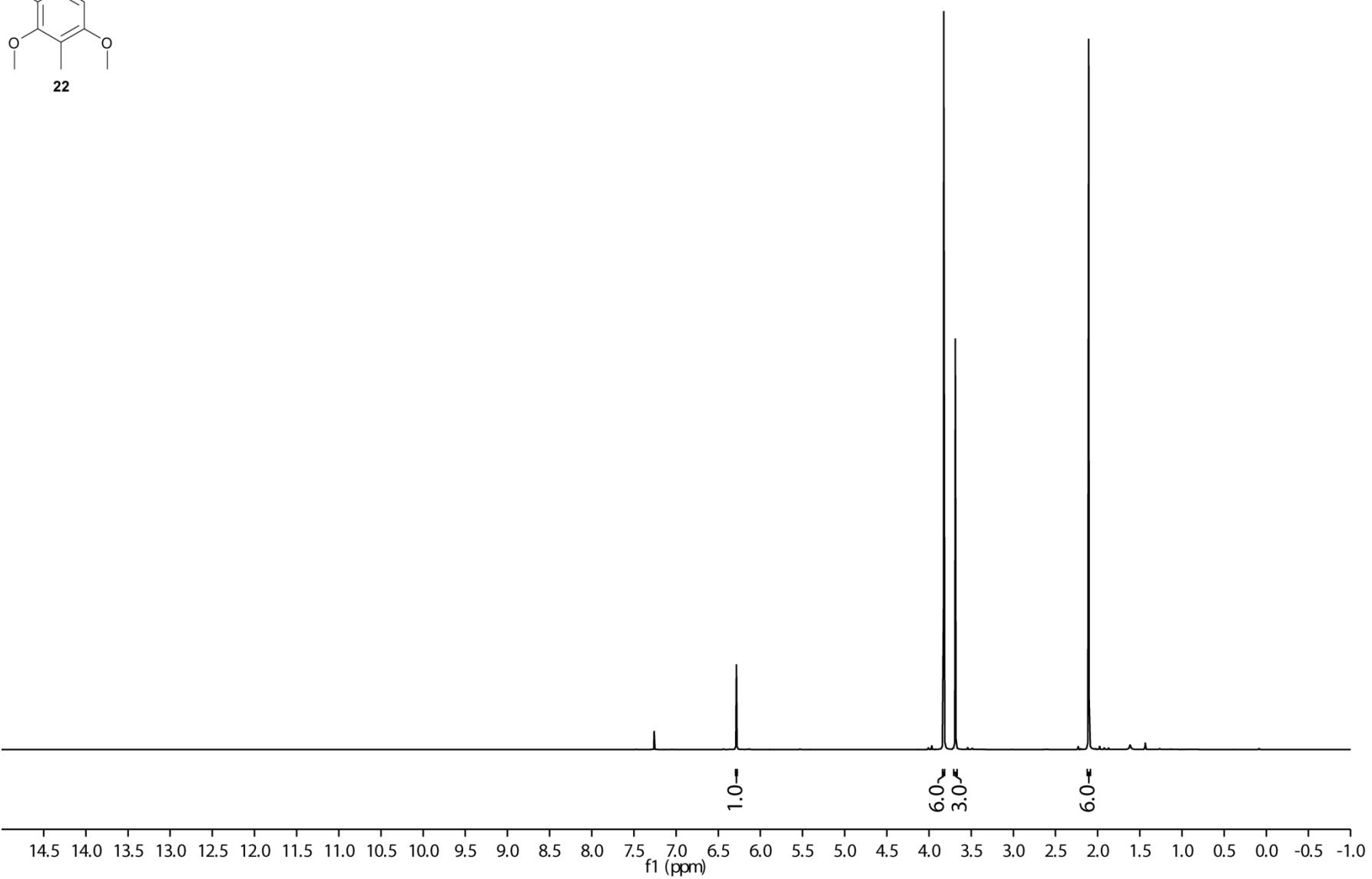
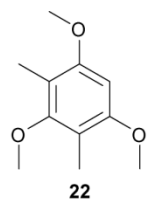


Figure S26. ¹H NMR spectrum of **22** (500 MHz, CDCl₃).

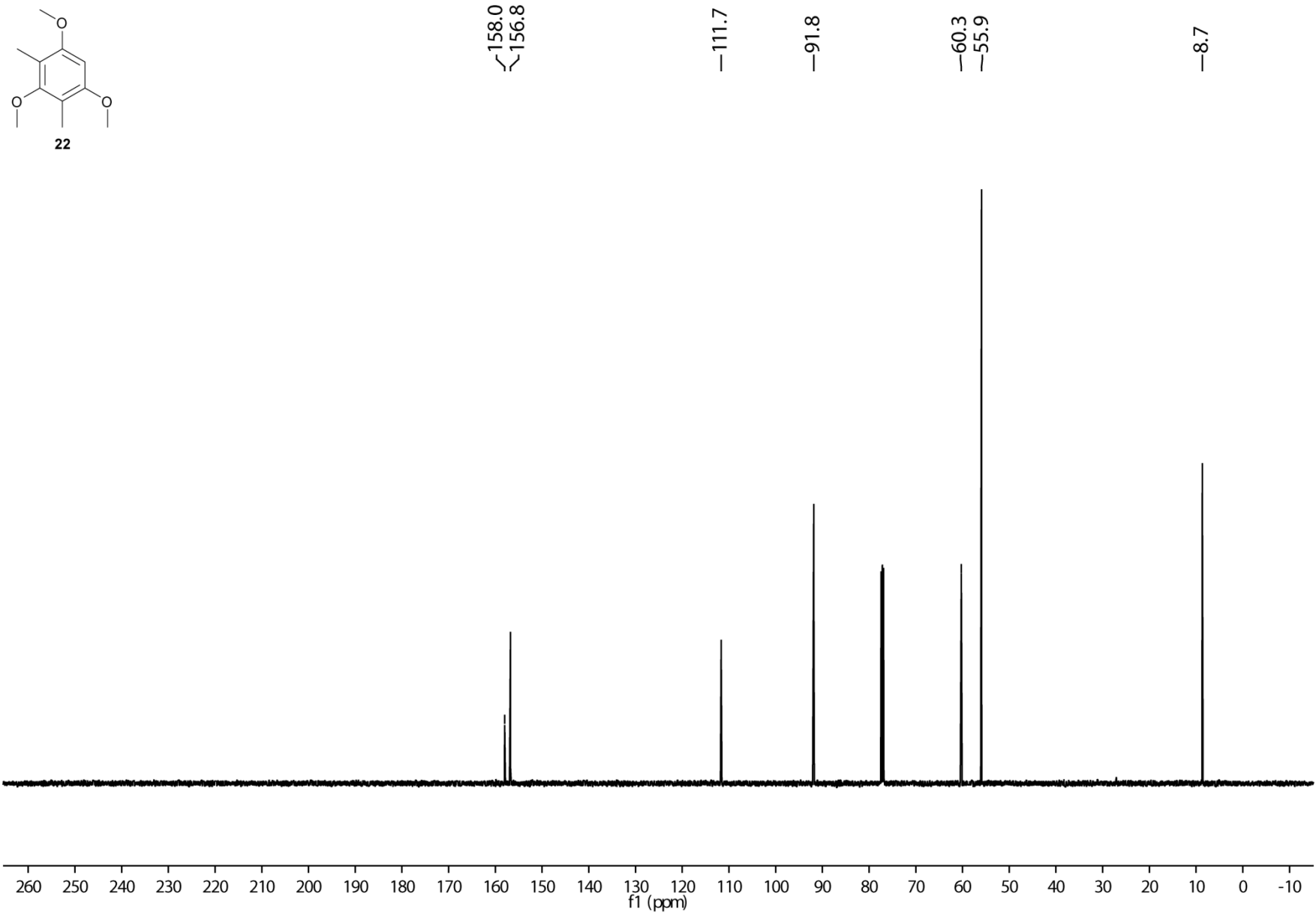
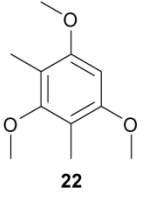


Figure S27. ^{13}C NMR spectrum of **22** (125 MHz, CDCl_3).

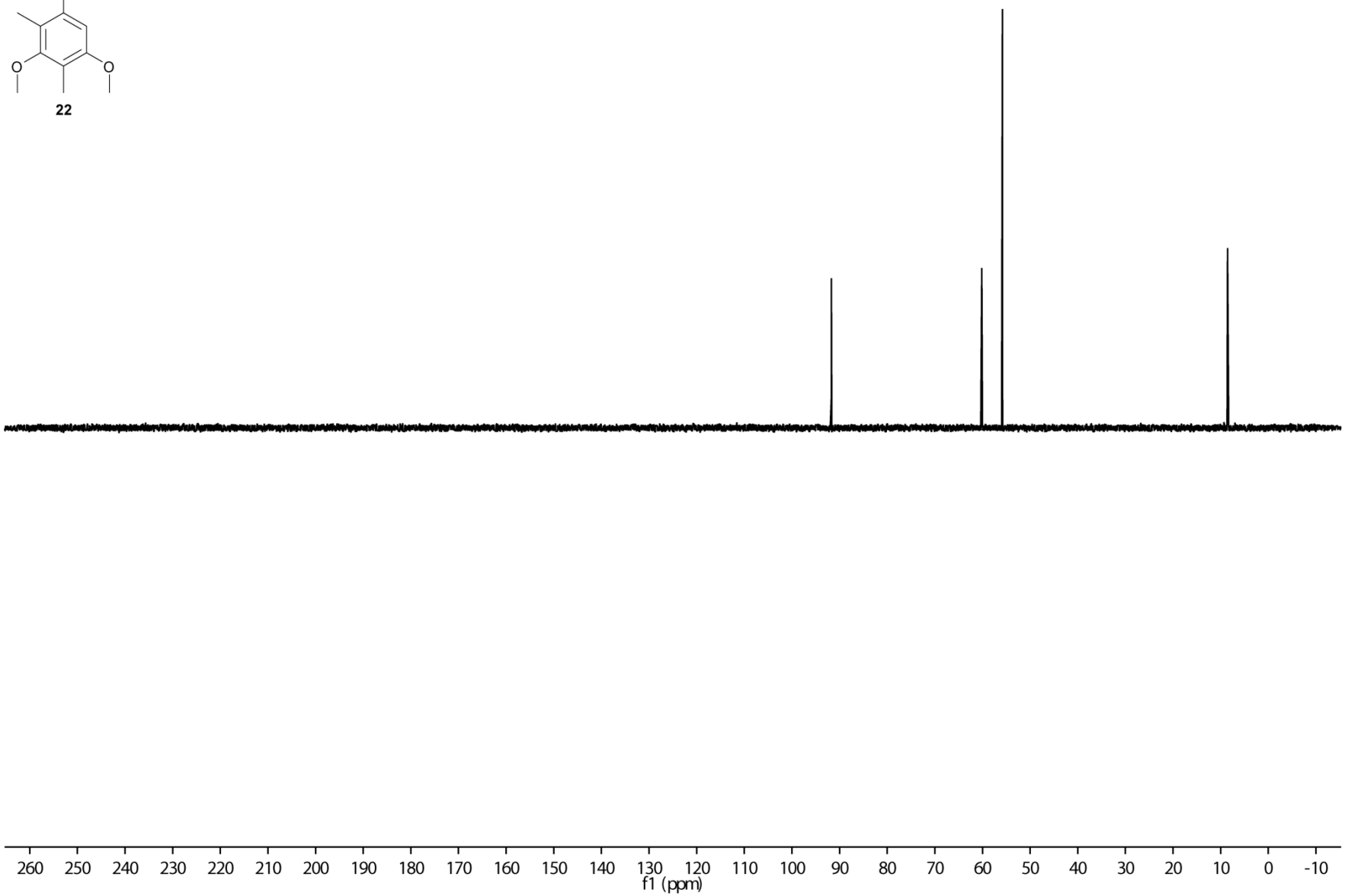
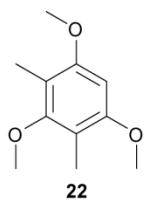


Figure S28. ^{13}C DEPT 135 spectrum of **22** (125 MHz, CDCl_3).

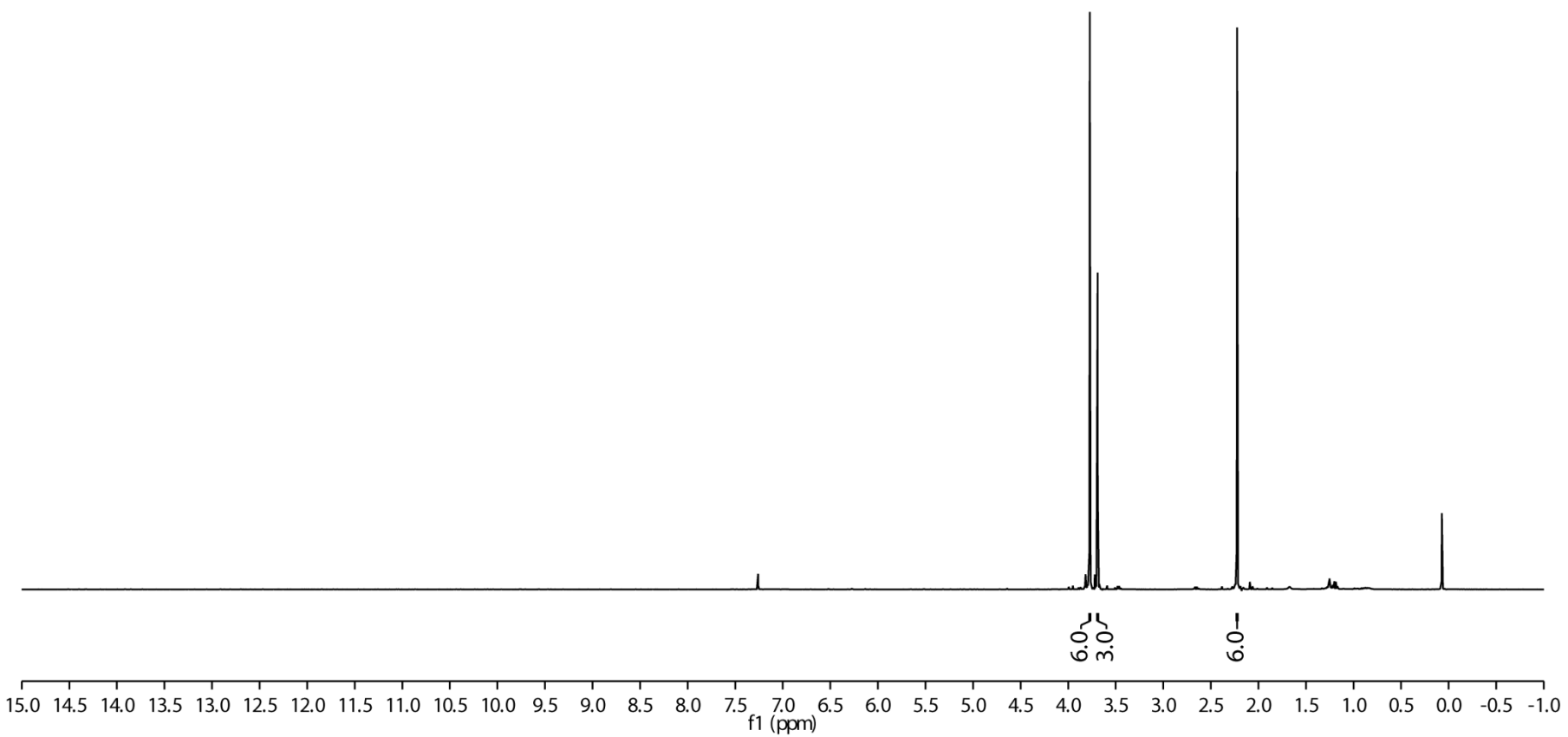
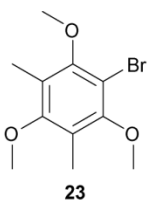


Figure S29. ¹H NMR spectrum of **23** (400 MHz, CDCl₃).

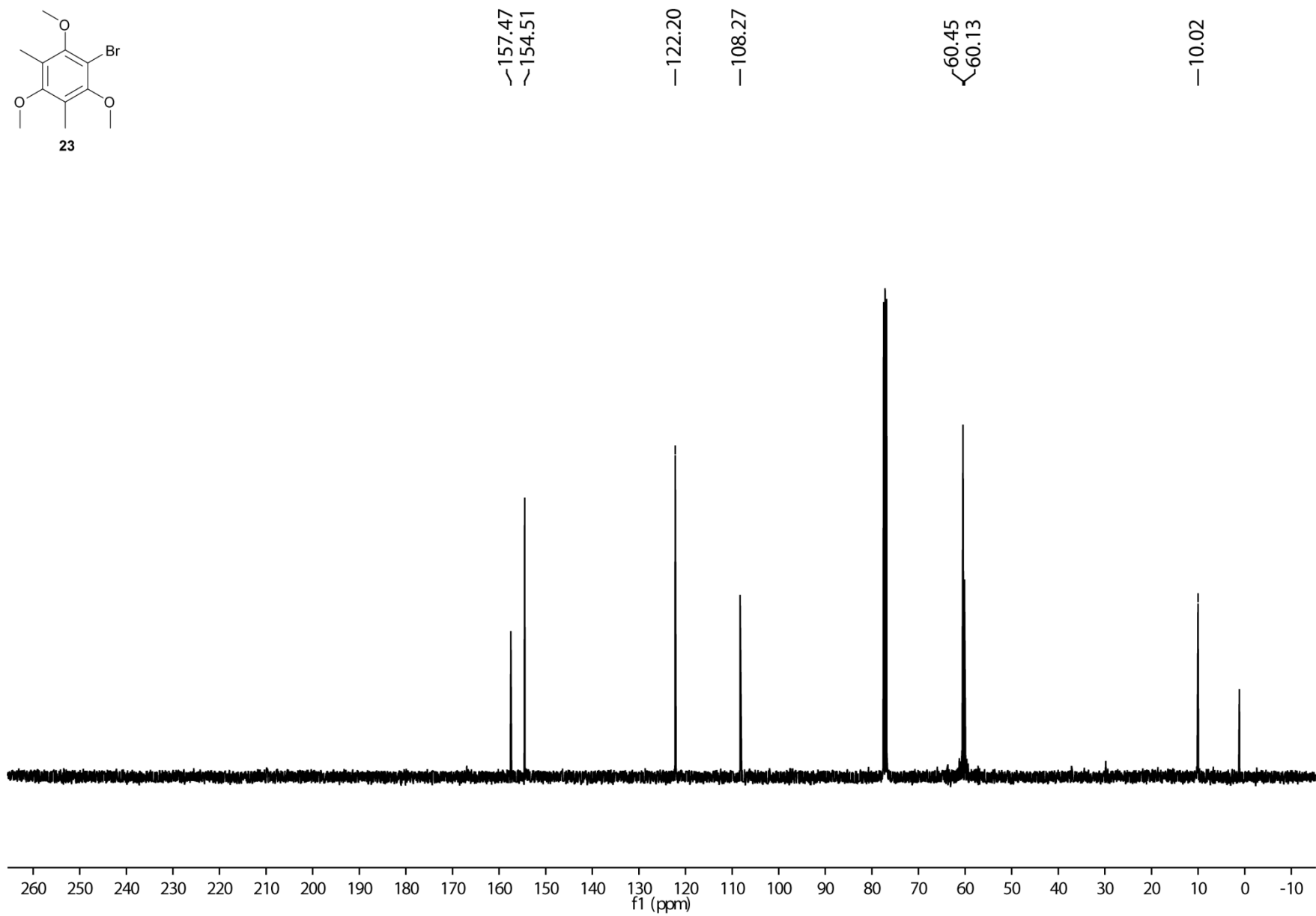
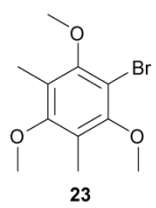


Figure S30. ^{13}C NMR spectrum of **23** (100 MHz, CDCl_3).

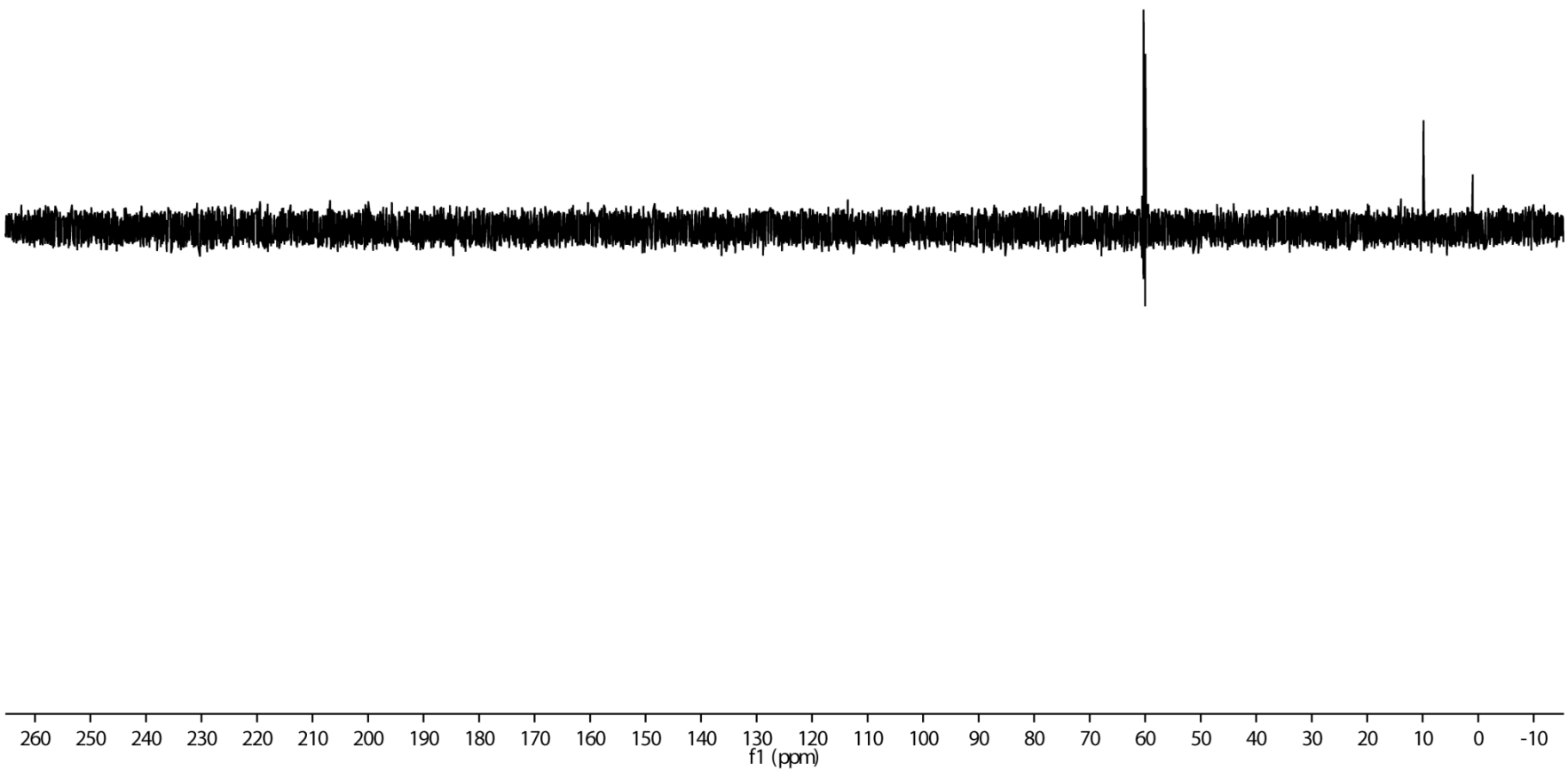
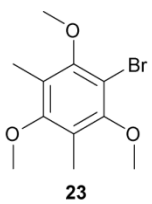


Figure S31. ^{13}C DEPT 135 spectrum of **23** (100 MHz, CDCl_3).

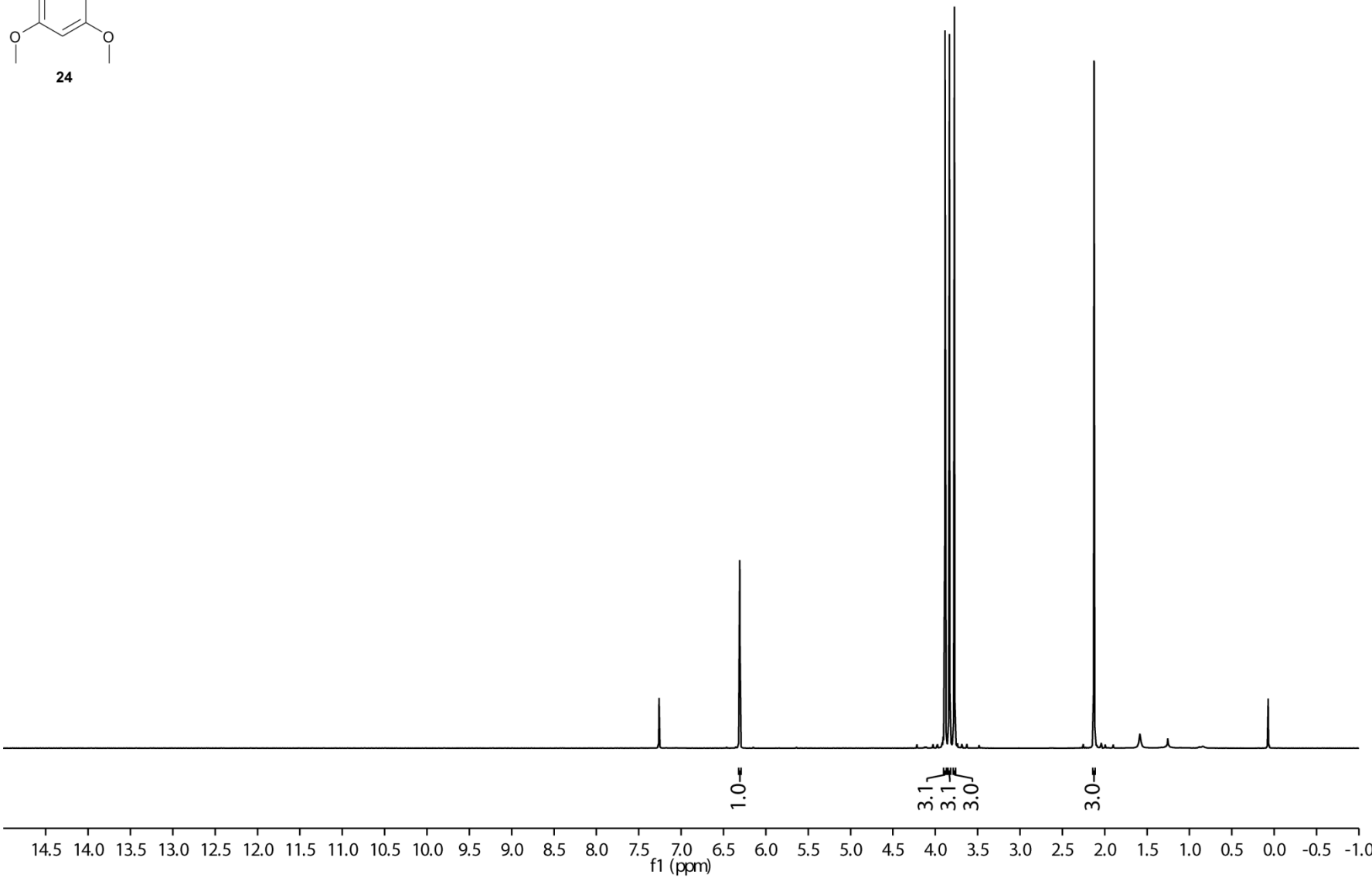
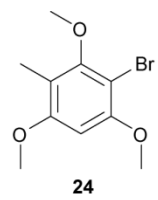


Figure S32. ^1H NMR spectrum of **24** (500 MHz, CDCl_3).

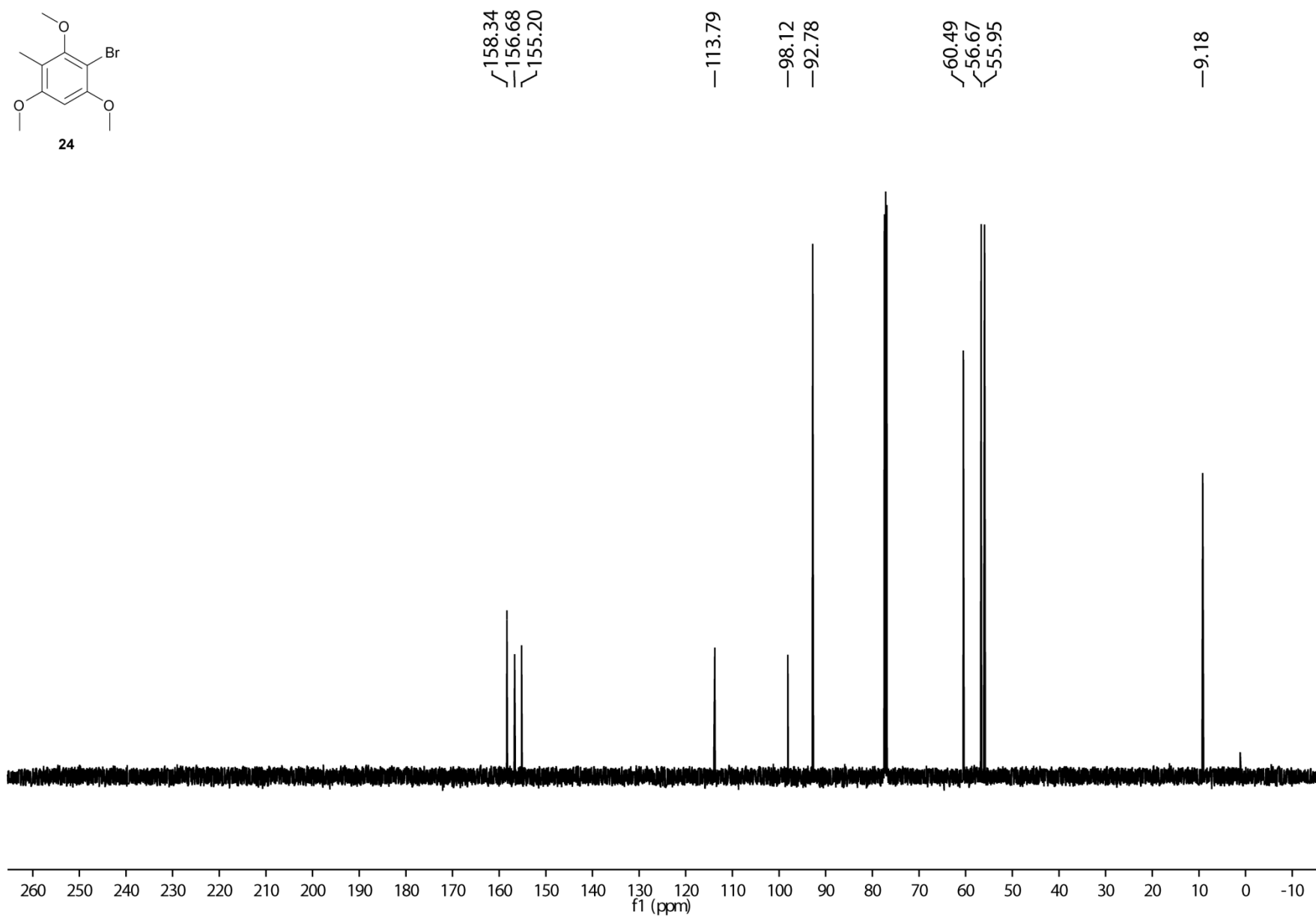
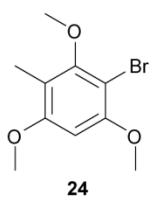


Figure S33. ^{13}C NMR spectrum of **24** (125 MHz, CDCl_3).

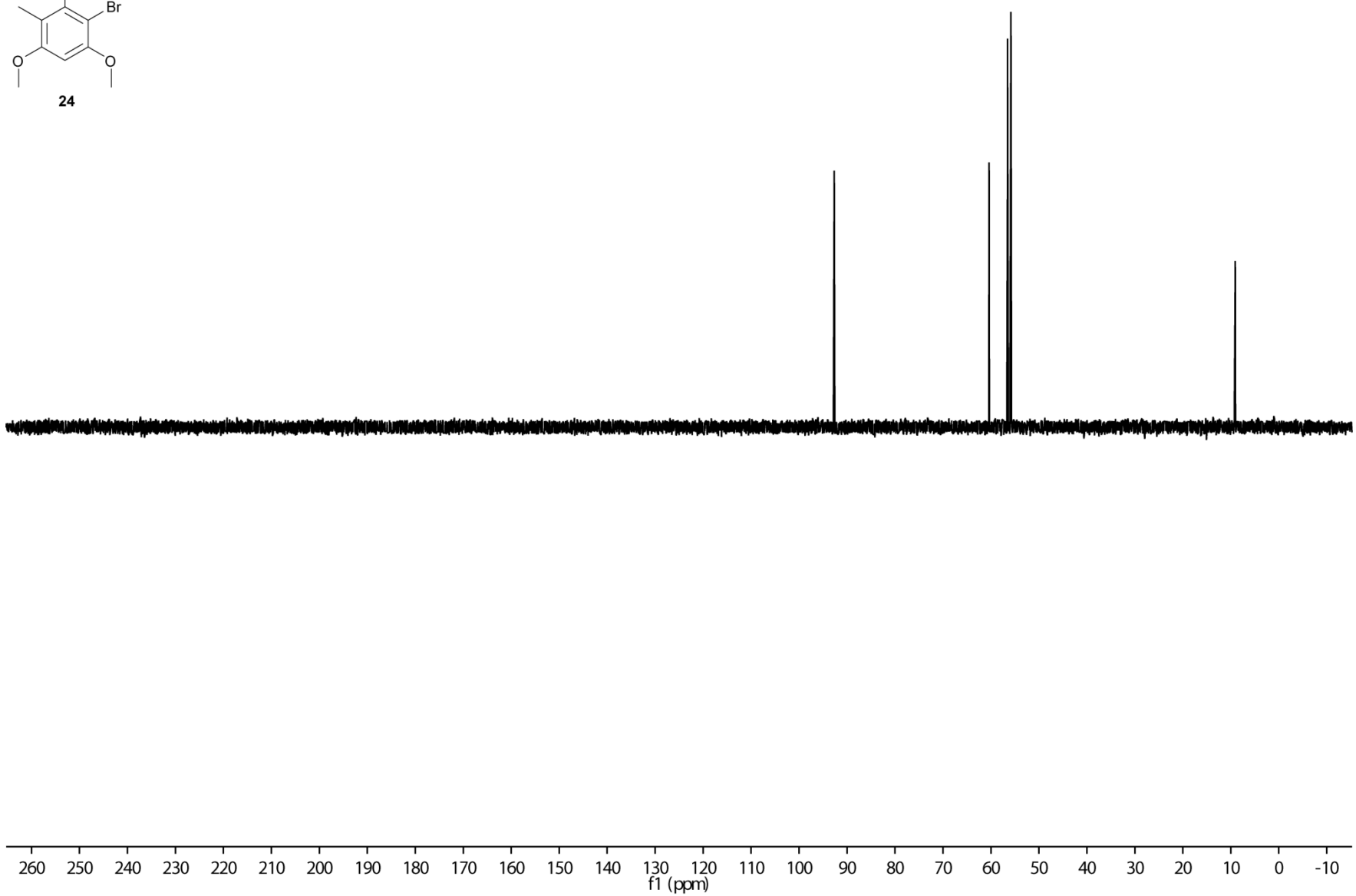
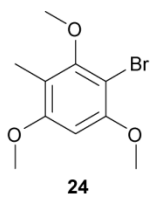


Figure S34. ¹³C DEPT 135 spectrum of **24** (125 MHz, CDCl₃).

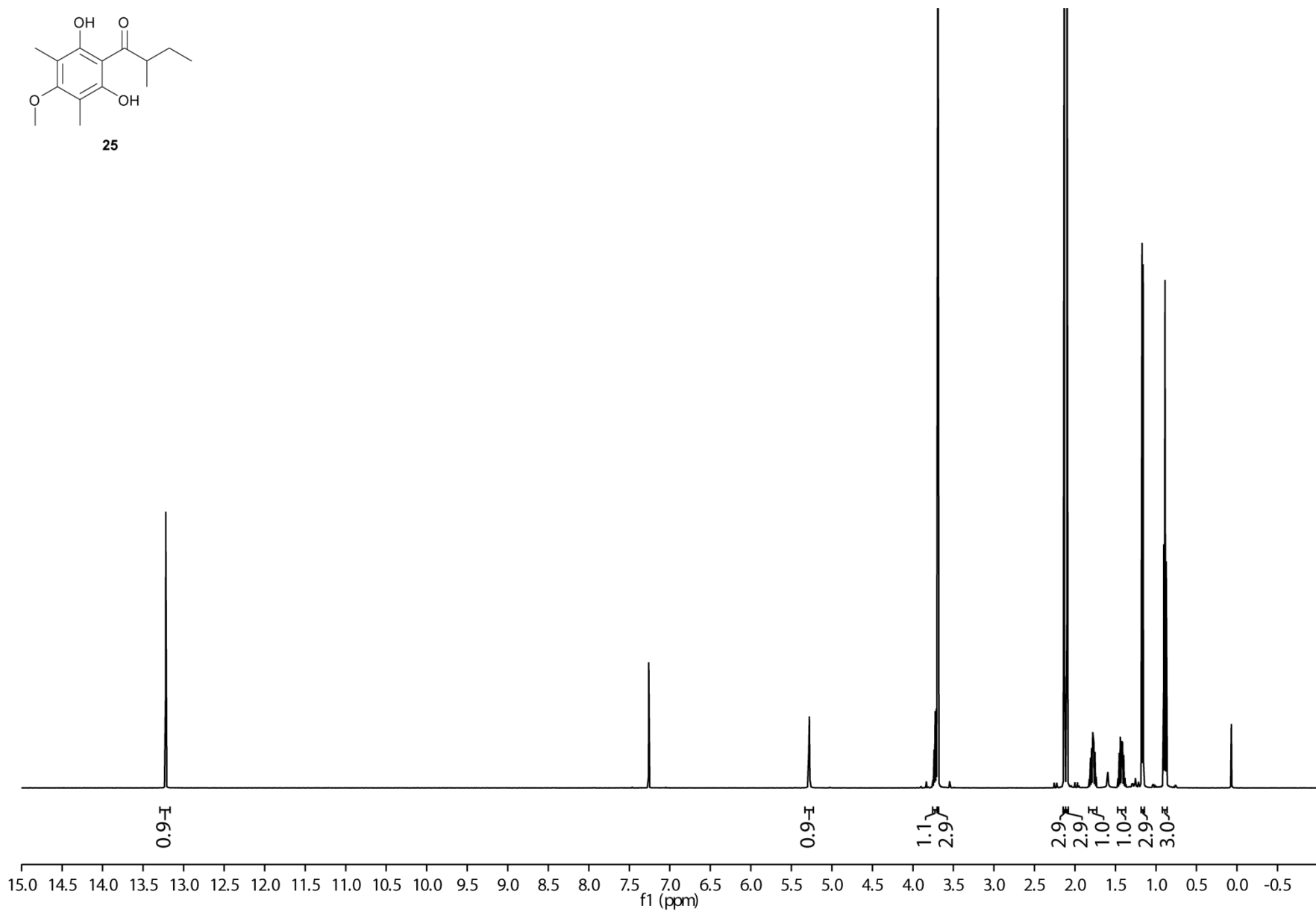
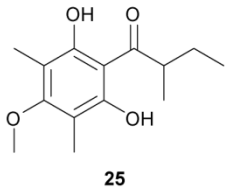


Figure S35. ¹H NMR spectrum of **25** (500 MHz, CDCl₃).

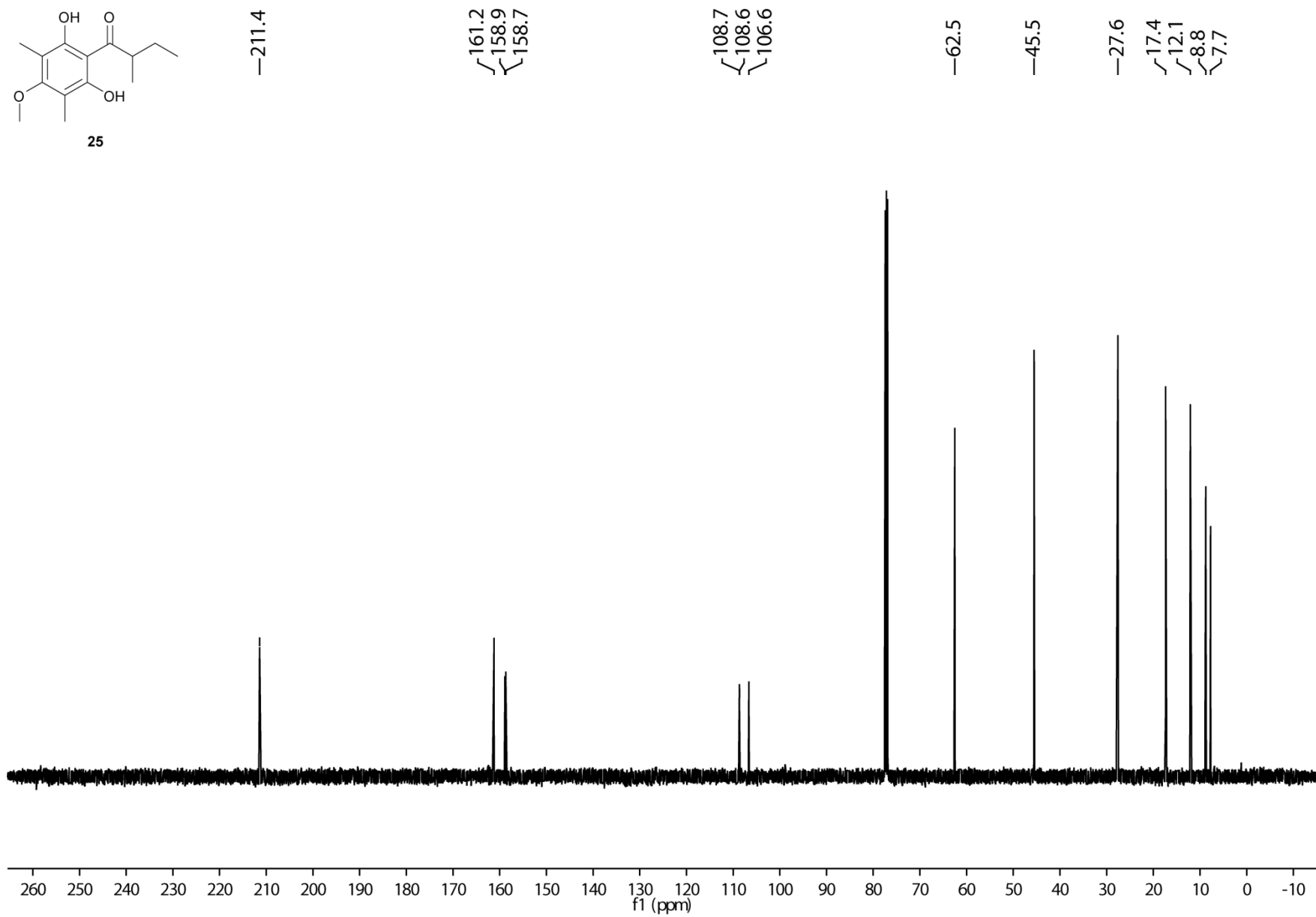
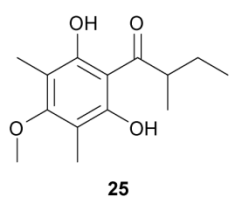


Figure S36. ¹³C NMR spectrum of **25** (125 MHz, CDCl₃).

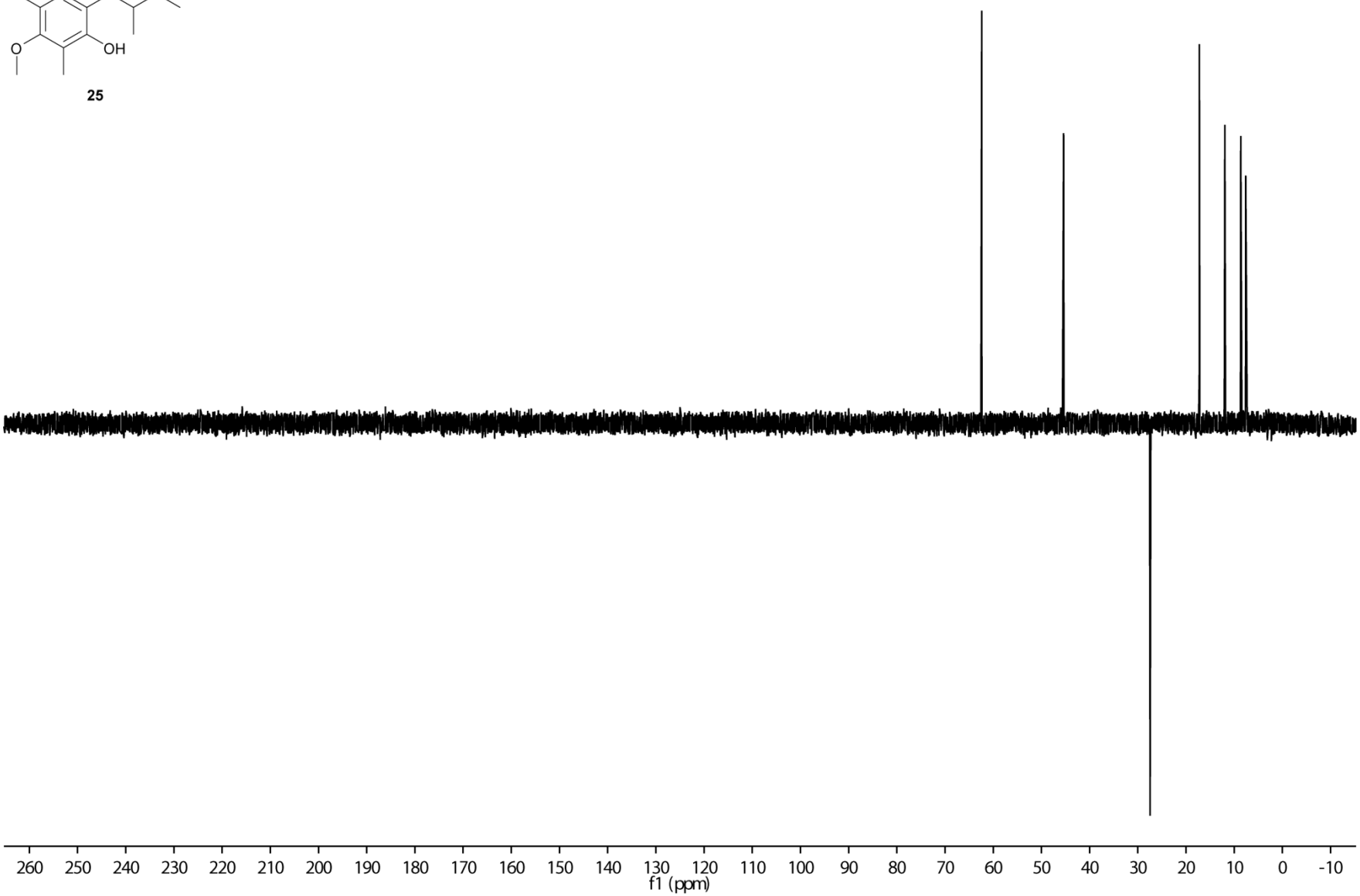
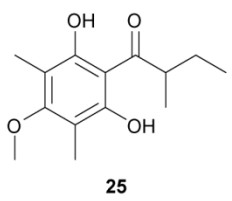


Figure S37. ¹³C DEPT 135 spectrum of **25** (125 MHz, CDCl₃).

Appendix E

Volatiles from Nineteen Recently Genome Sequenced Actinomycetes



Cite this: *Org. Biomol. Chem.*, 2015, **13**, 2673

Volatiles from nineteen recently sequenced actinomycetes†

Christian A. Citron,^a Lena Barra,^a Joachim Wink^b and Jeroen S. Dickschat^{*a}

The volatiles released by agar plate cultures of nineteen actinomycetes whose genomes were recently sequenced were collected by use of a closed-loop stripping apparatus (CLSA) and analysed by GC/MS. In total, 178 compounds from various classes were identified. The most interesting findings were the detection of the insect pheromone frontalin in *Streptomyces varsoviensis*, and the emission of the unusual plant metabolite 1-nitro-2-phenylethane. Its biosynthesis from phenylalanine was investigated in isotopic labelling experiments. Furthermore, the identified terpenes were correlated to the information about terpene cyclase homologs encoded in the investigated strains. The analytical data were in line with functionally characterised bacterial terpene cyclases and particularly corroborated the recently suggested function of a terpene cyclase from *Streptomyces violaceusniger* by the identification of a functional homolog in *Streptomyces rapamycinicus*.

Received 15th December 2014,
Accepted 6th January 2015

DOI: 10.1039/c4ob02609h

www.rsc.org/obc

Introduction

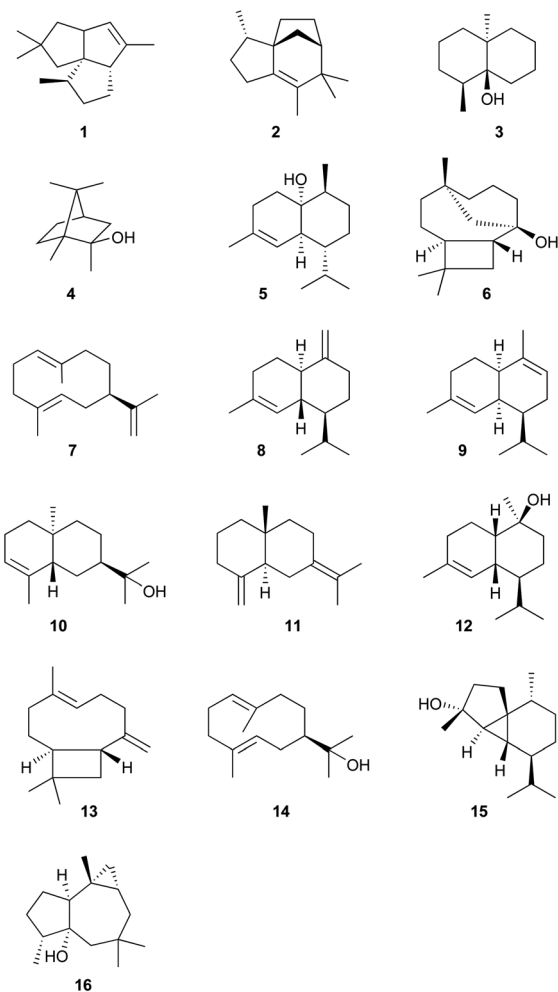
The first genome sequence of the bacterium *Haemophilus influenzae* was completely mapped in 1995.¹ Today, the modern sequencing techniques have enabled the rapid assembly of thousands of bacterial genome sequences. The accumulated sequencing data are stored on giant servers and bioinformatic online tools are available that allow for an efficient screening of these data for the presence of sequences with high homology to a probe sequence (basic local alignment search tool, BLAST).² The open access to genome data currently revolutionises many scientific fields including natural products chemistry. For each secondary metabolite produced by a bacterium a candidate biosynthetic gene or gene cluster can immediately be assigned, thus allowing for advanced genetic techniques such as heterologous gene expressions and DNA sequence manipulation that can confirm the involvement of genes in the biosynthesis of a secondary metabolite, may give detailed mechanistic insights, and can in some cases even result in an increased production.³ This approach is particularly interesting for high potential secondary metabolite producing bacteria

such as actinomycetes,⁴ myxobacteria,⁵ and cyanobacteria.⁶ Many bacteria particularly of these taxa encode terpene cyclases such as the synthases for pentalenene (**1**),⁷ *epi*-isozizaene (**2**),⁸ geosmin (**3**),⁹ 2-methylisoborneol (**4**),^{10,11} *epi*-cubenol (**5**),¹² and caryolan-1-ol (**6**, Scheme 1),¹³ but a large number of putative bacterial terpene cyclases is still not characterised. We have recently initiated a program to investigate the function of these bacterial terpene cyclases. Since mono-, sesqui- and diterpene hydrocarbons are volatile, this can be performed by gene cloning, heterologous expression in *Escherichia coli*, direct sampling of volatiles by use of a closed-loop stripping apparatus (CLSA) and GC/MS analysis of the obtained headspace extracts.¹⁴ For highly efficient cloning by homologous recombination in yeast we have recently developed a pET28c-derived expression vector that contains a yeast replication system and selectable marker.¹⁵ *Via* heterologous expression the terpene cyclases for germacrene A (**7**), γ -cadinene (**8**), α -amorphene (**9**), 7-*epi*- α -eudesmol (**10**), selina-4 (**15**), 7(11)-diene (**11**), T-muurolol (**12**), (*E*)- β -caryophyllene (**13**), hedyaryol (**14**), and *epi*-cubebol (**15**) were identified.^{15–18} As second part of this work the volatiles of more than 50 bacteria encoding terpene cyclases were analysed.^{19–21} If a completed genome reveals the presence of only one uncharacterised terpene cyclase, and if the headspace extracts of this organism contain only one terpene product for which no particular terpene cyclase has been assigned, the formation of this terpene by the respective uncharacterised terpene cyclase is a very plausible suggestion. By this approach the terpene cyclases for **5**,¹⁹ **13**,²¹ and isoafricanol (**16**)²² were uncovered. The function of the putative (*E*)- β -caryophyllene synthase and *epi*-cubenol synthase were subsequently corroborated by

^aKekulé-Institut für Organische Chemie und Biochemie, Universität Bonn, Gerhard-Domagk-Straße 1, 53121 Bonn, Germany. E-mail: dickschat@uni-bonn.de; Tel: +49 228 735797

^bHelmholtz-Zentrum für Infektionsforschung GmbH, Inhoffenstraße 7, 38124 Braunschweig, Germany

† Electronic supplementary information (ESI) available: Tabulated data of investigated strains and terpene cyclases encoded in their genomes and of results of headspace analyses, figures of representative total ion chromatograms for each investigated strain, and phylogenetic tree of bacterial terpene cyclase homologs. See DOI: 10.1039/c4ob02609h

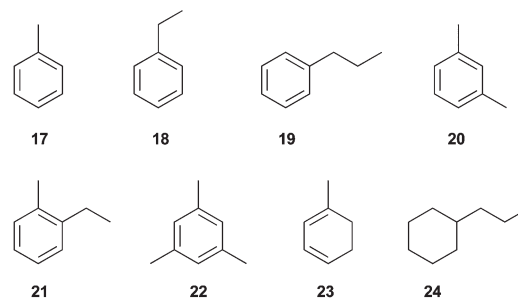


Scheme 1 Terpenes from characterised bacterial terpene cyclases.

heterologous expression and *in vitro* incubation experiments with the purified enzyme.^{12,15} Here we report on the volatiles from nineteen recently genome sequenced actinomycetes with a special focus on terpenes, but compounds from other classes will also be presented.

Results and discussion

The volatiles released by nineteen actinomycetes (Table 1 of ESI†) whose genomes were recently sequenced were collected on charcoal filters using a CLSA. The filters were extracted with dichloromethane and the headspace extracts were analysed by GC/MS. All strains were investigated in duplicate in order to check for reproducibility of the results. The identified compounds are summarised in Table 2 of ESI† and representative chromatograms for each strain are shown in Fig. 1 of ESI.† In total, 178 different compounds were detected, some of which occurred in multiple samples, while others were specific for a particular organism. The identified compounds belong to various compound classes including hydrocarbons, alcohols, aldehydes, ketones and ketals, carboxylic acids and esters,



Scheme 2 Hydrocarbons.

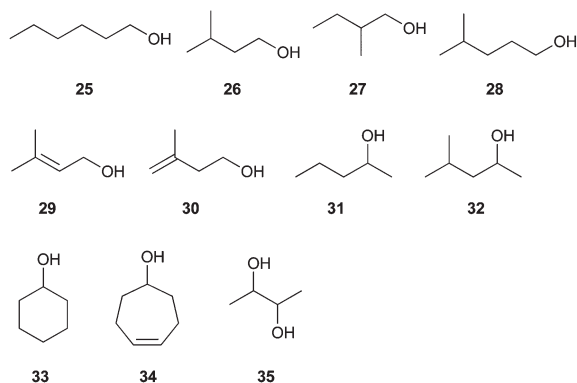
lactones, aromatic compounds, furans, nitrogen compounds, sulfur compounds, and terpenes. The volatiles from these different classes will be discussed separately.

Hydrocarbons

The identified hydrocarbons were mainly alkylated benzene derivatives that occurred in the CLSA headspace extracts of a few strains and generally in minor amounts (Scheme 2). The most widespread compound was toluene (17), showing up in five strains, followed by its partially reduced analog 1-methylcyclohexa-1,3-diene (23) that is a new bacterial metabolite and was observed in four strains. The other alkylated benzene derivatives 18–22 occurred less frequently. Particularly interesting is the detection of propylbenzene (19) in *Streptomyces cyaneofuscatus* NRRL B-2570 that was accompanied by the fully reduced analog propylcyclohexane (24) in this species. This organism released also all other hydrocarbons shown in Scheme 2, apart from 23. Both volatiles 19 and 24 have been reported before from *Chitinophaga pinensis* DSM 2588.²⁰

Alcohols

Among the alcohols the two branched compounds 3-methylbutan-1-ol (26) and 2-methylbutan-1-ol (27) that are likely derived from leucine and isoleucine, respectively, were the most widespread (Scheme 3). For some strains including *Pseudonocardia spinosipora* NRRL B-24156, *Streptomyces flavochromogenes* NRRL B-2684 and *Streptomyces mediolani* NRRL WC3934 the alcohol 26 was the principal compound. The unsaturated analogs of 26, 3-methylbut-2-en-1-ol (29) and 3-methylbut-3-en-1-ol (30), were also frequently found. These compounds may either also be derived from leucine, or by hydrolysis of the terpene precursors dimethylallyl diphosphate (DMAPP) and isopentenyl diphosphate (IPP). Hexanol (25) was emitted in trace amounts only by *P. spinosipora*, while its isomer 4-methylpentan-1-ol (28) was detected in *Streptomyces anulatus* NRRL B-2873. Secondary alcohols were represented by pentan-2-ol (31) from *Streptomyces varsoviensis* NRRL B-3589 and 4-methylpentan-2-ol (32) from *S. mediolani*. Cyclohexanol (33) occurred in *S. cyaneofuscatus* and *S. varsoviensis*. The unusual compound cyclohept-4-enol (34) that was previously reported from *Streptomyces svicensis*²⁰ was found in *Amycolatopsis nigriscens* DSM 44992 and *Streptomyces globisporus* NRRL B-2293. Finally, butan-2,3-diol (35) was released by *S. cyaneofuscatus* and *S. mediolani*. This diol is also known from various

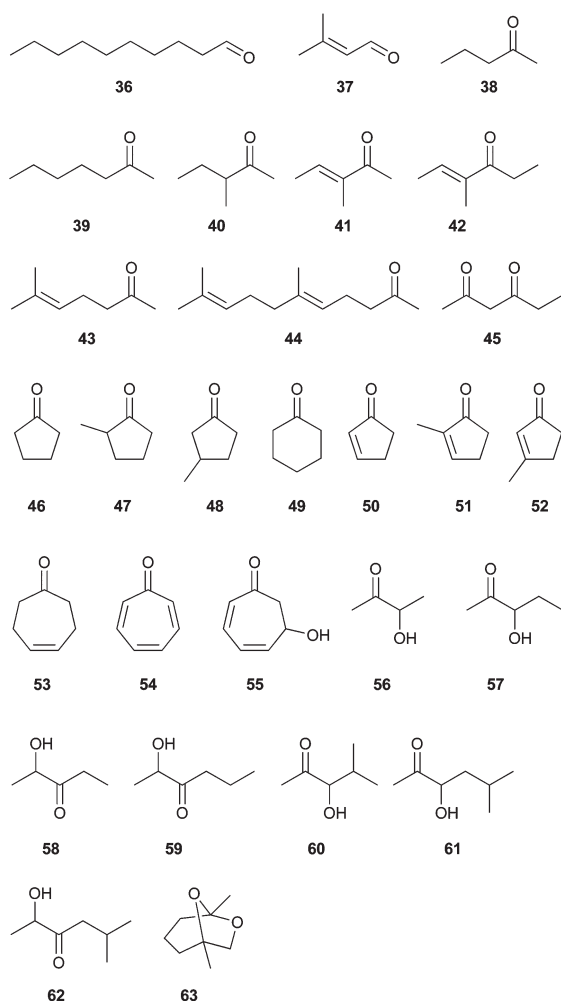


Scheme 3 Alcohols.

actinomycetes²⁰ and from *Bacillus*, where it was shown to promote growth and induce systemic resistance in *Arabidopsis thaliana*.^{23,24}

Aldehydes, ketones and ketals

Aldehydes were rarely found, with decanal (36) and prenal (37) as only representatives of this class (Scheme 4). In contrast,



Scheme 4 Aldehydes, ketones and ketals.

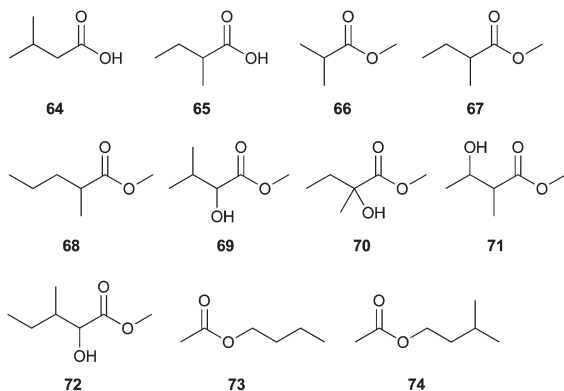
ketones ranging from unbranched to branched, saturated to unsaturated and cyclic compounds, occurred frequently and in nearly all investigated species, with the only exception of *Streptomyces rapamycinicus* NRRL 5491. The linear compounds were pentan-2-one (38) from *S. varsoviensis* and heptan-2-one (39) from *Streptomyces globisporus* NRRL B-2293. The branched ketones 3-methylpentan-2-one (40) and (*E*)-3-methylpent-3-en-2-one (41) were released by many strains, while (*E*)-4-methylhex-4-en-3-one (42) was only found in *Streptomyces afghaniensis* DSM 40228. All three compounds are likely derived from isoleucine via the coenzyme A thioester 2-methylbutyryl-SCoA. The occasionally detected volatiles 6-methylhept-5-en-2-one (43) and geranylacetone (44) may arise by oxidative degradation of terpenoids. Hexan-2,4-dione (45) was the only dione and was emitted by *Amycolatopsis alba* DSM 44262. Cyclopentanone (46) was widespread, while its alkylated and unsaturated derivatives were only found in a few strains and its higher homolog cyclohexanone (49) was only detected in *Streptomyces sclerotialis* NRRL ISP-5269. Cyclohept-4-enone (53) that corresponds to the alcohol 34 was present in many strains. Interestingly, one of these strains (*A. alba*) also produced tropone (54), while both 54 and tropone hydrate (55) were produced by *S. flavochromogenes*. Tropone was first reported as a natural product from the bacterium *Azoarcus Evansii* where it accumulated in a mutant with a blocked phenylacetate catabolon.²⁵ Tropone and its hydrate were later reported from marine bacteria of the *Roseobacter* clade^{26,27} and recently described as a biosynthetic shunt products of the antibiotic tropodithetic acid in *Phaeobacter inhibens*.²⁸

A widespread compound class in actinomycetes are hydroxy ketones including acetoin (56) and its derivatives 57–62. The parent compound itself was found in ten out of the nineteen investigated strains, while particularly the branched compounds 3-hydroxy-4-methylpentan-2-one (60), 3-hydroxy-5-methylhexan-2-one (61) and 2-hydroxy-5-methylhexan-3-one (62) were rare. The complete series of acetoin derivatives, with the exemption of 2-hydroxyhexan-3-one (59), was observed in *P. spinosipora*. As shown in investigations with the yeast *Zygosaccharomyces bisporus* and the actinomycete *Corynebacterium glutamicum* these compounds arise in thiamin diphosphate-dependent reactions from two α -oxoacids, e.g. 56 is generated from two units of pyruvic acid.^{29,30}

Surprisingly, the headspace extracts from *S. varsoviensis* contained the ketal frontalinalin (63) that is a known insect pheromone first identified from the bark beetle *Dendroctonus frontalis*.³¹ It was later also reported from many other coleoptera and even as a pheromone from elephants.³² In a previous study we have reported the production of other typical insect pheromones including conophthorin and chalcogran by streptomycetes. Together with known symbiotic relationships between streptomycetes and insects^{33–35} this raises the question, whether the true producers of insect pheromones may at least in some cases be bacteria.

Carboxylic acids and esters

Carboxylic acids and esters were only rarely emitted by the investigated actinomycetes. In fact, only the leucine and

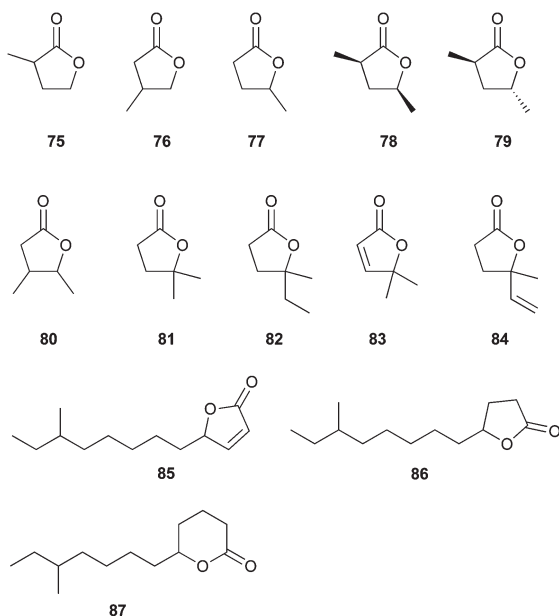


Scheme 5 Aldehydes, ketones and ketals.

isoleucine derived carboxylic acids 3-methylbutyric acid (**64**) and 2-methylbutyric acid (**65**) were found (Scheme 5). Both compounds occurred in *S. flavochromogenes*, while only **65** was present in extracts from *P. spinosipora*. A series of methyl esters and α -hydroxy methyl esters (**66–72**) was released by *Streptomyces prunicolor* NBRC 13075 with methyl 2-methylbutyrate as one of the main volatiles from this species. Methyl 3-hydroxy-2-methylbutyrate (**71**) was additionally detected in *S. varsoviensis*. The acetate esters butyl acetate (**73**) and 3-methylbutyl acetate (**74**) both occurred in only one strain, in *S. cyaneofuscatus* and in *S. globisporus*, respectively.

Lactones

As representatives of the lactones a series of alkylated butanolides (**75–82** and **84**) and the butenolide **83** was identified (Scheme 6). The most widespread compounds of this class were 3-methylbutan-4-olide (**76**), 2-methylbutan-4-olide (**75**), 4-methylpentan-4-olide (**81**) and 4-methylhexan-4-olide (**82**)

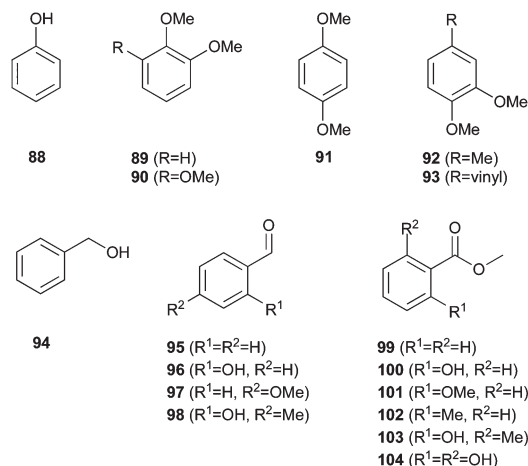


Scheme 6 Lactones.

that occurred in multiple strains. In contrast, all other lactones were found in only one particular strain, *i.e.* 4-methylhexan-4-olide (**82**) in *S. cyaneofuscatus*, *cis*- and *trans*-2-methylpentan-4-olide (**78** and **79**) in *S. rapamycinicus*, and 3-methylpentan-4-olide (**80**) and 4-methylpent-2-en-4-olide (**83**) in *S. sclerotialis*. Furthermore, three structurally related lactones with longer alkyl chains, 10-methyldodec-2-en-4-olide (**85**), 10-methyldodecan-4-olide (**86**) and 10-methyldodecan-5-olide (**87**), were present in *Streptomyces anulatus* NRRL B-2873 headspace extracts. The same lactones have been reported before from other streptomycetes,^{20,36} while the compounds **78** and **79** were recently reported from the marine bacterium *Ruegeria pomeroyi* DSS-3.³⁷ Various biological functions have been ascribed to lactones. Compounds such as the A-factor are well known as quorum sensing signals in streptomycetes.³⁸ Recent investigations showed that lactones with a high structural similarity to the compounds described here exhibit a significant seed germination inhibiting effect on plants,³⁹ or may in other cases promote seed germination.⁴⁰ Some lactones from streptomycetes may just be formed as shunt products of biosynthetic pathways to antibiotics,⁴¹ but it is also possible that their biological function has just not been uncovered so far. If the lactones from actinomycetes identified in this study have a function as signals in cell-to-cell communication, or affect other organisms in their ecological context, remains unknown.

Aromatic compounds

Among aromatic compounds 2-phenylethanol (**109**) and acetophenone (**105**) were the most widespread volatiles, followed by benzyl alcohol (**94**), benzaldehyde (**95**) and methyl benzoate (**99**, Scheme 7). Large quantities of **109** were emitted by *Allokutzneria albata* NRRL B-24461, *A. alba*, *S. afghaniensis*, and particularly by *Streptomyces fulvissimus* DSM 40593 and *S. prunicolor* where it occurred as the main compound. Phenol (**88**) was detected only in *S. flavochromogenes*, while veratrole (**89**) was a main compound of *A. nigrescens* and also found in traces in three other strains. Its isomer 1,4-dimethoxybenzene (**91**) only appeared in *S. anulatus*. A variety of aromatic compounds was present in headspace extracts from *A. alba*, including 1,2,3-trimethoxybenzene (**90**), 1,2-dimethoxy-4-methylbenzene (**92**), 3,4-dimethoxystyrene (**93**), 2-methoxybenzaldehyde (**97**), methyl salicylate (**100**), methyl 2-methoxybenzoate (**101**) and methyl 2,6-dihydroxybenzoate (**104**). Salicylaldehyde (**96**) was released by *S. prunicolor*, while 4-methylsalicylaldehyde (**98**) was produced by *P. spinosipora* and the structurally related ester methyl 6-methylsalicylate (**103**) by *Kitasatospora papulosa* NRRL B-16504. The corresponding methyl 2-methylbenzoate (**102**) was found in *Streptomyces californicus* NRRL B-3320. The free acid 6-methylsalicylic acid is one of the best studied polyketides and the fungal iterative polyketide synthase from *Penicillium patulum* is long known.⁴² Heterologous expression of its coding gene in *Streptomyces coelicolor* leads to product formation.⁴³ Furthermore, the methyl ester **103** has been reported before from the actinomycete *Saccharopolyspora erythraea*,²⁰ but a bacterial PKS for 6-methylsalicylic acid is unknown.



Scheme 7 Aromatic compounds.

In *S. erythraea* **103** may be generated as a side product of the recently characterised mellein synthase.⁴⁴

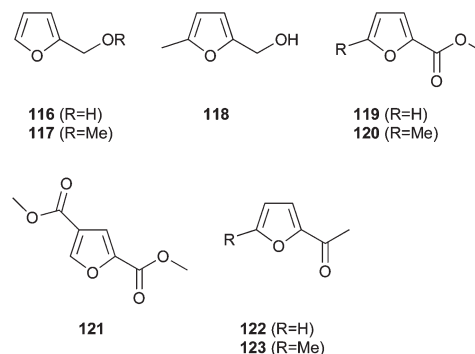
Other occasionally observed compounds included the acetophenones 2-hydroxyacetophenone (**106**), 2-methoxyacetophenone (**107**) and 2-methylacetophenone (**108**), the esters 2-phenylethyl acetate (**110**), methyl phenylacetate (**111**) and ethyl phenylacetate (**112**), and the phenylpropanoids 1-phenylpropan-2-ol (**113**), phenylacetone (**114**) and 1-phenylpropan-1,2-dione (**115**).

Furans

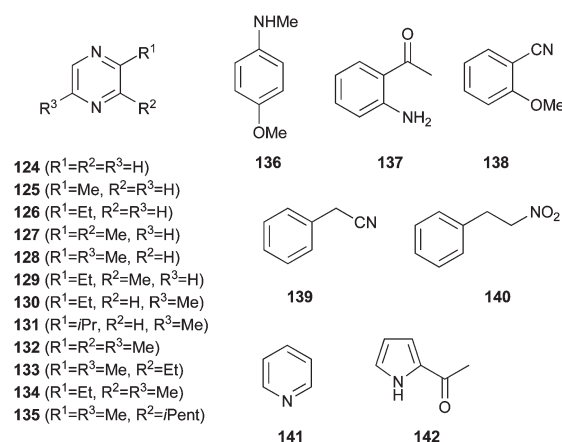
A small, but frequently from streptomycetes reported class of volatiles were furans (Scheme 8).^{20,45} The representatives 2-furan-methanol (**116**), 2-(methoxymethyl)furan (**117**), (5-methylfuran-2-yl)methanol (**118**), methyl furan-2-carboxylate (**119**) and 2-acetylfuran (**122**) were widespread, while methyl 5-methylfuran-2-carboxylate (**120**) and 2-acetyl-5-methylfuran (**123**) occurred less often, and dimethyl furan-2,4-dicarboxylate (**121**) only in *S. californicus*. It was recently reported that disruption of a gene coding for a non-ribosomal peptide synthetase (NRPS) involved in azinomycin biosynthesis resulted in the enhanced formation of **121** in *Streptomyces sahachiroi*,⁴⁶ but information about genes or enzymes for the biosynthesis of any of the volatile furans is lacking.

Nitrogen compounds

The largest class of nitrogen compounds was represented by pyrazines (**124–135**, Scheme 9). Most of these volatiles showed



Scheme 8 Furans.



Scheme 9 Nitrogen compounds.

up in many strains, while a few pyrazines were unique for a particular species, *i.e.* the parent compound **124** itself was found only in *S. sclerotialis*, 2-(1-methylethyl)-5-methylpyrazine (**131**) only in *S. mediolani*, and 2-(3-methylbutyl)-3,6-dimethylpyrazine (**135**) only in *P. spinosipora*. Gene knockout and feeding experiments with *C. glutamicum* demonstrated that pyrazines arise from acetoin and its derivatives in this species,³⁰ but an alternative pathway from amino acids is also known.⁴⁷

Phenylacetonitrile (**139**) and 2-acetylpyrrol (**142**), previously reported from a few other actinomycetes,²⁰ were also found in various strains. Other nitrogen compounds occurred less often, *e.g.* 4-methoxy-*N*-methylaniline (**136**) was only detected in *S. anulatus* and pyridine (**141**) only in *S. mediolani*. *A. alba* and *Streptomyces ochraceiscleroticus* NRRL ISP-5594 both emitted 2-aminoacetophenone (**137**), while 2-methoxybenzotrinitril (**138**) was produced by *A. albata* and *A. nigrescens*. This compound has never been reported from bacteria before and its identity was unequivocally established by comparison to a commercially available standard.

S. afghaniensis and *S. prunicolor* emitted the interesting nitrogen compound 1-nitro-2-phenylethane (**140**). For unambiguous identification **140** was synthesised according to a published procedure.⁴⁸ The synthetic material proved to be

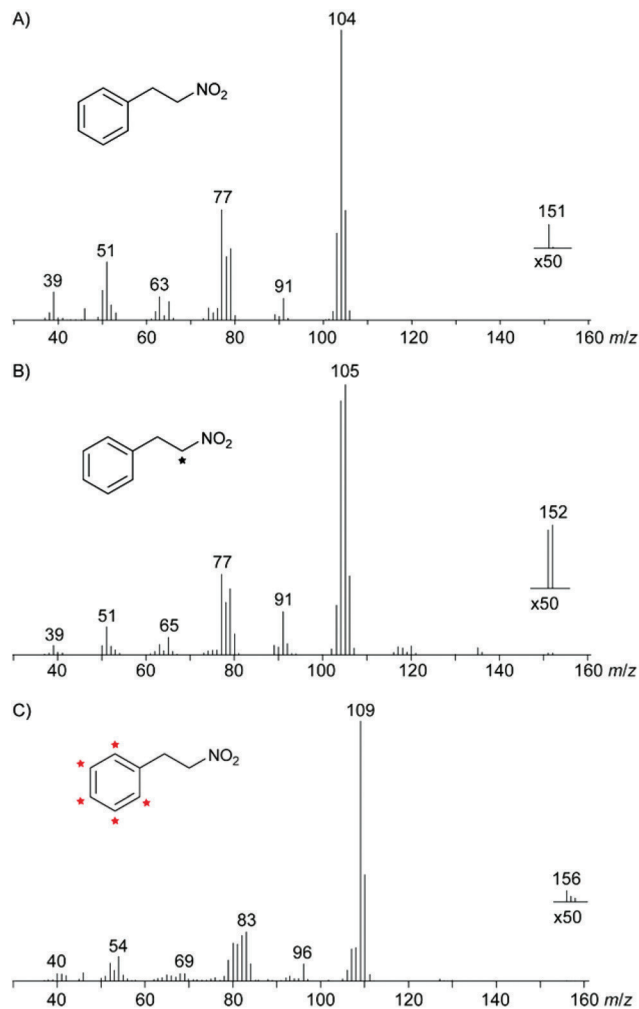
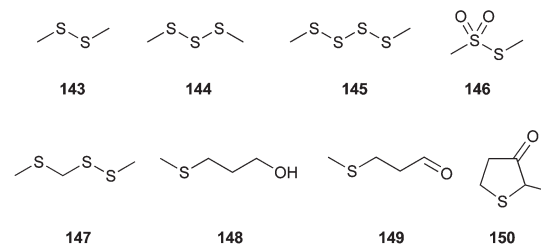


Fig. 1 Mass spectra of (A) synthetic **140**, (B) $[1-^{13}\text{C}]$ -**140** after feeding of $[2-^{13}\text{C}]$ phenylalanine, and (C) $[\text{ring-}^2\text{H}_5]$ -**140** after feeding of $[\text{ring-}^2\text{H}_5]$ phenylalanine. The black asterisk indicates a ^{13}C -labelled carbon and red asterisks indicated deuterated carbons.

identical to the natural volatile. The volatile **140** was first isolated from *Dennettia tripetala* fruits.⁴⁹ The compound is also known from several other plants such as tomato,⁵⁰ *Aniba canellilla*,⁵¹ *Parinari curatellifolia*⁵² and *Cananga odorata*,⁵³ but has never been reported from bacteria. Many interesting bioactivities have been attributed to **140** including antifungal,⁵¹ antinociceptive,⁵⁴ bradycardiac,⁵⁵ vasorelaxant,⁵⁶ antiinflammatory,⁵⁷ anticonvulsant and anxiolytic⁵⁸ effects. The biosynthesis of **140** was investigated by feeding of isotopically labelled precursors (Fig. 1). Feeding of $[2-^{13}\text{C}]$ phenylalanine to *S. prunicolor* resulted in the incorporation of isotopic labelling into **140** with *ca.* 50% incorporation rate as indicated by the molecular ion that increased from $m/z = 151$ to $m/z = 152$. Since the fragment ions representing the phenyl group (C_6H_5^+ , $m/z = 77$) and the benzyl group (C_7H_7^+ , $m/z = 91$) were not increased, the incorporation of isotopic labelling could be located at C-1 of **140**. Feeding of $[\text{ring-}^2\text{H}_5]$ phenylalanine also resulted in the incorporation of labelling into **140** with high rates (60%). The molecular ion and the base peak were observed at $m/z = 156$



Scheme 10 Sulfur compounds.

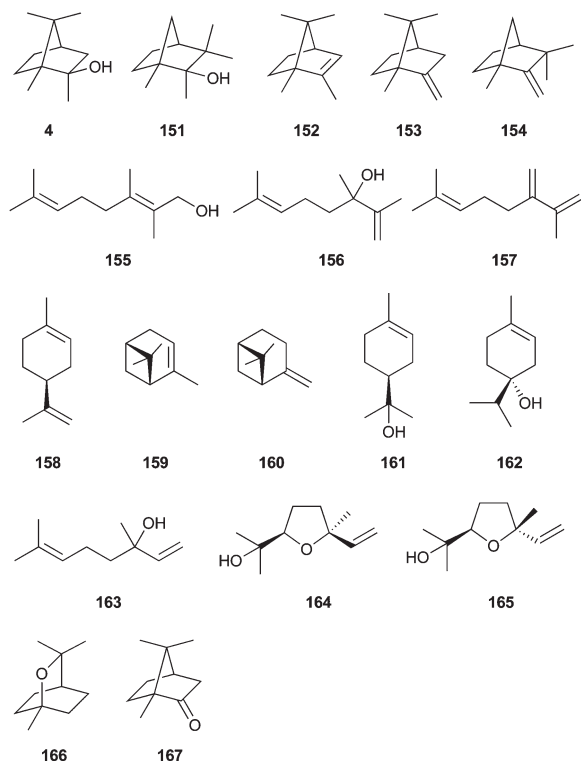
and $m/z = 109$, respectively, indicating the incorporation of all five deuterium atoms. Feeding of $[1-^{13}\text{C}]$ phenylalanine did not result in the incorporation of labelling into **140** (not shown). These experiments are in agreement with a biosynthesis of **140** from phenylalanine by decarboxylation to phenylethylamine and subsequent oxidation of the amino group.

Sulfur compounds

The sulfur volatiles dimethyl disulfide (**143**), its oxidation product *S*-methyl methanethiosulfonate (**146**), and dimethyl trisulfide (**144**) are widespread and also occur in many of the strains investigated in this study (Scheme 10). Higher polysulfides such as dimethyl tetrasulfide (**145**) are less frequent. Accordingly, this compound was only found in *A. albata* and *S. prunicolor*. Methyl methylthiomethyl disulfide (**147**) may be formed from **143** in a photochemical reaction⁵⁹ and was only detected in *A. albata*. Furthermore, the cultures of *P. spinospora* emitted 3-methylthiopropyl-1-ol (**148**), 3-methylthiopropylaldehyde (**149**) and 2-methyldihydrothiophen-3(2*H*)-one (**150**). The compound **150** was previously reported from the bacterium *Chitinophaga* Fx7914 and **149** was shown to be a biosynthetic intermediate from methionine to **150**.⁶⁰

Terpenes

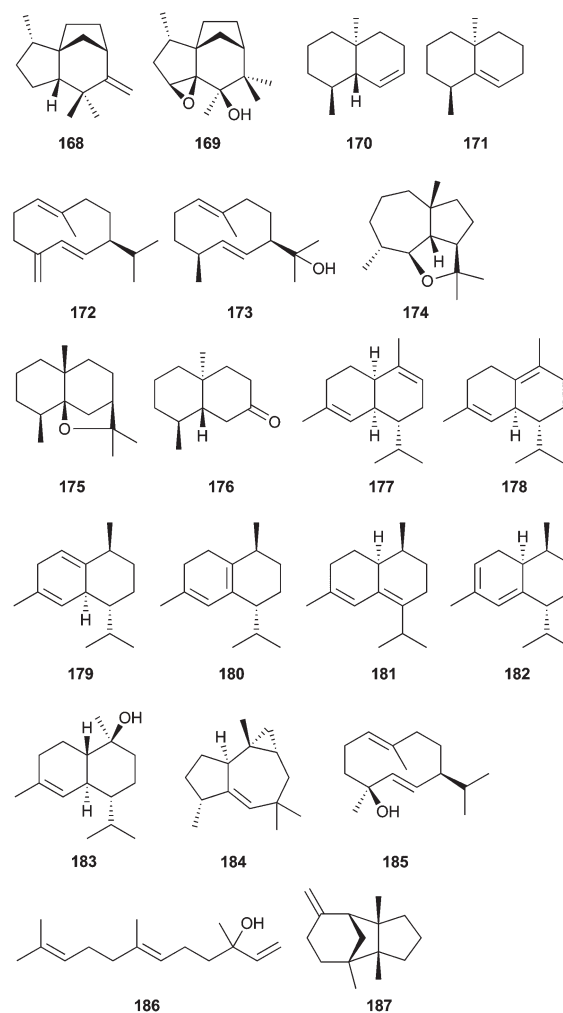
One of the best known volatiles from streptomycetes is the musty odour drinking water contaminant 2-methylisoborneol (**4**).⁶¹ Its biosynthesis proceeds by the *S*-adenosylmethionine (SAM) dependent methylation of geranyl diphosphate (GPP) and subsequent terpene cyclisation.⁶² The genes and enzymes for the biosynthesis of **4** have been extensively characterised.^{63,64} Recently, a series of additional homomonoterpenes that are made along the biosynthetic pathway to **4** has been characterised, including 2-methyl- β -fenchol (**151**), 2-methyl-2-bornene (**152**), 2-methylenebornane (**153**), 1-methylcamphene (**154**), (*E*)-2-methylgeraniol (**155**), 2-methylallinool (**156**) and 2-methylmyrcene (**157**) (Scheme 11).⁶⁵ 2-Methylisoborneol, the principal component of several of the investigated strains, and different combinations of its biosynthetic side products were detected in *A. albata*, *K. papulosa*, *S. flavochromogenes*, *S. globisporus*, *S. mediolani*, *S. ochraceiscleroticus*, *S. rapamycinicus*, *S. sclerotialis*, *S. varsoviensis* and *Streptomyces violens* NRRL B-3589. Their occurrence correlates nicely with the available genetic information, showing that genes for 2-methylisoborneol biosynthesis are encoded in the genomes of almost all of these strains (Table 1 of ESI†). Only for *K. papulosa* and



Scheme 11 Monoterpenes and homomonoterpenes.

S. mediolani a BLAST search does not show the presence of biosynthetic genes for **4**, possibly because the available genome sequence information is incomplete. Besides the homomonoterpenes a few regular monoterpenes were occasionally found, represented by limonene (**158**), α -pinene (**159**), β -pinene (**160**), α -terpineol (**161**), *p*-menth-1-en-4-ol (**162**), linalool (**163**), *cis*-linalool oxide (**164**), *trans*-linalool oxide (**165**) and 1,8-cineol (**166**). Although a monoterpene cyclase for **166** has recently been identified from *Streptomyces clavuligerus*,⁶⁶ a phylogenetic analysis of all bacterial terpene cyclase homologs (Fig. 2 of ESI†) reveals that no closely related homolog of the 1,8-cineol synthase is encoded in the strains producing **166** (*A. albata*, *S. ochraceiscleroticus*, *S. sclerotialis* and *S. varsoviensis*), suggesting that a more distantly related enzyme in these species may have the same function as the characterised terpene cyclase from *S. clavuligerus*.

The longest known sesquiterpenoid from streptomycetes is the earthy odorant geosmin (**3**, Scheme 12).⁶⁷ This widespread volatile is a sesquiterpene degradation product⁶⁸ that is frequently accompanied by its biosynthetic intermediates (8*S*,9*R*,10*S*)-8,10-dimethyl-1-octalin (**170**) and (1(10)*E*,5*E*)-germacradien-11-ol (**173**) and by the shunt products (8*S*,10*R*)-8,10-dimethyl-1(9)-octalin (**171**), germacrene D (**172**), 6,11-epoxyisodaucane (**174**) and isodihydroagarofuran (**175**).¹⁹ Within this study **3** and these biosynthetically related volatiles were detected in all strains apart from *P. spinosisporea*. The geosmin synthase is a bifunctional enzyme with two domains that was thoroughly characterised from *Streptomyces coelicolor*,⁹ and a close homolog of this enzyme was found to be encoded in all



Scheme 12 Sesquiterpenes and nor-sesquiterpenes.

geosmin producing actinomycetes, with the exception of *K. papulosa* (Table 1 of ESI†). Three organisms, *A. nigrescens*, *S. ochraceiscleroticus* and *S. violens*, even encode two geosmin synthases in their genomes. The decalone derivative **176** that was released by a few strains is also likely related to the geosmin biosynthetic pathway.⁶⁹

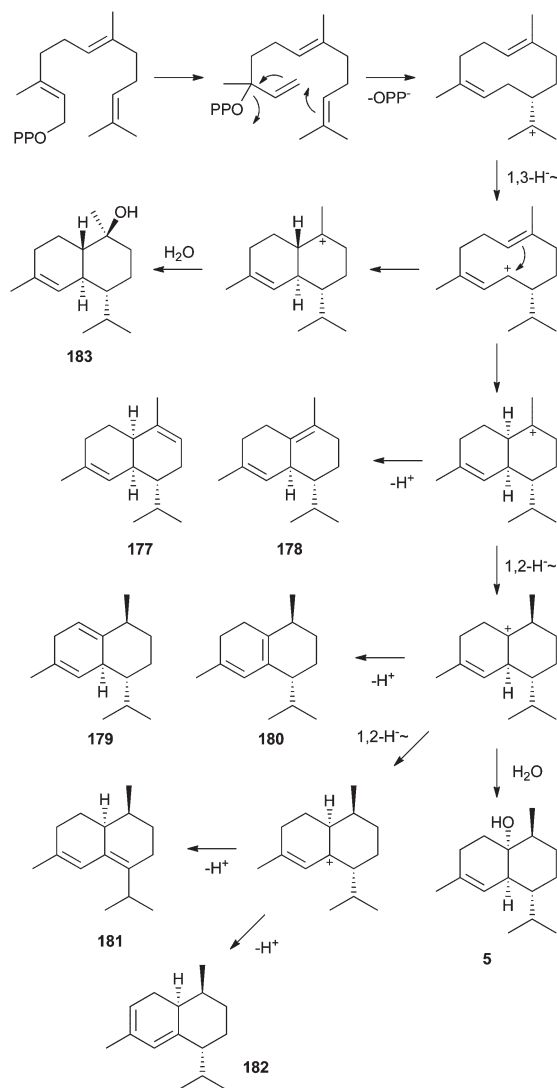
Another widespread sesquiterpene in streptomycetes is *epi*-isozizaene (**2**),^{8,19} the parent hydrocarbon of the antibiotic albaflavenone and related oxygenated products such as **169**.^{70,71} The *epi*-isozizaene synthase has been characterised from *S. coelicolor*,⁸ and homologs of this enzyme are encoded in *S. afghaniensis* and *S. prunicolor*, in agreement with the observed production of **2** and its oxidation product **169** or the shunt product *epi*-prezizaene (**168**).

As indicated by the phylogenetic tree (Fig. 2 of ESI†) the terpene cyclases for *epi*-cubenol (**5**) and caryolan-1-ol (**6**) are also very widespread among streptomycetes. These terpene cyclases have both first been characterised from *Streptomyces griseus*,^{12,13} and interestingly, in most cases both terpene cyclases co-occur in one organism. No common function *e.g.* in the biosynthesis of a secondary metabolite is known and

the two genes are usually not clustered, but the generality of the co-occurrence of the *epi*-cubenol synthase and the caryolan-1-ol synthase in streptomycetes suggests that they may be some kind of crosstalk between the two pathways. In this study genes for both enzymes were found in *S. anulatus*, *S. cyaneofuscatus*, *S. fulvissimus* and *S. mediolani*, while in *K. papulosa* only a gene for the *epi*-cubenol synthase was found and in *S. californicus* only a caryolan-1-ol synthase gene is present. Some of these terpene cyclases seemed not to be expressed under laboratory culture conditions, or the enzymes may be unfunctional, since no production of **5** was observed in *K. papulosa* and *S. mediolani*. Furthermore, neither **5** nor **6** was detected in *S. fulvissimus*, while on the other hand *S. californicus* did indeed release **5**, pointing to some missing genetic information. In all other cases the available genetic information matched the observed production of the volatiles **5** and **6**. The sesquiterpene **5** was in three strains found as principal component, and in these strong producers including *S. anulatus*, *S. californicus*, *S. cyaneofuscatus* **5** was accompanied by a few

structurally related sesquiterpenes. These compounds were α -muurolene (**177**), δ -cadinene (**178**), cadiena-1,4-diene (**179**), *trans*-cadiena-1(6),4-diene (**180**), zonarene (**181**), cadiena-3,5-diene (**182**) and α -cadinol (**183**). The formation of these compounds can be explained as side products of the *epi*-cubenol synthase (Scheme 13).

S. rapamycinicus emitted isoaffricanol (**16**) and african-1-ene (**184**). We have recently suggested the function of an unknown sesquiterpene cyclase from *Streptomyces violaceusniger* that also produces both compounds as isoaffricanol synthase.²² Although there is no direct evidence *e.g.* by incubation of farnesyl diphosphate with the purified enzyme, it is interesting to note that *S. rapamycinicus* encodes a terpene cyclase that is highly homologous to the putative isoaffricanol synthase from *S. violaceusniger*, thus further corroborating our hypothesis. The phylogenetic analysis of terpene cyclase homologs (Fig. 2 of ESI†) reveals that *S. afghaniensis* encodes an α -amorphene synthase homolog,¹⁶ and in agreement with this finding small amounts of α -amorphene (**9**) were found in the headspace extracts from this organism. Similarly, *S. prunicolor* encodes a terpene cyclase with close homology to a characterised 7-*epi*- α -eudesmol synthase,¹⁶ and production of small amounts of 7-*epi*- α -eudesmol (**10**) could also be observed. Finally, germacrene D-4-ol (**185**) was found in *S. globisporus*, nerolidol (**186**) was emitted by *P. spinospora*, and β -barbatene (**187**) occurred in *A. albata*, but the genetic background for these findings remained elusive. There are, however, in all three cases uncharacterised terpene cyclases encoded in the genomes of these organisms, and one of the respective genes will likely encode a terpene cyclase for the biosynthesis of these sesquiterpenes.



Scheme 13 Biosynthesis of *epi*-cubenol (**5**) and related sesquiterpenes.

Experimental

Strains, culture conditions, and feeding experiments

The bacterial strains *Allokutzneria albata* NRRL B-24461, *Kita-satospora papulosa* NRRL B-16504, *Pseudonocardia spinospora* NRRL B-24156, *Streptomyces anulatus* NRRL B-2873, *Streptomyces californicus* NRRL B-3320, *Streptomyces cyaneofuscatus* NRRL B-2570, *Streptomyces flavochromogenes* NRRL B-2684, *Streptomyces globisporus* NRRL B2293, *Streptomyces mediolani* NRRL WC-3934, *Streptomyces ochraceiscleroticus* NRRL ISP-5594, *Streptomyces sclerotialis* NRRL ISP-5269, *Streptomyces varsoviensis* NRRL B-3589 and *Streptomyces violens* NRRL ISP-5597 were obtained from the US department of agriculture (USDA ARS, Peoria, USA), the strains *Streptomyces afghanaensis* DSM 40228, *Streptomyces fulvissimus* DSM 40593, *Streptomyces prunicolor* DSM 40335, *Streptomyces rapamycinicus* DSM 41530, *Amycolatopsis alba* DSM 44262 and *Amycolatopsis nigrescens* DSM 44992 were obtained from the Deutsche Sammlung für Mikroorganismen und Zelllinien (DSMZ, Braunschweig, Germany). Bacterial strains were pre-cultured at 28 °C in liquid medium (generally medium 65, only *P. spinospora* was grown in medium 553 and *K. papulosa* in medium 547). After three days of growth 1 mL of the liquid culture was transferred onto

an agar plate containing the same medium. Incubation on solid medium was continued until sporulation occurred (usually ~7 days), then the volatiles were analysed by the CLSA method. The feeding experiments were performed by the addition of a sterile filtered aqueous solution of isotopically labelled precursors to a final concentration of 1 mmol L⁻¹. The following growth media were used as recommended by the DSMZ:⁷²

65. Glucose (4.0 g), yeast extract (4.0 g), malt extract (4.0 g), CaCO₃ (2.0 g), agar (12.0 g), H₂O (1000 mL), pH = 7.2. CaCO₃ and agar were deleted, when liquid medium was used.

553. Glucose (10.0 g), peptone from casein (5.0 g), yeast extract (5.0 g), beef extract (5.0 g), CaCl₂·2H₂O (0.74 g), agar (15.0 g), H₂O (1000 mL), pH = 7.2.

547. Solution A: soluble starch (10.0 g), H₂O (500 mL); solution B: CaCO₃ (2.0 g), K₂HPO₄ (1.0 g), MgSO₄·7H₂O (1.0 g), NaCl (1.0 g), (NH₄)₂SO₄ (2.0 g), H₂O (500 mL), trace salt solution: FeSO₄ (0.1 g), MnCl₂·4H₂O (0.1 g), ZnSO₄·7H₂O (0.1 g), H₂O (100 mL), pH = 7.0–7.4. Solutions A and B were mixed, trace salt solution (1 mL) and agar (20.0 g) were added before sterilisation.

Collection of volatiles

The volatiles from the agar plate cultures were collected by use of the closed-loop stripping analysis technique (CLSA). In a closed vessel an air stream was pumped over the agar plate and the emitted volatiles were trapped on charcoal filters (Chromtech GmbH, Idstein, Precision Char Coal Filter 5 mg). After 24 h the filter was eluted with ~50 µL dichloromethane and the extract was immediately analysed by GC/MS.

GC/MS

GC-MS analyses were carried out on an Agilent 7890B connected with an Agilent 5977A inert mass detector fitted with a HP-5 fused silica capillary column (30 m, 0.25 mm i.d., 0.25 µm film, Agilent). GC conditions were as follows: inlet pressure 77.1 kPa, He 23.3 mL min⁻¹, injection volume 1.5 µL, transfer line 300 °C, electron energy 70 eV. The operation mode was splitless (60 s valve time) and the carrier gas was He at 1.2 mL min⁻¹. The GC was programmed as follows: 5 min at 50 °C increasing with 5 °C min⁻¹ to 320 °C. Retention indices were calculated from retention times of a mixture of *n*-alkane standards (C₆–C₃₂).

Conclusions

In summary, we have investigated the volatiles released by nineteen genome sequenced actinomycetes. Many of the identified compounds have been reported from actinomycetes or other bacteria before,^{19–21,45,73,74} while the compounds 1-methylcyclohexa-1,3-diene (**23**), frontalin (**63**), 2-methoxybenzonitril (**138**) and 1-nitro-2-phenylethane (**140**) are new bacterial secondary metabolites and 4-methoxy-*N*-methylaniline (**136**) is a new natural product. In the present study we have shown in feeding experiments with isotopically labelled pre-

cursors that **140** is derived from phenylalanine by decarboxylation to 2-phenylethylamine and oxidation. Particularly interesting is the discovery of the insect pheromone frontalin from bacteria that is in line with our previous report about the bacterial production of other typical insect pheromones such as conophthorin and chalcogran.²⁰ Together with the known symbiotic relationship between insects and streptomycetes this suggests that insect pheromones may in some cases have a bacterial origin. Alternatively, this finding may point to a horizontal gene transfer event between insects and their symbiotic bacterial community. Finally, we have shown that all investigated actinomycetes encode several terpene cyclases in their genomes. Their phylogenetic analysis was in line with the production of terpenes, *i.e.* the production of geosmin, 2-methylisoborneol, *epi*-cubanol, caryolan-1-ol, *epi*-isozizaene, 7-*epi*- α -eudesmol and α -amorphene, for which highly homologous terpene cyclases from streptomycetes have been characterised, could be nicely correlated to the genomic information. Based on the finding that *S. violaceusniger* produces isoafrikanol and only one sesquiterpene cyclase of unknown function is encoded in this organism, we have recently suggested that this terpene cyclase is likely active as isoafrikanol synthase. This suggestion is now corroborated by the identification of isoafrikanol in *S. rapamycinicus* that encodes a closely related terpene cyclase in its genome. There are, however, several uncharacterised terpene cyclases with unknown products encoded in the genomes of the actinomycetes investigated in this study, and several of these do not seem to be expressed under laboratory conditions. We will address this question by heterologous expression of the respective terpene cyclase genes in our future experiments.

Acknowledgements

We thank the US Department of Agriculture for various strains of actinomycetes. This work was funded by the Deutsche Forschungsgemeinschaft DFG by the grant DI1536/2-1 (“Duftstoffe aus Actinomyceten”).

Notes and references

- R. D. Fleischmann, M. D. Adams, O. White, R. A. Clayton, E. F. Kirkness, A. R. Kerlavage, C. J. Bult, J.-F. Tomb, B. A. Dougherty, J. M. Merrick, K. McKenney, G. Sutton, W. FitzHugh, C. Fields, J. D. Gocayne, J. Scott, R. Shirley, L. Liu, A. Glodek, J. M. Kelley, J. F. Weidman, C. A. Phillips, T. Spriggs, E. Hedblom, M. D. Cotton, T. R. Utterback, M. C. Hanna, D. T. Nguyen, D. M. Saudek, R. C. Brandon, L. D. Fine, J. L. Fritchman, J. L. Fuhrmann, N. S. M. Geoghagen, C. L. Gnehm, L. A. McDonald, K. V. Small, C. M. Fraser, H. O. Smith and J. Craig Venter, *Science*, 1995, **269**, 496.
- S. F. Altschul, W. Gish, W. Miller, E. W. Myers and D. J. Lipman, *J. Mol. Biol.*, 1990, **215**, 403.

- 3 S. E. Ongley, X. Bian, B. A. Neilan and R. Müller, *Nat. Prod. Rep.*, 2013, **30**, 1121.
- 4 B. Aigle, S. Lautru, D. Spiteller, J. S. Dickschat, G. L. Challis, P. Leblond and J.-L. Pernodet, *J. Ind. Microbiol. Biotechnol.*, 2014, **41**, 251.
- 5 K. J. Weissman and R. Müller, *Nat. Prod. Rep.*, 2010, **27**, 1276.
- 6 J.-C. Kehr, D. Gatte Picchi and E. Dittmann, *Beilstein J. Org. Chem.*, 2011, **7**, 1622.
- 7 D. E. Cane, J.-K. Sohng, C. R. Lamberson, S. M. Rudnicki, Z. Wu, M. D. Lloyd, J. S. Oliver and B. R. Hubbard, *Biochemistry*, 1994, **33**, 5846.
- 8 X. Lin, R. Hopson and D. E. Cane, *J. Am. Chem. Soc.*, 2006, **128**, 6022.
- 9 J. Jiang, X. He and D. E. Cane, *Nat. Chem. Biol.*, 2007, **3**, 711.
- 10 M. Komatsu, M. Tsuda, S. Omura, H. Oikawa and H. Ikeda, *Proc. Natl. Acad. Sci. U. S. A.*, 2008, **105**, 7422.
- 11 C.-M. Wang and D. E. Cane, *J. Am. Chem. Soc.*, 2008, **130**, 8908.
- 12 C. Nakano, T. Tezuka, S. Horinouchi and Y. Ohnishi, *J. Antibiot.*, 2012, **65**, 551.
- 13 C. Nakano, S. Horinouchi and Y. Ohnishi, *J. Biol. Chem.*, 2011, **286**, 27980.
- 14 J. S. Dickschat, *Nat. Prod. Rep.*, 2014, **31**, 838.
- 15 J. S. Dickschat, K. A. K. Pahirulzaman, P. Rabe and T. A. Klapschinski, *ChemBioChem*, 2014, **15**, 810.
- 16 P. Rabe and J. S. Dickschat, *Angew. Chem., Int. Ed.*, 2013, **52**, 1810.
- 17 P. Baer, P. Rabe, C. A. Citron, C. C. de Oliveira Mann, N. Kaufmann, M. Groll and J. S. Dickschat, *ChemBioChem*, 2014, **15**, 213.
- 18 P. Baer, P. Rabe, K. Fischer, C. A. Citron, T. A. Klapschinski, M. Groll and J. S. Dickschat, *Angew. Chem., Int. Ed.*, 2014, **53**, 7652.
- 19 C. A. Citron, J. Gleitzmann, G. Laurenzano, R. Pukall and J. S. Dickschat, *ChemBioChem*, 2012, **13**, 202.
- 20 C. A. Citron, P. Rabe and J. S. Dickschat, *J. Nat. Prod.*, 2012, **75**, 1765.
- 21 P. Rabe, C. A. Citron and J. S. Dickschat, *ChemBioChem*, 2013, **14**, 2345.
- 22 R. Riclea, C. A. Citron, J. Rinkel and J. S. Dickschat, *Chem. Commun.*, 2014, **50**, 4228.
- 23 C.-M. Ryu, M. A. Farag, C.-H. Hu, M. S. Reddy, J. W. Kloepper and P. W. Paré, *Plant Physiol.*, 2004, **134**, 1017.
- 24 C.-M. Ryu, M. A. Farag, C.-H. Hu, M. S. Reddy, H.-X. Wei, P. W. Paré and J. W. Kloepper, *Proc. Natl. Acad. Sci. U. S. A.*, 2003, **100**, 4927.
- 25 R. Rost, S. Haas, E. Hammer, H. Herrmann and G. Burchhardt, *Mol. Genet. Genomics*, 2002, **267**, 656.
- 26 J. S. Dickschat, I. Wagner-Döbler and S. Schulz, *J. Chem. Ecol.*, 2005, **31**, 925.
- 27 V. Thiel, T. Brinkhoff, J. S. Dickschat, S. Wickel, J. Grunenberg, I. Wagner-Döbler, M. Simon and S. Schulz, *Org. Biomol. Chem.*, 2010, **8**, 234.
- 28 N. L. Brock, A. Nikolay and J. S. Dickschat, *Chem. Commun.*, 2014, **50**, 5487.
- 29 F. Neuser, H. Zorn and R. G. Berger, *Z. Naturforsch., C: Biosci.*, 2000, **55**, 560.
- 30 J. S. Dickschat, S. Wickel, C. J. Bolten, T. Nawrath, S. Schulz and C. Wittmann, *Eur. J. Org. Chem.*, 2010, 2687.
- 31 G. W. Kinzer, A. F. Fentiman, T. F. Page, R. L. Foltz, J. P. Vité and G. B. Pitman, *Nature*, 1969, **221**, 477.
- 32 D. R. Greenwood, D. Comeskey, M. B. Hunt and L. E. L. Rasmussen, *Nature*, 2005, **438**, 1097.
- 33 S. Haeder, R. Wirth, H. Herz and D. Spiteller, *Proc. Natl. Acad. Sci. U. S. A.*, 2009, **106**, 4742.
- 34 D.-C. Oh, M. Poulsen, C. M. Currie and J. Clardy, *Nat. Chem. Biol.*, 2009, **5**, 391.
- 35 J. M. Crawford and J. Clardy, *Chem. Commun.*, 2011, **47**, 7559.
- 36 J. S. Dickschat, T. Martens, T. Brinkhoff, M. Simon and S. Schulz, *Chem. Biodiversity*, 2005, **2**, 837.
- 37 R. Riclea, J. Gleitzmann, H. Bruns, C. Junker, B. Schulz and J. S. Dickschat, *Beilstein J. Org. Chem.*, 2012, **8**, 941.
- 38 A. S. Khokhlov, I. I. Tovarova, L. N. Borisova, S. A. Pliner, L. N. Shevchenko, E. Y. Kornitzkaya, N. S. Ivkina and I. A. Rapoport, *Dokl. Akad. Nauk SSSR*, 1967, **177**, 232.
- 39 C. A. Citron, C. Junker, B. Schulz and J. S. Dickschat, *Angew. Chem., Int. Ed.*, 2014, **53**, 4346.
- 40 A. Mandabi, H. Ganin, P. Krief, J. Rayo and M. M. Meijler, *Chem. Commun.*, 2014, **50**, 5322.
- 41 R. Riclea, B. Aigle, P. Leblond, I. Schoenian, D. Spiteller and J. S. Dickschat, *ChemBioChem*, 2012, **13**, 1635.
- 42 P. Dimroth, H. Walter and F. Lynen, *Eur. J. Biochem.*, 1970, **13**, 98.
- 43 D. J. Bedford, E. Schweizer, D. A. Hopwood and C. Khosla, *J. Bacteriol.*, 1995, **177**, 4544.
- 44 H. Sun, C. L. Ho, F. Ding, I. Soehano, X.-W. Liu and Z.-X. Liang, *J. Am. Chem. Soc.*, 2012, **134**, 11924.
- 45 K. Wilkins and C. Schöller, *Actinomycetologica*, 2009, **23**, 27.
- 46 D. Simkhada, H. Zhang, S. Mori, H. Williams and C. M. H. Watanabe, *Beilstein J. Org. Chem.*, 2013, **9**, 1768.
- 47 T. Nawrath, J. S. Dickschat, B. Kunze and S. Schulz, *Chem. Biodiversity*, 2010, **7**, 2129.
- 48 Y.-M. Shao, W.-B. Yang, T.-H. Kuo, K.-C. Tsai, C.-H. Lin, A.-S. Yang, P.-H. Liang and C.-H. Wong, *Bioorg. Med. Chem.*, 2008, **16**, 4652.
- 49 J. I. Okogun and D. E. U. Ekong, *Chem. Ind.*, 1969, **36**, 1272.
- 50 R. G. Buttery, R. Teranishi, R. A. Flath and L. C. Ling, *ACS Symp. Ser.*, 1989, **388**, 213.
- 51 J.-M. Oger, P. Richomme, H. Guinaudeau, J. P. Bouchara and A. Fournet, *J. Essent. Oil Res.*, 1994, **6**, 493.
- 52 D. Joulain, A. Casazza, R. Laurent, D. Portier, N. Guillaumon, R. Pandya, M. Le and A. Viljoen, *J. Agric. Food Chem.*, 2004, **52**, 2322.
- 53 C. Benini, M. Ringuet, J.-P. Wathelet, G. Lognay, P. du Jardin and M.-L. Fauconnier, *Flavour Fragrance J.*, 2012, **27**, 356.
- 54 A. B. de Lima, M. B. Santana, A. S. Cardoso, J. K. R. da Silva, J. G. S. Maia, J. C. T. Carvalho and P. J. C. Sousa, *Phytomedicine*, 2009, **16**, 555.

- 55 R. J. Bezerra de Siqueira, F. I. Bulcão Macedo, L. de Fátima Leal Interaminense, G. Pinto Duarte, P. J. Caldas Magalhães, T. Silva Brito, J. K. R. da Silva, J. G. S. Maia, P. J. C. Sousa, J. H. Leal-Cardoso and S. Lahlou, *Eur. J. Pharmacol.*, 2010, **638**, 90.
- 56 L. de Fátima Leal Interaminense, F. E. dos Ramos-Alves, R. J. Bezerra de Siqueira, F. E. Xavier, G. Pinto Duarte, P. J. Caldas Magalhães, J. G. S. Maia, P. J. C. Sousa and S. Lahlou, *Eur. J. Pharm. Sci.*, 2013, **48**, 709.
- 57 J. K. L. Vale, A. B. Lima, B. G. Pinheiro, A. S. Cardoso, J. K. R. Silva, J. G. S. Maia, G. E. P. de Sousa, A. B. F. da Silva, P. J. C. Sousa and R. S. Borges, *Planta Med.*, 2013, **79**, 628.
- 58 I. A. Oyemitan, C. A. Elusiyan, M. A. Akanmu and T. A. Olugbade, *Phytomedicine*, 2013, **20**, 1315.
- 59 R. G. Buttery and R. M. Seifert, *J. Agric. Food Chem.*, 1977, **25**, 434.
- 60 T. Nawrath, K. Gerth, R. Müller and S. Schulz, *ChemBioChem*, 2010, **11**, 1914.
- 61 L. L. Medsker, D. Jenkins, J. F. Thomas and C. Koch, *Environ. Sci. Technol.*, 1969, **3**, 476.
- 62 J. S. Dickschat, T. Nawrath, V. Thiel, B. Kunze, R. Müller and S. Schulz, *Angew. Chem., Int. Ed.*, 2007, **46**, 8287.
- 63 M. Komatsu, M. Tsuda, S. Omura, H. Oikawa and H. Ikeda, *Proc. Natl. Acad. Sci. U. S. A.*, 2008, **105**, 7422.
- 64 C.-M. Wang and D. E. Cane, *J. Am. Chem. Soc.*, 2008, **130**, 8908.
- 65 N. L. Brock, S. R. Ravella, S. Schulz and J. S. Dickschat, *Angew. Chem., Int. Ed.*, 2013, **52**, 2100.
- 66 C. Nakano, H.-K. Kim and Y. Ohnishi, *ChemBioChem*, 2011, **12**, 1988.
- 67 N. N. Gerber and H. A. Lechevalier, *Appl. Microbiol.*, 1965, **13**, 935.
- 68 J. S. Dickschat, H. B. Bode, T. Mahmud, R. Müller and S. Schulz, *J. Org. Chem.*, 2005, **70**, 5174.
- 69 S. Schulz, J. Fuhlendorff and H. Reichenbach, *Tetrahedron*, 2004, **60**, 3863.
- 70 B. Zhao, X. Lin, L. Lei, D. C. Lamb, S. L. Kelly, M. R. Waterman and D. E. Cane, *J. Biol. Chem.*, 2008, **283**, 8183.
- 71 S. Takamatsu, X. Lin, A. Nara, M. Komatsu, D. E. Cane and H. Ikeda, *Microbiol. Biotechnol.*, 2011, **4**, 184.
- 72 <http://www.dsmz.de/catalogues/catalogue-microorganisms/culture-technology/list-of-media-for-microorganisms.html>.
- 73 S. Schulz and J. S. Dickschat, *Nat. Prod. Rep.*, 2007, **24**, 814.
- 74 C. E. G. Schöller, H. Gürtler, R. Pedersen, S. Molin and K. Wilkins, *J. Agric. Food Chem.*, 2002, **50**, 2615.

Supporting Information for

Volatiles from Nineteen Recently Genome Sequenced Actinomycetes

Christian A. Citron,^a Lena Barra,^a Joachim Wink^b and Jeroen S. Dickschat*^a

^a Kekulé-Institut für Organische Chemie und Biochemie, Universität Bonn, Gerhard-Domagk-Straße 1, 53121 Bonn, Germany. Email: dickschat@uni-bonn.de; Tel: +49 228 735797.

^b Helmholtz-Zentrum für Infektionsforschung GmbH, Inhoffenstraße 7, 38124 Braunschweig, Germany.

Table 1 Investigated strains and terpene cyclases encoded in their genomes.

ID	Strain	Terpene cyclases
1	<i>Allokutzneria albata</i> NRRL B-24461	geosmin: WP_030430635 2-MIB: WP_030428809 unknown: WP_030426588 unknown: WP_030428809 unknown: WP_030430753 unknown: WP_030431358 unknown: WP_030432512 unknown: WP_030432932
2	<i>Amycolatopsis alba</i> DSM 44262	geosmin: WP_020631965 unknown: WP_020635617
3	<i>Amycolatopsis nigrescens</i> DSM 44992	geosmin: WP_020666924 geosmin: WP_020667245 unknown: WP_026359996
4	<i>Kitasatospora papulosa</i> NRRL B-16504	<i>epi</i> -cubenol: WP_030124319
5	<i>Pseudonocardia spinosipora</i> NRRL B-24156	unknown: WP_028934612 unknown: WP_028934660 unknown: WP_028934903
6	<i>Streptomyces afghaniensis</i> DSM 40228	geosmin: WP_020273180 α -amorphene: WP_020270655 <i>epi</i> -isozizaene: WP_020274234
7	<i>Streptomyces anulatus</i> NRRL B-2873	geosmin: WP_030593937 <i>epi</i> -cubenol: WP_030584158 caryolan-1-ol: WP_030581148
8	<i>Streptomyces californicus</i> NRRL B-3320	geosmin: WP_030116958/59 caryolan-1-ol: WP_030122040
9	<i>Streptomyces cyaneofuscatus</i> NRRL B-2570	geosmin: WP_030566077 <i>epi</i> -cubenol: WP_030573033 caryolan-1-ol: WP_030568864
10	<i>Streptomyces flavochromogenes</i> NRRL B-2684	geosmin: WP_030314776 2-MIB: WP_030312939 unknown: WP_030314165 unknown: WP_030319486
11	<i>Streptomyces fulvissimus</i> DSM 40593	geosmin: YP_007929188 <i>epi</i> -cubenol: YP_007929843 caryolan-1-ol: YP_007934038
12	<i>Streptomyces globisporus</i> NRRL B-2293	geosmin: WP_030688988 2-MIB: WP_030693045 unknown: WP_030690542 unknown: WP_030691789
13	<i>Streptomyces mediolani</i> NRRL WC3934	geosmin: WP_030809459 <i>epi</i> -cubenol: WP_030800135 caryolan-1-ol: WP_030811225

14	<i>Streptomyces ochraceiscleroticus</i> NRRL ISP-5594	geosmin: WP_031055842 geosmin: WP_031060696 2-MIB: WP_031053300 unknown: WP_031051181 unknown: WP_031064163 unknown: WP_031067610
15	<i>Streptomyces prunicolor</i> NBRC 13075	geosmin: WP_019062772 <i>epi</i> -isozizaene: WP_026150642 7- <i>epi</i> - α -eudesmol: WP_019057753 unknown: WP_019064917
16	<i>Streptomyces rapamycinicus</i> NRRL 5491	geosmin: WP_020870145 2-MIB: WP_020873136 isoafricanol: YP_008795010
17	<i>Streptomyces sclerotialis</i> NRRL ISP-5269	geosmin: WP_030613120 2-MIB: WP_030607882 unknown: WP_030624126 unknown: WP_030615021 unknown: WP_030617047
18	<i>Streptomyces varsoviensis</i> NRRL B-3589	geosmin: WP_030881645 2-MIB: WP_030891873 unknown: WP_030874469 unknown: WP_030877649
19	<i>Streptomyces violens</i> NRRL ISP-5597	geosmin: WP_030252760 geosmin: WP_030266576 2-MIB: WP_030263590 unknown: WP_030249874 unknown: WP_030250690 unknown: WP_030261827

Table 2 Identified volatile compounds and their occurrence in the investigated strains.

Compound ^a	<i>P</i>	<i>I</i> (Lit.) ^c	Ident. ^d	occurrence in strain ^e
pentan-2-one (38)	692	682 ¹	ms, ri, std	18
methyl 2-methylpropionate (66)	693	690 ⁷	ms, ri, std	15
pentan-2-ol (31)	698	689 ¹	ms, ri, std	18
acetoin (56)	706	709 ⁹	ms, ri, std	1, 4, 5, 7, 8, 9, 10, 12, 13, 15
3-methylbut-3-en-1-ol (30)	722	720 ¹¹	ms, ri, std	1, 4, 7, 8, 9, 12, 13, 15, 18, 19
3-methylbutan-1-ol (26)	724	733 ⁷	ms, ri, std	1, 4, 5, 7, 8, 9, 10, 12, 13, 15, 18, 19
pyrazine (124)	726	734 ⁹	ms, ri, std	17
2-methylbutan-1-ol (27)	728	733 ⁷	ms, ri, std	1, 4, 5, 7, 8, 9, 10, 12, 13, 18, 19
pyridine (141)	733	736 ¹⁵	ms, ri, std	13
dimethyl disulfide (143)	739	747 ⁹	ms, ri, std	1, 4, 7, 8, 10, 12, 14, 15, 17
3-methylpentan-2-one (40)	743	750 ¹²	ms, ri	9, 12, 13, 15, 17, 18, 19
3-methylpentan-2-ol (32)	747	745 ¹	ms, ri	13
toluene (17)	759	756 ¹¹	ms, ri, std	2, 9, 13, 17, 18
3-methylbut-2-en-1-ol (29)	766	770 ¹¹	ms, ri, std	1, 2, 5, 12, 13
butan-2,3-diol (35)	769	779 ¹⁶	ms, ri, std	9, 13
methyl 2-methylbutyrate (67)	772	780 ⁸	ms, ri, std	15
1-methylcyclohexa-1,3-diene (23)	773	771 ²¹	ms, ri	1, 8, 14, 17
3-methylbut-2-enal (37)	779	781 ¹⁸	ms, ri, std	1
cyclopentanone (46)	786	791 ¹⁹	ms, ri, std	1, 3, 7, 9, 12, 13, 15, 17, 18, 19
3-hydroxypentan-2-one (57)	800	800 ⁴	ms, ri, std	1, 2, 5, 7, 9, 10, 12, 13, 15
2-hydroxypentan-3-one (58)	807	810 ³⁷	ms, ri, std	1, 2, 5, 7, 9, 10, 12, 13, 15
butyl acetate (73)	814	807 ¹	ms, ri, std	9
methylpyrazine (125)	820	819 ¹	ms, ri, std	1, 2, 3, 5, 7, 8, 9, 10, 12, 13, 14, 15, 17, 18, 19
2-(methoxymethyl)furan (117)	829	823 ³⁸	ms, ri	4, 5, 8, 12, 13, 15, 17, 18
cyclopent-2-enone (50)	831	835 ²⁰	ms, ri, std	7, 9, 13
3-methylbutyric acid (64)	833	827 ¹	ms, ri, std	10
4-methylpentan-1-ol (28)	834	830 ¹	ms, ri, std	7
(<i>E</i>)-3-methylpent-3-en-2-one (41)	838	838 ³⁹	ms, ri	13, 17, 18
2-methylcyclopentanone (47)	838	836 ¹	ms, ri, std	7, 19
3-methylcyclopentanone (48)	845	848 ¹²	ms, ri	9, 17
2-methylbutyric acid (65)	845	846 ⁸	ms, ri, std	5, 10

3-hydroxy-4-methylpentan-2-one (60)	848	849 ³⁷	ms, ri	5, 9
methyl 2-hydroxy-2-methylbutyrate (70)	850	849 ³⁷	ms, ri, std	15
2-furanmethanol (116)	852	850 ²²	ms, ri, std	1, 2, 4, 5, 6, 9, 10, 11, 12, 15
ethylbenzene (18)	860	858 ²	ms, ri, std	9, 18
hexan-1-ol (25)	868	863 ¹	ms, ri, std	5
<i>m</i> -xylene (20)	868	866 ²	ms, ri, std	9, 18
methyl 2-methylvalerate (68)	870	871 ¹	ms, ri, std	15
3-methylbutyl acetate (74)	877	869 ¹	ms, ri	12
cyclohexanol (33)	882	886 ⁸	ms, ri, std	9, 18
hexan-2,4-dione (45)	888	880 ²⁷	ms, ri	2
heptan-2-one (39)	889	891 ¹	ms, ri, std	12
methyl 2-hydroxy-3-methylbutyrate (69)	892	889 ²⁶	ms, ri, std	15
cyclohexanone (49)	893	895 ⁸	ms, ri, std	17
2-hydroxyhexan-3-one (59)	901	900 ⁴	ms, ri, std	11, 15
2-methylcyclopent-2-enone (51)	904	905 ²⁷	ms, ri, std	7, 19
3-methylthiopropional (149)	905	901 ¹	ms, ri, std	5
2,5-dimethylpyrazine (128)	907	908 ¹	ms, ri, std	1, 2, 3, 5, 6, 7, 8, 9, 10, 11, 12, 13, 14, 15, 16, 17, 18, 19
2-acetylfuran (122)	909	909 ¹	ms, ri, std	1, 3, 4, 6, 7, 8, 9, 10, 12, 13, 15, 18, 19
ethylpyrazine (126)	913	912 ¹	ms, ri, std	5, 9, 13, 15, 19
2,3-dimethylpyrazine (127)	917	915 ¹	ms, ri, std	5, 7, 8, 9, 13, 14, 15, 19
methyl 3-hydroxy-2-methylbutyrate (71)	925	930 ²⁴	ms, ri	15, 18
propylcyclohexane (24)	929	928 ²⁹	ms, ri, std	9
α -pinene (159)	933	932 ¹	ms, ri, std	1, 2, 9, 14, 17, 18, 19
frontalin (63)	941	949 ²³	ms, ri	18
(<i>E</i>)-4-methylhex-4-en-3-one (42)	941	934 ³⁹	ms, ri	6
2-hydroxy-5-methylhexan-3-one (62)	943	944 ³⁷	ms, ri	5
3-hydroxy-5-methylhexan-2-one (61)	948	949 ³⁷	ms, ri	5
2-methylbutan-4-olide (75)	950	954 ⁶	ms, ri, std	2, 9, 16, 17, 18
pentan-4-olide (77)	951	941 ¹	ms, ri	9
(5-methylfuran-2-yl)methanol (118)	953	953 ²⁵	ms, ri	1, 6, 10, 12, 13
4-methylpent-2-en-4-olide (83)	953	953 ⁴²	ms, ri, std	17
propylbenzene (19)	953	954 ²	ms, ri, std	9
3-methylbutan-4-olide (76)	956	958 ³⁷	ms, ri	1, 9, 12, 13, 15, 16, 17, 18, 19
benzaldehyde (95)	959	952 ¹	ms, ri, std	1, 2, 3, 5, 9, 13, 15
3-methylcyclopent-2-enone (52)	965	973 ²⁸	ms, ri	13, 14
dimethyl trisulfide (144)	968	967 ⁵	ms, ri, std	1, 4, 6, 8, 10, 11, 12, 15, 17, 19

methyl furan-2-carboxylate (119)	976	969 ¹	ms, ri, std	4, 7, 8, 9, 12, 15
3-methylthiopropyl-1-ol (148)	976	969 ¹	ms, ri, std	5
β -pinene (160)	978	974 ¹	ms, ri, std	14, 17, 18, 19
1-ethyl-2-methylbenzene (21)	979	980 ²	ms, ri, std	9
phenol (88)	980	983 ¹⁹	ms, ri, std	10
2-methyl-2-bornene (152)	981	976 ³⁰	ms, ri	4, 14, 17, 18, 19
<i>cis</i> -2-methylpentan-4-olide (78)	983	n.a.	ms, std	16
4-methylpentan-4-olide (81)	985	992 ⁴³	ms, ri, std	2, 3, 9, 12, 15, 17
1-methylcamphene (154)	986	983 ³⁰	ms, ri	1, 14, 17, 18, 19
6-methylhept-5-en-2-one (43)	987	981 ¹	ms, ri, std	2, 3, 9, 13
2-methyldihydrothiophen-3(2 <i>H</i>)-one (150)	987	982 ³	ms, ri, std	5
<i>trans</i> -2-methylpentan-4-olide (79)	991	n.a.	ms, std	16
mesitylene (22)	993	994 ²	ms, ri, std	9
methyl 2-hydroxy-3-methylvalerate (72)	993	989 ¹	ms, ri	15
2-ethyl-5-methylpyrazine (130)	998	997 ³⁶	ms, ri	3, 9, 13, 15
trimethylpyrazine (132)	999	1000 ¹	ms, ri, std	1, 2, 5, 6, 8, 10, 12, 13, 14, 15, 18, 19
2-ethyl-3-methylpyrazine (129)	1001	1002 ¹	ms, ri	7, 8
cyclohept-4-enol (34)	1002	1002 ³⁷	ms, ri, std	3, 12
cyclohept-4-enone (53)	1005	1004 ³⁷	ms, ri, std	2, 3, 9, 12, 13, 14, 15, 17, 19
2-methylenebornane (153)	1017	1014 ³⁰	ms, ri	1, 4, 12, 14, 16, 17, 18, 19
2-acetyl-5-methylfuran (123)	1025	1031 ¹	ms, ri	8, 13, 15
limonene (158)	1028	1024 ¹	ms, ri, std	1
1,8-cineol (166)	1031	1026 ¹	ms, ri, std	1, 14, 17, 18
benzyl alcohol (94)	1034	1026 ¹	ms, ri, std	4, 5, 6, 9, 11, 12, 13, 15
3-methylpentan-4-olide (80)	1035	1034 ³⁷	ms, ri	17
4-methylhex-5-en-4-olide (84)	1039	1034 ¹	ms, ri, std	9
salicylaldehyde (96)	1043	1039 ¹	ms, ri, std	15
2-(1-methylethyl)-5-methylpyrazine (131)	1052	1059 ³³	ms, ri	13
2-acetylpyrrole (142)	1057	1054 ¹	ms, ri, std	1, 2, 8, 10, 13, 15
<i>S</i> -methyl methanethiosulfonate (146)	1062	1065 ⁵	ms, ri, std	1, 2, 9, 10, 11, 12
acetophenone (105)	1065	1059 ¹	ms, ri, std	1, 3, 6, 8, 9, 10, 12, 13, 14, 15, 17, 18, 19
<i>cis</i> -linalool oxide (164)	1072	1067 ¹	ms, ri	8, 9, 14
2-ethyl-3,6-dimethylpyrazine (133)	1076	1077 ⁴	ms, ri	1, 3, 5, 9, 10, 12, 13, 14
2-ethyl-3,5-dimethylpyrazine (134)	1078	1082 ⁴	ms, ri, std	2, 15, 19
2-methylmyrcene (157)	1081	1080 ³⁰	ms, ri, std	1
<i>trans</i> -linalool oxide (165)	1088	1084 ¹	ms, ri	8, 9

methyl 5-methylfuran-2-carboxylate (120)	1091	1092 ³⁷	ms, ri, std	9, 12
4-methylhexan-4-olide (82)	1092	1093 ³⁷	ms, ri, std	9
methyl benzoate (99)	1092	1088 ¹	ms, ri, std	2, 4, 7, 8, 10, 15
4-methylhexan-4-olide (82)	1094	1093 ³⁷	ms, ri, std	3, 9, 16, 17
linalool (163)	1098	1095 ¹	ms, ri, std	1, 3, 8, 9, 14, 15
2-phenylethanol (109)	1111	1107 ¹	ms, ri, std	1, 2, 4, 5, 6, 7, 8, 9, 10, 11, 12, 13, 14, 15, 18
methyl methylthiomethyl disulfide (147)	1126	1123 ⁵	ms, ri	1
phenylacetone (114)	1128	1124 ¹⁰	ms, ri, std	6, 7, 15, 18
1-phenylpropan-2-ol (113)	1135	n.a.	ms	15
2-methylacetophenone (108)	1136	1139 ³¹	ms, ri, std	7, 8
phenylacetonitrile (139)	1138	1134 ¹	ms, ri, std	3, 5, 6, 17
tropone hydrate (55)	1143	n.a.	ms, std	10
veratrole (89)	1145	1141 ¹	ms, ri	3, 7, 17, 19
camphor (167)	1146	1141 ¹	ms, ri, std	17
tropone (54)	1152	n.a.	ms, std	2, 10
2-hydroxyacetophenone (106)	1159	1155 ¹	ms, ri	3
4-methylsalicylaldehyde (98)	1161	n.a.	ms	5
1,4-dimethoxybenzene (91)	1163	1161 ¹	ms, ri	7
1-phenylpropan-1,2-dione (115)	1171	1175 ⁴¹	ms, ri	15
methyl phenylacetate (111)	1177	1175 ¹	ms, ri, std	1
methyl 2-methylbenzoate (102)	1178	1181 ³²	ms, ri	8
<i>p</i> -menth-1-en-4-ol (162)	1178	1174 ¹	ms, ri	14, 19
2-methylisoborneol (4)	1180	1178 ¹	ms, ri, std	1, 4, 10, 12, 13, 14, 16, 17, 18, 19
2-methyl- β -fenchol (151)	1184	1182 ³⁰	ms, ri, std	1, 4, 14, 16, 18, 19
α -terpineol (161)	1187	1186 ¹	ms, ri	14, 16, 17
methyl salicylate (100)	1190	1190 ¹	ms, ri, std	2, 3
2-methylinalool (156)	1193	n.a.	ms, std	4
decanal (36)	1202	1201 ¹	ms, ri, std	2, 3, 15
dimethyl tetrasulfide (145)	1218	1213 ⁵	ms, ri	1, 15
(8 <i>S</i> ,9 <i>R</i> ,10 <i>S</i>)-8,10-dimethyl-1-octalin (170)	1223	1223 ³⁰	ms, ri	1, 2, 3, 4, 6, 11, 12, 14, 15, 16, 17, 19
(8 <i>S</i> ,10 <i>R</i>)-8,10-dimethyl-1(9)-octalin (171)	1231	1230 ³⁰	ms, ri	1, 3, 6, 11, 14, 15, 16, 17, 19
1,2-dimethoxy-4-methylbenzene (92)	1237	1230 ¹⁷	ms, ri	2
ethyl phenylacetate (112)	1246	1243 ¹	ms, ri	6, 10, 11
2-methoxybenzaldehyde (97)	1250	1247 ¹	ms, ri	2
4-methoxy- <i>N</i> -methylaniline (136)	1255	n.a.	ms, std	7
2-phenylethyl acetate (110)	1256	1254 ¹	ms, ri	1, 11
2-methoxybenzonitrile (138)	1278	n.a.	ms, std	1, 3
2-methoxyacetophenone (107)	1289	1290 ¹	ms, ri	3
2-aminoacetophenone (137)	1296	1299 ¹³	ms, ri, std	2, 14

1-nitro-2-phenylethane (140)	1298	1294 ¹	ms, ri, std	6, 15
1,2,3-trimethoxybenzene (90)	1310	1315 ¹⁴	ms, ri, std	2, 3, 14
methyl 6-methylsalicylate (103)	1314	1317 ³⁷	ms, ri, std	4
2-(3-methylbutyl)-3,6-dimethylpyrazine (135)	1315	1321 ⁷	ms, ri, std	5
(<i>E</i>)-2-methylgeraniol (155)	1327	1325 ³⁰	ms, ri, std	4
methyl 2-methoxybenzoate (101)	1336	1334 ¹	ms, ri	2
african-1-ene (184)	1349	1356 ⁴⁴	ms, ri	16
dimethyl furan-2,4-dicarboxylate (121)	1356	1358 ³⁷	ms, ri, std	8
3,4-dimethoxystyrene (93)	1364	1368 ³⁴	ms, ri	2
methyl 2,6-dihydroxybenzoate (104)	1385	1386 ⁴⁰	ms, ri	2
geosmin (3)	1403	1399 ¹	ms, ri, std	1, 2, 3, 4, 6, 7, 8, 9, 10, 11, 12, 13, 14, 15, 16, 17, 18, 19
<i>epi</i> -isozizaene (2)	1444	1447 ³⁰	ms, ri	6, 15
geranylacetone (44)	1449	1453 ¹	ms, ri, std	2, 3
<i>epi</i> -prezizaene (168)	1452	1449 ³⁰	ms, ri	15
β -barbatene (187)	1453	1445 ⁴⁴	ms, ri	1
cadina-3,5-diene (182)	1453	1451 ³⁵	ms, ri	7
6,11-epoxyisodaucane (174)	1463	1469 ³⁰	ms, ri	3, 4, 8, 12, 15, 16
(1 <i>R</i> *,6 <i>S</i> *,10 <i>S</i> *)-6,10-dimethylbicyclo[4.4.0]decan-3-one (176)	1465	1469 ³⁵	ms, ri, std	3, 12, 14, 19
α -amorphenone (9)	1480	1483 ¹	ms, ri	6
<i>trans</i> -cadina-1(6),4-diene (180)	1475	1475 ¹	ms, ri	7
germacrene D (172)	1488	1479 ⁴⁴	ms, ri, std	1, 3, 6, 8, 11, 12, 13, 14, 15, 16, 17, 19
isodihydroagarofuran (175)	1503	1504 ³⁰	ms, ri, std	3, 6, 12, 14, 15, 16, 17
α -muurolene (177)	1500	1500 ¹	ms, ri	7, 8, 9
δ -cadinene (178)	1523	1522 ¹	ms, ri	7, 8
isoafricanol (16)	1526	n.a.	ms, std	16
zonarene (181)	1528	1528 ¹	ms, ri	7, 8
cadina-1,4-diene (179)	1534	1533 ¹	ms, ri	7, 8
nerolidol (186)	1566	1561 ¹	ms, ri, std	5
caryolan-1-ol (6)	1570	1564 ³⁵	ms, ri	7, 8, 9, 13
germacrene D-4-ol (185)	1582	1574 ¹	ms, ri	12
<i>epi</i> -cubenol (5)	1633	1627 ³⁵	ms, ri	4, 7, 8, 9
(1(10) <i>E</i> ,5 <i>E</i>)-germacradien-11-ol (173)	1640	1638 ³⁰	ms, ri	3, 4, 6, 8, 9, 11, 12, 13, 14, 15, 16, 17, 19
α -cadinol (183)	1655	1652 ¹	ms, ri	9
7- <i>epi</i> - α -eudesmol (10)	1664	1662 ¹	ms, ri	15
4 β ,5 β -epoxy-2- <i>epi</i> -zizaan-6 β -ol (169)	1673	1676 ³⁰	ms, ri	6
10-methyldodec-2-en-4-olide (85)	1729	1728 ³⁷	ms, ri, std	7
10-methyldodecan-4-olide (86)	1751	n.a.	ms, std	7
10-methyldodecan-5-olide (87)	1782	1780 ³⁷	ms, ri, std	7

^aCompound numbers refer to compound numbers in main text. Unidentified compounds, artifacts and medium constituents are not mentioned. ^bRetention index on a HP5-MS fused silica capillary column. ^cRetention index on the same or a similar column from tabulated data in the literature. ^dIdentification based on ms: mass spectrum (mass spectral match factor >850), ri: retention index on same or similar column (maximum deviation of 10 points), std: comparison to a synthetic or commercially available standard. For compound identification commercially available mass spectral databases (Adams, Joulain & König, Wiley, NIST)^{1,44-46} were used. ^eNumbers refer to strains listed in Table 1 of ESI.

References

- 1 R. P. Adams, *Identification of Essential Oil Components by Gas Chromatography/ Mass Spectrometry*, Allured, Carol Stream, **2009**.
- 2 E. Engel, C. Baty, D. L. Corre, I. Souchon and N. Martin, *J. Agric. Food Chem.*, 2002, **50**, 6459.
- 3 T. Nawrath, K. Gerth, R. Müller and S. Schulz, *ChemBioChem*, 2010, **11**, 1914.
- 4 J. S. Dickschat, S. Wickel, C. J. Bolten, T. Nawrath, S. Schulz and C. Wittmann, *Eur. J. Org. Chem.*, 2010, 2687.
- 5 J. S. Dickschat, C. Zell and N. L. Brock, *ChemBioChem*, 2010, **11**, 417.
- 6 N. L. Brock, B. Tudzynski and J. S. Dickschat, *ChemBioChem*, 2011, **12**, 2667.
- 7 J. C. Beaulieu and C. C. Grimm, *J. Agric. Food Chem.*, 2001, **49**, 1345.
- 8 J. A. Pino, J. Mesa, Y. Munoz, M. P. Marti and R. Marbot, *J. Agric. Food Chem.*, 2005, **53**, 2213.
- 9 L. Methven, M. Tsoukka, M. J. Oruna-Concha, J. K. Parker and D. S. Mottram, *J. Agric. Food Chem.*, 2007, **55**, 1427.
- 10 M. A. Ferhat, N. Tigrine-Kordjani, S. Schemat, B. Y. Meklati and F. Chemat, *Chromatographia*, 2007, **65**, 217.
- 11 R. Boulanger, D. Chassagne and J. Crouzet, *Flavour Fragr. J.*, 1999, **14**, 303.
- 12 X. Xu, L. L. P. Stee, J. Williams, J. Beens, M. Adahchour, R. J. J. Vreuls, U. A. Brinkman, and J. Lelieveld, *Atmos. Chem. Phys.*, 2003, **3**, 665.
- 13 S. L. Schwalmbach and D. G. Petersen, *J. Agric. Food Chem.*, 2006, **54**, 502.
- 14 D. Ansorena, I. Astiasaran, J. Bello, *J. Agric. Food Chem.*, 2000, **48**, 2395.
- 15 J. E. Premecz and M. E. Ford, *J. Chromatogr.*, 1987, **388**, 23.
- 16 J. J. Joffraud, F. Leroi, C. Roy and J. L. Berdague, *Int. J. Food Microbiol.*, 2001, **66**, 175.
- 17 R. J. V. Alves, A. C. Pinto, A. V. M. da Costa and C. M. Rezende, *J. Braz. Chem. Soc.*, 2005, **16**, 654.
- 18 N. Radulovic, P. Blagojevic and R. Palic, *Molecules*, 2010, **15**, 6168.
- 19 V. Vasta, J. Ratel and E. Engel, *J. Agric. Food Chem.*, 2007, **55**, 4630.
- 20 X. Xu, L. L. P. van Stee, J. Williams, J. Beens, M. Adahchour, R. J. J. Vreuls, U. A. T. Brinkman and J. Lelieveld, *Atmos. Chem. Phys.*, 2003, **3**, 665.
- 21 P. Bredael, *J. Hi. Res. Chromatogr. Chromatogr. Comm.*, 1982, **5**, 325.
- 22 D. Ansorena, I. Astiasaran and J. Bello, *J. Agric. Food Chem.*, 2000, **48**, 2395.
- 23 J. C. Leffingwell and E. D. Alford, *Electron. J. Environ. Agric. Food Chem.*, 2005, **4**, 899.
- 24 T. H. Kim, T. H. Kim, J. H. Shin, E. J. Yu, Y. S. Kim and H. J. Lee, *Biotechnol. Lett.*, 2002, **24**, 551.
- 25 A. D. Beal and D. S. Mottram, *J. Agric. Food Chem.*, 1994, **42**, 2880.
- 26 R. Boulanger and J. Crouzet, *Food Chem.*, 2000, **70**, 463.
- 27 F. B. Whitfield and D. S. Mottram, *J. Agric. Food Chem.*, 2001, **49**, 816.
- 28 J. Mateo and J. M. Zumalacarregui, *Meat Sci.*, 1996, **44**, 255.
- 29 S. K. Hoekman, *J. Chromatogr.*, 1993, **639**, 239.
- 30 P. Rabe, C. A. Citron and J. S. Dickschat, *ChemBioChem*, 2013, **14**, 2345.
- 31 J. A. Pino, R. Marbot and V. Fuentes, *J. Agric. Food Chem.*, 2003, **51**, 3836.

- 32 C. E. Rostad and W. E. Pereira, *J. Hi. Res. Chromatogr. Chromatogr. Comm.*, 1986, **9**, 328.
- 33 M. Solina, P. Baumgartner, R. L. Johnson and F. B. Whitfield, *Food Chem.*, 2005, **90**, 861.
- 34 C. X. Zhao, X. N. Li, Y. Z. Liang, H. Z. Fang, L. F. Huang and F. Q. Guo, *Chemom. Intell. Lab. Syst.*, 2006, **82**, 218.
- 35 C. A. Citron, J. Gleitzmann, G. Laurenzano, R. Pukall and J. S. Dickschat, *ChemBioChem*, 2012, **13**, 202.
- 36 A. D. Beal and D. S. Mottram, *J. Agric. Food Chem.*, 1994, **42**, 2880.
- 37 C. A. Citron, P. Rabe and J. S. Dickschat, *J. Nat. Prod.*, 2012, **75**, 1765.
- 38 B. R. Toledo, L. W. Hantao, T. D. Ho, F. Augusto and J. L. Anderson, *J. Chromatogr. A*, 2014, **1346**, 1.
- 39 N. L. Brock, B. Tudzynski and J. S. Dickschat, *ChemBioChem*, 2011, **12**, 2667.
- 40 S. Vitalini, G. Flamini, A. Valaguzza, G. Rodondi, M. Iriti and G. Fico, *Phytochemistry*, 2011, **72**, 1371.
- 41 Q. Wang, Y. Yang, X. Zhao, B. Zhu, P. Nan, J. Zhao, L. Wang, F. Chen, Z. Liu and Y. Zhong, *Food Chem.*, 2006, **98**, 52.
- 42 N. Radulovic, M. Dekic, M. Joksovic and R. Vukicevic, *Chem. Biodiversity*, 2012, **9**, 106.
- 43 J. C. Leffingwell and E. D. Alford, *Electron. J. Environ. Agric. Food Chem.*, 2005, **4**, 899.
- 44 D. Joulain and W. A. König, *The Atlas of Spectral Data of Sesquiterpene Hydrocarbons*, E. B.-Verlag, Hamburg, **1998**.
- 45 <http://www.sisweb.com/software/ms/wiley.htm>
- 46 <http://www.nist.gov/srd/nist1a.cfm>

Allokutzneria albata NRRL B-24461

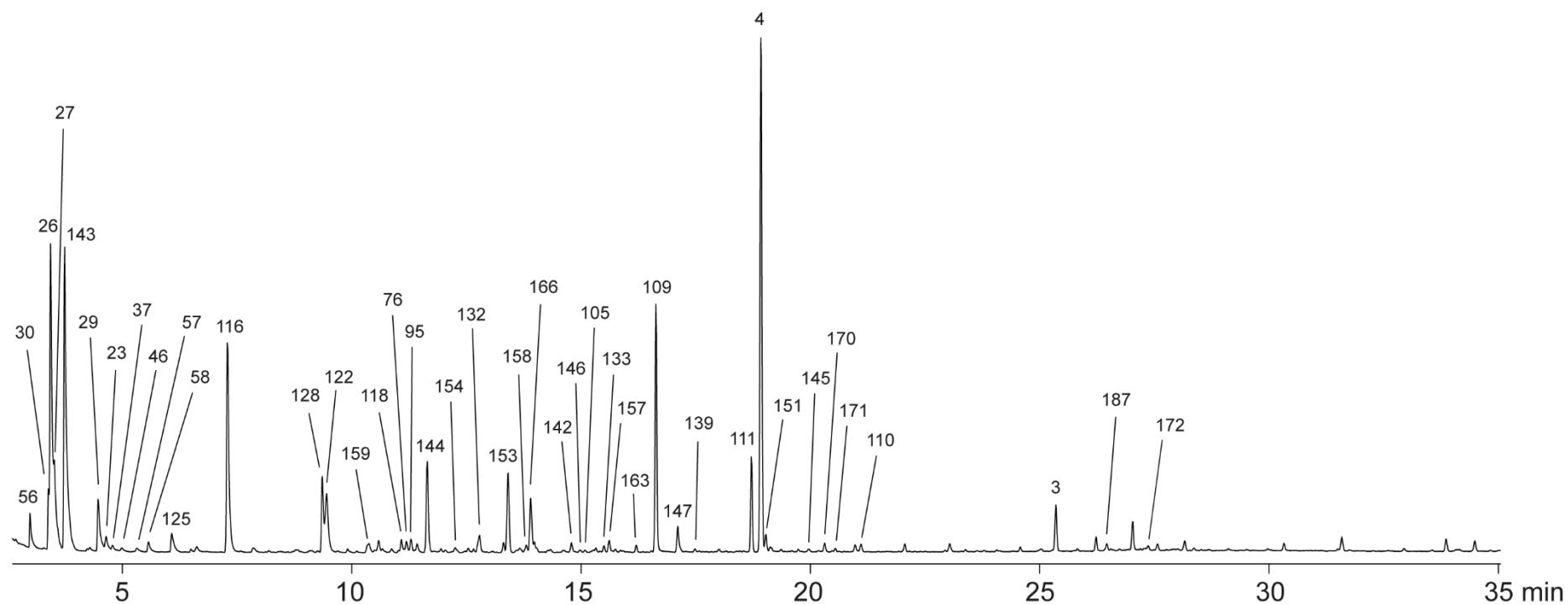


Figure 1 Total ion chromatograms of headspace extracts from investigated strains. Peak numbers refer to compound numbers in Table 2 of ESI and in main text.

Amycolatopsis alba DSM 44262

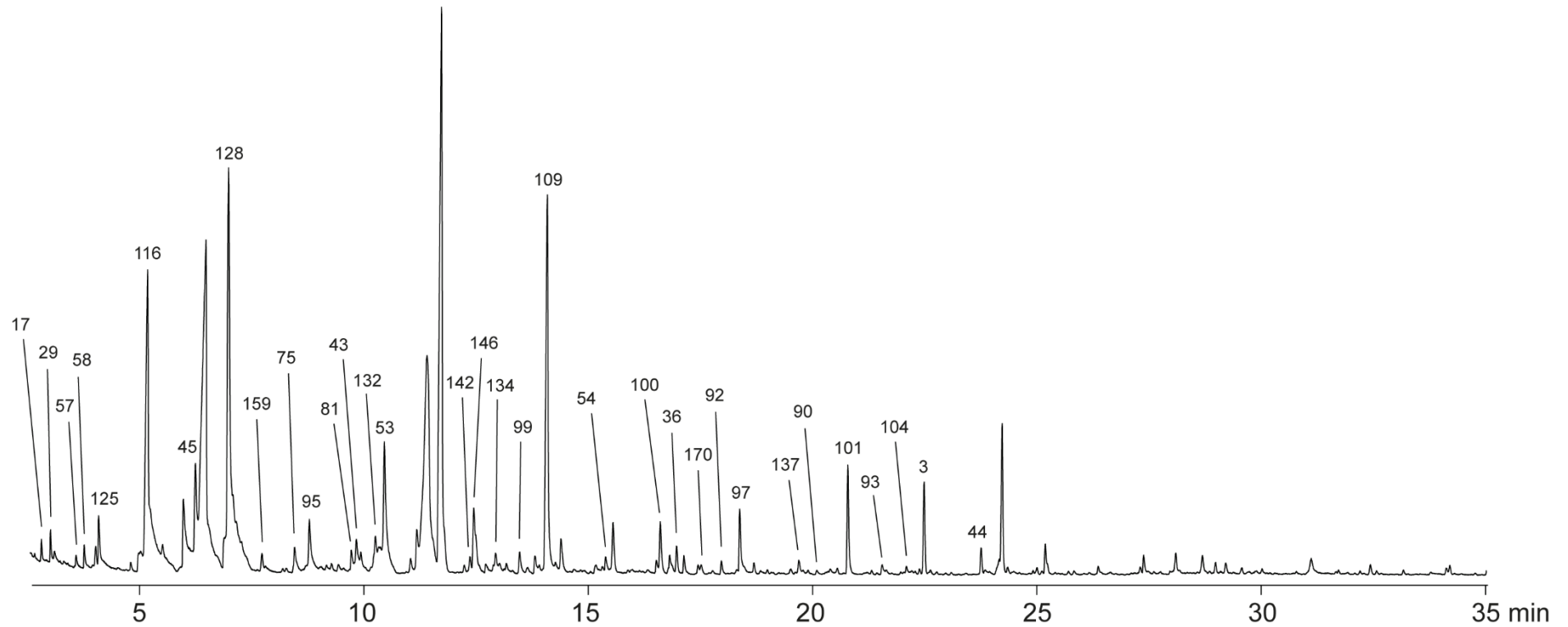


Figure 1 Total ion chromatograms of headspace extracts from investigated strains. Peak numbers refer to compound numbers in Table 2 of ESI and in main text.

Amycolatopsis nigrescens DSM 44992

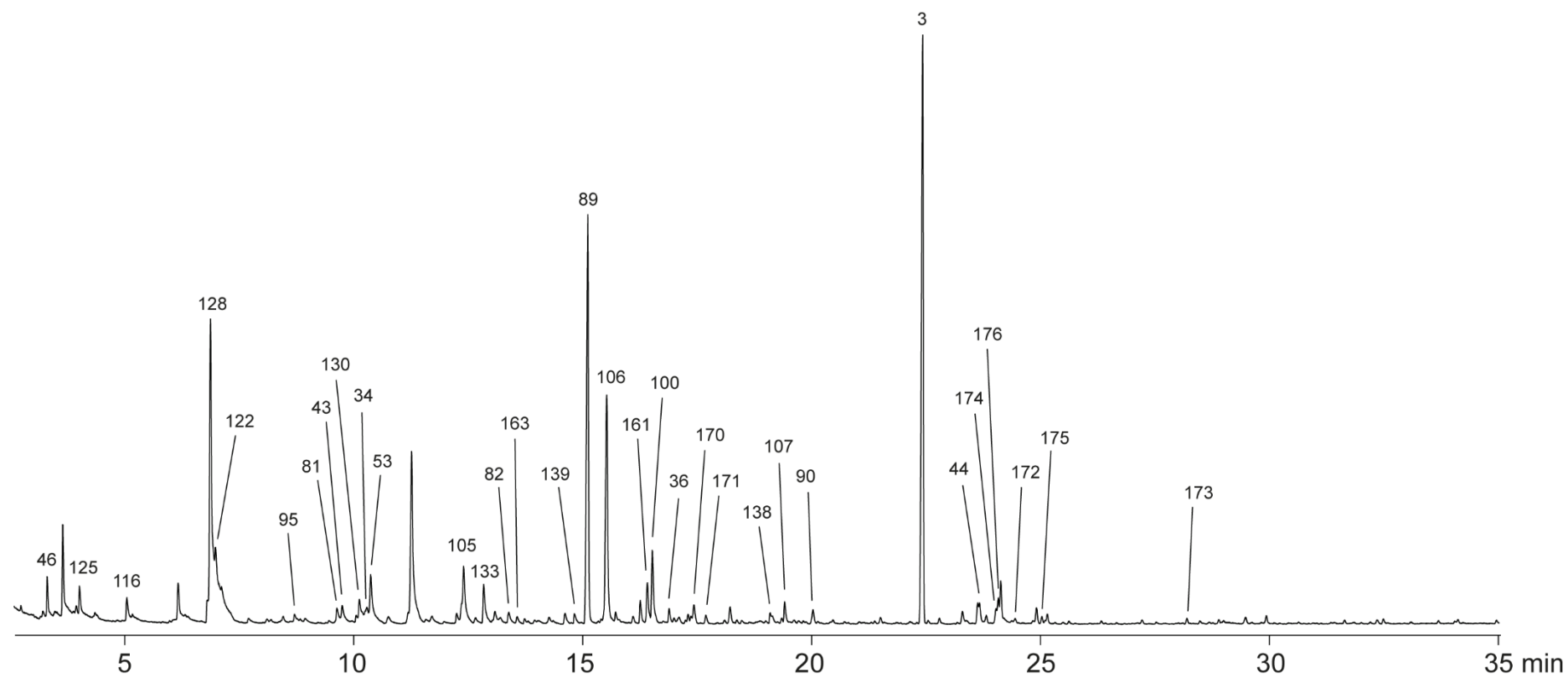


Figure 1 Total ion chromatograms of headspace extracts from investigated strains. Peak numbers refer to compound numbers in Table 2 of ESI and in main text.

Kitasatospora papulosa NRRL B-16504

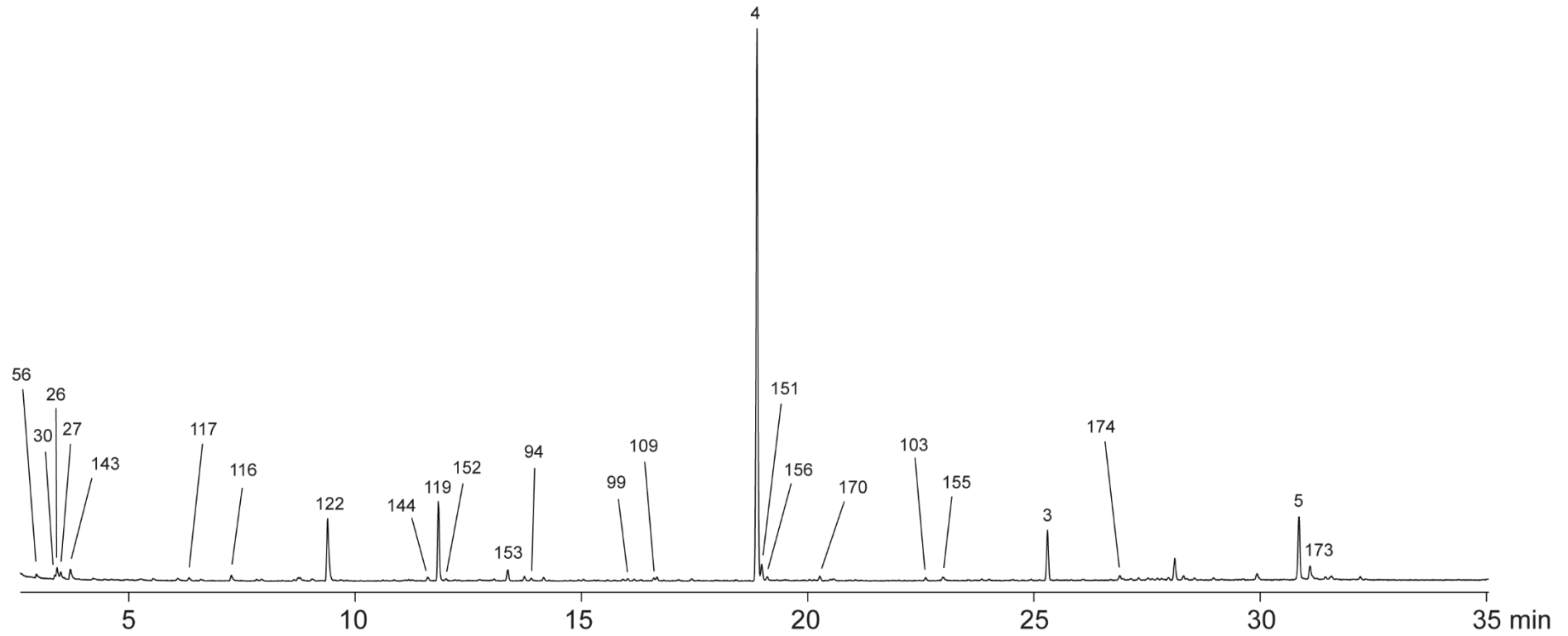


Figure 1 Total ion chromatograms of headspace extracts from investigated strains. Peak numbers refer to compound numbers in Table 2 of ESI and in main text.

Pseudonocardia spinosipora NRRL B-24156

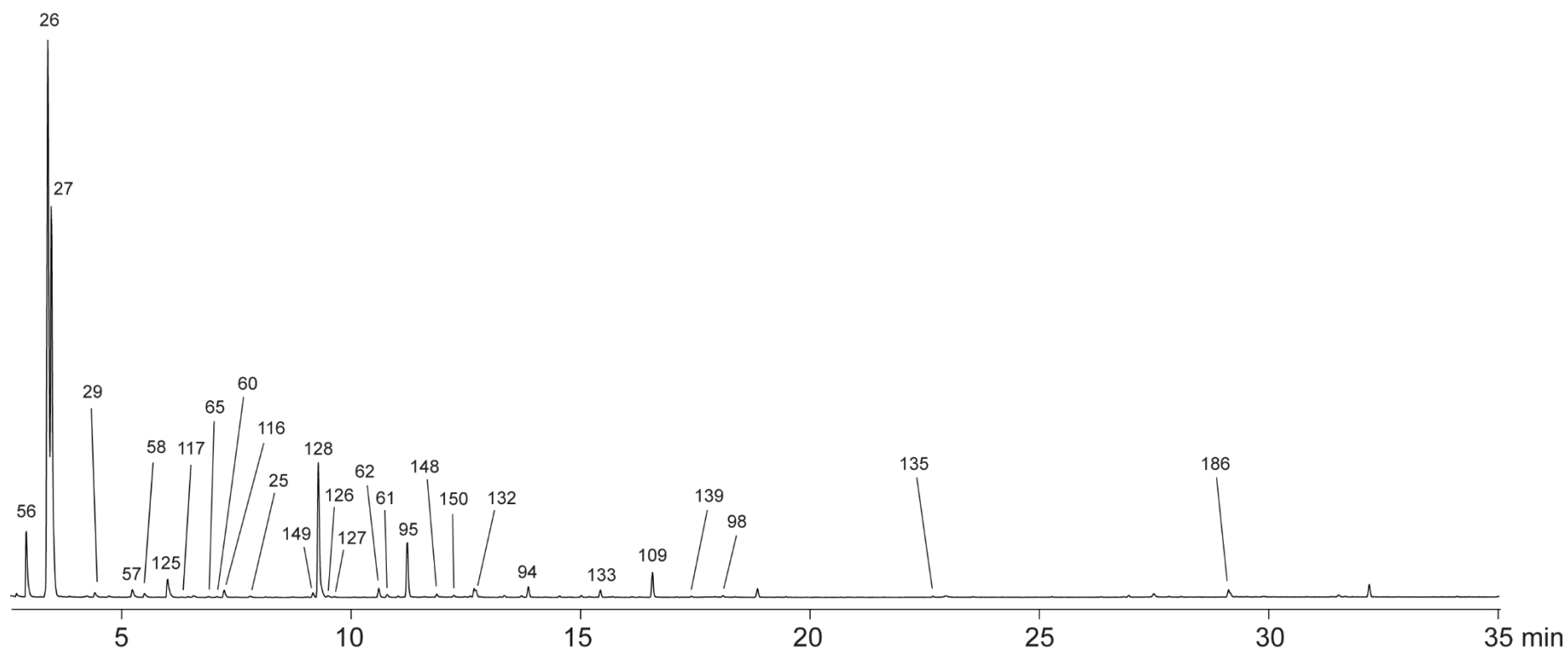


Figure 1 Total ion chromatograms of headspace extracts from investigated strains. Peak numbers refer to compound numbers in Table 2 of ESI and in main text.

Streptomyces afghaniensis DSM 40228

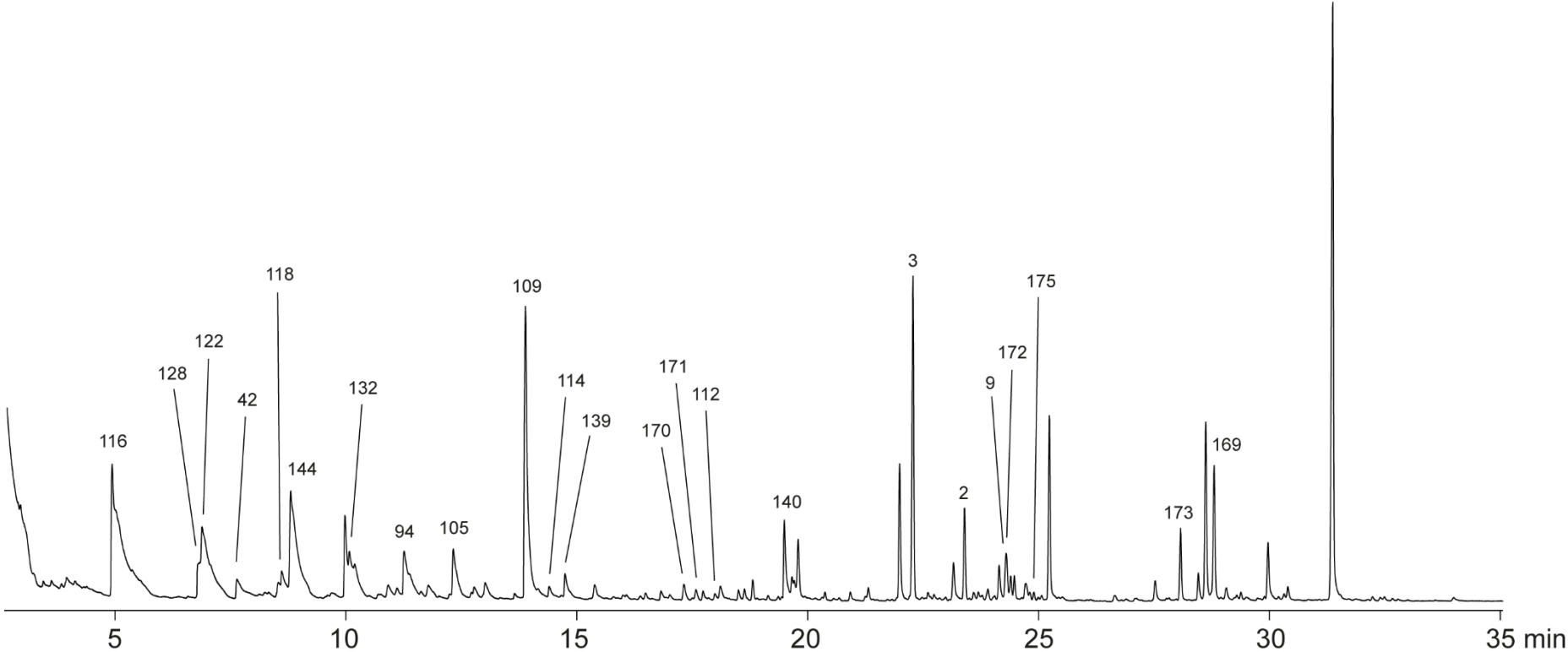


Figure 1 Total ion chromatograms of headspace extracts from investigated strains. Peak numbers refer to compound numbers in Table 2 of ESI and in main text.

Streptomyces anulatus NRRL B-2873

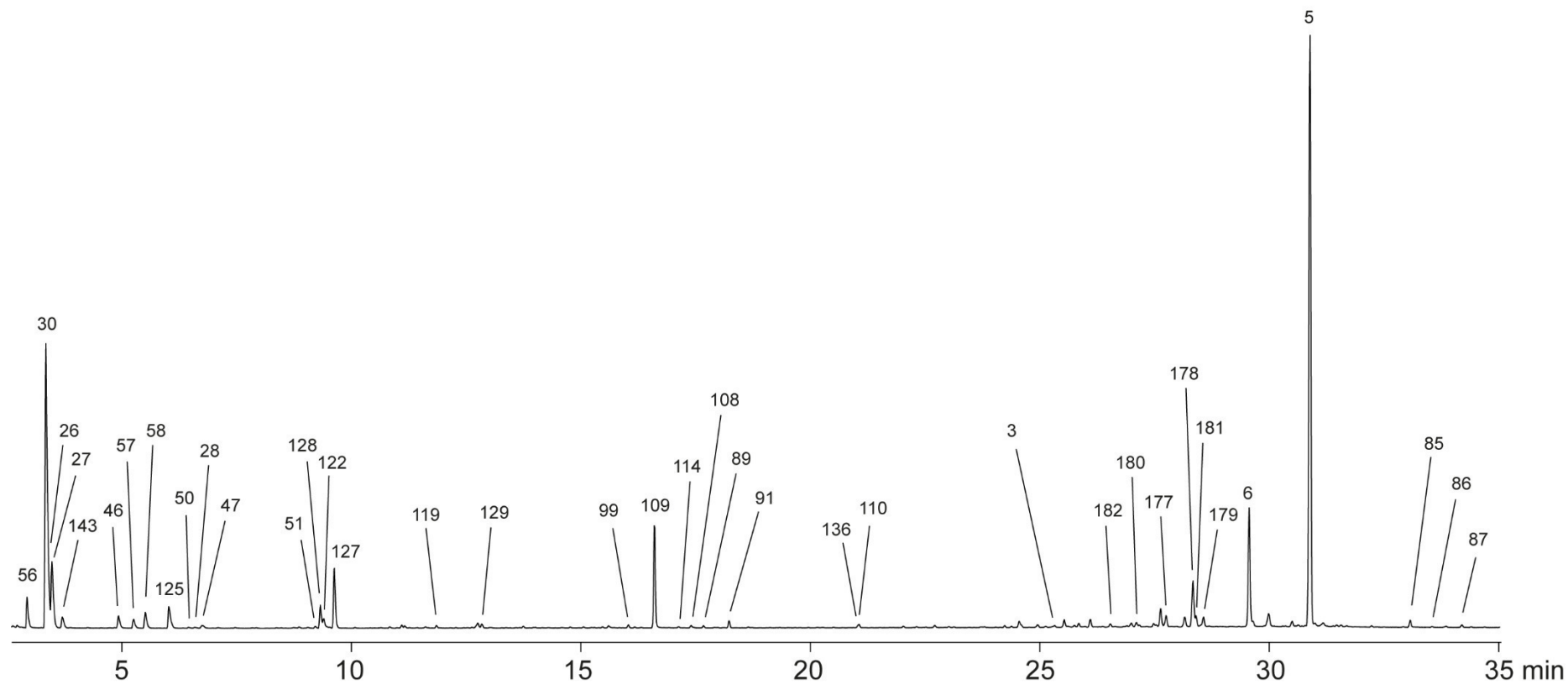


Figure 1 Total ion chromatograms of headspace extracts from investigated strains. Peak numbers refer to compound numbers in Table 2 of ESI and in main text.

Streptomyces californicus NRRL B-3320

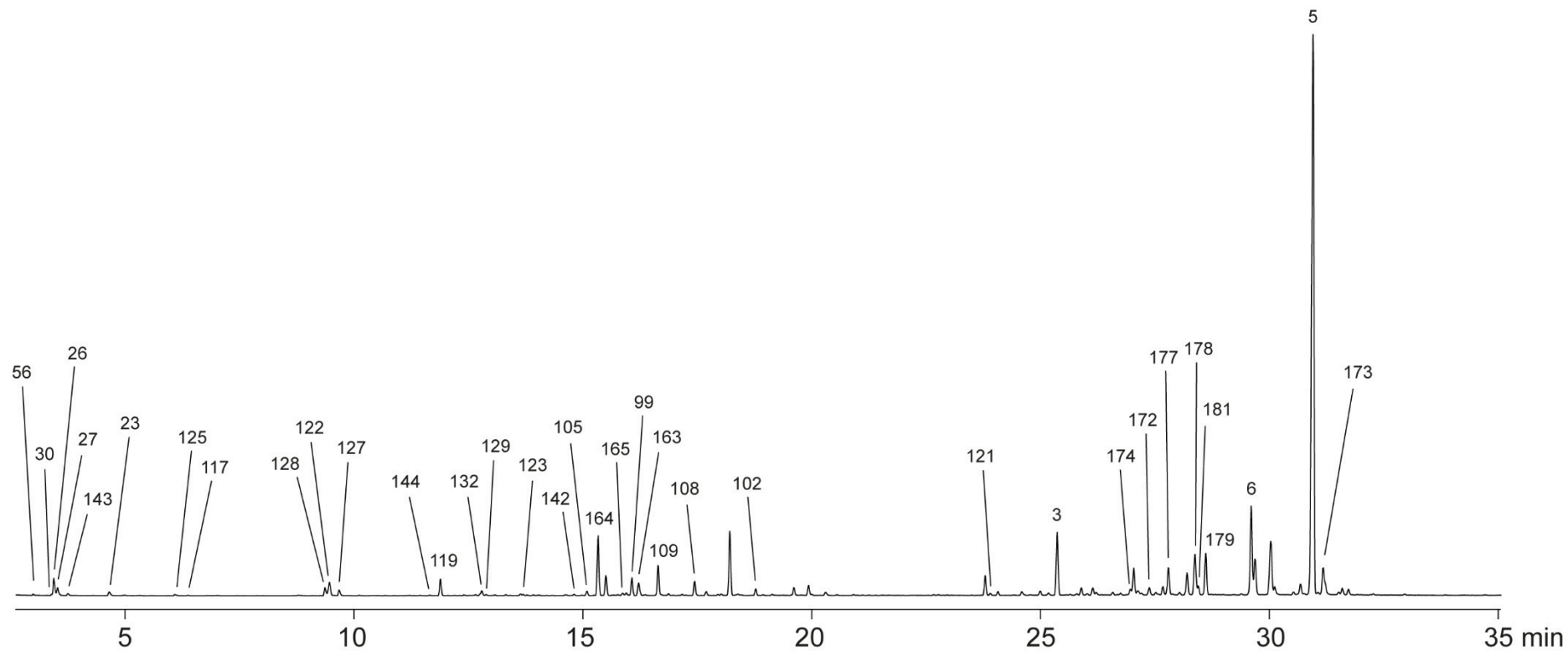


Figure 1 Total ion chromatograms of headspace extracts from investigated strains. Peak numbers refer to compound numbers in Table 2 of ESI and in main text.

Streptomyces cyaneofuscatus NRRL B-2570

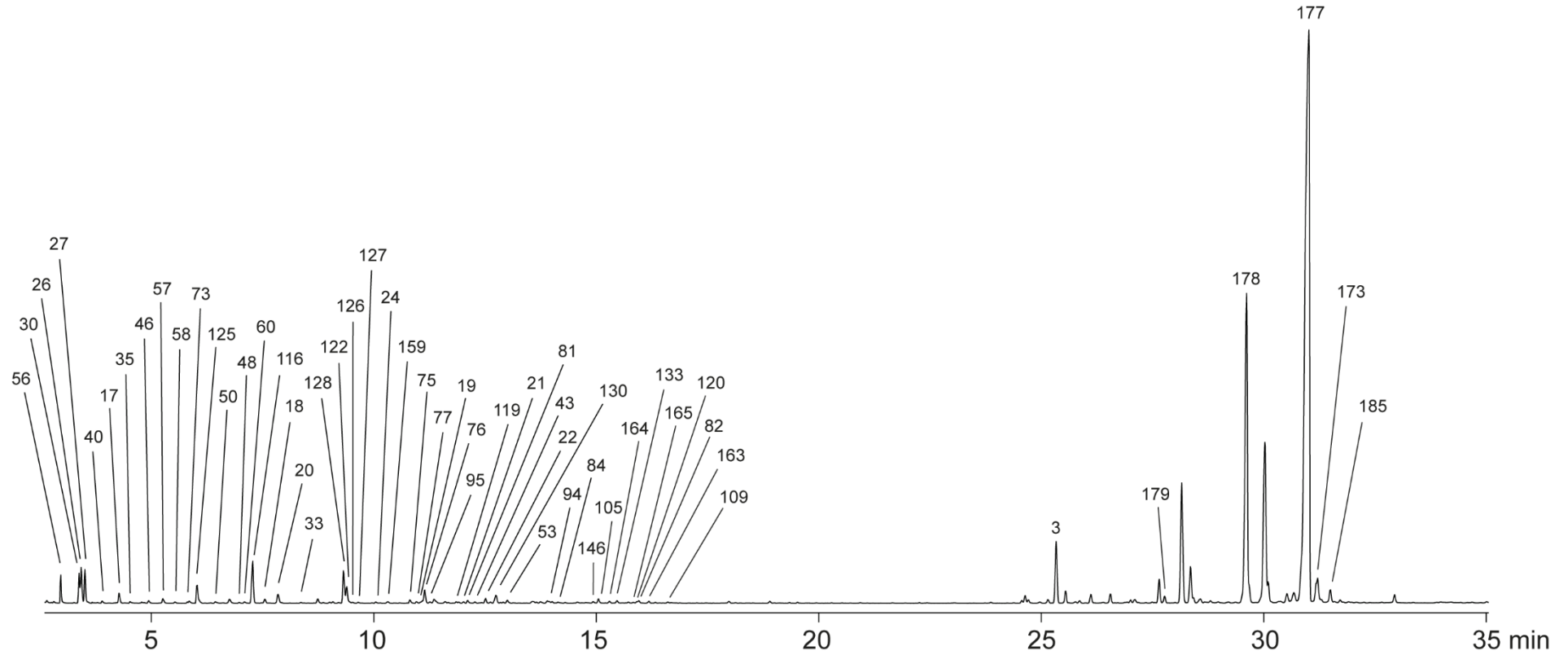


Figure 1 Total ion chromatograms of headspace extracts from investigated strains. Peak numbers refer to compound numbers in Table 2 of ESI and in main text.

Streptomyces flavochromogenes NRRL B-2684

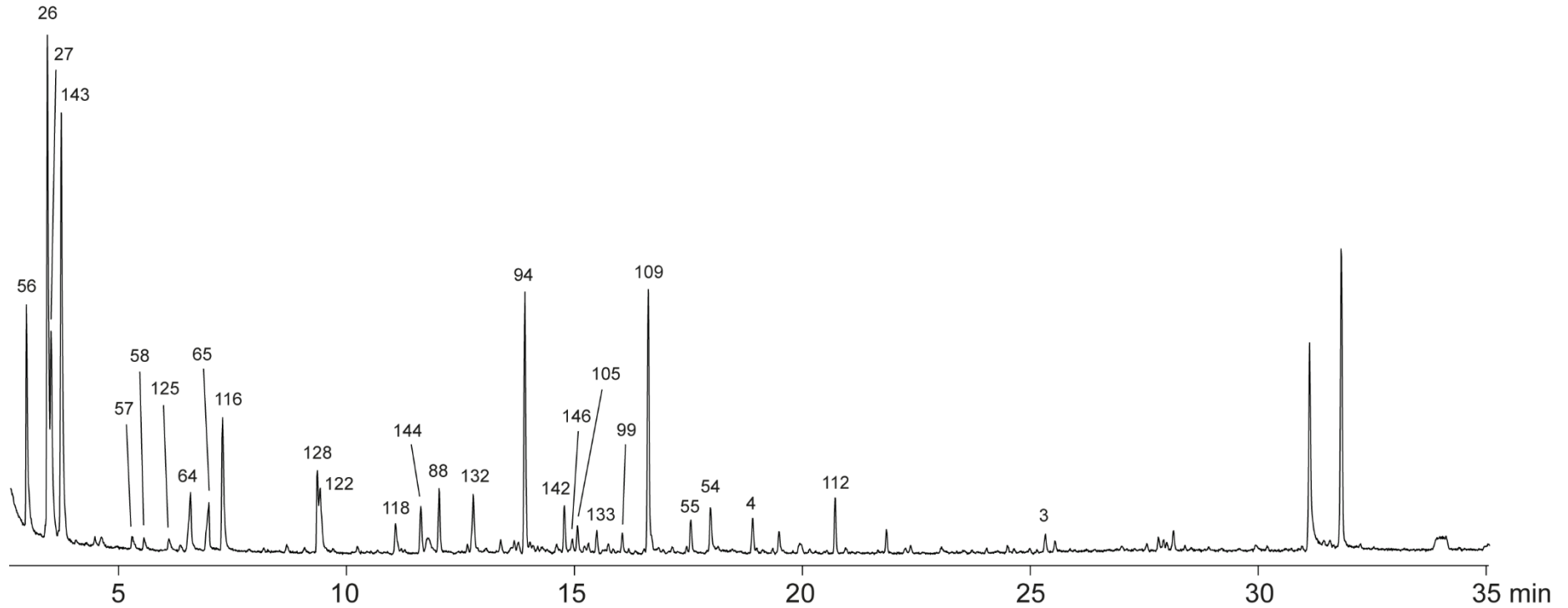


Figure 1 Total ion chromatograms of headspace extracts from investigated strains. Peak numbers refer to compound numbers in Table 2 of ESI and in main text.

Streptomyces fulvissimus DSM 40593

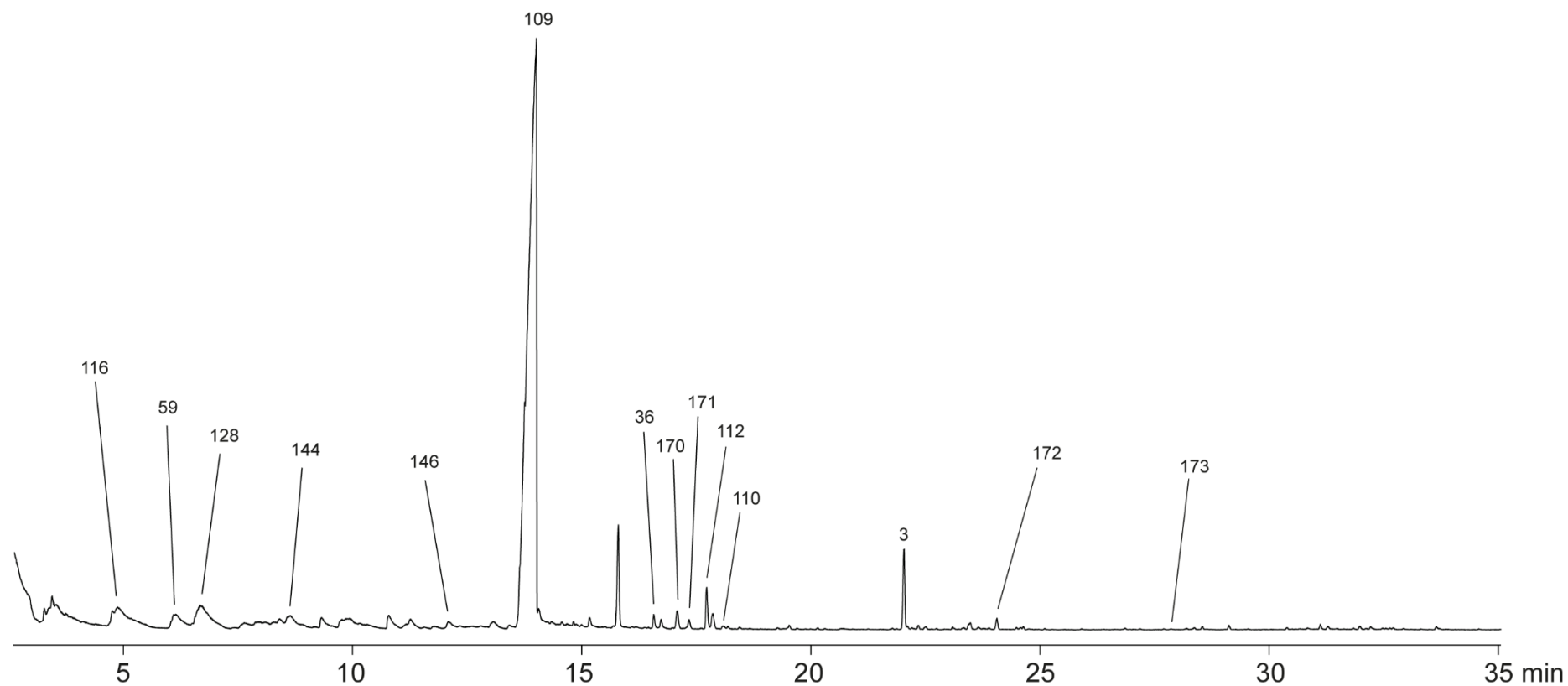


Figure 1 Total ion chromatograms of headspace extracts from investigated strains. Peak numbers refer to compound numbers in Table 2 of ESI and in main text.

Streptomyces globisporus NRRL B-2293

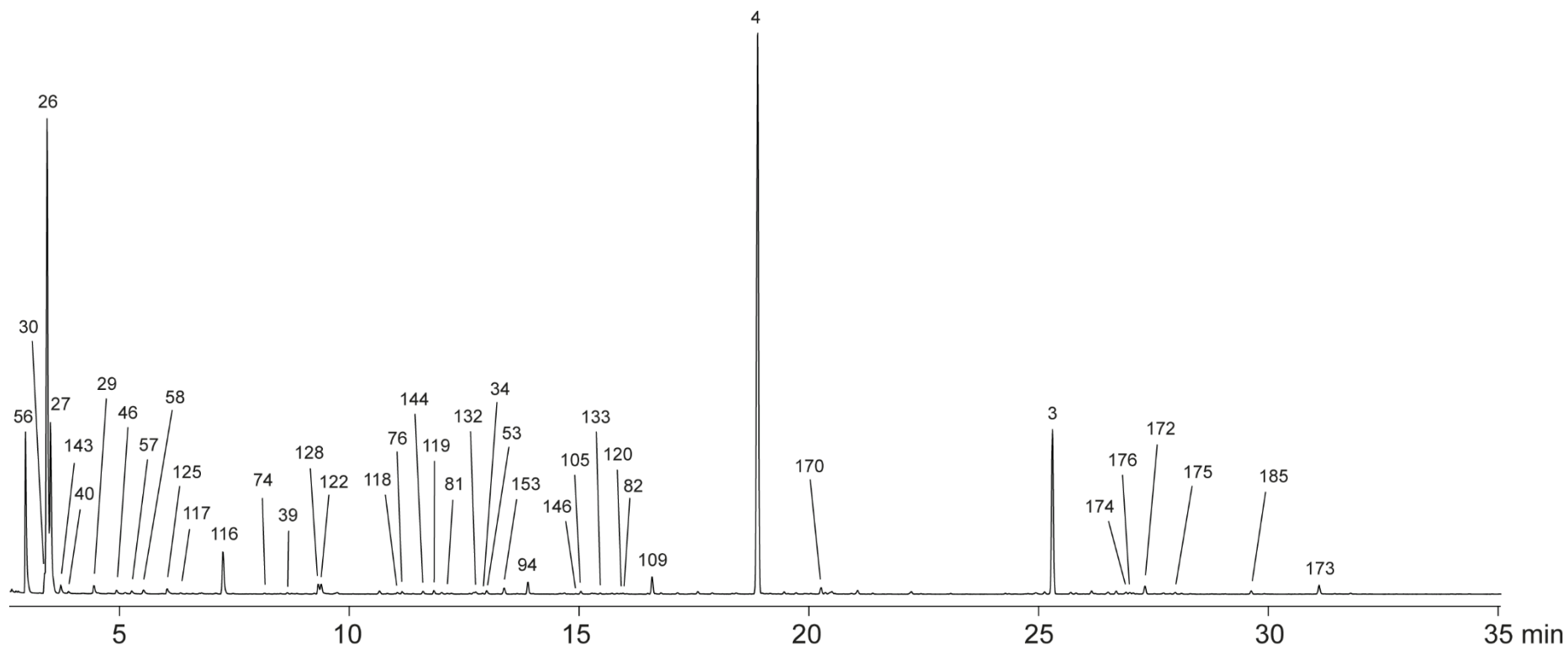


Figure 1 Total ion chromatograms of headspace extracts from investigated strains. Peak numbers refer to compound numbers in Table 2 of ESI and in main text.

Streptomyces mediolani NRRL WC3934

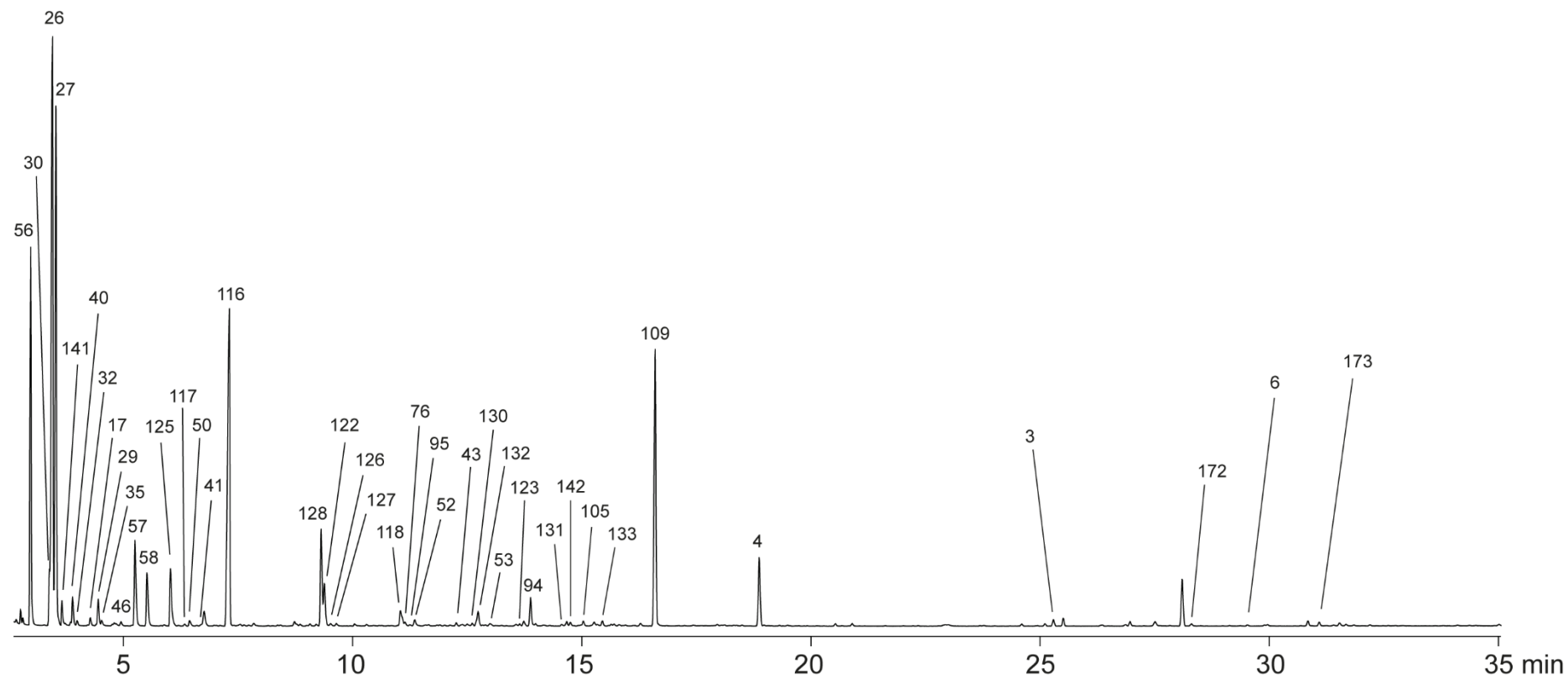


Figure 1 Total ion chromatograms of headspace extracts from investigated strains. Peak numbers refer to compound numbers in Table 2 of ESI and in main text.

Streptomyces ochraceiscleroticus NRRL ISP-5594

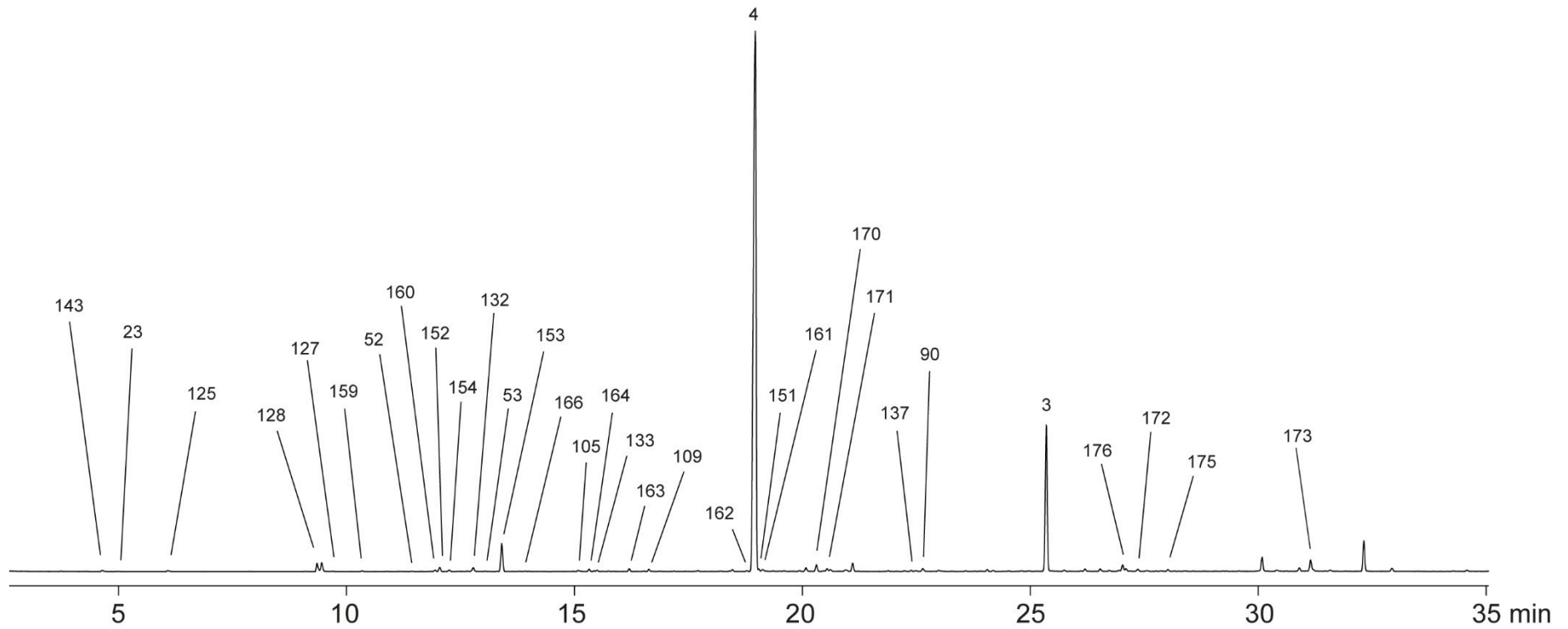


Figure 1 Total ion chromatograms of headspace extracts from investigated strains. Peak numbers refer to compound numbers in Table 2 of ESI and in main text.

Streptomyces prunicolor NBRC 13075

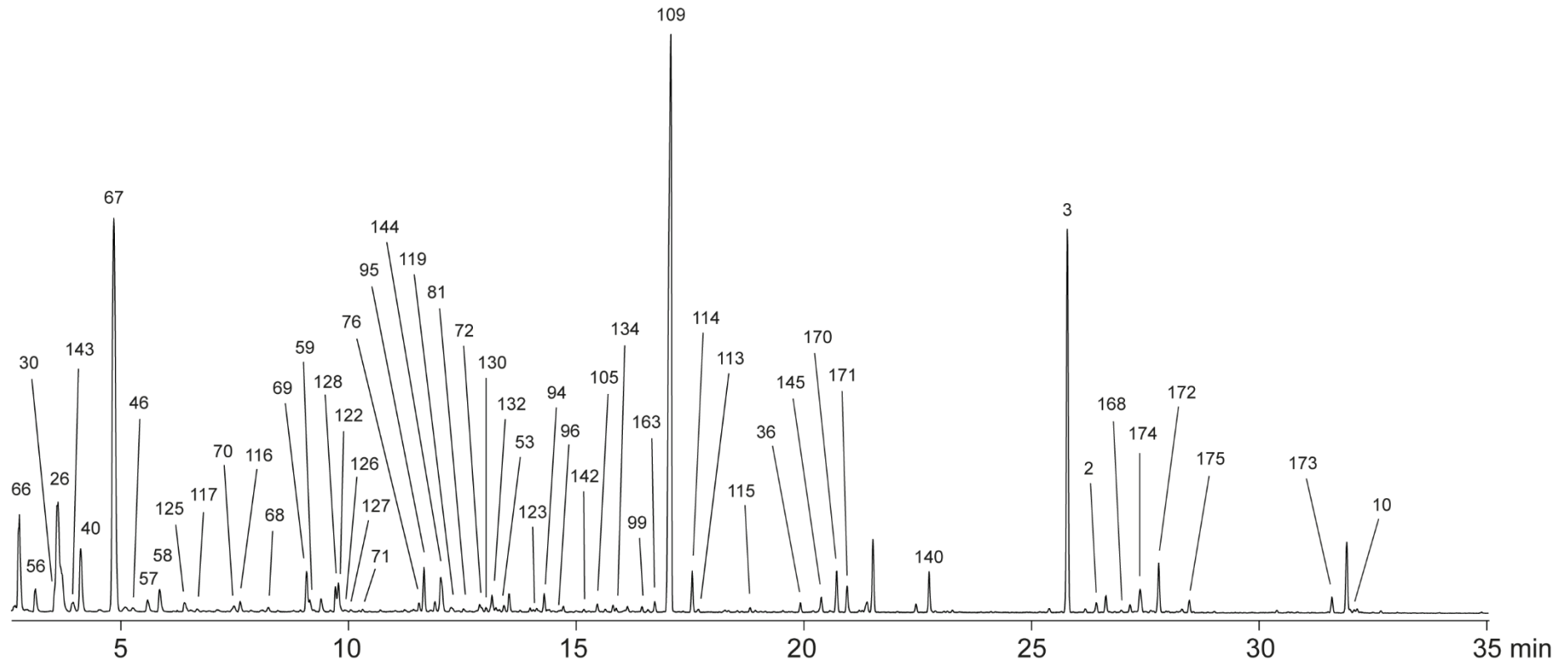


Figure 1 Total ion chromatograms of headspace extracts from investigated strains. Peak numbers refer to compound numbers in Table 2 of ESI and in main text.

Streptomyces rapamycinicus NRRL 5491

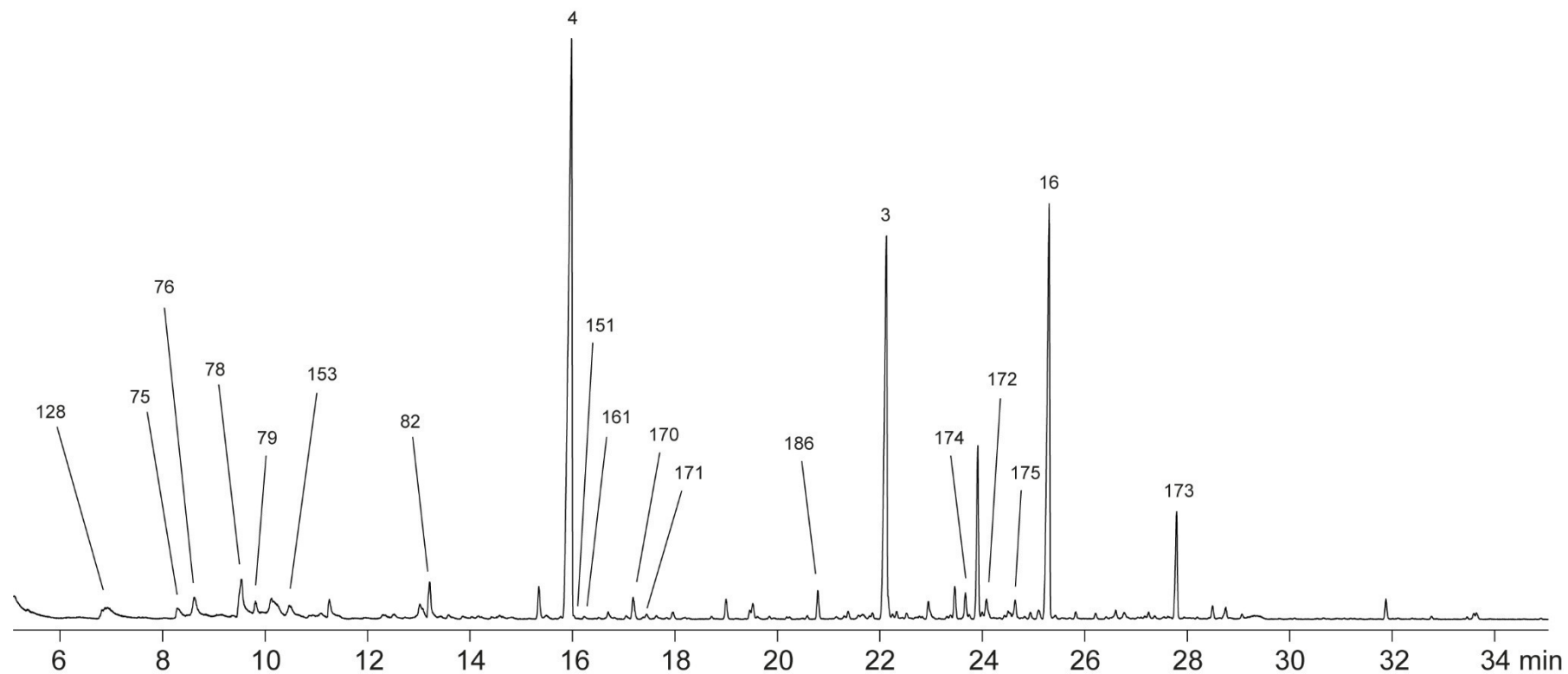


Figure 1 Total ion chromatograms of headspace extracts from investigated strains. Peak numbers refer to compound numbers in Table 2 of ESI and in main text.

Streptomyces sclerotialis NRRL ISP-5269

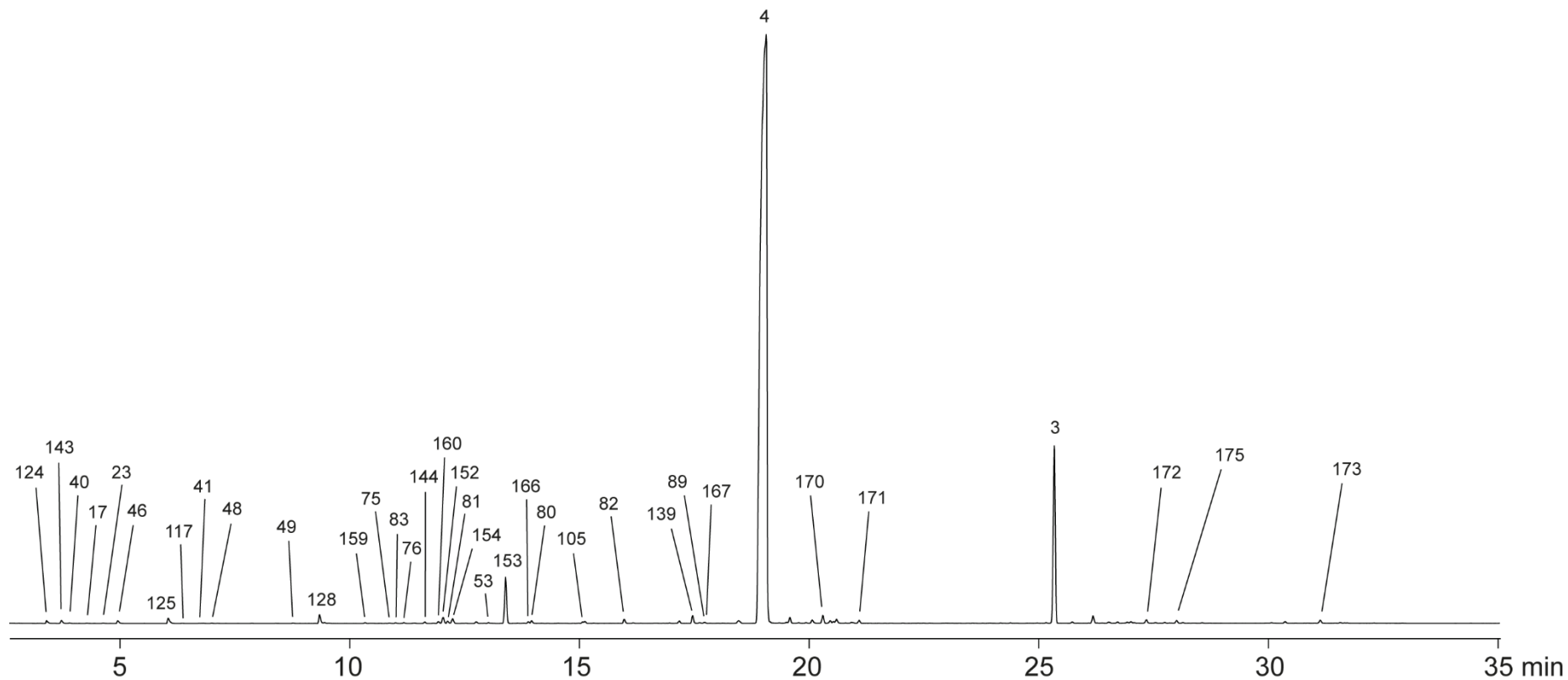


Figure 1 Total ion chromatograms of headspace extracts from investigated strains. Peak numbers refer to compound numbers in Table 2 of ESI and in main text.

Streptomyces varsoviensis NRRL B-3589

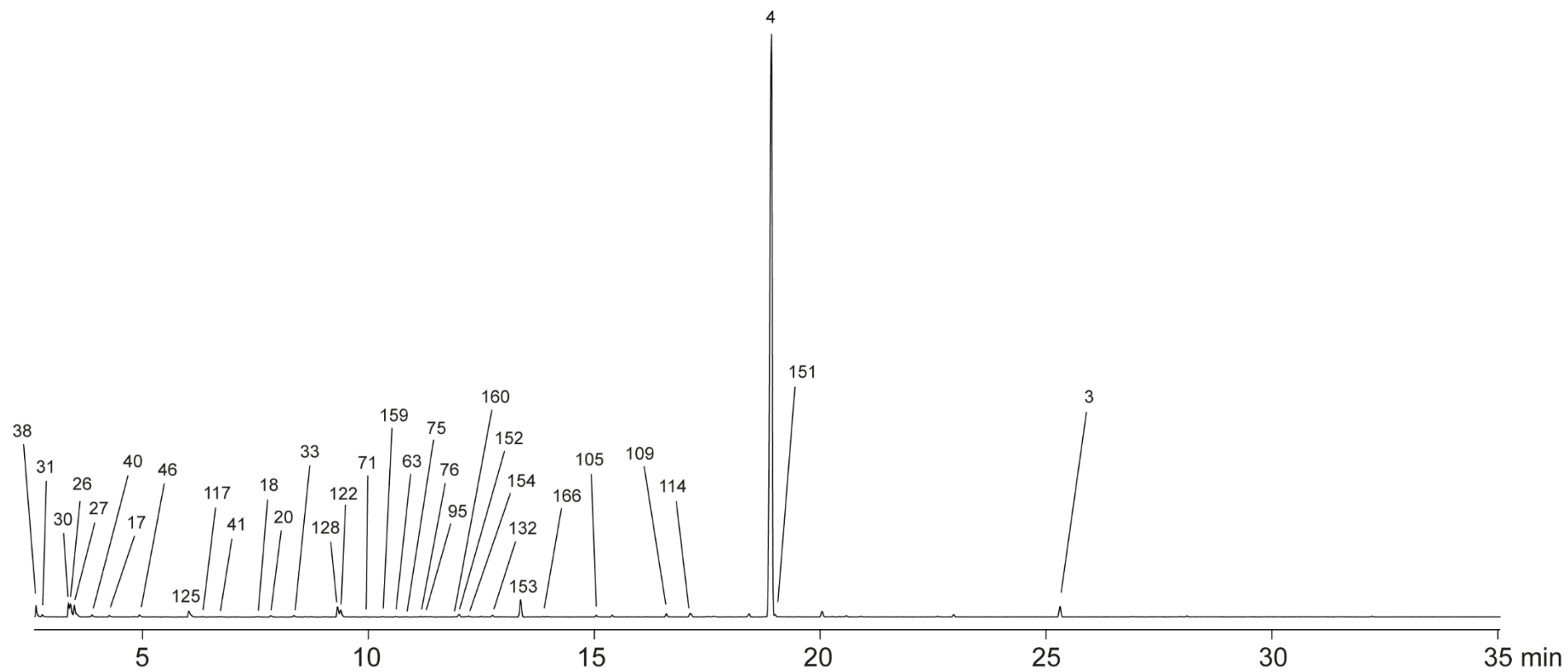


Figure 1 Total ion chromatograms of headspace extracts from investigated strains. Peak numbers refer to compound numbers in Table 2 of ESI and in main text.

Streptomyces violens NRRL ISP-5597

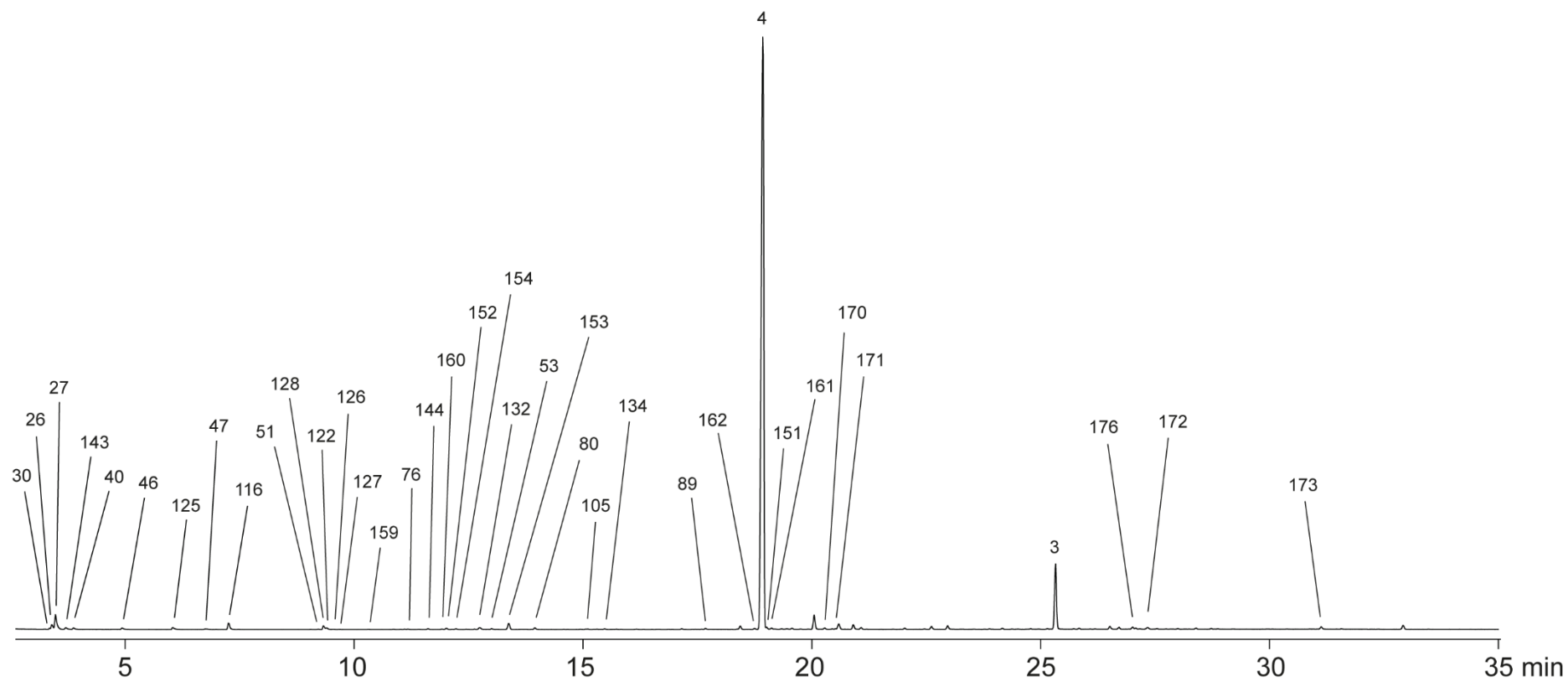


Figure 1 Total ion chromatograms of headspace extracts from investigated strains. Peak numbers refer to compound numbers in Table 2 of ESI and in main text.

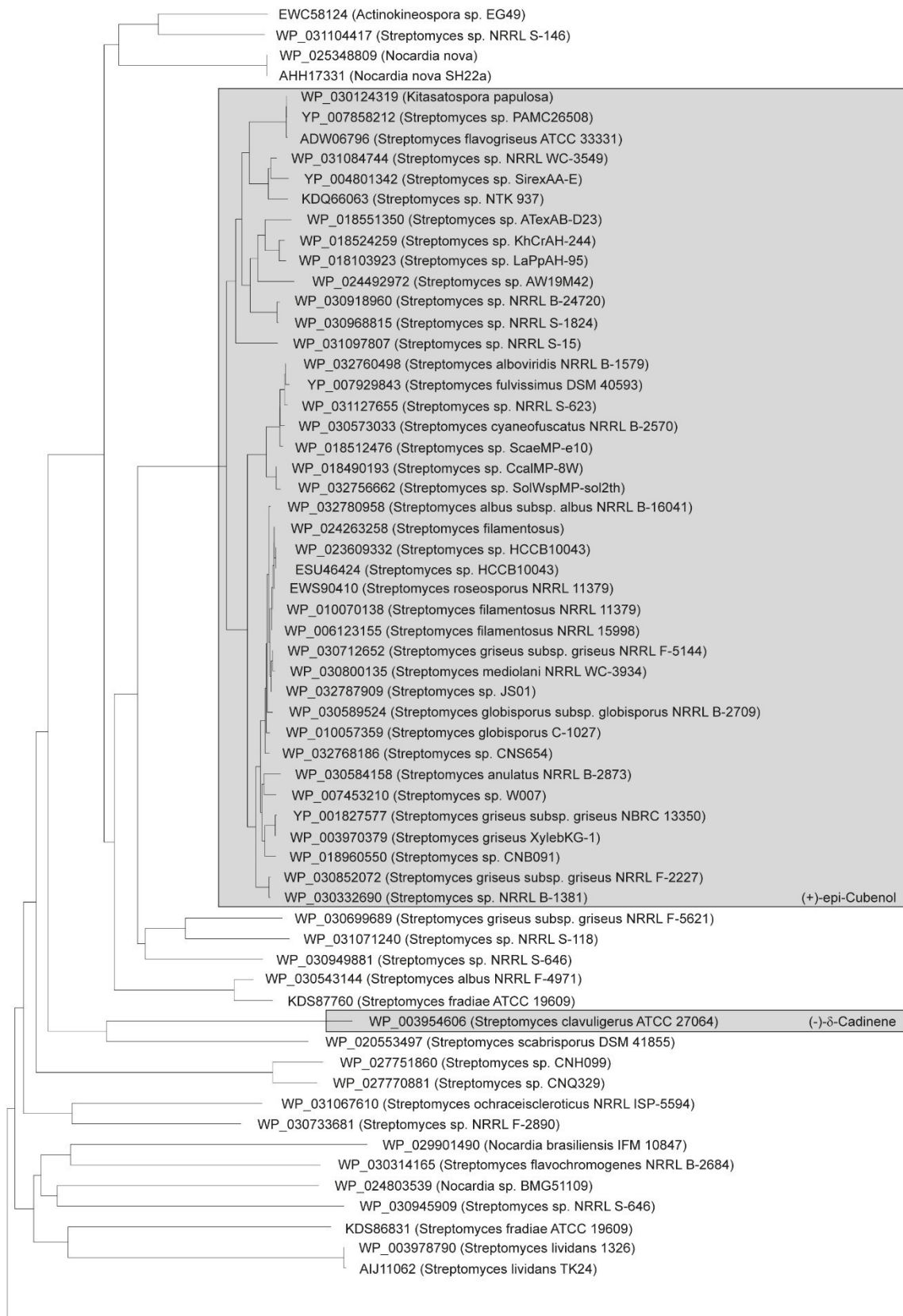


Figure 2 Phylogenetic tree of bacterial terpene cyclases.

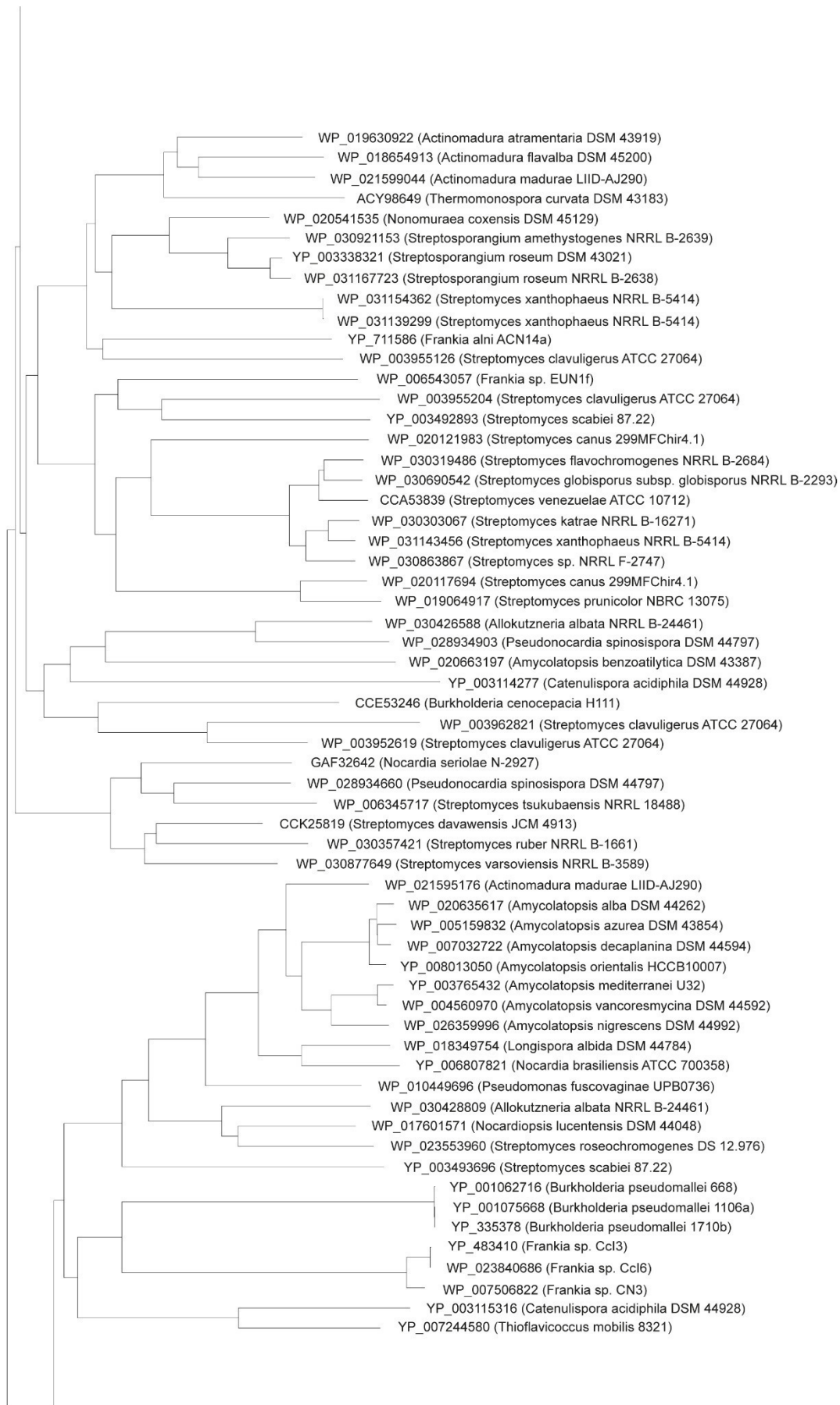


Figure 2 Phylogenetic tree of bacterial terpene cyclases.

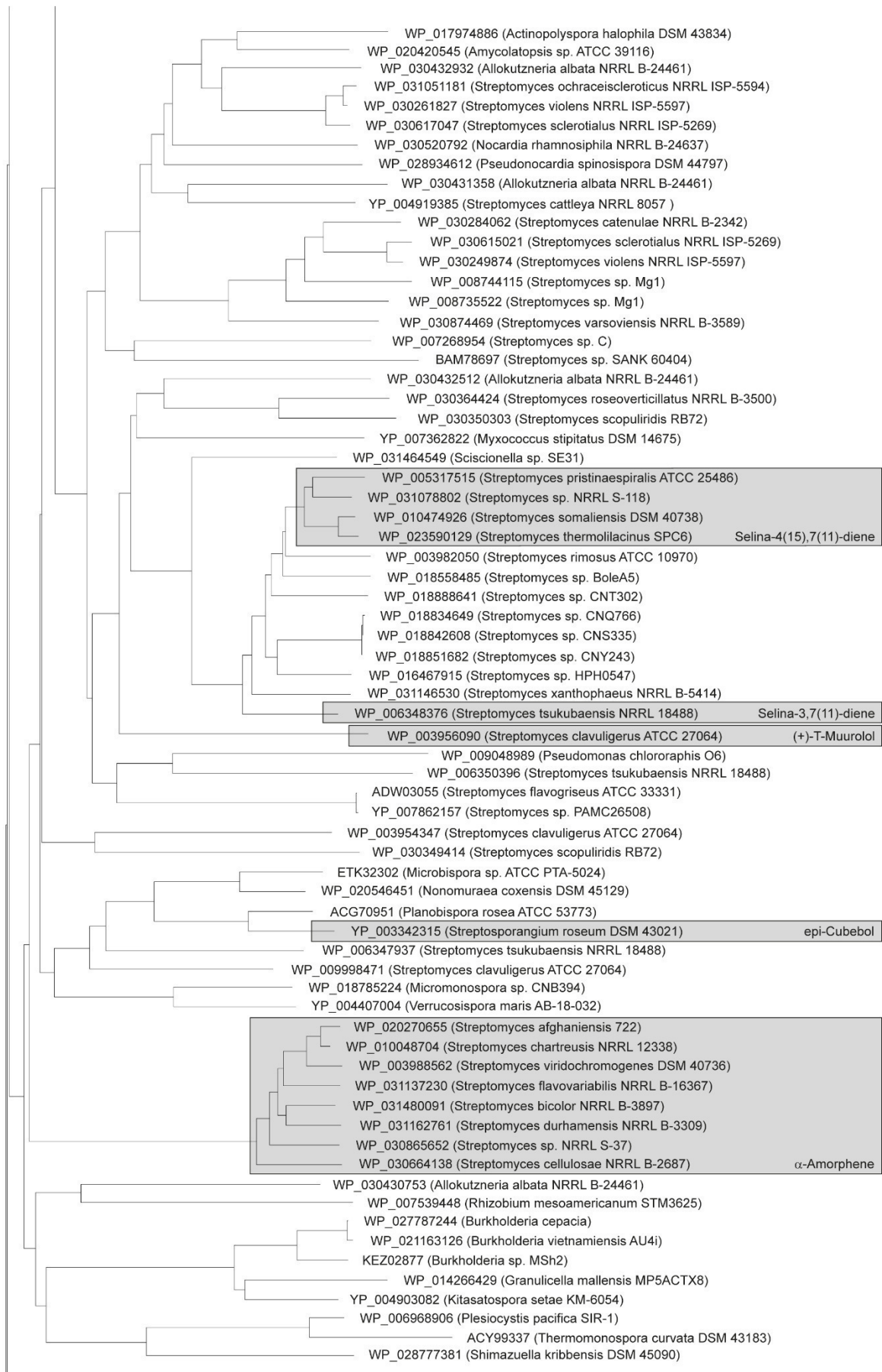


Figure 2 Phylogenetic tree of bacterial terpene cyclases.

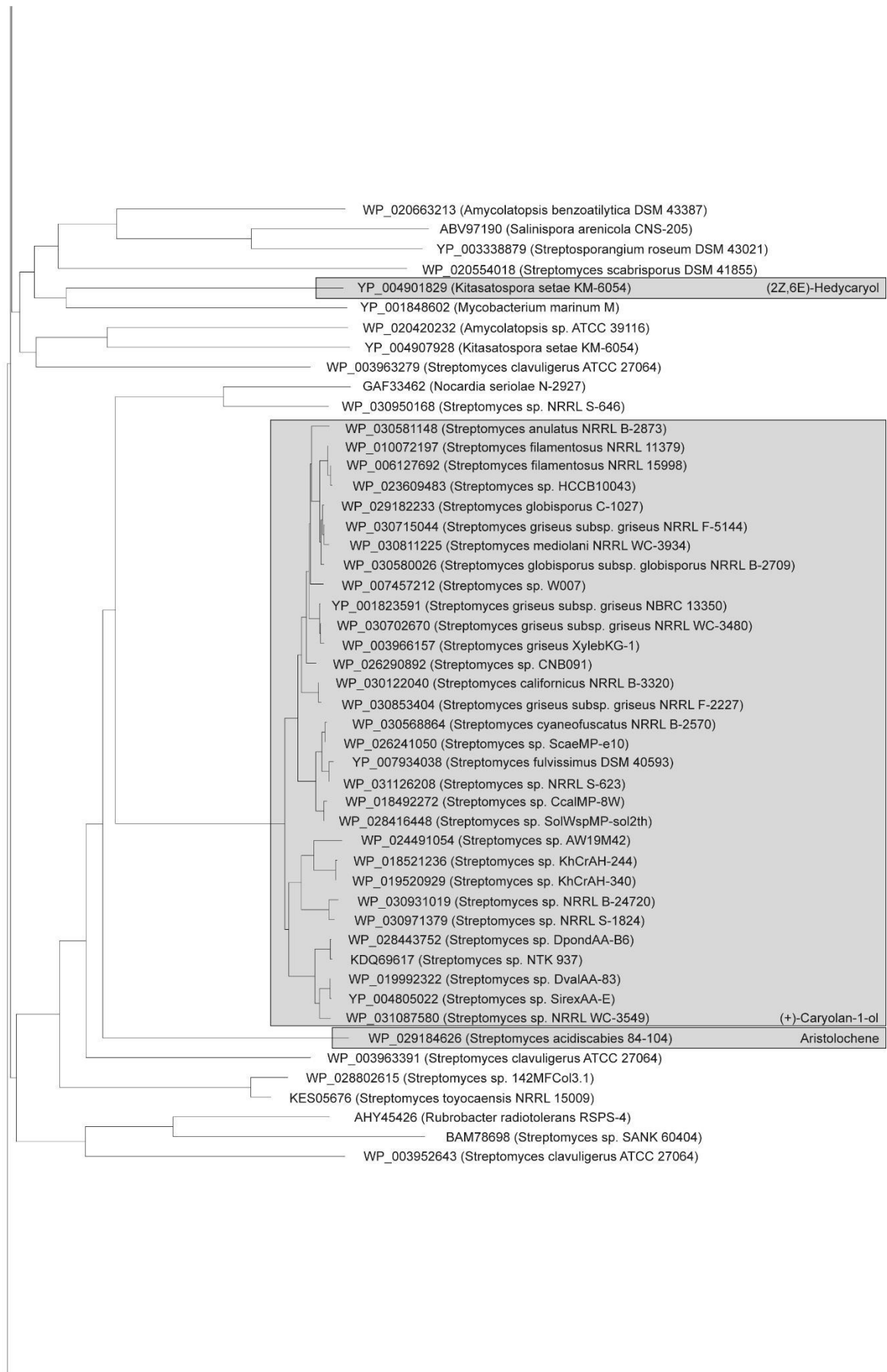


Figure 2 Phylogenetic tree of bacterial terpene cyclases.

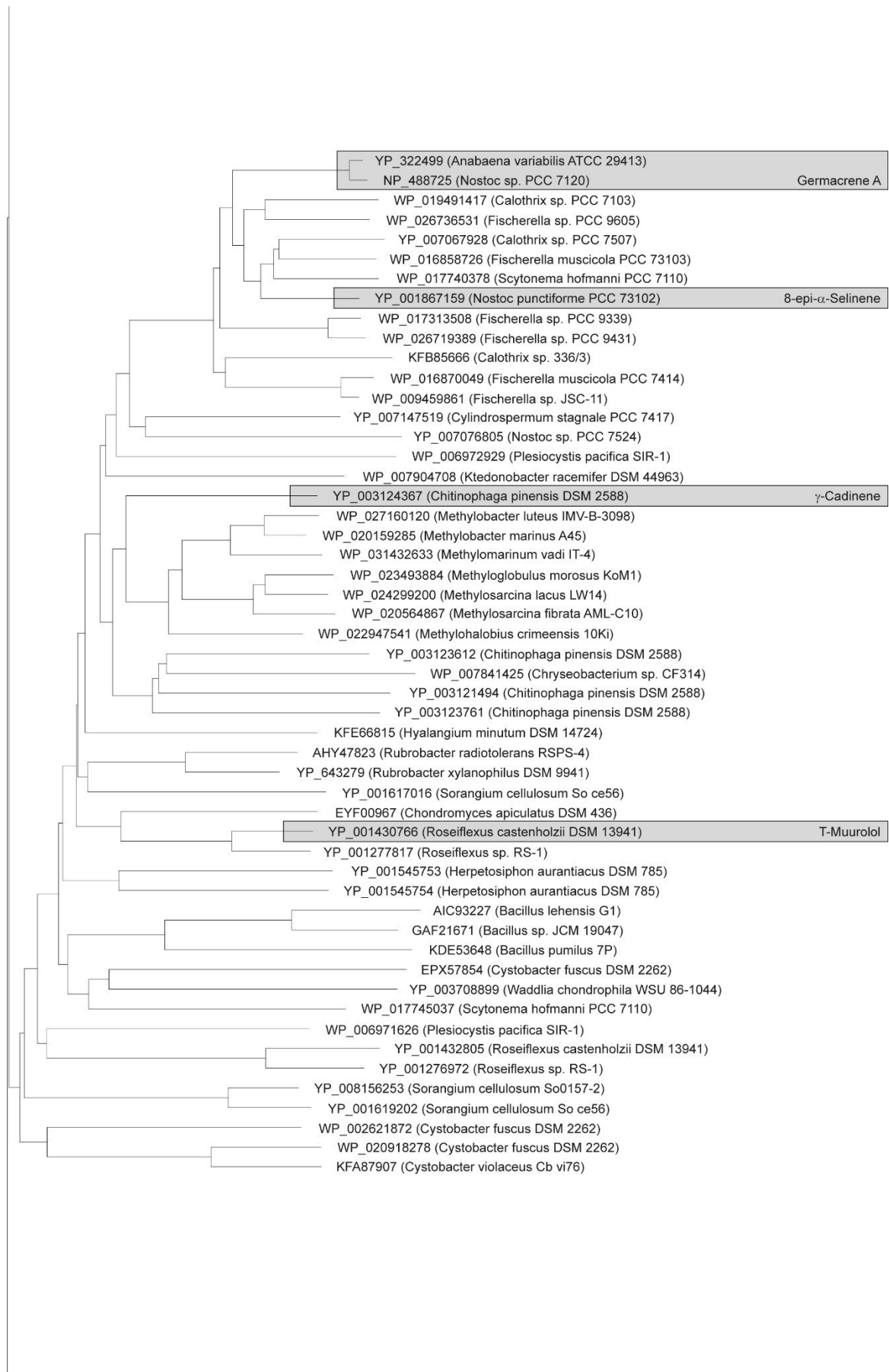


Figure 2 Phylogenetic tree of bacterial terpene cyclases.

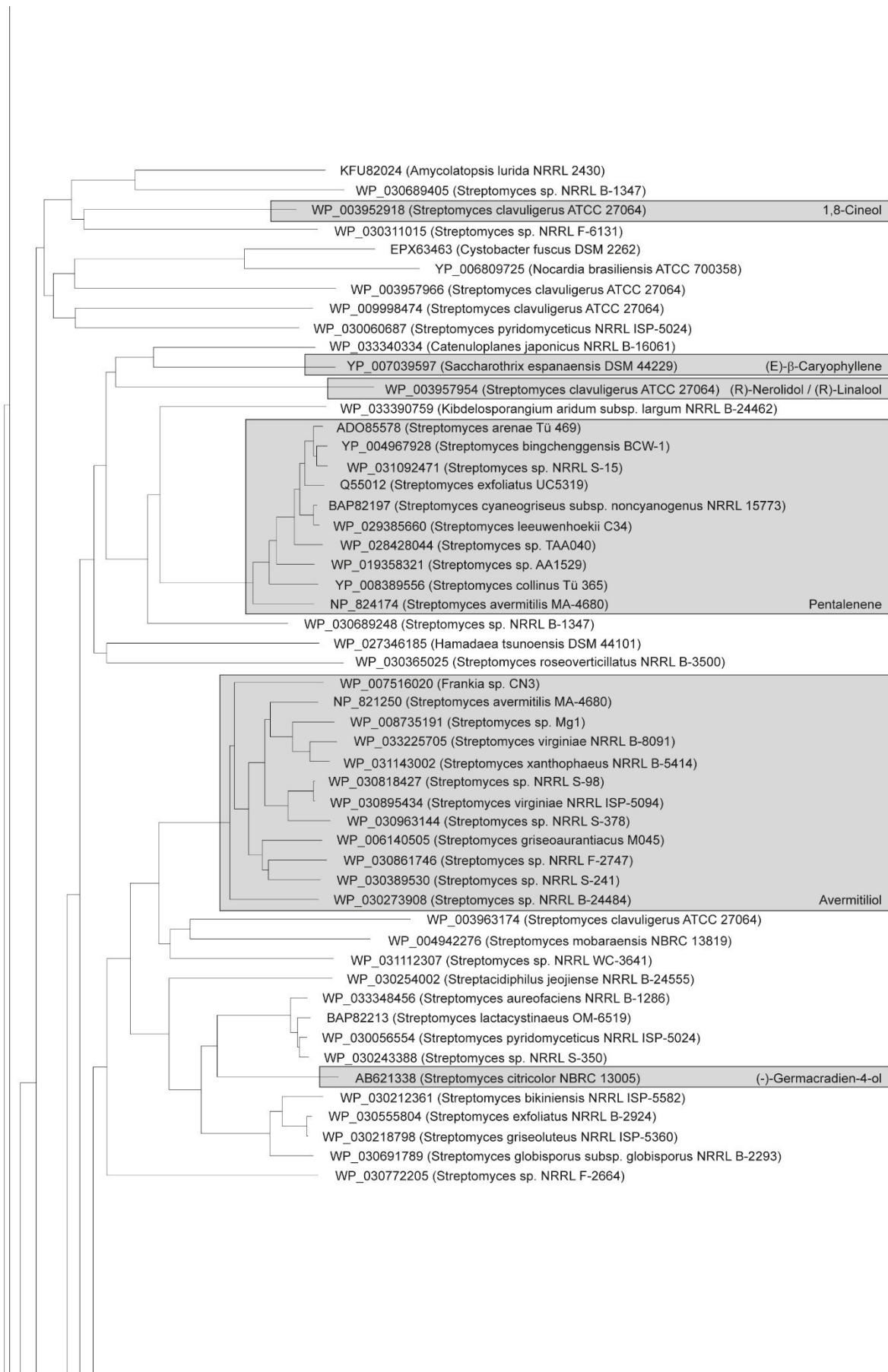


Figure 2 Phylogenetic tree of bacterial terpene cyclases.

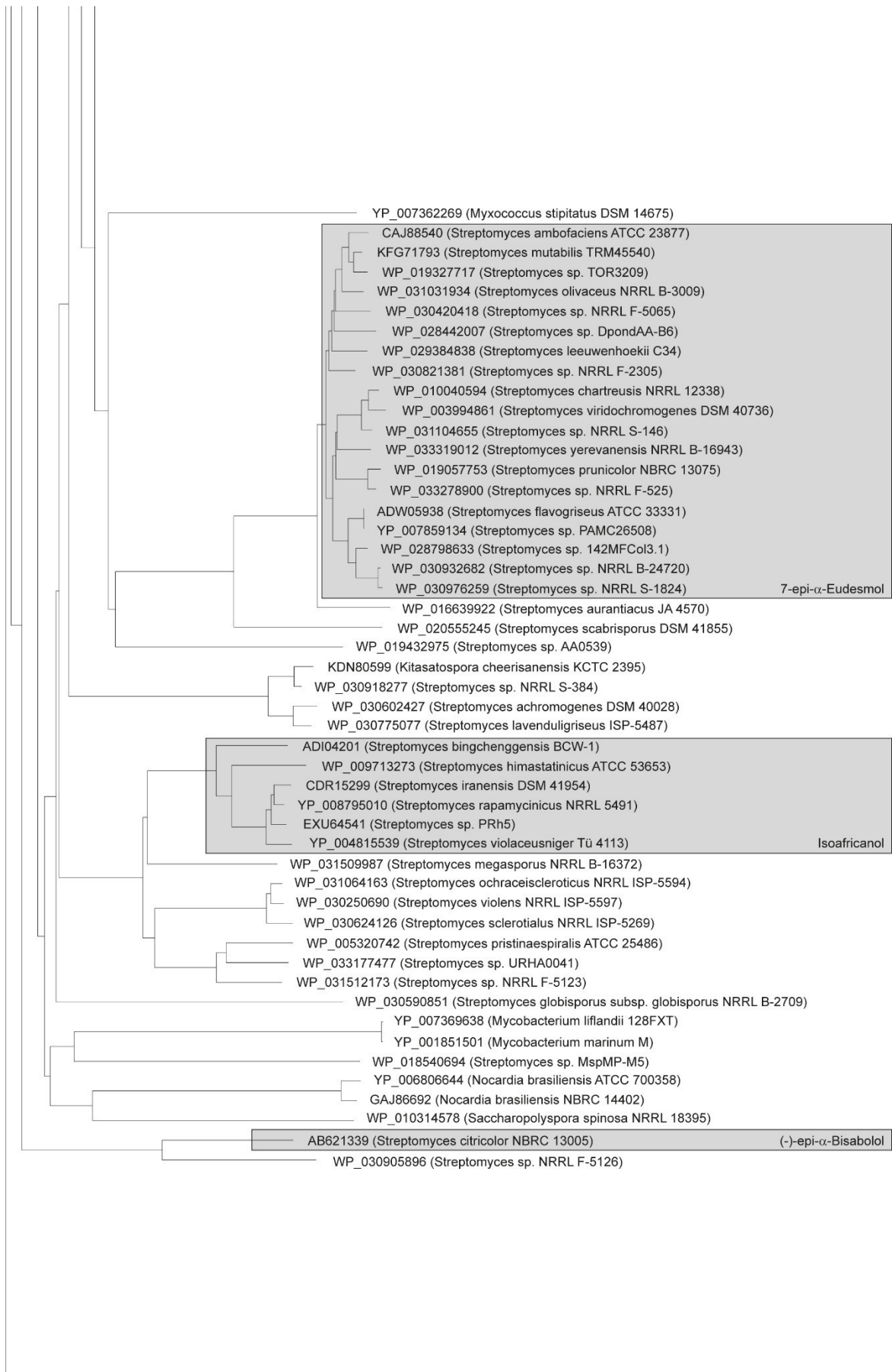


Figure 2 Phylogenetic tree of bacterial terpene cyclases.

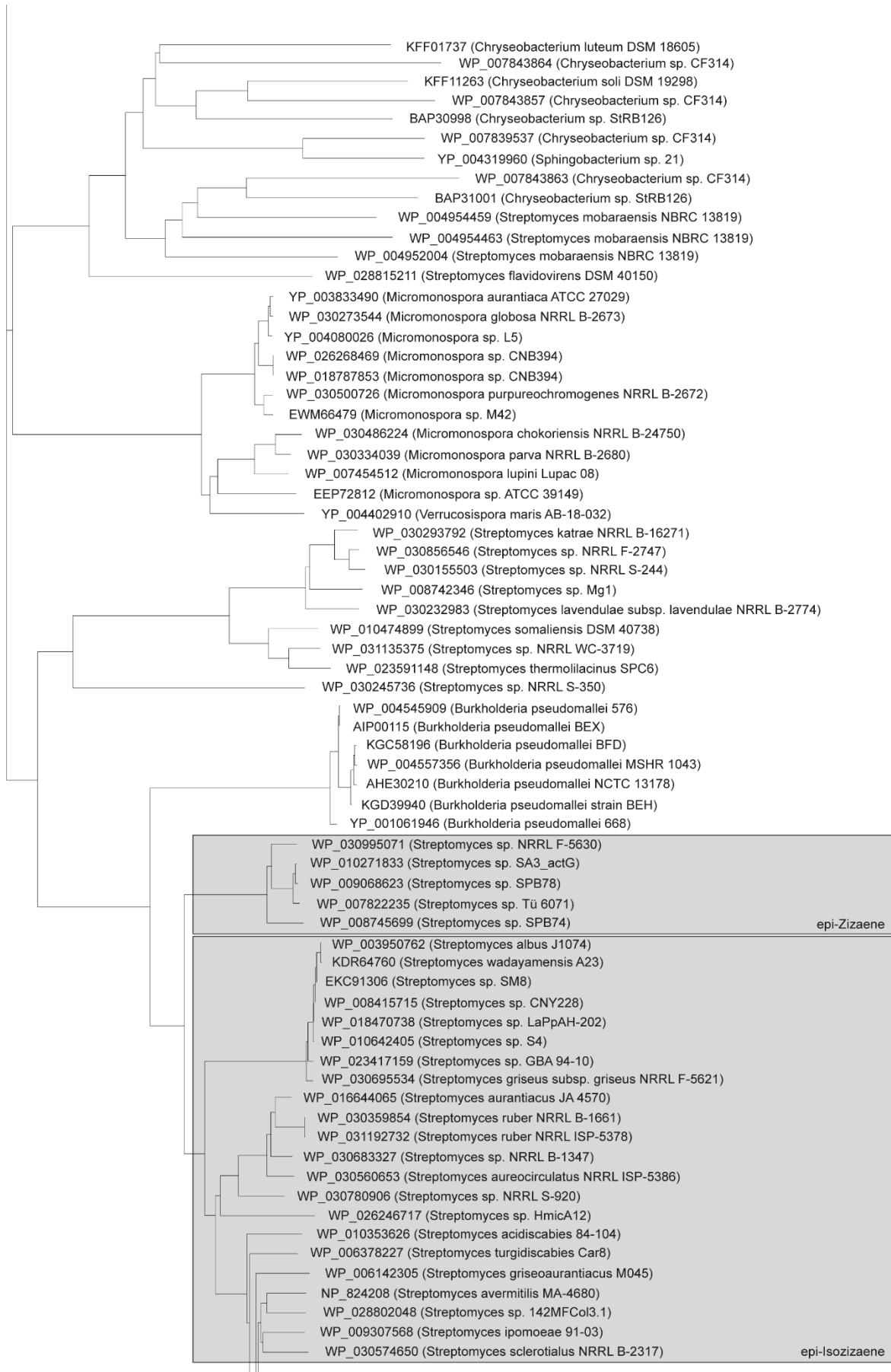


Figure 2 Phylogenetic tree of bacterial terpene cyclases.

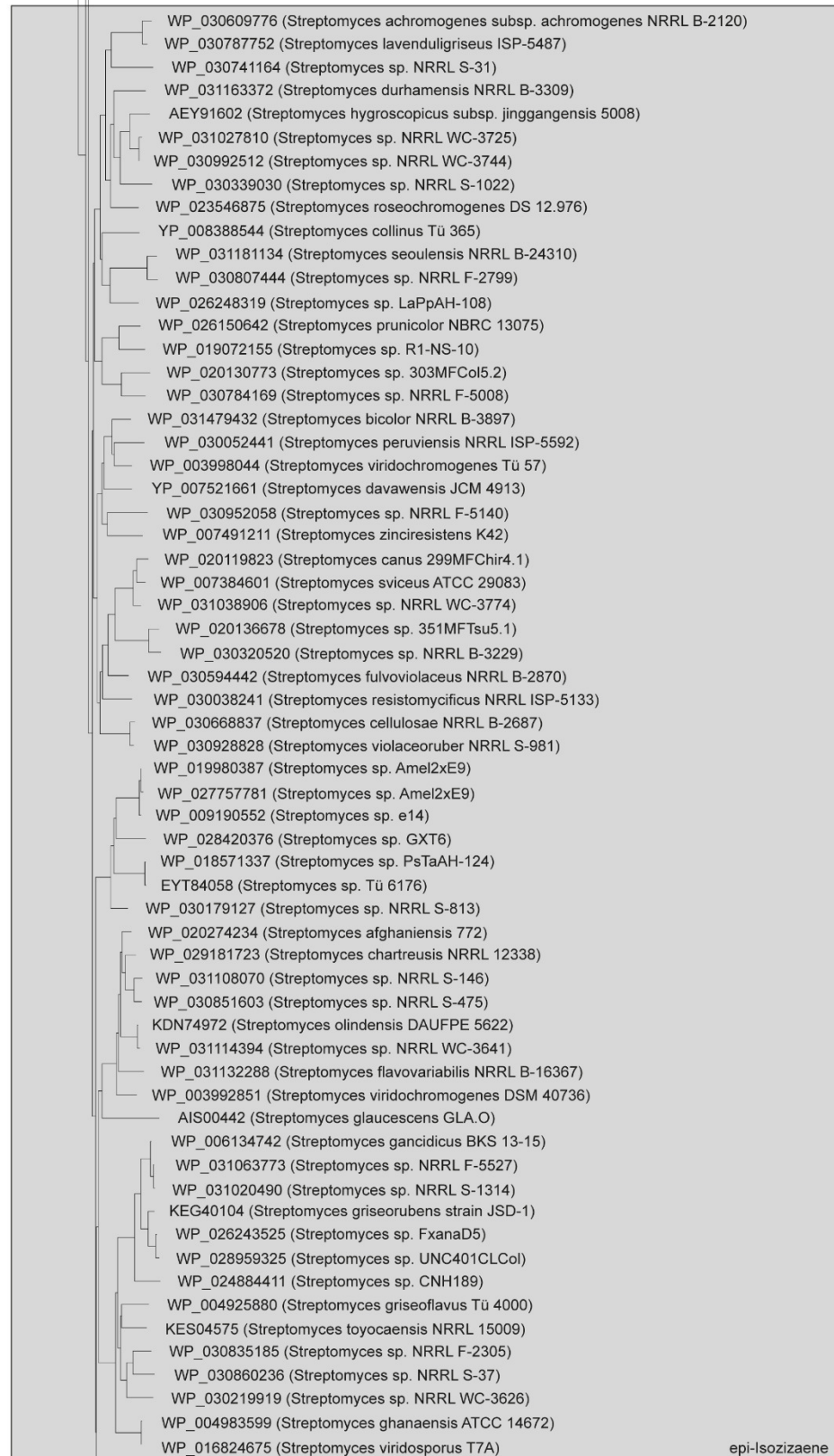


Figure 2 Phylogenetic tree of bacterial terpene cyclases.

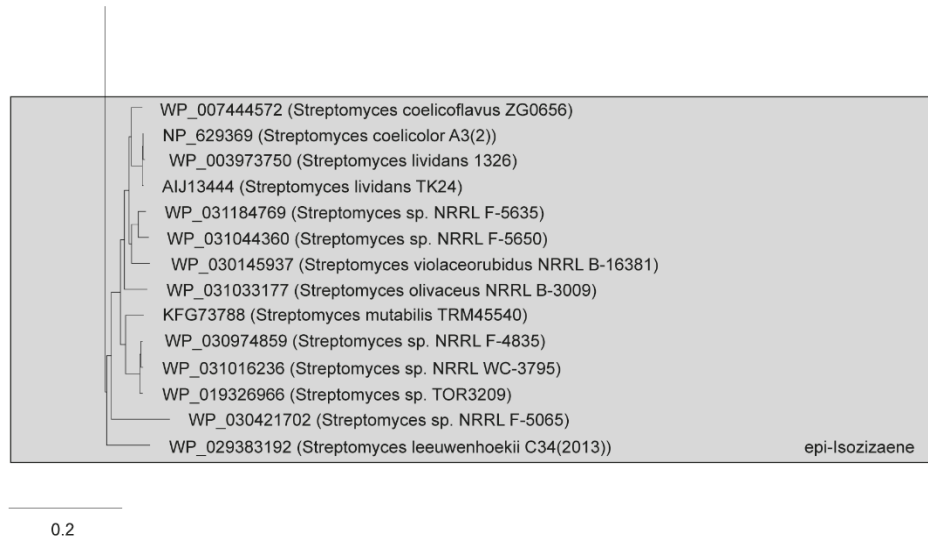


Figure 2 Phylogenetic tree of bacterial terpene cyclases.

Appendix F

Synthesis of Isotopically Labelled Oligoprenyl Diphosphates and Their Application in Mechanistic Investigations of Terpene Cyclases

Synthesis of Isotopically Labelled Oligoprenyl Diphosphates and Their Application in Mechanistic Investigations of Terpene Cyclases

Christian A. Citron,^[a] Patrick Rabe,^[a] Lena Barra,^[a] Chiaki Nakano,^[b] Tsutomu Hoshino,^[b] and Jeroen S. Dickschat*^[a]

Keywords: Synthetic methods / Biosynthesis / Terpenoids / Isotopic labelling / Phosphorylation

A flexible, efficient and robust method for the synthesis of isotopically labelled oligoprenyl diphosphates was developed. The method makes use of just a few building blocks (acetone, triethyl phosphonoacetate, and ethyl acetoacetate) from which several isotopomers with deuterium or ¹³C-labelling are commercially available or can be easily obtained by synthesis. Besides these building blocks, a few deuterated

reagents were used for the introduction of deuterium labelling. Furthermore, the synthesis of [14-²H]geranylgeranyl diphosphate is reported. The material was used for a stereochemical analysis of the cyclisation reaction catalysed by tuberculosinyl diphosphate synthase from *Mycobacterium tuberculosis*.

Introduction

The biosynthesis of terpenes starts with the formation of the universal C₅ building block dimethylallyl diphosphate (DMAPP) and isopentenyl diphosphate (IPP) that arise either via the mevalonate or the deoxyxylulose phosphate pathway. These monomers are subsequently fused by oligoprenyl diphosphate synthases to yield the linear precursors geranyl diphosphate (GPP, C₁₀), farnesyl diphosphate (FPP, C₁₅) and geranylgeranyl diphosphate (GGPP, C₂₀) with all-*E* configurations. These linear precursors are then cyclised by terpene cyclases in complex reaction cascades via cationic intermediates, usually into terpene hydrocarbons or terpene alcohols.^[1] Isotopomers of the linear terpene precursors labelled with stable (²H, ¹³C) or radioactive (³H, ¹⁴C) isotopes have been frequently used to follow the stereochemical course of terpene cyclisations,^[2,3] the regioselectivity of deprotonation steps,^[4,5] or other mechanistic aspects of terpene biosynthesis.^[6,7] For these purposes, numerous synthetic approaches to isotopomers of the linear terpene precursors DMAPP,^[8] GPP,^[2,4,6,9,10] FPP,^[5,7,11] and GGPP^[3] have been described, aiming at the introduction of isotope labels at specific and well-defined positions. Particularly interesting in addressing stereochemical problems of

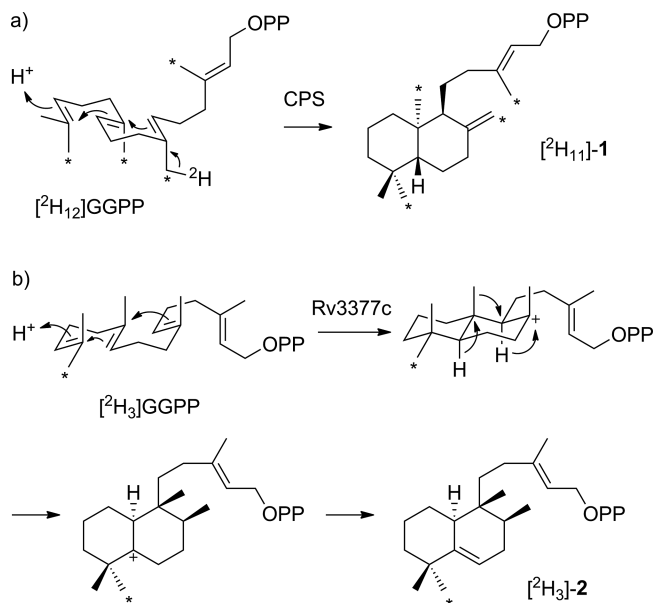
terpene biosynthesis^[12–15] are stereospecifically labelled precursors such as (1*S*)- and (1*R*)-[1-²H]FPP that have been made available by enzymatic reactions.^[12] All these isotopically labelled terpene precursors can be efficiently used in incubation experiments with recombinant terpene cyclases. Alternatively, for feeding experiments with actively growing cultures, isotopomers of the monomeric building blocks mevalonolactone or deoxyxylulose, depending on which pathway to terpenes is present in the particular organism, can be used, because these molecules are, in contrast to the oligoprenyl diphosphates, able to pass the cell membrane. For investigations on various problems of terpene biosynthesis via feeding experiments, we have recently developed flexible methods for the synthesis of various deuterated and ¹³C-labelled isotopomers of mevalonolactone^[16] and deoxyxylulose,^[17] including stereospecifically deuterated mevalonolactone isotopomers.^[18] In an exemplary investigation we have fed isotopically labelled [6,6,6-²H₃]mevalonolactone to *Fusarium fujikuroi*. This compound is transformed via the mevalonate pathway into [²H₁₂]GGPP with deuterated methyl groups as shown in Scheme 1 (a). The stereochemical course of its conversion into *ent*-copalyl diphosphate **1** by the *ent*-copalyl diphosphate synthase (CPS) with respect to the geminal methyl groups was demonstrated.^[19]

A recent example from our Japanese laboratories of using isotopically labelled oligoprenyl diphosphates for incubation experiments with purified recombinant terpene cyclases is shown in Scheme 1 (b). Incubation of [16,16,16-²H₃]GGPP with tuberculosinyl diphosphate synthase (Rv3377c) from *Mycobacterium tuberculosis* allowed us to follow the stereochemical course of the cyclisation reaction to tuberculosinyl diphosphate (**2**) via a chair-chair transition state (Scheme 1, b).^[3,20] Usually for the synthesis of

[a] Kekulé-Institut für Organische Chemie und Biochemie, Rheinische Friedrich-Wilhelms-Universität Bonn, Gerhard-Domagk-Straße 1, 53121 Bonn, Germany
E-mail: dickschat@uni-bonn.de
http://www.chemie.uni-bonn.de/oc/forschung/arbeitsgruppen/ak_dickschat

[b] Department of Applied Biological Chemistry, Faculty of Agriculture and Graduate School of Science and Technology, Niigata University, Nishi-ku, Ikarashi 2-8050, Niigata 950-2181, Japan

Supporting information for this article is available on the WWW under <http://dx.doi.org/10.1002/ejoc.201403002>.



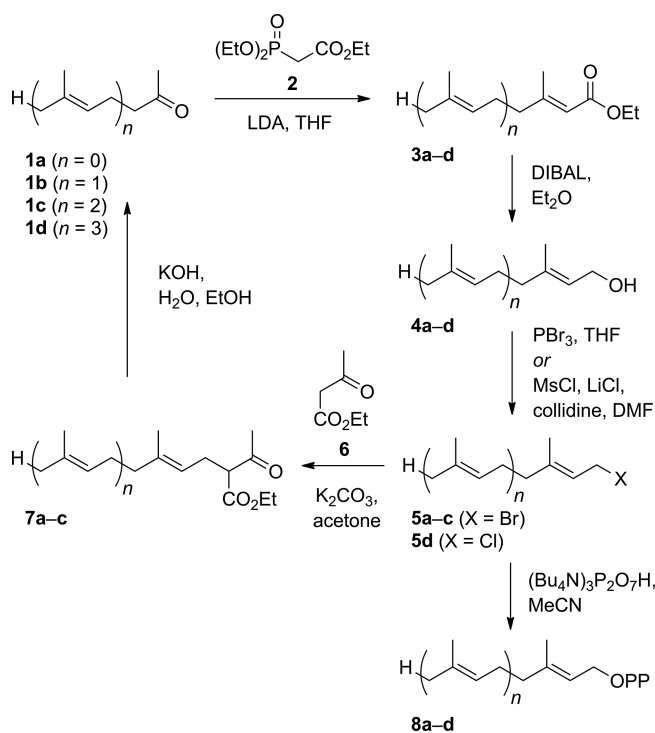
Scheme 1. Stereochemical course of cyclisation of GGPP a) to ent-copalyl diphosphate (**1**) by *Fusarium fujikuroi* ent-copalyl diphosphate synthase (CPS), and b) to tuberculosinyl diphosphate (**2**) by *Mycobacterium tuberculosis* tuberculosinyl diphosphate synthase (Rv3377c). Asterisks indicate completely deuterated methyl groups.

isotopically labelled oligoprenyl diphosphates with labelling in specific positions, a large number of steps is required, and a different strategy for the introduction of labelling for each position has to be developed. We now present a generally applicable approach for the synthesis of deuterium or ^{13}C -labelled oligoprenyl diphosphates (GPP, FPP, and GGPP) that can be used for the introduction of labelling into every position and all combinations of positions from cost-effective commercially available labelled building blocks. The compound $[14\text{-}^2\text{H}]\text{GGPP}$ was synthesised and used in an incubation experiment with tuberculosinyl diphosphate synthase, giving further insights into the stereochemical course of the reaction.

Results and Discussion

Our strategy for the synthesis of labelled oligoprenyl diphosphates with flexible introduction of stable isotope labelling is shown in Scheme 2. Starting from acetone (**1a**) we pursued a sequence of Horner–Wadsworth–Emmons (HWE) olefination with triethyl phosphonoacetate (**2**) to ethyl 3,3-dimethylacrylate (**3a**), DIBAL reduction to prenol (**4a**), transformation with PBr_3 into the corresponding bromide **5a**, alkylation with ethyl acetoacetate (**6**) to the β -keto ester **7a**, and saponification with spontaneous decarboxylation to sulcatone (**1b**). In summary, this five-step procedure results in chain elongation by one isoprene unit. We aimed at the higher homologs of **4a**, i.e. geraniol (**4b**), farnesol (**4c**), and geranylgeraniol (**4d**) by repeated analogous reactions. Their corresponding halides **5** were planned to be subjected to nucleophilic substitution with tris(tetra-butylammonium) hydrogen diphosphate to yield the desired

oligoprenyl diphosphates **8**. This route was previously used by us for the synthesis of unlabelled FPP and GGPP starting from **4b**, thus proving its practicability over two elongation cycles with an overall yield of 3% via 12 steps for the synthesis of GGPP (yields for each step are summarised in Table 1).^[21] A peculiar problem of the HWE reactions with **1c** and **1d** is the formation of *E*- and *Z*-stereoisomers, thus requiring rigorous product purification by repeated column chromatography (**3c**: *dr* = 4:1, **3d**: *dr* = 11:1, ratios based on isolated diastereomerically pure material).



Scheme 2. Synthetic strategy towards oligoprenyl diphosphates.

Table 1. Isolated yields of reactions according to Scheme 2.

Compd. ^[a]	a	b	c	d
1	n. a. ^[b]	18% ($^2\text{H}_{14}$)	93% ^[c]	88% ^[c]
3	72% ($^2\text{H}_7$)	45% ($^2\text{H}_{15}$)	93% ($^2\text{H}_1$)	88% ($^2\text{H}_1$)
4	79% ($^2\text{H}_9$)		55% ^[c]	56% ^[c]
5	(crude product was used without purification)		32% ($^2\text{H}_1$)	46% ($^2\text{H}_1$)
7	38% ($^2\text{H}_{13}$)	78% ^[c]	68% ^[c]	85% ^[c]
8		76% ($^2\text{H}_1$)	75% ($^2\text{H}_1$)	72% ($^2\text{H}_1$)
		83% ^[c]	76% ^[c]	38% ^[c]
				30% ($^2\text{H}_1$)

[a] Alphanumerical compound identifiers are according to bold numbers in Table lines to be combined with letters in Table columns. [b] n. a.: not applicable. [c] For comparison, the yields for unlabelled materials as reported previously were taken from reference.^[21]

A major advantage of the route presented in Scheme 2 is the possibility to incorporate ^{13}C -labellings into every position of the oligoprenyl diphosphates from commercially available building blocks: All three compounds used to

build the carbon frameworks, i.e. **1a**, **2**, and **6**, can be obtained with a single ^{13}C -labelling in each (incorporated) position or as multiply labelled compounds with various combinations of ^{13}C -labellings (Figure 1). The ^{13}C -labelling at the ester carbonyl carbon of **6** as it is present in two commercial isotopomers will be lost in the saponification/decarboxylation step from intermediates **7** to **1**. However, the respective isotopomers without a labelling of this lost carbon are not available from standard suppliers of fine chemicals. Therefore, the usage of the isotopomers as summarised in Figure 1 offers the most practical solution, if a synthesis aims at an introduction of the additional labellings at C-2 or at all three other carbons of **6**.

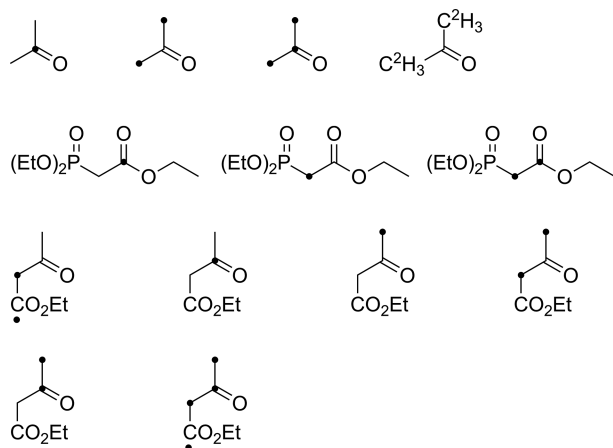
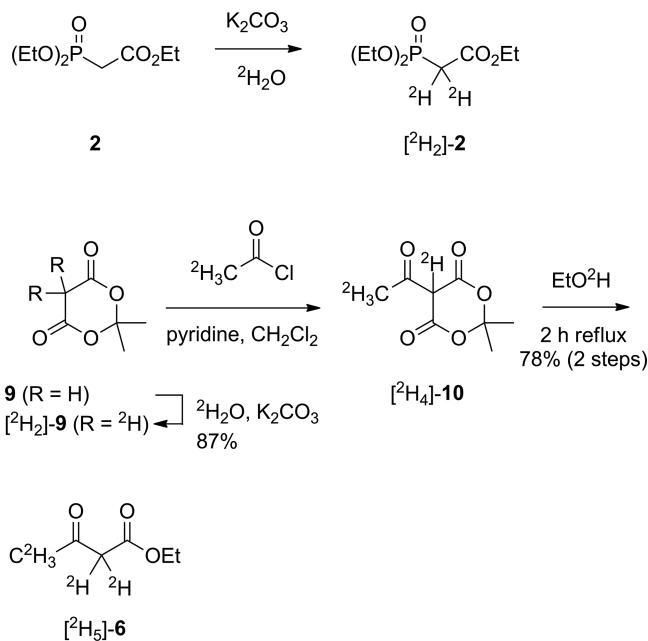


Figure 1. Commercially available deuterated and ^{13}C -labelled isotopomers of acetone (**1a**), triethyl phosphonoacetate (**2**), and ethyl acetoacetate (**6**).

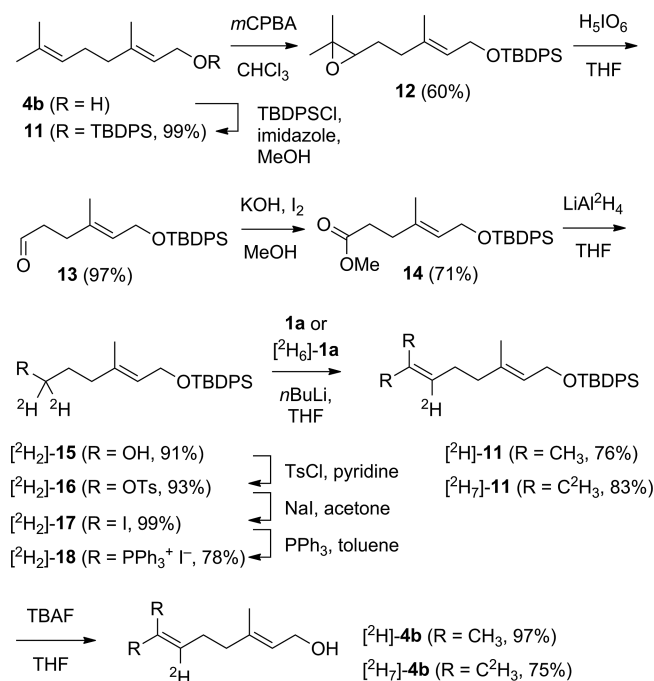
While the introduction of ^{13}C -labellings, although not performed in this study, is an obvious possibility, a special difficulty during the synthesis of analogous deuterated compounds arises by the danger of deuterium losses in ^2H , ^1H -exchange reactions, e.g. during aqueous workup. Therefore, we wanted to prove the operability of the route for the synthesis of all kinds of isotopomers of deuterated oligoprenyl diphosphates by the completion of one cycle from $^{2}\text{H}_6$ -**1a** to $^{2}\text{H}_{14}$ -**1b**. While $^{2}\text{H}_6$ -**1a** is commercially available, the other two required building blocks $^{2}\text{H}_2$ -**2** and $^{2}\text{H}_5$ -**6** were made available by synthesis (Scheme 3). Deuterated $^{2}\text{H}_2$ -**2** with a high deuterium content (>99%) was obtained from unlabelled **2** by basic ^1H , ^2H -exchange with K_2CO_3 in $^2\text{H}_2\text{O}$. The synthesis of $^{2}\text{H}_5$ -**6** was possible from Meldrum's acid (**9**), which can likewise be converted to $^{2}\text{H}_2$ -**9** by stirring in $^2\text{H}_2\text{O}$ and K_2CO_3 . Its acylation with commercially available $^{2}\text{H}_3$ acetyl chloride yielded $^{2}\text{H}_4$ -**10**, if $^2\text{H}_2\text{O}$ and ^2HCl were used for aqueous workup of the reaction. The crude product was stirred in boiling EtO^2H (deuterium content >99%) to yield the desired $^{2}\text{H}_5$ -**6**. All three deuterated building blocks $^{2}\text{H}_6$ -**1a**, $^{2}\text{H}_2$ -**2**, and $^{2}\text{H}_5$ -**6** were subsequently used to aim at a synthesis of fully deuterated $^{2}\text{H}_{14}$ -**1b**. Starting from $^{2}\text{H}_6$ -**1a**, the HWE reaction with $^{2}\text{H}_2$ -**2** to $^{2}\text{H}_7$ -**3a**, the reduction with LiAl^2H_4 to $^{2}\text{H}_9$ -**4a** and the conversion into $^{2}\text{H}_9$ -**5a** all resulted in completely deuterated materials. Surprisingly, the subsequent alkyl-



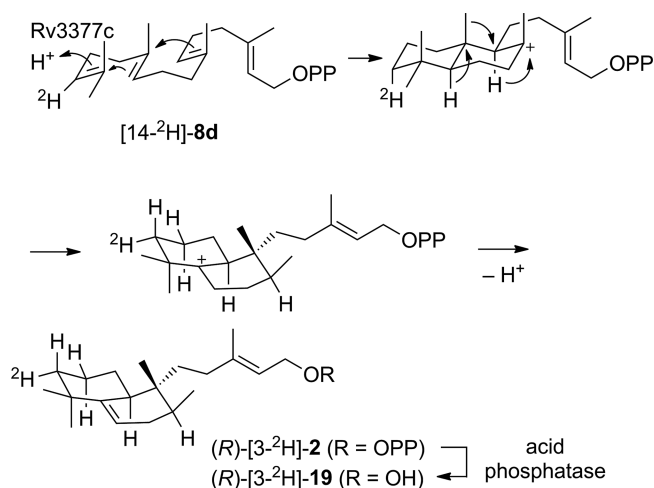
Scheme 3. Synthesis of $^{2}\text{H}_2$ -**2** and $^{2}\text{H}_5$ -**6**.

ation of $^{2}\text{H}_5$ -**6** with $^{2}\text{H}_9$ -**5a** proceeded with complete loss of the acidic deuterium at the α -carbon to yield $^{2}\text{H}_{12}$ -**7a** instead of the desired $^{2}\text{H}_{13}$ -**7a**, even if the reaction was performed in deuterated acetone as solvent. The most likely explanation for this finding is a $^2\text{H}/^1\text{H}$ -exchange with silanol groups of the silica gel in the chromatographic purification of deuterated **7a**. The lost deuterium could, however, be reintroduced in the subsequent deethoxycarbonylation with KO^2H in $^2\text{H}_2\text{O}/\text{EtO}^2\text{H}$ to $^{2}\text{H}_{12}$ -**1b** (herein, it is also crucial to use ^2HCl in the acidic workup). The yields for the overall procedure are summarised in Table 1 (cf. compounds $^{2}\text{H}_7$ -**3a**, $^{2}\text{H}_9$ -**4a**, $^{2}\text{H}_{13}$ -**7**, and $^{2}\text{H}_{14}$ -**1b**). In summary, this work demonstrated that the route of Scheme 2 can be used to incorporate deuterium into any of the positions of the oligoprenyl diphosphates with high incorporation rates. However, in contrast to the HWE reaction from $^{2}\text{H}_6$ -**1a** with $^{2}\text{H}_2$ -**2** to $^{2}\text{H}_7$ -**3a**, the corresponding conversion of $^{2}\text{H}_{14}$ -**1b** into $^{2}\text{H}_{15}$ -**3b** showed a 66% loss of deuterium at the olefinic C-2 carbon. This loss of deuterium was observed even under aqueous workup with $^2\text{H}_2\text{O}$, demonstrating that the HWE reaction is somewhat unreliable in terms of deuterium introduction.

A major disadvantage of the transformations from **1a** to **1b** as shown in Scheme 2 is the volatility of all products within this first elongation cycle which engenders significant losses of isotopically labelled material during product isolation. To overcome this problem, an easier-to-handle alternative approach for the introduction of labellings into the C-terminal portion of **4b** was developed (Scheme 4; a similar approach was reported by Stratakis and co-workers^[22]). The synthetic route starts from **4b** that was protected with TBDPSCl to yield the silyl ether **11**. Epoxidation to **12** and periodate cleavage resulted in **13**,^[23] which was converted with KOH and iodine in methanol into the methyl ester **14**. This reaction proved to be low-yielding on

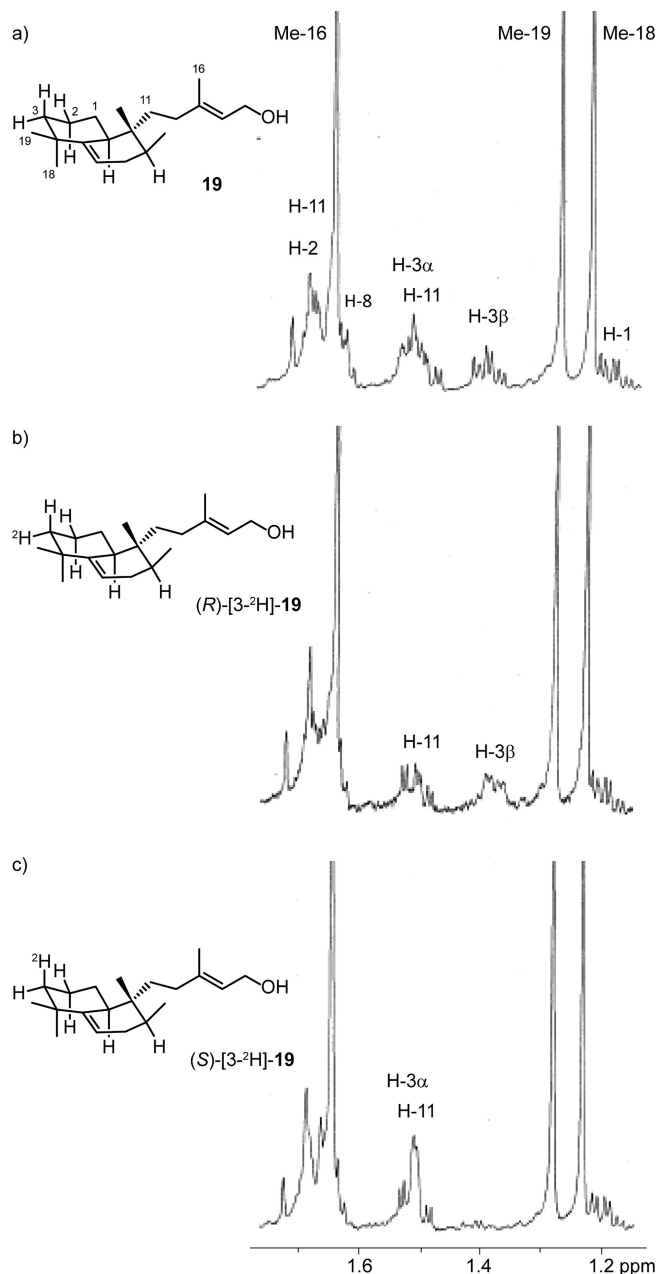
Scheme 4. Synthesis of $[\text{2H}]$ -**4b** and $[\text{2H}_7]$ -**4b**.

a large scale, and therefore, **13** was converted into **14** in ten separate ca. 20 mmol portions. Introduction of deuterium was performed by reduction with LiAlD_4 to the alcohol $[\text{2H}_2]$ -**15** which was followed by a sequence of tosylation and two subsequent nucleophilic substitutions with iodide and triphenylphosphane to the Wittig salt $[\text{2H}_2]$ -**18**. A Wittig reaction either with unlabelled **1a** or $[\text{2H}_6]$ -**1a** gave access to the TBDPS ethers $[\text{2H}]$ -**11** and $[\text{2H}_7]$ -**11**. A final deprotection with TBAF yielded the deuterated geraniol isotopomers $[\text{2H}]$ -**4b** and $[\text{2H}_7]$ -**4b** in 19% and 16% overall yield, respectively, via 10 steps. The compound $[\text{2H}]$ -**4b** was sub-

Scheme 5. Stereochemical course of cyclisation of GGPP to tuberculosinyl diphosphate (**2**) by *Mycobacterium tuberculosis* tuberculosinyl diphosphate synthase (Rv3377c). Incubation of $[\text{14-}^2\text{H}]$ GGPP, dephosphorylation by potato acid phosphatase, and ^1H NMR analysis of the product (Figure 2) demonstrated that protonation at C-14 proceeds from the *Si* side.

sequently converted into $[\text{14-}^2\text{H}]$ -**8d** by the methodology of Scheme 2. The obtained yields of this procedure are also summarised in Table 1.

The synthetic compound $[\text{14-}^2\text{H}]$ -**8d** was subsequently used in an incubation experiment with the tuberculosinyl diphosphate synthase from *M. tuberculosis* to investigate the stereochemical course of the reaction (Scheme). The product obtained was dephosphorylated with acid phosphatase from potato to tuberculosinol (**19**) and then analysed by ^1H NMR spectroscopy. In unlabelled **19**, the signal

Figure 2. a) ^1H NMR spectrum of **19**, b) ^1H NMR spectrum of (R) - $[\text{3-}^2\text{H}]$ -**19** obtained from the incubation of $[\text{14-}^2\text{H}]$ -**8d** with tuberculosinyl diphosphate synthase and dephosphorylation, and c) ^1H NMR spectrum of (S) - $[\text{3-}^2\text{H}]$ -**19** obtained from the incubation of **8d** with tuberculosinyl diphosphate synthase in deuterium oxide and dephosphorylation.

at $\delta_{\text{H}} = 1.39$ exhibited a ddd splitting pattern ($J = 12.5, 12.5, 5.4$ Hz), indicating that this signal can be assigned to H-3 β , while the signal at $\delta_{\text{H}} = 1.53$ was assignable to H-3 α (Figure 2, a). The latter signal overlapped with that of H-11, but these assignments were unambiguously confirmed by the HSQC spectrum. Feeding of [14- ^2H]-**8d** resulted in a missing signal for the 3-*pro-R* hydrogen (H-3 α) in the ^1H NMR spectrum (Figure 2, b), indicating that [14- ^2H]-**8d** is converted into (*R*)-[3- ^2H]-**19**, consistent with a protonation of the substrate from the *Si* side at C-14. This result was corroborated by a complementary experiment in which unlabelled **8d** was incubated with the tuberculosinyl diphosphate synthase in deuterium oxide followed by dephosphorylation. The signal for the 3-*pro-S* hydrogen (H-3 β) was missing in the ^1H NMR spectrum of the enzyme product (Figure 2, c), establishing its structure as (*S*)-[3- ^2H]-**19** which is in full agreement with the previous finding.

Conclusions

In summary, we have presented an efficient, flexible and robust protocol for the synthesis of oligoprenyl diphosphates with stable isotope labelling from just a few cost-effective, commercially available building blocks and reagents. Many of the reactions summarised in Table 1 have been performed several times in our laboratories, but not always with isotopically labelled material. Since yield optimisation with labelled compounds would be too expensive, the optimised yields for each step as they were obtained with unlabelled material^[21] are also included in Table 1. These data show which yields along the route are possible. We have shown that deuterium labelling can be efficiently introduced in any position of the isoprenoid precursors using the presented chemistry. Only the Horner–Wadsworth–Emmons reaction with [$^2\text{H}_2$]-**2** proved to be somewhat unreliable and proceeded in single cases with partial loss of deuterium labelling. The prepared compound [14- ^2H]GGPP was used in an incubation experiment with the tuberculosinyl diphosphate synthase from *M. tuberculosis*, followed by dephosphorylation. The ^1H NMR analysis of the enzyme's product demonstrated that the substrate was protonated from the *Si* face at C-14, which was further corroborated by the complementary experiment of GGPP incubation in deuterium oxide and dephosphorylation. These and similar experiments using other isotopically labelled oligoprenyl diphosphates prepared via our route are currently being performed in our laboratory.

Experimental Section

General Methods: Chemicals were purchased from Acros Organics (Geel, Belgium) or Sigma Aldrich Chemie GmbH (Steinheim, Germany) and used without further purification. All nonaqueous reactions were performed under an inert atmosphere (N_2) in flame-dried flasks. Solvents were purified by distillation and dried according to standard methods. Thin-layer chromatography was performed with 0.2 mm pre-coated plastic sheets Polygram[®] Sil G/UV254 (Machery–Nagel). Column chromatography was carried

out using Merck silica gel 60 (70–200 mesh). ^1H NMR and ^{13}C NMR spectra were recorded with Bruker DRX-400 (400 MHz) or AV III-400 (400 MHz) spectrometers, and were referenced against TMS ($\delta = 0.00$ ppm) for ^1H NMR and CDCl_3 ($\delta = 77.01$ ppm) for ^{13}C -NMR spectroscopy. IR spectra were recorded with a Bruker Tensor 27 ATR (attenuated total reflectance) instrument. GC–MS analyses were carried out with a HP 6890 gas chromatograph connected to a HP 5973 inert mass detector fitted with a BPX-5 (25 m, 0.25 mm i. d., 0.25 μm film) or HP5-MS (30 m, 0.25 mm i. d., 0.25 μm film) fused silica capillary column. Instrumental parameters were (1) inlet pressure, 77.1 kPa, He flow 23.3 mL min^{-1} , (2) injection volume, 2 μL , (3) transfer line, 300 $^\circ\text{C}$, and (4) electron energy 70 eV. The GC was programmed as follows: 5 min at 50 $^\circ\text{C}$ increasing at 10 $^\circ\text{C min}^{-1}$ to 320 $^\circ\text{C}$, and operated in split mode (20:1, 60 s valve time). The carrier gas was He at 1 mL min^{-1} . Retention indices (*I*) were determined from a homologous series of *n*-alkanes (C_8 – C_{38}).

(*E*)-*tert*-Butyl[(3,7-dimethylocta-2,6-dien-1-yl)oxy]diphenylsilane (11): A solution of geraniol (**4b**) (51.1 g, 331 mmol, 1.0 equiv.) in DMF (300 mL) was treated with imidazole (49.5 g, 729 mmol, 2.2 equiv.). After the imidazole was dissolved, the solution was cooled to 0 $^\circ\text{C}$ and TBDPS-Cl (100 g, 365 mmol, 1.1 equiv.) was added dropwise. The reaction mixture was stirred for 3 h at room temperature and afterwards quenched by the addition of H_2O . The aqueous layer was extracted three times with Et_2O , and the combined organic layers were washed with a satd. aqueous solution of NaHCO_3 . After drying with MgSO_4 and concentration under reduced pressure, the product **11** (129 g, 329 mmol, 99%) was obtained as a yellow oil. $R_f = 0.89$ [hexane/EtOAc (5:1)]. GC (BPX-5): $I = 2550$. ^1H NMR (400 MHz, CDCl_3 , TMS): $\delta = 7.72$ – 7.69 (m, 4 H, 4 \times CH), 7.43–7.23 (m, 6 H, 6 \times CH), 5.40–5.37 (m, 1 H, CH), 5.12–5.08 (m, 1 H, CH), 4.23 (d, $^3J_{\text{H,H}} = 6.3$ Hz, 2 H, CH_2), 2.09–2.04 (m, 2 H, CH_2), 1.99–1.96 (m, 2 H, CH_2), 1.68 (d, $^4J_{\text{H,H}} = 0.6$ Hz, 3 H, CH_3), 1.60 (s, 3 H, CH_3), 1.43 (s, 3 H, CH_3), 1.05 (s, 9 H, 3 \times CH_3) ppm. ^{13}C NMR (100 MHz, CDCl_3): $\delta = 137.0$ (C_q), 135.6 (4 \times CH), 134.1 (C_q), 131.5 (2 \times C_q), 129.5 (2 \times CH), 127.6 (4 \times CH), 124.1 (CH), 124.0 (CH), 61.2 (CH_2), 39.5 (CH_2), 26.8 (3 \times CH_3), 26.4 (CH_2), 25.7 (CH_3), 19.2 (C_q), 17.7 (CH_3), 16.3 (CH_3) ppm. MS (EI, 70 eV): m/z (%) = 392 (<1) [$\text{M}]^+$, 335 (27), 257 (3), 199 (100), 181 (5), 135 (5), 69 (3), 41 (3). IR (ATR): $\tilde{\nu} = 3071$ (w), 3050 (w), 2961 (w), 2930 (w), 2857 (w), 1428 (w), 1108 (s), 1056 (m), 822 (m), 738 (m), 700 (s), 610 (m) cm^{-1} . UV/Vis (CH_2Cl_2): λ_{max} (ϵ , $\text{L mol}^{-1} \text{cm}^{-1}$) = 271 (495), 265 (699), 260 (689), 228 (6229) nm.

(*E*)-*tert*-Butyl[5-(3,3-dimethyloxiran-2-yl)-3-methylpent-2-en-1-yl]oxy]diphenylsilane (12): Compound **11** (129 g, 329 mmol, 1.0 equiv.) was dissolved in CHCl_3 (1000 mL) and cooled to 0 $^\circ\text{C}$. In one portion, *m*CPBA (88.9 g, 362 mmol, 1.1 equiv.) was added, and the reaction mixture was stirred for 1 h at 0 $^\circ\text{C}$. The mixture was then washed with a satd. solution of NaHCO_3 , brine, and H_2O . The organic layer was dried with MgSO_4 and concentrated under reduced pressure. Column chromatography with hexane/EtOAc (10:1) yielded the desired epoxide **12** (80.5 g, 197 mmol, 60%) as a colorless oil. $R_f = 0.58$ [hexane/EtOAc (5:1)]. GC (BPX-5): $I = 2675$. ^1H NMR (400 MHz, CDCl_3 , TMS): $\delta = 7.73$ – 7.68 (m, 4 H, 4 \times CH), 7.43–7.35 (m, 6 H, 6 \times CH), 5.42 (tq, $^3J_{\text{H,H}} = 6.4$, $^4J_{\text{H,H}} = 1.2$ Hz, 1 H, CH), 4.23 (d, $^3J_{\text{H,H}} = 6.3$ Hz, 2 H, CH_2), 2.70 (t, $^3J_{\text{H,H}} = 6.3$ Hz, 1 H, CH), 2.15–2.03 (m, 2 H, CH_2), 1.68–1.57 (m, 2 H, CH_2), 1.46 (s, 3 H, CH_3), 1.30 (s, 3 H, CH_3), 1.26 (s, 3 H, CH_3), 1.04 (s, 9 H, 3 \times CH_3) ppm. ^{13}C NMR (100 MHz, CDCl_3): $\delta = 136.1$ (C_q), 135.6 (4 \times CH), 133.9 (2 \times C_q), 129.5 (2 \times CH), 127.6 (4 \times CH), 124.6 (CH), 64.0 (CH), 61.0 (CH_2), 58.3 (C_q), 36.1 (CH_2), 27.1 (CH_2), 26.8 (3 \times CH_3), 24.9 (CH_3), 19.1 (C_q), 18.7

(CH₃), 16.3 (CH₃) ppm. MS (EI, 70 eV): *m/z* (%) = 408 (<1) [M]⁺, 351 (2), 273 (6), 199 (100), 181 (7), 135 (24), 107 (5), 77 (4). IR (ATR): $\tilde{\nu}$ = 3071 (w), 3049 (w), 2959 (w), 2931 (w), 2891 (w), 2857 (w), 1428 (w), 1110 (m), 821 (m), 739 (m), 701 (s), 608 (m) cm⁻¹. UV/Vis (CH₂Cl₂): λ_{\max} (ϵ , L mol⁻¹ cm⁻¹) = 271 (461), 265 (686), 260 (686), 253 (641), 228 (6823) nm.

(E)-6-[(*tert*-Butyldiphenylsilyloxy)-4-methylhex-4-enal (13): Epoxide **12** (80.5 g, 197 mmol, 1.0 equiv.) was dissolved in THF (400 mL) and cooled to 0 °C. Within 90 min, a solution of H₅IO₆ (53.9 g, 236 mmol, 1.2 equiv.) in THF (400 mL) was added dropwise. After complete addition, the reaction mixture was stirred for an additional 2 h at 0 °C. The reaction was extracted with Et₂O, dried with MgSO₄ and concentrated under reduced pressure to give aldehyde **13** (69.9 g, 191 mmol, 97%) as a pale yellow oil. *R*_f = 0.44 [hexane/EtOAc (5:1)]. GC (BPX-5): *I* = 2493. ¹H NMR (400 MHz, CDCl₃, TMS): δ = 9.73 (t, ³*J*_{H,H} = 1.8 Hz, 1 H, CHO), 7.73–7.67 (m, 4 H, 4 × CH), 7.41–7.35 (m, 6 H, 6 × CH), 5.38 (tq, ³*J*_{H,H} = 6.2, ⁴*J*_{H,H} = 1.3 Hz, 1 H, CH), 4.22 (d, ³*J*_{H,H} = 6.3 Hz, 2 H, CH₂), 2.50–2.46 (m, 2 H, CH₂), 2.30–2.26 (m, 2 H, CH₂), 1.44 (s, 3 H, CH₃), 1.04 (s, 9 H, 3 × CH₃) ppm. ¹³C NMR (100 MHz, CDCl₃): δ = 202.1 (CHO), 135.6 (4 × CH), 134.8 (C_q), 133.9 (2 × C_q), 129.5 (2 × CH), 127.6 (4 × CH), 125.0 (CH), 60.9 (CH₂), 41.8 (CH₂), 31.4 (CH₂), 26.8 (3 × CH₃), 19.1 (C_q), 16.4 (CH₃) ppm. MS (EI, 70 eV): *m/z* (%) = 366 (<1) [M]⁺, 309 (9), 231 (24), 213 (6), 199 (100), 183 (10), 139 (14), 105 (4), 77 (9). IR (ATR): $\tilde{\nu}$ = 3071 (w), 3049 (w), 2957 (w), 2931 (w), 2891 (w), 2857 (w), 1725 (w), 1428 (w), 1110 (s), 1069 (m), 822 (m), 740 (m), 702 (s), 611 (m) cm⁻¹. UV/Vis (CH₂Cl₂): λ_{\max} (ϵ , L mol⁻¹ cm⁻¹) = 271 (354), 265 (687), 260 (649), 230 (4042) nm.

Methyl (E)-6-[(*tert*-Butyldiphenylsilyloxy)-4-methylhex-4-enoate (14): Aldehyde **13** (7.3 g, 20.0 mmol, 1.0 equiv.) was dissolved in MeOH (200 mL) and cooled 0 °C. Subsequently, solutions of KOH (2.9 g, 52.0 mmol, 2.6 equiv.) in MeOH (67 mL) and I₂ (6.6 g, 26.0 mmol, 1.3 equiv.) in MeOH (34 mL) were added, and stirring was continued for 90 min at 0 °C. The reaction mixture was diluted with EtOAc (1 L) and washed three times with satd. aqueous Na₂S₂O₃ and with brine. The organic layer was dried with MgSO₄ and concentrated under reduced pressure. Column chromatography with hexane/EtOAc (10:1) yielded product **14** (5.6 g, 14.0 mmol, 71%) as a yellowish oil. *R*_f = 0.32 [hexane/EtOAc (10:1)]. GC (BPX-5): *I* = 2592. ¹H NMR (400 MHz, CDCl₃, TMS): δ = 7.70–7.66 (m, 4 H, 4 × CH), 7.44–7.35 (m, 6 H, 6 × CH), 5.39 (tq, ³*J*_{H,H} = 6.5, ⁴*J*_{H,H} = 1.3 Hz, 1 H, CH), 4.21 (d, ³*J*_{H,H} = 6.3 Hz, 2 H, CH₂), 3.66 (s, 3 H, CH₃), 2.42–2.38 (m, 2 H, CH₂), 2.31–2.27 (m, 2 H, CH₂), 1.44 (s, 3 H, CH₃), 1.04 (s, 9 H, 3 × CH₃) ppm. ¹³C NMR (100 MHz, CDCl₃): δ = 173.7 (CO), 135.6 (4 × CH), 135.2 (C_q), 133.9 (2 × C_q), 129.5 (2 × CH), 127.6 (4 × CH), 124.8 (CH), 61.0 (CH₂), 51.5 (CH₃), 34.3 (CH₂), 32.6 (CH₂), 26.8 (3 × CH₃), 19.1 (C_q), 16.2 (CH₃) ppm. MS (EI, 70 eV): *m/z* (%) = 396 (<1) [M]⁺, 339 (68), 309 (39), 279 (5), 261 (16), 229 (12), 213 (75), 199 (100), 181 (16), 153 (9), 135 (11), 123 (15), 105 (5), 81 (10). IR (ATR): $\tilde{\nu}$ = 3071 (w), 2954 (w), 2932 (w), 2892 (w), 2857 (w), 1739 (m), 1429 (m), 1109 (s), 1056 (m), 822 (m), 740 (m), 701 (s), 609 (m) cm⁻¹. UV/Vis (CH₂Cl₂): λ_{\max} (ϵ , L mol⁻¹ cm⁻¹) = 271 (502), 265 (714), 260 (704), 230 (4609) nm.

(E)-[1,1-²H₂]-6-[(*tert*-Butyldiphenylsilyloxy)-4-methylhex-4-en-1-ol (15): A suspension of LiAlD₄ (3.6 g, 86 mmol, 1.2 equiv.) in THF (500 mL) was cooled to 0 °C, and methyl ester **14** (57.0 g, 144 mmol, 1.0 equiv.) was added dropwise. The reaction mixture was stirred for 2 h at 0 °C and overnight at room temperature. For workup, H₂O was added carefully, and the precipitate was dissolved by addition of 2 M HCl. The aqueous layer was extracted three

times with EtOAc, and the combined organic layers were dried with MgSO₄ and concentrated under reduced pressure to give compound [1,1-²H₂]-**15** (48.8 g, 131 mmol, 91%) as a yellowish oil. *R*_f = 0.26 [hexane/EtOAc (3:1)]. GC (BPX-5, MSTFA): *I* = 2580. ¹H NMR (400 MHz, CDCl₃, TMS): δ = 7.71–7.68 (m, 4 H, 4 × CH), 7.42–7.34 (m, 6 H, 6 × CH), 5.42 (tq, ³*J*_{H,H} = 6.3, ⁴*J*_{H,H} = 1.3 Hz, 1 H, CH), 4.22 (d, ³*J*_{H,H} = 6.3 Hz, 2 H, CH₂), 2.03 (t, ³*J*_{H,H} = 7.3 Hz, 2 H, CH₂), 1.81 (s, 1 H, OH), 1.62 (t, ³*J*_{H,H} = 7.9 Hz, 2 H, CH₂), 1.45 (d, ⁴*J*_{H,H} = 0.8 Hz, 3 H, CH₃), 1.05 (s, 9 H, 3 × CH₃) ppm. ¹³C NMR (100 MHz, CDCl₃): δ = 136.8 (C_q), 135.5 (4 × CH), 134.0 (2 × C_q), 129.5 (3 × CH), 127.5 (4 × CH), 124.3 (CH), 61.7 (quint., ¹*J*_{C,D} = 21.6 Hz, C²H₂), 61.0 (CH₂), 35.6 (CH₂), 30.3 (CH₂), 26.8 (3 × CH₃), 19.1 (C_q), 16.1 (CH₃) ppm. MS (EI, 70 eV, MSTFA): *m/z* (%) = 385 (5) [M]⁺, 370 (<1), 271 (98), 199 (100), 181 (11), 135 (10), 97 (53), 75 (11). IR (ATR): $\tilde{\nu}$ = 3358 (br), 3071 (w), 2931 (w), 2857 (w), 1428 (w), 1109 (m), 1050 (m), 822 (w), 700 (s) cm⁻¹. UV/Vis (CH₂Cl₂): λ_{\max} (ϵ , L mol⁻¹ cm⁻¹) = 271 (481), 265 (677), 260 (670), 230 (3961) nm.

(E)-[1,1-²H₂]-6-[(*tert*-Butyldiphenylsilyloxy)-4-methylhex-4-en-1-yl 4-methylbenzenesulfonate (16): Alcohol [1,1-²H₂]-**15** (48.8 g, 131 mmol, 1.0 equiv.) was dissolved in pyridine (165 mL) and cooled to 0 °C. TsCl (36.1 g, 190 mmol, 1.5 equiv.) was added in small portions, and stirring was continued for 3 h at 0 °C. The reaction mixture was poured onto ice and extracted three times with EtOAc. The combined organic layers were washed with a satd. solution of aqueous CuSO₄, 2 M HCl and H₂O. After drying with MgSO₄ and concentration under reduced pressure, tosylate [1,1-²H₂]-**16** (64.0 g, 122 mmol, 93%) was obtained as a yellow oil. *R*_f = 0.56 [hexane/EtOAc (3:1)]. ¹H NMR (400 MHz, CDCl₃, TMS): δ = 7.79–7.77 (m, 2 H, 2 × CH), 7.69–7.65 (m, 4 H, 4 × CH), 7.44–7.35 (m, 6 H, 6 × CH), 7.33–7.31 (m, 2 H, 2 × CH), 5.30 (tq, ³*J*_{H,H} = 6.3, ⁴*J*_{H,H} = 1.3 Hz, 1 H, CH), 4.16 (d, ³*J*_{H,H} = 6.3 Hz, 2 H, CH₂), 2.42 (s, 3 H, CH₃), 1.97 (t, ³*J*_{H,H} = 7.1 Hz, 2 H, CH₂), 1.71 (t, ³*J*_{H,H} = 8.1 Hz, 2 H, CH₂), 1.37 (s, 3 H, CH₃), 1.03 (s, 9 H, 3 × CH₃) ppm. ¹³C NMR (100 MHz, CDCl₃): δ = 144.6 (C_q), 135.5 (4 × CH), 135.1 (C_q), 133.9 (2 × C_q), 133.2 (C_q), 129.8 (2 × CH), 129.5 (2 × CH), 127.8 (2 × CH), 127.6 (4 × CH), 125.1 (CH), 69.5 (quint., ¹*J*_{C,D} = 22.9 Hz, C²H₂), 60.9 (CH₂), 34.9 (CH₂), 26.8 (3 × CH₃), 26.6 (CH₂), 21.6 (CH₃), 19.1 (C_q), 16.1 (CH₃) ppm. IR (ATR): $\tilde{\nu}$ = 3070 (w), 2957 (w), 2931 (w), 2891 (w), 2858 (w), 1359 (m), 1175 (m), 1111 (m), 815 (s), 700 (s), 607 (m), 553 (s) cm⁻¹. UV/Vis (CH₂Cl₂): λ_{\max} (ϵ , L mol⁻¹ cm⁻¹) = 265 (1292), 261 (1250), 231 (11676) nm.

(E)-[6,6-²H₂]-*tert*-Butyl[(6-iodo-3-methylhex-2-en-1-yl)oxy]diphenylsilane (17): Tosylate [1,1-²H₂]-**16** (64.0 g, 122 mmol, 1.0 equiv.) was dissolved in acetone (750 mL) and treated with NaI (34.8 g, 232 mmol, 1.9 equiv.). The reaction mixture was stirred overnight at room temperature under exclusion of light. The mixture was diluted with hexane, filtered and concentrated under reduced pressure to give [6,6-²H₂]-**17** (57.9 g, 121 mmol, 99%) as a pale red oil. *R*_f = 0.79 [hexane/EtOAc (5:1)]. GC (BPX-5): *I* = 2812. ¹H NMR (400 MHz, CDCl₃, TMS): δ = 7.70–7.68 (m, 4 H, 4 × CH), 7.44–7.36 (m, 6 H, 6 × CH), 5.42 (tq, ³*J*_{H,H} = 6.3, ⁴*J*_{H,H} = 1.2 Hz, 1 H, CH), 4.22 (d, ³*J*_{H,H} = 6.3 Hz, 2 H, CH₂), 2.05 (t, ³*J*_{H,H} = 7.1 Hz, 2 H, CH₂), 1.87 (t, ³*J*_{H,H} = 7.5 Hz, 2 H, CH₂), 1.42 (s, 3 H, CH₃), 1.04 (s, 9 H, 3 × CH₃) ppm. ¹³C NMR (100 MHz, CDCl₃): δ = 135.6 (4 × CH), 134.9 (C_q), 134.0 (2 × C_q), 129.5 (2 × CH), 127.6 (4 × CH), 125.4 (CH), 61.0 (CH₂), 39.8 (CH₂), 31.1 (CH₂), 26.8 (3 × CH₃), 19.1 (C_q), 16.1 (CH₃), 6.1 (quint., ¹*J*_{C,D} = 22.8 Hz, C²H₂) ppm. MS (EI, 70 eV): *m/z* (%) = 480 (<1) [M]⁺, 423 (40), 309 (18), 249 (4), 199 (100), 181 (9), 135 (4), 97 (12). IR (ATR): $\tilde{\nu}$ = 3070 (w), 2931 (w), 2891 (w), 2856 (w), 1427 (w), 1109 (s), 1062 (m), 822 (m), 739 (m), 700 (s), 610 (m) cm⁻¹. UV/Vis (CH₂Cl₂): λ_{\max} (ϵ , L mol⁻¹ cm⁻¹) = 265 (1078), 259 (1157), 229 (5598) nm.

(E)-[1,1-²H₂]-{6-[*tert*-Butyldiphenylsilyloxy]-4-methylhex-4-en-1-yl}triphenylphosphonium Iodide (18): Triphenylphosphine (38.0 g, 145 mmol, 1.2 equiv.) was dissolved in toluene (400 mL) and treated with [6,6-²H₂]-17 (57.9 g, 121 mmol, 1.0 equiv.). The reaction was refluxed for 3 h, cooled to room temperature, and filtered. The resulting solid was washed with toluene and dried under reduced pressure to give the Wittig salt [1,1-²H₂]-18 (69.5 g, 94 mmol, 78%) as a colorless solid. $R_f = 0.65$ [CH₂Cl₂/MeOH (10:1)]. ¹H NMR (400 MHz, CDCl₃, TMS): $\delta = 7.85$ – 7.62 (m, 19 H, 19 \times CH), 7.41–7.30 (m, 6 H, 6 \times CH), 5.38–5.34 (m, 1 H, CH), 4.17 (d, ³ $J_{H,H} = 6.3$ Hz, 2 H, CH₂), 2.32 (t, ³ $J_{H,H} = 7.1$ Hz, 2 H, CH₂), 1.86–1.72 (m, 2 H, CH₂), 1.34 (s, 3 H, CH₃), 0.99 (s, 9 H, 3 \times CH₃) ppm. ¹³C NMR (100 MHz, CDCl₃): $\delta = 135.3$ (4 \times CH), 135.0 (d, ⁴ $J_{PC} = 3.0$ Hz, 3 \times CH), 134.9 (C_q), 133.6 (2 \times C_q), 133.5 (d, ³ $J_{PC} = 10.0$ Hz, 6 \times CH), 130.4 (d, ² $J_{PC} = 12.5$ Hz, 6 \times CH), 129.4 (2 \times CH), 127.4 (4 \times CH), 125.9 (CH), 117.8 (d, ¹ $J_{PC} = 86.1$ Hz, 3 \times C_q), 60.6 (CH₂), 38.9 (d, ² $J_{PC} = 15.7$ Hz, CH₂), 26.6 (3 \times CH₃), 19.9 (d, ³ $J_{PC} = 3.9$ Hz, CH₂), 18.9 (C_q), 16.0 (CH₃) ppm. ³¹P NMR (122 MHz, CDCl₃): $\delta = 24.9$ ppm. IR (ATR): $\tilde{\nu} = 3052$ (w), 3014 (w), 2930 (w), 2856 (w), 2183 (w), 1437 (m), 1110 (s), 1064 (m), 917 (m), 731 (s), 703 (s), 687 (s), 610 (m) cm⁻¹. UV/Vis (CH₂Cl₂): λ_{max} (ϵ , L mol⁻¹ cm⁻¹) = 229 (33630) nm.

(E)-[6-²H]-*tert*-Butyl[(3,7-dimethylocta-2,6-dien-1-yl)oxy]diphenylsilane (11): Wittig salt [1,1-²H₂]-18 (20.0 g, 27 mmol, 1.0 equiv.) was suspended in THF (250 mL) and cooled to 0 °C. A solution of *n*BuLi (1.6 M, 18.6 mL, 29.7 mmol, 1.1 equiv.) in hexane was added, and stirring was continued for 90 min at 0 °C. After cooling to –78 °C, acetone (1.7 g, 29.7 mmol, 1.1 equiv.) was added dropwise, and the mixture was stirred overnight at room temperature. The reaction was quenched by the addition of H₂O and extracted three times with EtOAc. The combined organic layers were dried with MgSO₄ and concentrated under reduced pressure. Column chromatography with hexane/EtOAc (10:1) yielded [6-²H]-11 (8.1 g, 20.6 mmol, 76%) as a colorless oil (deuterium atom content: 90%). $R_f = 0.78$ [hexane/EtOAc (10:1)]. GC (BPX-5): $I = 2548$. ¹H NMR (400 MHz, CDCl₃, TMS): $\delta = 7.71$ – 7.68 (m, 4 H, 4 \times CH), 7.43–7.34 (m, 6 H, 6 \times CH), 5.38 (tq, ³ $J_{H,H} = 6.3$, ⁴ $J_{H,H} = 0.9$ Hz, 1 H, CH), 4.23 (d, ³ $J_{H,H} = 6.3$ Hz, 2 H, CH₂), 2.08–2.04 (m, 2 H, CH₂), 1.99–1.96 (m, 2 H, CH₂), 1.68 (s, 3 H, CH₃), 1.60 (s, 3 H, CH₃), 1.44 (s, 3 H, CH₃), 1.05 (s, 9 H, 3 \times CH₃) ppm. ¹³C NMR (100 MHz, CDCl₃): $\delta = 137.0$ (C_q), 135.6 (4 \times CH), 134.2 (2 \times C_q), 131.4 (C_q), 129.5 (2 \times CH), 127.6 (4 \times CH), 124.1 (CH), 123.8 (t, ¹ $J_{C,D} = 23.0$ Hz, C²H), 61.2 (CH₂), 39.5 (CH₂), 26.9 (3 \times CH₃), 26.3 (CH₂), 25.6 (CH₃), 19.2 (C_q), 17.7 (CH₃), 16.3 (CH₃) ppm. MS (EI, 70 eV): m/z (%) = 393 (3) [M]⁺, 336 (66), 258 (11), 199 (100), 181 (30), 135 (24), 121 (13), 70 (29), 41 (23). IR (ATR): $\tilde{\nu} = 3071$ (w), 2960 (w), 2857 (w), 1428 (w), 1109 (s), 1060 (m), 822 (w), 738 (m), 700 (s) cm⁻¹. UV/Vis (CH₂Cl₂): λ_{max} (ϵ , L mol⁻¹ cm⁻¹) = 271 (426), 265 (628), 259 (703), 230 (3306) nm.

(E)-[6-²H]-3,7-Dimethylocta-2,6-dien-1-ol (4b): Compound [6-²H]-11 (29.0 g, 73.6 mmol, 1.0 equiv.) was dissolved in THF (360 mL) and cooled to 0 °C. A solution of TBAF (1.0 M, 88.3 mL, 88.3 mmol, 1.2 equiv.) in THF was added and stirred for 3 h at 0 °C. The solution was diluted with Et₂O and washed with H₂O. The organic layer was dried with MgSO₄ and concentrated under reduced pressure. Column chromatography with hexane/EtOAc (5:1) yielded [6-²H]-4b (11.1 g, 71.4 mmol, 97%) as a colorless oil. $R_f = 0.26$ [hexane/EtOAc (5:1)]. GC (BPX-5, MSTFA): $I = 1363$. ¹H NMR (400 MHz, CDCl₃, TMS): $\delta = 5.31$ (tq, ³ $J_{H,H} = 7.0$, ⁴ $J_{H,H} = 1.3$ Hz, 1 H, CH), 4.15 (d, ³ $J_{H,H} = 7.0$ Hz, 2 H, CH₂), 2.12–2.08 (m, 2 H, CH₂), 2.05–2.01 (m, 2 H, CH₂), 1.68 (s, 3 H, CH₃), 1.67 (s, 3 H, CH₃), 1.60 (s, 3 H, CH₃) ppm. ¹³C NMR (100 MHz, CDCl₃): $\delta = 139.5$ (C_q), 131.6 (C_q), 123.5 (t, ¹ $J_{C,D} = 22.9$ Hz, C²H),

59.3 (CH₂), 39.5 (CH₂), 26.2 (CH₂), 25.5 (CH₃), 17.6 (CH₃), 16.2 (CH₃) ppm. MS (EI, 70 eV, MSTFA): m/z (%) = 227 (10) [M]⁺, 212 (15), 183 (8), 169 (23), 157 (27), 143 (55), 122 (62), 108 (11), 93 (34), 73 (100), 41 (47). IR (ATR): $\tilde{\nu} = 3323$ (br), 2967 (w), 2912 (m), 2857 (w), 1445 (m), 1375 (m), 1100 (w), 997 (s) cm⁻¹. UV/Vis (CH₂Cl₂): λ_{max} (ϵ , L mol⁻¹ cm⁻¹) = 227 (262) nm.

Isolation of (R)-[3-²H]-Tuberculosinol, and (S)-[3-²H]-Tuberculosinol: The purified Rv3377c protein was prepared as described previously.^[3] To isolate the product from the incubation of Rv3377c with [14-²H]-GGPP, the reaction mixture (300 mL) containing Tris-HCl buffer (pH 7.5, 50 mM), MgCl₂ (0.1 mM), [14-²H]-GGPP (6 mg), and purified Rv3377c protein (4 mg), was incubated at 30 °C for 20 h. To hydrolyze the diphosphate moiety of the product, the phosphatase reaction mixture (900 mL) containing Rv3377c reaction mixture (300 mL), acetate buffer (0.2 M, pH 5.6), 2-PrOH (20%, v/v), and acid phosphatase (0.25 mg mL⁻¹, Sigma) was then further incubated at 37 °C for 12 h. After addition of MeOH (400 mL), the reaction mixture was extracted with *n*-hexane (300 mL \times 3). The *n*-hexane layer was dried with Na₂SO₄ and the solvents were evaporated to dryness. The crude materials were dissolved in a small amount of hexane. The enzymatic product was purified by SiO₂ column chromatography with hexane/ethyl acetate (100:0 to 100:5) followed by reverse-phase HPLC [CAPCELL PAK C18 MG S5 column (250 \times 15 mm), SHISEIDO, Tokyo, Japan, mobile phase CH₃CN, flow rate 3 mL min⁻¹, detection at 210 nm], yielding 1.0 mg of (R)-[3-²H]-tuberculosinol (deuterium atom content: 93%). To isolate the product from the incubation of Rv3377c with non-labeled GGPP in deuterium oxide, the reaction mixture (150 mL) containing Tris-HCl buffer (1 M, pH 7.5, 7.5 mL), MgCl₂ (0.1 M, 0.15 mL), GGPP (3 mg mL⁻¹, 1 mL), purified Rv3377c protein (0.5 mg mL⁻¹, 4 mL), and D₂O (99.9 atom-% D, Aldrich, 137.35 mL) was incubated at 30 °C for 20 h. After the incubation, EDTA (0.5 M, pH 8.0, 3 mL) was added to terminate the reaction. The phosphatase reaction mixture (total volume 300 mL, same composition as described above) was incubated at 37 °C for 12 h. The enzymatic product was extracted with *n*-hexane and then purified by reverse-phase HPLC in CH₃CN, yielding 1.1 mg of (S)-[3-²H]-tuberculosinol (deuterium atom 91%).

Supporting Information (see footnote on the first page of this article): Synthetic procedures and spectroscopic data for compounds [2-²H₂]-2, [2-²H₂]-9, [2-²H₂]-6, [2-²H₂]-3a, [2-²H₂]-4a, [2-²H₂]-7a, [2-²H₂]-1b, [2-²H₂]-3b, [9-²H]-1c, [13-²H]-1d, [10-²H]-3c, [14-²H]-3d, [10-²H]-4c, [14-²H]-4d, [8-²H]-7b, [12-²H]-7c, and [14-²H]-8d. ¹H NMR, ¹³C NMR, and DEPT spectra of all synthesised compounds.

Acknowledgments

This work was funded by the Deutsche Forschungsgemeinschaft (DFG) with a Heisenberg fellowship (grant DI1536/4-1, to J. S. D. and project “Fragrants from Actinomycetes”, grant DI1536/2-1) and by the Beilstein Institut zur Förderung der Chemischen Wissenschaften with a Scholarship (to P. R.).

- [1] J. S. Dickschat, *Nat. Prod. Rep.* **2011**, *28*, 1917–1936.
- [2] M. L. Wise, H.-J. Pyun, G. Helms, B. Assink, R. M. Coates, R. B. Croteau, *Tetrahedron* **2001**, *57*, 5327–5334.
- [3] a) C. Nakano, T. Okamura, T. Sato, T. Dairi, T. Hoshino, *Chem. Commun.* **2005**, 1016–1018; b) C. Nakano, T. Hoshino, *ChemBioChem* **2009**, *10*, 2060–2071.
- [4] T. Suga, Y. Hiragata, M. Aihara, S. Izumi, *J. Chem. Soc., Chem. Commun.* **1992**, 1556–1558.
- [5] D. E. Cane, P. C. Prabhakaran, J. S. Oliver, D. B. McIlwaine, *J. Am. Chem. Soc.* **1990**, *112*, 3209–3210.

- [6] D. Arigoni, D. E. Cane, J. H. Shim, R. Croteau, K. Wagschal, *Phytochemistry* **1993**, *32*, 623–631.
- [7] D. J. Miller, J. Gao, D. G. Truhlar, N. J. Young, V. Gonzalez, R. K. Allemann, *Org. Biomol. Chem.* **2008**, *6*, 2346–2354.
- [8] H. V. Thulasiram, R. M. Phan, S. B. Rivera, C. D. Poulter, *J. Org. Chem.* **2006**, *71*, 1739–1741.
- [9] S. Izumi, M. Aihara, Y. Hiraga, T. Hirata, T. Suga, *J. Labelled Compd. Radiopharm.* **1991**, *29*, 591–597.
- [10] D. J. Comeskey, D. D. Rowan, A. J. Matich, *J. Labelled Compd. Radiopharm.* **2006**, *49*, 47–54.
- [11] T. Subramanian, K. L. Subramanian, M. Sunkara, F. O. Onono, A. J. Morris, H. P. Spielmann, *J. Labelled Compd. Radiopharm.* **2013**, *56*, 370–375.
- [12] D. E. Cane, J. S. Oliver, P. H. M. Harrison, C. Abell, B. R. Hubbard, C. T. Kane, R. Lattman, *J. Am. Chem. Soc.* **1990**, *112*, 4513–4524.
- [13] J. Jiang, X. He, D. E. Cane, *J. Am. Chem. Soc.* **2006**, *128*, 8128–8129.
- [14] W. K. W. Chou, I. Fanizza, T. Uchiyama, M. Komatsu, H. Ikeda, D. E. Cane, *J. Am. Chem. Soc.* **2010**, *132*, 8850–8851.
- [15] Y. Hu, W. K. W. Chou, R. Hopson, D. E. Cane, *Chem. Biol.* **2011**, *18*, 32–37.
- [16] a) J. S. Dickschat, C. A. Citron, N. L. Brock, R. Riclea, H. Kuhz, *Eur. J. Org. Chem.* **2011**, 3339–3346; b) C. A. Citron, N. L. Brock, B. Tudzynski, J. S. Dickschat, *Chem. Commun.* **2014**, *50*, 5224–5226.
- [17] a) C. A. Citron, N. L. Brock, P. Rabe, J. S. Dickschat, *Angew. Chem. Int. Ed.* **2012**, *51*, 4053–4057; b) N. L. Brock, S. R. Ravella, S. Schulz, J. S. Dickschat, *Angew. Chem. Int. Ed.* **2013**, *52*, 2100–2104.
- [18] C. A. Citron, J. S. Dickschat, *Org. Biomol. Chem.* **2013**, *11*, 7447–7450.
- [19] N. L. Brock, B. Tudzynski, J. S. Dickschat, *ChemBioChem* **2011**, *12*, 2667–2676.
- [20] C. Nakano, T. Okamura, T. Sato, T. Dairi, T. Hoshino, *Chem. Commun.* **2005**, 1016–1018.
- [21] P. Baer, P. Rabe, C. A. Citron, C. C. de Oliveira Mann, N. Kaufmann, M. Groll, J. S. Dickschat, *ChemBioChem* **2014**, *15*, 213–216.
- [22] C. Raptis, I. N. Lykakis, C. Tsangarakis, M. Stratakis, *Chem. Eur. J.* **2009**, *15*, 11918–11927.
- [23] C. Tsangarakis, M. Stratakis, *Eur. J. Org. Chem.* **2006**, 4435–4439.

Received: July 28, 2014
Published Online: October 24, 2014

SUPPORTING INFORMATION

DOI: 10.1002/ejoc.201403002

Title: Synthesis of Isotopically Labelled Oligoprenyl Diphosphates and Their Application in Mechanistic Investigations of Terpene Cyclases

Author(s): Christian A. Citron, Patrick Rabe, Lena Barra, Chiaki Nakano, Tsutomu Hoshino, and Jeroen S. Dickschat*

Experimental Procedures for Synthetic Compounds

Synthesis of triethyl [²H₂]phosphonoacetate (2): A solution of triethyl phosphonoacetate (2) (22.4 g, 100 mmol, 1.0 eq.) in 100 mL of ²H₂O was treated with a catalytic amount of K₂CO₃ (~130 mg) and stirred for 2 d at room temperature. The mixture was then extracted thrice with ethyl acetate, dried over MgSO₄ and concentrated under reduced pressure. Compound [²H₂]-2 (20.4 g, 90.4 mmol, 90%) was obtained as colourless oil. *R*_f = 0.84 (hexane/EtOAc (1:1)). GC (BPX-5): *I* = 1407. ¹H NMR (400 MHz, CDCl₃, TMS): δ = 4.23 – 4.14 (m, 6H, 3x CH₂), 1.37 – 1.27 (m, 9H, 3x CH₃) ppm. ¹³C NMR (100 MHz, CDCl₃): δ = 165.6 (d, ²*J*_{C,P} = 6.0 Hz, C_q), 62.5 (d, ²*J*_{C,P} = 6.2 Hz, 2x CH₂), 61.4 (CH₂), 16.2 (d, ³*J*_{C,P} = 6.2 Hz, 2x CH₃), 13.9 (CH₃) ppm. ³¹P NMR (162 MHz, CDCl₃): δ = 20.3 ppm. MS (EI, 70 eV): *m/z* (%) = 226 (<1) [M]⁺, 197 (97), 179 (82), 169 (43), 151 (82), 137 (17), 123 (100), 109 (57), 88 (37), 65 (11), 44 (35). IR (ATR): $\tilde{\nu}$ = 2984 (w), 2938 (w), 1732 (m), 1245 (s), 1016 (s), 964 (s) cm⁻¹.

Synthesis of [²H₂]meldrum's acid (9): A suspension of meldrum's acid (9) (7.2 g 50.0 mmol, 1.0 eq.) in 30 mL of ²H₂O was treated with K₂CO₃ (140 mg) and stirred at room temperature for 2 d. The mixture was then extracted three times with CH₂Cl₂, dried over MgSO₄ and concentrated under reduced pressure. Deuterated [²H₂]-9 (6.3 g, 43.4 mmol, 87%) was obtained as colourless solid. *R*_f = 0.30 (hexane/EtOAc (2:1)). GC (BPX-5): *I* = 1132. ¹H NMR (400 MHz, CDCl₃, TMS): δ = 1.79 (s, 6H, 2x CH₃) ppm. ¹³C NMR (100 MHz, CDCl₃): δ = 162.9 (2x C_q), 106.2 (C_q), 35.6 (quint., ¹*J*_{C,D} = 20.5 Hz, C²H₂), 27.5 (2x CH₃) ppm. MS (EI, 70 eV): *m/z* (%) = 146 (<1) [M]⁺, 129 (15), 100 (10), 72 (4), 58 (24), 43 (100). IR (ATR): $\tilde{\nu}$ = 2930 (w), 1787 (s), 1747 (s), 1354 (m), 1299 (s), 1280 (s), 1199 (s), 1068 (s), 1012 (s), 975 (s), 954 (s), 935 (m), 835 (s), 635 (m) cm⁻¹.

Synthesis of ethyl [²H₅]acetoacetate (6): According to Scherling and Pleiß,¹ compound [²H₂]-9 (6.3 g, 43.3 mmol, 1.01 eq.) was dissolved in 90 mL of abs. CH₂Cl₂ and cooled to 0 °C. Pyridine (7.8 mL, 86.7 mmol, 2.02 eq.) was added, followed by dropwise addition of [²H₃]acetyl chloride (3.0 mL, 42.9 mmol, 1.0 eq.). The reaction mixture was stirred for 1 h at 0 °C after which a 1 M solution of ²HCl in ²H₂O was added. The organic phase was separated, washed with ²HCl and with ²H₂O, dried with MgSO₄, and concentrated under reduced pressure. The residue was taken up with 100 mL of EtO²H and refluxed for 4 h. After cooling down to room temperature, the solvent was removed under reduced pressure to yield compound [²H₅]-6 (4.5 g, 32.9 mmol, 76%) as pale red liquid. *R*_f = 0.21 (hexane/EtOAc (10:1)). GC (BPX-5): *I* = 947. ¹H NMR (400 MHz, CDCl₃, TMS): δ = 4.21 (q, ³*J*_{H,H} = 7.1 Hz, 2H, CH₂), 1.29 (t, ³*J*_{H,H} = 7.1 Hz, 3H, CH₃) ppm. ¹³C NMR (100 MHz, CDCl₃): δ = 200.8 (C_q), 167.1 (C_q), 61.3 (CH₂), 49.5 (quint., ¹*J*_{C,D} = 20.0 Hz, C²H₂), 29.3 (sept., ¹*J*_{C,D} = 20.2 Hz, C²H₃), 14.0 (CH₃) ppm. MS (EI, 70 eV): *m/z* (%) = 135 (8) [M]⁺, 116 (2), 107 (8), 90 (43), 63 (12), 46 (100). IR (ATR): $\tilde{\nu}$ = 2985 (w), 2941 (w), 1737 (m), 1711 (s), 1316 (m), 1256 (m), 1150 (s), 1027 (m) cm⁻¹. UV-Vis (CH₂Cl₂): λ_{max} (ε, L mol⁻¹ cm⁻¹) = 244 (943) nm.

Synthesis of ethyl [²H₇]-3-methylbut-2-enoate (3a). A solution of diisopropylamine (9.6 g, 94.9 mmol, 1.05 eq.) in 250 mL of abs. THF was cooled to 0 °C and treated with *n*-butyl lithium (1.6 M in hexane, 59.3 mL, 94.9 mmol, 1.05 eq.). The reaction was stirred for 1 h at 0 °C and was then cooled to -78 °C. [²H₂]-2 (20.4 g, 90.4 mmol, 1.0 eq.) was added and stirring was continued for 1 h at -78 °C. Acetone [²H₆]-1a (5.79 g, 90.4 mmol, 1.0 eq.) was added dropwise and the reaction mixture was stirred over night at room temperature. The reaction was hydrolyzed by addition of distilled water, followed by threefold extraction with diethyl ether. The combined organic layers were dried over MgSO₄ and concentrated under reduced pressure. Column chromatography on silica gel with pentane/diethyl ether (10:1) yielded [²H₇]-3a (8.76 g, 64.9 mmol, 72%) as colorless liquid. *R*_f = 0.40 (hexane/EtOAc (10:1)). GC (HP-5): *I* = 922. ¹H NMR (400 MHz, CDCl₃, TMS): δ = 4.14 (q, ³*J*_{H,H} = 7.1 Hz, 2H, CH₂), 1.27 (t, ³*J*_{H,H} = 7.1 Hz, 3H, CH₃) ppm. ¹³C NMR (100 MHz, CDCl₃): δ = 166.7 (C_q), 156.1 (C_q), 115.9 (t, ¹*J*_{C,D} = 25.7 Hz, C²H), 59.4 (CH₂), 26.3 (sept., ¹*J*_{C,D} = 20.3 Hz, C²H₃), 19.2 (sept., ¹*J*_{C,D} = 20.3 Hz, C²H₃), 14.3 (CH₃) ppm. MS (EI, 70 eV): *m/z* (%) = 135 (40) [M]⁺, 107 (20), 90 (100), 62 (23) 42 (6). IR (ATR): $\tilde{\nu}$ = 2982 (w), 1710 (s), 1632 (m), 1276 (m), 1222 (s), 1104 (s), 1054 (s) 788 (m) cm⁻¹. UV-Vis (CH₂Cl₂): λ_{max} (ε, L mol⁻¹ cm⁻¹) = 230 (5428) nm.

Synthesis of [²H₉]-3-methylbut-2-en-1-ol (4a). LiAl²H₄ (2.2 g, 52.7 mmol, 1.0 eq.) was suspended in 50 mL of abs. diethyl ether and cooled to 0 °C. The ester [²H₂]-3a (7.1 g, 52.7 mmol, 1.0 eq.) was added dropwise and the reaction mixture stirred for 3 h at 0 °C. The reaction was quenched by addition of distilled water. The precipitate was dissolved by addition of aqueous hydrochloric acid. After extraction with diethyl ether, the combined organic layers were dried over MgSO₄ and concentrated under reduced pressure to yield [²H₉]-4a (3.95 g, 41.6 mmol, 79%) as colorless liquid. *R*_f = 0.10 (hexane/EtOAc (5:1)). ¹H NMR (400 MHz, CDCl₃, TMS): δ = 2.15 (br s, 1H, OH) ppm. ¹³C NMR (100 MHz, CDCl₃): δ = 135.8 (C_q), 123.2 (t, ¹*J*_{C,D} = 23.3 Hz, C²H), 58.3 (quint., ¹*J*_{C,D} = 21.7 Hz, C²H₂), 24.6 (sept., ¹*J*_{C,D} = 19.1 Hz, C²H₃), 16.8 (sept., ¹*J*_{C,D} = 19.1 Hz, C²H₃) ppm. MS (EI, 70 eV): *m/z* (%) = 95 (31) [M]⁺, 77 (100), 58 (16), 46 (22). IR (ATR): $\tilde{\nu}$ = 3323 (br), 2195 (w), 1265 (w), 1085 (s), 1041 (s), 961 (s) cm⁻¹.

Synthesis of ethyl [²H₁₂]-2-acetyl-5-methylhex-4-enoate (7a). The allyl bromide [²H₉]-5a (prepared from 3.95 g, 41.6 mmol, [²H₉]-4a) was dissolved in 50 mL of [²H₆]acetone and anhydrous K₂CO₃ (8.6g, 62.4 mmol, 1.5 eq.) and ethyl [²H₃]acetoacetate (4.4 g, 32.9 mmol, 0.8 eq.) were added. The mixture was refluxed for 4 h, cooled to room temperature, and filtered. The solution was concentrated under reduced pressure. Column chromatography on silica gel with hexane/ethyl acetate (5:1) yielded [²H₁₂]-7a (3.3 g, 15.9 mmol, 38%) as colorless oil. Inspection by ¹H NMR spectroscopy revealed the loss of one deuterium, most likely due to keto-enol tautomerism during column chromatography. Reintroduction of this deuterium in the next step was possible (vide infra). *R*_f = 0.48 (hexane/EtOAc (5:1)). GC (HP-5): *I* = 1317. ¹H NMR (400 MHz, CDCl₃, TMS): δ = 4.19 (q, ³*J*_{H,H} = 7.1 Hz, 2H, CH₂), 3.41 (br s, 1H, CH), 1.27 (t, ³*J*_{H,H} = 7.1 Hz, 3H, CH₃) ppm. ¹³C NMR (100 MHz, CDCl₃): δ = 203.2 (C_q), 169.6 (C_q), 119.3 (t, ¹*J*_{C,D} = 23.3 Hz, C²H), 61.2 (CH₂), 59.6 (CH), 28.2 (sept., ¹*J*_{C,D} = 20.5 Hz, C²H₃), 26.2 (quint., ¹*J*_{C,D} = 20.5 Hz, C²H₂), 24.7 (sept., ¹*J*_{C,D} = 19.1 Hz, C²H₃), 16.8 (sept., ¹*J*_{C,D} = 18.4 Hz, C²H₃), 14.0 (CH₃) ppm. MS (EI, 70 eV): *m/z* (%) = 211 (4) [M]⁺, 210 (4) [M-²H]⁺, 191 (3), 165 (63), 137 (29), 118 (100), 90 (40), 78 (34), 58 (9), 46 (63). IR (ATR): $\tilde{\nu}$ = 2984 (w), 1738 (m), 1712 (s), 1313 (m), 1262 (m), 1199 (m), 1030 (m) cm⁻¹.

Synthesis of [²H₁₄]-6-methylhept-5-en-2-one (1b). To a solution of the β-ketoester [²H₁₂]-7a (3.3 g, 15.9 mmol, 1.0 eq.) in 40 mL of [²H]ethanol was added KO²H (4.0 g, 70.1 mmol, 4.0 eq.) in 10 mL of ²H₂O. The reaction mixture was refluxed for 2 h and then quenched by the addition of 2 N ²HCl. The aqueous phase was extracted three times with diethyl ether. The combined organic layers were dried over

MgSO₄ and concentrated under reduced pressure. Column chromatography on silica gel with hexane/ethyl acetate (10:1) yielded [²H]₁₂-**1b** (393 mg, 2.81 mmol, 18%) as colorless liquid, with reintroduction of the deuterium that was lost in the preceding step. *R*_f = 0.53 (hexane/EtOAc (5:1)). GC (HP-5): *I* = 980. ¹H NMR (400 MHz, CDCl₃, TMS): δ = no product signals detectable ppm. ¹³C NMR (100 MHz, CDCl₃): δ = 209.2 (C_q), 132.5 (C_q), 122.2 (t, ¹J_{C,D} = 23.6 Hz, C²H), 42.8 (quint., ¹J_{C,D} = 19.0 Hz, C²H₂), 29.1 (sept., ¹J_{C,D} = 19.4 Hz, C²H₃), 24.6 (sept., ¹J_{C,D} = 19.9 Hz, C²H₃), 21.6 (quint., ¹J_{C,D} = 20.2 Hz, C²H₂), 16.7 (sept., ¹J_{C,D} = 19.0 Hz, C²H₃) ppm. MS (EI, 70 eV): *m/z* (%) = 140 (11) [M]⁺, 120 (76), 102 (20), 78 (60), 62 (36), 46 (100). IR (ATR): $\tilde{\nu}$ = 2225 (w), 2193 (w), 1708 (s), 1262 (m), 1048 (m) cm⁻¹.

Ethyl (2*E*/3*E*)-[²H]₁₅]-3,6-dimethylocta-2,6-dienoate (3b): A solution of HNⁱPr₂ (306 mg, 3.0 mmol, 1.3 eq.) in abs. THF (20 mL) was cooled to 0 °C and then treated with *n*-butyl lithium (1.6 M in hexane, 1.9 mL, 3.0 mmol, 1.3 eq.). After 1 h the reaction mixture was cooled to -78 °C and triethyl [²H]₂phosphonoacetate (683 mg, 3.0 mmol, 1.3 eq.) was added dropwise. Stirring was continued for 90 min after which **1b** (313 mg, 2.2 mmol, 1.0 eq.) was added dropwise. The reaction mixture was stirred over night at room temperature and was then quenched by addition of H₂O. The aqueous layer was extracted three times with diethyl ether, the combined organic layers were dried over MgSO₄ and concentrated under reduced pressure. Column chromatography on silica gel with hexane/ethyl acetate (20:1) yielded **3b** (213 mg, 1.0 mmol, 45%, mixture of isomers) as colourless liquid. NMR inspection revealed loss of 66% deuterium from the alpha position of the ester. *R*_f = 0.24 (*E*-isomer) / 0.21 (*E*-isomer). (hexane/EtOAc (5:1)). GC (HP-5): *I* = 1348 (*Z*-isomer), 1389 (*E*-isomer). ¹H NMR (400 MHz, CDCl₃, TMS): δ = 5.59 (br s, 0.33 H, CH of *E*-isomer), 5.57 (br s, 0.33 H, CH of *Z*-isomer) 4.10 – 4.04 (m, 2H, CH₂ of *E*- and *Z*-isomer), 1.22 – 1.18 (m, 3H, CH₃ of *E*- and *Z*-isomer) ppm. ¹³C NMR (100 MHz, CDCl₃): δ = 166.8 (C_q, *E*-isomer), 166.3 (C_q, *Z*-isomer), 159.9 (C_q, *Z*-isomer), 159.6 (C_q, *E*-isomer), 132.2 (C_q, *E*-isomer), 131.8 (C_q, *Z*-isomer), 123.2 (t, ¹J_{C,D} = 22.4 Hz, C²H, *Z*-isomer), 122.6 (t, ¹J_{C,D} = 23.3 Hz, C²H, *E*-isomer), 116.3 (CH, *Z*-isomer), 115.7 (CH, *E*-isomer), 59.4 (CH₂, *E*-isomer), 59.3 (CH₂, *Z*-isomer), 40.0 (quint., ¹J_{C,D} = 18.7 Hz, C²H₂), 25.1 (quint., ¹J_{C,D} = 19.3 Hz, C²H₂), 24.6 (sept., ¹J_{C,D} = 19.8 Hz, C²H₃), 17.9 (sept., ¹J_{C,D} = 20.0 Hz, C²H₃), 16.7 (sept., ¹J_{C,D} = 19.3 Hz, C²H₃), 14.3 (CH₃, *E*- and *Z*-isomer) ppm. MS (EI, 70 eV, *Z*-isomer): *m/z* (%) = 211 (2) [M]⁺, 210 (5) [M-1]⁺, 192 (2), 165 (14), 134 (33), 117 (13), 106 (22), 88 (14), 78 (100), 46 (41). MS (EI, 70 eV, *E*-isomer): *m/z* (%) = 211 (1) [M]⁺, 210 (3) [M-1]⁺, 195 (1), 165 (14), 134 (26), 117 (6), 106 (14), 88 (11), 78 (100), 46 (33).

General procedure for the synthesis of methyl ketones. To a solution of β-ketoesters [8-²H]-**7b** and [12-²H]-**7c** (1.0 eq., 0.5 M in ethanol) was added KOH (2.00 eq.) dissolved in distilled water (3 M). The reaction mixture was stirred under reflux for 2 h. After cooling to room temperature the solution was acidified with 2 M HCl and extracted three times with ethyl acetate. The combined organic layers were dried over MgSO₄ and concentrated under reduced pressure. Column chromatography with hexane/ethyl acetate (10:1) yielded the ketones [9-²H]-**1c** and [13-²H]-**1d** as pale yellow oils.

(*E*)-[9-²H]-6,10-dimethylundeca-5,9-dien-2-one (1c): Yield: (9.74 g, 50.0 mmol, 93%). *R*_f = 0.50 (hexane/EtOAc (5:1)). GC (BPX-5): *I* = 1435. ¹H NMR (400 MHz, CDCl₃, TMS): δ = 5.08 (tq, ³J_{H,H} = 7.2 Hz, ⁴J_{H,H} = 1.3 Hz, 1H, CH), 2.47 – 2.44 (m, 2H, CH₂), 2.29 – 2.23 (m, 2H, CH₂), 2.13 (s, 3H, CH₃), 2.07 – 2.02 (m, 2H, CH₂), 1.99 – 1.95 (m, 2H, CH₂), 1.67 (s, 3H, CH₃), 1.61 (s, 3H, CH₃), 1.59 (s, 3H, CH₃) ppm. ¹³C NMR (100 MHz, CDCl₃): δ = 208.8 (C_q), 136.3 (C_q), 131.2 (C_q), 123.8 (t, ¹J_{C,D} = 22.9 Hz, C²H), 122.5 (CH), 43.7 (CH₂), 39.6 (CH₂), 29.9 (CH₃), 26.5 (CH₂), 25.6 (CH₃), 22.4 (CH₂), 17.6 (CH₃), 15.9 (CH₃) ppm. MS (EI, 70 eV): *m/z* (%) = 195 (4) [M]⁺, 177 (4), 151 (24), 137 (22), 125 (25), 107 (40), 93 (16), 70 (77), 55 (12), 43 (100). IR (ATR): $\tilde{\nu}$ = 2966 (w), 2914 (w), 2855 (w), 1716 (s), 1445 (w), 1358 (m), 1157 (w) cm⁻¹. UV-Vis (CH₂Cl₂): λ_{max} (ε, L mol⁻¹ cm⁻¹) = 227 (335) nm.

(5*E*,9*E*)-[13-²H]-6,10,14-trimethylpentadeca-5,9,13-trien-2-one (1d): Yield: (1.72 g, 6.5 mmol, 88%). *R*_f = 0.85 (hexane/EtOAc (5:1)). GC (BPX-5): *I* = 1932. ¹H NMR (400 MHz, CDCl₃, TMS): δ = 5.11 – 5.06 (m, 2H, 2x CH), 2.45 (t, ³J_{H,H} = 7.7 Hz, 2H, CH₂), 2.26 (q, ³J_{H,H} = 6.7 Hz, 2H, CH₂), 2.13 (s, 3H, CH₃), 2.08 – 2.03 (m, 4H, 2x CH₂), 2.00 – 1.95 (m, 4H, 2x CH₂), 1.68 (s, 3H, CH₃), 1.62 (s, 3H, CH₃), 1.60 (s, 3H, CH₃), 1.59 (s, 3H, CH₃) ppm. ¹³C NMR (100 MHz, CDCl₃): δ = 208.8 (C_q), 136.4 (C_q), 135.0 (C_q), 131.1 (C_q), 124.0 (CH), 123.9 (t, ¹J_{C,D} = 23.1 Hz, C²H), 122.5 (CH), 43.7 (CH₂), 39.7 (CH₂), 39.6 (CH₂), 29.9 (CH₃), 26.7 (CH₂), 26.5 (CH₂), 25.6 (CH₃), 22.4 (CH₂), 17.6 (CH₃), 16.0 (CH₃), 15.9 (CH₃) ppm. MS (EI, 70 eV): *m/z* (%) = 263 (5) [M]⁺, 248 (1), 220 (2), 205 (4), 193 (5), 178 (11), 162 (6), 135 (32), 125 (24), 107 (42), 93 (27), 81 (36), 70 (100), 55 (13), 43 (99). IR (ATR): $\tilde{\nu}$ = 2965 (m), 2917 (m), 2855 (m), 1716 (s), 1445 (m), 1359 (m), 1158 (m) cm⁻¹. UV-Vis (CH₂Cl₂): λ_{max} (ε, L mol⁻¹ cm⁻¹) = 228 (1288) nm.

General procedure for the synthesis of esters. A solution of diisopropylamine (1.05 eq., 0.75 M in abs. THF) was cooled to 0 °C and treated with *n*-butyl lithium (1.6 M in hexane, 1.05 eq.). The mixture was stirred for 1 h at 0 °C and then cooled to -78 °C. Slowly triethyl phosphonoacetate (1.0 eq.) was added and stirring was continued for 2 h at -78 °C. Compounds [9-²H]-**1c** and [13-²H]-**1d** (1.0 eq.) were added dropwise and the reaction mixture was stirred over night at room temperature. The reaction was hydrolyzed by addition of distilled water, followed by extraction with ethyl acetate. The combined organic layers were dried over MgSO₄ and concentrated under reduced pressure. The corresponding esters were obtained as a mixture of 2*E* and 2*Z* diastereomers (4:1 for [10-²H]-**3c**, 11:1 for [14-²H]-**3d**) that were separated by repeated column chromatography with hexane/ethyl acetate (40:1).

Ethyl (2*E*,6*E*)-[10-²H]-3,7,11-trimethyldodeca-2,6,10-trienoate (3c): Yield: (4.2 g, 15.9 mmol, 32%). *R*_f = 0.45 (hexane/EtOAc (20:1)). GC (BPX-5): *I* = 1348. ¹H NMR (400 MHz, CDCl₃, TMS): δ = 5.67 – 5.66 (m, 1H, CH), 5.11 – 5.07 (m, 1H, CH), 4.14 (q, ³J_{H,H} = 7.1 Hz, 2H, CH₂), 2.17 – 2.16 (m, 3H, CH₃), 2.07 – 2.04 (m, 4H, 2x CH₂), 2.00 – 1.96 (m, 4H, 2x CH₂), 1.68 (s, 3H, CH₃), 1.60 (s, 6H, 2x CH₃), 1.27 (t, ³J_{H,H} = 7.1 Hz, 3H, CH₃) ppm. ¹³C NMR (100 MHz, CDCl₃): δ = 166.9 (C_q), 159.7 (C_q), 136.1 (C_q), 131.3 (C_q), 123.8 (t, ¹J_{C,D} = 23.2 Hz, C²H), 122.9 (CH), 115.6 (CH), 59.5 (CH₂), 41.0 (CH₂), 39.7 (CH₂), 26.6 (CH₂), 25.7 (CH₂), 25.6 (CH₃), 18.8 (CH₃), 17.6 (CH₃), 16.0 (CH₃), 14.3 (CH₃) ppm. MS (EI, 70 eV): *m/z* (%) = 265 (3) [M]⁺, 250 (1), 204 (3), 192 (3), 176 (3), 147 (5), 128 (37), 100 (12), 82 (42), 70 (100), 41 (48). IR (ATR): $\tilde{\nu}$ = 2977 (w), 2915 (w), 2855 (w), 1715 (m), 1648 (w), 1446 (w), 1371 (w), 1219 (m), 1141 (s), 1040 (w) cm⁻¹. UV-Vis (CH₂Cl₂): λ_{max} (ε, L mol⁻¹ cm⁻¹) = 230 (8914) nm.

Ethyl (2*Z*,6*E*)-[10-²H]-3,7,11-trimethyldodeca-2,6,10-trienoate: Yield: (860 mg, 3.2 mmol, 7%). *R*_f = 0.47 (hexane/EtOAc (20:1)). GC (BPX-5): *I* = 1809. ¹H NMR (400 MHz, CDCl₃, TMS): δ = 5.66 – 5.65 (m, 1H, CH), 5.17 (tq, ³J_{H,H} = 7.2 Hz, ⁴J_{H,H} = 1.3 Hz, 1H, CH), 4.14

(q, $^3J_{\text{HH}} = 7.2$ Hz, 2H, CH₂), 2.67 – 2.63 (m, 2H, CH₂), 2.21 – 2.15 (m, 2H, CH₂), 2.07 – 2.04 (m, 2H, CH₂), 1.99 – 1.96 (m, 2H, CH₂), 1.89 (d, $^4J_{\text{HH}} = 1.4$ Hz, 3H, CH₃), 1.67 (s, 3H, CH₃), 1.62 (s, 3H, CH₃), 1.60 (s, 3H, CH₃), 1.26 (t, $^3J_{\text{HH}} = 7.2$ Hz, 3H, CH₃) ppm. ¹³C NMR (100 MHz, CDCl₃): $\delta = 166.3$ (C_q), 160.1 (C_q), 135.7 (C_q), 131.1 (C_q), 124.0 (t, $^1J_{\text{CD}} = 23.7$ Hz, C²H), 123.5 (CH), 116.2 (CH), 59.3 (CH₂), 39.6 (CH₂), 33.4 (CH₂), 26.7 (CH₂), 26.5 (CH₂), 25.6 (CH₃), 25.3 (CH₃), 17.6 (CH₃), 15.9 (CH₃), 14.3 (CH₃) ppm. MS (EI, 70 eV): m/z (%) = 265 (9) [M]⁺, 250 (1), 221 (8), 204 (1) 192 (3), 176 (5), 149 (28), 128 (23) 121 (56), 109 (18), 91 (19), 82 (45), 70 (100), 53 (26), 41 (67). IR (ATR): $\tilde{\nu} = 2977$ (w), 2915 (w), 2855 (w), 1715 (m), 1648 (w), 1446 (w), 1371 (w), 1219 (m), 1141 (s), 1040 (w) cm⁻¹. UV-Vis (CH₂Cl₂): λ_{max} (ϵ , L mol⁻¹ cm⁻¹) = 230 (8914) nm.

Ethyl (2E,6E,10E)-[14-²H]-3,7,11,15-tetramethylhexadeca-2,6,10,14-tetraenoate (3d): Yield: (1.0 g, 3.0 mmol, 46%). $R_f = 0.46$ (hexane/EtOAc (20:1)). GC (BPX-5): $I = 2326$. ¹H NMR (400 MHz, CDCl₃, TMS): $\delta = 5.67 - 5.66$ (m, 1H, CH), 5.12 – 5.08 (m, 2H, 2x CH), 4.14 (q, $^3J_{\text{HH}} = 7.1$ Hz, 2H, CH₂), 2.17 (s, 3H, CH₃), 2.16 (s, 3H, CH₃), 2.09 – 2.06 (m, 6H, 3x CH₂), 2.04 – 1.95 (m, 6H, 3x CH₂), 1.68 (s, 3H, CH₃), 1.60 (s, 6H, 2x CH₃), 1.27 (t, $^3J_{\text{HH}} = 7.1$ Hz, 3H, CH₃) ppm. ¹³C NMR (100 MHz, CDCl₃): $\delta = 166.9$ (C_q), 159.7 (C_q), 136.1 (C_q), 135.0 (C_q), 131.1 (C_q), 124.1 (CH), 122.9 (CH), 115.6 (CH), 59.4 (CH₂), 41.0 (CH₂), 39.7 (CH₂), 39.6 (CH₂), 26.6 (CH₂), 26.5 (CH₂), 26.0 (CH₂), 25.6 (CH₃), 18.8 (CH₃), 17.6 (CH₃), 16.0 (CH₃), 15.9 (CH₃), 14.3 (CH₃) ppm. MS (EI, 70 eV): m/z (%) = 333 (7) [M]⁺, 318 (1), 288 (4), 263 (2), 247 (2), 219 (2), 206 (4), 189 (12), 175 (7), 161 (7), 147 (12), 136 (24), 128 (45), 121 (43), 107 (21), 93 (27), 81 (47), 70 (100), 53 (15), 41 (39). IR (ATR): $\tilde{\nu} = 2966$ (w), 2924 (w), 2855 (w), 1715 (m), 1648 (m), 1446 (w), 1379 (w), 1219 (m), 1142 (s), 1040 (w) cm⁻¹. UV-Vis (CH₂Cl₂): λ_{max} (ϵ , L mol⁻¹ cm⁻¹) = 229 (10069) nm.

Ethyl (2Z,6E,10E)-[14-²H]-3,7,11,15-tetramethylhexadeca-2,6,10,14-tetraenoate: Yield: (83 mg, 0.25 mmol, 4%). $R_f = 0.48$ (hexane/EtOAc (20:1)). GC (BPX-5): $I = 2281$. ¹H NMR (400 MHz, CDCl₃, TMS): $\delta = 5.66 - 5.65$ (m, 1H, CH), 5.17 (tq, $^3J_{\text{HH}} = 7.2$ Hz, $^4J_{\text{HH}} = 1.1$ Hz, 1H, CH), 5.13 – 5.09 (m, 1H, CH), 4.14 (q, $^3J_{\text{HH}} = 7.2$ Hz, 2H, CH₂), 2.65 (t, $^3J_{\text{HH}} = 7.5$ Hz, 2H, CH₂), 2.20 – 2.15 (m, 2H, CH₂), 2.08 – 2.04 (m, 4H, 2x CH₂), 2.00 – 1.95 (m, 4H, 2x CH₂), 1.89 (d, $^4J_{\text{HH}} = 1.4$ Hz, 3H, CH₃), 1.68 (s, 3H, CH₃), 1.62 (s, 3H, CH₃), 1.60 (s, 6H, 2x CH₃), 1.27 (t, $^3J_{\text{HH}} = 7.2$ Hz, 3H, CH₃) ppm. ¹³C NMR (100 MHz, CDCl₃): $\delta = 166.3$ (C_q), 160.1 (C_q), 135.8 (C_q), 135.0 (C_q), 131.1 (C_q), 124.2 (CH), 123.5 (CH), 59.4 (CH₂), 39.7 (CH₂), 33.4 (CH₂), 26.8 (CH₂), 26.7 (CH₂), 26.6 (CH₂), 25.6 (CH₃), 25.4 (CH₃), 17.6 (CH₃), 16.0 (2x CH₃), 14.3 (CH₃) ppm. MS (EI, 70 eV): m/z (%) = 333 (5) [M]⁺, 318 (1), 290 (2), 263 (2), 248 (2), 233 (1), 219 (3), 206 (4), 189 (20), 175 (8), 161 (7), 149 (31), 135 (18), 121 (55), 107 (20), 93 (26), 81 (31), 70 (100), 53 (16), 41 (44). IR (ATR): $\tilde{\nu} = 2967$ (w), 2920 (w), 2855 (w), 1716 (m), 1648 (w), 1445 (w), 1375 (w), 1238 (w), 1153 (s), 855 (w) cm⁻¹. UV-Vis (CH₂Cl₂): λ_{max} (ϵ , L mol⁻¹ cm⁻¹) = 230 (8536) nm.

General procedure for the synthesis of alcohols. The esters [10-²H]-**3c** and [14-²H]-**3d** (1.0 eq., 0.2 M in abs. Et₂O) were cooled to -78 °C and a solution of DIBAL-H (2.0 eq., 1.0 M in hexane) was added dropwise. The reaction mixture was stirred for 2 h at -78 °C, hydrolysed with distilled water and extracted three times with Et₂O. The combined organic layers were dried over MgSO₄ and concentrated under reduced pressure. Column chromatography with hexane/ethyl acetate (5:1) yielded the desired alcohols [10-²H]-**4c** and [14-²H]-**4d** as colorless oils.

(2E,6E)-[10-²H]-3,7,11-trimethyldodeca-2,6,10-trien-1-ol (4c): Yield: (2.6 g, 11.4 mmol, 72%). $R_f = 0.25$ (hexane/EtOAc (5:1)). GC (BPX-5): $I = 1846$. ¹H NMR (400 MHz, CDCl₃, TMS): $\delta = 5.42$ (tq, $^3J_{\text{HH}} = 6.9$ Hz, $^4J_{\text{HH}} = 1.3$ Hz, 1H, CH), 5.11 (tq, $^3J_{\text{HH}} = 7.0$ Hz, $^4J_{\text{HH}} = 1.3$ Hz, 1H, CH), 4.15 (d, $^3J_{\text{HH}} = 6.9$ Hz, 2H, CH₂), 2.15 – 1.96 (m, 8H, 4x CH₂), 1.68 (s, 6H, 2x CH₃), 1.60 (s, 6H, 2x CH₃), 1.49 (br s, 1H, OH) ppm. ¹³C NMR (100 MHz, CDCl₃): $\delta = 139.7$ (C_q), 135.3 (C_q), 131.2 (C_q), 123.9 (t, $^1J_{\text{CD}} = 23.1$ Hz, C²H), 123.7 (CH), 123.4 (CH), 59.3 (CH₂), 39.6 (CH₂), 39.5 (CH₂), 26.7 (CH₂), 26.3 (CH₂), 25.6 (CH₃), 17.6 (CH₃), 16.2 (CH₃), 16.0 (CH₃) ppm. MS (EI, 70 eV, MSTFA): m/z (%) = 295 (3) [M]⁺, 280 (2), 205 (7), 190 (14), 169 (12), 156 (19), 143 (29), 135 (31), 121 (16), 107 (29), 93 (46), 73 (100), 53 (12), 41 (40). IR (ATR): $\tilde{\nu} = 3321$ (br), 2965 (m), 2914 (s), 2854 (m), 1445 (s), 1377 (m), 998 (s) cm⁻¹. UV-Vis (CH₂Cl₂): λ_{max} (ϵ , L mol⁻¹ cm⁻¹) = 228 (591) nm.

(2E,6E,10E)-[14-²H]-3,7,11,15-tetramethylhexadeca-2,6,10,14-tetraen-1-ol (4d): Yield: (650 mg, 2.2 mmol, 75%). $R_f = 0.25$ (hexane/EtOAc (5:1)). GC (BPX-5): $I = 2376$. ¹H NMR (400 MHz, CDCl₃, TMS): $\delta = 5.42$ (tq, $^3J_{\text{HH}} = 6.9$ Hz, $^4J_{\text{HH}} = 1.3$ Hz, 1H, CH), 5.13 – 5.09 (m, 2H, 2x CH), 4.15 (d, $^3J_{\text{HH}} = 6.9$ Hz, 2H, CH₂), 2.13 – 1.95 (m, 12H, 6x CH₂), 1.68 (s, 6H, 2x CH₃), 1.60 (s, 9H, 3x CH₃) ppm. ¹³C NMR (100 MHz, CDCl₃): $\delta = 139.8$ (C_q), 135.4 (C_q), 135.0 (C_q), 131.1 (C_q), 124.2 (CH), 124.1 (t, $^1J_{\text{CD}} = 23.2$ Hz, C²H), 123.8 (CH), 123.3 (CH), 59.4 (CH₂), 39.7 (CH₂), 39.6 (CH₂), 39.5 (CH₂), 26.7 (CH₂), 26.6 (CH₂), 26.3 (CH₂), 25.6 (CH₃), 17.6 (CH₃), 16.3 (CH₃), 16.0 (CH₃), 15.9 (CH₃) ppm. MS (EI, 70 eV, MSTFA): m/z (%) = 363 (1) [M]⁺, 248 (1), 293 (1), 260 (1), 230 (2), 190 (3), 169 (5), 156 (9), 143 (12), 135 (12), 121 (11), 107 (17), 93 (22), 81 (26), 70 (100), 53 (9), 41 (30). IR (ATR): $\tilde{\nu} = 3314$ (br), 2965 (m), 2916 (s), 2853 (m), 1667 (w), 1444 (s), 1379 (m), 999 (s), 841 (w) cm⁻¹. UV-Vis (CH₂Cl₂): λ_{max} (ϵ , L mol⁻¹ cm⁻¹) = 227 (800) nm.

General procedure for the synthesis of allyl bromides. To a cooled (0 °C) solution of the alcohols [²H₉]-**4a**, [6-²H]-**4b**, and [10-²H]-**4c** (1.0 eq., 1.4 M in abs. THF) was added PBr₃ (0.4 eq.) dropwise. The mixture was stirred for 30 – 60 min at 0 °C and then poured onto ice-water. The aqueous phase was extracted three times with hexane. The combined organic layers were dried over MgSO₄ and concentrated under reduced pressure. The allyl bromides [²H₉]-**5a**, [6-²H]-**5b**, and [10-²H]-**5c** were obtained as yellow oils that were used in the next step without purification.

Synthesis of (2E,6E,10E)-[14-²H]-1-chloro-3,7,11,15-tetramethylhexadeca-2,6,10,14-tetraene (5d). A solution of the alcohol [14-²H]-**4d** (1.0 eq., 0.25 M in abs. DMF) was treated with *s*-collidine (1.1 eq.) and LiCl (3.0 eq.). The mixture was cooled to 0 °C and MsCl (1.1 eq.) was added dropwise. The reaction was stirred over night at room temperature and quenched by pouring onto ice-water. After extraction with pentane, drying with MgSO₄ and evaporation of the solvent the chloride [14-²H]-**5d** was obtained as pale yellow oil which was used in the next step without purification.

General procedure for the synthesis of β -ketoesters. The allyl bromides [6-²H]-**5b** and [10-²H]-**5c** (1.0 eq., 0.5 M in abs. acetone) were treated with ethyl acetoacetate (3.0 eq.) and K₂CO₃ (1.5 eq.). The mixture was stirred under reflux for 5 h and filtered after cooling to room

temperature. The solvent was removed under reduced pressure and the residue purified by column chromatography with hexane/ethyl acetate (20:1) to give the desired esters [8-²H]-**7b** and [12-²H]-**7c** as pale yellow oils.

Ethyl (E)-[8-²H]-2-acetyl-5,9-dimethyldeca-4,8-dienoate (7b): Yield: (14.5 g, 54.0 mmol, 76%, 2 steps). $R_f = 0.19$ (hexane/EtOAc (20:1). GC (BPX-5): $I = 1793$. ¹H NMR (400 MHz, CDCl₃, TMS): $\delta = 5.04$ (tq, ³ $J_{H,H} = 7.3$ Hz, ⁴ $J_{H,H} = 1.3$ Hz, 1H, CH), 4.18 (q, ³ $J_{H,H} = 7.2$ Hz, 2H, CH₂), 3.44 (t, ³ $J_{H,H} = 7.6$ Hz, 1H, CH), 2.57 – 2.53 (m, 2H, CH₂), 2.22 (s, 3H, CH₃), 2.06 – 1.97 (m, 4H, 2x CH₂), 1.67 (s, 3H, CH₃), 1.63 (s, 3H, CH₃), 1.59 (s, 3H, CH₃), 1.27 (s, ³ $J_{H,H} = 7.2$ Hz, 3H, CH₃) ppm. ¹³C NMR (100 MHz, CDCl₃): $\delta = 203.0$ (C_q), 169.5 (C_q), 138.3 (C_q), 131.3 (C_q), 123.6 (t, ¹ $J_{C,D} =$ Hz, C²H), 119.6 (CH), 61.2 (CH₂), 59.8 (CH), 39.6 (CH₂), 29.2 (CH₃), 26.9 (CH₂), 26.3 (CH₂), 25.5 (CH₃), 17.6 (CH₃), 16.0 (CH₃), 14.0 (CH₃) ppm. MS (EI, 70 eV): m/z (%) = 267 (5) [M]⁺, 249 (4), 224 (10), 197 (13), 178 (10), 155 (32), 137 (30), 123 (80), 109 (76), 93 (20), 81 (48), 70 (82), 55 (12), 43 (100). IR (ATR): $\tilde{\nu} = 2980$ (w), 2914 (w), 2856 (w), 1740 (s), 1715 (s), 1446 (w), 1360 (w), 1233 (m), 1145 (s), 1024 (m) cm⁻¹. UV-Vis (CH₂Cl₂): λ_{max} (ϵ , L mol⁻¹ cm⁻¹) = 228 (859) nm.

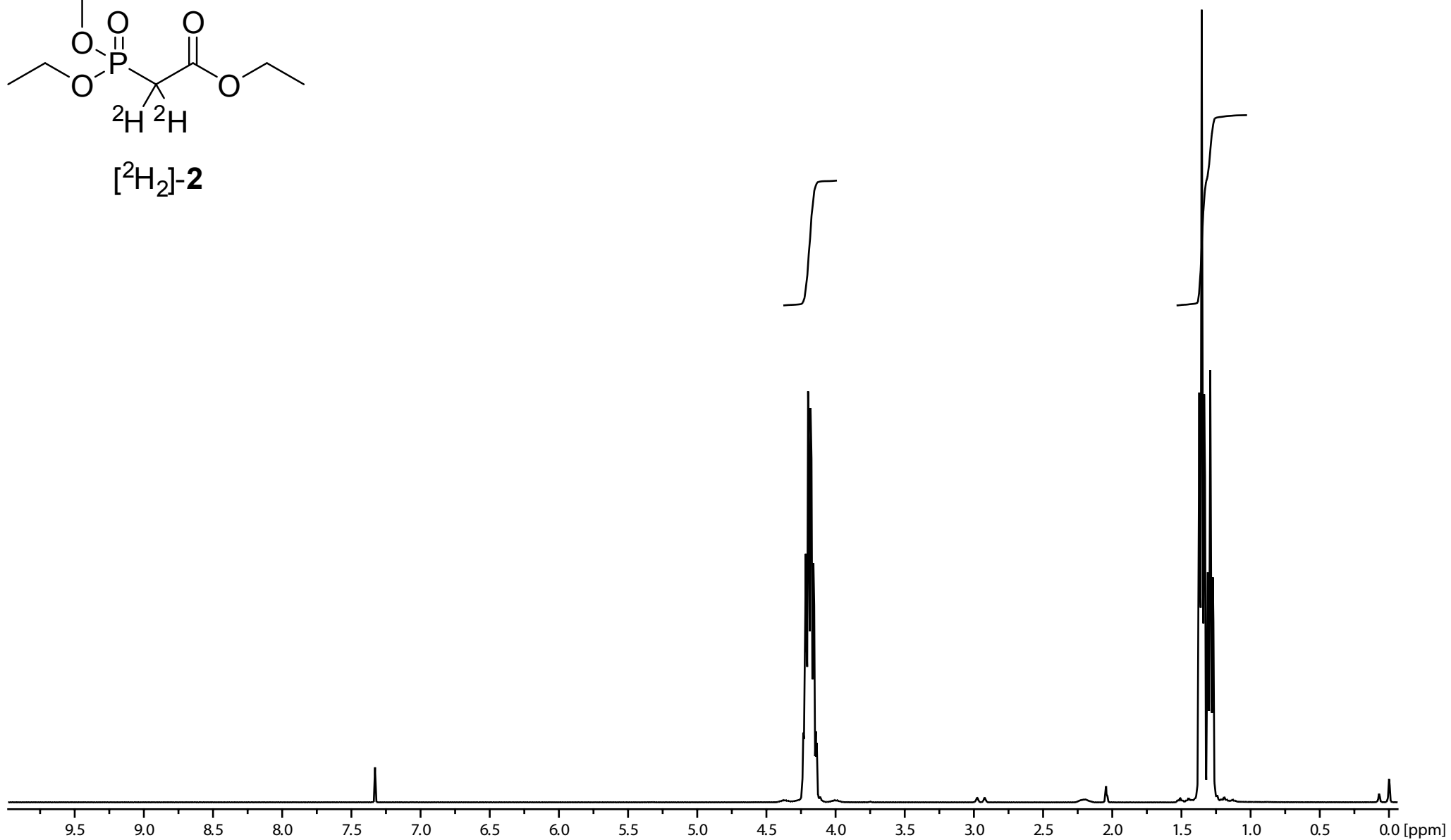
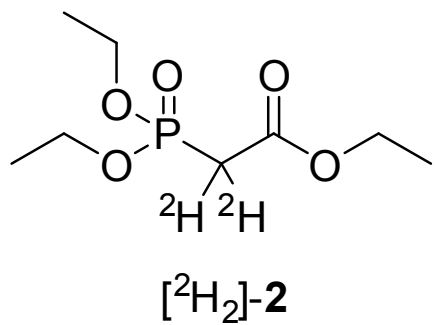
Ethyl (4E,8E)-[12-²H]-2-acetyl-5,9,13-trimethyltetradeca-4,8,12-trienoate (7c): Yield: (2.5 g, 7.4 mmol, 58%, 2 steps). $R_f = 0.85$ (hexane/EtOAc (5:1). GC (BPX-5): $I = 2244$. ¹H NMR (400 MHz, CDCl₃, TMS): $\delta = 5.09$ – 5.02 (m, 2H, 2x CH), 4.18 (q, ³ $J_{H,H} = 7.2$ Hz, 2H, CH₂), 3.44 (t, ³ $J_{H,H} = 7.6$ Hz, 1H, CH), 2.57 – 2.53 (m, 2H, CH₂), 2.22 (s, 3H, CH₃), 2.06 – 2.03 (m, 4H, 2x CH₂), 2.00 – 1.94 (m, 4H, 2x CH₂), 1.71 (s, 3H, CH₃), 1.63 (s, 3H, CH₃), 1.60 (s, 3H, CH₃), 1.59 (s, 3H, CH₃), 1.26 (t, ³ $J_{H,H} = 7.2$ Hz, 3H, CH₃) ppm. ¹³C NMR (100 MHz, CDCl₃): $\delta = 203.0$ (C_q), 169.6 (C_q), 138.4 (C_q), 135.2 (C_q), 131.1 (C_q), 124.0 (t, ¹ $J_{C,D} = 23.2$ Hz, C²H), 123.8 (CH), 119.6 (CH), 61.2 (CH₂), 59.8 (CH), 39.7 (CH₂), 29.1 (CH₃), 26.9 (CH₂), 26.6 (CH₂), 26.5 (CH₂), 25.6 (CH₃), 17.6 (CH₃), 16.1 (CH₃), 15.9 (CH₃), 14.1 (CH₃) ppm. MS (EI, 70 eV): m/z (%) = 335 (5) [M]⁺, 317 (1), 290 (1), 274 (1), 247 (3), 232 (2), 210 (3), 197 (8), 173 (7), 155 (15), 136 (25), 123 (36), 109 (30), 93 (22), 81 (45), 70 (100), 55 (12), 43 (78). IR (ATR): $\tilde{\nu} = 2974$ (w), 2914 (w), 2856 (w), 1715 (s), 1648 (m), 1445 (w), 1375 (w), 1238 (w), 1154 (s), 855 (w) cm⁻¹. UV-Vis (CH₂Cl₂): λ_{max} (ϵ , L mol⁻¹ cm⁻¹) = 229 (10426) nm.

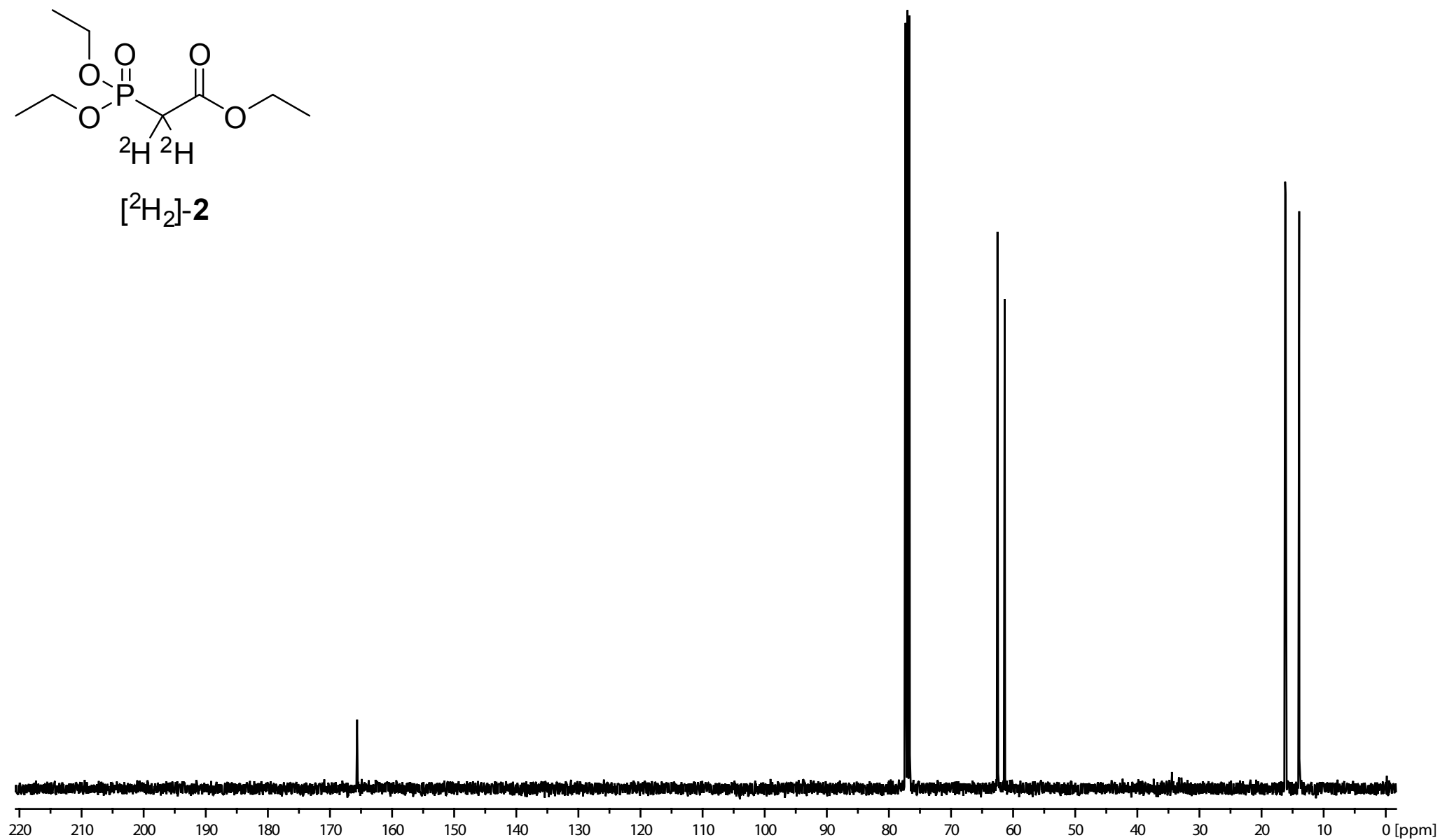
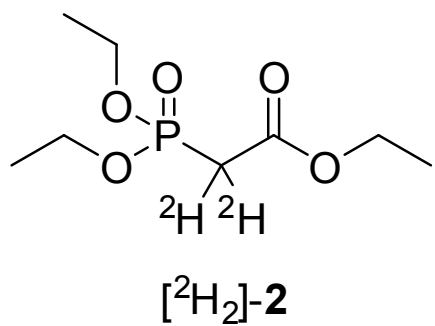
Procedure for the synthesis of the diphosphate. The halide [14-²H]-**5d** (1.0 eq.) was added to a solution of (NBu₄)₃HP₂O₇ (1.5 eq., 0.5 M in abs. CH₃CN). The reaction mixture was stirred over night at room temperature and then concentrated under reduced pressure. The residue was loaded onto a column containing ion exchange resin (DOWEX 50W-X8, NH₄⁺ form). Elution with two column volumes of ion exchange buffer (0.03 M NH₄HCO₃ in 2% *i*-PrOH/H₂O) and freeze drying yielded a yellowish solid. This material was dissolved in 0.05 M NH₄HCO₃ and *i*-PrOH/CH₃CN was added. The mixture was shaken until a white solid precipitated. After centrifugation the solution was transferred to a fresh flask and the solid again dissolved in 0.05 M NH₄HCO₃. The procedure was repeated twice. The collected solutions were pooled and freeze-dried to give the diphosphate [14-²H]-**8d** as colorless solid.

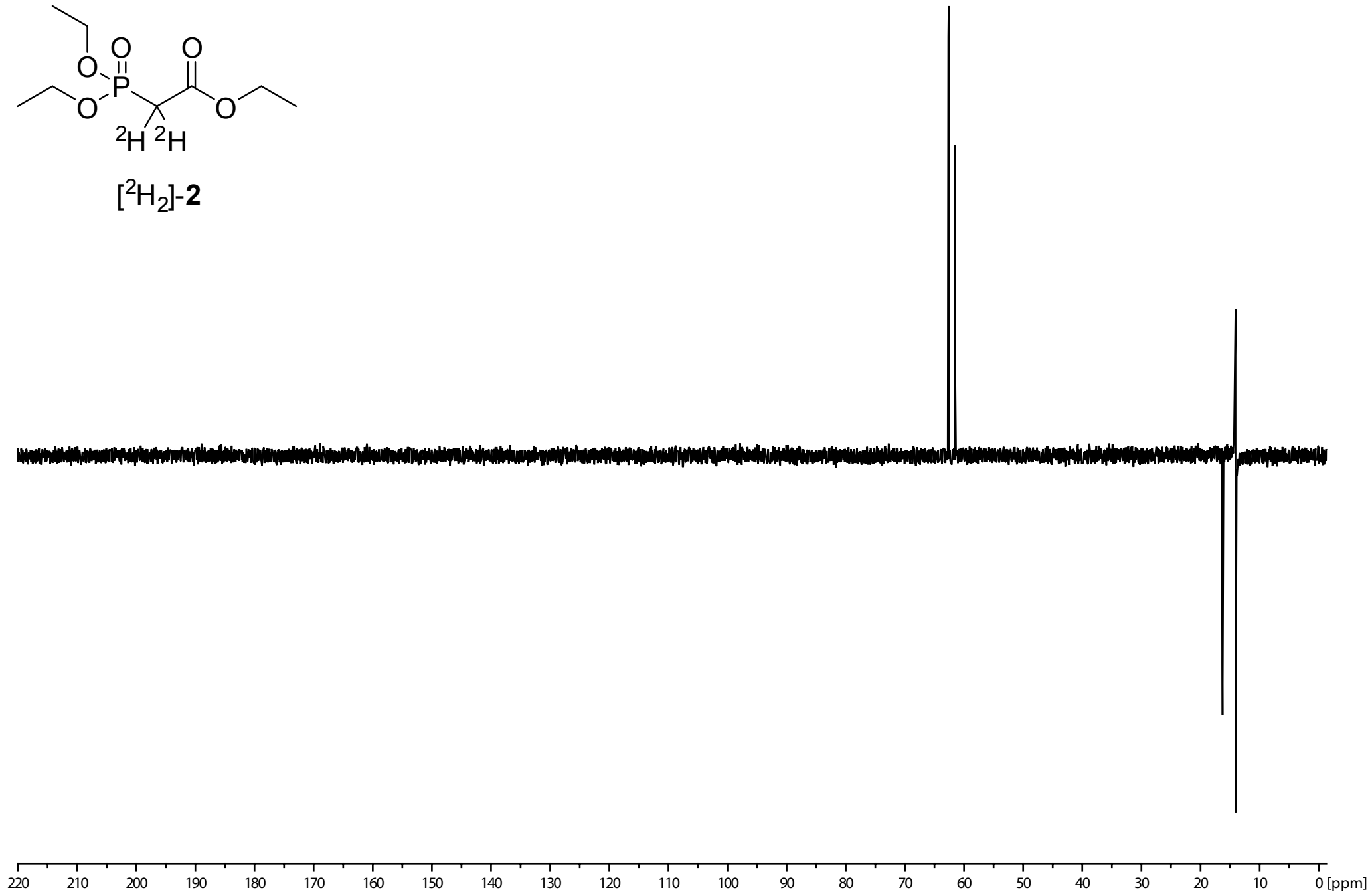
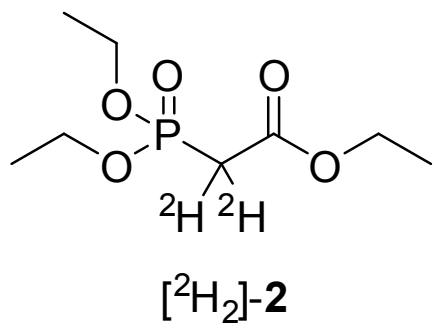
Trisammonium (2E,6E,10E)-[14-²H]geranylgeranyl diphosphate (8d): Yield: (130 mg, 0.26 mmol, 30%, 2 steps). ¹H NMR (400 MHz, ²H₂O, TMS): $\delta = 5.40$ (t, ³ $J_{H,H} = 6.6$ Hz, 1H, CH), 5.12 – 5.07 (m, 2H, 2x CH), 4.46 – 4.42 (m, 2H, CH₂), 2.09 – 1.92 (m, 12H, 6x CH₂), 1.73 (CH₃), 1.62 (CH₃), 1.58 (CH₃), 1.55 (CH₃), 1.54 (CH₃) ppm. ¹³C NMR (100 MHz, ²H₂O): $\delta = 145.0$ (C_q), 138.0 (C_q), 137.2 (C_q), 133.2 (C_q), 127.2 (CH), 126.9 (CH), 122.5 (d, ³ $J_{C,P} = 9.0$ Hz, CH), 65.5 (d, ² $J_{P,P} = 3.9$ Hz, CH₂), 42.6 (CH₂), 42.5 (CH₂), 42.4 (CH₂), 29.7 (CH₂), 29.6 (CH₂), 29.4 (CH₂), 28.2 (CH₃), 20.2 (CH₃), 18.9 (CH₃), 18.6 (2x CH₃) ppm. ³¹P NMR (162 MHz, ²H₂O): $\delta = -8.4$ (d, ² $J_{P,P} = 19.2$ Hz), -9.9 (d, ² $J_{P,P} = 19.2$ Hz) ppm. IR (ATR): $\tilde{\nu} = 3023$ (br), 2859 (m), 1442 (m), 1203 (m), 1161 (s), 1081 (s), 910 (s) cm⁻¹.

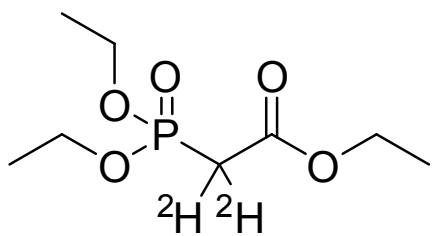
Literature

[1] D. Scherling, U. Pleiß, *J. Label. Compd. Radiopharm.* **1988**, *25*, 1393–1400.

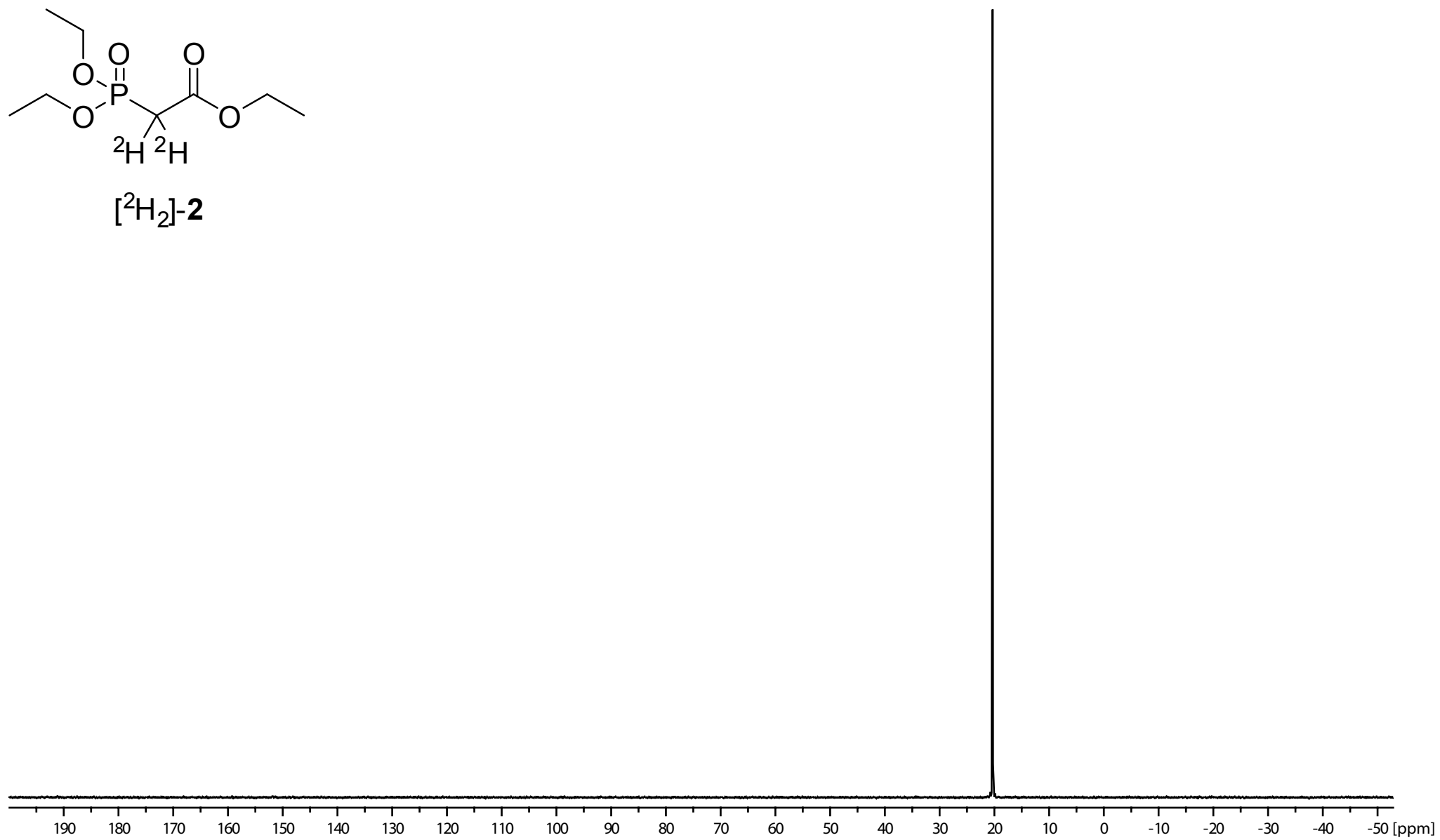


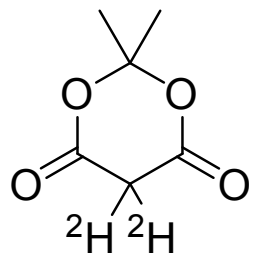




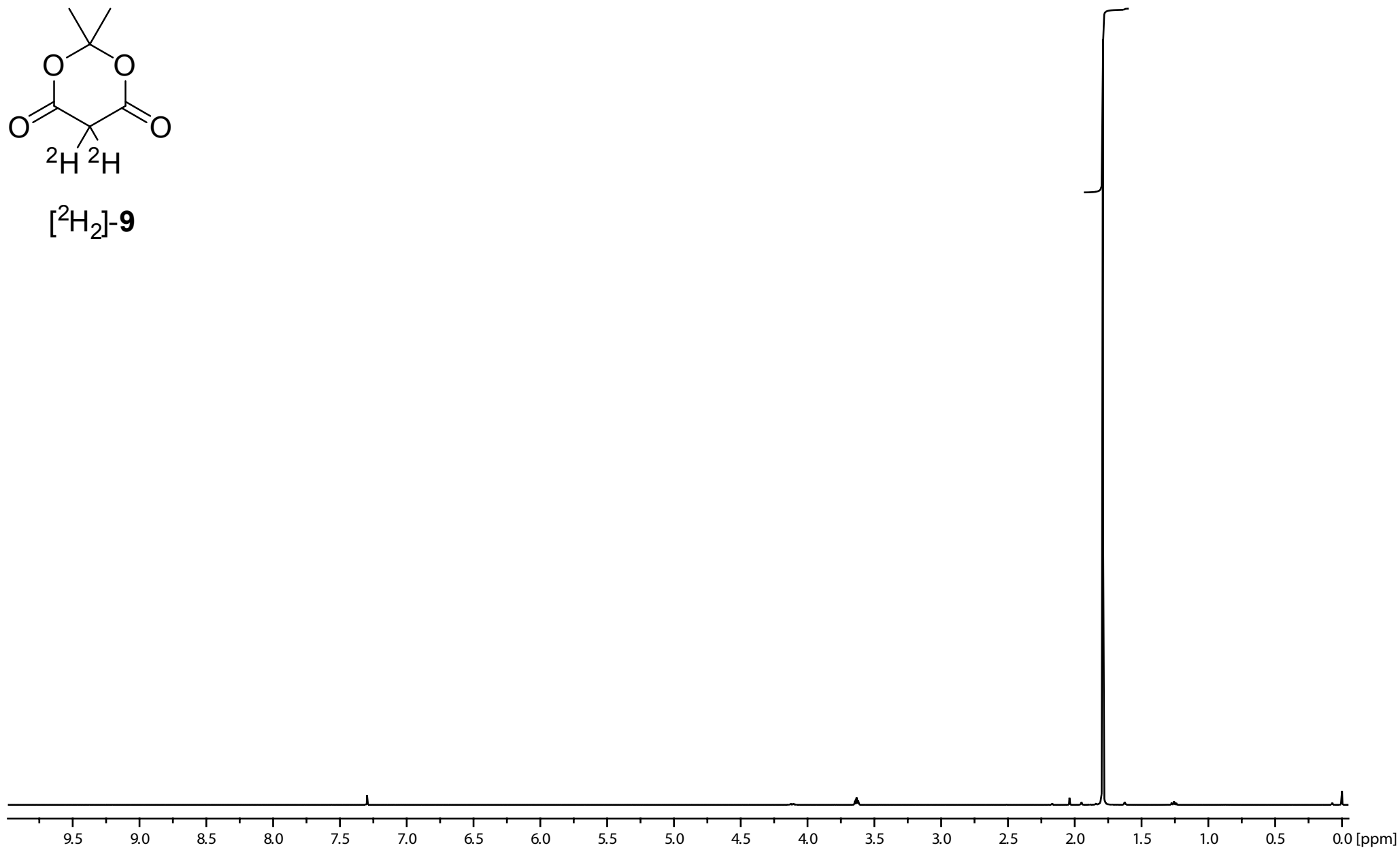


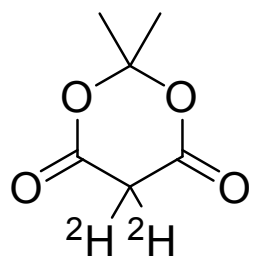
[$^2\text{H}_2$]-2



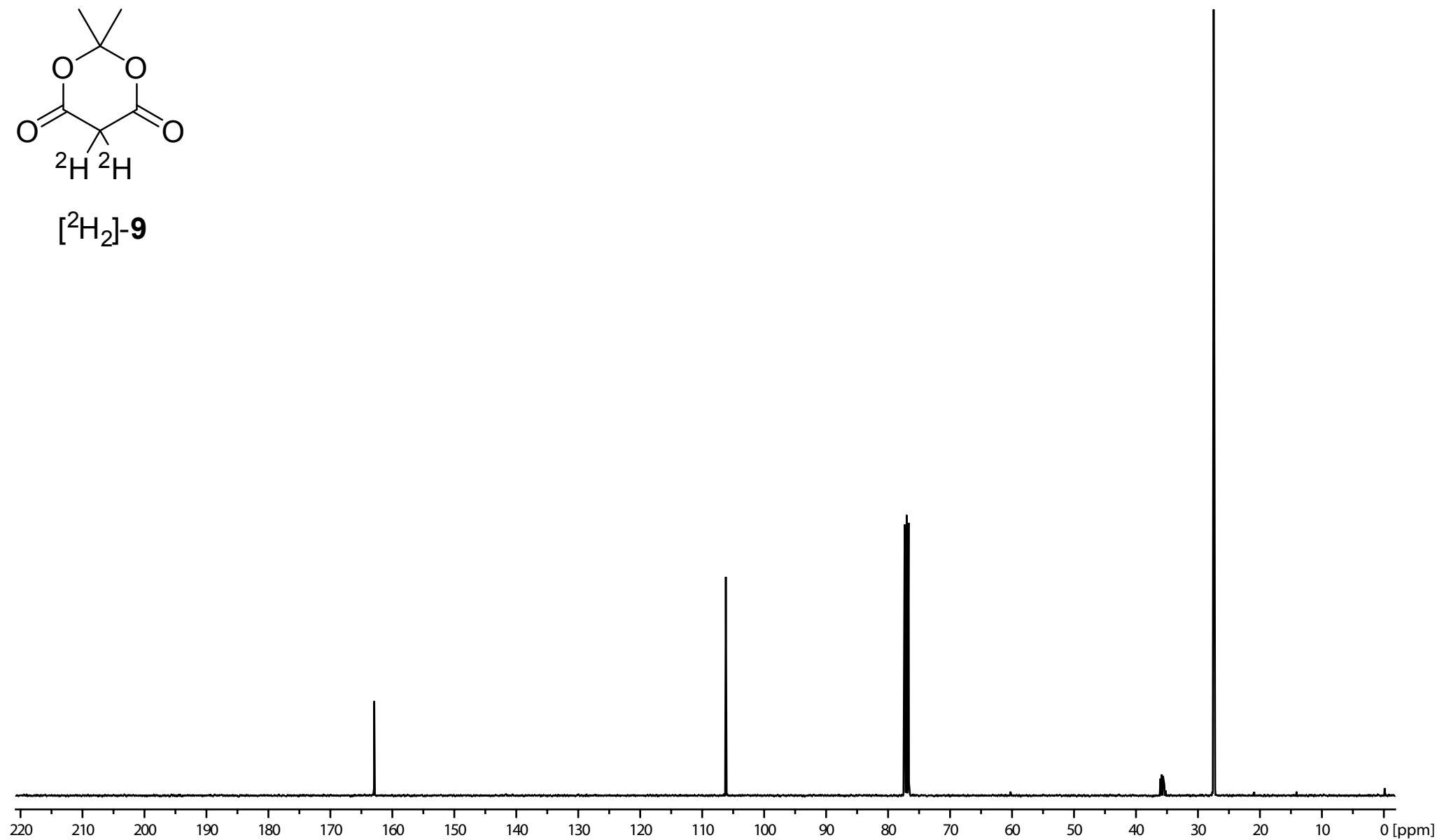


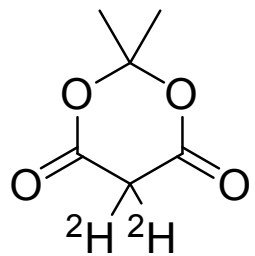
[²H₂]-**9**



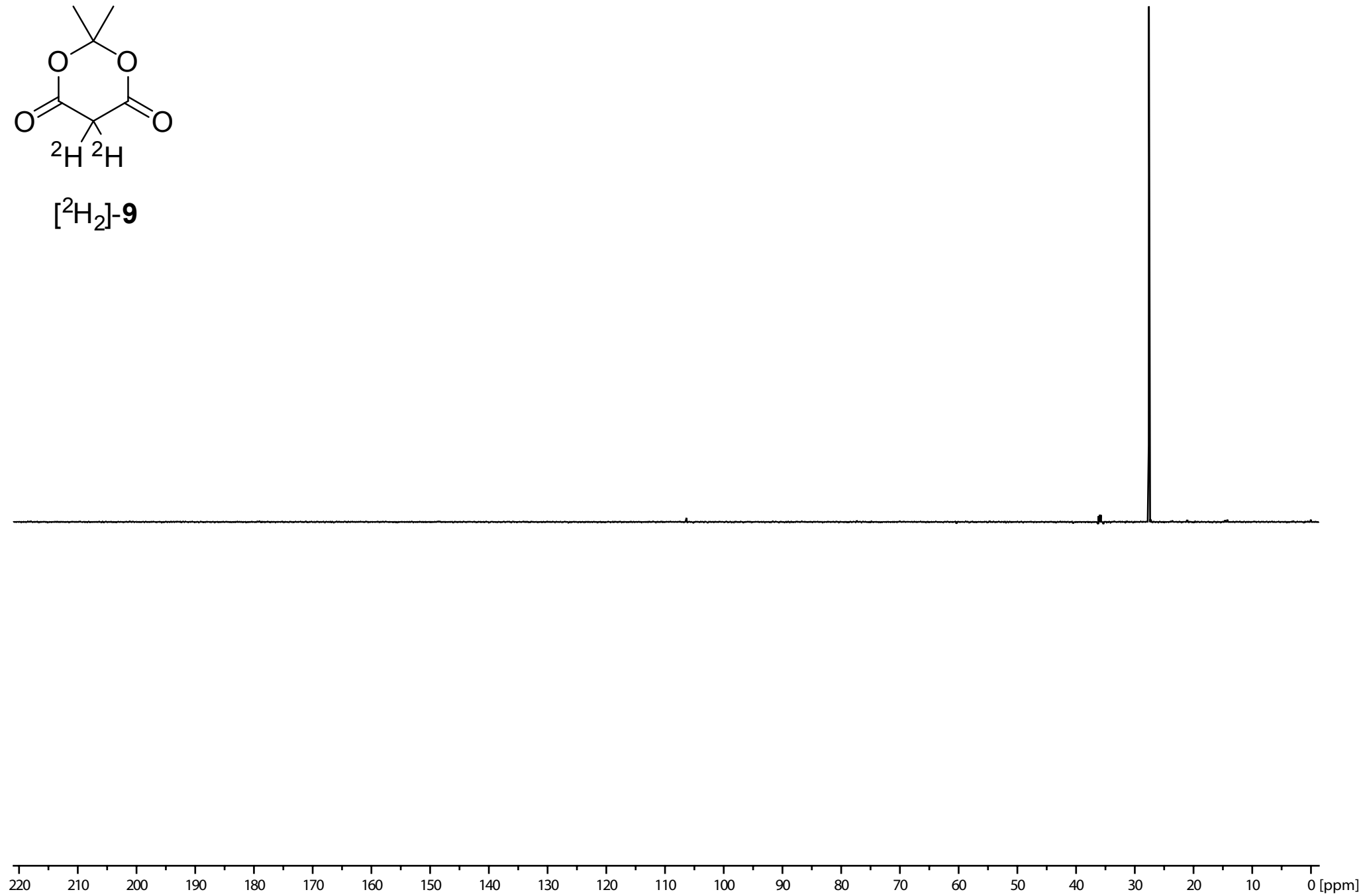


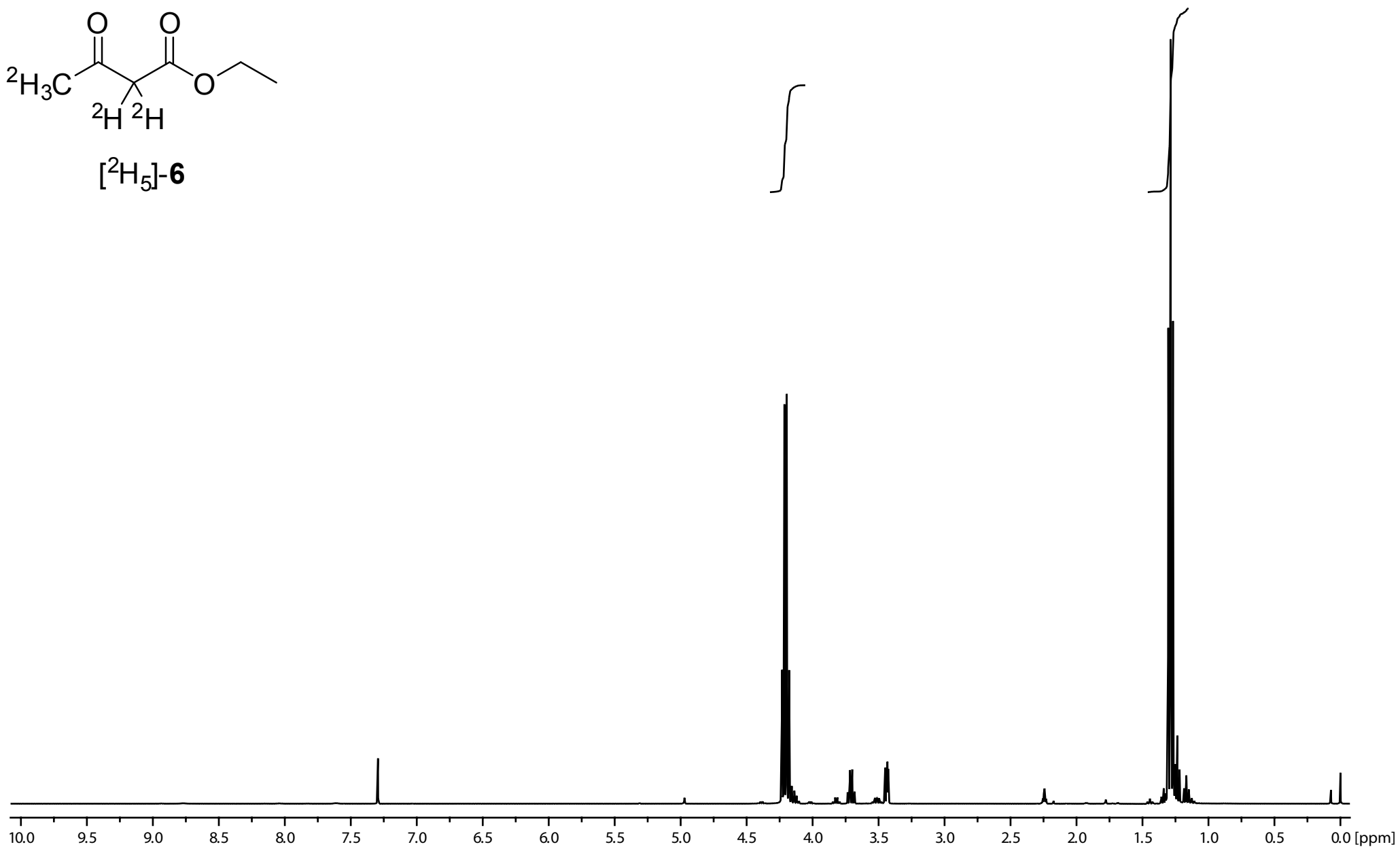
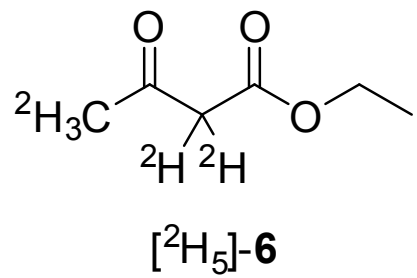
$[^2\text{H}_2]\text{-9}$

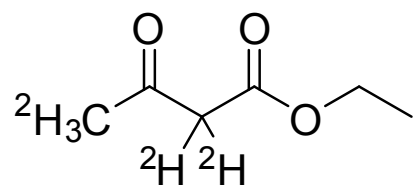




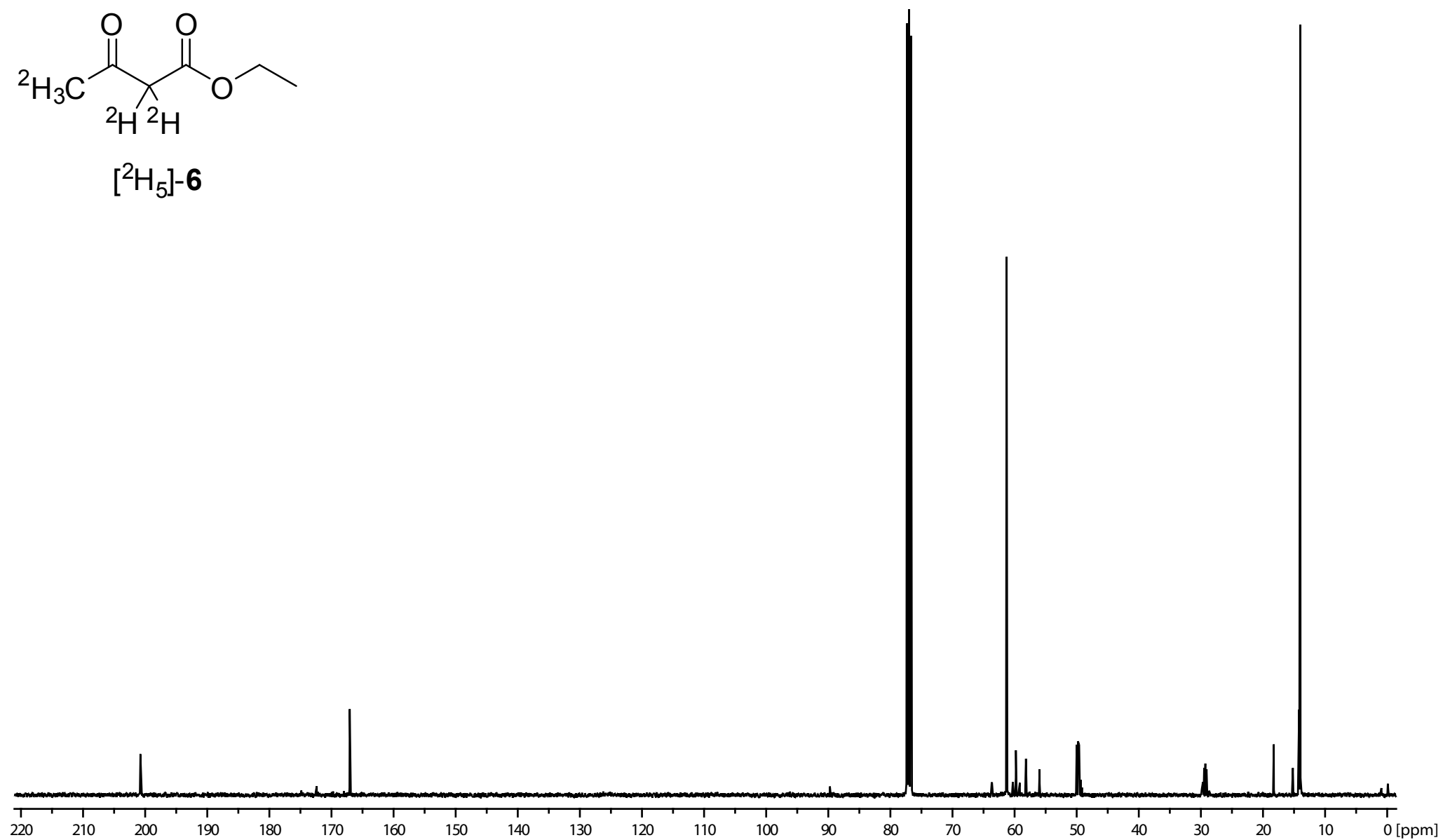
[²H₂]-9

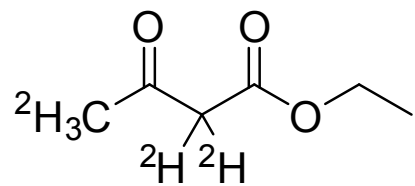




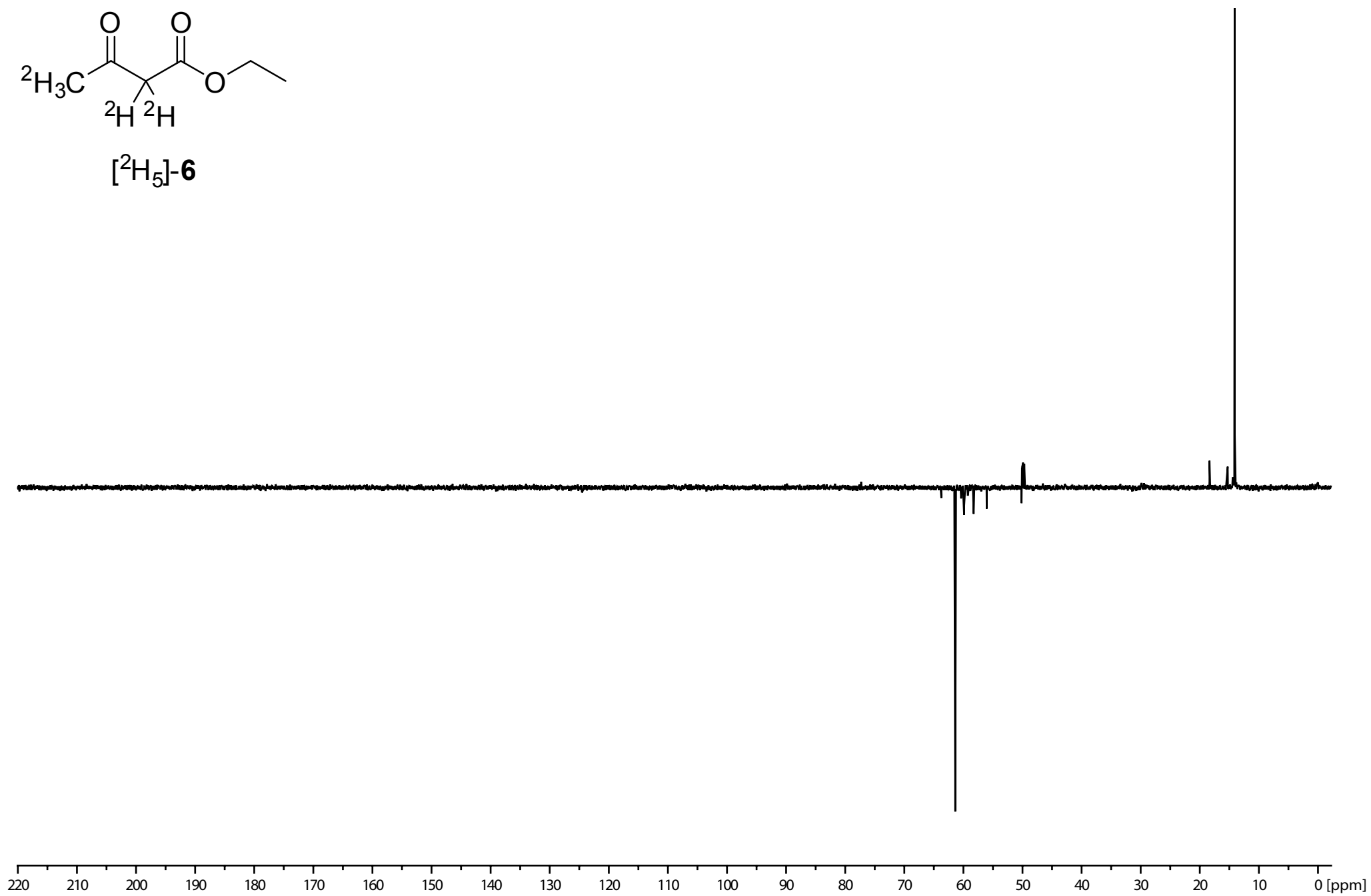


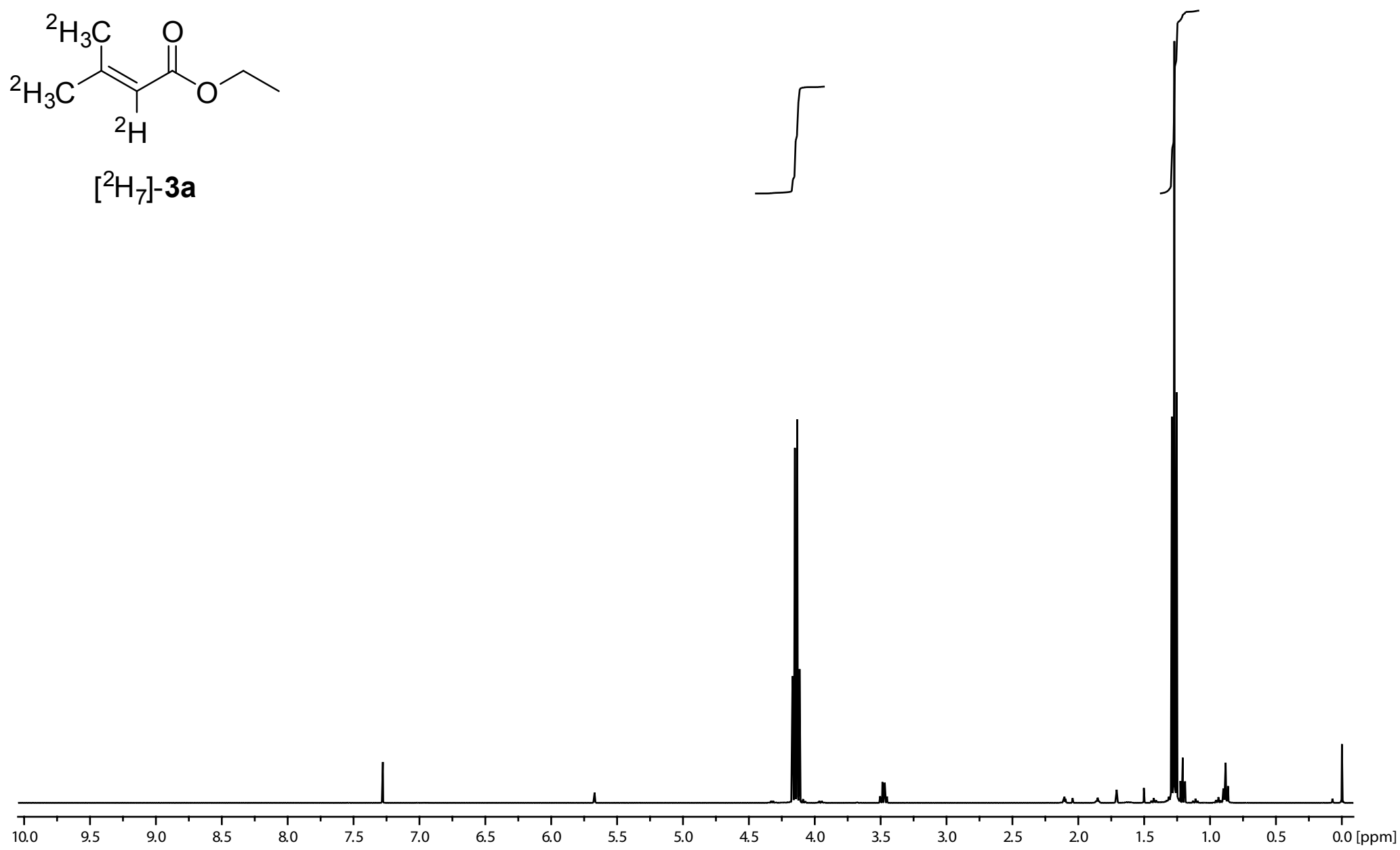
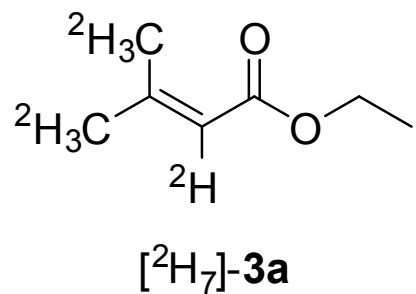
[²H₅]-**6**

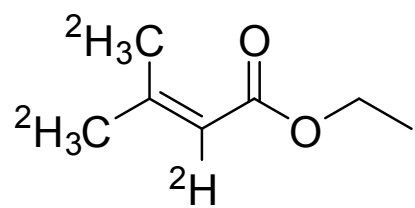




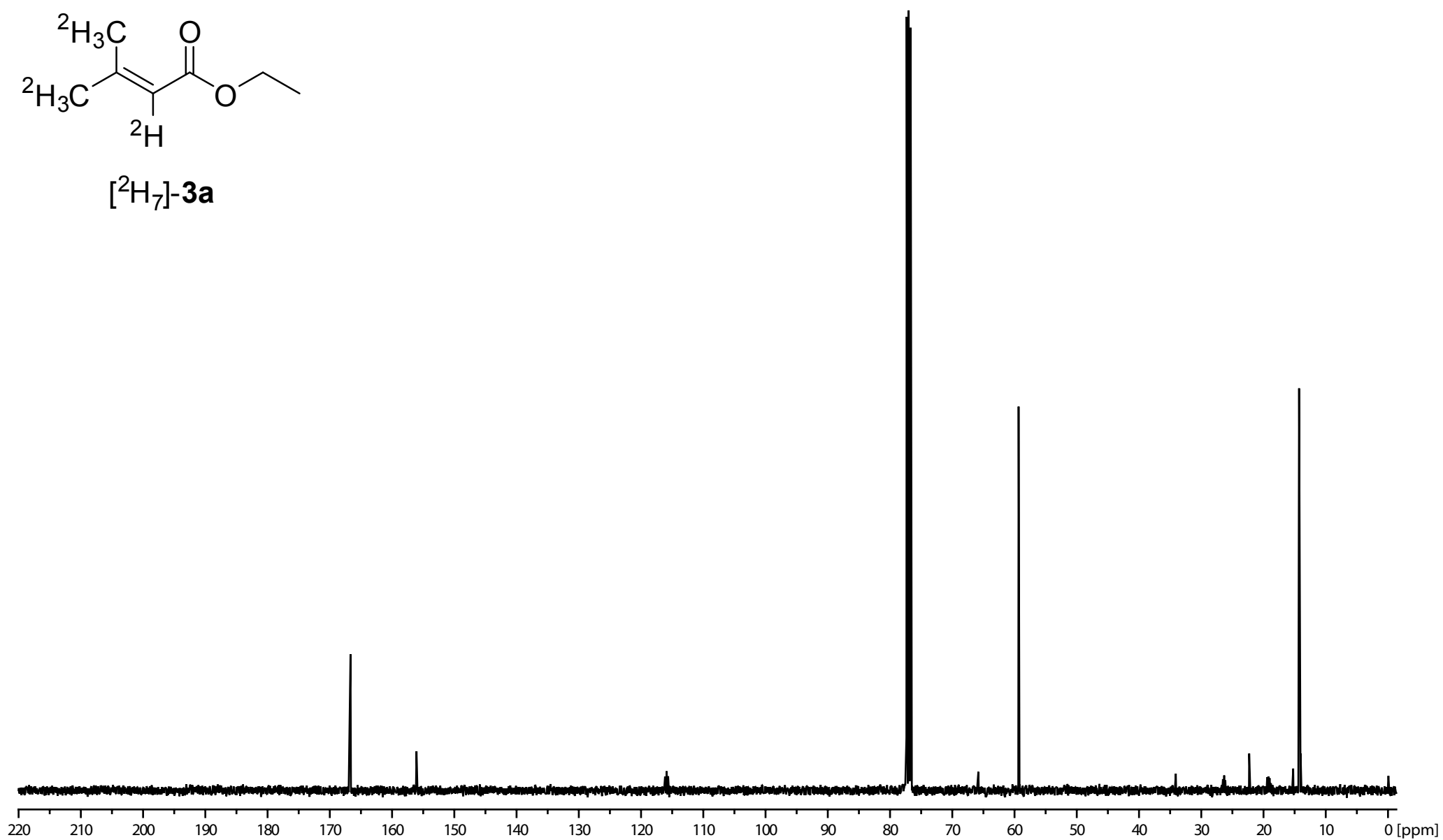
[²H₅]-**6**

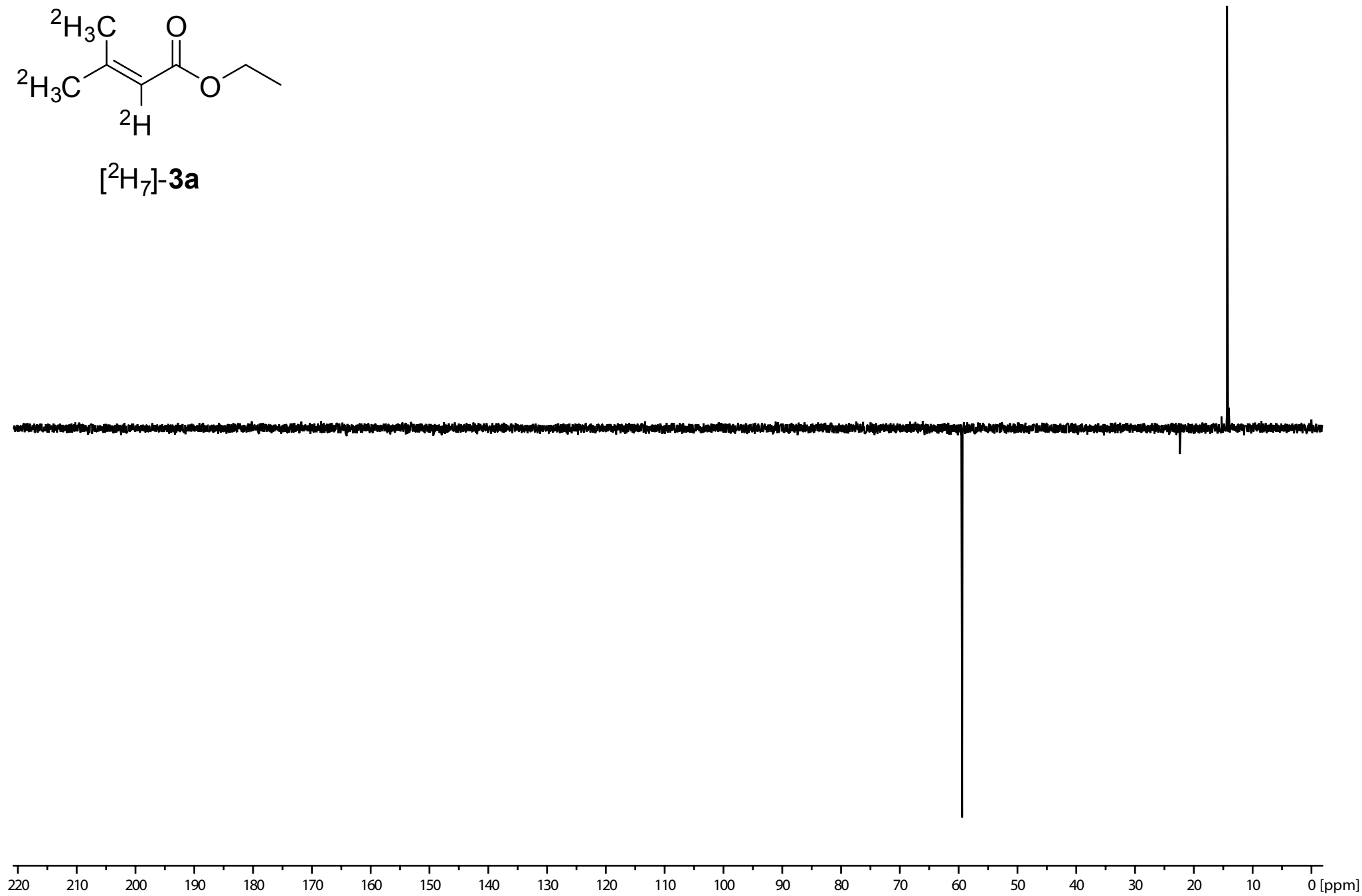
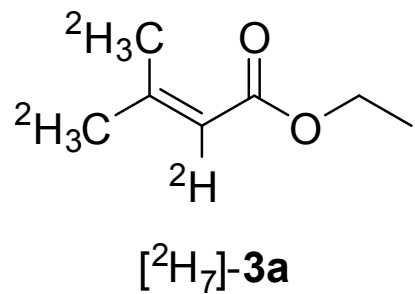


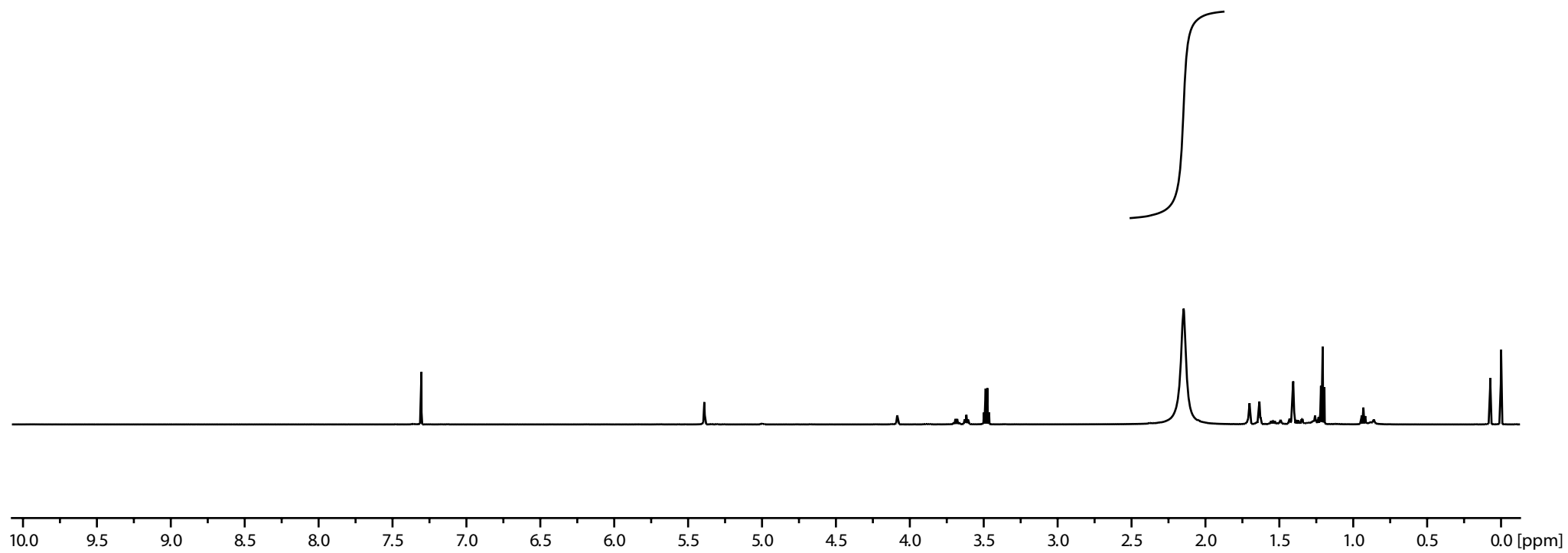
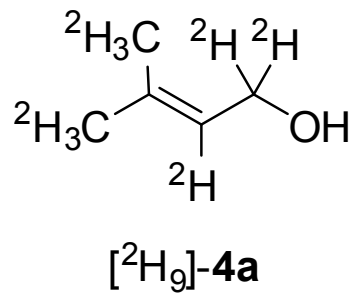


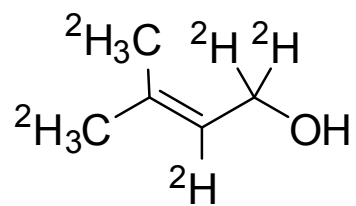


[²H₇]-3a

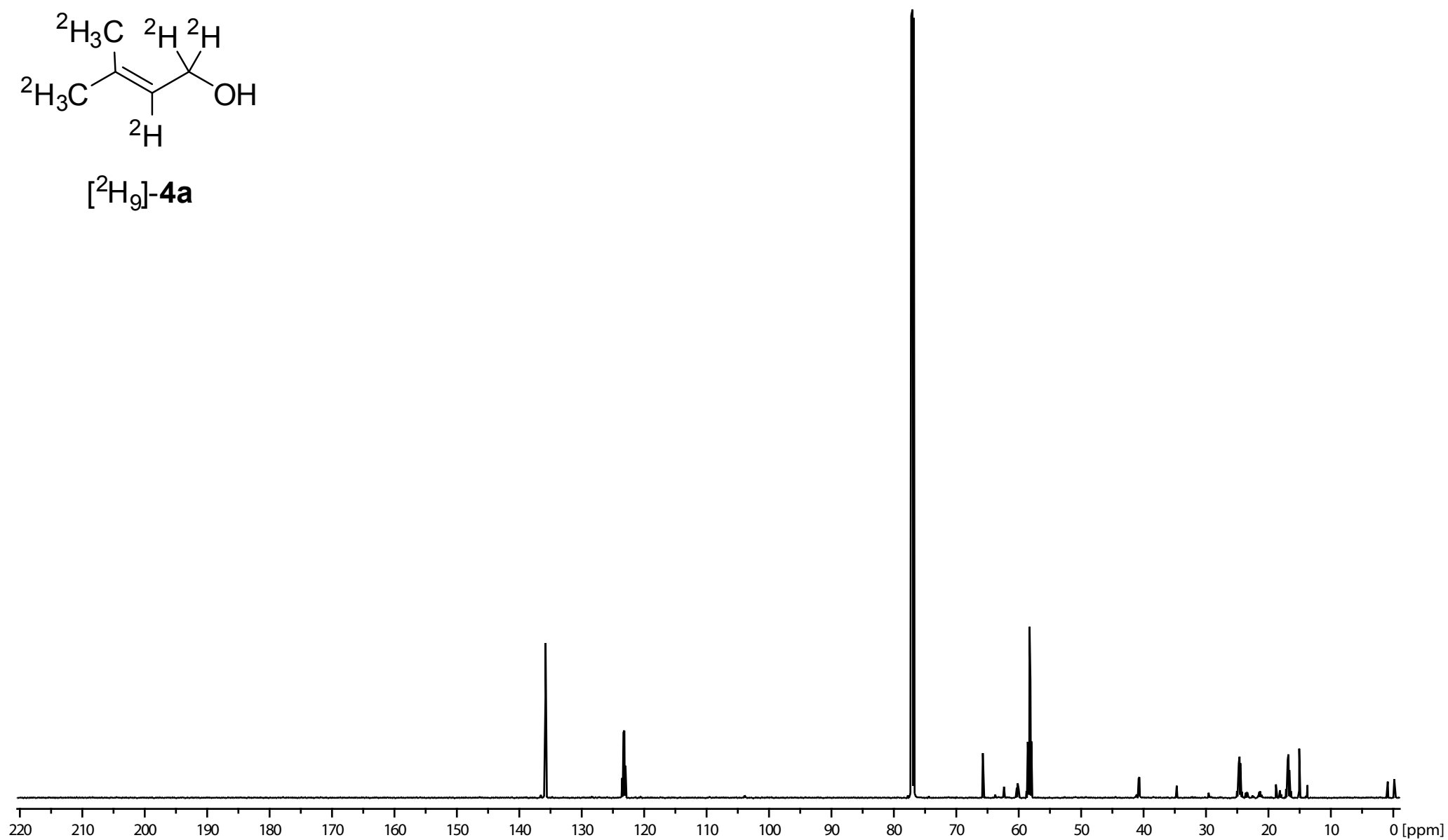


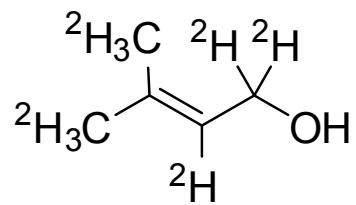




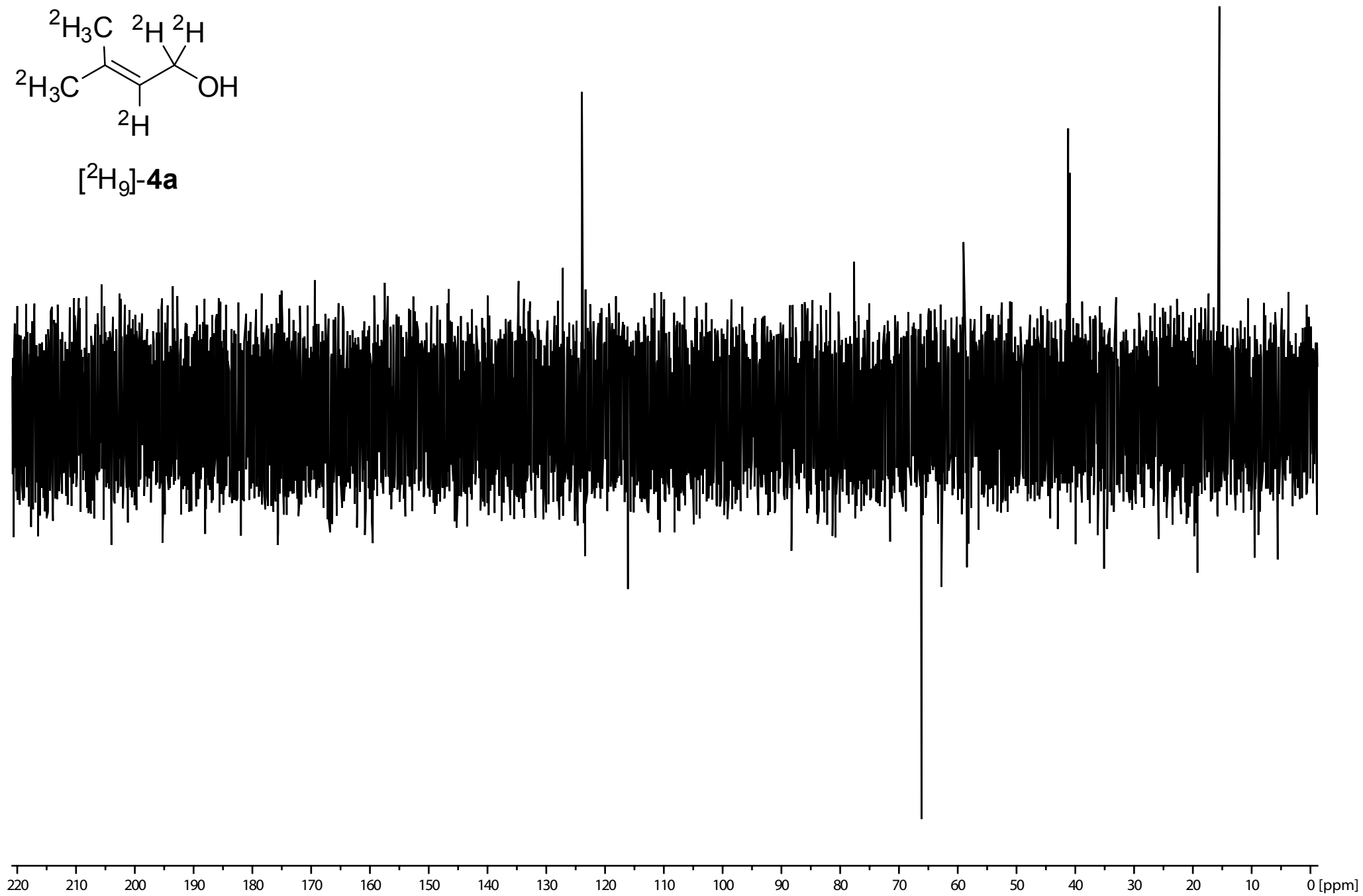


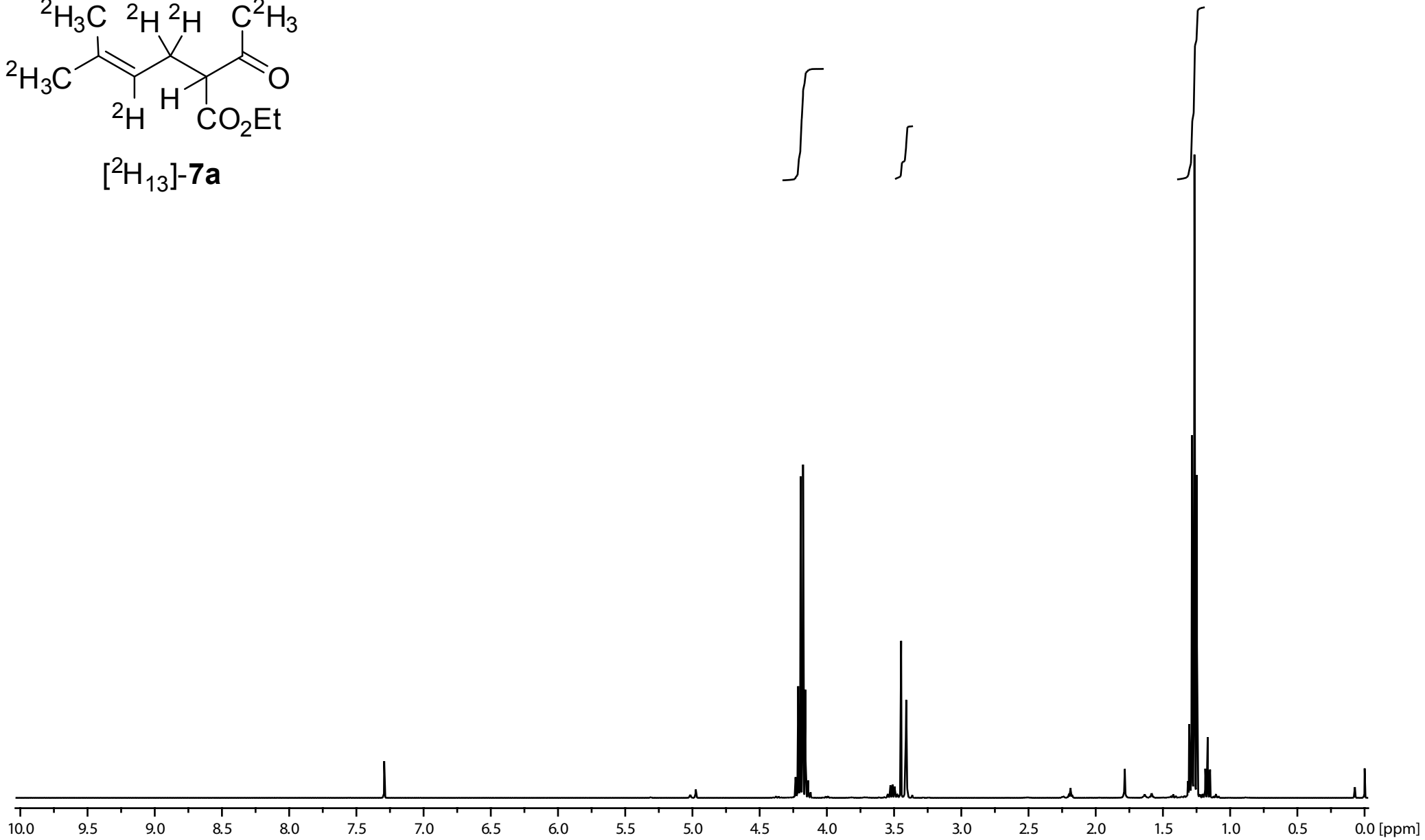
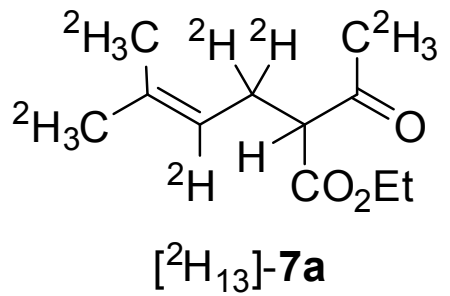
[²H₉]-4a

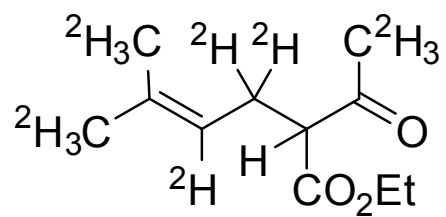




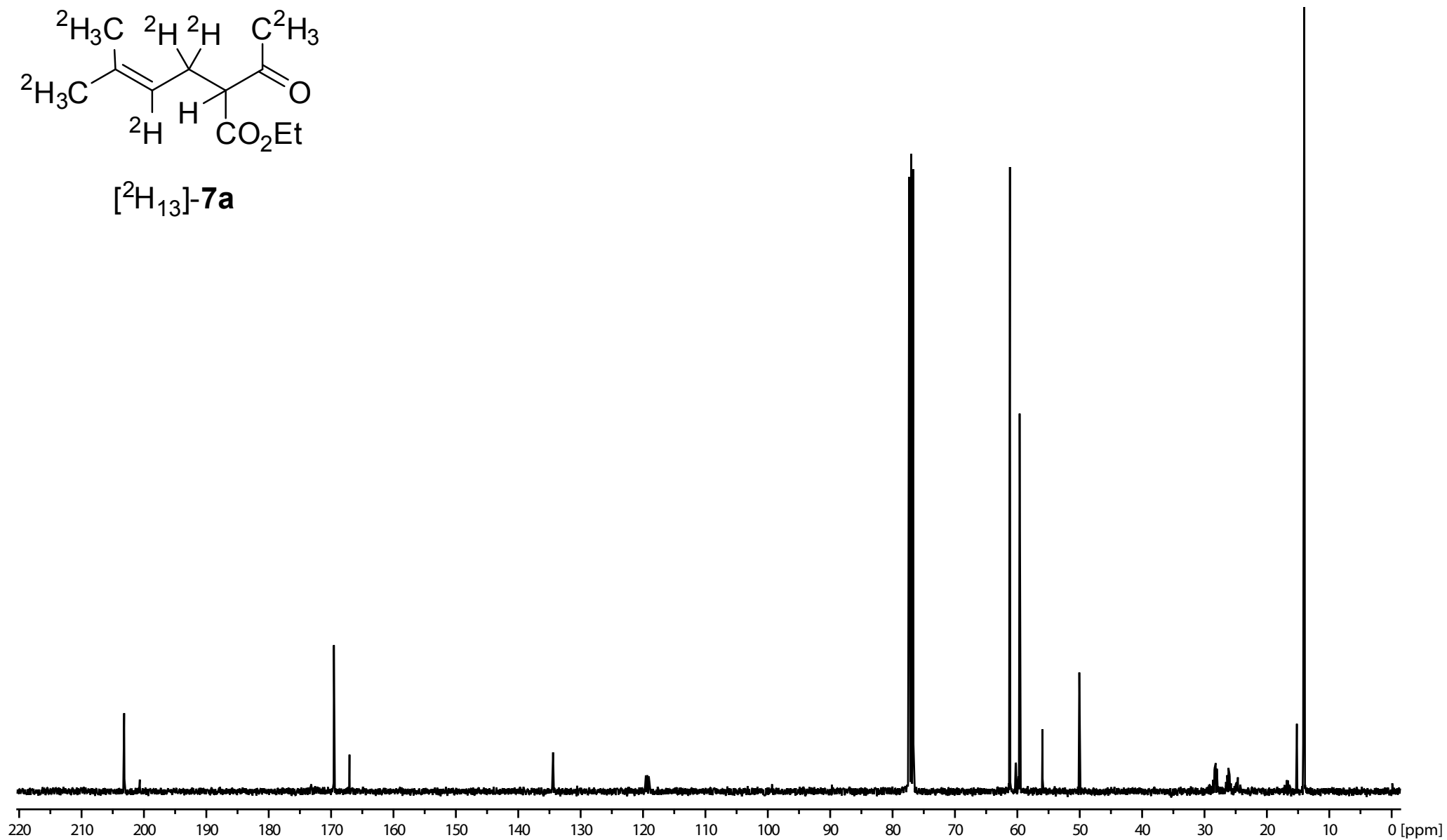
[²H₉]-4a

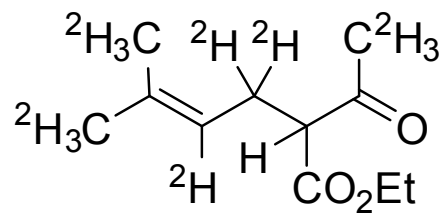




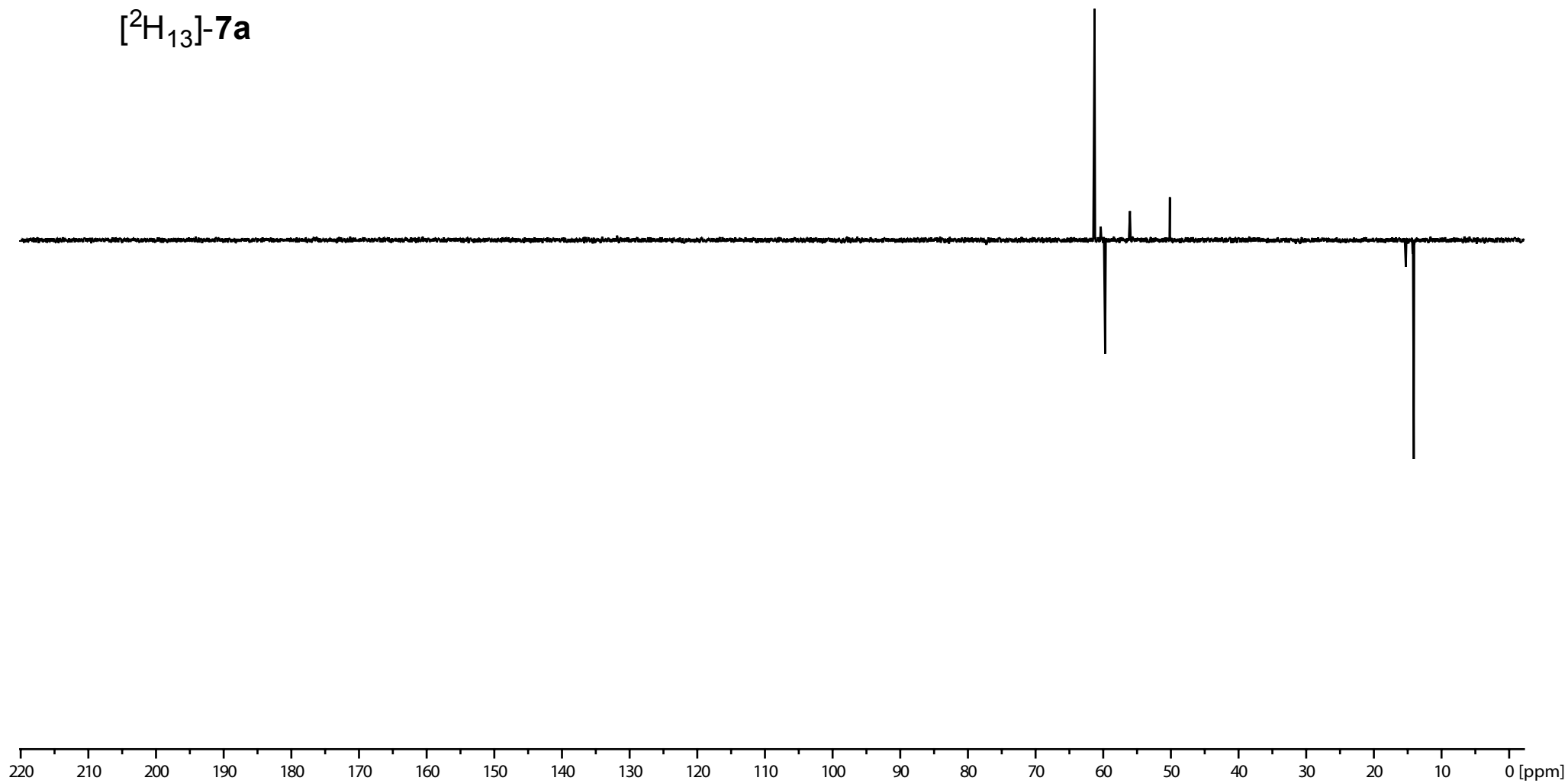


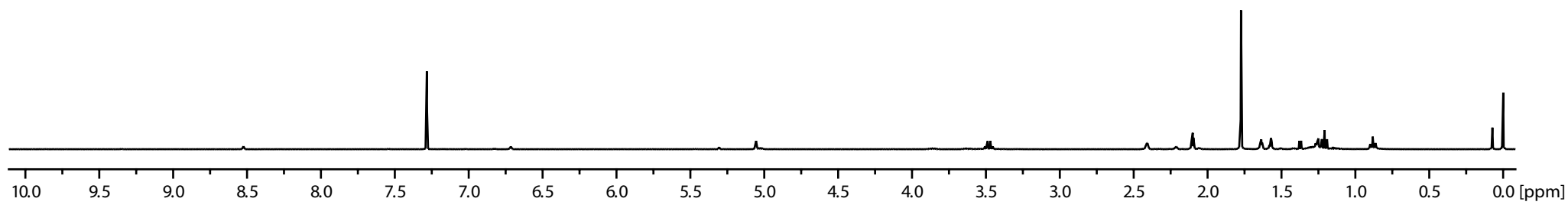
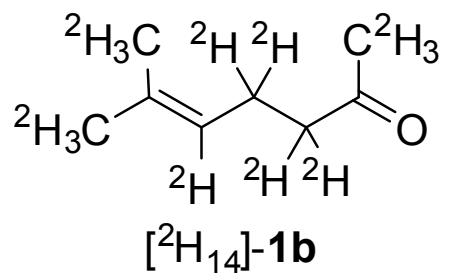
[²H₁₃]-7a

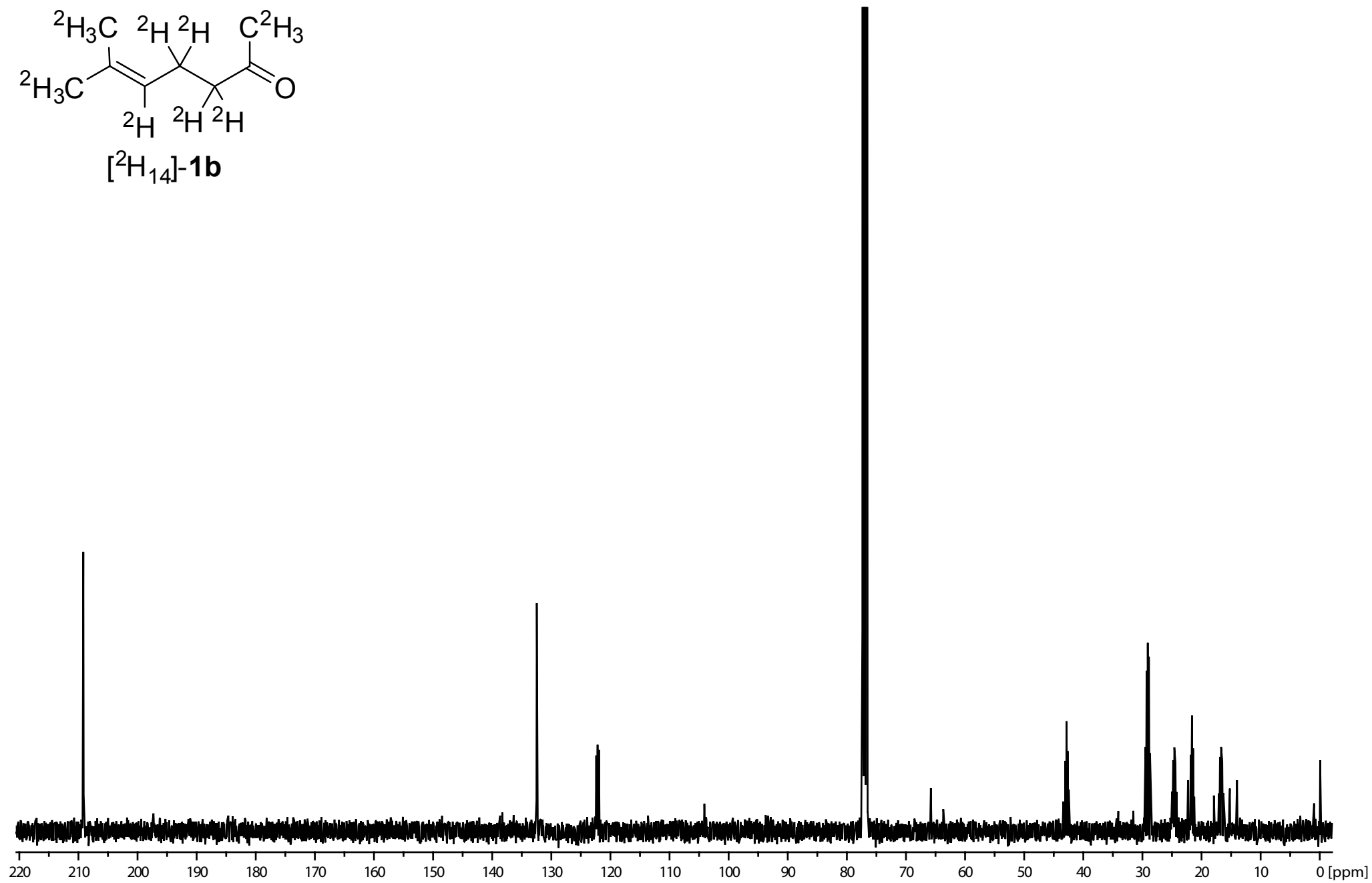
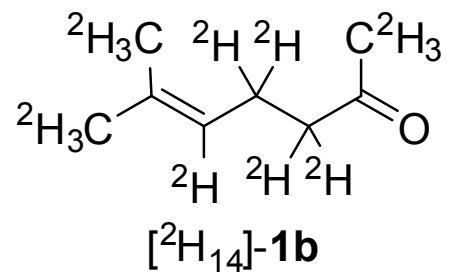


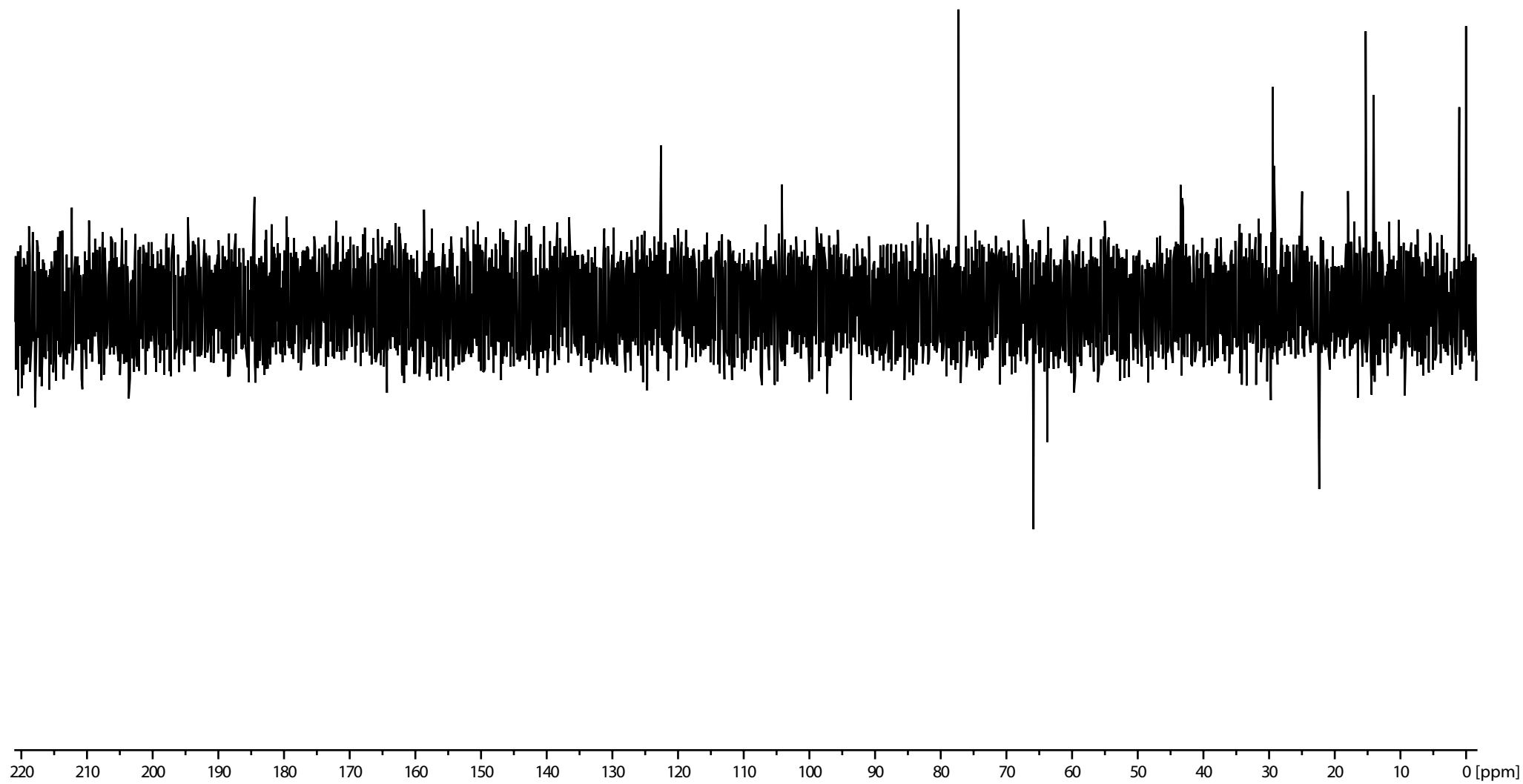
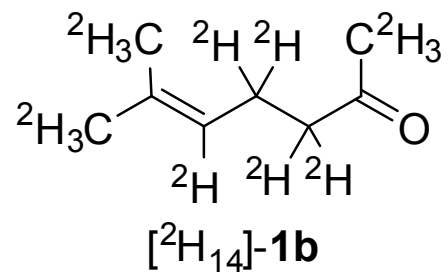


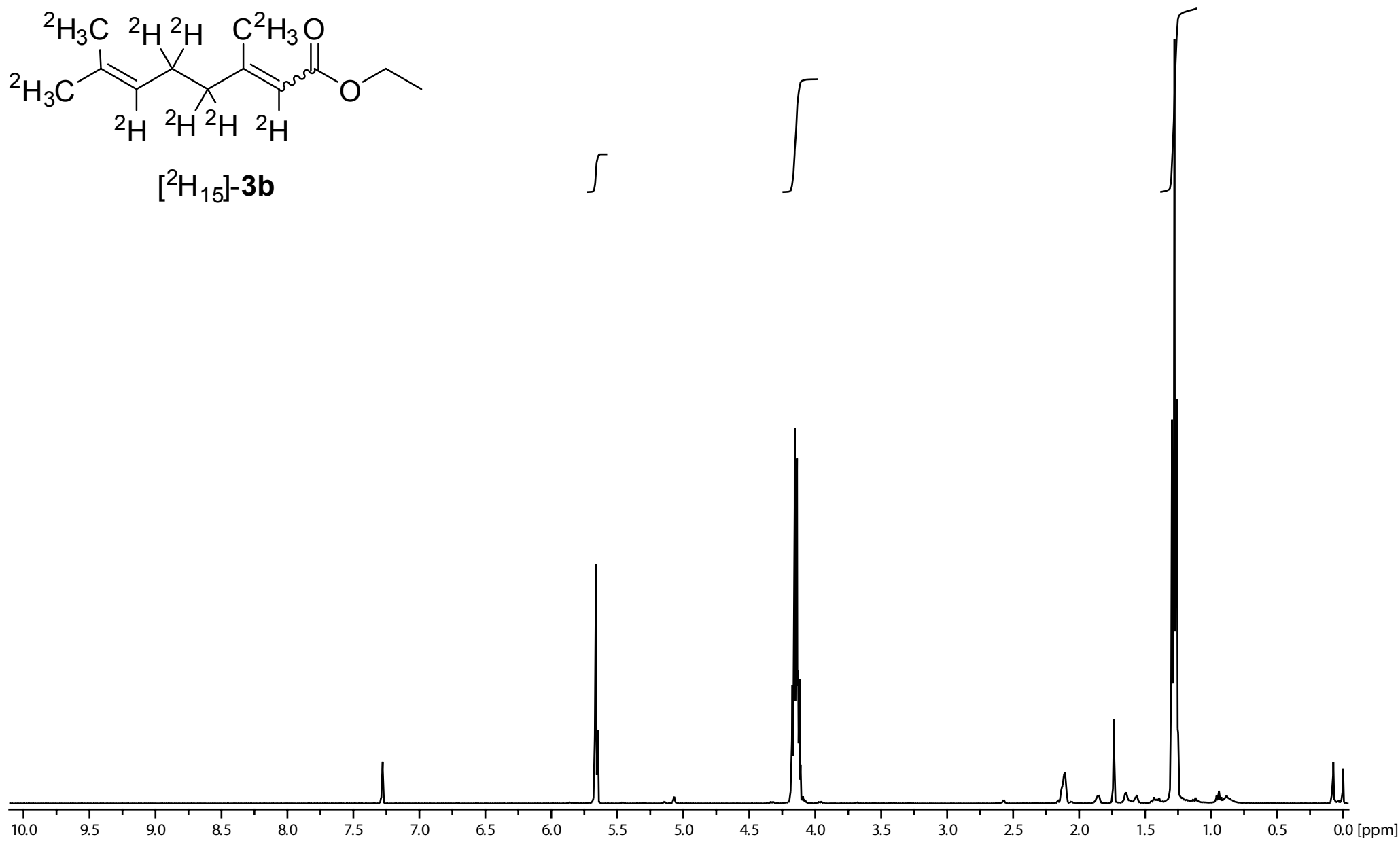
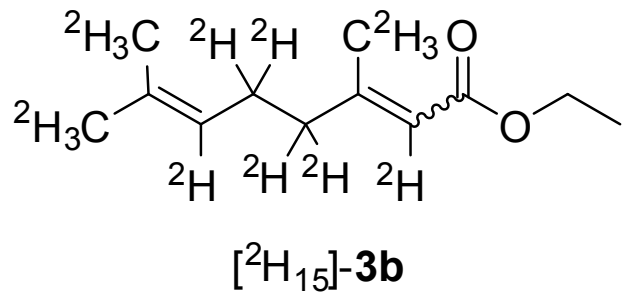
[²H₁₃]-7a

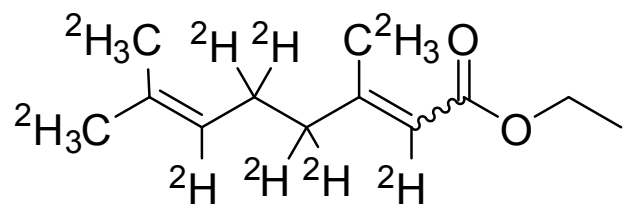




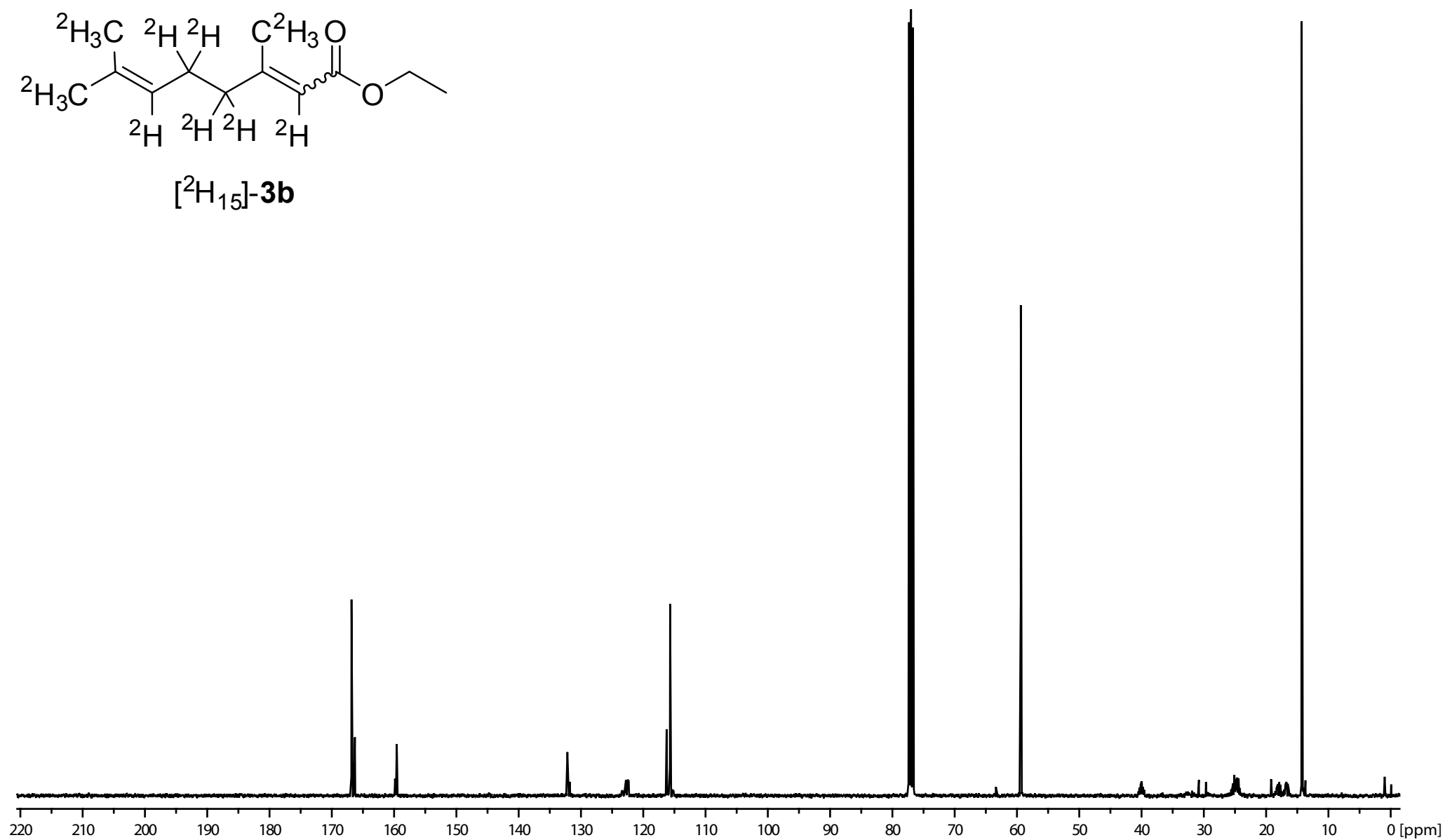


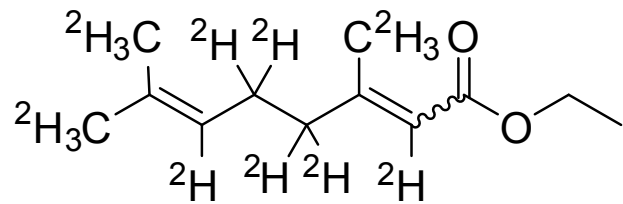




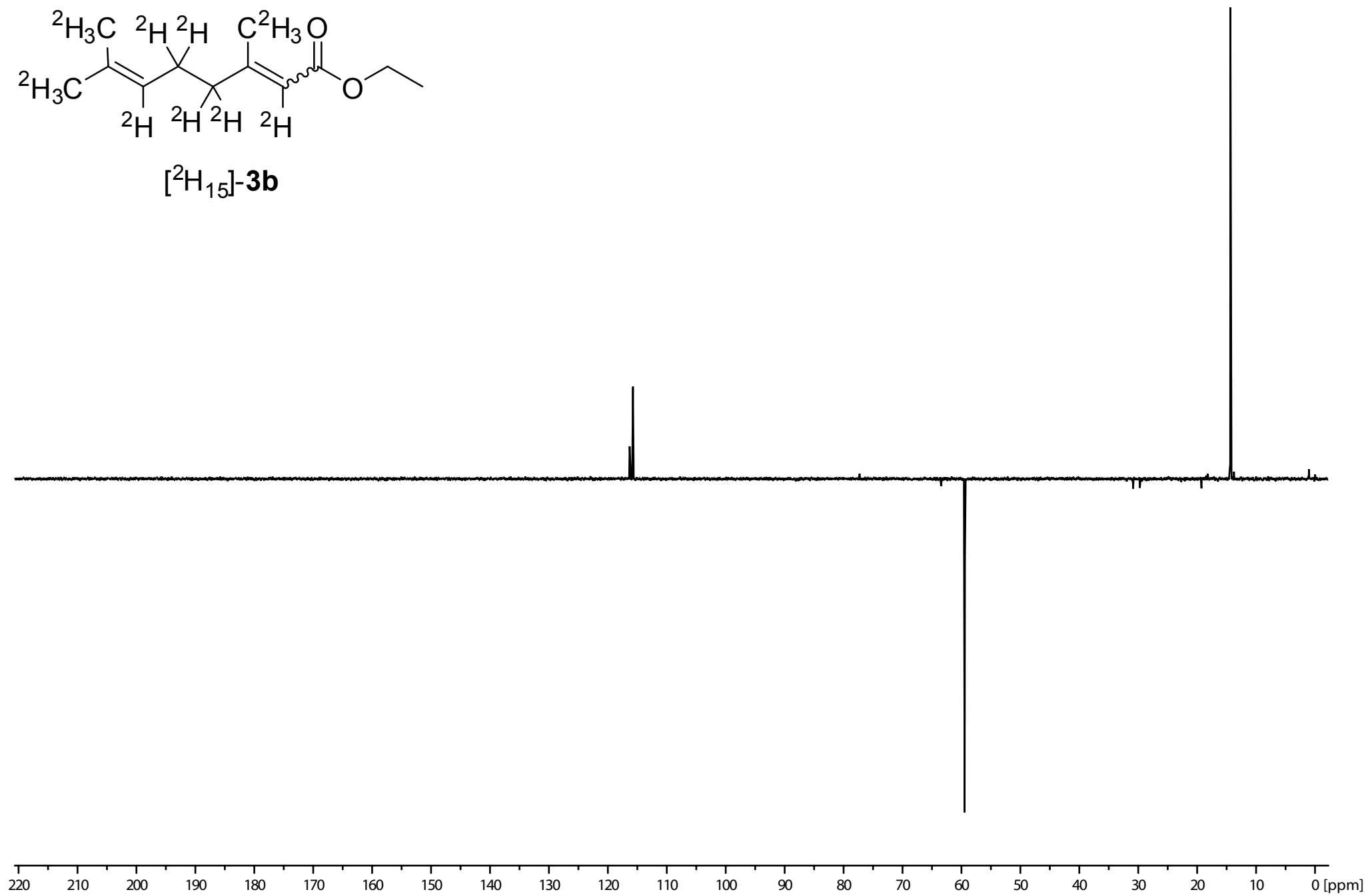


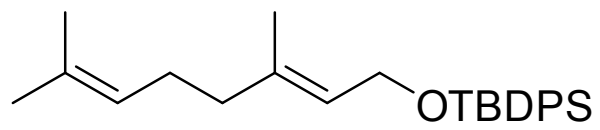
[²H₁₅]-3b



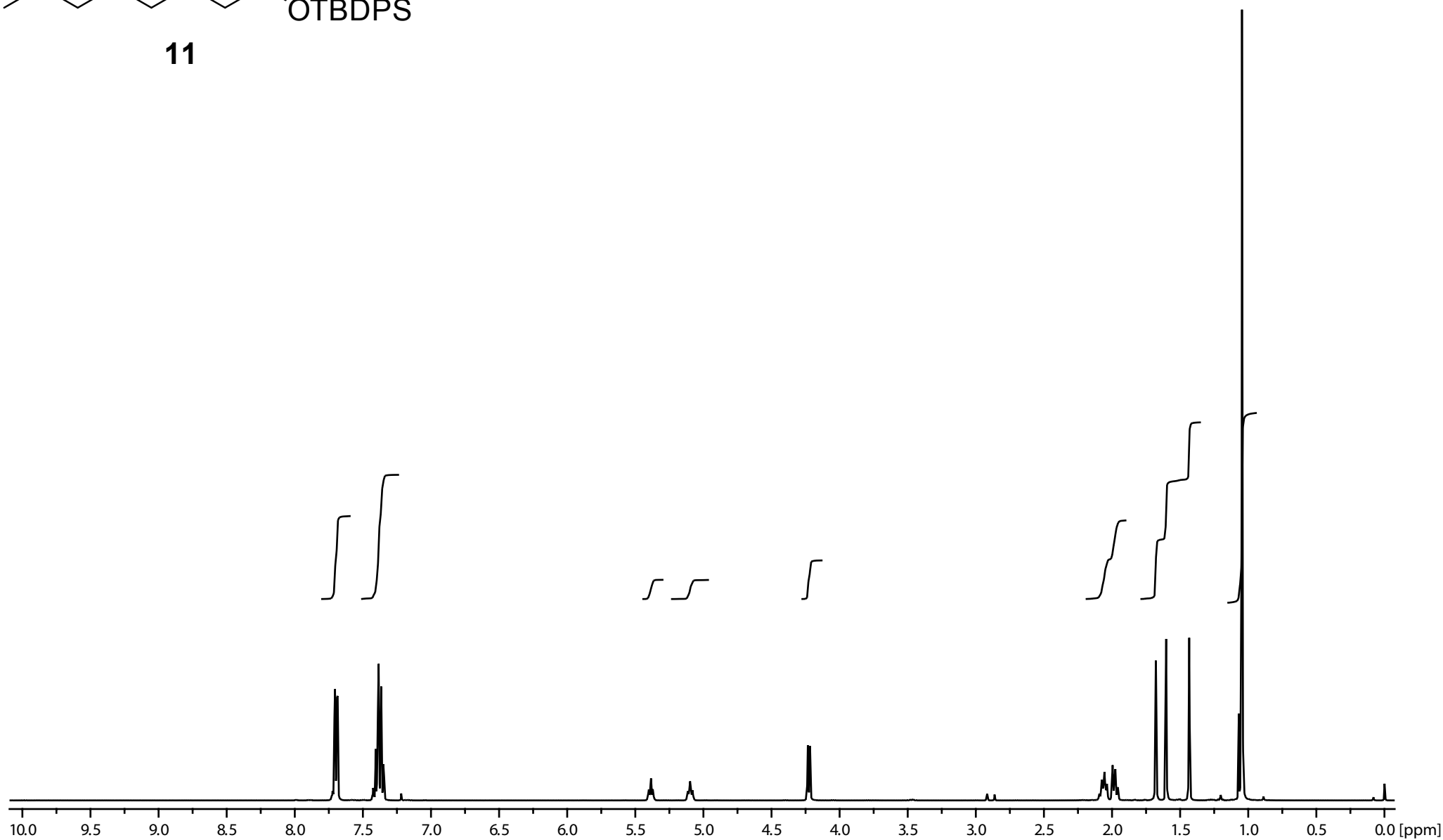


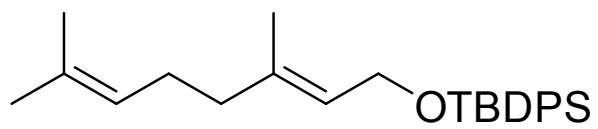
[²H₁₅]-3b



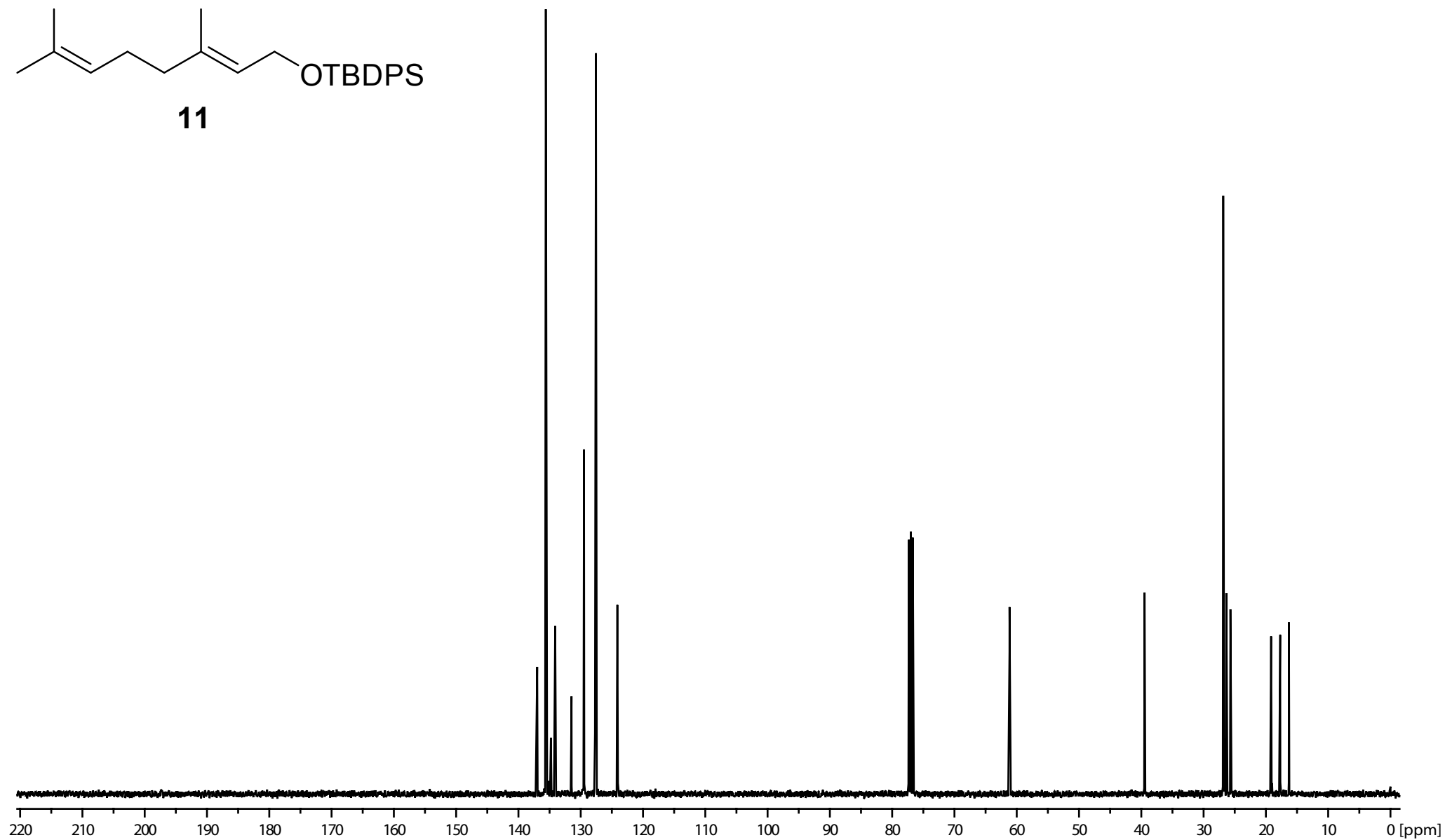


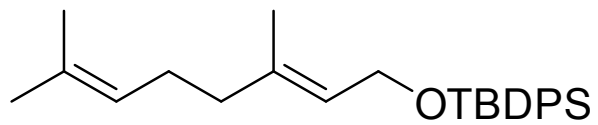
11



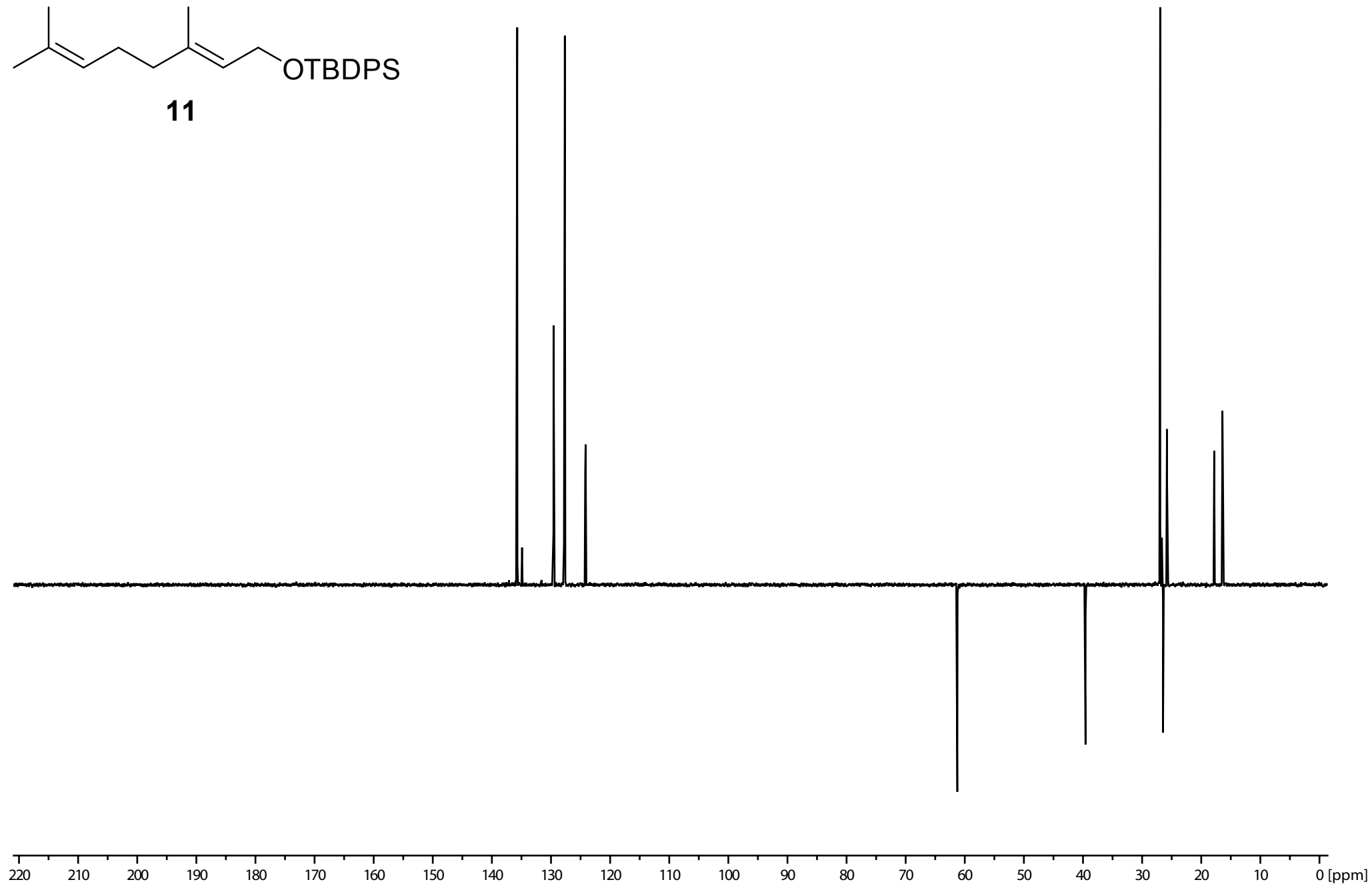


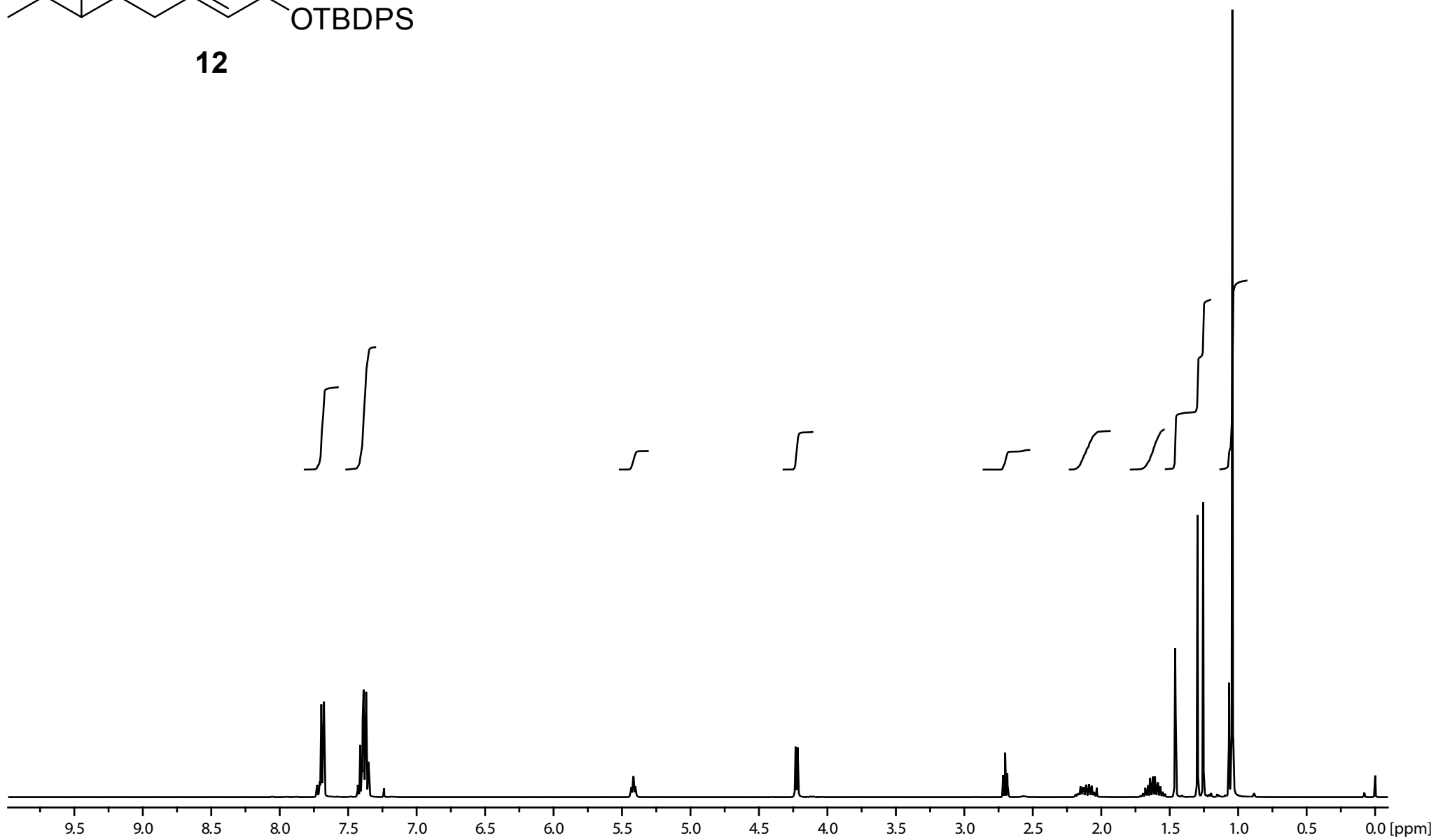
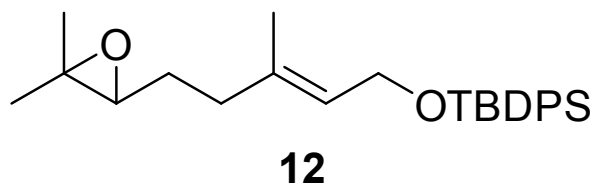
11

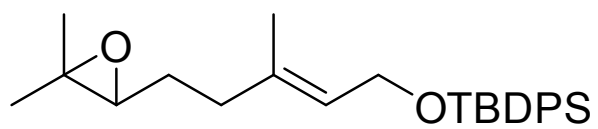




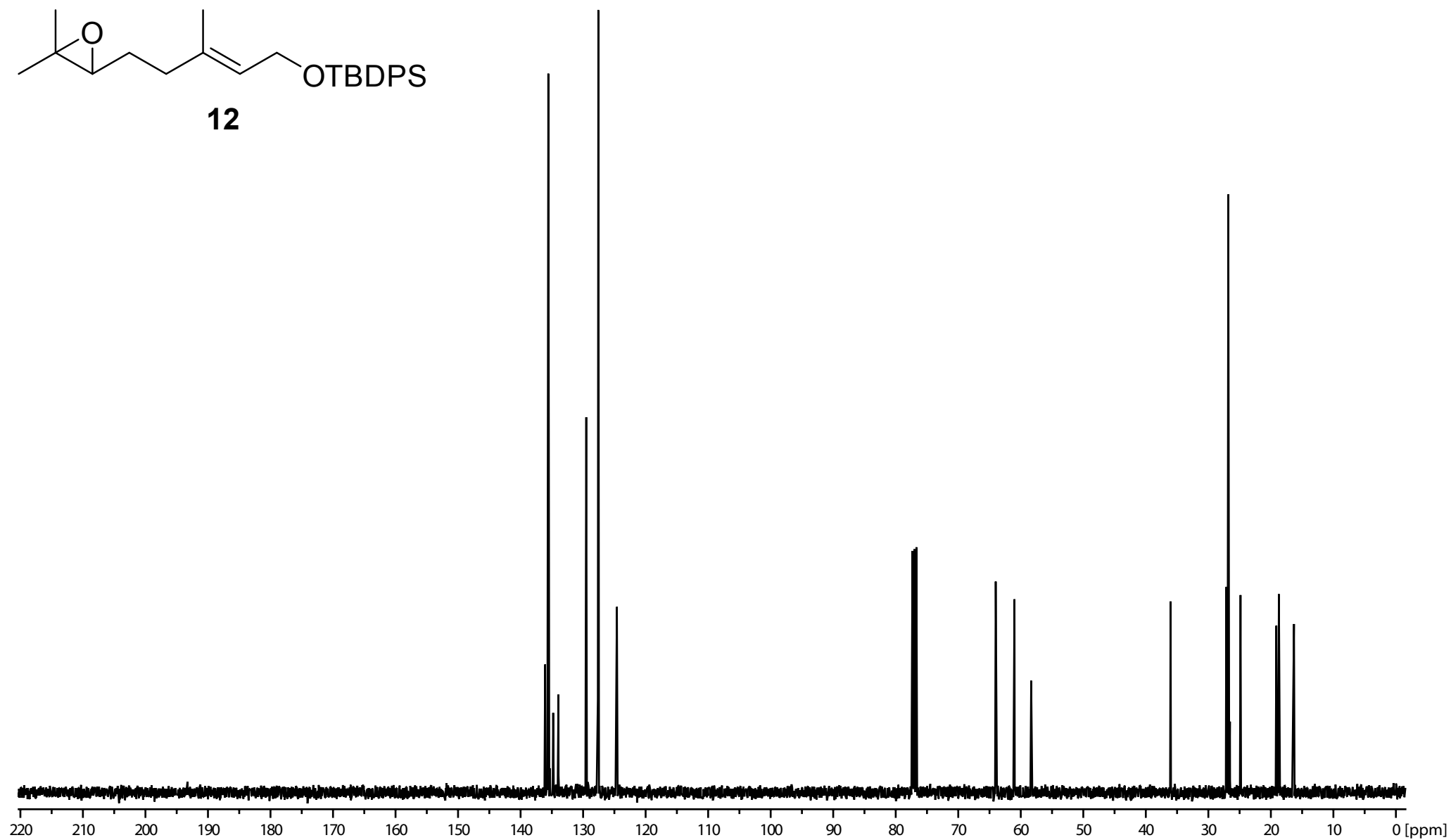
11

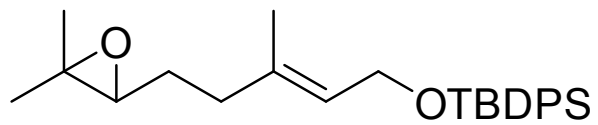




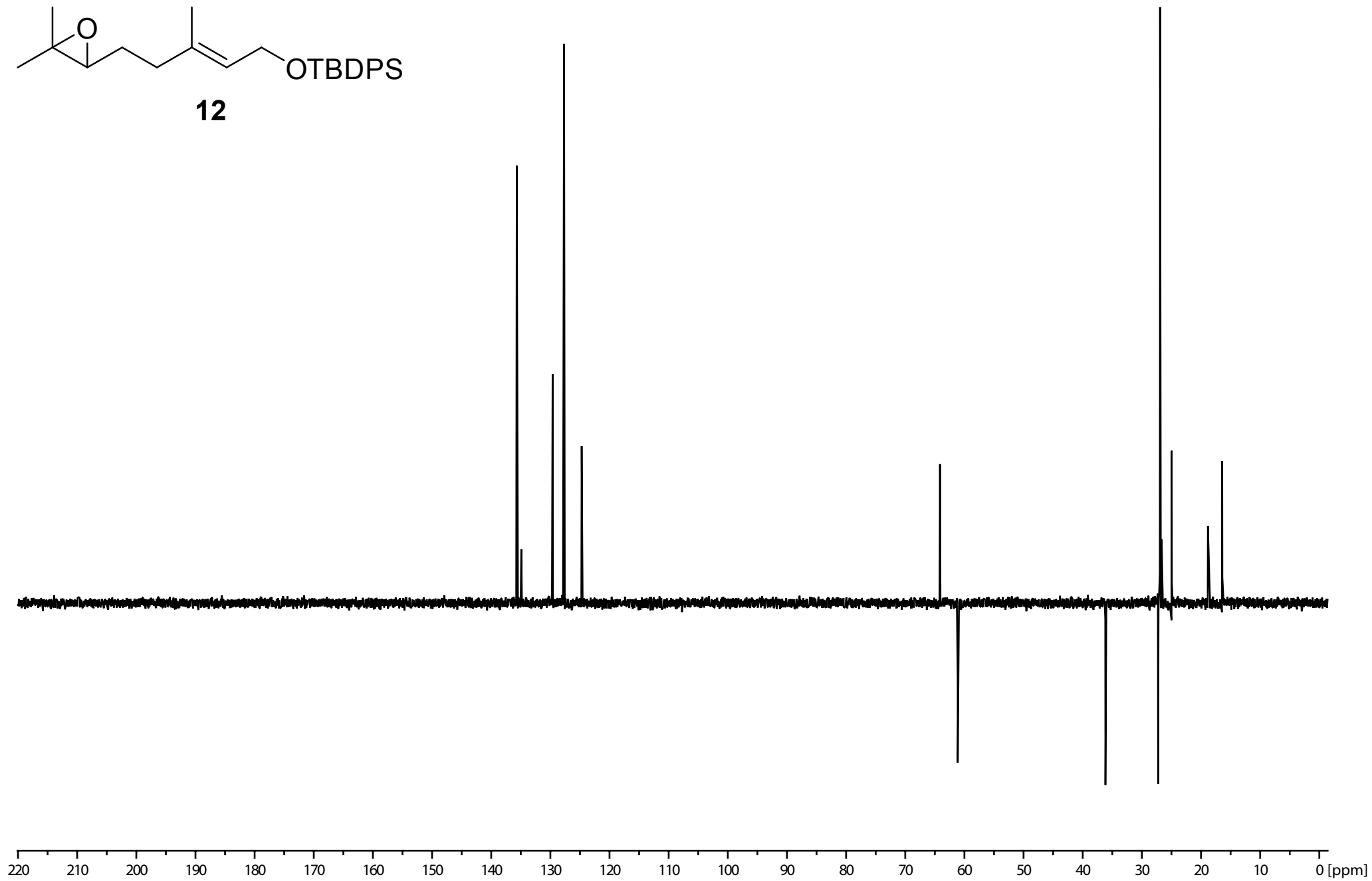


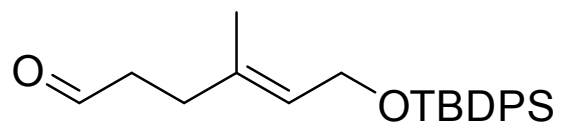
12



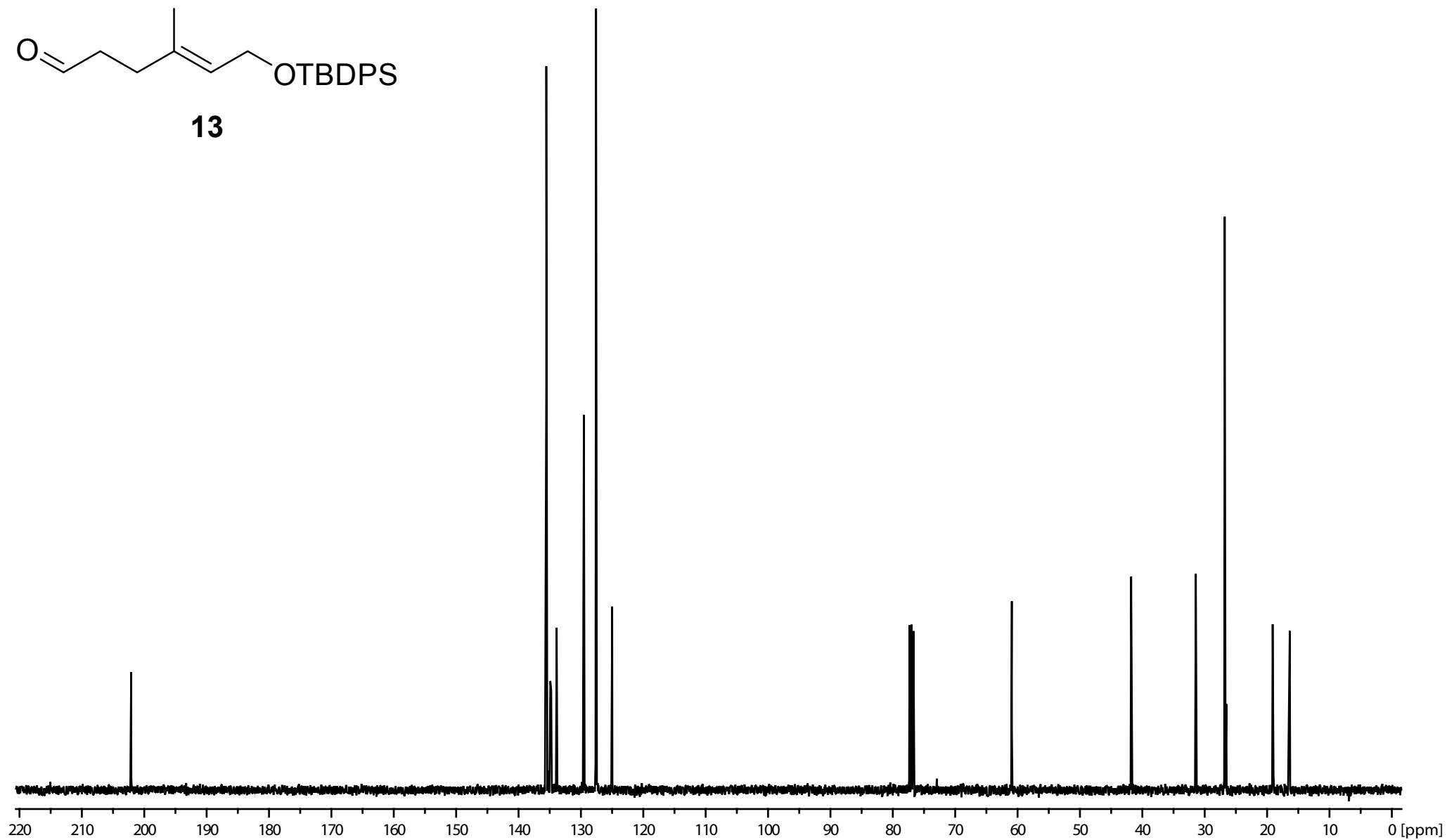


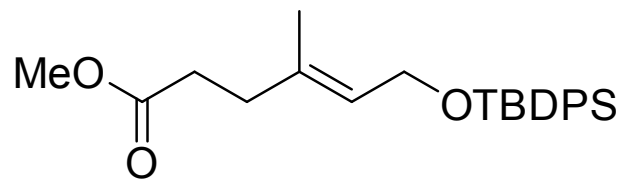
12



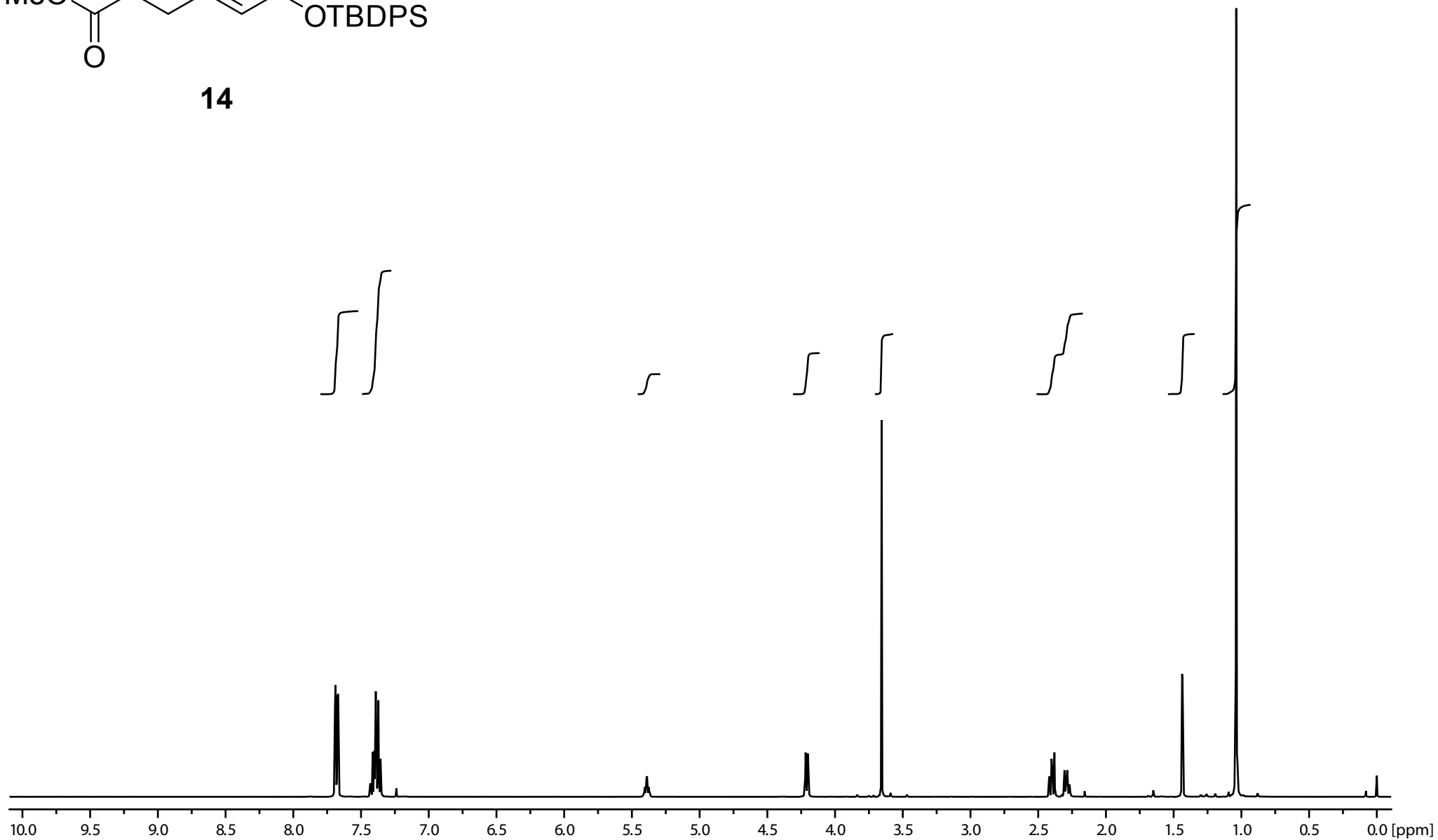


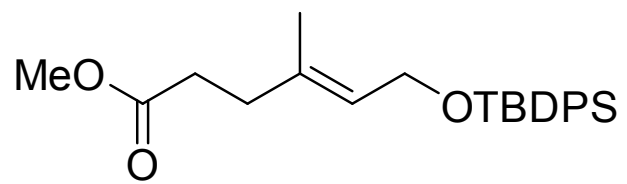
13



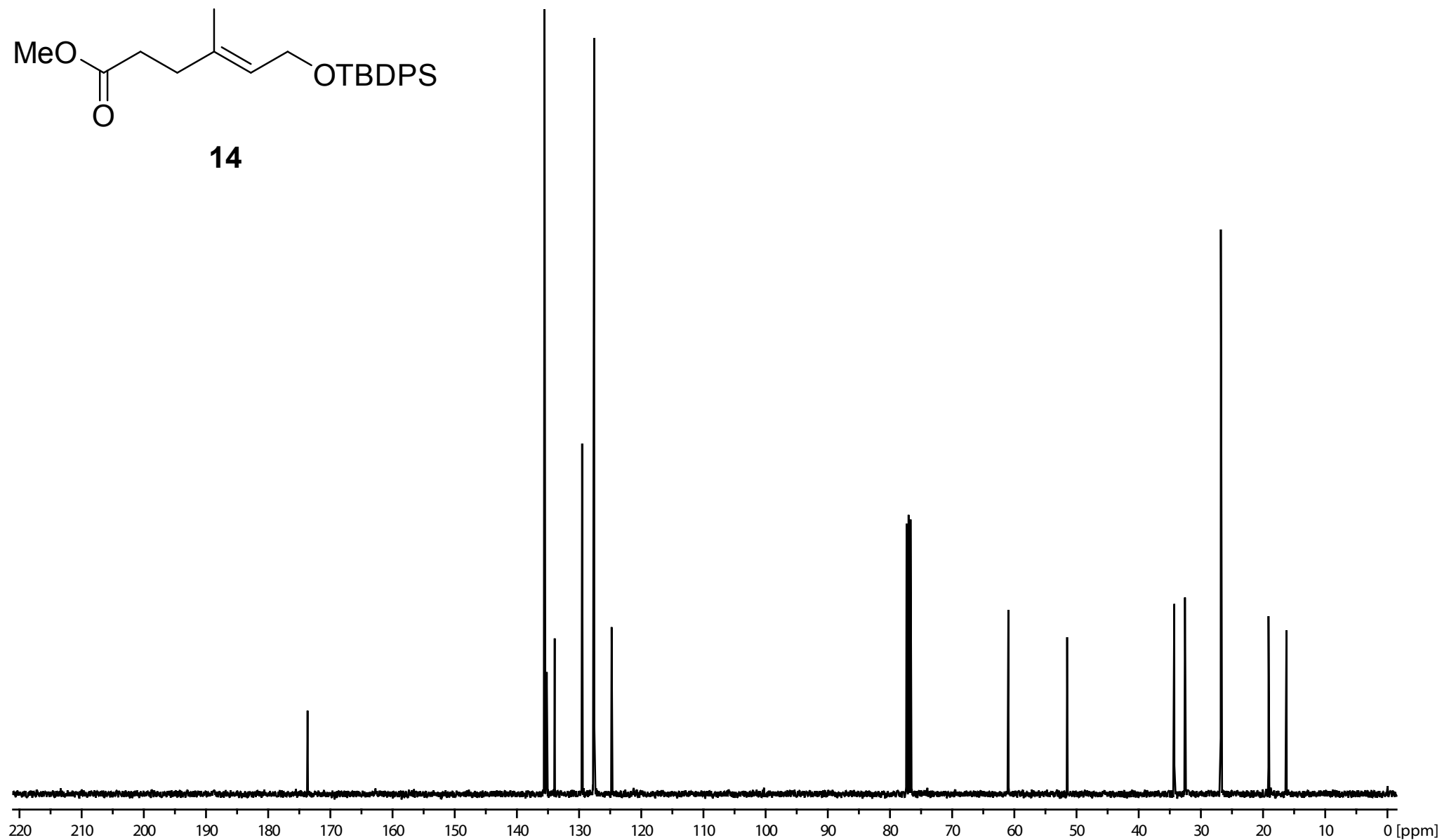


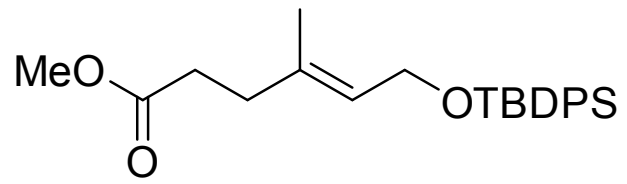
14



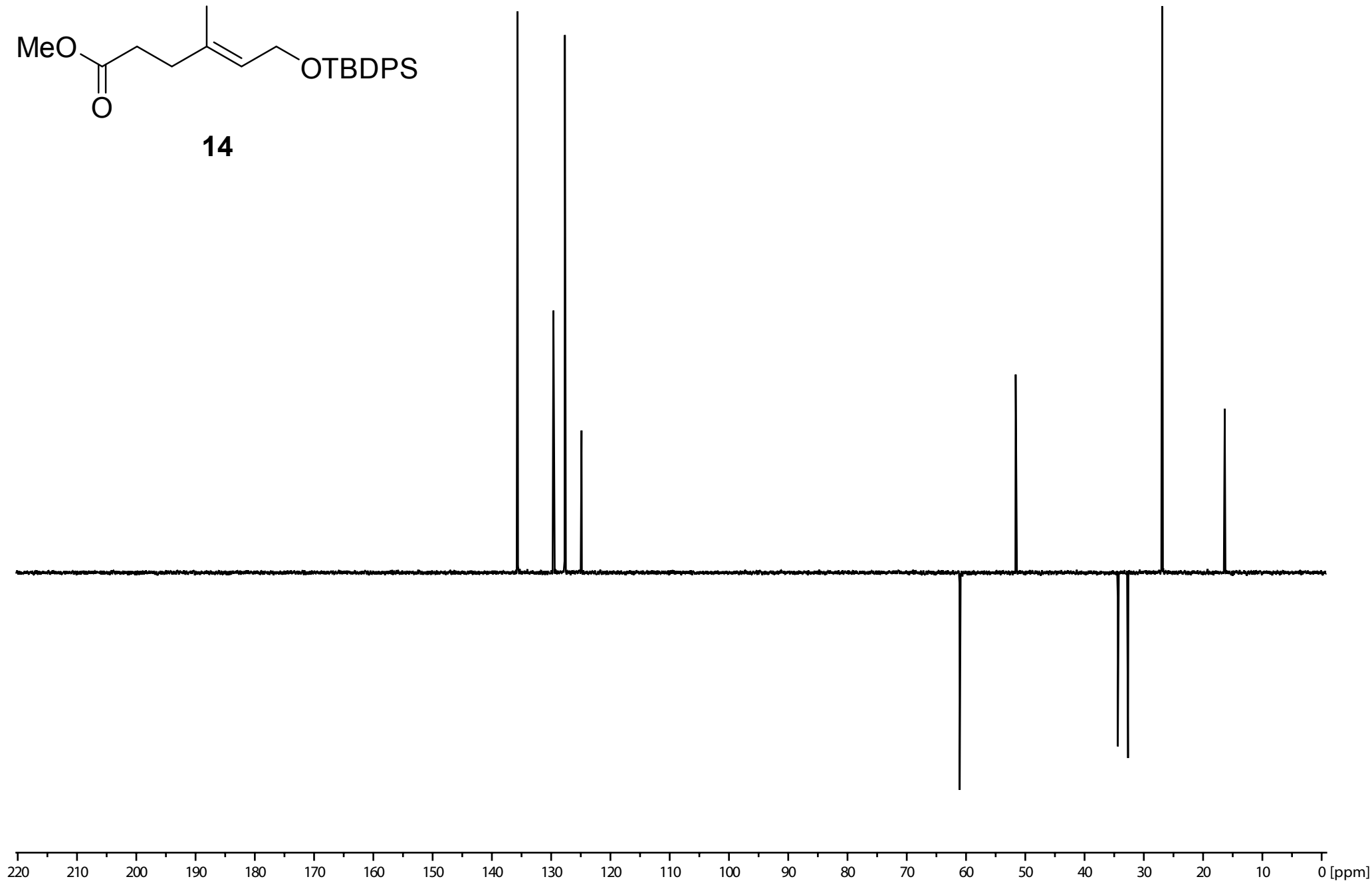


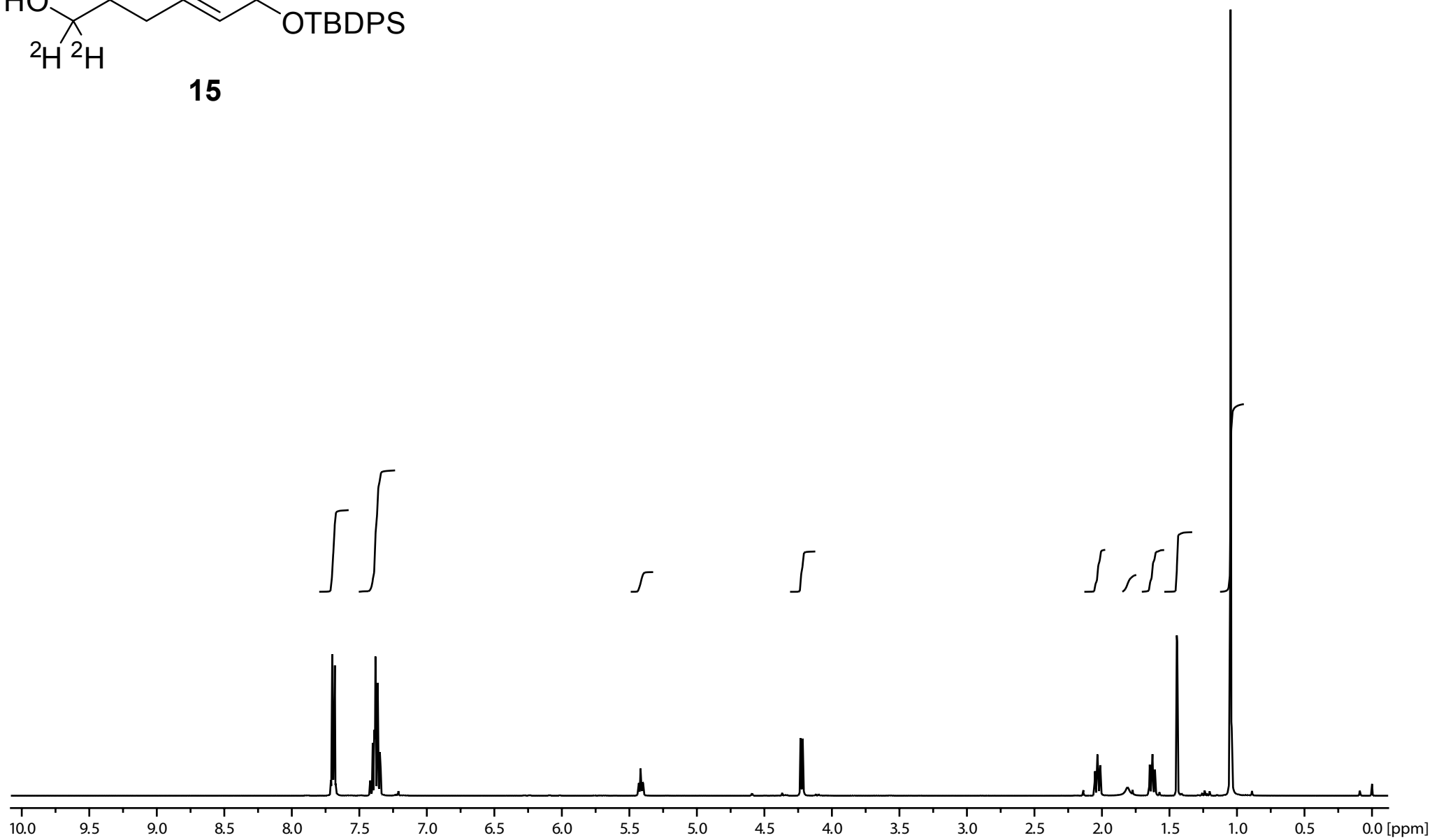
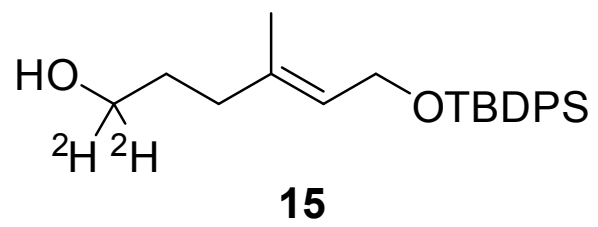
14

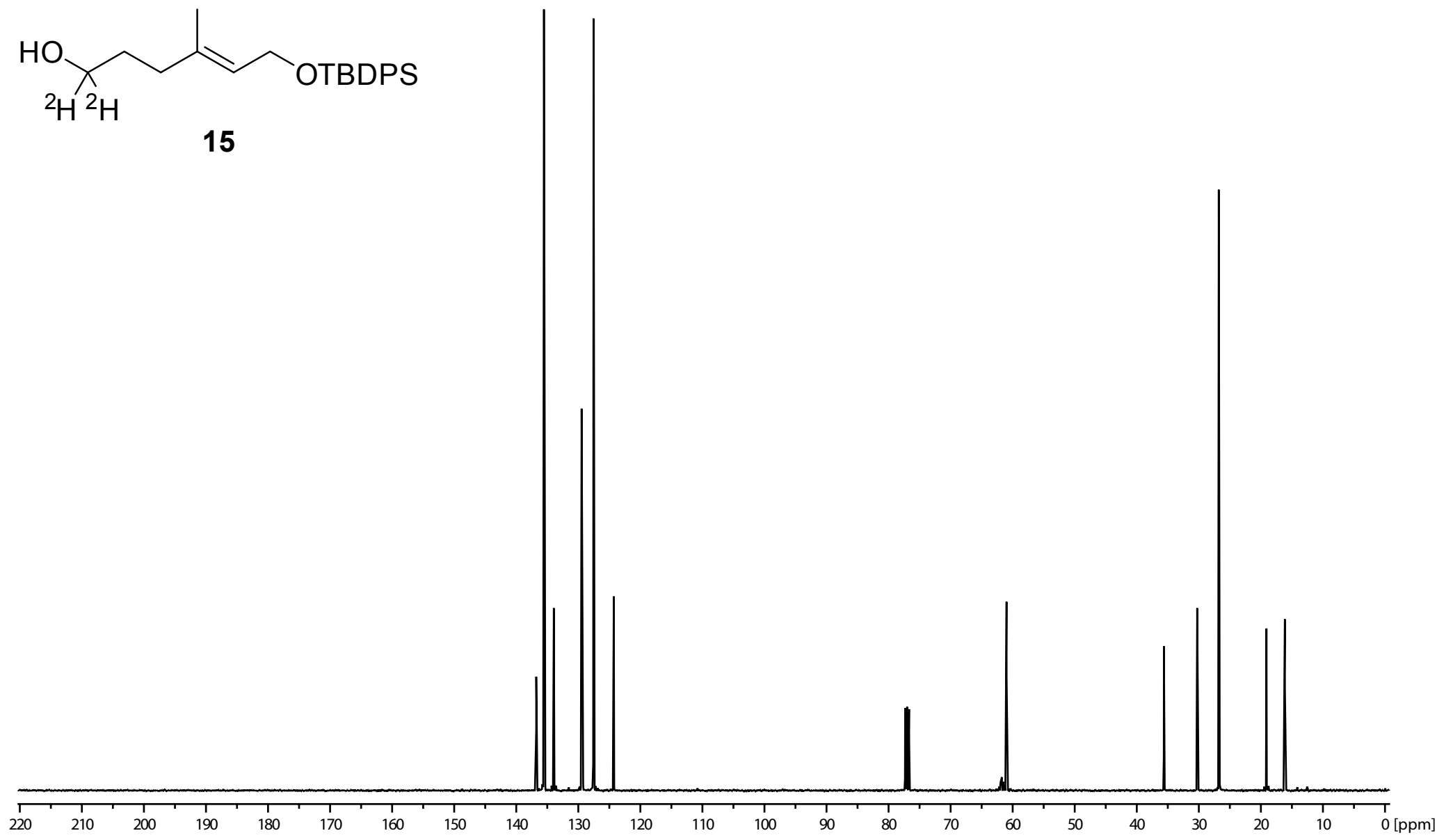
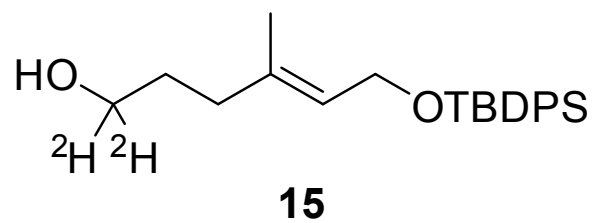


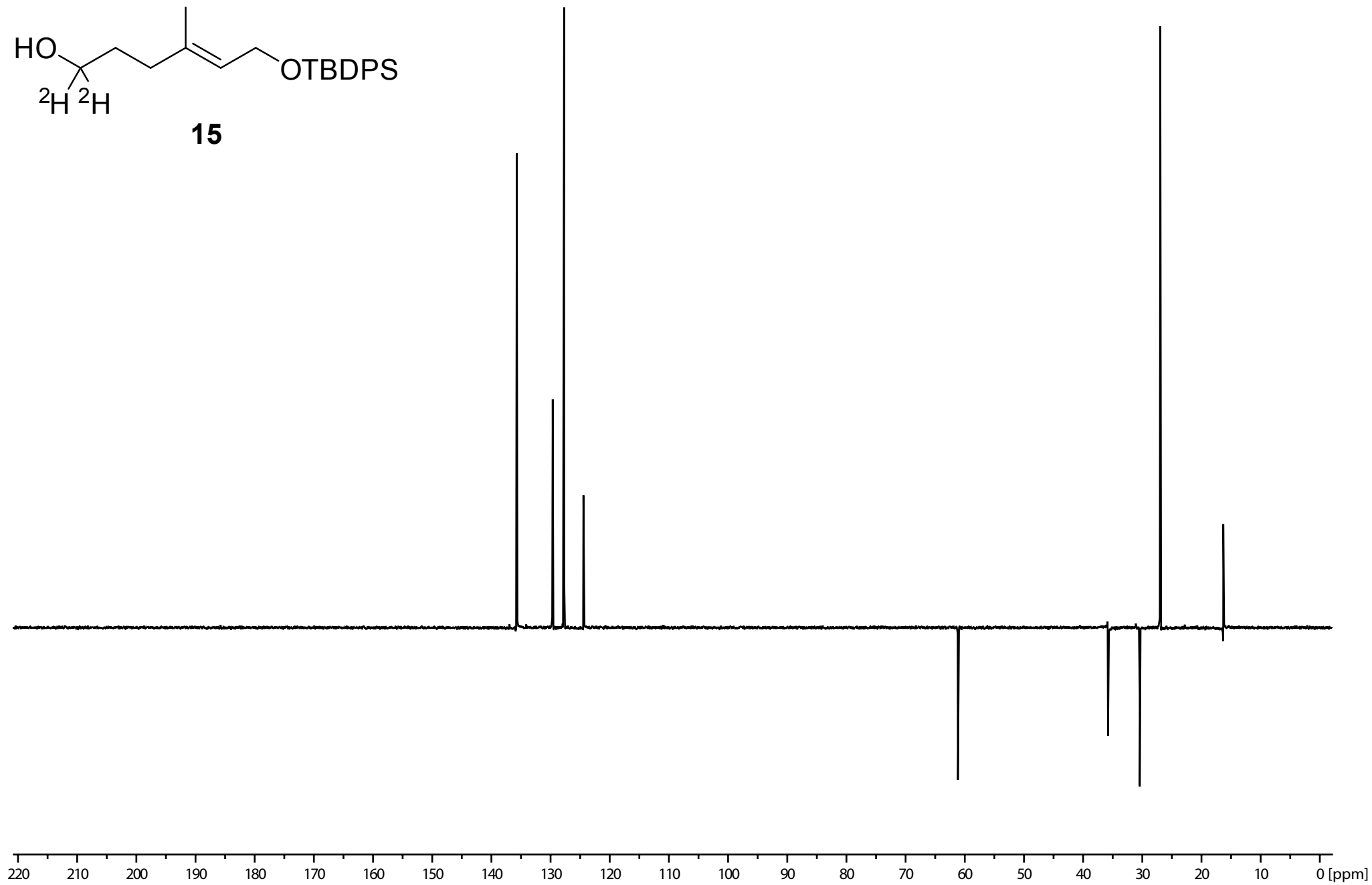
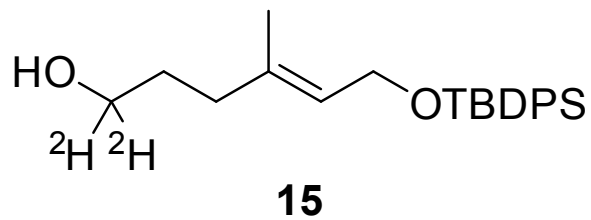


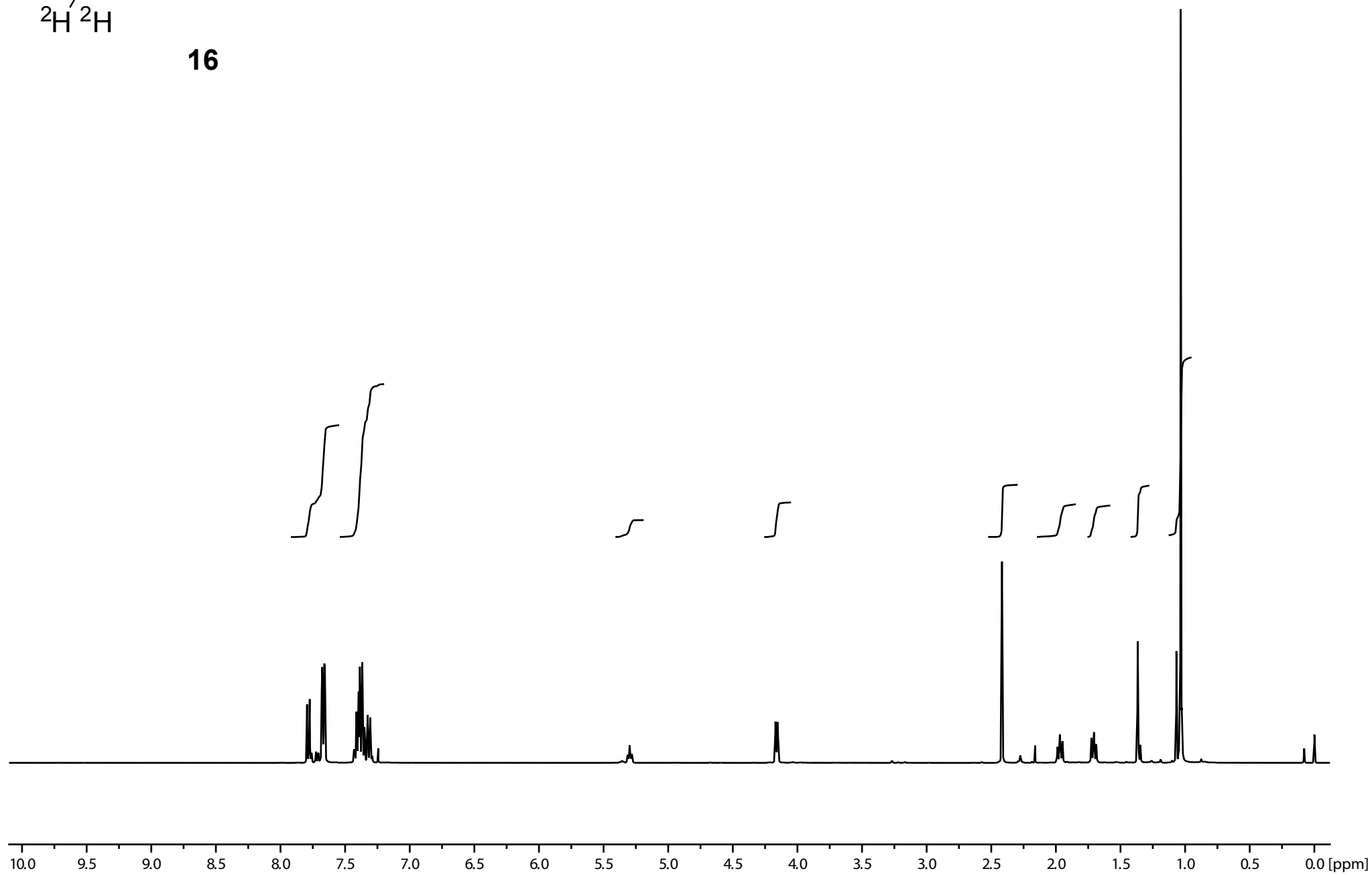
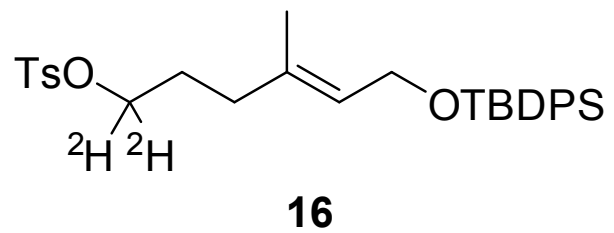
14

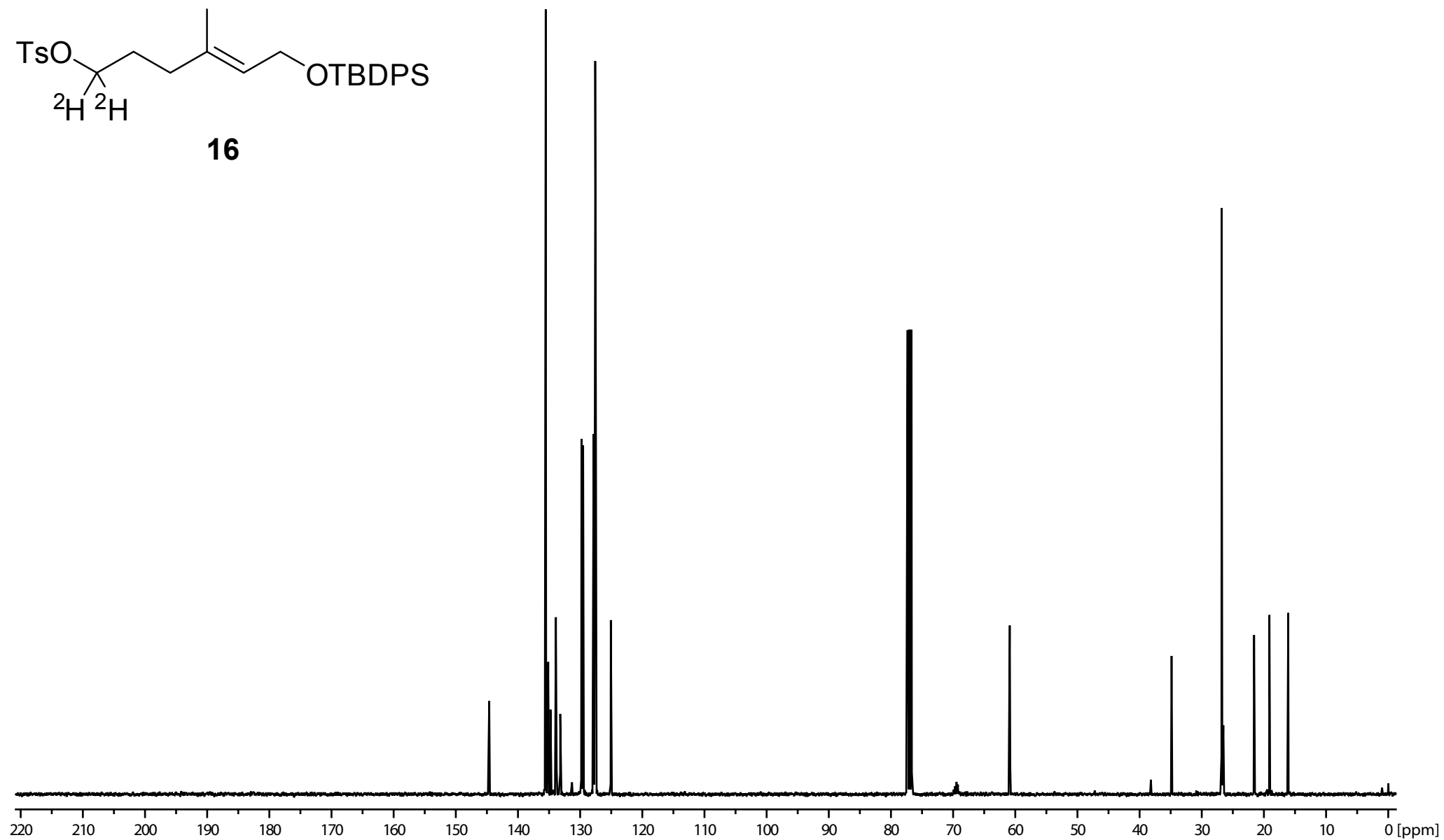
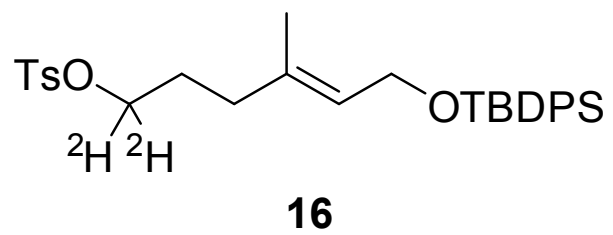


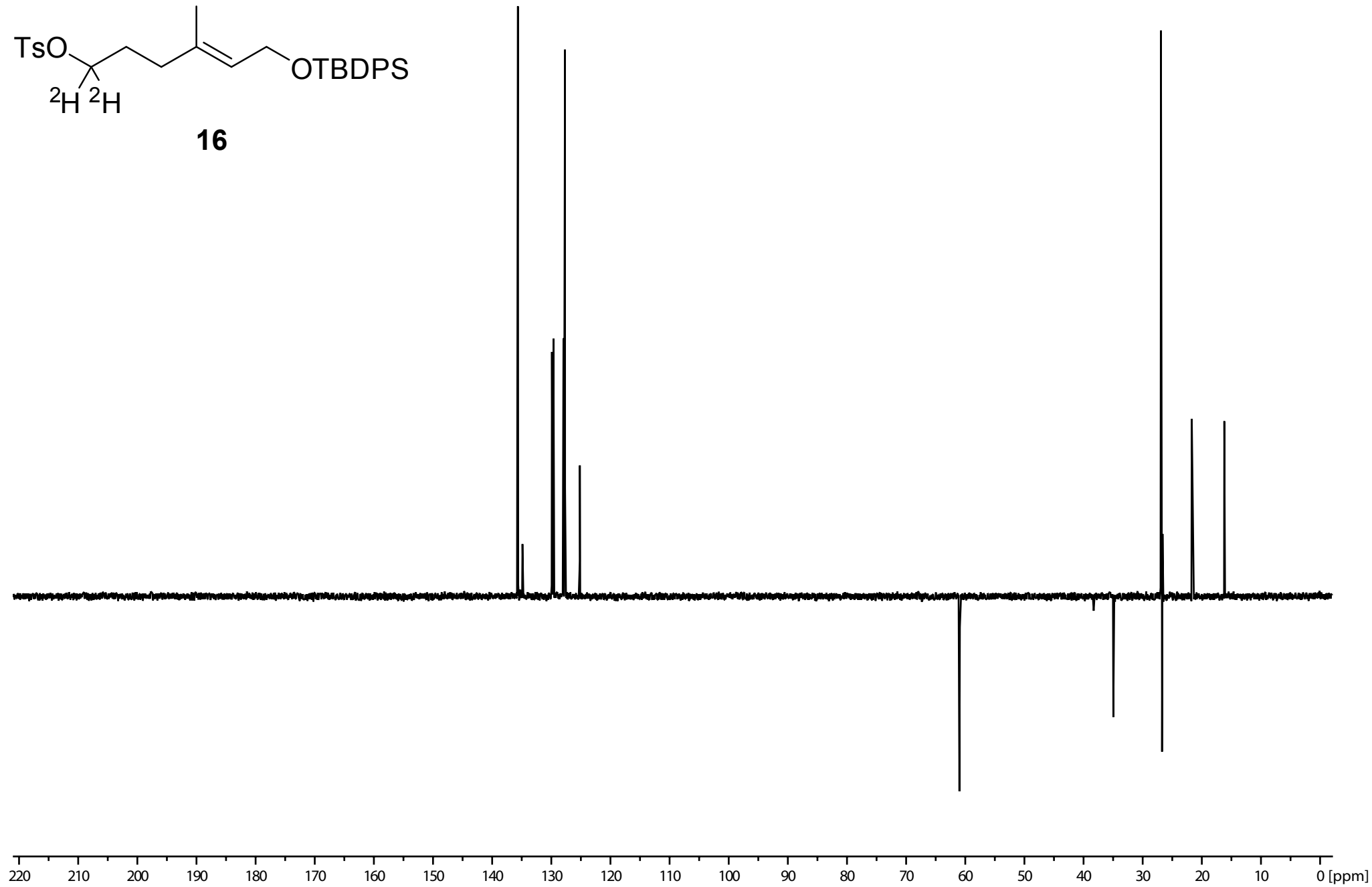
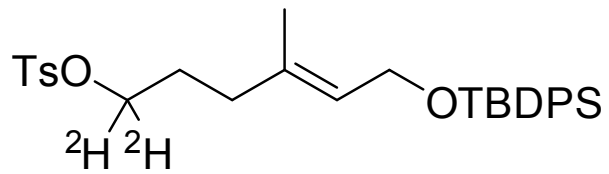


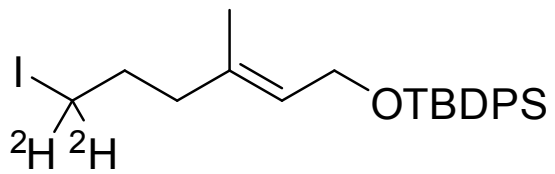




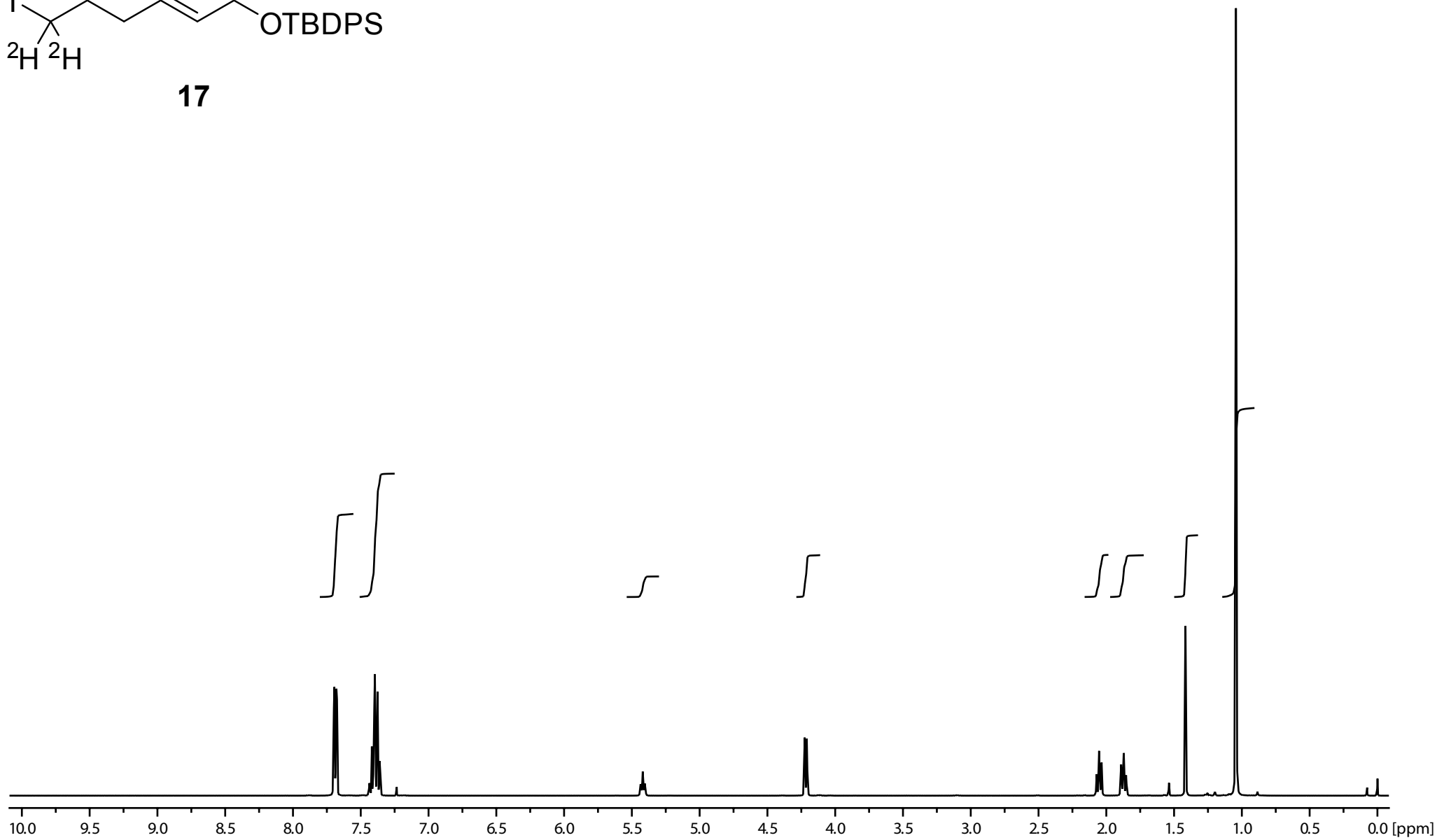


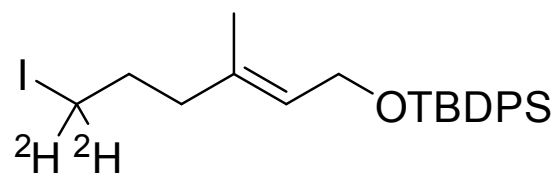




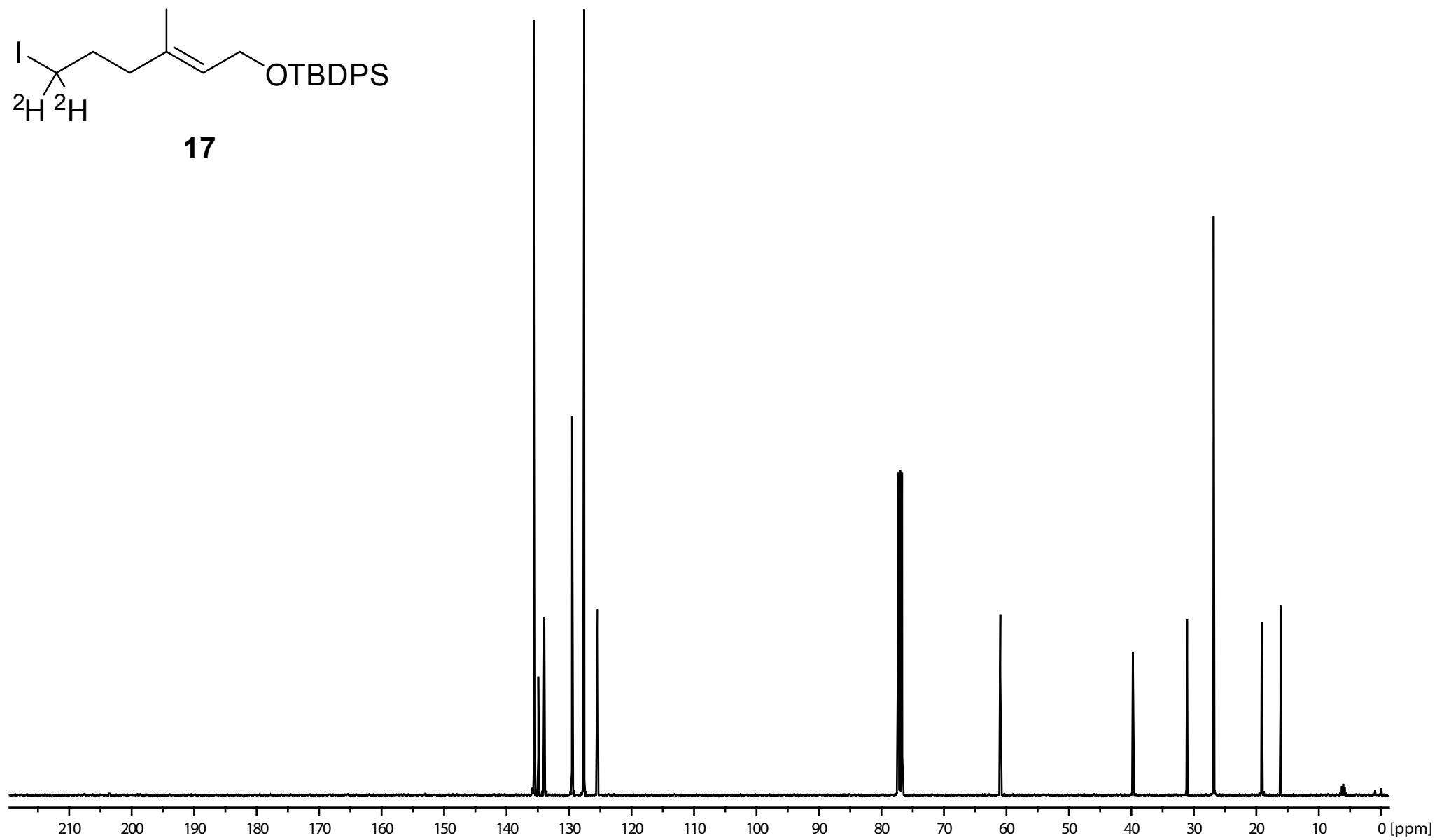


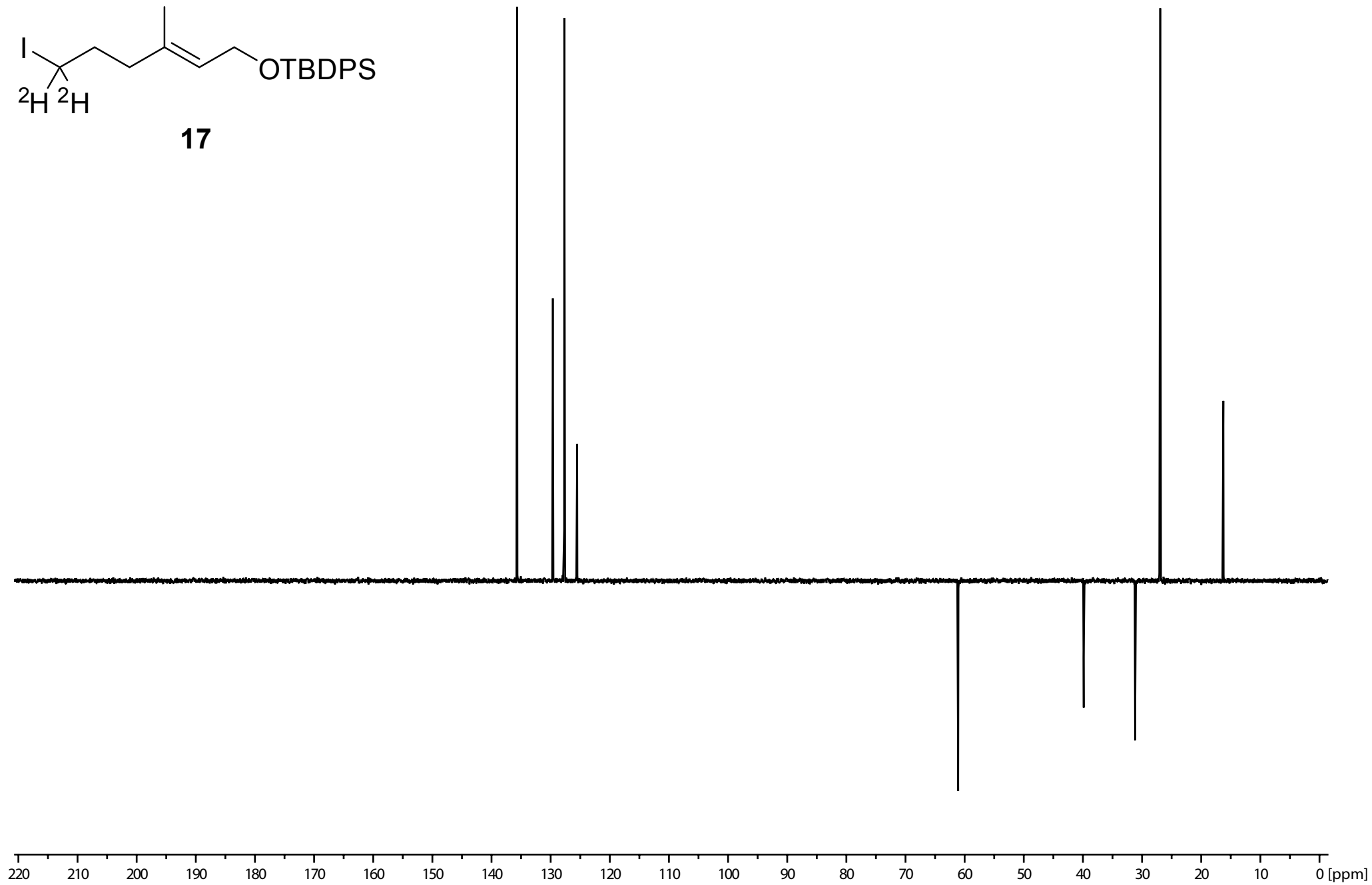
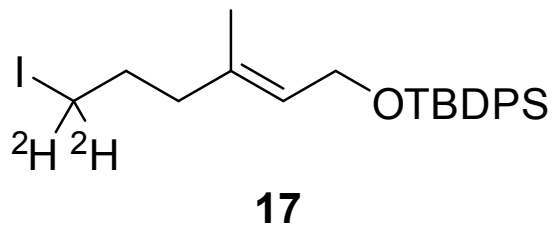
17

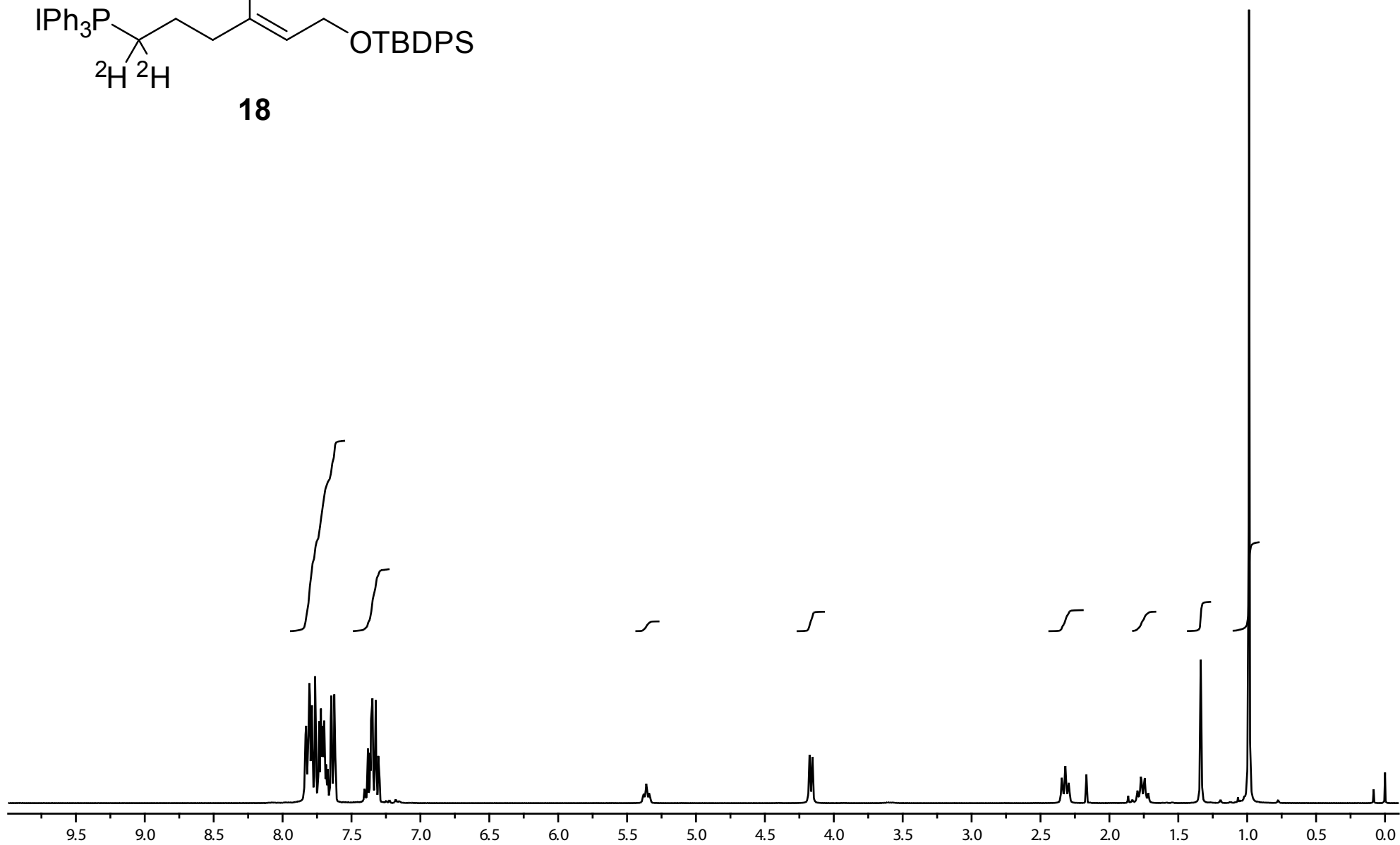
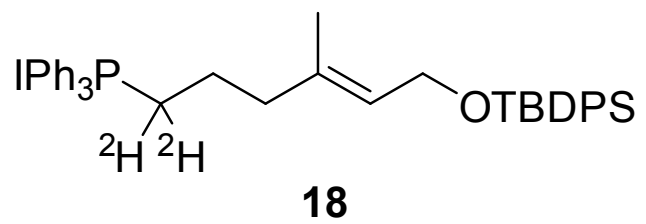


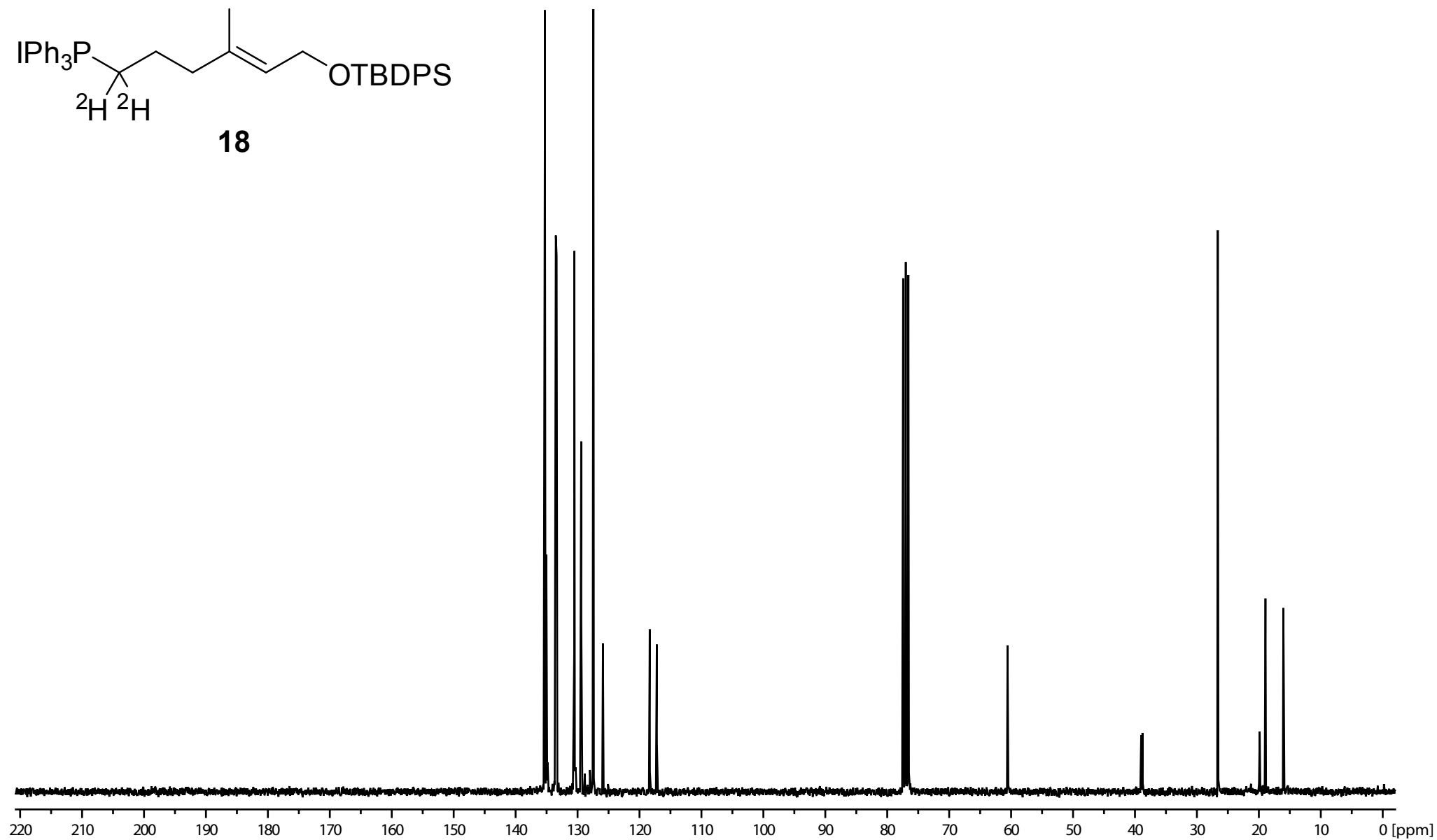
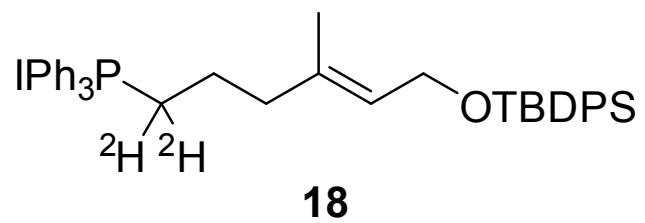


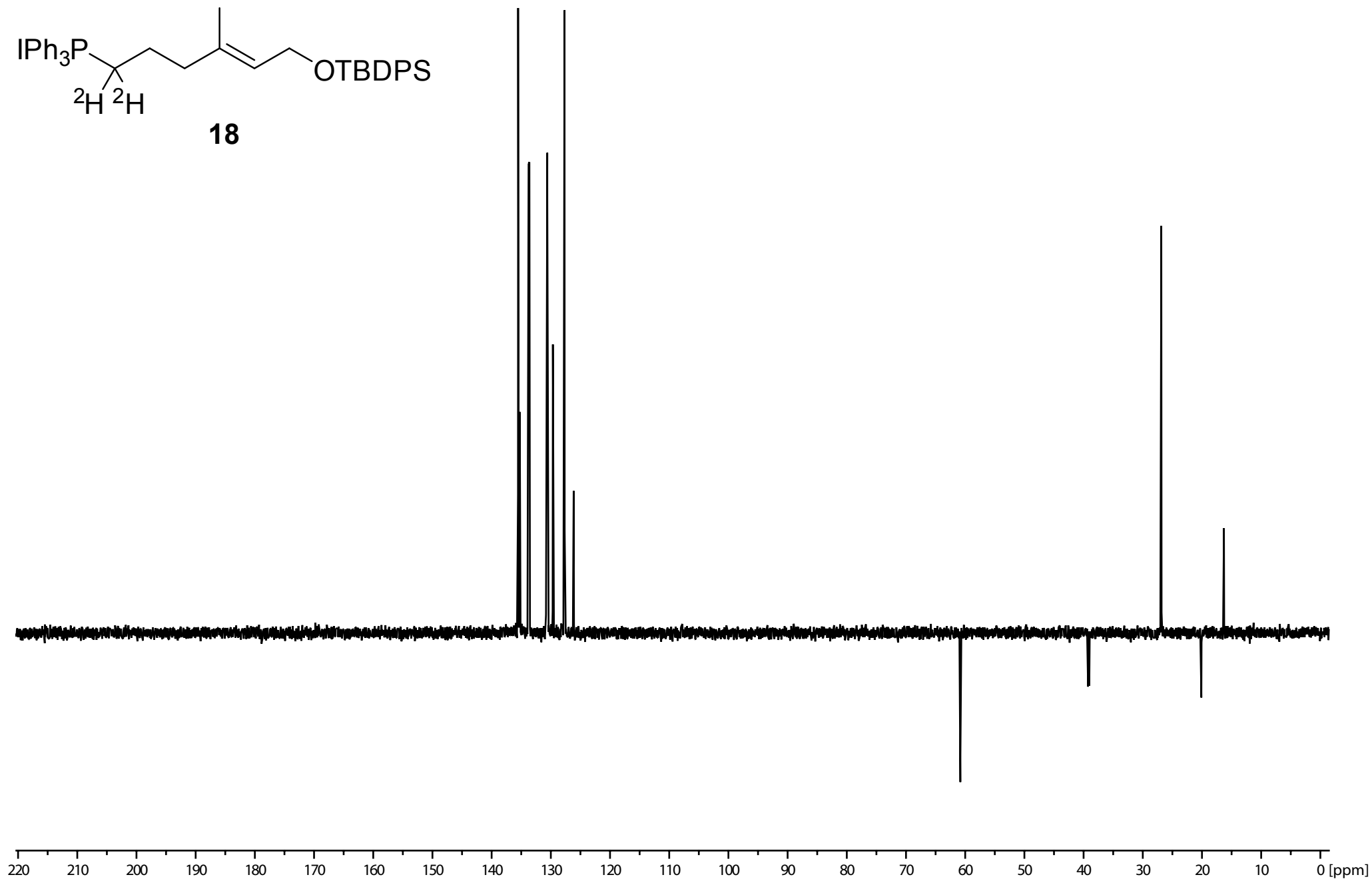
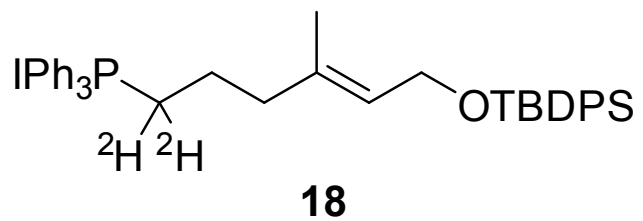
17

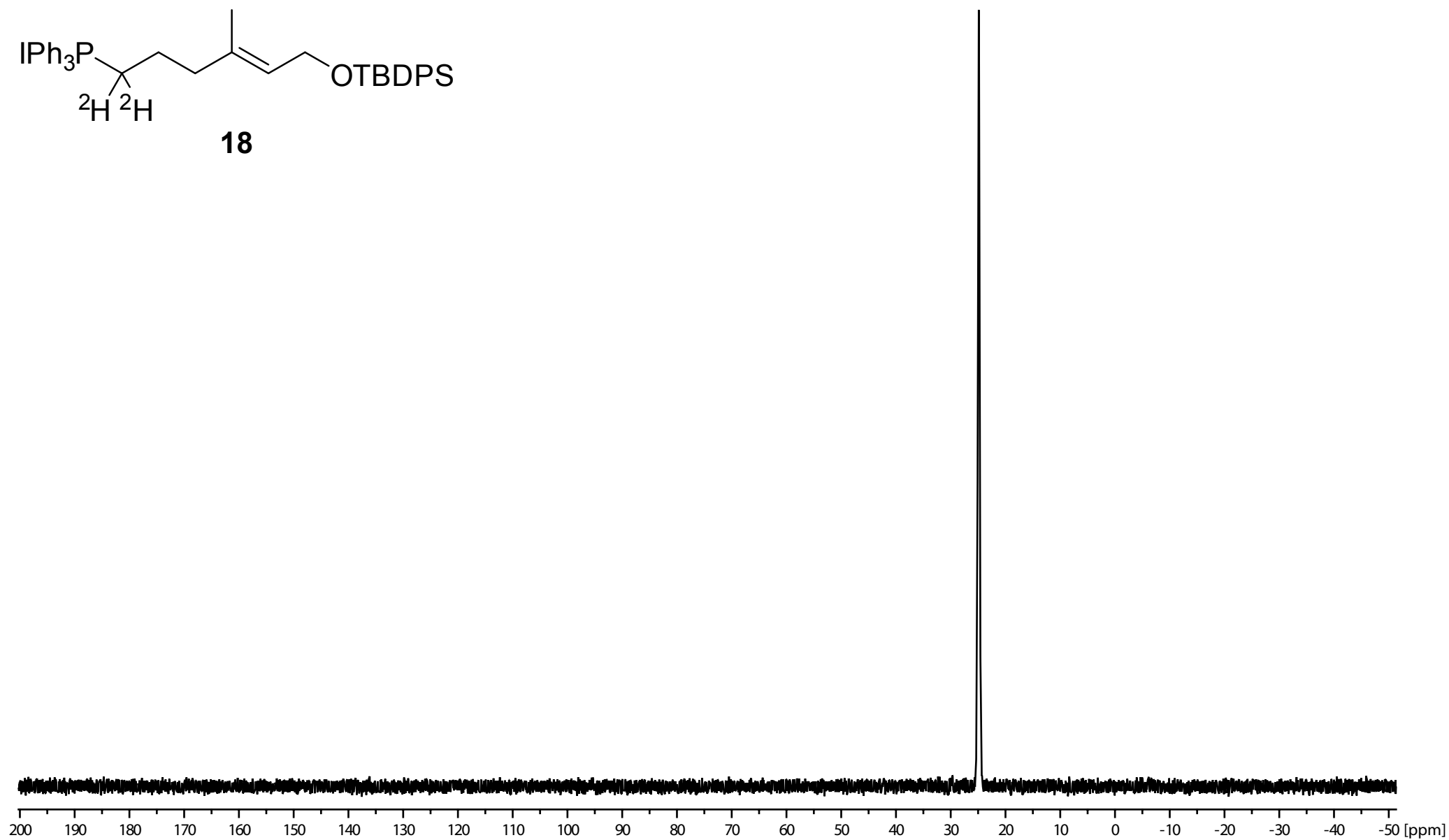
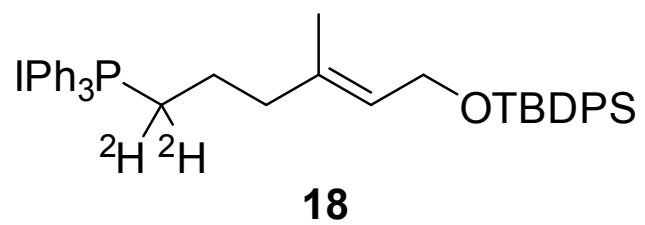


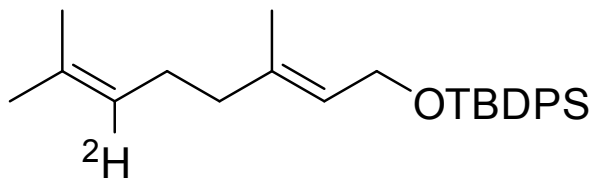




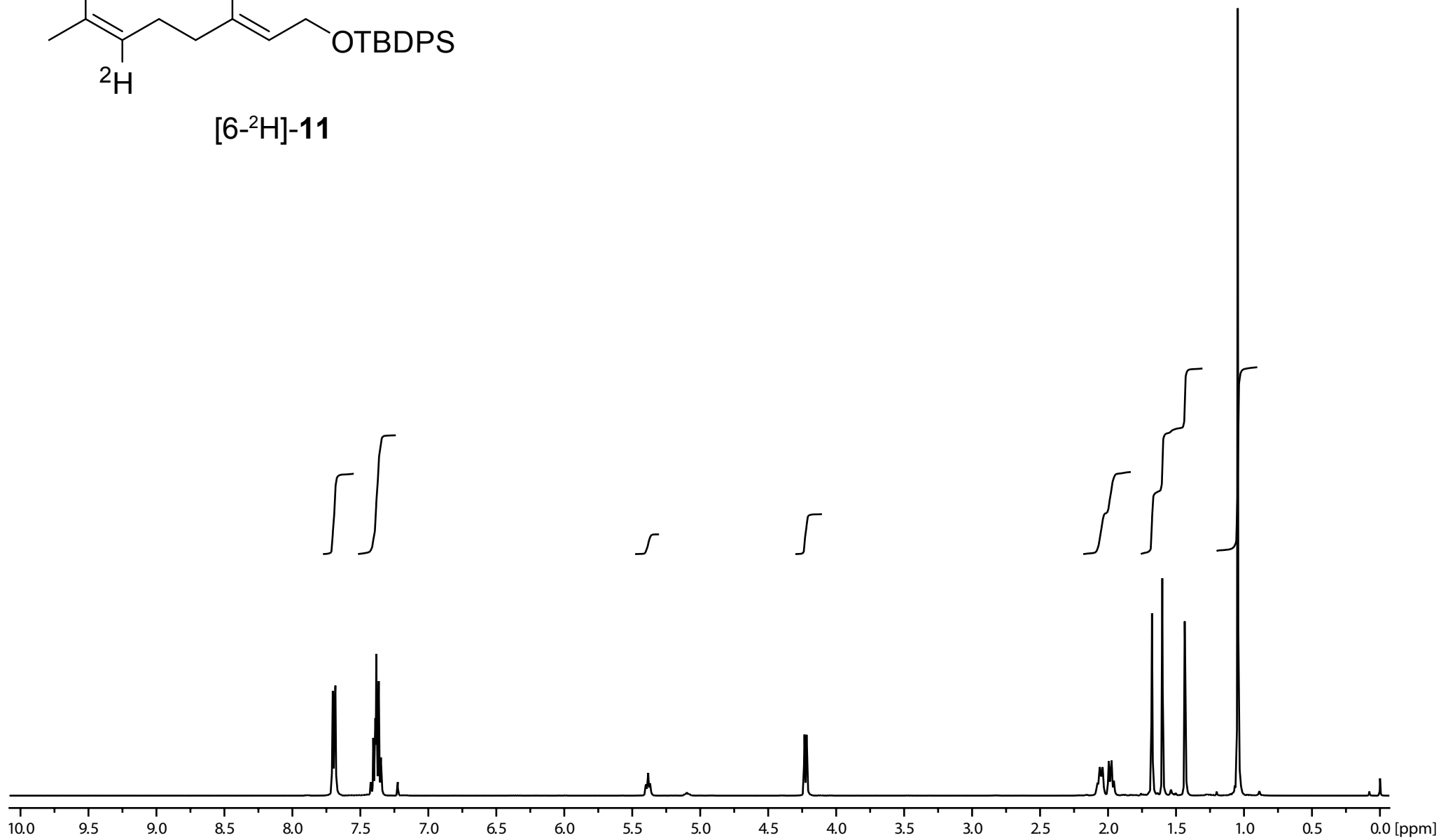


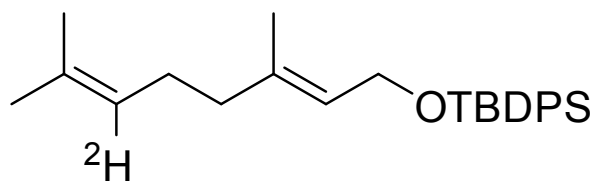




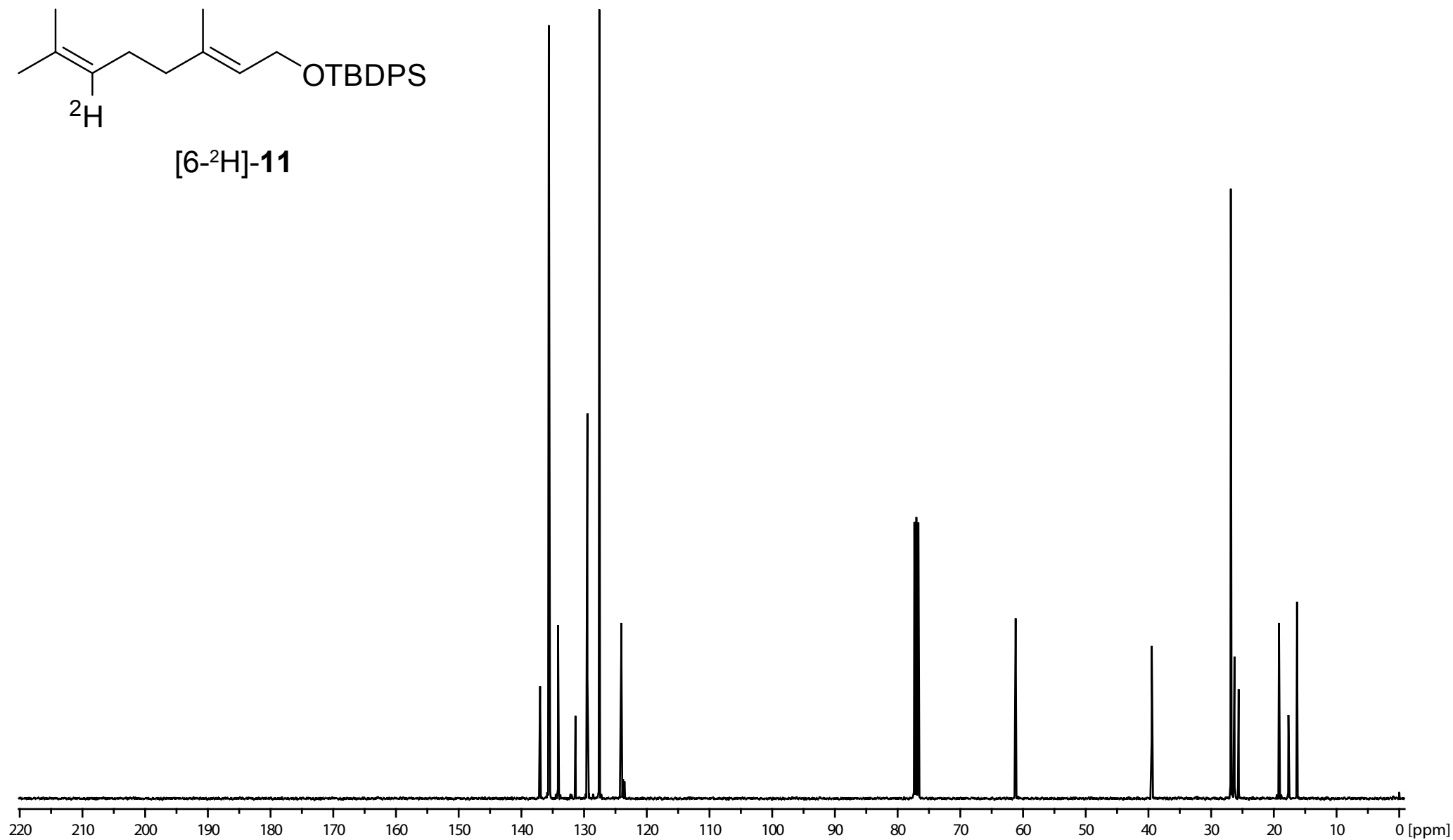


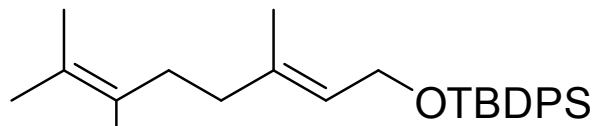
[6-²H]-11





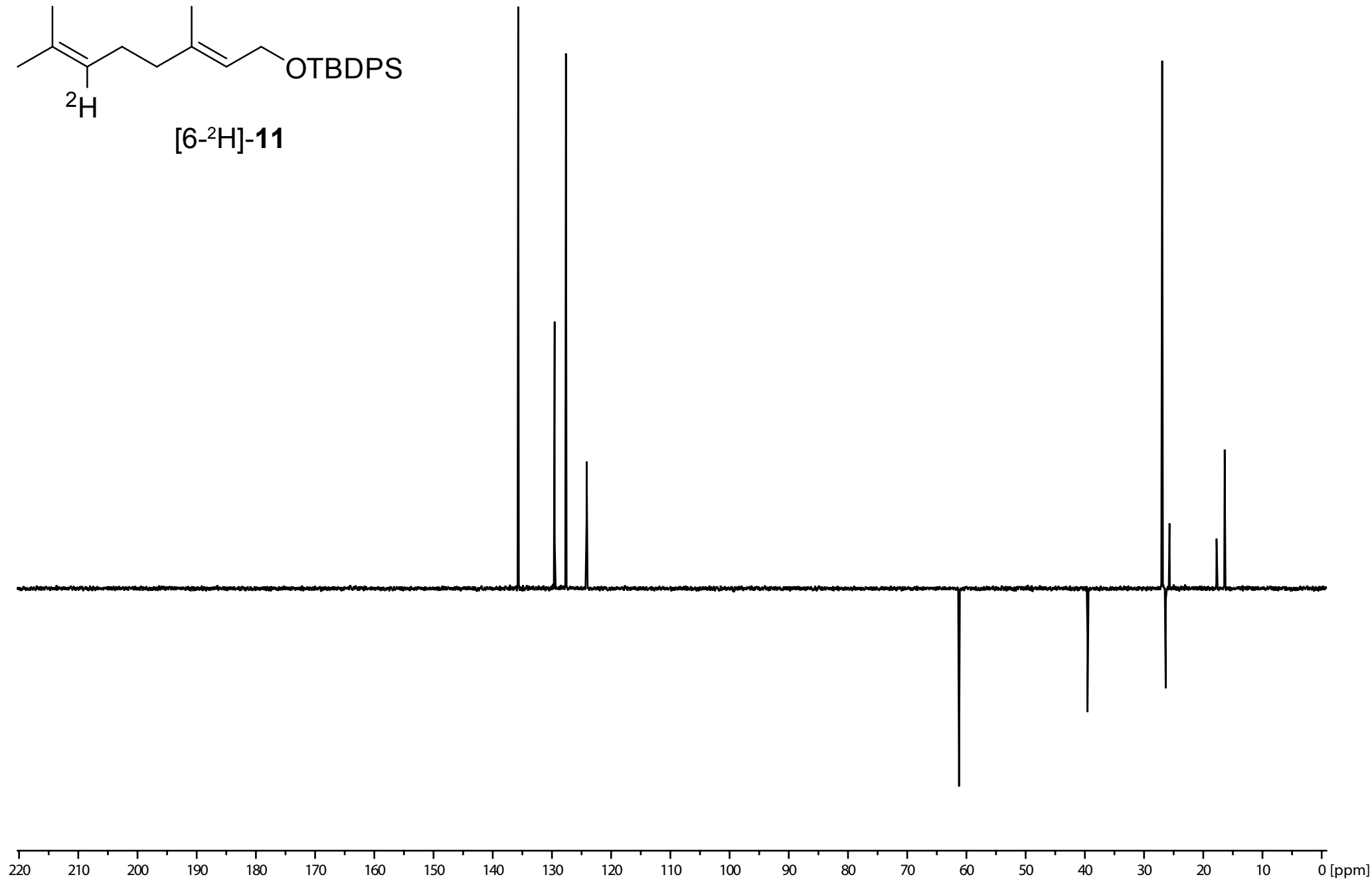
[6-²H]-11

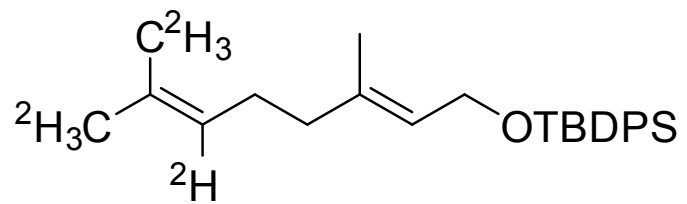




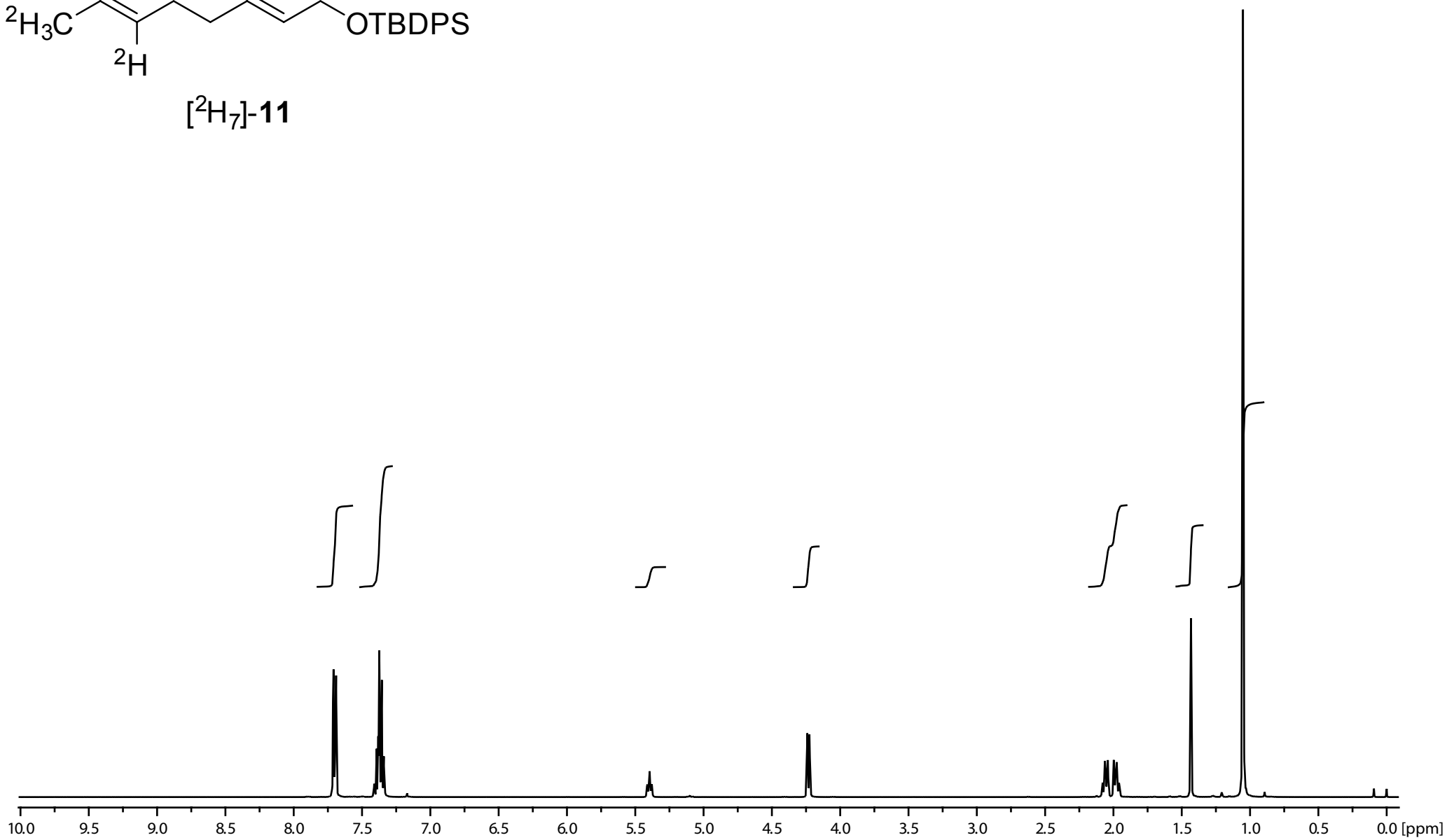
^2H

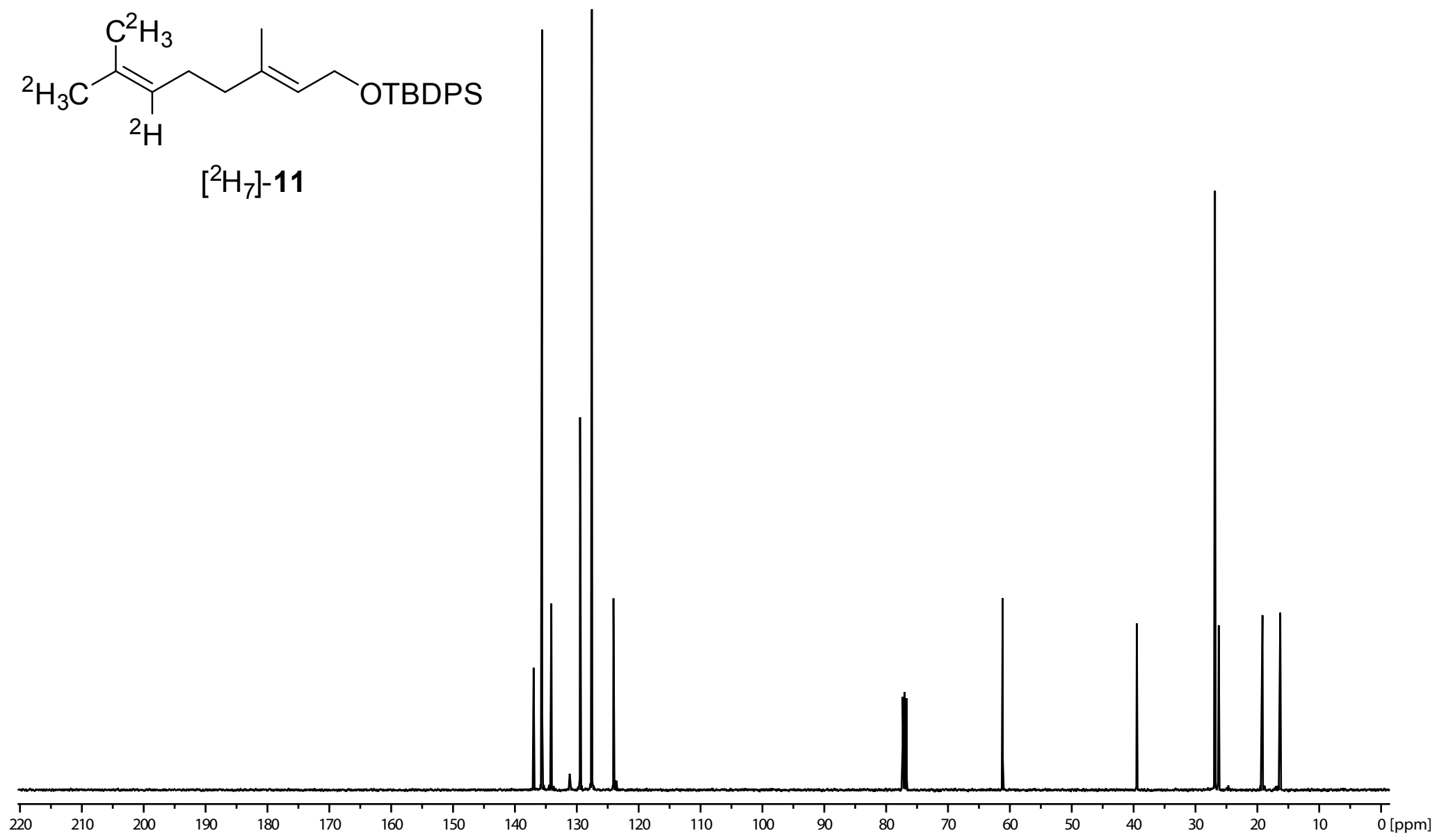
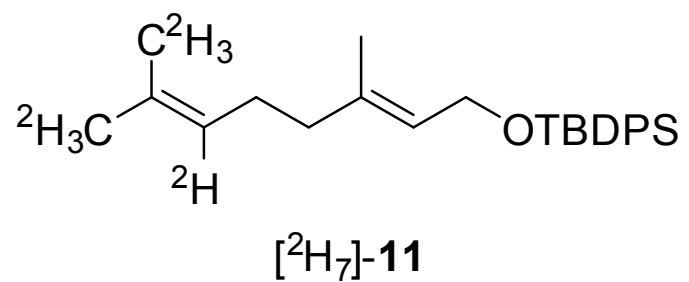
[6- ^2H]-11

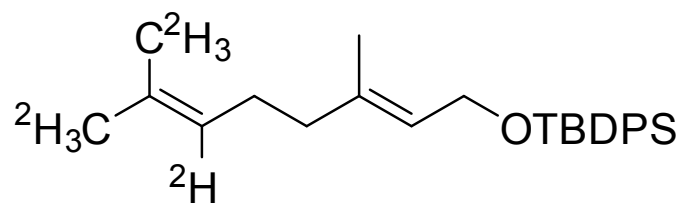




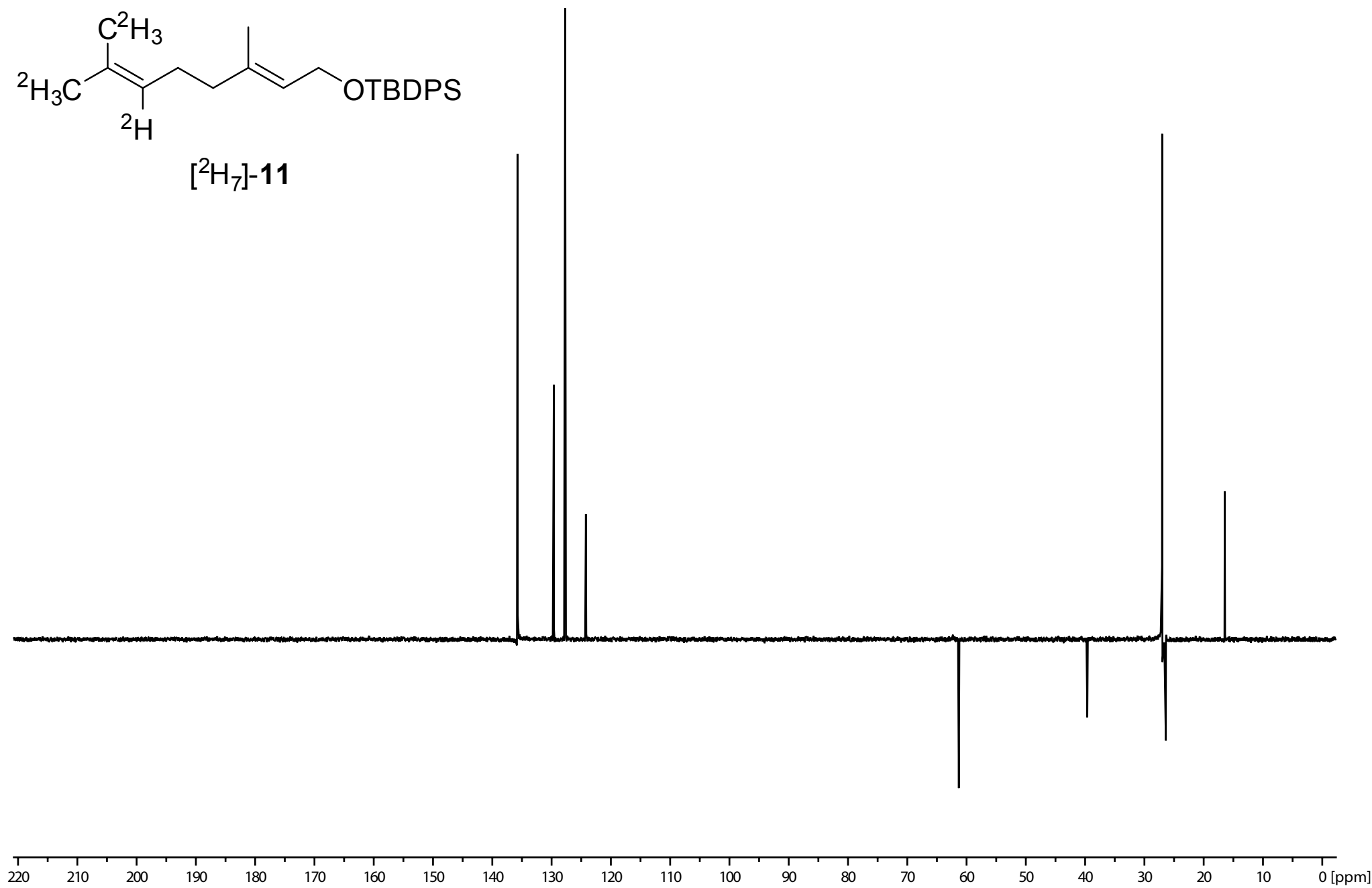
[$^2\text{H}_7$]-11

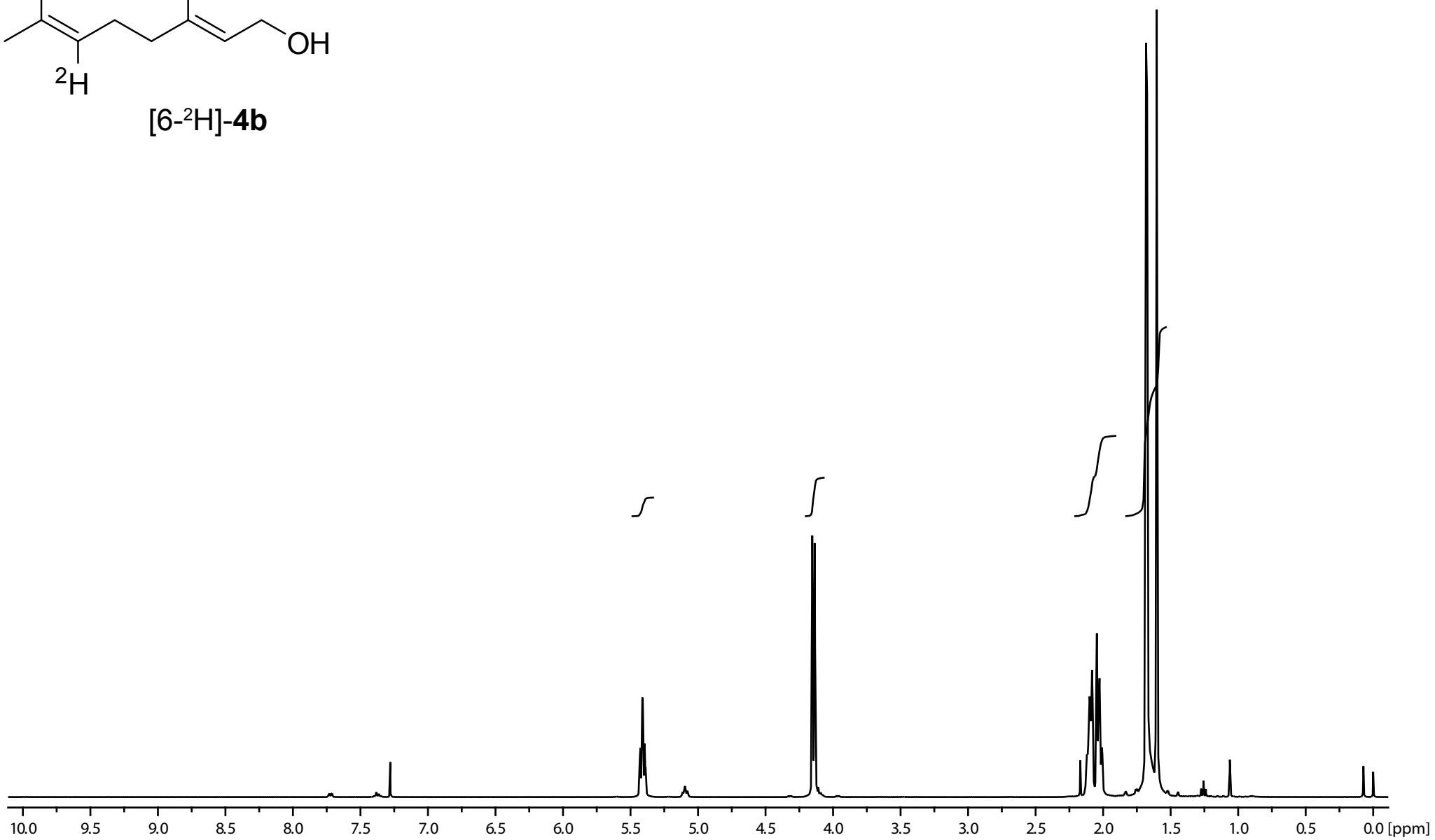
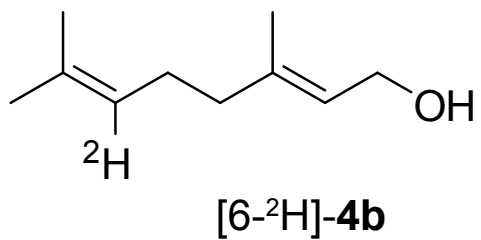


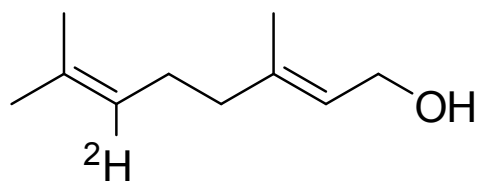




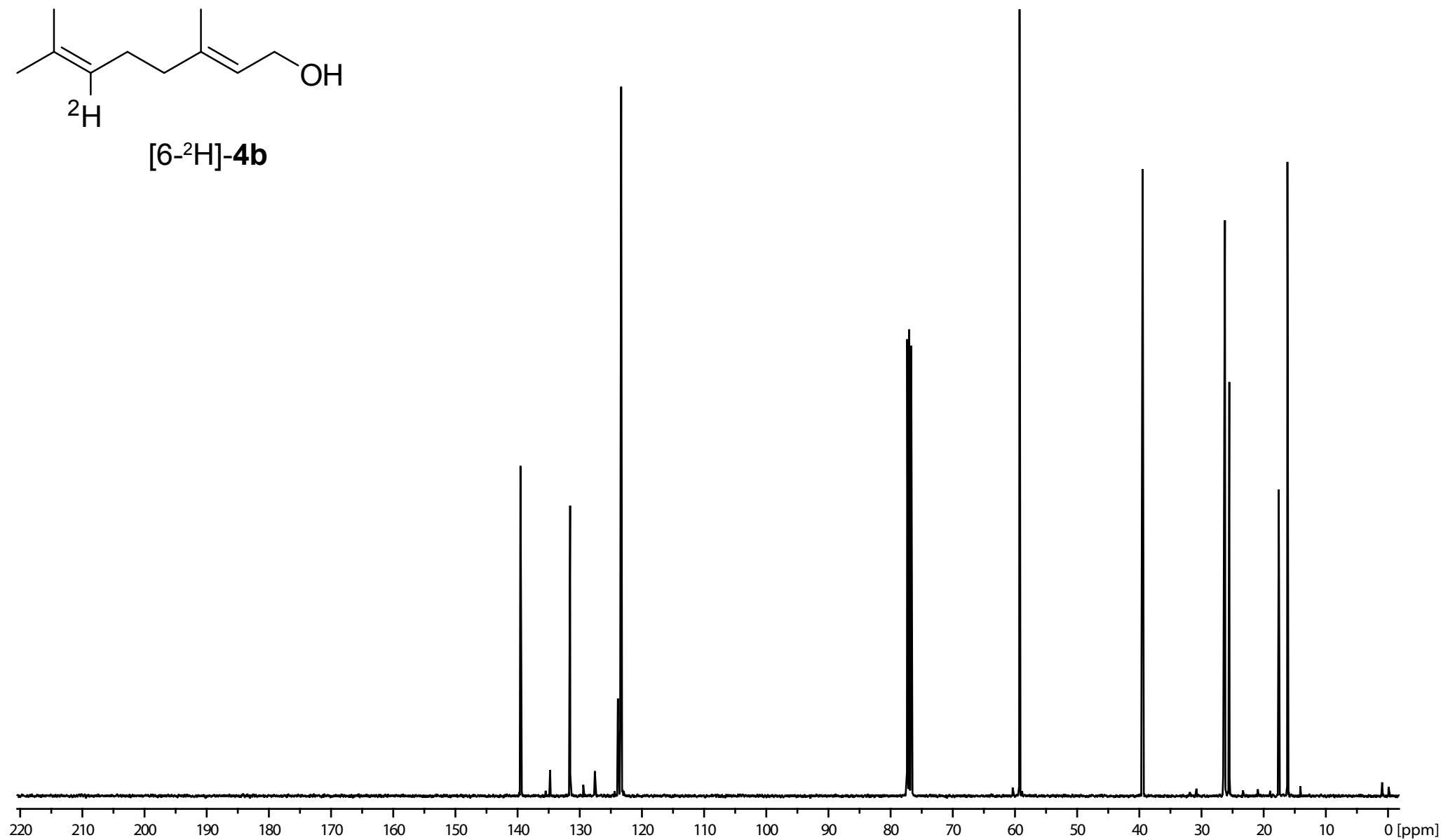
[²H₇]-11

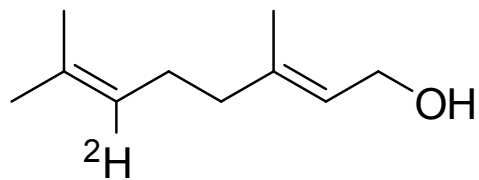




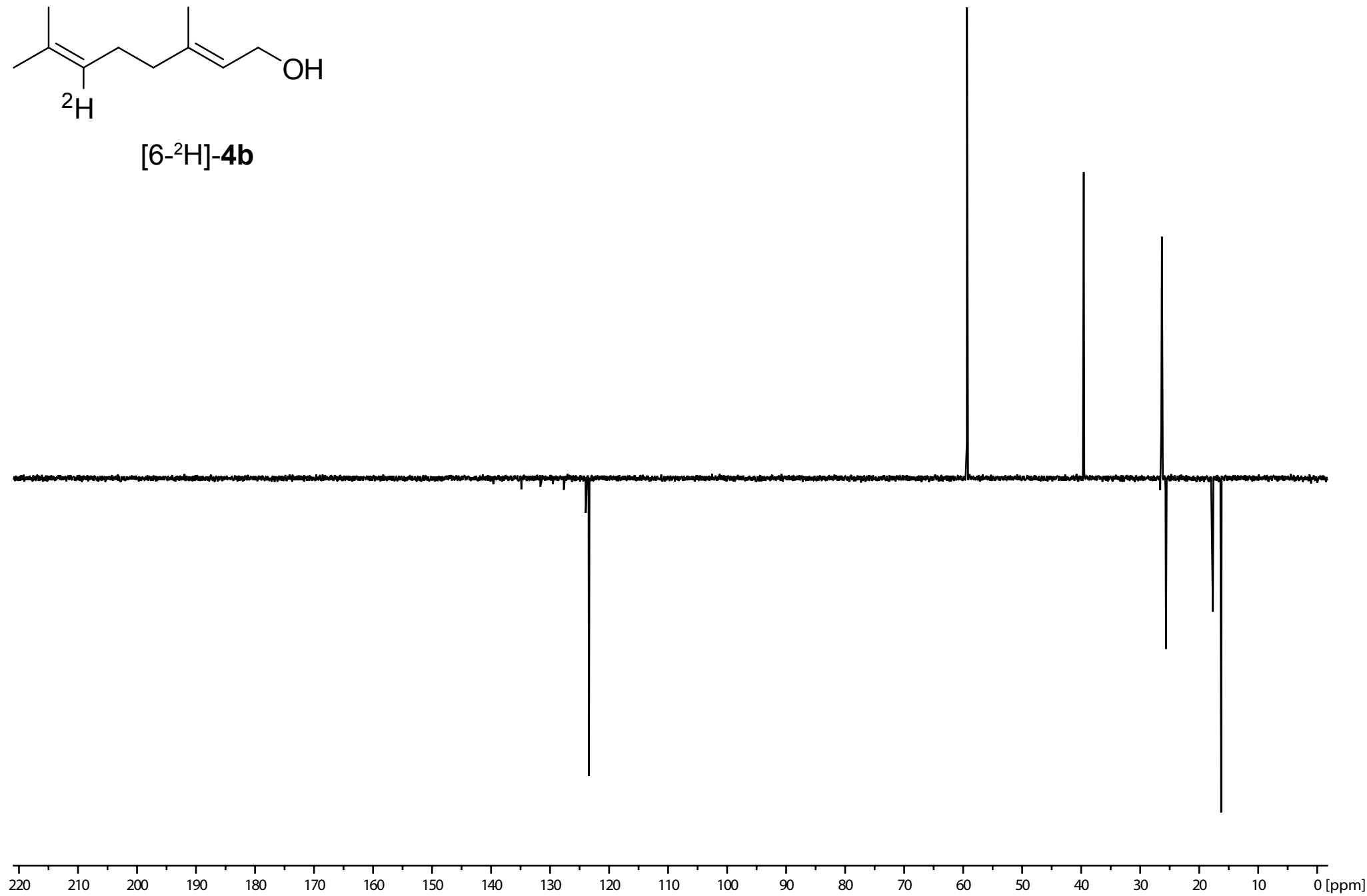


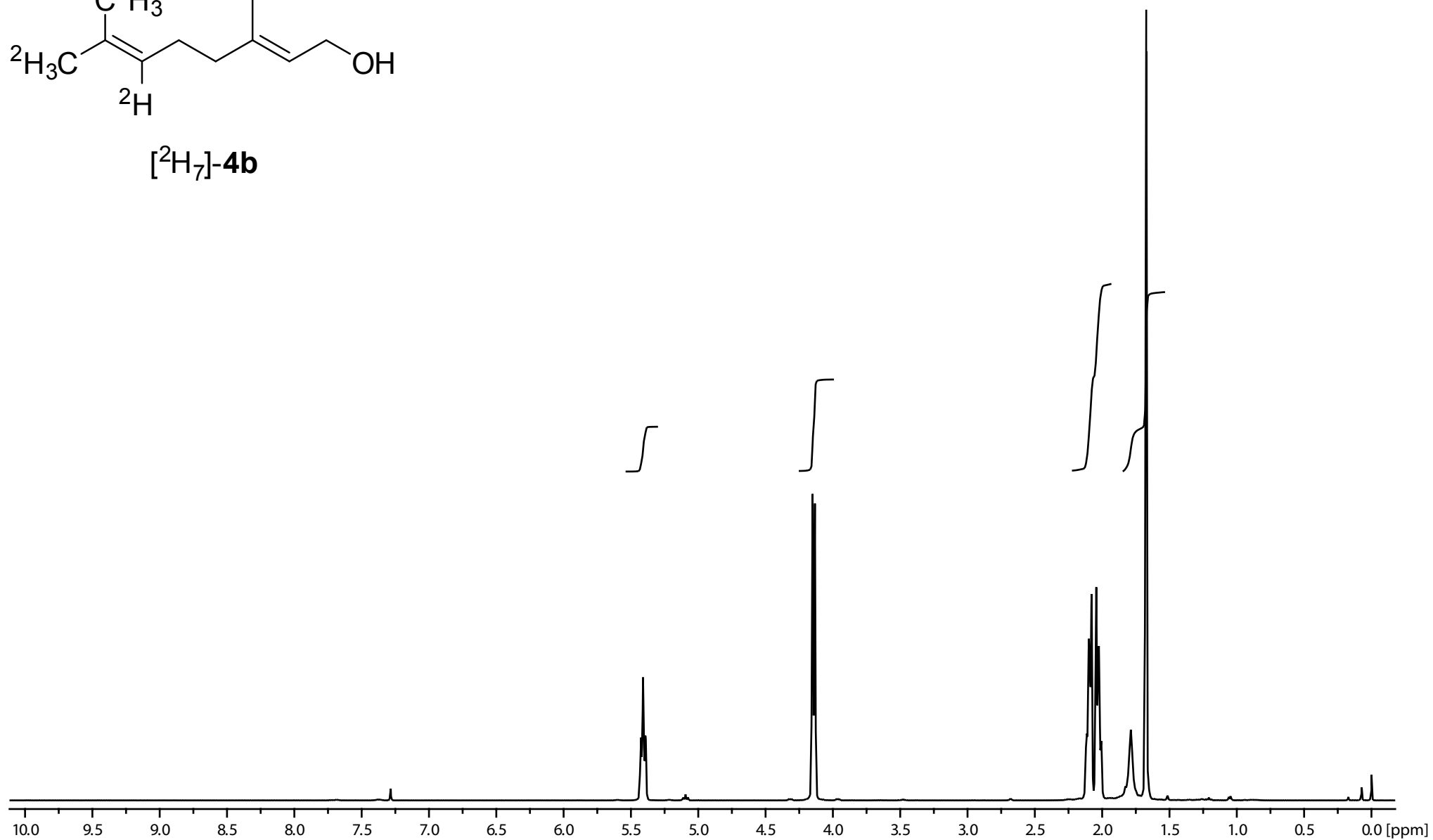
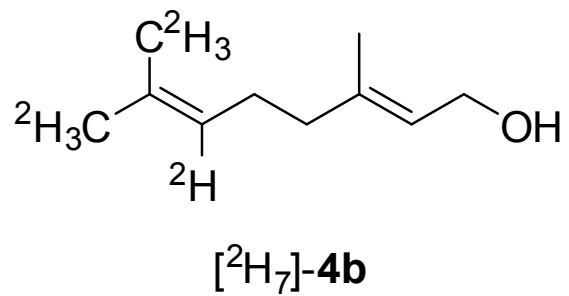
[6-²H]-4b

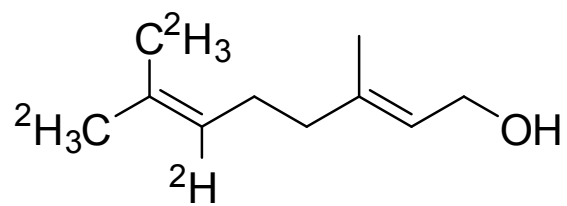




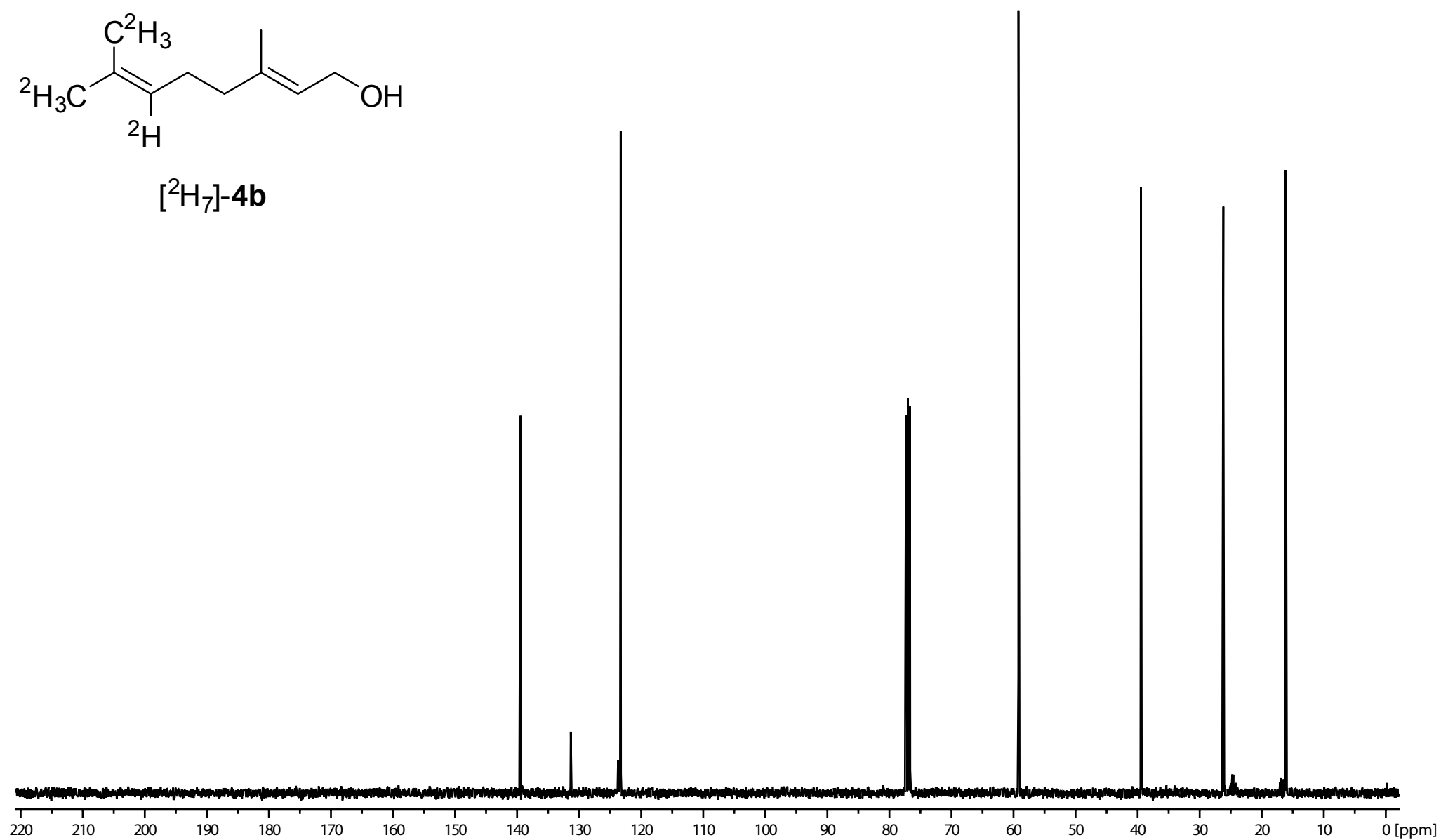
[6-²H]-4b

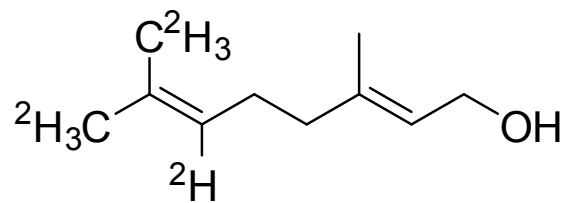




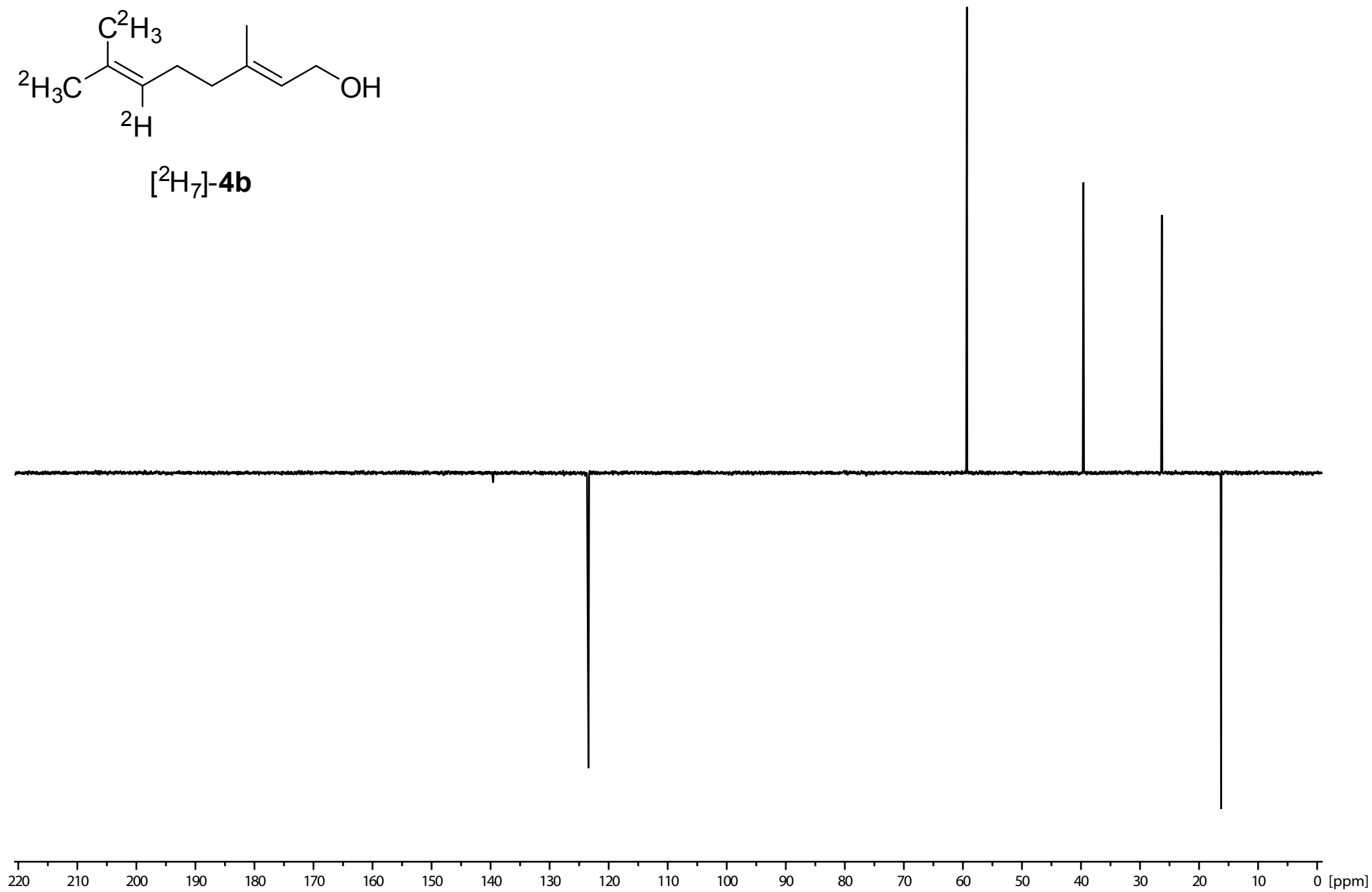


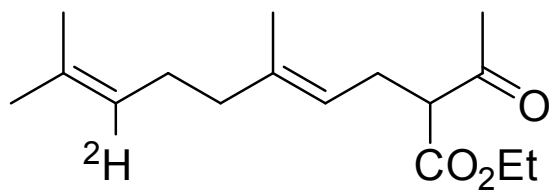
[²H₇]-4b



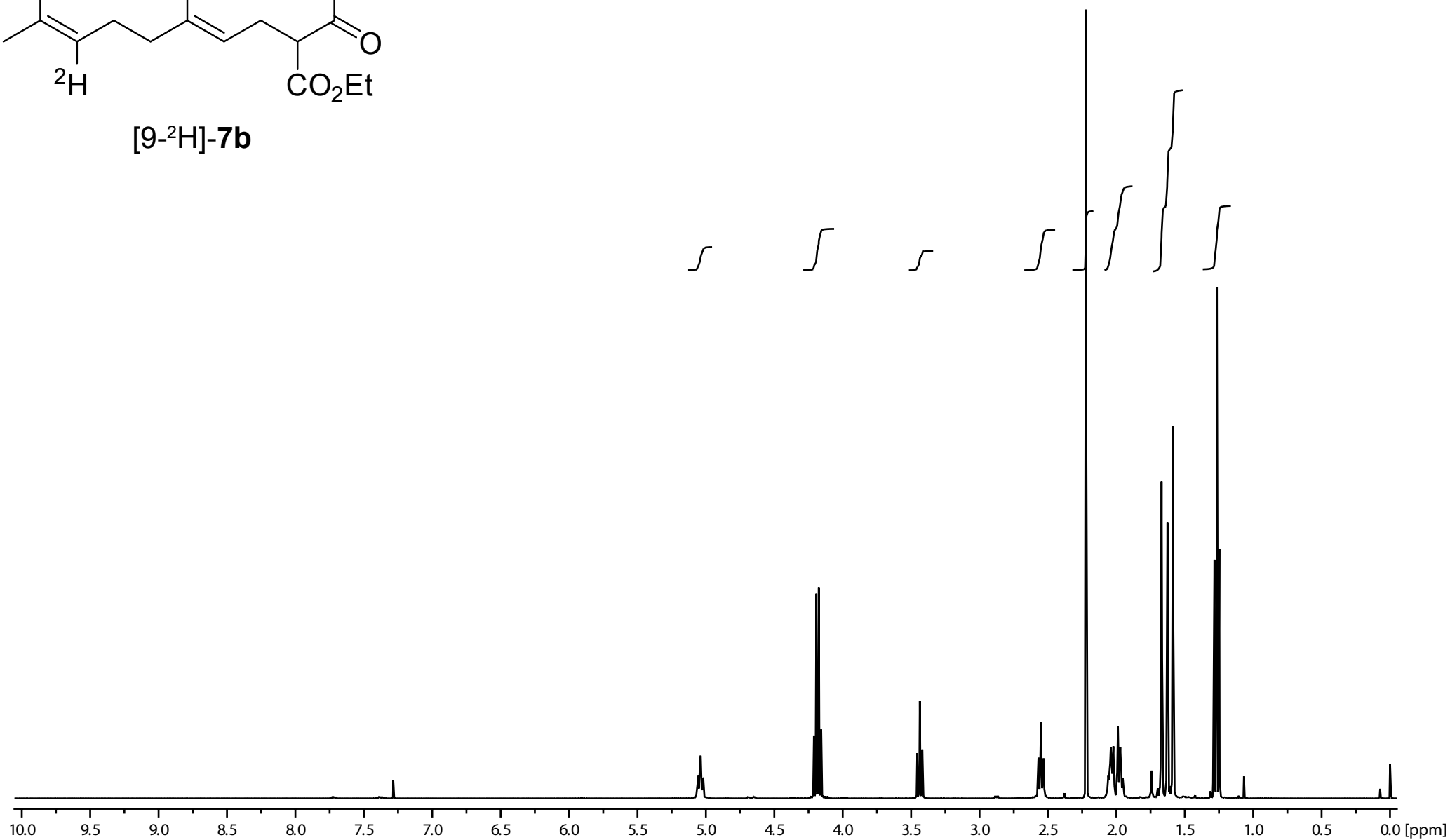


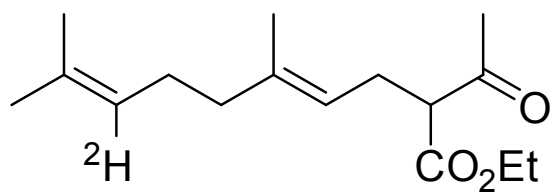
[²H₇]-4b



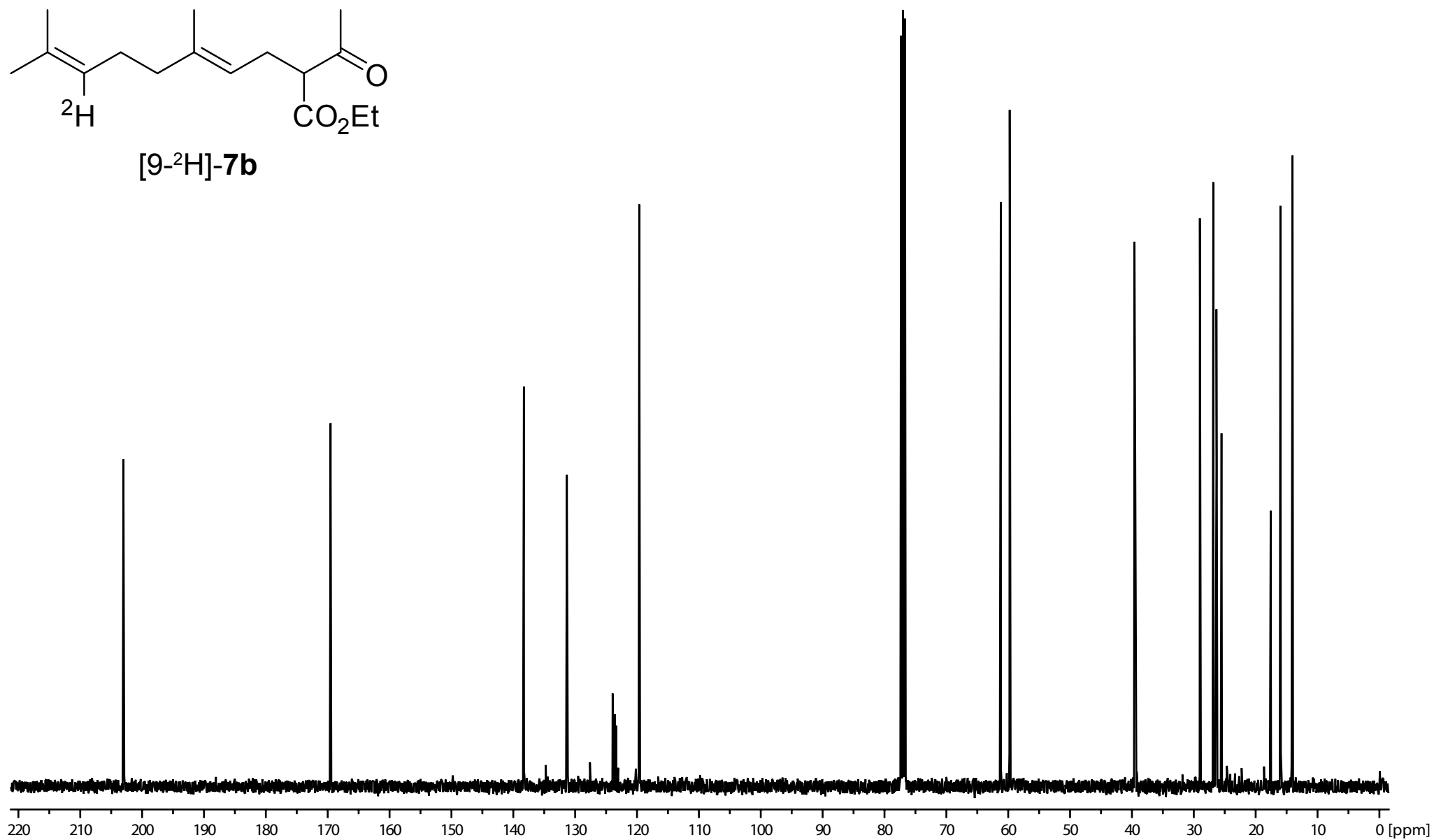


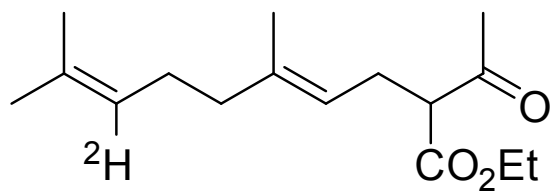
[9-²H]-7b



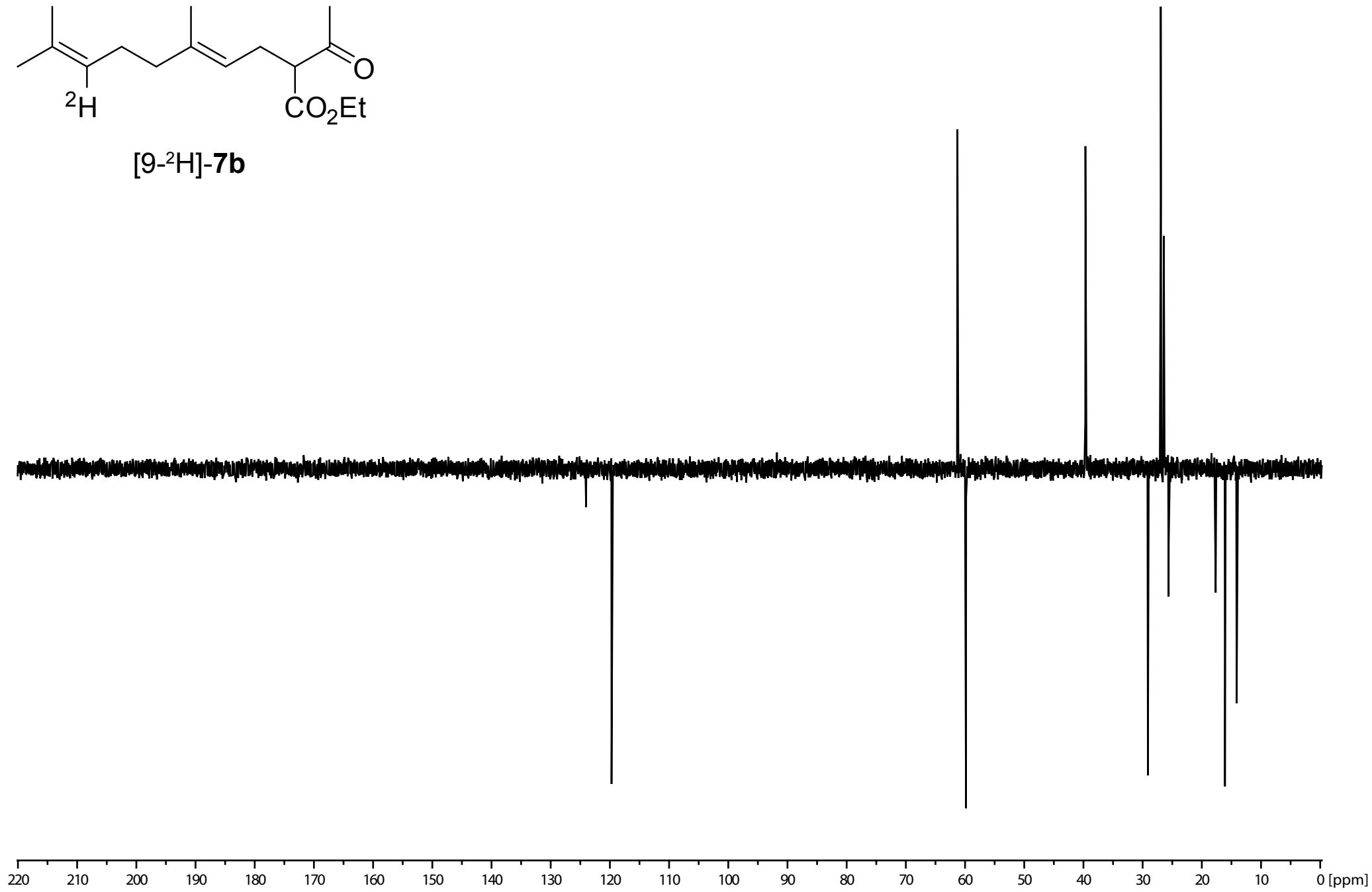


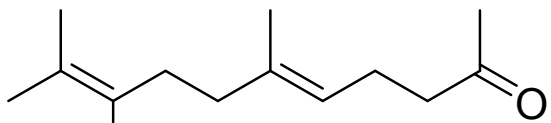
[9-²H]-7b





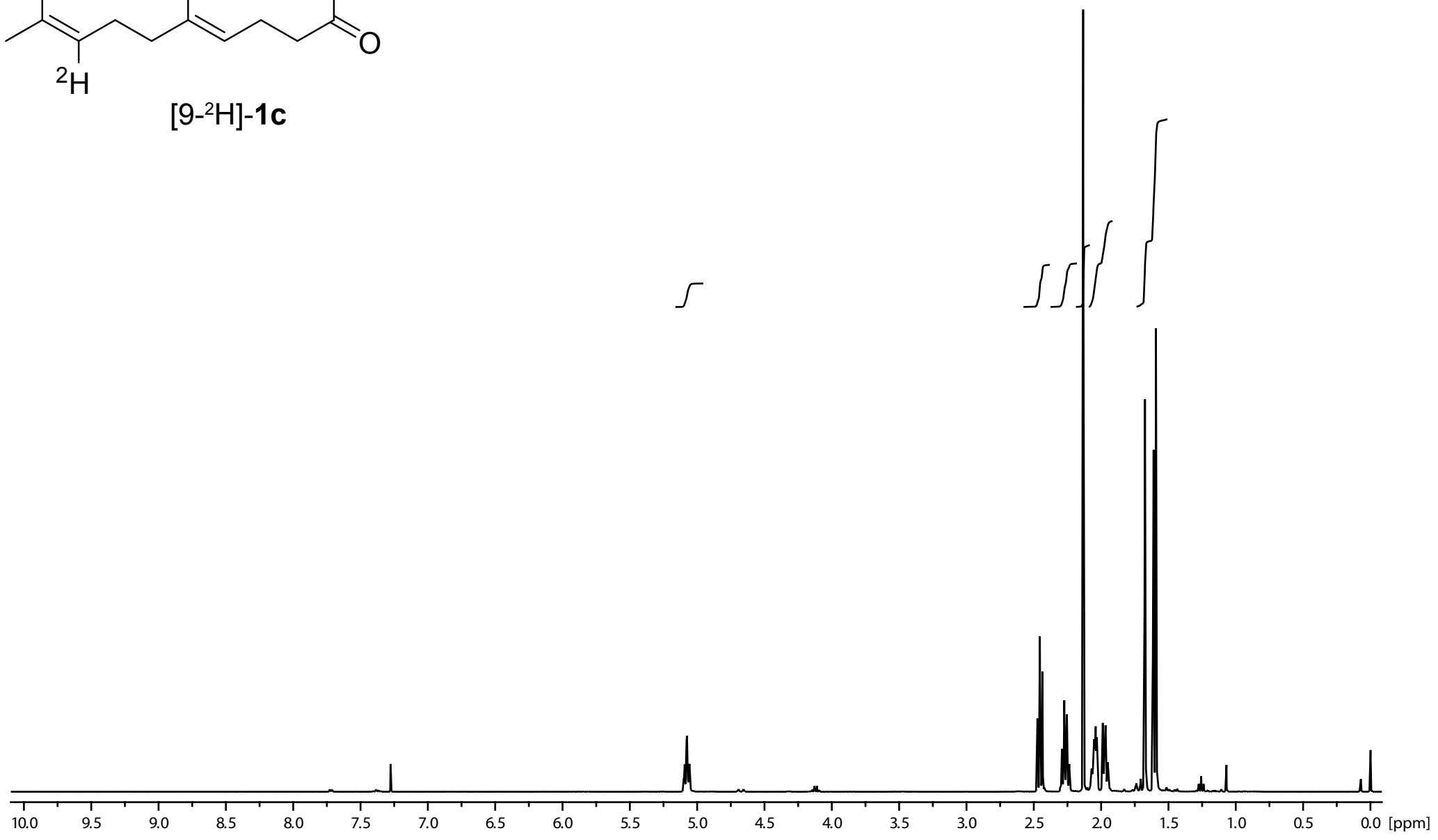
[9-²H]-7b

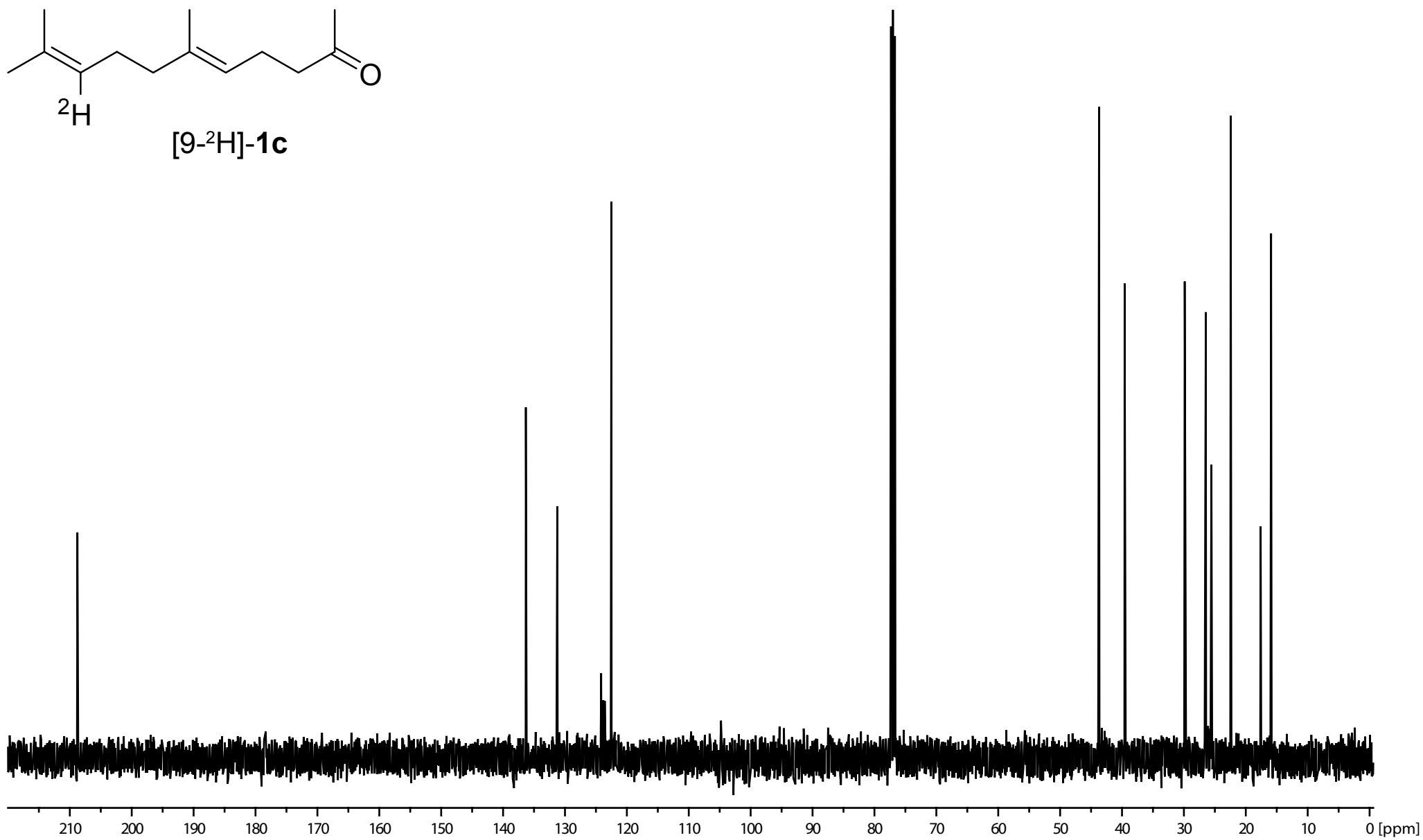
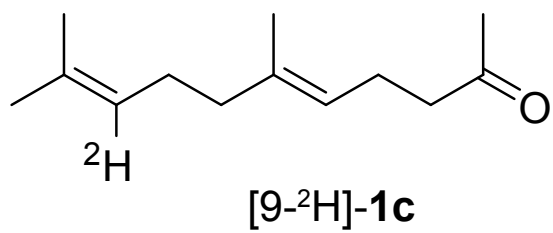


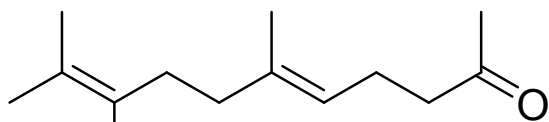


²H

[9-²H]-1c

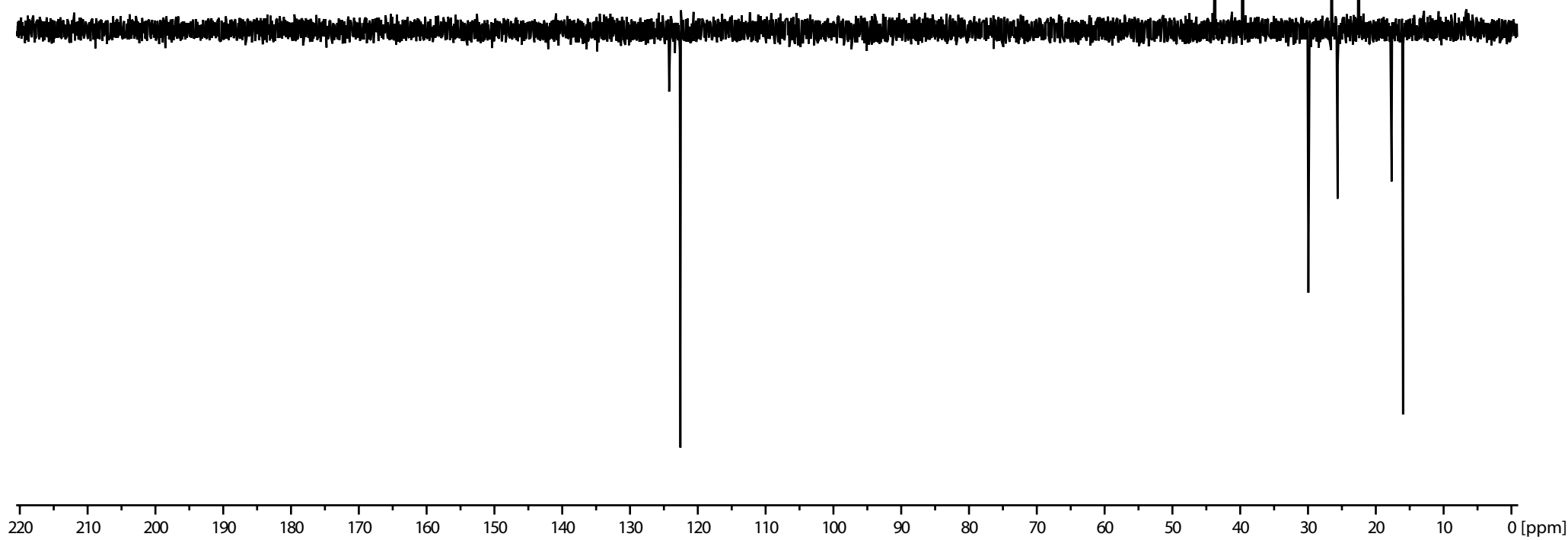


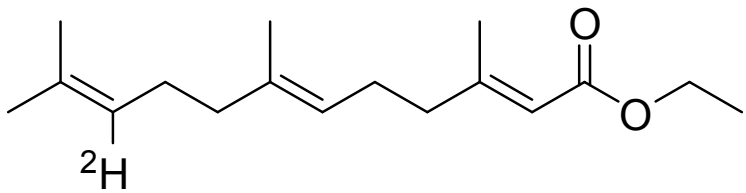




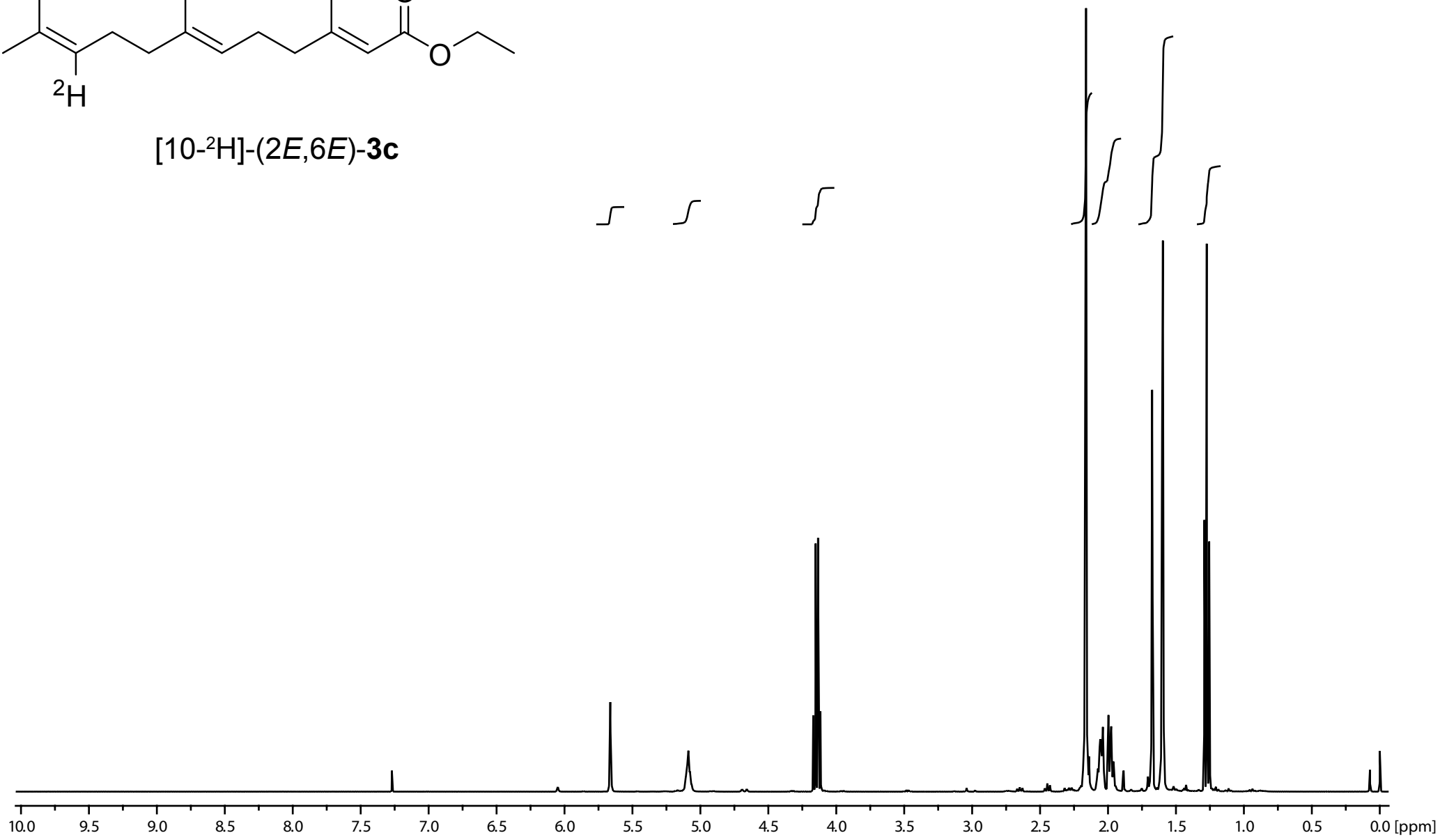
^2H

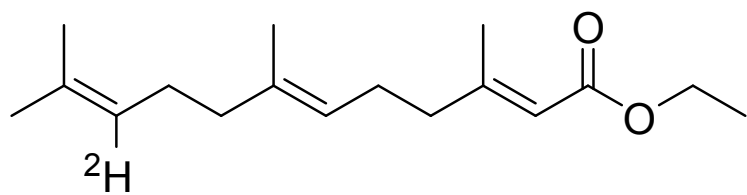
[9- ^2H]-1c



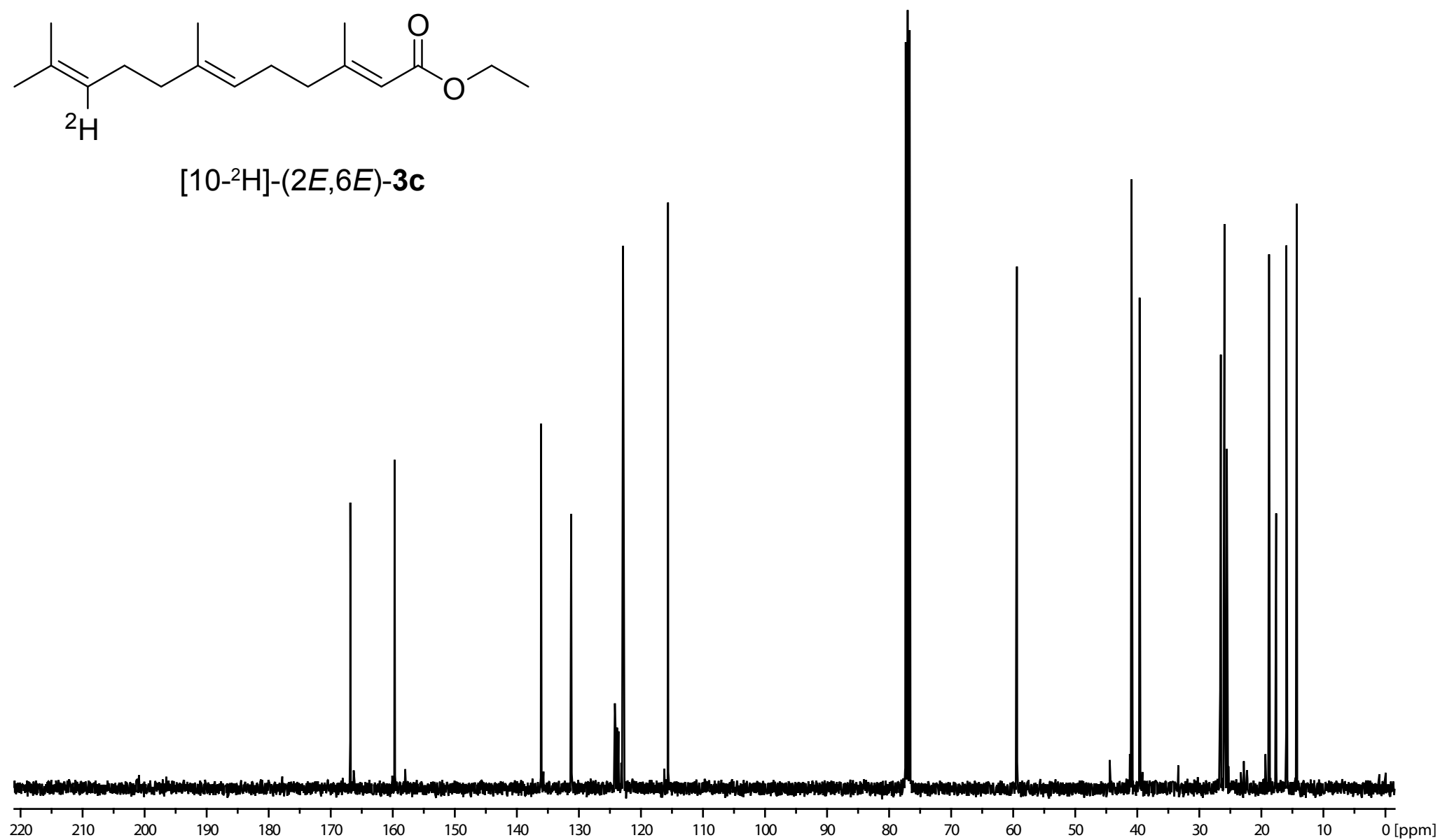


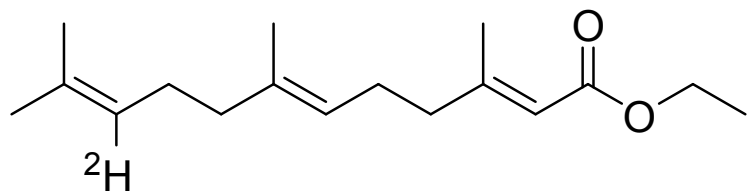
[10-²H]-(2*E*,6*E*)-3c



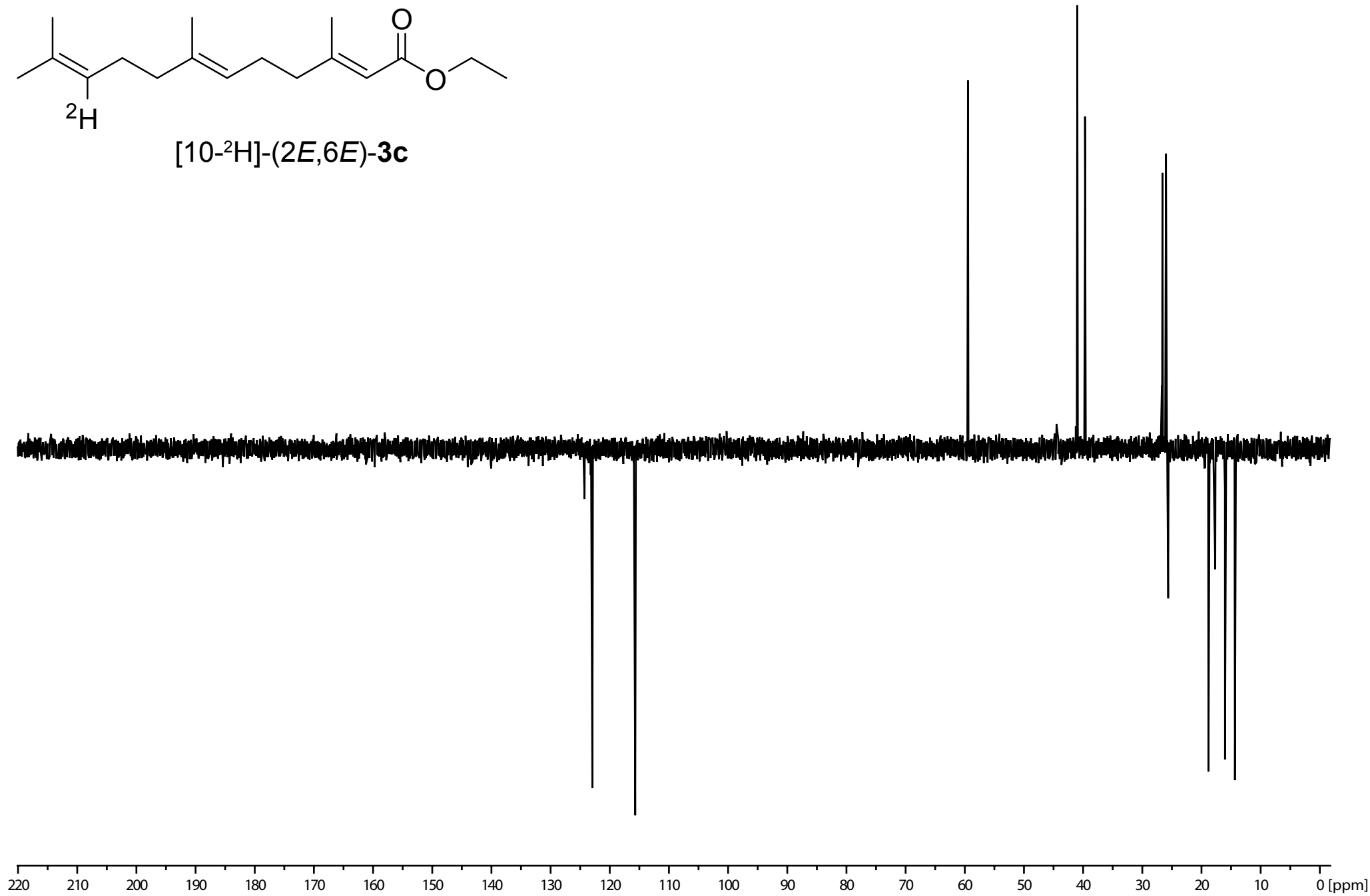


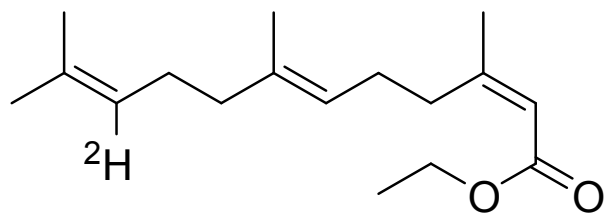
[10-²H]-(2*E*,6*E*)-3c



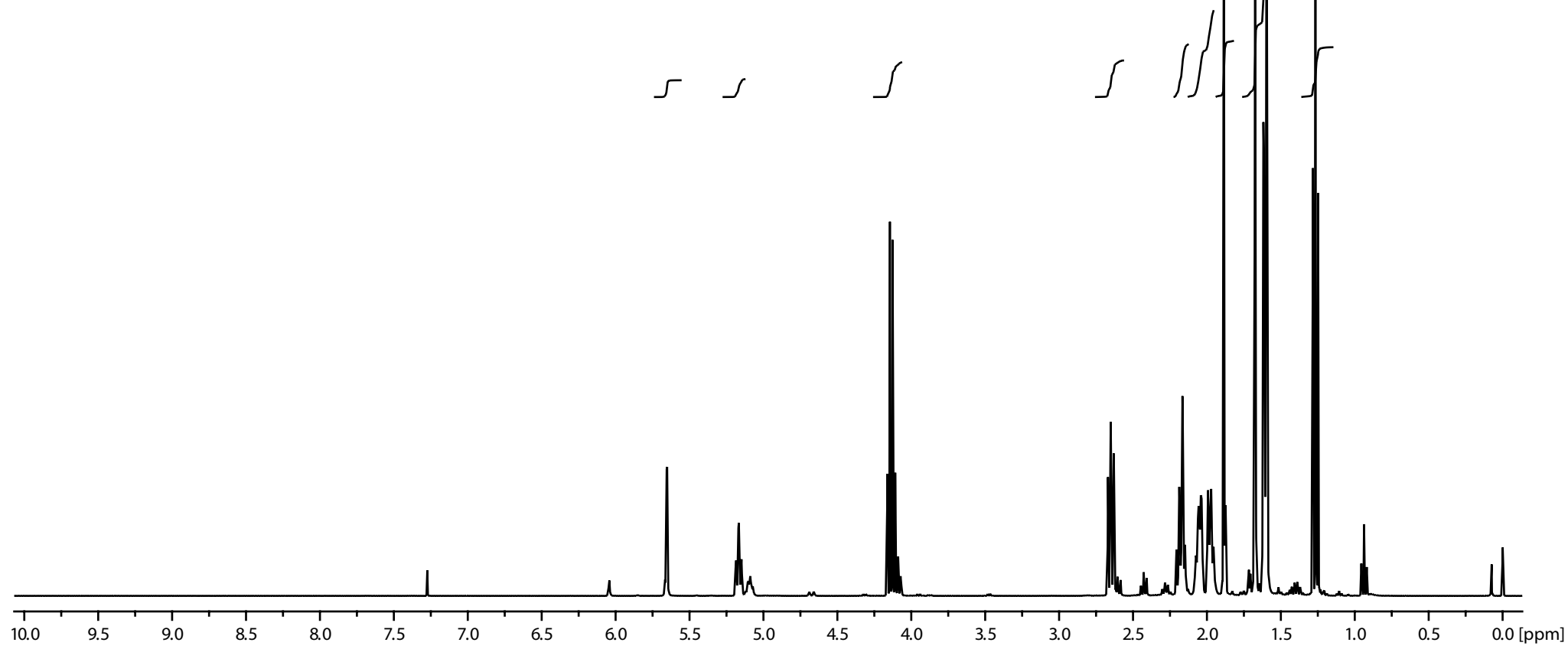


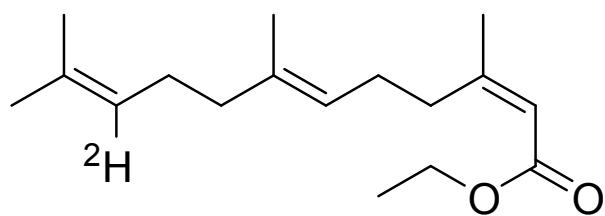
[10-²H]-(2*E*,6*E*)-3c



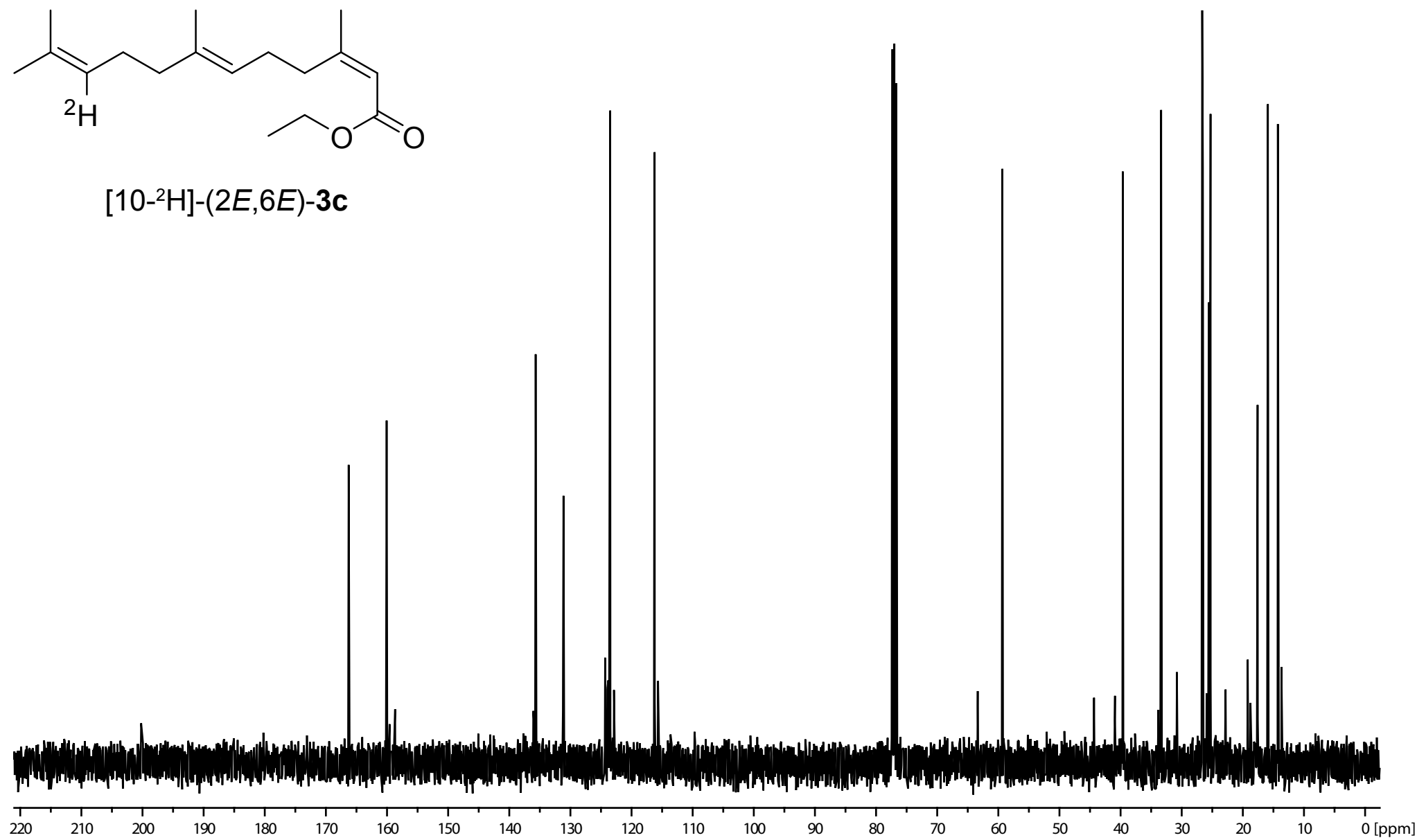


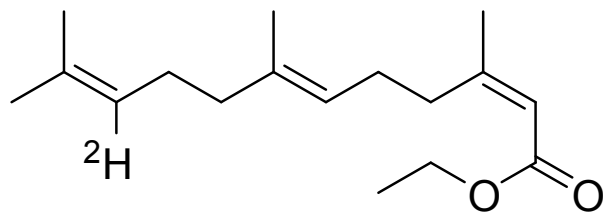
[10-²H]-(2*E*,6*E*)-3c



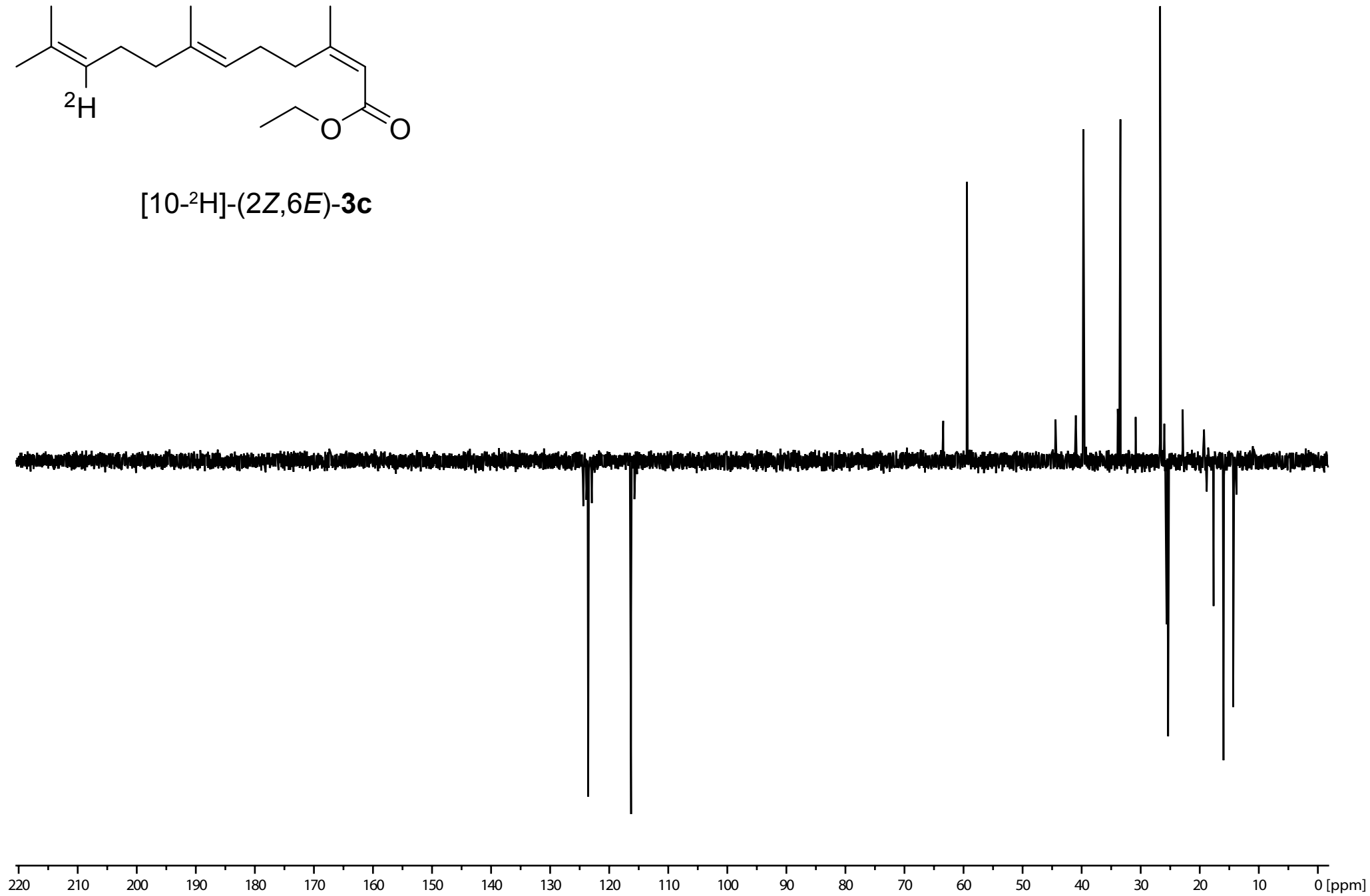


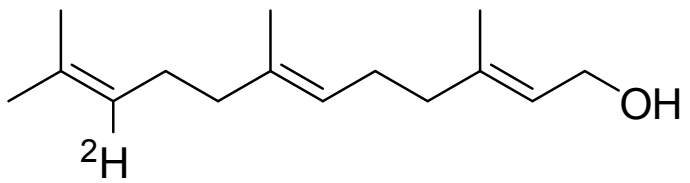
[10-²H]-(2*E*,6*E*)-**3c**



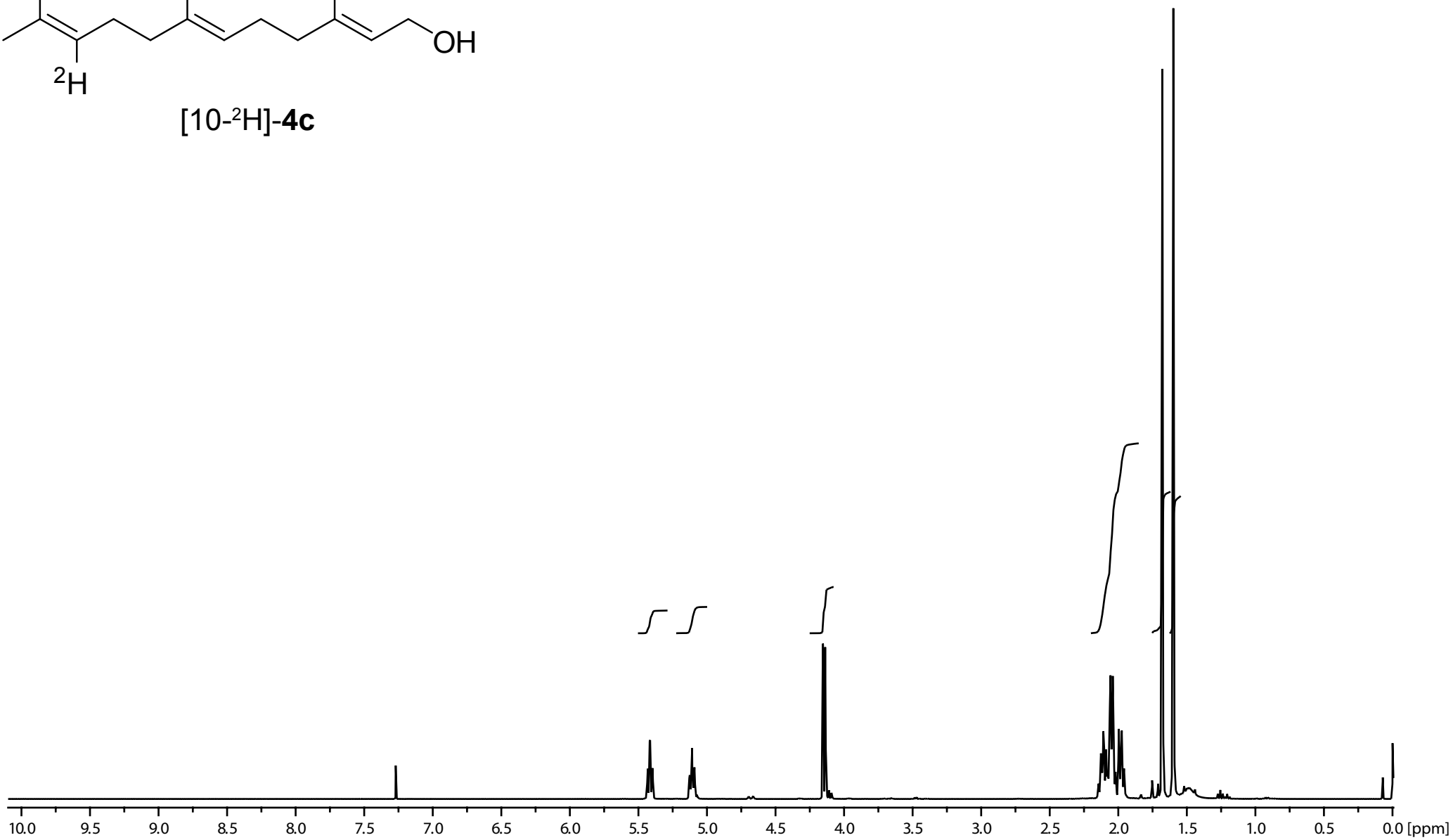


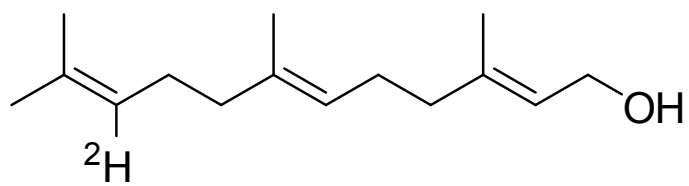
[10-²H]-(2Z,6E)-3c



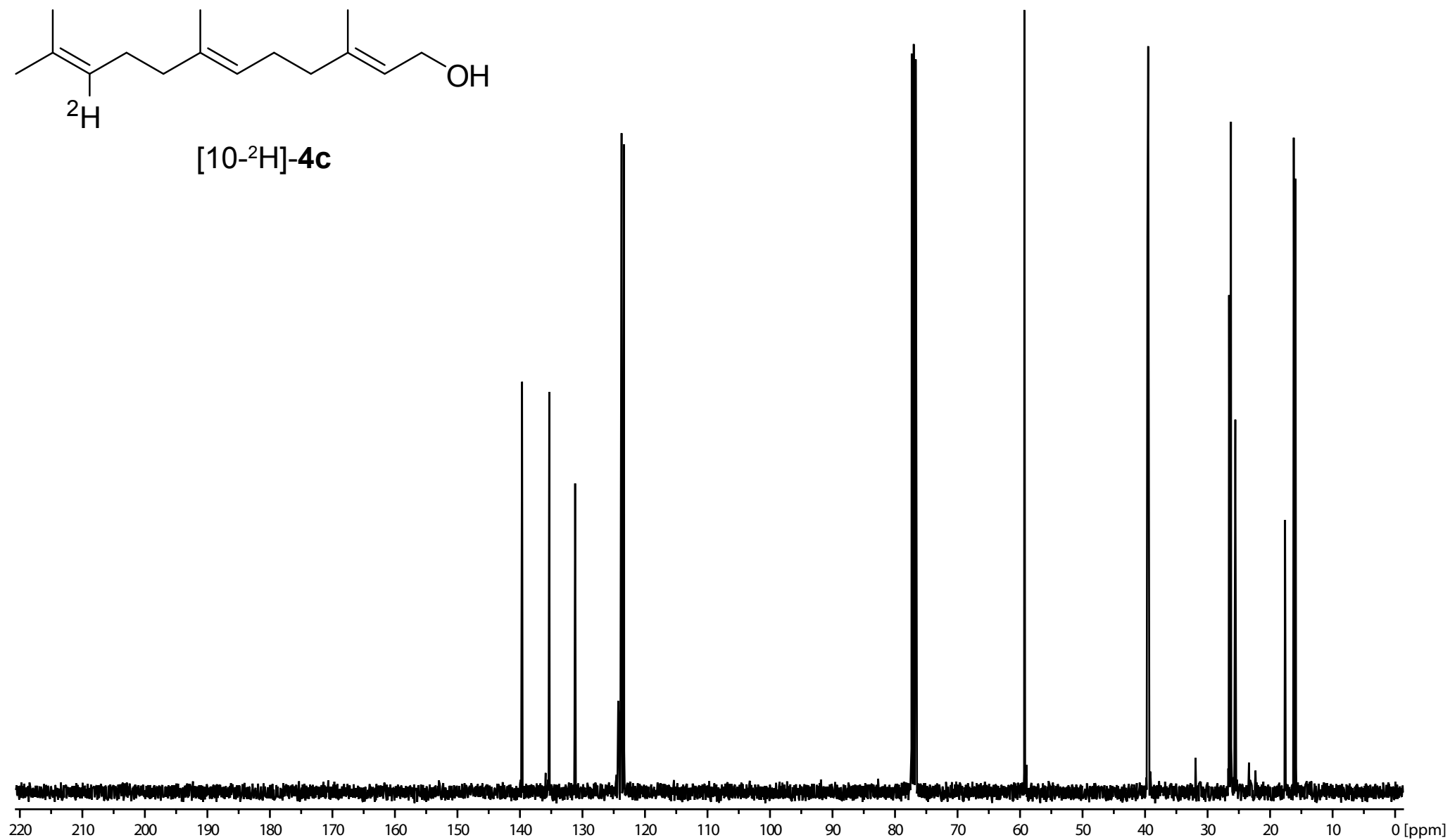


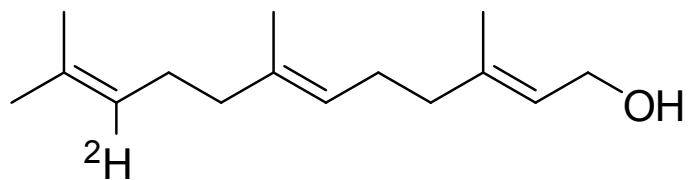
[10-²H]-4c



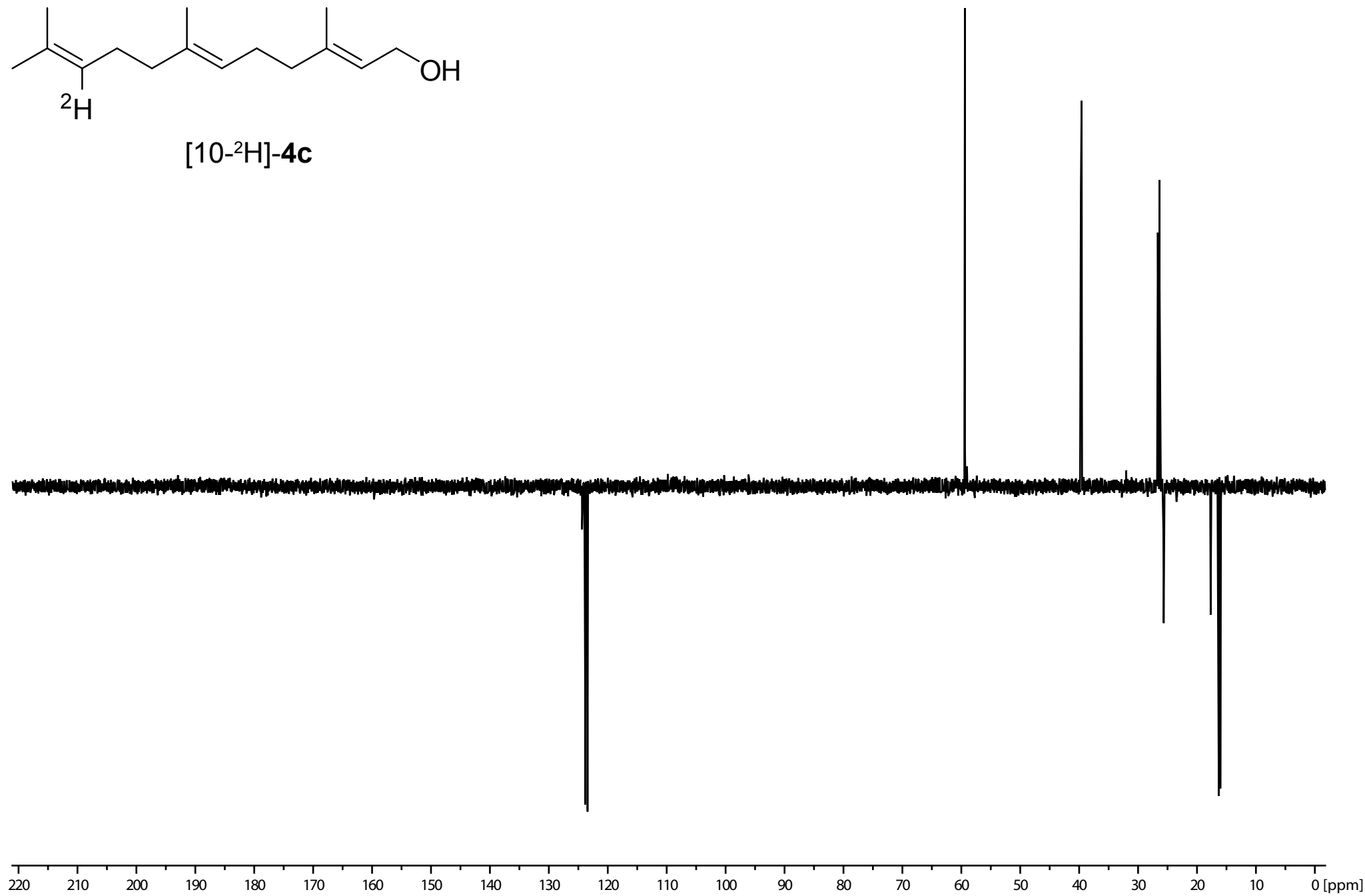


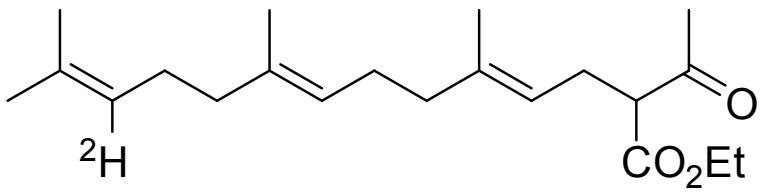
[10-²H]-4c



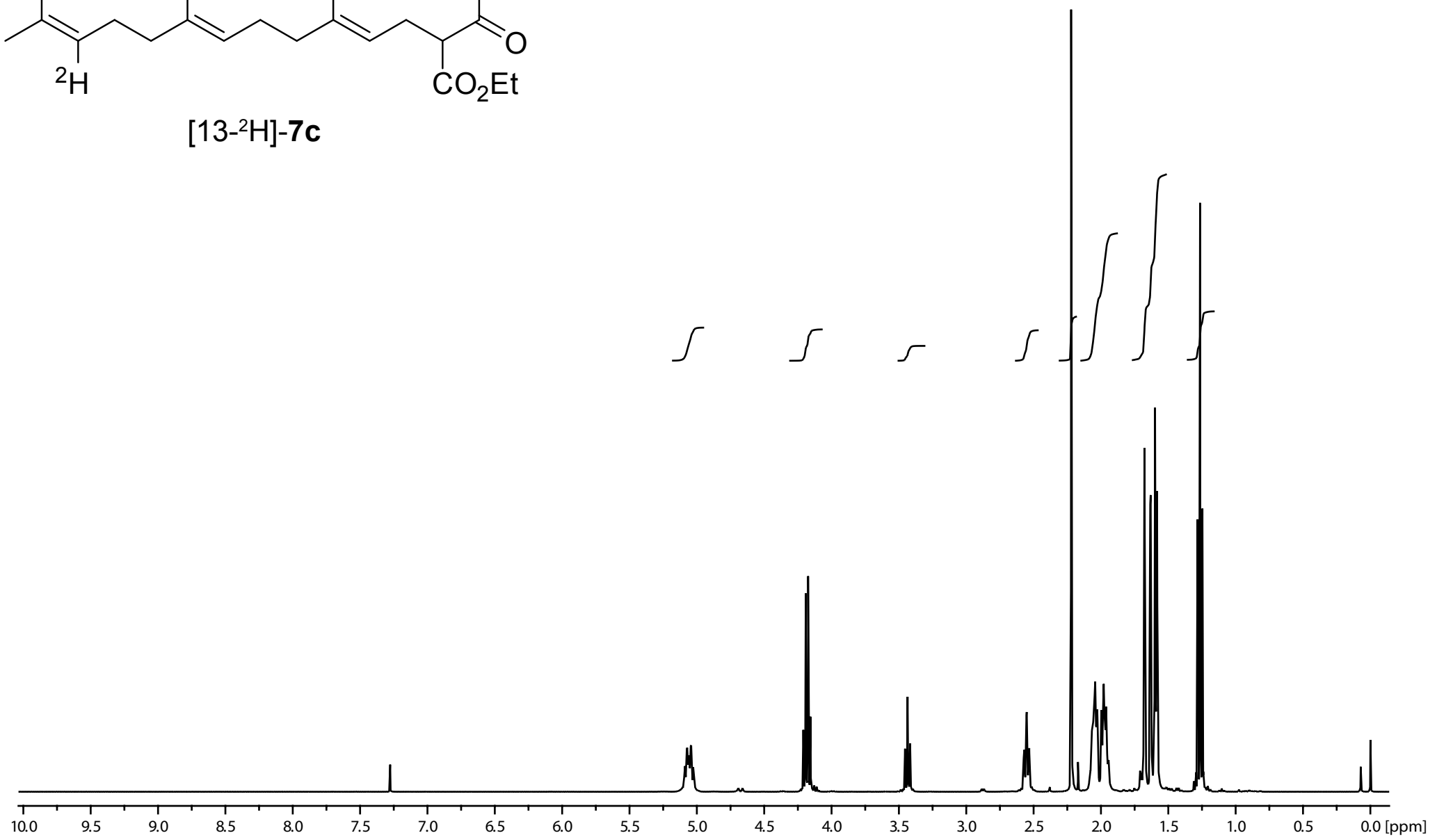


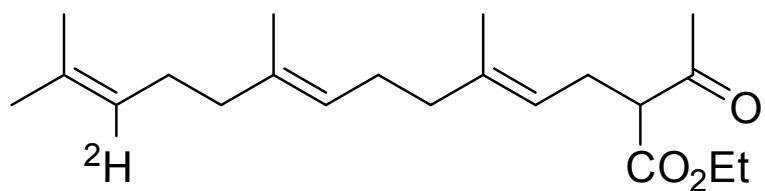
[10-²H]-4c



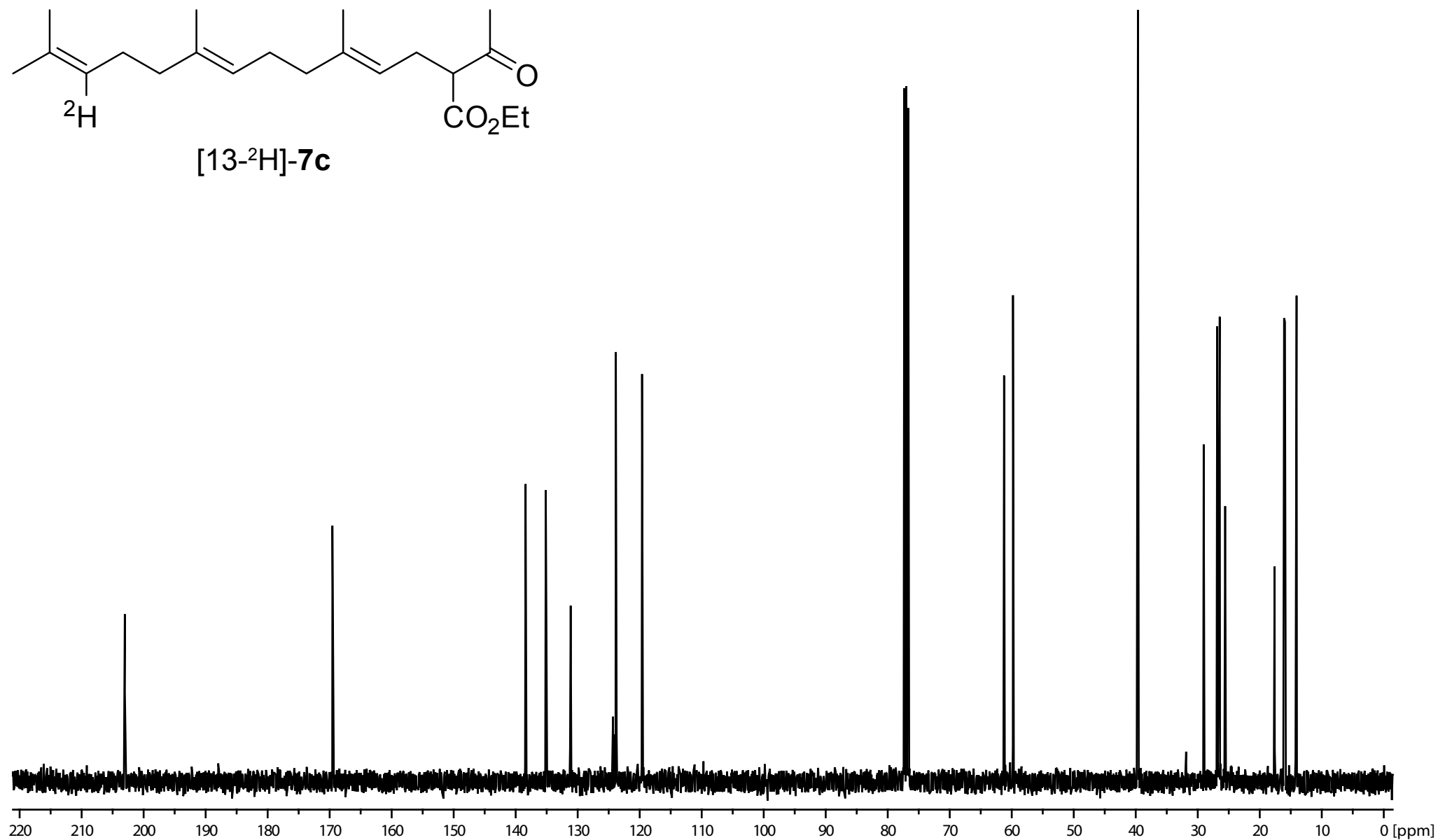


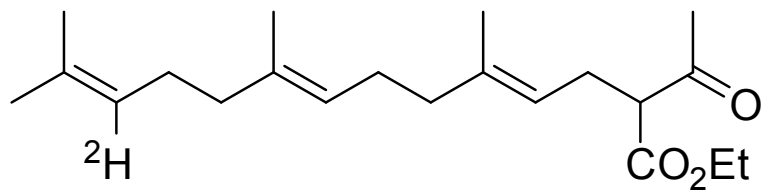
[13-²H]-7c



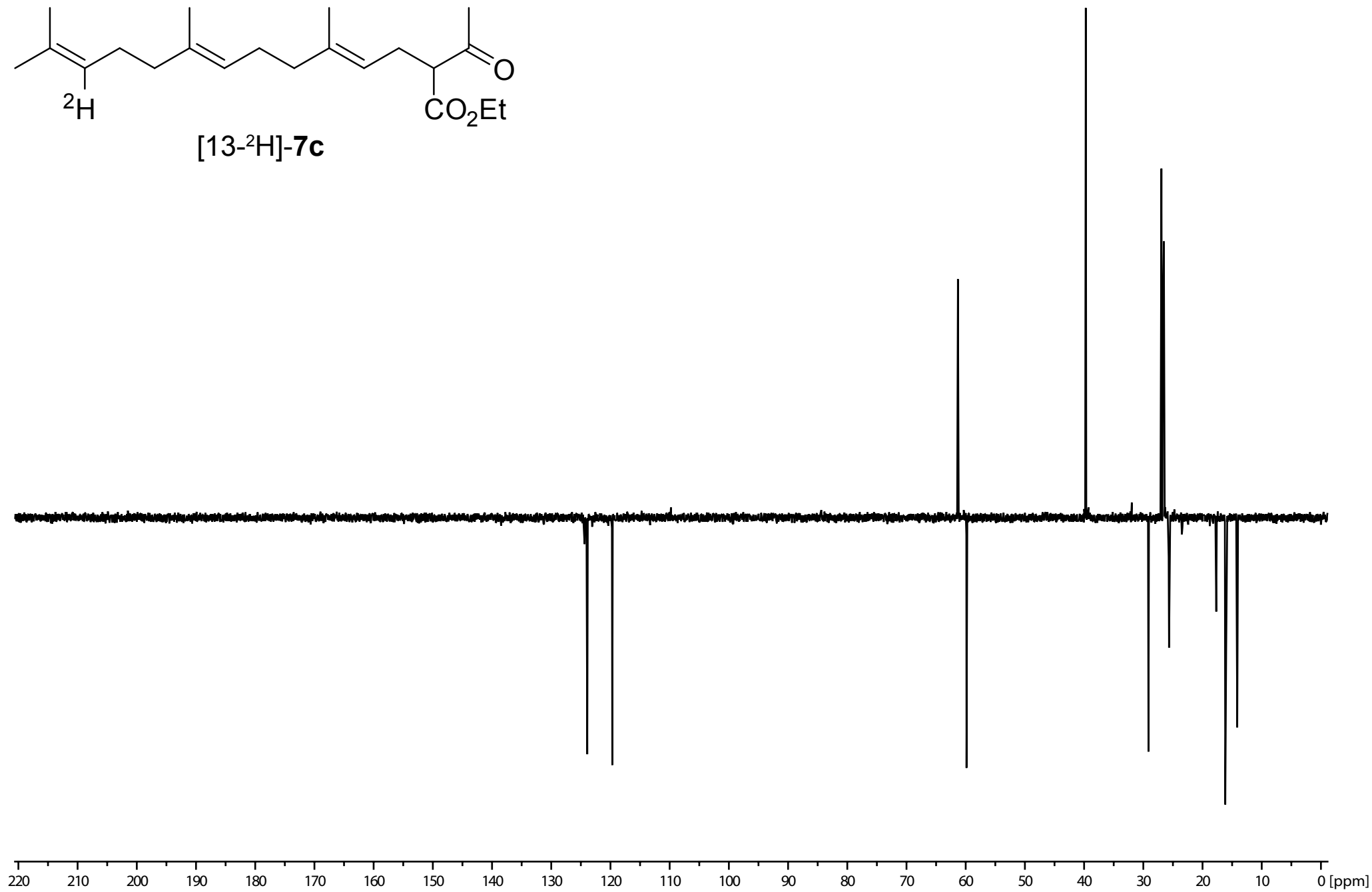


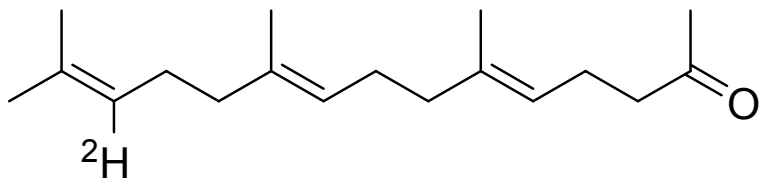
[13-²H]-7c



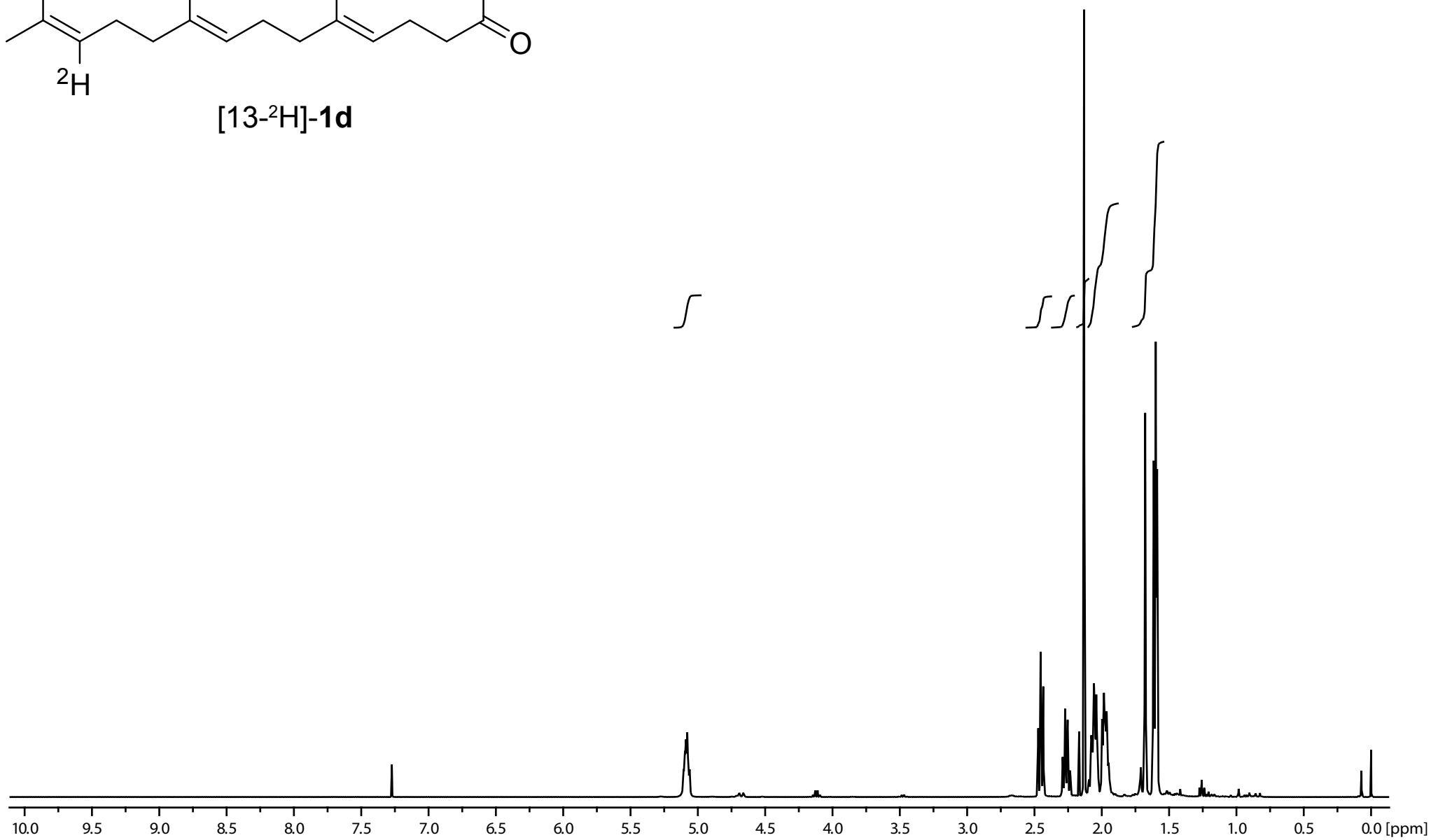


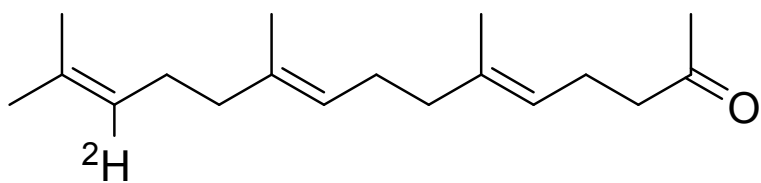
[13-²H]-7c



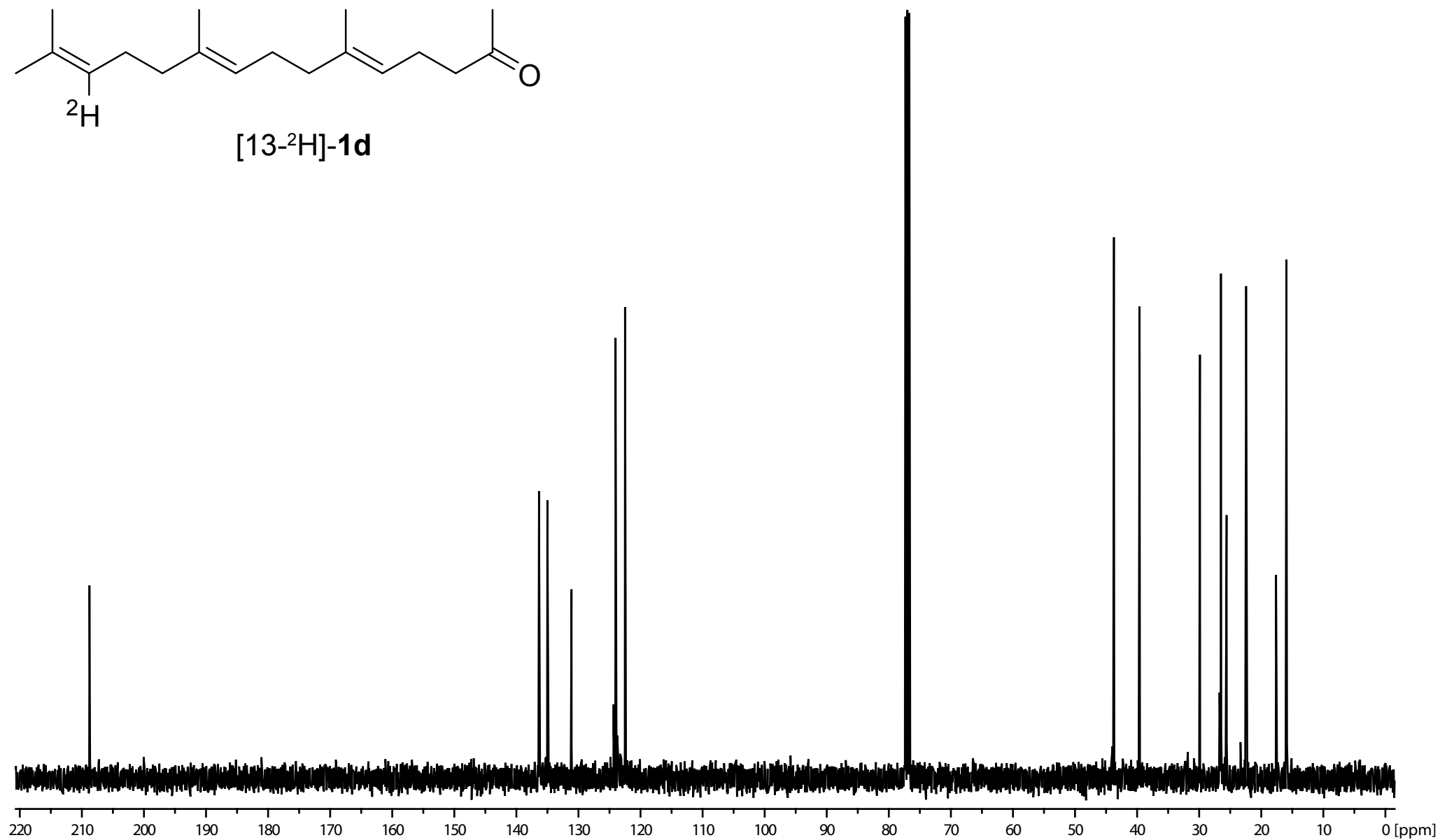


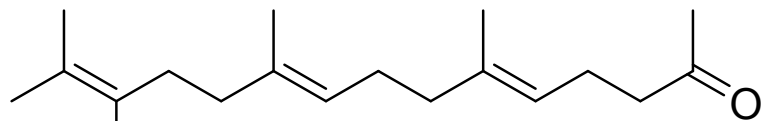
[13-²H]-1d





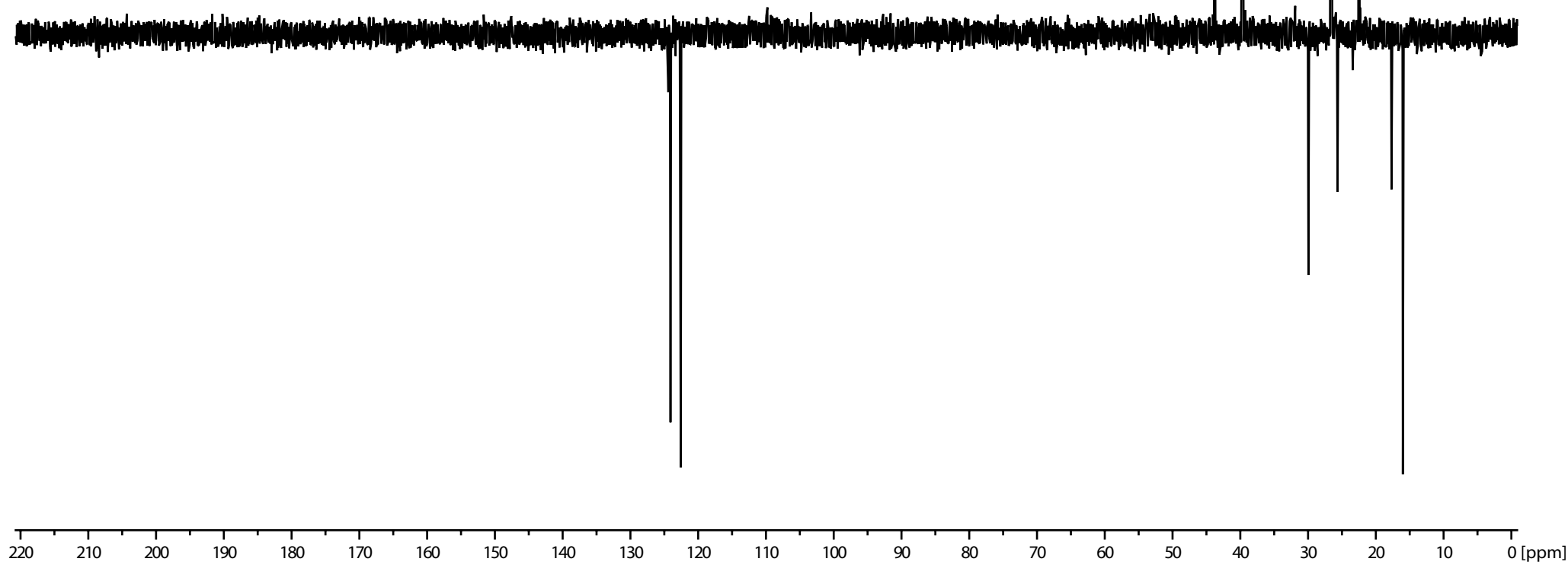
[13-²H]-1d

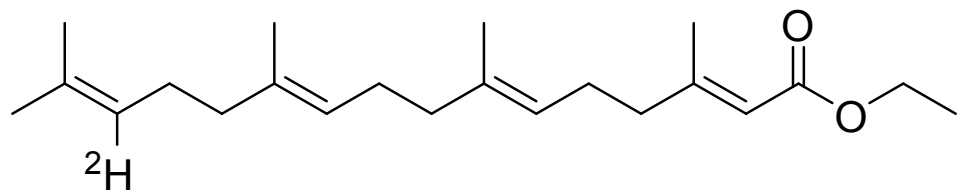




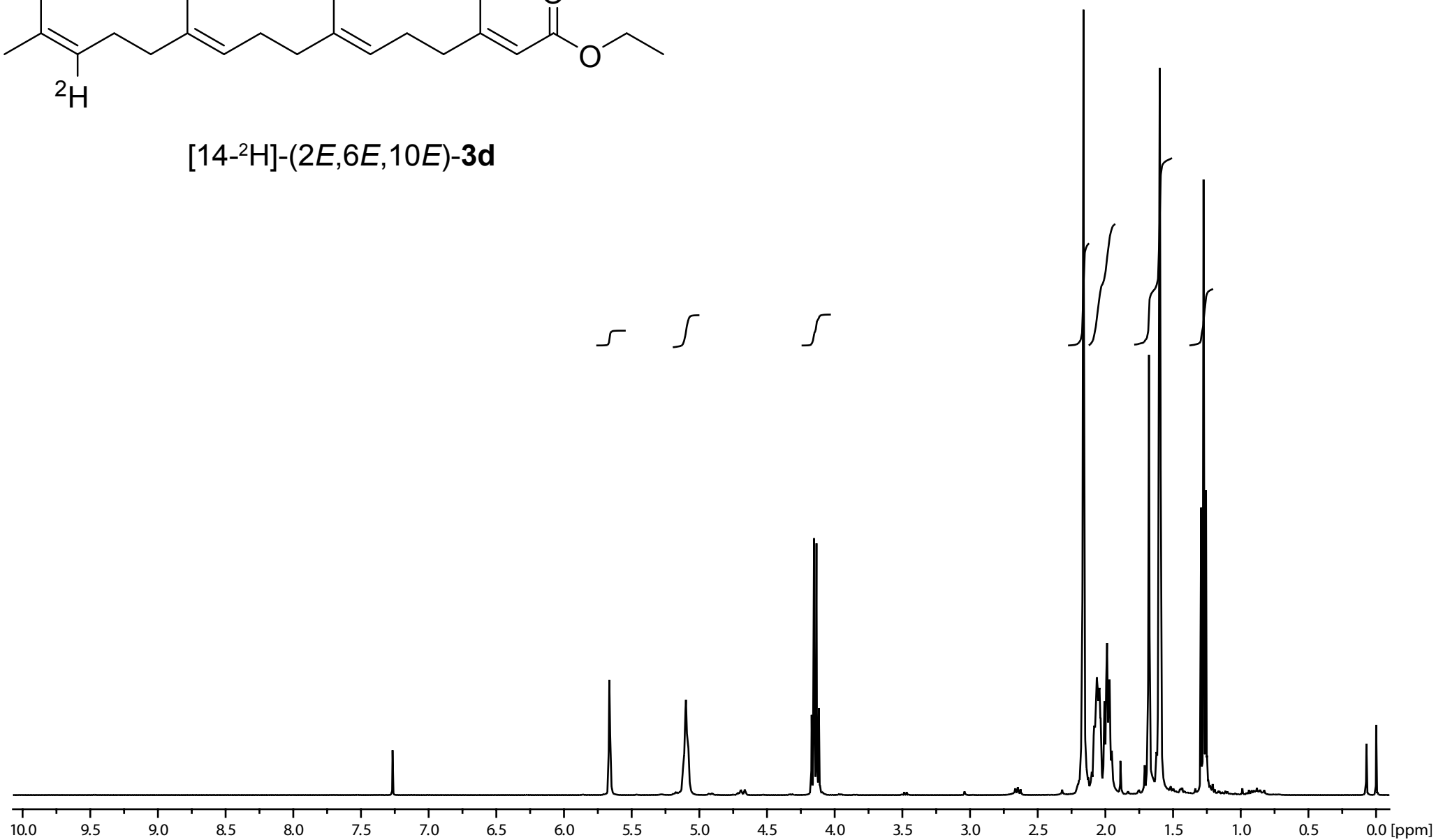
²H

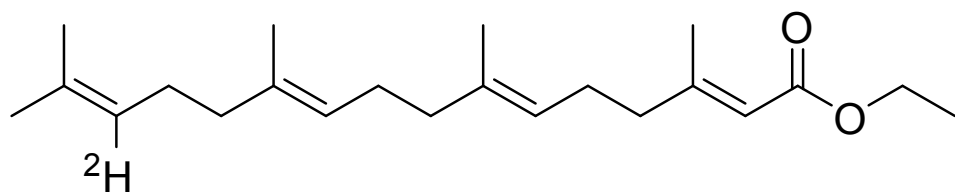
[13-²H]-1d



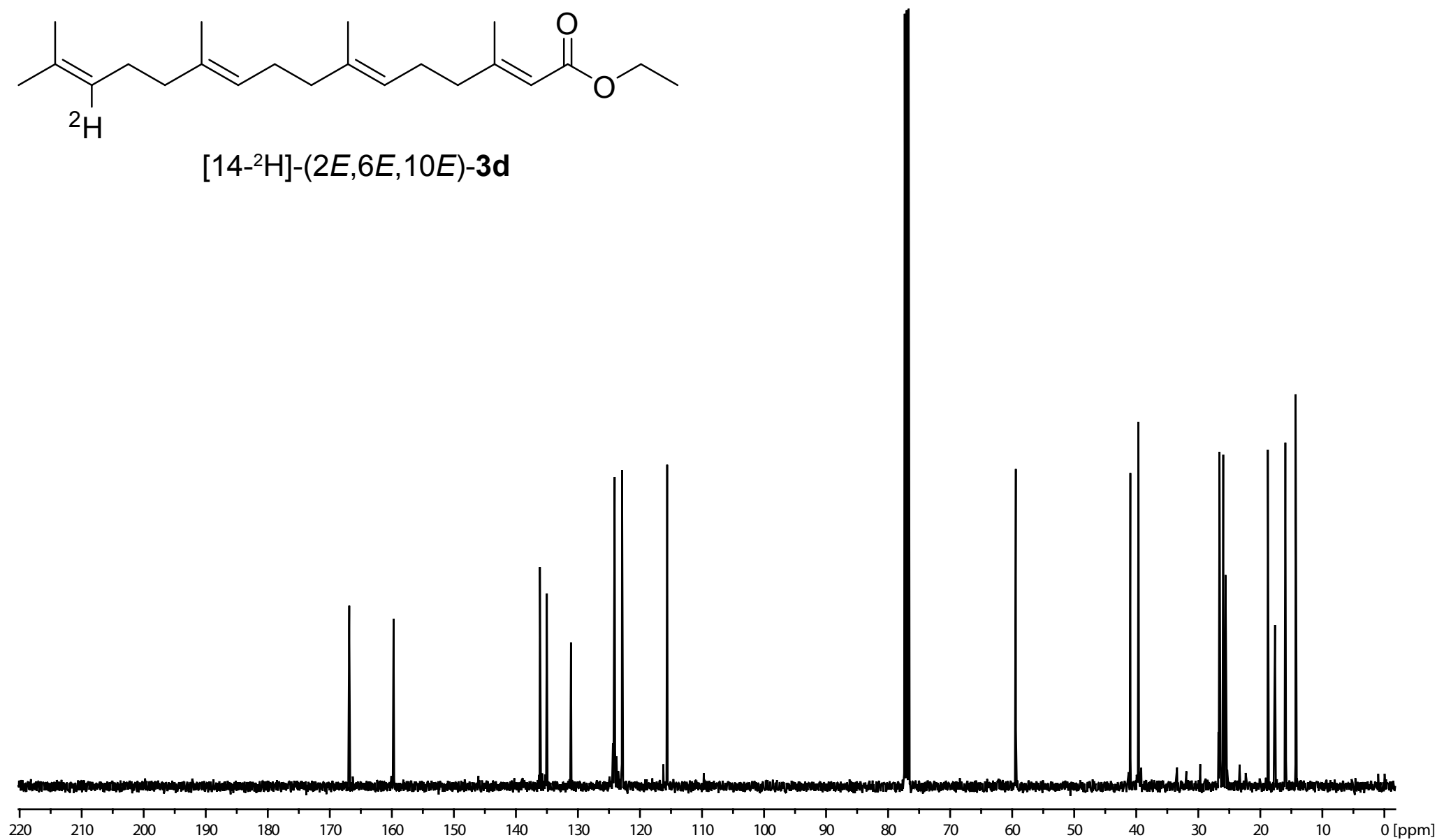


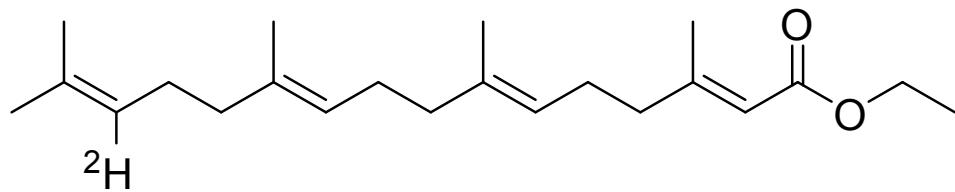
[14-²H]-(2*E*,6*E*,10*E*)-3d



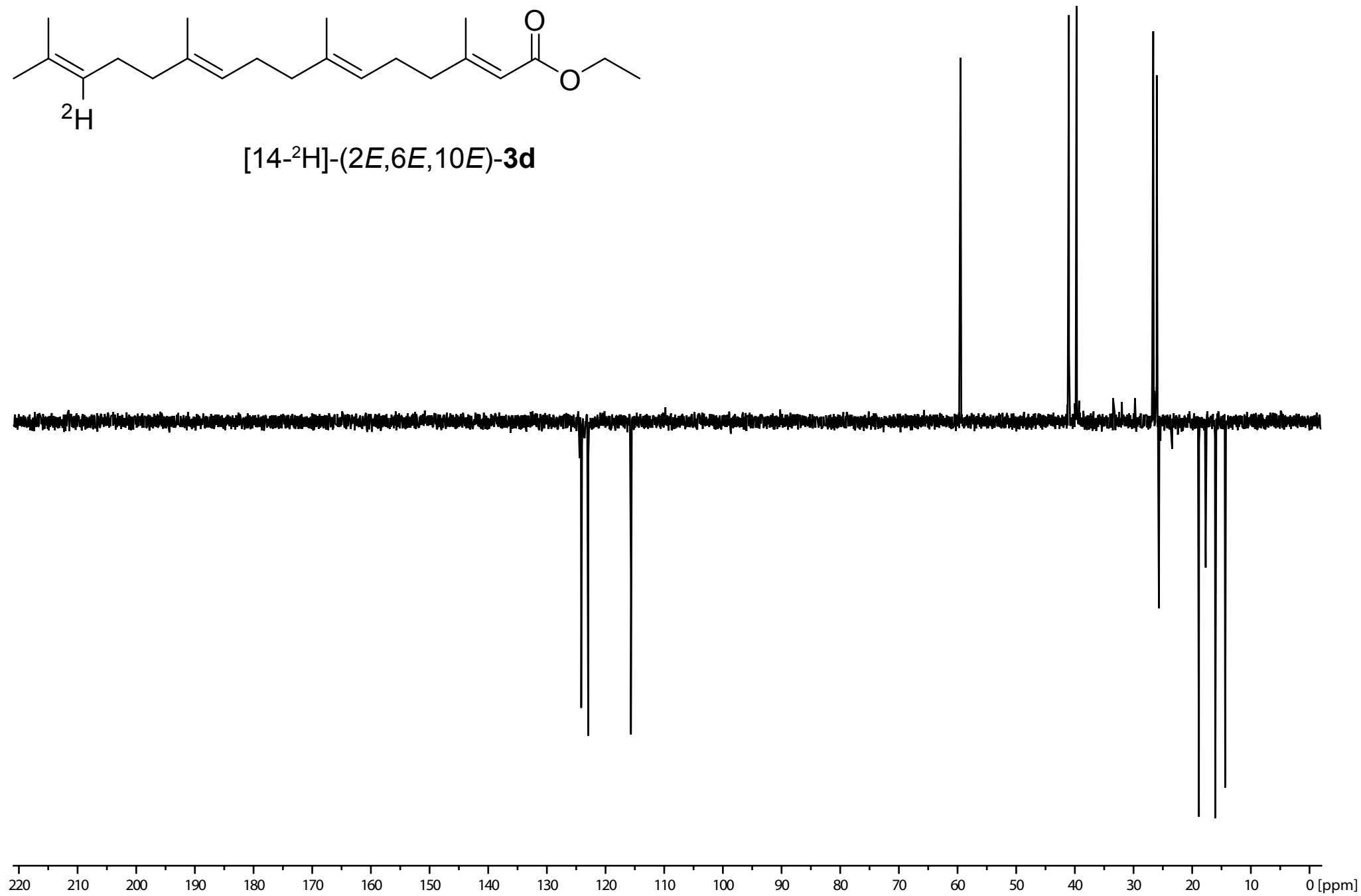


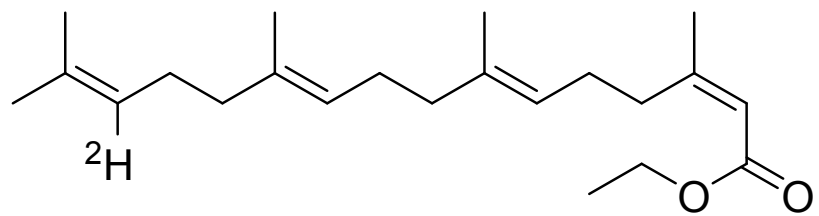
[14-²H]-(2*E*,6*E*,10*E*)-3d



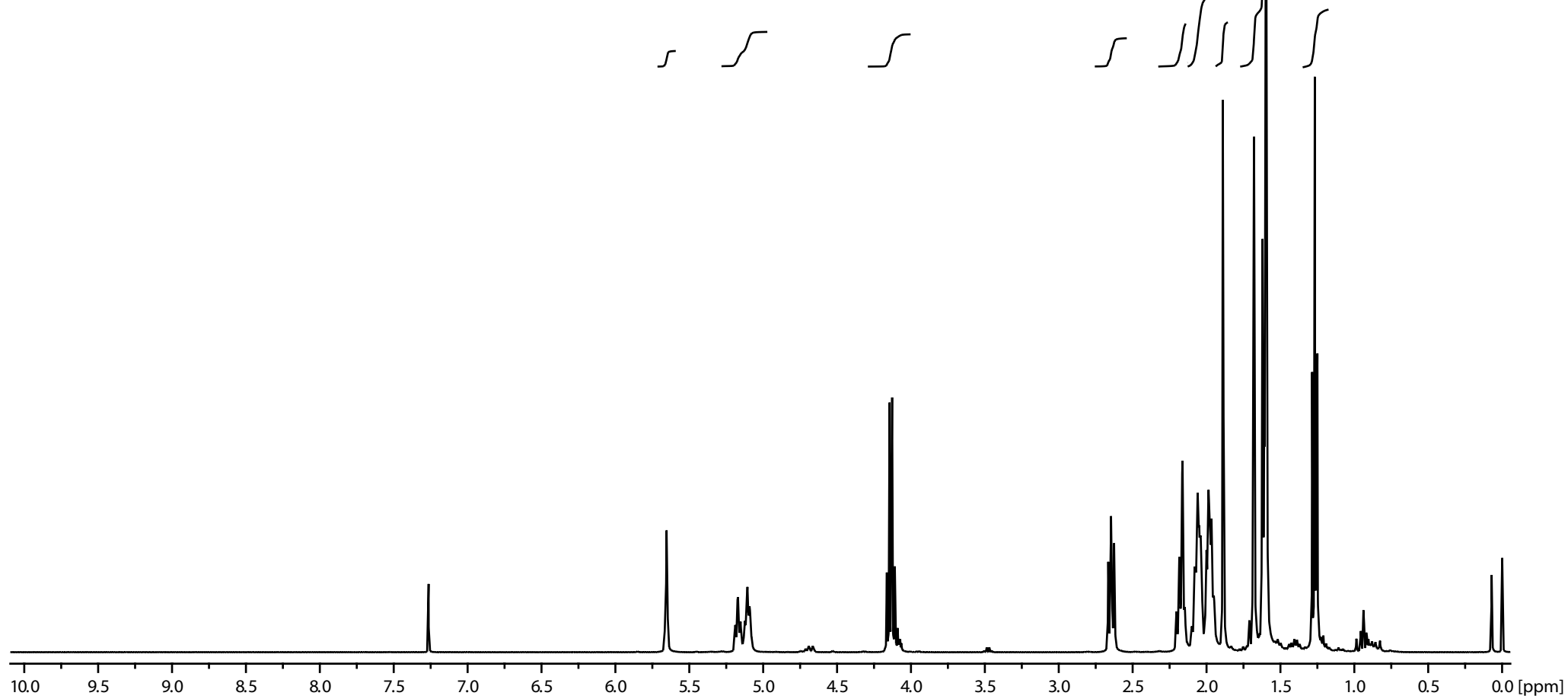


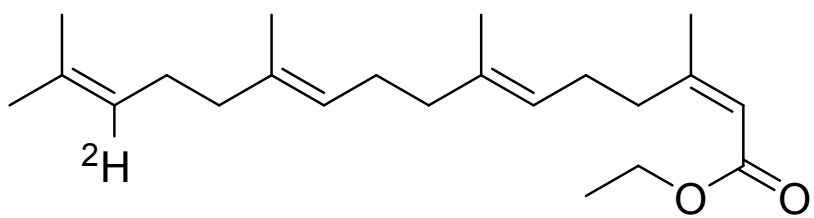
[14-²H]-(2*E*,6*E*,10*E*)-3d



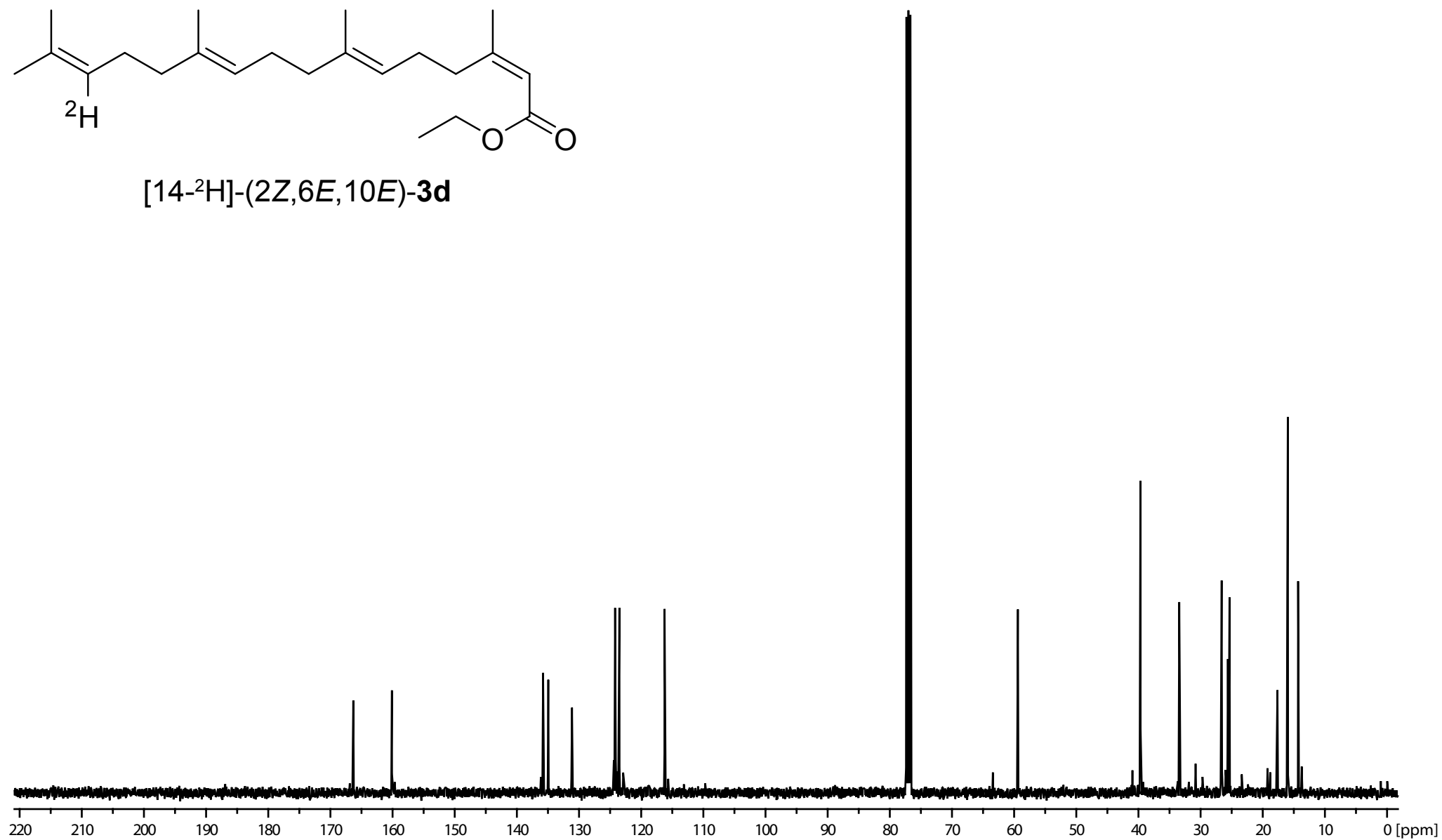


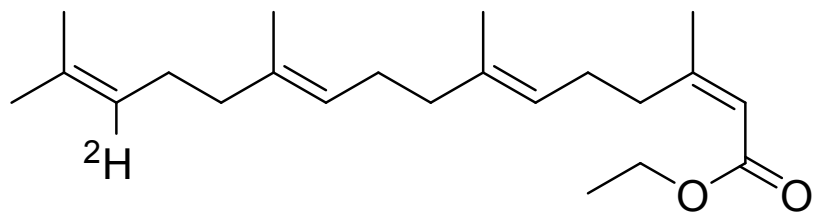
[14-²H]-(2Z,6E,10E)-3d



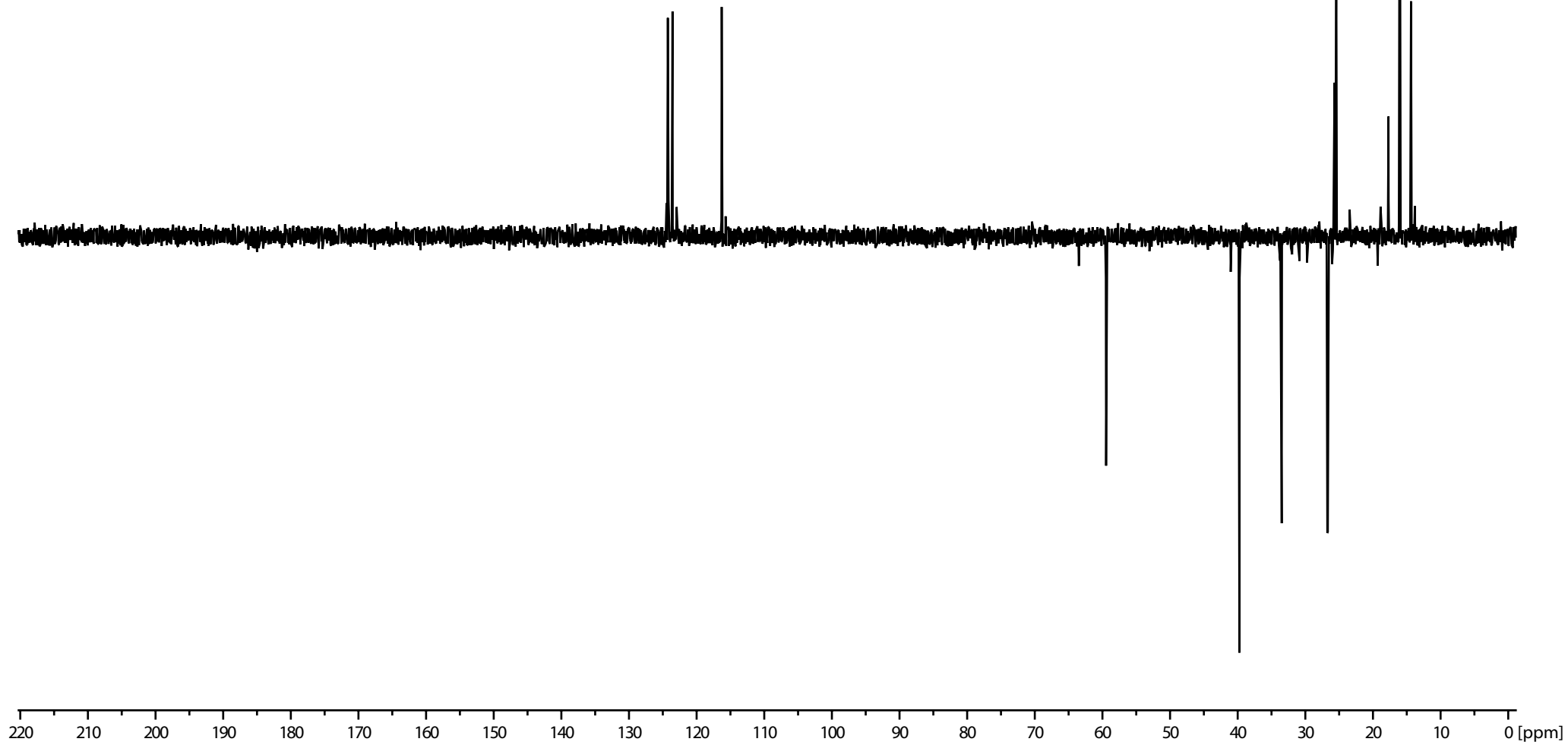


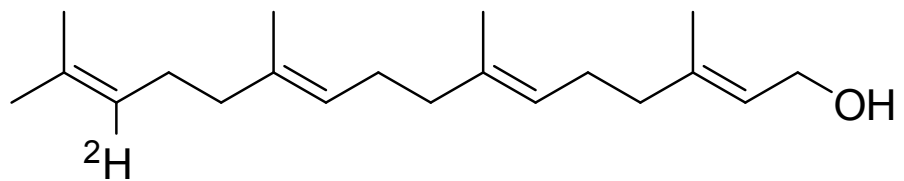
[14- ^2H]-*(2Z,6E,10E)*-3d



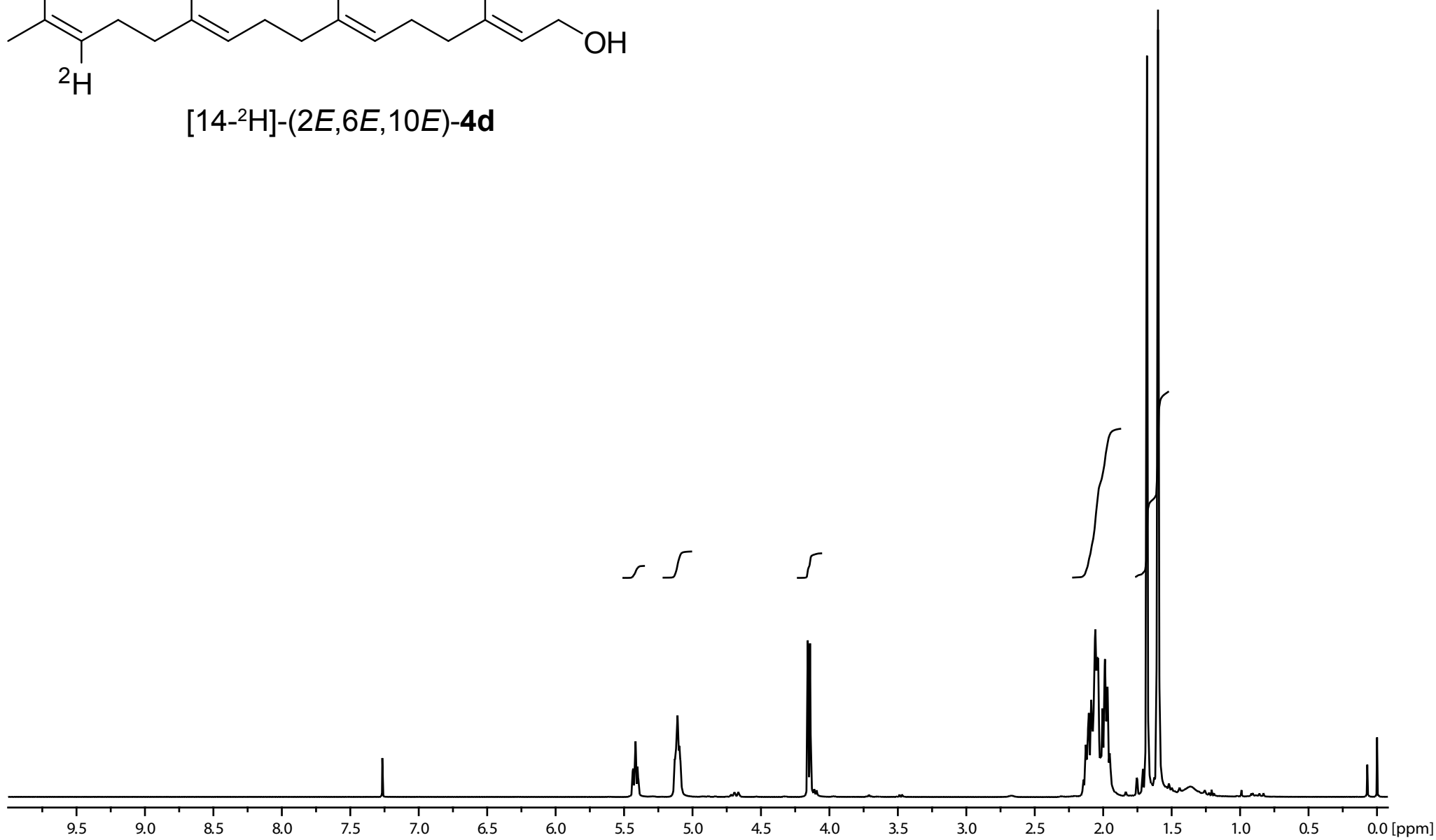


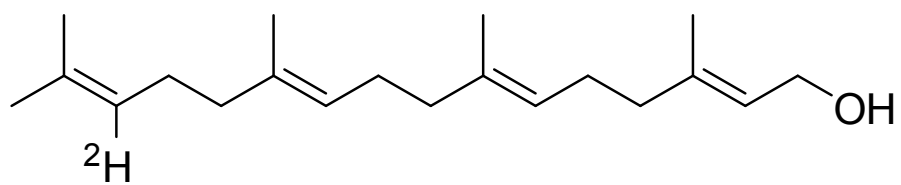
[14-²H]-(2Z,6E,10E)-3d



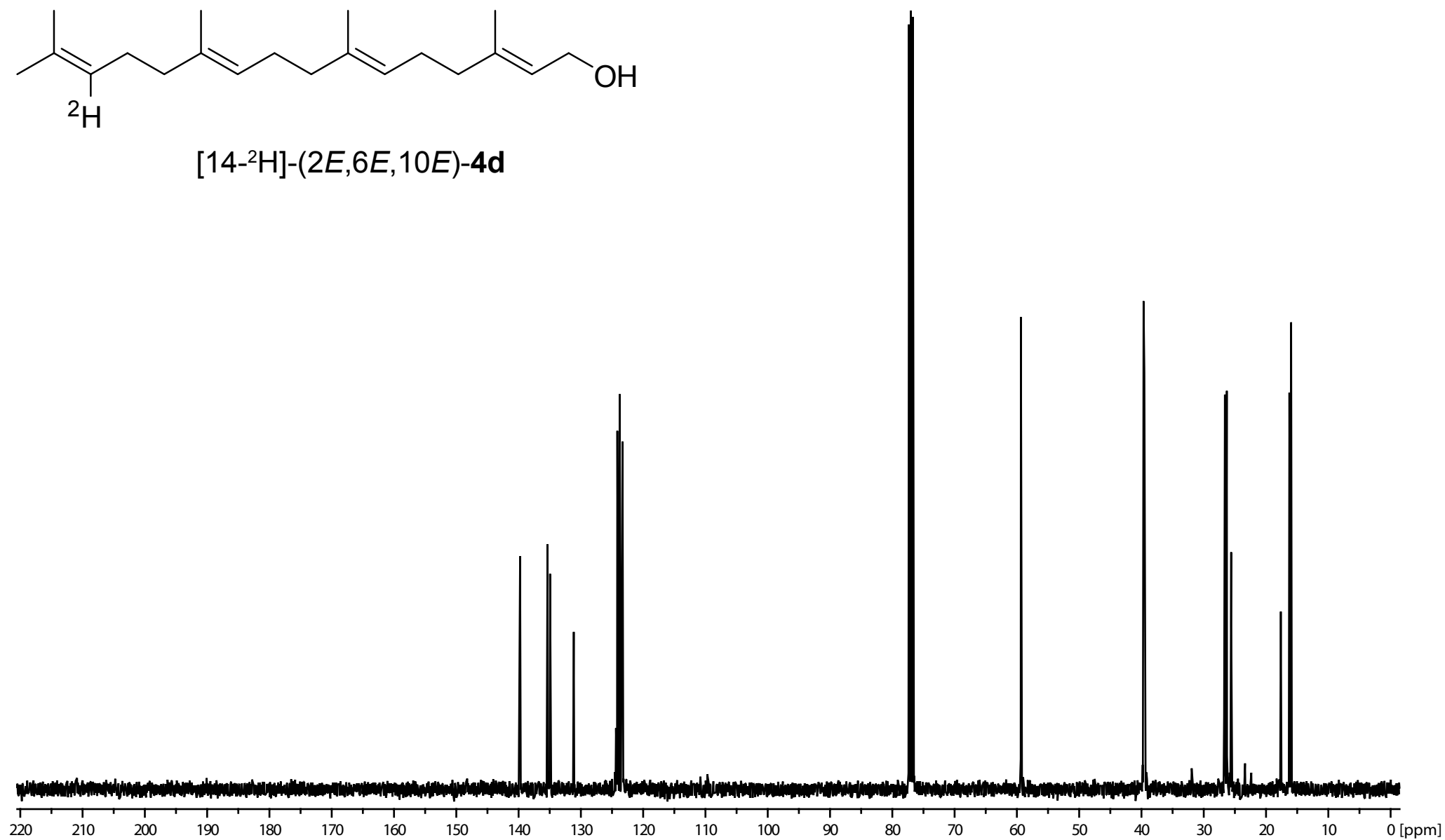


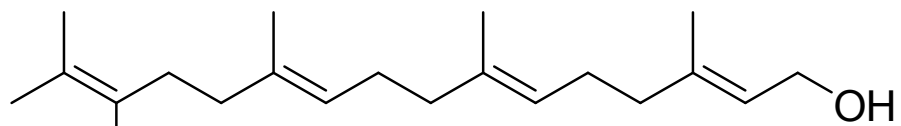
[14-²H]-(2*E*,6*E*,10*E*)-4d



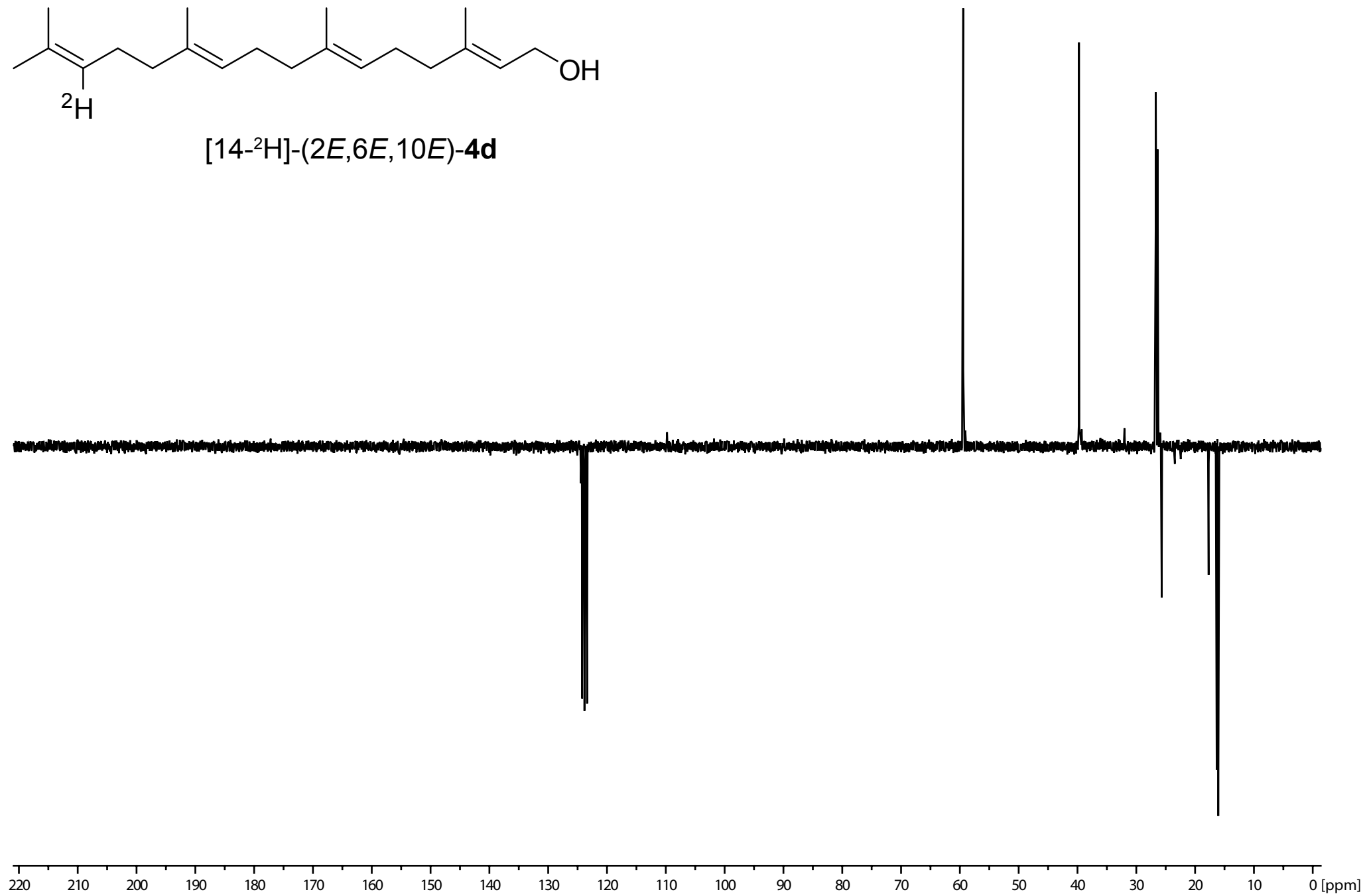


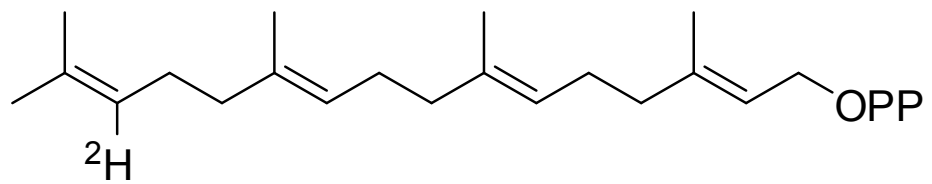
[14-²H]-(2*E*,6*E*,10*E*)-4d



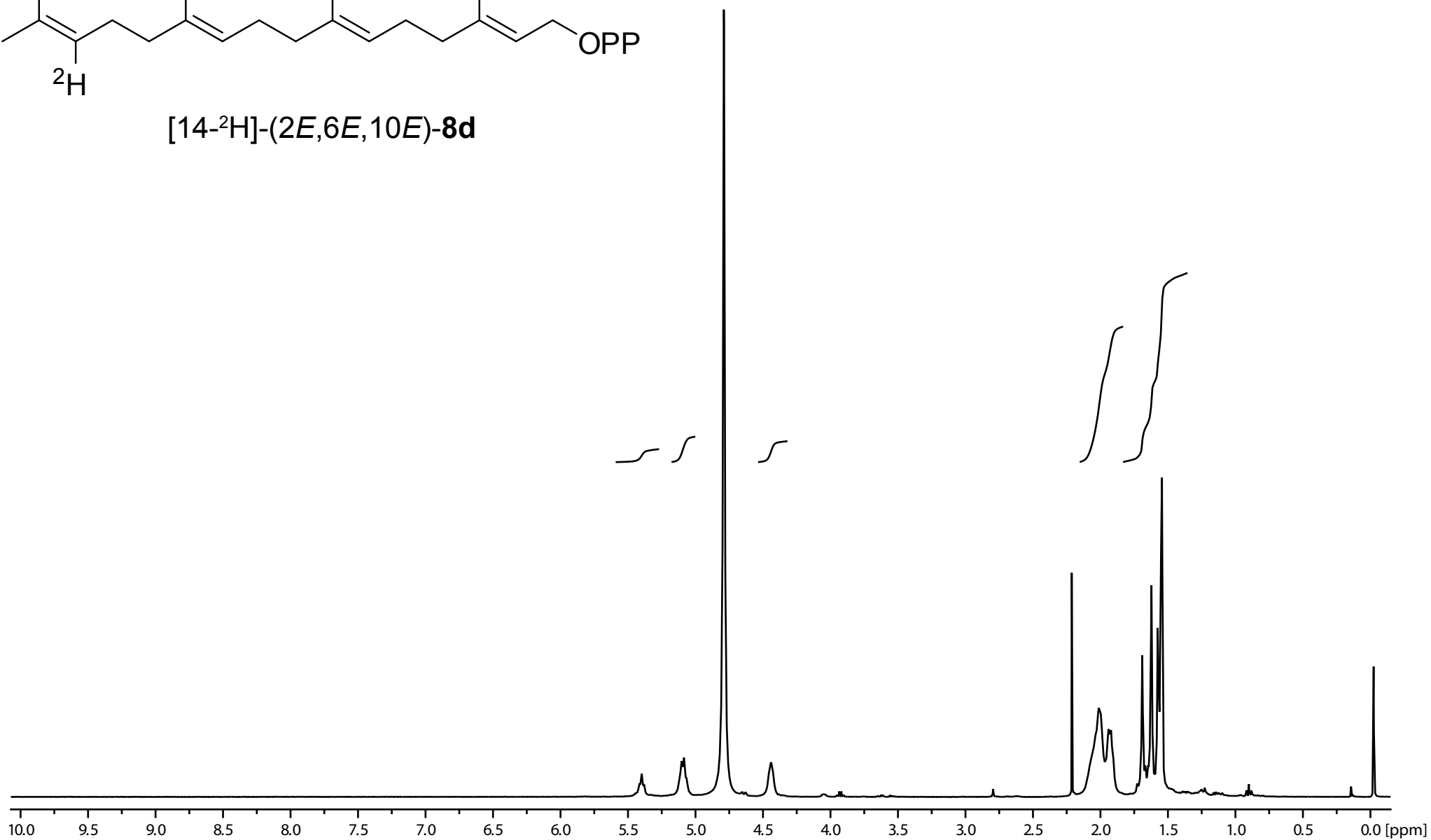


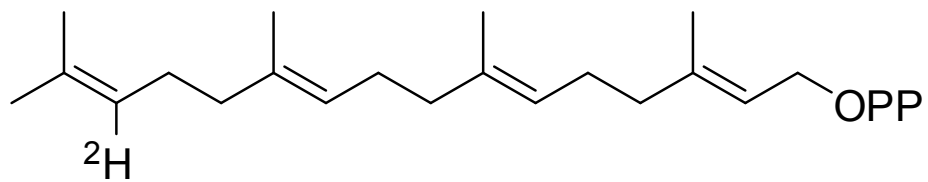
[14-²H]-(2*E*,6*E*,10*E*)-4d



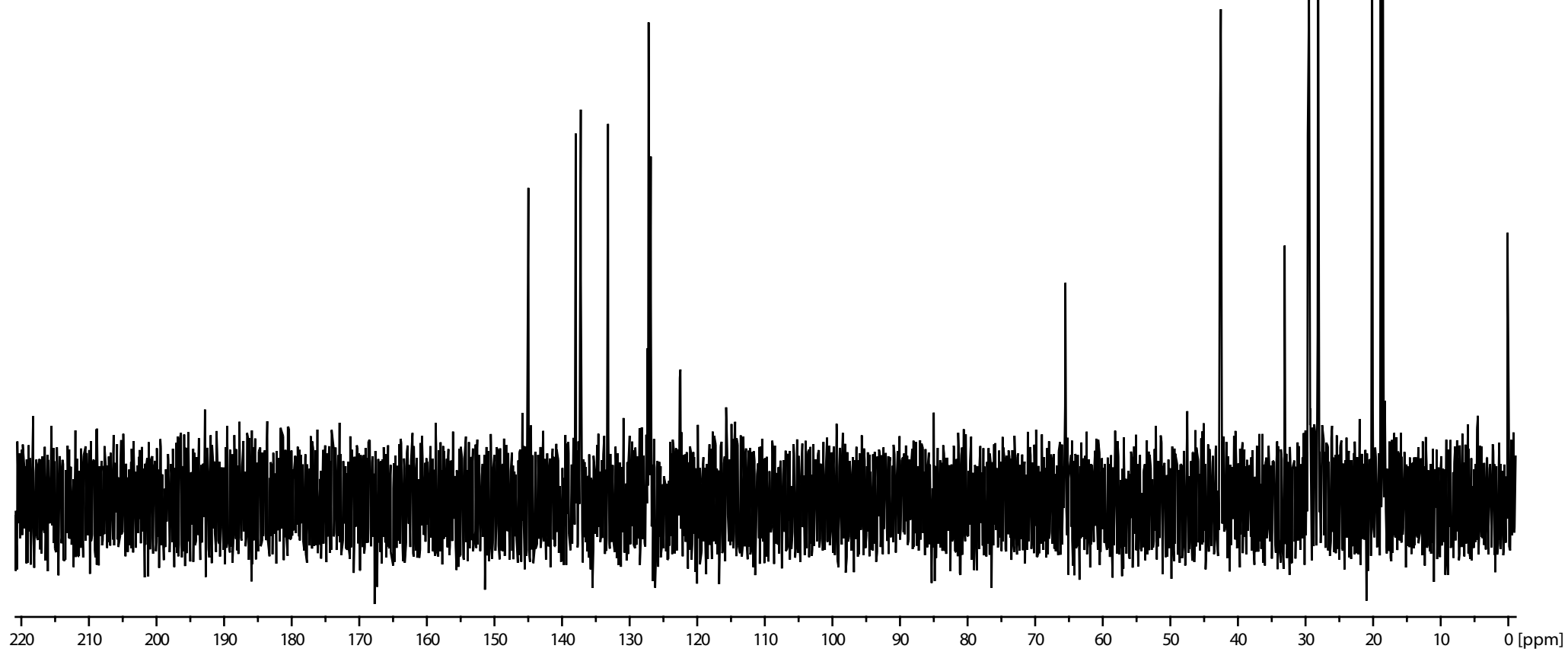


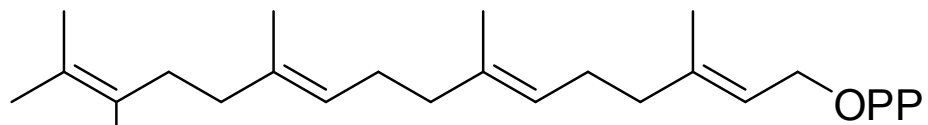
[14-²H]-(2*E*,6*E*,10*E*)-8d





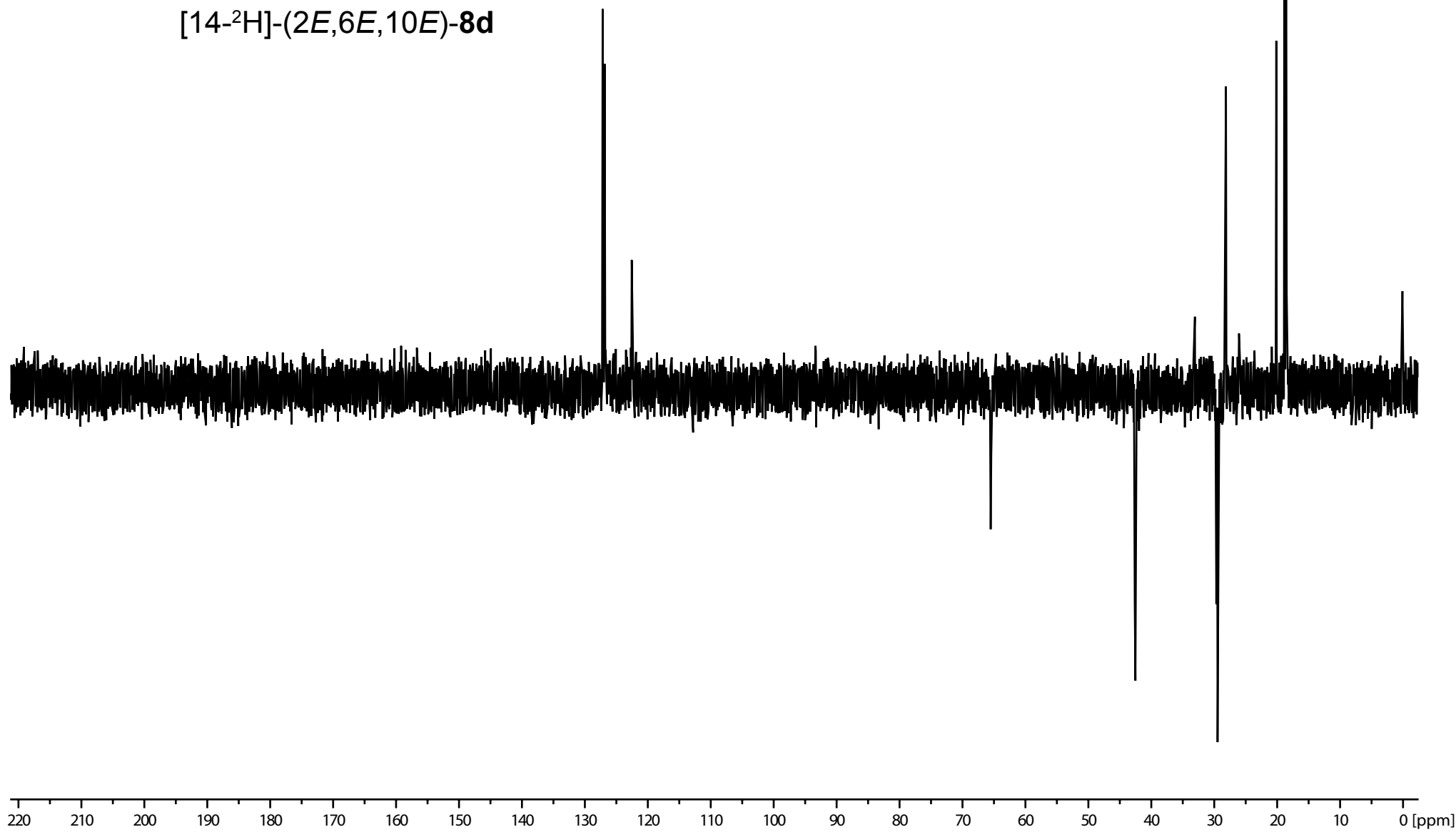
[14-²H]-(2*E*,6*E*,10*E*)-8d

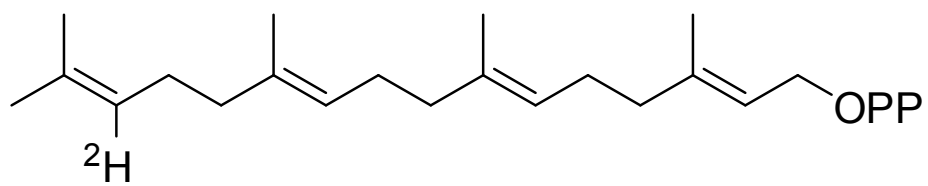




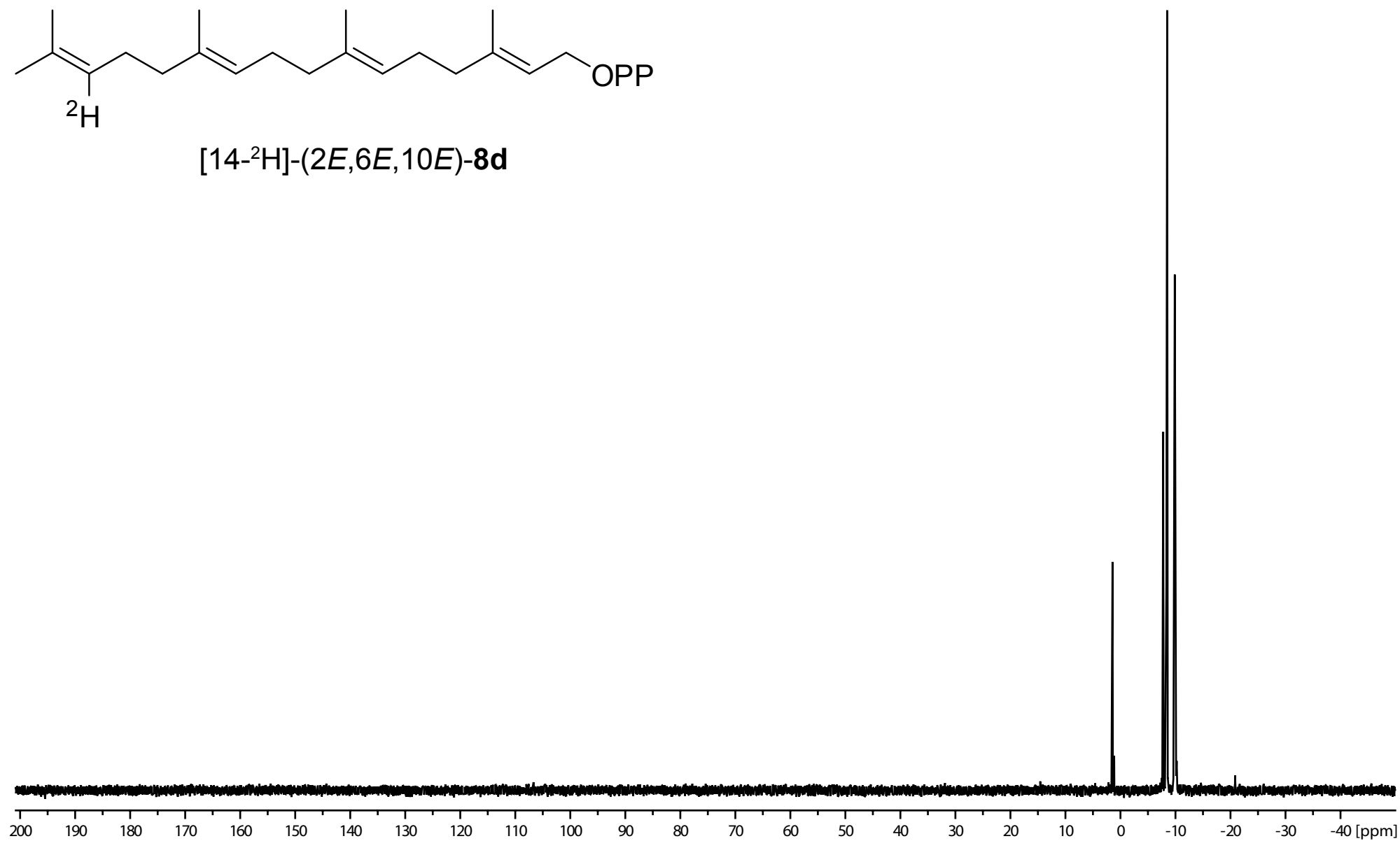
²H

[14-²H]-(2*E*,6*E*,10*E*)-8d





[14-²H]-(2*E*,6*E*,10*E*)-8d



Appendix G

Conformational Analysis, Thermal Rearrangement, and EI-MS
Fragmentation Mechanism of
(1(10)*E*,4*E*,6*S*,7*R*)-Germacradien-6-ol by ¹³C-Labeling
Experiments

Conformational Analysis, Thermal Rearrangement, and EI-MS Fragmentation Mechanism of (1(10)*E*,4*E*,6*S*,7*R*)-Germacradien-6-ol by ¹³C-Labeling Experiments

Patrick Rabe, Lena Barra, Jan Rinkel, Ramona Riclea, Christian A. Citron, Tim A. Klapschinski, Aron Janusko, and Jeroen S. Dickschat*

Abstract: An uncharacterized terpene cyclase from *Streptomyces pratensis* was identified as (+)-(1(10)*E*,4*E*,6*S*,7*R*)-germacradien-6-ol synthase. The enzyme product exists as two interconvertible conformers, resulting in complex NMR spectra. For the complete assignment of NMR data, all fifteen (¹³C₁)FPP isotopomers (FPP=farnesyl diphosphate) and (¹³C₁₅)FPP were synthesized and enzymatically converted. The products were analyzed using various NMR techniques, including ¹³C, ¹³C COSY experiments. The (¹³C)FPP isotopomers were also used to investigate the thermal rearrangement and EI fragmentation of the enzyme product.

Terpenoids are structurally and functionally fascinating natural products. The first identified compounds from bacteria, the earthy and musty odorants geosmin and 2-methylisoborneol,^[1] were isolated from streptomycetes in the 1960s, while recent research has shown that terpenes are particularly widespread in this taxon.^[2] The biosynthesis of terpenes starts from a linear oligoprenyl diphosphate that is converted by a terpene cyclase in a reaction cascade via cationic intermediates into a (poly)cyclic hydrocarbon or alcohol, which usually has several contiguous stereocenters. Crystal structures of terpene cyclases^[3] revealed that specific residues in the active site bind a trinuclear (Mg²⁺)₃ cluster that binds in turn to the substrate's diphosphate for ionization to a highly reactive cation. Hydrophobic residues shape a contour to force the substrate into a conformation for directed product formation and exclude water from the cavity to prevent quenching of immature intermediates. The products of several bacterial terpene cyclases have been characterized.^[3g,4] Additionally, our structure-based mechanistic understanding of bacterial terpene cyclases has been substantially refined by quantum chemical calculations,^[4s,5] site-specific mutations,^[3g,h,4c,6] and isotope-labeling studies.^[4b,g,q,7] Herein, we present a conformational analysis, the thermal rearrangement, and EI-MS fragmentation (EI-MS = electron impact mass spectrometry) of a sesquiterpene alcohol from *Streptomyces pratensis* by use of ¹³C-labeling techniques.

The genome of *S. pratensis* ATCC 33331 encodes five terpene cyclases, four of which show close homology to the synthases for geosmin,^[4c] 2-methylisoborneol,^[4f,g] 7-*epi*-α-eudesmol,^[4n] and *epi*-cubenol,^[4l] in agreement with the production of these terpenes by the bacterium.^[2a] The gene of the fifth uncharacterized terpene cyclase (accession number ADW03055; exhibiting the aspartate-rich motif ⁸⁶DDEYCD and the NSE triad ²²⁷NLVSYHKE) was cloned into the expression vector pYE-Express by homologous recombination in yeast.^[4o] The purified protein converted farnesyl diphosphate (FPP) into (1(10)*E*,4*E*)-germacradien-6-ol (**1**), identified by GC-MS (Figure 1A), while geranyl and geranylgeranyl diphosphate were not accepted. Two of the Cope rearrangement products of **1** (**2a** and **2b**) were also observed as a result of the thermal impact of the GC analysis (the mass spectra of **1**, **2a**, and **2b** are shown in Figure S1 in the Supporting Information). The ¹H and ¹³C NMR spectra of **1** recorded in CDCl₃ at room temperature showed broad and poorly resolved signals (Figure S2). In contrast, the NMR spectra at -50 °C and at 0 °C showed two sets of sharp signals for the known conformers **1a** and **1b** (as shown in Figure 1B by the “up/down” nomenclature for the methyl group pointing upwards (U) or downwards (D)).^[8] The NMR data corresponded to reported, but incomplete, data for (-)-**1** from *Santolina rosmarinifolia*.^[8a] The optical rotary power of [α]_D²⁴ = +21.4 for the compound pointed

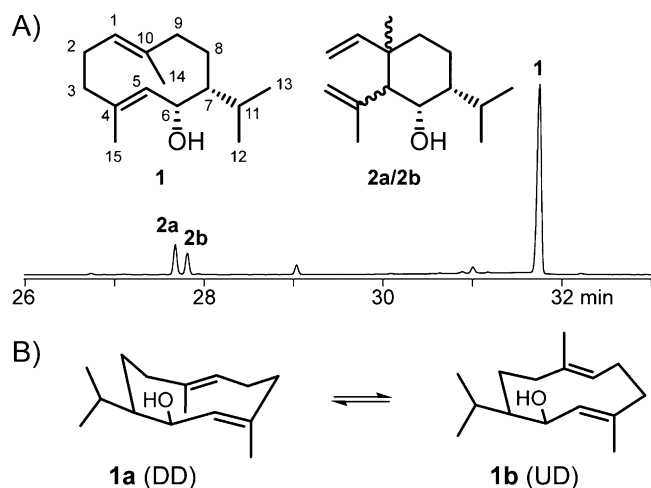


Figure 1. A) Total ion chromatogram of the sesquiterpene products from the *S. pratensis* (1(10)*E*,4*E*,6*S*,7*R*)-germacradien-6-ol (**1**) synthase. B) Structures of conformers **1a** and **1b**. U indicates that the methyl group is pointing up, D that the methyl group points downwards.

[*] P. Rabe, L. Barra, J. Rinkel, Dr. R. Riclea, Dr. C. A. Citron, T. A. Klapschinski, A. Janusko, Prof. Dr. J. S. Dickschat
Kekulé-Institut für Organische Chemie und Biochemie
Rheinische Friedrich-Wilhelms-Universität Bonn
Gerhard-Domagk-Strasse 1, 53121 Bonn (Germany)
E-mail: dickschat@uni-bonn.de

Supporting information for this article is available on the WWW under <http://dx.doi.org/10.1002/anie.201507615>.

to the opposite enantiomer as in the plant ($[\alpha]_D^{20} = -14.8$), establishing the terpene from *Streptomyces pratensis* as (+)-(1(10)*E*,4*E*,6*S*,7*R*)-germacradien-6-ol. The absolute configuration of the plant metabolite **1** was recently confirmed by total synthesis.^[9] Unlike the other terpene synthase products, **1** is not found in *S. pratensis* laboratory cultures (not shown).

The complex NMR spectra prevented a full assignment of the ¹H and ¹³C NMR signals to **1a** and **1b**, as in a previous report.^[8a] To overcome this problem, all fifteen (¹³C₁)FPP isotopomers were synthesized (Figures S3–6)^[10] and converted with germacradienol synthase. Each product was extracted with (²H₈)toluene and analyzed by ¹³C NMR spectroscopy, resulting in two strong signals for the labeled carbons of conformers **1a** and **1b** (Figure S7). These data unambiguously established which ¹³C NMR signals of **1** belonged to which carbon center, but it was not possible to assign which of the two ¹³C NMR signals observed in each single experiment belonged to which conformer. Therefore, completely labeled (¹³C₁₅)FPP was synthesized and incubated with germacradienol synthase and the product was analyzed by ¹³C, ¹³C COSY NMR experiments.^[11] This experiment revealed two distinct sets of cross-peaks (Figure 2; for an enlarged version see Figure S8) that allowed for an unambiguous assignment of all 30 carbon signals to each of the 15 carbon atoms of **1a** and **1b** (Table 1). The assignment of most ¹H NMR resonance signals was possible from ¹H, ¹H COSY, HSQC, and HMBC correlations (Figure 3) of the unlabeled compound. For a few cases, the HSQC spectra of the relevant (¹³C₁)-**1** isotopomers were very useful (Figure S9).

For structure elucidation of the two Cope rearrangement products observed during GC–MS analysis, **1** was subjected to a microwave reaction in toluene at 225 °C. The products were separable by column chromatography and proved to be

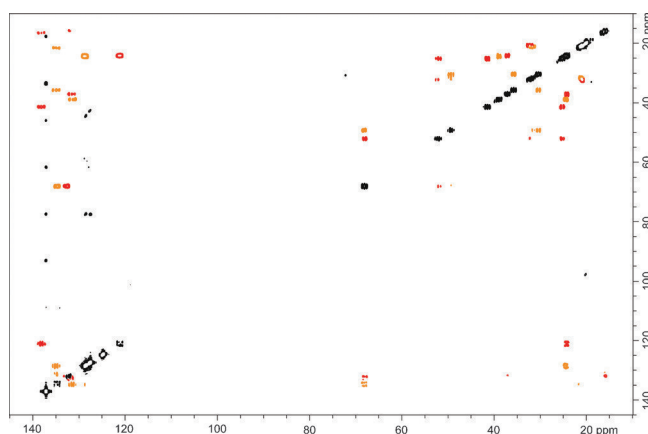


Figure 2. ¹³C, ¹³C COSY spectrum of (¹³C₁₅)-**1** obtained by enzymatic conversion of (¹³C₁₅)FPP. The two sets of cross-peaks for the conformers are shown in yellow (for **1a**) and red (for **1b**).

identical to **2a** and **2b** in terms of their mass spectra and GC retention times. Their structures were determined by one- and two-dimensional NMR spectroscopy (Table 1), resulting in their identification as shyobunol (**2a**) and 5,10-di-*epi*-shyobunol (**2b**).^[12] The relative configurations were determined from key NOESY correlations (Figure 4A). The assignment of NMR data was confirmed by Cope rearrangement of (¹³C₁₅)-**1**, obtained by enzymatic conversion of (¹³C₁₅)FPP, and subsequent analysis of the product by ¹³C, ¹³C COSY NMR experiments (Figure S10). From these experiments, two distinct sets of cross-peaks were detected for **2a** and **2b** that gave direct insights into the carbon–carbon connectivities. The absolute configurations of **2a** and **2b** can be deduced from the stereocenters at C-6 and C-7 of **1** that are not affected by the Cope rearrangement, as is known for various

Table 1: NMR data of the conformers **1a** and **1b** of (1(10)*E*,4*E*,6*S*,7*R*)-germacradien-6-ol in (²H₈)toluene recorded at –50 °C, and of **2a/2b** in (²H₆)benzene at 25 °C.^[a]

1+2 C ^[a]	1a (DD) ¹ H	¹³ C	1b (UD) ¹ H	¹³ C	2a ¹ H	¹³ C	2b ¹ H	¹³ C
1	CH 4.80 (d, <i>J</i> = 11.6, 1 H)	129.0	4.87 (t, <i>J</i> = 7.5, 1 H)	121.5	5.78 (dd, <i>J</i> = 17.5, 10.8, 1 H)	150.3	5.85 (dd, <i>J</i> = 17.6, 10.8, 1 H)	150.2
2	CH ₂ 2.17 (m, 1 H) 1.95 (m, 1 H)	24.8	2.24 (m, 1 H) 1.89 (m, 1 H)	24.6	4.98 (dd, <i>J</i> = 17.5, 1.2, 1 H, <i>E</i>) 4.94 (dd, <i>J</i> = 10.8, 1.2, 1 H, <i>Z</i>)	110.1	4.90 (dd, <i>J</i> = 17.6, 0.8, 1 H, <i>E</i>) 4.86 (dd, <i>J</i> = 10.8, 0.8, 1 H, <i>Z</i>)	110.4
3	CH ₂ 2.04 (m, 1 H) 2.00 (m, 1 H)	39.2	2.09 (m, 1 H) 1.94 (m, 1 H)	37.5	5.02 (br s, 1 H, <i>Z</i>) 4.91 (br s, 1 H, <i>E</i>)	113.3	4.90 (br s, 1 H) 4.70 (br s, 1 H)	113.9
4	C _q –	131.8	–	132.0	–	146.8	–	145.5
5	CH 5.06 (d, <i>J</i> = 7.0, 1 H)	135.1	5.04 (d, <i>J</i> = 8.5, 1 H)	133.0	1.69 (d, <i>J</i> = 1.7, 1 H)	56.6	2.32 (d, <i>J</i> = 6.8, 1 H)	57.4
6	CH 4.54 (d, <i>J</i> = 6.0, 1 H)	68.5	4.55 (d, <i>J</i> = 6.0, 1 H)	68.4	3.81 (br s, 1 H)	70.2	3.94 (m, 1 H)	71.9
7	CH 0.75 (d, <i>J</i> = 9.0, 1 H)	49.7	0.66 (d, <i>J</i> = 9.5, 1 H)	52.5	0.74 (m, 1 H)	49.8	1.54 (m, 1 H)	44.6
8	CH ₂ 1.95 (m, 2 H) 1.39 (d, <i>J</i> = 13.8, 1 H)	30.7	1.80 (m, 1 H) 1.30 (m, 1 H)	25.6	1.63 (m, 1 H) 1.49 (m, 1 H)	21.1	1.56 (m, 2 H)	22.3
9	CH ₂ 2.44 (d, <i>J</i> = 13.1, 1 H) 1.62 (t, <i>J</i> = 13.5, 1 H)	36.1	2.14 (m, 1 H) 1.79 (m, 1 H)	41.8	1.48 (m, 1 H) 1.29 (m, 1 H)	41.1	1.53 (m, 1 H) 1.25 (m, 1 H)	33.7
10	C _q –	135.3	–	138.5	–	40.2	–	30.3
11	CH 1.78 (m, 1 H)	32.0	1.73 (m, 1 H)	32.6	1.68 (m, 1 H)	29.4	1.88 (oct, <i>J</i> = 6.8, 1 H)	27.4
12	CH ₃ 1.00 (d, <i>J</i> = 6.0, 3 H)	21.4	1.09 (d, <i>J</i> = 6.3, 3 H)	21.2	0.92 (d, <i>J</i> = 6.8, 3 H)	20.8	0.94 (d, <i>J</i> = 6.8, 3 H)	21.9
13	CH ₃ 1.05 (d, <i>J</i> = 6.5, 3 H)	21.6	1.00 (d, <i>J</i> = 6.0, 3 H)	21.3	0.94 (d, <i>J</i> = 6.9, 3 H)	21.3	1.20 (d, <i>J</i> = 6.6, 3 H)	23.1
14	CH ₃ 1.55 (s, 3 H)	22.0	1.48 (s, 3 H)	16.9	1.46 (s, 3 H)	20.3	0.93 (s, 3 H)	23.1
15	CH ₃ 1.32 (s, 3 H)	16.3	1.30 (s, 3 H)	16.2	1.72 (s, 3 H)	27.8	1.68 (s, 3 H)	26.8

[a] Carbon numbering as shown in Figure 1. Chemical shifts δ in ppm, multiplicity *m* (*s* = singlet, *d* = doublet, *t* = triplet, *oct* = octet, *m* = multiplet, *br* = broad), coupling constants *J* are given in Hertz. Carbon assignments for **1** were deduced from incubation experiments with ¹³C-labeled FPP isotopomers (see the main text).

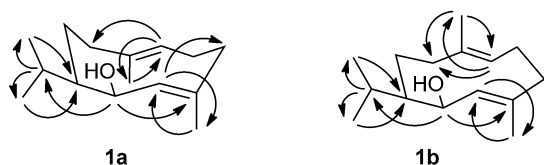


Figure 3. Key HMBC correlations that enabled the assignment of ^1H NMR signals of unlabeled **1**.

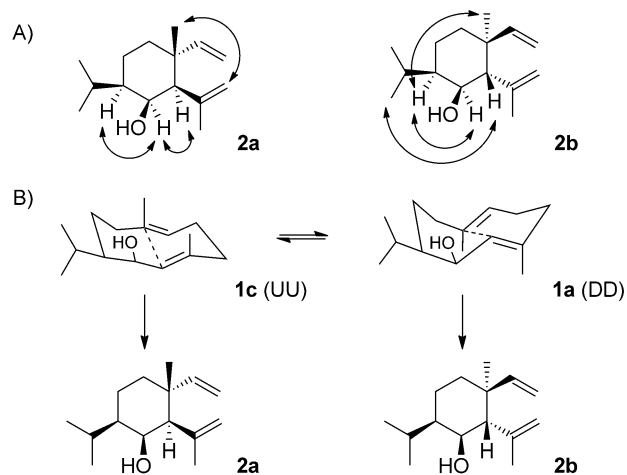


Figure 4. Cope rearrangement of **1**. A) Key NOESY correlations for determination of the relative configurations of **2a** and **2b**. B) Conformations of **1** explaining the formation of **2a** and **2b**.

germacranes.^[13] The bacterial shyobunol stereoisomers isolated here are the enantiomers of plant compounds from *Acorus calamus*,^[12] in agreement with the fact that also bacterial **1** is the optical antipode of a plant terpene. Whereas **2b** arises from the reported conformer **1a**,^[8a] the formation of **2a** is possible from the up/up conformer **1c** (Figure 4B, UU). Both rearrangement products are formed via chair-like transition states, similar to the Cope rearrangements of several other germacranes.^[8b,14]

The relative configurations of **2a** and **2b** gave additional support for the *syn* orientation of the hydroxy and isopropyl groups in **1**. In fact, the ^{13}C NMR chemical shifts of **1** and its *anti* stereoisomer kunzeaol are very similar (Table S11), and the *syn* or *anti* orientation of the substituents in the conformationally flexible compounds **1** and kunzeaol^[15] are difficult to determine. However, the NOESY spectra of the more rigid compounds **2a** and **2b** unambiguously proved the *syn* arrangement of the hydroxy and the isopropyl groups, thereby giving indirect evidence for the correct assignment of the relative configuration of **1**.

Since isotopically labeled compounds are very useful in studying MS fragmentation mechanisms,^[16] the products obtained from all fifteen isotopomers of (^{13}C)FPP with germacradienol synthase were also subjected to GC/EI-MS and GC/EI-MS-QTOF analysis. The observed fragment ion patterns for the isotopomers of (^{13}C)-**1** (Figure S11) gave direct insight into the fragmentation mechanism. Electron impact ionization of **1** proceeds preferably with the loss of one electron from an oxygen lone pair to yield the molecular ion

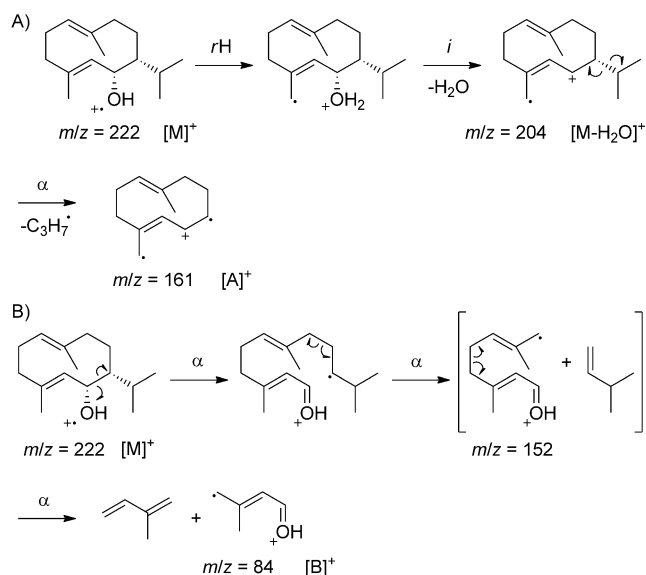


Figure 5. EI-MS fragmentation of **1**. Mechanisms for the formation of fragment ion $[\text{A}]^+$ ($m/z=161$) and the base peak ion $[\text{B}]^+$ ($m/z=84$).

$[\text{M}]^+$ (Figure 5A) that is observed at $m/z=222$ for unlabeled **1** and at $m/z=223$ for all ($^{13}\text{C}_1$)-**1** isotopomers (Table S12). Rearrangement of one hydrogen atom (*rH*) and inductive cleavage (*i*) with the neutral loss of water yields the fragment ion $[\text{M}-\text{H}_2\text{O}]^+$ that is detected at $m/z=204$ for natural **1** and at $m/z=205$ for all ($^{13}\text{C}_1$)-**1** isotopomers. A subsequent α cleavage (α) with loss of the isopropyl group is the only relevant mechanism that yields fragment ion $[\text{A}]^+$. This is evident from the observation of $[\text{A}]^+$ at $m/z=161$ in the mass spectrum for unlabeled **1** as well as for all isotopomers that contain ^{13}C labeling within the isopropyl group, that is, for the products obtained from ($11\text{-}^{13}\text{C}$)FPP, ($12\text{-}^{13}\text{C}$)FPP, and ($13\text{-}^{13}\text{C}$)FPP. All other ($^{13}\text{C}_1$)FPP isotopomers had a shifted signal for $[\text{A}]^+$ at $m/z=162$ (Figure S11). This mechanism was further supported by HRMS data for $[\text{A}]^+$, which established its molecular formula as $\text{C}_{12}\text{H}_{17}^+$ for all signals at $m/z=161$ or as $^{13}\text{C}_1^{12}\text{C}_{11}\text{H}_{17}^+$ for all at $m/z=162$ (Table S12), and by MS² analysis showing the direct formation of $[\text{A}]^+$ from $[\text{M}-\text{H}_2\text{O}]^+$.

For the formation of the base peak $[\text{B}]^+$ at $m/z=84$, the mechanism was shown to proceed by two α -cleavage reactions with the loss of the neutral molecule 3-methylbut-1-ene to form a fragment ion at $m/z=152$ and a third subsequent α cleavage with the neutral loss of isoprene (Figure 5B). The last step was confirmed by a shift of the signal for $[\text{B}]^+$ to $m/z=85$ for all ($^{13}\text{C}_1$)-**1** isotopomers in which the isotopic labeling appears in the $[\text{B}]^+$ forming portion, that is for **1** derived from ($1\text{-}^{13}\text{C}$)FPP, ($2\text{-}^{13}\text{C}$)FPP, ($3\text{-}^{13}\text{C}$)FPP, ($4\text{-}^{13}\text{C}$)FPP, and ($15\text{-}^{13}\text{C}$)FPP (Figure S11, Table S12). Furthermore, HRMS data established the molecular formulae for molecular fragments with $m/z=84$ ($\text{C}_5\text{H}_8\text{O}^+$) and $m/z=85$ ($^{13}\text{C}_1^{12}\text{C}_4\text{H}_8\text{O}^+$). The formation of $[\text{B}]^+$ as a daughter ion from the fragment ion at $m/z=152$ was investigated by MS² analysis, but because of the low abundance of this ion this experiment was inconclusive. The formation of $[\text{B}]^+$ is thus better described as a concerted process of three simultaneous α fragmentations.

In summary we have characterized a bacterial terpene cyclase from *S. pratensis* as (+)-(1(10)*E*,4*E*,6*S*,7*R*)-germacradien-6-ol synthase. Only one closely related homologue with 99.4% identical sites is found in *Streptomyces* sp. PAMC26508. As is typical for germacrane, **1** exists in different well-defined conformers that are observable by NMR at low temperatures. Extensive labeling experiments using synthetic ¹³C-labeled FPP isotopomers enabled a full assignment of ¹H and ¹³C NMR data of **1**, which had until this point not been possible for **1** and related germacrane as a result of their complex NMR spectra.^[8] A thermal rearrangement of **1** via chair-like transition states yielded two products whose absolute configurations were deduced from the absolute configuration of **1**, while the relative configurations of the rearrangement products reconfirmed that **1** is different from its epimer kunzeaol. Using ¹³C-labeled FPP isotopomers, we have also laid the groundwork for analyses of EI-MS fragmentation patterns of sesquiterpenes, and we present a first showcase study here. Future experiments in our laboratories will include the usage of the FPP isotopomers to address various other intricate problems of sesquiterpene chemistry.

Acknowledgements

This work was funded by the Deutsche Forschungsgemeinschaft (DI1536/7-1) and the Beilstein-Institut zur Förderung der Chemischen Wissenschaften with a Ph.D. scholarship to P.R. We thank Dr. Senada Nozinovic (Bonn) for NMR measurements.

Keywords: conformation analysis · isotopic labeling · mass spectrometry · NMR spectroscopy · terpenoids

How to cite: *Angew. Chem. Int. Ed.* **2015**, *54*, 13448–13451
Angew. Chem. **2015**, *127*, 13649–13653

- [1] a) N. N. Gerber, *Tetrahedron Lett.* **1968**, *9*, 2971; b) N. N. Gerber, *J. Antibiot.* **1969**, *22*, 508.
- [2] a) C. A. Citron, J. Gleitzmann, G. Laurenzano, R. Pukall, J. S. Dickschat, *ChemBioChem* **2012**, *13*, 202; b) P. Rabe, C. A. Citron, J. S. Dickschat, *ChemBioChem* **2013**, *14*, 2345; c) C. A. Citron, L. Barra, J. Wink, J. S. Dickschat, *Org. Biomol. Chem.* **2015**, *13*, 2673.
- [3] a) C. M. Starks, K. Back, J. Chappell, J. P. Noel, *Science* **1997**, *277*, 1815; b) C. A. Lesburg, G. Zhai, D. E. Cane, D. W. Christianson, *Science* **1997**, *277*, 1820; c) M. J. Rynkiewicz, D. E. Cane, D. W. Christianson, *Proc. Natl. Acad. Sci. USA* **2001**, *98*, 13543; d) E. Y. Shishova, L. Di Constanzo, D. E. Cane, D. W. Christianson, *Biochemistry* **2007**, *46*, 1941; e) J. A. Aaron, X. Lin, D. E. Cane, D. W. Christianson, *Biochemistry* **2010**, *49*, 1787; f) M. Köksal, Y. Jin, R. M. Coates, R. Croteau, D. W. Christianson, *Nature* **2011**, *469*, 116; g) P. Baer, P. Rabe, C. A. Citron, C. C. de Oliveira Mann, N. Kaufmann, M. Groll, J. S. Dickschat, *ChemBioChem* **2014**, *15*, 213; h) P. Baer, P. Rabe, K. Fischer, C. A. Citron, T. A. Klapschinski, M. Groll, J. S. Dickschat, *Angew. Chem. Int. Ed.* **2014**, *53*, 7652; *Angew. Chem.* **2014**, *126*, 7783.
- [4] a) D. E. Cane, J. K. Sohng, C. R. Lamberson, S. M. Rudnicki, Z. Wu, M. D. Lloyd, J. S. Oliver, B. R. Hubbard, *Biochemistry* **1994**, *33*, 5846; b) X. Lin, R. Hopson, D. E. Cane, *J. Am. Chem. Soc.* **2006**, *128*, 6022; c) J. Jiang, X. He, D. E. Cane, *Nat. Chem. Biol.* **2007**, *3*, 711; d) C.-M. Wang, D. E. Cane, *J. Am. Chem. Soc.* **2008**, *130*, 8908; e) S. A. Agger, F. Lopez-Gallego, T. R. Hoye, C. Schmidt-Dannert, *J. Bacteriol.* **2008**, *190*, 6084; f) M. Komatsu, M. Tsuda, S. Omura, H. Oikawa, H. Ikeda, *Proc. Natl. Acad. Sci. USA* **2008**, *105*, 7422; g) W. K. W. Chou, I. Fanizza, T. Uchiyama, M. Komatsu, H. Ikeda, D. E. Cane, *J. Am. Chem. Soc.* **2010**, *132*, 8850; h) Y. Hu, W. K. W. Chou, R. Hopson, D. E. Cane, *Chem. Biol.* **2011**, *18*, 32; i) C. Nakano, M. H.-K. Kim, Y. Ohnishi, *ChemBioChem* **2011**, *12*, 1988; j) C. Nakano, M. H.-K. Kim, Y. Ohnishi, *ChemBioChem* **2011**, *12*, 2403; k) C. Nakano, S. Horinouchi, Y. Ohnishi, *J. Biol. Chem.* **2011**, *286*, 27980; l) C. Nakano, T. Tezuka, S. Horinouchi, Y. Ohnishi, *J. Antibiot.* **2012**, *65*, 551; m) C. Nakano, F. Kudo, T. Eguchi, Y. Ohnishi, *ChemBioChem* **2011**, *12*, 2271; n) P. Rabe, J. S. Dickschat, *Angew. Chem. Int. Ed.* **2013**, *52*, 1810; *Angew. Chem.* **2013**, *125*, 1855; o) J. S. Dickschat, K. A. K. Pahirulzaman, P. Rabe, T. Klapschinski, *ChemBioChem* **2014**, *15*, 810; p) A. Schifrin, T. T. B. Ly, N. Günnewich, J. Zapp, V. Thiel, S. Schulz, F. Hannemann, Y. Khatri, R. Bernhardt, *ChemBioChem* **2015**, *16*, 337; q) P. Rabe, K. A. K. Pahirulzaman, J. S. Dickschat, *Angew. Chem. Int. Ed.* **2015**, *54*, 6041; *Angew. Chem.* **2015**, *127*, 6139; r) Y. Yamada, T. Kuzuyama, M. Komatsu, K. Shin-ya, S. Omura, D. E. Cane, H. Ikeda, *Proc. Natl. Acad. Sci. USA* **2015**, *112*, 857; s) J.-Y. Chow, B.-X. Tian, G. Ramamoorthy, B. S. Hillerich, R. D. Seidel, S. C. Almo, M. P. Jacobson, C. D. Poulter, *Proc. Natl. Acad. Sci. USA* **2015**, *112*, 5661.
- [5] a) P. Gutta, D. J. Tantillo, *J. Am. Chem. Soc.* **2006**, *128*, 6172; b) Y. J. Hong, D. J. Tantillo, *J. Am. Chem. Soc.* **2009**, *131*, 7999; c) Y. J. Hong, D. J. Tantillo, *Org. Lett.* **2011**, *13*, 1294.
- [6] M. Seemann, G. Zhai, J.-W. de Kraker, C. M. Paschall, D. W. Christianson, D. E. Cane, *J. Am. Chem. Soc.* **2002**, *124*, 7681.
- [7] a) D. E. Cane, C. Abell, P. H. M. Harrison, B. R. Hubbard, C. T. Kane, R. Lattman, J. S. Oliver, S. W. Weiner, *Philos. Trans. R. Soc. London Ser. B* **1991**, *332*, 123; b) L. Zu, M. Xu, M. W. Lodewyk, D. E. Cane, R. J. Peters, D. J. Tantillo, *J. Am. Chem. Soc.* **2012**, *134*, 11369.
- [8] a) A. F. Barrero, M. M. Herrador, J. F. Quilez, R. Alvarez-Manzaneda, D. Portal, J. A. Gavin, D. G. Gravalos, M. S. J. Simmonds, W. M. Blaney, *Phytochemistry* **1999**, *51*, 529; b) J. A. Faraldos, S. Wu, J. Chappell, R. M. Coates, *Tetrahedron* **2007**, *63*, 7733.
- [9] K. Foo, I. Usui, D. C. G. Götz, E. W. Werner, D. Holte, P. S. Barran, *Angew. Chem. Int. Ed.* **2012**, *51*, 11491; *Angew. Chem.* **2012**, *124*, 11659.
- [10] C. A. Citron, P. Rabe, L. Barra, C. Nakano, T. Hoshino, J. S. Dickschat, *Eur. J. Org. Chem.* **2014**, 7684.
- [11] L. Barra, K. Ibrom, J. S. Dickschat, *Angew. Chem. Int. Ed.* **2015**, *54*, 6637; *Angew. Chem.* **2015**, *127*, 6737.
- [12] R. Kaiser, D. Lamparski, *Helv. Chim. Acta* **1978**, *61*, 2671.
- [13] A. M. Adio, *Tetrahedron* **2009**, *65*, 5145.
- [14] a) A. J. Weinheimer, W. W. Youngblood, P. H. Washecheck, T. K. B. Karns, L. S. Chierszko, *Tetrahedron Lett.* **1970**, *11*, 497; b) J. A. Faraldos, Y. Zhao, P. E. O'Maille, J. P. Noel, R. M. Coates, *ChemBioChem* **2007**, *8*, 1826; c) S. Rosselli, A. Maggio, R. A. Raccuglia, M. Bruno, *Eur. J. Org. Chem.* **2003**, 2690.
- [15] a) C. P. Cornwell, N. Reddy, D. N. Leach, S. G. Wyllie, *Flavour Fragrance J.* **2001**, *16*, 263; b) B. Szafranek, K. Chrapkowska, D. Waligóra, R. Palavinskas, A. Banach, J. Szafranek, *J. Agric. Food Chem.* **2006**, *54*, 7729; c) B. Pickel, D. P. Drew, T. Manczak, C. Weitzel, H. T. Simonsen, D.-K. Ro, *Biochem. J.* **2012**, *448*, 261.
- [16] J. S. Dickschat, *Nat. Prod. Rep.* **2014**, *31*, 838.

Received: August 14, 2015

Published online: September 11, 2015

Supporting Information

**Conformational Analysis, Thermal Rearrangement, and EI-MS
Fragmentation Mechanism of (1(10)*E*,4*E*,6*S*,7*R*)-Germacradien-6-ol
by ¹³C-Labeling Experiments**

*Patrick Rabe, Lena Barra, Jan Rinkel, Ramona Riclea, Christian A. Citron, Tim A. Klapschinski,
Aron Janusko, and Jeroen S. Dickschat**

ange_201507615_sm_miscellaneous_information.pdf

Strains and culture conditions, cloning and homologous recombination

The bacterium *Streptomyces pratensis* ATCC 33331 was obtained from the Deutsche Sammlung von Mikroorganismen und Zellkulturen (DSMZ, Braunschweig, Germany). The strain was cultured on medium Gym 65 (Glucose 4.0 g, Yeast extract 4.0 g, Malt extract 4.0 g, 1L water, pH 7.2) for 5 d at 28°C. The terpene cyclase gene of *Streptomyces pratensis* ATCC 33331 (accession number ADW03055) was amplified from genomic DNA using the primers PR024f_ADW03055 (sequence is given below) and PR024r_ADW03055. The obtained PCR product was used as a template in a second PCR with elongated primers containing homology arms (PR023f_ADW03055 and PR023r_ADW03055, homology arms are underlined) for homologous recombination with the linearized (HindIII and EcoRI digestion) vector pYE-Express^[1] in *S. cerevisiae* FY834. Transformation of *S. cerevisiae* with the PCR product and the linearized vector pYE-Express for homologous recombination was carried out using the LiOAc/SS carrier DNA protocol.^[2] The transformed cells were plated on SM-URA agar plates and grown for three days at 28 °C. Plasmid DNA was isolated from the grown yeast using the kit Zymoprep Yeast Plasmid Miniprep II (Zymo Research, Irvine, USA), shuttled into *E. coli* BL 21 cells by electroporation and confirmed by sequencing.

PR024f_ADW03055: ATGACCTCCCAAGCTTCAGC

PR024r_ADW03055: CTAGTCCTTCAGCAGCGTCC

PR023f_ADW03055: GGCAGCCATATGGCTAGCATGACTGGTGGGAATGACCTCCCAAGCTTCAGC

PR023r_ADW03055: TCTCAGTGGTGGTGGTGGTGGTCTCGAGTCTAGTCCTTCAGCAGCGTCC

Incubation experiments of purified enzyme with FPP and isolation of products

E. coli BL 21 transformants were inoculated in a 2YT liquid preculture (tryptone 16 g, yeast extract 10 g, NaCl 5 g, water 1 L, pH 7.2) containing kanamycin (50 mg/L) overnight. *E. coli* BL 21 transformants from the preculture were inoculated in large scale 2YT liquid cultures (8 x 1 L) containing kanamycin (50 mg/L). Cells were grown to an OD₆₀₀ = 0.5 at 37 °C and 160 rpm, followed by cooling of the cultures to 18 °C for 30 minutes. IPTG (0.4 mM) was added and the culture was incubated at 18 °C and 160 rpm overnight. *E. coli* cells were harvested by centrifugation at 4 °C and 3600 rpm for 60 min. The pellets were resuspended in 2 x 10 mL lysis buffer (20 mM Na₂HPO₄, 0.5 M NaCl, 20 mM imidazole, 1 mM MgCl₂, pH 7.0) for each 1 L culture. Cell disruption was done by ultra-sonication on ice for 6 x 60 sec. The soluble enzyme fractions were harvested at 4 °C and 11000 rpm by repeated centrifugation (2 x 10 min). Protein purification was performed by Ni²⁺-NTA affinity chromatography with Ni²⁺-NTA superflow (Novagen) using binding buffer (20 mM Na₂HPO₄, 0.5 M NaCl, 20 mM imidazole, 1 mM MgCl₂, pH 7.0) and elution buffer (20 mM Na₂HPO₄, 0.5 M NaCl, 500 mM imidazole, 1 mM MgCl₂, pH 7.0). All wash and elution fraction were checked by SDS-PAGE. Incubation experiments were performed with the pure protein fractions (160 mL) and incubation buffer (100 mL, 50 mM Tris-HCl, 10 mM MgCl₂, 20 % glycerin, pH 7.0) containing FPP (100 mg, 0.5 mg/mL) at 28 °C overnight. The reaction mixture was extracted with 3 x 100 mL pentane. The combined organic layers were dried with MgSO₄ and concentrated under reduced pressure. Column chromatography on silica gel of the crude product (30 mg) with pentane/diethyl ether (5:1) yielded the pure sesquiterpene (15 mg) for structure elucidation by NMR.

GC-MS and GC-MS-QTOF analysis

GC-MS analyses were carried out with a 7890B gas chromatograph connected to a 5977A inert mass detector (Agilent) fitted with a HP5-MS fused silica capillary column (30 m, 0.25 mm i. d., 0.50 µm film). Instrumental parameters were (1) inlet pressure, 77.1 kPa, He 23.3 mL min⁻¹, (2) injection volume, 1-2 µL, (3) transfer line, 250 °C, and (4) electron energy 70 eV. The GC was programmed as follows: 5 min at 50 °C increasing at 10 °C min⁻¹ to 320 °C,

and operated in split mode (50:1, 60 s valve time). The carrier gas was He at 1 mL min⁻¹. Retention indices (I) were determined from a homologous series of n-alkanes (C8-C40). HRMS analyses were carried out with a 7890B gas chromatograph connected to a 7200 accurate-mass Q-TOF mass detector (Agilent) equipped with a HP5-MS fused silica capillary column (30 m, 0.25 mm i. d., 0.50 μm film). Instrumental parameters were (1) inlet pressure, 83.2 kPa, He 24.6 mL min⁻¹, (2) injection volume, 1 μL, (3) transfer line, 250 °C, and (4) electron energy 70 eV. The GC was programmed for HR-MS as follows: 5 min at 50 °C increasing at 10 °C min⁻¹ to 320 °C, and operated in split mode (50:1-100:1, 60 s valve time). The carrier gas was He at 1 mL min⁻¹. For targeted MS/MS the instrumental parameters were for (1) collision cell: collision gas flow 1 mL min⁻¹ N₂, collision energy: 10 V or 20 V and (2) MS1 scan resolution mode: narrow.

NMR spectroscopy

NMR spectra of synthetic compounds and isolated natural products were recorded on a Bruker DRX-400 (400 MHz), AV III-400 (400 MHz) or AV Avance DMX-500 (500 MHz) spectrometer, and were referenced against solvent signals (¹H NMR: (²H)chloroform δ = 7.26 ppm, (²H₆)benzene δ = 7.16 ppm, (²H₈)toluene δ = 2.08 ppm; ¹³C NMR: (²H)chloroform δ = 77.16 ppm, (²H₆)benzene δ = 128.06 ppm, (²H₈)toluene δ = 20.43 ppm). All temperature-dependent NMR analyses with the natural product were performed at -50 °C, 0 °C and 25 °C.

(+)-(1(10)*E*,4*E*,6*S*,7*R*)-germacradien-6-ol (1):

TLC (cyclohexane/ethyl acetate 5:1): *R*_f = 0.35. GC (HP 5): *I* = 1694 (literature (HP 5): *I* = 1697).^[3] [α]_D²⁰ = + 21.4 (CH₂Cl₂); MS (EI, 70 eV): *m/z* (%) = 222 (6), 207 (6), 204 (9), 189 (6), 179 (4), 161 (35), 151 (5), 147 (6), 140 (8), 138 (9), 137 (16), 136 (11), 133 (11), 123 (17), 121 (31), 119 (23), 111 (11), 109 (38), 108 (11), 107 (26), 105 (34), 97 (15), 95 (27), 93 (34), 91 (33), 84 (100), 83 (54), 81 (66), 79 (33), 77 (25), 69 (33), 68 (24), 67 (45), 55 (66), 53 (29), 43 (34), 41 (78), 39 (30). HRMS (TOF): obs. *m/z* (calcd., formula) = 222.1974 (222.1978, C₁₅H₂₆O⁺, [M]⁺), 207.1740 (207.1743, C₁₄H₂₃O⁺, [M-CH₃]⁺), 204.1875 (204.1873, C₁₅H₂₄⁺, [M-H₂O]⁺). IR (diamond ATR): $\tilde{\nu}$ = 3388 (br m), 2918 (s), 2867 (m), 2853 (m), 1663 (w), 1473 (m), 1446 (m), 1383 (m), 1366 (m), 1304 (w), 1248 (w), 1061 (m), 1014 (m), 982 (w), 847 (m), 675 (w), 551 (w), 507 (w), 493 (w) cm⁻¹.

¹H and ¹³C NMR data of both conformers are summarized in Table 1 of main text.

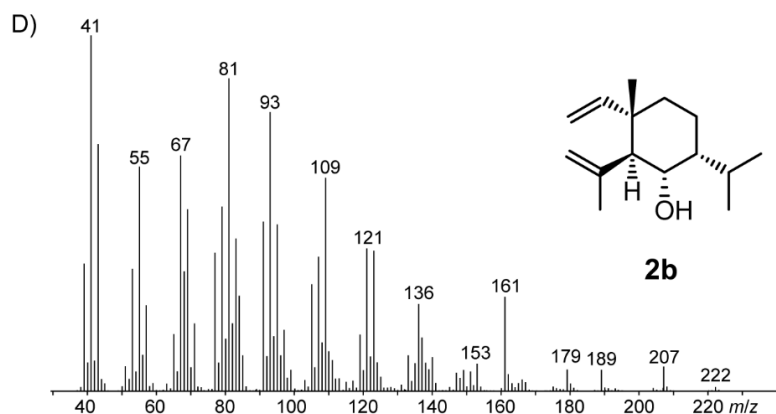
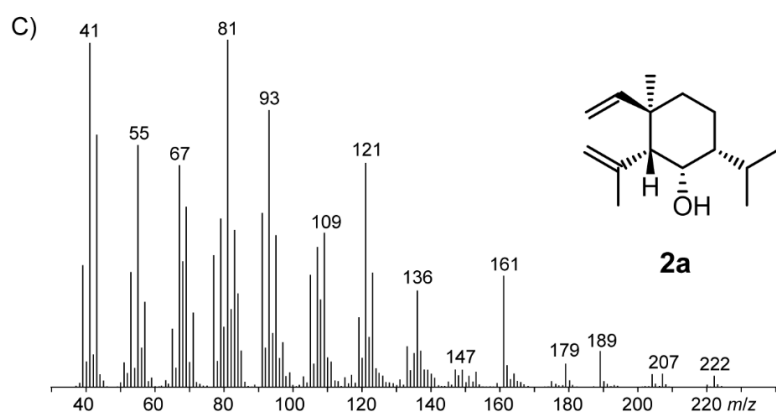
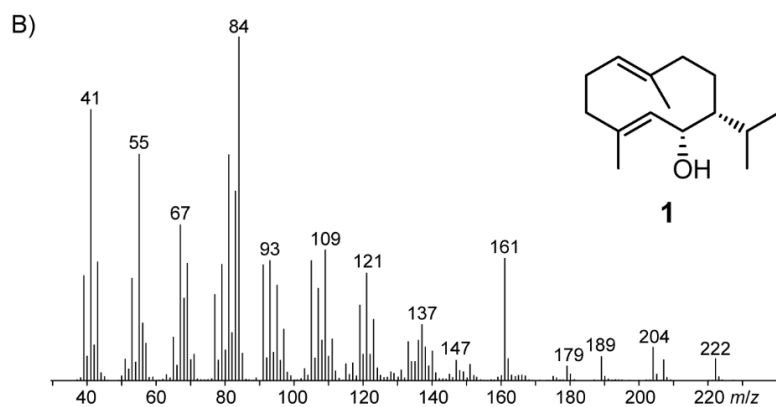
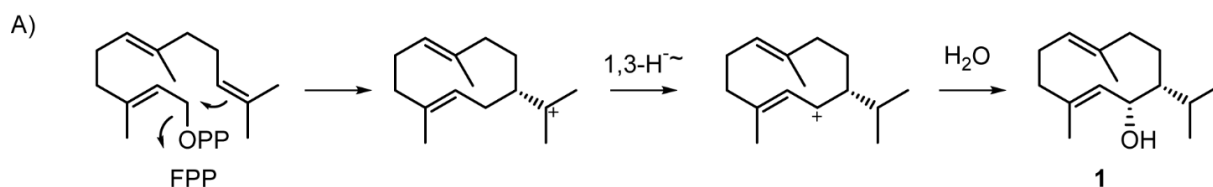


Figure 1. A) Cyclisation mechanism of FPP cyclisation to **1**. EI-MS spectra of B) the enzyme product (1(10)*E*,4*E*,6*S*,7*R*)-germacradien-6-ol (**1**) and of its Cope rearrangement products C) shyobunol (**2a**) and D) 5,10-di-*epi*-shyobunol (**2b**).

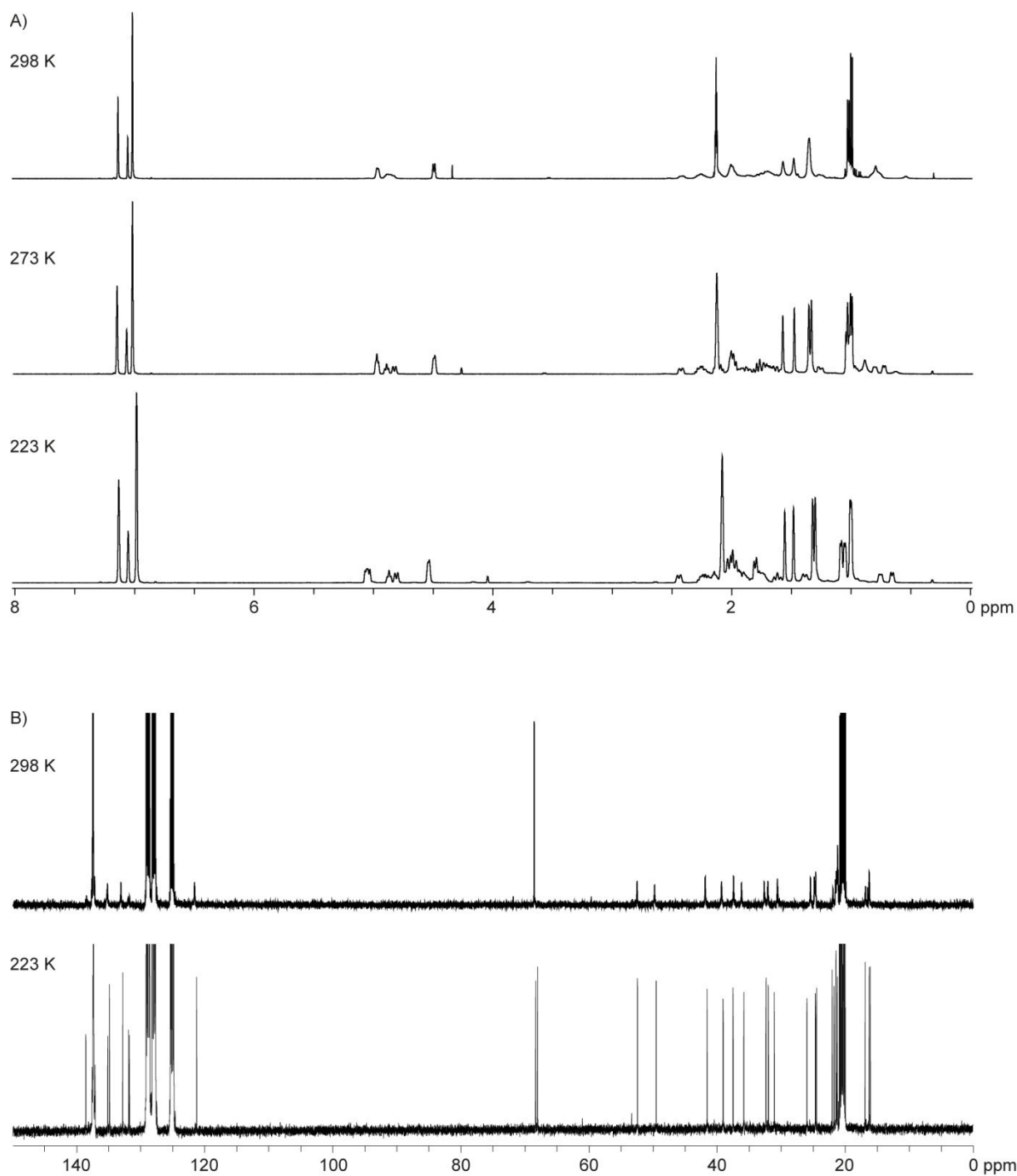


Figure 2. A) Recorded $^1\text{H-NMR}$ spectra of (1(10)*E*,4*E*,6*S*,7*R*)-germacradien-6-ol (**1**) at 298 K, 273 K and 223 K and B) $^{13}\text{C-NMR}$ spectra of (1(10)*E*,4*E*,6*S*,7*R*)-germacradien-6-ol (**1**) at 298 K and 223 K.

General synthetic methods

Chemicals were purchased from Acros Organics (Geel, Belgium) or Sigma Aldrich Chemie GmbH (Steinheim, Germany) and used without purification. All non-aqueous reactions were performed under an inert atmosphere (N_2 and Ar) in flame-dried flasks. Solvents were purified by distillation and dried according to standard methods. Thin-layer chromatography was performed with 0.2 mm precoated plastic sheets Polygram Sil G/UV254 (Machery-Nagel). Column chromatography was carried out using Merck silica gel 60 (70-200 mesh).

Synthesis of all fifteen isotopomers of ($^{13}C_1$)FPP and of ($^{13}C_{15}$)FPP

The synthesis of most ^{13}C -labeled isotopomers of FPP (with ^{13}C labeling at C-1, C-2, C-3, C-4, C-5, C-6, C-7, C-8, C-9, and C-10, and for completely labeled ($^{13}C_{15}$)FPP) was performed via a previously reported strategy (for FPPs with labeling at other carbons vide infra).^[4] Briefly, acetone (**3a**) was used in a Horner-Wadsworth-Emmons reaction with triethylphosphonoacetate to yield ethyl 3-methylbut-2-enoate (**4a**, Figure 3 of SI). A DIBAL-H reduction yielded prenol (**5a**) that was converted into the corresponding bromide (**6a**) with PBr_3 (or into the chloride with $MsCl$, $LiCl$ and collidine). The bromide or chloride was used for the alkylation of ethyl acetoacetate under basic conditions (K_2CO_3) to give the β -keto ester **7a**, that reacted upon saponification under spontaneous decarboxylation to sulcatone (**3b**), the analog of acetone elongated by one terpenoid isoprene unit. After a second round of this cycle, geranyl acetone (**3c**) was obtained that was further converted into farnesyl bromide or chloride (**6c**) and then with $(Bu_4N)_3P_2O_7H$ into FPP (**8**). For introduction of labeling the commercially available appropriate building blocks ($^{13}C_3$)acetone, triethyl ($1-^{13}C$)phosphonoacetate, triethyl ($2-^{13}C$)phosphonoacetate, triethyl ($^{13}C_2$)phosphonoacetate, ethyl ($1,2-^{13}C_2$)acetoacetate, ethyl ($3-^{13}C$)acetoacetate, ethyl ($4-^{13}C$)acetoacetate, and ethyl ($^{13}C_4$)acetoacetate were used (note that the seemingly more appropriate building blocks ethyl ($2-^{13}C$)acetoacetate and ethyl ($2,3,4-^{13}C_3$)acetoacetate are more expensive than ethyl ($1,2-^{13}C_2$)acetoacetate or not commercially available, respectively). All compounds along the route are known and the NMR data matched previously reported data,^[5-12] only the data for the portions influenced by the introduced ^{13}C -labeling deviated due to additional C,C- and C,H-couplings for which all coupling constants that could be determined are summarized in Tables 1 – 8 of SI.

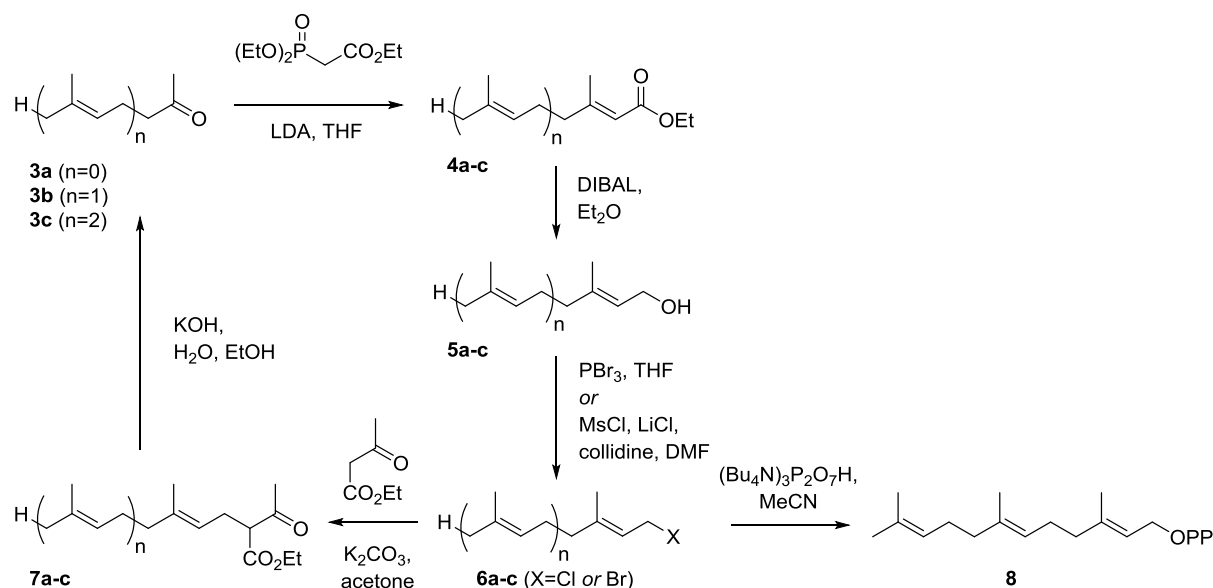
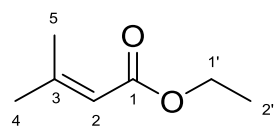
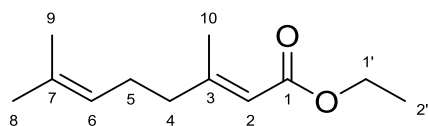


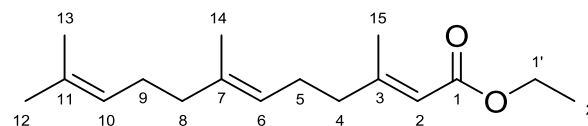
Figure 3. Synthesis of ^{13}C -labeled isotopomers of FPP.



4a



4b



4c

Table 1. Specific aspects of ^{13}C -NMR data of the ^{13}C -labeled isotopomers of **4a** – **4c**. All other ^{13}C -NMR data matched those reported for the unlabeled compounds.^[5,11,12] NMR data were recorded in CDCl_3 unless otherwise noted.

Compound ^[a]	C-1	C-2	C-3	C-4	C-5	C-6	C-7	C-8	C-9	C-10	C-11	C-12	C-13	C-14	C-15	C-1'	C-2'
(1- ^{13}C)- 4a	166.8*	116.2 d	156.4 d	27.5 d	20.3 d											59.5 d	14.4 d
		$^1J=75.9$	$^2J=2.2$	$^3J=7.6$	$^3J=1.4$											$^2J=2.3$	$^3J=2.2$
(2- ^{13}C)- 4a	166.8 d	116.2*	156.4 d	27.5 d													
	$^1J=75.8$		$^1J=72.2$	$^2J=4.0$													
($^{13}\text{C}_5$)- 4a	166.8* dddd	116.2* dddd	156.4* dddd	27.5* dddd	20.3* ddd											59.5 dd	14.4 d
	$^1J=75.5$ $^2J=1.9$ $^3J=7.6$ $^3J=1.9$	$^1J=73.9$ $^1J=73.9$ $^2J=4.0$ $^2J=4.0$	$^1J=72.3$ $^1J=40.3$ $^1J=40.3$ $^2J=2.2$	$^1J=40.7$ $^2J=3.7$ $^2J=3.7$ $^3J=3.7$	$^1J=40.1$ $J=3.3$ $J=1.0$											$^2J=1.6$ $^3J=1.6$	$^3J=2.3$
(1- ^{13}C)- 4b	167.0*	115.8 d	159.9 d	41.1 d												59.6 d	14.4 d
		$^1J=75.7$	$^2J=2.1$	$^3J=7.2$												$^2J=2.4$	$^3J=2.2$
(2- ^{13}C)- 4b	167.0 d	115.8*	159.9 d	41.1 d	26.2 d											59.6 d	
	$^1J=75.6$		$^1J=72.3$	$^2J=3.5$	$^3J=3.0$											$^3J=1.5$	
(3- ^{13}C)- 4b	167.0 d	115.8 d	159.9* d	41.1 d	26.2 d	123.2 d				18.9 d							
	$^2J=1.9$	$^1J=71.8$		$^1J=39.9$	$^2J=2.2$	$^3J=3.6$				$^1J=40.1$							
(4- ^{13}C)- 4b	167.0 d	115.8 d	159.9 d	41.1* d	26.2 d	123.2 d	132.6 d			18.9 d							
	$^3J=7.1$	$^2J=3.3$	$^1J=40.0$		$^1J=33.4$	$^2J=1.5$	$^3J=3.7$			$^1J=2.7$							

(5- ¹³ C)-4b		115.8 d ³ J=2.9	159.9 d ² J=2.1	41.1 d ¹ J=33.4	26.2*	123.2 d ¹ J=44.2		25.8 d ³ J=4.7	17.8 d ³ J=3.7	18.9 d ³ J=1.5						
(6- ¹³ C)-4b			159.9 d ³ J=3.4	41.1 d ² J=1.6	26.3 d ¹ J=44.1	123.2*	132.6 d ¹ J=73.9	25.8 d ² J=3.2	17.8 d ² J=1.9							
(10- ¹³ C)-4b	167.0 d ³ J=1.4		159.9 d ¹ J=40.0	41.1 d ² J=2.7	26.2 d ³ J=1.5					18.9*						
(¹³ C ₁₀)-4b	167.0* dddd ¹ J=75.8 ³ J=7.1 ² J=1.7 ² J=1.7	115.8* dd ¹ J=73.8 ¹ J=73.8	159.9* ddd ¹ J=72.5 ¹ J=38.2 ¹ J=38.2	41.1* dd ¹ J=36.4 ¹ J=36.5	26.3* dd ¹ J=34.7 ¹ J=43.6	123.2* dd ¹ J=74.0 ¹ J=44.0	132.6* dddd ¹ J=42.3 ¹ J=42.3 ¹ J=74.6 J=3.5	25.8* d ¹ J=42.6	17.8* d ¹ J=42.3	18.9* d ¹ J=40.3				59.6 dd ² J=1.6 ³ J=1.6	14.5 d ³ J=2.1	
(1- ¹³ C)-4c	167.0*	115.8 d ¹ J=75.8	159.9 d ² J=2.0	41.1 d ³ J=7.0										18.9 d ³ J=1.4	59.6 d ² J=2.3	14.5 d ³ J=2.3
(2- ¹³ C)-4c	167.0 d ¹ J=75.7	115.8*	159.9 d ¹ J=72.0	41.1 d ² J=3.4	26.1 d ³ J=2.9										59.6 d ³ J=1.4	
(3- ¹³ C)-4c	167.0 d ² J=1.9	115.8 d ¹ J=71.7	159.9*	41.1 d ¹ J=40.1	26.1 d ² J=2.2											
(4- ¹³ C)-4c	167.0 d ³ J=7.0	115.8 d ² J=3.3	159.9 d ¹ J=40.1	41.1* d ¹ J=33.2	26.1 d ² J=1.6	123.0 d ² J=1.6	136.3 d ³ J=3.8									
(5- ¹³ C)-4c		115.8 d ³ J=2.9	159.9 d ² J=2.1	41.1 d ¹ J=33.6	26.1* d ¹ J=44.0	123.0 d ¹ J=44.0		39.8 d ³ J=4.5					16.1 d ³ J=3.9			
(6- ¹³ C)-4c			159.9 d ³ J=3.2	41.1 d ² J=1.6	26.1 d ¹ J=67.9	123.0* d ¹ J=73.6	136.3 d ¹ J=73.6	39.8 d ² J=2.6	26.8 d ³ J=3.0							
(7- ¹³ C)-4c				41.1 d ³ J=3.6		123.0 d ¹ J=73.5	136.3* d ¹ J=42.5	39.8 d ² J=2.3	26.8 d ³ J=3.8	124.4 d ³ J=3.8			16.1 d ¹ J=42.2			

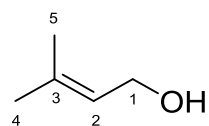
(8- ¹³ C)-4c					26.1 d ³ J=4.4	123.0 d ² J=2.6	136.3 d ¹ J=42.7	39.8*	26.8 d ¹ J=33.7	124.4 d ² J=1.6	131.5 d ³ J=3.7			16.1 d ² J=3.9			
(9- ¹³ C)-4c						123.0 d ³ J=3.0	136.3 d ² J=2.1	39.8 d ¹ J=33.4	26.8*	124.4 d ¹ J=44.2		25.8 d ³ J=4.5	17.8 d ³ J=3.5	16.1 d ³ J=1.2			
(10- ¹³ C)-4c							136.3 d ³ J=3.3	39.8 d ² J=1.6	26.8 d ¹ J=44.0	124.4*	131.5 d ¹ J=73.7	25.8 d ² J=3.2	17.8 d ² J=2.2				
(14- ¹³ C)-4c					26.1 d ³ J=3.9	123.0 d ² J=1.8	136.3 d ¹ J=42.3	39.8 d ² J=3.6	26.8 d ³ J=1.4					16.1*			
(15- ¹³ C)-4c	167.0 d ³ J=1.4		159.9 d ¹ J=40.1	41.1 d ² J=2.6	26.1 d ³ J=1.4										18.9*		
(¹³ C ₁₅)-4c	167.0* dddd ¹ J=75.6 ³ J=7.1 ² J=1.7 ² J=1.7	115.8* dd ¹ J=72.2 ¹ J=75.5	159.9* ddd ¹ J=72.0 ¹ J=39.5 ¹ J=39.5	41.1* dd ¹ J=36.4 ¹ J=36.4	26.1* dd ¹ J=35.6 ¹ J=43.3	123.0* dd ¹ J=73.9 ¹ J=44.0	136.3* ddd ¹ J=73.8 ¹ J=40.8 ¹ J=40.8	39.8* dd ¹ J=34.8 ¹ J=40.8	26.8* dd ¹ J=34.8 ¹ J=43.0	124.3* dd ¹ J=44.4 ¹ J=72.6	131.5* dddd ¹ J=73.8 ¹ J=42.3 ¹ J=42.3 J=3.5	25.8* d ¹ J=42.7	17.8* d ¹ J=42.1	16.1* d ¹ J=42.2	18.9* d ¹ J=40.0	59.6 dd ² J=1.7 ³ J=1.7	14.5 d ³ J=2.2

[a] Coupling constants ⁿJ are C,C-couplings via n bonds and given in Hertz (d = doublet, n.d. = not determinable due to signal overlappings). Asterisks indicate ¹³C-labeled carbons.

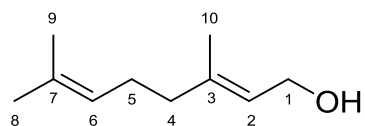
(6- ¹³ C)-4b				5.07 d ¹ J=150.9	1.60 d ³ J=4.3	1.68 d ³ J=5.5							
(10- ¹³ C)-4b	5.66 d ³ J=8.0						2.15 d ¹ J=127.7						
(¹³ C ₁₀)-4b	5.66 d ¹ J=159.3	2.15 d ¹ J=128.5	2.15 d ¹ J=128.5	5.07 d ¹ J=150.7	1.60 d ¹ J=125.2	1.68 d ¹ J=125.5	2.15 d ¹ J=128.5					4.14 d ³ J=3.0	
(1- ¹³ C)-4c												4.14 d ³ J=3.0	
(2- ¹³ C)-4c	5.66 d ¹ J=159.3										2.16 d ³ J=4.7		
(3- ¹³ C)-4c		2.16 d ¹ J=128.8											
(4- ¹³ C)-4c			n.d.										
(5- ¹³ C)-4c				5.09 d ¹ J=150.8									
(6- ¹³ C)-4c													
(7- ¹³ C)-4c					1.98 d ¹ J=120.4								
(8- ¹³ C)-4c						n.d.							
(9- ¹³ C)-4c							5.09 d ¹ J=150.0	1.67 d ³ J=5.9					
(10- ¹³ C)-4c													
(14- ¹³ C)-4c										1.60 d ¹ J=125.6			
(15- ¹³ C)-4c	5.65 d ³ J=8.2										2.17 d ¹ J=127.6		

$(^{13}\text{C}_{15})\text{-4c}$	5.66 d $^1J=159.4$	2.16 d $^1J=127.2$	2.16 d $^1J=127.2$	5.09 d $^1J=149.8$	1.98 d $^1J=123.6$	2.05 d $^1J=128.4$	5.09 d $^1J=150.6$	1.68 d $^1J=124.8$	1.60 d $^1J=125.5$	1.60 d $^1J=125.5$	2.17 d $^1J=127.7$	4.14 d $^3J=3.0$	
----------------------------------	--------------------------	--------------------------	--------------------------	--------------------------	--------------------------	--------------------------	--------------------------	--------------------------	--------------------------	--------------------------	--------------------------	------------------------	--

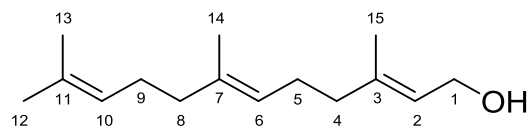
[a] Compound numbers refer to Figure 1. Coupling constants nJ are C,H-couplings via n bonds and given in Hertz (d = doublet, n.d. = not determinable due to signal overlappings).



5a



5b



5c

Table 3. Specific aspects of ^{13}C -NMR data of the ^{13}C -labeled isotopomers of **5a** – **5c**. All other ^{13}C -NMR data matched those reported for the unlabeled compounds.^[7,10,12] NMR data were recorded in CDCl_3 unless otherwise noted.

Compound ^[a]	C-1	C-2	C-3	C-4	C-5	C-6	C-7	C-8	C-9	C-10	C-11	C-12	C-13	C-14	C-15
(1- ^{13}C)- 5a	59.5*	123.7 d	136.6 d	25.9 d	17.9 d										
(2- ^{13}C)- 5a	59.5 d	123.7* $^1J=47.6$	136.5 d	25.9 d	17.9 d										
($^{13}\text{C}_5$)- 5a	59.5* dddd $^1J=47.6$ $^2J=1.6$ $^3J=4.1$ $^3J=5.1$	123.7* dddd $^1J=47.6$ $^1J=72.7$ $^2J=2.9$ $^2J=1.6$	136.5* dddd $^1J=73.0$ $^1J=41.4$ $^1J=42.5$ $^2J=1.6$	25.9* d $^1J=42.4$	17.9* dddd $^1J=41.4$ $^3J=4.1$ $^2J=5.9$ $^2J=1.6$										
(1- ^{13}C)- 5b	59.5*	123.4 d $^1J=47.5$	139.9 d $^2J=1.2$	39.7 d $^3J=4.8$						16.4 d $^3J=4.2$					
(2- ^{13}C)- 5b	59.5 d $^1J=47.5$	123.4* $^1J=47.5$	139.9 d $^1J=72.4$	39.7 d $^2J=2.5$	26.5 d $^3J=3.0$										
(3- ^{13}C)- 5b	59.5 d $^2J=1.6$	123.4 d $^1J=72.7$	139.9* $^1J=72.7$	39.7 d $^1J=41.9$	26.5 d $^2J=2.2$	124.0 d $^3J=3.8$				16.4 d $^1J=41.3$					
(4- ^{13}C)- 5b	59.5 d $^3J=4.8$	123.4 d $^2J=2.4$	139.9 d $^1J=41.7$	39.7* $^1J=41.7$	26.5 d $^1J=33.6$	124.0 d $^2J=1.6$	131.8 d $^3J=3.6$			16.4 d $^2J=3.5$					

(5- ¹³ C)-5b		123.4 d ³ J=3.0	139.9 d ² J=2.2	39.7 d ¹ J=33.6	26.5*	124.0 d ¹ J=44.0		25.8 d ³ J=4.5	17.8 d ³ J=3.8	16.4 d ³ J=1.4				
(6- ¹³ C)-5b			139.9 d ³ J=3.5	39.7 d ² J=1.6	26.5 d ¹ J=44.0	124.0*	131.9 d ¹ J=73.6	25.8 d ² J=3.2	17.8 d ² J=1.7					
(7- ¹³ C)-5b				39.7 d ³ J=3.7		124.0 d ¹ J=73.7	131.9*	25.8 d ¹ J=43.1	17.8 d ¹ J=42.1					
(10- ¹³ C)-5b	59.5 d ³ J=4.3	123.4 d ² J=1.6	139.9 d ¹ J=41.7	39.7 d ² J=3.5	26.5 d ³ J=1.5					16.4*				
(¹³ C ₁₀)-5b	59.5* dddd ¹ J=47.5 ³ J=4.6 ³ J=4.6 ² J=1.2	123.4* dd ¹ J=72.5 ¹ J=47.5	139.9* ddd ¹ J=41.7 ¹ J=41.7 ¹ J=72.6	39.7* dd ¹ J=33.6 ¹ J=41.7	26.5* dd ¹ J=34.5 ¹ J=43.8	124.0* dd ¹ J=73.7 ¹ J=44.0	131.9* dddd ¹ J=42.5 ¹ J=42.5 ¹ J=73.7 ² J=3.7	25.8* d ¹ J=42.9	17.8* d ¹ J=42.2	16.4* d ¹ J=41.6				
(1- ¹³ C)-5c	59.6*	123.5 d ¹ J=47.4	140.0 d ² J=1.2	39.7 d ³ J=4.7										16.4 d ³ J=4.2
(2- ¹³ C)-5c	59.6 d ¹ J=47.4	123.5*	140.0 d ¹ J=73.0	39.7 d ² J=2.4	26.4 d ³ J=3.1									16.4 d ² J=1.5
(3- ¹³ C)-5c	59.6 d ² J=1.3	123.5 d ¹ J=72.7	140.0* d ¹ J=41.8	39.7 d ¹ J=41.8	26.4 d ² J=2.2	123.9 d ³ J=3.5								16.4 d ¹ J=41.7
(4- ¹³ C)-5c	59.6 d ³ J=4.8	123.5 d ² J=2.3	140.0 d ¹ J=41.8	39.7* d ¹ J=34.5	26.4 d ¹ J=33.5	123.9 d ² J=1.6	135.5 d ³ J=3.6							
(5- ¹³ C)-5c		123.5 d ² J=3.0		39.7 d ¹ J=34.5	26.5* d ¹ J=44.0	123.9 d ¹ J=44.0		39.8 d ³ J=3.5					16.2 d ³ J=3.7	16.4 d ³ J=1.5
(6- ¹³ C)-5c			140.0 d ³ J=3.6	39.7 d ² J=1.6	26.4 d ¹ J=44.0	123.9*	135.5 d ¹ J=73.7	39.8 d ² J=2.6	26.9 d ³ J=3.1					

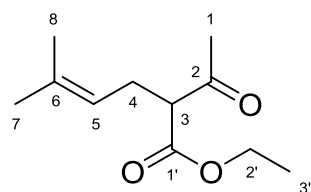
(7- ¹³ C)-5c				39.7 d ³ J=3.5		123.9 d ¹ J=73.4	135.5*	39.8 d ¹ J=42.4	26.9 d ² J=2.1	124.4 d ³ J=3.7				16.2 d ¹ J=42.4	
(8- ¹³ C)-5c					26.4 d ³ J=4.4	123.9 d ² J=2.6	135.5 d ¹ J=42.1	39.8*	26.8 d ¹ J=33.7	124.4 d ² J=1.6	131.5 d ³ J=3.6			16.2 d ² J=3.7	
(9- ¹³ C)-5c						123.9 d ³ J=2.9	135.5 d ² J=2.1	39.8 d ¹ J=34.2	26.8*	124.4 d ¹ J=44.1		25.8 d ³ J=4.7	17.8 d ³ J=3.7	16.2 d ³ J=1.4	
(10- ¹³ C)-5c							135.5 d ³ J=3.5	39.8 d ² J=1.7	26.9 d ¹ J=44.1	124.4*	131.5 d ¹ J=73.7	25.8 d ² J=3.2	17.8 d ² J=2.0		
(11- ¹³ C)-5c								39.8 d ³ J=3.7		124.4 d ¹ J=73.7	131.5*	25.8 d ¹ J=43.1	17.8 d ¹ J=42.2		
(12- ¹³ C)-5c									26.9 d ³ J=4.6	124.4 d ² J=3.1	131.5 d ¹ J=43.1	25.8* d ² J=4.5	17.8 d ² J=4.5		
(13- ¹³ C)-5c									26.9 d ³ J=3.6	124.4 d ² J=2.0	131.5 d ¹ J=42.2	25.8 d ² J=4.5	17.8*		
(14- ¹³ C)-5c					26.4 d ³ J=1.5	123.9 d ² J=1.8	135.5 d ¹ J=42.2	39.8 d ² J=3.8	26.9 d ³ J=1.5					16.2*	
(15- ¹³ C)-5c	59.6 d ³ J=4.3	123.5 d ² J=1.7	140.0 d ¹ J=41.7	39.7 d ² J=3.5	26.4 d ³ J=1.6										16.4*
(¹³ C ₁₅)-5c	59.6* dddd ¹ J=47.4 ¹ J=4.6 ¹ J=4.6 ¹ J=1.3	123.5* dd ¹ J=47.6 ¹ J=72.9	140.0* ddd ¹ J=72.6 ¹ J=41.8 ¹ J=41.8	39.7* dd ¹ J=36.6 ¹ J=36.6	26.4* dd ¹ J=43.5 ¹ J=36.5	123.9* dd ¹ J=44.0 ¹ J=73.7	135.5* ddd ¹ J=73.6 ¹ J=42.2 ¹ J=42.2	39.8* dd ¹ J=38.0 ¹ J=41.0	26.9* dd ¹ J=40.0 ¹ J=40.0	124.4* dd ¹ J=42.0 ¹ J=73.0	131.5* ddd ¹ J=73.6 ¹ J=42.3 ¹ J=42.3	25.8* d ¹ J=42.8	17.8* d ¹ J=42.0	16.2* d ¹ J=42.3	16.4* d ¹ J=41.7

[a] Coupling constants ⁿJ are C,C-couplings via n bonds and given in Hertz (d = doublet, n.d. = not determinable due to signal overlappings). Asterisks indicate ¹³C-labeled carbons.

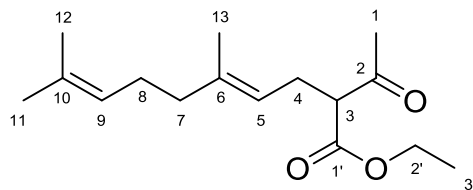
(5- ¹³ C)-5b				2.10 d ¹ J=127.9								
(6- ¹³ C)-5b					5.10 d ¹ J=150.3	1.60 d ³ J=4.58						
(10- ¹³ C)-5b								1.68 d ¹ J=125.9				
(¹³ C ₁₀)-5b	4.15 d ¹ J=142.0	5.41 d ¹ J=153.1	2.03 d ¹ J=126.3	2.10 d ¹ J=127.9	5.09 d ¹ J=150.5	1.60 d ¹ J=125.2	1.68 d ¹ J=126.0	1.68 d ¹ J=126.0				
(1- ¹³ C)-5c	4.15 d ¹ J=142.5											
(2- ¹³ C)-5c	4.15 d ² J=4.0	5.42 d ¹ J=153.2										
(3- ¹³ C)-5c	4.15 d ³ J=4.9											
(4- ¹³ C)-5c		5.42 d ³ J=6.5										
(5- ¹³ C)-5c				n.d.								
(6- ¹³ C)-5c					5.10 d ¹ J=150.2							
(7- ¹³ C)-5c											1.60 d ² J=5.5	
(8- ¹³ C)-5c						1.98 d ¹ J=130						
(9- ¹³ C)-5c							2.05 d ¹ J=126.8					

(10- ¹³ C)-5c							5.10 d ¹ J=150.1 n.d.				
(11- ¹³ C)-5c								n.d.	n.d.		
(12- ¹³ C)-5c								1.68 d ¹ J=125.2			
(13- ¹³ C)-5c									1.60 d ¹ J=125.1		
(14- ¹³ C)-5c										1.60 d ¹ J=125.4	
(15- ¹³ C)-5c		5.42 d ³ J=7.1									1.68 d ¹ J=126.1
(¹³ C ₁₅)-5c	4.15 d ¹ J=141.9	5.42 d ¹ J=153.5			5.10 d ¹ J=149.9		5.10 d ¹ J=149.9	1.68 d ¹ J=125.6	1.60 d ¹ J=125.0	1.60 d ¹ J=125.0	1.68 d ¹ J=125.6

[a] Coupling constants ⁿJ are C,H-couplings via n bonds and given in Hertz (d = doublet, n.d. = not determinable due to signal overlappings).



7a



7b

Table 5. Specific aspects of ^{13}C -NMR data of the ^{13}C -labeled isotopomers of **7a** and **7b**. All other ^{13}C -NMR data matched those reported for the unlabeled compounds.^[8,12] NMR data were recorded in CDCl_3 unless otherwise noted.

Compound ^[a]	via X=	C-1	C-2	C-3	C-4	C-5	C-6	C-7	C-8	C-9	C-10	C-11	C-12	C-13	C-1'	C-2'	C-3'
(2- ^{13}C)- 7a	Br	29.2 d $^1J=41.8$	203.2*	60.0 d $^1J=37.4$	27.1 d $^2J=1.3$	119.9 d $^3J=2.6$									169.6 d $^2J=1.6$		
(1',3- $^{13}\text{C}_2$)- 7a	Br	29.2 d $^2J=12.8$	203.2 dd $^1J=37.2$ $^2J=1.6$	60.0* d $^1J=56.2$	27.1 dd $^1J=33.7$ $^2J=1.5$	119.9 dd $^2J=1.3$ $^3J=2.7$	134.9 d $^3J=3.6$								169.6* d $^1J=56.1$	61.4 d $^2J=2.4$	14.2 d $^3J=2.1$
(4- ^{13}C)- 7a	Br		203.2 d $^2J=1.4$	60.0 d $^1J=33.8$	27.1* $^1J=44.3$	119.9 d $^1J=44.3$		25.9 d $^3J=4.8$	17.9 d $^3J=3.8$						169.7 d $^2J=1.6$		
(5- ^{13}C)- 7a	Br		203.2 d $^3J=2.7$	60.0 d $^2J=1.0$	27.1 d $^1J=44.6$	119.9* $^1J=74.1$	134.9 d $^2J=3.5$	25.9 d $^2J=1.9$	17.9 d $^2J=1.9$						169.6 d $^3J=2.7$		
($^{13}\text{C}_9$)- 7a in ($^2\text{H}_6$)benzene	Br	28.6* dd $^1J=42.0$ $^2J=13.1$	201.4* dd $^1J=37.2$ $^1J=42.0$	60.0* ddd $^1J=35.7$ $^1J=35.7$ $^1J=56.0$	27.3* dd $^1J=33.8$ $^1J=44.3$	120.8* dd $^1J=44.4$ $^1J=74.2$	134.3* dddd $^1J=72.2$ $^1J=42.7$ $^1J=42.7$ $^3J=3.6$	25.8* dddd $^1J=42.9$ $^2J=4.2$ $^2J=4.2$ $^3J=4.2$	17.7* dddd $^1J=42.1$ $^2J=1.9$ $^2J=1.8$						169.5* d $^1J=56.3$	61.0 d $^2J=2.4$	14.0 d $^3J=2.0$
(2- ^{13}C)- 7b	Br	29.2 d $^1J=41.8$	203.2*	60.0 d $^1J=37.2$	27.0 d $^2J=1.2$	119.8 d $^3J=2.6$									169.6 d $^2J=1.6$		

(1',3- ¹³ C ₂)- 7b	Br	29.2 d ³ J=12.7	203.2 dd ¹ J=37.3 ² J=1.4	60.0* d ¹ J=56.0	27.0 dd ¹ J=33.7 ² J=1.4	119.8 dd ² J=2.8 ³ J=1.1	138.5 d ³ J=3.5								169.6* d ¹ J=56.0	61.2 d ² J=2.4	14.1 d ³ J=2.0
(4- ¹³ C)- 7b	Br		203.2 d ² J=1.1	60.0 d ¹ J=33.6	27.0* 	119.8 d ¹ J=44.4		39.8 d ³ J=4.3						16.2 d ³ J=4.0			
(5- ¹³ C)- 7b	Br		203.2 d ³ J=2.7	60.0 d ² J=1.2	27.0 d ¹ J=44.2	119.8* 	138.5 d ¹ J=74.0	39.8 d ² J=3.0	26.6 d ³ J=3.0					16.2 d ² J=1.6	169.6 d ³ J=2.6		
(6- ¹³ C)- 7b				60.0 d ³ J=3.5		119.8 d ¹ J=73.9	138.5* 	39.8 d ¹ J=42.2	26.6 d ² J=2.2	124.1 d ³ J=3.4				16.2 d ¹ J=42.2			
(7- ¹³ C)- 7b	Br				27.0 d ³ J=4.5	119.8 d ² J=2.9	138.5 d ¹ J=42.4	39.8* 	26.6 d ¹ J=33.8	124.1 d ² J=1.5	131.7 d ³ J=3.6			16.2 d ² J=3.6			
(8- ¹³ C)- 7b	Br					119.8 d ³ J=3.1	138.5 d ² J=2.1	39.8 d ¹ J=33.6	26.6* 	124.1 d ¹ J=44.2		25.8 d ³ J=4.8	17.8 d ³ J=3.6	16.2 d ³ J=1.1			
(9- ¹³ C)- 7b	Br						138.5 d ³ J=3.2	39.8 d ² J=1.6	26.6 d ¹ J=44.1	124.1* 	131.7 d ¹ J=73.7	25.8 d ² J=3.2	17.8 d ² J=1.9				
(13- ¹³ C)- 7b	Br				27.0 d ³ J=4.0	119.8 d ² J=1.7	138.5 d ¹ J=42.1	39.8 d ² J=3.6	26.6 d ³ J=1.4					16.2*			
(¹³ C ₁₄)- 7b in (² H ₆)benzene	Br	28.7* dd ¹ J=42.0 ² J=13.3	201.4* dd ¹ J=37.2 ¹ J=42.0	60.0* dddd ¹ J=56.3 ¹ J=37.3 ¹ J=34.1 ² J=13.0 ³ J=3.4	27.1* dd ¹ J=44.1 ¹ J=34.1	120.8* dd ¹ J=44.3 ¹ J=74.3	138.0* ddd ¹ J=31.8 ¹ J=31.8 ¹ J=74.1	40.1* dd ¹ J=33.7 ¹ J=41.9	26.8* dd ¹ J=44.1 ¹ J=34.1	124.6* dd ¹ J=43.7 ¹ J=74.2	131.3* dd ¹ J=74.3 ¹ J=42.6	25.8* d ¹ J=43.2	17.7* d ¹ J=42.2	16.1* d ¹ J=42.2	169.6* d ¹ J=56.3	61.0 d ² J=2.4	14.1 d ¹ J=2.0

[a] Coupling constants ⁿJ are C,C-couplings via n bonds and given in Hertz (d = doublet, n.d. = not determinable due to signal overlappings). Asterisks indicate ¹³C-labeled carbons.

(1',3- ¹³ C ₂)- 7b	Br	2.22 d ² J=1.0	3.43 dd ¹ J=131.8 ² J=6.0										
(4- ¹³ C)- 7b	Br		3.43 t ² J=4.3	2.52 d ¹ J=150.5									
(5- ¹³ C)- 7b	Br		3.43 d ³ J=3.0		5.04 d ¹ J=152.3							1.63 d ³ J=5.1	
(6- ¹³ C)- 7b	Br											1.62 d ² J=6.0	
(7- ¹³ C)- 7b	Br					1.98 d ¹ J=120.4						1.63 d ³ J=3.9	
(8- ¹³ C)- 7b	Br						2.04 d ¹ J=125.1						
(9- ¹³ C)- 7b	Br							5.04 d ¹ J=150.4	1.67 d ³ J=6.0	1.58 d ³ J=5.0			
(13- ¹³ C)- 7b	Br											125.5 d ¹ J=125.5	
(¹³ C ₁₄)- 7b in (² H ₆)benzene	Br	1.87 ddd ¹ J=127.3 ² J=6.0 ³ J=1.2	3.28 d ¹ J=130.2	2.63 d ¹ J=130.1	5.14 d ¹ J=151.7	1.97 d ¹ J=125.3	2.07 d ¹ J=124.5	5.12 d ¹ J=30.2					3.88 dd ³ J=3.3 ⁴ J=1.0

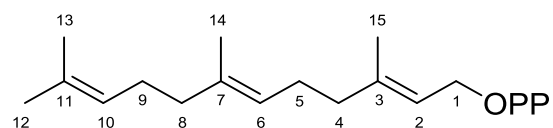
[a] Coupling constants ⁿJ are C,H-couplings via n bonds and given in Hertz (d = doublet, n.d. = not determinable due to signal overlappings).

(2- ¹³ C)- 3c	30.1 d ¹ J=40.1	208.8*	43.9 d ¹ J=39.1	22.5 d ² J=1.7	122.6 d ³ J=3.3								
(3- ¹³ C)- 3c	30.1 d ² J=13.8	208.8 d ¹ J=39.5	43.9*	22.6 d ¹ J=34.7	122.7 d ² J=1.5	136.5 d ³ J=3.7							
(4- ¹³ C)- 3c	30.1 d ³ J=0.6	208.8 d ² J=1.8	43.9 d ¹ J=34.8	22.5* d ¹ J=44.0	122.6 d ¹ J=44.0		39.8 d ³ J=4.5						16.1 d ³ J=3.9
(5- ¹³ C)- 3c		208.8 d ³ J=3.3	43.9 d ² J=1.7	22.6 d ¹ J=44.3	122.6* d ¹ J=74.0	136.5 d ¹ J=74.0	39.8 d ² J=2.6	26.7 d ³ J=3.0					16.1 d ² J=1.8
(6- ¹³ C)- 3c			43.9 d ³ J=3.6		122.6 d ¹ J=73.7	136.5* d ¹ J=73.7	39.8 d ¹ J=42.8	26.7 d ² J=2.2	124.3 d ³ J=3.6				16.1 d ¹ J=42.2
(7- ¹³ C)- 3c ^[b]						136.5 d ¹ J=42.8	39.8* d ¹ J=33.7	26.7 d ¹ J=33.7					
(8- ¹³ C)- 3c					122.6 d ³ J=3.0	136.5 d ² J=2.2	39.8 d ¹ J=33.7	26.7* d ¹ J=44.2	124.3 d ¹ J=44.2		25.8 d ³ J=4.6	17.8 d ³ J=3.7	16.1 d ³ J=1.4
(9- ¹³ C)- 3c						136.5 d ³ J=3.6	39.8 d ² J=1.6	26.7 d ¹ J=44.1	124.3* d ¹ J=73.7	131.5 d ¹ J=73.7	25.8 d ² J=3.1	17.8 d ² J=1.9	
(13- ¹³ C)- 3c				22.6 d ³ J=4.0	122.6 d ² J=1.8	136.5 d ¹ J=42.2	39.8 d ² J=3.7	26.7 d ³ J=1.5					16.1*
(¹³ C ₁₅)- 3c	30.1* dd ¹ J=40.0 ¹ J=14.0	208.8* dddd ¹ J=40.0 ¹ J=40.0 ² J=1.8 ³ J=3.4	43.9* dddd ¹ J=38.3 ¹ J=34.9 ² J=14.0 ³ J=3.4	22.6* dd ¹ J=34.7 ¹ J=44.0	122.6* dd ¹ J=73.7 ¹ J=44.1	136.5* dddddd ¹ J=74.0 ¹ J=42.4 ¹ J=42.4 ² J=2.2 ³ J=3.6 ³ J=3.6	39.8* dd ¹ J=42.2 ¹ J=34.1	26.7* dd ¹ J=34.9 ¹ J=43.3	124.3* dddddd ¹ J=73.7 ¹ J=44.2 ² J=1.9 ² J=1.9 ² J=3.4 ³ J=3.4	131.5* dddd ¹ J=73.6 ¹ J=42.6 ¹ J=42.6 ³ J=3.6	25.8* dddd ¹ J=43.0 ² J=3.3 ² J=4.3 ³ J=4.3	17.8* dddd ¹ J=42.2 ² J=2.1 ² J=4.3 ³ J=4.3	16.1* dddd ¹ J=42.2 ² J=1.6 ² J=3.5 ³ J=1.6 ³ J=3.5

[a] Coupling constants ⁿJ are C,C-couplings via n bonds and given in Hertz (d = doublet, n.d. = not determinable due to signal overlappings). Asterisks indicate ¹³C-labeled carbons. [b] Not recorded, data inferred from coupling constants observed for (6-¹³C)- and (8-¹³C)-FPP.

(2- ¹³ C)- 3c	2.13 d ² J=5.8	2.45 d ² J=5.2								
(3- ¹³ C)- 3c	2.13 d ³ J=1.2	2.45 d ¹ J=129.0								
(4- ¹³ C)- 3c (5- ¹³ C)- 3c			n.d.	5.07 d ¹ J=151.1					1.61 d ³ J=5.0	
(6- ¹³ C)- 3c (7- ¹³ C)- 3c					1.97 d ¹ J=129.2					1.61 d ³ J=3.9
(8- ¹³ C)- 3c						2.05 d ¹ J=127.4				
(9- ¹³ C)- 3c							5.06 d ¹ J=150.1	1.67 d ³ J=5.5	1.58 d ³ J=4.9	
(13- ¹³ C)- 3c										1.60 d ¹ J=126.1
(¹³ C ₁₅)- 3c	2.13 dd ¹ J=127.0 ² J=5.7	2.45 d ¹ J=125.4	2.26 d ¹ J=127.4	5.07 d ¹ J=150.4	1.97 d ¹ J=130.6	2.05 d ¹ J=126	5.07 d ¹ J=150.4	1.67 d ¹ J=125.1	1.59 d ¹ J=125.1	1.61 d ¹ J=125.1

[a] Coupling constants ⁿJ are C,H-couplings via n bonds and given in Hertz (d = doublet, n.d. = not determinable due to signal overlappings).



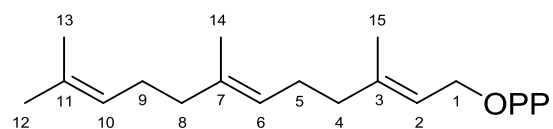
8

Table 9. Specific aspects of ^{13}C -NMR data of the ^{13}C -labeled isotopomers of **8**. All other ^{13}C -NMR data matched those reported for the unlabeled compound.^[12] NMR data were recorded in CDCl_3 unless otherwise noted.

Compound ^[a]	C-1	C-2	C-3	C-4	C-5	C-6	C-7	C-8	C-9	C-10	C-11	C-12	C-13	C-14	C-15
(1- ^{13}C)- 8 in $^2\text{H}_2\text{O}$	65.2*	122.5 d $^1J=50.0$		41.5 d $^3J=4.6$											18.3 d $^3J=4.1$
(2- ^{13}C)- 8 in $^2\text{H}_2\text{O}$		122.4*	145.6 d $^1J=72.4$	41.6 d $^2J=2.7$	28.4 d $^3J=3.1$										18.4 d $^2J=1.6$
(3- ^{13}C)- 8 in $^2\text{H}_2\text{O}$		122.6 d $^1J=72.2$	145.0*	41.6 d $^1J=41.6$	28.4 d $^2J=2.1$	126.9 d $^3J=3.6$									18.3 d $^1J=41.4$
(4- ^{13}C)- 8 in $^2\text{H}_2\text{O}$			145.3 d $^1J=41.8$	41.5*	28.3 d $^1J=35.0$										18.3 d $^2J=2.0$
(5- ^{13}C)- 8 in $^2\text{H}_2\text{O}$		122.3 d $^3J=2.7$	145.7 d $^2J=1.8$	41.6 d $^1J=33.5$	28.4*	127.0 d $^1J=43.4$		41.6 d $^3J=4.2$						18.0 d $^3J=3.4$	18.4 d $^3J=1.3$
(6- ^{13}C)- 8 in $^2\text{H}_2\text{O}$															
(7- ^{13}C)- 8 in $^2\text{H}_2\text{O}$							138.8*								
(8- ^{13}C)- 8 in $^2\text{H}_2\text{O}$					28.6 d $^3J=5.0$	126.8 d $^2J=2.0$	138.3 d $^1J=42.6$	41.7* d $^1J=42.8$	28.7 d $^1J=42.8$	127.0 d $^2J=1.2$	134.4 d $^3J=3.1$			17.9 d $^2J=3.0$	
(9- ^{13}C)- 8 in $^2\text{H}_2\text{O}$							139.4 d $^2J=1.8$	41.5 d $^1J=33.7$	28.5* d $^1J=41.0$	127.2 d $^1J=41.0$		27.6 d $^3J=4.6$	19.7 d $^3J=3.5$		

(10- ¹³ C)- 8 in ² H ₂ O							138.9 d ³ J=3.2		28.7 d ¹ J=42.4	127.2* s	135.4 d ¹ J=72.5	27.7 d ² J=3.2	19.8 d ² J=1.9		
(11- ¹³ C)- 8 in ² H ₂ O								41.8 d ³ J=3.6		127.0 d ¹ J=73.1	134.4* s	27.7 d ¹ J=42.9	19.8 d ¹ J=42.0		
(12- ¹³ C)- 8 in ² H ₂ O									28.8 d ³ J=4.6	127.1 d ² J=3.0	134.8 d ¹ J=41.9	27.7* d			
(13- ¹³ C)- 8 in ² H ₂ O									28.8 d ³ J=3.5	126.9 d ² J=2.0	134.0 d ¹ J=42.2	27.7 d ² J=2.0	19.6* s		
(14- ¹³ C)- 8 in ² H ₂ O				28.3 d ³ J=3.0	126.8 d ² J=1.5			41.5 d ² J=2.3	28.5 d ³ J=3.5					17.9*	
(15- ¹³ C)- 8 in ² H ₂ O			144.9 d ¹ J=41.6	41.8 d ² J=3.4											18.4*
(¹³ C ₁₅)- 8 in ² H ₂ O	65.2 d ¹ J=49.2	122.5 dd ¹ J=72.6 ¹ J=50.0	145.4 ddd ¹ J=72.6 ¹ J=41.7 ¹ J=41.7	41.5 dd ¹ J=38.0 ¹ J=38.0	28.4 dd ¹ J=42.5 ¹ J=37.0	126.7 dd ¹ J=71.9 ¹ J=43.3	139.3 ddd ¹ J=72.0 ¹ J=41.7 ¹ J=41.7	41.4 dd ¹ J=38.0 ¹ J=38.0	28.6 dd ¹ J=42.5 ¹ J=37.0	127.1 dd ¹ J=71.9 ¹ J=43.3	135.1 dddd ¹ J=72.0 ¹ J=41.8 ¹ J=41.8 ³ J=3.4	27.5 d ¹ J=42.2	19.6 d ¹ J=41.8	17.9 d ¹ J=41.6	18.3 d ¹ J=41.6

[a] Coupling constants ⁿJ are C,C-couplings via n bonds and given in Hertz (d = doublet, n.d. = not determinable due to signal overlappings). Asterisks indicate ¹³C-labeled carbons.



8

Table 10. Specific aspects of $^1\text{H-NMR}$ data of the ^{13}C -labeled isotopomers of **8**. All other $^1\text{H-NMR}$ data matched those reported for the unlabeled compound.^[12] NMR data were recorded in CDCl_3 unless otherwise noted.

Compound ^[a]	H-1	H-2	H-4	H-5	H-6	H-8	H-9	H-10	H-12	H-13	H-14	H-15
(1- ^{13}C)- 8 in $^2\text{H}_2\text{O}$	4.46 d $^1J=145.7$											
(2- ^{13}C)- 8 in $^2\text{H}_2\text{O}$	4.48 d $^2J=3.6$	5.45 d $^1J=156.7$										1.73 d $^3J=4.7$
(3- ^{13}C)- 8 in $^2\text{H}_2\text{O}$												
(4- ^{13}C)- 8 in $^2\text{H}_2\text{O}$			n.d.									
(5- ^{13}C)- 8 in $^2\text{H}_2\text{O}$				2.12 d $^1J=126.7$								
(6- ^{13}C)- 8 in $^2\text{H}_2\text{O}$					5.24 d $^1J=150.0$							
(7- ^{13}C)- 8 in $^2\text{H}_2\text{O}$												
(8- ^{13}C)- 8 in $^2\text{H}_2\text{O}$						2.00 d $^1J=127.0$					1.62 d $^3J=3.1$	
(9- ^{13}C)- 8 in $^2\text{H}_2\text{O}$							2.11 d $^1J=126.0$					

(10- ¹³ C)- 8 in ² H ₂ O								5.14 d ¹ J=149.3					
(11- ¹³ C)- 8 in ² H ₂ O									1.68 d ² J=6.2	1.62 d ² J=6.3			
(12- ¹³ C)- 8 in ² H ₂ O									1.68 d ¹ J=125.1				
(13- ¹³ C)- 8 in ² H ₂ O										1.62 d ¹ J=126.0			
(14- ¹³ C)- 8 in ² H ₂ O											1.60 d ¹ J=125.4		
(15- ¹³ C)- 8 in ² H ₂ O												1.71 d ¹ J=125.6	
(¹³ C ₁₅)- 8 in ² H ₂ O	4.48 d ¹ J=145.6	5.48 d ¹ J=156.1	2.14 d ¹ J=124.6	2.11 d ¹ J=126.5	5.19 d ¹ J=151.9	2.02 d ¹ J=127.0	2.11 d ¹ J=126.5	5.19 d ¹ J=151.9	1.68 d ¹ J=125.2	1.62 d ¹ J=125.4	1.63 d ¹ J=125.4	1.72 d ¹ J=125.5	

[a] Coupling constants ⁿJ are C,H-couplings via n bonds and given in Hertz (d = doublet, n.d. = not determinable due to signal overlappings).

Synthesis of (15-¹³C)FPP

The synthesis of (15-¹³C)FPP was performed via the route shown in Figure 4 of SI with usage of (¹³C)methyl iodide that is much cheaper than ethyl (4-¹³C)acetoacetate that would be required for a synthesis via the strategy shown in Figure 3 of SI. Ethyl acetate was treated with LDA to form the ester enolate that was alkylated with freshly prepared geranyl bromide (**6b**, prepared from geraniol **5b** with PBr₃) to yield the ester **9**. DIBAL-H reduction to the alcohol **10** was followed by IBX oxidation to the aldehyde **11** that was used in a Grignard reaction with freshly prepared (¹³C)methylmagnesium iodide to yield the alcohol **12**. IBX oxidation afforded (1-¹³C)geranyl acetone (**3c**) that was converted into (1-¹³C)FPP through the methods shown in Figure 1 of SI.

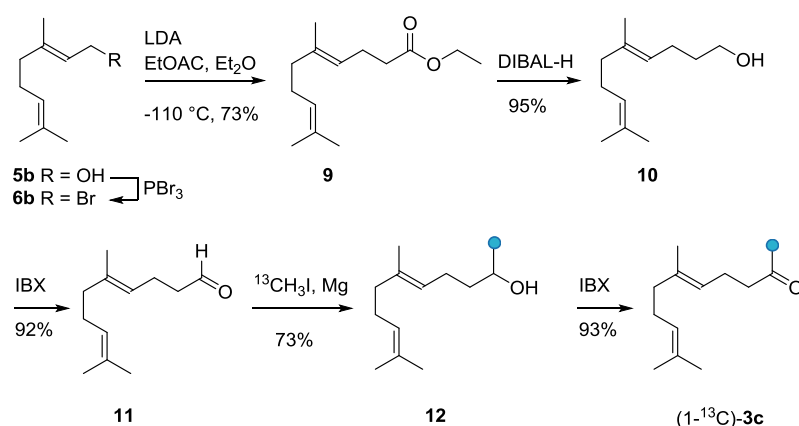


Figure 4. Alternative synthesis of (1-¹³C)geranyl acetone (**3c**).

Synthesis of ethyl (*E*)-5,9-dimethyldeca-4,8-dienoate (**9**)

According to a literature procedure^[13] to a cooled solution (0 °C) of geraniol (**5b**) (3.09 g, 20 mmol, 1.0 eq., 0.35 M in abs. THF) was added PBr₃ (2.17 g, 8 mmol, 0.4 eq.) dropwise. The reaction mixture was stirred for 45 min at 0 °C and then poured into ice-water. The aqueous phase was extracted three times with EtOAc. The combined organic layers were dried with MgSO₄ and concentrated under reduced pressure to yield analytically pure geranyl bromide (**6b**). In a second flask a solution of diisopropylamine (4.14 g, 41 mmol, 2.05 eq.) in abs. THF (50 mL) was cooled to 0 °C and treated with *n*-butyllithium (1.6 M in hexane, 25.6 mL, 41 mmol, 2.05 eq.). The reaction mixture was stirred for 1 h at 0 °C. In a third flask ethyl acetate (3.61 g, 41 mmol, 2.05 eq.) was dissolved in abs. THF (150 mL), CuI (15.23 g, 80 mmol, 4.0 eq.) was added, and the mixture was cooled to -110 °C. The freshly prepared LDA from flask 2 was cannulated to flask 3 with stirring at -110 °C. The reaction mixture was warmed to -50 °C and further stirred for 1.5 h. The freshly prepared geranyl bromide (**6b**) in abs. THF (20 mL) was added dropwise and the reaction was stirred for another 2 h at -30 °C. The reaction mixture was then hydrolyzed by the addition of a saturated aqueous NH₄Cl solution (200 mL), followed by extraction with ethyl acetate (3 x 200 mL). The combined organic layers were dried over MgSO₄ and concentrated under reduced pressure. The residue was purified by column chromatography with hexane/ethyl acetate (20:1) to give the desired ester **9** (3.25g, 14.5 mmol, 73%) as colorless oil.

TLC (hexane/ethyl acetate 20:1): *R*_f = 0.35. ¹H-NMR (400 MHz, CDCl₃, TMS): δ = 5.11-5.03 (m, 2H, 2xCH), 4.10 (q, 2H, ³J_{H,H} = 7.13 Hz, ¹J_{C,H} = 147.1 Hz, CH₂), 2.30 (m, 4H, 2xCH₂), 2.00 (m, 4H, 2xCH₂), 1.65 (d, 3H, ⁴J_{H,H} = 1.2 Hz, 1xCH₃), 1.60 (d, 3H, ⁴J_{H,H} = 1.1 Hz, 1xCH₃),

1.57 (d, 3H, $^4J_{H,H} = 1.0$ Hz, 1xCH₃), 1.24 (t, 3H, $^3J_{H,H} = 7.2$ Hz) ppm. ¹³C-NMR (100 MHz, CDCl₃): $\delta = 173.5$ (CO), 136.7 (C_q), 131.5 (C_q), 124.3 (CH), 122.5 (CH), 60.3 (CH₂), 39.8 (CH₂), 34.6 (CH₂), 26.7 (CH₂), 25.8 (CH₃), 23.7 (CH₂), 17.8 (CH₃), 16.1 (CH₃), 14.4 (CH₃) ppm. GC (HP 5): $I = 1554$. MS (EI, 70 eV): m/z (%) = 224 (5) [M]⁺, 181 (89), 155 (10), 123 (26), 135 (33), 123 (10), 109 (68), 93 (13), 81 (52), 69 (100), 55 (12), 41 (33).

Synthesis of (*E*)-5,9-dimethyldeca-4,8-dien-1-ol (**10**)

The ester **9** (3.2 g, 14.3 mmol, 1.0 eq.) was dissolved in dry diethyl ether (70 mL) and the solution was cooled to -78 °C. A solution of DIBAL-H (2.2 eq., 1.0 M in hexane, 31.4 mmol, 31.4 mL) was added dropwise. The reaction mixture was stirred for 1 h at -78 °C, followed by hydrolysis with a saturated aqueous sodium potassium tartrate solution. The aqueous layer was extracted three times with diethyl ether (100 mL). The combined organic layers were dried with MgSO₄ and concentrated under reduced pressure. Column chromatography with hexane/ethyl acetate (5:1) yielded the desired alcohol **10** (2.47 g, 13.6 mmol, 95%) as colorless oil.

TLC (hexane/ethyl acetate 5:1): $R_f = 0.25$. ¹H-NMR (400 MHz, CDCl₃, TMS): $\delta = 5.16$ -5.10 (m, 1H, 1xCH), 5.10-5.05 (m, 1H, 1xCH), 3.62 (t, 2H, $^3J_{H,H} = 6.5$ Hz, CH₂), 2.09-1.95 (m, 8H, 4xCH₂), 1.67 (d, 3H, $^4J_{H,H} = 1.2$ Hz, 1xCH₃), 1.60 (s, 3H, 1xCH₃), 1.59 (s, 3H, 1xCH₃) ppm. ¹³C-NMR (100 MHz, CDCl₃): $\delta = 135.9$ (C_q), 131.5 (C_q), 124.4 (CH), 123.9 (CH), 62.8 (CH₂), 39.8 (CH₂), 32.9 (CH₂), 26.8 (CH₂), 25.8 (CH₃), 24.4 (CH₂), 17.8 (CH₃), 16.1 (CH₃) ppm. GC (HP 5): $I = 1437$. MS (EI, 70 eV): m/z (%) = 182 (4) [M]⁺, 147 (9), 139 (60), 123 (26), 109 (10), 95 (79), 81 (14), 69 (100), 55 (19), 41 (38).

Synthesis of (*E*)-5,9-dimethyldeca-4,8-dienal (**11**)

The alcohol **10** (2.2 g, 12.1 mmol, 1.0 eq.) was dissolved in abs. DMSO (60 mL) and IBX (4.15 g, 14.7 mmol, 1.2 eq.) was added in one portion. The reaction mixture was stirred for 2 h at room temperature, hydrolyzed with water (200 mL) and extracted three times with ethyl acetate (200 mL). The organic phase was washed twice with saturated aqueous NaHCO₃ solution. The combined organic layers were dried with MgSO₄ and concentrated under reduced pressure. Column chromatography with cyclohexane/ethyl acetate (10:1) yielded the desired aldehyde (**11**) (1.93 g, 11.1 mmol, 92%) as pale yellow oil.

TLC (hexane/ethyl acetate 5:1): $R_f = 0.63$. ¹H-NMR (400 MHz, CDCl₃, TMS): $\delta = 9.74$ (t, 1H, $^3J_{H,H} = 1.7$ Hz, 1xCH), 5.12-5.02 (m, 2H, 2xCH), 2.47-2.42 (m, 2H, 1xCH₂), 2.35-2.28 (m, 2H, 1xCH₂), 2.08-1.94 (m, 4H, 2xCH₂), 1.66 (d, 3H, $^4J_{H,H} = 1.1$ Hz, 1xCH₃), 1.61 (m, 3H, 1xCH₃), 1.59 (s, 3H, 1xCH₃) ppm. ¹³C-NMR (100 MHz, CDCl₃): $\delta = 202.7$ (CHO), 136.9 (C_q), 131.6 (C_q), 124.2 (CH), 122.1 (CH), 44.1 (CH₂), 39.7 (CH₂), 26.7 (CH₂), 25.8 (CH₃), 21.0 (CH₂), 17.8 (CH₃), 16.1 (CH₃) ppm. GC (HP 5): $I = 1376$. MS (EI, 70 eV): m/z (%) = 180 (3) [M]⁺, 162 (2), 147 (6), 137 (21), 121 (8), 109 (6), 93 (28), 81 (9), 69 (100), 55 (23), 41 (34).

Synthesis of (1-¹³C)-(*E*)-6,10-dimethylundeca-5,9-dien-2-ol (**12**)

Mg (106 mg, 5.75 mmol, 1.0 eq.) was covered with dry Et₂O (1 mL) in a flame-dried flask and (¹³C)MeI (797 mg, 5.75 mmol, 1.0 eq.) in abs. Et₂O (5.2 mL) was added dropwise. After consumption of the Mg the aldehyde **11** (936 mg, 5.75 mmol, 1.0 eq.) was added dropwise at 0 °C and the reaction mixture was stirred overnight. The reaction mixture was hydrolyzed with saturated aqueous NH₄Cl solution (50 mL) and extracted three times with ethyl acetate

(100 mL). The combined organic layers were dried with MgSO_4 and concentrated under reduced pressure. Column chromatography on silica gel with cyclohexane/ethyl acetate (8:1) yielded the desired alcohol **12** (824 mg, 4.2 mmol, 73%) as pale yellow oil.

TLC (cyclohexane/ethyl acetate 3:1): $R_f = 0.39$. $^1\text{H-NMR}$ (400 MHz, CDCl_3 , TMS): $\delta = 5.16$ - 5.10 (m, 1H, 1xCH), 5.10 - 5.04 (m, 1H, 1xCH), 3.78 (qtd, 1H, 1xCH, $^3J_{\text{H,H}} = 6.2$ Hz, $^3J_{\text{H,H}} = 6.2$ Hz, $^2J_{\text{C,H}} = 1.0$ Hz), 2.15 - 1.95 (m, 6H, 3xCH₂), 1.67 (d, 3H, $^4J_{\text{H,H}} = 1.0$ Hz, 1xCH₃), 1.61 (d, 3H, $^4J_{\text{H,H}} = 1.0$ Hz, 1xCH₃), 1.59 (s, 3H, 1xCH₃), 1.55 - 1.41 (m, 2H, 1xCH₂), 1.17 (dd, 3H, $^3J_{\text{H,H}} = 6.11$ Hz, $^1J_{\text{C,H}} = 124.9$ Hz, 1xCH₃) ppm. $^{13}\text{C-NMR}$ (100 MHz, CDCl_3): $\delta = 135.7$ (C_q), 131.5 (C_q), 124.4 (CH), 124.1 (CH), 68.0 (d, $^1J_{\text{C,C}} = 38.5$ Hz, CH), 39.8 (CH₂), 39.3 (CH₂), 26.8 (CH₂), 25.8 (CH₃), 24.5 (d, $^3J_{\text{C,C}} = 2.6$ Hz, CH₂), 23.6 ($^{13}\text{CH}_3$), 17.8 (CH₃), 16.1 (CH₃) ppm. GC (HP 5): $I = 1460$. MS (EI, 70 eV): m/z (%) = 197 (3) [M]⁺, 179 (5), 164 (7), 154 (38), 123 (30), 110 (89), 95 (19), 82 (28), 69 (100), 55 (33), 46 (35), 41 (83).

Synthesis of (1- ^{13}C)geranylacetone (**3c**)

The alcohol **12** (610 mg, 3.1 mmol, 1.0 eq.) was dissolved in abs. DMSO (15 mL) and IBX (962 mg, 3.41 mmol, 1.1 eq.) was added in one portion. The reaction mixture was stirred overnight at room temperature, hydrolyzed with water (50 mL) and extracted three times with diethyl ether (100 mL). The organic phase was washed twice with saturated aqueous NaHCO_3 solution. The combined organic layers were dried with MgSO_4 and concentrated under reduced pressure. Column chromatography with cyclohexane/ethyl acetate (5:1) yielded the desired methyl ketone **3c** (559 mg, 2.87 mmol, 93 %) as pale yellow oil.

NMR data are presented in Tables 1 and 2 of SI.

Synthesis of (14-¹³C)FPP

Due to the high costs of ethyl (4-¹³C)acetoacetate the synthesis of (14-¹³C)FPP was also performed via an alternative route (Figure 5 of SI). The allyl alcohol **13** was converted into ethyl 5-methylhex-4-enoate (**14**) via a Claisen orthoester rearrangement. The ester **14** was then converted into the Weinreb amide **15** via a standard method, followed by a reaction with freshly prepared (¹³C)methylmagnesium iodide to yield the methyl ketone **3b** that was further converted into (14-¹³C)FPP using the strategy presented in Figure 1 of SI.

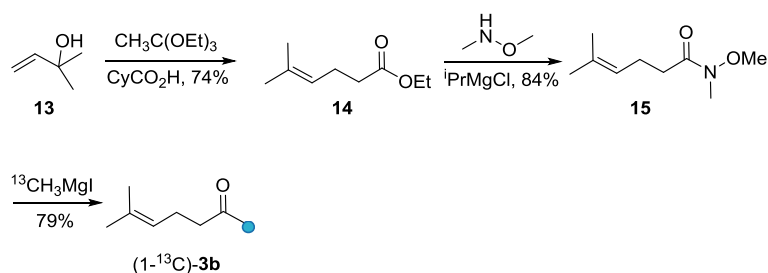


Figure 5. Alternative synthesis of (1-¹³C)-6-methyl-5-hepten-2-one (**3b**).

Synthesis of ethyl 5-methylhex-4-enoate (**14**)

According to a literature procedure^[14] a solution of 1,1-dimethylallyl alcohol (**13**) (2.0 g, 23.3 mmol, 1.0 eq.), triethyl orthoacetate (37.8 g, 233 mmol, 10 eq.) and cyclohexanecarboxylic acid (297 mg, 2.32 mmol, 0.1 eq.) was stirred under reflux conditions for 3 h. The reaction mixture was then cooled to room temperature and extracted three times with diethyl ether (100 mL). The combined organic layers were washed with 10 % aqueous HCl, saturated aqueous NaHCO₃ solution, water and brine (each 100 mL). The organic layer was dried with MgSO₄ and concentrated under reduced pressure. The residue was purified by silica gel column chromatography using hexane/ethyl acetate (30:1) as eluent to afford the corresponding ester **14** (6.67 g, 17.1 mmol, 74%).

¹H-NMR (400 MHz, CDCl₃): δ = 5.08-5.02 (m, 1H, CH), 4.08 (q, ³J_{H,H} = 7.1 Hz, 2H, CH₂), 2.28-2.25 (m, 4H, 2xCH₂), 1.65 (d, ⁴J_{H,H} = 0.9 Hz, 3H, CH₃), 1.58 (s, 3H, CH₃), 1.25 (t, ³J_{H,H} = 7.1 Hz, 3H, CH₃) ppm. ¹³C-NMR (100 MHz, CDCl₃): δ = 173.5 (CO), 133.0 (C_q), 122.6 (CH), 60.2 (CH₂), 34.6 (CH₂), 25.7 (CH₃), 23.7 (CH₂), 17.7 (CH₃), 14.3 (CH₃) ppm. GC (HP-5): *I* = 1093. MS (EI, 70 eV): *m/z* (%) = 156 (77), 141 (1), 127 (6), 111 (25), 101 (11), 95 (6), 88 (22), 85 (56), 82 (100), 73 (6), 69 (83), 60 (15), 55 (21), 41 (31).

Synthesis of *N*-methoxy-*N*,5-dimethylhex-4-enamide (**15**)

According to a literature procedure^[15] to a solution of ester **14** (2.58 g, 16.5 mmol, 1 eq.) in dry THF (30 mL) and *N*,*O*-dimethylhydroxylamide hydrochloride (3.03 g, 49.6 mmol, 3 eq.) was slowly added a freshly prepared solution of iPrMgCl in THF (66.1 mL, 66.1 mmol, 1.0 M, 4 eq.) at -20 °C. The mixture was stirred for 30 min at -10 °C and then hydrolyzed with NH₄Cl solution (20 wt % in H₂O, 100 mL), followed by three times extraction with diethyl ether (100 mL). The combined organic layers were dried with MgSO₄ and concentrated under reduced pressure. The resulting residue was purified by flash column chromatography to afford the desired Weinreb amide **15** (2.37 g, 13.9 mmol, 84%).

$^1\text{H-NMR}$ (400 MHz, CDCl_3): δ = 5.14 (tq, $^3J_{\text{H,H}} = 7.2$ Hz, $^4J_{\text{H,H}} = 1.5$ Hz, $^4J_{\text{H,H}} = 1.4$ Hz, 1H, CH), 3.65 (s, 3H, OCH_3), 3.15 (s, 3H, NCH_3), 2.41 (t, $^3J_{\text{H,H}} = 7.6$ Hz, 2H, CH_2), 2.28 (dt, $^3J_{\text{H,H}} = 7.2$ Hz, $^3J_{\text{H,H}} = 7.6$ Hz, 2H, CH_2), 1.66 (d, $^4J_{\text{H,H}} = 1.1$ Hz, 3H, CH_3), 1.60 (s, 3H, CH_3) ppm. $^{13}\text{C-NMR}$ (100 MHz, CDCl_3): δ = 174.4 (CO), 132.7 (C_q), 123.2 (CH), 61.3 (CH_3), 32.2 (CH_2), 25.7 ($2\times\text{CH}_3$), 23.3 (CH_2), 17.7 (CH_3) ppm. GC (HP-5): t_r = 1297. MS (EI, 70 eV): m/z (%) = 171 (31), 140 (12), 111 (25), 103 (19), 98 (10), 83 (50), 79 (3), 73 (7), 69 (100), 61 (69), 55 (33), 41 (36).

Synthesis of (1- ^{13}C)-6-methyl-5-hepten-2-one (**3b**)

To a stirred solution of amide **15** (2.46 g, 13.5 mmol, 1.0 eq.) in dry THF (100 mL) at 0 °C, was added dropwise a solution of freshly prepared $^{13}\text{CH}_3\text{MgI}$ (33.0 mmol, 33 mL, 2.5 eq., 1.0 M in Et_2O). After 2 h stirring at 0 °C, the reaction mixture was hydrolyzed by dropwise addition of 1 M HCl (30 mL). The layers were separated and the aqueous layer was extracted three times with Et_2O (50 mL). The combined organic layers were dried with MgSO_4 , filtered and concentrated under reduced pressure. The resulting residue was purified by flash column chromatography using hexane/ EtOAc (15:1-7:1) as eluent to give the ketone **3b** as colorless oil (1.33g, 10.5 mmol, 79%).

NMR data are presented in Tables 1 and 2 of SI.

Synthesis of (11-¹³C)FPP, (12-¹³C)FPP and (13-¹³C)FPP

For the synthesis of (12-¹³C)FPP and (13-¹³C)FPP with a stereoselective labeling at the terminal (*E*- or *Z*-)methyl groups the strategy shown in Figure 1 is inappropriate. The synthetic route that was used instead to prepare these compounds (Figure 6 of SI) proceeded via an intermediate that could also be used to prepare (11-¹³C)FPP in just a few steps that was therefore also not made via the route of Figure 1 of SI.

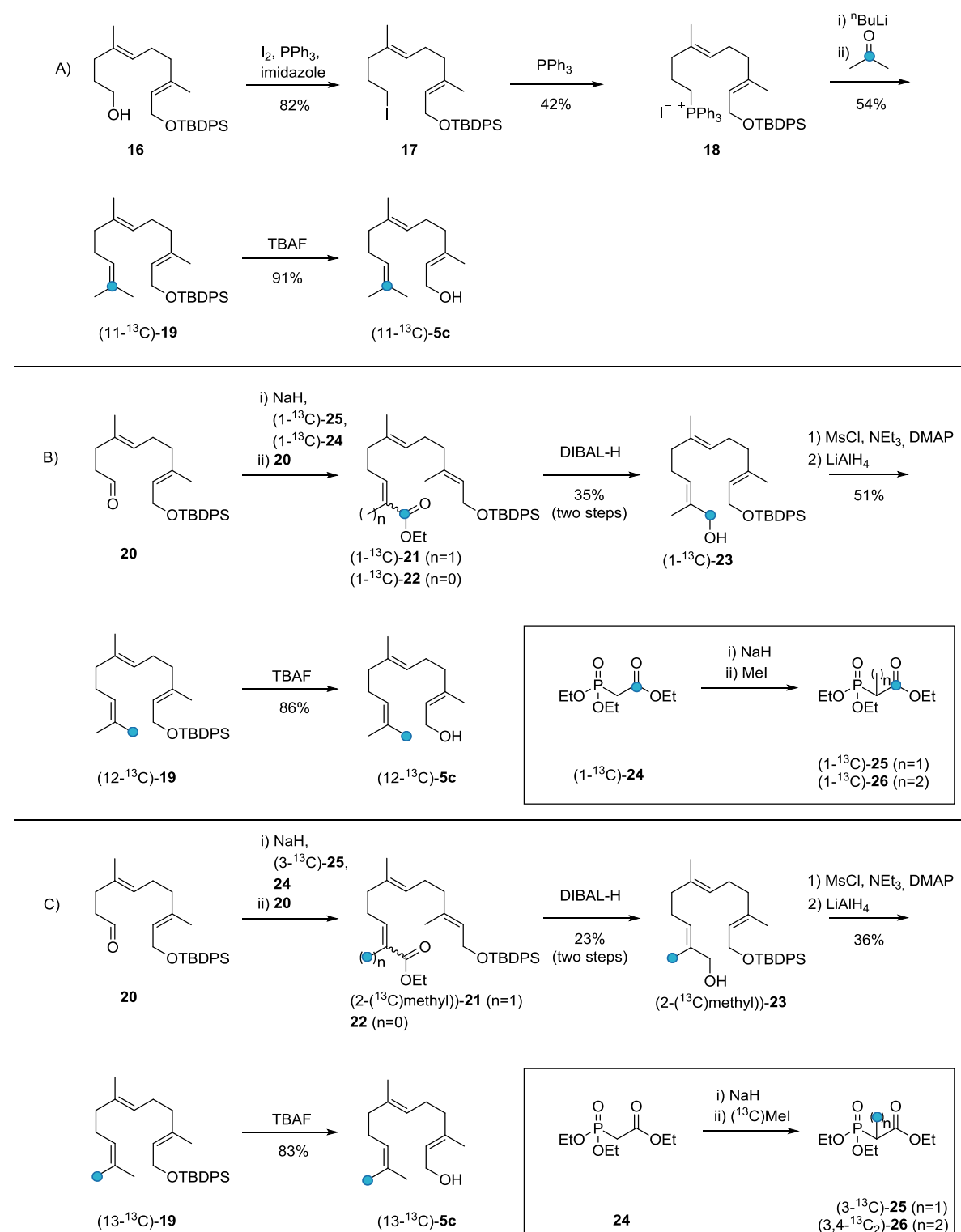


Figure 6. Alternative synthesis of A) (11-¹³C)-5c, B) (12-¹³C)-5c and C) (13-¹³C)-5c.

Briefly, for the synthesis of (11-¹³C)FPP alcohol **16**^[16] was converted into the iodide **17** with I₂, PPh₃ and imidazole, followed by conversion into the Wittig salt **18**. A Wittig reaction with (2-¹³C)acetone resulted in **19** that was deprotected with TBAF to yield (11-¹³C)-**5c**. The transformation into (11-¹³C)FPP was performed as shown in Figure 1.

Labeling of the terminal methyl groups was introduced via a HWE reaction of aldehyde **20**^[16] with (1-¹³C)- and (3-¹³C)triethylphosphonopropionate, made from commercially available (1-¹³C)triethylphosphonoacetate and methyl iodide respectively triethylphosphonoacetate and (¹³C)methyl iodide.^[17] The esters **21** were reduced to alcohol **23** using DIBAL-H and further defunctionalized via reduction of the mesylate with LiAlH₄^[18] to **19**. Both isotopomers were deprotected with TBAF to give (12-¹³C)- and (13-¹³C)-**5c** which were converted into the corresponding diphosphates **8** (Figure 1 of SI).

Synthesis of *tert*-butyl(((2*E*,6*E*)-10-iodo-3,7-dimethyldeca-2,6-dien-1-yl)oxy)diphenylsilane (**17**)

As described in the literature,^[19] PPh₃ (2.38 g, 9.1 mmol, 1.2 eq.) was dissolved in abs. CH₂Cl₂ (40 mL) and added imidazole (640 mg, 9.1 mmol, 1.2 eq.). After that alcohol **16** (3.30 g, 7.6 mmol, 1.0 eq.), which was synthesized via a literature-known procedure starting from farnesol,^[16] was added dropwise. After addition of I₂ (2.30 g, 9.1 mmol, 1.2 eq.), the mixture was stirred 2 h at room temperature, concentrated under reduced pressure and purified by column chromatography [cyclohexane/ethyl acetate (20:1)] to give iodide **17** (3.40 g, 6.2 mmol, 82%) as a colorless oil.

TLC (hexane/ethyl acetate 20:1): *R*_f = 0.90. ¹H-NMR (400 MHz, CDCl₃, TMS): δ = 7.74-7.68 (m, 4H, CH), 7.45-7.35 (m, 6H, CH), 5.43-5.36 (m, 1H, CH), 5.22-5.15 (m, 1H, CH), 4.23 (d, ³*J* = 6.2 Hz, 2H, CH₂), 3.14 (t, ³*J* = 7.0 Hz, 2H, CH₂), 2.14-1.97 (m, 6H, 3xCH₂), 1.95-1.86 (m, 2H, CH₂), 1.60 (s, 3H, CH₃), 1.45 (s, 3H, CH₃), 1.06 (s, 9H, 3xCH₃) ppm. ¹³C-NMR (101 MHz, CDCl₃): δ = 137.0 (C_q), 135.8 (4xCH), 134.2 (2xC_q), 133.2 (C_q), 129.6 (2xCH), 127.7 (4xCH), 125.7 (CH), 124.4 (CH), 61.3 (CH₂), 40.2 (CH₂), 39.5 (CH₂), 31.7 (CH₂), 27.0 (3xCH₃), 26.4 (CH₂), 19.3 (C_q), 16.5 (CH₃), 16.0 (CH₃), 6.8 (CH₂) ppm.

Synthesis of ((4*E*,8*E*)-10-((*tert*-butyldiphenylsilyl)oxy)-4,8-dimethyldeca-4,8-dien-1-yl)-triphenylphosphonium iodide (**18**)

The iodide **17** (3.40 g, 6.2 mmol, 1.0 eq.) and PPh₃ (2.00 g, 7.4 mmol, 1.2 eq.) were dissolved in abs. toluene (30 mL) and heated for 16 h under reflux conditions. The mixture was concentrated under reduced pressure. Column chromatography [CH₂Cl₂/MeOH (20:1)] yielded the Wittig salt **18** (2.10 g, 2.3 mmol, 42%) as a yellow gel.

TLC (CH₂Cl₂/MeOH 10:1): *R*_f = 0.52. ¹H-NMR (300 MHz, CD₂Cl₂, TMS): δ = 7.89-7.64 (m, 19H, 19xCH), 7.43-7.32 (m, 6H, 6xCH), 5.37 (tq, ³*J* = 6.4 Hz, ⁴*J* = 1.2 Hz, 1H, CH), 5.19 (t, ³*J* = 6.9 Hz, 1H, CH), 4.19 (d, ³*J* = 6.4 Hz, 2H, CH₂), 3.44-3.31 (m, CH₂), 2.27 (t, ³*J* = 7.1 Hz, 2H, CH₂), 2.14-2.03 (m, 2H, CH₂), 2.03-1.93 (m, 2H, CH₂), 1.85-1.69 (m, 2H, CH₂), 1.50 (s, 3H, CH₃), 1.45 (s, 3H, CH₃), 1.02 (s, 9H, 3xCH₃) ppm. ¹³C-NMR (75 MHz, CD₂Cl₂): δ = 137.5 (C_q), 135.8 (4xCH), 135.6 (d, *J*_{C,P} = 3.0 Hz, 3xCH), 134.3 (2xC), 133.9 (d, *J*_{C,P} = 10.0 Hz, 6xCH), 132.9 (C_q), 130.8 (d, *J*_{C,P} = 12.6 Hz, 6xCH), 129.8 (2xCH), 127.9 (4xCH), 127.2 (CH), 124.2 (CH), 118.3 (d, ¹*J*_{C,P} = 86.3 Hz, 3xC_q), 61.3 (CH₂), 39.9 (d, *J*_{C,P} = 15.8 Hz, CH₂), 39.6 (CH₂), 26.9 (3xCH₃), 26.7 (CH₂), 22.5 (d, *J*_{C,P} = 51.2 Hz, CH₂), 20.8 (d, *J*_{C,P} = 4.0 Hz, CH₂), 19.3 (C_q), 16.4 (CH₃), 15.8 (CH₃) ppm.

Synthesis of (11-¹³C)*tert*-butyldiphenyl(((2*E*,6*E*)-3,7,11-trimethyldodeca-2,6,10-trien-1-yl)-oxy)silane (**19**)

Wittig salt **18** (2.10 g, 2.3 mmol, 1.0 eq.) was dissolved in abs. THF (20 mL) and cooled to 0 °C. A solution of *n*-butyllithium (1.6 M in hexane, 1.6 mL, 2.5 mmol, 1.1 eq.) was added dropwise and the mixture was stirred for 90 min at 0 °C. After cooling to -78 °C, (2-¹³C)acetone (133 mg, 2.3 mmol, 1.0 eq.) was added slowly and stirring was continued overnight at constant temperature. The reaction was quenched with H₂O (20 mL) and the mixture was extracted three times with Et₂O. The combined organic layers were dried over MgSO₄, concentrated under reduced pressure and purified by column chromatography [cyclohexane/ethyl acetate (20:1)] to give the protected farnesol **19** (0.57 g, 1.2 mmol, 54%) as colorless oil.

TLC (hexane/ethyl acetate 20:1): *R*_f = 0.69. ¹H-NMR (300 MHz, CDCl₃, TMS): δ = 7.74-7.67 (m, 4H, 4xCH), 7.46-7.34 (m, 6H, 6xCH), 5.40 (tq, ³*J* = 6.3 Hz, ⁴*J* = 1.1 Hz, 1H, CH), 5.17-5.06 (m, 2H, 2xCH), 4.23 (d, ³*J* = 6.3 Hz, 2H, CH₂), 2.14-2.04 (m, 4H, 2xCH₂), 2.03-1.94 (m, 4H, 2xCH₂), 1.69 (d, ²*J*_{C,H} = 6.2 Hz, 3H, CH₃), 1.61 (s, 3H, CH₃), 1.60 (d, ²*J*_{C,H} = 4.2 Hz, 3H, CH₃), 1.45 (s, 3H, CH₃), 1.05 (s, 9H, 3xCH₃) ppm. ¹³C-NMR (75 MHz, CDCl₃): δ = 137.2 (C_q), 135.8 (4xCH), 135.3 (C_q), 134.3 (2xC_q), 131.4 (¹³C_q), 129.6 (2xCH), 127.7 (4xCH), 124.5 (d, ¹*J*_{C,C} = 73.8 Hz, CH), 124.2 (CH), 124.1 (CH), 61.3 (CH₂), 39.9 (d, ²*J*_{C,C} = 3.6 Hz, CH₂), 39.7 (CH₂), 27.0 (3xCH₃), 26.9 (CH₂), 26.5 (CH₂), 25.9 (d, ¹*J*_{C,C} = 43.1 Hz, CH₃), 19.3 (C_q), 17.8 (d, ¹*J*_{C,C} = 42.2 Hz, CH₃), 16.5 (CH₃), 16.2 (CH₃) ppm. GC (HP 5): *I* = 3045. MS (EI, 70 eV): *m/z* (%) = 405 (4), 404 (11), 326 (3), 205 (4), 204 (12), 201 (15), 200 (53), 199 (100), 197 (8), 188 (4), 181 (7), 176 (4), 135 (18), 121 (4), 110 (3), 105 (2), 93 (3), 81 (4), 77 (7), 70 (19), 42 (5), 41 (5).

Synthesis of (11-¹³C)farnesol (**5c**)

The oxysilane (11-¹³C)-**19** (570 mg, 1.24 mmol, 1.0 eq.) was dissolved in abs. THF (10 mL) and cooled to 0 °C. A solution of TBAF in THF (1.0 M, 1.5 mL, 1.5 mmol, 1.2 eq.) was added dropwise. The reaction mixture was stirred for 2.5 h at 0 °C, diluted with H₂O (10 mL) and extracted three times with Et₂O. After drying of the combined organic layers over MgSO₄ and concentration of the solution under reduced pressure, column chromatography [cyclohexane/ethyl acetate (8:1)] yielded the desired alcohol (11-¹³C)-**5c** as colorless liquid.

NMR data are presented in Tables 3 and 4 of SI.

Synthesis of (1-¹³C)- and (2-(¹³C)methyl)-(2*E*,6*E*,10*E*)-12-((*tert*-butyldiphenylsilyl)oxy)-2,6,10-trimethyldodeca-2,6,10-trien-1-ol (**23**)

A suspension of 60% NaH in mineral oil (542 mg, 13.6 mmol, 2.0 eq.) was suspended in abs. THF (35 mL) and cooled to 0 °C. After that, (1-¹³C)triethyl phosphonopropionate, prepared from (1-¹³C)triethyl phosphonoacetate by methylation with methyl iodide (vide infra) and contaminated with inseparable starting material and (1-¹³C)-2-methyltriethylphosphonopropionate, (2.92 g) was added dropwise and the reaction mixture was stirred for 1 h at 0 °C, cooled to -78 °C and aldehyde **20** (2.95 g, 6.8 mmol, 1.0 eq., synthesized according to ref. 16) was added slowly. The reaction was stirred at -78 °C for 19 h, warmed to room temperature and quenched with H₂O (40 mL). The mixture was extracted with Et₂O (three times), the organic layers were dried with MgSO₄ and concentrated under reduced pressure. Column chromatography gave a mixture of the two

diastereomeric esters (*E*)- and (*Z*)-(1-¹³C)-**21** and (1-¹³C)-**22** as colorless oil that was inseparable by column chromatography and used directly in the next step.

The mixture of esters (*E*)- and (*Z*)-(1-¹³C)-**21** and (1-¹³C)-**22** (3.40 g) was dissolved in THF (65 mL) and cooled to -78 °C. A 1 M solution of DIBAL-H in hexane (15.7 mL, 15.7 mmol) was added slowly and cooling was removed. The reaction mixture was stirred for 3 h and hydrolysed by addition of saturated aqueous Na-K-tartrate solution (70 mL). The mixture was extracted four times with Et₂O (100 mL), the organic layers were washed with Na-K-tartrate solution, dried with MgSO₄ and concentrated under reduced pressure. Repeated column chromatography gave the desired pure alcohol (1-¹³C)-**23** (1.12 g, 2.3 mmol, 35% over two steps) as colorless oil.

TLC (hexane/ethyl acetate 3:1): *R*_f = 0.44. ¹H-NMR (400 MHz, CDCl₃, TMS): δ = 7.74-7.68 (m, 4H, 4xCH), 7.45-7.35 (m, 6H, 6xCH), 5.43-5.35 (m, 2H, 2xCH), 5.13 (tq, ³*J* = 6.7 Hz, ⁴*J* = 1.2 Hz, 1H, CH), 4.23 (d, ³*J* = 6.3 Hz, 2H, CH₂), 3.99 (d, ¹*J*_{C,H} = 141.5 Hz, 2H, CH₂), 2.18-1.96 (m, 8H, 4xCH₂), 1.67 (d, ³*J*_{C,H} = 4.2 Hz, 3H, CH₃), 1.61 (s, 3H, CH₃), 1.44 (s, 3H, CH₃), 1.05 (s, 9H, 3xCH₃) ppm. ¹³C-NMR (101 MHz, CDCl₃): δ = 137.1 (C_q), 135.8 (4xCH), 134.9 (C_q), 134.8 (d, ¹*J*_{C,C} = 45.8 Hz, C_q), 134.2 (2xC_q), 129.6 (2xCH), 127.7 (4xCH), 126.2 (d, ²*J*_{C,C} = 3.5 Hz, CH), 124.5 (CH), 124.2 (CH), 69.2 (¹³CH₂), 61.3 (CH₂), 39.6 (CH₂), 39.4 (CH₂), 27.0 (3xCH₃), 26.4 (CH₂), 26.3 (d, ³*J*_{C,C} = 4.8 Hz, CH₂), 19.3 (C_q), 16.5 (CH₃), 16.2 (CH₃), 13.8 (d, ²*J*_{C,C} = 4.5 Hz, CH₃) ppm.

The synthesis of (2-(¹³C)methyl)-**23** was performed in a similar way, only unlabeled triethyl phosphonoacetate was methylated with (¹³C)methyl iodide in the preparation of (3-¹³C)triethyl phosphonopropionate (**25**, vide infra). Yield: 1.15 g, 2.41 mmol (23% over two steps).

¹H-NMR (400 MHz, CDCl₃, TMS): δ = 7.74-7.67 (m, 4H, 4xCH), 7.45-7.35 (m, 6H, 6xCH), 5.44-5.36 (m, 2H, 2xCH), 5.14 (tq, ³*J* = 6.7 Hz, ⁴*J* = 1.1 Hz, 1H, CH), 4.23 (d, ³*J* = 6.3 Hz, 2H, CH₂), 3.99 (d, ³*J*_{C,H} = 2.8 Hz, 2H, CH₂), 2.19-1.95 (m, 8H, 4xCH₂), 1.67 (d, ¹*J*_{C,H} = 126.1 Hz, 3H, CH₃), 1.62 (s, 3H, CH₃), 1.45 (s, 3H, CH₃), 1.41 (br s, 1H, OH), 1.05 (s, 9H, 3xCH₃) ppm. ¹³C-NMR (101 MHz, CDCl₃): δ = 137.1 (C_q), 135.8 (4xCH), 134.9 (C_q), 134.8 (d, ¹*J*_{C,C} = 43.2 Hz, C_q), 134.2 (2xC_q), 129.6 (2xCH), 127.7 (4xCH), 126.2 (d, ²*J*_{C,C} = 1.6 Hz, CH), 124.4 (CH), 124.2 (CH), 69.1 (d, ²*J*_{C,C} = 4.5 Hz, CH₂), 61.3 (CH₂), 39.6 (CH₂), 39.4 (CH₂), 27.0 (3xCH₃), 26.4 (CH₂), 26.4 (d, ³*J*_{C,C} = 3.5 Hz, CH₂), 19.3 (C_q), 16.5 (CH₃), 16.2 (CH₃), 13.8 (¹³CH₃) ppm.

Synthesis of (12-¹³C)- and (13-¹³C)*tert*-butyldiphenyl(((2*E*,6*E*)-3,7,11-trimethyldodeca-2,6,10-trien-1-yl)oxy)silane (**19**)

Following a known procedure,^[18] alcohol (1-¹³C)-**23** (1100 mg, 2.31 mmol, 1.0 eq.) was dissolved in CH₂Cl₂ (70 mL) and cooled to 0 °C. To the solution was added Et₃N (467 mg, 4.61 mmol, 2.0 eq.), DMAP (564 mg, 4.61 mmol, 2.0 eq.) and slowly MsCl (529 mg, 4.61 mmol, 2.0 eq.). After stirring 1 h at 0 °C, another portion of Et₃N (2.0 eq) and MsCl (2.0 eq) was added. After additional 40 min, the reaction mixture was stirred 2 h at room temperature, poured into ice water (100 mL) and was extracted six times with hexane. The combined organic layers were sequentially washed with 5%-HCl solution and saturated aqueous solutions of NaHCO₃ and NaCl. After drying over MgSO₄, solvent was removed under reduced pressure to give the crude mesylate as yellowish oil. This material was used without further purification and added slowly to a suspension of LiAlH₄ (1.60 g, 42.1 mmol, 18.3 eq.) in THF (380 mL). The reaction mixture was stirred for 2 h at room temperature and quenched by slow addition of ethyl acetate (saturated with H₂O, 200 mL). After stirring over night, saturated aqueous NH₄Cl solution (300 mL) was added, the suspension was filtered and extracted four times with hexane. The combined organic layers were dried with MgSO₄ and concentrated under reduced pressure. Column chromatography [cyclohexane/ethyl

acetate (20:1)] gave the protected farnesol (12-¹³C)-**19** (545 mg, 1.18 mmol, 51%) as colorless oil.

TLC (hexane/ethyl acetate 20:1): R_f = 0.69. ¹H-NMR (400 MHz, CDCl₃, TMS): δ = 7.73-7.67 (m, 4H, 4xCH), 7.45-7.34 (m, 6H, 6xCH), 5.39 (tq, ³ J = 6.3 Hz, ⁴ J = 1.2 Hz, 1H, CH), 5.16-5.06 (m, 2H, 2xCH), 4.23 (d, ³ J = 6.3 Hz, 2H, CH₂), 2.13-2.03 (m, 4H, 2xCH₂), 2.03-1.95 (m, 4H, 2xCH₂), 1.67 (dq, ¹ $J_{C,H}$ = 125.1 Hz, ⁴ J = 1.0 Hz, 3H, CH₃), 1.62-1.59 (m, 6H, 2xCH₃), 1.45 (s, 3H, CH₃), 1.05 (s, 9H, 3xCH₃) ppm. ¹³C-NMR (101 MHz, CDCl₃): δ = 137.2 (C_q), 135.8 (4xCH), 135.3 (C_q), 134.3 (2xC_q), 131.4 (d, ¹ $J_{C,C}$ = 43.1 Hz, C_q), 129.6 (2xCH), 127.7 (4xCH), 124.5 (d, ² $J_{C,C}$ = 3.1 Hz, CH), 124.2 (CH), 124.1 (CH), 61.3 (CH₂), 39.9 (CH₂), 39.7 (CH₂), 27.0 (3xCH₃), 26.9 (d, ³ $J_{C,C}$ = 4.6 Hz, CH₂), 26.5 (CH₂), 25.9 (¹³CH₃), 19.3 (C_q), 17.9 (d, ² $J_{C,C}$ = 4.5 Hz, CH₃), 16.5 (CH₃), 16.2 (CH₃) ppm. GC (HP 5): I = 3029. MS (EI, 70 eV): m/z (%) = 405 (5), 404 (17), 326 (3), 251 (3), 205 (6), 204 (20), 201 (26), 200 (82), 199 (100), 197 (16), 188 (8), 183 (7), 181 (13), 176 (8), 161 (3), 137 (8), 135 (29), 123 (4), 121 (10), 119 (3), 110 (6), 107 (3), 105 (5), 95 (3), 93 (4), 91 (3), 81 (7), 77 (12), 70 (33), 68 (6), 67 (5), 55 (3), 42 (10), 41 (10).

For the synthesis of (13-¹³C)-**19** the same procedure starting from (2-(¹³C)methyl)-**23** was used. Yield: 398 mg, 0.86 mmol (36%).

¹H-NMR (400 MHz, CDCl₃, TMS): δ = 7.73-7.67 (m, 4H, 4xCH), 7.45-7.35 (m, 6H, 6xCH), 5.40 (tq, ³ J = 6.3 Hz, ⁴ J = 1.2 Hz, 1H, CH), 5.16-5.06 (m, 2H, 2xCH), 4.23 (d, ³ J = 6.3 Hz, 2H, CH₂), 2.13-2.03 (m, 4H, 2xCH₂), 2.03-1.95 (m, 4H, 2xCH₂), 1.69 (d, ³ $J_{C,H}$ = 3.9 Hz, 3H, CH₃), 1.61 (s, 3H, CH₃), 1.60 (d, ¹ $J_{C,H}$ = 129.3 Hz, 3H, CH₃), 1.45 (s, 3H, CH₃), 1.05 (s, 9H, 3xCH₃) ppm. ¹³C-NMR (101 MHz, CDCl₃): δ = 137.2 (C_q), 135.8 (4xCH), 135.3 (C_q), 134.3 (2xC_q), 131.4 (d, ¹ $J_{C,C}$ = 42.2 Hz, C_q), 129.6 (2xCH), 127.7 (4xCH), 124.5 (d, ² $J_{C,C}$ = 2.0 Hz, CH), 124.2 (CH), 124.1 (CH), 61.3 (CH₂), 39.9 (CH₂), 39.7 (CH₂), 27.0 (3xCH₃), 26.9 (d, ³ $J_{C,C}$ = 3.6 Hz, CH₂), 26.5 (CH₂), 25.9 (d, ² $J_{C,C}$ = 4.5 Hz, CH₃), 19.3 (C_q), 17.9 (¹³CH₃), 16.5 (CH₃), 16.2 (CH₃) ppm. MS (EI, 70 eV): m/z (%) = 404 (5), 199 (100), 181 (3), 135 (6), 77 (3), 70 (9), 42 (3), 41 (3).

Synthesis of (12-¹³C)- and (13-¹³C)farnesol (**5c**)

The oxysilanes (12-¹³C)-**19** (527 mg, 1.14 mmol) and (13-¹³C)-**19** (398 mg, 0.86 mmol) were converted into farnesols (12-¹³C)-**5c** (218 mg, 0.98 mmol, 86%) and (13-¹³C)-**5c** (160 mg, 0.72 mmol, 83%) with TBAF following the same procedure as described above for (11-¹³C)-**19**. NMR data for both isotopomers are presented in Tables 3 and 4.

Synthesis of (1-¹³C)- and (3-¹³C)triethylphosphonopropionate (**25**)

According to the literature,^[17] a suspension of 60% NaH in mineral oil (658 mg, 16.45 mmol, 1.03 eq.) was suspended in abs. THF (9 mL) and cooled to 0 °C. After that a solution of (1-¹³C)triethylphosphonoacetate **24** (3.60 g, 16.0 mmol, 1.00 eq.) in dry THF (9 mL) was added slowly during a period of 20 min. The reaction was stirred at room temperature for 2.5 h, cooled to -5 °C and added a solution of MeI (2.39 g, 16.87 mmol, 1.06 eq.) in abs. THF (9 mL) during 10 min. The mixture was stirred for additional 1 h at room temperature, quenched by addition of H₂O (14 mL) and extracted four times with CH₂Cl₂. The combined organic layers were dried over MgSO₄ and concentrated under reduced pressure to give an inseparable mixture of the starting material (1-¹³C)-**24** and the two methylation products (1-¹³C)-**25** and (1-¹³C)-**26** (2.94 g) as a yellow, biphasic oil.

Analytical data for main compound (1-¹³C)-**25** in the mixture are: ¹H-NMR (500 MHz, CDCl₃, TMS): δ = 4.25-4.10 (m, 6H, 3xCH₂), 3.01 (ddq, ² $J_{H,P}$ = 23.4 Hz, ² $J_{H,C}$ = 7.7 Hz, ³ $J_{H,H}$ = 7.4 Hz, 1H, CHMe), 1.48-1.39 (m, 3H, CH₃), 1.36-1.23 (m, 9H, 3xCH₃) ppm. ¹³C-NMR (126 MHz, CDCl₃): δ = 169.9 (d, ² $J_{C,P}$ = 4.7 Hz, ¹³CO), 62.8 (d, ² $J_{C,P}$ = 6.6 Hz, 2xCH₂), 61.5 (d, ² $J_{C,C}$ =

2.6 Hz, CH₂), 39.5 (dd, ¹J_{C,P} = 133.4 Hz, ¹J_{C,C} = 57.1 Hz, CH), 16.6-16.4 (m, 2xCH₃), 14.2 (d, ³J_{C,C} = 2.0 Hz, CH₃), 11.8 (dd, ²J_{C,P} = 6.3 Hz, ²J_{C,C} = 1.9 Hz, CH₃) ppm. ³¹P-NMR (203 MHz, CDCl₃): δ = 23.8 (d, ²J_{C,P} = 4.7 Hz) ppm. GC (HP 5): *I* = 1428. MS (EI, 70 eV): *m/z* (%) = 239 (10), 212 (17), 210 (9), 194 (70), 193 (13), 166 (84), 165 (34), 164 (9), 155 (41), 139 (16), 138 (85), 137 (32), 136 (15), 127 (37), 120 (13), 111 (38), 109 (100), 103 (34), 99 (54), 92 (18), 91 (32), 82 (20), 81 (65), 75 (20), 65 (27), 57 (30), 56 (29), 45 (22), 43 (7).

(3-¹³C)Triethylphosphonopropionate (**25**) was synthesized with the same procedure using triethylphosphonoacetate and (¹³C)methyl iodide.

Analytical data for main compound (3-¹³C)-**25** in the mixture are: ¹H-NMR (400 MHz, CDCl₃, TMS): δ = 4.21-4.04 (m, 6H, 3xCH₂), 3.02-2.89 (m, 1H, CHMe), 1.59-1.49 (m, 3H, CH₃), 1.31-1.17 (m, 9H, 3xCH₃) ppm. ¹³C-NMR (101 MHz, CDCl₃): δ = 169.7 (d, ²J_{C,P} = 4.6 Hz, CO), 62.6 (d, ²J_{C,P} = 6.7 Hz, 2xCH₂), 61.4 (CH₂), 39.4 (dd, ¹J_{C,P} = 133.5 Hz, ¹J_{C,C} = 32.5 Hz, CH), 16.5-16.3 (m, 2xCH₃), 14.1 (CH₃), 11.7 (d, ²J_{C,P} = 6.3 Hz, ¹³CH₃) ppm. ³¹P-NMR (203 MHz, CDCl₃): δ = 24.3 (d, ²J_{C,P} = 6.3 Hz) ppm. GC (HP 5): *I* = 1430. MS (EI, 70 eV): *m/z* (%) = 239 (9), 212 (26), 210 (13), 194 (89), 193 (18), 167 (40), 166 (98), 165 (18), 155 (42), 138 (100), 137 (33), 127 (31), 110 (42), 109 (51), 103 (27), 99 (41), 81 (41), 75 (14), 65 (14), 57 (14), 44 (14).

Incubation experiments of purified enzyme with (¹³C)FPPs.

For each incubation a 0.5 L 2YT liquid culture (containing kanamycin (50 mg/L)) of *E. coli* BL 21 transformants was inoculated. The cultivation and protein isolation conditions are performed as reported above. Each pure protein fraction from 0.5 L 2YT liquid culture was concentrated with a Vivaspın20 concentration tube (MWCO 30000, Sartorius Stedim, Göttingen) for 0.5 to 1.5 h at 6000 rpm to 2 mL enzyme fraction. Incubation experiments were performed with the pure protein (2 mL) and incubation buffer (2 mL, 50 mM Tris·HCl, 10 mM MgCl₂, 20 % glycerin, pH 7.0) containing the (¹³C)FPP (3 mg, 1.5 mg/mL) at 28 °C overnight. The reaction mixture was extracted with 0.6 mL (²H₈)toluene and directly measured by NMR.

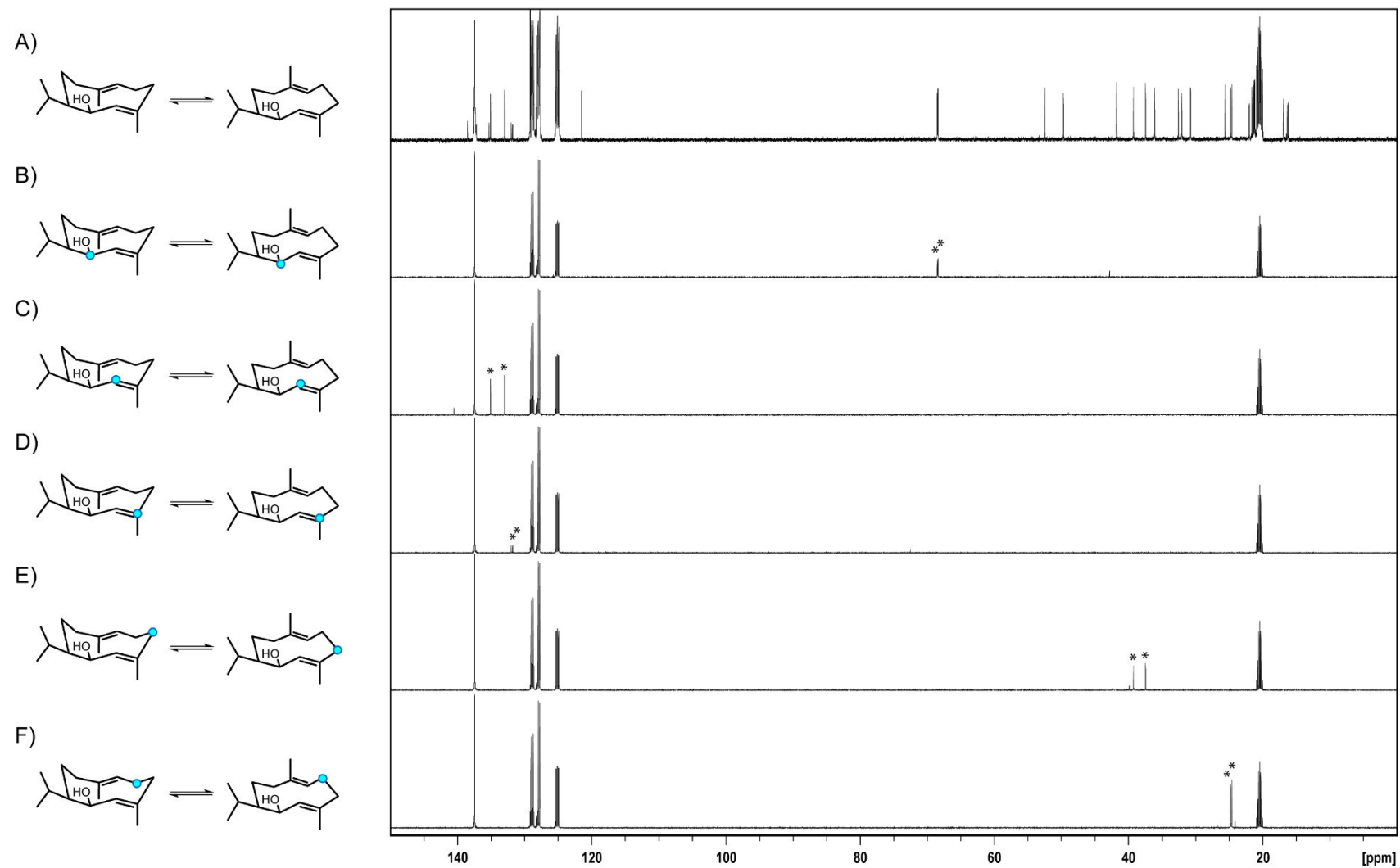


Figure 7. A) ^{13}C -NMR spectrum of unlabelled 1(10)*E*,4*E*,6*S*,7*R*-germacradien-6-ol (**1**), and NMR spectra of isotopomers of ($^{13}\text{C}_1$)-**1** obtained from B) (1- ^{13}C)FPP, C) (2- ^{13}C)FPP, D) (3- ^{13}C)FPP, E) (4- ^{13}C)FPP and F) (5- ^{13}C)FPP. Blue circles indicate ^{13}C -labelled carbons and asterisks indicate signals of ^{13}C -labelled carbons for the two conformers of **1** observed in each experiment. Spectra were recorded in $(^2\text{H}_8)$ toluene.

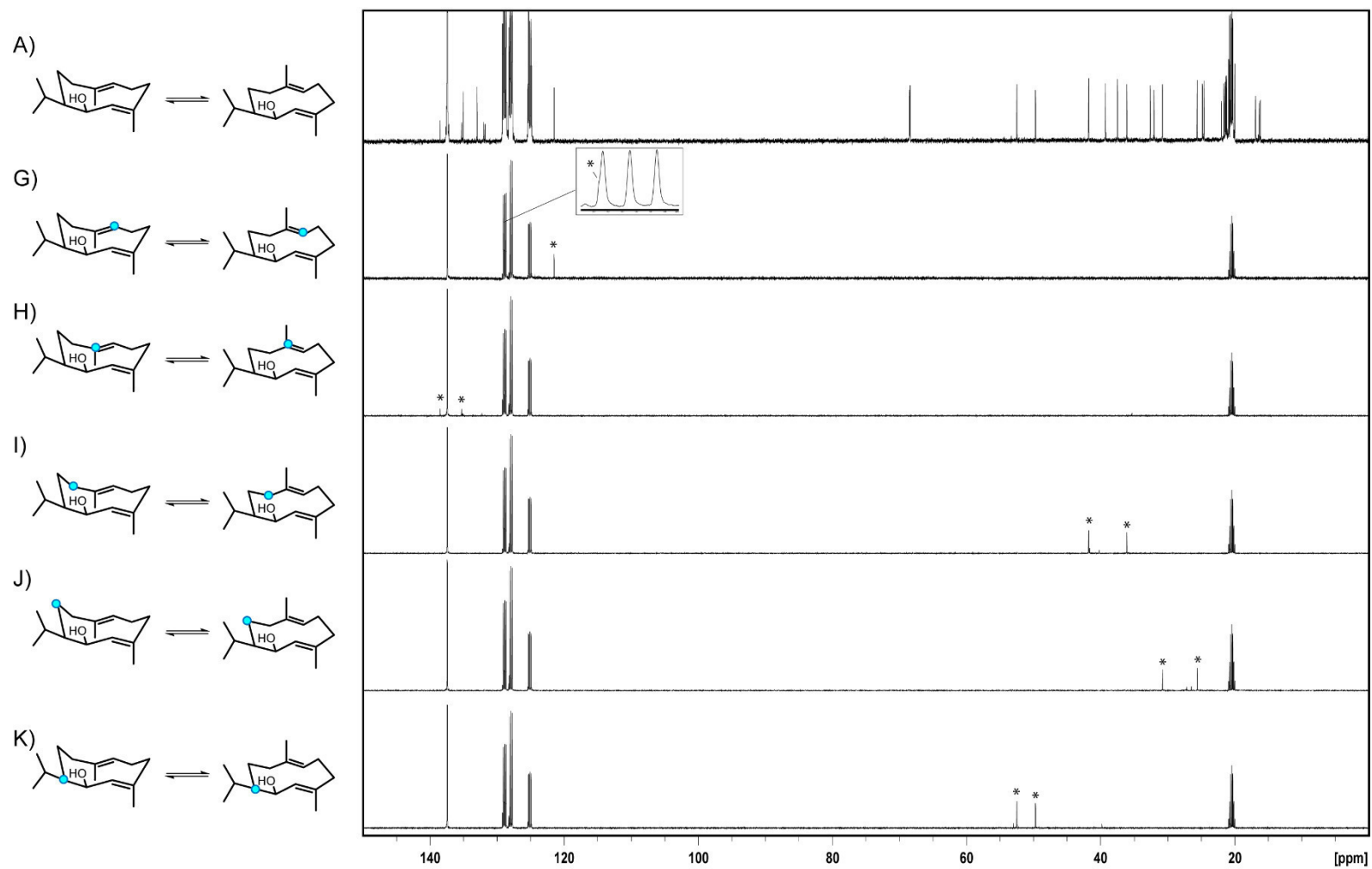


Figure 7. A) ^{13}C -NMR spectrum of unlabelled 1(10)*E*,4*E*,6*S*,7*R*-germacradien-6-ol (**1**), and NMR spectra of isotopomers of ($^{13}\text{C}_1$)-**1** obtained from G) (6- ^{13}C)FPP (one signal observed as a shoulder, a solvent signal (shown in the box), H) (7- ^{13}C)FPP, I) (8- ^{13}C)FPP, J) (9- ^{13}C)FPP and K) (10- ^{13}C)FPP. Blue circles indicate ^{13}C -labeled carbons and asterisks indicate signals of ^{13}C -labelled carbons for the two conformers of **1** observed in each experiment. Spectra were recorded in ($^2\text{H}_8$)toluene.

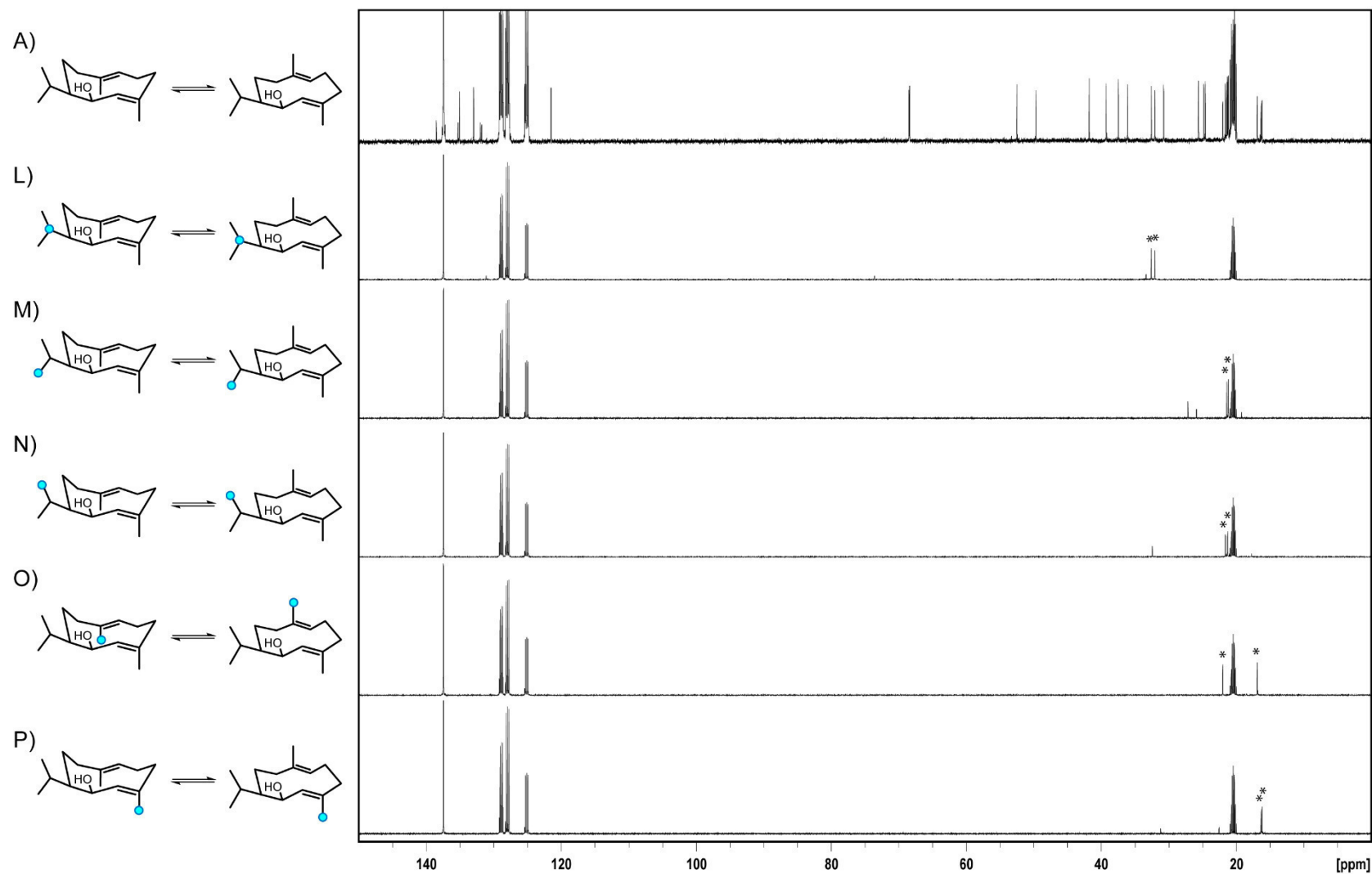


Figure 7. A) ^{13}C -NMR spectrum of unlabelled 1(10)*E*,4*E*,6*S*,7*R*-germacradien-6-ol (**1**), and NMR spectra of isotopomers of ($^{13}\text{C}_1$)-**1** obtained from L) (11- ^{13}C)FPP, M) (12- ^{13}C)FPP, N) (13- ^{13}C)FPP, O) (14- ^{13}C)FPP and P) (15- ^{13}C)FPP. Blue circles indicate ^{13}C -labeled carbons and asterisks indicate signals of ^{13}C -labelled carbons for the two conformers of **1** observed in each experiment. Spectra were recorded in ($^2\text{H}_3$)toluene.

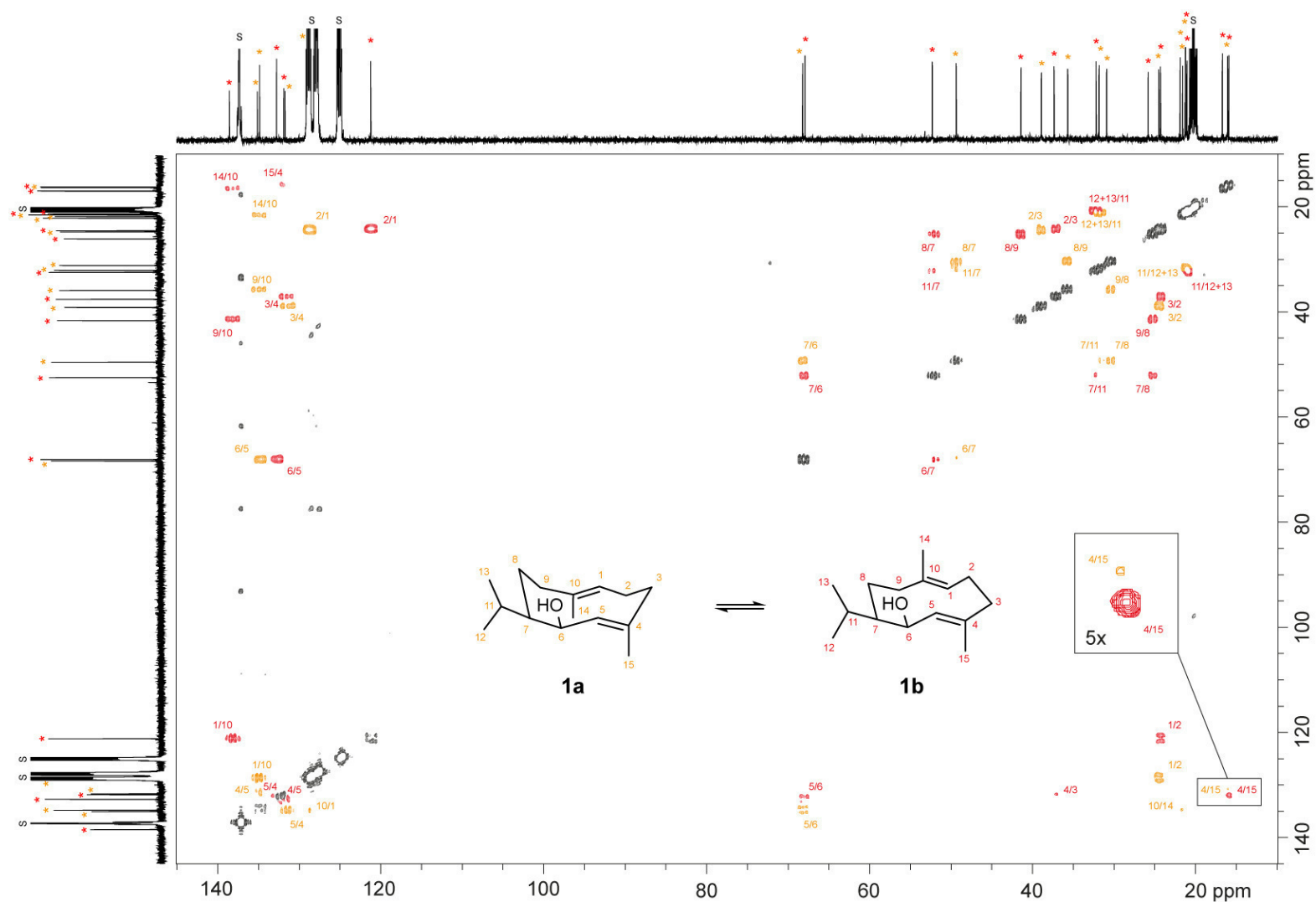


Figure 8. $^{13}\text{C},^{13}\text{C}$ -COSY NMR spectrum of $(^{13}\text{C}_{15})$ -**1** obtained by enzymatic conversion of $(^{13}\text{C}_{15})$ FPP with germacradienol synthase recorded in $(^2\text{H}_8)$ toluene (S = solvent signals). The two sets of crosspeaks for the conformers are shown in yellow (for **1a**) and red (for **1b**) and numbers next to crosspeaks indicate which carbons are coupling (e. g. 1/2 in yellow is a crosspeak for coupling of C-1 with C-2 of conformer **1a**)

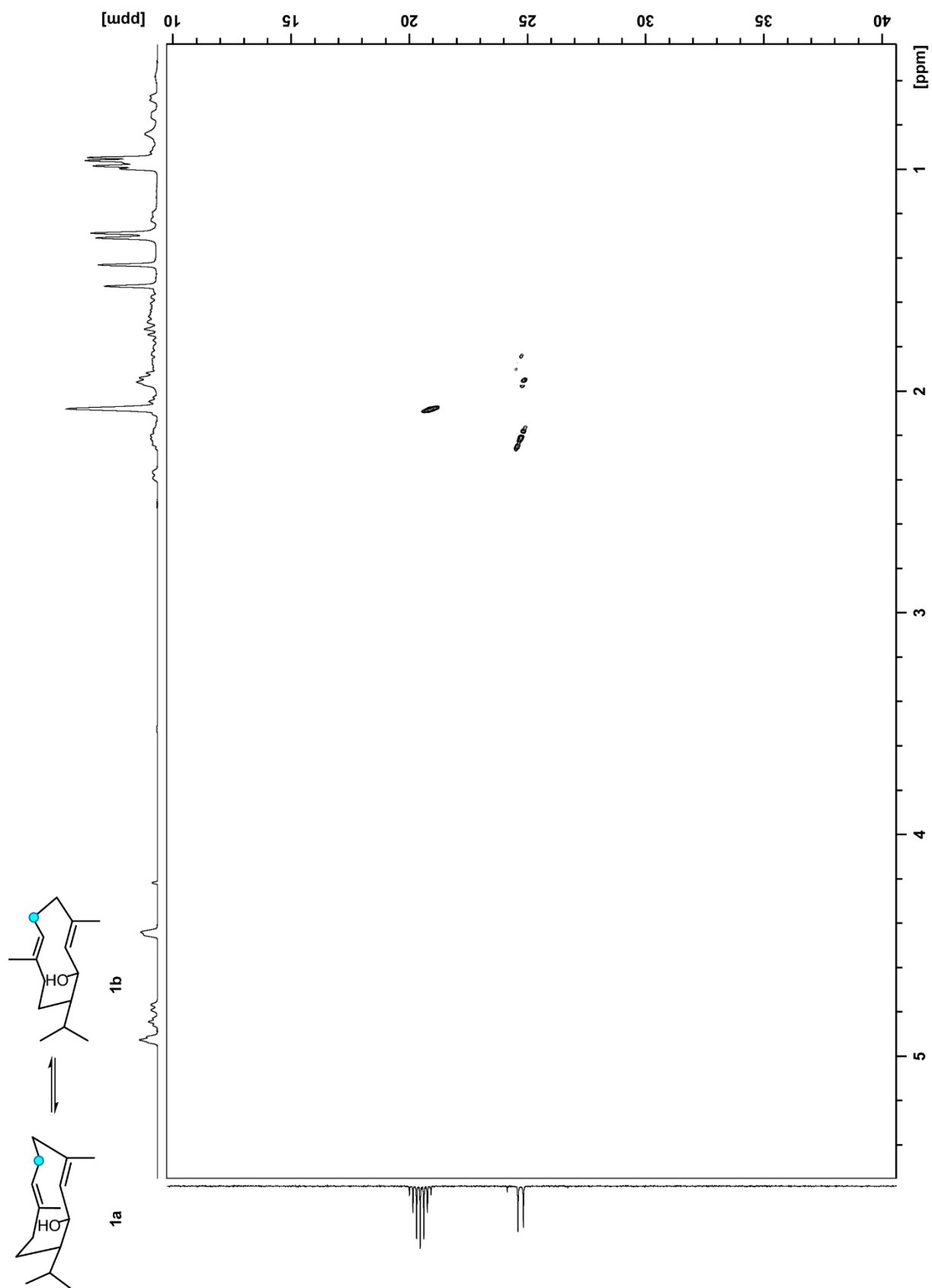


Figure 9. HSQC spectrum of $(2\text{-}^{13}\text{C}_1)\text{-}(1(10)E,4E,6S,7R)\text{-germacradien-6-ol}$ (**1**) recorded in $(^2\text{H}_8)\text{toluene}$ at 223K. Blue circles indicate ^{13}C -labeled carbons.

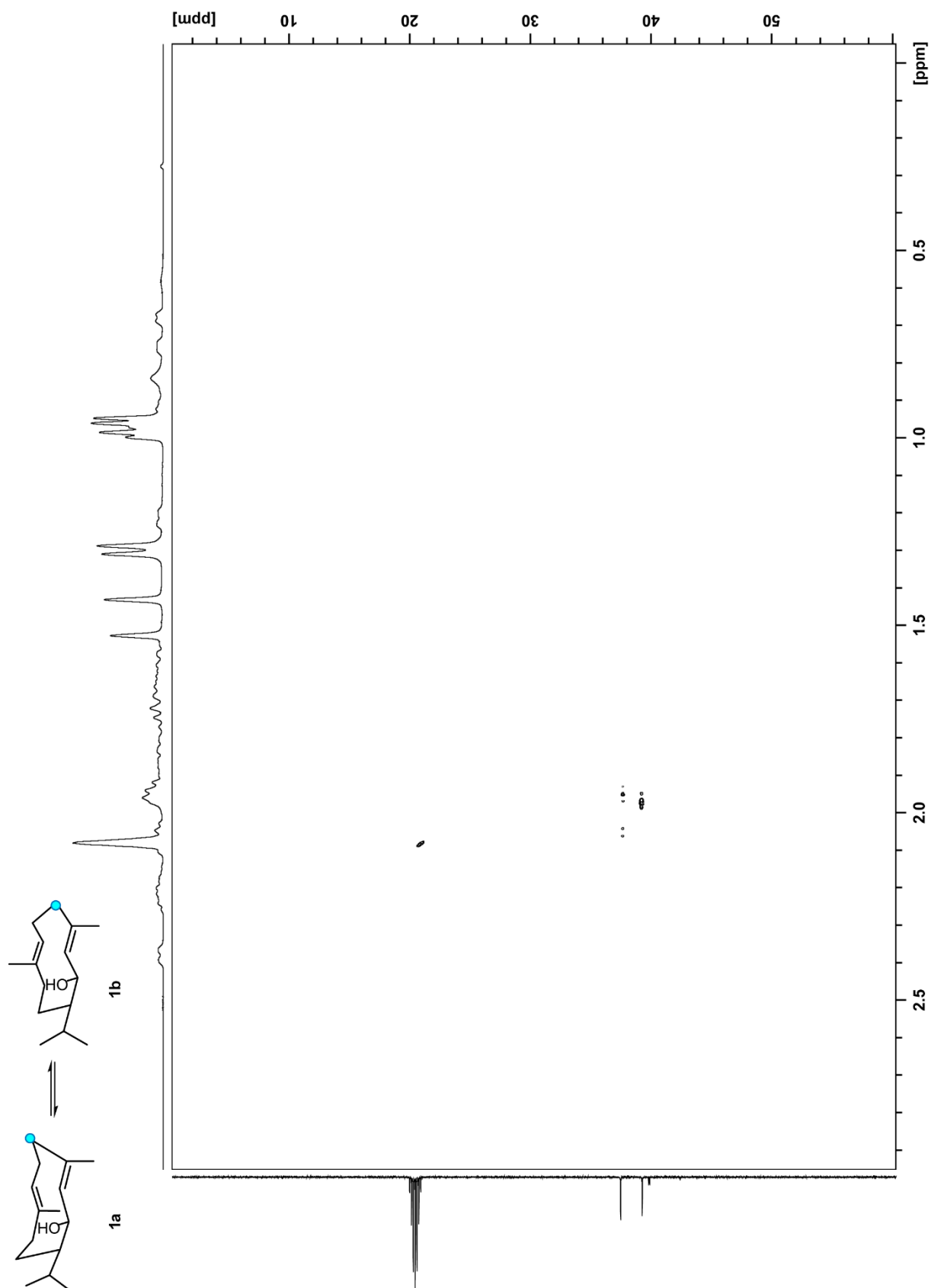


Figure 9 (continued). HSQC spectrum of $(3\text{-}^{13}\text{C}_1)\text{-}(1(10)E,4E,6S,7R)\text{-germacradien-6-ol (1)}$ recorded in $(^2\text{H}_8)\text{toluene}$ at 223K. Blue circles indicate ^{13}C -labeled carbons.

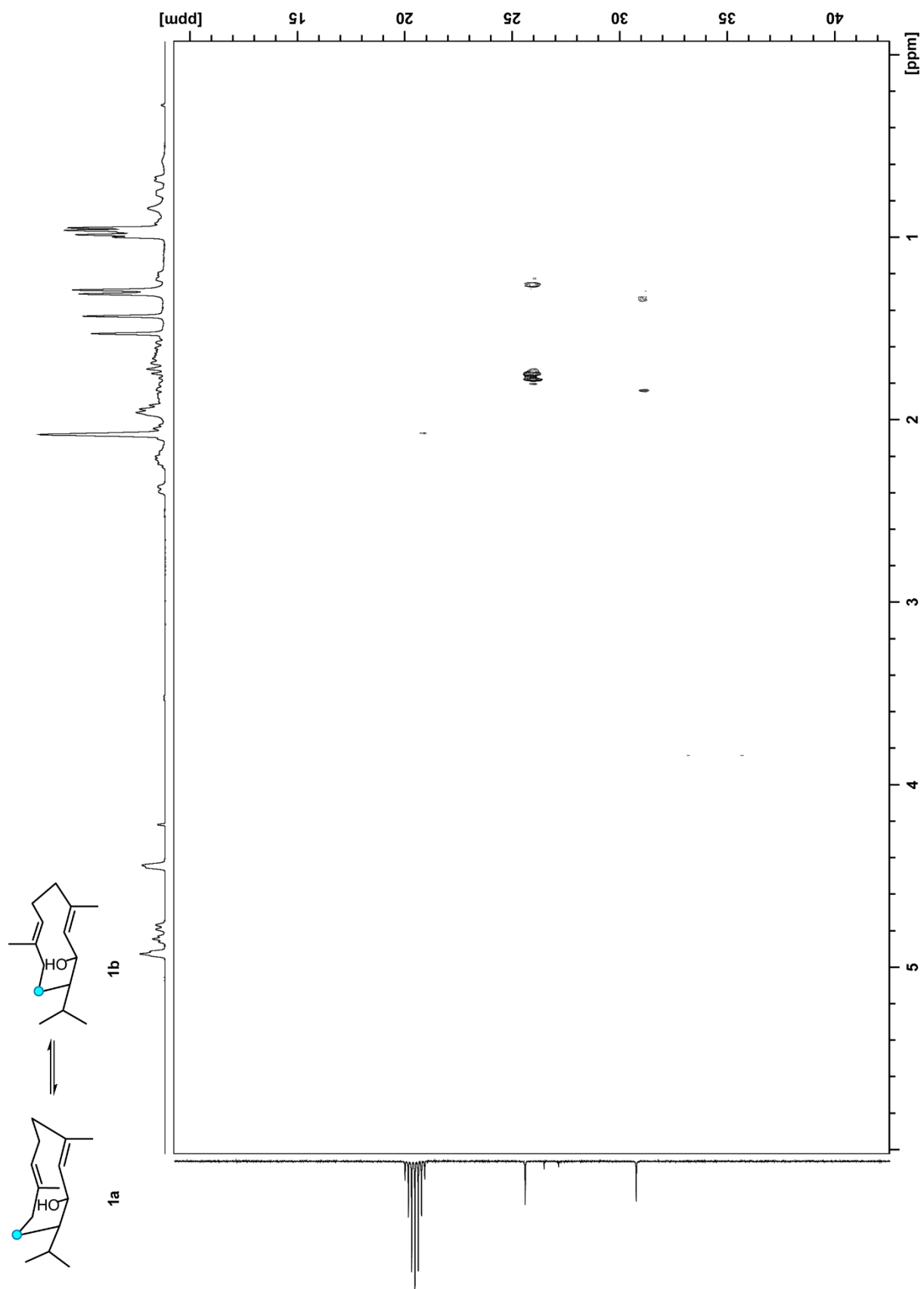


Figure 9 (continued). HSQC spectrum of $(8\text{-}^{13}\text{C}_1)\text{-}(1(10)E,4E,6S,7R)\text{-germacradien-6-ol (1)}$ recorded in $(^2\text{H}_8)\text{toluene}$ at 223K. Blue circles indicate ^{13}C -labeled carbons.

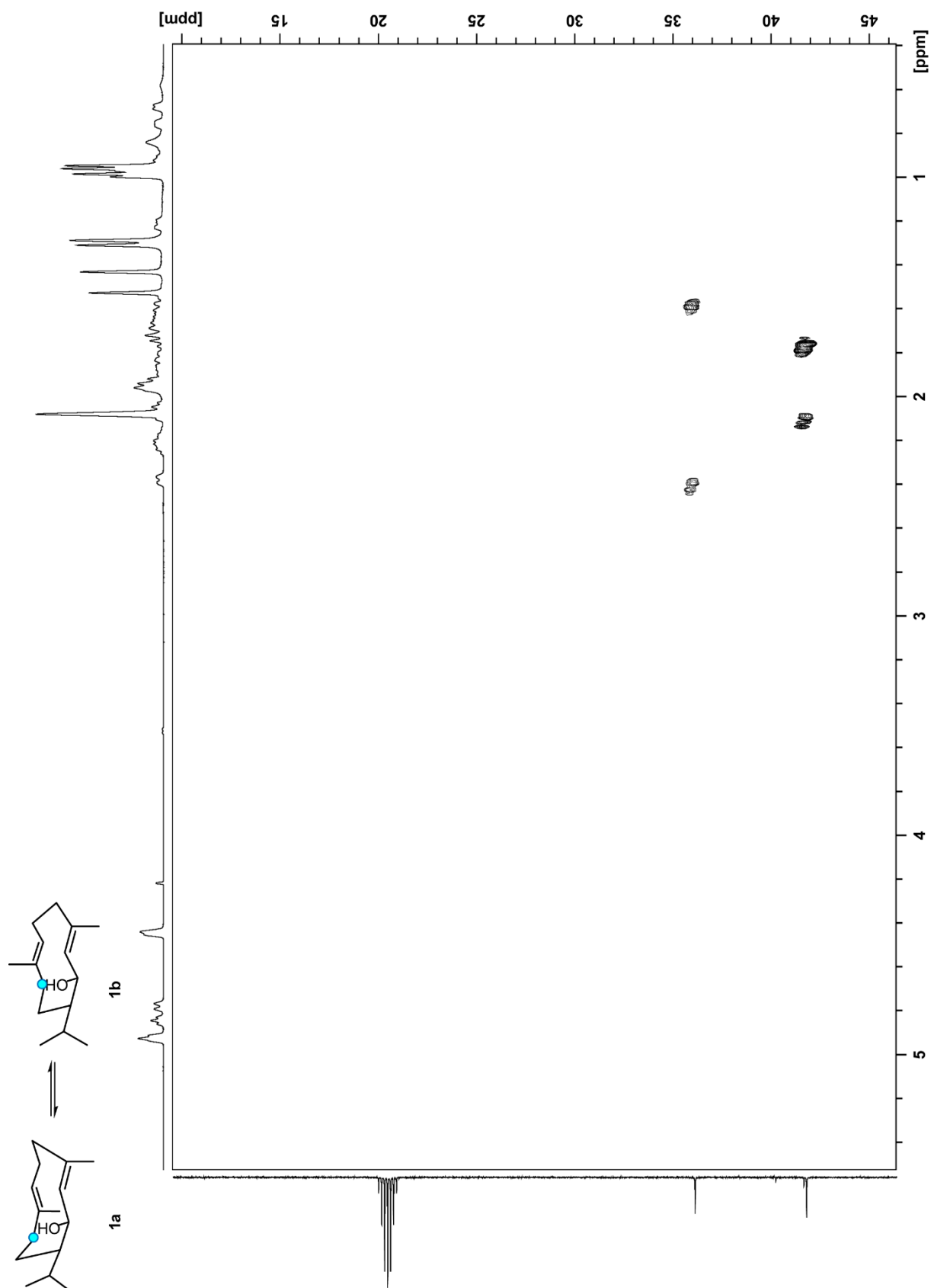


Figure 9 (continued). HSQC spectrum of (9-¹³C₁)-(1(10)*E*,4*E*,6*S*,7*R*)-germacradien-6-ol (**1**) recorded in (²H₈)toluene at 223K. Blue circles indicate ¹³C-labeled carbons.

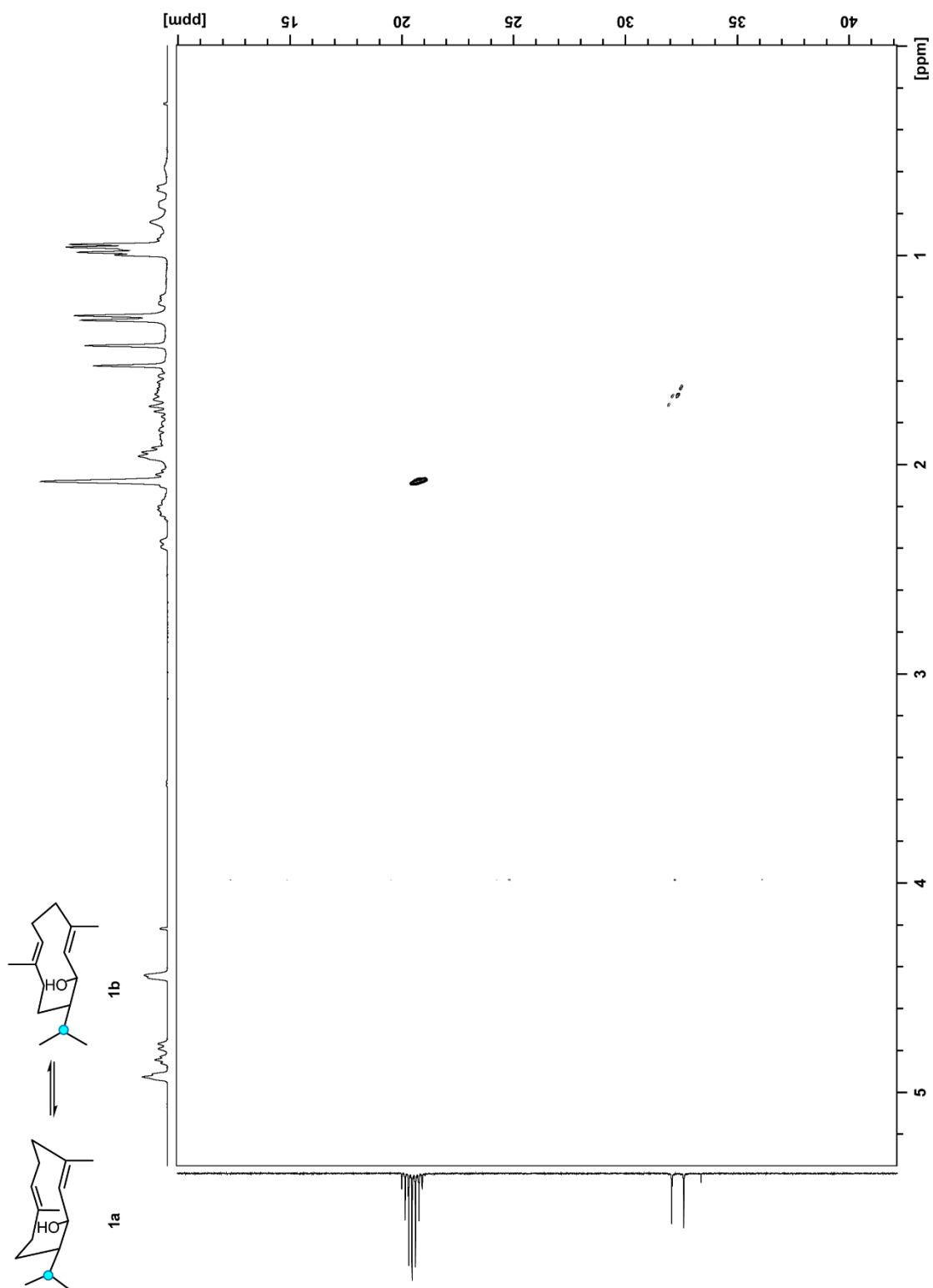


Figure 9 (continued). HSQC spectrum of $(11\text{-}^{13}\text{C}_1)\text{-}(1(10)E,4E,6S,7R)\text{-germacradien-6-ol}$ (**1**) recorded in $(^2\text{H}_8)\text{toluene}$ at 223K. Blue circles indicate ^{13}C -labeled carbons.

Cope rearrangement

The Cope rearrangement from 6.8 mg of (+)-(1(10)*E*,4*E*,6*S*,7*R*)-germacradien-6-ol was performed at 225°C for 20 h in (²H₈)toluene in a CEM Discover microwave reactor. After cooling to room temperature the solvent was evaporated under reduced pressure. Column chromatography with pentane/diethyl ether (10:1) yielded the products **2a** (2 mg, 29%) and **2b** (1.8 mg, 26%).

2a:

TLC (cyclohexane/ethyl acetate 2:1): *R_f* = 0.85. GC (HP 5): *I* = 1521. MS (EI, 70 eV): *m/z* (%) = 222 (3), 207 (4), 204 (4), 189 (10), 179 (6), 161 (32), 137 (10), 136 (27), 133 (11), 123 (33), 121 (64), 119 (20), 109 (43), 108 (25), 107 (40), 105 (32), 95 (43), 93 (80), 91 (50), 83 (45), 81 (100), 79 (48), 77 (37), 71 (22), 69 (51), 67 (64), 57 (25), 55 (70), 53 (33), 43 (72), 41 (98), 39 (35). HRMS (TOF): *m/z* = 222.1975 (calcd. 222.1978, C₁₅H₂₆O⁺). IR (diamond ATR): $\tilde{\nu}$ = 3357 (br m), 3060 (w), 2956 (m), 2927 (m), 2869 (w), 1636 (w), 1601 (w), 1520 (s), 1483 (m), 1348 (s), 1217 (w), 1162 (w), 1108 (w), 1016 (w), 1003 (w), 965 (w), 906 (m), 873 (m), 850 (s), 820 (m), 748 (m), 723 (m), 704 (m), 638 (w), 555 (w) cm⁻¹.

2b:

TLC (cyclohexane/ethyl acetate 2:1): *R_f* = 0.79. GC (HP 5): *I* = 1526. MS (EI, 70 eV): *m/z* (%) = 222 (1), 207 (6), 189 (6), 179 (6), 161 (26), 137 (14), 136 (24), 123 (39), 121 (40), 119 (20), 109 (60), 107 (37), 105 (30), 95 (46), 93 (79), 91 (48), 83 (42), 81 (89), 79 (52), 77 (39), 71 (19), 69 (51), 67 (66), 57 (24), 55 (63), 53 (34), 43 (70), 41 (100), 39 (36). HRMS (TOF): *m/z* = 222.1967 (calcd. 222.1978). IR (diamond ATR): $\tilde{\nu}$ = 3447 (br w), 3079 (w), 2955 (s), 2925 (s), 2869 (m), 1730 (w), 1673 (w), 1510 (m), 1378 (m), 1259 (m), 1085 (m), 1014 (s), 951 (w), 894 (s), 799 (s) cm⁻¹.

¹H and ¹³C NMR data of both Cope rearrangement products are summarized in Table 1 of main text.

Cope rearrangement of (¹³C₁₅)-(1(10)*E*,4*E*,6*S*,7*R*)-germacradien-6-ol:

The NMR sample of (¹³C₁₅)-(1(10)*E*,4*E*,6*S*,7*R*)-germacradien-6-ol in (²H₈)toluene was heated to 225°C for 16 h in a CEM Discover microwave reactor. After cooling to room temperature the product was immediately measured on NMR. The ¹³C,¹³C-COSY NMR spectrum of the mixture of (¹³C₁₅)-**2a** and (¹³C₁₅)-**2b** is presented in Figure 10 of SI.

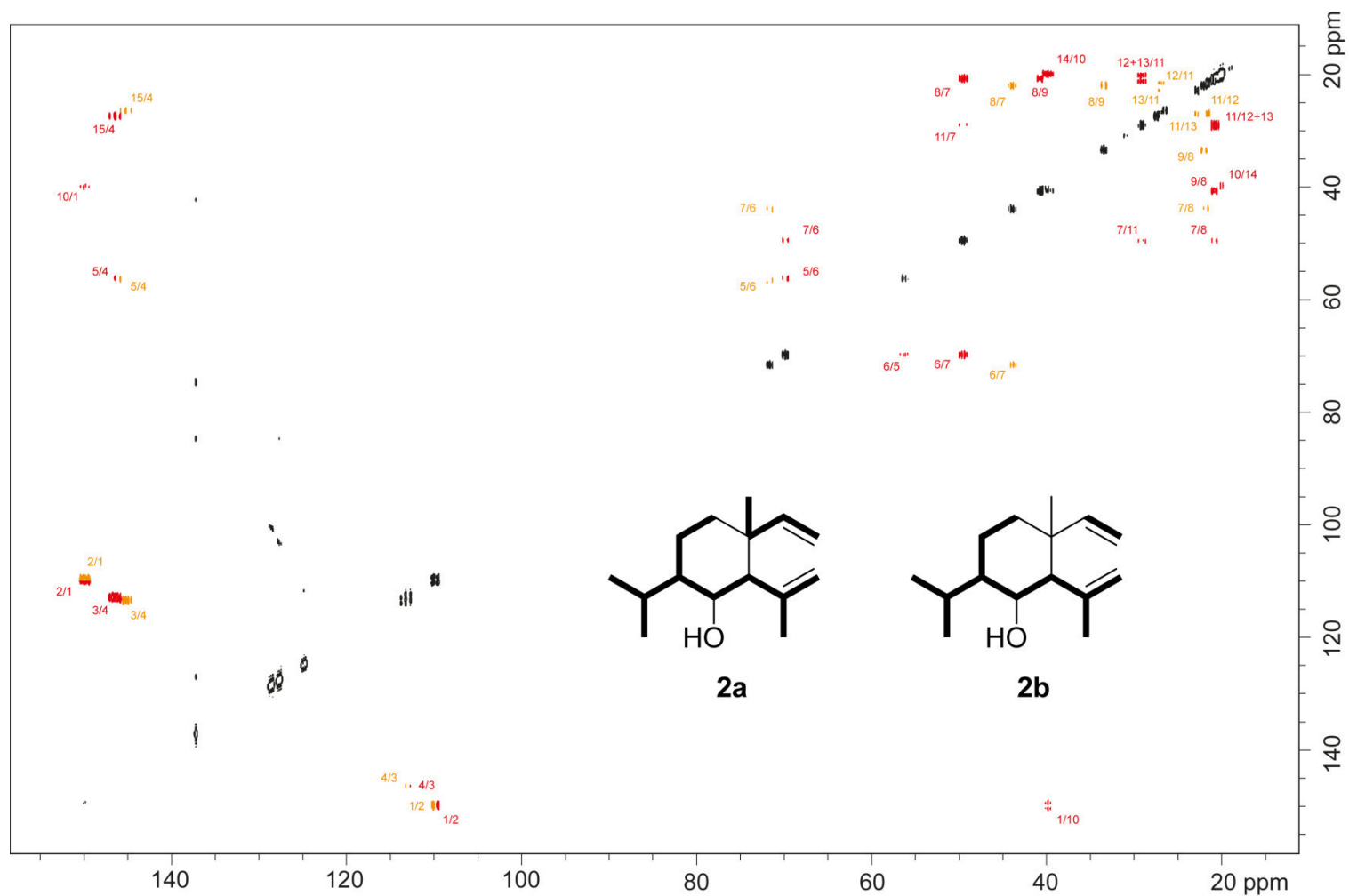


Figure 10. $^{13}\text{C}, ^{13}\text{C}$ -COSY NMR spectrum of $(^{13}\text{C}_{15})$ -**2a** and $(^{13}\text{C}_{15})$ -**2b** obtained after COPE rearrangement of $(^{13}\text{C}_{15})$ -**1** in $(^2\text{H}_8)$ toluene after microwave reaction at 225°C . Bold lines in the structures of **2a** and **2b** show contiguous ^{13}C -spin systems. Crosspeaks of **2a** are shown in red and crosspeaks of **2b** are in yellow.

Table 11. Compared ^{13}C -NMR data sets of (1(10)*E*,4*E*,6*S*,7*R*)-germacradien-6-ol (**1**) and its stereoisomer kunzeaol (*anti*-**1**) measured in (^2H)chloroform.

1 (this work) ^[a]	1 (Baran et al.) ^[20]	1 (Blaney et al.) ^[21]	<i>anti</i> - 1 (Kunzeaol, Ro et al.) ^[22]	<i>anti</i> - 1 (Kunzeaol, Wyllie et al.) ^[23]	<i>anti</i> - 1 (Kunzeaol, Szafranek et al.) ^[24]
138.9	138.8 (-0.1)	138.9	138.7 (-0.2)	138.4 (-0.5)	138.9
135.8	135.8	135.7 (-0.1)	135.7 (-0.1)	135.3 (-0.4)	
133.5	133.8 (+0.3)	133.5	133.6 (+0.1)	133.8 (+0.3)	133.6 (+0.1)
133.4	133.4	133.3 (-0.1)	133.2 (-0.2)	132.3 (-1.1)	132.4 (-1.0)
133.2	133.0 (-0.2)	133.0 (-0.2)	132.9 (-0.3)	132.2 (-1.0)	
131.3	131.6 (+0.3)	131.4 (+0.1)	131.5 (+0.2)	131.7 (+0.3)	131.5 (+0.2)
128.8	128.9 (+0.1)	128.7 (-0.1)	128.8	128.5 (-0.3)	128.8
121.4	121.5 (+0.1)	121.3 (-0.1)	121.3 (-0.1)	121.1 (-0.3)	121.4
68.9	69.0 (+0.1)	68.8 (-0.1)	68.8 (-0.1)	68.5 (-0.4)	68.8 (-0.1)
68.8		68.6 (-0.2)	-	-	
52.2	52.3 (+0.1)	52.2	52.2	51.9 (-0.3)	52.2
49.4	49.5 (+0.1)	49.3 (-0.1)	49.4	49.2 (-0.2)	49.4
41.4	41.5 (+0.1)	41.3 (-0.1)	41.4	41.2 (-0.2)	41.4
39.1	39.2 (+0.1)	39.0 (-0.1)	39.1	38.8 (-0.3)	39.1
37.2	37.3 (+0.1)	37.2	37.1 (-0.1)	36.9 (-0.3)	37.1 (-0.1)
35.8	35.9 (+0.1)	35.7 (-0.1)	35.8	35.6 (-0.2)	35.8
32.2	32.3 (+0.1)	32.1 (-0.1)	32.2	31.9 (-0.3)	32.2
31.8	31.9 (+0.1)	31.7 (-0.1)	31.7 (-0.1)	31.5 (-0.3)	31.7 (-0.1)
30.3	30.2 (-0.1)	30.3	30.1 (-0.2)	29.9 (-0.4)	30.1 (-0.2)
25.3	25.2 (-0.1)	25.2 (-0.1)	25.0 (-0.3)	24.9 (-0.4)	25.1 (-0.2)
24.6	24.7 (+0.1)	-			
24.3	24.4 (+0.1)	24.3	24.3	24.3	24.3
22.1	22.1	22.1	21.9 (-0.2)	21.7 (-0.4)	22.0 (-0.1)
21.5	21.5	21.5	21.3 (-0.2)	20 (-1.5)	21.1 (-0.4)
21.3	21.4 (+0.1)	21.3	21.2 (-0.1)	20 (-1.3)	21.1 (-0.2)
21.2	21.3 (+0.1)	21.2	21.1 (-0.1)		
21.0	21.1 (+0.1)	21.0	21.0		
17.1	17.1	17.0 (-0.1)	16.9 (-0.2)	16.7 (-0.4)	16.9 (-0.2)
16.5	16.5	16.5			
16.4		16.4	16.3 (-0.1)	16.2 (-0.2)	16.4

[a] All signals are given in ppm. Deviations of reported ^{13}C -NMR shifts from data measured in this work are shown in brackets.

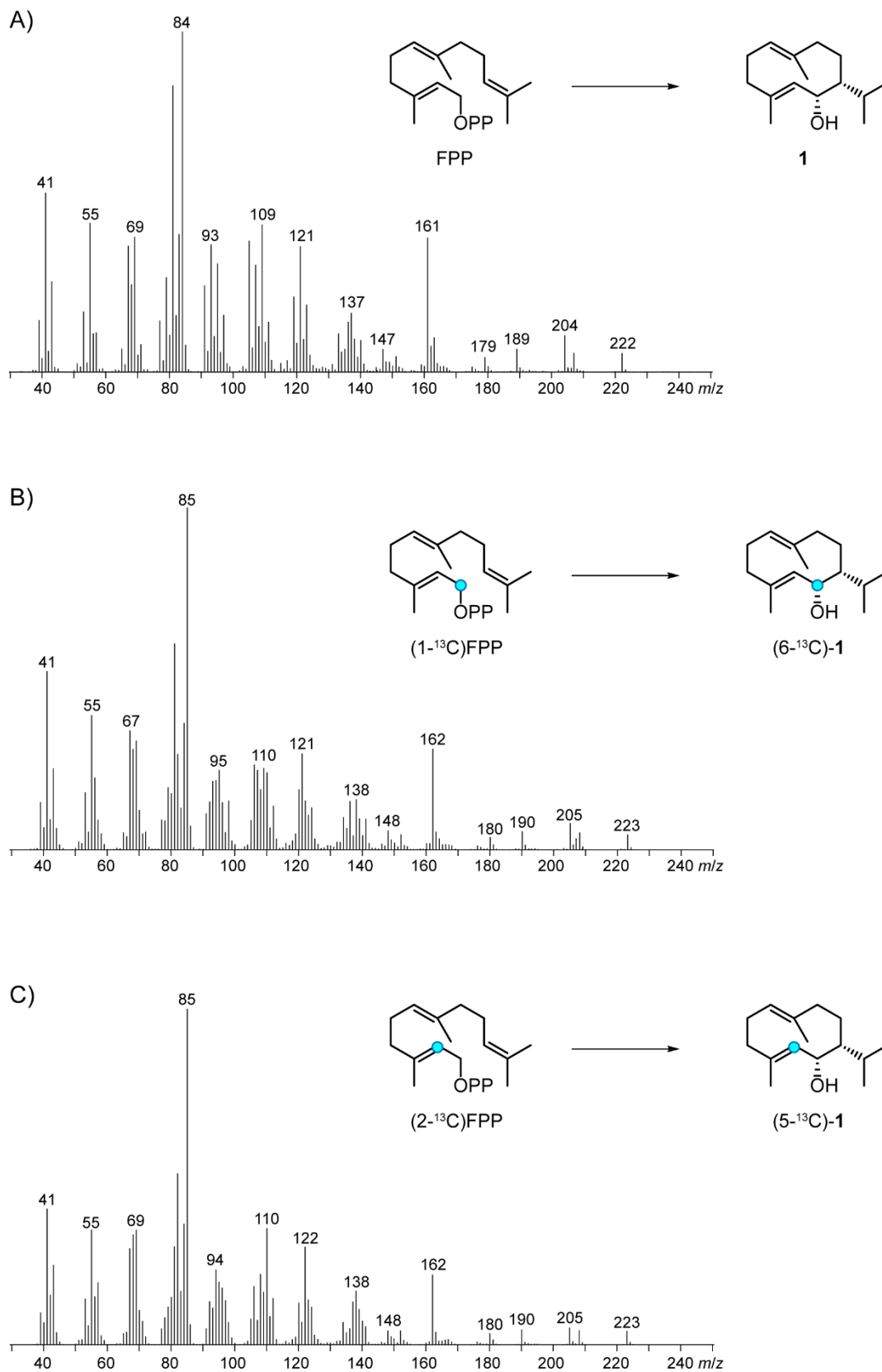


Figure 11. EI mass spectra of (1(10)*E*,4*E*,6*S*,7*R*)-germacradien-6-ol (**1**). A) Unlabeled **1**, B) (6-¹³C)-**1** obtained from (1-¹³C)FPP, C) (5-¹³C)-**1** obtained from (2-¹³C)FPP. Blue circles indicate ¹³C-labeled carbons.

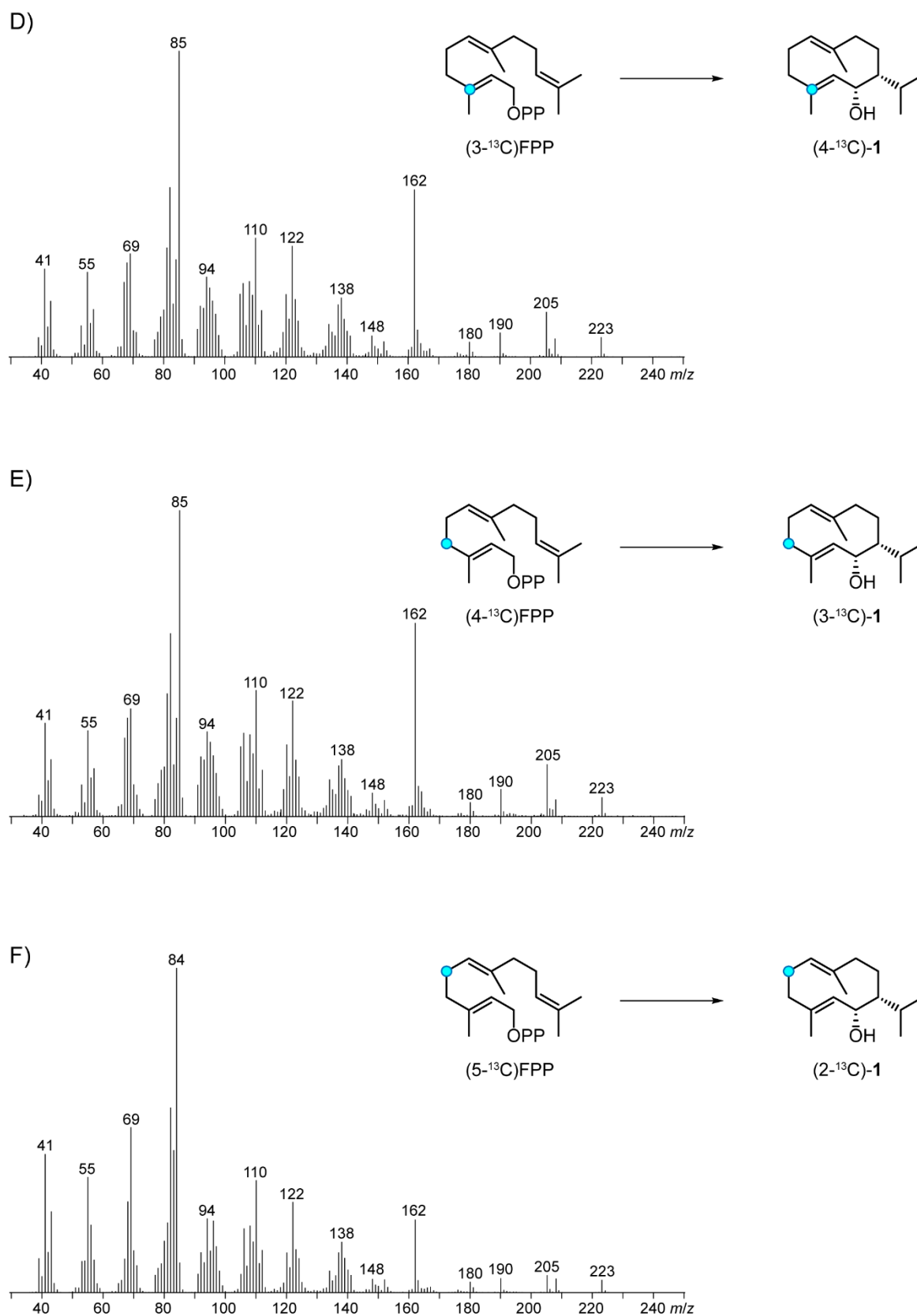


Figure 11 (continued). EI mass spectra of (1(10)*E*,4*E*,6*S*,7*R*)-germacradien-6-ol (**1**). D) (4-¹³C)-**1** obtained from (3-¹³C)FPP, E) (3-¹³C)-**1** obtained from (4-¹³C)FPP, F) (2-¹³C)-**1** obtained from (5-¹³C)FPP. Blue circles indicate ¹³C-labeled carbons.

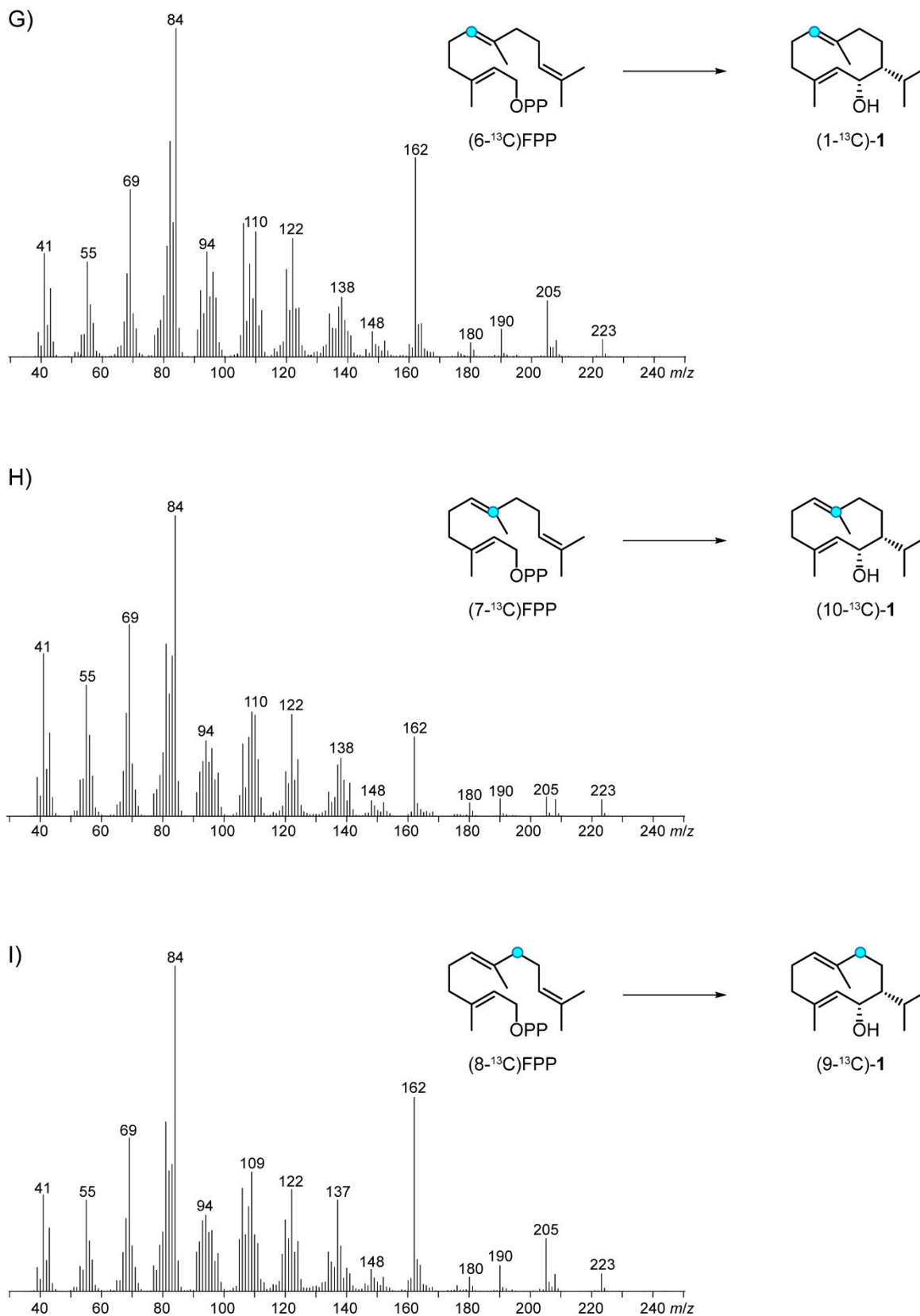


Figure 11 (continued). EI mass spectra of (1(10)*E*,4*E*,6*S*,7*R*)-germacradien-6-ol (**1**). G) (1-¹³C)-**1** obtained from (6-¹³C)FPP, H) (10-¹³C)-**1** obtained from (7-¹³C)FPP, I) (9-¹³C)-**1** obtained from (8-¹³C)FPP. Blue circles indicate ¹³C-labeled carbons.

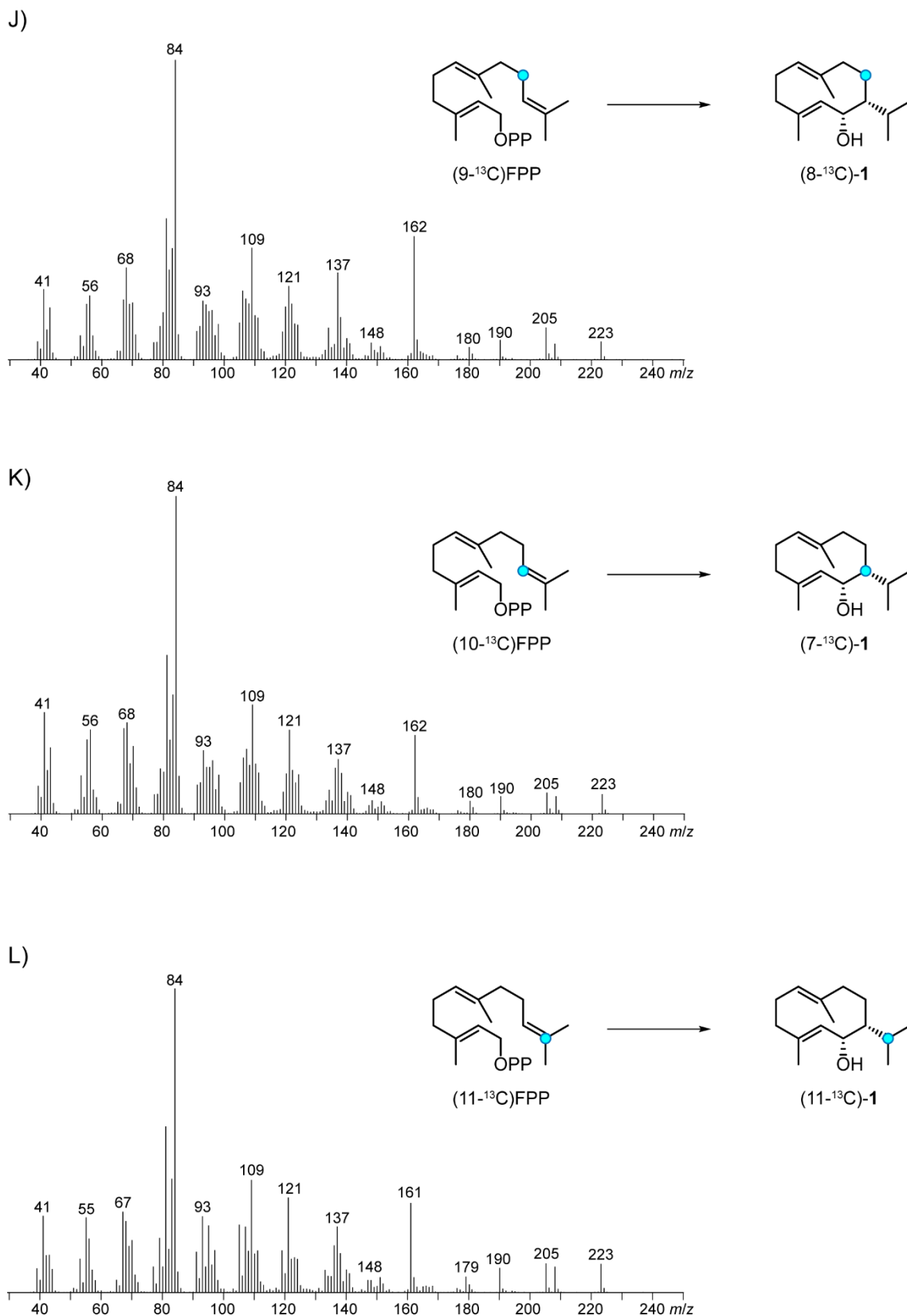


Figure 11 (continued). EI mass spectra of (1(10)*E*,4*E*,6*S*,7*R*)-germacradien-6-ol (**1**). J) (8-¹³C)-**1** obtained from (9-¹³C)FPP, K) (7-¹³C)-**1** obtained from (10-¹³C)FPP, L) (11-¹³C)-**1** obtained from (11-¹³C)FPP. Blue circles indicate ¹³C-labeled carbons.

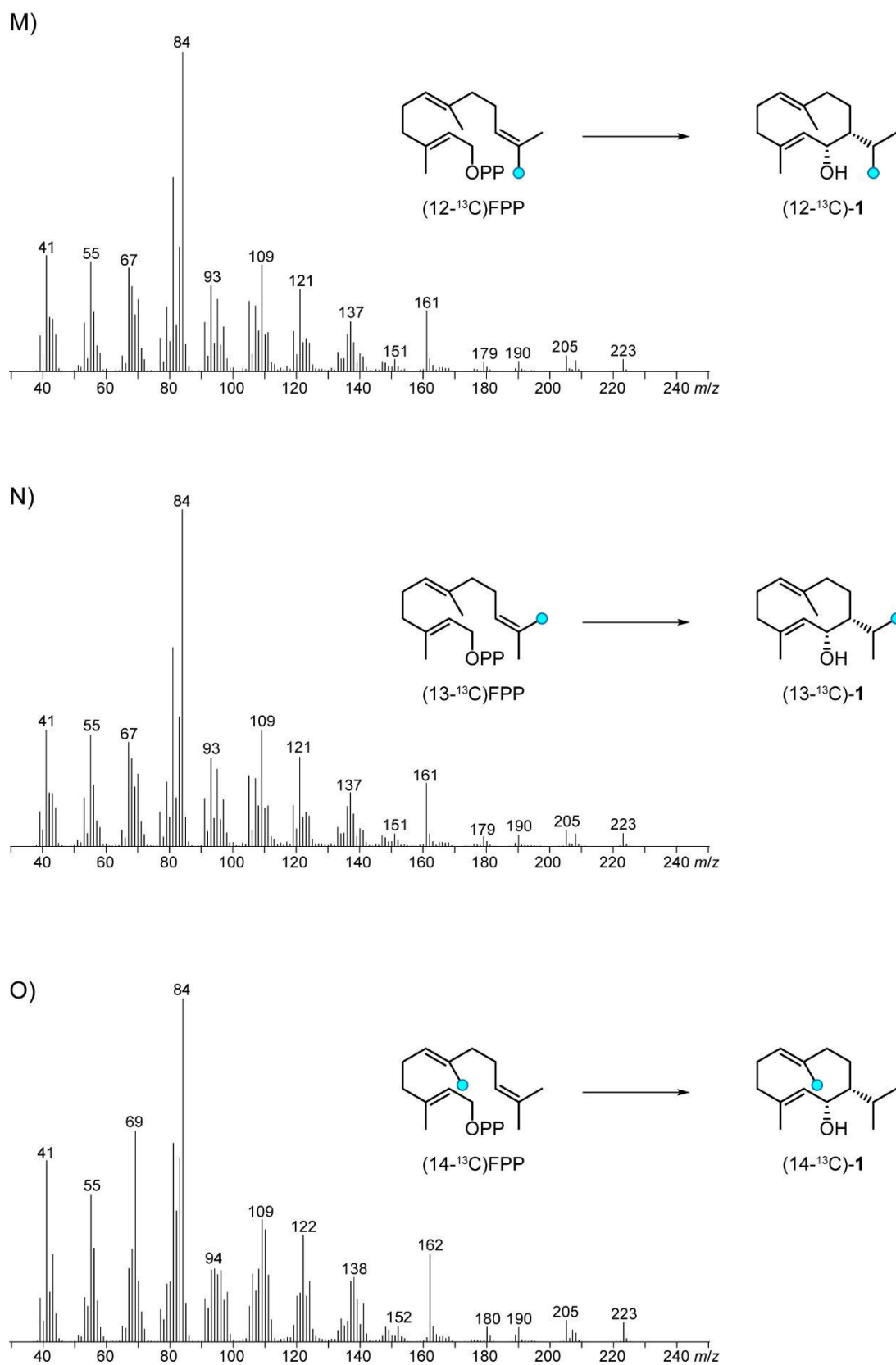


Figure 11 (continued). EI mass spectra of (1(10)*E*,4*E*,6*S*,7*R*)-germacradien-6-ol (**1**). M) (12-¹³C)-**1** obtained from (12-¹³C)FPP, N) (13-¹³C)-**1** obtained from (13-¹³C)FPP, O) (14-¹³C)-**1** obtained from (14-¹³C)FPP. Blue circles indicate ¹³C-labeled carbons.

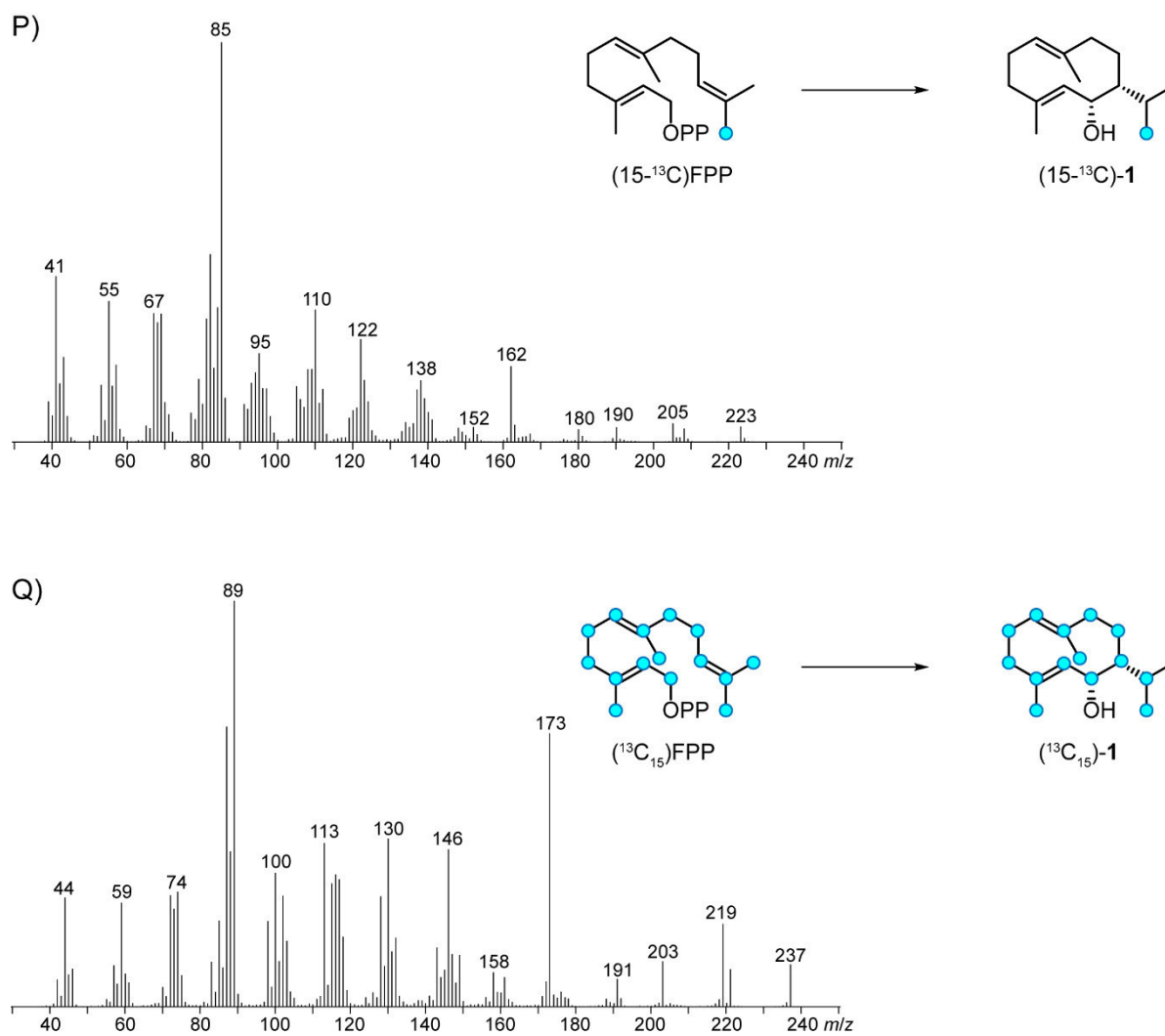


Figure 11 (continued). EI mass spectra of (1(10)*E*,4*E*,6*S*,7*R*)-germacradien-6-ol (**1**). P) (15-¹³C)-**1** obtained from (15-¹³C)FPP, Q) (¹³C₁₅)-**1** obtained from (¹³C₁₅)FPP. Blue circles indicate ¹³C-labeled carbons.

Table 12. Molecular and fragment ions of **1** observed in the EI mass spectra after enzymatic conversion of FPP, all fifteen (¹³C)FPP isotopomers, and (¹³C₁₅)FPP. The structures of fragment ions [A]⁺ and [B]⁺ are shown in Figure 5 of main text.

Compd.	Product	[M] ⁺	[M-H ₂ O] ⁺	[A] ⁺	[A] ⁺ (HR-MS) ^[a]	[B] ⁺	[B] ⁺ (HR-MS) ^[b]
FPP	1	222	204	161	161.1336	84	84.0574
(1- ¹³ C)FPP	(6- ¹³ C)- 1	223	205	162	162.1354	85	85.0599
(2- ¹³ C)FPP	(5- ¹³ C)- 1	223	205	162	162.1357	85	85.0601
(3- ¹³ C)FPP	(4- ¹³ C)- 1	223	205	162	162.1362	85	85.0606
(4- ¹³ C)FPP	(3- ¹³ C)- 1	223	205	162	162.1356	85	85.0601
(5- ¹³ C)FPP	(2- ¹³ C)- 1	223	205	162	162.1359	84	84.0567
(6- ¹³ C)FPP	(1- ¹³ C)- 1	223	205	162	162.1357	84	84.0568
(7- ¹³ C)FPP	(10- ¹³ C)- 1	223	205	162	162.1356	84	84.0565
(8- ¹³ C)FPP	(9- ¹³ C)- 1	223	205	162	162.1356	84	84.0566
(9- ¹³ C)FPP	(8- ¹³ C)- 1	223	205	162	162.1355	84	84.0567
(10- ¹³ C)FPP	(7- ¹³ C)- 1	223	205	162	162.1358	84	84.0565
(11- ¹³ C)FPP	(11- ¹³ C)- 1	223	205	161	161.1321	84	84.0565
(12- ¹³ C)FPP	(12- ¹³ C)- 1	223	205	161	161.1320	84	84.0567
(13- ¹³ C)FPP	(13- ¹³ C)- 1	223	205	161	161.1323	84	84.0568
(14- ¹³ C)FPP	(14- ¹³ C)- 1	223	205	162	162.1358	84	84.0567
(15- ¹³ C)FPP	(15- ¹³ C)- 1	223	205	162	162.1357	85	85.0602
(¹³ C ₁₅)FPP	(¹³ C ₁₅)- 1	237	219	173	173.1728	89	89.0738

[a] Calculated masses for [A]⁺: 161.1325 (C₁₂H₁₇⁺), 162.1358 (¹³C₁¹²C₁₁H₁₇⁺), 173.1727 (¹³C₁₂H₁₇⁺). [b] Calculated masses for [B]⁺: 84.0570 (C₅H₈O⁺), 85.0603 (¹³C₁¹²C₄H₁₇O⁺), 89.0737 (¹³C₅H₈O⁺).

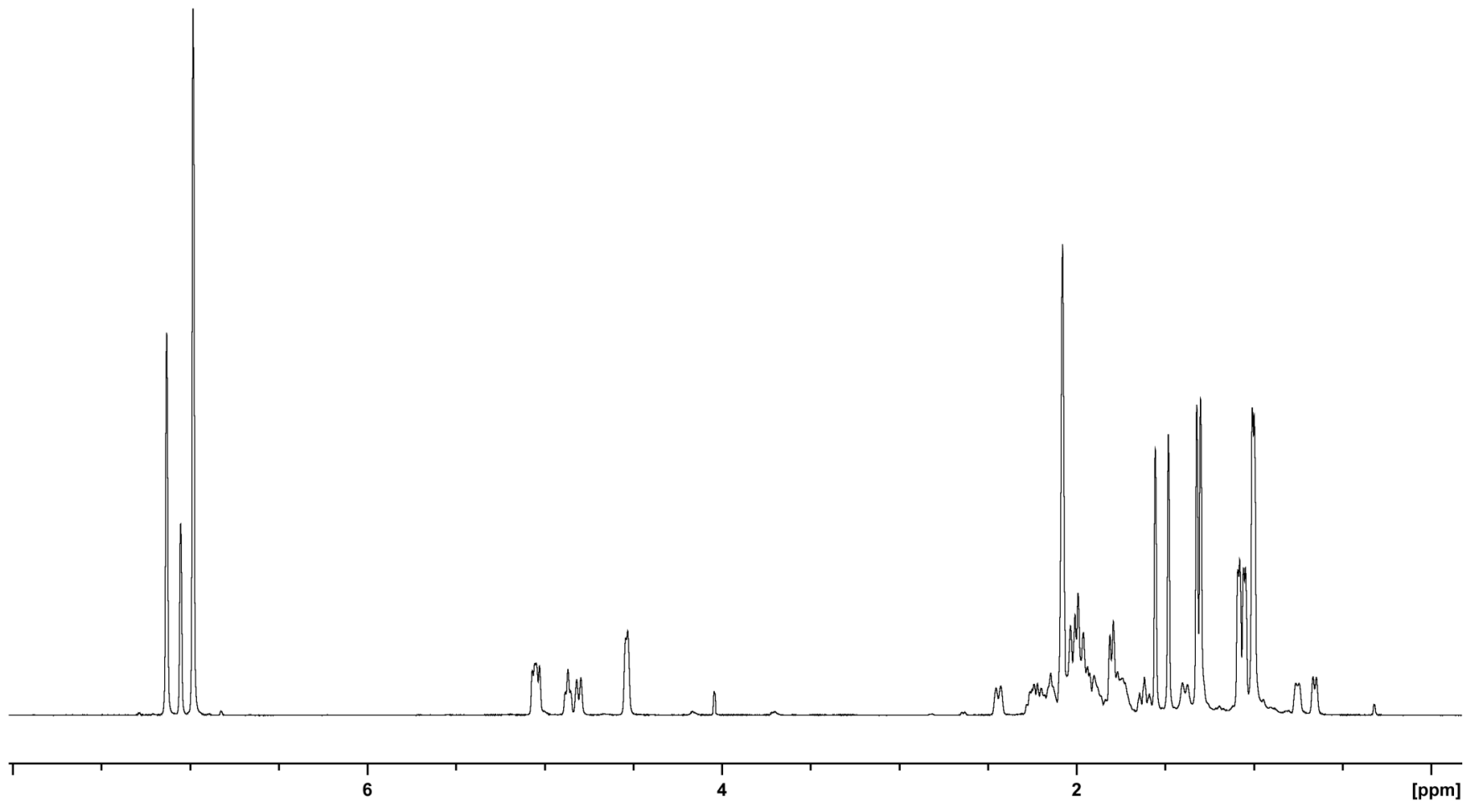
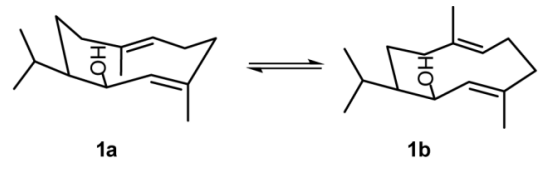


Figure 12. ¹H-NMR spectrum of (1(10)*E*,4*E*,6*S*,7*R*)-germacradien-6-ol (**1**) in (²H₈)toluene at 223K.

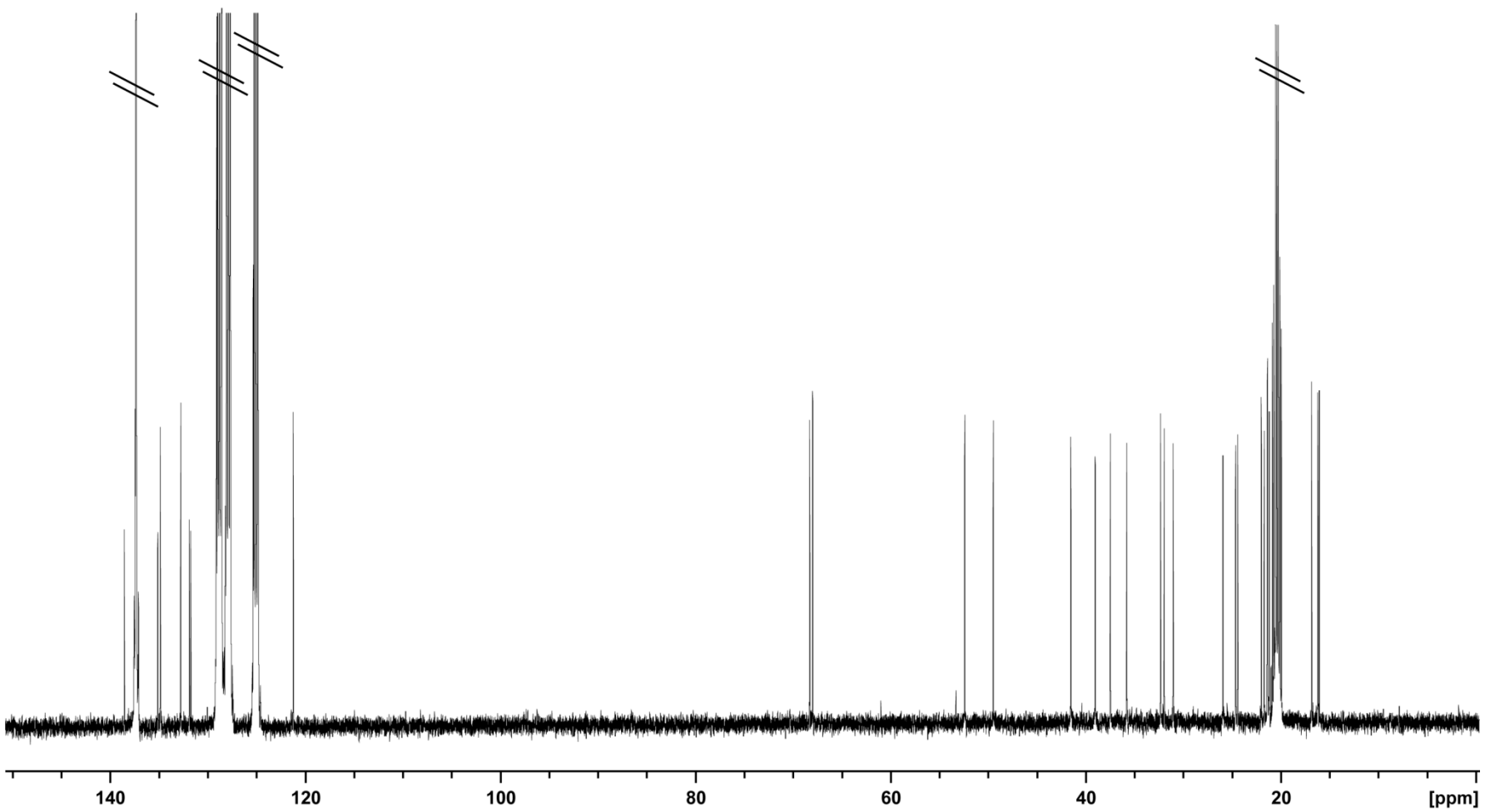
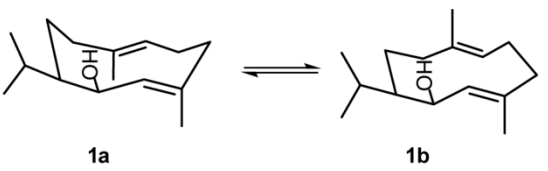


Figure 12 (continued). ^{13}C -NMR spectrum of (1(10)*E*,4*E*,6*S*,7*R*)-germacradien-6-ol (**1**) in $(^2\text{H}_8)$ toluene at 223K. Solvent signals are crossed out.

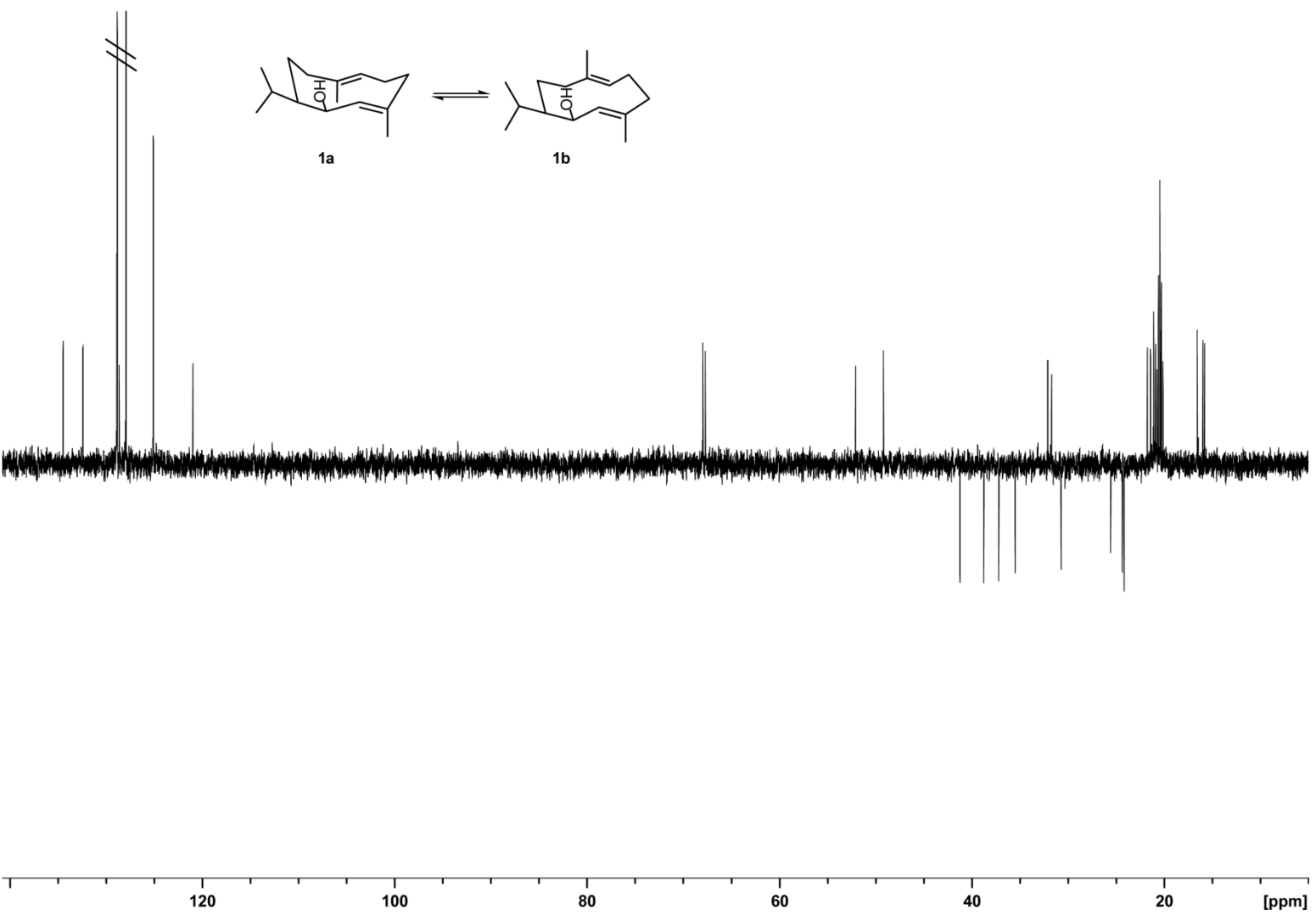


Figure 12 (continued). ^{13}C -DEPT135 spectrum of (1(10)*E*,4*E*,6*S*,7*R*)-germacradien-6-ol (1) in $(^2\text{H}_8)$ toluene at 223K. Solvent signals are crossed out.

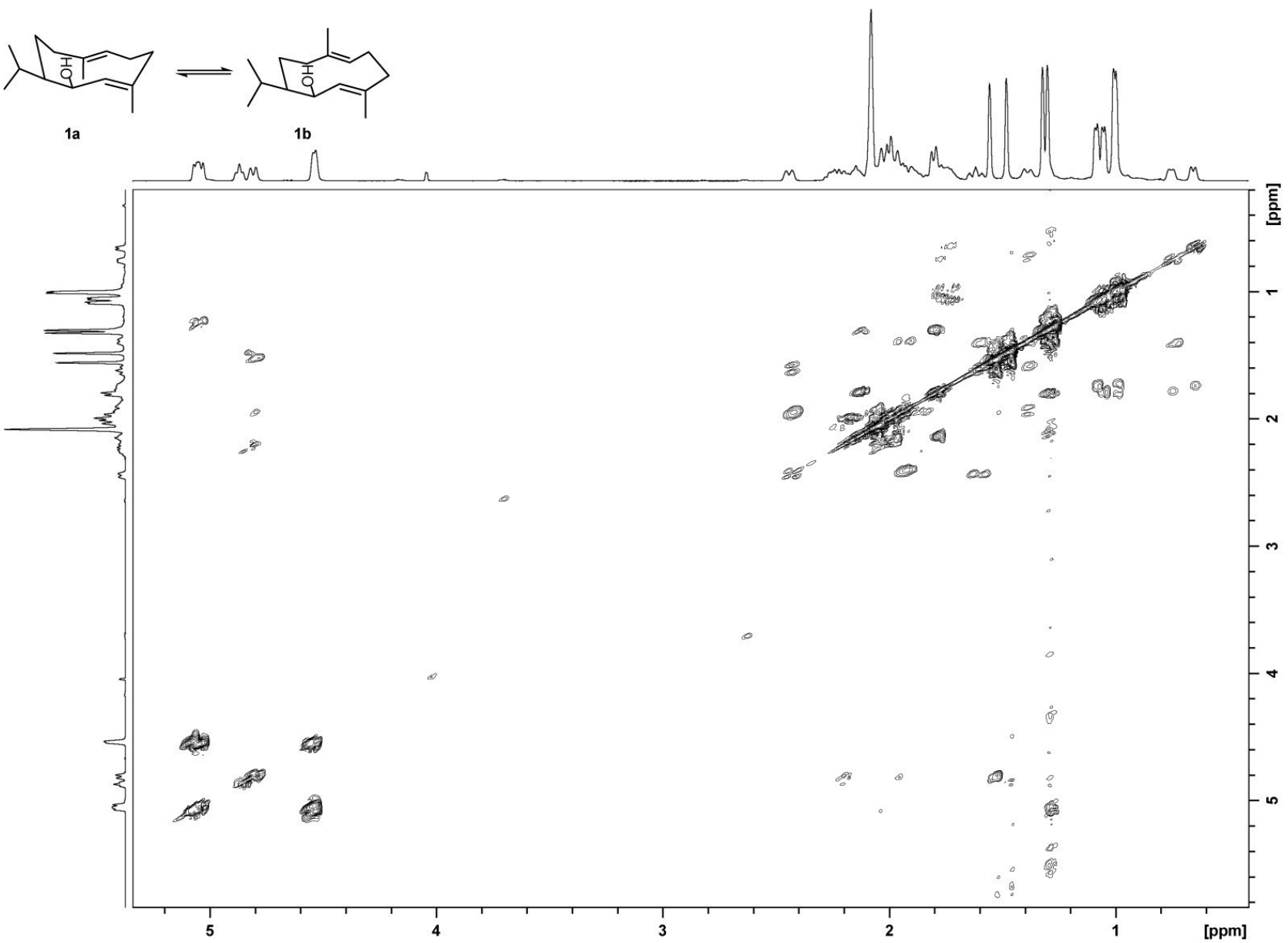


Figure 12 (continued). ^1H , ^1H -COSY spectrum of (1(10)*E*,4*E*,6*S*,7*R*)-germacradien-6-ol (1) in ($^2\text{H}_8$)toluene at 223K.

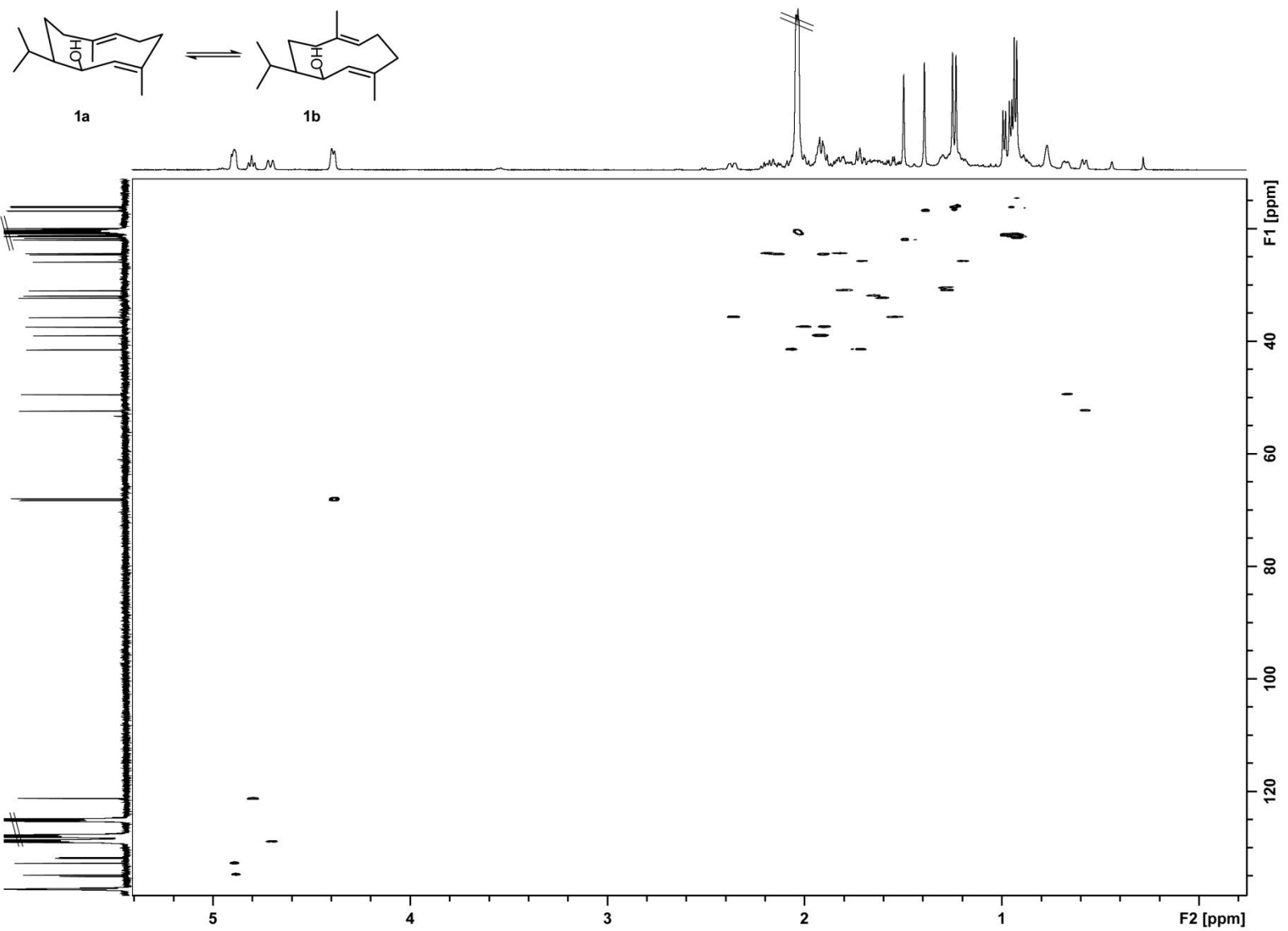


Figure 12 (continued). HSQC spectrum of (1(10)*E*,4*E*,6*S*,7*R*)-germacradien-6-ol (**1**) in (²H₈)toluene at 223K. Solvent signals are crossed out.

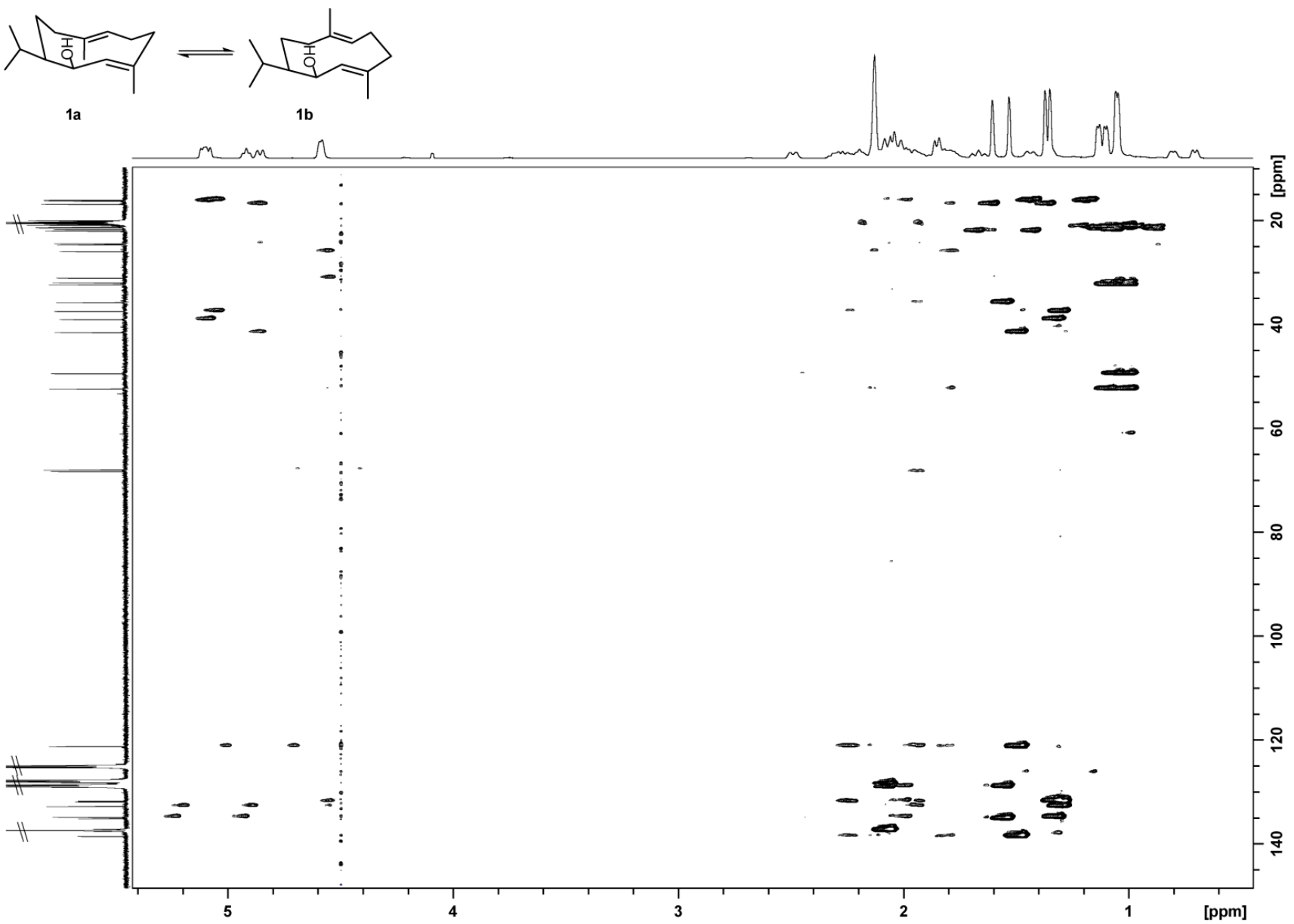


Figure 12 (continued). HMBC spectrum of (1(10),*E*,4*E*,6*S*,7*R*)-germacradien-6-ol (**1**) in (²H₈)toluene at 223K. Solvent signals are crossed out.

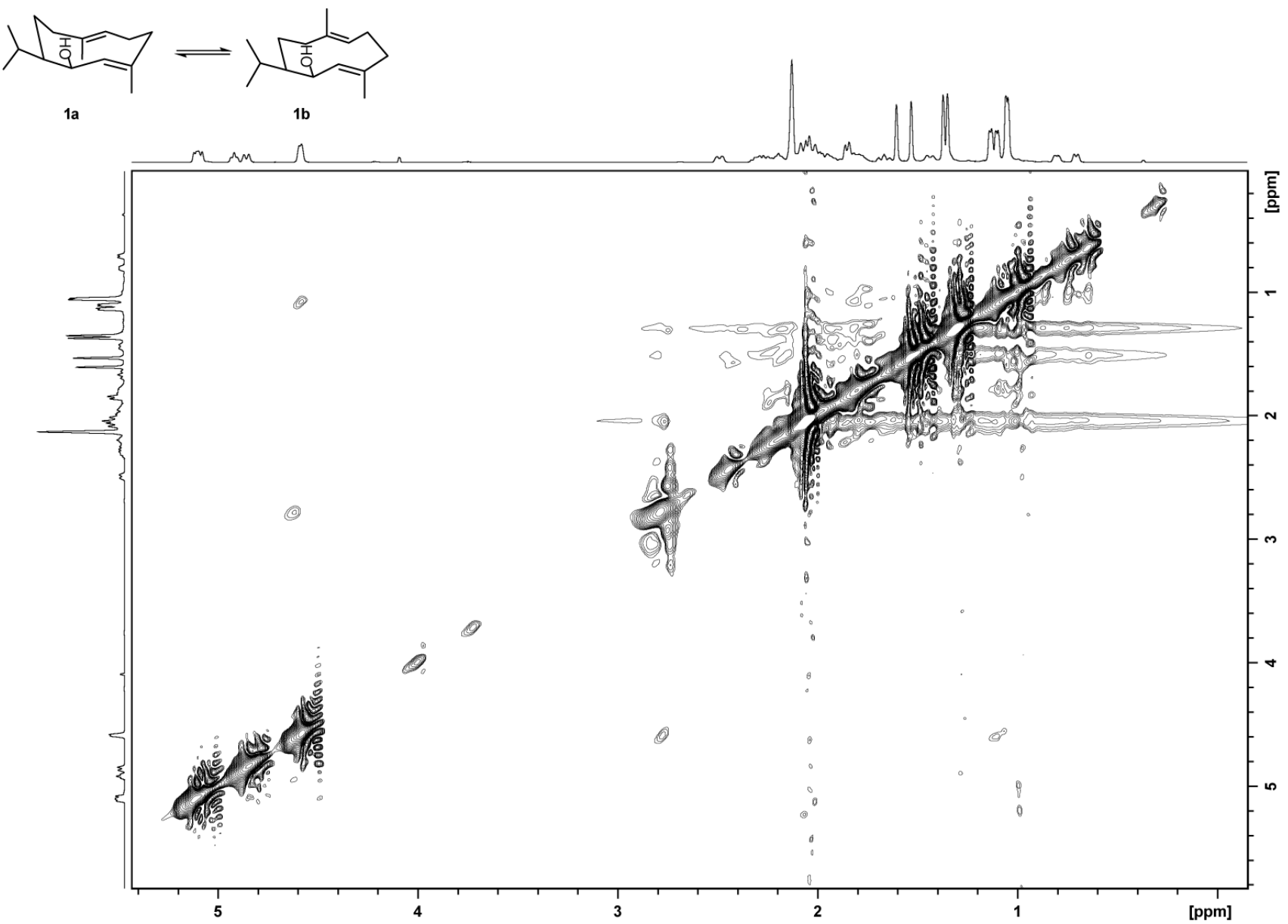
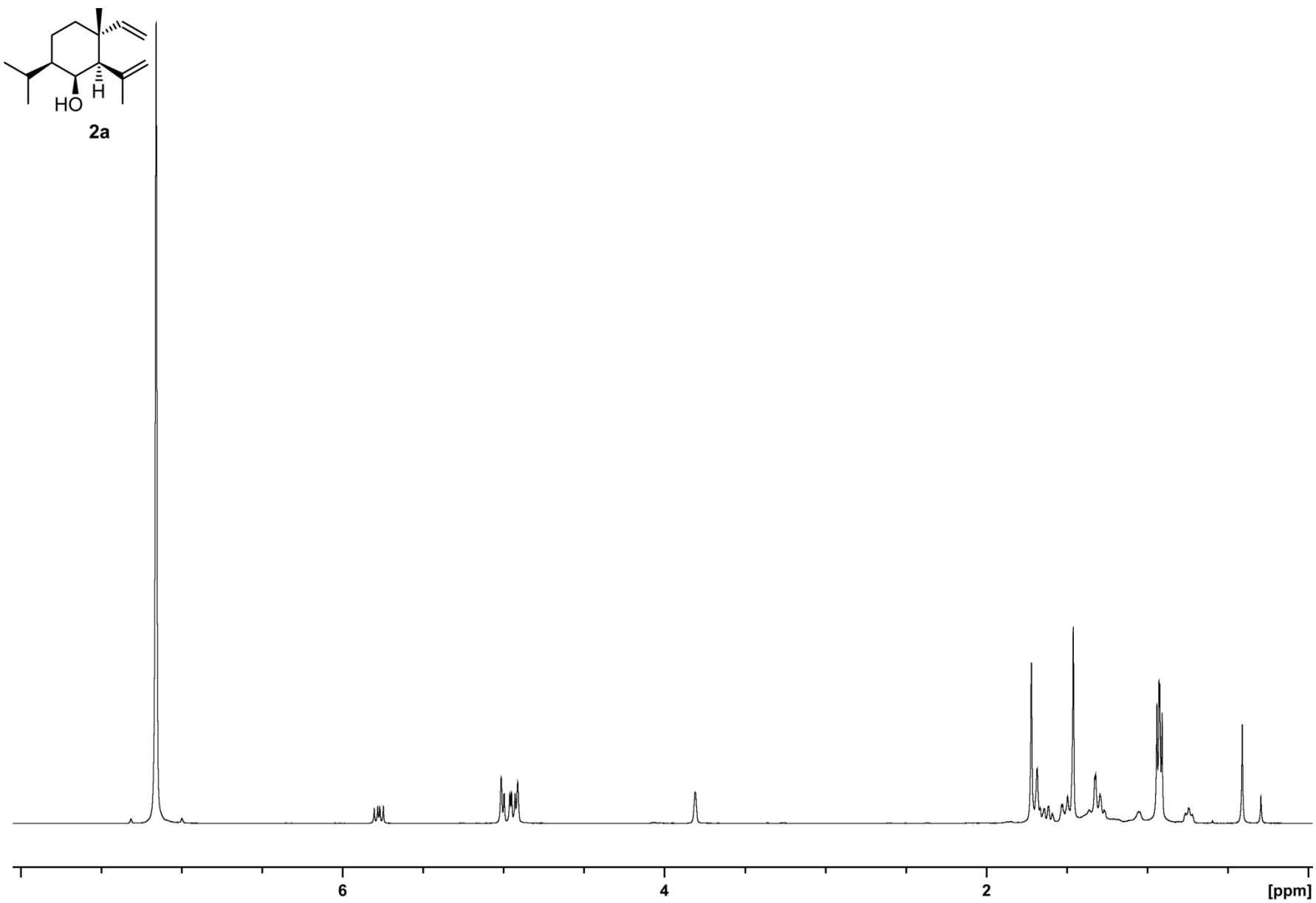


Figure 12 (continued). NOESY-NMR spectrum of (1(10),E,4E,6S,7R)-germacradien-6-ol (1) in (2H₈)toluene at 223K.

Figure 13. $^1\text{H-NMR}$ spectrum of **2a** in ($^2\text{H}_6$)benzene at 298K.



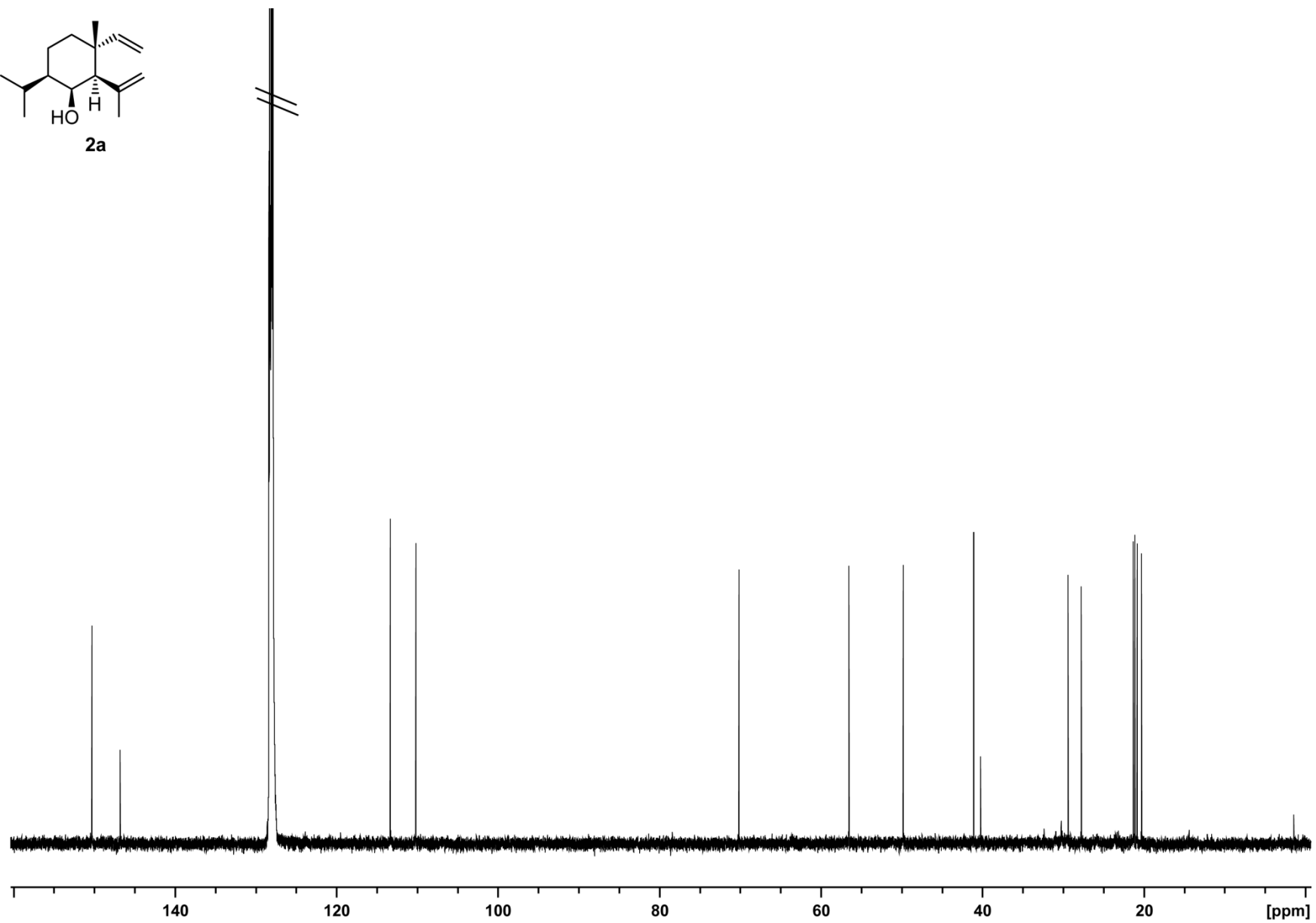
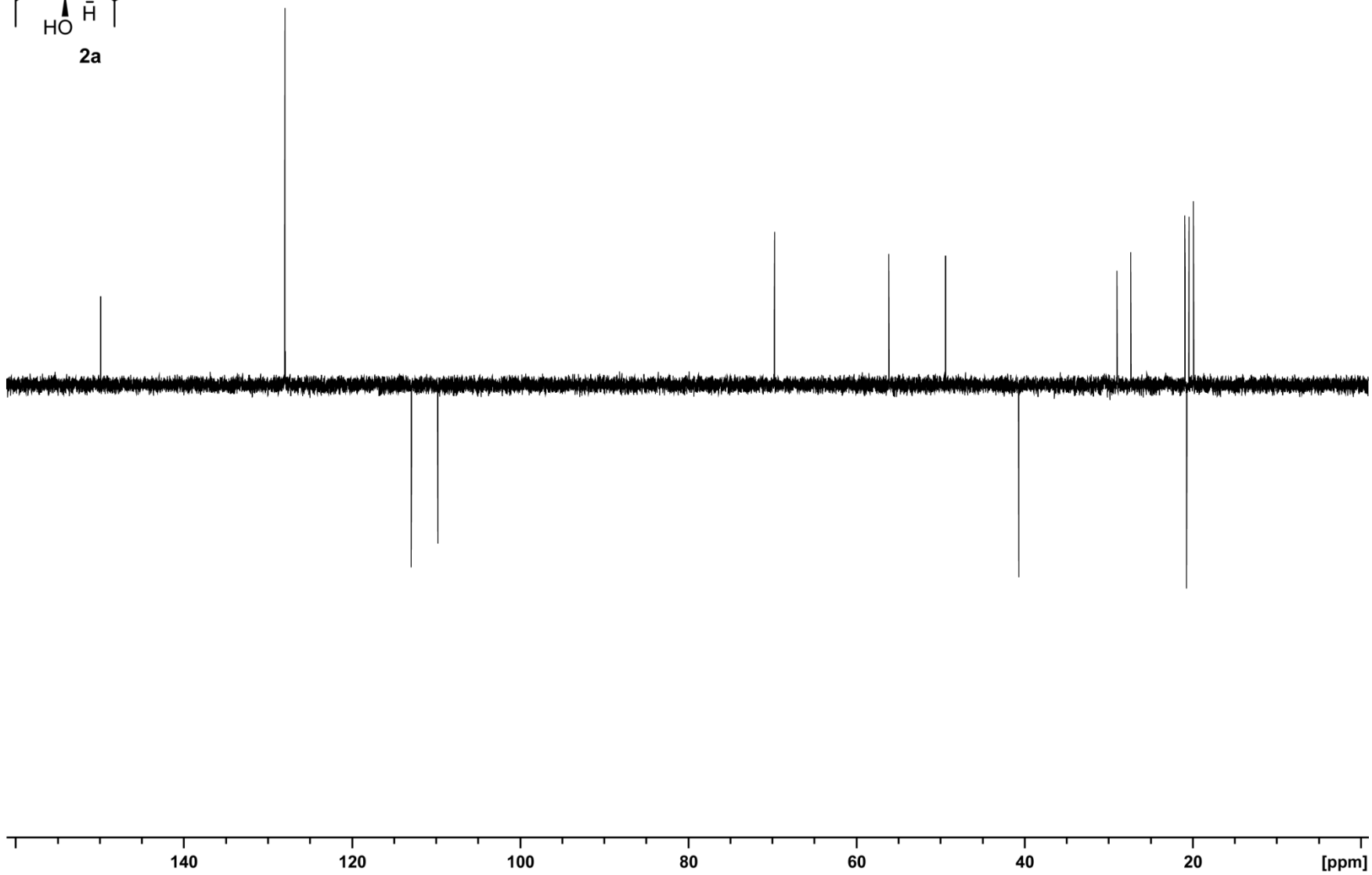
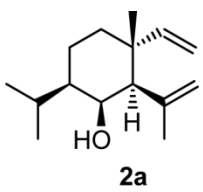


Figure 13 (continued). ^{13}C -NMR spectrum of **2a** in $(^2\text{H}_6)$ benzene at 298K. Solvent signals are crossed out.

Figure 13 (continued). ^{13}C -DEPT135 spectrum of **2a** in ($^2\text{H}_6$)benzene at 298K.



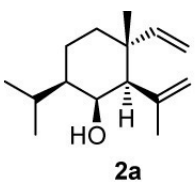
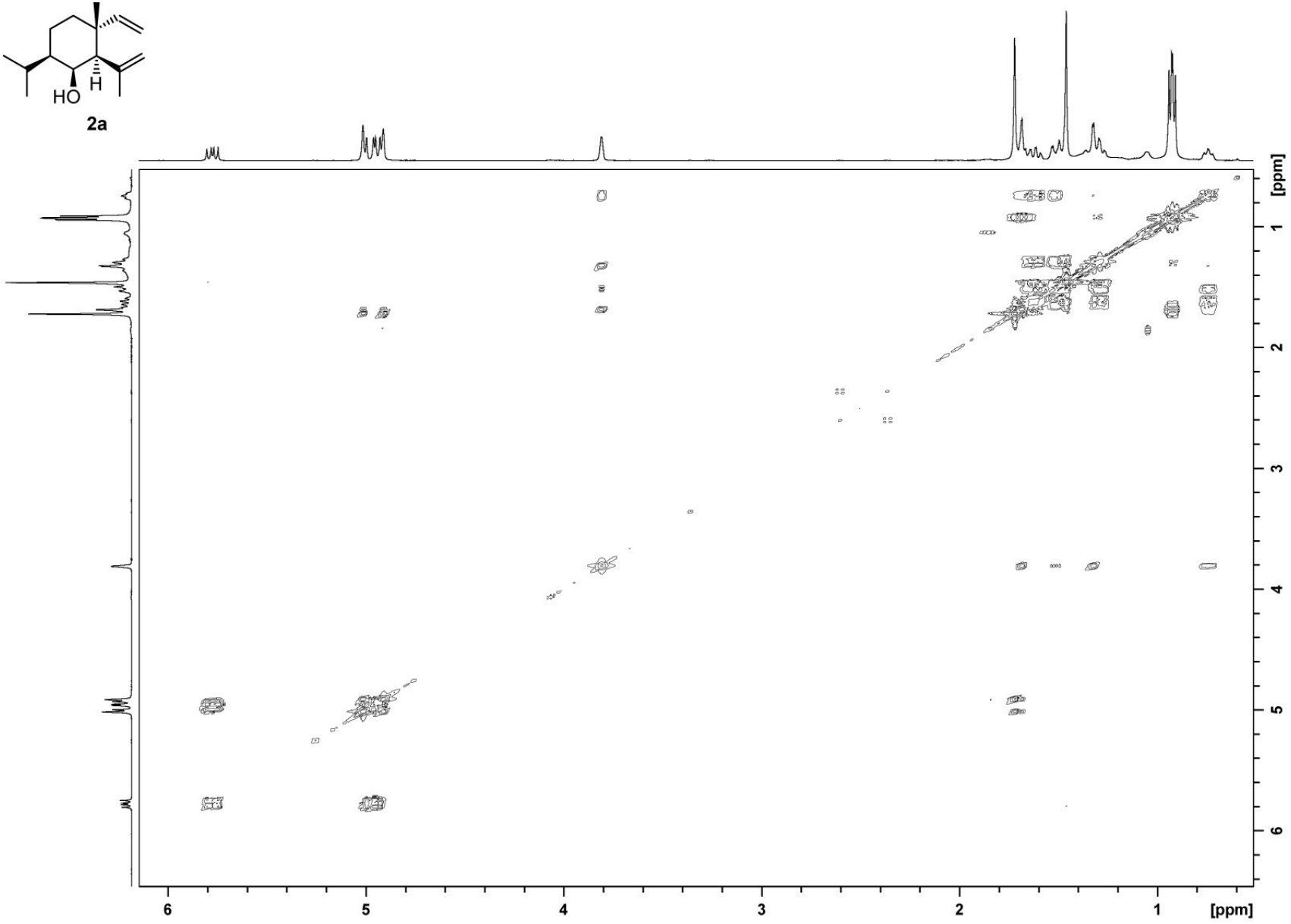
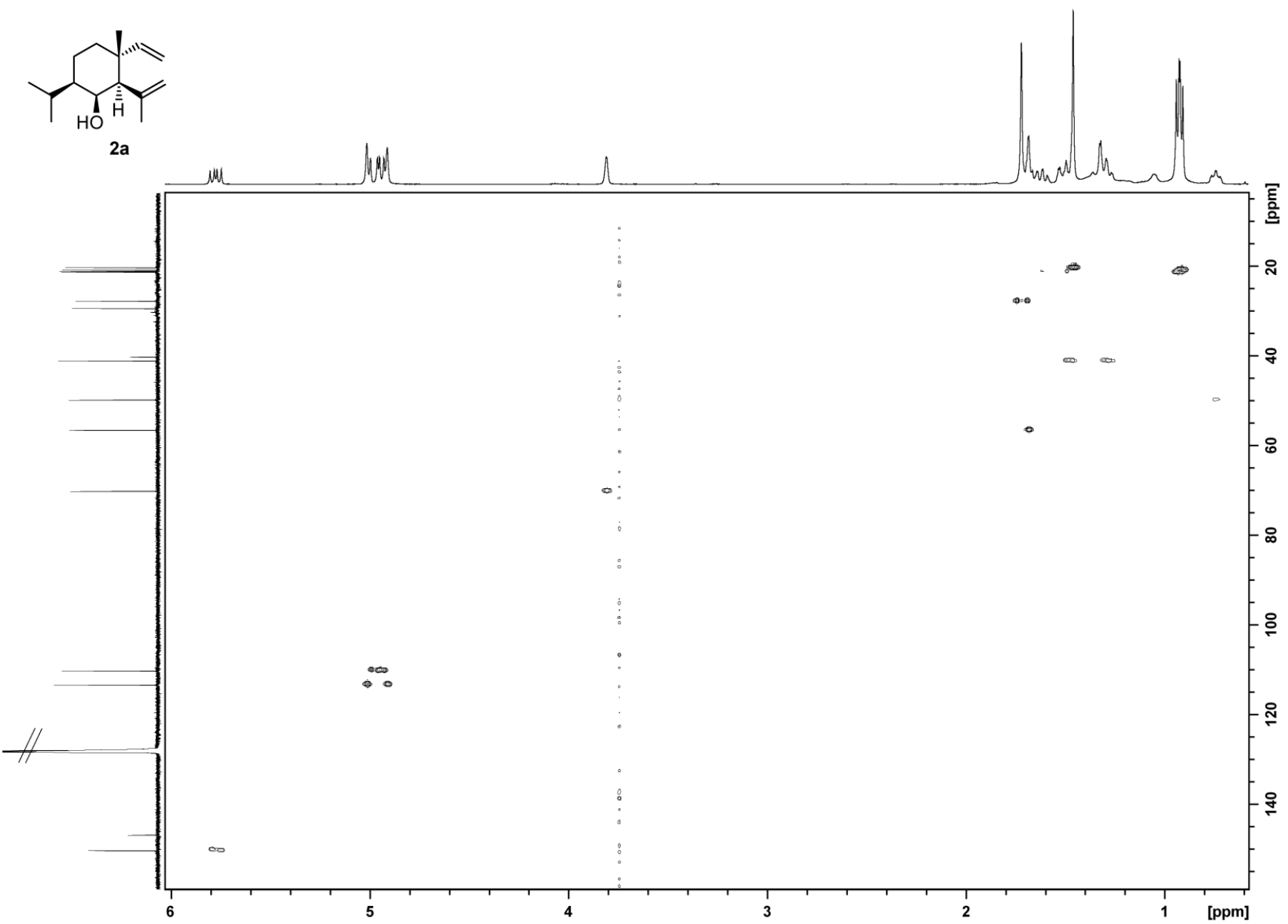


Figure 13 (continued). ^1H , ^1H -COSY spectrum of **2a** in $(^2\text{H}_6)$ benzene at 298K.





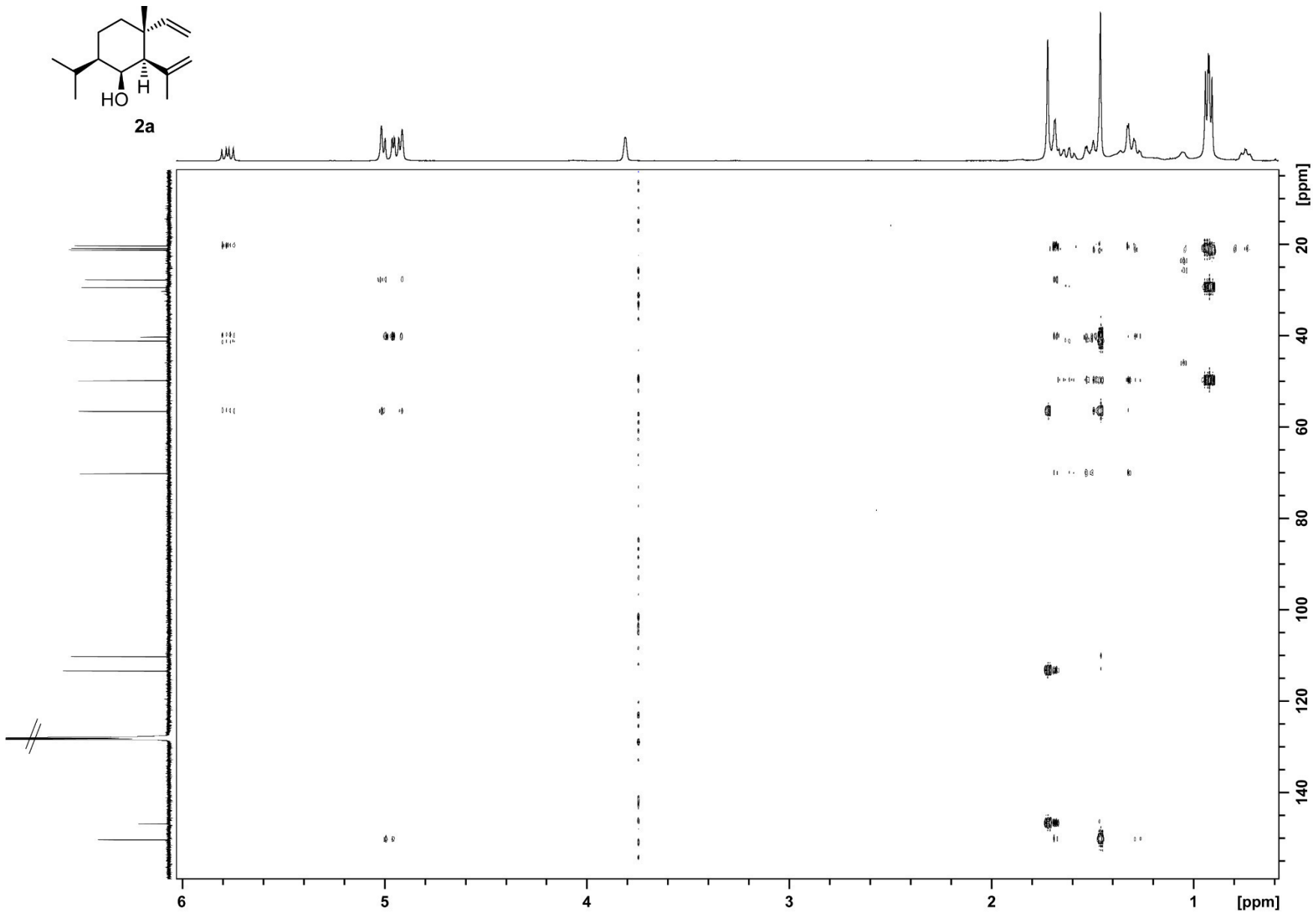
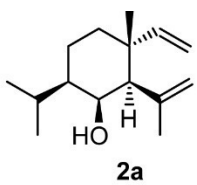


Figure 13 (continued). HMBC spectrum of **2a** in ($^2\text{H}_6$)benzene at 298K. Solvent signals are crossed out.

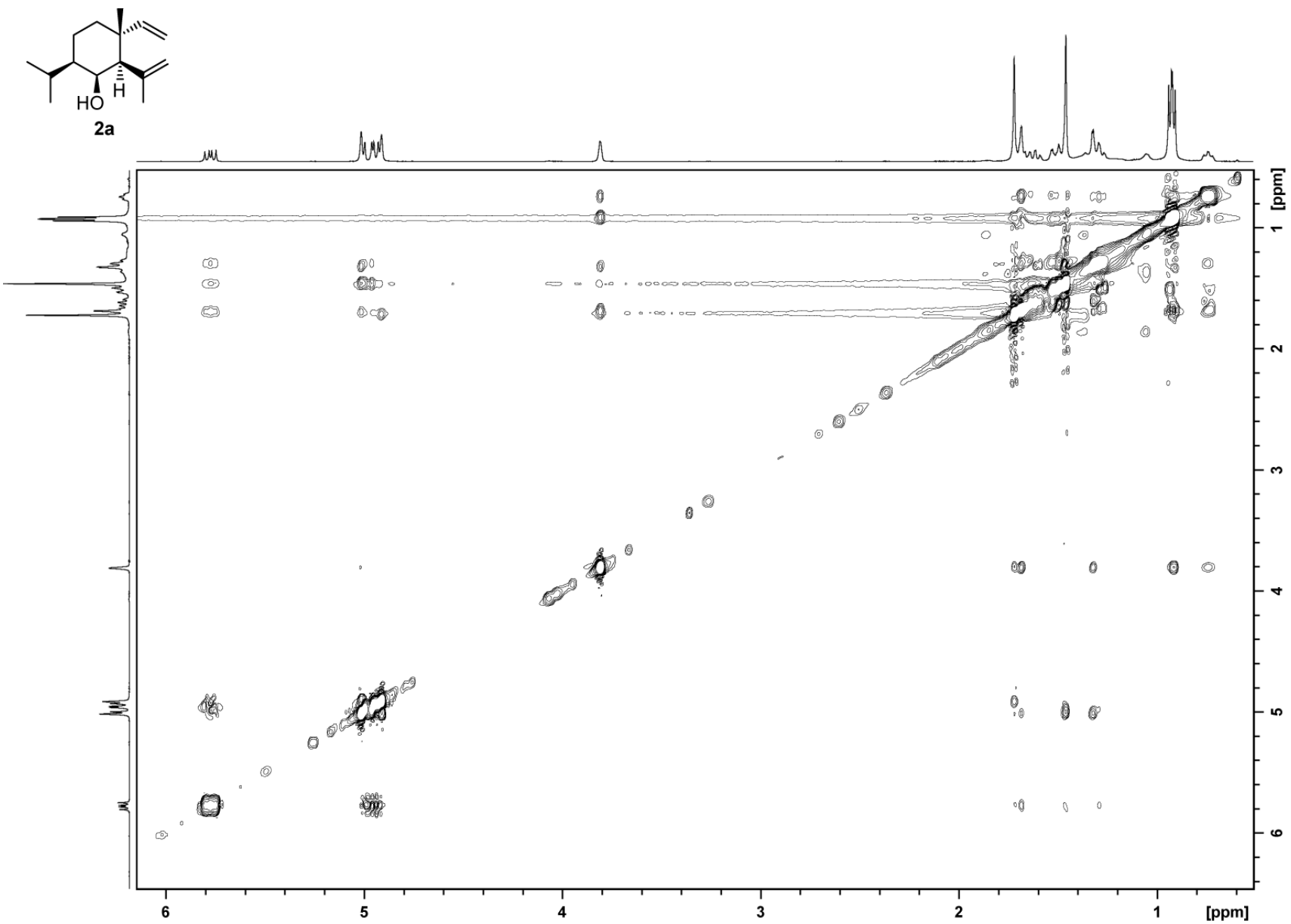


Figure 13 (continued). NOESY spectrum of **2a** in $(^2\text{H}_6)$ benzene at 298K.

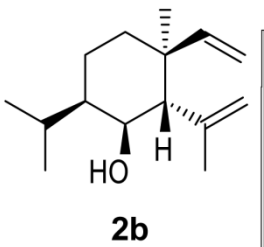
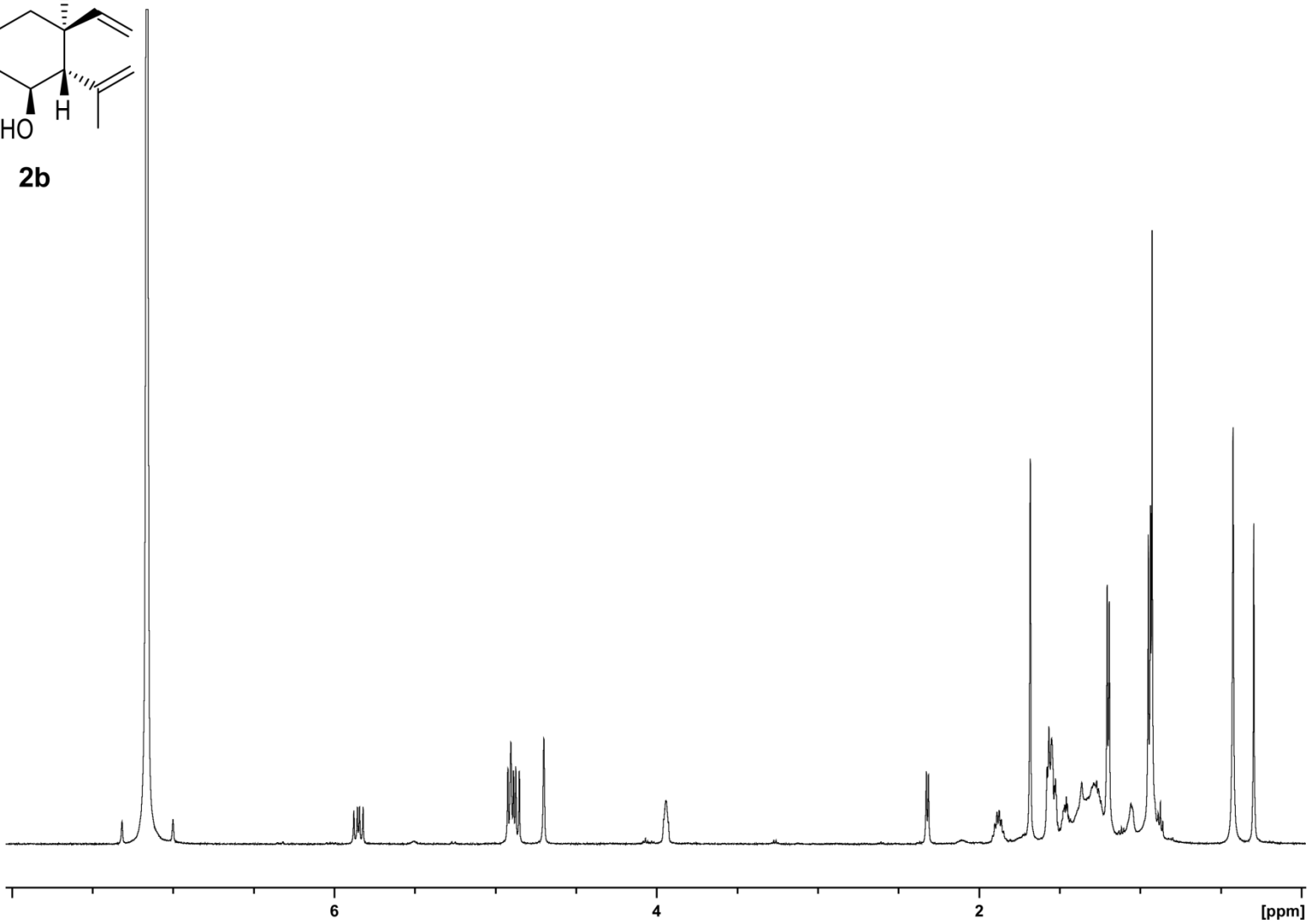
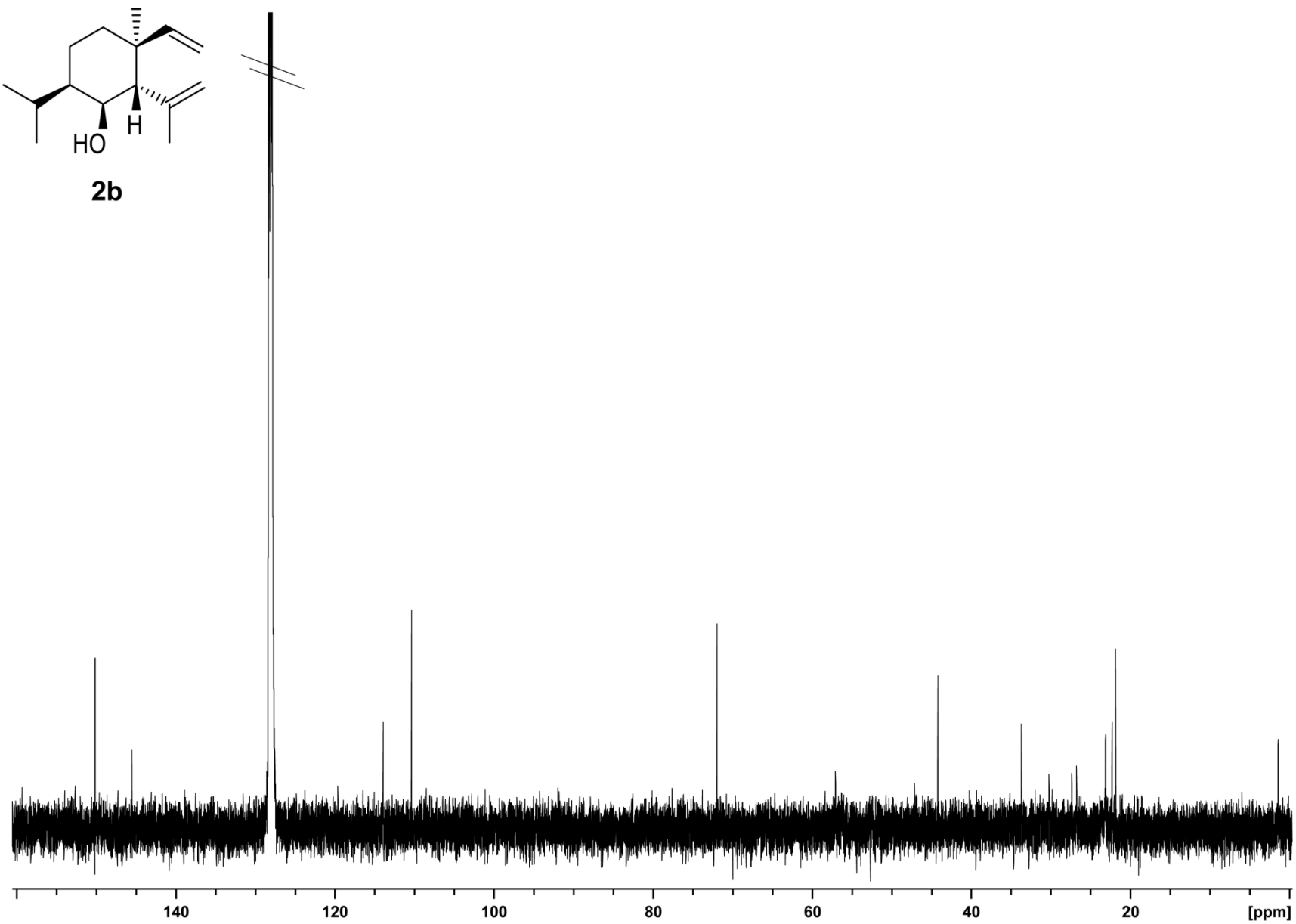
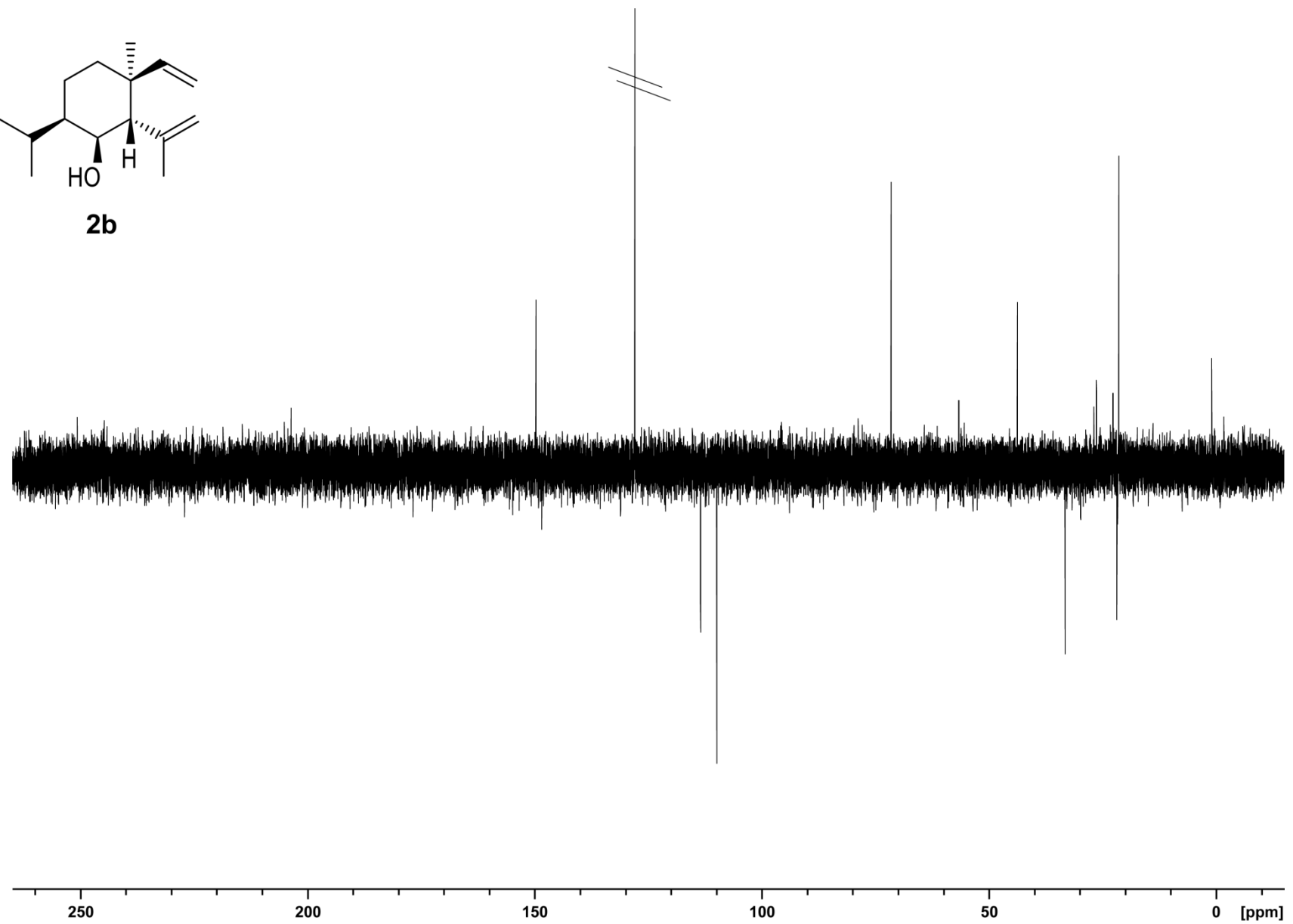
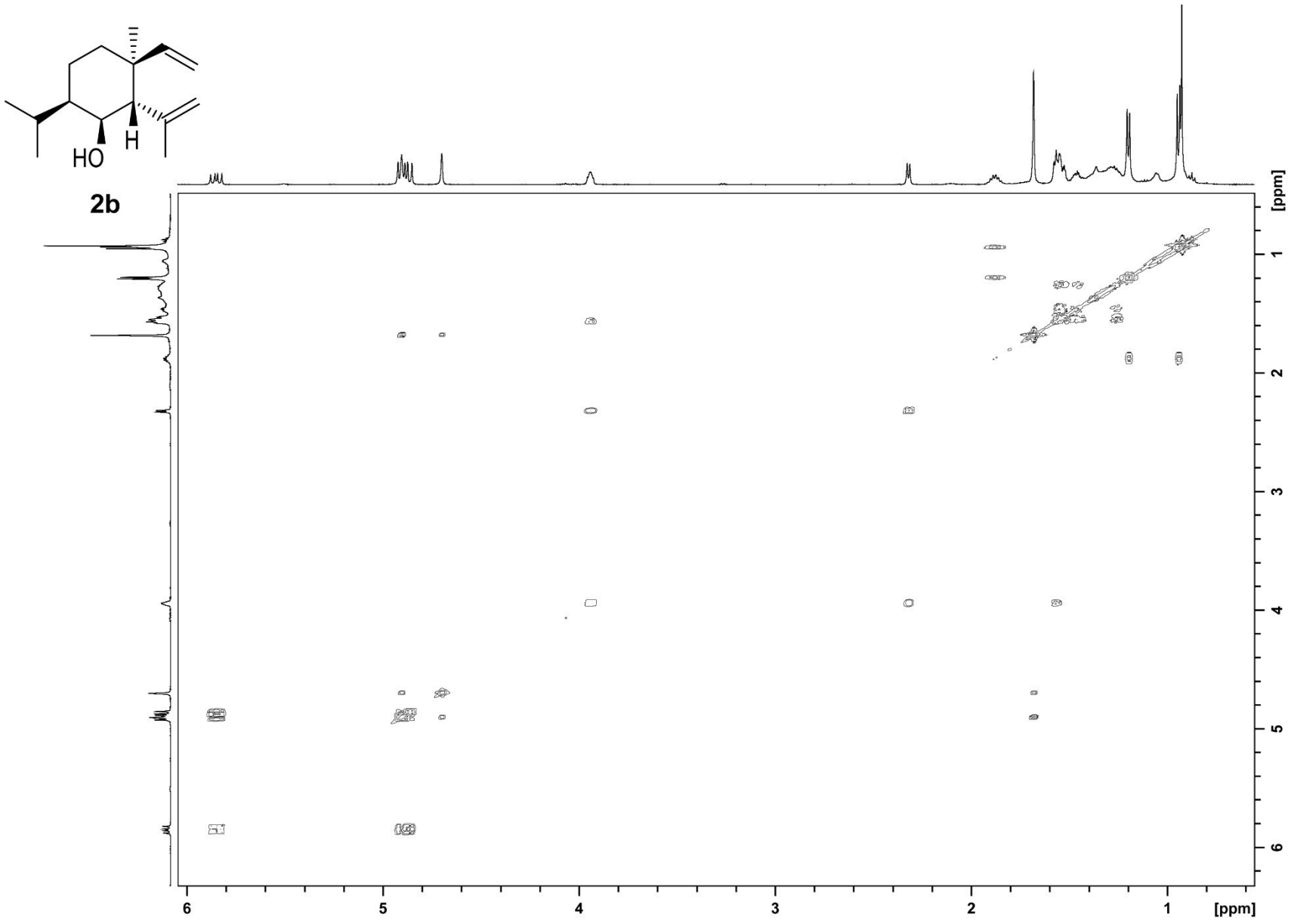


Figure 14. $^1\text{H-NMR}$ spectrum of **2b** in ($^2\text{H}_6$)benzene at 298K.









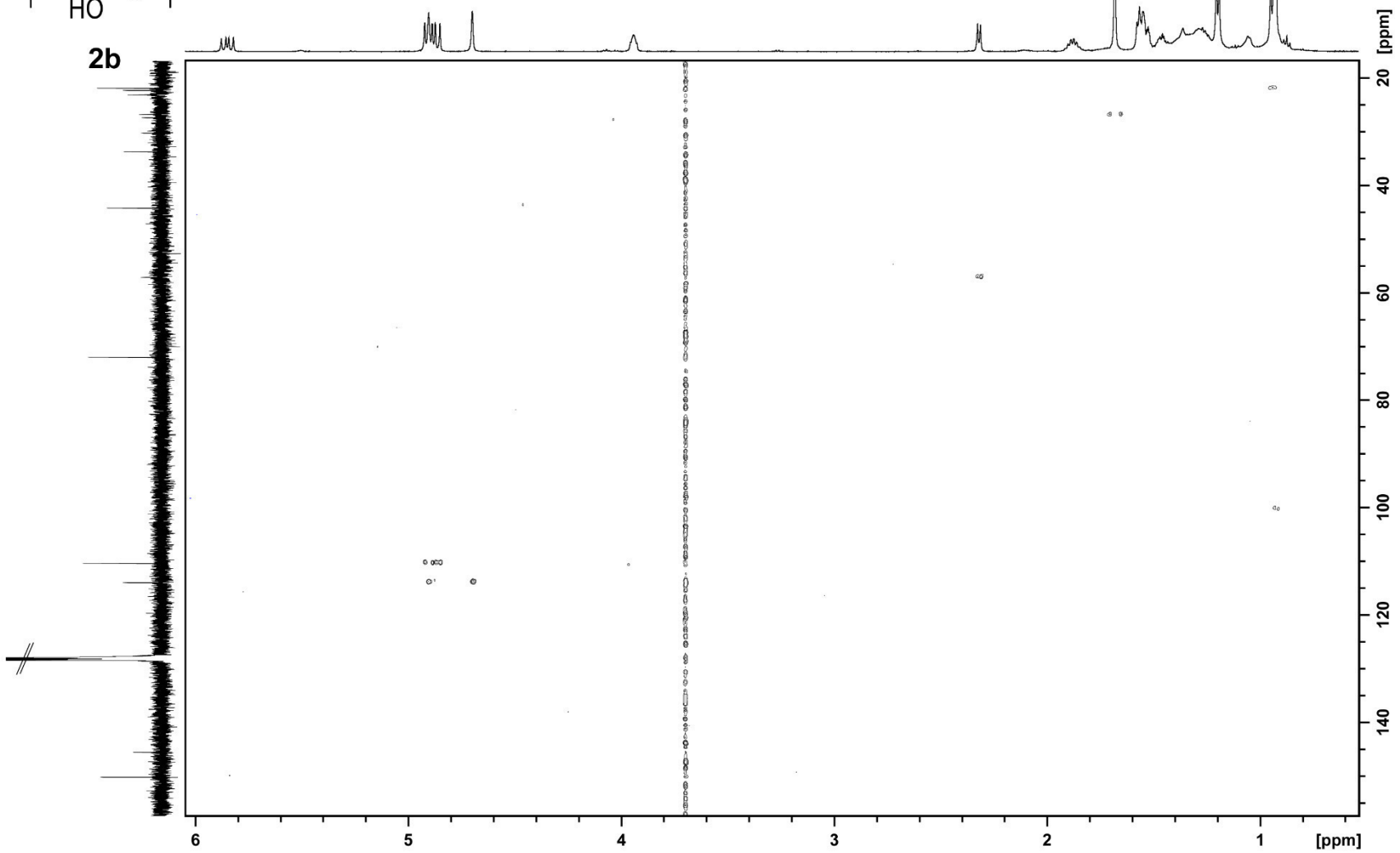
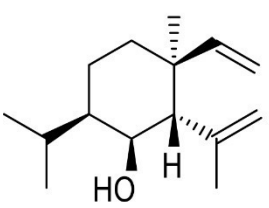


Figure 14 (continued). HSQC spectrum of **2b** in $^{2}H_6$ benzene at 298K. Solvent signals are crossed out.

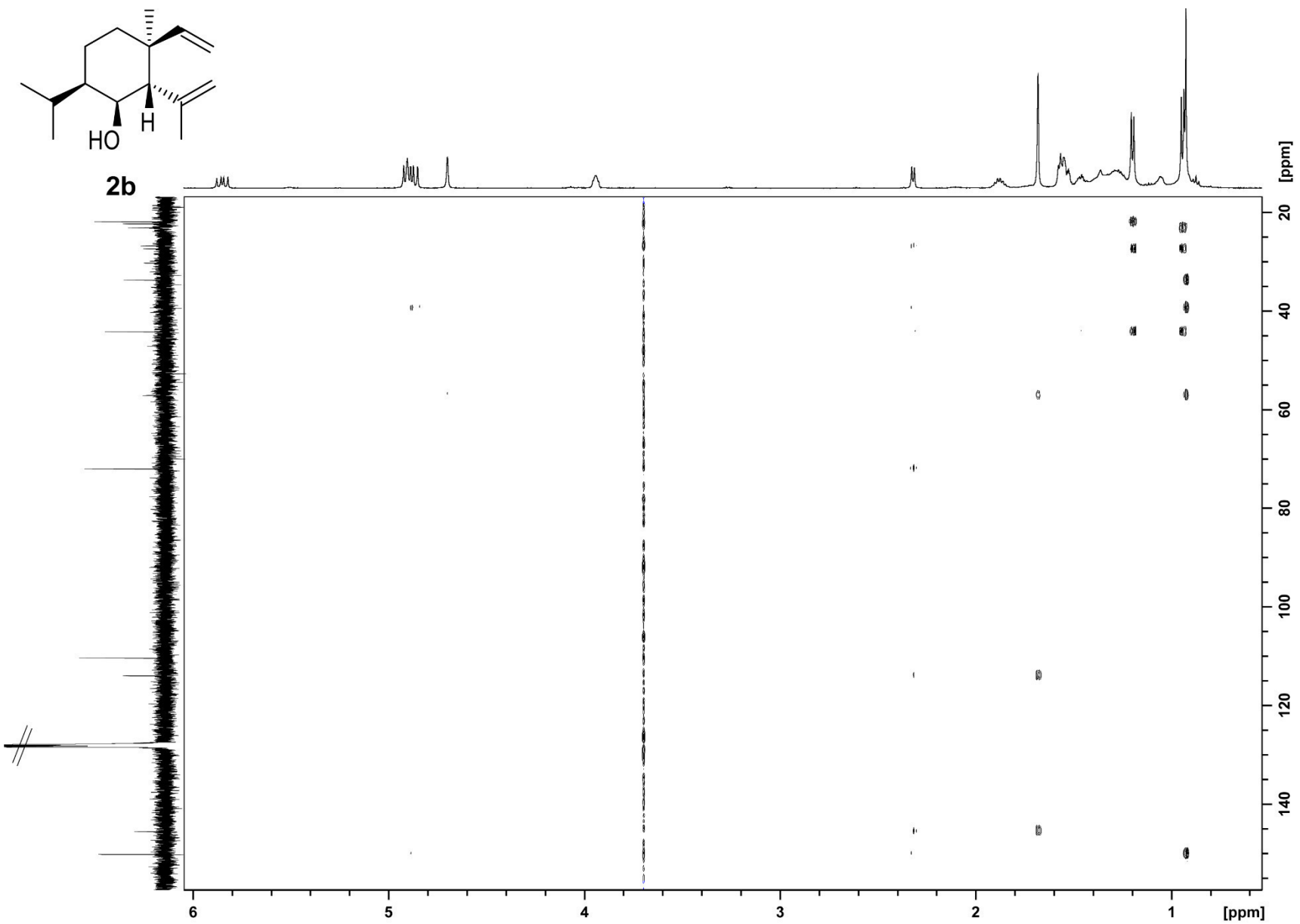
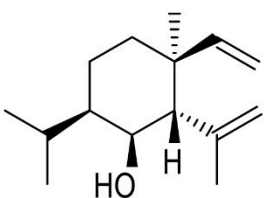
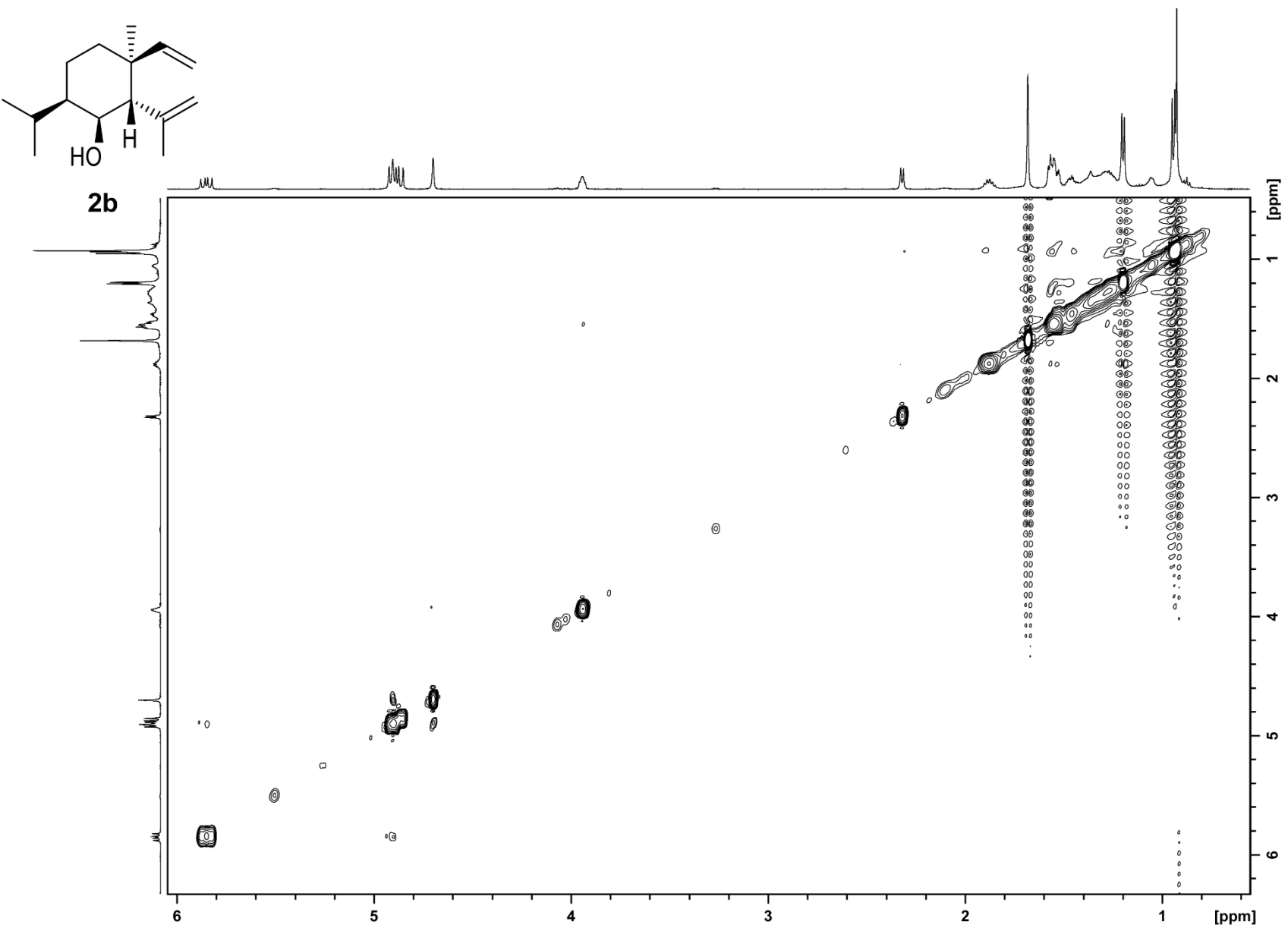


Figure 14 (continued). HMBC spectrum of **2b** in $(^2\text{H}_6)$ benzene at 298K. Solvent signals are crossed out.



References

- [1] J. S. Dickschat, K. A. K. Pahirulzaman, P. Rabe, T. A. Klapschinski, *ChemBioChem* **2014**, *15*, 810–814.
- [2] R. D. Gietz, R. H. Schiestl, *Nat. Protoc.* **2007**, *2*, 31–34.
- [3] N. S. Radulović, A. B. Miltojević, M. McDermott, S. Waldren, J. A. Parnell, M. Martins G. Pinheiro, P. Dias Fernandes, F. de Sousa Menezes, *J. Ethnopharmacol.* **2011**, *135*, 610–619.
- [4] C. A. Citron, P. Rabe, L. Barra, C. Nakano, T. Hoshino, J. S. Dickschat, *Eur. J. Org. Chem.* **2014**, 7684–7691.
- [5] V. Sharma, G. T. Kelly, C. M. H. Watanabe, *Org. Lett.* **2008**, *10*, 4815–4818.
- [6] E. L. Clennan, D. Zhang, J. Singleton, *Photochem. Photobiol.* **2006**, *82*, 1226–1232.
- [7] E. Wenkert, M. J. Gašić, E. W. Hagaman, L. D. Kwart, *Org. Magn. Resonance* **1975**, *7*, 51–53.
- [8] M. Peña-López, M. M. Martínez, L. A. Sarandeses, J. P. Sestelo, *J. Org. Chem.* **2010**, *75*, 5337–5339.
- [9] A. Michrowska, Ł. Gułajski, K. Grela, *Chem. Commun.* **2006**, 841–843.
- [10] T. Iwasaki, K. Agura, Y. Maegawa, Y. Hayashi, T. Ohshima, K. Mashima, *Chem. Eur. J.* **2010**, *16*, 11567–11571.
- [11] W. B. Motherwell, G. Bégis, D. E. Cladingboel, L. Jerome, T. D. Sheppard, *Tetrahedron* **2007**, *63*, 6462–6476.
- [12] P. Baer, P. Rabe, C. A. Citron, C. C. de Oliveira Mann, N. Kaufmann, M. Groll, J. S. Dickschat, *ChemBioChem* **2014**, *15*, 213–216.
- [13] D. M. Cermak, D. F. Wiemer, K. Lewis, R. J. Hoh, *Bioorg. Med. Chem.* **2000**, *8*, 2729–2737.
- [14] D. C. Braddock, G. Cansell, S. A. Hermitage, *Chem. Commun.* **2006**, 2483–2485.
- [15] J. S. Dickschat, S. C. Wenzel, H. B. Bode, R. Müller, S. Schulz, *ChemBioChem* **2004**, *5*, 778–787.
- [16] S. E. Sen, G. M. Garvin, *J. Label. Compd. Radiopharm.* **1995**, *36*, 1063–1069.
- [17] F. Khachik, G. R. Beecher, B. W. Li, G. Englert, *J. Label. Compd. Radiopharm.* **1995**, *36*, 1157–1172.
- [18] C. Nakano, T. Hoshino, *ChemBioChem* **2009**, *10*, 2060–2071.
- [19] G. L. Lange, C. Gottardo, *Synth. Commun.* **1990**, *20*, 1473–1479.
- [20] K. Foo, I. Usui, D. C. G. Götz, E. W. Werner, D. Holte, P. S. Baran, *Angew. Chem. Int. Ed.* **2012**, *51*, 11491–11495.
- [21] A. F. Barrero, M. Mar Herrador, J. F. Quilez, R. Alvarez-Manzaneda, D. Portal, J. A. Gavin, D. G. Gravalos, M. S. J. Simmonds, W. M. Blaney, *Phytochemistry* **1999**, *51*, 529–541.
- [22] B. Pickel, D. P. Drew, T. Manczak, C. Weitzel, H. T. Simonsen, D.-K. Ro, *Biochem. J.* **2012**, *448*, 261–271.
- [23] C. P. Cornwell, N. Reddy, D. N. Leach, S. G. Wyllie, *Flavor Fragr. J.* **2001**, *16*, 263–273.
- [24] B. Szafranek, K. Chrapkowska, D. Waligóra, R. Palavinskas, A. Banach, J. Szafranek, *J. Agr. Food Chem.* **2006**, *54*, 7729–7734.

Appendix H

A Method for Investigating the Stereochemical Course of Terpene Cyclisations



Cite this: *Org. Biomol. Chem.*, 2016, **14**, 158

A method for investigating the stereochemical course of terpene cyclisations†

Patrick Rabe, Jan Rinkel, Tim A. Klapschinski, Lena Barra and Jeroen S. Dickschat*

Three sesquiterpene cyclases from *Streptomyces scabiei* 87.22, *Streptomyces venezuelae* ATCC 10712 and *Streptomyces clavuligerus* ATCC 27064 were characterised and their products were identified as (–)-neomeranol B, (+)-isodauc-8-en-11-ol and (+)-intermedeol, respectively. The stereochemical courses of the terpene cyclisations were investigated by use of various ¹³C-labelled FPP isotopomers. A quick and easy test was developed that allows to distinguish reprotonations of olefinic double bonds in neutral intermediates from the two stereoheterotopic faces. The method makes use of incubating ¹³C-FPP isotopomers labelled at the reprotonated carbon in deuterium oxide and subsequent HSQC analysis of the product. A 1,7-cyclisation towards (+)-isodauc-8-en-11-ol was followed by use of (1,7-¹³C₂)-FPP. Surprisingly, the (+)-isodauc-8-en-11-ol also accepted (2Z,6E)-FPP resulting in the same product profile as obtained from (2E,6E)-FPP.

Received 25th September 2015,
Accepted 12th October 2015

DOI: 10.1039/c5ob01998b

www.rsc.org/obc

Introduction

Terpenes are a structurally diverse class of natural products which are present in all kingdoms of life. Their biosynthesis proceeds *via* the linear precursors geranyl diphosphate (monoterpenes, C₁₀), farnesyl diphosphate (sesquiterpenes, C₁₅) or geranylgeranyl diphosphate (diterpenes, C₂₀) that are converted into (poly)cyclic terpene hydrocarbons or alcohols by terpene cyclases. As crystallographic data reveal,^{1–8} class 1 enzymes exhibit, despite an overall low sequence conservation, a highly conserved α -helical fold, and in their active sites the highly conserved aspartate-rich motif (DDXX(X)(D,E)) near position 90 and approximately 130 residues downstream the NSE triad (NDXXSXX(R,K)(E,D)) for binding of a trinuclear Mg²⁺ cluster. The substrate binds in turn with its diphosphate moiety to the Mg²⁺ cations for formation of a highly reactive allyl cation. A reaction cascade involving cyclisations, carbon backbone rearrangements, hydride migrations and a terminal deprotonation or nucleophilic attack of water yields a terpene hydrocarbon or alcohol.^{9,10} The recently obtained crystal structure of selina-4(15),7(11)-diene synthase from *Streptomyces pristinaespiralis* in combination with site-specific mutations

demonstrated the additional involvement of a highly conserved arginine (pyrophosphate sensor) that is part of an effector triad located at the helix G break, in most bacterial enzymes exactly 46 residues upstream of the NSE triad, and a RY dimer near the enzyme's C-terminus that are both important for substrate recognition.⁸ Cationic intermediates along the cyclisation cascade can be stabilised by cation- π -interactions with aromatic residues.^{4,5,7,8,11} To date, the products of nearly 50 bacterial type I terpene synthases have been characterized,^{11–31} and the functions of many enzymes can be delineated from their high sequence identity to these known enzymes. This work has resulted in the assignment of a function to nearly half of the *ca.* 600 presumptive terpene cyclases encoded in the genomes of sequenced bacteria, while the other half of these enzymes still awaits functional characterisation. Here we present the molecular cloning and expression of three bacterial terpene cyclases and structure elucidation of the products made by these enzymes. Furthermore, the enzyme mechanisms were investigated by isotopic labelling experiments.

Results and discussion

The gene of an unidentified terpene synthase from *Streptomyces scabiei* 87.22 (WP_013004899) was cloned into the expression vector pYE-Express by homologous recombination in yeast.²⁶ The His-tagged recombinant protein was expressed in *E. coli*, purified by Ni-NTA chromatography and incubated with oligoprenyl diphosphates for functional characterisation. While GPP and GGPP were not accepted as substrates, FPP

Kekulé-Institut für Organische Chemie und Biochemie, Rheinische Friedrich-Wilhelms-Universität Bonn, Gerhard-Domagk-Straße 1, 53121 Bonn, Germany.

E-mail: dickschat@uni-bonn.de

† Electronic supplementary information (ESI) available: Strains, culture conditions, gene cloning and expression conditions, details of incubation experiments and synthesis of (1,7-¹³C₂)FPP including spectroscopic data, and gas chromatograms, mass spectra and NMR spectra of terpene cyclase products. See DOI: 10.1039/c5ob01998b

conversion yielded a product with an EI mass spectrum that was not included in our mass spectral libraries (Fig. 1a of ESI†). EI-MS-QTOF analysis pointed to a sesquiterpene alcohol ($m/z = 222.1970$, calc. for $C_{15}H_{26}O^+$: 222.1978). The compound was purified from an enzymatic conversion of 80 mg FPP, yielding 4.1 mg of the pure sesquiterpene alcohol, and its structure was determined by one- and two-dimensional NMR spectroscopy (Table 1).

The ^{13}C -NMR and ^{13}C -DEPT135-NMR spectra of **1** exhibited fifteen carbon signals (four methyl, five methylene, two methine, one oxygenated methine and three quaternary carbons). The absence of signals for sp^2 carbons suggested a tricyclic ring system. The signals for the corresponding protons for each carbon were assigned by heteronuclear single quantum correlation (HSQC) spectroscopy. 1H , 1H -correlation spectroscopy (COSY) revealed two contiguous spin systems (C-5-6-7-8-9 and C-1-2-3, Fig. 2a). The 1H -NMR signals for all four methyl groups appeared as singlets revealing their attachment to quaternary carbons. The highfield shifts of the protons attached to C-6 and C-7 ($\delta = 0.48$ and 0.52 ppm) suggested the presence of a cyclopropane ring. Heteronuclear multiple bond correlation (HMBC) spectroscopy showed cross peaks from C-12 and C-13 to C-6, C-7 and C-11, from C-14 to

C-1, C-4, C-8, C-9 and C-10, and from C-15 to C-3, C-4, C-5 and C-10. These and all other HMBC correlations (including C-6 to C-5, C-7 and C-8; C-10 to C-2 and C-1 to C-3) were in agreement with the structure of **1**. The relative configuration was determined by nuclear Overhauser spectroscopy (NOESY, Fig. 2a). Key correlations were observed between H-12, H-6 and H-7, indicating the *cis*-orientation of H-6 and H-7. Correlations between both bridgehead methyl groups H-14 and H-15 supported the *cis*-fused 7-5 ring system. Further diagnostic cross-peaks were observed between H-5 and H-13 and between H-6 and H-15, resulting in a fully assigned relative stereochemistry. The optical rotary power was determined as $[\alpha]_D^{24} = -10.2$ ($c = 0.082$, CH_2Cl_2).

The sesquiterpene alcohol **1** (neomeranol B) is a new natural product with a neomerane-type carbon backbone as previously described for neomeranol (**2**), a compound that was isolated from the green alga *Neomeris annulata* and has cytotoxic activity against brine shrimp.^{32,33} A series of oxidised neomeranes was recently isolated from *Valeriana officinalis*.³⁴ Compound **1** is also present in headspace extracts of *Streptomyces scabiei* 87.22 (Fig. 2 of ESI†), demonstrating that the neomeranol B synthase is expressed under laboratory culture conditions.

Table 1 NMR data of (–)-neomeranol B (**1**), (+)-isodauc-8-en-11-ol (**3**) and (+)-intermedeol (**4**) in (2H_6)benzene

1 C ^a	¹ H (δ , m, J, int) ^b	¹³ C (δ) ^c	3 C ^a	¹ H (δ , m, J, int) ^b	¹³ C (δ) ^c	4 C ^a	¹ H (δ , m, J, int) ^b	¹³ C (δ) ^c
1a	1.78 (dt, ³ J = 9.4, ² J = 12.5, 1H)	35.7 (CH ₂)	1	—	42.5 (C _q)	1a	1.22 (m, 1H)	41.7 (CH ₂)
1b	1.09 (m, 1H)					1b	0.98 (m, 1H)	
2a	1.63 (m, 1H)	19.2 (CH ₂)	2a	1.33 (m, 1H)	41.9 (CH ₂)	2	1.33 (m, 2H)	22.5 (CH ₂)
2b	1.65 (m, 1H)		2b	1.20 (m, 1H)				
3a	2.49 (m, 1H)	34.9 (CH ₂)	3a	1.55 (m, 1H)	27.5 (CH ₂)	3a	1.58 (m, 1H)	43.8 (CH ₂)
3b	1.46 (m, 1H)		3b	1.50 (m, 1H)		3b	1.17 (m, 1H)	
4	—	52.3 (C _q)	4	2.13 (dt, ³ J = 11.4, ³ J = 9.2, 1H)	53.55 (CH)	4	—	71.3 (C _q)
5	3.19 (d, ³ J = 9.1, 1H)	69.5 (CH)	5	1.71 (dt, ³ J = 12.5, ³ J = 2.2, 1H)	57.4 (CH)	5	1.38 (m, 1H)	49.1 (CH)
6	0.48 (dd, ³ J = 9.5, ³ J = 9.2, 1H)	31.2 (CH)	6a	1.43 (ddt, ² J = 13.5, ³ J = 11.8, ³ J = 2.4, 1H)	23.9 (CH ₂)	6a	1.81 (m, 1H)	23.9 (CH ₂)
			6b	2.31 (ddt, ² J = 13.5, ³ J = 5.6, ³ J = 2.4, 1H)		6b	1.63 (m, 1H)	
7	0.52 (dt, ³ J = 9.5, ³ J = 6.2, 1H)	27.9 (CH)	7a	2.03 (m, 1H)	36.5 (CH ₂)	7	2.34 (br, 1H)	39.8 (CH)
			7b	1.97 (m, 1H)				
8a	1.03 (m, 1H)	20.5 (CH ₂)	8	—	139.4 (C _q)	8a	2.15 (dtt, ³ J = 12.6, ³ J = 1.8, 1H)	23.1 (CH ₂)
8b	1.51 (m, 1H)					8b	1.27 (m, 1H)	
9a	1.37 (m, 1H)	37.3 (CH ₂)	9	5.48 (m, 1H)	123.3 (CH)	9a	1.42 (m, 1H)	40.7 (CH ₂)
9b	1.42 (m, 1H)					9b	1.05 (m, 1H)	
10	—	46.1 (C _q)	10a	1.86 (m, 1H)	42.9 (CH ₂)	10	—	35.4 (C _q)
			10b	2.07 (m, 1H)				
11	—	19.3 (C _q)	11	—	73.7 (C _q)	11	—	146.9 (C _q)
12	0.95 (s, 3H)	29.0 (CH ₃)	12	1.06 (s, 3H)	27.7 (CH ₃)	12	1.78 (dt, ⁴ J = 0.7, ⁴ J = 0.6, 3H)	23.0 (CH ₃)
13	1.02 (s, 3H)	15.2 (CH ₃)	13	1.02 (s, 3H)	32.4 (CH ₃)	13	5.08 (dm, ² J = 9.4, ⁴ J = 0.7, 2H)	111.4 (CH ₂)
14	0.87 (d, ⁴ J = 0.8, 3H)	28.0 (CH ₃)	14	1.75 (m, 3H)	27.3 (CH ₃)	14	0.79 (t, ⁴ J = 0.8, 3H)	18.6 (CH ₃)
15	1.04 (s, 3H)	15.2 (CH ₃)	15	0.85 (s, 3H)	19.4 (CH ₃)	15	0.98 (d, ⁴ J = 0.7, 3H)	22.7 (CH ₃)

^aCarbon numbering as in Fig. 1. ^bChemical shifts δ in ppm, multiplicity m (s = singlet, d = doublet, t = triplet, m = multiplet, br = broad), coupling constants J are given in Hertz (spectra of **1** and **3** recorded at 500 MHz, spectra of **4** recorded at 600 MHz). ^cChemical shifts δ in ppm and assignment of carbons by ^{13}C -DEPT135 spectroscopy. For NMR data of **3** in (2H)chloroform cf. Table 1 of ESI.

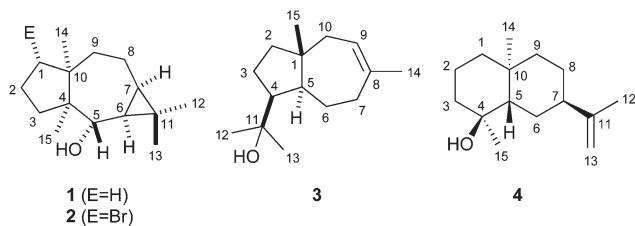


Fig. 1 Structures of neomeranol B (**1**), neomeranol (**2**), isodauc-8-en-11-ol (**3**) and (+)-intermedeol (**4**).

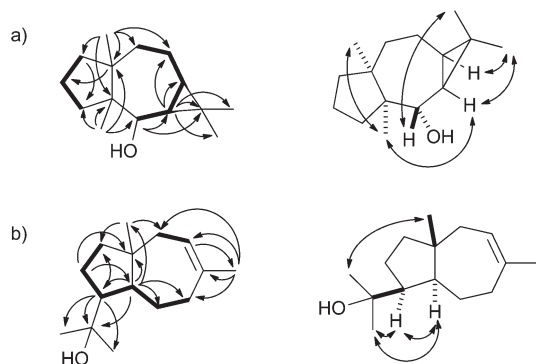


Fig. 2 Key HMBC (single headed arrows) and NOESY correlations (double headed arrows) for (a) neomeranol B (**1**) and (b) isodauc-8-en-11-ol (**3**). Contiguous ^1H -spin systems are shown in bold.

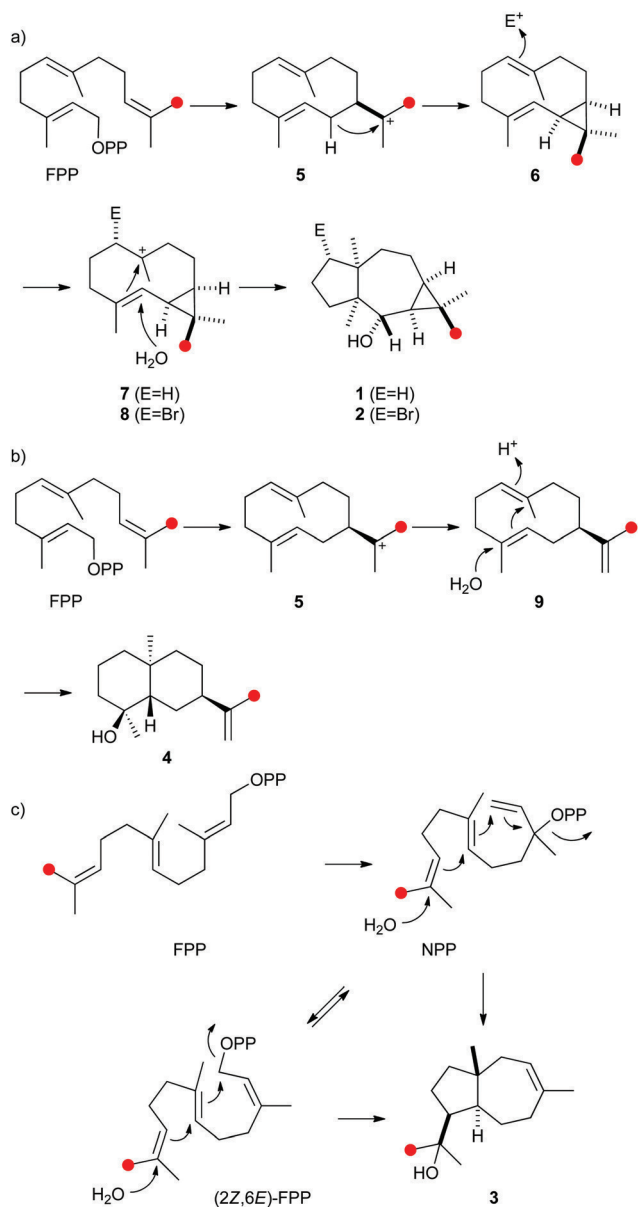
Using the same approach a terpene synthase from *Streptomyces venezuelae* ATCC 10712 (CCA53839) also yielded an unknown sesquiterpene alcohol (EI-MS-QTOF: $m/z = 222.1973$, the EI mass spectrum is shown in Fig. 1b of ESI †) from FPP, while GPP and GGPP were not accepted. The enzymatic conversion of 90 mg FPP followed by purification *via* column chromatography yielded 12 mg of the pure compound **3**. Its ^{13}C -NMR and ^{13}C -DEPT135 spectra showed fifteen carbon signals for four methyl, five methylene, three methine and three quaternary carbons (Table 1). One of the quaternary carbons ($\delta = 73.7$ ppm) carried the alcohol function, while the signals of two carbons appeared in the olefinic region, indicating a bicyclic system. HSQC allowed for a correlation of the ^1H signals with the ^{13}C signals, while the $^1\text{H}, ^1\text{H}$ -COSY spectrum revealed two spin systems (C-9-10 and C-2-3-4-5-6-7, Fig. 2b). HMBC connectivities from C-4 to C-11, C-12 and C-13 indicated the 1-hydroxy-1-methylethyl moiety, while further key HMBC correlations from C-5 to C-3, C-4, C-6, C-7, C-11 and C-15, and from C-14 to C-7, C-8, C-9 and C-10 explained the bicyclo[5.3.0]decene system. The relative configuration was determined by NOESY (Fig. 2b) that showed diagnostic correlations between H-15 and H-12, and between H-5, H-4 and H-13, in agreement with a *trans*-fused ring system and the *cis*-orientation of H-4 and H-5. The optical rotary power was determined as $[\alpha]_{\text{D}}^{22} = +19.4$ ($c = 0.505$, CH_2Cl_2). In summary, compound **3** was identified as the new natural product (+)-isodauc-8-en-11-ol.

Recently, Ikeda and coworkers reported on the production of (+)-dauca-8,11-diene by the same terpene cyclase during heterologous expression in *Streptomyces avermitilis*.²⁹ This compound was observed as a minor product (3%) of the purified recombinant enzyme in the conversion of FPP (Fig. 3a of ESI †). In agreement with this finding only the sesquiterpene alcohol **3**, but not dauca-8,11-diene is present in headspace extracts of *S. venezuelae* ATCC 10712 (Fig. 3b of ESI †).³⁵ In conclusion, the function of the sesquiterpene cyclase from *S. venezuelae* must be reassigned as (+)-isodauc-8-en-11-ol synthase.

The incubation of FPP with a third terpene cyclase from *S. clavuligerus* ATCC 27064 (WP_003955204) yielded a sesquiterpene alcohol, whereas GPP and GGPP were not converted by the enzyme. Its EI mass spectrum (Fig. 1c of ESI †) and all NMR data were in agreement with literature data for intermedeol (**4**) (Tables 1 and 2 of ESI †).^{36,37} The absolute configuration was determined as (+)-(4*S*,5*S*,7*R*,10*S*)-**4** based on the measured optical rotary power of $[\alpha]_{\text{D}}^{25} = +11.9$ ($c = 0.50$, CH_2Cl_2) in comparison to reported data for (+)-**4** of $[\alpha]_{\text{D}}^{22} = +18.0$ ($c = 2.80$, CHCl_3).³⁶ The sesquiterpene alcohol **4** is also found in the volatiles fraction of *S. clavuligerus* ATCC 27064 (Fig. 4 of ESI †).

The biosynthetic mechanisms of the three characterised bacterial sesquiterpene cyclases were investigated by isotopic labelling experiments. For the biosynthesis of **2** a pathway *via* cyclisation of FPP to the (*E,E*)-germacradienyl cation (**5**) followed by deprotonation to bicyclogermacrene (**6**) was proposed (Scheme 1a).³² Several types of halogenases including vanadium-dependent chloroperoxidases or FADH₂-dependent halogenases provide Hal⁺ equivalents in the biosynthesis of halogenated natural products.^{38,39} The halogenation of **6** with an electrophilic bromine species to the cationic intermediate **8** may initiate a second cyclisation with attack of water, either in a concerted process or *via* a cyclopropylcarbinyl cation as discussed for the biosynthesis of avermitilol,⁴⁰ to yield **2**. For the biosynthesis of **1** a very similar cyclisation cascade can be assumed in which the electrophile "Br⁺" is substituted by a proton. Such a cyclisation cascade *via* the neutral intermediate **6** can be catalysed by a single terpene cyclase, while the biosynthesis of **2** likely requires two enzymes: a terpene cyclase for the formation of **6** from FPP and a halogenase for the conversion of **6** into **2**. The pathway for the formation of **1** by the terpene cyclase from *S. scabiei* *via* the neutral intermediate **6** is supported by its occurrence as a trace compound in enzyme incubations of FPP (Fig. 2a of ESI †).

The protonation of **6** at C-1 was evident from incubations of ($6\text{-}^{13}\text{C}$)FPP³¹ in water and in deuterium oxide followed by direct ^{13}C -NMR analysis of the product that was simply extracted with ($^2\text{H}_6$)benzene, resulting in a strongly enhanced singlet for C-1 of **1** in the incubation experiment in water and a triplet due to $^2\text{H}, ^{13}\text{C}$ -coupling in the experiment in deuterium oxide (Fig. 3a and b). The stereochemical course of the protonation was followed by HSQC analysis of the two obtained samples. While ($1\text{-}^{13}\text{C}$)-**1** gave two distinct crosspeaks for coupling of C-1 with the two directly bound diastereotopic



Scheme 1 Proposed biosynthesis of (a) neomeranols **1** and **2**, (b) (+)-(4*S*,5*S*,7*R*,10*S*)-intermedeol (**4**) and (c) isodauc-8-en-11-ol (**3**). Red circles indicate ¹³C-labelled carbons.

protons at $\delta_{\text{H}} = 1.09$ and 1.78 ppm, only one crosspeak at $\delta_{\text{H}} = 1.78$ ppm was observed for (1-¹³C,1-²H)-**1** obtained from the incubation of FPP in deuterium oxide (Fig. 3c). Thus, the proton at $\delta_{\text{H}} = 1.09$ was substituted by deuterium, which is *cis*-oriented to Me-14, as was established by NOESY with the unlabelled compound (this hydrogen shows a crosspeak with the neighbouring methyl group (H-14), while the second proton at C-1 shows a crosspeak to H-5, next to the hydroxy function; Fig. 12 of ESI†). In summary, this experiment revealed a strict stereochemical course for the reprotonation of the neutral intermediate **6** to yield **1** with a *cis*-orientation of the introduced hydrogen and Me-14. Because of the unknown

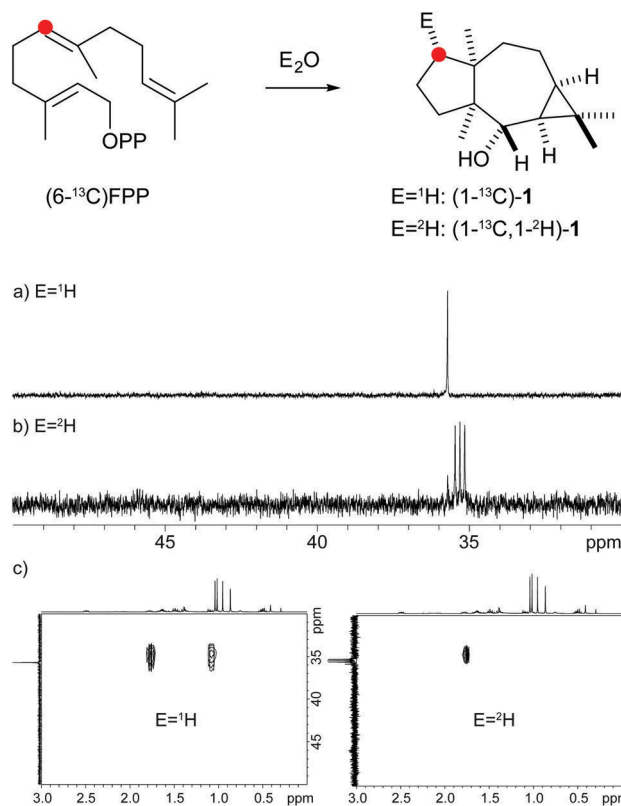


Fig. 3 Incubation experiments with (6-¹³C)FPP and the neomeranol B synthase in water and in deuterium oxide. Red circles indicate ¹³C-labelled carbons.

absolute configuration of **1** it remains unknown whether this corresponds to a *Re* or a *Si* face attack to intermediate **6**.

A model for the biosynthesis of (4*S*,5*S*,7*R*,10*S*)-**4** starts with a 1,10-cyclisation of FPP to the germacradienyl cation (**5**) that forms germacrene A (**9**) upon loss of a proton (Scheme 1b). Reprotonation at C-1 initiates a second cyclisation and subsequent attack of water to yield **4**. This suggested mechanism was studied using the same approach as described above for the neomeranol B synthase, *i.e.* via the incubation of (6-¹³C)-FPP with the intermedeol synthase in water and in deuterium oxide. NMR analysis of the extracted product resulted in a strongly enhanced singlet (incubation in water) or triplet for the ¹³C-labelled carbon due to ²H, ¹³C-coupling (incubation in deuterium oxide), thereby proving the reprotonation at C-1 (Fig. 4a and b). The stereochemistry of the protonation step was again evident from HSQC analysis of both samples, revealing that the crosspeak at $\delta_{\text{H}} = 0.98$ ppm (*pro-R* proton as evident from the NOESY spectrum, Fig. 26 of ESI†) is retained in the deuterated sample, while the crosspeak at $\delta_{\text{H}} = 1.22$ ppm (*pro-S* proton) is lost (Fig. 4c). Here, reprotonation of the neutral intermediate **9** from the *Si* face can be concluded, since the absolute configuration of **4** is known.

A biosynthetic proposal for the formation of **3** includes the initial isomerisation of FPP to NPP that may react in a zipper mechanism in two concerted 1,7- and 6,10-cyclisations with

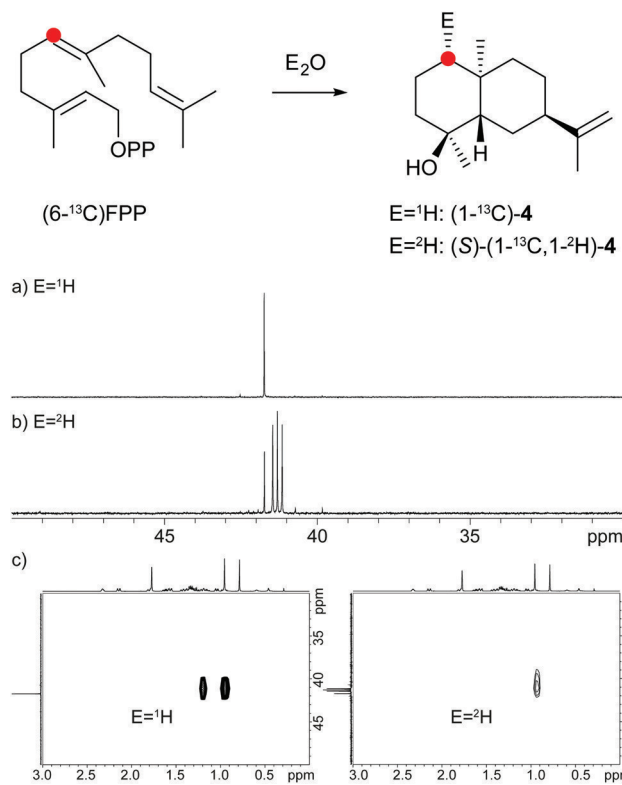


Fig. 4 Incubation experiments with (6-¹³C)FPP and the intermediol synthase in water and in deuterium oxide. Red circles indicate ¹³C-labelled carbons.

concomitant attack of water at C-11 (Scheme 1c). Experimental evidence for this mechanism was obtained by incubation of (1,7-¹³C₂)FPP (for synthesis *cf.* Fig. 5 of ESI†) with the purified recombinant isodauc-8-en-11-ol synthase that gave two doublets for ¹J_{C,C}-coupling in the ¹³C-NMR spectrum with a coupling constant of 35.0 Hz and a strong roof effect (Fig. 5).

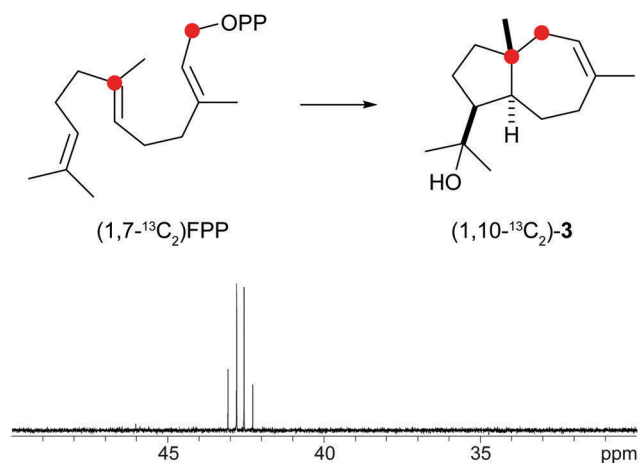


Fig. 5 Incubation of (1,7-¹³C₂)FPP with isodauc-8-en-11-ol synthase. The two doublets in the ¹³C-NMR spectrum show a strong roof effect. Red circles indicate ¹³C-labelled carbons.

The biosynthesis of related sesquiterpenoids from *Ferula jaeshkeana* was suggested by Dev *et al.* in 1973 to proceed *via* (2Z,6E)-FPP.⁴¹ Although the generally accepted mechanism for the biosynthesis of sesquiterpenes with an initial 1,6- or 1,7-cyclisation proceeds *via* NPP, the possibility of an enzymatic conversion of (2Z,6E)-FPP by the isodauc-8-en-11-ol synthase was tested. (2Z,6E)-FPP⁷ was indeed accepted as substrate and converted into the same main product 3 and all minor side products as observed from (2E,6E)-FPP (Fig. 3c of ESI†). In previous work the conversion of (2Z,6E)-FPP was also demonstrated for tobacco 5-*epi*-aristolochene synthase^{42,43} and δ-cadinene synthase from cotton,⁴⁴ but in contrast to our findings for the isodauc-8-en-11-ol synthase these experiments yielded different product spectra as obtained from (2E,6E)-FPP. Whether the results presented here mean that (2Z,6E)-FPP is a true intermediate in the biosynthesis of 3 that may itself be formed from (2E,6E)-FPP *via* NPP (Scheme 1c),⁴⁵ or just fits with a similar conformation as NPP into the enzyme's active site and is thus transformed, is a question that will be difficult to address experimentally.

Finally, the stereochemical course of all three bacterial sesquiterpene cyclases in terms of the fate of the terminal *E*- and *Z* methyl groups (C-12 and C-13) of FPP was investigated by incubation experiments with (13-¹³C)FPP (red circles in Scheme 1). As was followed by ¹³C-NMR spectroscopy (Fig. 6) the isotopic labelling from (13-¹³C)FPP showed up at C-13 (δ = 15.2 ppm), but not at C-12 of 1 (δ = 29.0 ppm) in the incubation experiment with neomeranol B synthase, while the enzymatic conversion of (13-¹³C)FPP with intermediol synthase produced 4 with specific introduction of labelling into C-12 (δ = 23.0 ppm) and not C-13 (δ = 111.4 ppm; a very small peak is visible here that likely originates from a small contamination (<1%) of synthetic (13-¹³C)FPP with (12-¹³C)-FPP). Finally, the incubation of (13-¹³C)FPP with the isodauc-8-en-11-ol synthase resulted in a specific labelling at C-13 (δ = 32.4 ppm), but not at C-12 of 3 (δ = 27.7 ppm). In conclusion, all three enzymes revealed a very strict stereochemical course.

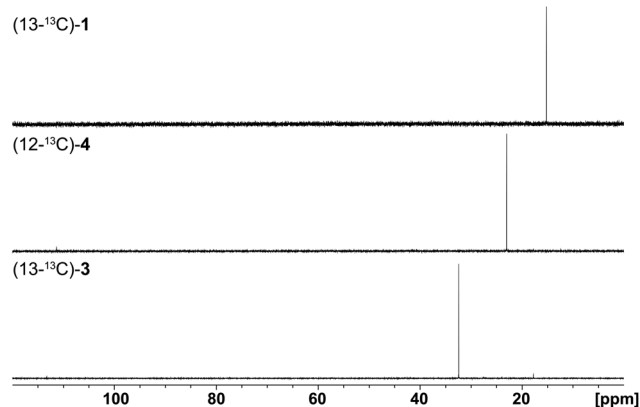


Fig. 6 Results (¹³C-NMR spectra) obtained from incubation experiments with (13-¹³C)FPP. The corresponding isotopic labellings are shown in Scheme 1.

Conclusions

We have characterised the enzyme products of three bacterial terpene cyclases as (–)-neomeranol B (**1**), (+)-isodauc-8-en-11-ol (**3**) and (+)-intermedeol (**4**). The compounds **1** and **3** have been isolated from natural sources for the first time. The terpene cyclisations of FPP to **1** and **4** proceed *via* the neutral intermediates bicyclogermacrene and germacrene A, that are reprotonated for further conversion into the final products. We provide here a fast and easy method to investigate the stereochemical courses, *i.e.* to distinguish reprotonations from the two stereochemically different faces of an olefinic double bond, by using a ¹³C-FPP isotopomer with labelling at the reprotonated carbon for incubations in deuterium oxide. A simple HSQC spectrum in combination with NOESY analysis of the unlabelled enzyme product gives then information about the stereochemical course. Furthermore, we have investigated the stereochemical courses of terpene cyclisations with respect to the fate of the stereochemically different *E*- and *Z* methyl groups of FPP (C-12 and C-13) by usage of (13-¹³C)FPP. A similar experiment using deuterium labels has previously been performed, *inter alia*, with the *epi*-isozizaene synthase from *Streptomyces coelicolor* A3(2).⁴⁶ As demonstrated here and in previous work from our and other groups isotopic labellings are very useful for structure elucidations and mechanistic biosynthetic investigations.^{28,31,47–52} We will continue to investigate interesting aspects of terpene cyclisations *via* this approach.

Acknowledgements

This work was funded by the Deutsche Forschungsgemeinschaft DFG (DI1536/7-1) and by the Beilstein-Institut zur Förderung der Chemischen Wissenschaften with a PhD scholarship to PR. We thank Dr Senada Nozinovic (Bonn) for recording the NMR spectra.

Notes and references

- C. M. Starks, K. Back, J. Chappell and J. P. Noel, *Science*, 1997, **277**, 1815–1820.
- C. A. Lesburg, G. Zhai, D. E. Cane and D. W. Christianson, *Science*, 1997, **277**, 1820–1824.
- M. J. Rynkiewicz, D. E. Cane and D. W. Christianson, *Proc. Natl. Acad. Sci. U. S. A.*, 2001, **98**, 13543–13548.
- E. Y. Shishova, L. Di Constanzo, D. E. Cane and D. W. Christianson, *Biochemistry*, 2007, **46**, 1941–1951.
- J. A. Aaron, X. Lin, D. E. Cane and D. W. Christianson, *Biochemistry*, 2010, **49**, 1787–1797.
- M. Köksal, Y. Jin, R. M. Coates, R. Croteau and D. W. Christianson, *Nature*, 2011, **469**, 116–120.
- P. Baer, P. Rabe, C. A. Citron, C. C. de Oliveira Mann, N. Kaufmann, M. Groll and J. S. Dickschat, *ChemBioChem*, 2014, **15**, 213–216.
- P. Baer, P. Rabe, K. Fischer, C. A. Citron, T. A. Klapschinski, M. Groll and J. S. Dickschat, *Angew. Chem., Int. Ed.*, 2014, **53**, 7652–7656.
- J. S. Dickschat, *Nat. Prod. Rep.*, 2011, **28**, 1917–1936.
- N. L. Brock and J. S. Dickschat, *Biosynthesis of Terpenoids*, in *Handbook of Natural Products*, ed. K. G. Ramawat and J.-M. Mérillon, Springer, 2013, pp. 2693–2732.
- M. Seemann, G. Zhai, J.-W. de Kraker, C. M. Paschell, D. W. Christianson and D. E. Cane, *J. Am. Chem. Soc.*, 2002, **124**, 7861–7869.
- D. E. Cane, J. K. Sohng, C. R. Lamberson, S. M. Rudnicki, Z. Wu, M. D. Lloyd, J. S. Oliver and B. R. Hubbard, *Biochemistry*, 1994, **33**, 5846–5857.
- X. Lin, R. Hopson and D. E. Cane, *J. Am. Chem. Soc.*, 2006, **128**, 6022–6023.
- J. Jiang, X. He and D. E. Cane, *Nat. Chem. Biol.*, 2007, **3**, 711–715.
- C.-M. Wang and D. E. Cane, *J. Am. Chem. Soc.*, 2008, **130**, 8908–8909.
- S. A. Agger, F. Lopez-Gallego, T. R. Hoyer and C. Schmidt-Dannert, *J. Bacteriol.*, 2008, **190**, 6084–6096.
- M. Komatsu, M. Tsuda, S. Omura, H. Oikawa and H. Ikeda, *Proc. Natl. Acad. Sci. U. S. A.*, 2008, **105**, 7422–7427.
- W. K. W. Chou, I. Fanizza, T. Uchiyama, M. Komatsu, H. Ikeda and D. E. Cane, *J. Am. Chem. Soc.*, 2010, **132**, 8850–8851.
- Y. Hu, W. K. W. Chou, R. Hopson and D. E. Cane, *Chem. Biol.*, 2011, **18**, 32–37.
- C. Nakano, M. H.-K. Kim and Y. Ohnishi, *ChemBioChem*, 2011, **12**, 1988–1991.
- C. Nakano, F. Kudo, T. Eguchi and Y. Ohnishi, *ChemBioChem*, 2011, **12**, 2271–2275.
- C. Nakano, M. H.-K. Kim and Y. Ohnishi, *ChemBioChem*, 2011, **12**, 2403–2407.
- C. Nakano, S. Horinouchi and Y. Ohnishi, *J. Biol. Chem.*, 2011, **286**, 27980–27987.
- C. Nakano, T. Tezuka, S. Horinouchi and Y. Ohnishi, *J. Antibiot.*, 2012, **65**, 551–558.
- P. Rabe and J. S. Dickschat, *Angew. Chem., Int. Ed.*, 2013, **51**, 1810–1812.
- J. S. Dickschat, K. A. K. Pahirulzaman, P. Rabe and T. Klapschinski, *ChemBioChem*, 2014, **15**, 810–814.
- A. Schiffrin, T. T. B. Ly, N. Günnewich, J. Zapp, V. Thiel, S. Schulz, F. Hannemann, Y. Khatri and R. Bernhardt, *ChemBioChem*, 2015, **16**, 337–344.
- P. Rabe, K. A. K. Pahirulzaman and J. S. Dickschat, *Angew. Chem., Int. Ed.*, 2015, **54**, 6041–6045.
- Y. Yamada, T. Kuzuyama, M. Komatsu, K. Shin-ya, S. Omura, D. E. Cane and H. Ikeda, *Proc. Natl. Acad. Sci. U. S. A.*, 2015, **112**, 857–862.
- J.-Y. Chow, B.-X. Tian, G. Ramamoorthy, B. S. Hillerich, R. D. Seidel, S. C. Almo, M. P. Jacobson and C. D. Poulter, *Proc. Natl. Acad. Sci. U. S. A.*, 2015, **112**, 5661–5666.

- 31 P. Rabe, L. Barra, J. Rinkel, R. Riclea, C. A. Citron, T. A. Klapschinski, A. Janusko and J. S. Dickschat, *Angew. Chem., Int. Ed.*, 2015, **53**, DOI: 10.1002/anie.201507615R1.
- 32 D. E. Barnekow, J. H. Cardellina, A. S. Zektzer and G. E. Martin, *J. Am. Chem. Soc.*, 1989, **111**, 3511–3517.
- 33 V. J. Paul, J. M. Cronan and J. H. Cardellina, *J. Chem. Ecol.*, 1993, **19**, 1847–1860.
- 34 Z.-Z. Han, X.-P. Zu, J.-X. Wang, H.-L. Li, B.-Y. Chen, Q.-X. Liu, X.-Q. Hu, Z.-H. Yan and W.-D. Zhang, *Tetrahedron*, 2014, **70**, 962–966.
- 35 C. A. Citron, J. Gleitzmann, G. Laurenzano, R. Pukall and J. S. Dickschat, *ChemBioChem*, 2012, **13**, 202–214.
- 36 A. San Feliciano, M. Medarde, B. Del Rey, J. M. M. Del Corral and A. F. Barrero, *Phytochemistry*, 1990, **29**, 3207–3211.
- 37 R. P. W. Kesselmans, J. B. P. A. Wijnberg, A. J. Minnaard, R. E. Walinga and A. de Groot, *J. Org. Chem.*, 1991, **56**, 7237–7244.
- 38 P. Bernhardt, T. Okino, J. M. Winter, A. Miyanaga and B. S. Moore, *J. Am. Chem. Soc.*, 2011, **133**, 4268.
- 39 C. Wagner, M. El Omari and G. M. König, *J. Nat. Prod.*, 2009, **72**, 540.
- 40 Y. J. Hong and D. J. Tantillo, *Org. Lett.*, 2011, **13**, 1294–1297.
- 41 M. C. Sriraman, B. A. Nagasampagi, R. C. Pandey and S. Dev, *Tetrahedron*, 1973, **29**, 985–991.
- 42 J. A. Faraldos, P. E. O'Maille, N. Dellas, J. P. Noel and R. M. Coates, *J. Am. Chem. Soc.*, 2010, **132**, 4281–4289.
- 43 J. P. Noel, N. Dallas, J. A. Faraldos, M. Zhao, B. A. Hess Jr., L. Smentek, R. M. Coates and P. E. O'Maille, *ACS Chem. Biol.*, 2010, **5**, 377–392.
- 44 J. A. Faraldos, D. J. Miller, V. Gonzalez, Z. Yoosuf-Aly, O. Cascon, A. Li and R. K. Allemann, *J. Am. Chem. Soc.*, 2012, **134**, 5900–5908.
- 45 D. Arigoni, *Pure Appl. Chem.*, 1975, **41**, 219–245.
- 46 X. Lin and D. E. Cane, *J. Am. Chem. Soc.*, 2009, **131**, 6332–6333.
- 47 L. Barra, K. Ibrom and J. S. Dickschat, *Angew. Chem., Int. Ed.*, 2015, **54**, 6637–6640.
- 48 R. Riclea and J. S. Dickschat, *Angew. Chem., Int. Ed.*, 2015, **54**, 12167–12170.
- 49 H. B. Bode, D. Reimer, S. W. Fuchs, F. Kirchner, C. Dauth, C. Kegler, W. Lorenzen, A. O. Brachmann and P. Grin, *Chem. – Eur. J.*, 2012, **18**, 2342–2348.
- 50 H. B. Bode, A. O. Brachmann, K. B. Jadhav, L. Seyfarth, C. Dauth, S. W. Fuchs, M. Kaiser, N. R. Waterfield, H. Sack, S. H. Heinemann and H.-D. Arndt, *Angew. Chem., Int. Ed.*, 2015, **54**, 10352–10355.
- 51 A. Meguro, Y. Motoyoshi, K. Teramoto, S. Ueda, Y. Totsuka, Y. Ando, T. Tomita, S.-Y. Kim, T. Kimura, M. Igarashi, R. Sawa, T. Shinada, M. Nishiyama and T. Kuzuyama, *Angew. Chem., Int. Ed.*, 2015, **54**, 4353–4356.
- 52 A. Ear, S. Amand, F. Blanchard, A. Blond, L. Dubost, D. Buisson and B. Nay, *Org. Biomol. Chem.*, 2015, **13**, 3662–3666.

Incubation experiments of purified enzyme with FPP and isolation of products

E. coli BL 21 transformants were inoculated in a 2YT liquid preculture (tryptone: 16 g, yeast extract: 10 g, NaCl: 5 g, water: 1 L, pH 7.2) containing kanamycin (50 mg/L) overnight. *E. coli* BL 21 transformants from the preculture were inoculated in large scale 2YT liquid cultures (6-8 x 1 L) containing kanamycin (50 mg/L). Cells were grown to an $OD_{600} = 0.4$ at 37 °C and 160 rpm, followed by cooling of the cultures to 18 °C for 30 minutes. IPTG (0.4 mM) was added and the culture was incubated at 18 °C and 160 rpm overnight. *E. coli* cells were harvested by centrifugation at 4 °C and 3600 rpm for 60 min. The pellets were resuspended in 2 x 10 mL lysis buffer (20 mM Na_2HPO_4 , 0.5 M NaCl, 20 mM imidazole, 1 mM $MgCl_2$, pH 7.0) for each 1 L culture. Cell disruption was done by ultra-sonication on ice for 6 x 60 sec. The soluble enzyme fractions were harvested at 4 °C and 8000 rpm by repeated centrifugation (2 x 10 min). Protein purification was performed by Ni^{2+} -NTA affinity chromatography with Ni^{2+} -NTA superflow (Novagen) using binding buffer (20 mM Na_2HPO_4 , 0.5 M NaCl, 20 mM imidazole, 1 mM $MgCl_2$, pH 7.0) and elution buffer (20 mM Na_2HPO_4 , 0.5 M NaCl, 500 mM imidazole, 1 mM $MgCl_2$, pH 7.0). All wash and elution fraction were checked by SDS-PAGE. Incubation experiments were performed with the pure protein fractions (80-160 mL) and incubation buffer (100 mL, 50 mM Tris-HCl, 10 mM $MgCl_2$, 20 % glycerin, pH 7.0) containing FPP (50-80 mg, 0.4-0.6 mg/mL) at 28 °C overnight. The reaction mixture was extracted with 3 x 100 mL pentane. The combined organic layers were dried with $MgSO_4$ and concentrated under reduced pressure. Column chromatography on silica gel of the crude products with pentane/diethyl ether (5:1) yielded the pure sesquiterpene alcohols for structure elucidation by NMR.

Neomeranol B (1). Yield: 4.1 mg. HRMS (TOF): obs. m/z (calcd., formula) = 222.1970 (222.1978, $C_{15}H_{26}O^+$, $[M]^+$). GC (HP5-MS): $I = 1607$. MS (EI, 70 eV): m/z (%) = 222 (0.3) $[M]^+$, 204 (2), 189 (3), 161 (4), 137 (5), 123 (4), 109 (24), 97 (35), 85(100), 69 (18), 55 (20), 41 (18). IR (diamond ATR): $\tilde{\nu} = 3385$ (br m), 2953 (s), 2923 (s), 2891 (m), 2873 (m), 1725 (w), 1453 (m), 1378 (m), 1298 (w), 1261 (w), 1164 (w), 1136 (w), 1019 (s), 1002 (s), 951 (w), 827 (w), 804 (w), 712 (w), 600 (w), 529 (w) cm^{-1} . $[\alpha]_D^{24} = -10.2$ (CH_2Cl_2 , $c = 0.082$).

Intermedeol (4). Yield: 9.6 mg. HRMS (TOF): obs. m/z (calcd., formula) = 222.1970 (222.1978, $C_{15}H_{26}O^+$, $[M]^+$). GC (HP5-MS): $I = 1664$. MS (EI, 70 eV): m/z (%) = 222 (3) $[M]^+$, 204 (100), 189 (95), 175 (17), 161 (94), 147 (34), 133 (38), 122 (46), 107 (46), 107 (45), 93 (45), 81 (65), 71 (30), 55 (26), 43 (34). IR (diamond ATR): $\tilde{\nu} = 3438$ (br m), 3085 (w), 2969 (m), 2929 (s), 2867 (m), 2850 (m), 1738 (w), 1638 (w), 1452 (m), 1381 (m), 1229 (w), 1168 (w), 1095 (m), 1064 (w), 931 (w), 907 (m), 887 (m), 803 (w), 575 (w), 527 (w) cm^{-1} . $[\alpha]_D^{25} = +11.9$ (CH_2Cl_2 , $c = 0.50$).

Isodauc-8-en-11-ol (3). Yield: 11.8 mg. HRMS (TOF): obs. m/z (calcd., formula) = 222.1973 (222.1978, $C_{15}H_{26}O^+$, $[M]^+$). GC (HP5-MS): $I = 1669$. MS (EI, 70 eV): m/z (%) = 222 (x) $[M]^+$, 204 (35), 189 (14), 163 (18), 161 (16) 149 (41), 135 (16), 121 (27), 107 (41), 95 (77), 81 (44), 67 (29), 59 (100), 55 (20), 42 (32). IR (diamond ATR): $\tilde{\nu} = 3364$ (br m), 2966 (m), 2923 (m), 2886 (m), 1738 (w), 1454 (w), 1440 (w), 1383 (m), 1364 (m), 1147 (s), 945 (m), 928 (m), 883 (s), 840 (m), 802 (m), 660 (w), 587 (w), 519 (w), 476 (w) cm^{-1} . $[\alpha]_D^{22} = +19.4$ (CH_2Cl_2 , $c = 0.505$).

NMR data of all natural products are presented in Table 1 of main text.

Incubation experiments of purified enzyme with ¹³C-labelled FPPs.

For each incubation a 0.5 L 2YT liquid culture (containing kanamycin (50 mg/L)) of *E. coli* BL 21 transformants was inoculated from an overnight preculture. Cells were grown to an OD₆₀₀ = 0.4 at 37 °C and 160 rpm, followed by cooling of the cultures to 18 °C for 30 minutes. IPTG (0.4 mM) was added and the culture was incubated at 18 °C and 160 rpm overnight. *E. coli* cells were harvested by centrifugation at 4 °C and 8000 rpm for 10 min. The pellets were resuspended in 10 mL lysis buffer (20 mM Na₂HPO₄, 0.5 M NaCl, 20 mM imidazole, 1 mM MgCl₂, pH 7.0) and lysed by ultra-sonication on ice for 5 x 30 sec. The soluble enzyme fractions were harvested at 4°C and 11000 rpm by centrifugation (1 x 10 min). Protein purification was performed by Ni²⁺-NTA affinity chromatography with Ni²⁺-NTA superflow (Novagen) using binding buffer (20 mM Na₂HPO₄, 0.5 M NaCl, 20 mM imidazole, 1 mM MgCl₂, pH 7.0) and elution buffer (20 mM Na₂HPO₄, 0.5 M NaCl, 500 mM imidazole, 1 mM MgCl₂, pH 7.0). Each pure protein fraction (checked by SDS) was concentrated with a Vivaspin20 concentration tube (MWCO 30000, Sartorius Stedim, Göttingen) for 1.5 h at 6000 rpm to 2 mL enzyme fraction. Incubation experiments were performed with the pure protein (2 mL) and incubation buffer (2 mL, 50 mM Tris·HCl, 10 mM MgCl₂, 20 % glycerin, pH 7.0) containing the ¹³C-labelled FPP (3 mg, 1.5 mg/mL) at 28 °C overnight. The reaction mixture was extracted with 0.6 mL (²H₆)benzene and directly measured by NMR.

The protein purifications of intermedeol synthase and neomeranol B synthase in D₂O were performed by Ni²⁺-NTA affinity chromatography with Ni²⁺-NTA superflow (Novagen) using binding buffer (20 mM Na₂HPO₄, 0.5 M NaCl, 20 mM imidazole, 1 mM MgCl₂, pH 7.0 in D₂O) and elution buffer (20 mM Na₂HPO₄, 0.5 M NaCl, 500 mM imidazole, 1 mM MgCl₂, pH 7.0 in D₂O). Each pure protein fraction (checked by SDS) was concentrated with a Vivaspin20 concentration tube (MWCO 30000, Sartorius Stedim, Göttingen) for 1.5 at 6000 rpm to 2 mL enzyme fraction. Incubation experiments were performed with the pure protein (2 mL) and D₂O (2 mL) containing the (6-¹³C)FPP (3 mg, 1.5 mg/mL) at 28 °C overnight. The reaction mixture was extracted with 0.6 mL (²H₆)benzene and directly measured by NMR.

Incubation experiments of purified isodaucen-11-ol synthase with (2Z,6E)FPP

For the incubation experiment of isodaucen-11-ol synthase with the substrate analogue (2Z,6E)FPP a 0.5 L 2YT liquid culture (containing kanamycin (50 mg/L)) of *E. coli* BL 21 transformants was inoculated. The cultivation and protein isolation conditions are performed as reported above. The pure protein fraction of isodaucen-11-ol synthase was used for an incubation experiment with the pure protein (2 mL) and incubation buffer (2 mL, 50 mM Tris·HCl, 10 mM MgCl₂, 20 % glycerin, pH 7.0) containing the (2Z,6E)FPP³ (0.6 mg, 0.3 mg/mL) at 28 °C overnight. The reaction mixture was extracted with 0.5 mL *n*hexane and directly injected in GC/MS.

GC-/MS and GC/Q-TOF analysis

GC-MS analyses were carried out with a 7890B gas chromatograph connected to a 5977A inert mass detector (Agilent) fitted with a HP5-MS fused silica capillary column (30 m, 0.25 mm i. d., 0.50 μm film). Instrumental parameters were (1) inlet pressure, 77.1 kPa, He 23.3 mL min⁻¹, (2) injection volume, 1-2 μL, (3) transfer line, 250 °C, and (4) electron energy 70 eV. The GC was programmed as follows: 5 min at 50 °C increasing at 10 °C min⁻¹ to 320 °C, and operated in split mode (50:1, 60 s valve time). The carrier gas was He at 1 mL min⁻¹. Retention indices (*I*) were determined from a homologous series of n-alkanes (C8-C40). HRMS analyses were carried out with a 7890B gas chromatograph connected to a 7200 accurate-mass Q-TOF mass detector (Agilent) equipped with a HP5-MS fused silica capillary

column (30 m, 0.25 mm i. d., 0.50 μm film). Instrumental parameters were (1) inlet pressure, 83.2 kPa, He 24.6 mL min^{-1} , (2) injection volume, 1 μL , (3) transfer line, 250 $^{\circ}\text{C}$, and (4) electron energy 70 eV. The GC was programmed for HR-MS as follows: 5 min at 50 $^{\circ}\text{C}$ increasing at 10 $^{\circ}\text{C min}^{-1}$ to 320 $^{\circ}\text{C}$, and operated in split mode (50:1-100:1, 60 s valve time). The carrier gas was He at 1 mL min^{-1} .

CLSA headspace sampling

The volatiles released by *Streptomyces scabiei* 87.22, *Streptomyces venezuelae* ATCC 10712 and *Streptomyces clavuligerus* ATCC 27064 were trapped by use of the CLSA (closed-loop stripping analysis) technique after cultivation of *Streptomyces scabiei* 87.22 on medium Gym 65 (glucose: 4.0 g, yeast extract: 4.0 g, malt extract: 4.0 g, water: 1 L, pH 7.2) and *Streptomyces venezuelae* ATCC 10712 on medium SFM (mannitol: 20.0 g, soya flour: 20.0 g, water: 1 L, pH 7.2) for 3 d at 28 $^{\circ}\text{C}$ as reported previously.⁴

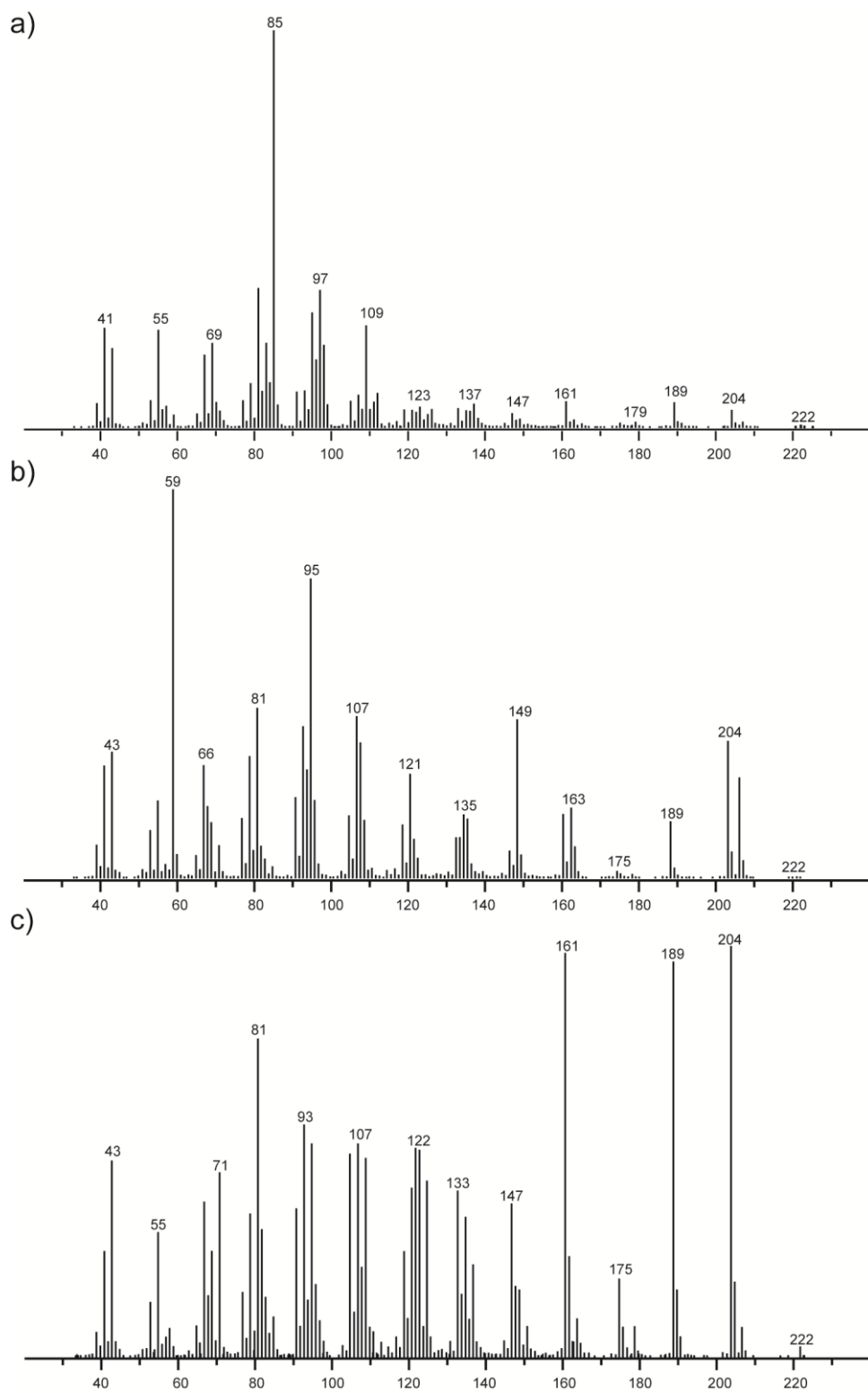


Fig. 1 EI-MS spectra of a) neomeranol B (**1**), b) isodauc-8-en-11-ol (**3**) and c) intermedeol (**4**).

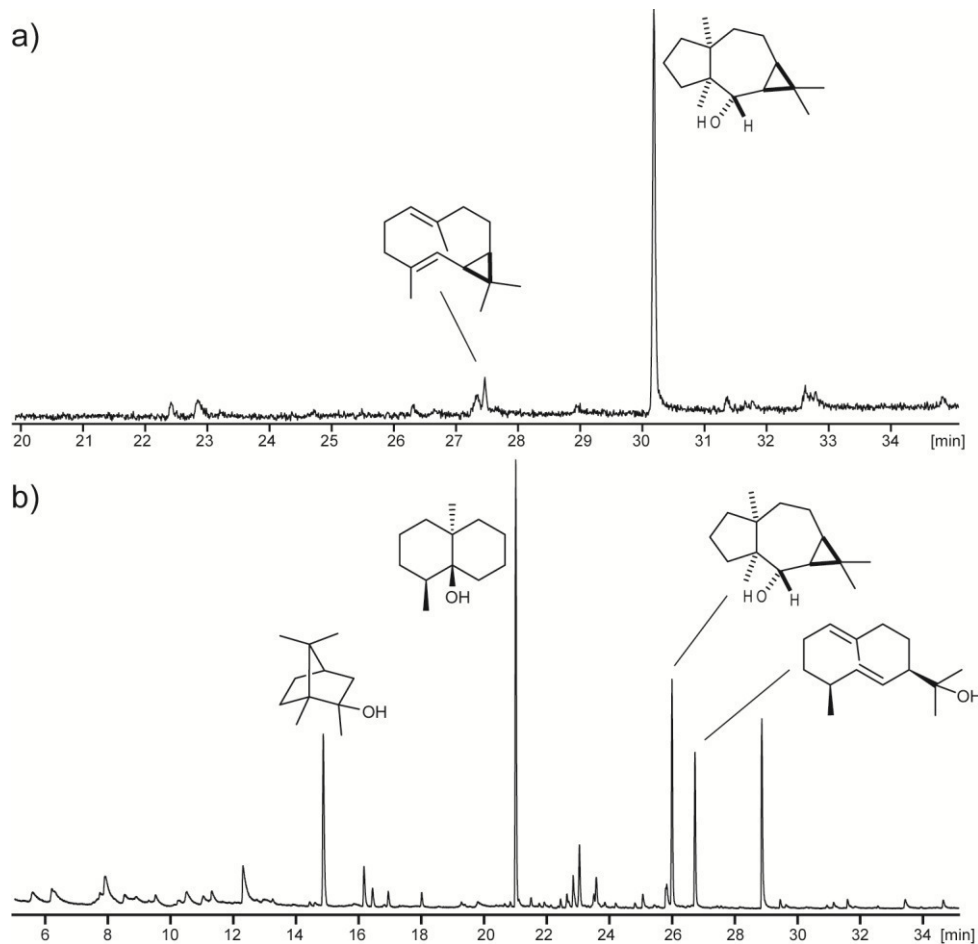


Fig. 2 Total ion chromatograms of a) a hexane extract of an incubation experiment of neomeranol B synthase with FPP at pH 7.0 and b) of a CLSA headspace extract of wildtype *Streptomyces scabiei* 87.22⁴ on medium SFM demonstrating the production of **1**. The slightly deviating retention times for one and the same compound in the three samples are due to usage of different GCs, but retention indices matched.

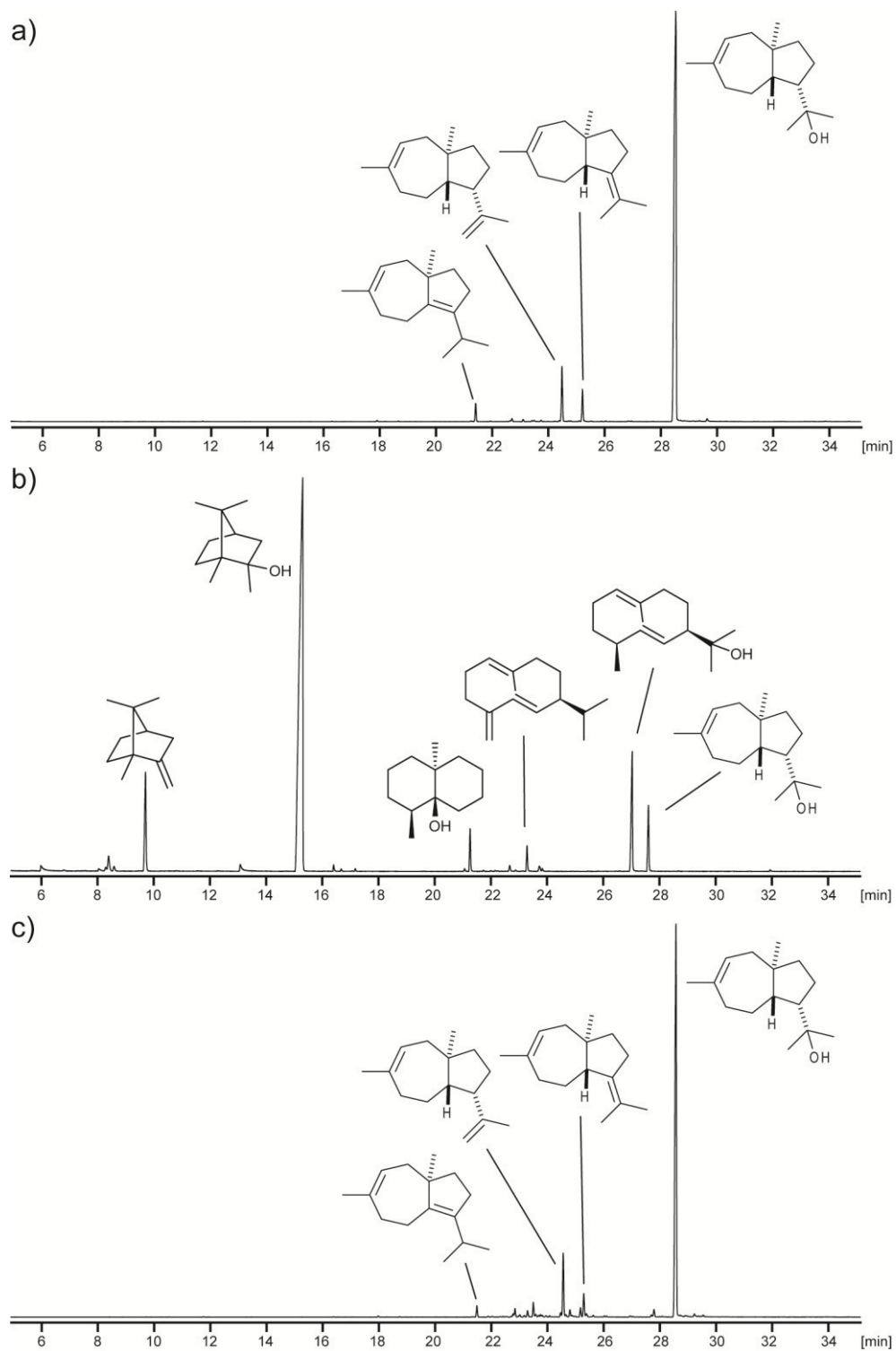


Fig. 3 Total ion chromatograms a) of a hexane extract of an incubation experiment of isodauc-8-en-11-ol synthase with (2*E*,6*E*)-FPP at pH 7.0, b) of a CLSA headspace extract of wildtype *S. venezuelae* ATCC 10712⁴ on medium Gym 65 demonstrating the production of **3**, and c) of a hexane extract of an incubation experiment of isodauc-8-en-11-ol synthase with (2*Z*,6*E*)-FPP at pH 7.0. The slightly deviating retention times for one and the same compound in the three samples are due to usage of different GCs, but retention indices matched.

Table 2 Comparison of measured and reported NMR data of intermedeol (**4**) in (²H)chloroform, confirming the identity of isolated **4** and intermedeol.

4 (this study, 100 MHz) ^[a]	4 (de Groot et al., 50 MHz) ⁵	4 (San Feliciano et al., 50 MHz) ⁶
146.9	146.6	146.8
110.8	110.7	110.7
72.1	72.0	71.9
49.2	49.1	49.1
43.6	43.4	43.5
41.4	41.3	41.4
40.4	40.2	40.4
39.3	39.2	39.4
35.3	35.2	35.2
23.5	23.4	23.5
22.8	22.7	22.7
22.7	22.7	22.7
22.3	22.2	22.3
20.2	20.1	20.1
18.5	18.4	18.4

[a] All signals are given in ppm. Deviations of reported ¹³C-NMR shifts from data measured in this work are shown in brackets.

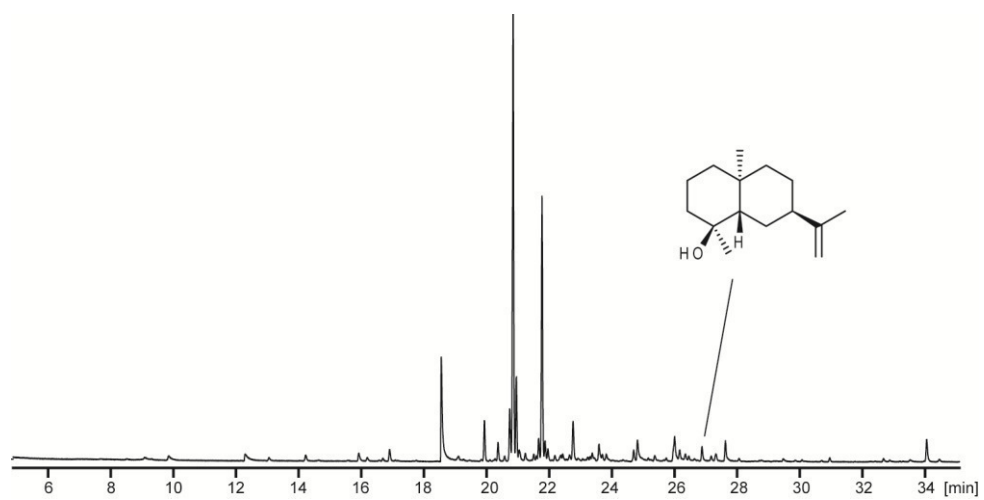
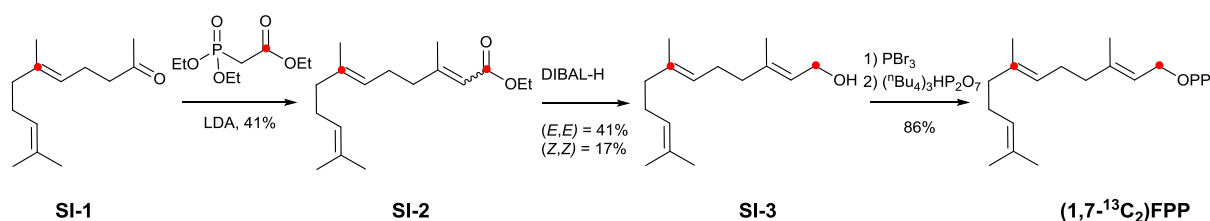


Fig. 4 Total ion chromatogram of a CLSA headspace extract of wildtype *Streptomyces clavuligerus* ATCC 27064⁴ on medium SFM demonstrating the production of **4**.

Fig. 5 Synthesis of (1,7-¹³C₂)FPP.



General synthetic methods

Chemicals were purchased from Acros Organics (Geel, Belgium) or Sigma Aldrich Chemie GmbH (Steinheim, Germany) and used without purification. All non-aqueous reactions were performed under an inert atmosphere (N₂ or Ar) in flame-dried flasks. Solvents were purified by distillation and dried according to standard methods. Thin-layer chromatography was performed with 0.2 mm precoated plastic sheets Polygram Sil G/UV254 (Machery-Nagel). Column chromatography was carried out using Merck silica gel 60 (70-200 mesh). NMR spectra of synthetic compounds and isolated natural products were recorded on a Bruker DRX-400 (400 MHz), AV III-400 (400 MHz) or AV Avance DMX-500 (500 MHz) spectrometer, and were referenced against solvent signals (¹H NMR: (²H)chloroform δ = 7.26 ppm, (²H₆)benzene δ = 7.16 ppm, ¹³C NMR: (²H)chloroform δ = 77.16 ppm, (²H₆)benzene δ = 128.06 ppm).

Synthesis of ethyl (1,7-¹³C₂)-(6E)-3,7,11-trimethyldodeca-2,6,10-trienoate (SI-2)

A solution of diisopropylamine (95 mg, 0.93 mmol, 1.1 eq.) in abs. THF (5 mL) was cooled to 0 °C and treated with *n*-butyl lithium (59.4 μ L, 0.93 mmol, 1.6 M in hexane, 1.1 eq.). It was stirred for 30 min at 0 °C and then the reaction was cooled to -78 °C. Slowly (1-¹³C)triethyl phosphonoacetate (210 mg, 0.93 mmol, 1.1 eq.) was added and stirring was continued for 2 h at -78 °C. (6-¹³C)Geranylacetone⁷ (SI-1) (164 mg, 0.84 mmol, 1.0 eq.) was added dropwise at -78 °C and the reaction mixture was stirred over night at room temperature. The reaction was hydrolyzed by addition of distilled water, followed by extraction with ethyl acetate. The combined organic layers were dried over MgSO₄ and concentrated under reduced pressure. Column chromatography on silica gel with cyclohexane/ethyl acetate (45:1) resulted in a mixture of diastereoisomers SI-2 (*E*/*Z*: 4/1; 92 mg, 0.35 mmol, 41%).

¹H-NMR (400 MHz, CDCl₃): δ = 5.68-5.62 (m, 1H, CH), 5.12-5.05 (m, 2H, 2xCH), 4.14 (dq, ³J_{H,H} = 7.1 Hz, ³J_{C,H} = 3.0 Hz, 2H, CH₂), 2.19-2.15 (m, 7H, 2xCH₂ + CH₃), 2.09-2.02 (m, 2H, 1xCH₂), 2.01-1.94 (m, 2H, 1xCH₂), 1.27 (t, ³J_{H,H} = 7.1 Hz, 3H, CH₃), 1.68 (s, 3H, CH₃), 1.60 (br, 3H, CH₃), 1.59 (s, 3H, CH₃) ppm. ¹³C-NMR (100 MHz, CDCl₃): δ = 167.0 (¹³C_q), 159.9 (d, ²J_{C,C} = 2.0 Hz, C_q), 136.3 (¹³C_q), 131.5 (C_q), 124.4 (d, ³J_{C,C} = 3.7 Hz, CH), 123.0 (d, ¹J_{C,C} = 73.6 Hz, CH), 115.7 (d, ¹J_{C,C} = 75.7 Hz, CH), 59.6 (d, ²J_{C,C} = 2.3 Hz, CH₂), 41.1 (dd, ³J_{C,C} = 7.0 Hz, ³J_{C,C} = 3.6 Hz, CH₂), 39.8 (d, ¹J_{C,C} = 42.6 Hz, CH₂), 26.8 (d, ²J_{C,C} = 2.3 Hz, CH₂), 26.1 (CH₂), 25.8 (CH₃), 18.9 (d, ³J_{C,C} = 1.5 Hz, CH₃), 17.8 (CH₃), 16.1 (d, ¹J_{C,C} = 42.1 Hz, CH₃), 14.5 (d, ³J_{C,C} = 2.2 Hz, CH₃) ppm. MS (EI, 70 eV): *m/z* (%) = 266 (11) [M]⁺, 251 (4), 221 (18), 205 (8), 192 (12), 177 (14), 148 (20), 137 (39), 129 (100), 122 (87), 101 (45), 82 (91), 69 (99), 54 (18), 41 (93).

Synthesis of (1,7-¹³C₂)-(2E,6E)-farnesol (SI-3)

The mixture of diastereoisomers **SI-2** (92 mg, 0.34 mmol, 1.0 eq.) in abs. THF (3.5 mL) was cooled to -78 °C and a solution of DIBAL-H (0.75 mmol, 0.75 mL 2.2 eq., 1.0 M in hexane) was added dropwise. The reaction mixture was stirred for 2 h at -78 °C. It was hydrolyzed with saturated potassium sodium tartrate solution in water and extracted three times with diethyl ether. The combined organic layers were dried over MgSO₄ and concentrated under reduced pressure. Repeated column chromatography with cyclohexane/ethyl acetate (9:1) yielded in the alcohols (1,7-¹³C₂)-(2E,6E)-farnesol (30 mg, 0.14 mmol, 41%) and (1,7-¹³C₂)-(2Z,6E)-farnesol (**SI-3**) (13 mg, 0.06 mmol, 17%) as colorless oils.

¹H-NMR (400 MHz, CDCl₃): δ = 5.42 (tdq, ³J_{H,H} = 6.9 Hz, ²J_{C,H} = 1.3 Hz, ⁴J_{H,H} = 1.3 Hz, 1H, CH), 5.14-5.06 (m, 2H, 2xCH), 4.15 (dd, ¹J_{C,H} = 142.2 Hz, ³J_{H,H} = 6.9 Hz, 2H, CH₂), 2.16-1.94 (m, 8H, 4xCH₂), 1.68 (s, 6H, 2xCH₃), 1.60 (s, 3H, 1xCH₃), 1.60 (d, ²J_{C,H} = 5.9 Hz, 3H, 1xCH₃) ppm. ¹³C-NMR (100 MHz, CDCl₃): δ = 140.0 (d, ²J_{C,C} = 1.3 Hz, C_q), 133.5 (¹³C_q), 131.5 (C_q), 124.4 (d, ³J_{C,C} = 3.4 Hz, CH), 123.9 (d, ¹J_{C,C} = 73.5 Hz, CH), 123.5 (d, ¹J_{C,C} = 47.1 Hz, CH), 59.6 (¹³CH₂), 39.8 (d, ¹J_{C,C} = 42.7 Hz, CH₂), 39.7 (cd, ³J_{C,C} = 4.7 Hz, ³J_{C,C} = 3.6 Hz, CH₂), 26.9 (d, ²J_{C,C} = 2.2 Hz, CH₂), 26.4 (CH₂), 25.8 (CH₃), 17.8 (CH₃), 16.4 (d, ³J_{C,C} = 4.3 Hz, CH₃), 16.2 (d, ¹J_{C,C} = 42.4 Hz, CH₃) ppm. MS (EI, 70 eV): *m/z* (%) = 224 (5) [M]⁺, 206 (6), 192 (14), 181 (10), 163 (20), 137 (77), 124 (63), 110 (56), 94 (93), 82 (100), 69 (98), 55 (38), 41 (99).

Synthesis of (1,7-¹³C₂)-(2E,6E)-farnesyl diphosphate (FPP)

A solution of (1,7-¹³C₂)-(2E,6E)-farnesol (**SI-3**) (30 mg, 0.14 mmol, 1.0 eq.) in abs. THF (0.4 mL) was treated with PBr₃ (15 mg, 0.056 mmol, 5.3 μL, 0.4 eq.) at 0°C. The reaction was stirred for 30 min at 0°C and quenched by pouring into ice-water. After extraction with pentane the combined organic layers were dried with MgSO₄. The solvent was removed under reduced pressure and the pale yellow oil was subsequently added to a solution of (ⁿBu₄)₃HP₂O₇ (190 mg, 0.21 mmol, 1.5 eq.) in abs. CH₃CN (0.8 mL). The reaction mixture was stirred over night at room temperature and then concentrated under reduced pressure. The yellow oil was loaded onto a column containing ion exchange resin (DOWEX 50W-X8, NH₄⁺ form). Elution with two column volumes of ion exchange buffer (0.03 M NH₄HCO₃ in 2% ⁱPrOH/H₂O) and freeze drying yielded a yellowish solid. This material was dissolved in 0.05 M NH₄HCO₃ and ⁱPrOH/CH₃CN (1/1) was added. The mixture was shaken until a white solid precipitated. After centrifugation the solution was transferred to a fresh flask and the solid again dissolved in 0.05 M NH₄HCO₃. The procedure was repeated twice. The solvent was pooled and concentrated under reduced pressure and again resolved in 5 mL H₂O. Freeze-drying give (1,7-¹³C₂)FPP (54 mg, 0.12 mmol, 85%) as pale yellow solid.

¹H-NMR (400 MHz, CDCl₃): δ = 5.46 (br, 1H, CH), 5.24-5.14 (m, 2H, 2xCH), 4.46 (d, ¹J_{C,H} = 147.9, 2H, CH₂), 2.15-1.95 (m, 8H, 4xCH₂), 1.73 (br, 3H, CH₃), 1.68 (s, 3H, CH₃), 1.62 (d, 3H, CH₃), 1.62 (s, 3H, CH₃) ppm. ¹³C-NMR (100 MHz, CDCl₃): δ = 145.6 (d, ²J_{C,C} = 1.7 Hz, C_q), 138.4 (¹³C_q), 134.4 (C_q), 127.0 (CH), 126.9 (d, ³J_{C,C} = 3.4 Hz, CH), 122.4 (dd, ¹J_{C,C} = 50.7 Hz, ³J_{C,P} = 1.8 Hz, CH), 65.2 (br, ¹³C_q), 41.6 (dd, ³J_{C,C} = 4.0 Hz, ³J_{C,C} = 4.2 Hz, CH₂), 41.5 (d, ¹J_{C,C} = 42.7 Hz, CH₂), 28.7 (d, ³J_{C,C} = 1.6 Hz, CH₂), 28.4 (CH₂), 27.7 (CH₃), 19.8 (CH₃), 18.5 (d, ³J_{C,C} = 4.2 Hz, CH₃), 18.0 (d, ¹J_{C,C} = 42.2 Hz, CH₃) ppm.

References

- 1 J. S. Dickschat, K. A. K. Pahirulzaman, P. Rabe and T. A. Klapschinski, *ChemBioChem*, 2014, **15**, 810-814.
- 2 R. D. Gietz and R. H. Schiestl, *Nat. Protoc.* 2007, **2**, 31–34.
- 3 P. Baer, P. Rabe, C. A. Citron, C. C. de Oliveira Mann, N. Kaufmann, M. Groll and J. S. Dickschat, *ChemBioChem*, 2014, **15**, 213-216.
- 4 C. A. Citron, J. Gleitzmann, G. Laurenzano, R. Pukall and J. S. Dickschat, *ChemBioChem*, 2012, **13**, 202-214.
- 5 R. P. W. Kesselmans , J. B. P. A. Wijnberg , A. J. Minnaard , R. E. Walinga and A. de Groot, *J. Org. Chem.*, 1991, **56**, 7237–7244.
- 6 A. San Feliciano, M. Medarde, B. Del Rey, J. M. Miguel Del Corral and A. F. Barrero, *Phytochemistry*, 1990, **29**, 3207-3211.
- 7 P. Rabe, L. Barra, J. Rinkel, R. Riclea, C. A. Citron, T. A. Klapschinski, A. Janusko and J. S. Dickschat, *Angew. Chem. Int. Ed.*, 2015, **53**, accepted.

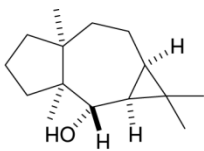
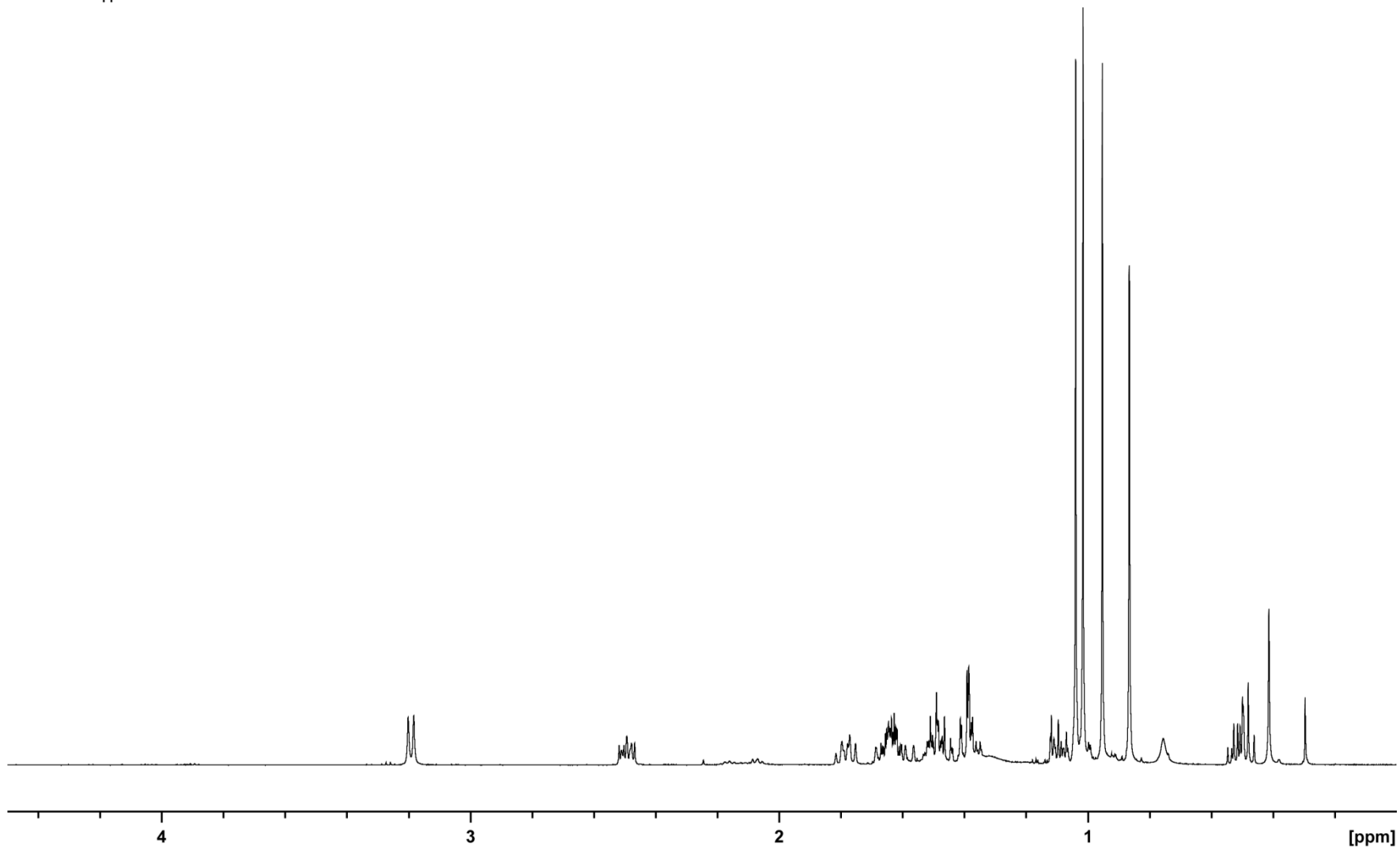


Fig. 6 $^1\text{H-NMR}$ -spectrum of neomeranol B (**1**) in ($^2\text{H}_6$)benzene at 298K at 500 MHz.



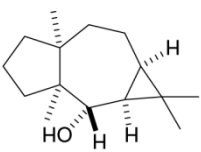
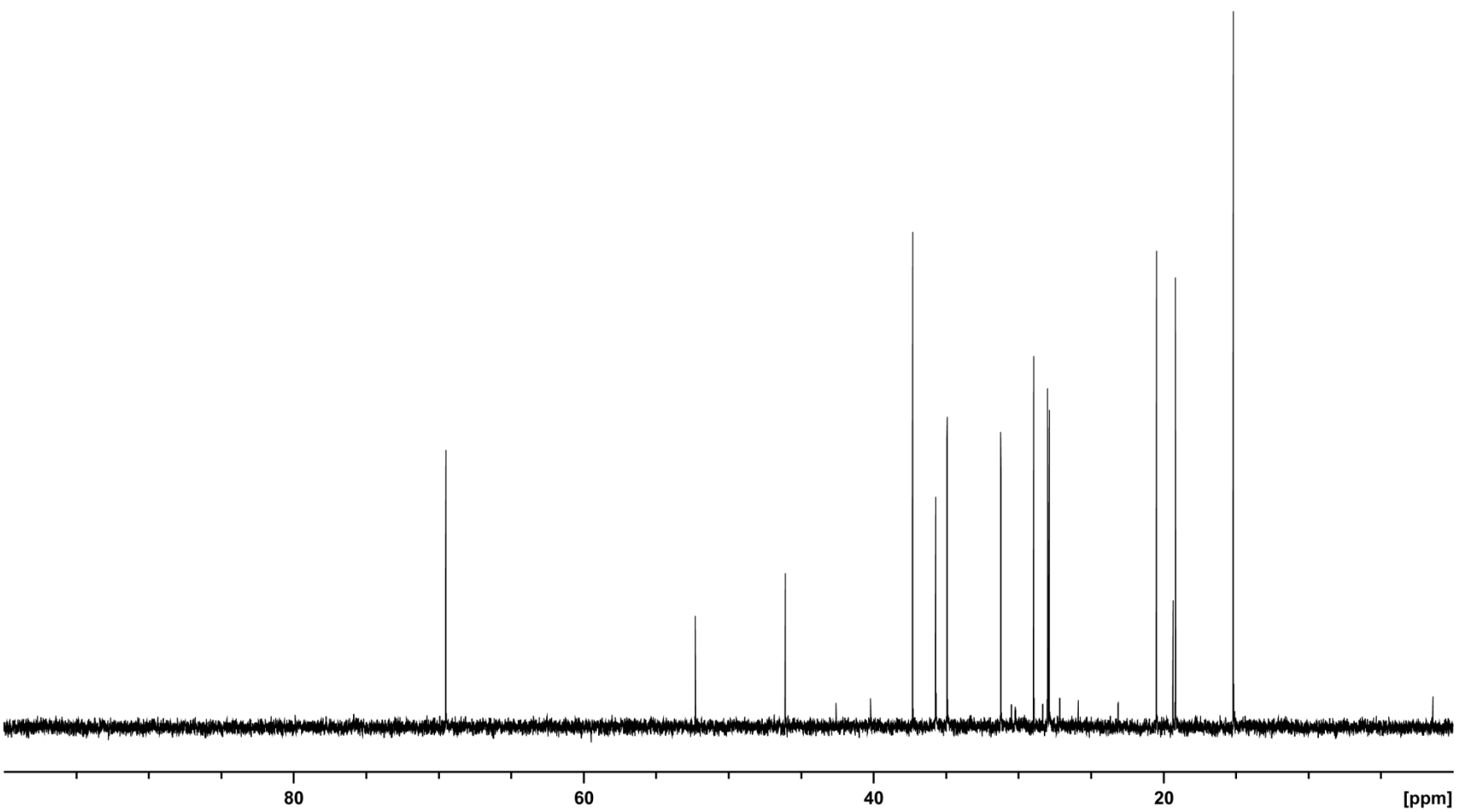


Fig. 7 ^{13}C -NMR-spectrum of neomeranol B (**1**) in ($^2\text{H}_6$)benzene at 298K at 500 MHz.



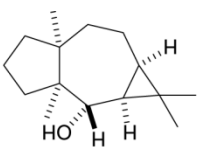
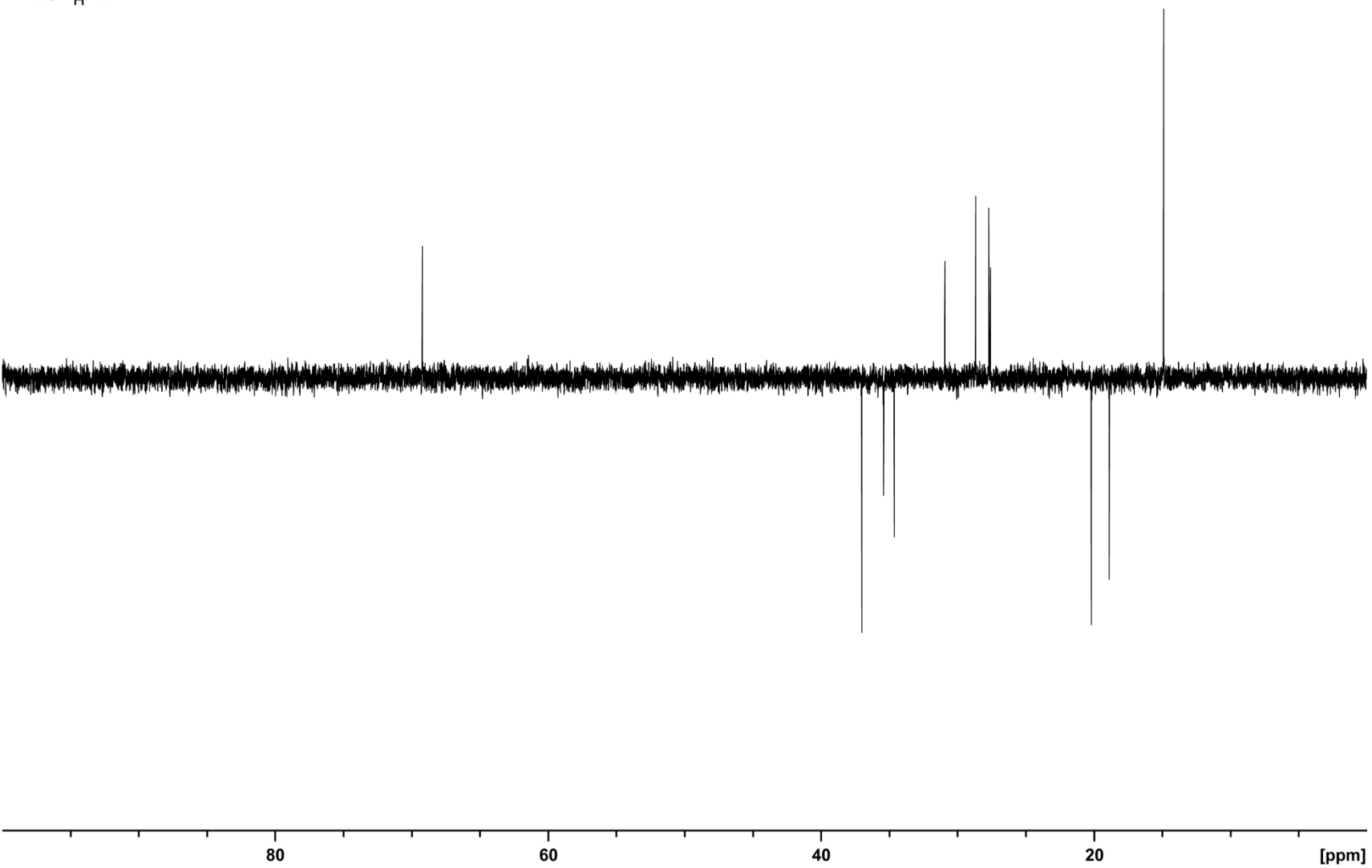


Fig. 8 ^{13}C -DEPT135-NMR-spectrum of neomeranol B (**1**) in ($^2\text{H}_6$)benzene at 298K at 500 MHz.



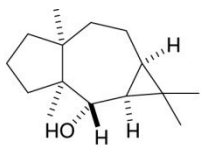
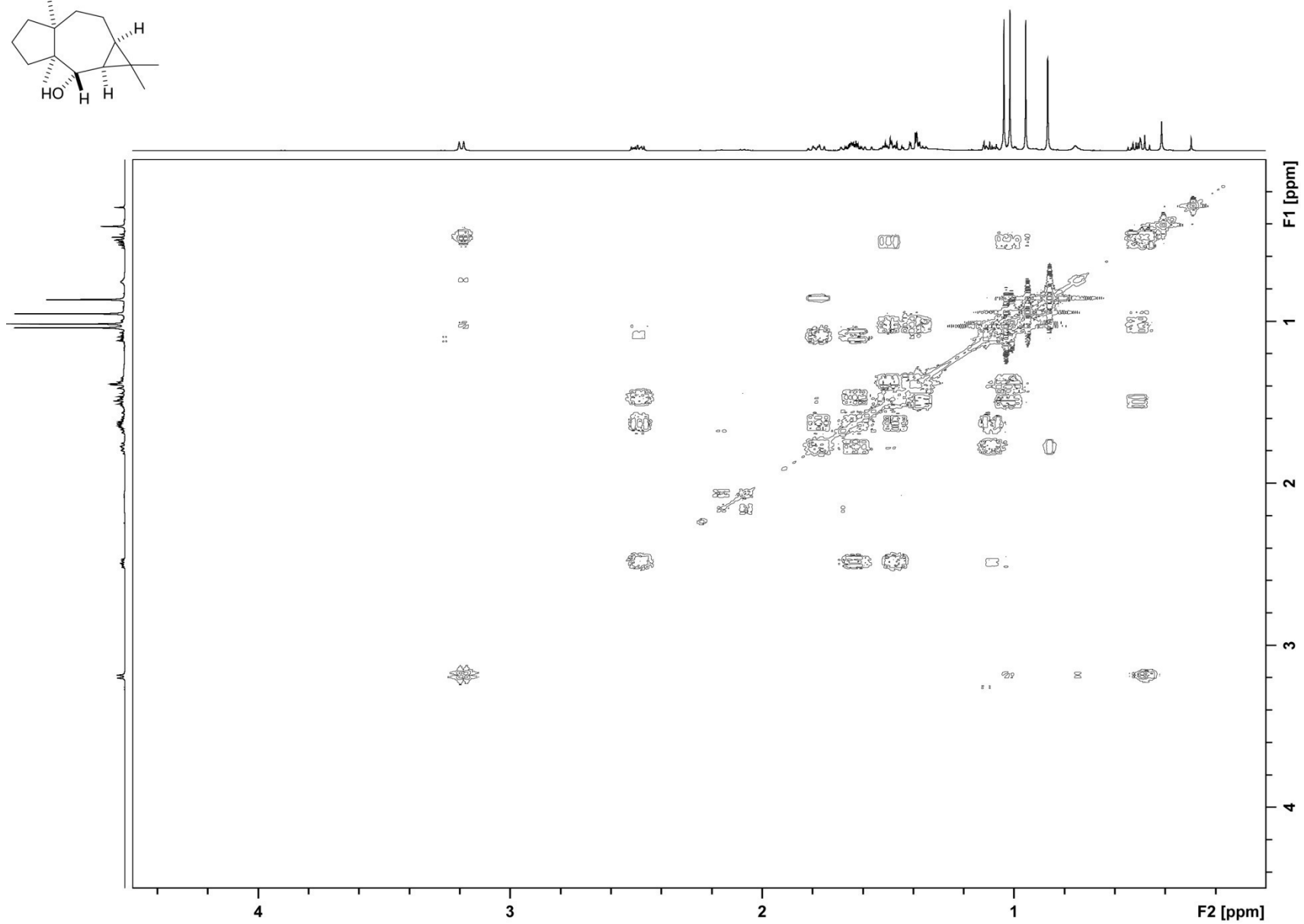


Fig. 9 ¹H, ¹H-COSY spectrum of neomeranol B (**1**) in (²H₆)benzene at 298K at 500 MHz.



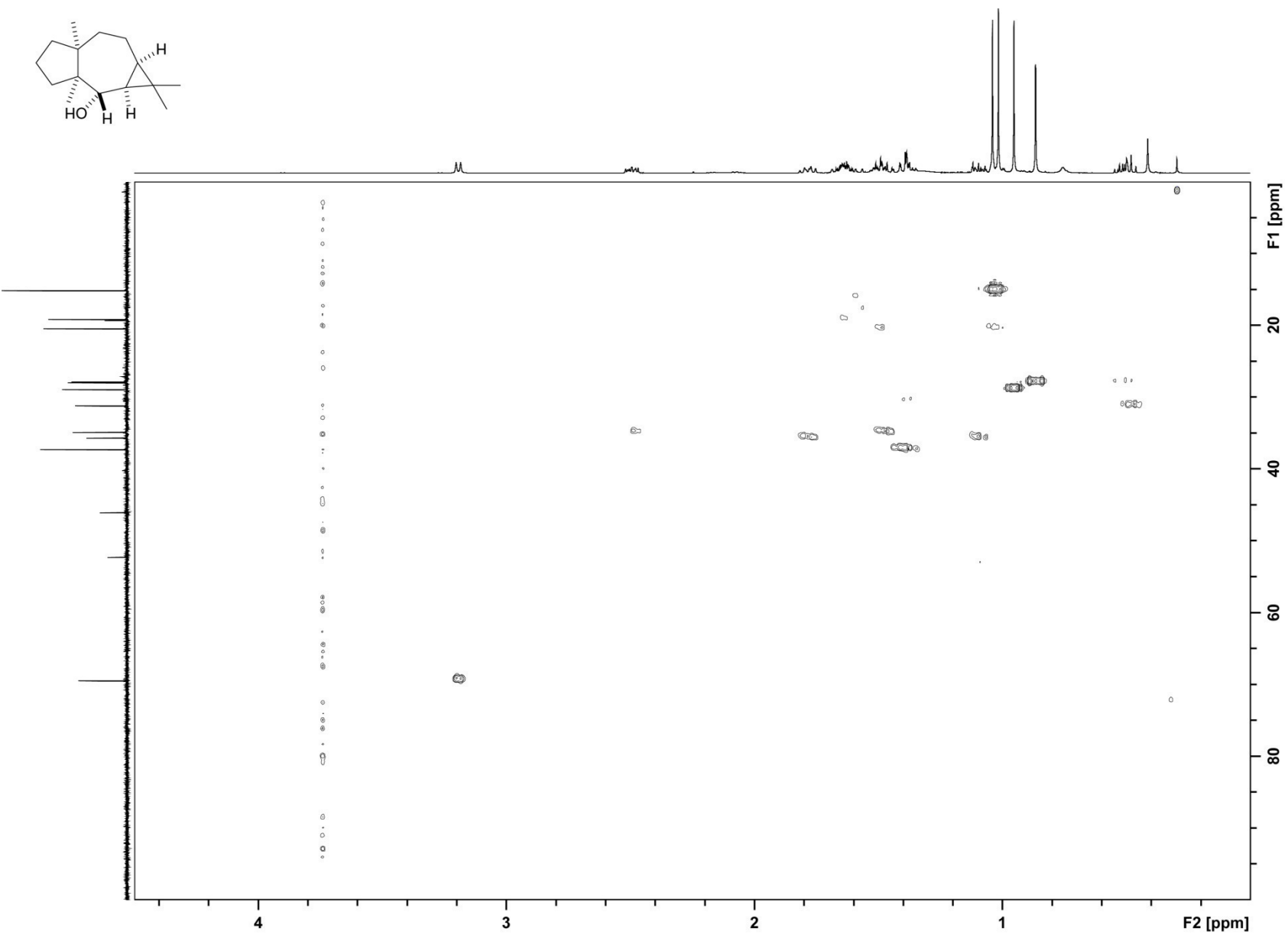


Fig. 10 HSQC spectrum of neomeranol B (**1**) in $^{12}\text{H}_6$ benzene at 298K at 500 MHz.

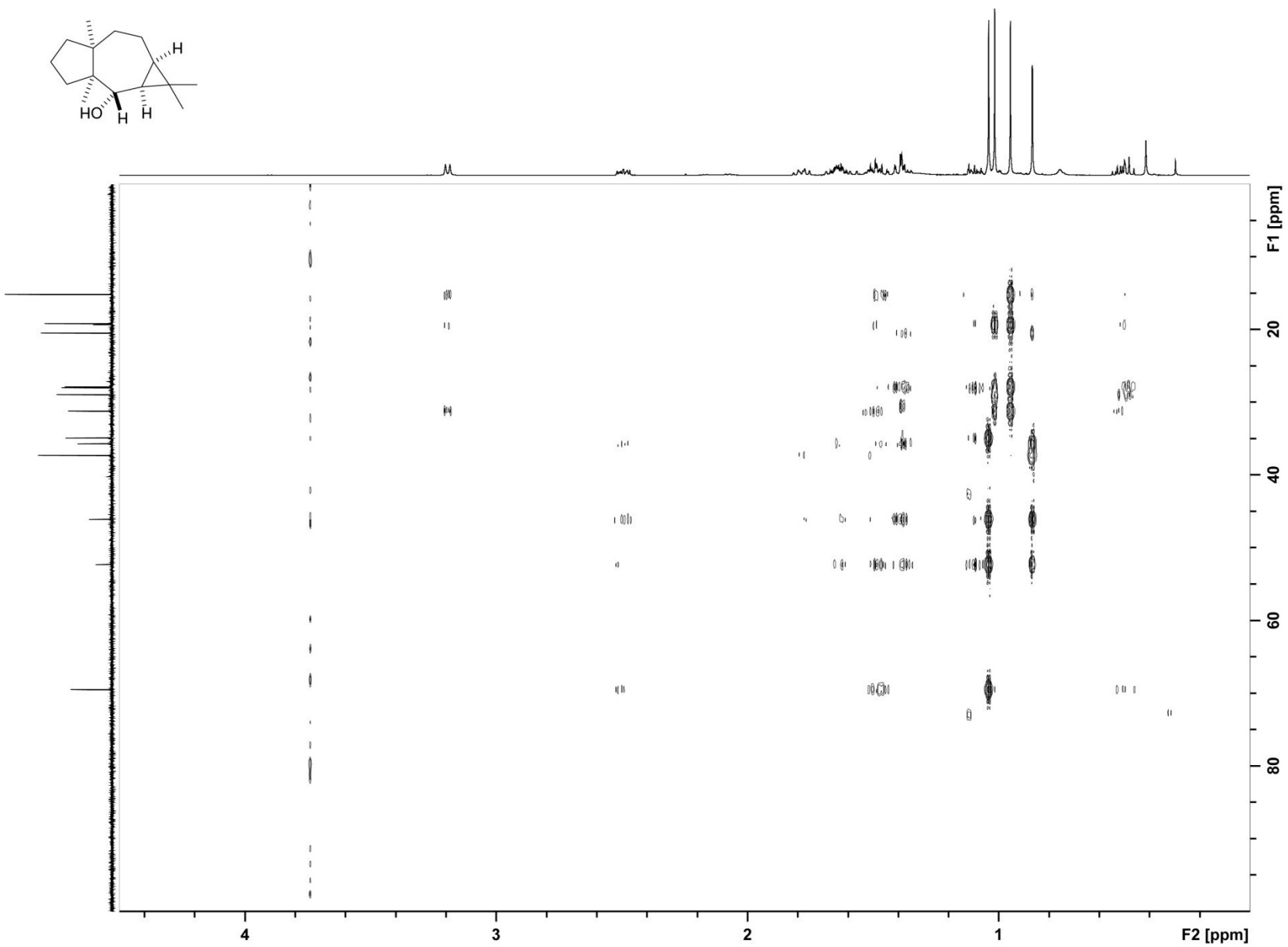


Fig. 11 HMBC spectrum of neomeranol B (**1**) in $^2\text{H}_6$ benzene at 298K at 500 MHz.

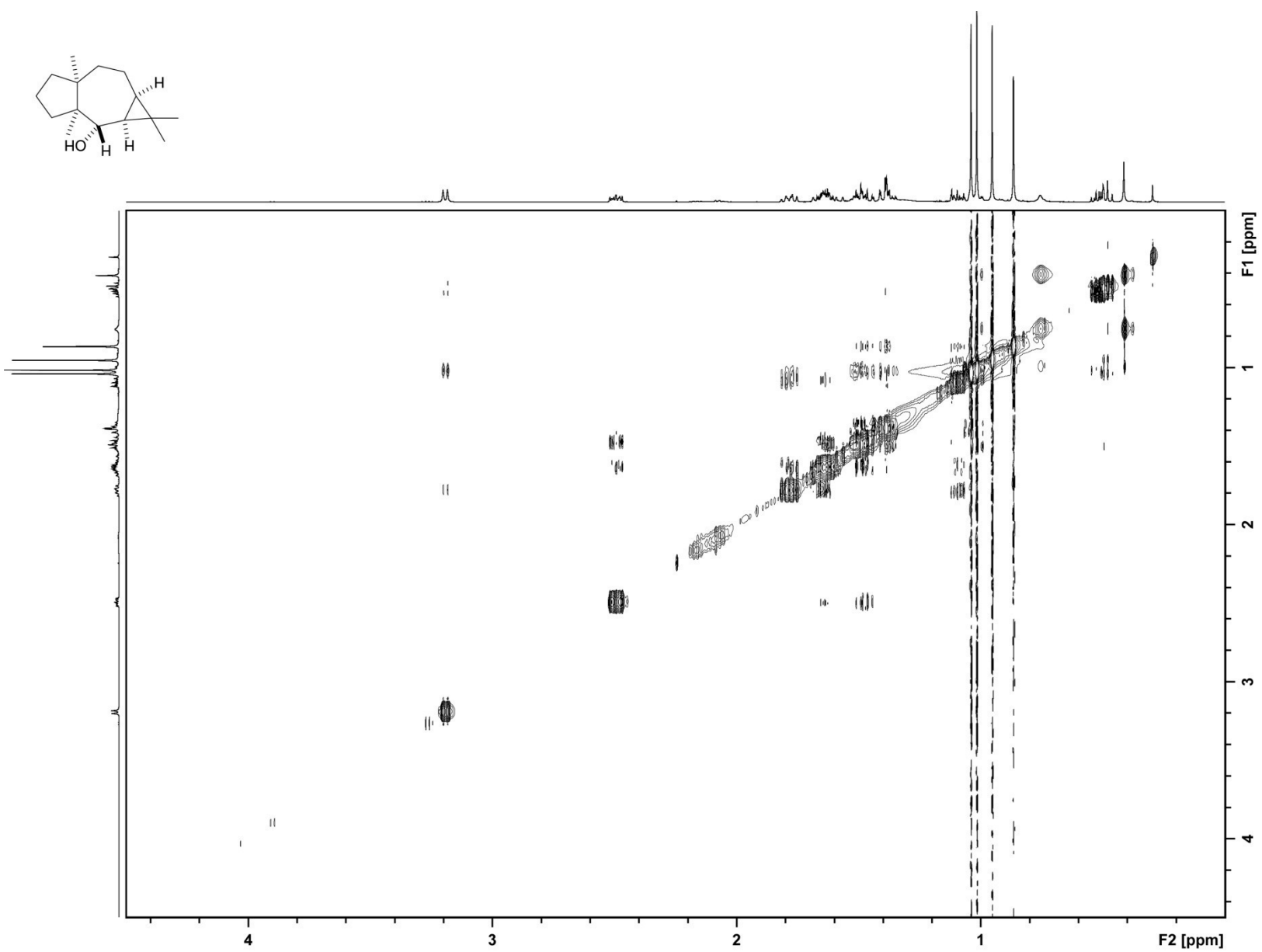


Fig. 12 NOESY spectrum of neomeranol B (**1**) in $(^2\text{H}_6)$ benzene at 298K at 500 MHz.

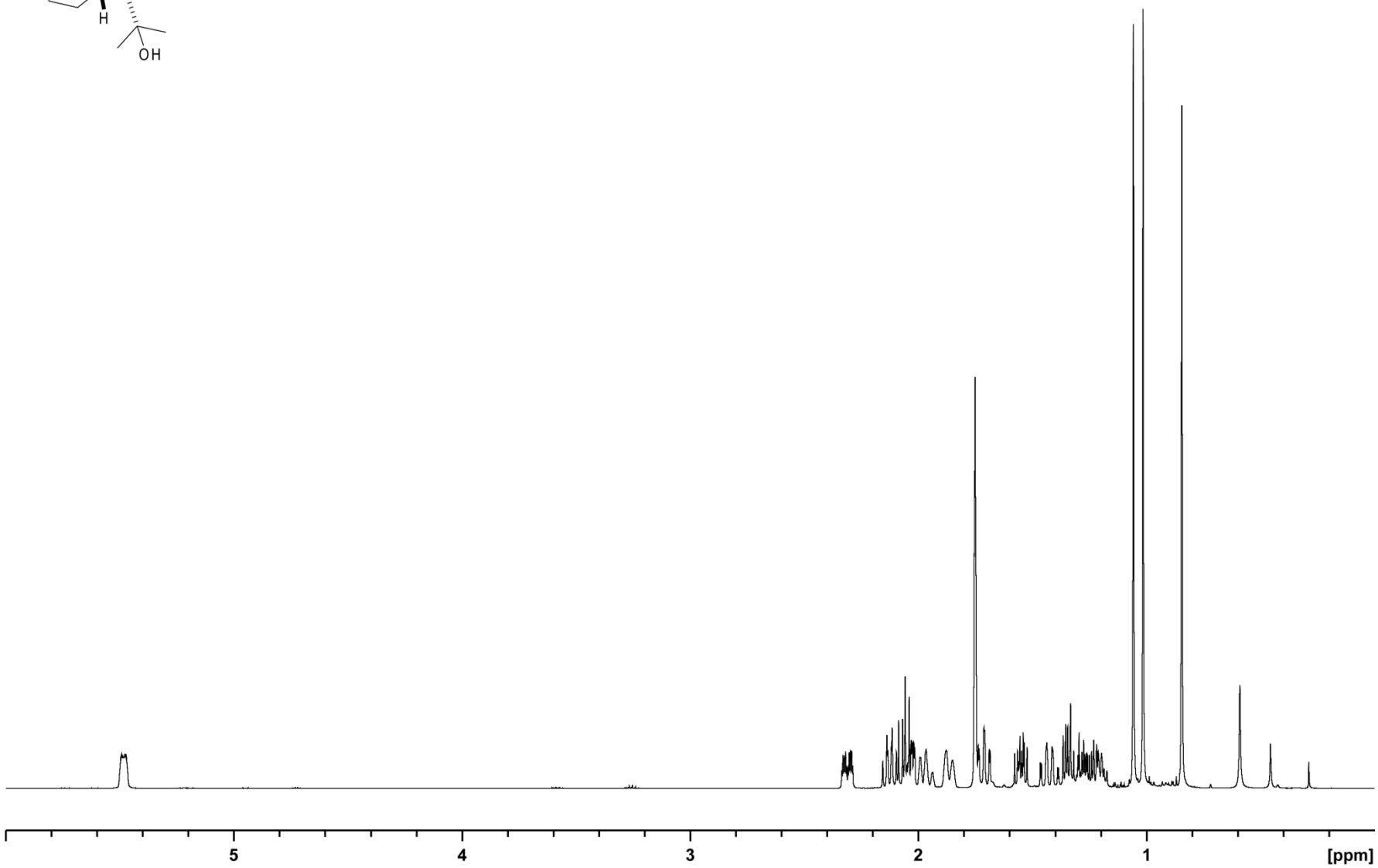
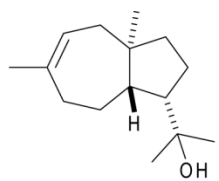


Fig. 13 ¹H-NMR spectrum of isodauc-8-en-11-ol (**3**) in (2H₆)benzene at 298K at 500 MHz.

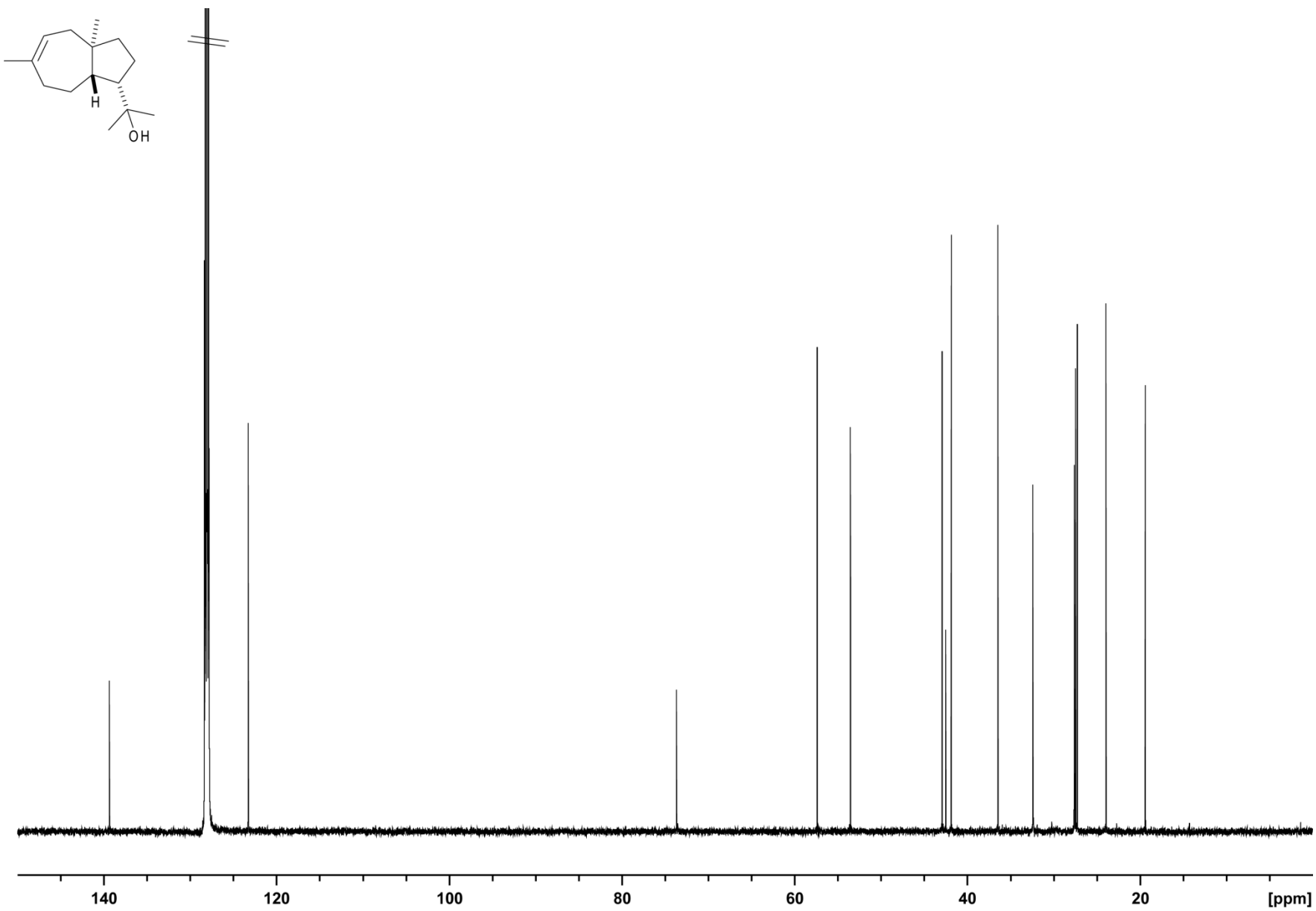
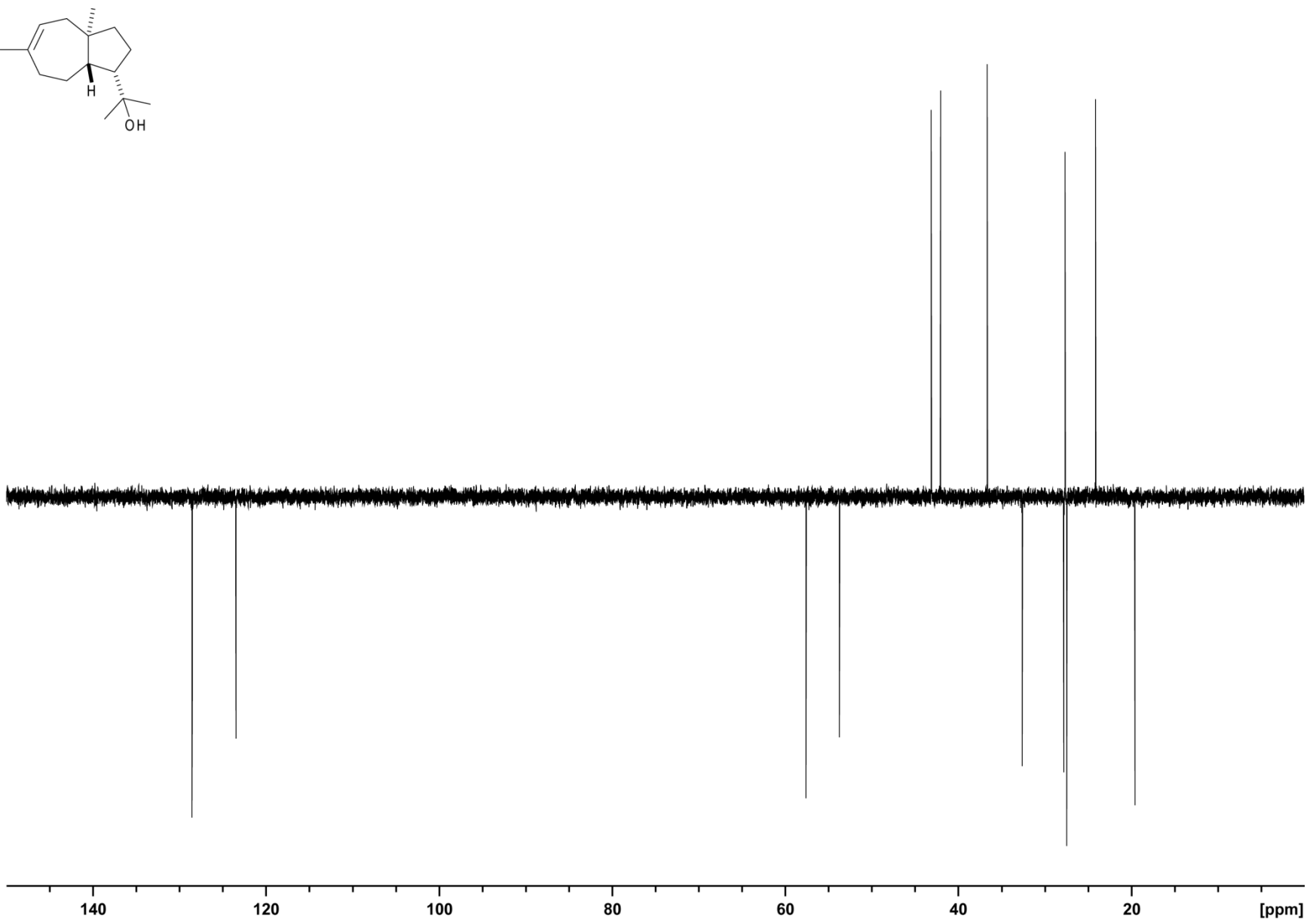


Fig. 14 ^{13}C -NMR spectrum of isodauc-8-en-11-ol (**3**) in $(^2\text{H}_6)$ benzene at 298K at 500 MHz.



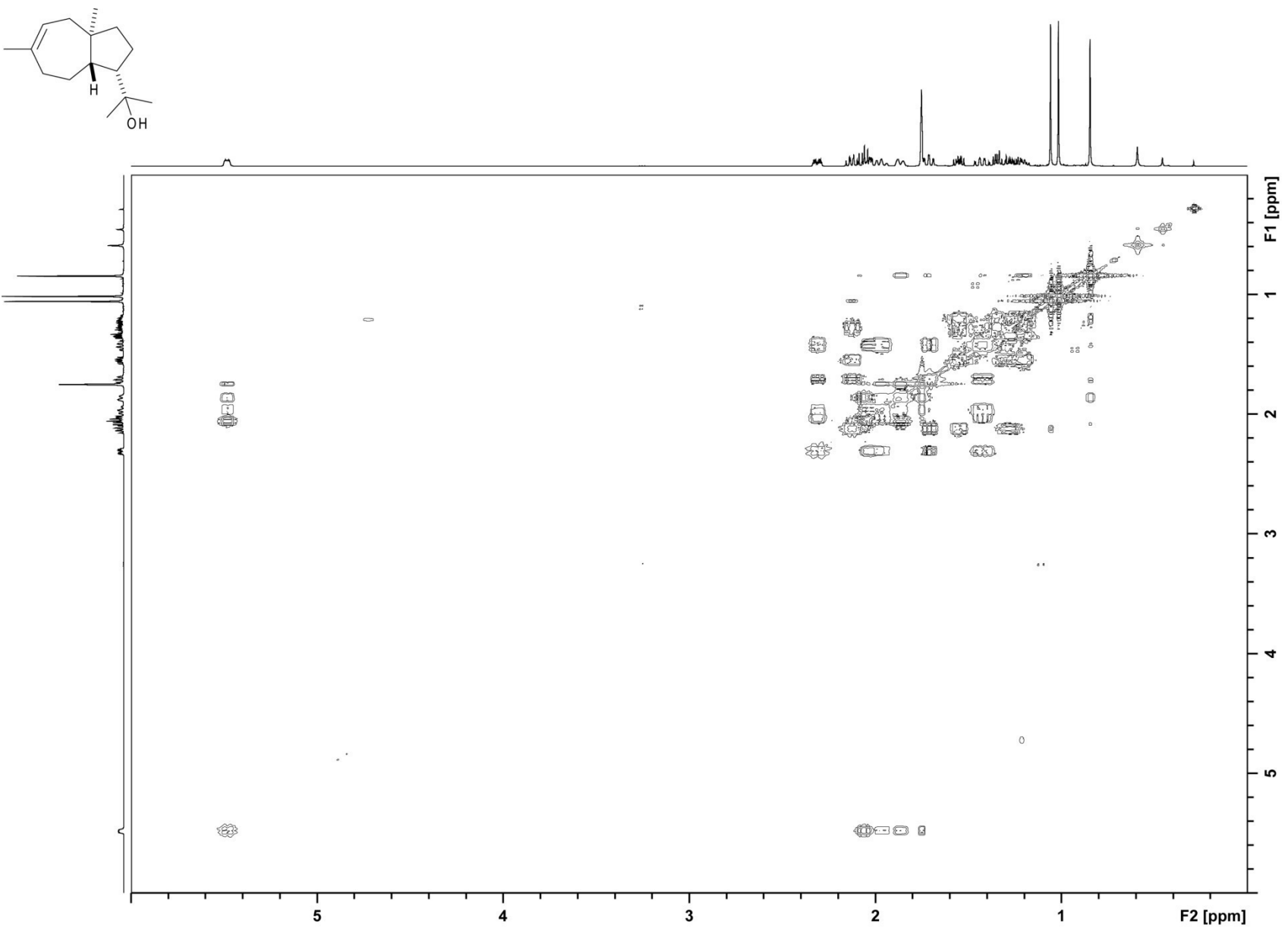


Fig. 16 $^1\text{H}, ^1\text{H}$ -COSY spectrum of isodauc-8-en-11-ol (**3**) in $(^2\text{H}_6)$ benzene at 298K at 500 MHz.

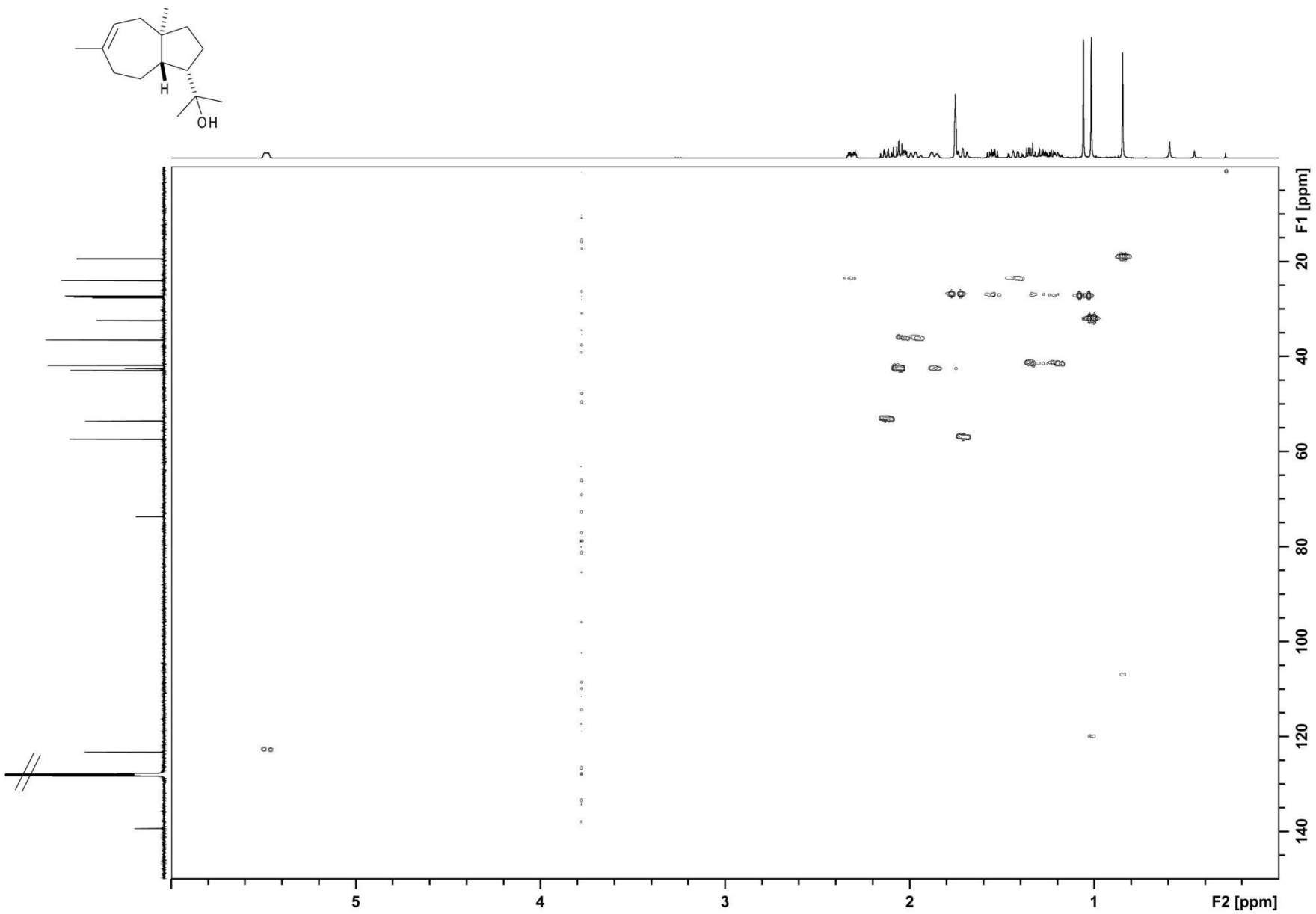


Fig. 17 HSQC spectrum of isodauc-8-en-1-ol (**3**) in $(^2\text{H}_6)$ benzene at 298K at 500 MHz.

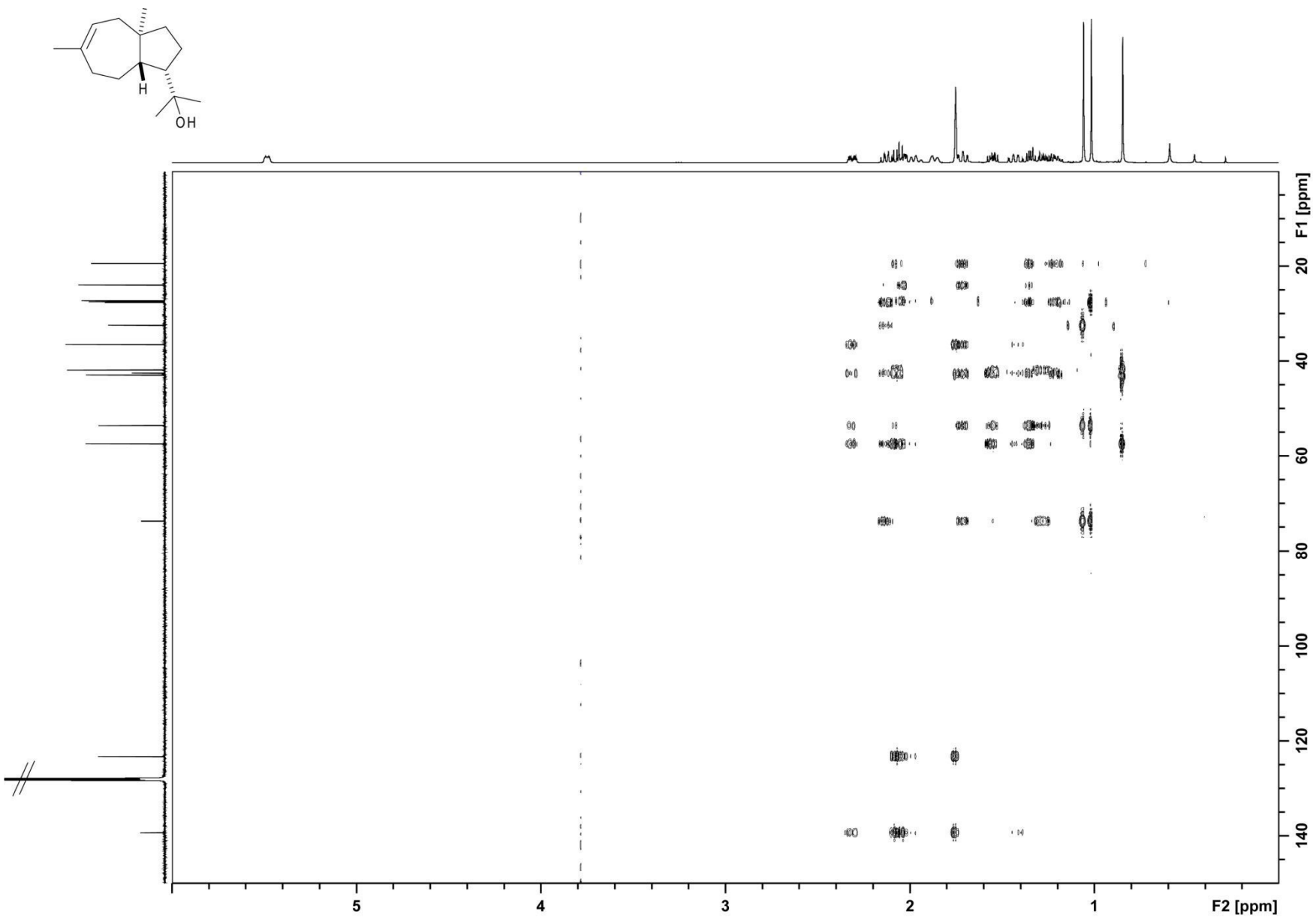


Fig. 18 HMBC spectrum of isodauc-8-en-1-ol (**3**) in $(^2\text{H}_6)$ benzene at 298K at 500 MHz.

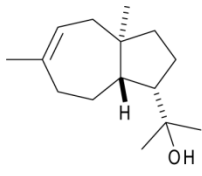
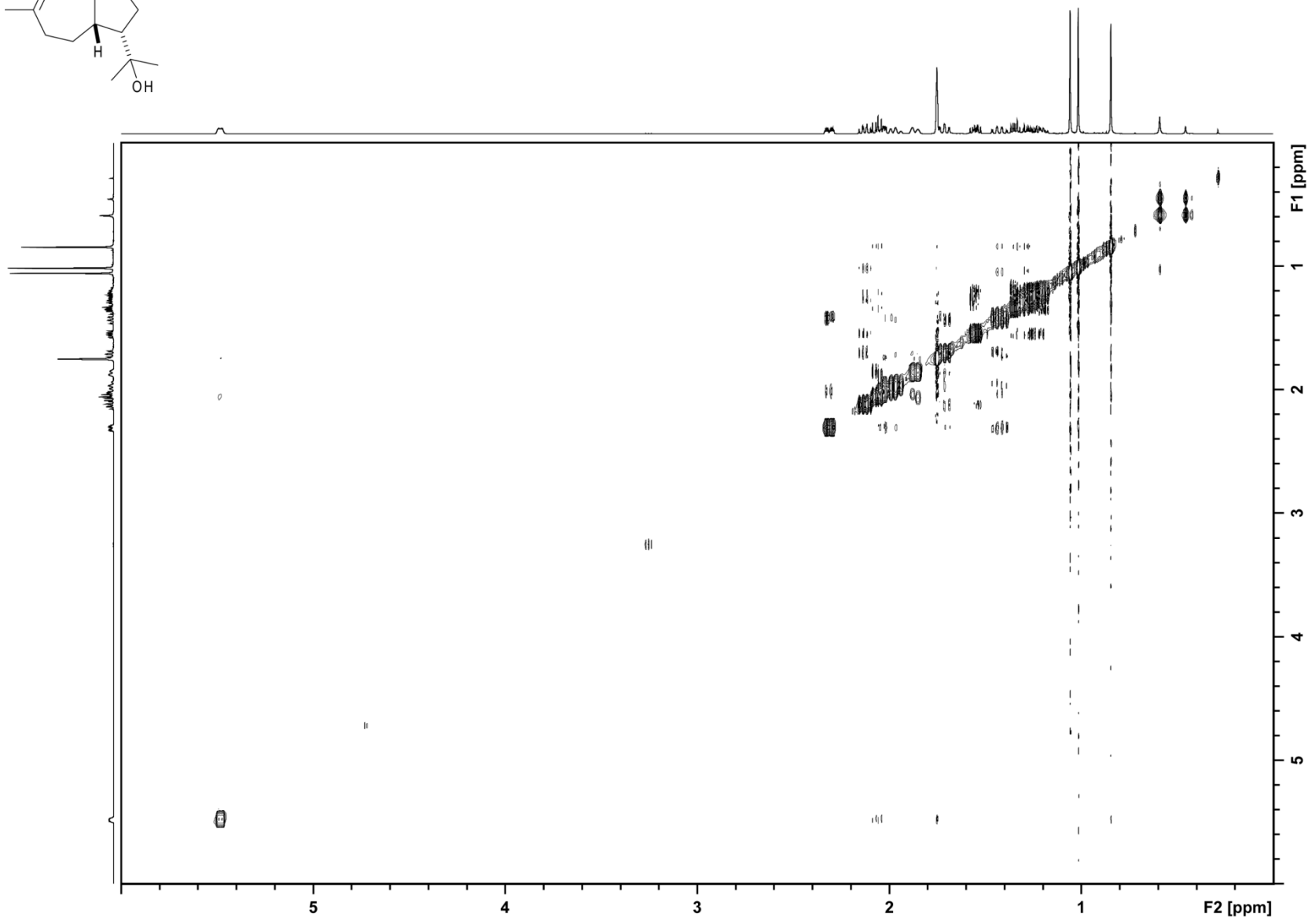


Fig. 19 NOESY spectrum of isodauc-8-en-1-ol (**3**) in ²H₆benzene at 298K at 500 MHz.



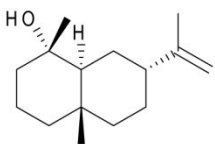


Fig. 20 $^1\text{H-NMR}$ spectrum of intermediateol (**4**) in $(^2\text{H}_6)$ benzene at 298K at 300 MHz.

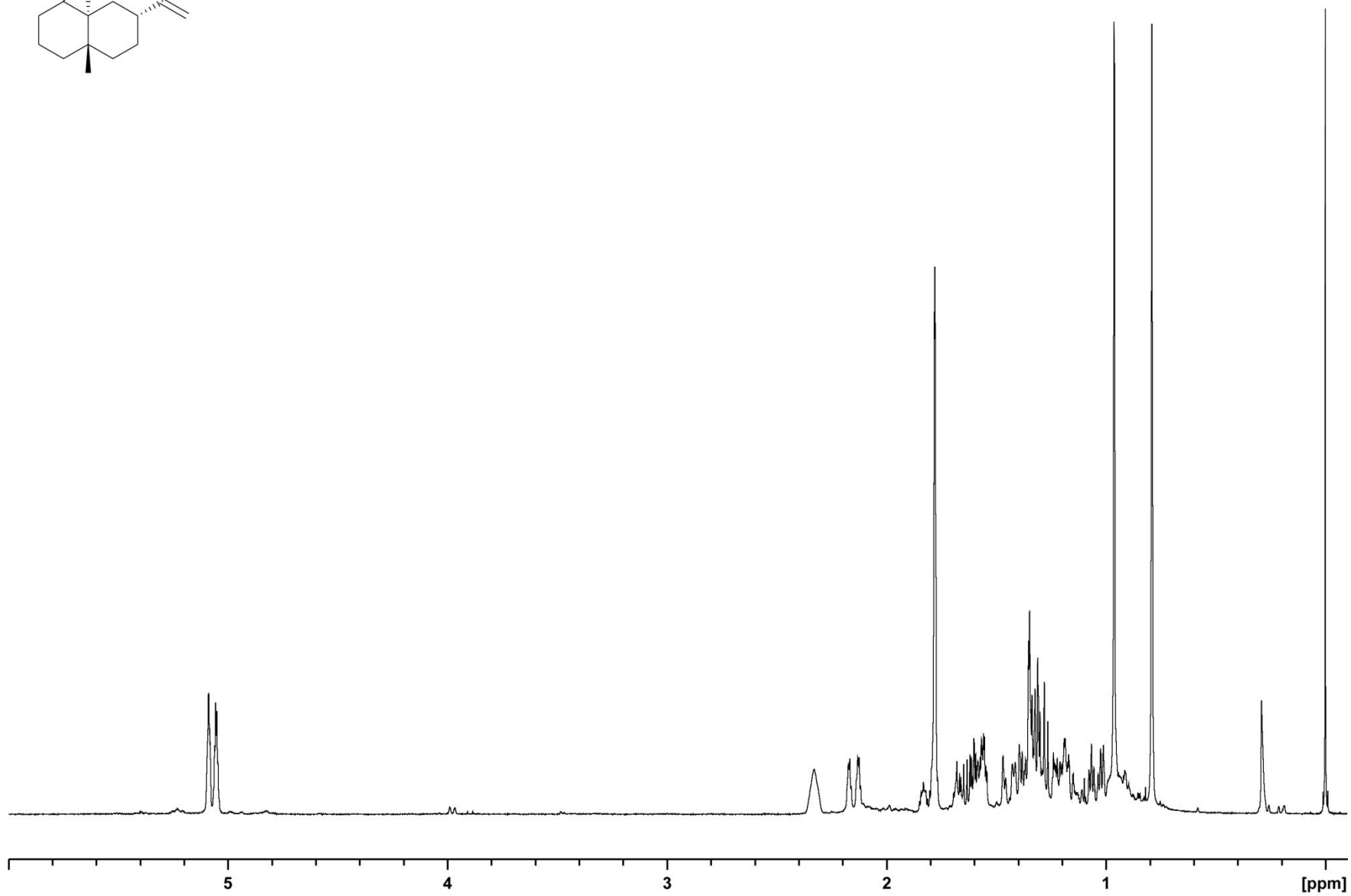
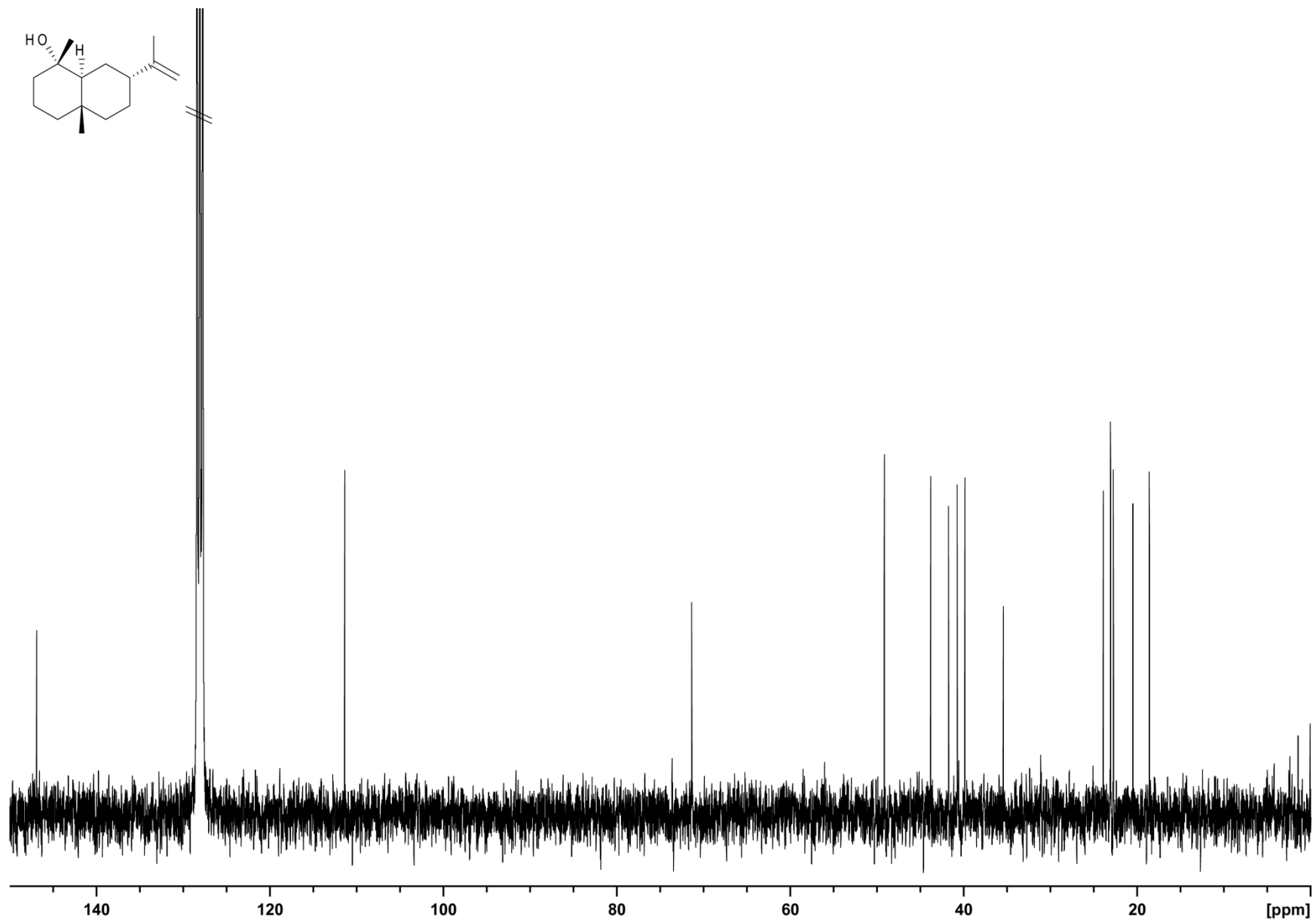


Fig. 21 ^{13}C -NMR spectrum of intermedeol (**4**) in $(^2\text{H}_6)$ benzene at 298K at 300 MHz.



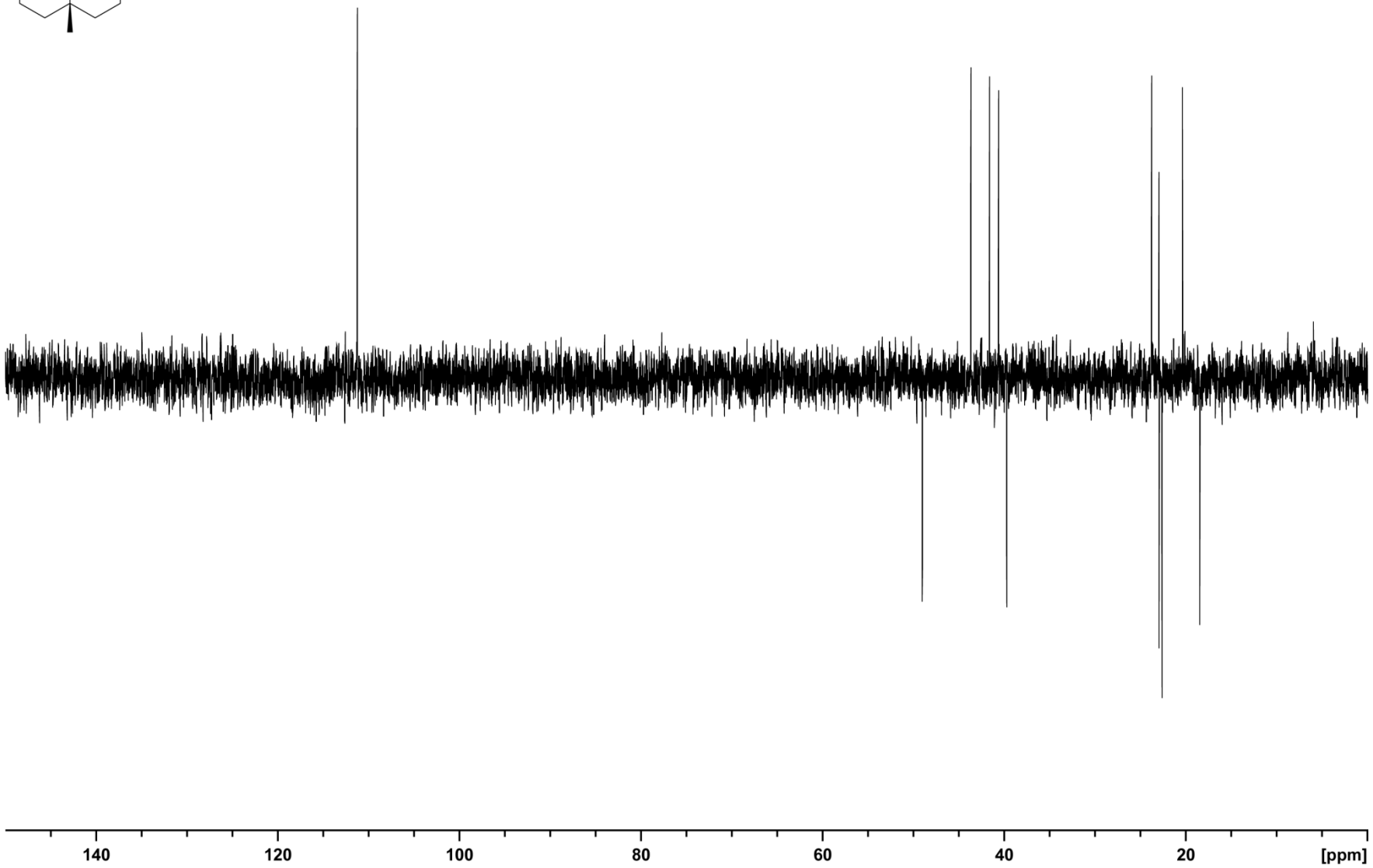
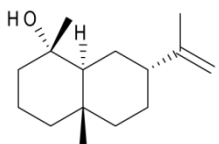


Fig. 22 ^{13}C -DEPT135-NMR spectrum of intermediate (**4**) in ($^2\text{H}_6$)benzene at 298K at 300 MHz.

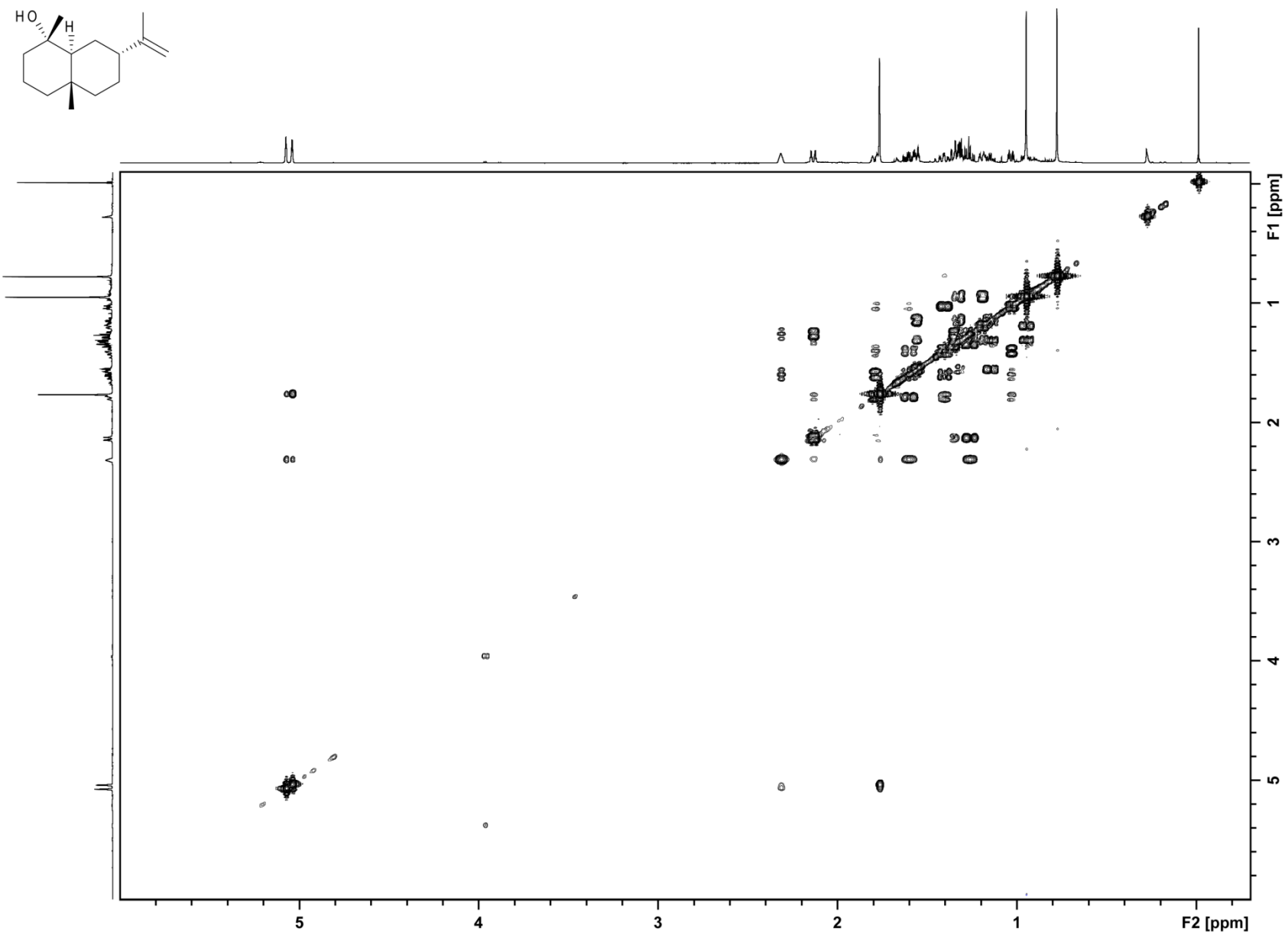


Fig. 23 ^1H , ^1H -COSY spectrum of intermediate **4** in $(^2\text{H}_6)$ benzene at 298K at 600 MHz.

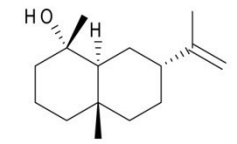
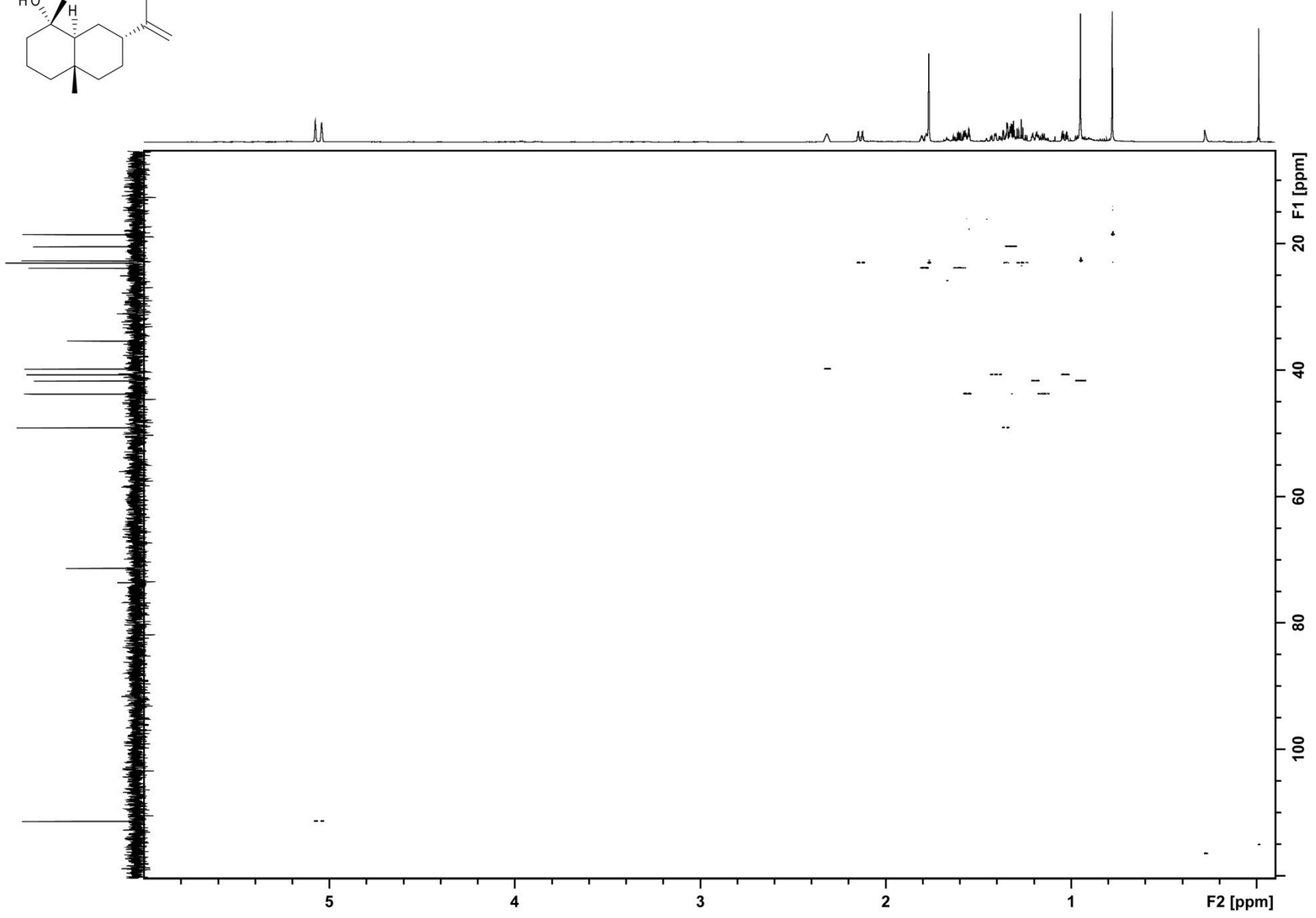


Fig. 24 HSQC spectrum of intermediateol (**4**) in ($^2\text{H}_6$)benzene at 298K at 600 MHz.



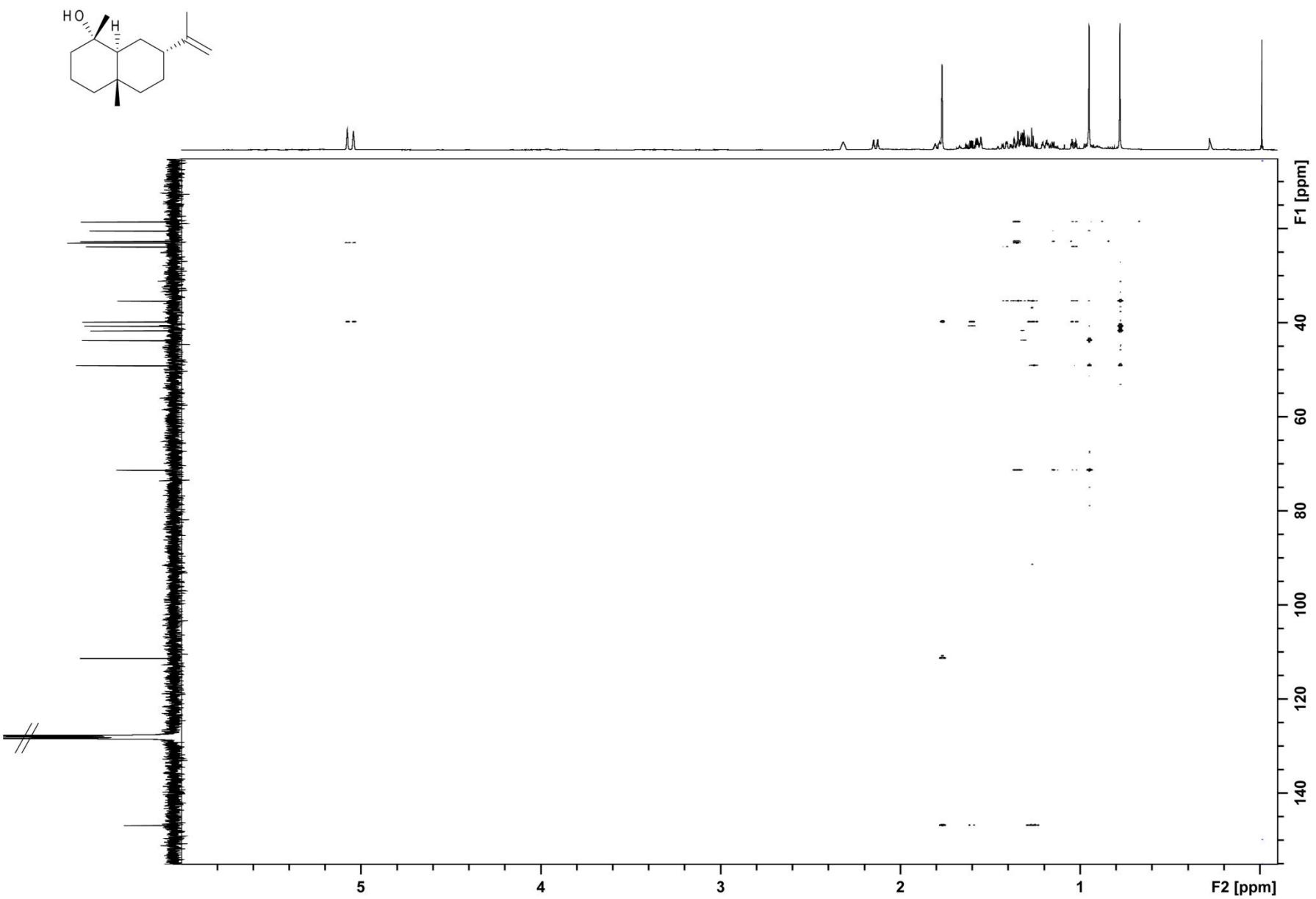


Fig. 25 HMBC spectrum of intermediate **4** in (C₆H₆) benzene at 298 K at 600 MHz.

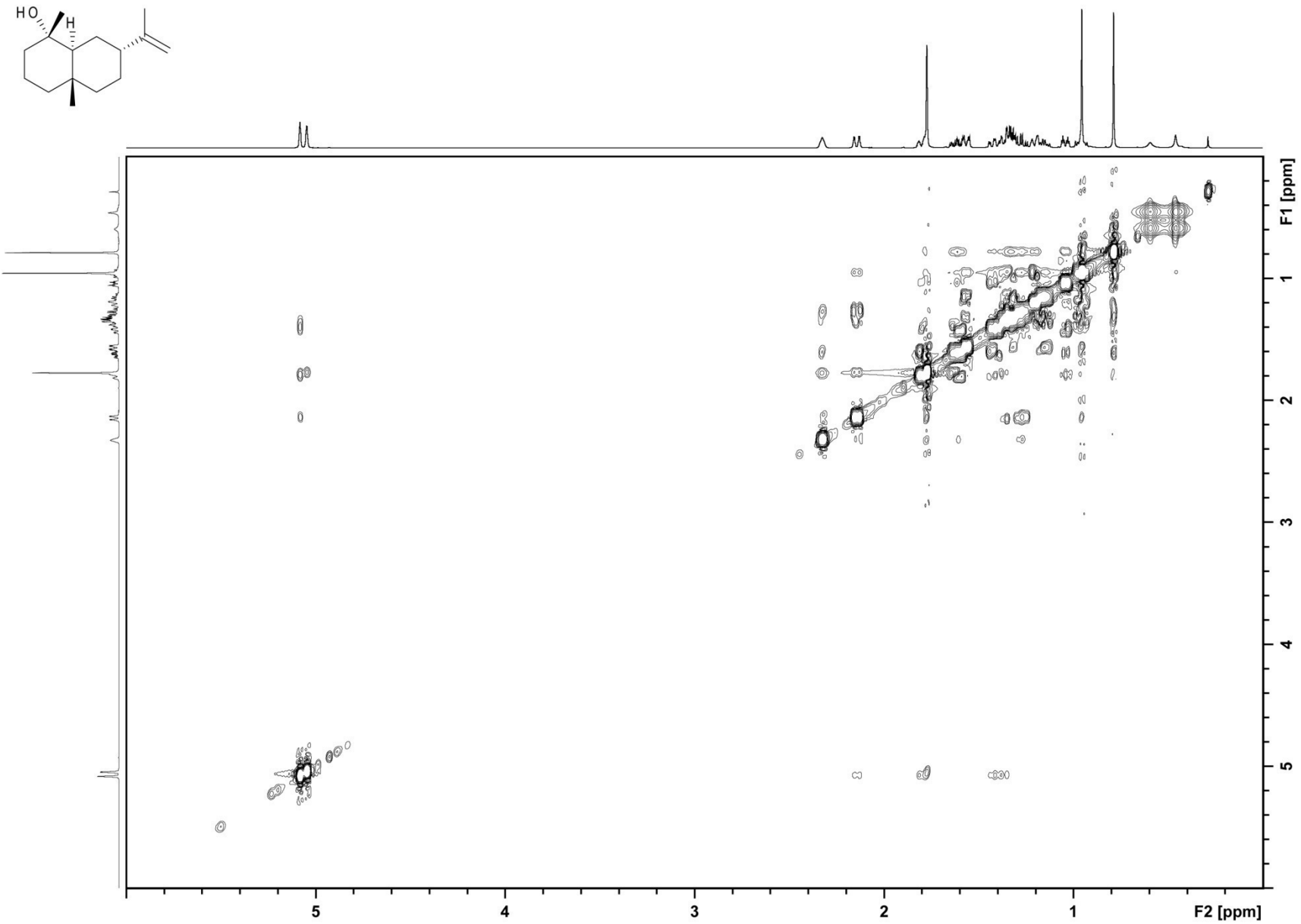


Fig. 26 NOESY spectrum of intermediate (4) in $(^2\text{H}_6)$ benzene at 298K at 500 MHz.

Appendix I

Discovery of a Mosaic-Like Biosynthetic Assembly Line with a
Decarboxylative Off-Loading Mechanism through a
Combination of Genome Mining and Imaging

Discovery of a Mosaic-Like Biosynthetic Assembly Line with a Decarboxylative Off-Loading Mechanism through a Combination of Genome Mining and Imaging

Mahsa Mir Mohseni[†], Thomas Höver[†], Lena Barra, Marcel Kaiser, Pieter C. Dorrestein, Jeroen S. Dickschat, and Till F. Schäberle*

Abstract: The biosynthetic gene cluster for the antiplasmodial natural product siphonazole was identified by using a combination of genome mining, imaging, and expression studies in the natural producer *Herpetosiphon* sp. B060. The siphonazole backbone is assembled from an unusual starter unit from the shikimate pathway that is extended by the action of polyketide synthases and non-ribosomal peptide synthetases with unusual domain structures, including several split modules and a large number of duplicated domains and domains predicted to be inactive. Product release proceeds through decarboxylation and dehydration independent of the thioesterase SphJ and yields the diene terminus of siphonazole. High variation in terms of codon-usage within the gene cluster, together with the dislocated domain organization, suggest a recent emergence in evolutionary terms.

For decades natural products have played major roles as biological probes, inspiration for organic chemists and, most prominently, an important source of therapeutic compounds.^[1,2] But natural product research currently struggles with two dilemmas. On the one hand, the development of resistance renders many drugs useless, while on the other hand, the development of innovative drugs has been deadlocked over the last two decades, since doubts have arisen concerning the usefulness of natural products as a basis for

new leads. One reason is that known compounds are frequently re-isolated in bioactivity-based screening approaches. A still promising approach for today is offered by so far poorly studied groups of organisms, for example, microorganisms associated with insects or from marine habitats, or the diverse group of gliding bacteria that usually exhibit complex life cycles and harbor great potential to produce bioactive compounds.^[3-7] Herein, we report on the discovery of the siphonazole biosynthetic gene cluster from *Herpetosiphon* sp. B060, a strain that we isolated from a soil sample from the intertidal zone, through a combination of genome mining, expression analysis, and imaging mass spectrometry (IMS). The gene cluster shows a mosaic-like structure, combines parts from the shikimate pathway and polyketide and non-ribosomal peptide biosynthesis,^[8] and makes use of an unusual termination mechanism that was studied in detail.

Siphonazole was isolated from *Herpetosiphon* sp. B060 and its structure elucidated a decade ago,^[8] and strategies for its total synthesis have also been developed,^[9,10] but details of the biosynthesis, including the timing and the corresponding gene cluster, are unknown. Besides expression analysis, an interesting and fast method to follow the production of a natural product is offered by imaging mass spectrometry (IMS), which can be directly performed on an agar-plate culture. To investigate product distribution and to identify the siphonazole biosynthetic gene cluster, IMS analysis of *Herpetosiphon* sp. B060 grown on agar was performed (Figure 1 a). Siphonazole production was specifically detected at the outer edge of the swarming colonies, that is, only in young cells. Hence, it was shown that this method can be successfully used to investigate strains for which no genetic tools exist.

The draft genome of *Herpetosiphon* sp. B060 was screened for polyketide synthase (PKS) and nonribosomal peptide synthetase (NRPS) sequences, resulting in two contigs that encoded gene clusters for hybrid PKS/NRPS metabolites. One of these gene clusters showed high similarity to a pathway present in the related strain *Herpetosiphon aurantiacus*, which does not produce siphonazole. Furthermore, prediction of the adenylation (A) domain substrate specificities for this cluster pointed to the incorporation of ornithine, asparagine, and leucine, but none of these amino acids correlated to the structure of siphonazole (Scheme 1), which is assembled from a methylated 3,4-dihydroxybenzoate starter unit, one glycine and two threonines, three intact acetate units, and C2 of a fourth acetate (Figure S1 in the Supporting Information).^[8] The second candidate PKS/NRPS gene cluster contained

[*] Dr. M. Mir Mohseni,^[†] Dr. T. Höver,^[†] Dr. T. F. Schäberle
Institut für Pharmazeutische Biologie, Universität Bonn
53115 Bonn (Germany)
E-mail: till.schaerberle@uni-bonn.de

L. Barra, Prof. J. S. Dickschat
Kekulé-Institut für Organische Chemie und Biochemie
Universität Bonn, 53121 Bonn (Germany)

M. Kaiser
Schweizerisches Tropen- und Public-Health-Institut (Swiss TPH)
Basel CH-4002 (Switzerland)

M. Kaiser
Universität Basel, CH-4003 Basel (Switzerland)

Prof. P. C. Dorrestein
Collaborative Mass Spectrometry Innovation Center
Skaggs School of Pharmacy and Pharmaceutical Sciences
University of California at San Diego, La Jolla, CA (USA)

[†] These authors contributed equally

Supporting information for this article (details about the biosynthetic gene cluster, analysis of enzymes, and experimental) can be found under:

<http://dx.doi.org/10.1002/anie.201606655>. Accession number of the siphonazole biosynthetic gene cluster: KX765816.

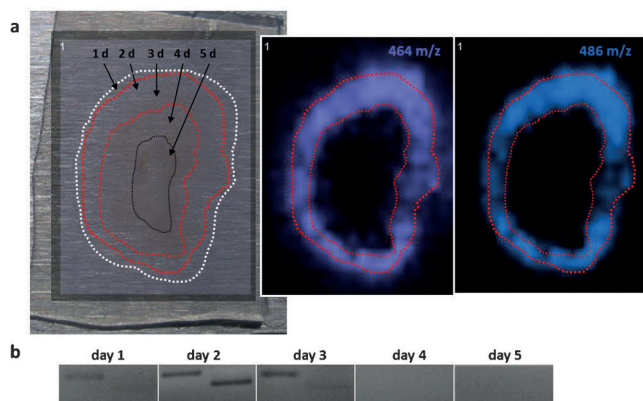
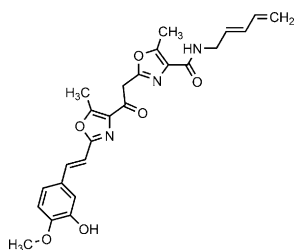


Figure 1. a) IMS analysis of an actively growing agar-plate culture of *Herpetosiphon* sp. B060. The detected ions m/z 464 and m/z 486 correspond to siphonazole $[M+H]^+$ and the sodium adduct $[M+Na]^+$. The culture was inoculated in the area indicated by the black line. The red lines indicate the area of the swarming colony, in which the cells are 2–3 days old. b) Time course of the expression of the siphonazole genes *sphA* and *sphB*.



Scheme 1. The structure of siphonazole.

A domains predicted to be specific for glycine and threonine activation, as expected for siphonazole. Furthermore, oxidation domains were identified within the NRPS modules, which are required for oxazole ring formation. Expression level analysis for the cluster genes *sphA* and *sphB* revealed strong expression in young cells, with a maximum at day two (Figure 1b), which is in line with the results of IMS analysis.

A fosmid library of *Herpetosiphon* sp. B060 genomic DNA was generated and screened with primers designed for specific parts of the cluster, resulting in the identification of three fosmids carrying partial cluster information. DNA sequencing of the three fosmids yielded large parts of the cluster sequence, and the gaps were closed by PCR amplification of genomic DNA, finally yielding the putative biosynthetic gene cluster for siphonazole biosynthesis (Figure 2). The hybrid NRPS/*trans*-AT PKS cluster consists of ten genes, *sphA* to *sphJ*, and spans 50 kb in total (Table S1 in the Supporting Information). RT-PCR with primer pairs covering the end of one gene and the start of the downstream following one revealed that *sphA* and *sphB*, as well as *sphC* to *sphJ*, are transcriptionally coupled units (Figure S2).

The core of the siphonazole biosynthetic gene cluster consists of twelve modules, including four NRPS and eight *trans*-AT PKS modules. Further, the *O*-methyltransferase *SphB*, a C-terminal hydrolase domain of *SphH*, and the aldolase *SphI* are integral parts of the cluster (Figure 2). The

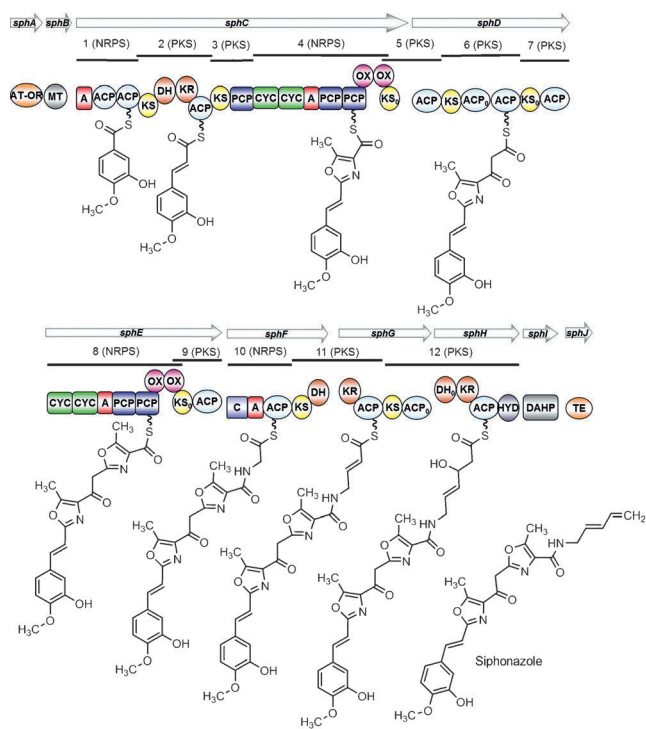
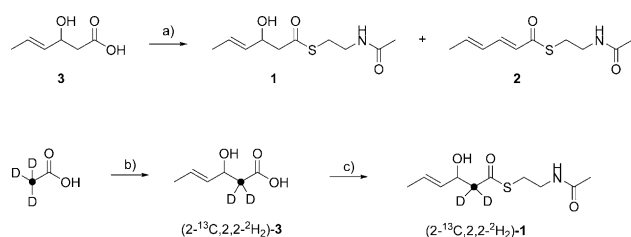


Figure 2. The biosynthetic gene cluster and a biosynthetic model for the assembly of siphonazole. A: adenylation domain, ACP: acyl carrier protein, AT-OR: acyltransferase–oxidoreductase, C: condensation domain, CYC: cyclisation domain, DAHP: 3-deoxy-D-arabinoheptulosonate-7-phosphate synthase, DH: dehydratase, HYD: hydrolase, KR: ketoreductase, KS: ketosynthase, MT: methyltransferase, OX: oxidation domain, PCP: peptidyl carrier protein, TE: thioesterase. Domains that are predicted through bioinformatics to be inactive are indicated by the index 0.

activities of these enzymes/domains, as well as activation of the starter unit, were analyzed in detail (see the Supporting Information).

Feeding experiments with (1^{13}C)acetate revealed that the last acetate is decarboxylated after its incorporation.^[8] The last module shows the unusual domain organization KS-ACP₀-DH₀-KR-ACP-HYD, with a C-terminal hydrolase that is unique to the siphonazole cluster. A bioinformatic analysis of the discrete thioesterase (TE) *SphJ* reveals that this enzyme may have a proof-reading function to release misprimed substrates from ACPs of the siphonazole pathway instead of being responsible for product release. To investigate how the domains of the last module participate in the processing of the fourth incorporated malonyl-CoA unit, and which domains of this module are relevant for product off-loading, possibly together with the discrete TE *SphJ*, the C-terminal part of *SphH* (ACP-HYD, referred to as *SphH*_{Cterm}) and *SphJ* were heterologously expressed in *E. coli* and purified (Figures S21, S22). Since the natural substrate in its bound state with the ACP of *SphH*_{Cterm} is difficult to obtain, enzyme incubation experiments were performed with short substrate mimics that were synthesized starting from 3-hydroxyhex-4-enoic acid (**3**).^[11] The acid was transformed into the respective *N*-acetylcysteamine thioester (SNAC ester) **1** by using EDC as a coupling reagent (Scheme 2). As



Scheme 2. Synthesis of substrate analogues **1–3** used for the in vitro incubation experiments. a) EDC, DMAP, HSNAC, 70% of **1** and 4% of **2**; b) *n*BuLi (1 equiv), LDA (1 equiv);, then (*E*)-crotonaldehyde, 85%; c) DCC, DMAP, HSNAC, 47%. EDC = 1-ethyl-3-(3-dimethylaminopropyl)carbodiimide, DMAP = 4-dimethylaminopyridine, HSNAC = *N*-acetylcystamine, LDA = lithium diisopropylamide, DCC = *N,N'*-dicyclohexylcarbodiimide.

a side product of this reaction the SNAC ester of sorbic acid (**2**) was isolated. Furthermore, for investigation of the enzyme mechanism, the isotopically labelled compound (2-¹³C,2,2-²H₂)-**1** was synthesized through aldol addition of (2-¹³C,2,2-²H₃)acetic acid to (*E*)-crotonaldehyde and conversion into the SNAC ester.

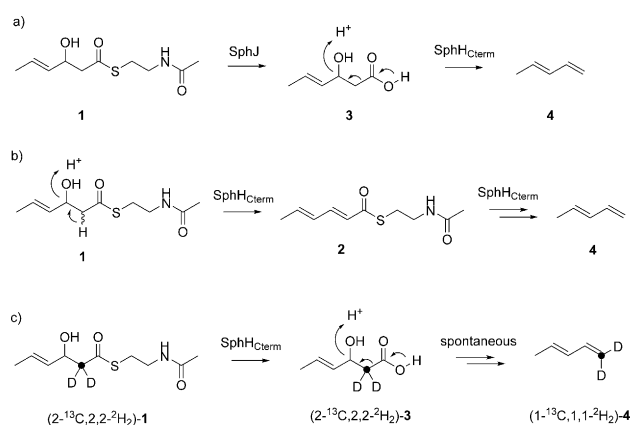
The synthetic substrate analogues were incubated with different enzyme preparations, and the production of pentadiene, which is formed analogously to the natural product siphonazole, was detected by capturing the volatiles from the incubation reaction on a solid-phase microextraction (SPME) fiber followed by GC/MS analysis.^[12] Incubation of **1** with SphH_{Cterm} and SphJ resulted in a strong production of pentadiene (**4**; Table 1 and Figure S14), which is in line with

Table 1: Results from incubation experiments with substrates **1–3**, (2-¹³C,2,2-²H₂)-**1**, and different enzyme combinations.

Substrate	SphH _{Cterm} + SphJ	SphJ	SphH _{Cterm}	Control
1	+	–	+	–
(2- ¹³ C,2,2- ² H ₂)- 1	n.d.	n.d.	+	–
2	–	–	–	–
3	n.d.	n.d.	+	+

+ : pentadiene production, – : no pentadiene production, n.d. : not determined

a mechanism of initial hydrolysis of the thioester **1** to the acid **3** by SphJ, followed by a decarboxylation and dehydration by SphH (Scheme 3 a), but this experiment does not always allow exclusion of the possibility that only one of the enzymes participates in the reaction. Therefore, the thioester **1** was also incubated with either SphJ or SphH_{Cterm} alone, and indeed incubation of **1** with SphJ did not result in the production of **4** (only traces were detected, as in the control experiment without enzyme), while incubation with SphH_{Cterm} alone resulted in the formation of **4** in similar amounts to those observed following incubation with both enzymes. These data call into question the involvement of the TE SphJ in the termination mechanism of siphonazole biosynthesis and further support a sole proof-reading function for this enzyme, while suggesting that product release, decarboxylation, and dehydration are all catalyzed by SphH_{Cterm}.



Scheme 3. Possible mechanisms for product release in siphonazole biosynthesis. a) Thioester hydrolysis by SphJ and dehydration/decarboxylation by SphH_{Cterm}. b) Initial dehydration by SphH_{Cterm} followed by thioester hydrolysis and decarboxylation by the same enzyme. c) Thioester hydrolysis by SphH_{Cterm} followed by spontaneous/concerted dehydration and decarboxylation.

The question of which of these three reactions occurs first was investigated through incubation experiments with substrates (2-¹³C,2,2-²H₂)-**1**, **2**, and **3**. If thioester hydrolysis were first, then the subsequent steps of dehydration and decarboxylation could be a concerted process (Scheme 3 b). This was studied by using the isotopically labelled substrate (2-¹³C,2,2-²H₂)-**1**, which may first be hydrolyzed to the free acid (2-¹³C,2,2-²H₂)-**3**. Protonation of the hydroxy function in (2-¹³C,2,2-²H₂)-**3** and elimination of water could induce spontaneous decarboxylation, and in this mechanism, both deuterium atoms and the ¹³C-labelling should be retained in the product (1-¹³C,1,1-²H₂)-**4**. As shown in an incubation experiment with SphH_{Cterm} and (2-¹³C,2,2-²H₂)-**1**, this was the case (Figure S15; a mass spectrum of the obtained (1-¹³C,1,1-²H₂)-**4** is shown in in Figure S16). The results of this labelling experiment also speak against a mechanism in which the dehydration of **1** to **2** is the first step, because this would require the loss of one deuterium from C_α. Furthermore, incubation of **2** with neither SphH_{Cterm}, SphJ, nor both yielded **4** (Table 1 and Figure S17), which is in agreement with the function of SphJ as proof-reading TE. If ester hydrolysis is the first step, then substrate **3** should be converted into **4** by SphH_{Cterm}, as was experimentally observed (Table 1 and Figure S18), but similar amounts of **4** were detected in the control experiment without enzyme, thus suggesting that SphH_{Cterm} only catalyzes the thioester hydrolysis, while the decarboxylation–dehydration of **3** to **4** is likely a spontaneous reaction in water. However, it cannot be excluded that catalysis by SphH_{Cterm} is required for conversion of the natural substrate.

Siphonazole was tested for its biological activity. Cytotoxic activity was observed, but the effect (the mean IC₅₀ value against a panel of 36 cancer cell lines was 5.90 μg mL⁻¹, 12.74 μM) was too weak for further evaluation as an anticancer agent. At non-cytotoxic concentrations, no antiviral activity was observed (tested: coxsackie virus B3, influenza virus A, herpes simplex virus type 1). Antibacterial or anti-

fungal effects were not observed. Instead, siphonazole showed activity against *Plasmodium falciparum* (IC₅₀: 0.59 μg mL⁻¹, 1.27 μM; Table S2).

The siphonazole biosynthetic gene cluster shows many idiosyncrasies, which is typical for *trans*-AT PKSs and hints at recombination events through horizontal gene transfer. Until now, most approaches to mutate a cluster in a target-oriented way have remained ineffective. *Herpetosiphon* sp. B060 is an example where nature has relatively recently performed recombinatorial biosynthesis, and obtained a natural product—the desired output for synthetic biology. Future investigation of the siphonazole cluster might provide new insight into this field to create “unnatural natural products”. Furthermore, new tools for synthetic biology are desirable. The investigated thioester hydrolysis, which is a prerequisite for the terminal, presumably spontaneous decarboxylation–dehydration of the released molecule, by SphH_{Cterm} represents such a novel functionality within PKS systems. A similar terminal alkene moiety was observed in the biosynthesis of the anticancer compound curacin A.^[13] However, in curacin A biosynthesis, a sulfotransferase encoded in the terminal module first transfers a sulfonate group to the β-hydroxy group, making it a better leaving group. The subsequent decarboxylative elimination is catalyzed by a TE. By contrast, in siphonazole biosynthesis, SphH_{Cterm} is sufficient, and the simplified substrate mimic used indicates promiscuity of this enzyme, which could be used in further transformations. The promising antiplasmodial activity of siphonazole will be subject of future investigations, since additional economically priced treatment options are still needed to achieve reductions in the *Plasmodium falciparum* malaria burden.^[14]

In this report, a work flow is illustrated that allows one to link a metabolite of interest directly to its biosynthetic gene cluster. Such approaches are needed to speed up gene cluster identification, even when only draft genomes are available. This holds especially true for organisms that are not genetically accessible. Using a mass spectrometry based technology such as IMS, which was established to observe the chemical output and metabolic exchange between an organism and the environment directly on agar plates,^[15,16] facilitates the linking of a metabolite to its biosynthetic gene cluster. Increasing sequencing efforts make clear the discrepancy between computationally identified biosynthetic gene clusters and known metabolites, and this resource should be made use of. New microorganisms, preferably from under-investigated ecological niches, should be domesticated, as recently shown for the teixobactin producer,^[17] and metagenomics approaches should be intensified to create a basis for identifying gene loci for new lead compounds. Then, a mass spectrometry based analysis in combination with expression profiles should enable the prompt linking of genes and metabolites.

Acknowledgments

M.M.M. was funded by NRW International Graduate Research School BIOTECH-PHARMA. Work in the lab of T.F.S. was funded by the Federal Ministry of Education and Research (BMBF). Boehringer Ingelheim Fonds is thanked for a travel grant to T.F.S.

Keywords: biosynthesis · genome mining · imaging mass spectrometry (IMS) · natural products · siphonazole

How to cite: *Angew. Chem. Int. Ed.* **2016**, *55*, 13611–13614
Angew. Chem. **2016**, *128*, 13809–13813

- [1] C. T. Walsh, M. A. Fischbach, *J. Am. Chem. Soc.* **2010**, *132*, 2469–2493.
- [2] D. J. Newman, G. M. Cragg, *J. Nat. Prod.* **2012**, *75*, 311–335.
- [3] T. F. Schäberle, F. Lohr, A. Schmitz, G. M. König, *Nat. Prod. Rep.* **2014**, *31*, 953–972.
- [4] S. C. Wenzel, R. Müller, *Curr. Opin. Drug Discovery Dev.* **2009**, *12*, 220–230.
- [5] C. Beemelmanns, H. Guo, M. Rischer, M. Poulsen, *Beilstein J. Org. Chem.* **2016**, *12*, 314–327.
- [6] A. Dávila-Céspedes, P. Hufendiek, M. Crüsemann, T. F. Schäberle, G. M. König, *Beilstein J. Org. Chem.* **2016**, *12*, 969–984.
- [7] J. Korp, M. S. V. Gurovic, M. Nett, *Beilstein J. Org. Chem.* **2016**, *12*, 594–607.
- [8] M. Nett, O. Erol, S. Kehraus, M. Köck, A. Krick, E. Eguereva, E. Neu, G. M. König, *Angew. Chem. Int. Ed.* **2006**, *45*, 3863–3867; *Angew. Chem.* **2006**, *118*, 3947–3951.
- [9] J. Linder, C. J. Moody, *Chem. Commun.* **2007**, 1508–1509.
- [10] J. Zhang, M. A. Ciufolini, *Org. Lett.* **2009**, *11*, 2389–2392.
- [11] B. D. Ames, C. Nguyen, J. Bruegger, P. Smith, W. Xu, S. Ma, E. Wong, S. Wong, X. Xie, J. W. Li, J. C. Vederas, Y. Tang, S. C. Tsai, *Proc. Natl. Acad. Sci. USA* **2012**, *109*, 11144–11149.
- [12] J. S. Dickschat, *Nat. Prod. Rep.* **2014**, *31*, 838–861.
- [13] L. Gu, B. Wang, A. Kulkarni, J. J. Gehret, K. R. Lloyd, L. Gerwick, W. H. Gerwick, P. Wipf, K. Håkansson, J. L. Smith, D. H. Sherman, *J. Am. Chem. Soc.* **2009**, *131*, 16033–16035.
- [14] P. G. Walker, J. T. Griffin, N. M. Ferguson, A. C. Ghani, *Lancet Glob. Health.* **2016**, Jun 3, pii: S2214-109X(16)30073-0.
- [15] Y. L. Yang, Y. Xu, P. Straight, P. C. Dorrestein, *Nat. Chem. Biol.* **2009**, *5*, 885–887.
- [16] a) Y. L. Yang, Y. Xu, R. D. Kersten, W. T. Liu, M. J. Meehan, B. S. Moore, N. Bandeira, P. C. Dorrestein, *Angew. Chem. Int. Ed.* **2011**, *50*, 5839–5842; *Angew. Chem.* **2011**, *123*, 5961–5964.
- [17] L. L. Ling, T. Schneider, A. J. Peoples, A. L. Spoering, I. Engels, B. P. Conlon, A. Mueller, T. F. Schäberle, D. E. Hughes, S. Epstein, M. Jones, L. Lazarides, V. A. Steadman, D. R. Cohen, C. R. Felix, K. A. Fetterman, W. P. Millett, A. G. Nitti, A. M. Zullo, C. Chen, K. Lewis, *Nature* **2015**, *517*, 455–459.

Received: July 12, 2016

Revised: August 29, 2016

Published online: September 26, 2016

Supporting Information

Discovery of a Mosaic-Like Biosynthetic Assembly Line with a Decarboxylative Off-Loading Mechanism through a Combination of Genome Mining and Imaging

*Mahsa Mir Mohseni[†], Thomas Höver[†], Lena Barra, Marcel Kaiser, Pieter C. Dorrestein, Jeroen S. Dickschat, and Till F. Schäberle**

[ange_201606655_sm_miscellaneous_information.pdf](#)

Content

Description of the biosynthetic gene cluster and biosynthetic hypothesis

Analysis of specific protein(domain)s

General material and methods

General synthetic methods

Synthesis of (*E*)-*S*-(2-acetamidoethyl) 3-hydroxyhex-4-enethioate (**1**)

Synthesis of (2-¹³C,2,2-²H₂)-(*E*)-3-hydroxyhex-4-enoic acid ((2-¹³C,2,2-²H₂)-**3**)^[36]

Synthesis of (2-¹³C,2,2-²H₂)-(*E*)-*S*-(2-acetamidoethyl) 3-hydroxyhex-4-enethioate ((2-¹³C,2,2-²H₂)-**1**)

SPME sampling

Extracted ion chromatograms of *in vitro* studies

NMR chromatograms

Figures and Tables

Figure S1. Molecular structure of siphonazole and its deduced building blocks

Figure S2. Test PCRs for RNA expression analysis

Figure S3. Conserved motifs of SphA which indicate malonyl-CoA as substrate

Figure S4. Conserved C-H-H catalytic triad of the KS domains

Figure S5. Multiple sequence alignment of the ACP and PCP domains

Figure S6. Multiple sequence alignment of the KR domains

Figure S7. Multiple sequence alignment of the DH domains

Figure S8. Multiple sequence alignment of the thioesterase SphJ with the sequence of type II TEs associated with bacterial PKSs, NRPSs.

Figure S9. SDS-PAGE of a typical purification of SphI

Figure S10. pH dependency and metal requirements of SphI

Figure S11. Signature motifs and multiple sequence alignment of SphB

Figure S12. Methylation activity of SphB

Figure S13. Results of the ATP-PP_i exchange assay

Figure S14. *in vitro* experiments with substrate mimic **1**

Figure S15. *in vitro* experiments with substrate mimic (2-¹³C,2,2-²H₂)-**1**.

Figure S16. Mass spectrum of 1,3-pentadiene reference (A) and mass spectrum of labeled pentadiene after incubation of (2-¹³C,2,2-²H₂)-**1** with SphH_{Cterm} (*holo*-ACP) (B).

Figure S17. *in vitro* experiments with substrate mimic **2**

Figure S18. *in vitro* experiments with substrate mimic **3**

Figure S19. SDS-PAGE of a typical purification of SphB

Figure S20. SDS-PAGE of a typical purification of the SphC A domain

Figure S21. SDS-PAGE of a typical purification of SphH_{Cterm}

Figure S22. SDS-PAGE of a typical purification of SphJ

Table S1. Predicted functionalities of the proteins encoded in the siphonazole biosynthetic gene cluster

Table S2. Antiprotozoal activities of siphonazole

Table S3. mRNA screening primers

Table S4. Primers for protein expression constructs

Table S5. Bacterial strains and plasmids used in this study

NMR chromatograms

Siphonazole biosynthetic gene cluster

All individual domains were screened for the presence of signature motifs that are known to be required for catalytic activity (Figures S3 – S8). This analysis revealed that several KS domains (KS5, KS7 and KS9 and ACPs (ACP6₁ and ACP12₁), and the dehydratase domain DH12 are likely inactive because of critical mutations.^[18-20] Therefore, modules 3, 5 and 6 merely pass on the intermediate without elongation, while the product of module 12 is likely an ACP-bound 3-hydroxy intermediate and not an enoyl-S-ACP. The three KR_s identified in the siphonazole gene cluster are all regarded as active, even though the conserved asparagine of KR12 is replaced by a cysteine residue (Figure S6). However, this is also the case in the first PksM-KR from *Bacillus subtilis*, which has been reported as functional.^[21] In silico prediction of the substrate specificities for the four A domains pointed to the group of hydrophobic-aromatic substrates for the loading A domain (A1), while the domains A4 and A8 have identical sequences and were predicted to activate threonine, and the substrate of A10 was tentatively identified as glycine. In the NRPS modules 4 and 8 no C domains are found, but instead two pairs of cyclisation (Cyc) domains are present that usually catalyze the formation of heterocycles from serine, threonine or cysteine residues.^[22] The unusual arrangement of tandem Cyc domains has its precedence in the biosynthesis of vibriobactin and leinamycin, in which the first domain is responsible for heterocyclisation and the second one substitutes for a regular C domain for peptide bond formation.^[23,24] A similar mechanism can be assumed for siphonazole biosynthesis. Modules 4 and 8 also contain tandem oxidation (Ox) domains for the conversion of initially formed oxazoline/thiazoline into oxazole/thiazole rings. As exemplified for epothilone biosynthesis,^[25] one such domain is sufficient for this transformation. Indeed, analysis of the signature motifs revealed that the second Ox domains of modules 4 and 8 both lack the NADPH-binding site,^[26] indicating that these are non-functional due to impaired cofactor binding. Another peculiarity of modules 4 and 8 is the 98% identity of their nucleotide sequences over a range of 4,750 bp, suggesting either a duplication event or a double integration into the cluster. Furthermore, the GC-

content of these modules is much higher (68%) than the average over the whole gene cluster (53%), which also points to their recent acquisition and integration into a hypothetical parental gene cluster. This hypothesis is also reflected by the non-functional modules 5, 7 and 9 surround modules 4 and 8, representing a mosaic-like architecture that is also frequently seen in other *trans*-AT PKS clusters that generally seem to develop by extensive horizontal gene transfers.^[27] The *trans*-AT domain SphA of the siphonazole cluster is predicted to load malonyl-CoA onto the ACP domains of the PKS modules 2, 6, 11 and 12 (Figure S3), in agreement with the results from feeding experiments with labelled acetate.^[9] The C-terminal part of SphA contains an oxidoreductase domain, but the catalytic histidine is replaced by tyrosine, suggesting the oxidoreductase as non-functional.

Off-loading of the nascent molecule is done by the action of a thioesterase (TE). In the present cluster sphJ encodes a free-standing TE which contains the conserved G-x-S-x-G motif and shows highest identity to TEs from *Bacillus* species. SphJ also shows the motif for proof-reading TEs (Figure S8) that have the function to edit miss-primed domains and thereby ensure the loading of the correct substrate. Hence, the TE domain may not be involved in substrate off-loading, but another mechanism may be relevant for siphonazole, as will be discussed later. In addition to the described proteins forming the PKS/NRPS core of the biosynthetic gene cluster, the *O*-methyltransferase (*O*-MT) SphB, a C-terminal hydrolase domain of SphH, and the aldolase SphI are integral parts of the cluster (Figure 2).

In silico analysis of **SphI** revealed its homology to 3-deoxy-D-arabino-heptulosonate 7-phosphate (DAHP) synthases, enzymes catalyzing the condensation of phosphoenolpyruvate (PEP) and erythrose 4-phosphate (E4P) to yield chorismate.^[28] SphI showed 54% identity to a hypothetical aldolase from an unclassified bacterium (accession number: PRJNA192319), and ensures the precursor supply from the versatile shikimate pathway, as was shown for other metabolites using shikimate pathway derived starter units such as the glycopeptide antibiotic balhimycin.^[29] Heterologous expression of sphI in *E. coli* and incubation of the purified protein (Figure S9) with E4P and PEP yielded DAHP. Optimal conditions were pH7 and 30°C, while addition of EDTA abolished enzyme activity, revealing SphI to be a metallo-enzyme (Figure S10). The kinetic properties of SphI were determined under optimal conditions using Mn²⁺ as co-factor (K_M 377.9 ±20.8 μM; k_{cat} 0.0088 ±0.0003 s⁻¹).

SphB showed homology to *S*-adenosylmethionine (SAM)-dependent *O*-MTs with highest identity (65%) to a SAM-dependent MT from *Paenibacillus sonchi* (accession number: WP_039835538). The three conserved motifs that participate in SAM-binding were identified within the protein sequence (Figure S11). For siphonazole either 3,4-dihydroxybenzoic acid

(protocatechuic acid) or its 4'-*O*-methyl derivative isovanillic acid may act as the biosynthetic starter unit. Feeding experiments with (methyl-¹³C)methionine identified SAM as the methyl group donor.^[9] The methylation of the 4'-hydroxyl group by SphB was verified by protein expression in *E. coli* and incubation of the purified enzyme with protocatechuic acid and SAM. HPLC and UV/Vis analysis revealed formation of the product isovanillic acid (Figure S12). The optimal enzyme conditions were determined to be 45 °C and pH8 with kinetic parameters of K_M 1.325 μ M and k_{cat} of 1.54 min^{-1} .

As discussed above, the amino acid sequence of the **loading domain A1** pointed to the group of hydrophobic-aromatic substrates, but its precise specificity could not be predicted with certainty. Hence, the activity of A1 was tested towards the candidate substrates protocatechuic acid and isovanillic acid, as well as selected amino acids *in vitro* by an ATP-PP_i exchange assay. Therefore, N-terminal parts of SphC were heterologously expressed in *E. coli*. Interestingly, only protocatechuic acid, but not isovanillic acid, was accepted as a substrate (Figure S13). Furthermore, the tridomain A1-PCP1-PCP1₂ yielded a ten-fold higher exchange rate than the didomain A1-PCP1, while the single A1 domain was inactive. These data point to activation and loading of protocatechuic acid by the A1 domain and implicate a post-loading methylation by SphB.

General material and methods

Imaging mass spectrometry

Thin layer ISP2 agar plates were prepared. ISP2 media was prepared as described. Briefly, yeast extract 4 g, malt extract 10 g, dextrose 4 g, and agar 20 g, were added to 1 L of deionized water. For *S. coelicolor* growth, an aqueous suspension of spores was spotted onto the agar. For gliding bacteria the inoculum consisted of a part (0.5x0.5 cm) of a pre-grown plate placed upside down on the ISP2 medium. The bacterial colonies were allowed to form for the times indicated in the paper. Incubation was performed at 28°C. A photograph of the colonies was taken before they were subjected to further sample preparation for IMS. Afterwards, a region of agar was cut, laid on top of a cleaned and washed MALDI target plate, and covered by sprinkling the matrix consisting of a 1:1 mixture of α -cyano-4-hydroxycinnamic acid and 2,5-dihydroxybenzoic acid on top of the culture using a 20 μ m sieve. Once the sample was completely covered with matrix, it was dried in a 37 °C oven. The matrix is required for the ionization of the molecules present along the surface of the sample. At the same time, the matrix effectively fixes the organisms in place when applied. The natural product IMS was performed as described earlier²⁸. Briefly, the Bruker MSP 96 anchor plate containing the sample was inserted into a Microflex Bruker Daltonics mass

spectrometer outfitted with Compass 1.2 software suite (Consists of FlexImaging 2.0, FlexControl 3.0, and FlexAnalysis 3.0). A photomicrograph of the colonies to be imaged by mass spectrometry was loaded onto the Fleximaging command window. Three teach points were selected in order to align the background image with the sample target plate, before the sample was run in positive mode. After data acquisition, the data was analyzed using the FlexImaging software. The resulting mass spectra were filtered manually and individual colors were assigned to the specific masses.

Genomic mining and expression analysis

Fosmid library. Chromosomal DNA derived from a liquid culture of *Herpetosiphon spec.* B060 was used for the construction of a fosmid library construction using pCC1FOS (Epicenter, Madison, USA). The genomic library was constructed according to manufacturer's instructions. The resulting colonies with an average insert length of 36 kb were generated and transferred into 96-well microtiter plates. For long term storage at -80 °C the fosmid cultures were mixed with an equal volume of 100 % glycerol.

Genome sequencing. Genomic DNA for sequencing was isolated with the Qiagen DNeasy Blood & Tissue Kit according to the manufacturer's protocol. The resulting DNA with a concentration of ~400 ng/μL was submitted to 454 whole genome sequencing on a Roche GS FLX Titanium sequencer. The output was 158,535,259 bp which were assembled to 1,663 contigs. The average contig size was 7,809 bp with the largest contig stretching over 121,725 bp.

Genomic mining. A local Blast database was set up containing all the contigs obtained by sequencing. In previous work three fosmids were found to carry NRPS or PKS parts. DNA sequences of subclones from these fosmids as well as end sequences of the inserts were used as queries for Blast analysis. In that way identified contigs were subsequently analyzed more profound manually. Genes were annotated and the therefrom encoded proteins were analyzed in respect to siphonazole biosynthesis. In this analysis further all contigs showing homology to PKS and NRPS coding sequences were included. *In silico* prediction of A domain specificity was performed using NRSPredictor.^[30]

Gap closure. To close the initially remaining gaps in the putative biosynthetic gene cluster, specific primers were designed and used for PCRs using genomic DNA of *Herpetosiphon spec.* B060 as template. The resulting amplicates were subjected to Sanger sequencing, and the obtained sequence information was aligned with the existing one. In addition specific primers were designed and used for direct sequencing using the corresponding fosmid as template.

Molecular cloning

SphB. The primer pair OMT-fwd-BamHI and OMT-rev-HindIII, was used to amplify the *sphB*-gene, whereby each primer carried the sequence for the desired restriction site for subsequent cloning into the expression vector pET28. In brief, the target sequence was amplified using fosmid DNA as template. The gel purified fragment was ligated into the cloning vector pGEM-T (Promega), and the resulting construct was transferred to CaCl₂-competent *E. coli* XL1 Blue cells. The identity of the fragment was verified by sequencing, before it was restricted from the construct using *Bam*HI and *Hind*III. The restricted fragment was gel-purified and ligated into likewise restricted pET28. The resulting construct (pET28_SphB) was subsequently transferred in CaCl₂-competent *E. coli* BL21 cells.

However, the protein precipitated rapidly when exposed to low temperatures. Therefore, purification had to be carried out at room temperature and the following assays were performed directly afterwards to avoid activity loss.

SphC. For the expression of the SphC A domain several constructs were created, *i.e.* the single A domain (primer pair: sphC-A-fwd and sphC-A-rev), the A-PCP1 didomain (primer pair: sphC-A-fwd and sphC-A+ACP1), and the A-PCP1-PCP1₂ tridomain (primer pair: sphC-A-fwd and sphC-A+ACP1&2). For all the constructs the targeted DNA-fragment was amplified by PCR using *Pfu*-polymerase, directly cloned into pET151, and transferred to *E. coli* Top10 cells. Then, the constructs were verified by sequencing, and positive ones were transferred in CaCl₂-competent *E. coli* BL21* cells.

SphI. Primers showing homology to the 5' start region (sphI-fwd) and the 3' end region (sphI-rev) of the *sphI*-gene have been designed carrying 5'-prime overhangs for subsequent cloning into the vector pET151 (Invitrogen). PCR using *Pfu*-polymerase (Promega) in combination with these primers yielded an amplificate of 736 bps. This was cloned into pET151, and transferred into *E. coli* cells. The identity of the final construct (pET151_SphI) was verified by Sanger sequencing.

SphH. To amplify the coding sequence of the SphH_{Cterm}, the primer pair SphH_end_fw and SphH_end_dn was designed. Forward primer contains a 3' single strand end (CAAC) overhang which is identical to the 5' end of TOPO[®]-charged vector. pCC1FOS containing the complete siphonazole gene cluster was used as template for amplification of the target gene. Using *Pfu*-polymerase in the PCR reaction resulted in a blunt-ended fragment. The amplified fragment with the correct size of 1378 bp was extracted from the agarose gel. The yielded DNA was cloned into the pET-TOPO[®] vector by topoisomerase cloning. The ready construct of pET151 harboring SphH_{Cterm} was transferred to Top 10 chemically competent *E. coli* cells. The grown colonies on LB medium supplied with ampicillin were picked and inoculated in 3 mL liquid medium. Subsequently, plasmids were isolated from these cultures

and subjected to sequencing. The accurate construct (pET151-SphH_{Cterm}) was transferred to the expression host *E. coli* BAP1.

SphJ. The primer pair, *SphJ*-topo-Up and *SphJ*-topo-Down was used to amplify the SphJ-coding sequence. The resulting fragment (736 bp) was cloned in pET151 and used to transform *E. coli* XL1-Blue. The positive colony containing the accurate construct with the exact nucleotide sequence of *sphJ*, as deduced from the restriction pattern and the sequencing result, was selected for further experiments. The resulting construct pET151_SphJ was isolated from the corresponding colony and used to transform the expression host *E. coli* BL21 star.

Protein expression

A single colony of the respective cells, i.e. *E. coli* BL21 or *E. coli* BAP1, containing the desired construct was inoculated in 10 mL LB medium supplemented with the appropriate antibiotic. After 16 h this culture was used for inoculation of 1 L LB medium at 37°C on a shaker. Once the cells reached an OD₆₀₀ of ~0.4–0.6 the flask was cooled down to 16°C and protein expression was induced by adding IPTG (final concentration 0.4–0.5 mM); further incubation was performed at 16°C over night. Cells were harvested by centrifugation (4,000 rpm, 20 min, 4°C) and resuspended in lysis buffer (50 mM NaH₂PO₄, 300 mM NaCl, 10 mM imidazole, pH 8). After disruption of the cells by sonification and subsequent centrifugation (8,500 rpm, 20 min, 4°C) the supernatant was applied to Ni-NTA columns (equilibrated in lysis buffer). To increase the binding efficiency, the flow-through was re-loaded on the column at least three times. The column was washed twice with 2.5 ml washing buffers (50 mM NaH₂PO₄, 300 mM NaCl, pH 8) with 30 and 50 mM imidazole, respectively. Subsequently, the elution of the protein was performed in five elution steps using 500 µl elution buffer (50 mM NaH₂PO₄, 300 mM NaCl, pH 8) with 100, 150, 200, 300 and 300 mM imidazole, respectively. All collected fractions were analyzed by SDS-PAGE.

Heterologous expression and purification of SphB.

SphB was expressed in good amounts with an N-terminal his-tag and purified from BL21 *E. coli* cells (Figure S19). The visible band between 20 and 30 kDa is in accordance with the calculated mass of 28.95 kDa. Elution fractions 3 – 5 were pooled and used for subsequent assays. The soluble protein precipitated rapidly when exposed to low temperatures or during concentration procedures. Therefore, purification had to be carried out at room temperature and assays performed directly afterwards to avoid loss of activity.

Heterologous expression and purification of the SphC A domain.

The constructs were based on pET151 cloning vector and BL21 starTM expression cells were used. Using these constructs it was possible to generate soluble proteins (Figure S20).

Heterologous expression and purification of SphI.

After optimization, the strain containing the (pET151-SphI) construct was incubated at 16°C and induced with 0.4 mM IPTG at an OD₆₀₀ of 0.5 (Figure S9). The His-tagged protein (41.3 kDa) was purified by affinity chromatography using higher concentrations of imidazole in washing and elution steps.

Heterologous expression and purification of SphH_{Cterm}.

Heterologous expression of SphH_{Cterm} in the *apo*- as well as in the *holo*-form was performed in *E.coli* BL21 or *E.coli* BAP1, respectively. The desired proteins were overexpressed and purified from 1 L cultures. A prominent band corresponding to SphH_{Cterm} with the expected size of 53.5 kDa was enriched during purification (Figure S21).

Heterologous expression and purification of SphJ.

Expression and purification of recombinant SphJ was accomplished in an analogous way to SphH_{Cterm} expression. Analytic SDS-PAGE revealed a band in the elution fractions corresponding to the expected size of 31.2 kDa (Figure S22).

Protein assays

SphB-activity was observed by an *in vitro* methylation assay in 50 mM Tris-HCl buffer, pH 7.5. Reagents and protein solution were always prepared freshly and used directly. A typical reaction mixture (100 µL final volume) consisted of: SphB 25 µM, protocatechuic acid (substrate) 1 mM, *S*-adenosylmethionine 500 µM, MgCl₂ 10 mM, and 50 mM Tris/HCl (pH 7.5). Incubation was performed at 30°C. HPLC analysis of the methylation assay was carried out on a Merck-Hitachi system consisting of a D-6000A interface with an L-6200A Intelligent Pump, a Rheodyne 7725i injection system and an L-4500A diode array detector. Column was a Waters XTerra™ C18 (5 µm, 4.6 x 250 mm). The complete reaction mix was injected without further preparation and separated using a gradient of 0.1% TFA and acetonitrile as liquid phase in the following setup. Solvent A: H₂O with 0.1% TFA, solvent B: acetonitrile, gradient: from 90% A, 10% B in 20 min to 40% A, 60% B, with a flow rate of 1 mL/min.

SphC-activity was measured using an ATP-PP_i exchange assay. The assay used is based on the consumption of γ-¹⁸O₄-labelled ATP and the formation of ¹⁶O₄-ATP by an excess of unlabeled PP_i.^[31] In brief, 200 nM purified A domain (solved in 20 mM Tris-HCl (pH 7.5), 5% glycerol, 1mM DTT) was incubated with 1 mM γ-¹⁸O₄-ATP, 1mM substrate, 5 mM MgCl₂ and 5 mM PP_i in a reaction volume of 6 µL for 30 min at room temperature. The assay was stopped by the addition of 6 µL 9-aminoacridine in acetone (10 mg/mL). The subsequent analysis was performed by MALDI-TOF-MS. Therefore, the ratio of γ-¹⁶O₄-ATP (m/z=506) and the sum of all ATP species, including unlabeled, partially labeled, fully labeled (m/z=514), and monosodium-coordinated ions (m/z 506, 508, 510, 512, 514, 528, 530, 532,

534, and 536, respectively) was determined. The percent exchange was normalized with the following modifier: % exchange = $(100/0.833) \times {}^{16}\text{O}/({}^{18}\text{O}+{}^{16}\text{O})$.

SphI-activity was analyzed using a continuous spectrophotometric method. A typical reaction mixture consisted of the freshly purified enzyme, PEP (80 μM), erythrose-4-phosphate (350 μM), and MnSO_4 (100 μM) in 50 mM BTP buffer (pH 7). The sample was incubated in a quartz cuvette and the absorption was observed at 232 nm using a LAMBDA 40 UV/Vis Spectrophotometer (Perkin Elmer). One unit of enzyme activity was defined as consumption of 1 μmol PEP per minute.^[32] To get metal-free SphI, the enzyme was pre-treated with EDTA for 10 minutes prior reaction. The reaction was started by adding pre-treated SphI to the reaction mixture. The latter was supplemented with different divalent cations, *i.e.* Mg^{2+} , Zn^{2+} , Cu^{2+} , and Cd^{2+} , and Mn^{2+} (100 μM). Enzyme activity was monitored at room temperature as described before. To determine the effect of temperature on the enzymatic activity of SphI, the assay was incubated for 10 min at the respective temperature between 10°-70° C. Reactions were started by SphI-addition. To investigate the pH dependence of SphI, the pH of the buffer used was varied between pH 5-9. Further, the beforehand determined optimal conditions were used for kinetic studies of SphI. The concentration of E4P was varied (between 0.025 – 1 mM), whereas the PEP concentration was kept constantly (80 μM). The reaction mixtures containing 100 μM MnCl_2 were initiated by adding freshly purified enzyme and incubation was performed at 30° C. To determine K_m , V_{max} and K_{cat} various E4P concentrations (0.025-1.0 mM) and steady concentration of PEP (80 μM) were used. The values were calculated using double-reciprocal plots (software: Graf Pad Prism 5).

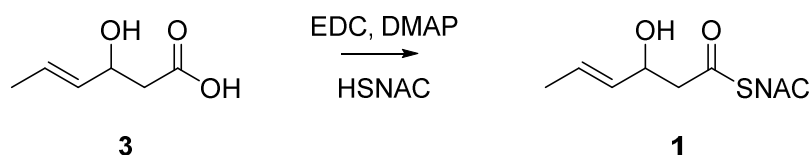
Anti-plasmodial assay

Antiplasmodial activity was determined against the NF54 strain of *Plasmodium falciparum*, using a modified [^3H] hypoxanthine incorporation assay.^[33] Briefly, infected human erythrocytes were exposed to serial drug dilutions in microtiter plates for 48 h at 37 °C in a gas mixture with reduced oxygen and elevated CO_2 . [^3H] hypoxanthine was added to each well and after further incubation for 24 h the wells were harvested on glass fiber filters and counted in a liquid scintillation counter. From the sigmoidal inhibition curve the IC_{50} value was calculated. Chloroquine was used as positive control in each test series.

General synthetic methods. Chemicals were obtained from Acros Organics (Geel, Belgium) or Sigma Aldrich Chemie GmbH (Steinheim, Germany) and used without purification. All reactions were performed under argon atmosphere in dried reaction vessels. Solvents were purified by distillation and dried according to standard methods. Thin-layer chromatography was performed with 0.2 mm precoated plastic sheets Polygram® Sil G/UV254 (Machery-Nagel). Column chromatography was carried out using Merck silica gel 60 (70-200 mesh). ^1H

NMR and ^{13}C NMR spectra were recorded on Bruker Avance DMX-500 (500 MHz), Bruker Avance DPX-400 (400 MHz) spectrometers, and were referenced against solvent signals (^1H NMR: (^2H)dichloromethane $\delta = 5.32$ ppm; ^{13}C NMR: (^2H)dichloromethane $\delta = 53.84$ ppm). GC-MS analyses of synthetic compounds were carried out with a 7890B gas chromatograph connected to a 5977A inert mass detector (Agilent) fitted with a HP5-MS fused silica capillary column (30 m, 0.25 mm i. d., 0.25 μm film). Instrumental parameters were (1) inlet pressure, 77.1 kPa, He 23.3 mL min^{-1} , (2) injection volume, 1 μL , (3) transfer line, 250 $^\circ\text{C}$, and (4) electron energy 70 eV. The GC was programmed as follows: 5 min at 50 $^\circ\text{C}$ increasing at 10 $^\circ\text{C min}^{-1}$ to 320 $^\circ\text{C}$, and operated in split mode (50:1, 60 s valve time). The carrier gas was He at 1 mL min^{-1} . Retention indices (*I*) were determined from a homologous series of n-alkanes (C8-C38).

Synthesis of (*E*)-*S*-(2-acetamidoethyl) 3-hydroxyhex-4-enethioate (**1**).

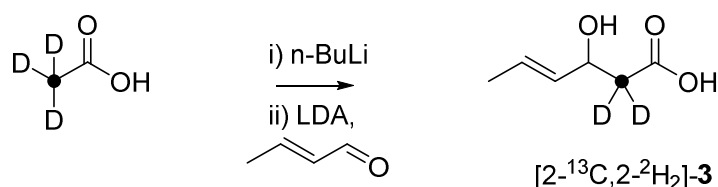


Acid **3** (105 mg, 0.81 mmol, 1 eq) was dissolved in 3 mL absolute DCM and HSNAC (115 mg, 0.97 mmol, 1.2 eq) was added. Afterwards EDC·HCl (186 mg, 0.97 mmol, 1.2 eq) and DMAP (22 mg, 0.18 mmol, 0.2 eq) were added and the reaction was stirred for 1h at room temperature. The solvent was removed under reduced pressure and the crude material was purified by HPLC (KNAUER Eurospher II 100-5 C18A; 5 μm ; 250 x 16 mm, MeCN/ H_2O , v/v 20:80, $R_t = 6.02$ min). Thioester **1** (142 mg, 0.62 mmol, 70%) was obtained as a colorless liquid. As a side product, the SNAC ester of sorbic acid (**2**) was isolated (6 mg, 0.03 mmol, 4%).

Analytical data for **1**: ^1H -NMR (400 MHz, [$^2\text{H}_2$]-DCM): $\delta = 5.88$ (s br, 1H, NH), 5.73 (dq, $^3J(\text{H,H}) = 15.3$ Hz, $^3J(\text{H,H}) = 6.5$ Hz, $^4J(\text{H,H}) = 1.1$ Hz, 1H, CH), 5.49 (ddq, $^3J(\text{H,H}) = 15.3$ Hz, $^3J(\text{H,H}) = 6.3$ Hz, $^4J(\text{H,H}) = 1.6$ Hz, 1H, CH), 4.51 (dt, $^3J(\text{H,H}) = 6.2$ Hz, $^3J(\text{H,H}) = 6.3$ Hz, 1H, CH), 3.39 (m, 2H, CH_2), 3.02 (m, 2H, CH_2), 2.75 (d, $^3J(\text{H,H}) = 6.3$ Hz, 2H, CH_2), 2.60 (s br, 1H, OH), 1.91 (s, 3H, CH_3), 1.69 (m, 3H, CH_3) ppm. ^{13}C -NMR (100 MHz, [$^2\text{H}_2$]-DCM): $\delta = 198.8$ (s, C_q), 170.5 (s, C_q), 132.4 (s, CH), 127.7 (s, CH), 69.9 (s, CH), 51.6 (s, CH_2), 39.5 (s, CH_2), 29.3 (s, CH_2), 23.3 (s, CH_3), 17.8 (s, CH_3) ppm. IR (ATR): $\tilde{\nu} = 3433, 3269, 3087, 2945, 2856, 1684, 1618, 1556, 1431, 1299, 1120, 1054, 924, 867, 763, 628, 609$ cm^{-1} . HR MS (ESI $^+$): calcd. for $\text{C}_{10}\text{H}_{17}\text{NNaO}_3\text{S}^+$ [M-Na^+] 254.0821, found 254.0821.

Analytical data for **2**: $^1\text{H-NMR}$ (400 MHz, $[\text{D}_2\text{H}_2]\text{-DCM}$): $\delta = 7.21$ (dd, $^3J(\text{H,H}) = 10.4$ Hz, $^3J(\text{H,H}) = 15.2$ Hz, 1H, CH), 6.26 (dq, $^3J(\text{H,H}) = 6.5$ Hz, $^3J(\text{H,H}) = 15.0$ Hz, 1H, CH), 6.18 (dd, $^3J(\text{H,H}) = 10.5$ Hz, $^3J(\text{H,H}) = 15.0$ Hz, 1H, CH), 6.10 (d, $^3J(\text{H,H}) = 15.2$ Hz, 1H, CH), 5.88 (s br, 1H, NH), 3.40 (dt, $^3J(\text{H,H}) = 6.3$ Hz, $^3J(\text{H,H}) = 6.4$ Hz, 2H, CH_2), 3.07 (t, $^3J(\text{H,H}) = 6.4$ Hz, 2H, CH_2), 1.90 (s, 3H, CH_3), 1.87 (d, $^3J(\text{H,H}) = 6.3$ Hz, 3H, CH_3) ppm. $^{13}\text{C-NMR}$ (100 MHz, $[\text{D}_2\text{H}_2]\text{-DCM}$): $\delta = 190.4$ (C_q), 170.4 (C_q), 142.5 (CH), 142.1 (CH), 130.0 (CH), 126.2 (CH), 40.2 (CH_2), 29.0 (CH_2), 23.5 (CH_3), 19.2 (CH_3) ppm. MS (EI, 70 eV): m/z (%) = 213 (<1), 185 (4), 154 (4), 127 (7), 95 (100), 67 (41), 43 (32). GC (HP-5MS): $I = 1939$.

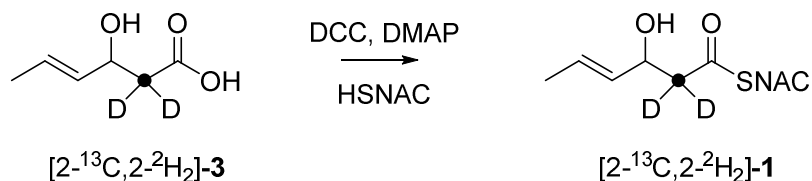
Synthesis of $[(2\text{-}^{13}\text{C}, 2, 2\text{-}^2\text{H}_2)\text{-(E)-3-hydroxyhex-4-enoic acid } (2\text{-}^{13}\text{C}, 2, 2\text{-}^2\text{H}_2)\text{-3}]^{\text{[1]}}$



(2- ^{13}C , 2, 2, 2- $^2\text{H}_3$)acetic acid (0.10 g, 1.56 mmol, 1 eq) was dissolved in 1.5 mL of absolute THF and cooled to -78°C under argon atmosphere. n-butyllithium (1.6M in hexane, 0.98 mL, 1.56 mmol, 1 eq) was added dropwise by use of a syringe pump. The reaction was stirred for 1h at -78°C and then warmed to 0°C . Freshly prepared LDA solution (2M in THF, 0.94 mL, 1.87 mmol, 1.2 eq) was added dropwise and after stirring for 10 minutes the reaction was warmed to 45°C for 1h. After cooling to -78°C , crotonaldehyde (0.13 g, 1.87 mmol, 1.2 eq) was added dropwise as a THF solution (10M). After stirring for 2h at -78°C the reaction was quenched with water, warmed to room temperature and acidified with 2M HCl. The aqueous phase was extracted three times with ethyl acetate and the combined organic phases were dried over MgSO_4 . The solvent was removed under reduced pressure and the product isolated as colorless, waxy oil (0.37g, 2.84 mmol, 85%).

$^1\text{H-NMR}$ (400 MHz, $\text{C}^2\text{H}_2\text{Cl}_2$): $\delta = 5.75$ (dq, $^3J(\text{H,H}) = 15.3$ Hz, $^3J(\text{H,H}) = 6.5$ Hz, 1H, CH), 5.52 (m, 1H, CH), 4.47 (d, $^3J(\text{H,H}) = 6.3$ Hz, 1H, CH), 1.70 (d, $^3J(\text{H,H}) = 6.5$ Hz, 3H, CH_3) ppm. $^{13}\text{C-NMR}$ (100 MHz, $\text{C}^2\text{H}_2\text{Cl}_2$): $\delta = 176.9$ (d, $^1J(\text{C,C}) = 54.1$ Hz, C_q), 132.0 (CH), 128.2 (d, $J(\text{C,C}) = 3.3$ Hz, CH), 69.1 (d, $^1J(\text{C,C}) = 37.7$ Hz, CH), 41.2 (quin, $^1J(\text{C},^2\text{H}) = 19.8$ Hz, C^2H_2), 17.8 (CH_3) ppm. IR (ATR): $\tilde{\nu} = 3430$ (br), 3015, 2970, 2920, 2641, 1736, 1712, 1438, 1367, 1258, 1229, 1217, 1130, 1073, 1010, 963, 920, 826, 798, 764, 660, 566, 517, 490 cm^{-1} . HR MS (ESI): calcd. for $^{13}\text{CC}_5^2\text{H}_2\text{H}_7\text{O}_3^-$ $[\text{M-H}]^-$ 132.0716, found 132.0730.

Synthesis of (2-¹³C,2,2-²H₂)-(E)-S-(2-acetamidoethyl) 3-hydroxyhex-4-enethioate ((2-¹³C,2,2-²H₂)-1).



(2-¹³C,2,2-²H₂)-**3** (85 mg, 0.64 mmol, 1 eq) was dissolved in 2 mL absolute DCM and HSNAC (91 mg, 0.77 mmol, 1.2 eq) was added. Afterwards DCC (158 mg, 0.77 mmol, 1.2 eq) and DMAP (16 mg, 0.13 mmol, 0.2 eq) were added and the reaction was stirred for 1h at room temperature. After filtration the solvent was removed under reduced pressure and the crude material was purified by HPLC (KNAUER Eurospher II 100-5 C18A; 5 μm; 250 x 16 mm, MeCN/H₂O, v/v 20:80, R_t = 6.02 min). The product **1** (70 mg, 0.3 mmol, 47%) was obtained as a colorless liquid.

¹H-NMR (400 MHz, C²H₂Cl₂): δ = 5.97 (s br, 1H, NH), 5.76 (dddq, ³J(H,H) = 15.3 Hz, ³J(H,H) = 6.5 Hz, ⁴J(H,C) = 1.1 Hz, ⁴J(H,H) = 1.1 Hz, 1H, CH), 5.53 (dddq, ³J(H,H) = 15.3 Hz, ⁴J(H,H) = 1.6 Hz, ⁴J(H,C) = 2.2 Hz, ³J(H,H) = 6.3 Hz, 1H, CH), 4.53 (d, ³J(H,H) = 6.3 Hz, 1H, CH), 3.43 (m, 2H, CH₂), 3.05 (m, 2H, CH₂), 1.95 (s, 3H, CH₃), 1.72 (m, 3H, CH₃) ppm. ¹³C-NMR (100 MHz, C²H₂Cl₂): δ = 198.8 (C_q), 170.6 (C_q), 132.4 (CH), 127.7 (d, ³J(C,C) = 3.3 Hz, CH), 69.8 (d, ¹J(H,H) = 36.5 Hz, CH), 51.0 (quin, ¹J(C,²H) = 19.8 Hz, CH₂), 39.5 (CH₂), 29.2 (CH₂), 23.3 (CH₃), 17.8 (CH₃) ppm. Degree of deuteration: 84 %. IR (ATR): $\tilde{\nu}$ = 3434, 3270, 3086, 2968, 2943, 2855, 1680, 1621, 1555, 1374, 1300, 1268, 1237, 1202, 1142, 1085, 1032, 1006, 971, 939, 892, 848, 763, 752, 731, 634, 543, 505, 479 cm⁻¹. HR MS (ESI⁺): calcd. for ¹³CC₉²H₂H₁₅NNaO₃S⁺ [M-Na⁺] 257.0980, found 257.0982.

SPME sampling. Substrate mimics **1**, **2**, **3** and [2-¹³C,2,2-²H₂]-**1** (c=0.09 mg/μL) were incubated with the respective enzymes for 1h at 30°C in a closed reaction tube furnished with a septum. The SPME assembly needle (d_f = 75 μm, Carboxen/Polydimethylsiloxane, fused silica, 24Ga, 3pk) was placed through the septum above the reaction headspace for the complete reaction time and was directly analyzed by GC-MS. The GC-MS parameters were as follows: 7890B gas chromatograph connected to a 5977A inert mass detector (Agilent) fitted with a HP5-MS fused silica capillary column (30 m, 0.25 mm i. d., 0.25 μm film). Instrumental parameters were (1) inlet pressure, 77.1 kPa, He 23.3 mL min⁻¹, (2) transfer line, 250 °C, and (3) electron energy 70 eV. The GC was programmed as follows: 5 min at 25 °C increasing at 1 °C min⁻¹ to 30 °C, followed by increasing at 10 °C min⁻¹ to 80 °C and operated in split mode (10:1 or 100:1, 60 s valve time). The carrier gas was He at 1 mL min⁻¹.

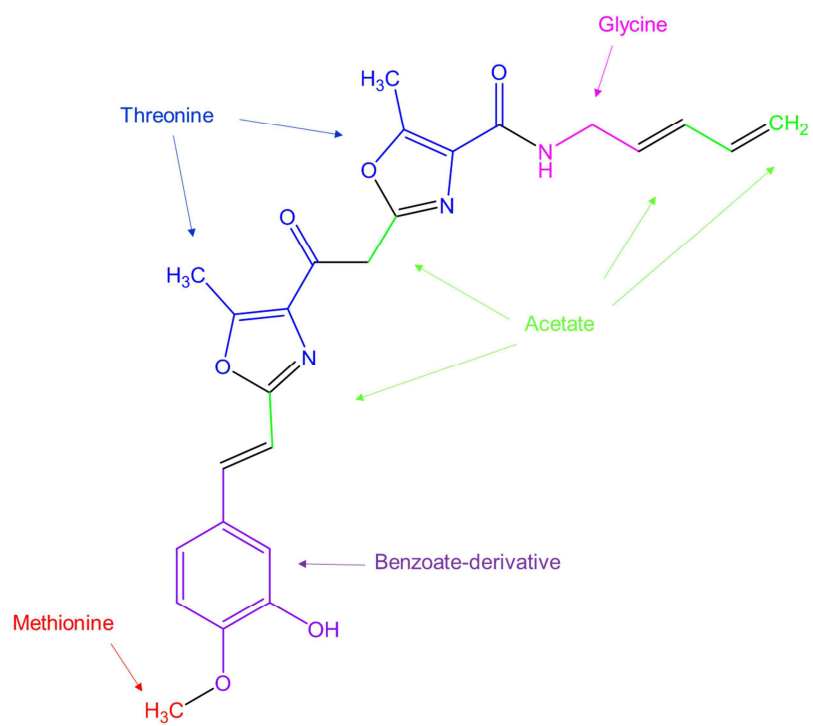


Figure S1. Molecular structure of siphonazole and its deduced building blocks.

Origins of building blocks are marked according to feeding experiments.

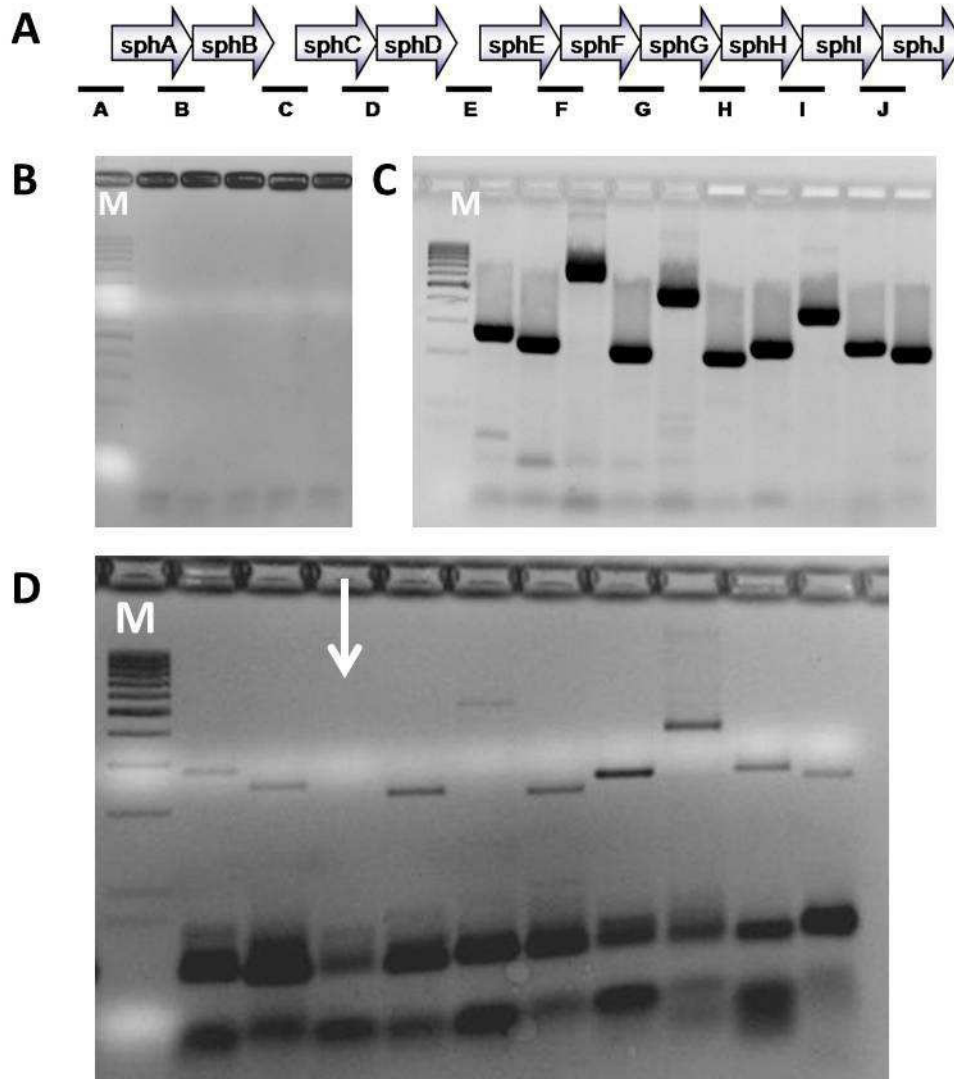


Figure S2. Test PCRs for RNA expression analysis.

A) Schematic representation of PCR probes; B) PCR from isolated mRNA from days 1, 2, 3, 4 and 7 with primer pair gap1; M, marker; C) PCRs from fosmid DNA; D) RT-PCR from RNA; In C and D the fragments are loaded in alphabetical order; The white arrow highlights the missing amplificate of the intergenic region between *sphB* and *sphC*. This finding suggests that two transcriptionally coupled units exist, i.e. *sphA-sphB*, and *sphC-sphJ*.

Motif 1										
SphA	G	H	S	V	G	90				
BaeE	G	H	S	L	G	87				
PksE	G	H	S	L	G	92				
DfnA	G	H	S	L	G	89				
ChiA	G	H	S	L	G	89				

Motif 2						Motif 3						
SphA	Q	T	Q	Y	T	Q	60	G	A	F	H	193
BaeE	Q	T	Q	F	T	Q	56	G	A	F	H	191
PksE	Q	T	Q	Y	T	Q	61	G	A	F	H	196
DfnA	K	T	Q	F	T	Q	58	G	A	F	H	192
ChiA	Q	T	Q	Y	T	Q	58	G	A	F	H	192

Figure S3. Multiple sequence alignment of the acyltransferase SphA.

Residues corresponding to the consensus motifs are coloured yellow; reference sequences were taken from the biosynthesis of bacillaene (BaeE, YP_001421287), difficidin (DfnA, YP_001421800) and similar proteins from *Paenibacillus mucilaginosus* (PksE, YP_004640302) and *Pseudomonas fluorescens* (ChiA, AAM12912).

	Motif 1						Motif 2					Motif 3				
KS2	G	P	(X) ₇	C	S	S	17	H	G	T	G	T	302	G	H	341
KS3	G	P	(X) ₇	C	S	S	17	H	G	T	G	T	303	G	H	344
KS5	G	P	(X) ₇	C	S	S	17	A	A	T	G	S	303	G	H	340
KS6	G	P	(X) ₇	C	S	S	17	H	G	T	G	T	305	G	H	343
KS7	G	P	(X) ₇	C	S	S	17	Q	G	T	G	T	302	G	H	341
KS9	G	P	(X) ₇	C	S	S	17	A	A	N	G	T	304	G	H	342
KS11	G	P	(X) ₇	C	S	S	17	H	G	T	G	T	300	G	H	344
KS12	G	P	(X) ₇	C	S	S	17	H	G	T	G	T	302	G	H	340

Figure S4. Multiple sequence alignment of the KS domains.

Highly conserved residues are coloured yellow; residues of the catalytic triad are coloured green; deviations in the catalytic core are printed in red. The numbering corresponds to the module in which the domains are located.

ACP1	E	L	G	F	D	S	V	32
ACP1 ₂	E	L	G	F	D	S	V	32
ACP2	E	F	G	L	D	S	I	32
ACP5	I	Y	G	I	N	S	Q	32
ACP6	E	Y	G	F	D	A	I	32
ACP6 ₂	E	Y	G	F	D	S	V	32
ACP7	N	Y	G	I	D	S	V	32
ACP9	R	Y	G	F	N	S	L	32
ACP10	N	Y	G	F	D	S	I	32
ACP11	S	Y	G	V	D	S	V	32
ACP12	E	Y	G	L	D	A	P	32
ACP12 ₂	N	Y	G	V	D	S	L	32

PCP3	A	Y	G	L	D	S	I	32
PCP4	S	A	G	A	T	S	L	30
PCP4 ₂	S	A	G	A	T	S	L	30
PCP8	S	A	G	A	T	S	L	30
PCP8 ₂	S	A	G	A	T	S	L	30

Figure S5. Multiple sequence alignment of the ACP and PCP domains

Residues corresponding to the consensus motifs are coloured yellow; the essential serine moiety is coloured green; deviations in this location are printed in red.

NADPH-binding motif

KR2	G	L	G	G	V	G	L	L	C	A	1889
KR11	G	K	G	A	L	G	A	I	F	A	166
KR12	G	A	G	N	V	G	F	K	L	C	504
<i>A.var.</i>	G	T	S	A	V	G	T	E	I	A	1220
PksM	G	A	G	Y	I	G	E	A	W	S	1540
<i>H.che.</i>	G	L	G	K	I	G	L	A	L	A	1125

Catalytic Core

KR2	K [23]	S [12]	Y	G	Y	A	N	2024
KR11	K [23]	S [12]	Y	A	Y	A	N	297
KR12	K [23]	S [12]	Y	A	A	G	C	639
<i>A.var.</i>	K [23]	S [14]	Y	A	A	A	N	1373
PksM	K [23]	S [12]	Y	A	S	G	C	1675
<i>H.che.</i>	K [23]	S [12]	Y	A	A	A	N	1347

Figure S6. Multiple sequence alignment of the KR domains

Residues corresponding to the consensus motif are highlighted in yellow; catalytic residues are highlighted in green, deviations in these locations are printed in red; reference sequences were taken from similar proteins from *Anabaena variabilis* (*A.var.*, YP_324485), *Bacillus subtilis* (PksM, P40872) and *Hahella chejuensis* (*H.che.*, YP_434161).

DH2	H	R	W	E	G	Q	A	L	L	P	40
DH11	H	I	V	Q	G	Q	R	V	L	P	40
DH12	Y	Q	V	A	D	S	Q	R	L	P	43
SorB	H	R	V	L	D	M	H	L	L	P	33
Ery chain A	H	V	V	G	G	R	T	L	V	P	42
<i>Beggiatoa</i>	H	V	V	G	S	Q	K	T	L	P	39

Figure S7. Multiple sequence alignment of the DH domains

Residues corresponding to the consensus motif are coloured yellow; catalytic residues are coloured green, deviations in these locations are printed in red; reference sequences were taken from the biosynthesis of sorangicin (SorB, ADN68477), erythromycin (Ery chain A, 3EL6_A) and a similar protein from *Beggiatoa* sp. SS (*Beggiatoa*, ZP_01997443).

SphJ	F	G	H	S	L	G	89	S	G	P	H	199
GrsT	L	G	H	S	M	G	97	P	G	D	H	212
RifR	F	G	H	S	M	G	96	P	G	G	H	214
PikAV	F	G	H	S	L	G	101	S	G	G	H	215

Figure S8. Multiple sequence alignment of the thioesterase SphJ with the sequence of type II TEs associated with bacterial PKSs, NRPSs.

Residues corresponding to the consensus motif are coloured yellow; catalytic residues are coloured green; the hydrolase signature sequence (G-X-S-X-G) of SphJ matches to the conserved sequence of type II TEs (G-H-S-M-G), while while the Met residue in the signature sequence of SphJ and TE PikAV are replaced by Leu. Reference sequences were taken from the biosynthesis of rifamycin (*A. mediterranei*, AAG52991), gramicidin (*B. brevis*, AAA58717) and pikromycin (*S. venezuelae*, AAC69333).^[36]

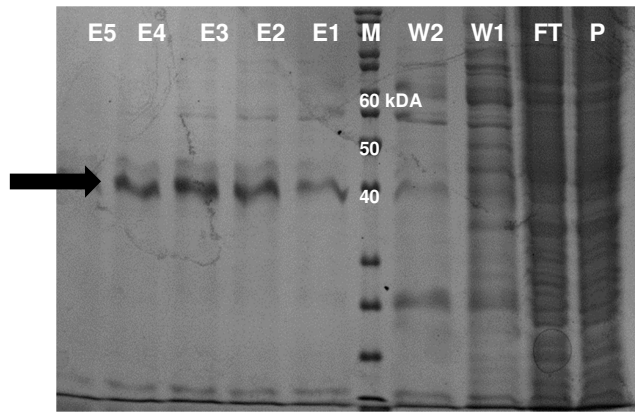


Figure S9. SDS-PAGEs of a typical SphI purification by affinity-chromatography on a Ni-NTA column

FT: flow through; W1 and W2, (washing steps with 50 and 100 mM imidazole, respectively); E1–E5, elution fractions; M, marker; P: pellet. The black arrow indicates SphI (calculated mass of 41.3 kDa).

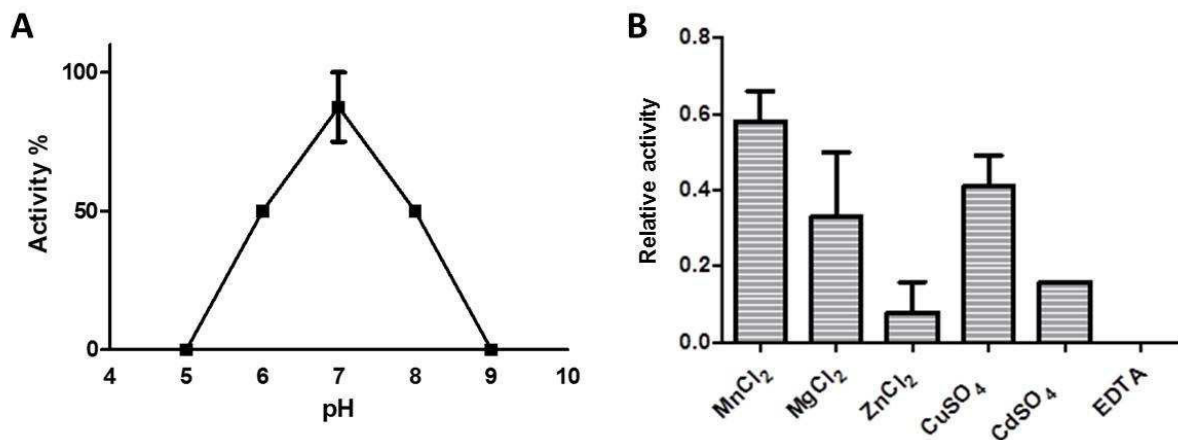


Figure S10. A) pH dependency; B) metal requirements of SphI

The enzymatic activity was determined between pH 5-9. The mean value of two independent enzyme purifications is given; error bar indicates standard deviation.

Disappearance of PEP in the reaction mixture containing 80 μ M PEP, 350 μ M E4P, 100 μ M MnSO₄ and BTP buffer (pH 5-9) were observed by adding SphI at room temperature and the values were recorded 30 minutes after reaction start. 100% activity are equivalent to a consumption of 80 μ M PEP in 30 minutes. To investigate the metal dependence of SphI, the reaction was started by adding SphI to the mixture (80 μ M PEP, 350 μ M E4P, EDTA 100 μ M or divalent cations, 50 mM BTP buffer; pH 7). Divalent cations tested: Cd²⁺, Cu²⁺, Mg²⁺, Mn²⁺ and Zn²⁺ (100 μ M).

Motif1 (VIL)-(LV)-(DE)-(IV)-G-(GC)-G-(TP)-G
 Motif2 (PG)-(QT)-(FYA)-D-A-(IVY)-(FI)-(CVL)
 Motif3 L-L-(RK)-P-G-G-(RIL)-(LI)-(LFIV)-(IL)

	Motif 1								Motif 2										
SphB	M	L	E	I	G	T	F	T	G	72	N	Y	F	D	F	V	Y	I	142
<i>N. punct.</i>	T	L	E	V	G	V	F	T	G	72	E	T	F	D	F	A	F	I	142
<i>R. brookii</i>	T	L	D	I	G	V	F	T	G	72	E	T	F	D	F	A	F	I	142
<i>B. cereus</i>	V	L	E	V	G	T	F	T	G	76	N	I	F	D	F	I	F	I	146

Motif 3

SphB	L	V	R	P	G	G	I	I	G	I	168
<i>N. punct.</i>	L	L	R	P	G	G	L	I	A	I	168
<i>R. brookii</i>	L	I	R	S	G	G	L	I	A	V	168
<i>B. cereus</i>	L	I	R	P	G	G	I	V	A	V	172

Figure S11. Signature motifs and multiple sequence alignment of SphB.

Residues corresponding to the consensus motifs are coloured yellow; reference sequences were taken from similar proteins from *Nostoc punctiforme* (*N. punct.*, YP_001867016), *Raphidiopsis brookii* D9 (*R. brookii*, ZP_06306391) and *Bacillus cereus* BGSC 6E1 (*B. cereus*, EEK53069).

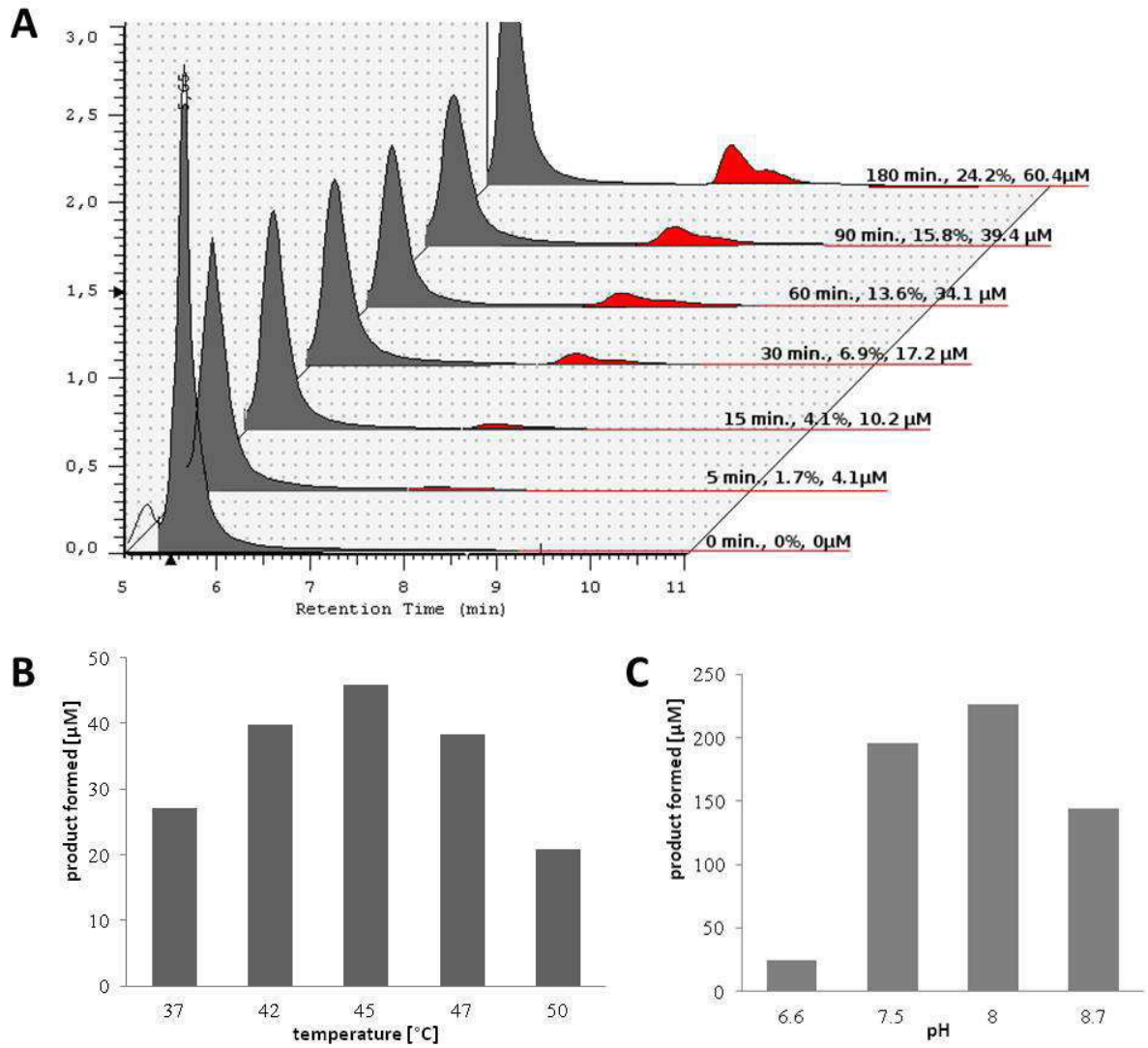


Figure S12. Methylation activity of SphB

A) Time course of a methylation assay. The grey peak represents the substrate protocatechuic acid and the red peak the product isovanillic acid, respectively. B) Optimal temperature of SphB. C) pH dependency of SphB.

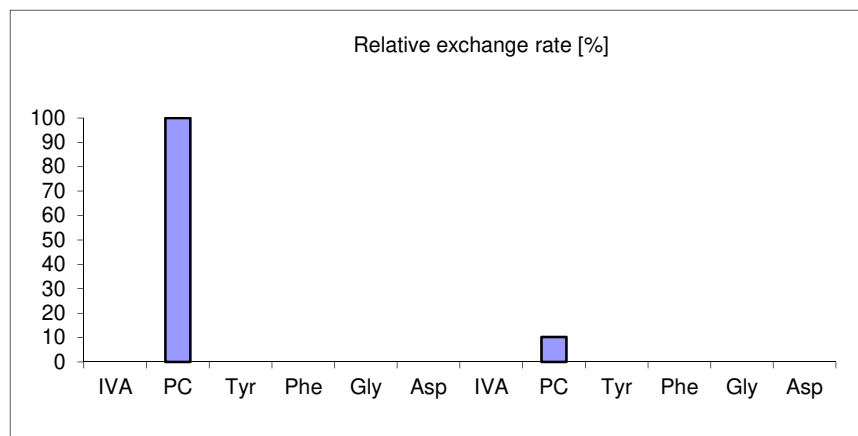


Figure S13. Results of the ATP-PP_i exchange assay

The best conversion was set to 100%. The first six rows show the result for the tridomain A1-PCP1-PCP1₂, while the next rows show the result for the didomain A1-PCP1. IVA, isovanillic acid; PC, protocatechuic acid.

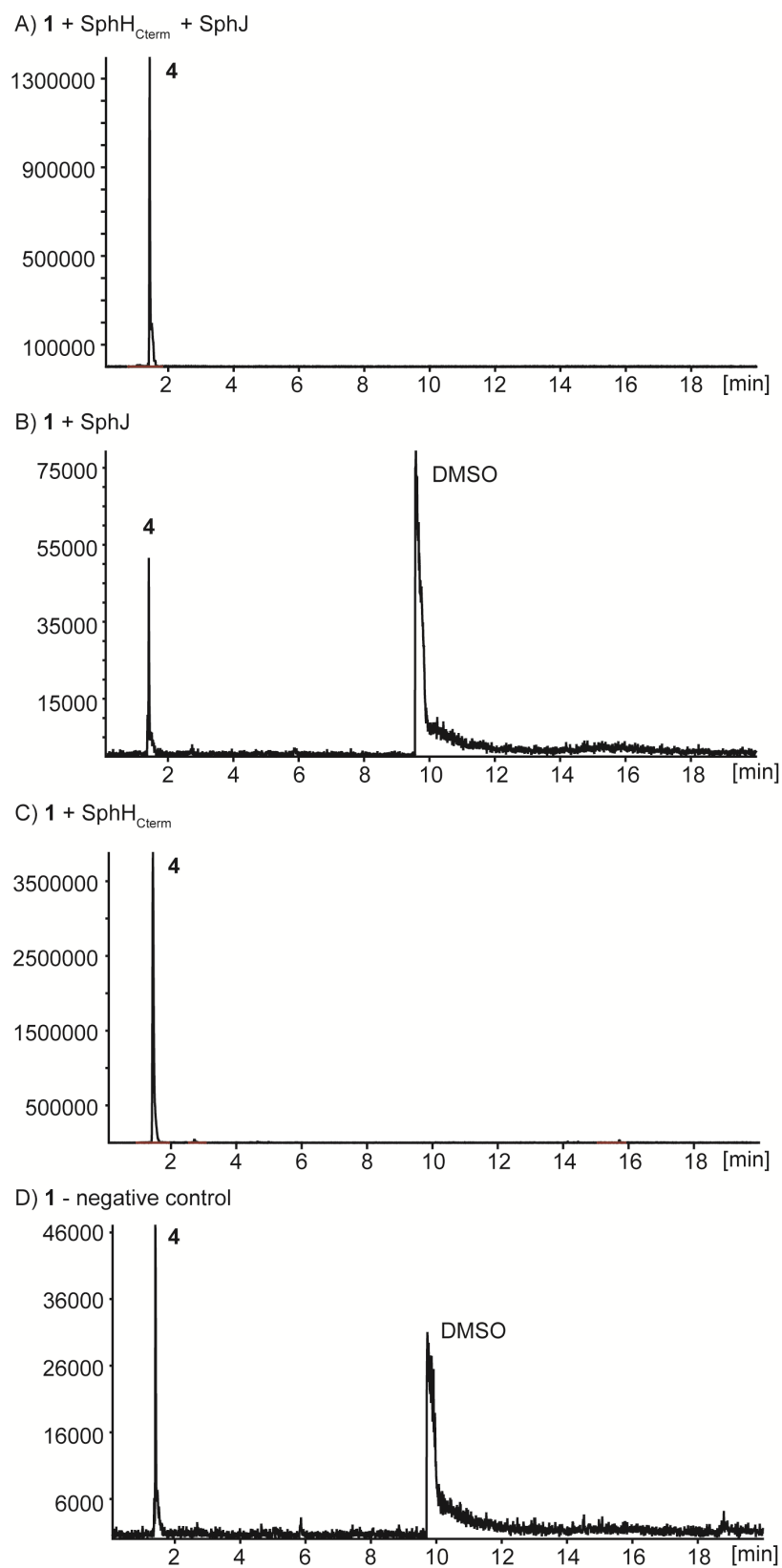
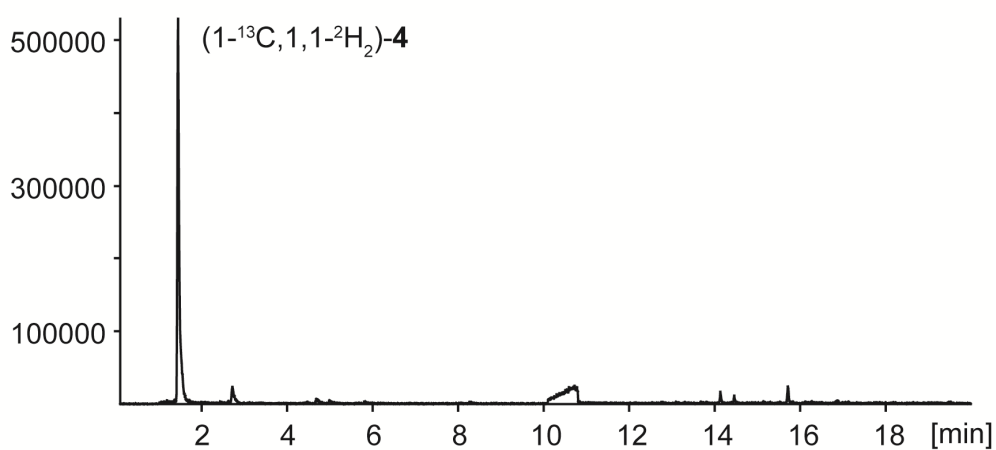


Figure S14. Extracted ion chromatograms of the base peak ion of pentadiene **4** (m/z 67) for *in vitro* experiments with substrate mimic **1**. The relative intensities for experiments A – D are directly comparable.

A) $(2\text{-}^{13}\text{C}, 2, 2\text{-}^2\text{H}_2)\text{-1}$ + SphH_{Cterm}



B) $(2\text{-}^{13}\text{C}, 2, 2\text{-}^2\text{H}_2)\text{-1}$ - negative control

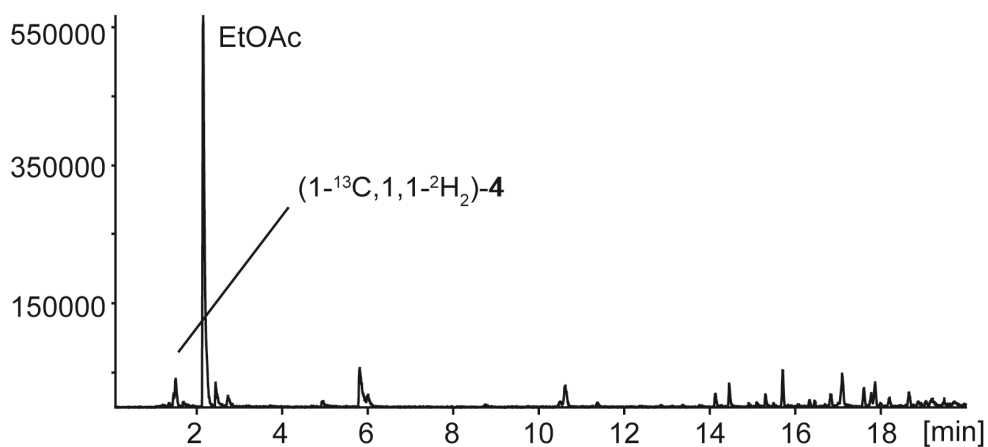


Figure S15. Extracted ion chromatograms of the base peak ion of labelled pentadiene $(1\text{-}^{13}\text{C}, 1, 1\text{-}^2\text{H}_2)\text{-4}$ (m/z 70) of *in vitro* experiments with substrate mimic $(2\text{-}^{13}\text{C}, 2, 2\text{-}^2\text{H}_2)\text{-1}$. The relative intensities for experiments A and B are directly comparable.

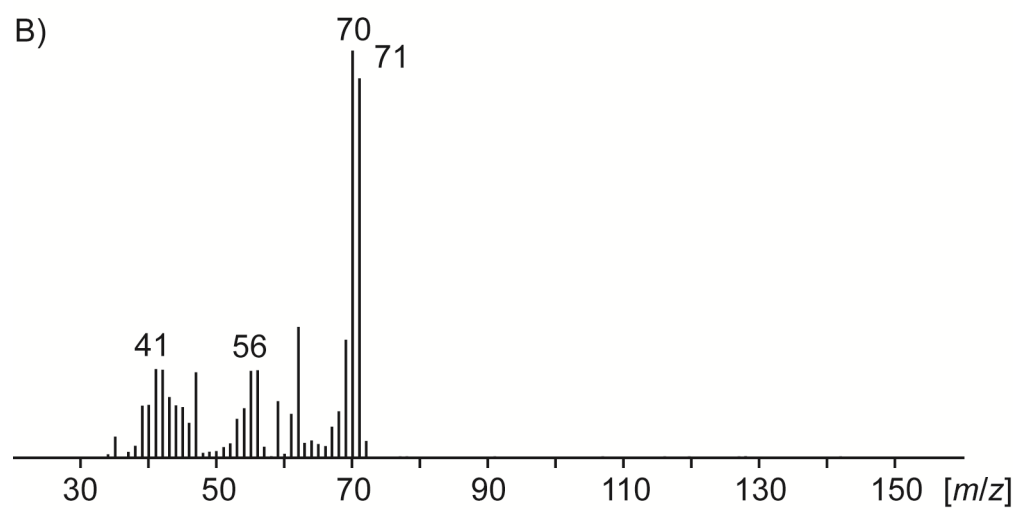
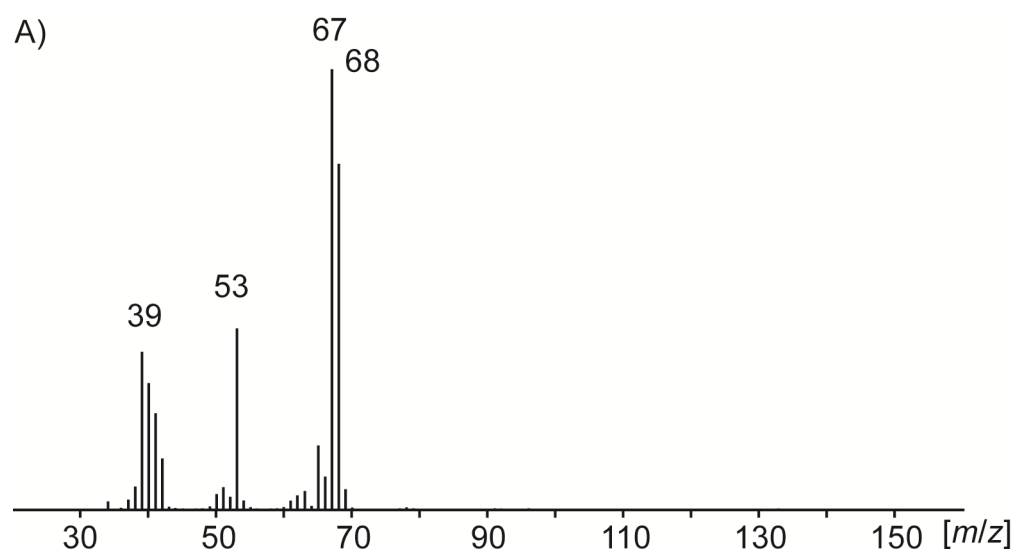


Figure S16. Mass spectrum of A) 1,3-pentadiene **4** and B) of labelled pentadiene ($1\text{-}^{13}\text{C}, 1,1\text{-}^2\text{H}_2$)-**4** obtained by incubation of ($2\text{-}^{13}\text{C}, 2,2\text{-}^2\text{H}_2$)-**1** with SphH_{Cterm} (B).

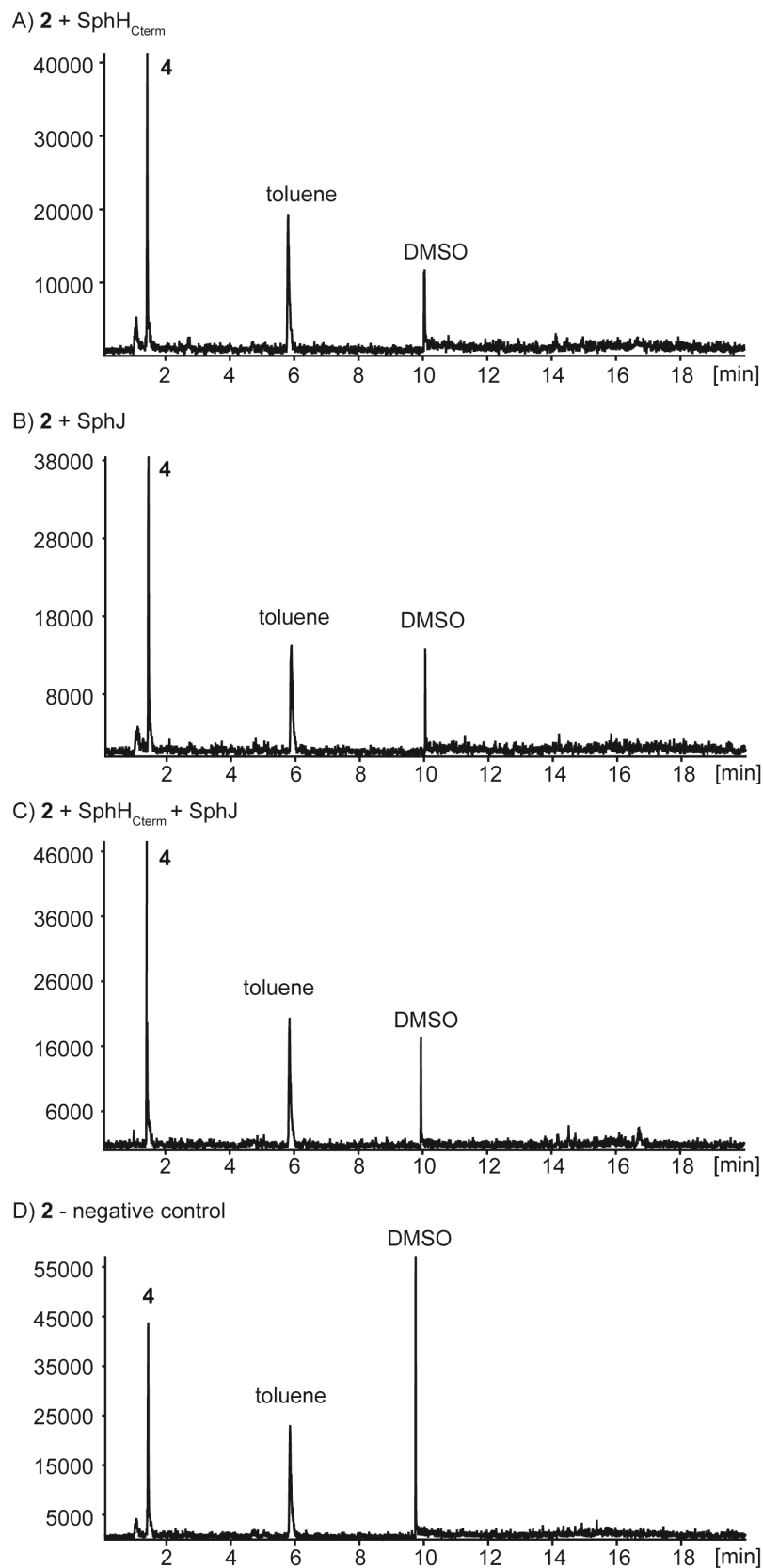
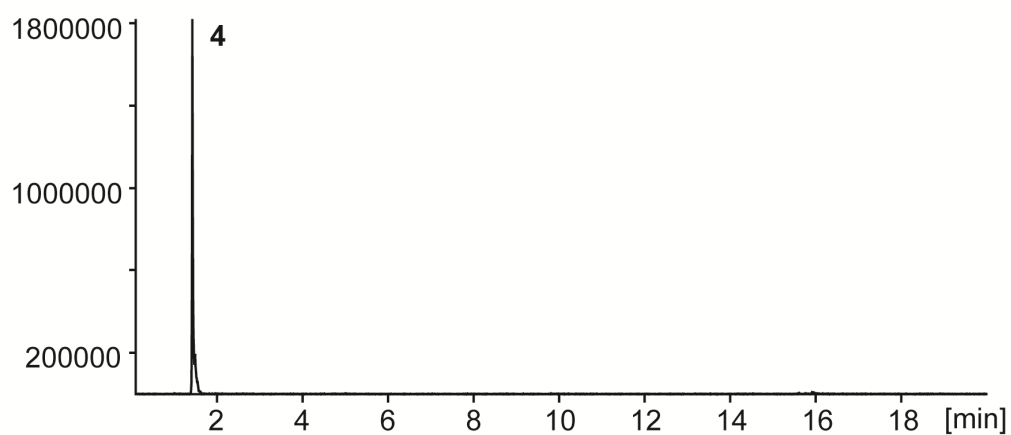


Figure S17. Extracted ion chromatograms of the base peak ion of pentadiene **4** (m/z 67) for *in vitro* experiments with substrate mimic **2**. The relative intensities for experiments A – D are directly comparable.

A) **3** + SphH_{Cterm}



B) **3** - negative control

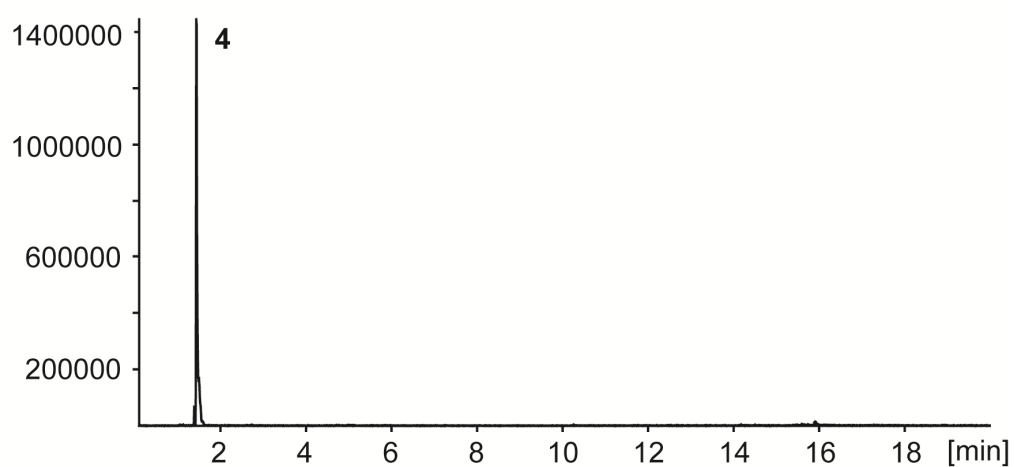


Figure S18. Extracted ion chromatograms of the base peak ion of pentadiene **4** (m/z 67) for *in vitro* experiments with substrate mimic **3**. The relative intensities for experiments A and B are directly comparable.

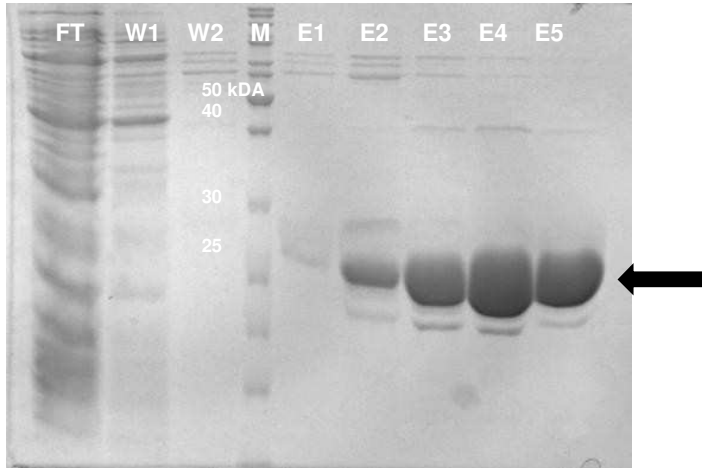


Figure S19. SDS-PAGE of a typical purification of SphB by affinity-chromatography on Ni-NTA column.

Protein gel shows fraction from the purification; Ft, flow through; W1, wash1 (20 mM imidazole); W2, wash2 (40 mM imidazole); E1 – E5, elution fractions with 100 to 300 mM imidazole; M, size marker. Black arrow indicates SphB (calculated mass of 28.9 kDa).

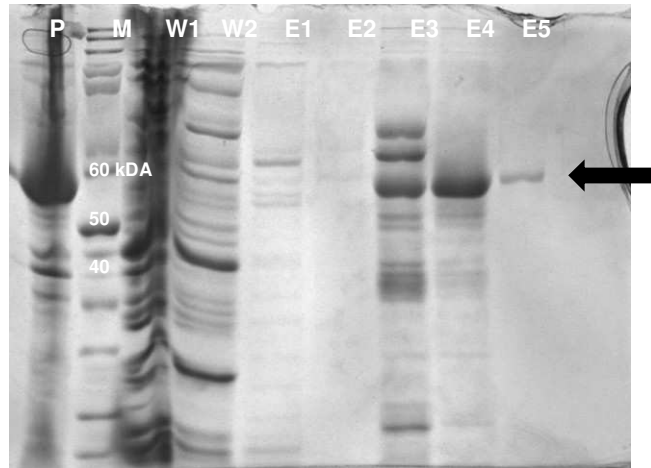


Figure S20. SDS-PAGE of a typical purification of SphC by affinity-chromatography on Ni-NTA column.

Protein gel shows fraction from the purification; W1, wash1 (20 mM imidazole); W2, wash2 (40 mM imidazole); E1 – E5, elution fractions with 100 to 300 mM imidazole; M, marker. Black arrow indicates calculated mass of 58,1 kDa for the SphC.

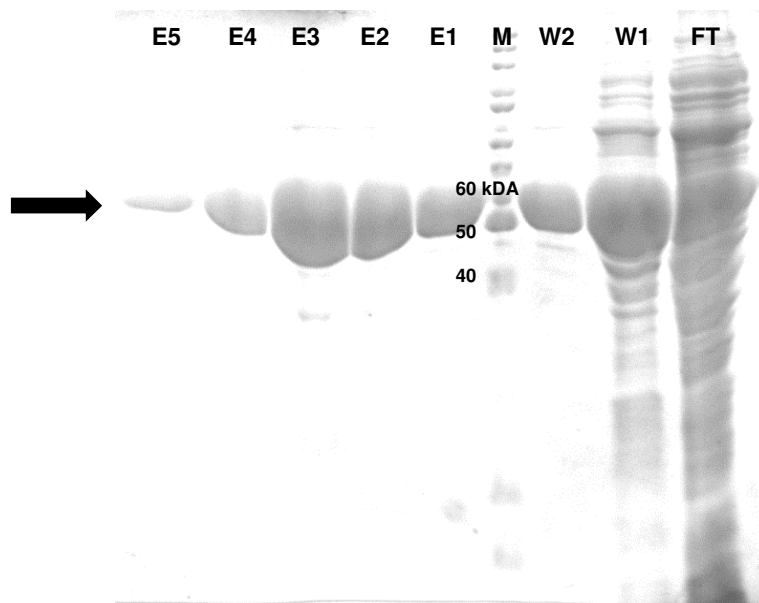


Figure S21. SDS-PAGE of a typical purification of SphH_{Cterm} by affinity-chromatography on a Ni-NTA column.

FT, flow through; W1 and W2, (washing steps with 30 and 50 mM imidazole, respectively); E1–E5, elution fractions (100-350 mM imidazole) once at 100 mM, once at 150 mM, once at 200 mM, and twice at 300 mM).; M, marker. Black arrow indicates calculated mass of 53.5 kDa for the SphH Hyd-ACP.

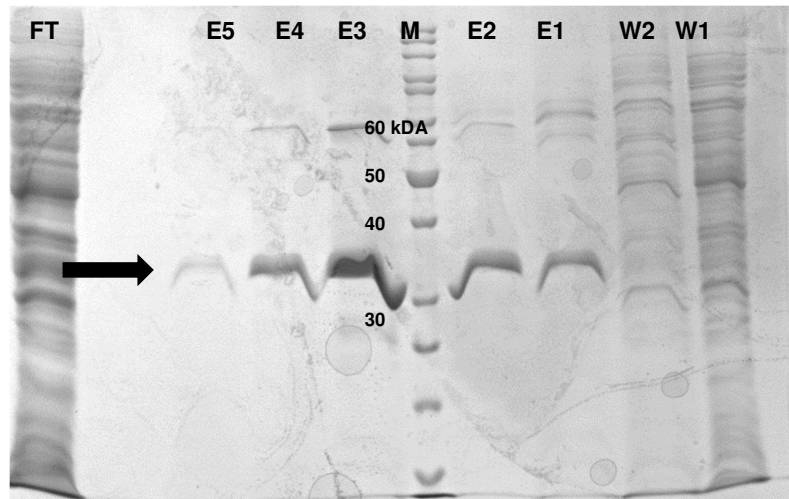


Figure S22. SDS-PAGE of a typical purification of SphJ by affinity-chromatography on a Ni-NTA column.

FT, flow through; W1 and W2, (washing steps with 30 and 50 mM imidazole, respectively); E1–E5, elution fractions (100–350 mM imidazole); M, marker. The black arrow indicates the calculated mass of 31.2 kDa for the SphJ.

Table S1. Predicted functionalities of the proteins encoded in the siphonazole biosynthetic gene cluster

Gene	Size ^a	Highest homology ^b	Identity ^c	Predicted domains ^d
<i>sphA</i>	762	malonyl CoA-ACP transacylase [<i>Pelosinus fermentans</i>]	389/765 (51%)	<i>trans</i> -AT-OR
<i>sphB</i>	221	SAM-dependent methyltransferase [<i>Paenibacillus sonchi</i>]	144/220 (65%)	O-methyltransferase
<i>sphC</i>	5451	hypothetical protein [<i>Fischerella</i> sp. PCC 9339]	135/339 (40%)	A-ACP-ACP-KS-DH-KR- ACP-KS-PCP-Cyc-Cyc- A- PCP-PCP-Ox-Ox-KS
<i>sphD</i>	2089	beta-ketoacyl synthase [<i>Clostridium</i>] <i>cellulolyticum</i>]	719/1951 (37%)	ACP-KS-ACP-ACP-KS- ACP
<i>sphE</i>	2693	hypothetical protein [<i>Paenibacillus polymyxa</i>]	662/2120 (31%)	Cyc-Cyc-A-PCP-PCP- Ox-Ox-KS-ACP
<i>sphF</i>	2059	mixed polyketide synthase/non- ribosomal peptide synthetase, partial [<i>Streptomyces avermitilis</i>]	862/2013 (43%)	C-A-ACP-KS-DH
<i>sphG</i>	1186	hypothetical protein, partial [<i>Clostridium</i>] <i>cellulolyticum</i>]	479/1031 (46%)	KR-ACP-KS-ACP
<i>sphH</i>	1228	putative Carboxyl esterase [<i>Xenorhabdus bovienii</i> str. <i>oregonense</i>]	270/915 (30%)	DH-KR-ACP-Hydrolase
<i>sphI</i>	348	hypothetical protein [<i>Atribacteria</i> <i>bacterium</i> JGI 0000059-114]	183/342 (54%)	Aldolase
<i>sphJ</i>	243	MULTISPECIES: thioesterase [<i>Bacillus</i>]	100/231 (43%)	TE

^a The size of the proteins is given in amino acids. ^b BLASTp results for the amino acid sequences from the siphonazole biosynthetic gene cluster. ^c The numbers of amino acids identical to the highest homologue are given. ^d Column five shows the predicted protein functions.

Table S2. Antiprotozoal activities of siphonazole.

Parasite	Siphonazole		Reference drug ¹	
	IC ₅₀ (µg/mL)	IC ₅₀ (µM)	IC ₅₀ (µg/mL)	IC ₅₀ (µM)
<i>T. brucei rhodesiense</i>	5.36	11.57	0.0013	0.0032
<i>Trypanosoma cruzi</i>	22.40	48.36	0.30	1.15
<i>Leishmania donovani</i>	28.40	61.32	0.14	0.34
<i>Plasmodium falciparum</i>	0.59	1.27	0.04	0.11
Cytotoxicity (L6 cells)	23.80	51.38	0.01	0.02

¹ (melarsoprol, benznidazole, miltefosine, chloroquine, podophyllotoxin)

Table S3. mRNA screening primers.

Primer	Sequence (5'–3')
A-fwd A-rev	GCGAGGCATACCATGAAAGG CCTGCTTCTGTGATCCTTG
B-fwd B-rev	CAGGCTCGTCATGTCGATAC TTCTGGTGGCGTTTGCATGG
C-fwd C-rev	TTGGTGATGGCTTGA CTCTC CGGGCTTGGTTGGTAAACAG
D-fwd D-rev	TGGCGTAATTCAGCCACGTC GCAATCGCGGTTAAATCAGG
E-fwd E-rev	TTCAGGAACTGCGCTTGATG GCAGTCGCGAATGGTTGGTG
F-fwd F-rev	AATCCCGCCCACCCAGATTC AATGCCATGCCGACGCTAAG
G-fwd G-rev	GGAGCAGGTTGGCATCTACG GTTTCAGGCACCATCCCTTG
H-fwd H-rev	TTGTTATTTGAGCGCCACCC AACGCTGACTATCAGCAACC
I-fwd I-rev	TTCTGCGCGAGCAAGAAGCC CTTTGGCAACGCCACAATG
J-fwd J-rev	CCGACA ACTCAATCCCAATG TCAAGCAGCGGCTCTTGACG

Table S4. Primers for protein expression constructs

Primer	Sequence (5'–3')
OMt-fwd-BamHI OMt-rev-HindIII	GCGGATCCATGGCAAAGGCATCATTGAAC CGAAGCTTGT TATTTGCGAATAACGAGAG
SphI-fwd SphI-rev	CACCATGATCGTAACGATAGAGC CTAACTGACCACAAGTGC
SphH_end_fw SphH_end_dn	CACCTTGTATGGCTATATTCTTGG CTAGACAAGCGTTGACATTA
SphJ-topo-Up SphJ-topo-Down	CACCATGGCAAGCTTGATCAAG CTATTCGTCAACTATGCTAATC
sphC-A-fwd sphC-A-rev sphC-A+ACP1 sphC-A+ACP1&2	CACCATGGTGCAACAAGATTTAC CTAATCAATTTTGCCATTGGGAAG CTAAAGGGCGCTGGCCAAATC CTACAATGCCAGCGCAAGATC

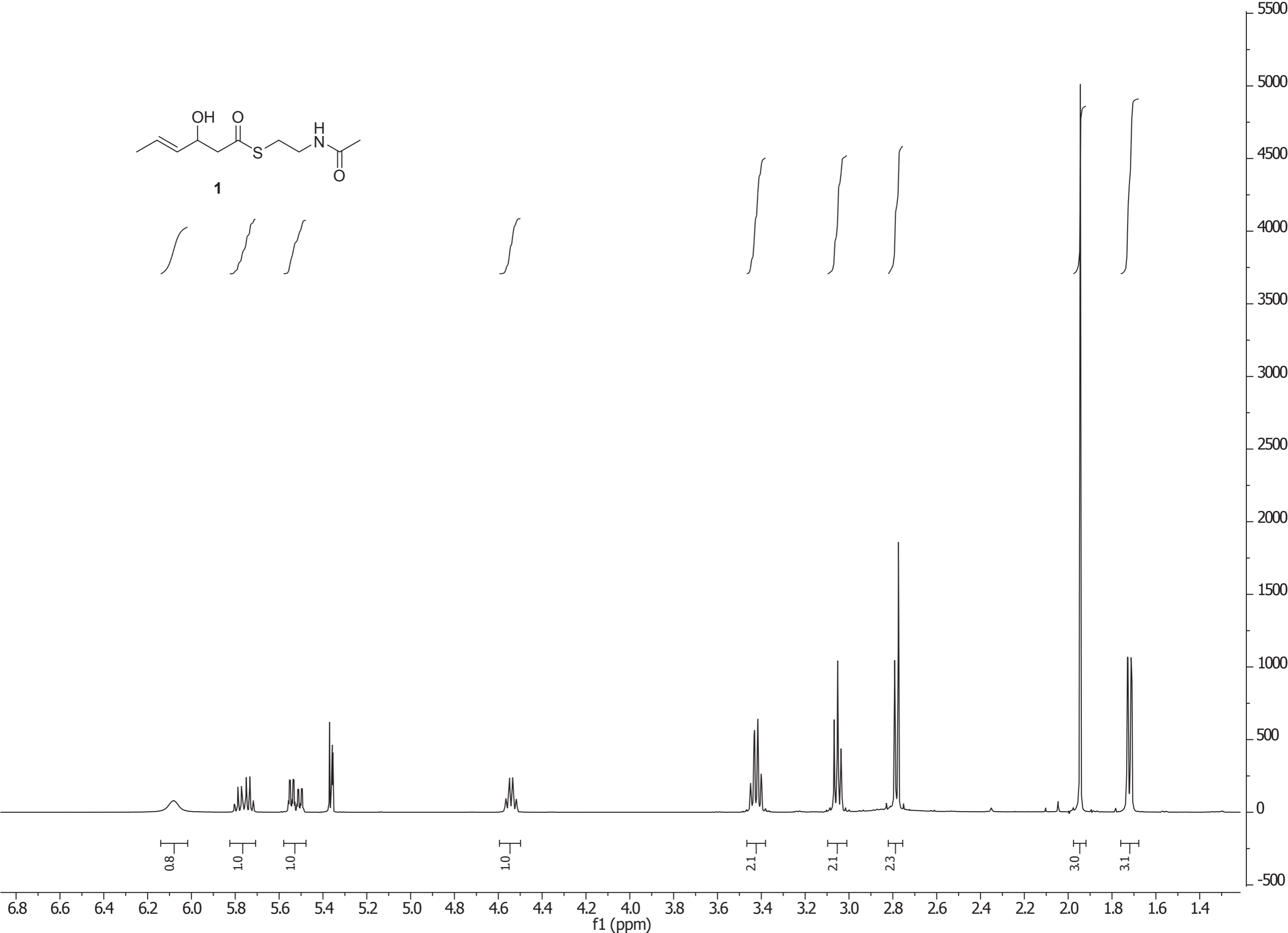
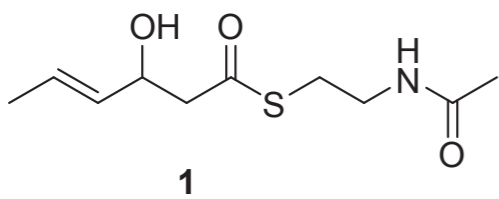
Table S5. Bacterial strains and plasmids used in this study

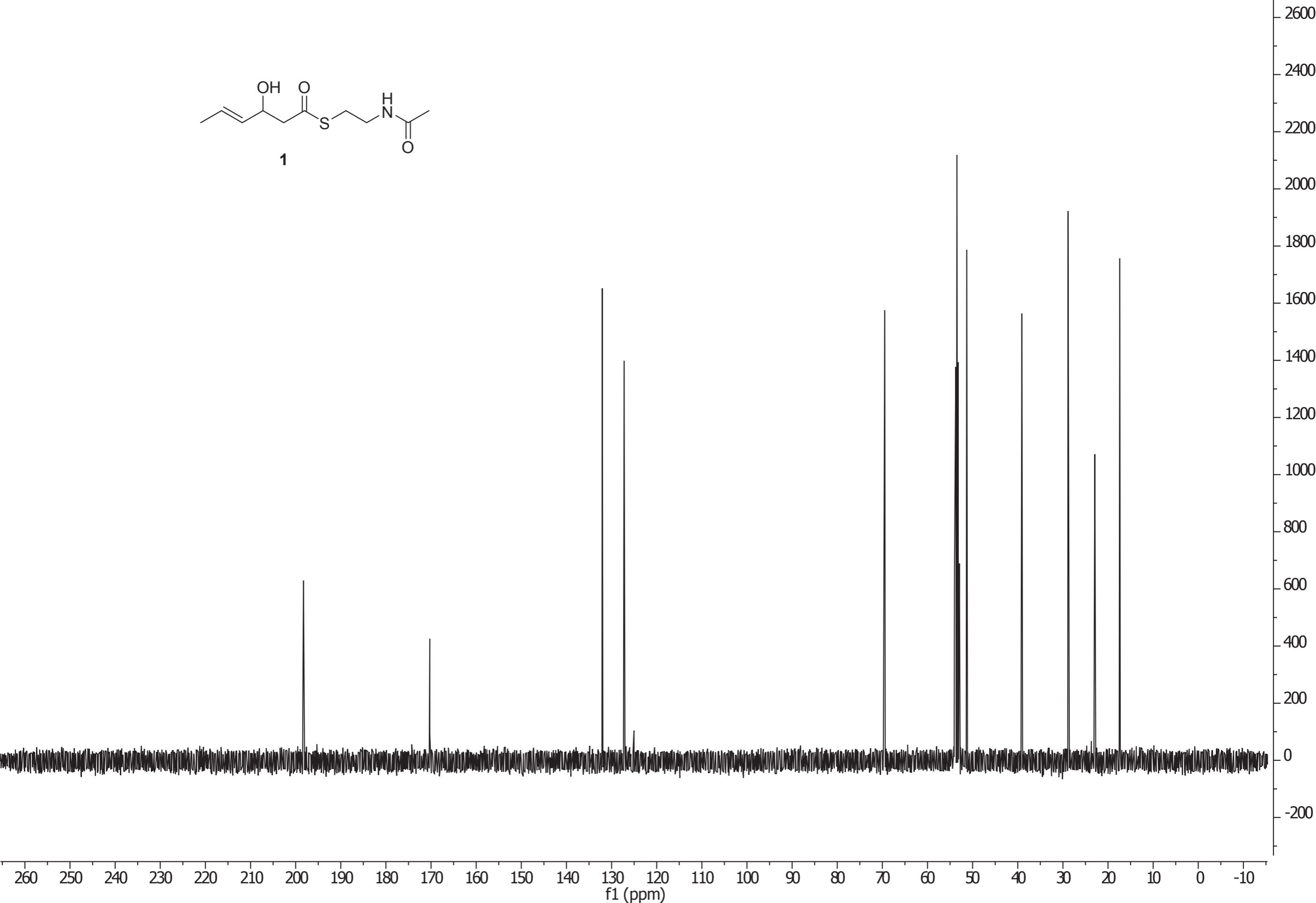
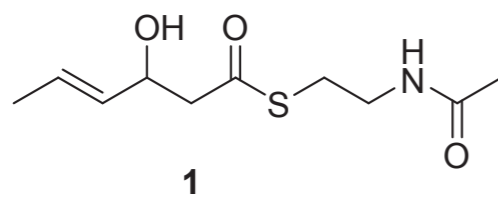
Organism	Genotype of interest	Provider
XL1-Blue <i>E. coli</i>	<i>recA1 endA1 gyrA96 thi-1 hsdR17 supE44 relA1 lac [F' proAB lacIqZΔM15 Tn10 (Tetr)</i>	Stratagene (La Jolla, CA, USA)
BL21 <i>E. coli</i>	<i>F- ompT gal dcm lon hsdSb (rB-mB-) λ(DE3 [lac lacUV5-T7 gene1 ind 1 sam7 nin5])</i>	Invitrogen Life Technologies Corporation (Germany)
BAP1 <i>E. coli</i>	BL21(DE3) ΔprpRBCD::T7psfp-T7pprpE	Pfeifer et al., 2001 ^[36]
TOP10 <i>E. coli</i>	<i>F- mcrA Δ(mrr-hsdRMS-mcrBC) Φ80lacZΔM15 ΔlacX74 recA1 araD139 Δ(ara-leu)7697 galU galK rpsL (StrR) endA1 nupG)</i>	Invitrogen Life Technologies Corporation (Germany)
pET28a(+)	kanR, His tag cds (6xHis)	Merck KGaA (Germany)
pET151/D-TOPO	ampR, His tag cds (6xHis)	Invitrogen Life Technologies Corporation (Germany)
pET28_SphB	<i>sphB</i>	This study
pET151_SphC	<i>sphC</i> (N-terminal A domain)	This study
pET151_SphC_ACP1	<i>sphC</i> (A + ACP1 domains)	This study
pET151_SphC_ACP1&2	<i>sphC</i> (A + ACP1+ACP1 ₂ domains)	This study
pET151_SphI	<i>sphI</i>	This study
pET151_SphH _{Cterm}	<i>sphH</i> (C-terminal part)	This study
pET151_SphJ	<i>sphJ</i>	This study

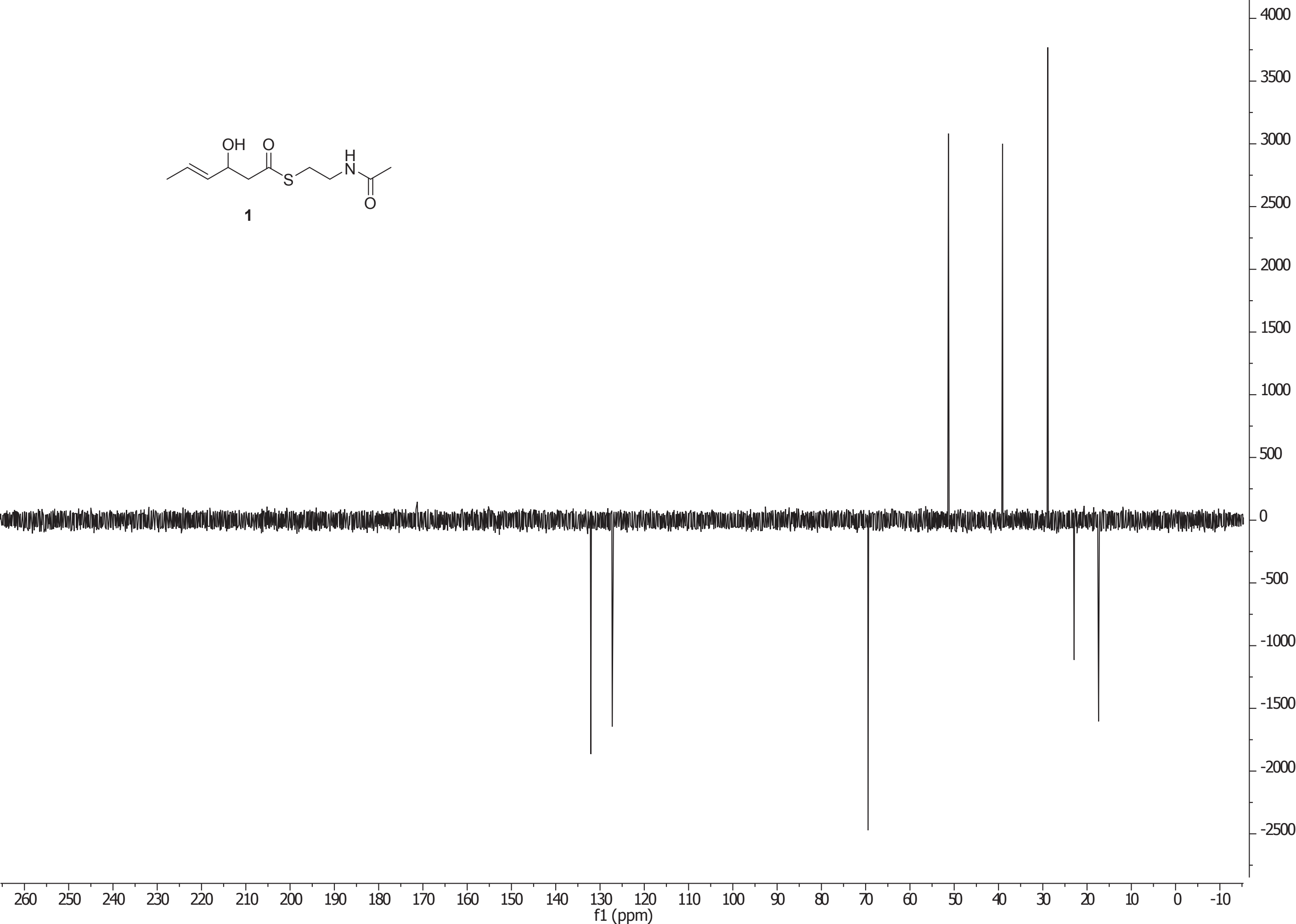
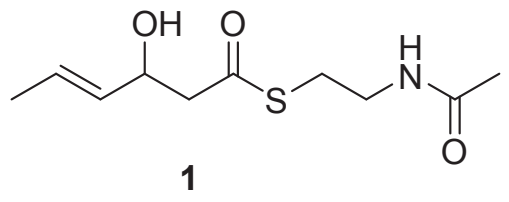
References

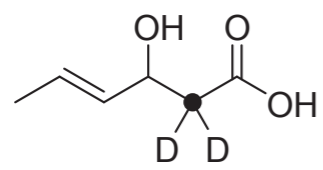
- [18] S. Donadio, M. J. Staver, J. B. McAlpine, S. J. Swanson, L. Katz *Science* **1991**, *252*, 675–679.
- [19] S. Donadio, L. Katz *Gene* **1992**, *111*, 51–60.
- [20] Y. M. Zhang, J. Hurlbert, S. W. White, C. O. Rock *J. Biol. Chem.* **2006**, *281*, 17390–17399.

- [21] R. Butcher, F. C. Schroeder, M. Fischbach, P. D. Straight, R. Kolter, C. T. Walsh, J. Clardy *Proc. Natl. Acad. Sci.* **2007**, *104*, 1506–1509.
- [22] R. S. Roy, M. Gehring, J. C. Milne, P. J. Belshaw, C. T. Walsh *Nat. Prod. Rep.* **1999**, *16*, 249-263.
- [23] C. G. Marshall, N. J. Hillson, C. T. Walsh *Biochemistry* **2002**, *41*, 244–250.
- [24] Y. Q. Cheng, G. L. Tang, B. Shen *J. Bac.* **2002**, *184*, 7013–7024.
- [25] I. Molnar, T. Schupp, M. Ono, R. Zirkle, M. Milnamow, B. Nowak-Thompson, N. Engel, C. Toupet, A. Stratmann, D. D. Cyr, J. Grolach, J. M. Mayo, A. Hu, S. Goff, J. Schmid, J. M. Ligon *Chem. Biol.* **2000**, *7*, 97–109.
- [26] T. Kobori, H. Sasaki, W. C. Lee, S. Zenno, K. Saigo, M. E. P. Murphy, M. Tanokura *J. Biol. Chem.* **2001**, *276*, 2816–2823.
- [27] J. Piel *Nat. Prod. Rep.* **2010**, *27*, 996–1047.
- [28] S. G. van Lanen, S. Lin, B. Shen *Proc. Natl. Acad. Sci.* **2008**, *105*, 494–499.
- [29] J. Thykaer, J. Nielsen, W. Wohlleben, T. Weber, M. Gutknecht, A. E. Lantz, E. Stegmann *Metab. Eng.* **2010**, *12*, 455–461.
- [30] Röttig, M., Medema, M. H., Blin, K., Weber, T., Rausch, C., & Kohlbacher, O. *Nucleic Acids Res.* **2011**, *39* (Web Server issue), W362-367.
- [31] Phelan, V. V., Du, Y., McLean, J. A., & Bachmann, B. O. *Chem. Biol.* **2009**, *16*, 473–478.
- [32] Schofield, L. R., Patchett, M. L., & Parker, E. J. *Protein Expr. Purif.* **2004**, *34*, 17–27.
- [33] Snyder, C. Chollet, J. Santo-Tomas, J. Scheurer, C. Wittlin, S. *Exp. Parasitol.* **2007**, *115*, 296.
- [34] Henrick, C. A., Willy, W. E., McKean, D. R., Baggiolini, E. & Siddall, J. B. *J. Org. Chem.* **1975**, *40*, 8-14.
- [35] Kotowska, M., Pawlik, K., Smulczyk-Krawczynszyn, A., Bartosz-Bechowski, H., & Kuczek, K. *Appl. Environ. Microbiol.* **2009**, *75*, 887-896.
- [36] Pfeifer, B. A., Admiraal, S. J., Gramajo, H., Cane, D. E. & Khosla, C. *Science* **2011**, *291*, 1790-1792.

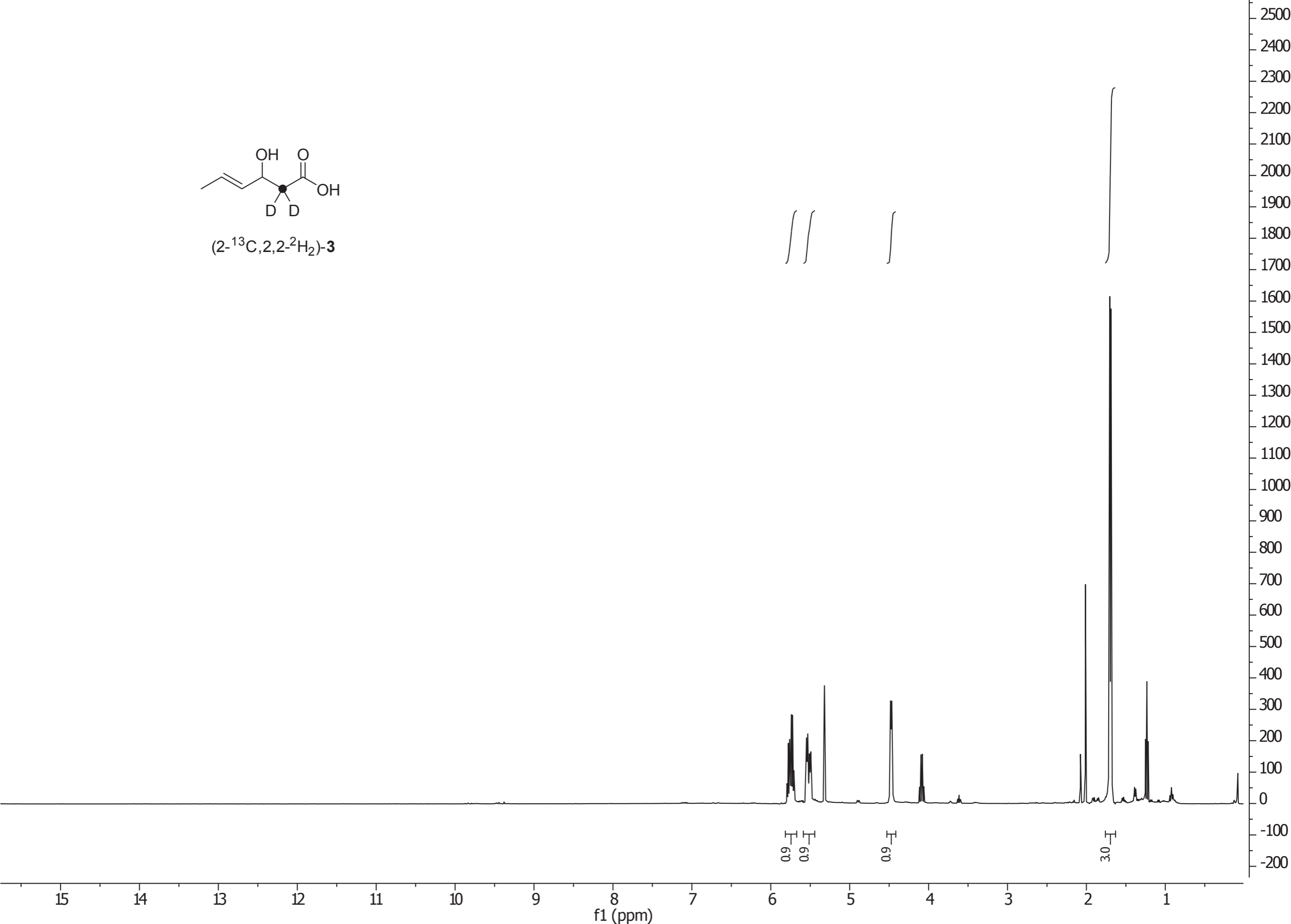


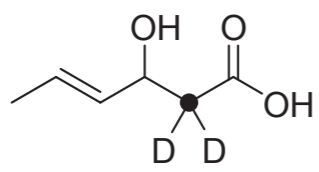




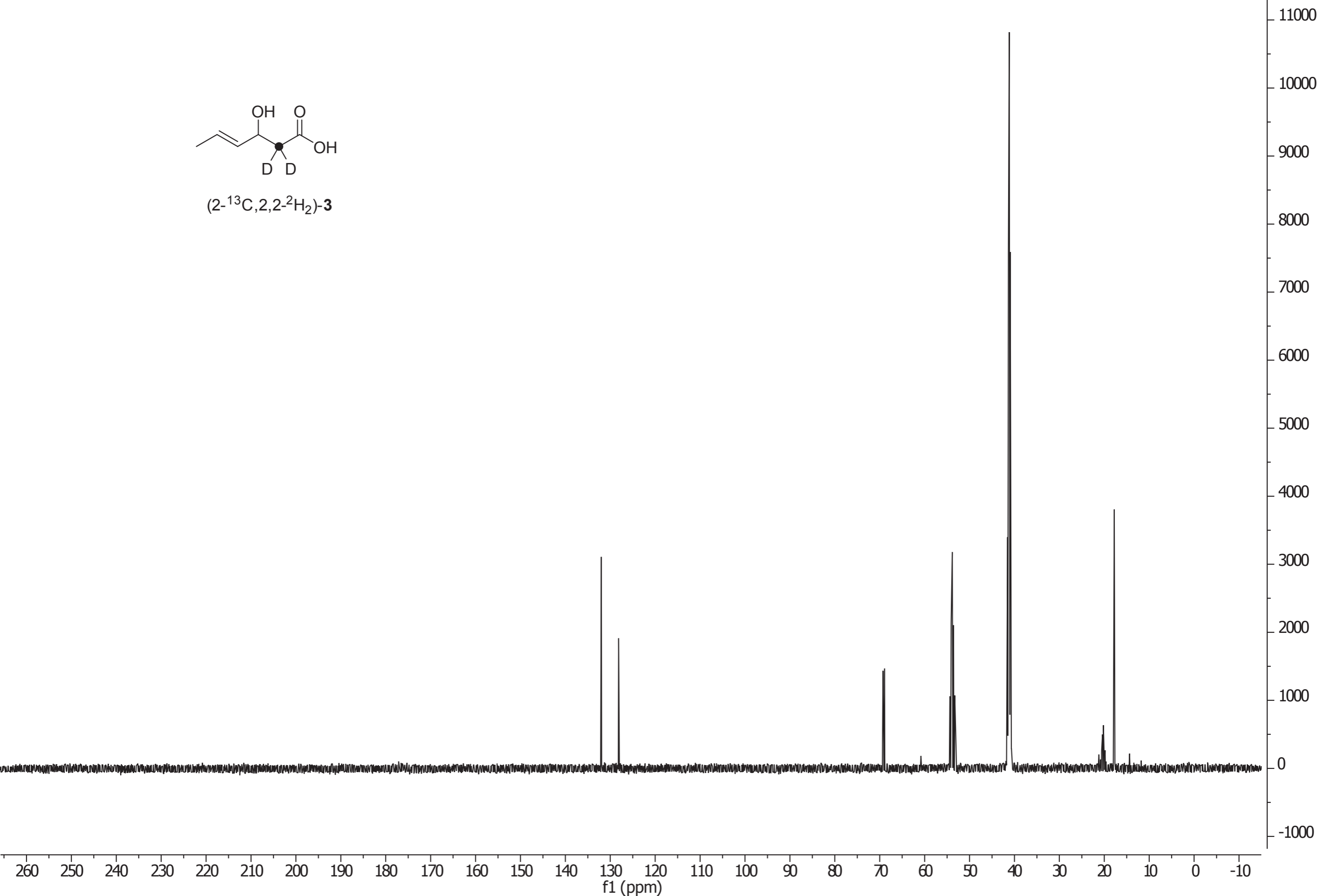


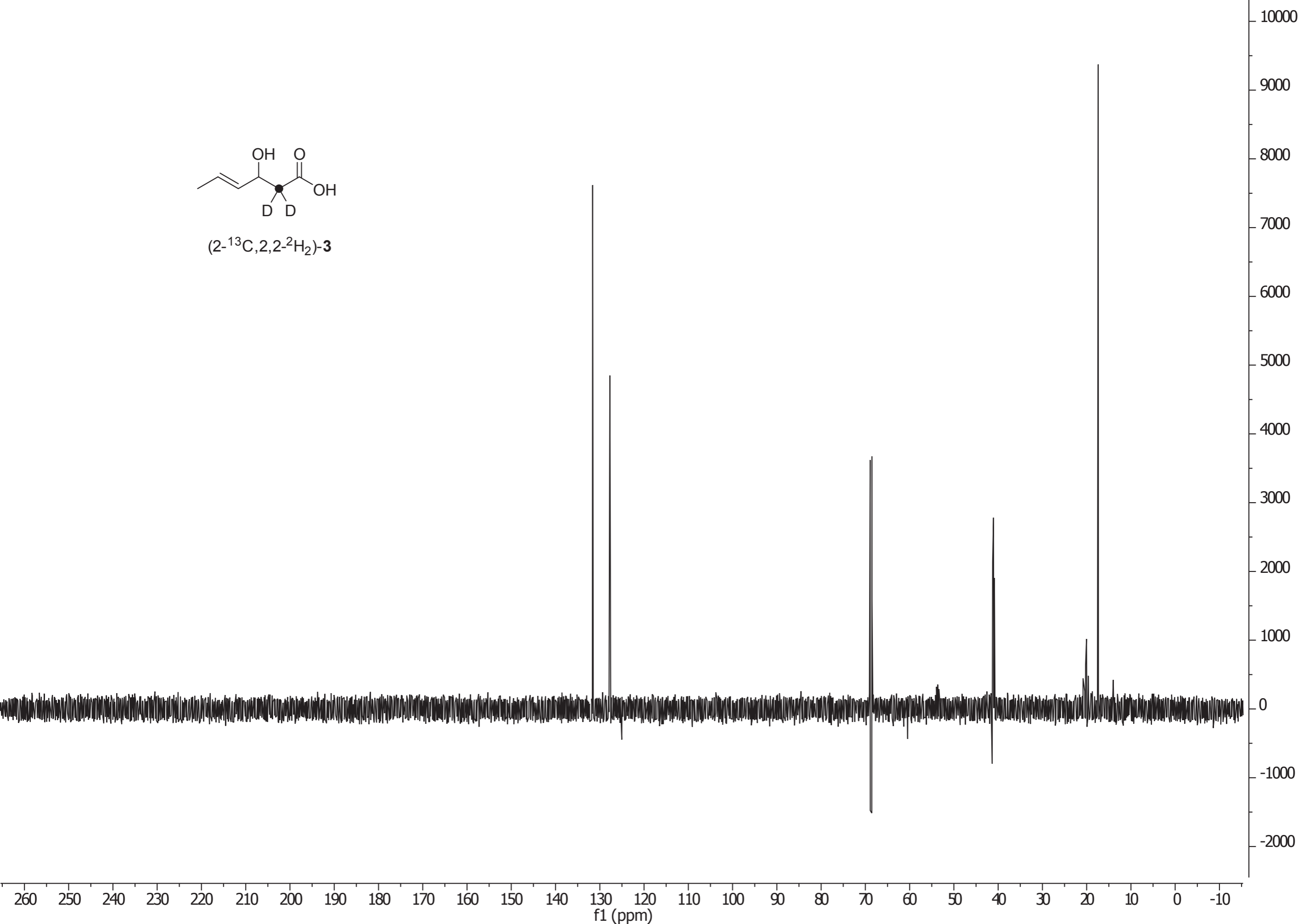
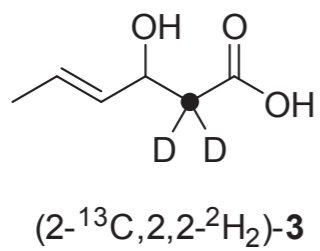
(2-¹³C,2,2-²H₂)-3

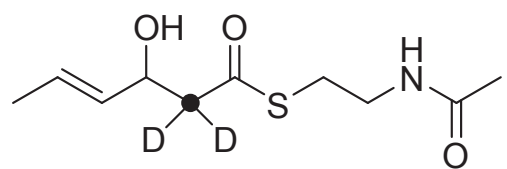




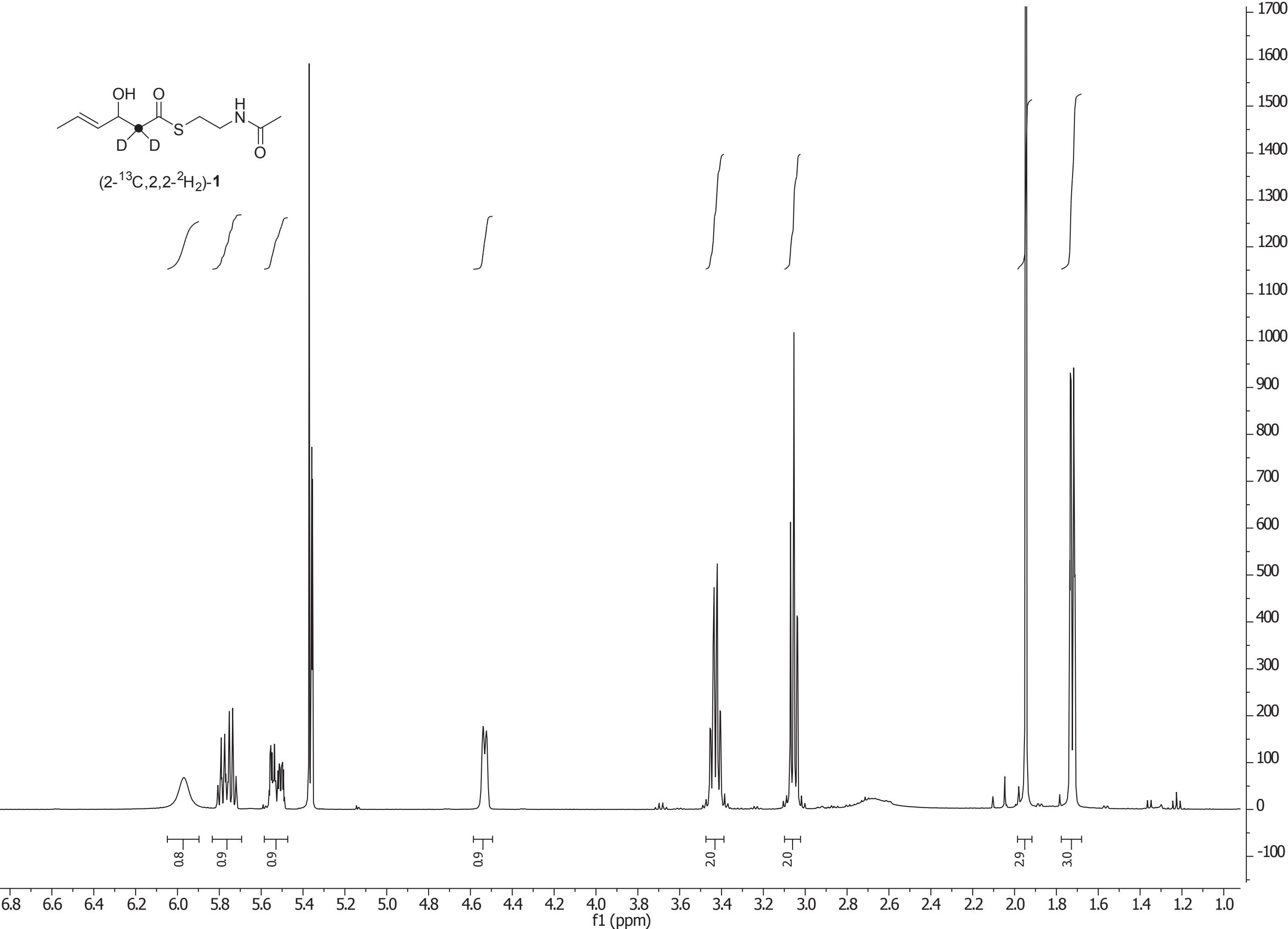
(2-¹³C,2,2-²H₂)-3

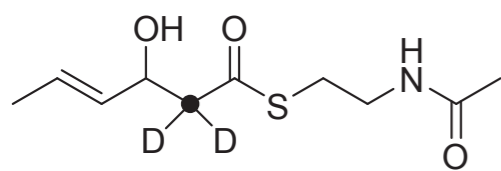




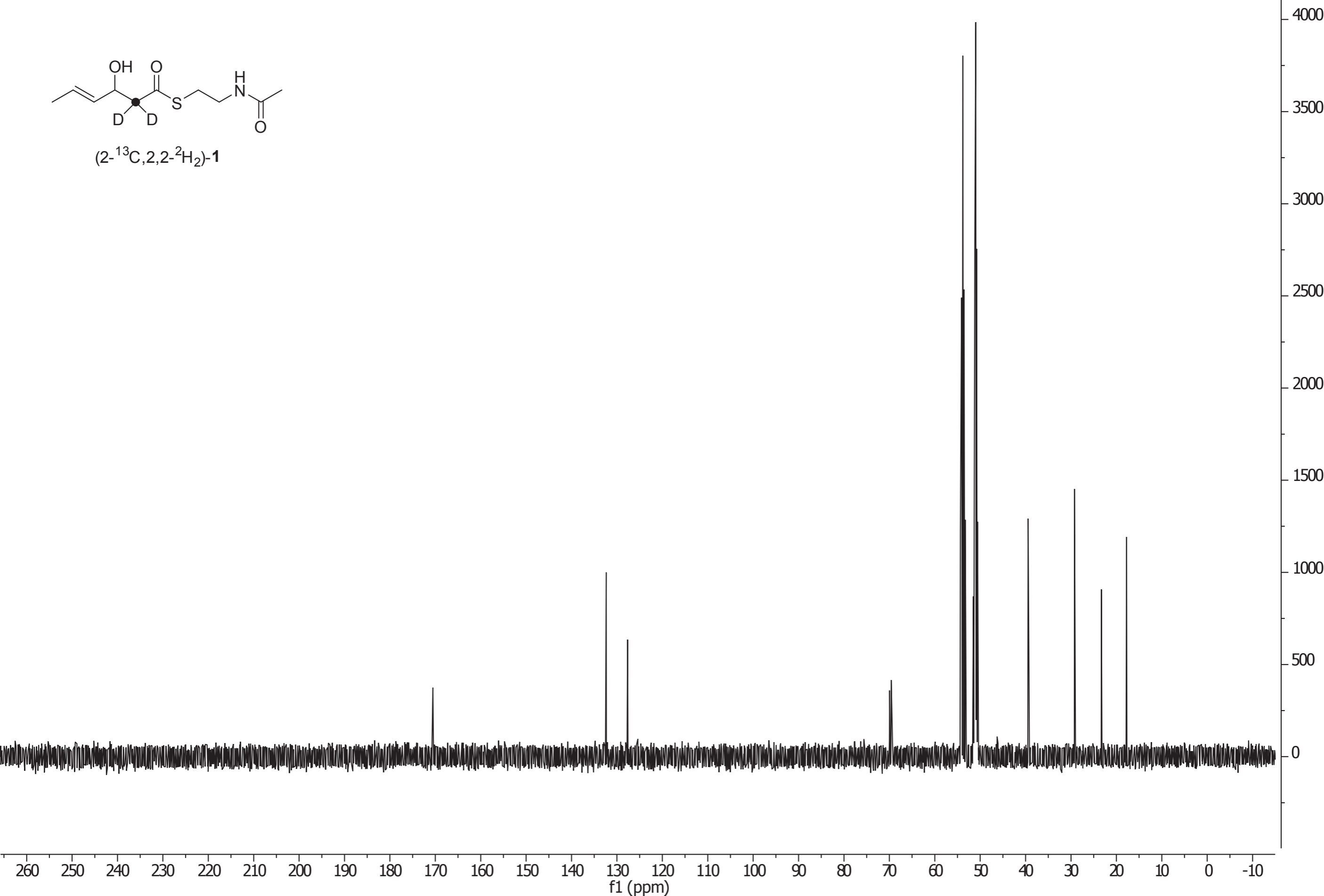


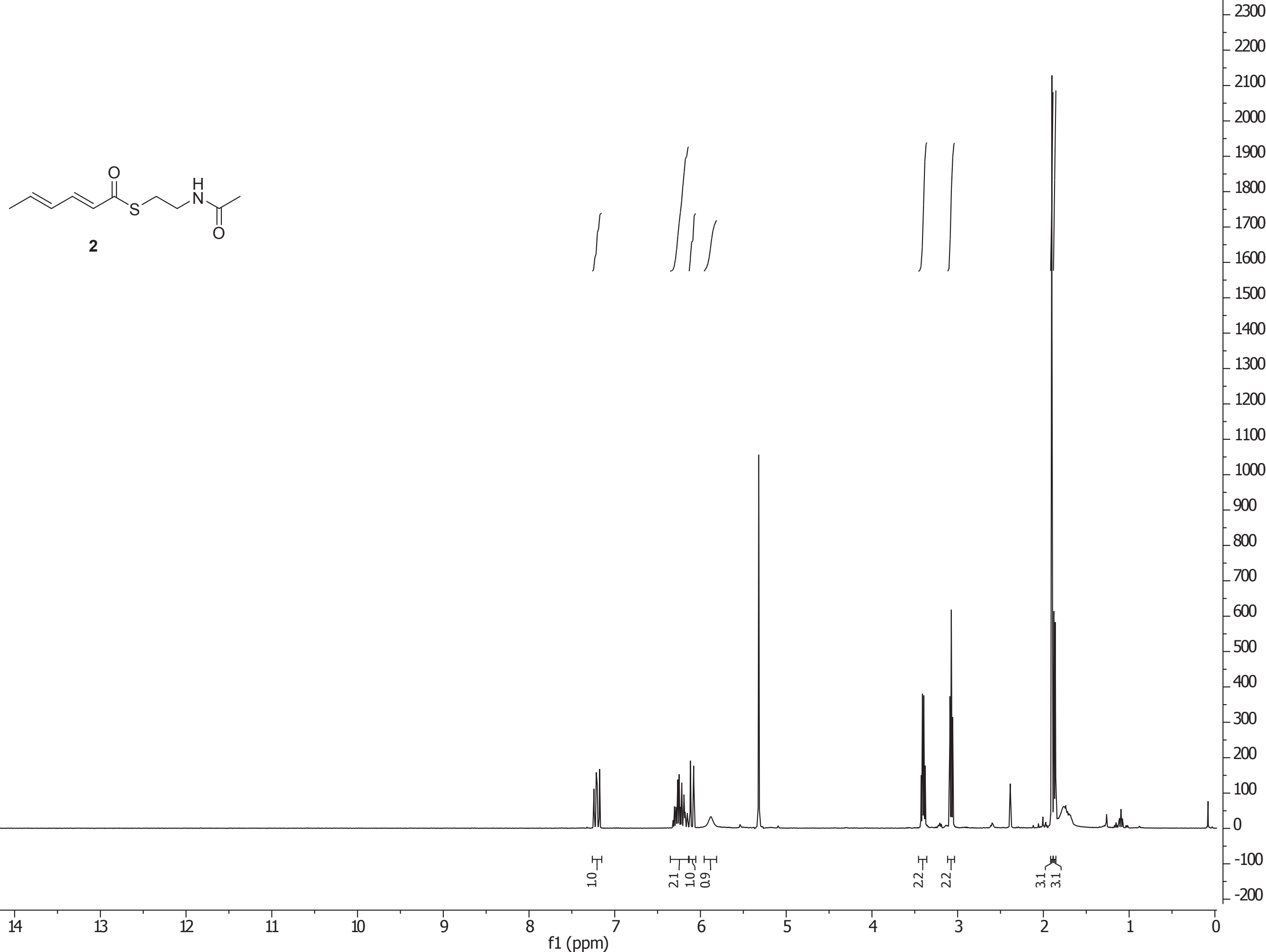
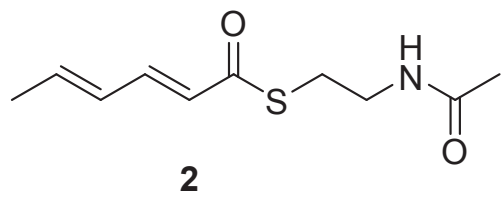
(2-¹³C,2,2-²H₂)-1

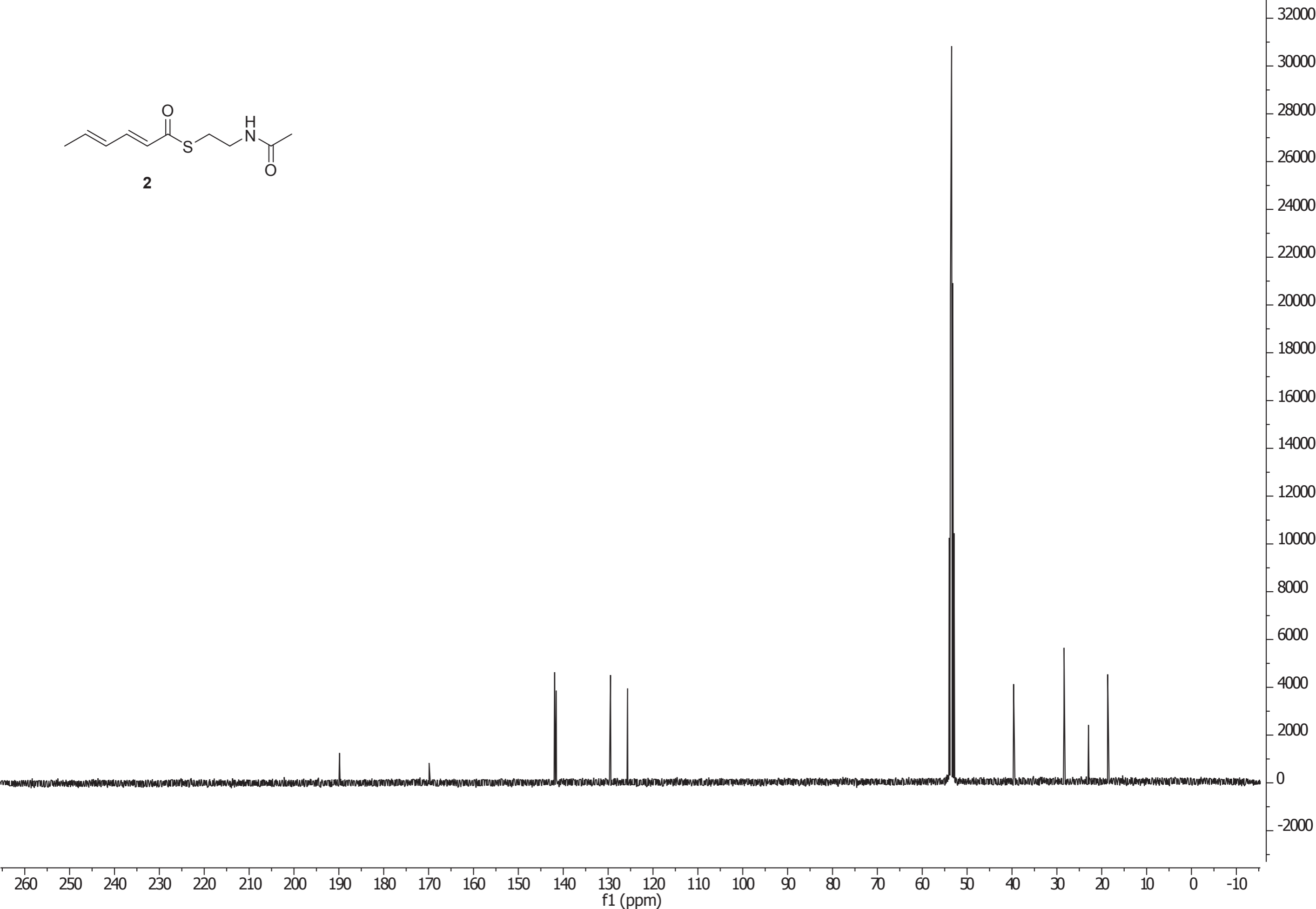
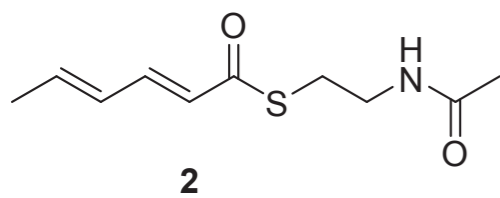


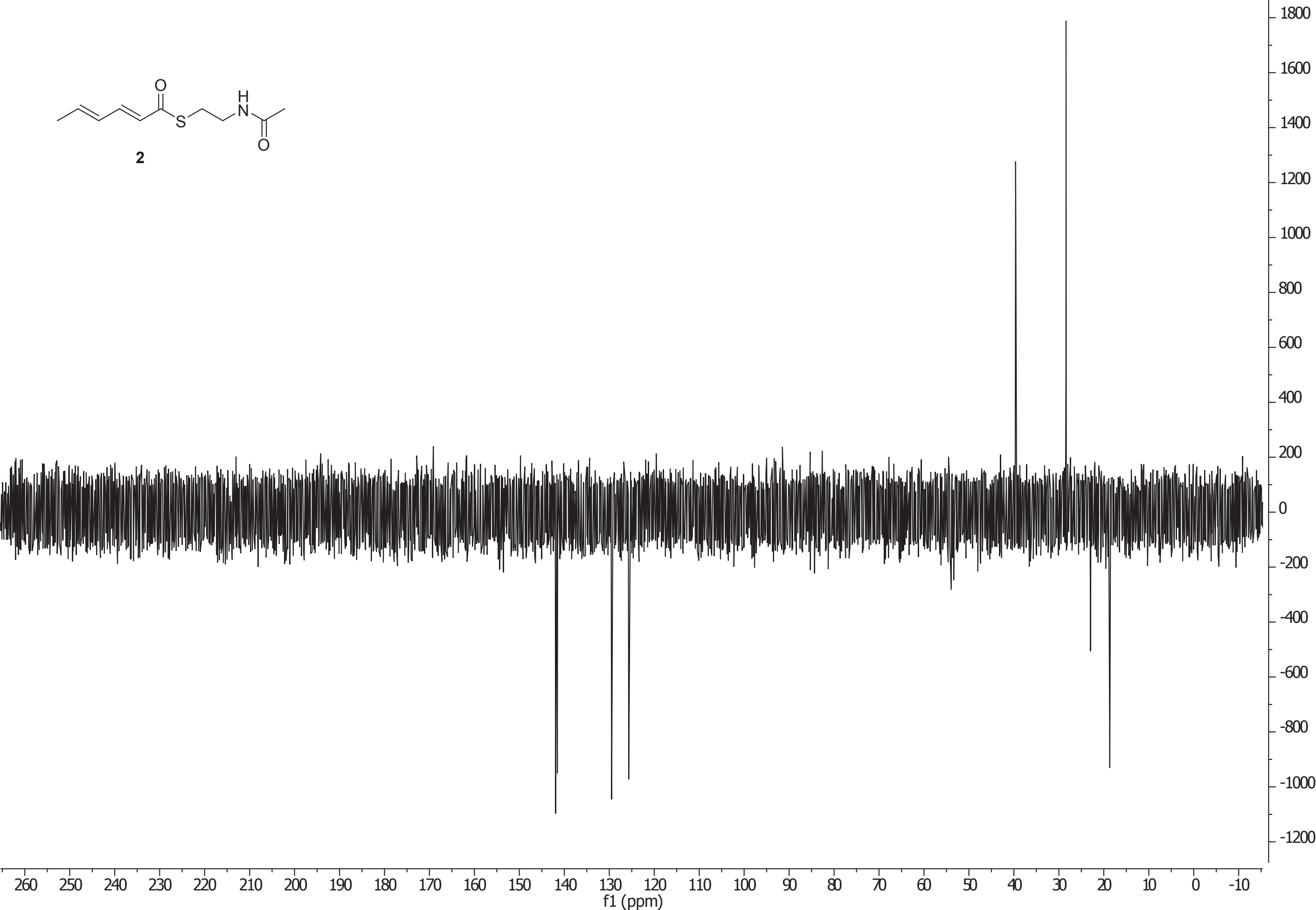
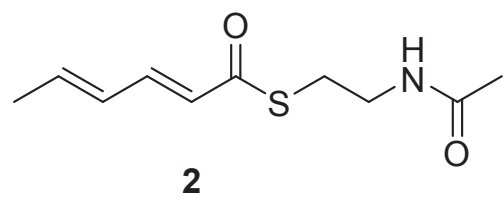


(2-¹³C,2,2-²H₂)-1









Appendix J

Sceptrin – Enantioselective Synthesis of a Tetrasubstituted
all-trans Cyclobutane Key Intermediate

Cyclobutane Synthesis | Very Important Paper |

VIP Sceptrin – Enantioselective Synthesis of a Tetrasubstituted all-*trans* Cyclobutane Key IntermediateLena Barra^[a] and Jeroen S. Dickschat^{*[a]}

Abstract: The asymmetric synthesis of both enantiomers of tetrasubstituted all-*trans* dimethyl 3,4-diacetylcyclobutane-1,2-dicarboxylate with high enantiomeric purity (>98 % ee) using a valine-derived chiral auxiliary in a diastereoselective photodimerization is reported. The absolute configuration was assigned

by single-crystal X-ray diffraction analysis. Because this cyclobutane is a key intermediate in the total synthesis of (–)-sceptrin and ageliferin, our findings strengthen the recently revised absolute configurations of these pyrrole-imidazole alkaloids.

Introduction

The cyclobutane ring is a widespread structural motif that occurs in all classes of natural products including terpenes, alkaloids, fatty acids, nucleosides and polyketides.^[1] Particularly intriguing are cyclobutane-centred symmetric (or pseudo-symmetric) natural products that are presumably formed by an intermolecular [2+2] cycloaddition of two identical (or structurally related) monomers that can usually result in a variety of regio- and stereoisomers. Well-known examples are the pseudo-symmetric all-*trans* compound anisumic acid (**1**) from the Chinese medicinal plant *Clausena anisum-olens* (Rutaceae)^[2] and sceptrin (**2**), which was isolated in 1981 by Faulkner and Clardy and co-workers from the marine sponge *Agelas sceptrum* (Figure 1).^[3] This dimer of hymenidin (**3**) belongs to a large group of marine pyrrole-imidazole alkaloids that exhibit remarkable structural architectures and a broad spectrum of bioactivities,^[4] including anti-microbial, anti-muscarinic and anti-histaminic activities, and inhibition of the cell motility of cancer cell lines without showing cytotoxicity at the effective concentrations.^[5] Besides **2**, a series of related compounds can be isolated from different *Agelas* species, such as ageliferin (**4**),^[6] which can be rationalized as the [4+2] cycloadduct of **3**, and nakamuric acid (**5**),^[7] for which the absolute configuration was recently clarified.^[8] From a synthetic point of view, these chiral natural products are challenging targets because methods for the asymmetric construction of cyclobutane scaffolds are limited.^[9] The first total synthesis of (*rac*)-**2** was reported in 2004 and proceeded via the tetrasubstituted all-*trans* cyclobutane (*rac*)-**6** as a key intermediate that was transformed into (*rac*)-**2** in 12 linear steps.^[10] A subsequent enantioselective synthesis of (+)-**6** gave

access to natural (–)-**2** and confirmed the initially assigned absolute configuration,^[11] but a more recent synthetic route starting from L-glutamic acid resulted in a revision of the absolute configuration for sceptrin and, consequently, for the key intermediate (+)-**6** of the first enantioselective approach towards sceptrin.^[12] Here we describe an alternative procedure for the synthesis of both enantiomers of **6** from L- or D-valine that confirms the recently revised absolute configuration of sceptrin.

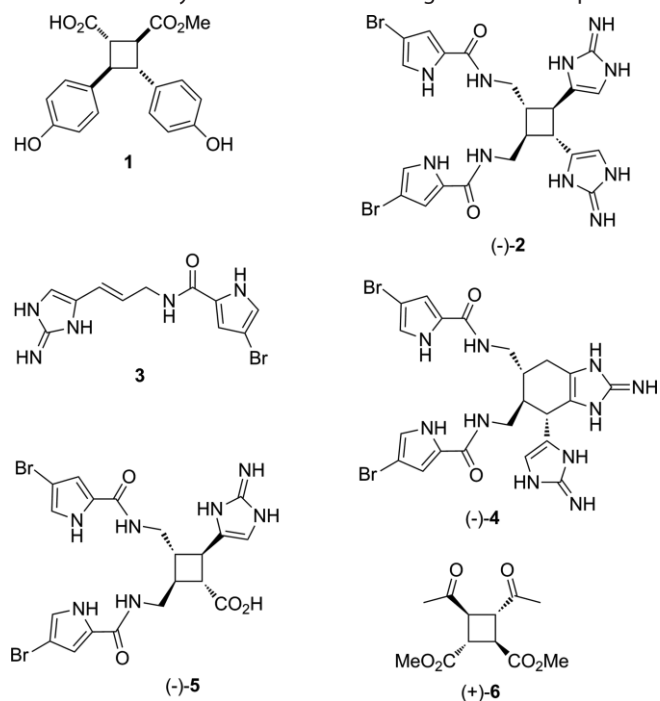


Figure 1. Structures of anisumic acid (**1**), sceptrin (**2**), hymenidin (**3**), ageliferin (**4**), nakamuric acid (**5**) and of the synthetic key intermediate (+)-**6** towards sceptrin and ageliferin.

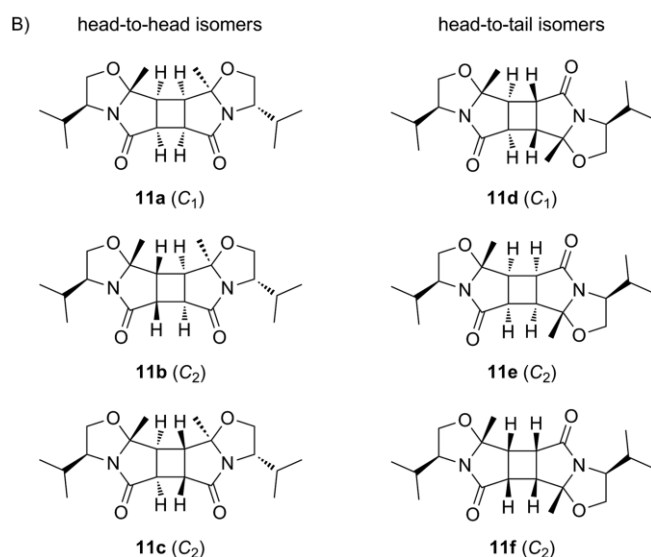
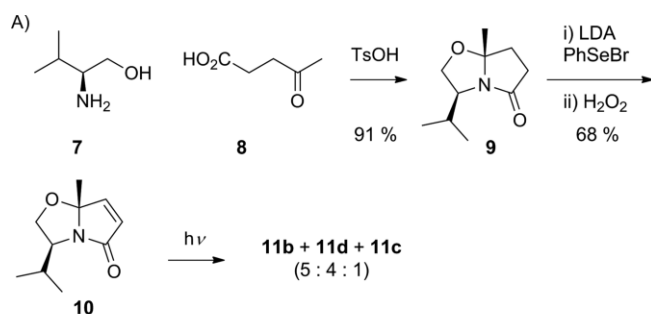
Results and Discussion

For the enantioselective synthesis of **6**, L-valinol (**7**) and levulinic acid (**8**) were converted into the bicyclic lactam **9**, which is a

[a] Kekulé-Institute of Organic Chemistry and Biochemistry, Rheinische Friedrich Wilhelms University of Bonn, Gerhard-Domagk-Straße 1, 53121 Bonn, Germany
E-mail: dickschat@uni-bonn.de
https://www.chemie.uni-bonn.de/oc/forschung/arbeitsgruppen/ak_dickschat

Supporting information and ORCID(s) from the author(s) for this article are available on the WWW under <https://doi.org/10.1002/ejoc.201700882>.

known intermediate in the total synthesis of (-)-grandisol (Scheme 1A).^[13] Introduction of an α,β -unsaturation by Grieco elimination yielded the enone **10**, a compound that was previously applied in face-selective cyclopropanation reactions.^[14] UV irradiation of **10** at 250 nm in dichloromethane resulted in the formation of two products in yields of 15 % and 8 % that were tentatively identified as [2+2] dimerization products by GC-MS (Table 1).



Scheme 1. Synthesis of photodimers: A) synthesis of monomer **10** from valinol and subsequent irradiation to photodimers **11** and B) representation of all possible photodimers with their point groups given in parentheses.

Table 1. Optimization of the reaction conditions for the photodimerization of **10**.^[a]

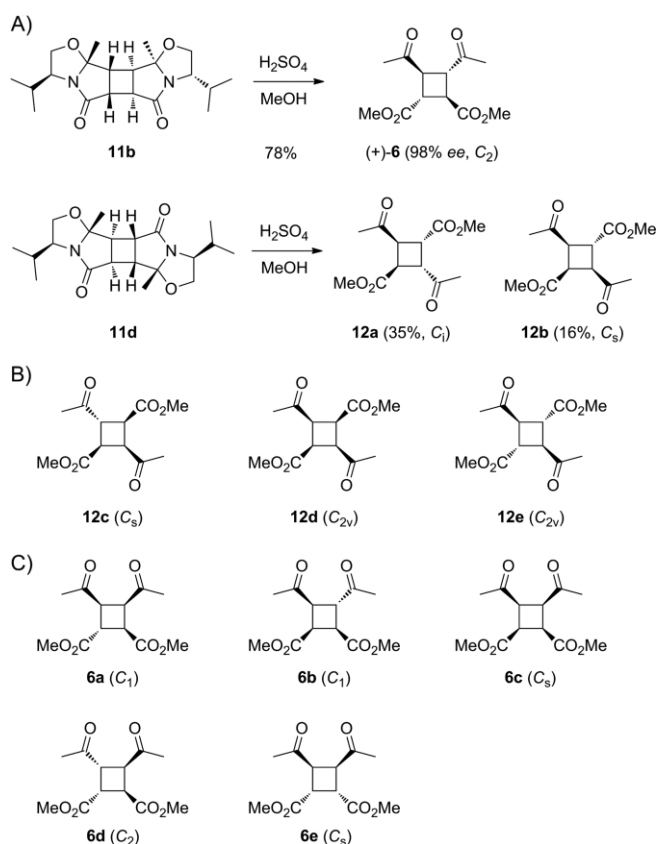
λ [nm]	Solvent	Additive	Time [h]	Yield [%]		
				11b	11c	11d
250	DCM	–	24	15	n.d.	8
250	MeCN	–	24	19	n.d.	10
250	neat	–	48	0	0	0
350	MeCN	–	48	0	0	0
350	MeCN	acetophenone	12	37	5	32
350	MeCN	benzophenone	48	0	0	0
350	MeCN	acetone	48	0	0	0

[a] DCM = dichloromethane, MeCN = acetonitrile, n.d. = not determined.

During optimization of the reaction conditions, moderately increased yields were obtained in acetonitrile, whereas neat conditions did not give any [2+2] cycloadducts, even after prolonged reaction times. Changing to a wavelength of 350 nm

did not yield any photodimerization products, but with the addition of acetophenone as photosensitizer significantly improved yields could be obtained, even with reduced reaction times, and also minor quantities (5 %) of a third product were obtained. When applied under the same conditions, benzophenone and acetone proved to be ineffective as photosensitizers.

The structures of the three compounds obtained under the optimized reaction conditions were elucidated by the following rationale. In theory, the photodimerization of **10** can lead to six isomers, namely three head-to-head connected isomers **11a–c** and three head-to-tail cycloadducts **11d–f** (Scheme 1B, the symmetry properties of the molecules discussed in the following section are summarized in Tables S1 and S2 in the Supporting Information). Among the head-to-head compounds the *cis-syn-cis* stereoisomer **11a** exhibits C_1 symmetry, whereas the two *cis-anti-cis* stereoisomers **11b** and **11c** both represent the point group C_2 . Analogously, the head-to-tail isomer **11d** is of C_1 symmetry, whereas **11e** and **11f** belong to the C_2 point group. The main product of the photodimerization shows 10 signals in its ^{13}C NMR spectrum, in agreement with one of the C_2 -symmetric structures. The acid-catalysed cleavage of this product in methanol resulted in (+)-**6** (Scheme 2A), the reported intermediate in the synthesis of sceptrin, which can only be formed from **11b** with epimerization of both methyl ketones or from **11c** with epimerization of both methyl ester groups to yield the



Scheme 2. Methanolysis of photodimers: A) acid-catalyzed cleavage of photodimers **11b** and **11d**, B) further possible methanolysis products from head-to-tail photodimers and C) from head-to-head photodimers with their point groups given in parentheses.

thermodynamically most stable all-*trans* cyclobutane. Epimerization of the methyl ketones was assumed to be faster than epimerization of the methyl esters, thereby favouring the structure of **11b** for the main product. Indeed, the cleavage in (²H₄)methanol with ²H₂SO₄ proceeded with H/D exchange of only the cyclobutane hydrogens at the α positions with respect to the methyl ketones and not the methyl esters (Figure 2, for incorporation rates, ¹³C NMR and HSQC spectra see Table S3 and Figures S1–S3 in the Supporting Information). The structure of **11b** is further supported by X-ray diffraction analysis, with the crystallographic data of its lysis product pointing to a (1*R*,2*R*,3*S*,4*S*) configuration for (+)-**6** (Figure 3).

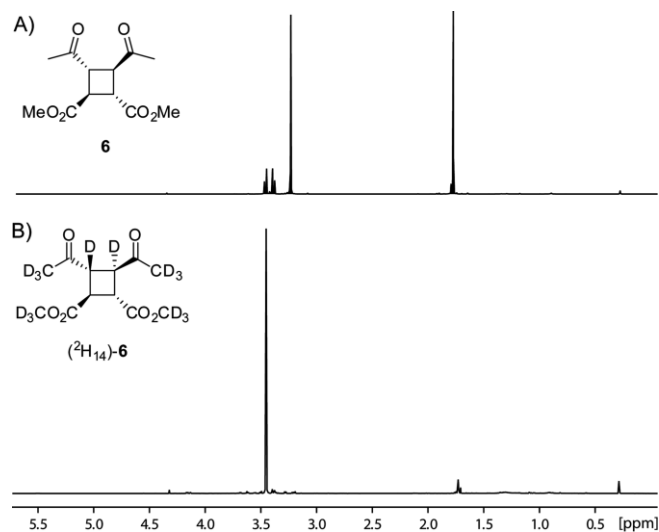


Figure 2. Result of the H/D exchange experiment. A) ¹H NMR spectrum of **6** (700 MHz, C₆D₆) and B) ¹H NMR spectrum of (²H₁₄)-**6** (700 MHz, C₆D₆).

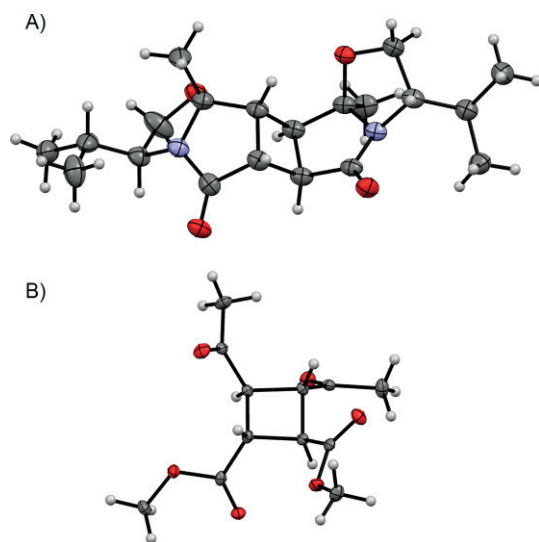


Figure 3. X-ray structures of **11b** and its cleavage product (+)-**6**. ORTEP representations of A) **11b** and B) (1*R*,2*R*,3*S*,4*S*)-**6** (crystallographic data are given in Tables S4 and S5 in the Supporting Information).

Starting from *D*-valinol, *ent*-(-)-**6** was obtained by the same route. Both enantiomers were isolated with high enantiomeric purity (>98 % *ee*), as revealed by HPLC analysis on a homochiral

stationary phase (Figure 4). The delineated structure of **11b** is also supported by 2D NMR spectroscopy, including ¹H,¹H COSY, HSQC, HMBC and NOESY, but many of the observed correlations are also in line with the other C₂-symmetric isomers. This was also a major problem in the identification of the other two photodimers.

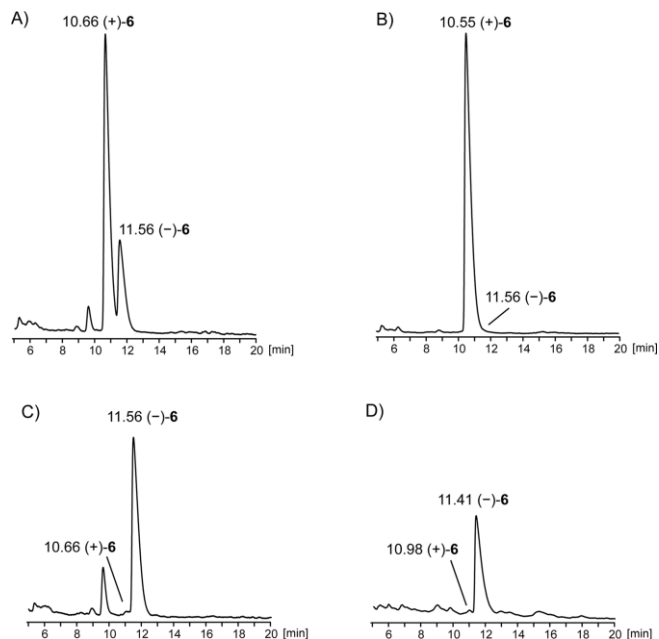


Figure 4. Analysis of the enantiomeric excess of **6** by HPLC on a chiral stationary phase. A) Mixture of (+)- and (-)-**6**, B) (+)-**6** obtained from the cleavage of (+)-**11b**, C) (-)-**6** obtained from the cleavage of (-)-**11b** and D) (-)-**6** obtained from the cleavage of (+)-**11c**.

The second most abundant photodimerization product from **10** exhibits 20 signals in its ¹³C NMR spectrum, which points to one of the two possible structures of C₁ symmetry (**11a** or **11d**). Methanolysis of this product yielded two achiral or chiral racemic products, as indicated by a missing optical rotation. One of these products reveals six and the other one nine signals in their ¹³C NMR spectra, requiring the presence of symmetric elements in both cases. Taking epimerizations (preferably at the methyl ketones) into account, the only possible structures for the minor product with nine ¹³C NMR signals are the achiral compounds **12b** or **12c** (see Table S2 in the Supporting Information). For all the other stereoisomers of **12** with either C_i or C_{2v} symmetry, six carbon signals are expected, whereas none of the stereoisomers of **6** that could potentially arise from a head-to-head isomer such as **11a** has the correct symmetry properties to explain the observed ¹³C NMR spectrum. The product **12b** was finally identified, because two sets of signals for the diastereotopic methyl ester functions and coinciding signals for the enantiotopic methyl ketones are observed, whereas **12c** would require two sets of signals for the methyl ketones and just one for the methyl esters. The major product of this methanolysis is likely to be **12a**, and the initial mixture of these two products pointed to the structure of **11d** for the second photodimer of **10**. The formation of **12b** shows again the preferential epimerization of the methyl ketone functions, whereas the hypothetical isomerization of one methyl ester group would

produce **12c**. No formation of the all-*trans* cyclobutane **12e** was observed, which also demonstrates the difficulties associated with the epimerization of the methyl ester groups under the applied reaction conditions.

The third minor product of the photodimerization of **10** exhibits 10 signals in the ^{13}C NMR spectrum, in agreement with the structures of **11c**, **11e** or **11f**. Methanolysis resulted in (–)-**6**, which is only explainable from the second C_2 -symmetric head-to-head dimer **11c**, again requiring epimerization of both methyl ketones.

Conclusions

An alternative approach to the synthesis of both pure enantiomers of the tetrasubstituted all-*trans* cyclobutane **6** in five steps and 19 % overall yield has been developed. The stereoinformation is transferred from valinol, guiding a diastereoselective photodimerization that yields three products with interesting stereochemical properties. Also, their methanolysis with potential epimerization of the methyl ketones is a peculiar and intellectually challenging stereochemical problem. As outlined, the cyclobutane (+)-**6** is a key intermediate in the total synthesis of the pyrrole-imidazole alkaloid scorpionin (**2**) that serves itself as a precursor for the synthesis of the related natural products ageliferin (**4**) and nakamuric acid (**5**).^[15] In the work presented here, the absolute configuration of (+)-**6** was re-examined, including by X-ray diffraction analysis, which confirmed the recently revised absolute configurations of this compound and all the natural products that were synthetically obtained from it. The efficient enantioselective approach to both enantiomers of **6** from cheap L- and D-valinol may be of use for the total synthesis of other cyclobutane natural products.

Experimental Section

General Synthetic Methods: All chemicals were obtained from Acros Organics (Geel, Belgium), Sigma Aldrich Chemie GmbH (Steinheim, Germany) or TCI Deutschland GmbH (Eschborn, Germany). All solvents were purified by distillation. Whenever necessary, reactions were carried out under inert atmosphere (Ar) using vacuum-heated flasks and dried solvents (dried according to standard protocols). TLC was performed on 0.20 mm silica plates (Polygram SIL G/UV254) obtained from Macherey–Nagel (Düren, Germany). Column chromatography was performed on Merck silica gel (0.040–0.063 Mesh). NMR spectra were recorded with Bruker AV I (400 MHz), AV III HD Prodigy (500 MHz) and AV III HD Cryo (700 MHz) spectrometers, and were referenced against CDCl_3 ($\delta = 7.26$ ppm), C_6D_6 ($\delta = 7.16$ ppm) and $[\text{D}_3]\text{DMSO}$ ($\delta = 2.50$ ppm) for ^1H NMR, and CDCl_3 ($\delta = 77.01$ ppm), C_6D_6 ($\delta = 128.06$ ppm) and $[\text{D}_6]\text{DMSO}$ ($\delta = 39.52$ ppm) for ^{13}C NMR spectroscopy. The multiplicities are specified as follows: singlet (s), doublet (d), triplet (t), quartet (q), septet (sept.), multiplet (m). GC–MS analyses were carried out with an Agilent HP7890B gas chromatograph connected to a HP5977A mass detector fitted with a HP-5MS silica capillary column (30 m, 0.25 mm i.d., 0.50 μm film). The GC–MS conditions were as follows: 1) inlet pressure: 77.1 kPa, He flow 23.3 mL/min; 2) injection volume: 1 μL ; 3) injection mode: split 50:1, valve time 60 s; 4) oven temperature ramp: 5 min at 50 $^\circ\text{C}$ increasing at 10 $^\circ\text{C}/\text{min}$ to 320 $^\circ\text{C}$; 5) carrier gas He at 1 mL/min; 6) transfer line: 250 $^\circ\text{C}$; 7) electron energy: 70 eV. Retention indices (*I*) were determined from a homologous

series of *n*-alkanes (C_8 – C_{40}). Optical rotary powers were recorded with a P8000 Polarimeter (Krüss). UV/Vis spectra were recorded with a Cary 100 UV/Vis spectrometer (Agilent). IR spectra were recorded with an Alpha FT-IR spectrometer from Bruker. The intensities of the signals are specified as follows: strong (s), medium (m), weak (w), broad (br).

(3S,7aR)-3-Isopropyl-7a-methyltetrahydropyrrolo[2,1-b]oxazol-5(6H)-one [(+)-9]: L-Valinol (7.20 g, 69.8 mmol, 1.0 equiv.) and levulinic acid (8.11 g, 69.8 mmol, 1.0 equiv.) were dissolved in toluene (400 mL) and *p*-toluenesulfonic acid (0.60 g, 3.49 mmol, 0.05 equiv.) was added. The reaction mixture was heated at reflux for 16 h using a Dean–Stark trap. After completion of the reaction the mixture was concentrated and washed with NaHCO_3 (sat. aqueous solution). The organic phase was dried with MgSO_4 and the solvent was removed under reduced pressure. The crude product was purified by column chromatography on silica gel (cyclohexane/ethyl acetate, 3:1) and (+)-**9** (12.0 g, 65.6 mmol, 94 %) was isolated as a colourless oil. $[\alpha]_{\text{D}}^{25} = +84.2$ ($c = 1$, acetone). $R_f = 0.2$. GC (HP-5MS): $I = 1379$. ^1H NMR (400 MHz, CDCl_3): $\delta = 4.14$ (dd, $^2J_{\text{H,H}} = 8.7$, $^3J_{\text{H,H}} = 7.3$ Hz, 1 H, CHH), 3.85 (dd, $^2J_{\text{H,H}} = 8.7$, $^3J_{\text{H,H}} = 6.1$ Hz, 1 H, CHH), 3.59 (ddd, $^3J_{\text{H,H}} = 6.3$, $^3J_{\text{H,H}} = 7.3$, $^3J_{\text{H,H}} = 10.4$ Hz, 1 H, CH), 2.73 (ddd, $^2J_{\text{H,H}} = 17.0$, $^3J_{\text{H,H}} = 9.8$, $^3J_{\text{H,H}} = 9.8$ Hz, 1 H, CHH), 2.46 (ddd, $^2J_{\text{H,H}} = 17.0$, $^3J_{\text{H,H}} = 7.0$, $^3J_{\text{H,H}} = 5.6$ Hz, 1 H, CHH), 2.20–2.12 (m, 2 H, CH_2), 1.73–1.61 (m, 1 H, CH), 1.47 (s, 3 H, CH_3), 1.03 (d, $^3J_{\text{H,H}} = 6.7$ Hz, 3 H, CH_3), 0.88 (d, $^3J_{\text{H,H}} = 6.7$ Hz, 3 H, CH_3) ppm. ^{13}C NMR (100 MHz, CDCl_3): $\delta = 179.0$ (C_q), 100.0 (C_q), 71.1 (CH_2), 61.8 (CH), 34.2 (CH_2), 33.6 (CH), 33.1 (CH_2), 25.1 (CH_3), 20.6 (CH_3), 19.2 (CH_3) ppm. IR (ATR): $\tilde{\nu} = 2959$ (w), 2931 (w), 2872 (w), 1704 (s), 1466 (w), 1347 (s), 1247 (w), 1190 (w), 1020 (m), 879 (m) cm^{-1} . MS (EI, 70 eV): m/z (%) = 183 (32), 168 (87), 154 (18), 140 (100), 126 (19), 112 (32), 100 (46), 82 (55), 69 (23), 55 (24), 43 (30). HRMS (ESI): calcd. for $\text{C}_{10}\text{H}_{17}\text{NNaO}_2^+$ 206.1151; found 206.1151 [M + Na] $^+$.

(3R,7aS)-3-Isopropyl-7a-methyltetrahydropyrrolo[2,1-b]oxazol-5(6H)-one [(–)-9]: Lactam (–)-**9** was synthesized analogously from D-valinol (5.00 g, 48.5 mmol). Yield: 8.08 g (44.1 mmol, 91 %). All recorded spectroscopic data, with the exception of the optical rotary power, were identical to those for (+)-**9**. $[\alpha]_{\text{D}}^{25} = -81.9$ ($c = 1$, acetone).

(3S,7aR)-3-Isopropyl-7a-methyl-2,3-dihydropyrrolo[2,1-b]oxazol-5(7aH)-one [(+)-10]: Diisopropylamine (0.61 g, 6.00 mmol, 2.2 equiv.) was dissolved in dry THF (15 mL) under Ar and cooled to 0 $^\circ\text{C}$. A solution of *n*-butyllithium (1.6 M in hexane, 3.80 mL, 6.00 mmol, 2.2 equiv.) was added dropwise and the mixture was stirred for 30 min and afterwards cooled to –78 $^\circ\text{C}$. A solution of (+)-**9** (0.50 g, 2.73 mmol, 1.0 equiv.) in dry THF (1 mL) was added dropwise and the mixture was stirred for 2 h, followed by dropwise addition of a cooled solution (–78 $^\circ\text{C}$) of PhSeBr (0.77 g, 3.28 mmol, 1.2 equiv.) in dry THF (10 mL). The mixture was warmed to room temperature and stirred overnight, quenched with water and extracted with EtOAc. The combined organic phases were dried with MgSO_4 and the solvent was removed under reduced pressure. The crude selenylation product and pyridine (0.54 g, 6.82 mmol, 2.5 equiv.) were dissolved in DCM (15 mL) and cooled to 0 $^\circ\text{C}$. A 35 % aqueous H_2O_2 solution (0.80 mL, 8.18 mmol, 3.0 equiv.) was added dropwise and the mixture was stirred for 3 h. After completion of the reaction the mixture was quenched with 1 M HCl solution. The organic phase was washed with water and brine and dried with MgSO_4 . After removal of the solvent under reduced pressure, the crude product was purified by column chromatography on silica gel (petroleum ether/diethyl ether, 3:1) and (+)-**10** was obtained as a pale-yellow solid, which was repeatedly washed with cold pentane until a colourless product was obtained (0.34 g, 1.86 mmol,

68 %). $[\alpha]_D^{21} = +48.6$ ($c = 1$, acetone). $R_f = 0.2$. GC (HP-5MS): $l = 1320$. M.p. 49–51 °C. $^1\text{H NMR}$ (500 MHz, C_6D_6): $\delta = 6.37$ (d, $^3J_{\text{H,H}} = 5.8$ Hz, 1 H, CH), 5.64 (d, $^3J_{\text{H,H}} = 5.8$ Hz, 1 H, CH), 3.88 (dd, $^2J_{\text{H,H}} = 8.8$, $^3J_{\text{H,H}} = 7.3$ Hz, 1 H, CHH), 3.64 (dd, $^2J_{\text{H,H}} = 8.8$, $^3J_{\text{H,H}} = 6.0$ Hz, 1 H, CHH), 3.44 (ddd, $^3J_{\text{H,H}} = 10.1$, $^3J_{\text{H,H}} = 7.2$, $^3J_{\text{H,H}} = 6.3$ Hz, 1 H, CH), 1.45 (dsept., $^3J_{\text{H,H}} = 10.1$, $^3J_{\text{H,H}} = 6.6$ Hz, 1 H, CH), 1.17 (s, 3 H, CH_3), 1.10 (d, $^3J_{\text{H,H}} = 6.6$ Hz, 3 H, CH_3), 0.58 (d, $^3J_{\text{H,H}} = 6.6$ Hz, 3 H, CH_3) ppm. $^{13}\text{C NMR}$ (125 MHz, C_6D_6): $\delta = 177.6$ (C_q), 150.6 (CH), 127.9 (CH), 100.4 (C_q), 73.7 (CH_2), 62.7 (CH), 33.2 (CH), 22.3 (CH_3), 20.8 (CH_3), 19.2 (CH_3) ppm. IR (ATR): $\tilde{\nu} = 3089$ (w), 2959 (w), 2930 (w), 2875 (w), 1708 (s), 1671 (m), 1320 (s), 1105 (s), 1011 (m), 892 (s), 833 (m) cm^{-1} . UV/Vis (MeCN): λ_{max} [$\log(\epsilon/\text{M}^{-1}\text{cm}^{-1})$] = 245 [3.187] nm. MS (EI, 70 eV): m/z (%) = 181 (6), 166 (49), 151 (60), 138 (100), 124 (11), 110 (54), 96 (27), 80 (11), 59 (17), 53 (11), 41 (16). HRMS (ESI): calcd. for $\text{C}_{10}\text{H}_{15}\text{NNaO}_2^+$ 204.0995; found 204.0999 [M + Na] $^+$.

(3R,7aS)-3-Isopropyl-7a-methyl-2,3-dihydropyrrolo[2,1-b]-oxazol-5(7aH)-one [(–)-10]: Compound (–)-**10** was synthesized analogously from (–)-**9** (5.00 g, 27.3 mmol). Yield: 3.26 g (18.0 mmol, 66 %). All recorded spectroscopic data, with the exception of the optical rotary power, were identical to those for (+)-**10**. $[\alpha]_D^{21} = -49.3$ ($c = 1$, acetone).

General procedure for the photochemical dimerization of 10: Enone **10** was dissolved at a concentration of 0.1 M in freshly degassed solvent according to Table 1 and irradiated by use of a Rayonet RPR-200 photoreactor. When utilized, photosensitizers were added (5 equiv.) directly to **10**. When irradiation with $\lambda = 250$ nm was conducted, reaction vessels made of fused silica glass were used. The reaction progress was monitored by GC and carried out until all starting material was consumed or after no product formation was detected after 48 h. The solvent was removed under reduced pressure and the crude products were directly subjected to HPLC separation [system: Fa. KNAUER GmbH (Berlin, Germany), two pumps S-1800, assistant 6000 with feedpump S-100 (10 mL pump-head) and electronic injection valve (6 port), UV/Vis detector S-2550 (190–900 nm); column: KNAUER Eurospher II 100-5 C18P, 5 μm , 250 \times 20 mm; solvent: MeCN/ H_2O (45:55); flow rate: 24.0 mL/min]. Fractions containing the target compound were pooled and the solvent was removed by lyophilization. For the different tested reaction conditions, see Table 1.

Photodimers (+)-11b, (+)-11d and (+)-11c: Enone (+)-**10** (0.20 g, 1.10 mmol, 1.0 equiv.) was dissolved in freshly degassed dry MeCN (10 mL) and acetophenone (0.66 g, 5.52 mmol, 5.0 equiv.) was added. The solution was irradiated with $\lambda = 350$ nm until all starting material was consumed (12 h). The solvent was removed under reduced pressure and the crude product mixture was purified by HPLC. After lyophilization (+)-**11b** (74.0 mg, 0.20 mmol, 37 %), (+)-**11d** (64 mg, 0.18 mmol, 32 %) and (+)-**11c** (10 mg, 0.03 mmol, 5 %) were isolated as colourless solids.

Analytical data for (+)-**11b**: $[\alpha]_D^{21} = +193.6$ ($c = 1$, MeOH). GC (HP-5MS): $l = 2642$. M.p. 196–198 °C. $^1\text{H NMR}$ (400 MHz, C_6D_6): $\delta = 3.99$ –3.89 (m, 2 H, 2 CHH), 3.58–3.51 (m, 4 H, 2 CHH, 2 CH), 3.57–3.48 (m, 2 H, 2 CH), 3.31 (m, 2 H, 2 CH), 2.99 (m, 2 H, 2 CH), 1.39–1.27 (m, 2 H, 2 CH), 1.08 (s, 6 H, 2 CH_3), 1.07 (d, $^3J_{\text{H,H}} = 6.7$ Hz, 6 H, 2 CH_3), 0.57 (d, $^3J_{\text{H,H}} = 6.6$ Hz, 6 H, 2 CH_3) ppm. $^{13}\text{C NMR}$ (100 MHz, C_6D_6): $\delta = 176.9$ (2 C_q), 97.8 (2 C_q), 73.0 (2 CH_2), 61.0 (2 CH), 46.1 (2 CH), 42.2 (2 CH), 34.5 (2 CH), 25.5 (2 CH_3), 20.9 (2 CH_3), 19.0 (2 CH_3) ppm. IR (ATR): $\tilde{\nu} = 2957$ (w), 2940 (w), 2875 (w), 1703 (s), 1466 (w), 1352 (s), 1227 (w) 1148 (w), 1047 (w), 1007 (m), 899 (w), 769 (m), 609 (w) cm^{-1} . MS (EI, 70 eV): m/z (%) = 362 (7), 347 (100), 319 (25), 291 (4), 279 (8), 261 (3), 236 (3), 219 (2), 207 (9), 193 (8), 182 (12), 166 (17), 151 (46), 138 (33), 128 (54), 108 (44), 96 (32), 80 (20), 69 (45), 55 (16), 43 (52). HRMS (ESI): calcd. for $\text{C}_{20}\text{H}_{31}\text{N}_2\text{O}_4^+$ 363.2278; found

363.2278 [M + H] $^+$. Optical rotary power of (–)-**11b**: $[\alpha]_D^{21} = -184.2$ ($c = 1$, MeOH).

Analytical data for (+)-**11d**: $[\alpha]_D^{21} = +89.0$ ($c = 1$, acetone). GC (HP-5MS): $l = 2690$. M.p. 189–192 °C. $^1\text{H NMR}$ (500 MHz, C_6D_6): $\delta = 3.87$ (dd, $^2J_{\text{H,H}} = 8.5$, $^3J_{\text{H,H}} = 7.6$ Hz, 1 H, CHH), 3.79 (dd, $^2J_{\text{H,H}} = 8.2$, $^3J_{\text{H,H}} = 8.2$ Hz, 1 H, CHH), 3.67 (ddd, $^3J_{\text{H,H}} = 10.8$, $^3J_{\text{H,H}} = 7.2$, $^3J_{\text{H,H}} = 7.0$ Hz, 1 H, CH), 3.56 (m, 1 H, CH), 3.53 (m, 1 H, CHH), 3.46 (ddd, $^3J_{\text{H,H}} = 10.2$, $^3J_{\text{H,H}} = 7.1$, $^3J_{\text{H,H}} = 7.1$ Hz, 1 H, CH), 3.36 (dd, $^2J_{\text{H,H}} = 8.5$, $^3J_{\text{H,H}} = 6.9$ Hz, 1 H, CHH), 3.00 (m, 1 H, CH), 2.99 (m, 1 H, CH), 2.63 (m, 1 H, CH), 1.43–1.30 (m, 2 H, 2 CH), 1.23 (s, 3 H, CH_3), 1.15 (d, $^3J_{\text{H,H}} = 6.6$ Hz, 3 H, CH_3), 1.07 (d, $^3J_{\text{H,H}} = 6.6$ Hz, 3 H, CH_3), 1.05 (s, 3 H, CH_3), 0.57 (d, $^3J_{\text{H,H}} = 6.6$ Hz, 3 H, CH_3), 0.56 (d, $^3J_{\text{H,H}} = 6.6$ Hz, 3 H, CH_3) ppm. $^{13}\text{C NMR}$ (125 MHz, C_6D_6): $\delta = 182.0$ (C_q), 178.2 (C_q), 100.8 (C_q), 97.9 (C_q), 72.6 (CH_2), 69.0 (CH_2), 64.0 (CH), 61.9 (CH), 45.7 (CH), 44.9 (CH), 44.1 (CH), 41.4 (CH), 34.4 (CH), 34.1 (CH), 25.9 (CH_3), 21.2 (CH_3), 20.9 (CH_3), 20.4 (CH_3), 19.0 (CH_3), 18.9 (CH_3) ppm. IR (ATR): $\tilde{\nu} = 2924$ (w), 2903 (w), 2868 (w), 1694 (s), 1463 (w), 1329 (m), 1138 (w), 1030 (w), 873 (w), 751 (w) cm^{-1} . MS (EI, 70 eV): m/z (%) = 362 (23), 347 (100), 319 (60), 279 (11), 236 (21), 220 (3), 207 (7), 182 (20), 166 (7), 151 (72), 138 (21), 128 (45), 126 (44), 108 (21), 96 (23), 84 (12), 69 (21), 56 (7), 43 (21). HRMS (ESI): calcd. for $\text{C}_{20}\text{H}_{30}\text{N}_2\text{NaO}_4^+$ 385.2098; found 385.2098 [M + Na] $^+$. Optical rotary power of (–)-**11d**: $[\alpha]_D^{21} = -91.5$ ($c = 0.6$, acetone).

Analytical data for (+)-**11c**: $[\alpha]_D^{21} = +5.2$ ($c = 1$, acetone). GC (HP-5MS): $l = 2738$. M.p. 192–193 °C. $^1\text{H NMR}$ (500 MHz, $[\text{D}_6]\text{DMSO}$): $\delta = 4.10$ (dd, $^2J_{\text{H,H}} = 8.4$, $^3J_{\text{H,H}} = 8.4$ Hz, 2 H, 2 CHH), 3.76 (dd, $^2J_{\text{H,H}} = 8.4$, $^3J_{\text{H,H}} = 6.9$ Hz, 2 H, 2 CHH), 3.50 (ddd, $^3J_{\text{H,H}} = 10.7$, $^3J_{\text{H,H}} = 7.5$, $^3J_{\text{H,H}} = 7.5$ Hz, 2 H, 2 CH), 3.04 (m, 2 H, 2 CH), 2.98 (m, 2 H, 2 CH), 1.76–1.64 (m, 2 H, 2 CH), 1.50 (s, 6 H, 2 CH_3), 0.98 (d, $^3J_{\text{H,H}} = 6.6$ Hz, 6 H, 2 CH_3), 0.85 (d, $^3J_{\text{H,H}} = 6.6$ Hz, 6 H, 2 CH_3) ppm. $^{13}\text{C NMR}$ (125 MHz, $[\text{D}_6]\text{DMSO}$): $\delta = 181.2$ (2 C_q), 100.3 (2 C_q), 68.0 (2 CH_2), 63.8 (2 CH), 42.6 (2 CH), 42.1 (2 CH), 32.8 (2 CH), 20.9 (2 CH_3), 19.3 (2 CH_3), 18.8 (2 CH_3) ppm. IR (ATR): $\tilde{\nu} = 2963$ (w), 2951 (w), 2872 (w), 1718 (s), 1459 (w), 1296 (m), 1280 (m), 1181 (m), 1071 (w), 999 (w), 986 (w), 863 (s), 695 (w) cm^{-1} . MS (EI, 70 eV): m/z (%) = 362 (21), 347 (27), 319 (40), 295 (5), 279 (5), 235 (13), 182 (9), 151 (100), 138 (19), 128 (60), 108 (60), 96 (20), 84 (10), 69 (16), 56 (6), 43 (20). HRMS (ESI): calcd. for $\text{C}_{20}\text{H}_{30}\text{N}_2\text{NaO}_4^+$ 385.2098; found 385.2098 [M + Na] $^+$.

Dimethyl (1R,2R,3S,4S)-3,4-Diacetylcyclobutane-1,2-dicarboxylate [(+)-6]: Photodimerization product (+)-**11b** (62.0 mg, 0.17 mmol, 1.0 equiv.) was dissolved in MeOH (10 mL) and conc. H_2SO_4 (1 mL) was added carefully. The reaction mixture was heated at 70 °C for 6 h. After completion of the reaction, the mixture was diluted with EtOAc and washed with water. The organic phase was dried with MgSO_4 and the solvent was removed under reduced pressure. The crude product was purified by column chromatography on silica gel (petroleum ether/diethyl ether, 1:1) and (+)-**6** (34.0 mg, 0.13 mmol, 78 %, 98 % ee, Figure 4) was isolated as a colourless solid. $[\alpha]_D^{21} = +30.3$ ($c = 1$, CHCl_3). $R_f = 0.3$. GC (HP-5MS): $l = 1663$. M.p. 76–78 °C. $^1\text{H NMR}$ (500 MHz, CDCl_3): $\delta = 3.75$ (s, 6 H, 2 CH_3), 3.51 (dd, $J = 9.5$, 2.4 Hz, 2 H, 2 CH), 3.40 (dd, $J = 9.5$, 2.4 Hz, 2 H, 2 CH), 2.20 (s, 6 H, 2 CH_3) ppm. $^{13}\text{C NMR}$ (125 MHz, CDCl_3): $\delta = 205.0$ (C_q), 171.8 (C_q), 52.7 (CH_3), 46.6 (CH), 39.1 (CH), 27.9 (CH_3) ppm. IR (ATR): $\tilde{\nu} = 2964$ (w), 2922 (w), 2903 (w), 2865 (w), 1695 (s), 1461 (w), 1347 (m), 1168 (m), 1114 (m), 874 (w), 773 (w), 683 (w) cm^{-1} . MS (EI, 70 eV): m/z (%) = 256 (3), 241 (7), 224 (33), 213 (19), 196 (1), 182 (21), 171 (10), 164 (5), 153 (25), 140 (22), 123 (12), 111 (26), 95 (14), 85 (6), 59 (11), 43 (100). HRMS (ESI): calcd. for $\text{C}_{12}\text{H}_{16}\text{NaO}_6^+$ 279.0839; found 279.0839 [M + Na] $^+$.

Dimethyl (1S,2S,3R,4R)-3,4-Diacetylcyclobutane-1,2-dicarboxylate [(–)-6]: Compound (–)-**6** was synthesized by acidic cleavage of

either (+)-**11c** (yield: 8.00 mg, 0.03 mmol, 71 %, 98 % *ee*, Figure 4) or (–)-**11b** (yield: 12.0 mg, 0.05 mmol, 78 %, 98 % *ee*, Figure 4) following the same procedure as used for (+)-**6**. All recorded spectroscopic data, with the exception of the optical rotary power, were identical to those for (+)-**6**. $[\alpha]_D^{25} = -30.0$ ($c = 1$, CHCl_3).

Dimethyl (1R,2R,3S,4S)-2,4-Diacetylcyclobutane-1,3-dicarboxylate (12a) and Dimethyl (1R,2R,3S,4S)-2,4-Diacetylcyclobutane-1,3-dicarboxylate (12b): Photodimerization product (+)-**11d** (36.0 mg, 0.10 mmol, 1.0 equiv.) was dissolved in MeOH (3 mL) and conc. H_2SO_4 (0.3 mL) was added carefully. The reaction mixture was heated at 70 °C for 16 h. After complete reaction, the mixture was diluted with EtOAc and washed with water. The organic phase was dried with MgSO_4 and the solvent was removed under reduced pressure. The crude product was purified by column chromatography on silica gel (petroleum ether/diethyl ether, 1:2) and **12a** (9.00 mg, 0.035 mmol, 35 %) and **12b** (4.00 mg, 0.016 mmol, 16 %) were isolated as colourless solids.

Analytical data for **12a**: $R_f = 0.3$. GC (HP-5MS): $I = 1729$. M.p. 77–78 °C. ^1H NMR (500 MHz, CDCl_3): $\delta = 3.84\text{--}3.77$ (m, 2 H, 2 CH), 3.73–3.67 (m, 2 H, 2 CH), 3.69 (s, 6 H, 2 CH_3), 2.20 (s, 6 H, 2 CH_3) ppm. ^{13}C NMR (125 MHz, CDCl_3): $\delta = 205.7$ (2 C_q), 171.8 (2 C_q), 52.5 (2 CH_3), 47.2 (2 CH), 40.4 (2 CH), 29.4 (2 CH_3) ppm. IR (ATR): $\tilde{\nu} = 3005$ (w), 2954 (w), 2921 (w), 2851 (w), 1722 (s), 1706 (s), 1440 (m), 1358 (m), 1298 (w), 1233 (s), 1193 (s), 1073 (m), 1038 (w), 982 (w), 953 (w), 935 (w), 797 (m), 724 (w), 661 (w), 510 (w) cm^{-1} . MS (EI, 70 eV): m/z (%) = 256 (3), 241 (9), 225 (22), 214 (9), 209 (3), 196 (10), 182 (26), 171 (19), 155 (6), 150 (43), 140 (35), 139 (35), 123 (20), 111 (25), 95 (14), 79 (2), 69 (2), 59 (4), 43 (100). HRMS (ESI): calcd. for $\text{C}_{12}\text{H}_{16}\text{NaO}_6^+$ 279.0839; found 279.0839 [M + Na] $^+$.

Analytical data for **12b**: $R_f = 0.2$. GC (HP-5MS): $I = 1689$. M.p. 99–101 °C. ^1H NMR (500 MHz, CDCl_3): $\delta = 4.06$ (dd, $^3J_{\text{H,H}} = 10.0$, $^3J_{\text{H,H}} = 10.0$ Hz, 1 H, CH), 3.78 (s, 3 H, CH_3), 3.67 (s, 3 H, CH_3), 3.67 (dd, $^3J_{\text{H,H}} = 9.0$, $^3J_{\text{H,H}} = 9.0$ Hz, 1 H, CH), 3.40 (dd, $^3J_{\text{H,H}} = 9.5$, $^3J_{\text{H,H}} = 9.5$ Hz, 2 H, 2 CH), 2.13 (s, 6 H, 2 CH_3) ppm. ^{13}C NMR (125 MHz, CDCl_3): $\delta = 204.6$ (2 C_q), 172.9 (C_q), 172.0 (C_q), 52.7 (CH_3), 52.4 (CH_3), 46.4 (2 CH), 42.9 (CH), 41.4 (CH), 27.5 (2 CH_3) ppm. IR (ATR): $\tilde{\nu} = 3003$ (w), 2942 (w), 2919 (w), 2851 (w), 1717 (s), 1706 (s), 1441 (m), 1378 (w), 1358 (w), 1282 (s), 1184 (m), 1158 (s), 1132 (s), 1054 (m), 1040 (w), 996 (w), 934 (m), 806 (w), 589 (w), 486 (w) cm^{-1} . MS (EI, 70 eV): m/z (%) = 256 (<1), 241 (9), 224 (56), 214 (3), 209 (4), 193 (12), 181 (15), 171 (12), 165 (4), 155 (4), 150 (40), 139 (30), 123 (12), 111 (25), 95 (13), 85 (9), 59 (5), 59 (12), 43 (100). HRMS (ESI): calcd. for $\text{C}_{12}\text{H}_{16}\text{NaO}_6^+$ 279.0839; found 279.0839 [M + Na] $^+$.

($^2\text{H}_6$)Dimethyl (1R,2R,3S,4S)-($^2\text{H}_8$)-3,4-Diacetylcyclobutane-1,2-dicarboxylate [($^2\text{H}_{14}$)-6**]:** Photodimer (+)-**11b** (19.0 mg, 0.05 mmol) was dissolved in ($^2\text{H}_4$)methanol (3 mL) and ($^2\text{H}_2$)sulfuric acid (98 % in D_2O , 0.3 mL) was added carefully. The reaction was heated for 16 h at 70 °C, diluted with D_2O (10 mL) and extracted with DCM. The organic phase was dried with MgSO_4 and the solvent was removed under reduced pressure to yield ($^2\text{H}_{14}$)-**6** (11.0 mg, 0.04 mmol, 78 %). GC (HP-5MS): $I = 1650$. MS (EI, 70 eV): m/z (%) = 270 (3), 252 (7), 235 (33), 224 (17), 216 (5), 206 (4), 200 (4), 188 (5), 180 (5), 172 (3), 161 (10), 155 (9), 146 (11), 116 (41), 100 (8), 62 (8), 46 (100). For the NMR spectroscopic data, see Table S1 in the Supporting Information.

Analysis of the Enantiomeric Excess of 6: The enantiomeric excesses of (+)- and (–)-**6** obtained from acidic cleavage of either (+)-**11b**, (–)-**11b** or (+)-**11c** were analysed by HPLC using the following conditions: system: Fa. Knauer GmbH (Berlin, Germany), HPG-pump P6.1L, oven CT 2.1, photodiode array detector DAD 6.1L (190–

1020 nm); column: DAICEL Chiralpak IB; 5 μm , 4.6 mm \times 250 mm; solvent: *n*-hexane/2-propanol (85:15); flow rate: 1.0 mL/min; pressure: 42 bar; temperature: 25 °C.

CCDC 1552548 [for (+)-**11b**], and 1552549 [for (+)-**6**] contain the supplementary crystallographic data for this paper. These data can be obtained free of charge from The Cambridge Crystallographic Data Centre.

Acknowledgments

This work was funded by the Deutsche Forschungsgemeinschaft (DFG) (DI1536/9-1). We thank Dr. Gregor Schnakenburg for X-ray analysis and Prof. Dr. Alexander C. Filippou for access to the instruments for these analyses.

Keywords: Photochemistry · Small ring systems · Chiral auxiliaries · Natural products

- [1] a) Y. J. Hong, D. J. Tantillo, *Chem. Soc. Rev.* **2014**, *43*, 5042–5050; b) Y.-Y. Fan, X.-H. Gao, J.-M. Yue, *Sci. China Chem.* **2016**, *59*, 1126–1141; c) V. M. Dembitsky, *Phytomedicine* **2014**, *21*, 1559–1581.
- [2] Y.-S. Wang, B.-T. Li, S.-X. Liu, Z.-Q. Wen, J.-H. Yang, H.-B. Zhang, X.-J. Hao, *J. Nat. Prod.* **2017**, *80*, 798–804.
- [3] R. P. Walker, D. J. Faulkner, D. Van Engen, J. Clardy, *J. Am. Chem. Soc.* **1981**, *103*, 6772–6773.
- [4] a) T. Lindel, *Alkaloids* **2017**, *77*, 117–219; b) M. A. Beniddir, L. Evanno, D. Joseph, A. Skiredj, E. Poupon, *Nat. Prod. Rep.* **2016**, *33*, 820–842; c) V. M. Dembitsky, *J. Nat. Med.* **2008**, *62*, 1–33.
- [5] a) V. S. Bernan, D. M. Roll, C. M. Ireland, M. Greenstein, W. M. Maiese, D. A. Steinberg, *J. Antimicrob. Chemother.* **1993**, *32*, 539–550; b) R. Rosa, W. Silva, G. Escalona de Motta, A. D. Rodriguez, J. J. Morales, M. Ortiz, *Experientia* **1992**, *48*, 885–887; c) R. Mohammed, J. Peng, M. Kelly, M. T. Hamann, *J. Nat. Prod.* **2006**, *69*, 1739–1744; d) A. Vassas, G. Bourdy, J. J. Paillard, J. Lavayre, M. Pais, J. C. Quirion, C. Debitus, *Planta Med.* **1996**, *62*, 28–30; e) P. A. Keifer, R. E. Schwartz, M. E. S. Koker, R. G. Hughes, D. Rittschof, K. L. Rinehart, *J. Org. Chem.* **1991**, *56*, 2965–2975; f) A. D. Rodriguez, M. J. Lear, J. J. La Clair, *J. Am. Chem. Soc.* **2008**, *130*, 7256–7258; g) A. Cipres, D. P. O'Malley, K. Li, D. Finlay, P. S. Baran, K. Vuori, *ACS Chem. Biol.* **2010**, *5*, 195–202.
- [6] J. Kobayashi, M. Tsuda, T. Murayama, H. Nakamura, Y. Ohizumi, M. Ishibashi, M. Iwamura, T. Ohta, S. Nozoe, *Tetrahedron* **1990**, *46*, 5579–5586.
- [7] C. Eder, P. Proksch, V. Wray, R. W. M. van Soest, E. Ferdinandus, L. A. Pattisina, *Sudarsono, J. Nat. Prod.* **1999**, *62*, 1295–1297.
- [8] Y.-T. Sun, B. Lin, S.-G. Li, M. Liu, Y.-J. Zhou, Y. Xu, H.-M. Hua, H. W. Lin, *Tetrahedron* **2017**, *73*, 2786–2792.
- [9] a) S. Poplata, A. Tröster, Y.-Q. Zou, T. Bach, *Chem. Rev.* **2016**, *116*, 9748–9815; b) W. R. Gutekunst, P. S. Baran, *J. Org. Chem.* **2014**, *79*, 2430–2452; c) T. Bach, J. P. Hehn, *Angew. Chem. Int. Ed.* **2011**, *50*, 1000–1045; *Angew. Chem.* **2011**, *123*, 1032; d) E. Lee-Ruff, G. Mladenova, *Chem. Rev.* **2003**, *103*, 1449–1483.
- [10] P. S. Baran, A. L. Zografos, D. P. O'Malley, *J. Am. Chem. Soc.* **2004**, *126*, 3726–3727.
- [11] P. S. Baran, K. Li, D. P. O'Malley, C. Mitsos, *Angew. Chem. Int. Ed.* **2006**, *45*, 255–258; *Angew. Chem.* **2006**, *118*, 261.
- [12] Z. Ma, X. Wang, X. Wang, R. A. Rodriguez, C. E. Moore, S. Gao, X. Tan, Y. Ma, A. L. Rheingold, P. S. Baran, C. Chen, *Science* **2014**, *346*, 219–224.
- [13] A. I. Meyers, S. A. Fleming, *J. Am. Chem. Soc.* **1986**, *108*, 306–307.
- [14] A. I. Meyers, J. L. Romine, S. A. Fleming, *J. Am. Chem. Soc.* **1988**, *110*, 7245–7247.
- [15] D. P. O'Malley, K. Li, M. Maue, A. L. Zografos, P. S. Baran, *J. Am. Chem. Soc.* **2007**, *129*, 4762–4775.

Received: June 20, 2017

Eur. J. Org. Chem. **2017** • ISSN 1099–0690

<https://doi.org/10.1002/ejoc.201700882>

SUPPORTING INFORMATION

Title: Sceptin – Enantioselective Synthesis of a Tetrasubstituted all-*trans* Cyclobutane Key Intermediate

Author(s): Lena Barra, Jeroen S. Dickschat*

TABLE OF CONTENTS

1. SYMMETRY PROPERTIES OF PHOTODIMERS AND HYDROLYSIS PRODUCTS	3
2. LABELING STUDY	4-6
3. CRYSTALLOGRAPHIC DATA	7-8
4. NMR SPECTRA OF SYNTHETIC COMPOUNDS	9-56
5. REFERENCES	57

1. SYMMETRY PROPERTIES OF PHOTODIMERS AND HYDROLYSIS PRODUCTS

Table S1. Symmetry properties of photodimers.

Dimer	Point group	Expected no. of ^{13}C -NMR signals	Hydrolysis product(s) ^[a]
11a	C_1	20	6c (6b, 6e)
11b	C_2	10	6d (6a, 6)
11c	C_2	10	<i>ent</i> - 6d (ent-6a, ent-6)
11d	C_1	20	12a (12b)
11e	C_2	10	12d (12c, 12e)
11f	C_2	10	12d (12c, 12e)

[a] Initial hydrolysis product plus products formed by epimerisation(s) at α -carbons of methyl ketones (in brackets).

Table S2. Symmetry properties of hydrolysis products.

Compound	Point group	Expected no. of ^{13}C -NMR signals	Equivalent groups ^[a]
6	C_2	6	esters, ketones
12a	C_i	6	esters, ketones
12b	C_s	9	ketones
12c	C_s	9	esters
12d	C_{2v}	6	esters, ketones
12e	C_{2v}	6	esters, ketones
6a	C_1	12	–
6b	C_1	12	–
6c	C_s	6	esters, ketones
6d	C_2	6	esters, ketones
6e	C_s	6	esters, ketones

[a] Superimposable by symmetry operation and magnetically equivalent in NMR.

2. LABELING STUDY

Table S3. NMR data of **6** and (²H₁₄)-**6**.

C ^[a]	¹³ C (δ) of 6 ^[b]	¹ H (δ, m, <i>J</i>) of 6	¹³ C (δ, m, <i>J</i>) of (² H ₁₄)- 6 ^[b]	¹ H (δ, m) of (² H ₁₄)- 6
1	171.7 (C _q)	–	171.7 (s)	–
2	39.3 (CH)	3.46 (m)	39.2 (s)	3.45 (s)
3	46.8 (CH)	3.39 (m)	CH (8%): 46.7 (s) CD (92%): 46.3 (t, ¹ <i>J</i> _{C,D} = 21.4)	–
4	203.8 (C _q)	–	203.9 (s)	–
5	27.2 (CH ₃)	1.78 (s)	CHD ₂ (18%): 26.8 (quin, ¹ <i>J</i> _{C,D} = 19.5) CD ₃ (82%): 26.5 (sept, ¹ <i>J</i> _{C,D} = 19.6)	–
6	51.9 (CH ₃)	3.23 (s)	51.1 (sept, ¹ <i>J</i> _{C,D} = 22.4)	–

[a] Carbon numbering as shown in Figure S1. [b] ¹³C NMR data (175 MHz) recorded in C₆D₆. Chemical shifts δ in ppm, multiplicities m, coupling constants *J* are given in Hertz, differing degree of deuteration given in % by peak integration, assignment of carbons by ¹³C DEPT 135 and HSQC spectroscopy. [c] ¹H NMR data (700 MHz) recorded in C₆D₆. Chemical shifts δ in ppm, multiplicities m, coupling constants *J* are given in Hertz.

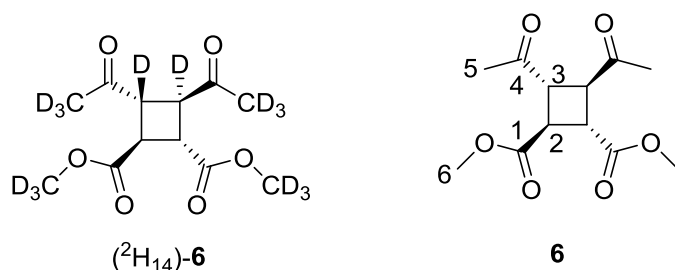


Figure S1. Structure of (²H₁₄)-**6** and carbon numbering for **6**.

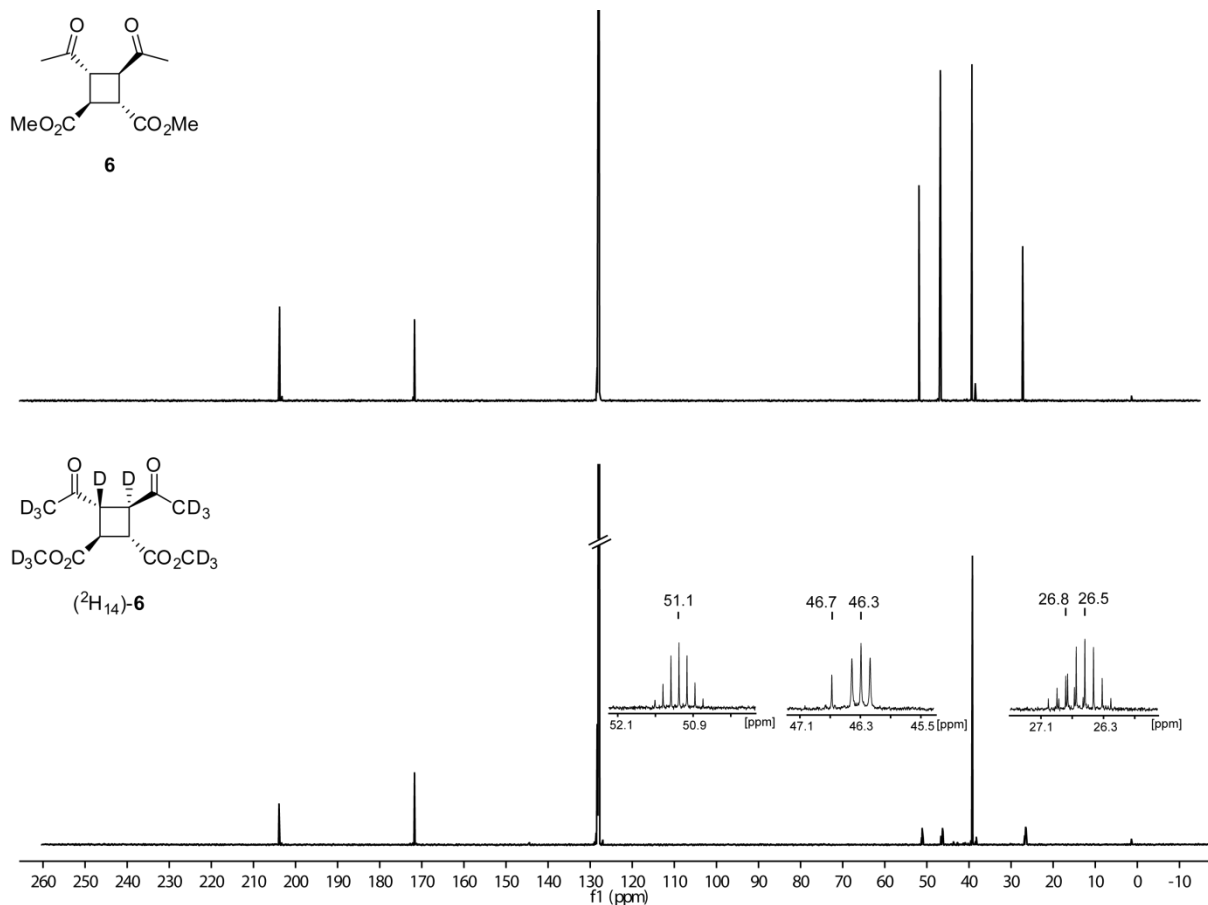


Figure S2. Comparison of ^{13}C NMR data of **6** and $(^2\text{H}_{14})\text{-6}$ (175 MHz, C_6D_6).

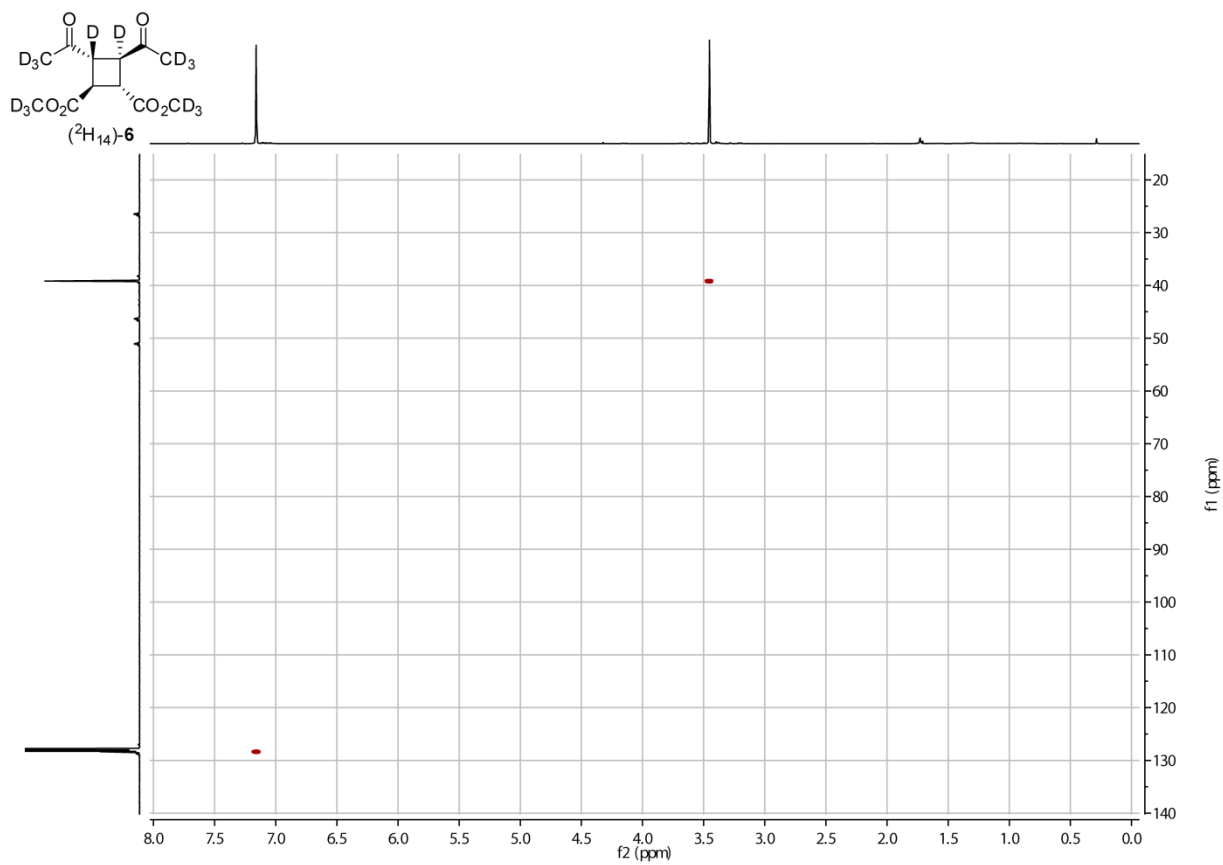


Figure S3. HSQC spectrum of $(^2\text{H}_{14})\text{-6}$.

3. CRYSTALLOGRAPHIC DATA

For both (+)-**6** and (+)-**11b** clear colorless needles were obtained from slow evaporation of a concentrated solution in C₆D₆. The data collections were performed on a Bruker D8-Venture diffractometer ((Bruker CMOS-Photon100 detector)) equipped with a low temperature device (Oxford Cryostream 800er series, Oxford Cryosystems, 100K) using Cu K_α radiation ($\lambda = 1.54178 \text{ \AA}$, monochromated by a HELIOS multilayer optics). Intensities were measured by fine-slicing ω - and ϕ -scans and corrected for background, polarization and Lorentz effects. A semi-empirical (mulabs) absorption correction¹ was carried out on both data sets. The structures were solved by a dual-space method (SHELXT-2014)² and refined by full-matrix least squares on F² (SHELXL-2014).³ All non-hydrogen atoms were refined anisotropically. Hydrogen atoms at carbon were placed in calculated positions and refined isotropically using a riding model. CCDC-1552549 {(+)-**6**} and CCDC-1552548 {(+)-**11b**} contain the supplementary data for these structures. These data can be obtained free of charge via www.ccdc.cam.ac.uk/data_request/cif, or by emailing data_request@ccdc.cam.ac.uk, or by contacting The Cambridge Crystallographic Data Centre, 12, Union Road, Cambridge CB2 1EZ, UK; fax: +44 1223 336033.

Table S4. Details of X-ray crystal structure determination of (+)-**6**.

Crystal habitus	clear colorless needle	μ/mm^{-1}	0.919
Device type	Bruker D8-Venture	F(000)	272.0
Empirical formula	C ₁₂ H ₁₆ O ₆	Crystal size/mm ³	0.18 x 0.08 x 0.04
Moiety formula	C ₁₂ H ₁₆ O ₆	Absorption correction	empirical
Formula weight	256.25	Tmin; Tmax	0.4435; 0.7535
Temperature/K	100	Radiation	CuK α ($\lambda = 1.54178$)
Crystal system	monoclinic	2 range for data collection/°	10.806 to 135.464
Space group	P2 ₁	Completeness to theta	0.998
a/Å	5.0361(3)	Index ranges	-6≤h≤6, -18≤k≤18, -10≤l≤9
b/Å	15.3716(9)	Reflections collected	9291
c/Å	8.4503(5)	Independent reflections	2269 [R _{int} = 0.0793, R _{sigma} = 0.0615]
α /°	90	Data/restrain/parameters	2269/1/167
β /°	104.335(4)	Goodness-of-fit F ²	1.054
γ /°	90	Final R indexes [I>2 σ (I)]	R ₁ = 0.0401, wR ₂ = 0.0920
Volume/ Å ³	633.79(7)	Final R indexes [all data]	R ₁ = 0.0484, wR ₂ = 0.0968
Z	2	Largest diff. peak/hole / eÅ ⁻³	0.20/-0.30
ρ_{calc} [g/cm ³]	1.343	Flack parameter	0.12(16)

Table S5. Details of X-ray crystal structure determination of (+)-**11b**.

Crystal habitus	clear colorless needle	μ/mm^{-1}	0.693
Device type	Bruker D8- Venture	F(000)	392.0
Empirical formula	$\text{C}_{20}\text{H}_{30}\text{N}_2\text{O}_4$	Crystal size/ mm^3	0.3 x 0.15 x 0.1
Moiety formula	$\text{C}_{20}\text{H}_{30}\text{N}_2\text{O}_4$	Absorption correction	empirical
Formula weight	362.46	Tmin; Tmax	0.4153; 0.7536
Temperature/K	122.99	Radiation	$\text{CuK}\alpha$ ($\lambda = 1.54178$)
Crystal system	monoclinic	2 range for data collection/ $^\circ$	7.236 to 135.444
Space group	$\text{P}2_1$	Completeness to theta	1.000
a/ Å	12.3155(12)	Index ranges	$-14 \leq h \leq 14, -7 \leq k \leq 6, -14 \leq l \leq 14$
b/ Å	6.4811(6)	Reflections collected	26213
c/ Å	12.3723(11)	Independent reflections	3443 [$R_{\text{int}} = 0.0817, R_{\text{sigma}} = 0.0448$]
$\alpha/^\circ$	90	Data/restrain/parameters	3443/2/242
$\beta/^\circ$	99.081(6)	Goodness-of-fit F^2	1.048
$\gamma/^\circ$	90	Final R indexes [$I \geq 2\sigma(I)$]	$R_1 = 0.0457, wR_2 = 0.1071$
Volume/ Å^3	975.16(16)	Final R indexes [all data]	$R_1 = 0.0534, wR_2 = 0.1141$
Z	2	Largest diff. peak/hole / $\text{e}\text{Å}^{-3}$	0.18/-0.28
ρ_{calc} [g/cm^3]	1.234	Flack parameter	0.3(3)

4. NMR SPECTRA OF SYNTHETIC COMPOUNDS

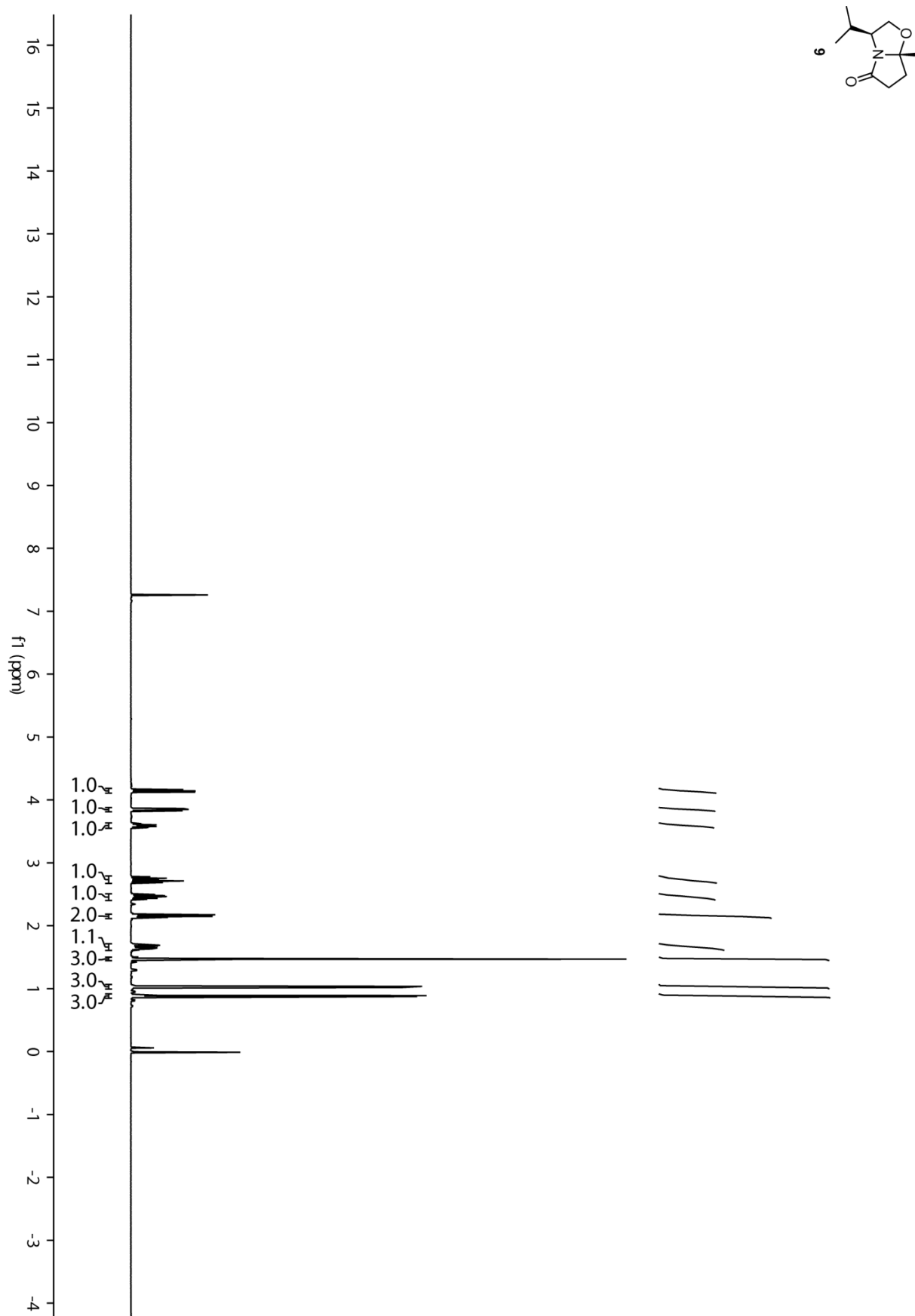


Figure S4. ^1H NMR spectrum of **9** (400 MHz, CDCl_3).

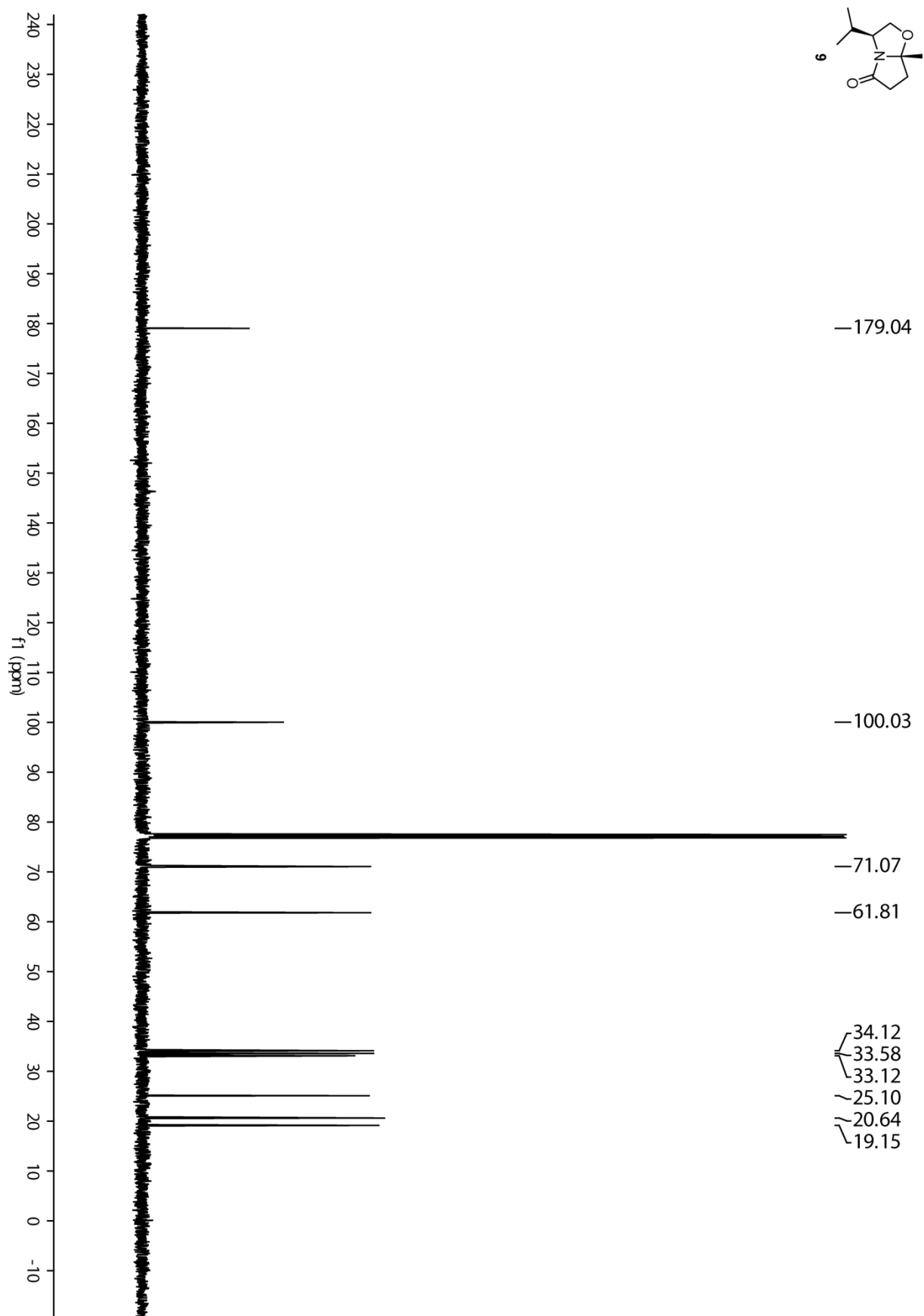


Figure S5. ^{13}C NMR spectrum of **9** (100 MHz, CDCl_3).

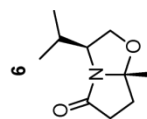
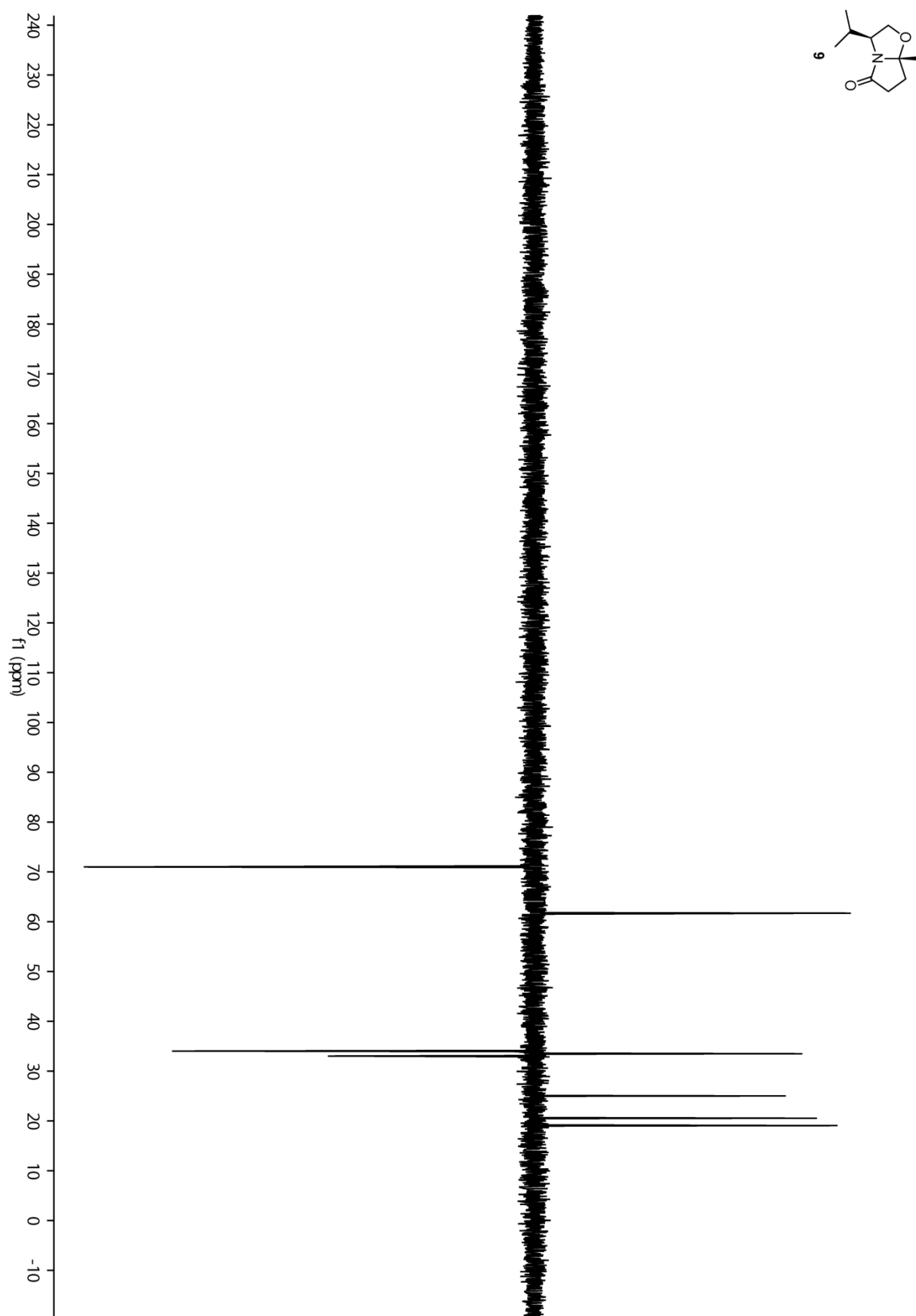


Figure S6. ^{13}C DEPT 135 spectrum of **9** (100 MHz, CDCl_3).

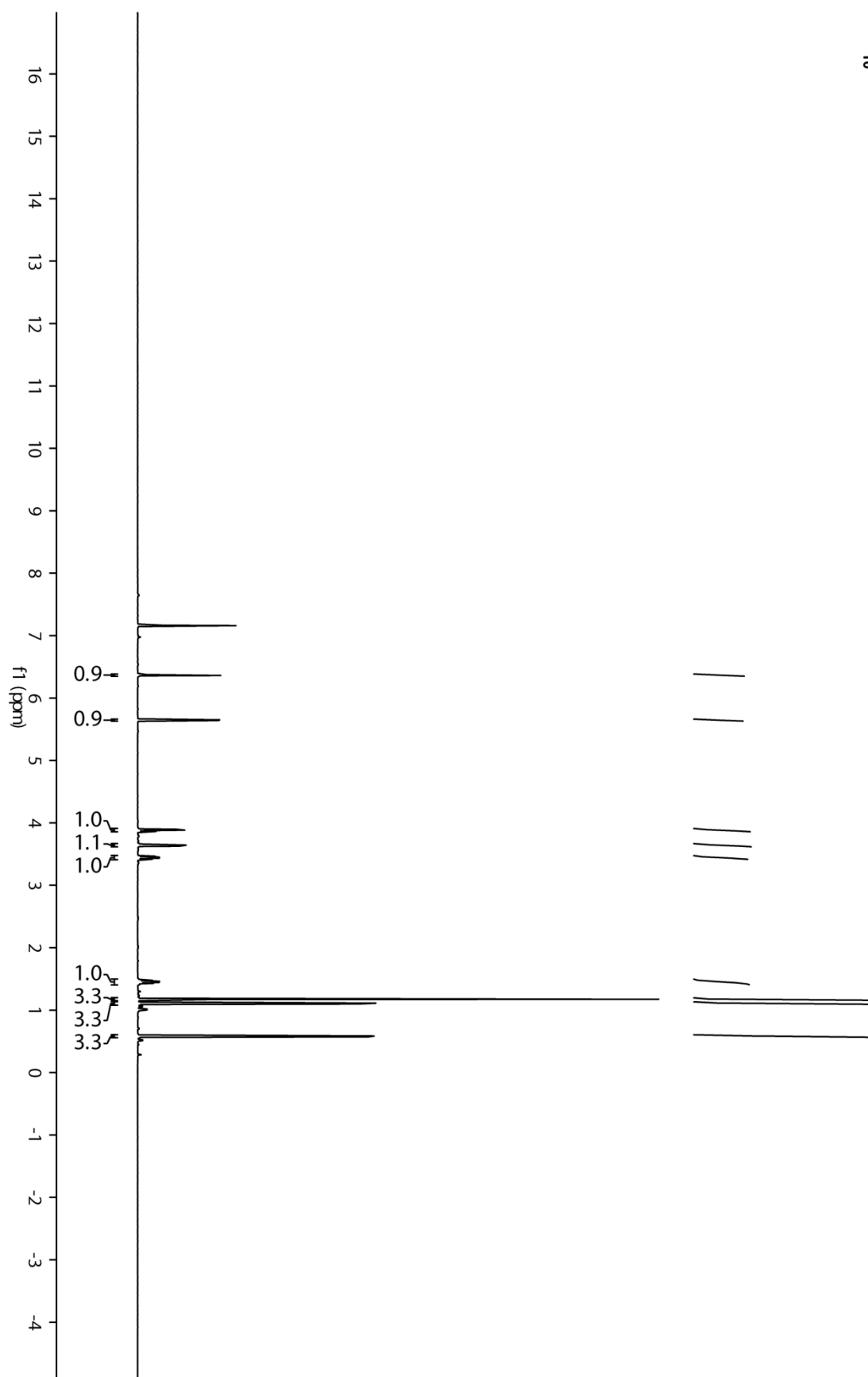
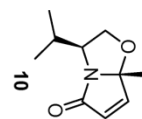


Figure S7. ^1H NMR of **10** (500 MHz, C_6D_6).

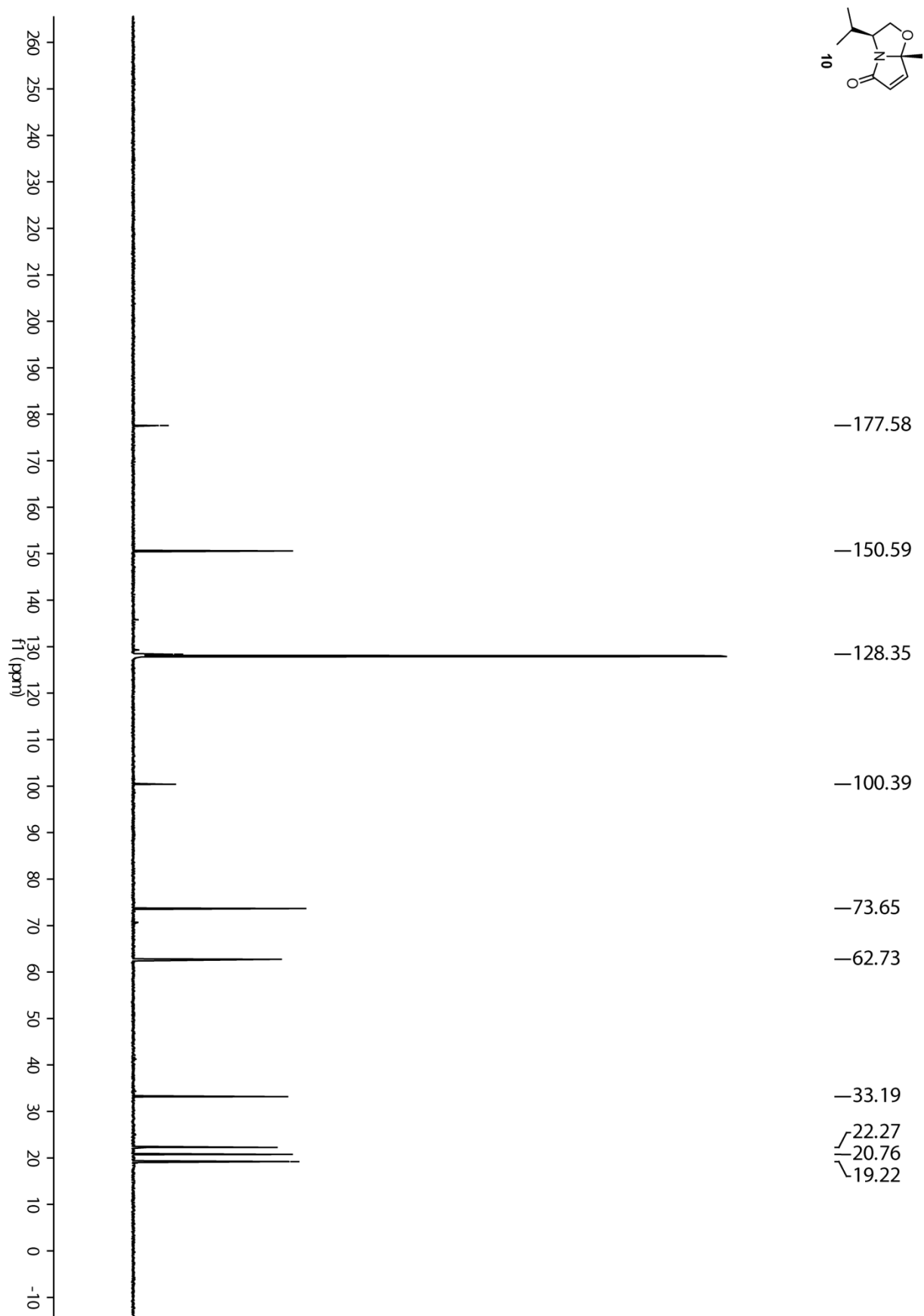


Figure S8. ^{13}C NMR spectrum of **10** (125 MHz, C_6D_6).

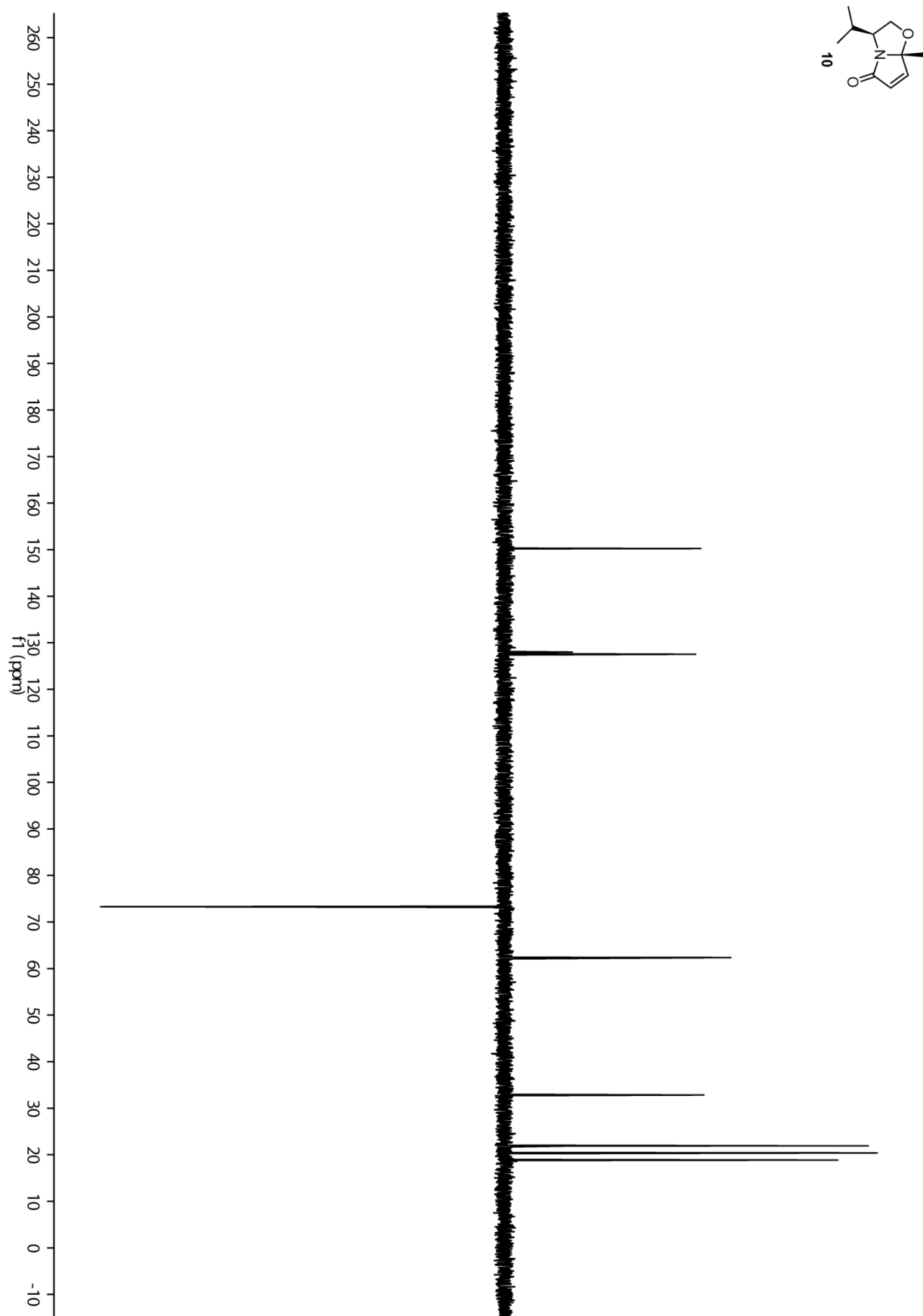


Figure S9. ^{13}C DEPT 135 spectrum of **10** (125 MHz, C_6D_6).

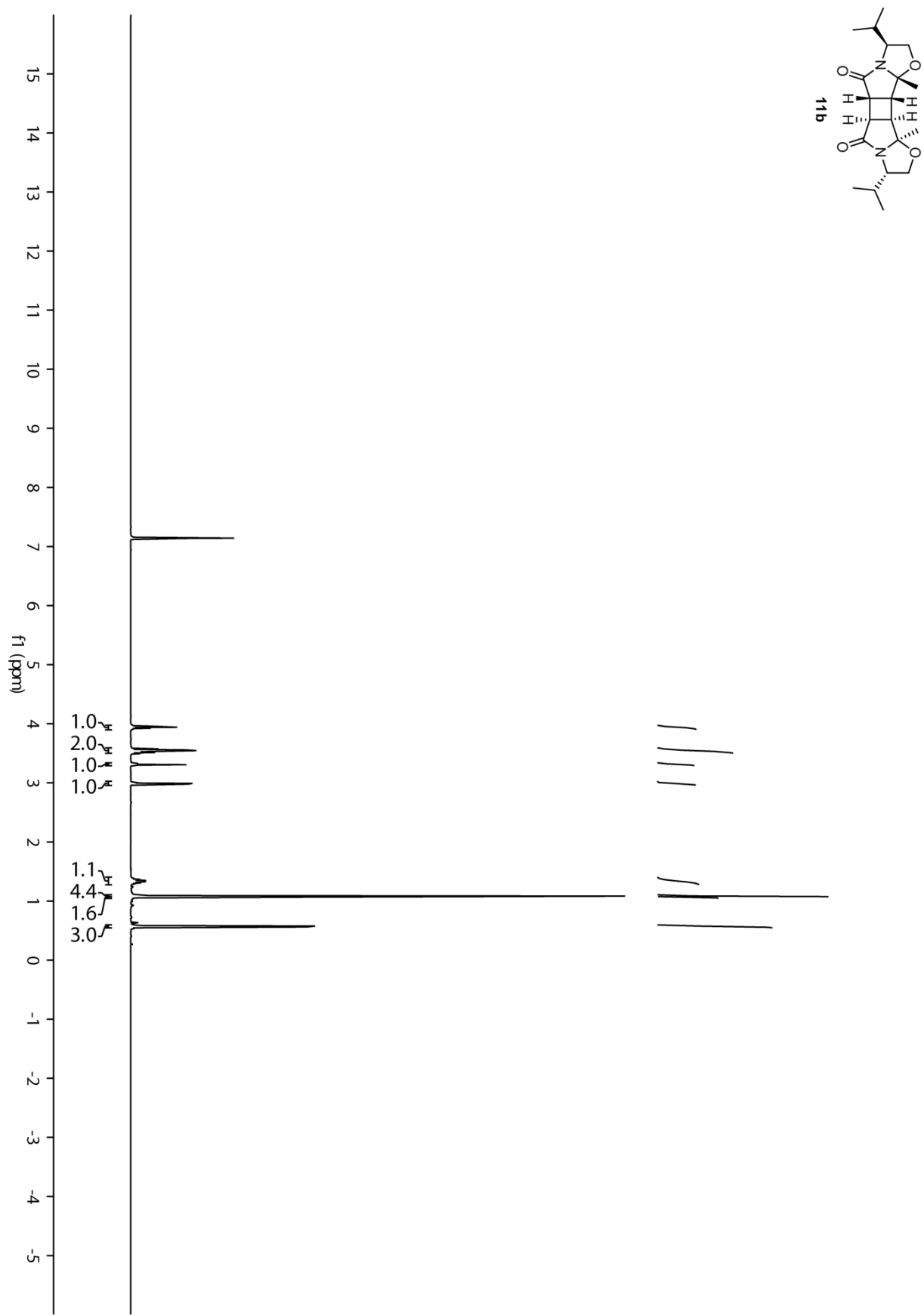


Figure S10. ¹H NMR spectrum of **11b** (400 MHz, C₆D₆).

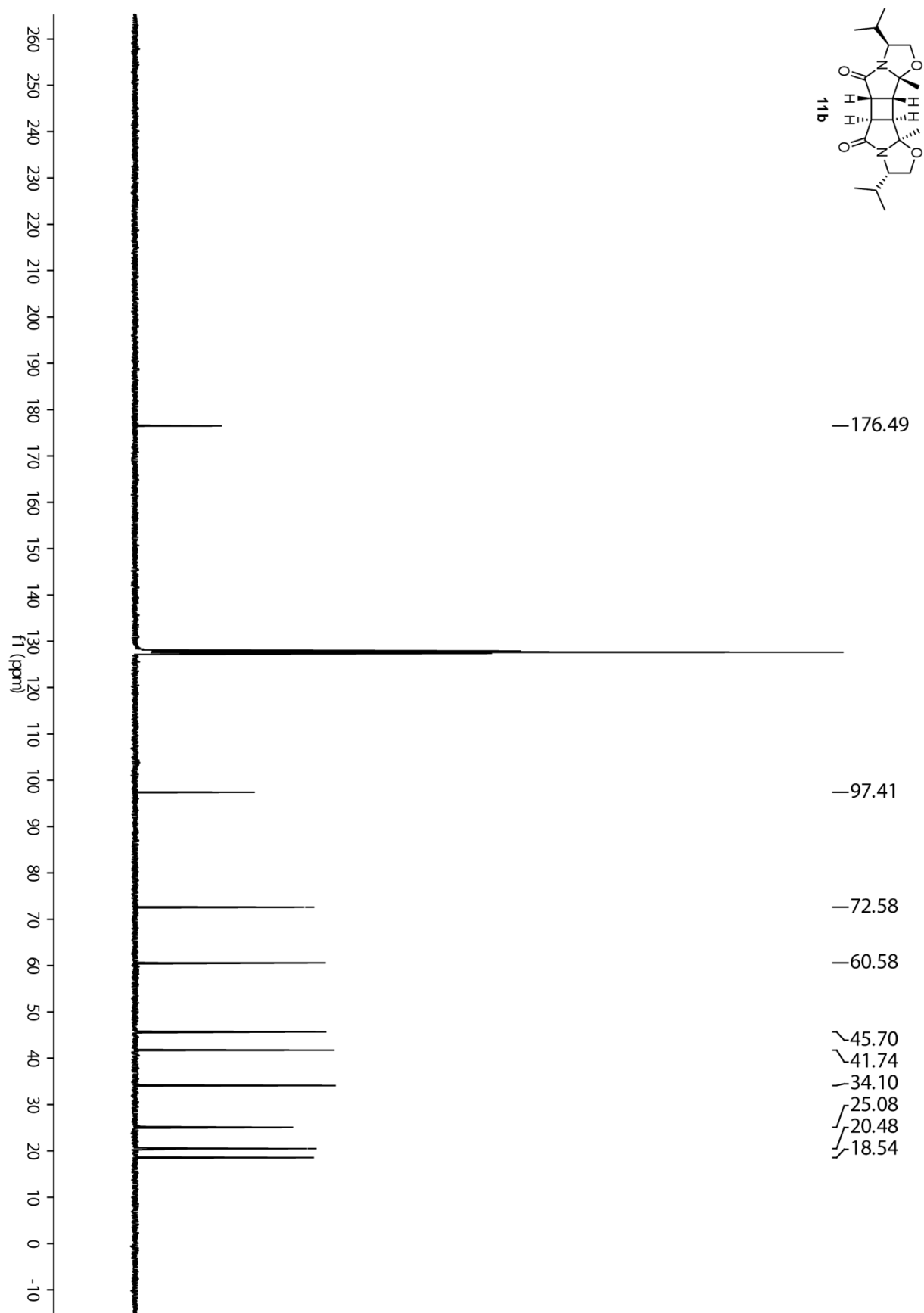


Figure S11. ^{13}C NMR spectrum of **11b** (125 MHz, C_6D_6).

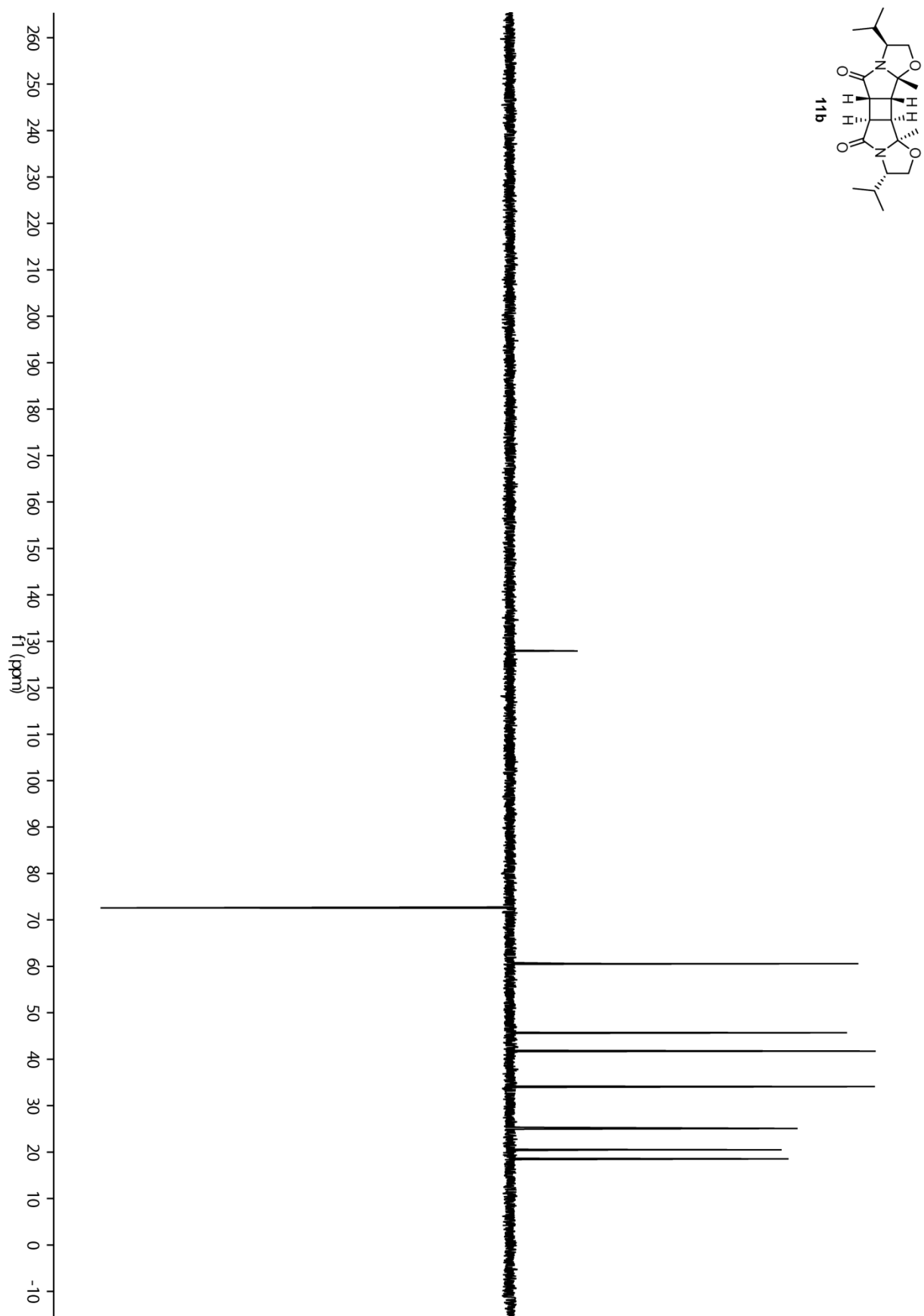
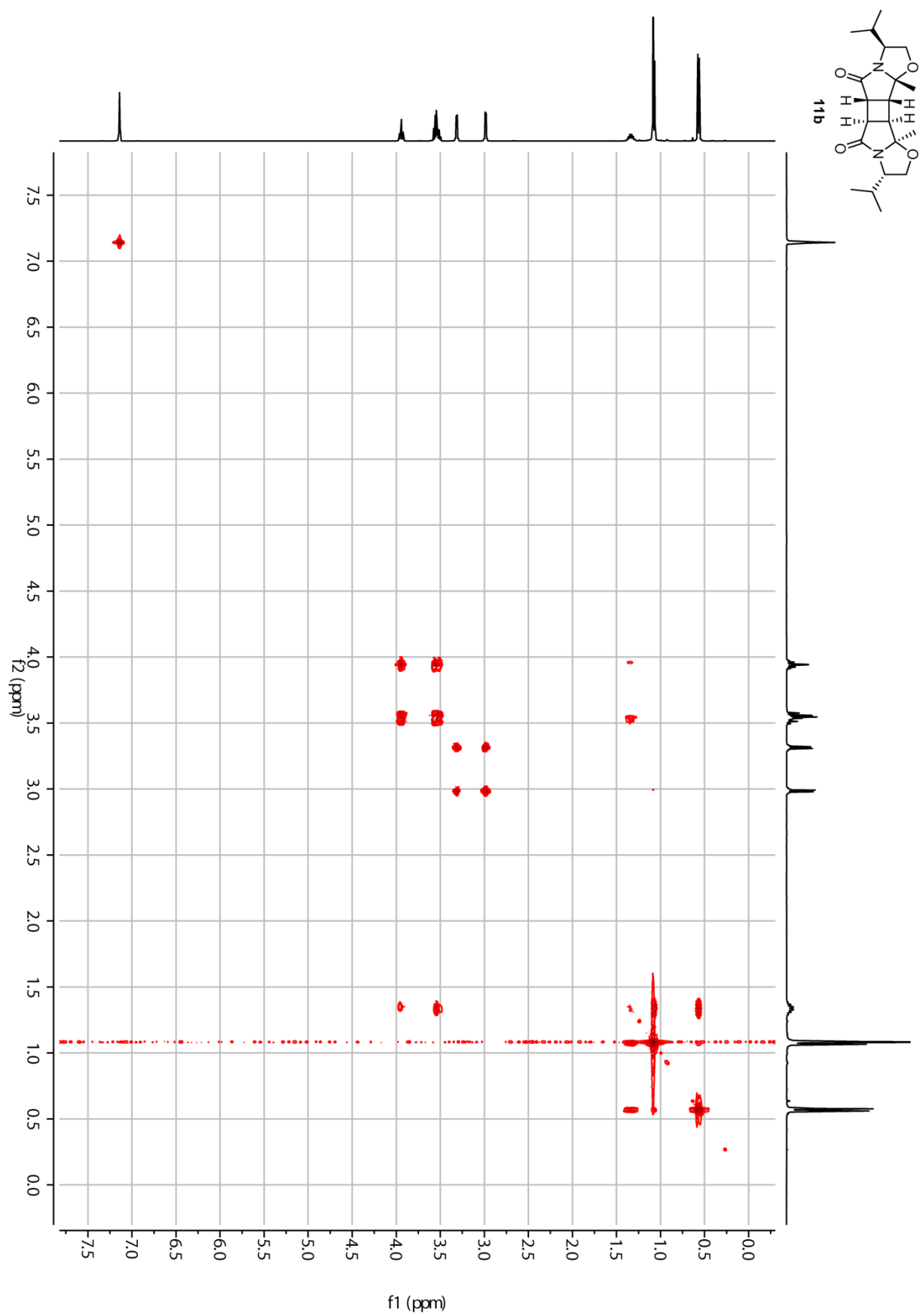


Figure S1. ^{13}C DEPT 135 spectrum of **11b** (125 MHz, C_6D_6).



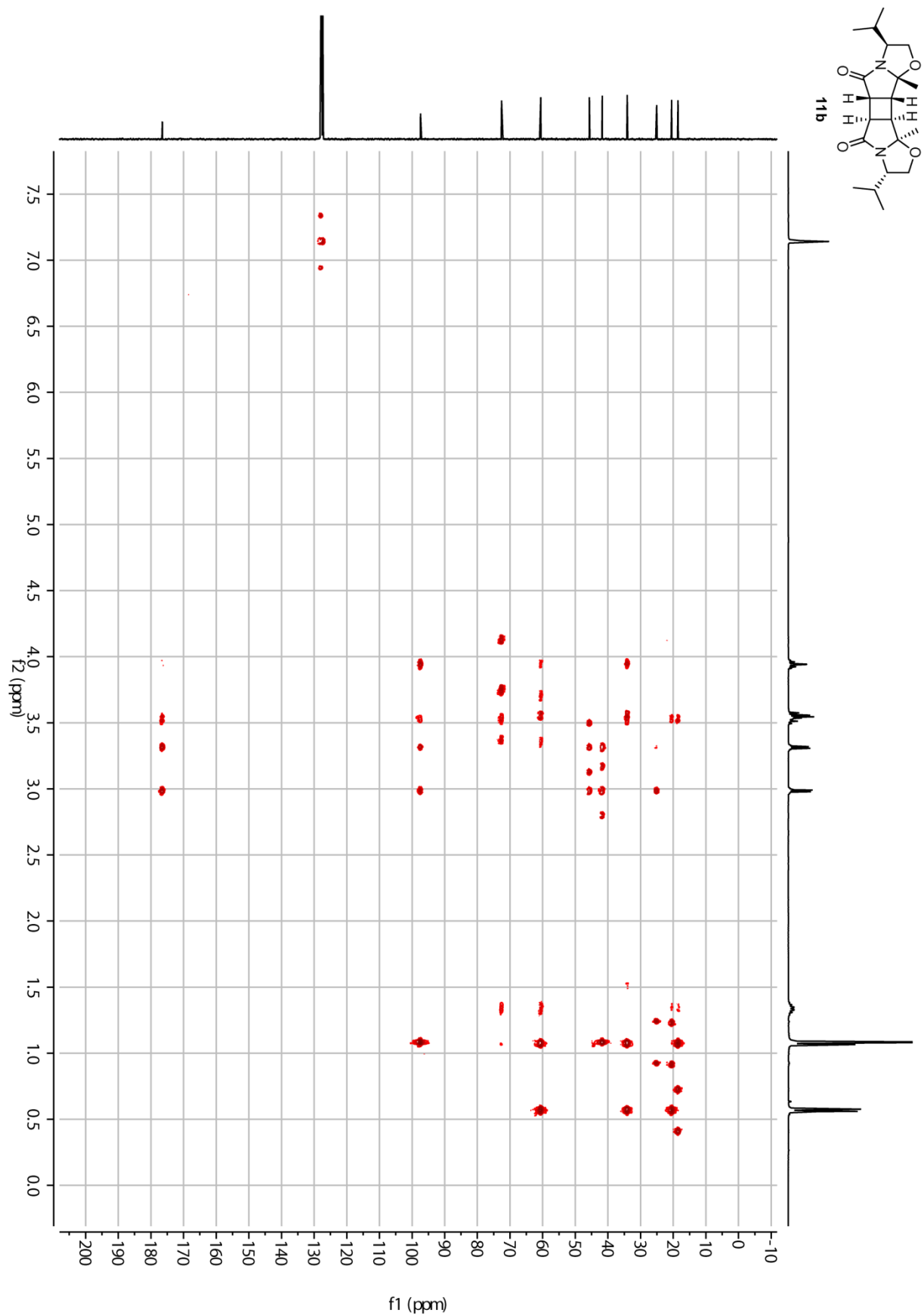


Figure S3. HMBC spectrum of **11b** (C_6D_6).

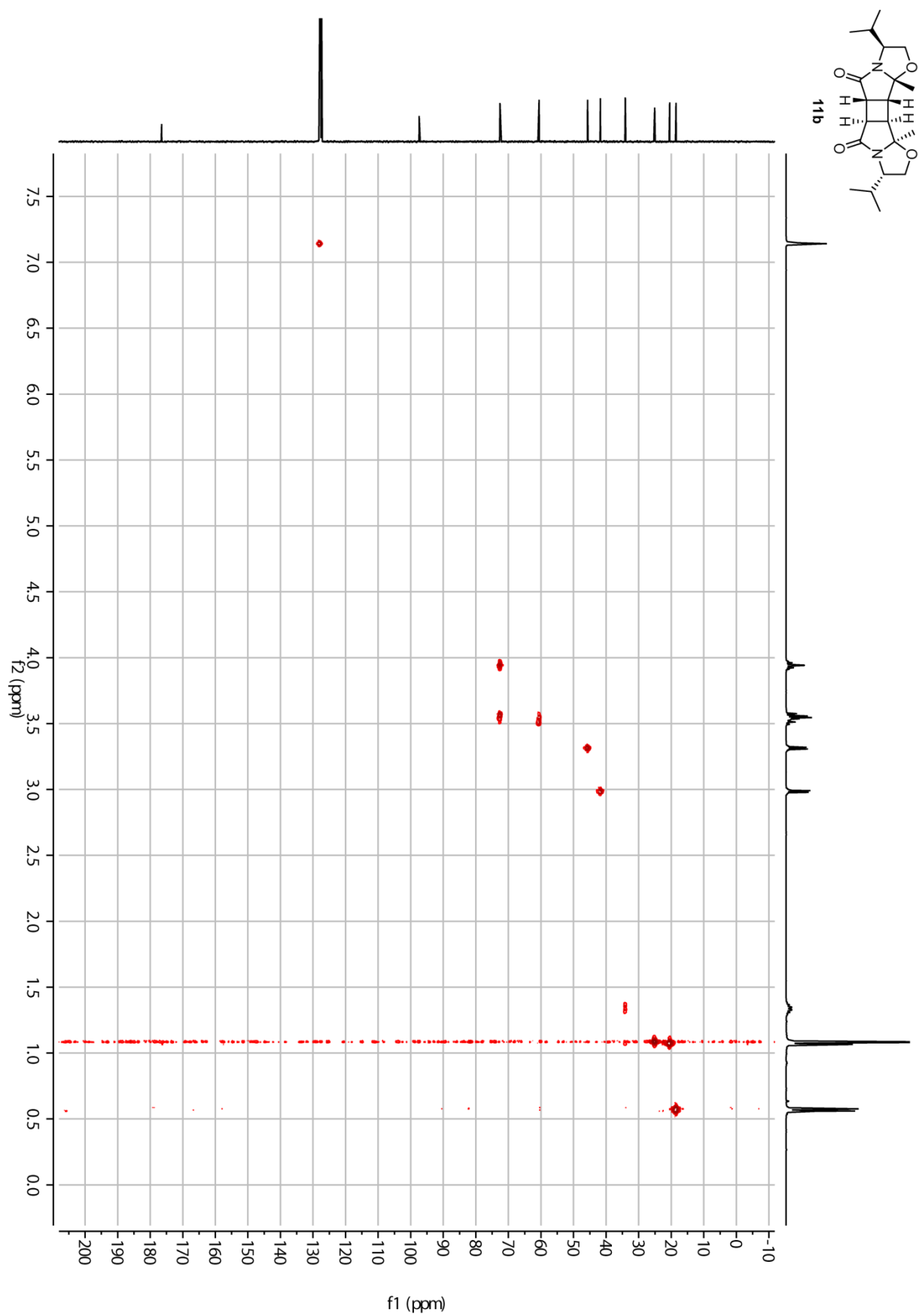


Figure S4. HSCQ spectrum of **11b** (C_6D_6).

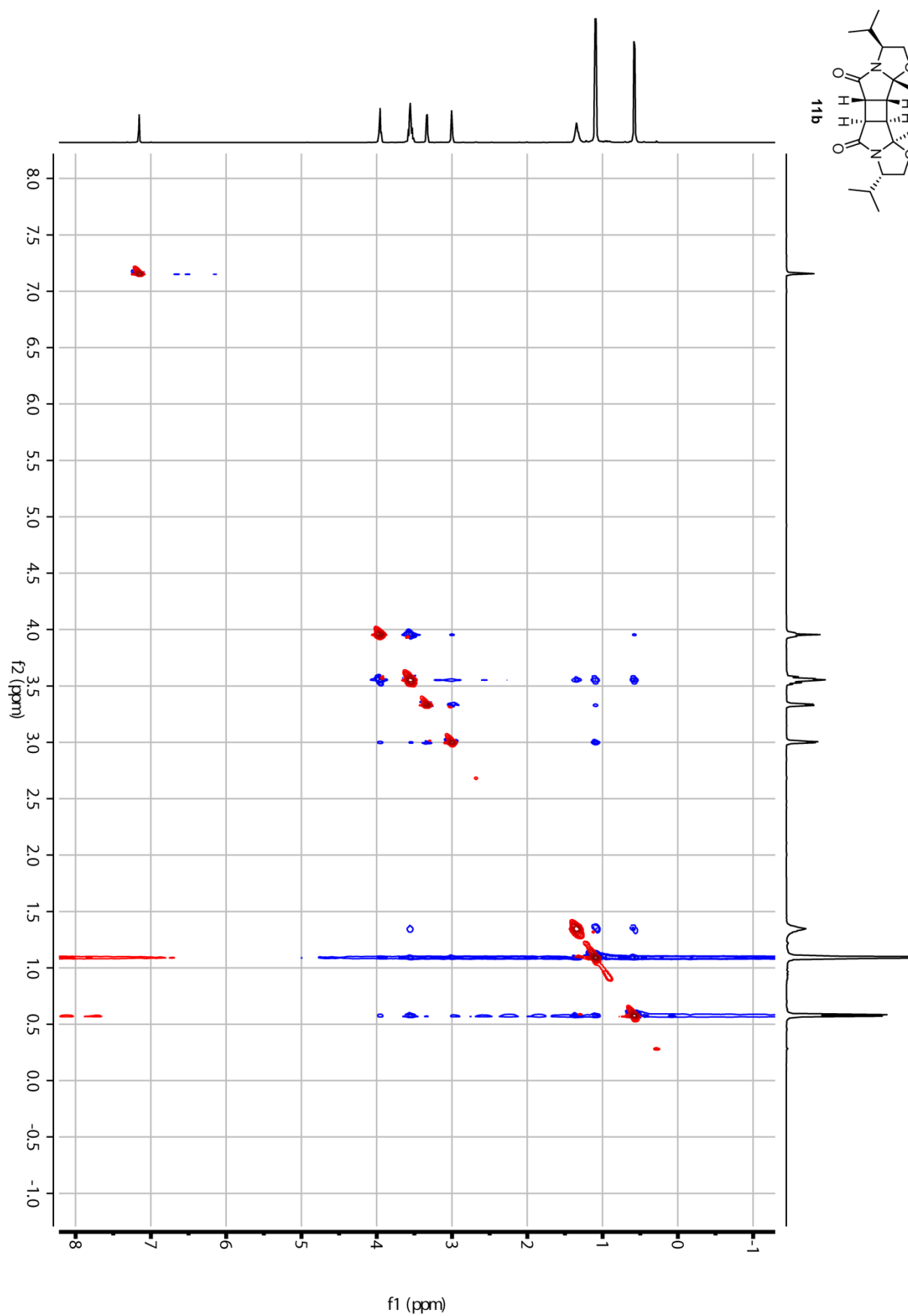


Figure S5. NOESY spectrum of **11b** (C_6D_6).

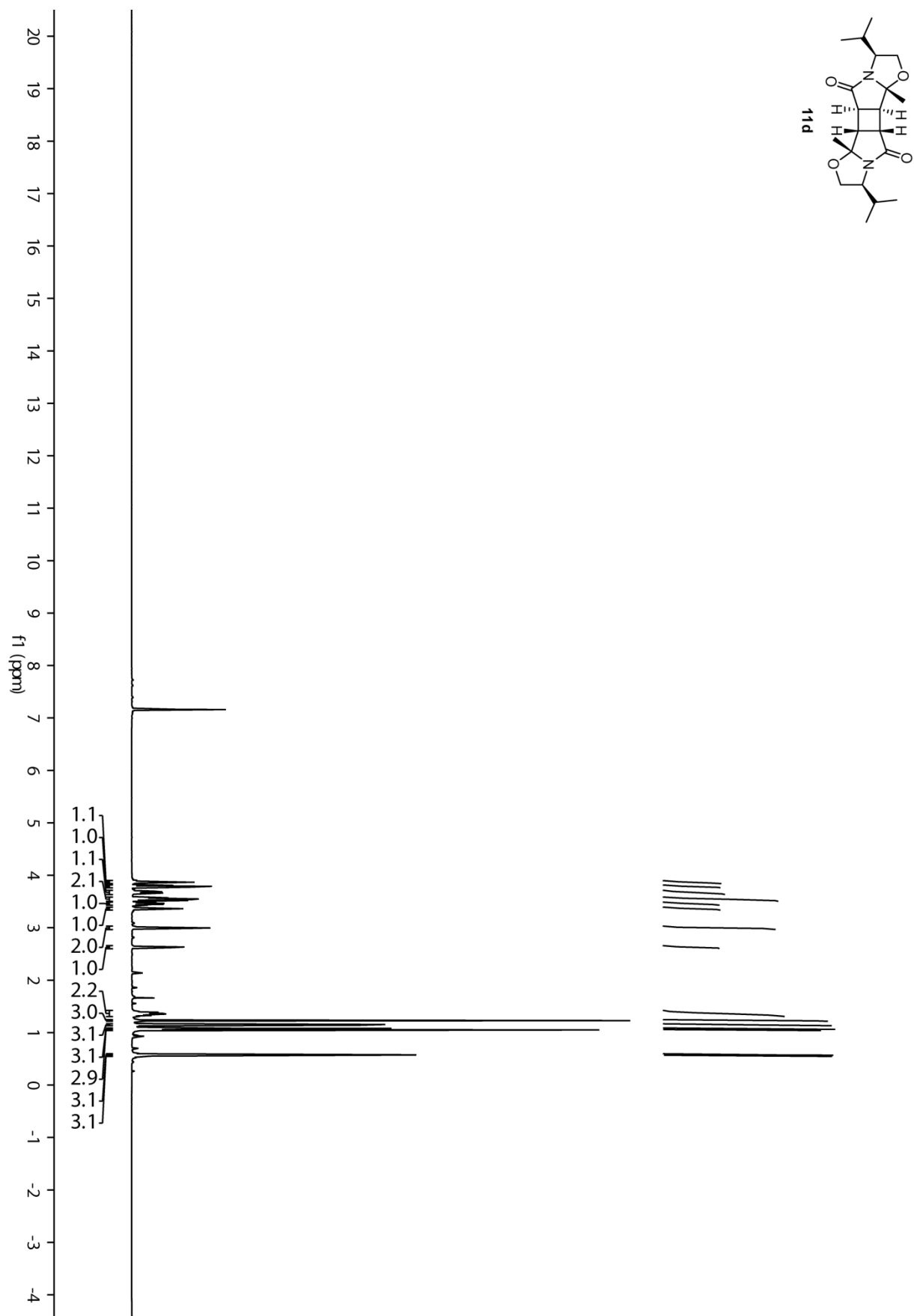


Figure S6. ^1H NMR spectrum of **11d** (500 MHz, C_6D_6).

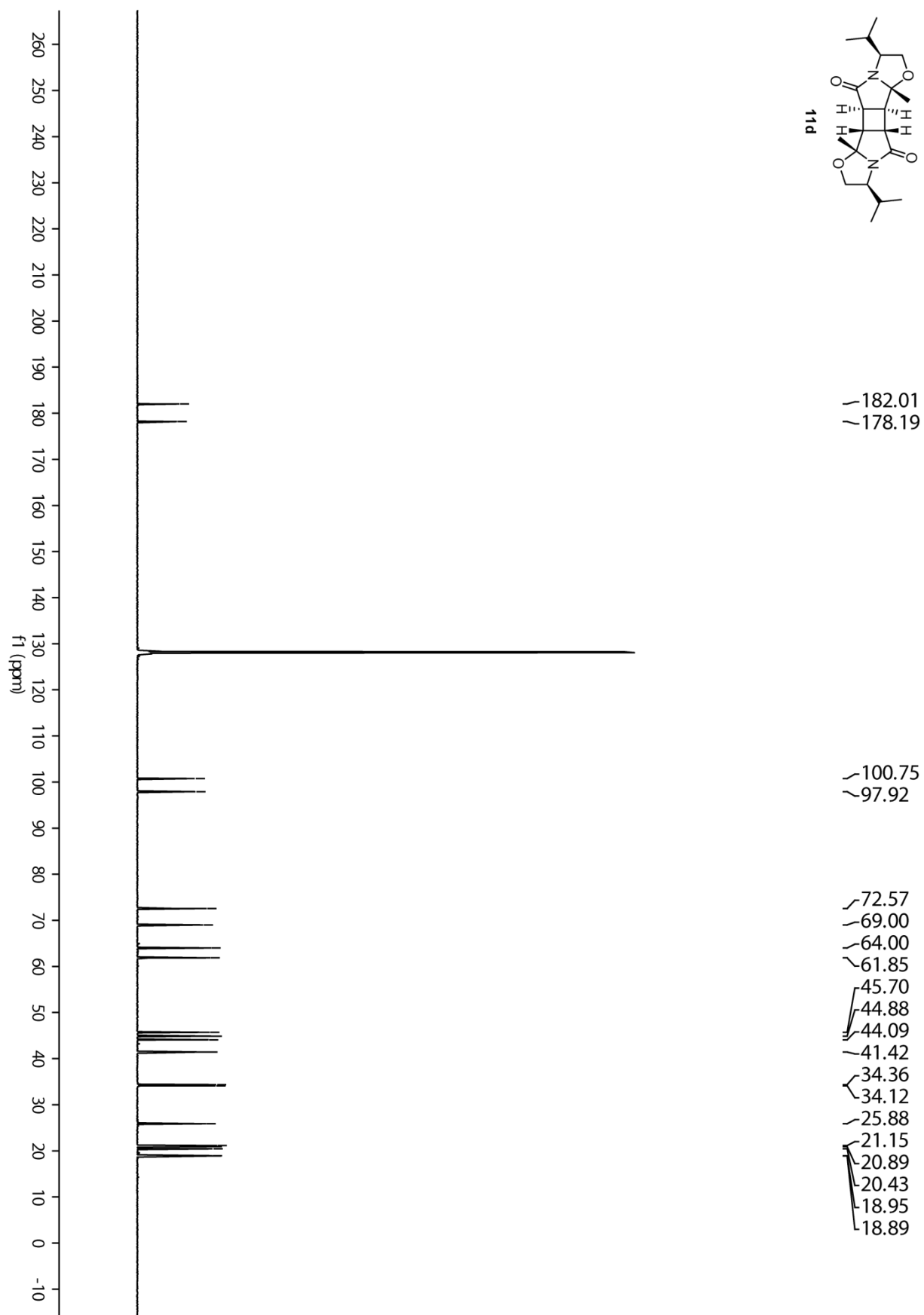


Figure S18. ^{13}C NMR spectrum of **11d** (125 MHz, C_6D_6).

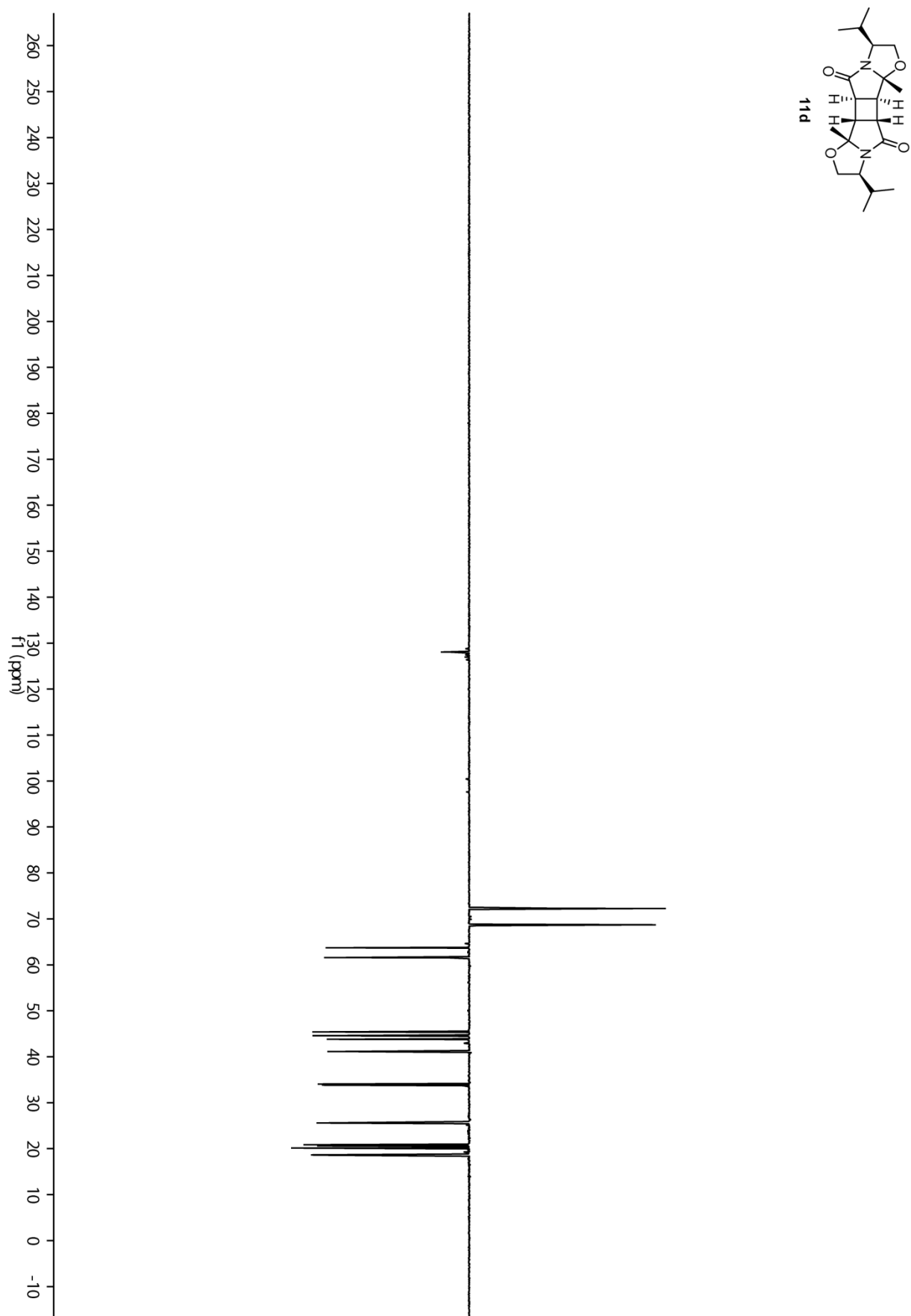


Figure S19. ^{13}C DEPT 135 spectrum of **11d** (125 MHz, C_6D_6).

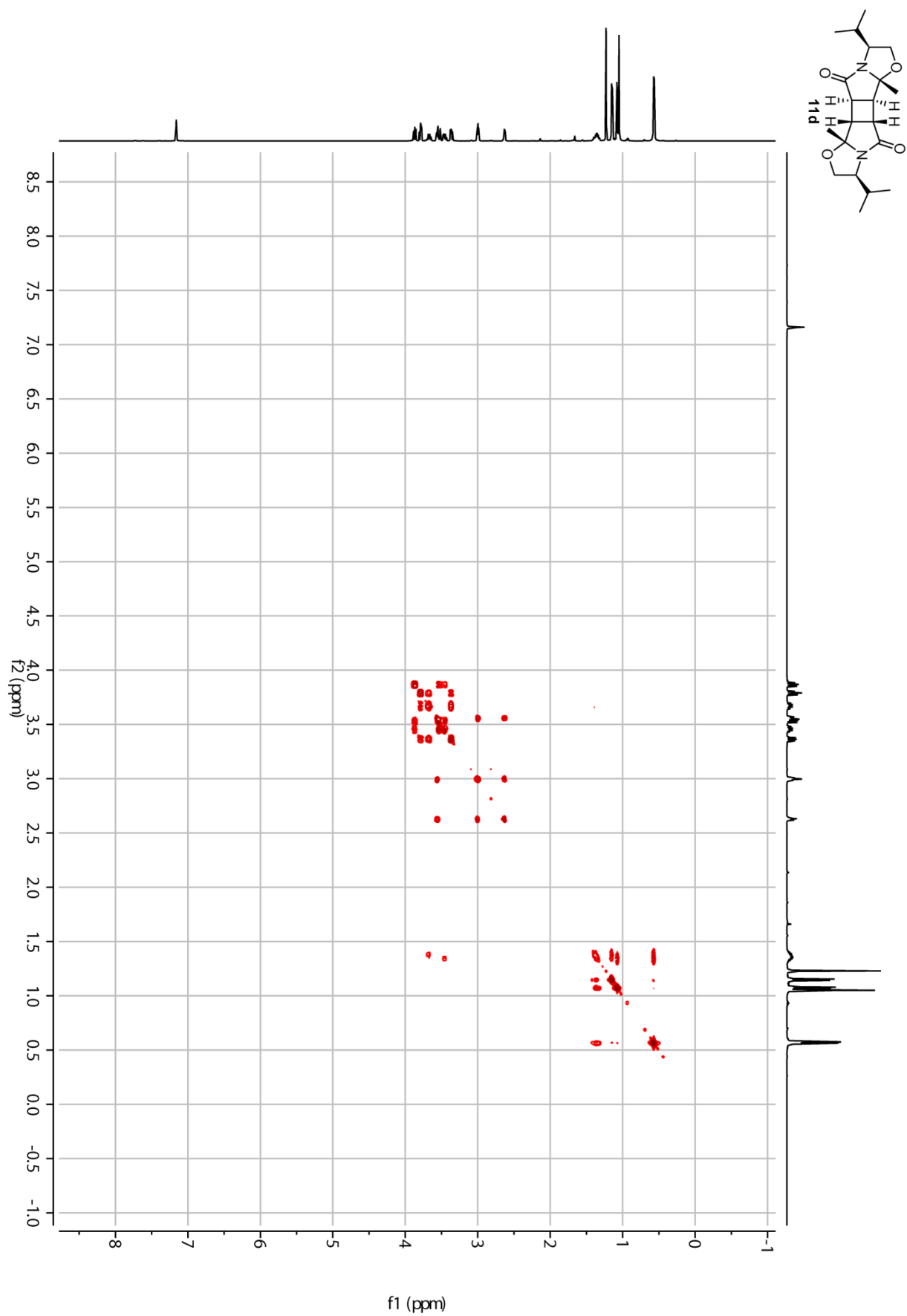


Figure S7. $^1\text{H}, ^1\text{H}$ -COSY spectrum of **11d** (C_6D_6).

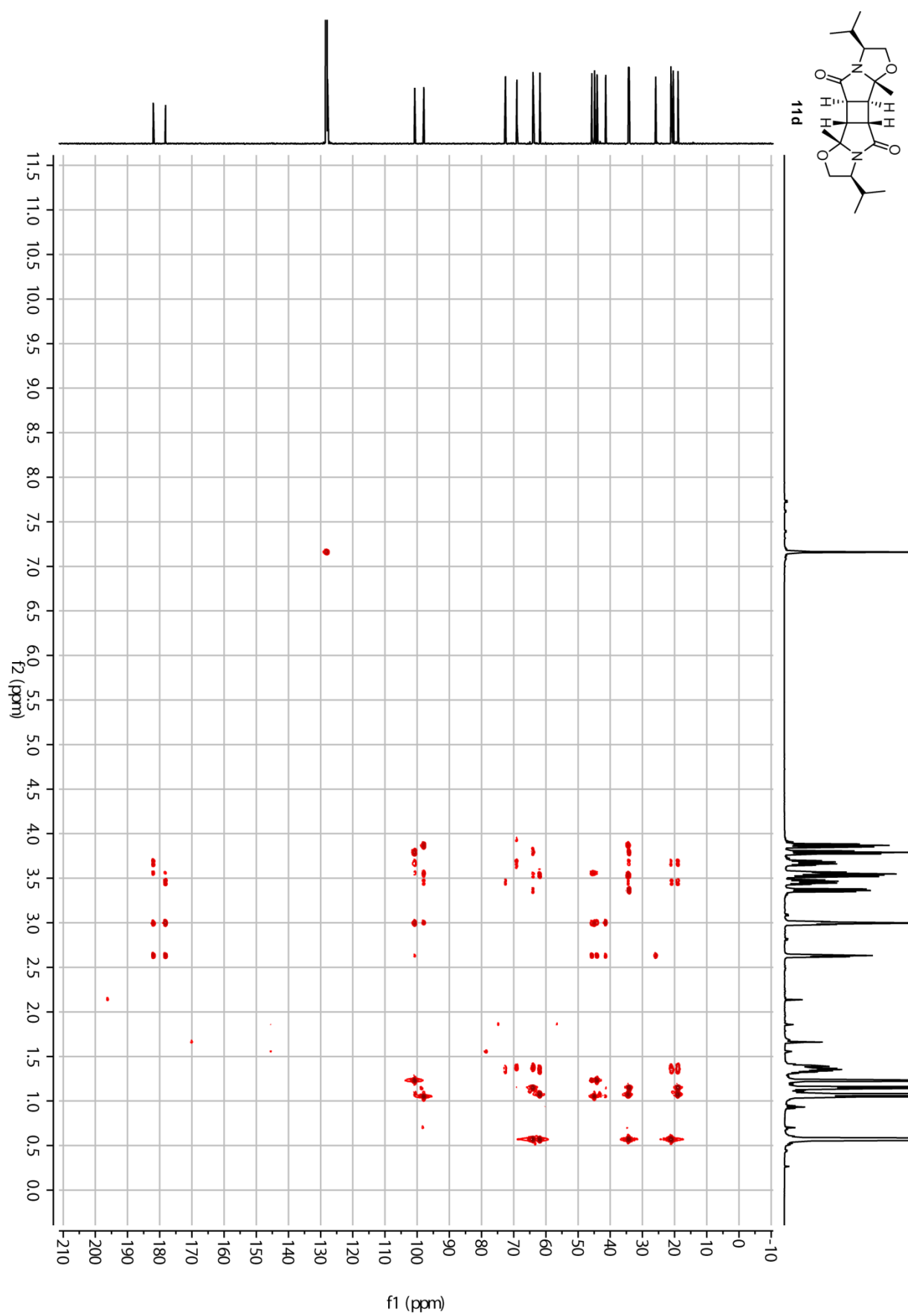


Figure S8. HMBC spectrum of **11d** (C_6D_6).

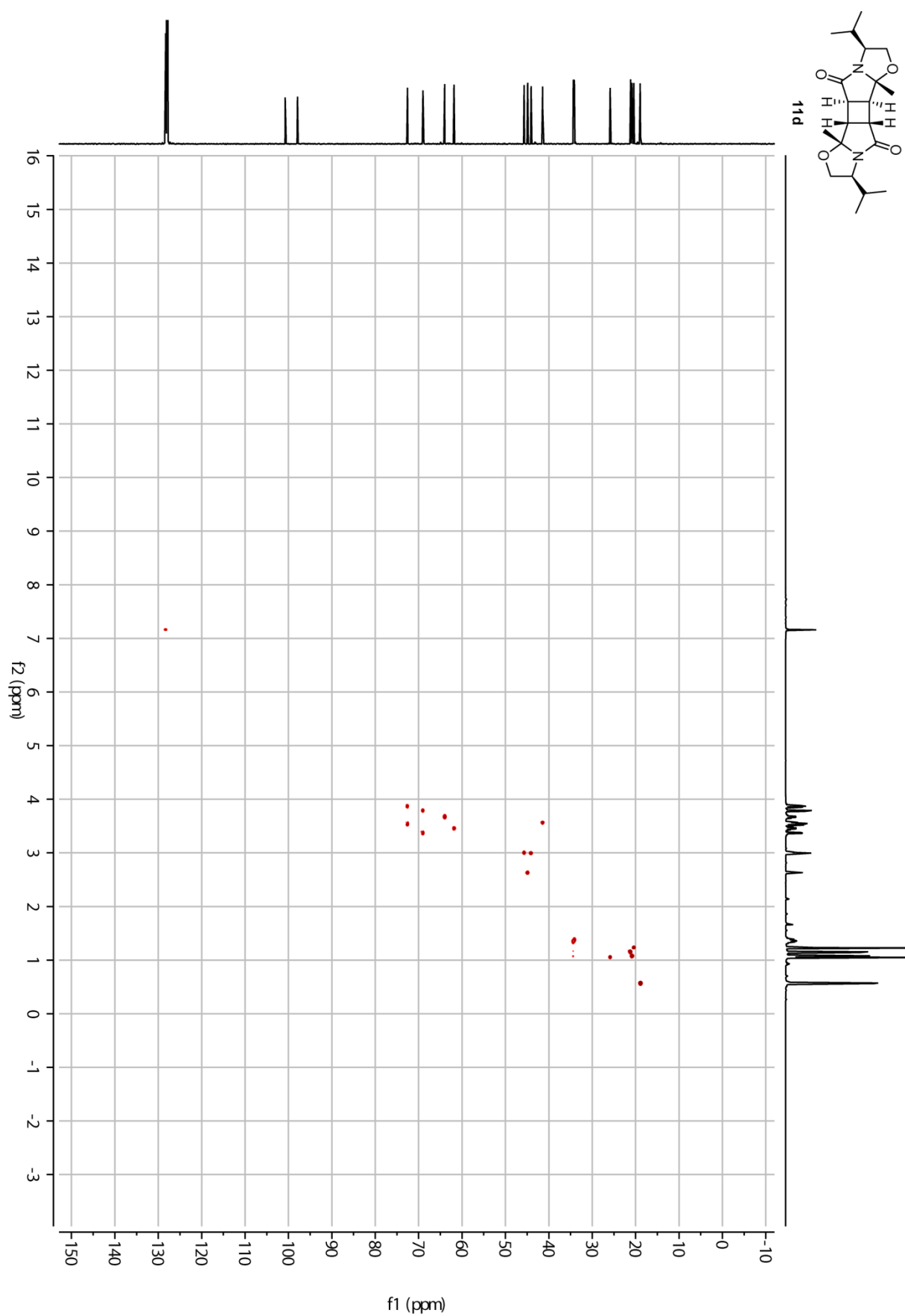


Figure S9. HSQC spectrum of **11d** (C_6D_6).

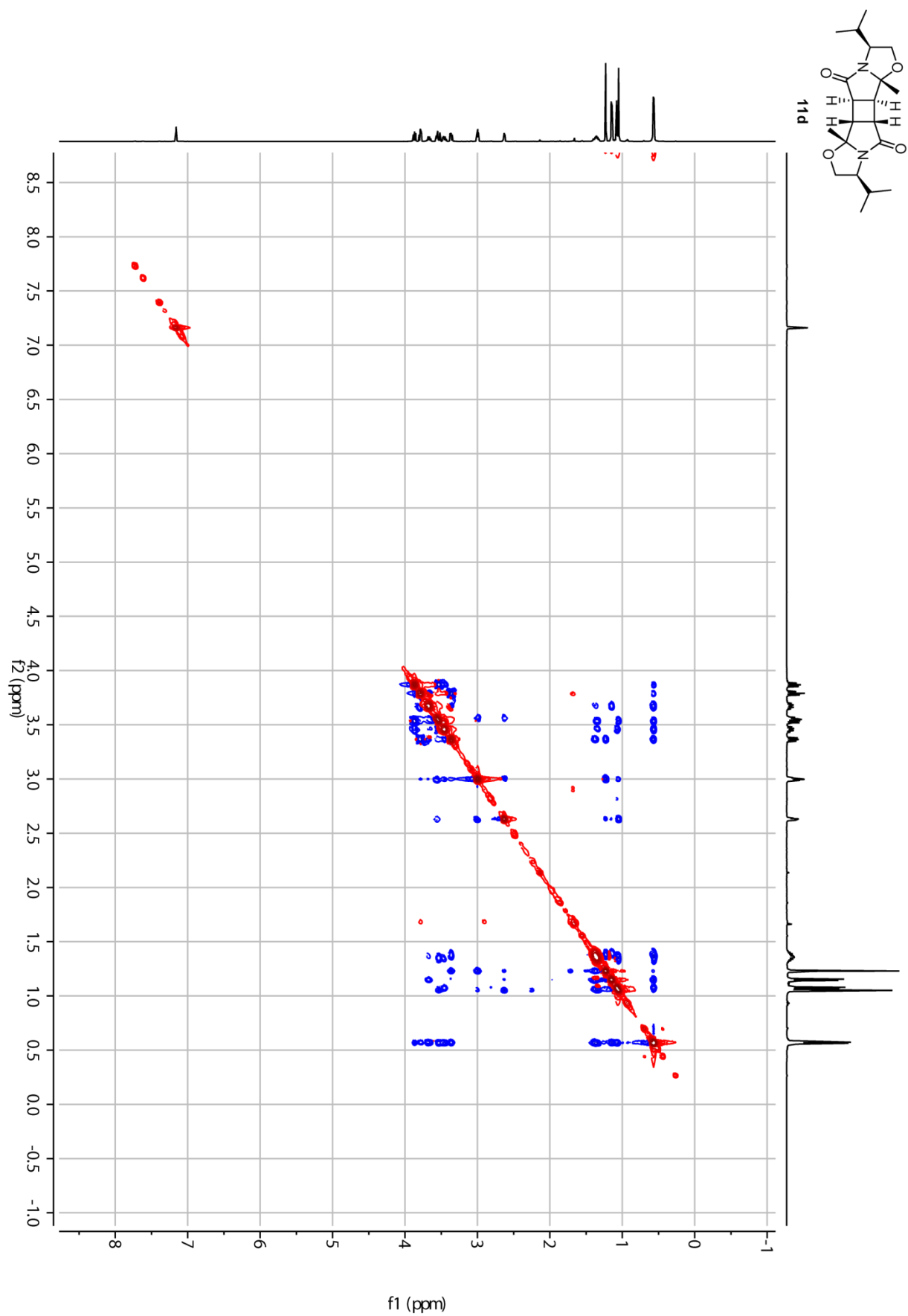


Figure S10. NOESY spectrum of **11d** (C_6D_6).

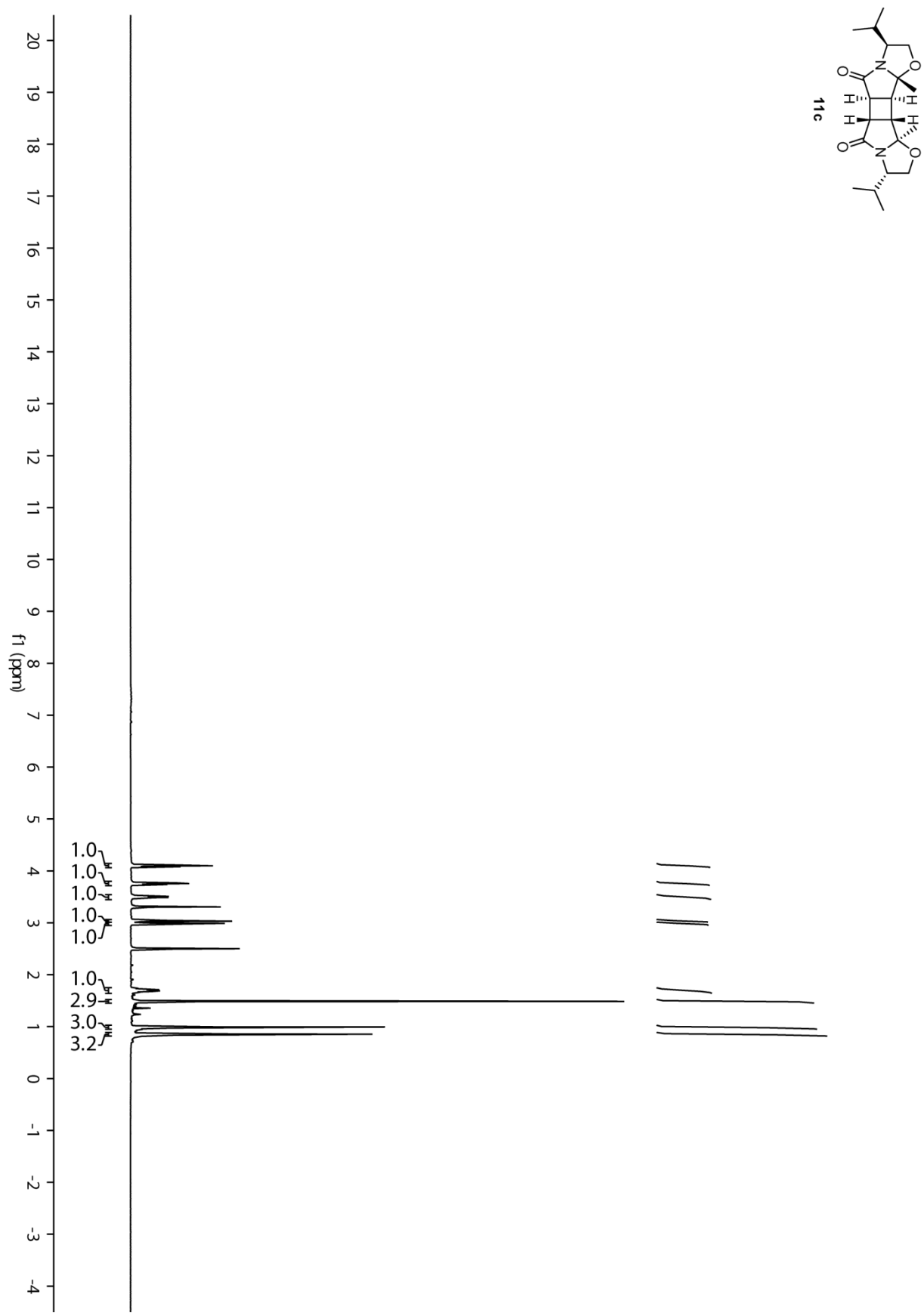


Figure S11. ¹H NMR spectrum of **11c** (500 MHz, *d*₆-DMSO).

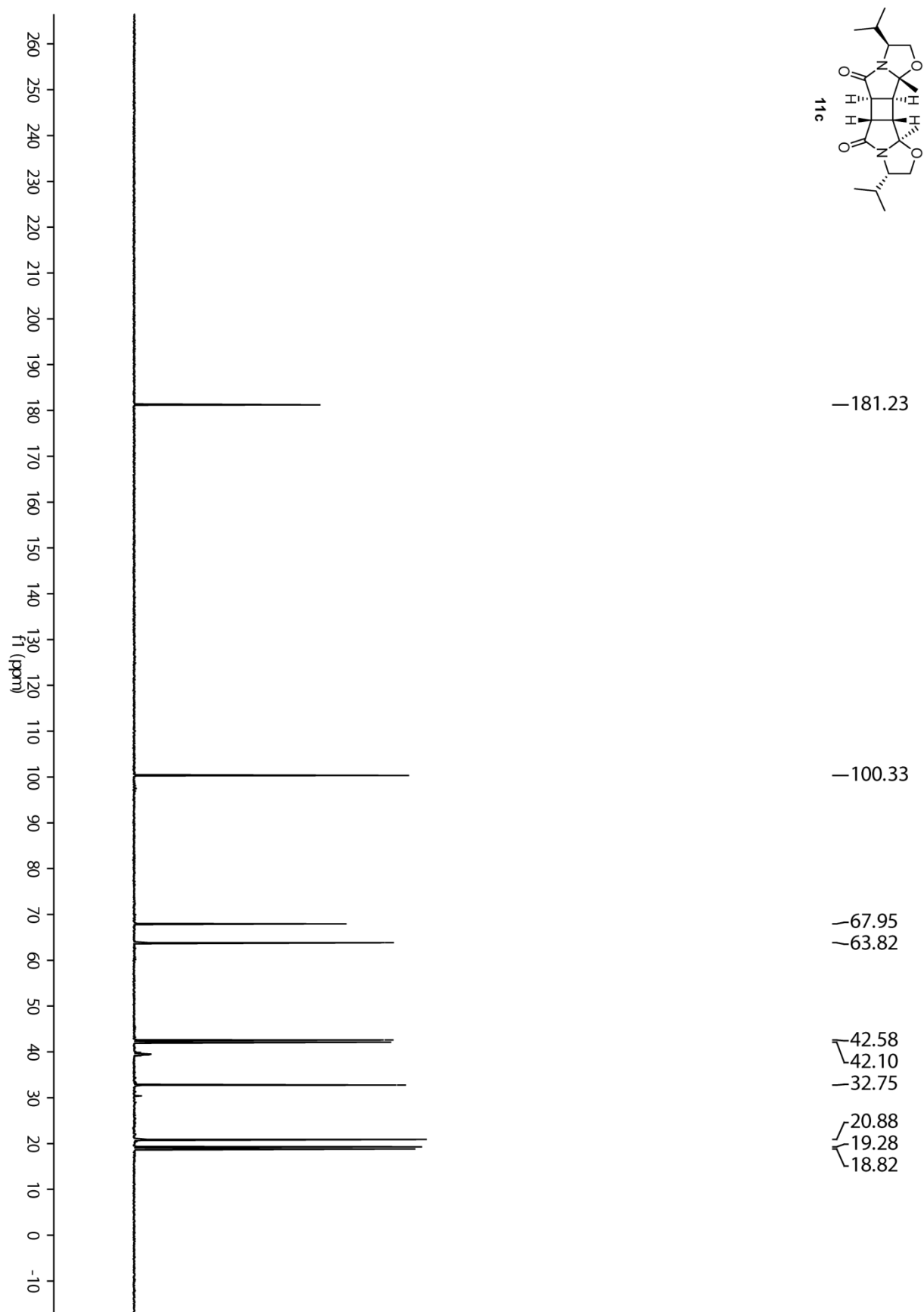


Figure S12. ^{13}C NMR spectrum of **11c** (125 MHz, d_6 -DMSO).

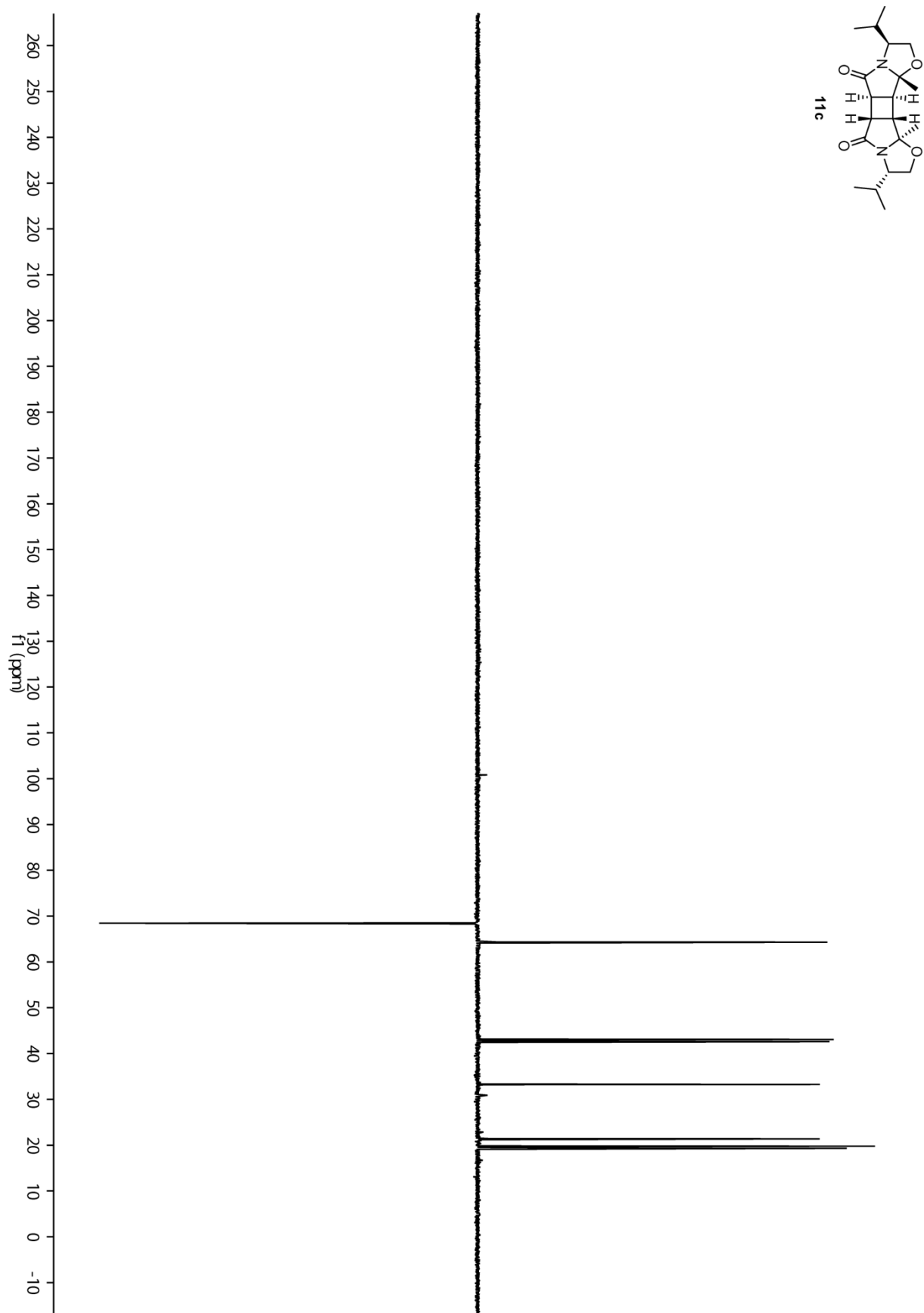


Figure S13. ^{13}C DEPT 135 spectrum of **11c** (125 MHz, d_6 -DMSO).

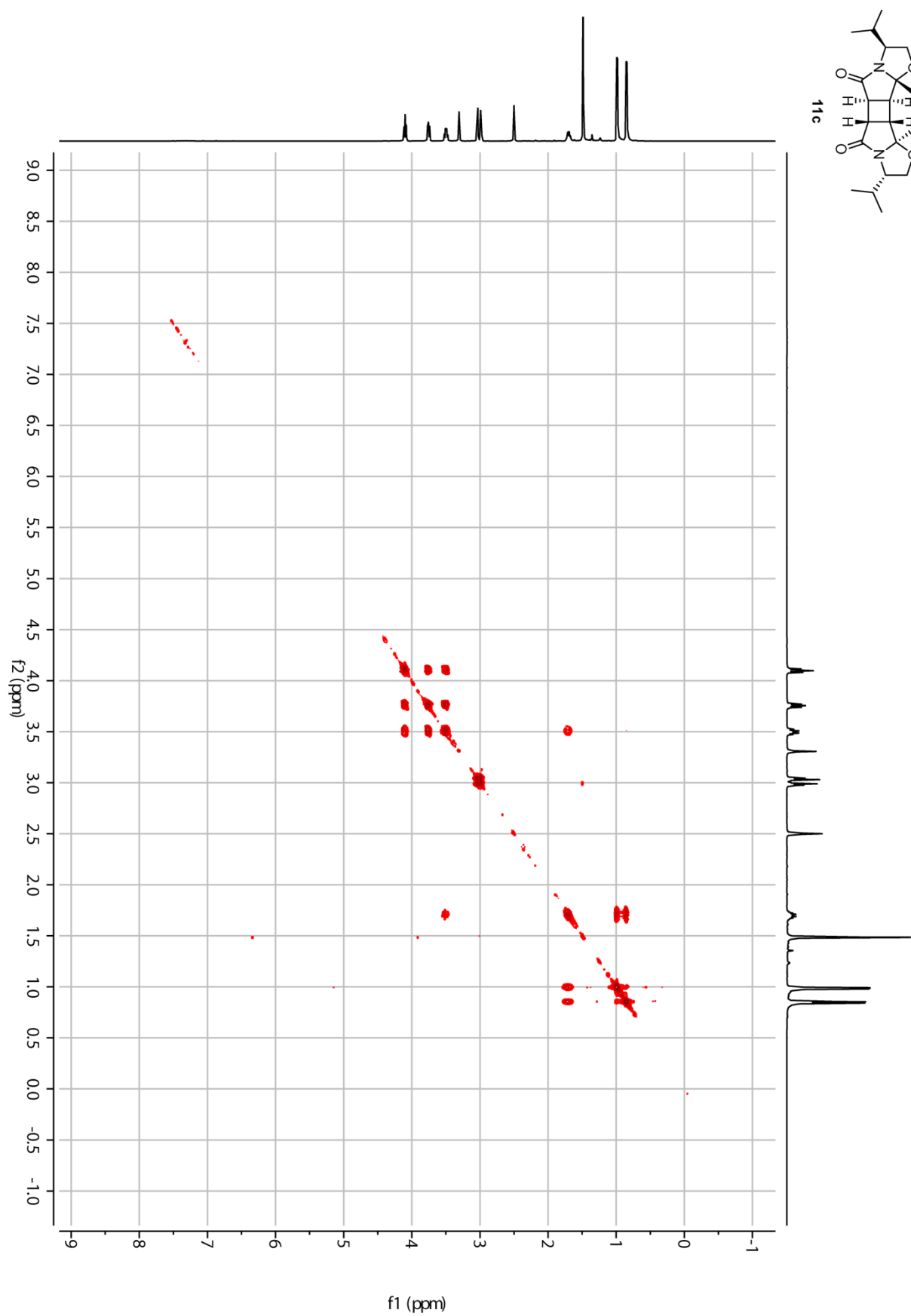


Figure S14. $^1\text{H}, ^1\text{H}$ -COSY spectrum of **11c** (500 MHz, d_6 -DMSO).

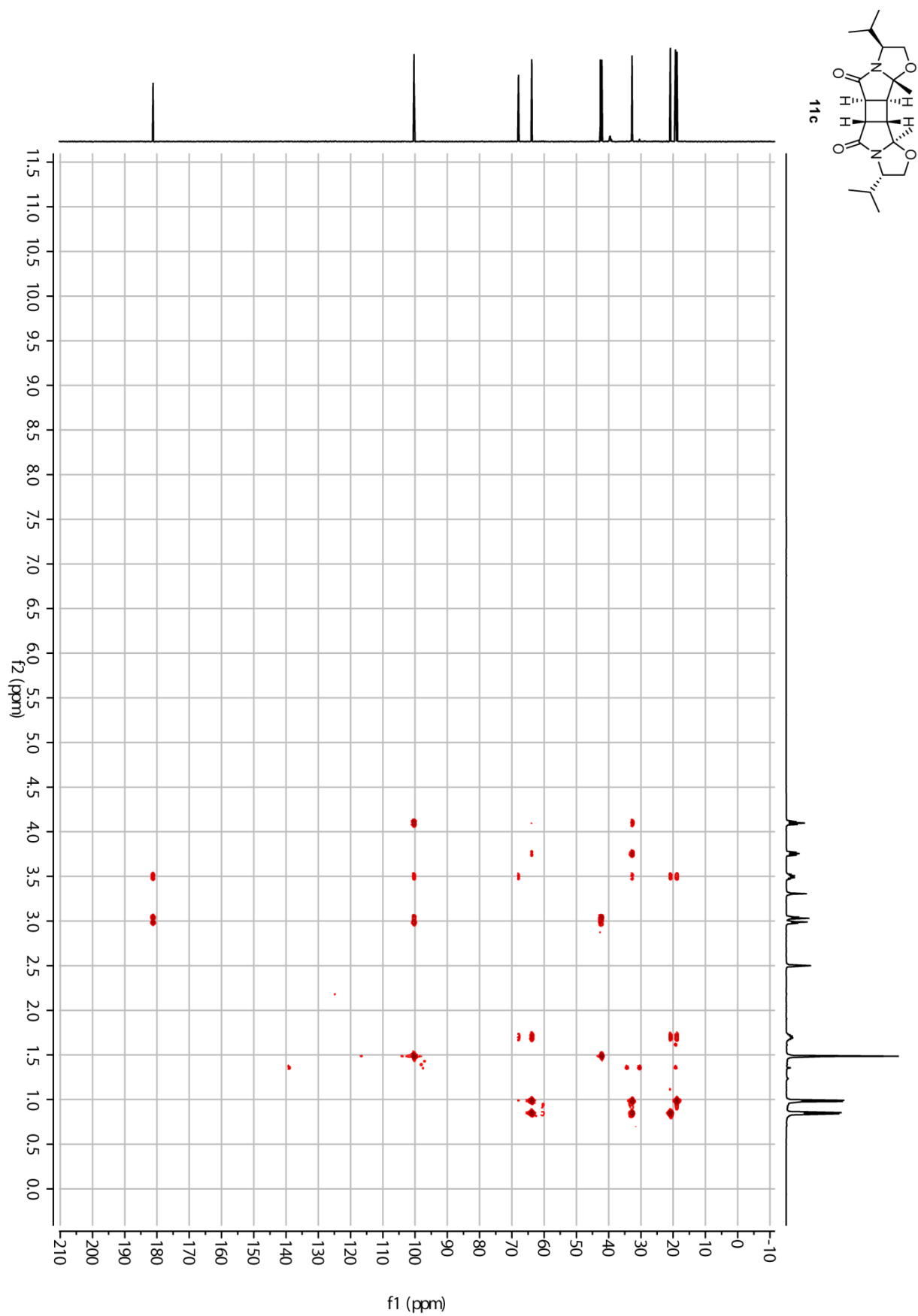


Figure S28. HMBC spectrum of **11c** (d_6 -DMSO).

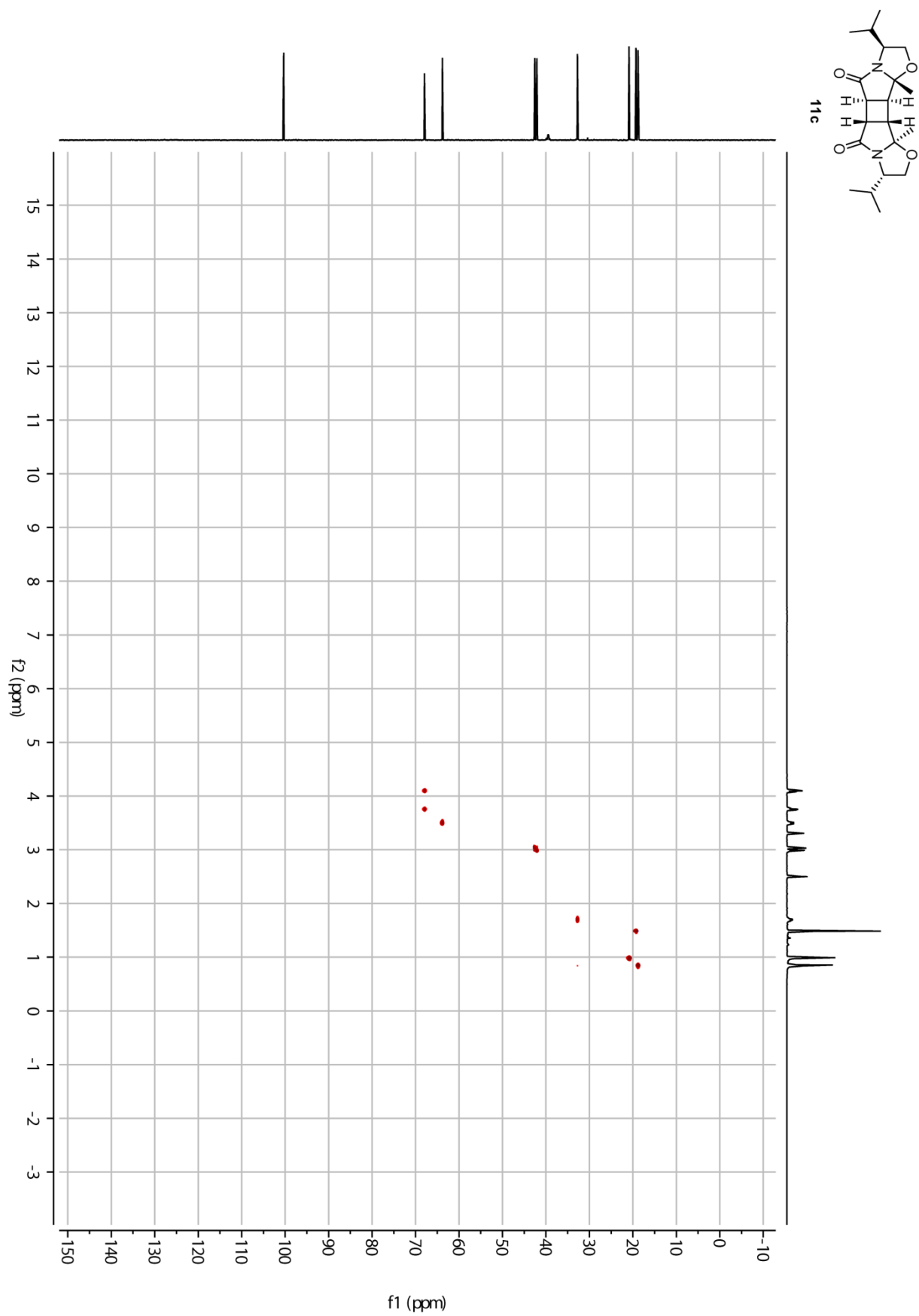


Figure S29. HSQC spectrum of **11c** (d_6 -DMSO).

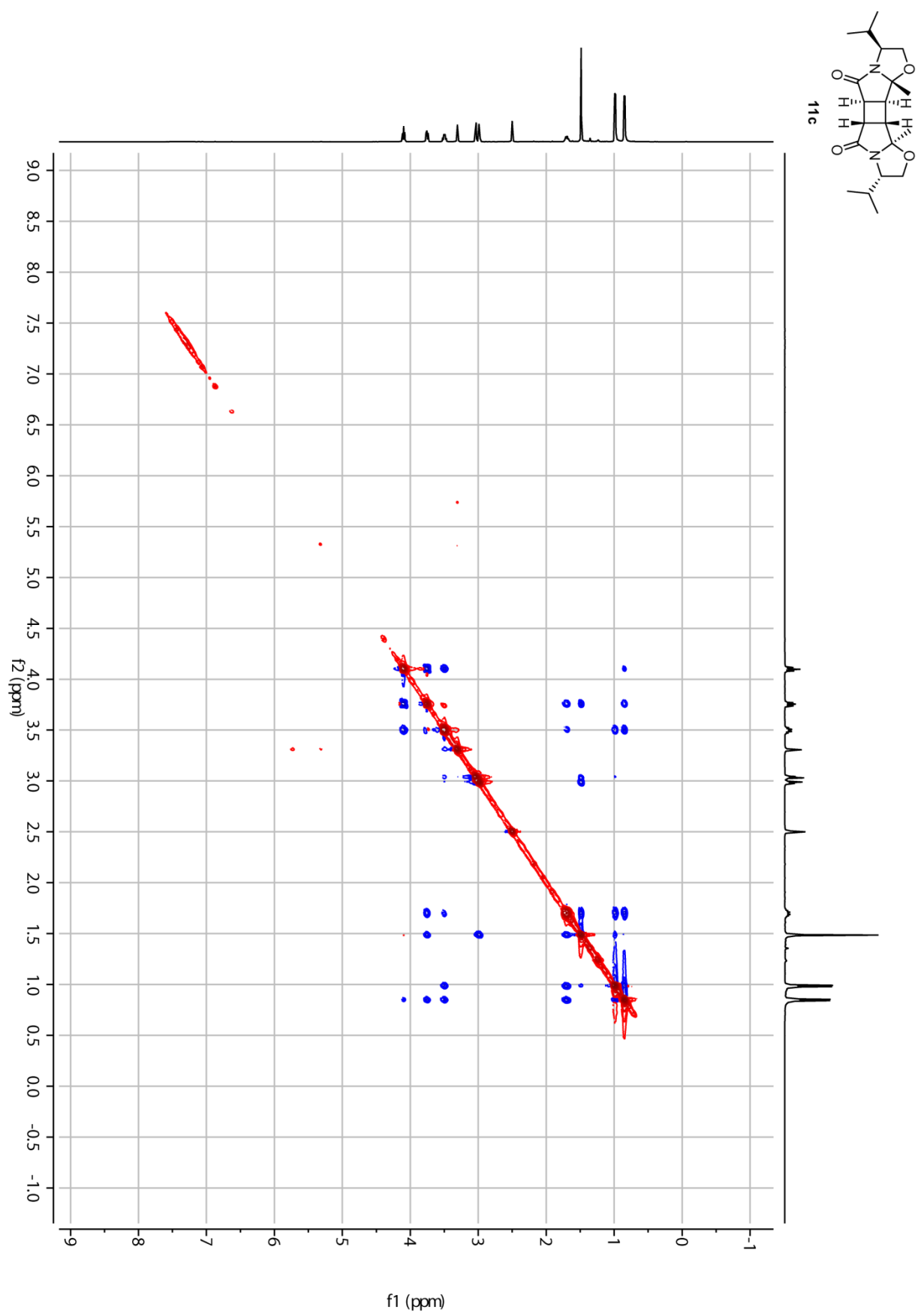


Figure S15. NOESY spectrum of **11c** (d_6 -DMSO).

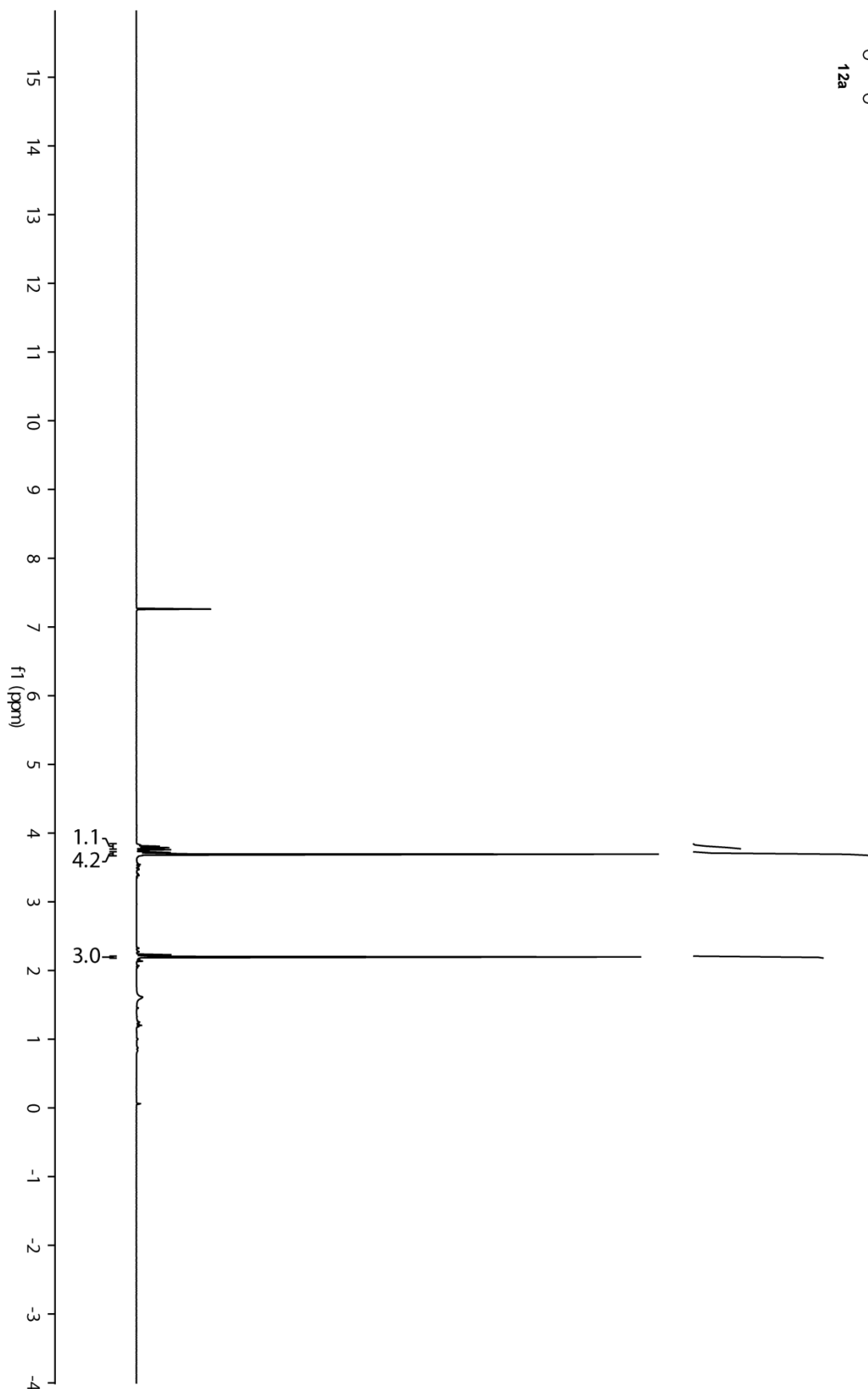
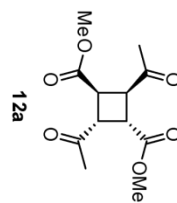


Figure S16. ¹H NMR spectrum of **12a** (500 MHz, CDCl₃).

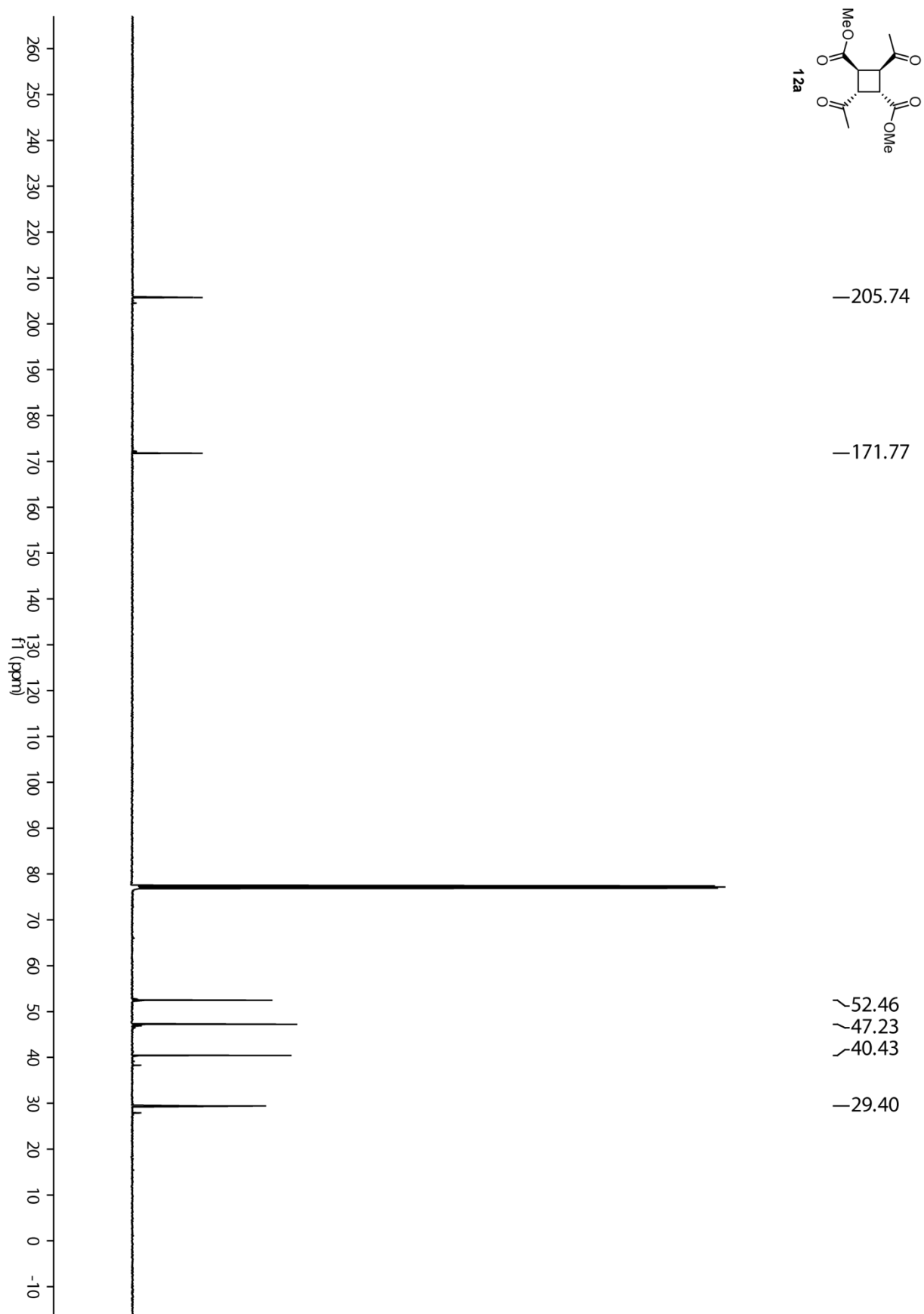


Figure S17. ^{13}C NMR spectrum of **12a** (125 MHz, CDCl_3).

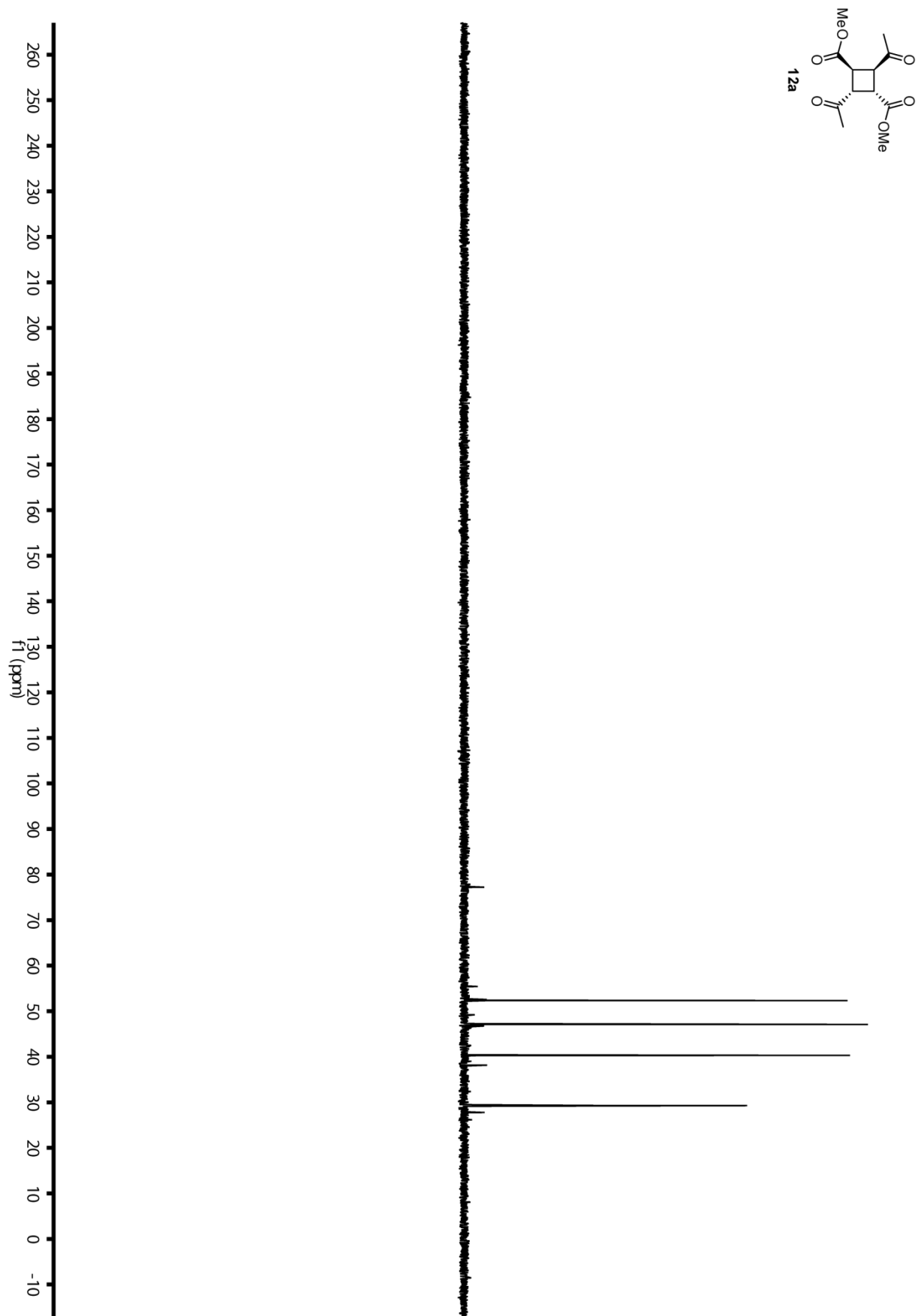


Figure S18. ^{13}C DEPT 135 spectrum of **12a** (125 MHz, CDCl_3).

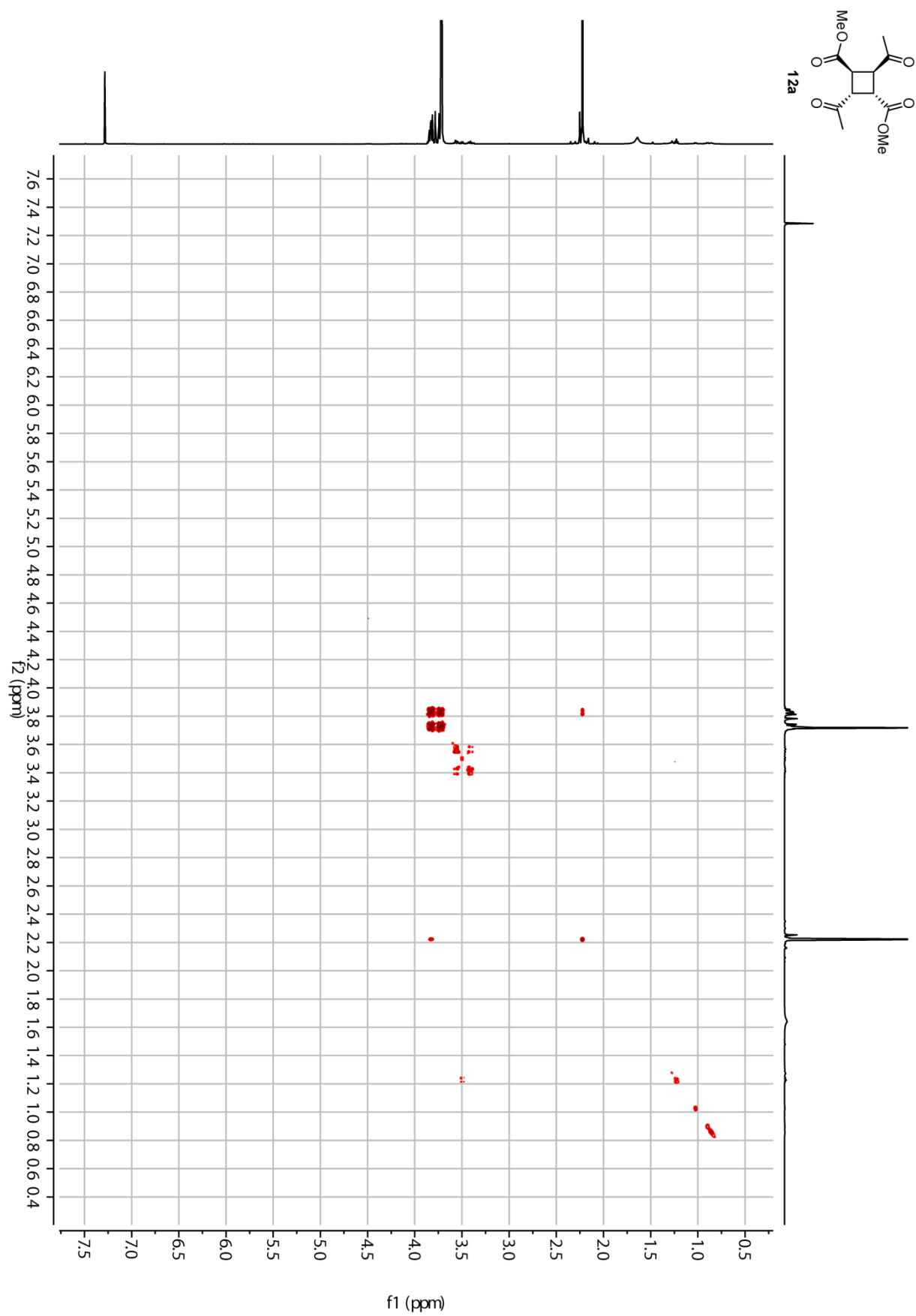


Figure S19. ^1H , ^1H COSY spectrum of **12a** (500 MHz, CDCl_3).

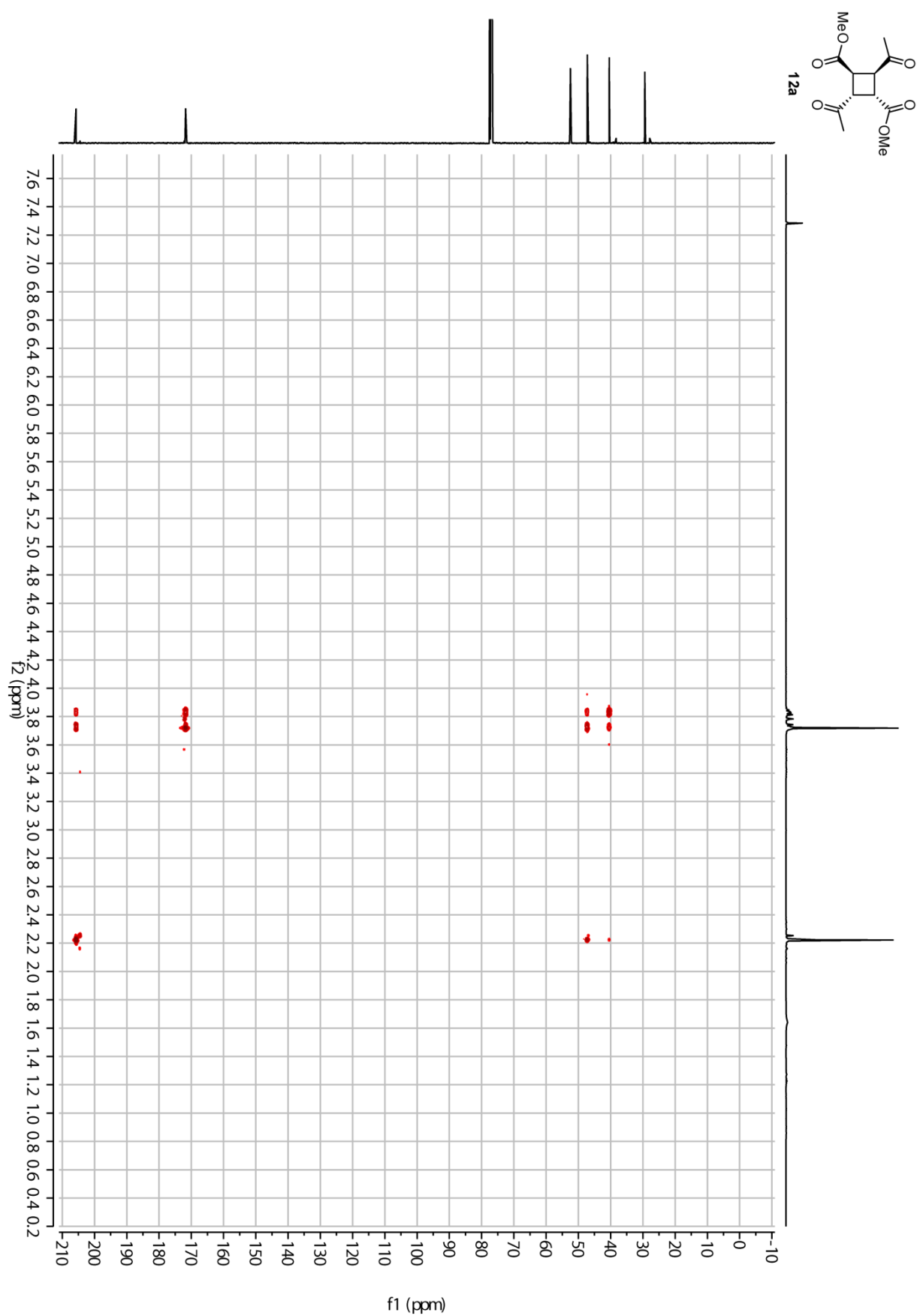


Figure S20. HMBC spectrum of **12a** (CDCl₃).

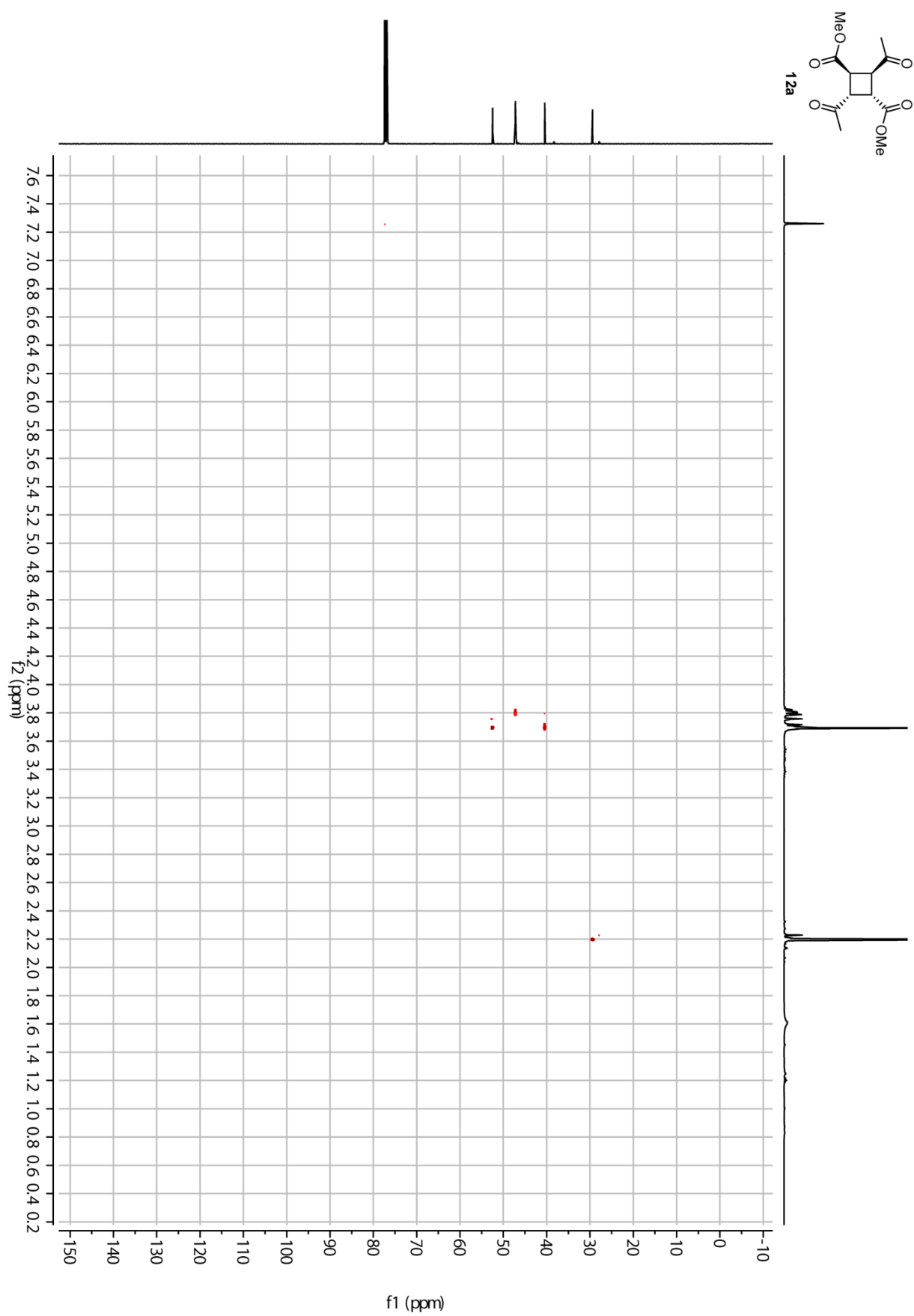


Figure S21. HSQC spectrum of **12a** (CDCl₃).

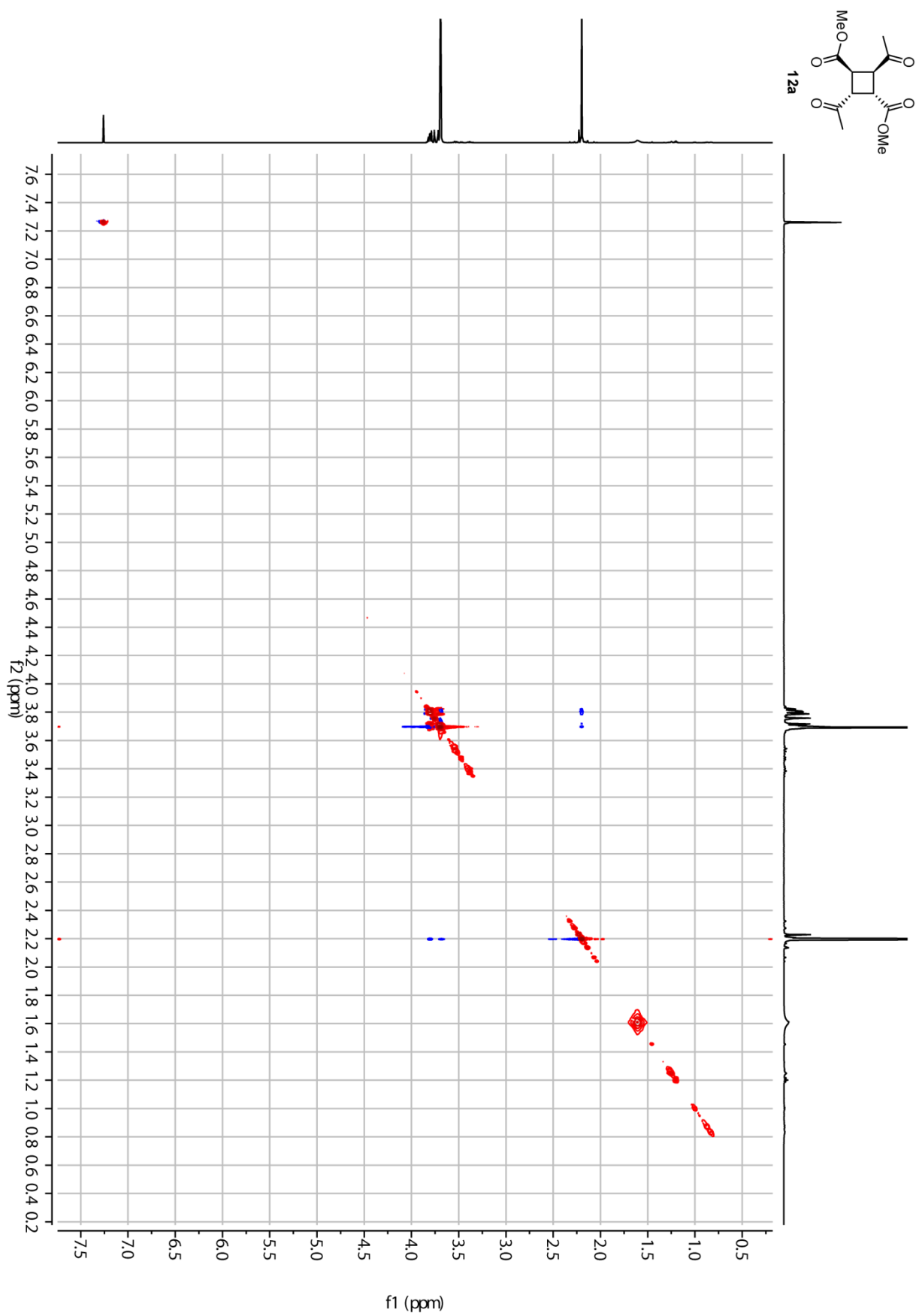


Figure S22. NOESY spectrum of **12a** (CDCl₃).

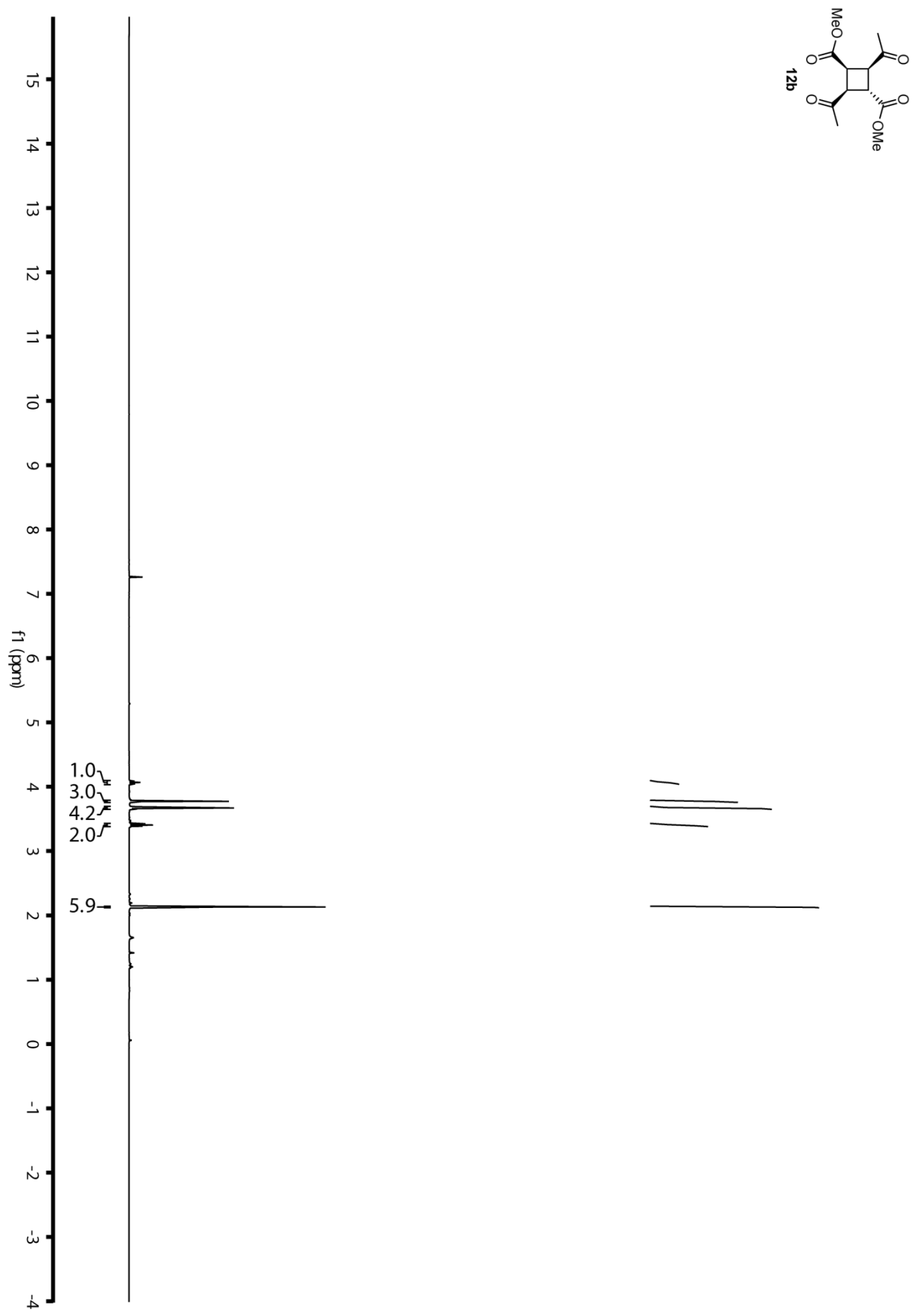


Figure S38. ¹H NMR spectrum of **12b** (500 MHz, CDCl₃).

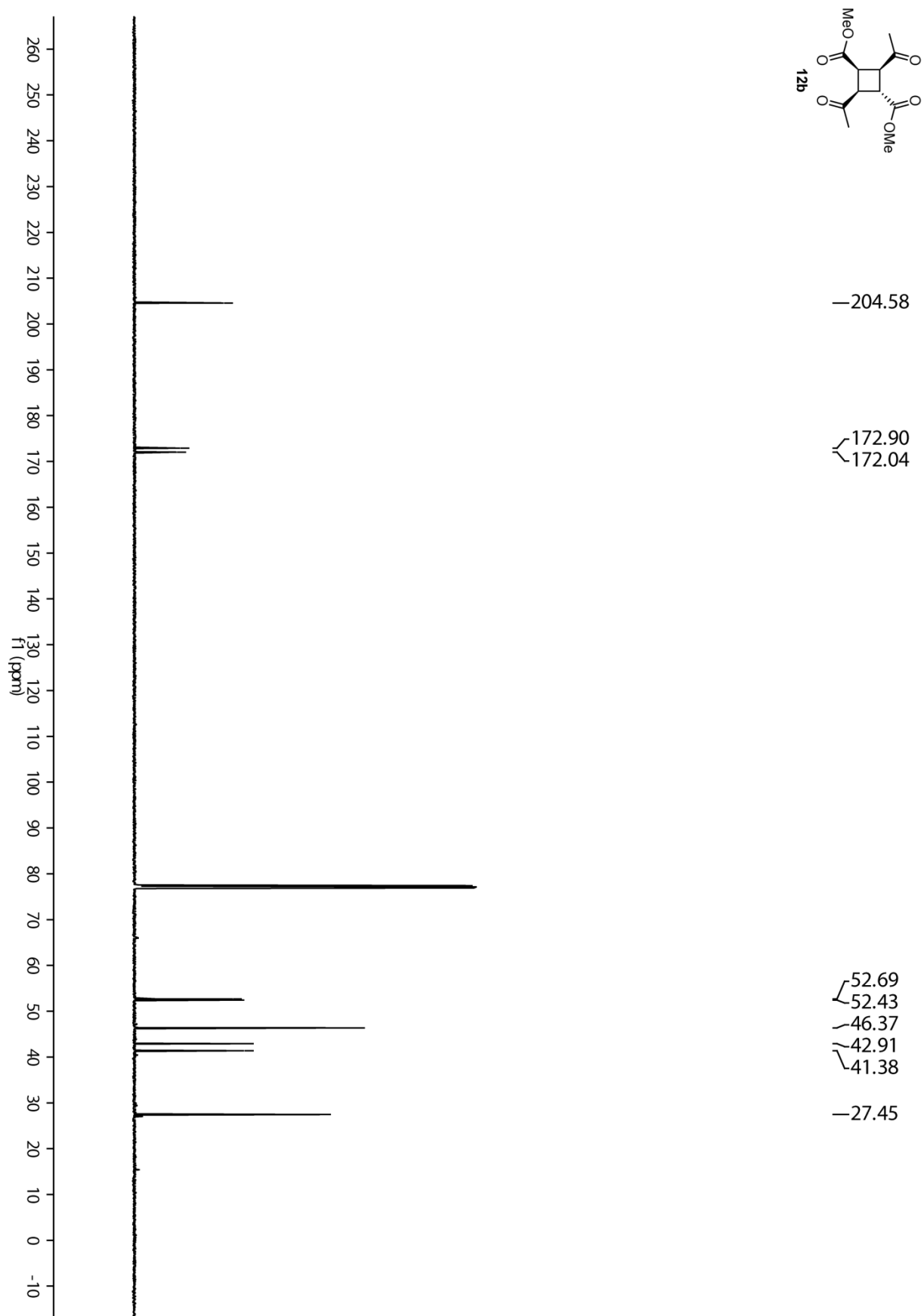


Figure S39. ¹³C NMR spectrum of **12b** (125 MHz, CDCl₃).

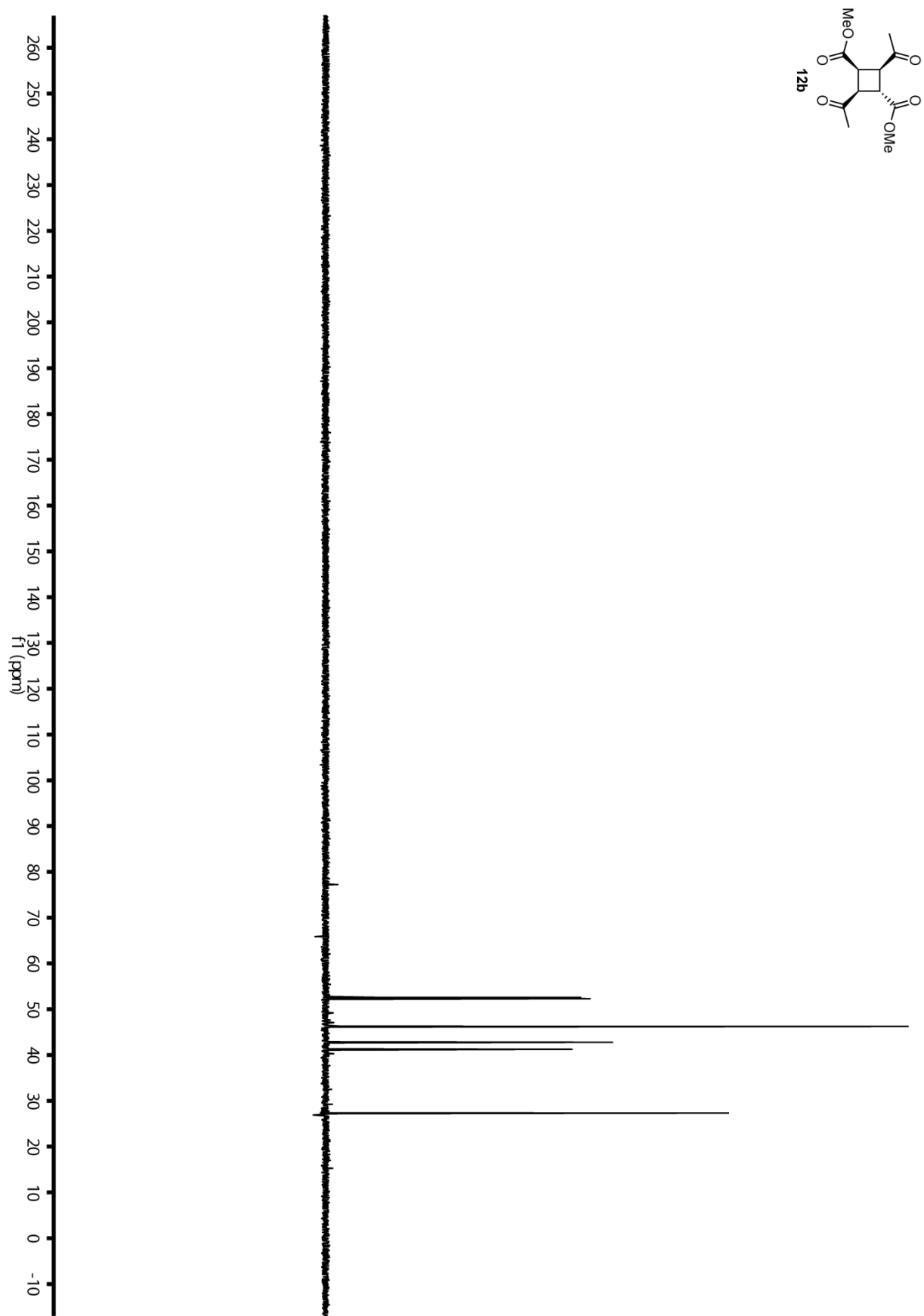


Figure S23. ^{13}C DEPT 135 spectrum of **12b** (125 MHz, CDCl_3).

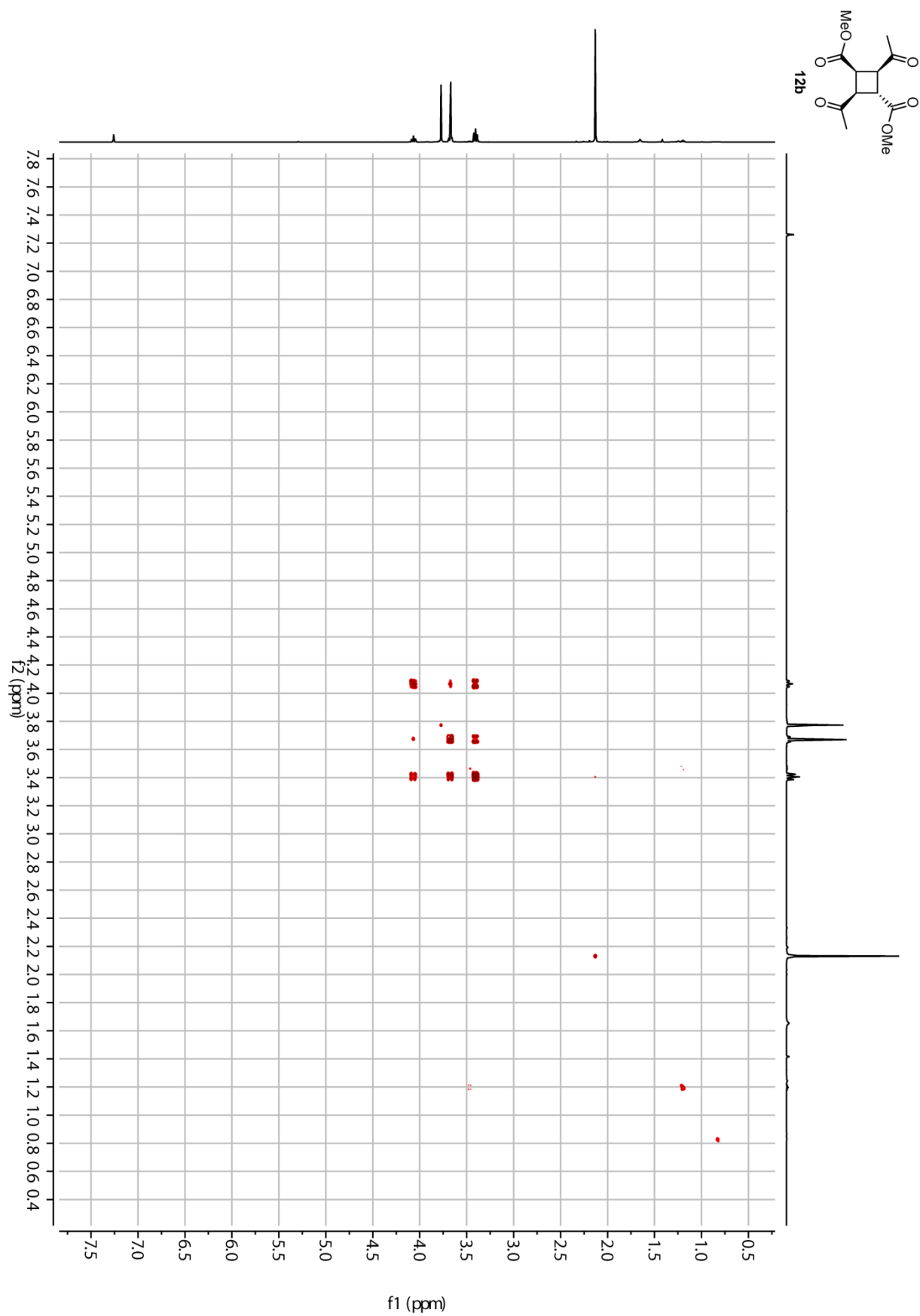


Figure S24. $^1\text{H}, ^1\text{H}$ -COSY spectrum of **12b** (500 MHz, CDCl_3).

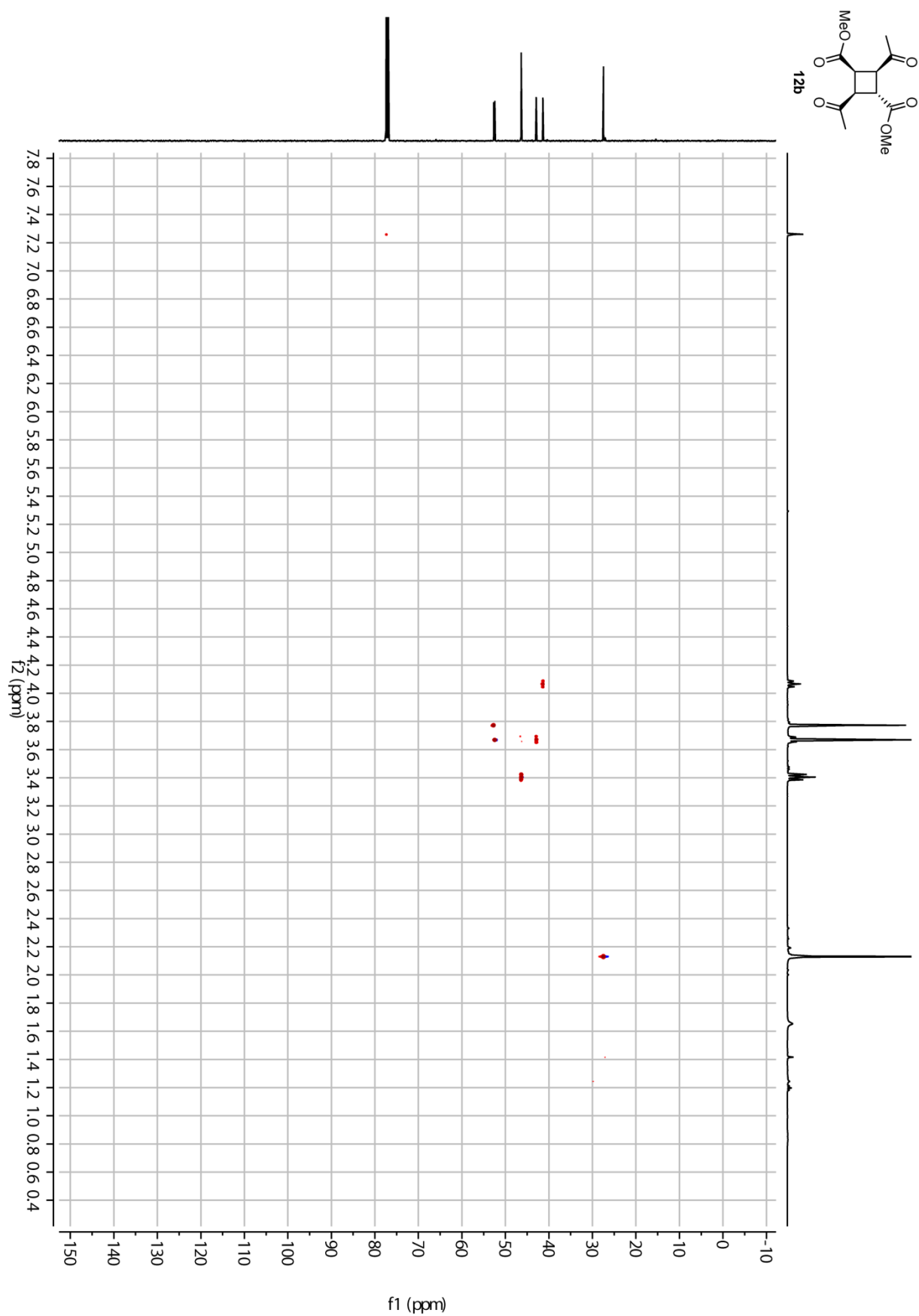


Figure S26. HSQC spectrum of **12b** (CDCl₃).

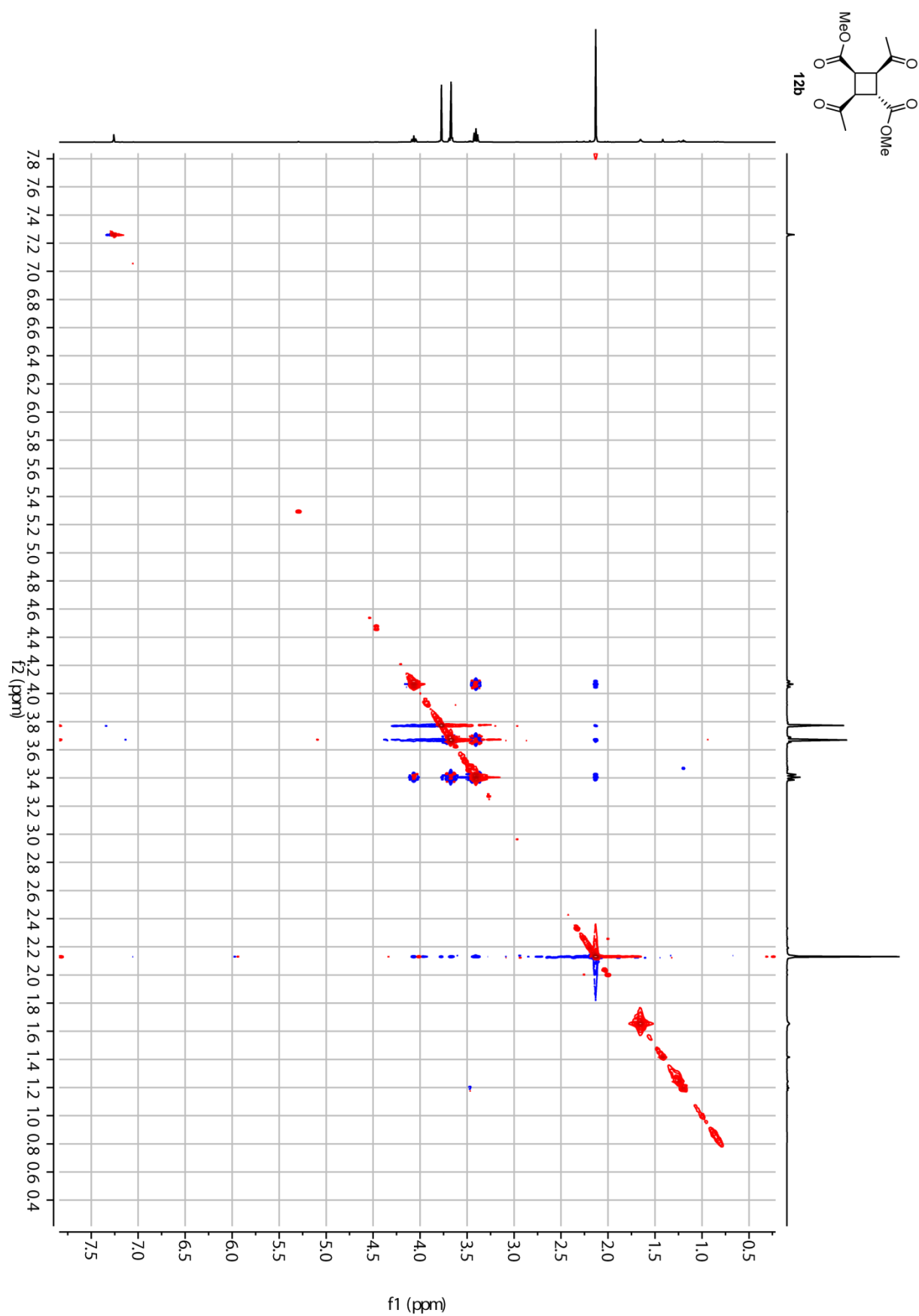


Figure S27. NOESY spectrum of **12b** (CDCl_3).

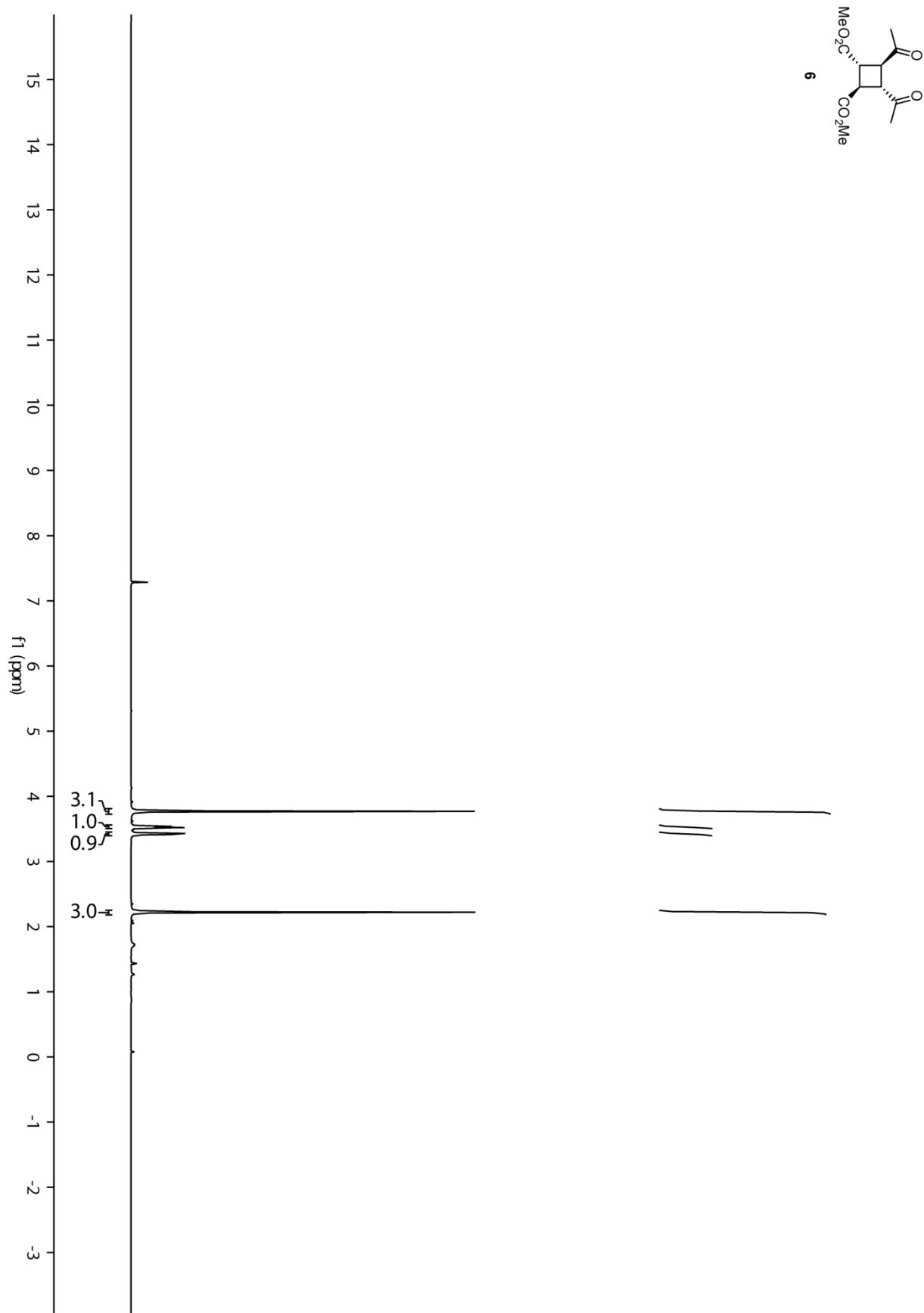


Figure S28. ^1H NMR spectrum of **6** (500 MHz, CDCl_3).

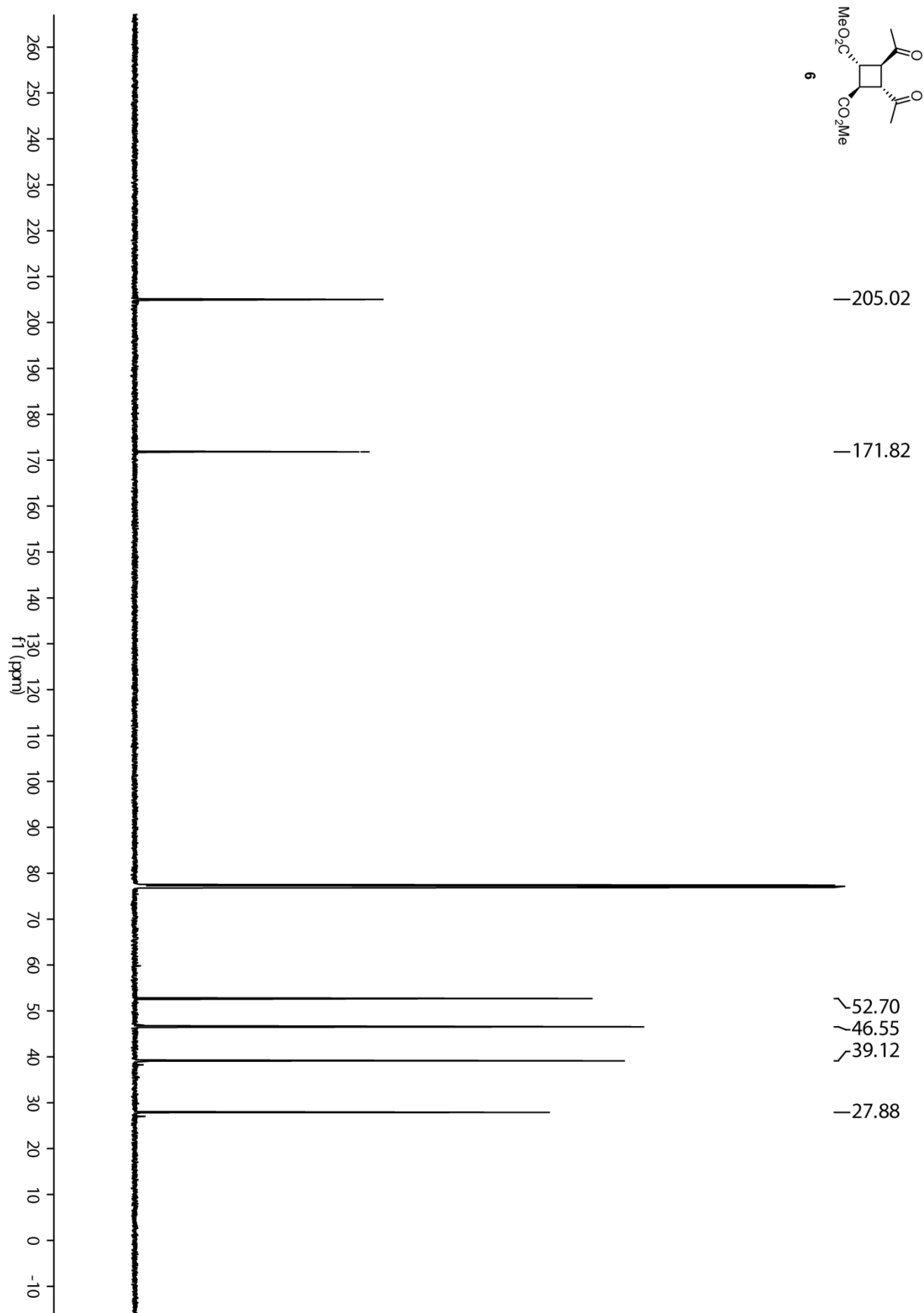


Figure S29. ^{13}C NMR spectrum of **6** (125 MHz, CDCl_3).

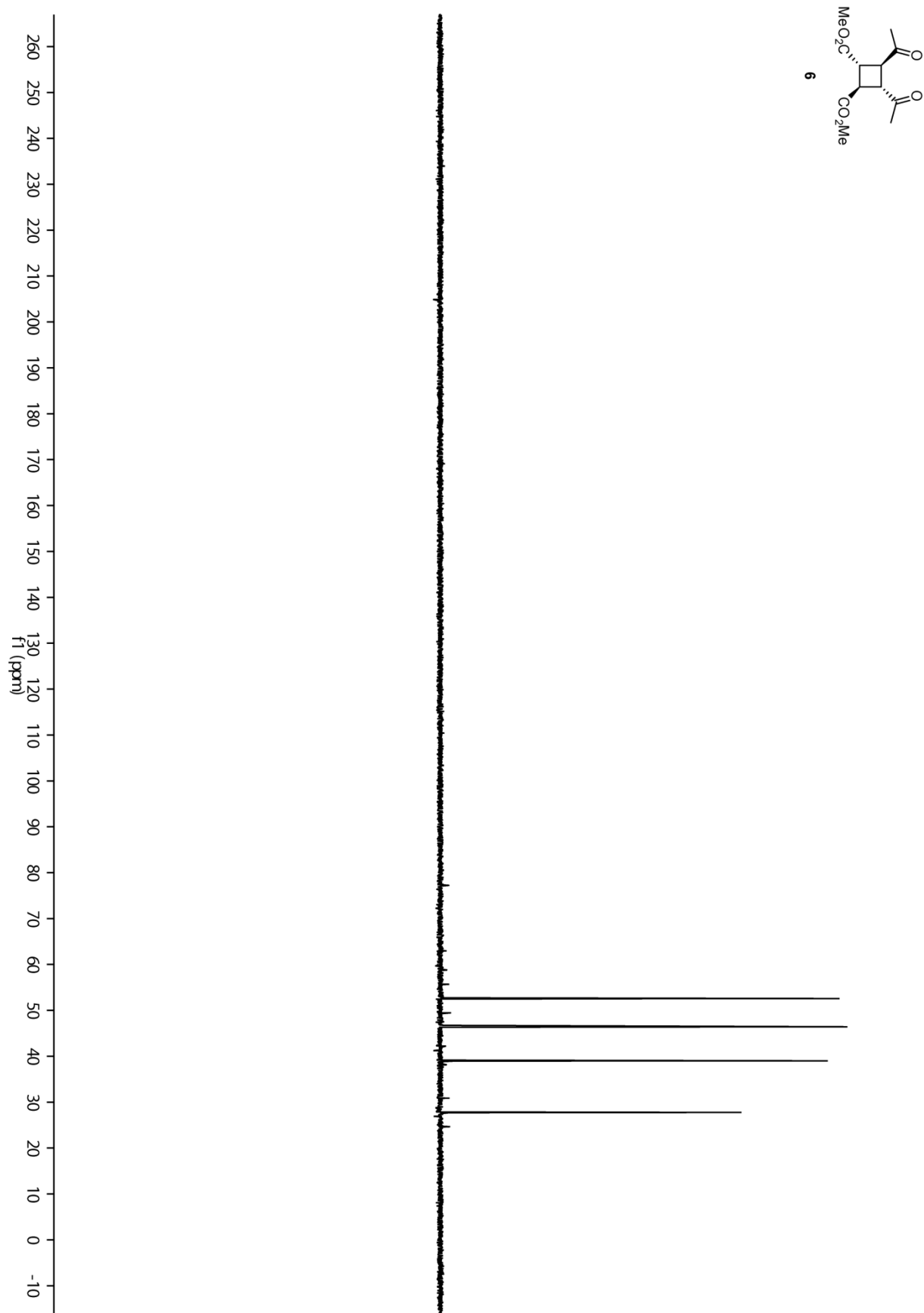


Figure S30. ^{13}C DEPT 135 spectrum of **6** (125 MHz, CDCl_3).

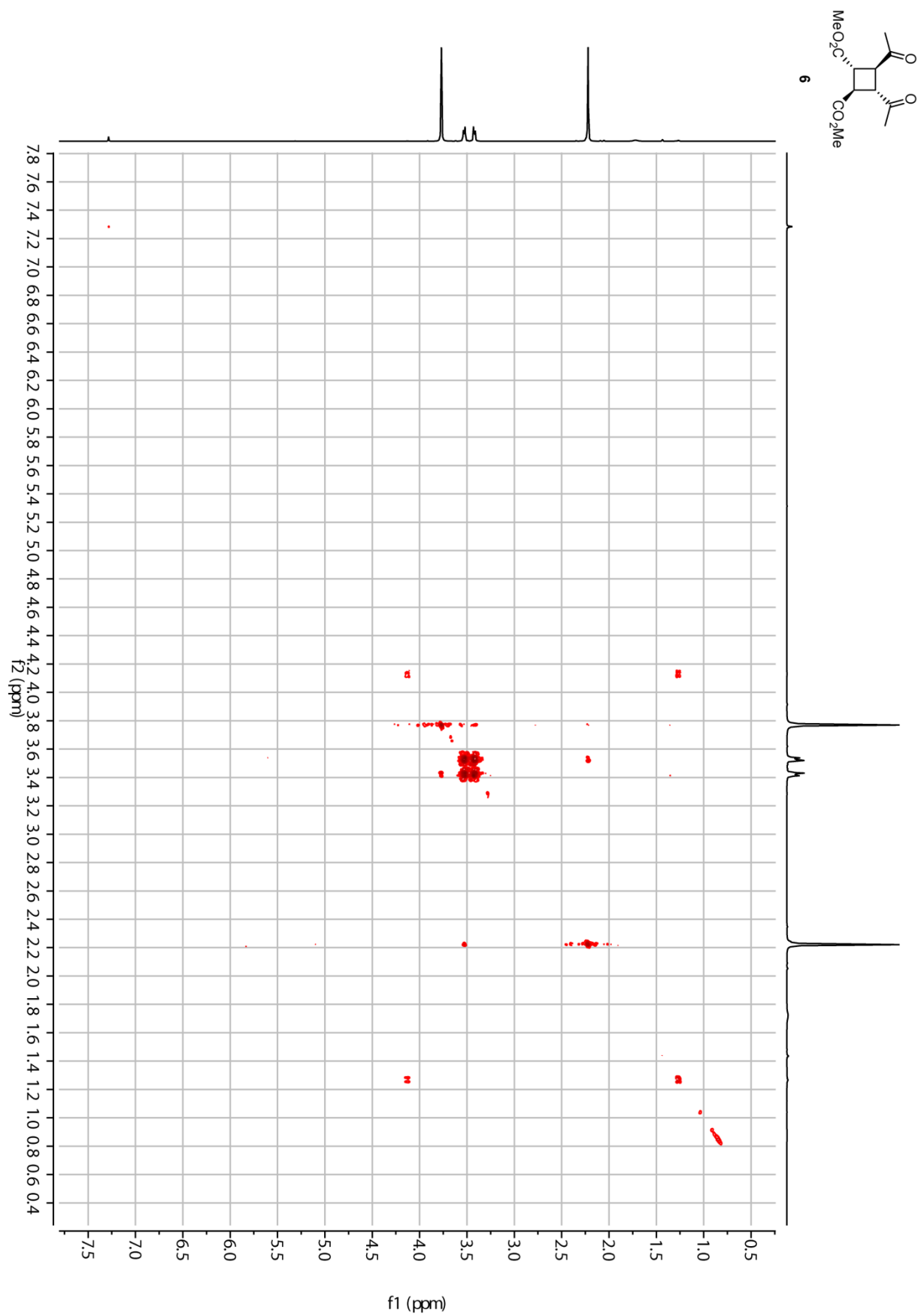
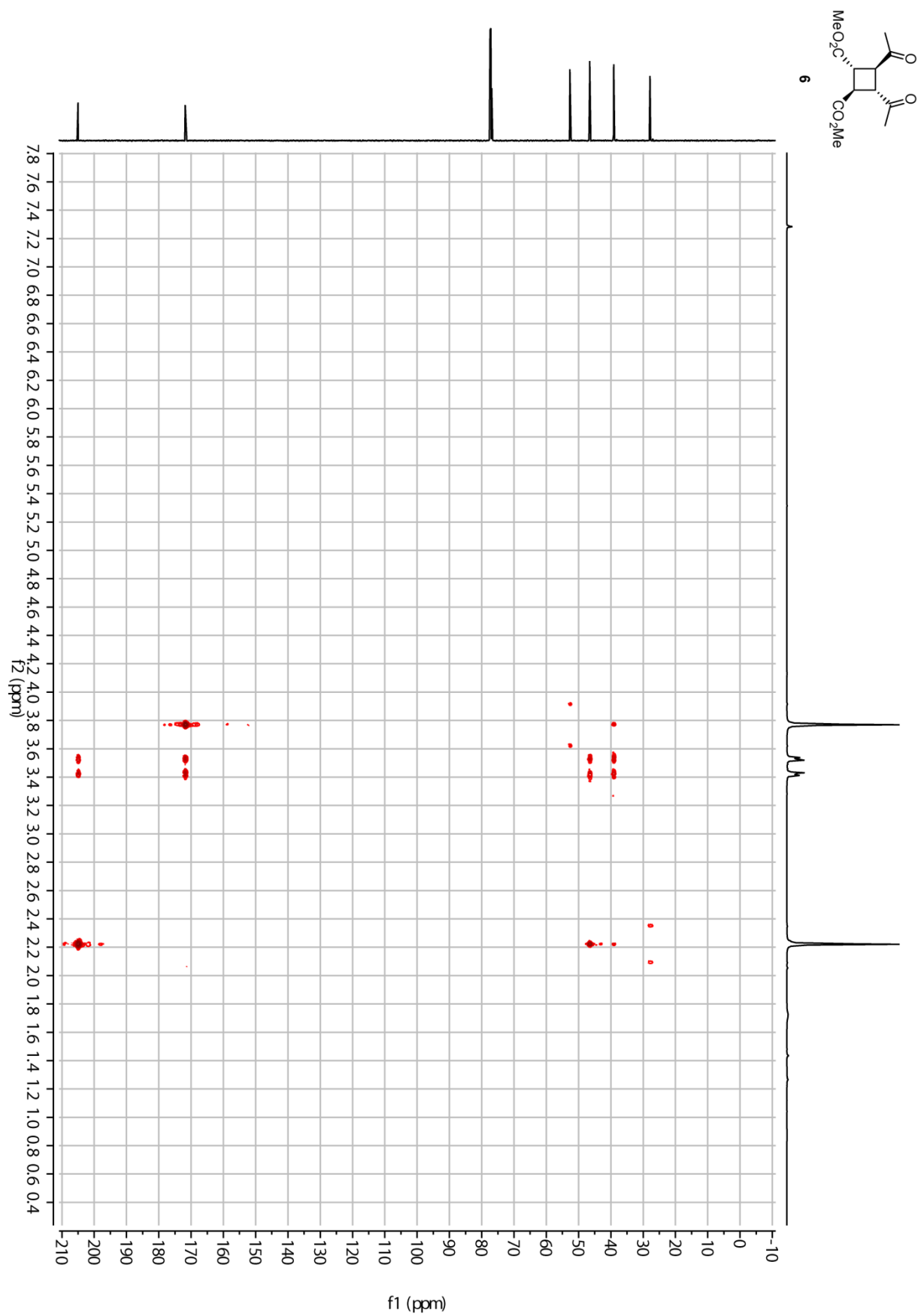


Figure S48. ^1H , ^1H -COSY spectrum of **6** (500 MHz, CDCl_3).



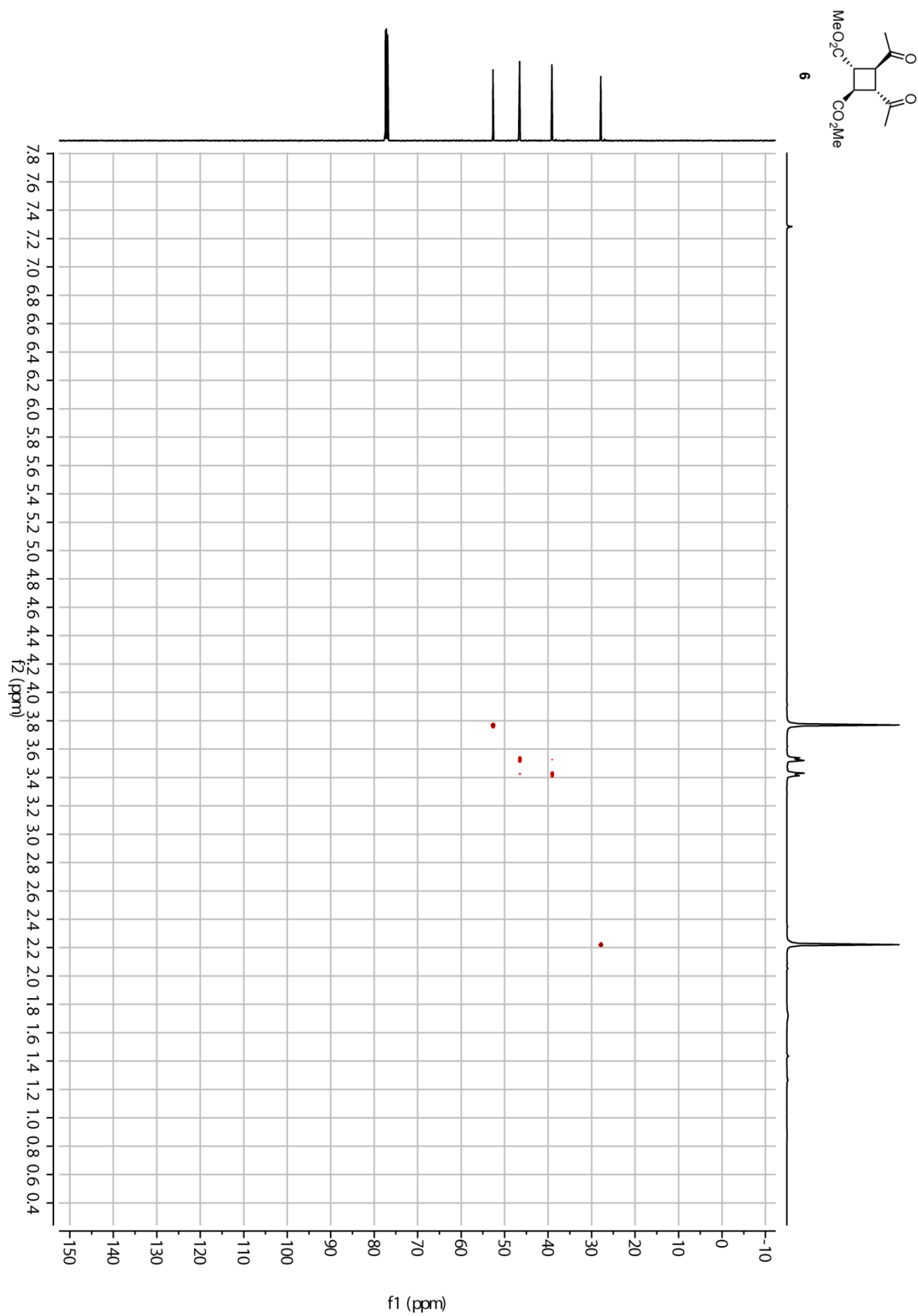


Figure S31. HSQC spectrum of **6** (CDCl_3).

5. REFERENCES

- (1) Blessing, R. H. *Acta Crystallogr.* **1995**, *A51*, 33-38.
- (2) Sheldrick, G. M. *Acta Crystallogr.* **2015**, *A71*, 3-8.
- (3) Sheldrick, G. M. *Acta Crystallogr.* **2015**, *C71*, 3-8.

LEBENS LAUF

PERSÖNLICHE DATEN

Name	Lena Barra
Adresse	Im Krausfeld 45, 53111 Bonn
E-Mail-Adresse	lena.barra@uni-bonn.de
Familienstand	ledig
Staatsangehörigkeit	deutsch
Geburtsdaten	11. Mai 1988 in Braunschweig

SCHULISCHE AUSBILDUNG/STUDIUM

1994 - 1998	Grundschule Denkte, Groß Denkte
1998 - 2000	Orientierungsstufe Cranachstraße, Wolfenbüttel
2000 - 2007	Theodor-Heuss-Gymnasium, Wolfenbüttel Abschluss: Allgemeine Hochschulreife
2007 - 2011	Studium an der TU Braunschweig, Abschluss: Bachelor of Science, Chemie
2011 - 2013	Studium an der TU Braunschweig, Abschluss: Master of Science, Chemie
seit 01.09.2013	Promotionsvorhaben, TU Braunschweig, seit 07.2014 Universität Bonn, Arbeitskreis: Prof. Dr. J. S. Dickschat

PUBLIKATIONSLISTE

- [1] L. Barra, B. Schulz, J. S. Dickschat, *Pogostol Biosynthesis by the Endophytic Fungus Geniculosporium*, *ChemBioChem* **2014**, *15*, 2379-2383.
- [2] C. A. Citron, P. Rabe, L. Barra, C. Nakano, T. Hoshino, J. S. Dickschat, *Synthesis of Isotopically Labelled Oligoprenyl Diphosphates and Their Application in Mechanistic Investigations of Terpene Cyclases*, *Eur. J. Org. Chem.* **2014**, 7684-7691.
- [3] C. A. Citron, L. Barra, J. Wink, J. S. Dickschat, *Volatiles from Nineteen Recently Genome Sequenced Actinomycetes*, *Org. Biomol. Chem.* **2015**, *13*, 2673-2683.

- [4] L. Barra, K. Ibrom, J. S. Dickschat, *Structural Revision and Elucidation of the Biosynthesis of Hypodoratoxide by ^{13}C , ^{13}C COSY NMR Spectroscopy*, *Angew. Chem. Int. Ed.* **2015**, *54*, 6637-6640.
- L. Barra, K. Ibrom, J. S. Dickschat, *Strukturrevision und Aufklärung der Biosynthese von Hypodoratoxid durch ein ^{13}C , ^{13}C -COSY-NMR-Experiment*, *Angew. Chem.* **2015**, *127*, 6737-6740.
- [5] P. Rabe, L. Barra, J. Rinkel, R. Riclea, C. A. Citron, T. A. Klapschinski, A. Janusko, J. S. Dickschat, *Conformational Analysis, Thermal Rearrangement, and EI-MS Fragmentation Mechanism of (1(10)E,4E,6S,7R)-Germacradien-6-ol by ^{13}C -Labeling Experiments*, *Angew. Chem. Int. Ed.* **2015**, *54*, 13448-13451.
- P. Rabe, L. Barra, J. Rinkel, R. Riclea, C. A. Citron, T. A. Klapschinski, A. Janusko, J. S. Dickschat, *Konformationsanalyse, thermische Umlagerung und EI-MS-Fragmentierungsmechanismus von (1(10)E,4E,6S,7R)-Germacradien-6-ol durch ^{13}C -Markierungsexperimente*, *Angew. Chem.* **2015**, *127*, 13649-13653.
- [6] P. Rabe, J. Rinkel, T. A. Klapschinski, L. Barra, J. S. Dickschat, *A method for investigating the stereochemical course of terpene cyclisations*, *Org. Biomol. Chem.* **2016**, *14*, 158-164.
- [7] M. M. Mohseni, T. Höver, L. Barra, M. Kaiser, P. C. Dorrestein, J. S. Dickschat, T. F. Schäberle, *Discovery of a Mosaic-Like Biosynthetic Assembly Line with a Decarboxylative Off-Loading Mechanism through a Combination of Genome Mining and Imaging*, *Angew. Chem. Int. Ed.* **2016**, *55*, 13611-13614.
- M. M. Mohseni, T. Höver, L. Barra, M. Kaiser, P. C. Dorrestein, J. S. Dickschat, T. F. Schäberle, *Entdeckung einer Mosaik-ähnlichen Biosynthesemaschinerie mit einem decarboxylierenden Entladungsmechanismus durch die Kombination von Genom-Mining und bildgebenden Verfahren*, *Angew. Chem.* **2016**, *128*, 13809-13813.
- [8] L. Barra, J. S. Dickschat, *Sceptrin – Enantioselective Synthesis of a Tetrasubstituted all-trans Cyclobutane Key Intermediate*, *Eur. J. Org. Chem.* **2017**, 4566-4571.
- [9] L. Barra, P. Barac, G. M. König, M. Crüsemann, J. S. Dickschat, *Volatiles from the fungal microbiome of the marine sponge *Callyspongia cf. flammea**, *Org. Biomol. Chem.* **2017**, *15*, 7411-7421.
- [10] L. Barra, J. S. Dickschat, *Harzianone Biosynthesis by the Biocontrol Fungus *Trichoderma**, *ChemBioChem*, **2017**, accepted.

Summary

The cumulative doctoral thesis “Studies on the Biosynthesis and Structure Elucidation of Terpene Natural Products by Isotopic Labeling Experiments” deals with the application of stable isotopes for structure elucidation and biosynthesis studies of terpenoids from microorganisms. Additionally, analytic and synthetic studies on volatile natural products were conducted.

A highly sensitive method for the identification of terpenes from fungal organisms, based on *in vivo* incorporation of ^{13}C -labeled biosynthetic precursors was developed. This method was successfully applied for the identification of pogostol from the endophytic fungus *Geniculosporium*, of harzianone from the biocontrol fungus *Trichoderma* and of hypodoratoxide from the mycophilic fungus *Hypomyces odoratus*. The results gave additional insights into the biosynthesis of these metabolites. Isotopically labeled substrates were also designed, synthesized and utilized for *in vitro* experiments with recombinant enzymes from bacterial sources.

Additionally, two studies on volatile metabolites from microorganisms were conducted. Nineteen recently genome sequenced actinomycetes were investigated and the chemical analysis was correlated to genome sequencing data. The volatiles of five sponge-associated fungi were analyzed and a series of bioactive metabolites, like the quorum sensing inhibitor protoanemonin, a highly phytotoxic lactone and algicidal phloroglucinol derivatives were identified.

During studies towards the total synthesis of the sesquiterpene koraiol, an enantioselective approach for the synthesis of a pseudosymmetric, tetrasubstituted all-*trans* cyclobutane was developed. The method makes use of a chiral auxiliary in a diastereoselective photodimerization. The obtained cyclobutane derivative is a key intermediate in the total synthesis of the highly bioactive sponge-derived metabolite scep trin.